

Project No. 17-45

Copy No.

**SAFETY PREDICTION METHODOLOGY
AND ANALYSIS TOOL
FOR FREEWAYS AND INTERCHANGES**

FINAL REPORT

**Prepared For
National Cooperative Highway Research Program
Transportation Research Board
of
The National Academies**

TRANSPORTATION RESEARCH BOARD
OF THE NATIONAL ACADEMIES
PRIVILEGED DOCUMENT

This report, not released for publication, is furnished only for review to members of or participants in the work of the CRP. This report is to be regarded as fully privileged, and dissemination of the information included herein must be approved by the CRP.

**Texas Transportation Institute
Texas A&M University**

In Association with:
CH2M-Hill

May 2012

ACKNOWLEDGMENT OF SPONSORSHIP

This work was sponsored by the American Association of State Highway and Transportation Officials, in cooperation with the Federal Highway Administration, and was conducted in the National Cooperative Highway Research Program which is administered by the Transportation Research Board of the National Academies.

DISCLAIMER

This is an uncorrected draft as submitted by the research agency. The opinions and conclusions expressed or implied in the report are those of the research agency. They are not necessarily those of the Transportation Research Board, the National Academies, or the program sponsors.

NATIONAL COOPERATIVE HIGHWAY RESEARCH PROGRAM

Project 17-45

Safety Prediction Methodology and Analysis Tool for Freeways and Interchanges

James A. Bonneson
Srinivas Geedipally
Michael P. Pratt
Texas Transportation Institute
College Station, Texas

Dominique Lord
Texas A&M University
College Station, Texas

Subject Areas

Highway and Facility Design
Highway Operations, Highway Safety

Research Sponsored by the American Association of State
Highway and Transportation Officials in Cooperation with the
Federal Highway Administration

**Transportation Research Board
of the National Academies**

Washington, D.C.

May 2012

CONTENTS

	<u>page</u>
LIST OF FIGURES	vi
LIST OF TABLES	ix
ACKNOWLEDGMENTS	xiii
ABSTRACT	xiv
EXECUTIVE SUMMARY	1
CHAPTER 1: INTRODUCTION	3
Research Objectives	3
Research Scope	3
Organization of this Report	4
CHAPTER 2: LITERATURE REVIEW	5
Background	5
Freeway and Interchange Safety	12
CHAPTER 3: FRAMEWORK FOR SAFETY PREDICTION	57
Overview of <i>HSM</i> Methodology	57
Prioritized List of SPFs and CMFs	60
CHAPTER 4: DATABASE DEVELOPMENT	69
Data Collection Procedures	69
Database Summary	79
CHAPTER 5: PREDICTIVE MODEL FOR FREEWAY SEGMENTS	101
Background	102
CMF Development	108
Methodology	113
Model Calibration for FI Crashes	119
Model Calibration for PDO Crashes	158
Nomenclature	177
CHAPTER 6: PREDICTIVE MODEL FOR RAMP SEGMENTS	183
Background	184
CMF Development	188
Methodology	196
Model Calibration for FI Crashes	199
Model Calibration for PDO Crashes	223
Nomenclature	234
CHAPTER 7: PREDICTIVE MODEL FOR CROSSROAD RAMP TERMINALS	237
Background	238
CMF Development	242
Methodology	254
Model Calibration for FI Crashes	259
Model Calibration for PDO Crashes	294
Nomenclature	318
CHAPTER 8: SEVERITY DISTRIBUTION FUNCTIONS	321
Literature Review	321
Freeway Segments	323
Ramp Segments	336
Crossroad Ramp Terminals	342
CHAPTER 9: CONCLUSIONS AND RECOMMENDATIONS	351

REFERENCES	353
APPENDIX A Practitioner Interviews	
APPENDIX B Database Enhancement	
APPENDIX C Proposed HSM Freeways Chapter	
APPENDIX D Proposed HSM Ramps Chapter	
APPENDIX E Proposed HSM Appendix B for Part C	
APPENDIX F Algorithm Description	

LIST OF FIGURES

	<u>page</u>
Figure 1. Typical interchange types.....	7
Figure 2. Distribution of interchange types used in the United States.....	7
Figure 3. Typical diamond and parclo interchange types.....	8
Figure 4. Typical ramp configurations.....	9
Figure 5. Freeway and interchange design components.....	10
Figure 6. Disaggregated alignment for a diamond ramp.....	12
Figure 7. Ramp-configuration-based SPFs based on total crashes.....	17
Figure 8. Relationship between CMF value and ramp radius based on total crashes.....	19
Figure 9. Relationship between CMF value and ramp lane width based on total crashes.....	20
Figure 10. Relationship between ramp crash frequency and crash type based on total crashes...	21
Figure 11. Typical speed-change lanes.....	22
Figure 12. Relationship between CMF value and acceleration length based on total crashes.	25
Figure 13. Relationship between CMF value and deceleration length based on total crashes.	26
Figure 14. Relationship between crash rate, traffic demand, and number of lanes.....	29
Figure 15. Freeway segment SPFs based on FI crashes.....	30
Figure 16. Relationship between CMF value and curve radius.....	32
Figure 17. Relationship between CMF value and lane width based on total crashes.....	33
Figure 18. Illustrative interaction between shoulder width and lane width.....	34
Figure 19. Relationship between CMF value and outside shoulder width based on total crashes.....	34
Figure 20. Relationship between CMF value and inside shoulder width based on total crashes.....	35
Figure 21. Relationship between CMF value and median width.....	35
Figure 22. Relationship between CMF value and horizontal clearance based on FI crashes.....	37
Figure 23. Percent of lane changes as a function of distance from ramp gore.....	39
Figure 24. Total crash rate as a function of distance from ramp gore.....	40
Figure 25. Relationship between CMF value and distance from gore.....	41
Figure 26. Relationship between CMF value and weaving length.....	42
Figure 27. Relationship between CMF value and interchange spacing.....	43
Figure 28. Relationship between total crash rate and volume-to-capacity ratio for highways.....	45
Figure 29. Relationship between total crash rate and volume-to-capacity ratio for freeways.....	45
Figure 30. Relationship between traffic demand, crash type, and total crash frequency.....	46
Figure 31. Relationship between CMF value and volume-to-capacity ratio.....	47
Figure 32. High-occupancy vehicle travel direction types.....	49
Figure 33. Relationship between FI crash rate and speed differential.....	51
Figure 34. SPF for two interchange types based on total crashes.....	53
Figure 35. Designs to discourage wrong-way maneuvers.....	56

Figure 36. Highway Safety Manual predictive method.....	58
Figure 37. Ramp terminal configurations.....	91
Figure 38. Illustrative freeway facility analysis sites.....	103
Figure 39. Hourly volume distribution for two freeway segments.....	110
Figure 40. Proportion-of-volume statistic for freeway segments in three states.....	111
Figure 41. Relationship between crash rate and side friction demand.....	112
Figure 42. Weaving section types.....	114
Figure 43. Weaving section length measurement.....	115
Figure 44. Predicted vs. reported multiple-vehicle freeway FI crashes.....	135
Figure 45. Predicted vs. reported single-vehicle freeway FI crashes.....	137
Figure 46. Predicted vs. reported ramp-entrance-related FI crashes.....	138
Figure 47. Predicted vs. reported ramp-exit-related FI crashes.....	139
Figure 48. Calibrated freeway horizontal curve CMF for FI crashes.....	141
Figure 49. Calibrated freeway lane width CMF for FI crashes.....	142
Figure 50. Calibrated freeway outside shoulder width CMF for FI crashes.....	143
Figure 51. Calibrated freeway inside shoulder width CMF for FI crashes.....	144
Figure 52. Calibrated freeway median width CMF for FI crashes.....	145
Figure 53. Calibrated freeway outside clearance CMF for FI crashes.....	147
Figure 54. Lane change CMF as a function of distance from ramp gore.....	149
Figure 55. Lane change CMF for segments between a pair of interchanges.....	150
Figure 56. Average CMF value for FI crashes as a function of weaving section length.....	151
Figure 57. Calibrated freeway ramp entrance CMF for right-side ramps and FI crashes.....	152
Figure 58. Calibrated freeway ramp exit CMF for right-side ramps and FI crashes.....	153
Figure 59. Calibrated freeway high-volume CMF for FI crashes.....	154
Figure 60. Freeway FI model components.....	155
Figure 61. Freeway FI model.....	156
Figure 62. Predicted vs. reported multiple-vehicle freeway PDO crashes.....	161
Figure 63. Predicted vs. reported single-vehicle freeway PDO crashes.....	163
Figure 64. Predicted vs. reported ramp-entrance-related PDO crashes.....	164
Figure 65. Predicted vs. reported ramp-exit-related PDO crashes.....	165
Figure 66. Calibrated freeway horizontal curve CMF for PDO crashes.....	167
Figure 67. Calibrated freeway outside shoulder width CMF for PDO crashes.....	168
Figure 68. Calibrated freeway inside shoulder width CMF for PDO crashes.....	168
Figure 69. Calibrated freeway median width CMF for PDO crashes.....	169
Figure 70. Calibrated freeway outside barrier CMF for PDO crashes.....	171
Figure 71. Average CMF value for PDO crashes as a function of weaving section length.....	173
Figure 72. Calibrated freeway ramp entrance CMF for right-side ramps and PDO crashes.....	174
Figure 73. Calibrated freeway high-volume CMF for PDO crashes.....	175
Figure 74. Freeway PDO model components.....	176
Figure 75. Freeway PDO model.....	177
Figure 76. Illustrative interchange analysis sites.....	184
Figure 77. Starting milepost location on ramps and C-D roads.....	189
Figure 78. Diagonal ramp configuration for example application.....	195
Figure 79. Speed-change lane location on ramps and C-D roads.....	197
Figure 80. Predicted vs. reported multiple-vehicle ramp FI crashes.....	210
Figure 81. Predicted vs. reported single-vehicle ramp FI crashes.....	211
Figure 82. Calibrated ramp horizontal curve CMF for FI crashes.....	213
Figure 83. Calibrated ramp lane width CMF for FI crashes.....	214

Figure 84. Calibrated ramp right shoulder width CMF for FI crashes.	215
Figure 85. Calibrated ramp left shoulder width CMF for FI crashes.	216
Figure 86. Calibrated ramp right side barrier CMF for FI crashes.	217
Figure 87. Calibrated ramp left side barrier CMF for FI crashes.	218
Figure 88. Calibrated ramp weaving section CMF for FI crashes.	219
Figure 89. Calibrated ramp speed-change lane CMF for FI crashes.	220
Figure 90. Calibrated ramp lane add or drop CMF for FI crashes.	221
Figure 91. Ramp FI model components.	222
Figure 92. Ramp FI model.	222
Figure 93. Predicted vs. reported multiple-vehicle ramp PDO crashes.	225
Figure 94. Predicted vs. reported single-vehicle ramp PDO crashes.	226
Figure 95. Calibrated ramp horizontal curve CMF for PDO crashes.	228
Figure 96. Calibrated ramp right shoulder width CMF for PDO crashes.	228
Figure 97. Calibrated ramp left shoulder width CMF for PDO crashes.	229
Figure 98. Calibrated ramp right side barrier CMF for PDO crashes.	230
Figure 99. Calibrated ramp left side barrier CMF for PDO crashes.	231
Figure 100. Calibrated ramp weaving section CMF for PDO crashes.	232
Figure 101. Ramp PDO model components.	233
Figure 102. Ramp PDO model.	234
Figure 103. Illustrative crossroad ramp terminal boundary.	239
Figure 104. Comparison of predicted turn lane CMFs with standardized residuals - total crashes.	247
Figure 105. Relationship between median width and CMF value at unsignalized intersections.	251
Figure 106. Effective number of lanes for various exit ramp configurations.	252
Figure 107. Relationship between exit ramp volume, control, and CMF value at signalized terminals.	253
Figure 108. Relationship between skew angle and CMF value at unsignalized intersections. ..	254
Figure 109. Right-turn channelization length.	255
Figure 110. Crossroad median width.	256
Figure 111. Simulation results for the inverse dispersion parameter.	258
Figure 112. Predicted vs. reported FI crashes at signalized A2 and B2 configurations.	269
Figure 113. Predicted vs. reported FI crashes at signalized A4 and D3ex configurations.	270
Figure 114. Predicted vs. reported FI crashes at signalized B4 and D3en configurations.	271
Figure 115. Predicted vs. reported FI crashes at signalized D4 configurations.	272
Figure 116. Calibrated segment length CMF for FI crashes–signalized.	277
Figure 117. Calibrated median width CMF for FI crashes–signalized.	278
Figure 118. Terminal FI models–signalized.	279
Figure 119. Predicted vs. reported FI crashes at unsignalized A2 and B2 configurations.	287
Figure 120. Predicted vs. reported FI crashes at unsignalized A4 and D3ex configurations.	288
Figure 121. Predicted vs. reported FI crashes at unsignalized B4 and D3en configurations.	289
Figure 122. Predicted vs. reported FI crashes at unsignalized D4 configurations.	290
Figure 123. Calibrated exit ramp capacity CMF for FI crashes–unsignalized.	291
Figure 124. Calibrated segment length CMF for FI crashes–unsignalized.	293
Figure 125. Terminal FI models–unsignalized.	295
Figure 126. Predicted vs. reported PDO crashes at signalized A2 and B2 configurations.	298
Figure 127. Predicted vs. reported PDO crashes at signalized A4 and D3ex configurations.	299
Figure 128. Predicted vs. reported PDO crashes at signalized B4 and D3en configurations.	300

Figure 129. Predicted vs. reported PDO crashes at signalized D4 configurations.	301
Figure 130. Calibrated segment length CMF for PDO crashes–signalized.	306
Figure 131. Calibrated median width CMF for PDO crashes–signalized.	307
Figure 132. Terminal PDO models–signalized.	308
Figure 133. Predicted vs. reported PDO crashes at unsignalized A2 and B2 configurations.	311
Figure 134. Predicted vs. reported PDO crashes at unsignalized A4 and D3ex configurations.	312
Figure 135. Predicted vs. reported PDO crashes at unsignalized B4 and D3en configurations.	313
Figure 136. Predicted vs. reported PDO crashes at unsignalized D4 configurations.	314
Figure 137. Terminal PDO models–unsignalized.	317
Figure 138. Freeway severity distribution based on the proportion of segment with barrier.	329
Figure 139. Freeway severity distribution based on the proportion of AADT during high-volume hours.	330
Figure 140. Freeway severity distribution based on the proportion of segment with rumble strips.	331
Figure 141. Freeway severity distribution based on the proportion of segment with horizontal curve.	332
Figure 142. Freeway severity distribution based on lane width.	333
Figure 143. Ramp severity distribution based on the proportion of segment with barrier.	340
Figure 144. Crossroad ramp terminal severity distribution based on access point frequency.	347

LIST OF TABLES

	<u>page</u>
TABLE 1. Freeway mileage and number of interchanges in the United States	6
TABLE 2. Crash distribution among interchange ramp components	13
TABLE 3. Crash distribution among interchange ramp components	13
TABLE 4. Comparison of total crash rates for exit ramps with a lane drop	27
TABLE 5. CMFs for shoulder rumble strips	36
TABLE 6. Elements that may influence the safety of crossroad ramp terminals	55
TABLE 7. Prioritized list of SPFs and CMFs for freeway segments	63
TABLE 8. Prioritized list of SPFs and CMFs for interchange ramp	65
TABLE 9. Prioritized list of SPFs and CMFs for crossroad ramp terminals	66
TABLE 10. Prioritized list of SPFs and CMFs for freeway speed-change lanes	67
TABLE 11. Base FI crash rates for minimum exposure criteria	72
TABLE 12. SAS Processing Effort	73
TABLE 13. Database attributes	74
TABLE 14. Database target sample size	75
TABLE 15. Criteria for defining crossroad-ramp-terminal-related crashes	79
TABLE 16. Database sample size	80
TABLE 17. Summary characteristics for freeway segments	81
TABLE 18. Barrier and ramp characteristics for freeway segments	82
TABLE 19. Crash data summary for freeway segments	84
TABLE 20. Summary characteristics for ramp segments	86
TABLE 21. Barrier and cross section characteristics for ramp segments	87
TABLE 22. Crash data summary for ramp segments	89

TABLE 23. Crash data summary by ramp configuration	90
TABLE 24. Summary characteristics for crossroad ramp terminals	94
TABLE 25. Crash data summary for crossroad ramp terminals.....	95
TABLE 26. Crash data summary by ramp terminal configuration.....	97
TABLE 27. Sample size considerations for crossroad ramp terminals	97
TABLE 28. Summary characteristics for freeway speed-change lane segments	99
TABLE 29. Freeway variables from HSIS database	105
TABLE 30. Freeway variables from supplemental data sources.....	106
TABLE 31. Freeway FI model statistical description–combined model–two states.....	130
TABLE 32. Freeway model validation statistics	132
TABLE 33. Freeway FI model statistical description–combined model–three states.....	133
TABLE 34. Freeway FI model statistical description–multiple-vehicle model–three states	134
TABLE 35. Freeway FI model statistical description–single-vehicle model–three states	136
TABLE 36. Freeway FI model statistical description–ramp entrance model–three states.....	137
TABLE 37. Freeway FI model statistical description–ramp exit model–three states	138
TABLE 38. Distribution of FI crashes on freeways	140
TABLE 39. Freeway PDO model statistical description–combined model –three states	159
TABLE 40. Freeway PDO model statistical description–multiple-vehicle model–three states.	160
TABLE 41. Freeway PDO model statistical description–single-vehicle model–three states.....	162
TABLE 42. Freeway PDO model statistical description–ramp entrance model–three states	163
TABLE 43. Freeway PDO model statistical description–ramp exit model–three states	164
TABLE 44. Distribution of PDO crashes on freeways.....	166
TABLE 45. Ramp variables from HSIS database	186
TABLE 46. Ramp variables from supplemental data sources.....	187
TABLE 47. Input data for ramp curve speed prediction	191
TABLE 48. Input data for example application.....	195
TABLE 49. Results for example application.....	196
TABLE 50. Ramp FI model statistical description–combined model–two states	205
TABLE 51. Ramp model validation statistics	207
TABLE 52. Ramp FI model statistical description–combined model–three states	208
TABLE 53. Ramp FI model statistical description–multiple-vehicle model–three states.....	209
TABLE 54. Ramp FI model statistical description–single-vehicle model–three states	210
TABLE 55. Distribution of FI crashes on ramps.....	212
TABLE 56. Ramp PDO model statistical description–combined model–three states.....	224
TABLE 57. Ramp PDO model statistical description–multiple-vehicle model–three states	224
TABLE 58. Ramp PDO model statistical description–single-vehicle model–three states	226
TABLE 59. Distribution of PDO crashes on ramps	227
TABLE 60. Terminal variables from HSIS database	241
TABLE 61. Variables from supplemental data sources.....	242
TABLE 62. Turn lane CMF model statistical description - total crashes.....	246
TABLE 63. Leg-specific turn lane CMFs - total crashes	247
TABLE 64. Leg-specific turn lane CMFs - FI crashes.....	248
TABLE 65. Leg-specific turn lane CMFs - PDO crashes	249
TABLE 66. Indicator variable values for typical ramp terminal configurations.....	264
TABLE 67. Terminal FI model statistical description–combined model–two states–signalized	265
TABLE 68. Terminal model validation statistics–signalized.....	266
TABLE 69. Terminal FI model statistical description–combined model–three states–signalized	267

TABLE 70. Terminal FI model statistical description–A2 and B2 configuration–signalized ...	268
TABLE 71. Terminal FI model statistical description–A4 and D3ex configuration–signalized	269
TABLE 72. Terminal FI model statistical description–B4 and D3en configuration–signalized	270
TABLE 73. Terminal FI model statistical description–D4 configuration–signalized.....	272
TABLE 74. Calibrated protected left-turn operation CMF for FI crashes	274
TABLE 75. Calibrated right-turn channelization CMF for FI crashes–signalized.....	275
TABLE 76. Calibrated access point frequency CMF for FI crashes–signalized.....	276
TABLE 77. Terminal FI model statistical description–combined model–two states–unsignalized	283
TABLE 78. Terminal model validation statistics–unsignalized.....	284
TABLE 79. Terminal FI model statistical description–combined model–three states–unsignalized	285
TABLE 80. Terminal FI model statistical description–A2 and B2 configuration–unsignalized	286
TABLE 81. Terminal FI model statistical description–A4 and D3ex configuration–unsignalized	287
TABLE 82. Terminal FI model statistical description–B4 and D3en configuration–unsignalized	288
TABLE 83. Terminal FI model statistical description–D4 configuration–unsignalized.....	289
TABLE 84. Calibrated access point frequency CMF for FI crashes–unsignalized.....	292
TABLE 85. Terminal PDO model statistical description–combined model–three states– signalized	296
TABLE 86. Terminal PDO model statistical description–A2 and B2 configuration–signalized	297
TABLE 87. Terminal PDO model statistical description–A4 and D3ex configuration–signalized	298
TABLE 88. Terminal PDO model statistical description–B4 and D3en configuration–signalized	299
TABLE 89. Terminal PDO model statistical description–D4 configuration–signalized	301
TABLE 90. Calibrated left-turn CMF for PDO crashes–signalized.....	302
TABLE 91. Calibrated right-turn CMF for PDO crashes–signalized.....	303
TABLE 92. Calibrated protected left-turn operation CMF for PDO crashes	303
TABLE 93. Calibrated right-turn channelization CMF for PDO crashes–signalized	304
TABLE 94. Calibrated access point frequency CMF for PDO crashes–signalized	305
TABLE 95. Terminal PDO model statistical description–combined model–three states– unsignalized	309
TABLE 96. Terminal PDO model statistical description–A2 and B2 configuration–unsignalized	311
TABLE 97. Terminal PDO model statistical description–A4 and D3ex configuration– unsignalized	312
TABLE 98. Terminal PDO model statistical description–B4 and D3en configuration– unsignalized	313
TABLE 99. Terminal PDO model statistical description–D4 configuration–unsignalized	314
TABLE 100. Calibrated left-turn CMF for PDO crashes–unsignalized.....	315
TABLE 101. Calibrated right-turn CMF for PDO crashes–unsignalized.....	316
TABLE 102. Summary statistics for freeway SDF development.....	326
TABLE 103. Parameter estimation for freeway SDF.....	327
TABLE 104. Freeway severity distribution based on area type and state	334
TABLE 105. Example application of SDF local calibration procedure	336
TABLE 106. Summary statistics for ramp SDF development	338

TABLE 107. Parameter estimation for ramp SDF.....	339
TABLE 108. Ramp severity distribution based on lanes, area type, and ramp type	341
TABLE 109. Summary statistics for crossroad ramp terminal SDF development.....	344
TABLE 110. Parameter estimation for crossroad ramp terminal SDF	345
TABLE 111. Crossroad ramp terminal severity distribution–signalized.....	347
TABLE 112. Crossroad ramp terminal severity distribution–unsignalized.....	349

ACKNOWLEDGMENTS

The research reported herein was performed under NCHRP Project 17-45 by the Texas Transportation Institute (TTI); and CH2M-Hill. Dr. James Bonneson of TTI served as the Principal Investigator for the project and supervised the research conducted by TTI. Mr. Jason Moller supervised the research conducted by CH2M-Hill. The research supervisors were assisted by the following individuals:

- Dr. Srinivas Geedipally Texas Transportation Institute
- Dr. Dominique Lord Texas A&M University
- Mr. Tim Neuman CH2M-Hill
- Mr. Michael P. Pratt Texas Transportation Institute

ABSTRACT

Safety prediction procedures have been developed for rural two-lane highways, rural multilane highways, and urban and suburban arterials, and are included in the *Highway Safety Manual (HSM)*. However, the *HSM* does not include a safety prediction methodology for freeways and interchanges. This research was undertaken to address this need by developing methodologies suitable for inclusion in the *HSM*. To accomplish this objective, data were assembled that included a wide range of geometric design features, traffic control features, traffic characteristics, and crash records for freeway segments, ramp segments, and crossroad ramp terminals. The data were used to calibrate predictive models, each of which included a safety performance function and several crash modification factors. Separate severity distribution functions were also calibrated using this data. These functions are used with the predictive models to estimate the expected crash frequency for each of five severity levels (i.e., fatal, incapacitating injury, non-incapacitating injury, possible injury, and property damage only crash).

EXECUTIVE SUMMARY

INTRODUCTION

Prior to this research project, state highway agencies did not have tools for reflecting safety in their decisions concerning freeway and interchange projects. This research was undertaken to address this need by developing safety prediction methods for freeways and interchanges that can be used to quantify the influence of design and operational decisions on safety.

There were several objectives of this research project. One key objective was to develop an overall framework for safety prediction methods for freeways and interchanges. A second key objective was to develop analytical models and procedures within the overall framework, and then document them as a predictive method in a chapter for the future edition of the *HSM*.

The project's secondary objectives were to develop a software tool and training materials to facilitate the implementation of the safety prediction methods developed for this project. One objective was to develop a software tool that automated the framework, models, and procedures for safety evaluation. A second objective was to develop workshop training materials that inform practitioners about techniques for effectively using the software tool to evaluate alternative freeway designs. A third objective was to document the method's algorithms in a manner that would support their inclusion in the FHWA's Interactive Highway Safety Design Model (IHSDM).

FINDINGS

Interviews with practitioners were conducted for the purpose of identifying important safety issues related to freeway and interchange design. Based on these interviews, it was determined that separate predictive methods were needed for freeway segments, freeway speed-change lanes, interchange ramps, and crossroad ramp terminals.

Information was obtained from the practitioners about the importance of having specific design and traffic control features addressed by the methodology. Features ranking highest for freeway segments included ramp separation distance, median width, barrier location, and horizontal curvature. A need to better understand the effect of recurring congestion on safety was also noted as being important. Features that ranked highest for interchange ramps include barrier location and horizontal curvature. Features that ranked highest for crossroad ramp terminals included terminal configuration, control mode, left-turn bay presence, and number of lanes on each approach.

The data used to calibrate the predictive models was based on the road inventory data available from the Highway Safety Information System (HSIS). Data for three states were combined for model calibration. These data were enhanced through the inclusion of additional road inventory data extracted from aerial photographs. The enhanced database was then combined with the crash data (also obtained from HSIS) to form the highway safety database needed for model development and calibration.

The data enhancement activity was found to be helpful for several reasons. First, a comparison of the HSIS data with that collected from aerial photographs frequently showed sufficient disagreement in key variables to be of concern when used for model calibration. Also, several variables often had subtly different definitions among the states represented in the combined database. Moreover, the state databases often did not include variables for road-related factors known to be associated with crash frequency (e.g., rumble strip presence). To overcome these limitations, the study-state databases were enhanced using data from aerial photographs.

CONCLUSIONS

This report documents a safety prediction method for freeways that is suitable for incorporation in the *HSM*. The method addresses freeway segments and freeway speed-change lanes. It includes crash modification factors that describe the observed relationship between crash frequency and horizontal curvature, lane width, shoulder width, median width, barrier length and offset, ramp-related lane changes, rumble strip presence, clear zone width, and the extent of recurring congestion.

This report also documents a safety prediction method for ramps that is suitable for incorporation in the *HSM*. The method addresses ramp segments, C-D road segments, and crossroad ramp terminals. For segments, it includes crash modification factors that describe the observed relationship between crash frequency and horizontal curvature, lane width, shoulder width, barrier length and offset, a change in the number of basic lanes, presence of a ramp-to-ramp merge or diverge point, and ramp-related lane changes on a C-D road.

The safety prediction method for crossroad ramp terminals includes crash modification factors that describe the observed relationship between crash frequency and exit ramp control, exit ramp lanes, presence of turn lanes on the crossroad, presence of driveway access points, distance to the adjacent ramp terminal, median width, presence of protected-only left-turn operation, presence of right-turn channelization, and skew angle.

RECOMMENDATIONS

The safety prediction methods developed in this research should be incorporated into the *HSM*.

The analysis of freeway crash data indicated that crashes on curved freeway segments with shoulder rumble strips were more frequent than on curved segments without shoulder rumble strips. This finding is partially supported by other research documented in the literature. Additional research is needed to quantify the safety effect of shoulder rumble strips on freeway curves.

The safety prediction method for ramps does not address frontage roads. Frontage roads are sufficiently unique in their design and operation that a separate safety prediction method should be developed to specifically address them. This method would include predictive models that separately address one-way frontage-road segments, two-way frontage-road segments, frontage-road ramp terminals, and frontage-road crossroad terminals.

CHAPTER 1: INTRODUCTION

State highway agencies, and others responsible for road systems, do not currently have useful tools for reflecting safety in their decisions concerning freeway and interchange projects. This diminishes the weight placed on safety considerations in these decisions. When difficult choices must be made, greater confidence is often placed on predictions of cost, operational impacts, and environmental impacts, which are expressed in quantitative terms.

Safety prediction procedures have been developed for rural two-lane highways, rural multilane highways, and urban and suburban arterials, and are included in the *Highway Safety Manual (HSM)* (Highway, 2010). Base safety models were developed by the Federal Highway Administration for freeways and interchanges, and these are included in the network screening module of the SafetyAnalyst software (Harwood et al., 2010) and in the Interchange Safety Analysis Tool (ISAT) (Torbic et al., 2007). ISAT was developed as an interim tool to meet immediate needs. The ISAT tool provides crash estimates of three typical interchange configurations (diamond, partial cloverleaf, and full cloverleaf), but has limited capabilities and flexibility.

The aforementioned issues led to the conclusion that research was needed to develop a comprehensive safety prediction methodology and safety analysis tool for freeway corridor and site-specific analysis. The research results would lead to the development of a new chapter for the *HSM*, and documentation to facilitate implementation of the new methodology in the Interactive Highway Safety Design Model (IHSDM).

RESEARCH OBJECTIVES

The objectives of this research are identified in the following list.

- Develop an overall framework for the enhancement of safety prediction methodologies for freeways and interchanges to support decision making for planning, network, corridor analysis, and individual site analysis.
- Develop analytical models and procedures within the overall framework.
- Develop a safety analysis tool that automates the framework, models, and procedures.
- Develop a chapter for the future edition of the *HSM* that documents the methodology.
- Document the models to support their inclusion in the IHSDM.

RESEARCH SCOPE

To achieve the project objectives, the research scope included consideration of the following freeway and interchange components.

- freeway segment,
- interchange ramp,
- crossroad ramp terminal, and
- freeway speed-change lane.

The safety prediction methodology was developed to address a wide range of freeway and interchange conditions. A sample of such conditions is identified in the following list:

- freeway-freeway (i.e., system) and freeway-crossroad (i.e., service) interchanges;
- freeway and interchange facilities in urban and rural areas; and
- crossroad ramp terminals that are signal or stop controlled.

The methodology developed in this project can be used to support decision making in the planning and design of freeways and interchanges. The temporal scope of the methodology is also broad to the extent that it includes procedures for evaluating the safety of a segment or corridor for a single year or a specified analysis period consisting of several consecutive years. The methodology supports the following types of design decisions:

- interchange spacing;
- interchange and ramp configuration (e.g., ramp type, location, radius); and
- arrangement of ramps (e.g., successive entrance ramps, weaving section versus collector-distributor road).

ORGANIZATION OF THIS REPORT

This report presents the results of the research undertaken to develop a safety prediction methodology for freeways and interchanges. Chapter 2 documents the findings from a review of the literature addressing freeway and interchange safety. Chapter 3 presents a framework for safety prediction and summarizes the findings from a series of practitioner interviews. Chapter 4 documents the development of a database suitable for calibrating the predictive models that comprise the predictive method. Chapters 5, 6, and 7 describe the calibration of the predictive models for freeway segments, ramp segments, and crossroad ramp terminals, respectively. Chapter 8 summarizes the steps taken to make the research products ready for implementation. Chapter 9 presents the conclusions and recommendations of the research.

Appendix A presents the findings from the practitioner interviews. These interviews identified a range of freeway safety issues and analysis needs. Appendix B describes the activities undertaken to add additional variables to the database assembled for model calibration. Appendix C presents a proposed *HSM* chapter for freeways and Appendix D presents a proposed *HSM* chapter for ramps.

CHAPTER 2: LITERATURE REVIEW

This chapter describes the findings from a review of the literature related to freeway and interchange safety. The objective of this review was to identify the highway infrastructure-related factors that influence the safety of freeways and interchanges. The findings were used to identify design and operational elements that have a significant effect on safety, knowledge gaps, and alternative model forms. This information was used to develop a methodological framework for safety prediction. The framework is described in Chapter 3.

This chapter consists of two parts. The first part provides background information on interchange design, operation, and safety in the United States. The second part describes the findings from a review of the literature on freeway and interchange safety.

BACKGROUND

This part of the chapter provides background information on the interchanges that are in service on the U.S. highway system. The objectives of this section are to provide some context for the discussion in subsequent parts of the chapter and to establish a vocabulary for this discussion. Topics addressed include interchange safety, interchange type, and ramp configuration. The last section describes the freeway and interchange area in terms of its disaggregated component parts. The purpose of this section is to identify components that have a unique operational character.

Data from *Highway Statistics* for 2007 (Federal, 2009) were used to characterize the distribution of freeway mileage by functional system and area type. These data are shown in the top part of Table 1. They indicate that there are about 46,700 miles on the Interstate Highway System and 13,400 miles on other access-controlled highways. About 58 percent of this mileage is in rural areas. An examination of *Highway Statistics* data for recent years indicates that freeway mileage has increased by about 1 percent per year since 2004, almost exclusively in urban areas.

The number of interchanges on the highway system is not indicated in *Highway Statistics*. However, an estimate of this number can be obtained using the average interchange spacing values for rural and urban areas derived by Torbic et al. (2007). The resulting distribution of interchanges is shown in the middle part of Table 1. It is estimated that there are about 17,800 interchanges on the Interstate Highway System and 6,900 interchanges on other access-controlled highways. In contrast to the freeway mileage distribution, only about 32 percent of interchanges are in rural areas.

Torbic et al. (2007) also derived estimates of the proportion of freeway-to-freeway (i.e., system) interchanges by area type. These estimates were used to compute the number of system and service interchanges on freeways. The distribution is shown in the bottom part of Table 1. The data shown suggest that there are about 3,400 system interchanges and 21,300 service interchanges on the freeway system.

TABLE 1. Freeway mileage and number of interchanges in the United States

Attribute	Functional System	Rural	Urban	Total
Freeway length, mi ¹	Interstate	30,313	16,396	46,709
	Non-interstate ²	4,575	8,809	13,384
	Total:	34,888	25,205	60,093
Number of interchanges ³	Interstate	6,900	10,900	17,800
	Non-interstate	1,000	5,900	6,900
	Total:	7,900	16,800	24,700
Number of interchanges ⁴	Freeway-to-freeway (system)	400	3,000	3,400
	Freeway-to-arterial (service)	7,500	13,800	21,300
	Total:	7,900	16,800	24,700

Notes:

1 - Data from *Highway Statistics* for 2007 (Federal, 2009).

2 - Includes “Other Freeways and Expressways” and “Other Principal Arterials” with full access control.

3 - Based on an average spacing of 4.4 and 1.5 miles per interchange for rural and urban areas, respectively.

4 - Based on an estimated 5.3 and 17.6 percent freeway-to-freeway interchanges in rural and urban areas, respectively.

Interchange Safety

The characteristics of crashes in interchange areas were tabulated by Torbic et al. (2007). They examined the Fatality Analysis Reporting System (FARS) and the General Estimates System (GES) for the years 2000 through 2004. The data they reported indicate that interchange-related crashes represent 22 percent of all fatal crashes occurring on freeways. It is noted that the interchange area constitutes about 20 percent of the freeway mileage (at 0.5 mi/interchange). They estimated that there is an average 0.05 fatal crashes/yr per interchange and 12.5 total crashes/yr per interchange (all severities).

Interchange Types

Typical interchange types are illustrated in Figure 1 (Policy, 2004). The ramps associated with these interchanges vary widely in their geometry. Sharp curvature is common at one or more points along the ramp’s length. Also, some ramps that serve two traffic movements (e.g., right- and left-turn from freeway to crossroad) have an intermediate ramp-to-ramp merge (or diverge) point that makes their operation different from those serving only one movement.

A survey of state DOTs was conducted by Garber and Fontaine (1999) for the purpose of developing guidelines for interchange selection. They received completed surveys from 36 of the 50 state DOTs. One survey question related to the types of interchanges being used in the respondent’s jurisdiction. The responses to this question are summarized in Figure 2.

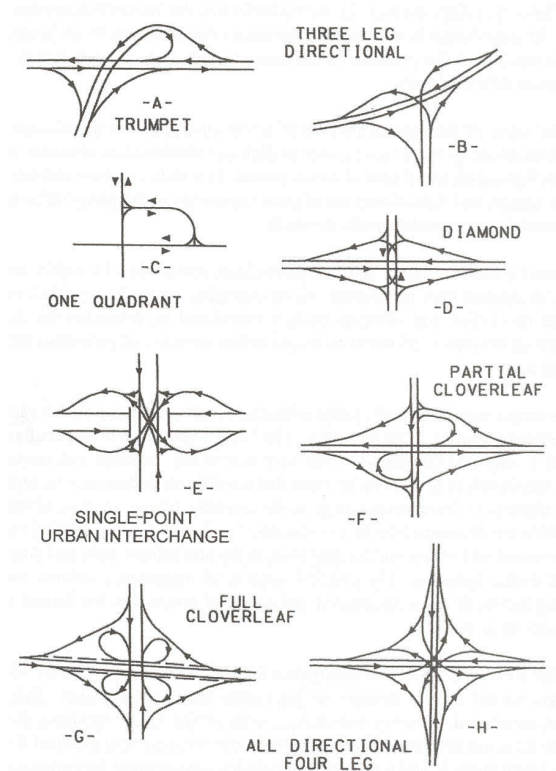


Figure 1. Typical interchange types.

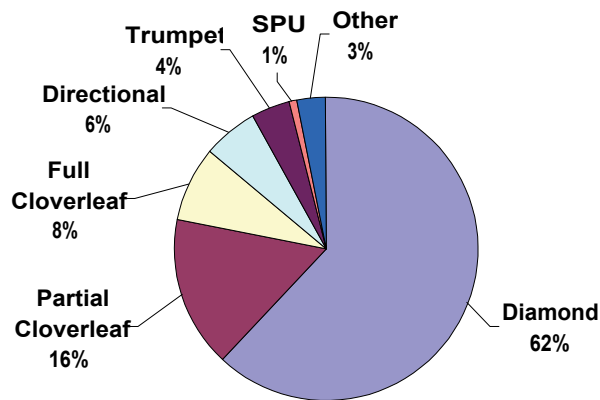


Figure 2. Distribution of interchange types used in the United States.

The trends in Figure 2 suggest that the diamond is the most widely used interchange type, followed by the partial cloverleaf (or “parclo”). Together, these two interchange types account for 78 percent of all interchanges. Based on the previous estimate of 24,700 interchanges in the U.S., the distribution in Figure 2 indicates that there are about 15,300 diamond interchanges, 4,000 partial cloverleaf interchanges, 2,000 full cloverleaf interchanges, 1,000 trumpet interchanges, 250 single-point urban interchanges (SPUIs), and 700 “other” interchanges.

Typical variations of the diamond and parclo interchange types are shown in Figure 3. It is noted that the SPUI is generally considered to be a diamond-type interchange, but was separately categorized in the distribution shown in Figure 2. Frontage-road variations exist for the tight urban diamond and SPUI but are not shown in Figure 3. The parclo AB (with loop ramps on the same side of the crossroad) is also not shown.

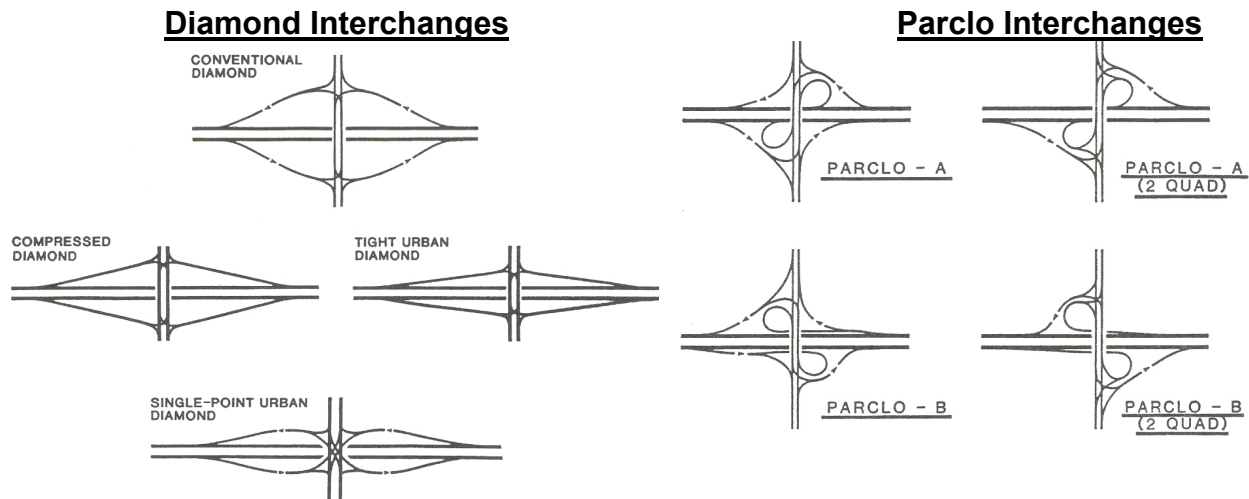


Figure 3. Typical diamond and parclo interchange types.

Ramp Configuration

Typical ramp configurations used at interchanges in non-frontage-road settings are shown in Figure 4. The ramp configurations used in frontage-road settings are not shown, but can be described as slip, buttonhook, and scissor.

The diamond ramp configuration in Figure 4 is shown to have two alternative alignments. The alignment shown using the solid line is straight with a skew at the crossroad ramp terminal and possibly one short curve near the freeway ramp terminal. The alignment shown using dashed lines has two curves and negligible skew at the crossroad ramp terminal. These alternatives are likely to have a different influence on the safety of the diamond configuration and possibly the ramp terminal.

The parclos shown in Figure 3 (and the directional interchanges shown in Figure 1) each have two or more ramps with a ramp-to-ramp junction at some point along their length. This treatment is not shown in Figure 4 but is found on ramps with the diamond or connector configuration. The ramp-to-ramp merge or diverge point associated with this ramp configuration is likely to have a negative influence on ramp safety, relative to a ramp without such points.

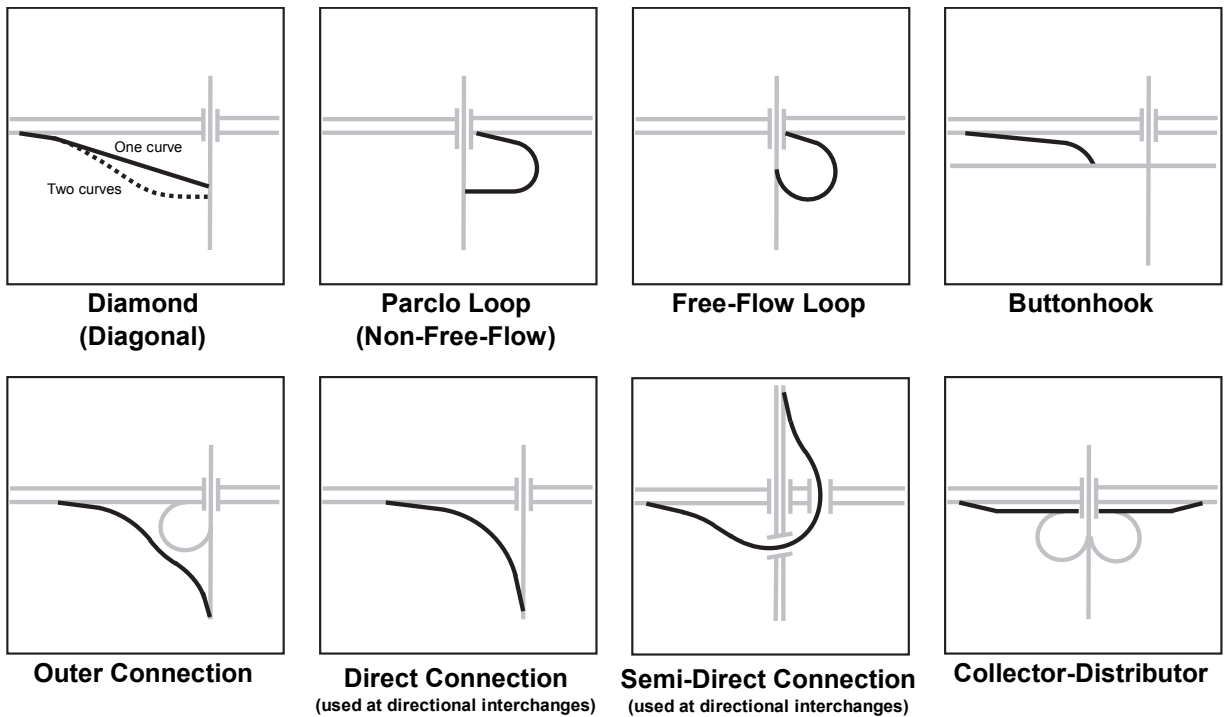


Figure 4. Typical ramp configurations.

The full cloverleaf interchange is sometimes designed to have a collector-distributor (C-D) road configuration that removes ramp-related weaving from the main lanes. The geometry of this configuration is shown in the lower right corner of Figure 4. It is often used with the outer connection ramp.

Freeway and Interchange Design Components

A section of freeway with one or more interchanges can be disaggregated into the following components:

- freeway segment,
- interchange ramp,
- crossroad ramp terminal,
- freeway speed-change lane,
- crossroad segment, and
- crossroad speed-change lane.

These components are shown in Figure 5 for a hypothetical freeway section. The section has a constant number of basic lanes. Various combinations of entrance and exit ramps are shown on the west side of the facility (similar ramps are provided on the east side but are not shown to simplify the figure). Some of the ramps are associated with a conventional interchange and other ramps serve surface roadways but do not represent one of the typical interchange types shown in Figure 1.

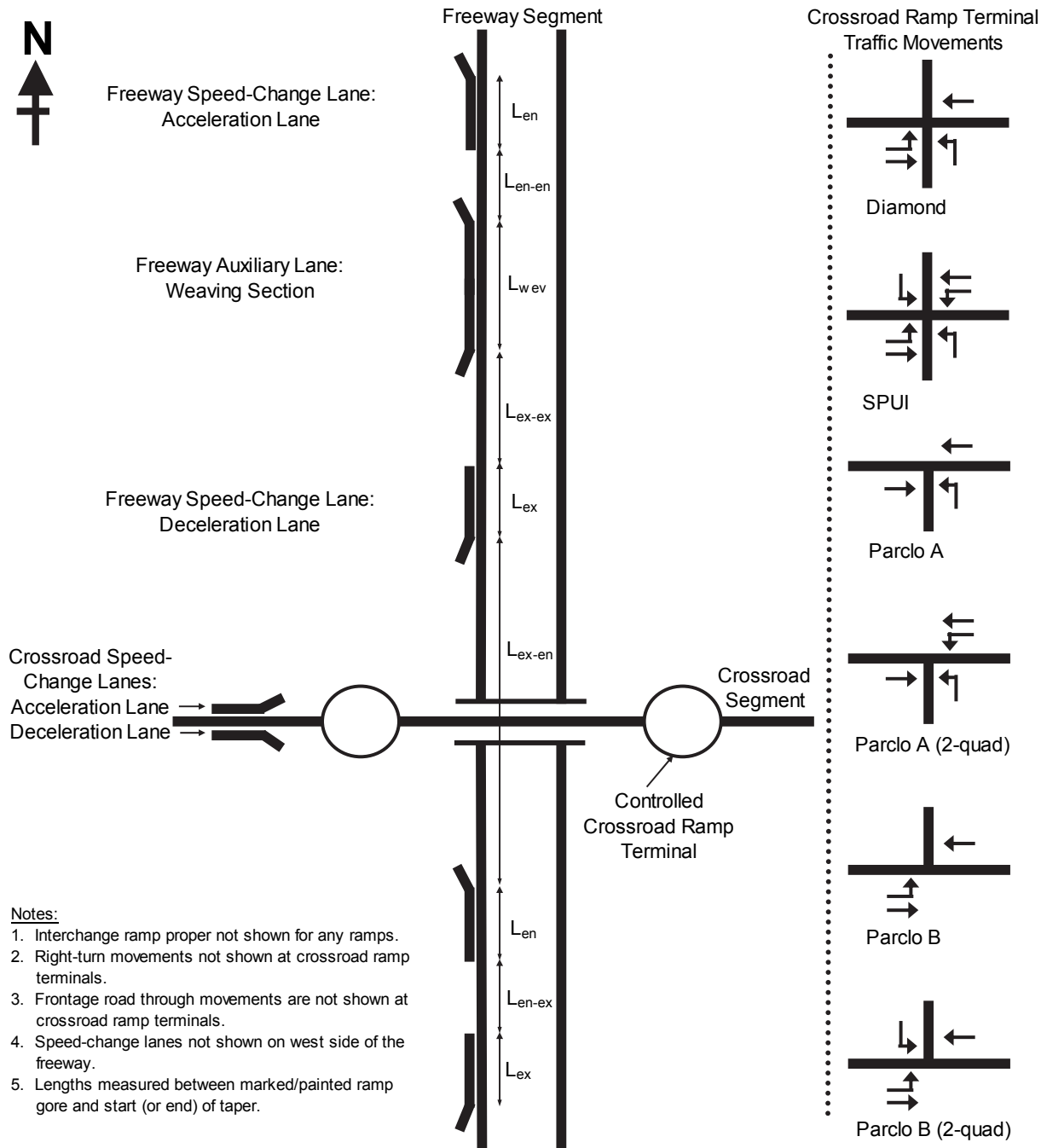


Figure 5. Freeway and interchange design components.

Freeway Segment and Speed-Change Lane

Figure 5 illustrates several types of freeway components. For example, there are two speed-change lanes shown, each is associated with a ramp entrance (with length L_{en}). There are two speed-change lanes associated with a ramp exit (with length L_{ex}). The freeway section is shown to consist of several segments. There is a segment formed by an entrance-exit ramp pair with a weaving section (with length L_{wv}). There is a segment between two ramp entrances (with

length L_{en-en}), between two ramp exits (with length L_{ex-ex}), between a ramp entrance and exit (with length L_{en-ex}), and between a ramp exit and entrance (with length L_{ex-en}).

Within the lengths of roadway between ramps, lane changes can occur directly or indirectly as a result of the entering (or exiting) ramp traffic. Lane-change frequency and concentration (i.e., intensity) is likely correlated with ramp volume, length of roadway between ramps (i.e., L_{en-en} , L_{ex-ex} , L_{en-ex} , L_{ex-en}), and main lane volume. Crash frequency is likely correlated with lane-change intensity.

Crossroad Ramp Terminal

The crossroad segment shown in Figure 5 has two “controlled” crossroad ramp terminals. These terminals are typically associated with service interchanges, such as the diamond, parclo, SPUI, and one-quadrant interchange types. A service interchange is used at the intersection of a major and minor roadway, and has one or more traffic movements that are stop- or signal-controlled.

The right-hand side of Figure 5 illustrates the traffic movements that intersect at the controlled crossroad ramp terminals of the diamond and parclo interchanges. The north and south legs represent ramps. Right-turn movements are not shown. They may be served at the intersection or externally using a channelized speed-change lane. If Figure 5 is extended to include frontage-road settings, then through movements would also be shown on the ramp approaches at each crossroad ramp terminal.

With one exception, the traffic movement patterns at crossroad ramp terminals are *not* the same as found at traditional 3-leg or 4-leg intersections. Hence, the use of a safety prediction model calibrated using traditional 3-leg or 4-leg intersections to estimate ramp terminal crash frequency should be viewed with skepticism until it can be shown statistically that this extrapolation yields acceptably accurate predictions. The one exception is the parclo A (2-quad) terminal, which has traffic patterns that are similar to a traditional 3-leg intersection.

Interchange Ramp

Ramp configurations are not shown in Figure 5. However, schematic drawings for these ramps were provided previously in Figure 4. The interchange ramp alignment is comprised of tangent and curved segments. These segments are shown in Figure 6 for a diamond ramp. Logically, the crash history of a ramp is likely to be influenced by the number of ramp curves and their radii. It may also be influenced by the operating speed on the ramp segments. This speed is likely to change along the length of the ramp.

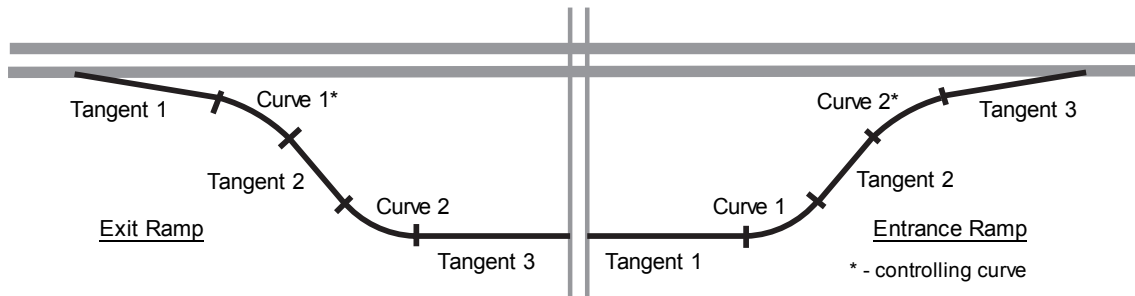


Figure 6. Disaggregated alignment for a diamond ramp.

FREEWAY AND INTERCHANGE SAFETY

This part of the chapter describes the findings from a review of the literature related to the topic of freeway and interchange safety. In many instances, the findings are described in terms of safety performance functions (SPFs) or crash modification factors (CMFs). An SPF describes the relationship between traffic volume and crash frequency for a roadway or intersection. A CMF is used to describe the safety effect of a geometric design or traffic control device.

The review is focused on the following topics: ramp proper, freeway speed-change lane, freeway segment, and high-occupancy-vehicle (HOV) facilities. Relatively little information was found on crossroad ramp terminal safety.

Table 2 provides some insight as to the relative intensity of crashes for seven selected ramp configurations and area types. The crash rates shown are based on data provided in Appendix B of the report by Bauer and Harwood (1998). Traffic volume data were not provided in the report so comparisons among columns are not fully normalized by exposure. Nevertheless, the following trends are noted from inspection of the rates in Table 2:

- A normal deceleration lane tends to have a lower crash rate than the ramp proper.
- A diverge area on a direct or semi-direct connection ramp tends to have a higher crash rate than the ramp proper.
- The crash rate for a normal acceleration lane tends to be larger than the ramp proper rate when the likely speed increase is large, and vice versa when the speed increase is small.
- The rural diamond exit ramp has a higher crash rate on the ramp proper and at the crossroad ramp terminal approach than the rural diamond entrance ramp.

An early study of interchange crash data was undertaken by Cirillo (1968). She examined crash data at 718 urban interchanges and 942 rural interchanges on the Interstate Highway System. The crash rates reported for the ramp components are listed in Table 3. The following trends are noted from inspection of the rates in this table:

- A deceleration lane tends to have a lower crash rate than the ramp proper.
- The rural exit ramp has a higher crash rate on the ramp proper than the rural entrance ramp; however, the reverse trend holds for the urban ramp combination.
- An acceleration lane tends to have a lower crash rate than the ramp proper.

TABLE 2. Crash distribution among interchange ramp components

Interchange Ramp Component	Rural			Urban			
	Entrance			Exit Ramp			
	Diamond	Diamond	Diamond	Parclo	Free-Flow Loop	Outer Connection	Direct & Semi-Direct
Total Crashes (All Severities) per Mile per Year by Ramp Type¹							
Normal deceleration lane	--	0.34	3.2	5.8	5.9	2.7	2.8
Deceleration lane with mainline lane drop	--	--	12	--	--	--	2.1
Ramp proper	0.09	0.76	8.4	13	6.1	11	6.2
Normal acceleration lane	0.48	--	--	--	7.5	2.1	3.1
Acceleration lane with mainline lane addition	0.0	--	--	--	--	--	2.9
Diverge area on ramp	--	--	--	--	--	--	11
Merge area on ramp	--	--	--	--	--	--	5.8
Two-way road on ramp	--	--	--	6.1	--	7.6	--
Total crashes:	79	184	998	50	183	422	511
Total miles:	84.8	91.3	47.6	1.9	9	16	34.8
Total Crashes (All Severities) per Ramp per Year by Ramp Type¹							
Crossroad ramp terminal (stop)	0.11	0.25	1.72	2.8	--	0.97	--
Crossroad ramp terminal (free)	--	--	--	--	0.91	1.1	--
Total crashes:	64	155	721	59	101	275	--
Total ramps:	194	204	139	7	37	45	68

Note:

1 - Based on three years of crash data. Crashes cited occurred in the speed-change lane, ramp proper, or ramp approach to the crossroad ramp terminal. Rates are not computed for interchange components for which there is less than 0.3 miles of total length for all components combined. Source: Bauer and Harwood (1998).

TABLE 3. Crash distribution among interchange ramp components

Interchange Ramp Component	Rural		Urban	
	Exit	Entrance	Exit	Entrance
Total Crashes (All Severities) per 100 mvm by Ramp Type¹				
Deceleration lane	137	--	186	--
Ramp proper	346	--	370	719
Acceleration lane	--	--	76	174
Total crashes:	547	--	375	2,620
Total 100 million-vehicle-miles:	3.11	--	4.27	10.0

Note:

1 - mvm: million vehicle miles. Source: Cirillo (1968).

Interchange Ramp Proper

This subsection describes the findings from a review of the safety literature related to the interchange ramp proper. The ramp proper is defined to be the portion of the ramp between the freeway speed-change lane and the crossroad ramp terminal.

Travel along a ramp requires the driver to change speed and direction relatively often and to varying degrees. The frequency and extent of these changes varies by ramp configuration, traffic composition, crossroad ramp terminal control, and the design speed differential of the two intersecting roadways. The ramp design elements of note are represented by horizontal curvature, superelevation rate, ramp grade, and ramp-to-ramp merge (or diverge) points. In addition to these changing conditions, travel along the ramp presents the driver with complex conditions and multiple decision points. These changes and complexities can increase the potential for conflict or crash, especially for larger vehicles (Garber et al., 1992).

Basic Descriptors

This subsection describes various fundamental descriptors of ramp proper design and operation. Topics addressed include: area type, ramp type, entrance/exit side, ramp configuration, number of lanes, and ramp length.

Area Type. This descriptor indicates the population density in the vicinity of the ramp. The categories used are urban and rural. The rates listed in Table 3 indicate that urban ramps have a higher crash rate than rural ramps; however, the relative increase varies by ramp type (i.e., exit or entrance).

More recently, Bauer and Harwood (1998) examined crash data for five ramp configurations on Washington freeways. All total, 551 ramps are represented in the database. Their regression analysis of the data indicated that ramps in urban areas have 40 percent more crashes than those in rural areas, given the same traffic volume and ramp configuration. The Interchange Safety Analysis Tool (ISAT) acknowledges a possible difference between urban and rural ramps; however, the SPFs in ISAT are identical for both area types (Torbic et al., 2007).

Ramp Type. This descriptor indicates whether the ramp is used to enter or exit from the freeway. The categories used are entrance and exit. The ramp proper rates listed in Table 3 indicate that rural exit ramps have a higher crash rate than rural entrance ramps. However, the reverse trend applies to urban ramp combinations.

A report by Lundy (1966) describes crash and exposure data for ten ramp configurations on California freeways. All total, 582 ramps were represented in the database. These data were re-analyzed for this report using regression analysis. The objective of this analysis was to quantify the relationship between ramp type and crash frequency. Based on this analysis, it was determined that exit ramps have about 42 percent more crashes than entrance ramps, given the same traffic volume and ramp configuration. This trend was consistent for all ten of the ramp configurations considered (although the relative increase varied by configuration).

More recently, Khorashadi (1998) examined crash data for nine ramp configurations found in California. All total, 13,325 ramps were included in the database, representing a mixture of rural and urban areas. A re-analysis of the reported crash data indicates that exit ramps have about 64 percent more crashes than entrance ramps, given the same traffic volume and ramp configuration.

Bauer and Harwood's (1998) regression analysis of Washington ramp data indicated that exit ramps have about 65 percent more crashes than entrance ramps, given the same traffic volume and ramp configuration. This percentage is consistent with that found in the data reported by Khorashadi (1998) for ramps in California. Bauer and Harwood offered that this trend was partly due to crashes occurring on the exit ramp that are related to the operation of the crossroad ramp terminal (most notably rear-end crashes) and thus, are not directly attributable to ramp geometry.

The SPFs in ISAT indicate that exit ramps have more crashes than entrance ramps when the configuration is a diamond, free-flow loop, or parclo loop. The amount of increase varies with traffic volume. They also indicate that there is no safety difference between entrance and exit ramps for the direct or semi-direct connection configurations.

Entrance/Exit Side. This descriptor indicates whether the ramp is entered on the right side of the freeway and curves to the right, or is entered on the left side and curves to the left. The dominance of right-hand ramps on the freeway system has led drivers to develop an expectation for right-hand ramps. As a result, left-hand ramps are unexpected by unfamiliar drivers and tend to be associated with an increased level of lane changing and speed change. These attributes are believed to explain the increased frequency of crashes observed with left-hand ramps, relative to right-hand ramps, especially in the vicinity of the freeway speed-change lane.

A survey of ramp configurations on the Interstate Highway System taken in the late 1960s indicates that left-hand ramps represented about 4.7 percent of the 5,088 ramps found in 22 states (Yates, 1970). This percentage did not vary appreciably for ramps in urban or rural areas.

A more recent survey of ramp configurations on freeways in North Carolina was undertaken by Moon and Hummer (2009). They found that left-hand ramps represent about 1.8 percent of the 1837 ramps surveyed. North Carolina was one of the states included in the survey by Yates (1970) so it can be used to examine the change in left-hand ramp presence over time. An examination of Yates' data indicates that left-hand ramps represented 3.7 percent of the 696 ramps found in North Carolina in the late 1960s. By comparing the two percentages, it appears that about half of the left-hand ramps have been removed from North Carolina freeways in the last 40 years.

Two reports were found that address ramp safety and that distinguish between the ramp entrance and exit side in the analysis. However, in these two reports, it is difficult to determine the extent to which crashes in the speed-change lane have also been included in the reported data. Hence, the findings cited in the next two paragraphs reflect a mix of crashes on both the ramp proper and the speed-change lane. A discussion of entrance/exit side and its influence on

crashes in the speed-change lane is provided in a subsequent section titled Freeway Speed-Change Lane.

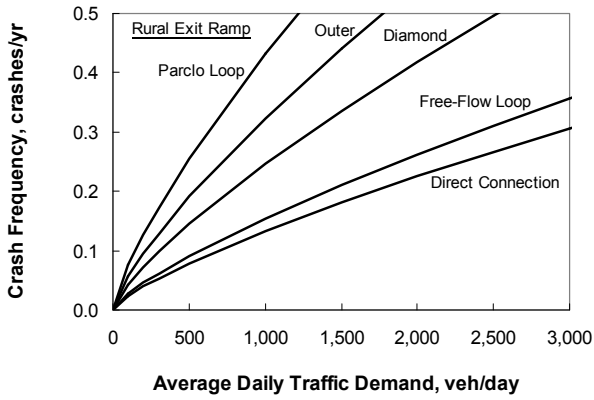
Yates (1970) examined crash data for loop and outer connection ramps in 22 states. Only 17 loop ramps with a left-hand entrance or exit were identified, so his analysis focused on the 223 outer connection ramps with a left-hand entrance or exit. The reported data were re-analyzed for this report. The results indicate that total crash frequency is 25 percent *lower* on left-hand outer connection ramps. This finding is contrary to the aforementioned concern about driver expectancy; however, it is likely dominated by crash trends on the ramp proper (as opposed to the speed-change lane) and reflects only the outer connection ramp.

Lundy (1966) also examined total crash data for a range of ramp configurations and ramp types, some of which were designated as “left-side” ramps. The data were specific to under-crossing and over-crossing interchanges and are believed to include speed-change-related crashes. The typical under-crossing interchange has the freeway at grade and the crossroad below the freeway. The typical over-crossing interchange has the freeway at grade and the crossroad above the freeway. A re-analysis of the reported data indicates that left-hand ramps at under-crossing interchanges have about 95 percent more crashes than right-hand ramps, given the same volume and ramp type. Similarly, left-hand ramps at over-crossing interchanges have about 54 percent more crashes than right-hand ramps.

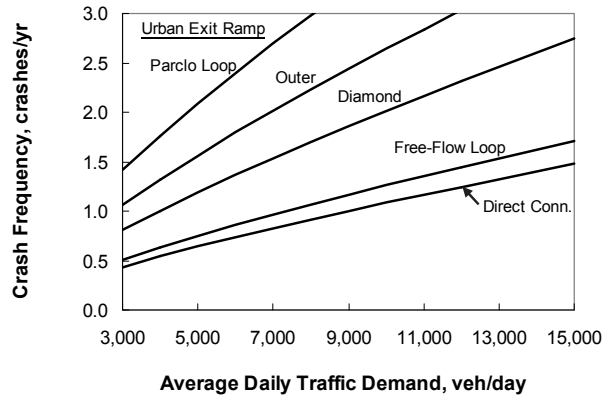
Ramp Configuration. This descriptor describes the general shape of the ramp. Typical configurations are shown in Figure 4. Several previous studies have examined the frequency and severity of crashes on interchange ramps. These examinations focused on the individual ramps (as opposed to the overall interchange) because of the unique influence of individual ramp element design on crash potential. The findings of many of these studies are summarized by Twomey et al. (1992). For example, they reported total crash rates that compared “curved” and “straight” ramp alignments. Their data indicate that curved ramps have 14 percent more crashes than straight ramps.

SPFs have been developed by Bauer and Harwood (1998) and by Torbic et al. (2007). Several configuration-based SPFs were also developed for this report using the data reported by Khorashadi (1998). These SPFs are compared in Figure 7 for exit ramps in rural and urban areas. Similar trends are obtained for entrance ramps. Crash frequency is defined to include total crashes occurring on the ramp (i.e., all severities). A typical ramp length of 0.20 mi was used with the SPFs developed by Torbic et al.

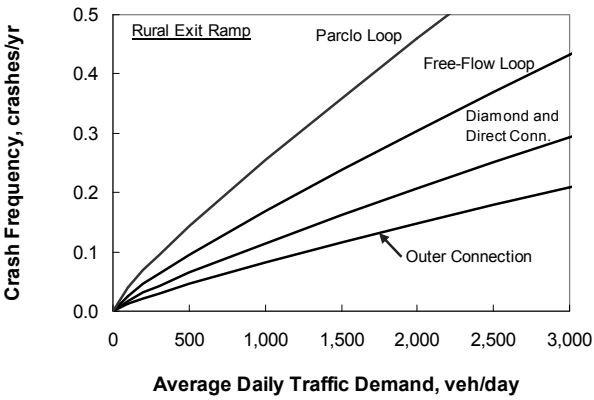
An examination of Figure 7 indicates that a consistent trend among ramp configurations is difficult to find. The only trend that is consistent among all SPFs is that the diamond ramp has fewer crashes than the parclo loop ramp, given the same traffic volume. A comparison of the Bauer and Harwood SPFs with those from the Khorashadi data indicates that parclo loops tend to have more frequent crashes than other ramp configurations. Also, diamond ramps tend to be in the “middle” in terms of having fewer crashes than some ramp configurations and more than others. The Khorashadi SPFs tend to predict fewer crashes than the Bauer and Harwood SPFs for a given volume and configuration. The Torbic et al. SPFs suggest that direct connection ramps have more crashes than other configurations, which is in contrast to the trend indicated for this ramp by the other two researchers.



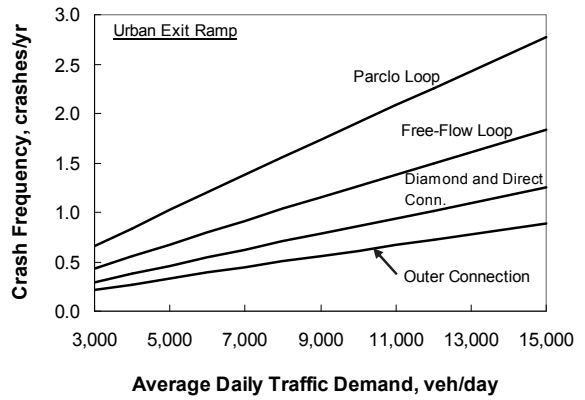
a. Bauer and Harwood rural ramp SPFs.



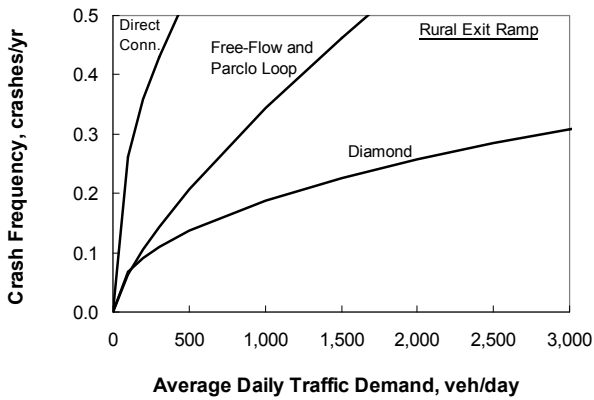
b. Bauer and Harwood urban ramp SPFs.



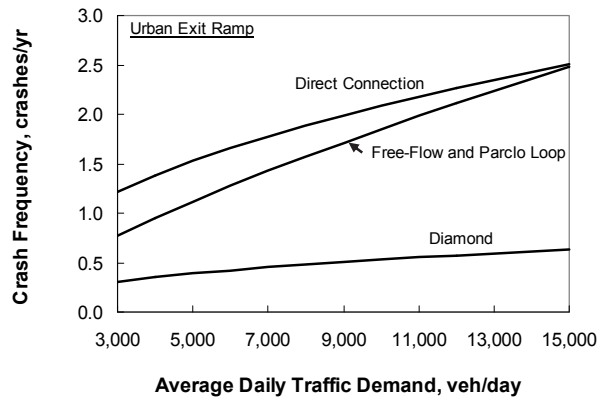
c. Khorashadi rural ramp SPFs.



d. Khorashadi urban ramp SPFs.



e. ISAT rural ramp SPFs.



f. ISAT urban ramp SPFs.

Figure 7. Ramp-configuration-based SPFs based on total crashes.

The trends shown in Figure 7 suggest that ramp configuration alone may not provide a sufficient basis upon which to develop SPFs. For example, ramp configuration does not distinguish between ramps that do, and do not, have a ramp-to-ramp merge or diverge point along their length. Moreover, traffic volume is typically not available for the ramp segments before and after the merge or diverge point. This limitation makes the calibration of an SPF for an entire ramp problematic (Bauer and Harwood, 1998; Bahar et al., 2001). The variation in curvature that can exist among ramps with the same configuration (see Figures 4 and 6) may also explain some of the variations observed in Figure 7.

Number of Lanes. This descriptor indicates the number of lanes in the ramp cross section. Data reported by Bauer and Harwood (1998) indicate that 84 percent of interchange ramps in Washington have one lane and 16 percent have two lanes. They developed a regression model that indicates single-lane ramps have more than twice as many crashes as two-lane ramps, for a given traffic volume and configuration.

Ramp Length. This descriptor indicates the length of the ramp, as measured along a portion (or all) of the ramp proper. Most ramp SPFs found in the literature do not include ramp length. Similarly, most reported ramp crash rates are not based on ramp length.

Bauer and Harwood (1998) developed a regression model for ramp segments (i.e., a piece of the ramp proper that is shorter than its total length) that included a variable for segment length. They found that crash frequency increased with segment length. The SPFs in ISAT include a variable for ramp length. The form of the ISAT SPFs indicates a one-to-one correlation between ramp length and crash frequency.

Elements with Quantified Relationship

This subsection describes various associations between safety and ramp proper design or operation that have been quantified through an analysis of crash data. Topics addressed include horizontal curve radius, grade, lane width, and ramp meter operation.

Horizontal Curve Radius. In the late 1960s, Yates (1970) gathered data for 5,088 ramps on the Interstate Highway System in 22 states. One element of his examination was the relationship between crash rate and ramp curve radius. His examination focused on the ramp curve with the sharpest radius. These data were re-analyzed for this report using regression analysis. The results are shown in Figure 8 using the trend line labeled “Ramp.”

The lines shown in Figure 8 illustrate the relationship between crash risk and curve radius. The line labeled “Ramp” is based on data reported by Yates (1970). The line labeled “Two-Lane Highway” is obtained from an equation derived by Harwood et al. (2000) and is based on the curve having a 90-degree deflection angle. It is shown to provide a basis of comparison with the ramp relationship. The two lines suggest that a two-lane highway curve has more crash risk than a ramp curve for any radius smaller than 2,000 ft. It is likely that this difference between the two curves can be explained by the lower speeds and different driver expectations on ramp curves, relative to two-lane highway curves.

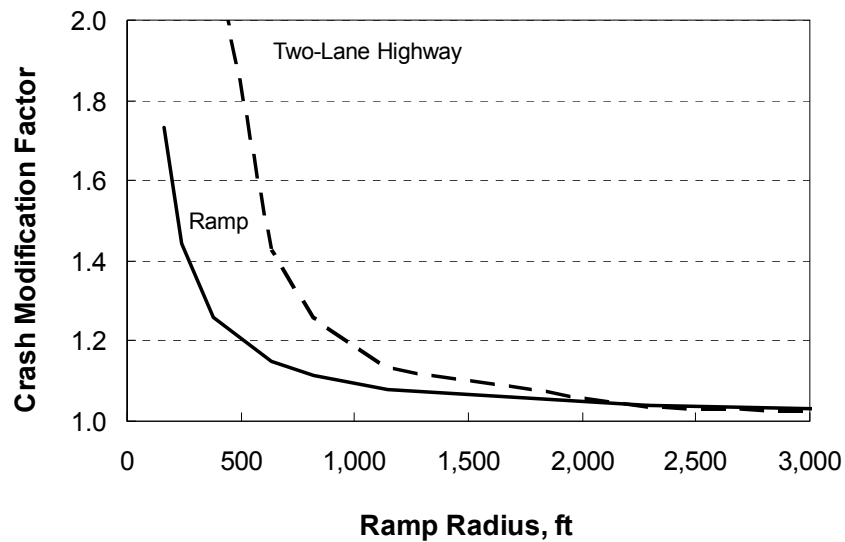


Figure 8. Relationship between CMF value and ramp radius based on total crashes.

Ramp Grade. Bahar et al. (2007) synthesized safety research on the effect of various geometric and traffic control elements. Their review indicated that some research has been conducted on the topic of grade for two-lane highways. The research cited indicates that crash risk increases with increasing grade (up or down).

Lundy (1966) examined crash data for 582 ramps on California freeways. The data were specific to under-crossing and over-crossing interchanges. The typical under-crossing interchange has the freeway at grade and the crossroad below the freeway (i.e., exit ramp on downgrade). The typical over-crossing interchange has the freeway at grade and the crossroad above the freeway (i.e., exit ramp on upgrade). The reported data were re-analyzed for this report. The analysis separately considered ramp type (i.e., entrance or exit) and grade (i.e., up or down). The findings indicate that grade does not have a significant effect on ramp crash frequency.

Lane Width. Bauer and Harwood (1998) examined the effect of ramp lane width and found that wider lanes were associated with fewer crashes on exit ramps. They calibrated a regression model for ramp segments using all ramp crashes, except those identified as rear end. They rationalized that rear-end crashes on exit ramps were more likely related to the crossroad ramp terminal than the ramp geometry. The average lane width was 15 ft. A CMF was derived from the reported regression model. It is shown in Figure 9 using the trend line labeled “Ramp.”

The lines shown in Figure 9 illustrate the relationship between crash risk and average ramp lane width. The line labeled “Ramp” is based on the factor derived from the Bauer and Harwood (1998) model. The two lines labeled “Two-Lane Highway” were obtained from an equation derived by Harwood et al. (2000) and are based on a proportion of “related crashes” equal to 0.55. This proportion represents the proportion of single-vehicle crashes on exit ramps reported by Bauer and Harwood (1998). The equation derived by Harwood et al. was “shifted” to a base lane width of 15 ft to facilitate its comparison with the line labeled “Ramp.”

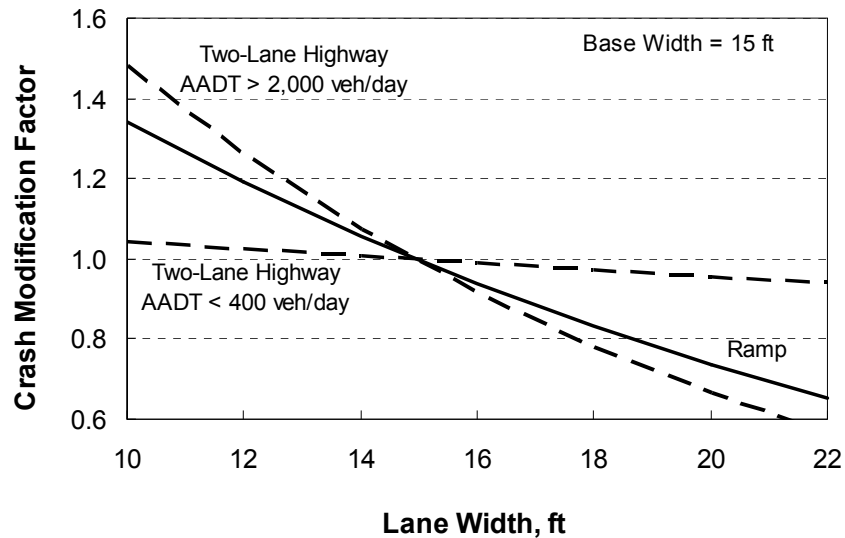


Figure 9. Relationship between CMF value and ramp lane width based on total crashes.

The two-lane highway lines are shown in Figure 9 to provide a basis of comparison with the ramp relationship. These lines suggest that a two-lane highway with an annual average daily traffic (AADT) volume in excess of 2,000 veh/day has more crash risk than a ramp curve. The reverse trend is true for a highway with an AADT volume less than 400 veh/day.

Ramp Meter Operation. Ramp metering is a freeway traffic management strategy that is generally recognized to improve freeway operation and safety. However, its effect on ramp safety and operation has not been as closely examined. One research project by Upchurch and Cleavenger (1999) specifically examined the effect of ramp metering on ramp-related crashes. They conducted a before-after study using the non-metered hours as a comparison group. They examined ramp-related crashes during a period of three years before and three years after ramp meters were installed on nine ramps of an Arizona freeway. A log-odds analysis of the reported data was conducted for this report. The results indicate that total ramp-related crashes increased 500 percent during the hours when ramp metering was operational. The increase is largely related to the increase in rear-end crashes on the ramp.

Related Topics

This subsection describes the influence of ramp configuration on manner of collision.

Khorashadi (1998) examined crash data for nine ramp configurations found in California. All total, 13,325 ramps were represented in the database. Included in the reported data was the number of multiple-vehicle crashes. These data were re-analyzed for this report. Single-vehicle crash frequency was estimated by subtracting multiple-vehicle crashes from the reported total crash frequency. A regression model was fit to each data set. These models are shown in Figure 10.

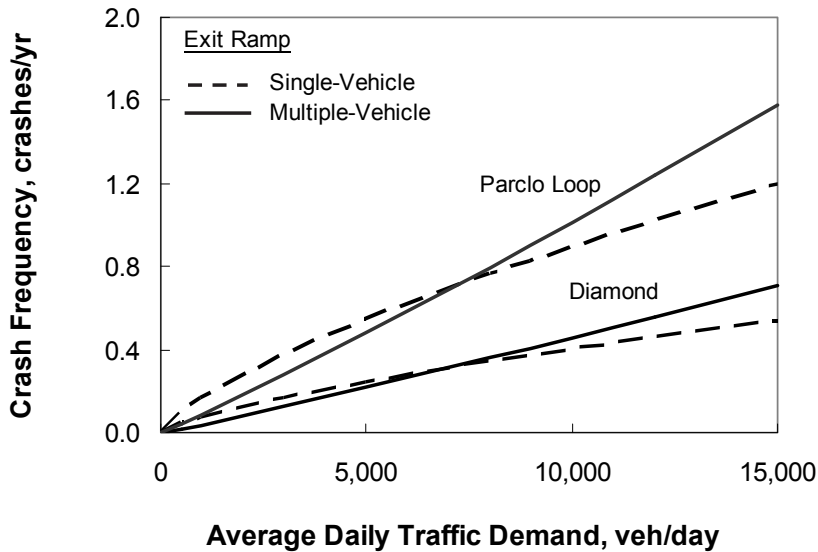


Figure 10. Relationship between ramp crash frequency and crash type based on total crashes.

The lines in Figure 10 indicate that the distribution of collision type varies with traffic volume. This trend is consistent among all ramp configurations. It suggests that multiple-vehicle crashes account for a larger portion of all crashes when ramp volume exceeds about 8,000 veh/day. These trends logically reflect the effect of traffic exposure, such that single-vehicle crashes are more common when there are few vehicles on the road and multiple-vehicle crashes are more common when there are more vehicles on the road.

Freeway Speed-Change Lane

This subsection describes the findings from a review of the literature related to the freeway speed-change lane. The AASHTO document *A Policy on Geometric Design of Highways and Streets (Green Book)* (2004) defines the speed-change lane to be an auxiliary lane, including tapered areas, that provides for the acceleration or deceleration of vehicles entering or exiting the freeway lanes.

Speed-change lanes have two design types, the parallel design and the taper design. Both designs are shown in Figure 11. The acceleration and deceleration lengths referenced in the figure are defined in the *Green Book*. The acceleration length and speed-change lane length begin at the end of the controlling curve on an entrance ramp. The deceleration length and speed-change lane length end at the start of the controlling curve on an exit ramp.

Hereafter in this chapter, the entrance ramp speed-change lane is referred to as an “acceleration lane” and the exit ramp speed-change lane is referred to as a “deceleration lane.” Alternative speed-change lane lengths and terms were developed for use in Chapters 3 to 9 because of the difficulty of consistently locating the end of the controlling curve in the field or on aerial photographs. The terms used in Chapters 3 to 9 are “ramp entrance length” and “ramp exit length.” They are shown in Figure 11. They are defined by the gore point and taper point.

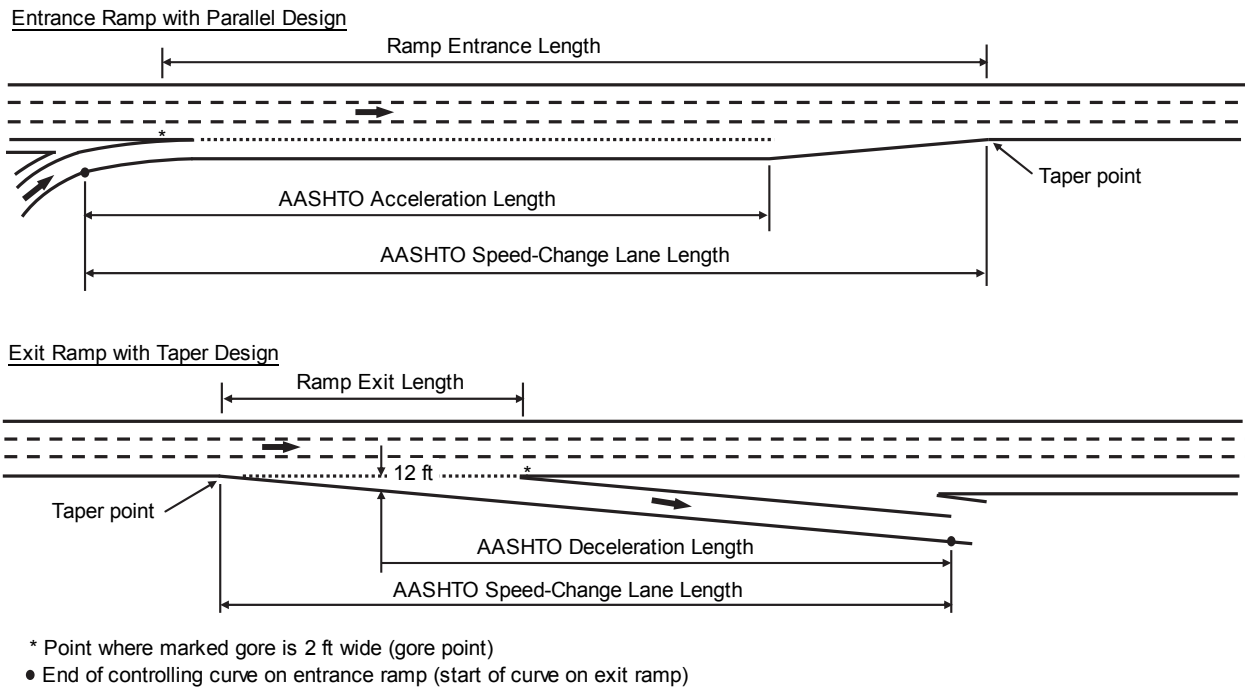


Figure 11. Typical speed-change lanes.

Basic Descriptors

This subsection describes various descriptors of speed-change lane design and operation. Topics addressed include area type, ramp type, entrance/exit side, and speed-change lane design.

Area Type. This descriptor indicates the population density in the vicinity of the speed-change lane. The categories used are urban and rural. The rates listed in Table 3 indicate that speed-change lanes in rural areas have a lower crash rate than those in urban areas.

Bauer and Harwood (1998) examined crash data representing 551 ramps on Washington freeways. They specifically identified crashes that occurred in entrance and exit ramp speed-change lanes. Their regression analysis of the data indicated that deceleration lanes in rural areas have 70 percent fewer crashes than those in urban areas, given the same traffic volume. Similarly, acceleration lanes in rural areas have 45 percent fewer crashes than those in urban areas, given the same traffic volume and length.

Ramp Type. This descriptor indicates whether the ramp is used to enter or exit from the freeway. The categories used are entrance and exit. The previous examination of crash rates in Tables 2 and 3 indicated that the crash rate for the speed-change lane tends to be lower than that of the ramp proper. One exception is that the crash rate for acceleration lanes can be higher than that of the ramp proper when the speed increase is large.

Sarhan et al. (2006) examined crash data for 26 interchanges on a freeway in Canada. The crash data included crashes on the freeway segment within the interchange area plus those in the speed-change lanes. They developed a regression model that included a sensitivity to

acceleration length and a second model that included a sensitivity to deceleration length. By comparing these two models, it was found that there were more crashes associated with the acceleration lane, relative to the deceleration lane, for daily freeway traffic volumes in excess of about 70,000 veh/day and equal speed-change lane lengths. This trend is consistent with the crash rates shown in Table 3.

Entrance/Exit Side. This descriptor indicates whether the ramp is entered on the right side of the freeway and curves to the right, or is entered on the left side and curves to the left. The focus of this discussion is on crashes that occur in the speed-change lane and in an adjacent segment of the freeway in which ramp-related lane changes occur. A discussion of the association between entrance/exit side and crashes on the ramp is provided in a previous section titled Interchange Ramp Proper.

Worrall (1969) examined total crash rates for 139 ramps (of which 29 had a left-side entrance or exit) on urban freeways in Illinois. He found that the left-side entrance ramps had a 60 percent higher crash rate than right-side entrance ramps. Left-side exit ramps had a 90 percent higher crash rate than right-side exit ramps. Based on an examination of operational characteristics for a series of case-study locations, he found that left-side entrance ramps were particularly problematic when the ramp served a large number of trucks. He also found that left-side ramps located just beyond a crest curve or within a short distance of a right-side ramp were also problematic.

Moon and Hummer (2009) gathered crash data for 158 ramps (of which 33 ramps had a left-side entrance or exit) on freeways in North Carolina. Crashes in the speed-change lane and on the freeway for a distance up to 1,500 ft from the ramp gore were included in the database. They calibrated a regression model using the data. Model coefficients indicate that left-side entrances or exits have 70 to 150 percent more total crashes than right-side entrances or exits.

Zhao and Zhou (2009) gathered crash data for 19 ramps (of which four had a left-side exit) on freeways in Florida. Crashes in the speed-change lane and on the freeway for a distance up to 1,000 ft from the start of the deceleration length were included in the database. A re-analysis of these data was undertaken for this report to quantify the correlation between entrance/exit side and crash frequency. The analysis indicates that left-side exits have 180 percent more total crashes than right-side exits. This percentage is slightly larger than the range reported by Moon and Hummer.

Speed-Change Lane Design. As noted in the discussion of Figure 11, speed-change lanes have two design types—the parallel design and the taper design. A key difference between these two designs is the ramp entrance length and the ramp exit length.

No research reports or papers were identified that explicitly examined the association between crashes and speed-change lane design. However, there were several documents that described an examination of the relationship between acceleration length (or deceleration length) and crash frequency. The findings reported in these documents are reviewed in the next subsection.

Koepke (1993) conducted a survey of 45 state DOTs regarding their ramp design practice and existing ramp designs. He found that 9 percent of the DOTs use the parallel design, 24 percent use the taper design, and 67 percent use both designs. He pointed out that the 1990 *Green Book* noted a decided trend toward the use of the taper type, although some DOTs use the taper design for exits and the parallel design for entrances.

Elements with Quantified Relationship

This subsection describes various associations between safety and speed-change lane design that have been quantified through an analysis of crash data. Topics addressed include acceleration length, deceleration length, and ramp exits with a lane drop.

Acceleration Length. Five research reports or papers were identified that addressed the relationship between acceleration length and crash frequency. Cirillo (1970) assembled crash data for 3,516 acceleration lanes at interchanges on the Interstate Highway System in 22 states. The analysis unit was a freeway segment with a speed-change lane. Hence, the database included both freeway-segment crashes and speed-change-related crashes.

The Cirillo data were re-analyzed for the purpose of deriving a CMF for acceleration length. The derivation of this equation is described in the section titled Freeway Segments. The calibrated equation for total crashes is provided in Equation 1. It is shown in Figure 12. The equation converges to a value of 1.0 as acceleration length increases.

$$CMF_{enr} = 1.0 + \frac{(0.001 AADT_{ramp})^{0.83}}{22.3 L_{enr}} (1.0 - e^{-22.3 L_{enr}}) \quad (1)$$

where,

- CMF_{enr} = crash modification factor for acceleration length;
- $AADT_{ramp}$ = ramp AADT volume, veh/day; and
- L_{enr} = acceleration length, mi.

Equation 1 predicts a factor value of 1.12 for an acceleration length of 2,000 ft. A length of 2,000 ft or more is generally recognized as more than adequate for most freeway ramp entrances. However, the fact that the value exceeds 1.0 for this length and longer indicates that there are additional crashes occurring in the freeway mainlines as a result of ramp-related lane changes that occur downstream of the ramp entrance.

Bauer and Harwood (1998) gathered three years of crash data for 276 acceleration lanes and 192 deceleration lanes at interchanges in Washington. Only crashes identified as occurring in the speed-change lane were included in the database. They used a regression analysis to examine the relationship between acceleration length and total crash frequency. They found that speed-change lane crash frequency *increased* with increasing acceleration length.

Bauer and Harwood (1998) also examined acceleration length using total crash data for the combined ramp proper and speed-change lane. In this analysis, they found that the combined crash frequency decreased as speed-change lane length increased. A CMF was derived from their regression model, as shown in Figure 12. It yields a factor value of 1.0 at the average speed-change lane length of 950 ft. The factor converges to a value of 0.0 as length increases.

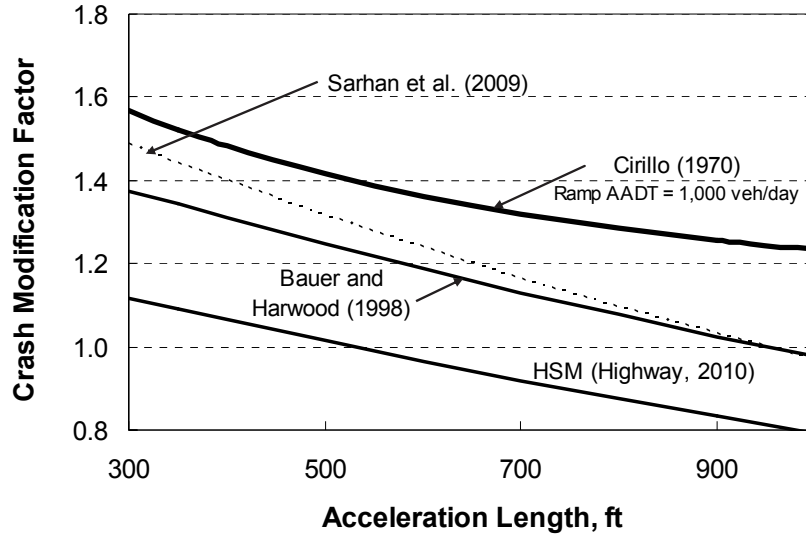


Figure 12. Relationship between CMF value and acceleration length based on total crashes.

Sarhan et al. (2006) examined total crash data for 26 interchanges on a freeway in Canada. The crash data included crashes on the freeway segment within the interchange area plus those in the speed-change lanes. They developed a regression model that included a sensitivity to acceleration length. A CMF was derived from their model, as shown in Figure 12. It yields a value of 1.0 at the average length of 950 ft. The factor converges to a value of 0.0 as entrance length increases.

The *HSM* (Highway, 2010) provides a CMF for acceleration lane length. It is shown in Figure 12. A review of the reference sources for this model indicates that it was derived from the aforementioned Bauer and Harwood (1998) regression model. Hence, the “acceleration length” in reference is actually the ramp entrance length shown in Figure 11. In addition, the base length is stated as 528 ft, which is about one-half of the average length reported by Bauer and Harwood (1998). The factor converges to a value of 0.0 as entrance length increases.

Deceleration Length. Four research reports or papers were identified that addressed the relationship between deceleration length and crash frequency. Cirillo (1970) assembled crash data for 3,516 deceleration lanes at interchanges on the Interstate Highway System. The analysis unit was a freeway segment with a speed-change lane. Hence, the database included both freeway segment crashes and speed-change-related crashes.

The Cirillo data were re-analyzed for the purpose of deriving a CMF for deceleration length. The derivation of this equation is described in the section titled Freeway Segments. The calibrated equation is provided in Equation 2. It is shown in Figure 13. The equation converges to a value of 1.0 as deceleration length increases.

$$CMF_{exr} = 1.0 + \frac{(0.001 AADT_{ramp})^{0.35}}{22.9 L_{exr}} (1.0 - e^{-22.9 L_{exr}}) \quad (2)$$

where,

CMF_{exr} = crash modification factor for deceleration length; and
 L_{exr} = deceleration length, mi.

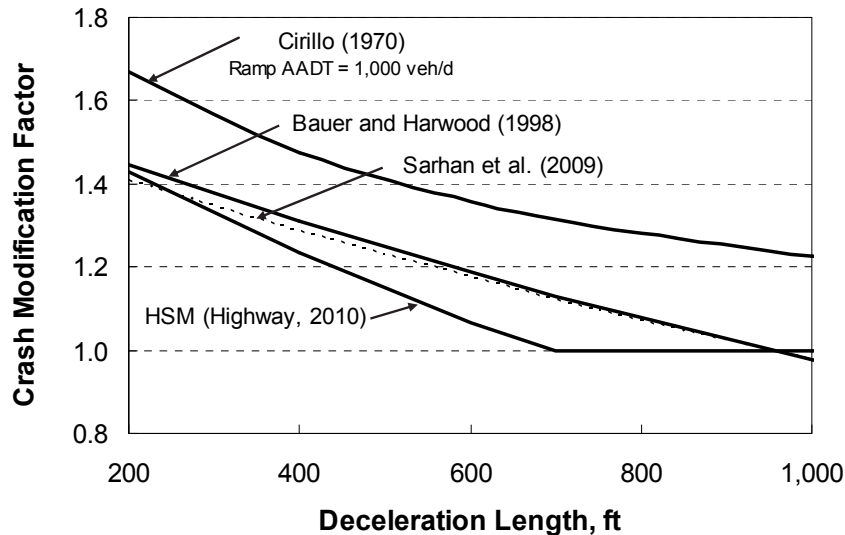


Figure 13. Relationship between CMF value and deceleration length based on total crashes.

Bauer and Harwood (1998) gathered three years of crash data for 276 acceleration lanes and 192 deceleration lanes at interchanges in Washington. Only crashes identified as occurring in the speed-change lane were included in the database. They used regression analysis to examine the relationship between deceleration length and crash frequency. The correlation with deceleration length was not statistically significant, so it was not quantified.

Bauer and Harwood (1998) also examined deceleration length using crash data for the combined ramp proper and speed-change lane. In this analysis, they found that the combined crash frequency decreased with increasing speed-change lane length. A CMF was derived from their regression model, as shown in Figure 13. It yields a factor value of 1.0 at the average speed-change lane length of 950 ft. The factor converges to a value of 0.0 as length increases.

Sarhan et al. (2006) examined total crash data for 26 interchanges on a freeway in Canada. The crash data included crashes on the freeway segment within the interchange area plus those in the speed-change lanes. They developed a regression model that included a sensitivity to deceleration length. A CMF was derived from their model, as shown in Figure 13. It yields a factor value of 1.0 at the average length of 950 ft. The factor converges to a value of 0.0 as exit length increases.

The *HSM* (Highway, 2010) provides information about the effect of deceleration length. In Exhibit 15-5, it indicates that the extension of a lane by 100 ft corresponds to a 7 percent reduction in crashes, provided that the lane does not exceed 690 ft. The guidance in the manual is not clear whether this factor applies to the speed-change lane, speed-change lane and ramp proper, or speed-change lane and freeway segment. The guidance is reproduced as a CMF in Figure 13.

Exit Ramps with a Lane Drop. A lane drop at an exit ramp is often a result of the need for two lanes to serve ramp traffic demand. The additional lane is added to the freeway segment as an auxiliary lane in advance of the ramp and then dropped from the freeway cross section at the ramp. This approach maintains the basic number of lanes through the interchange area. Occasionally, the outside lane on the freeway segment is dropped at a single-lane ramp (or two outer lanes are dropped at a dual-lane exit ramp). This approach does not maintain lane balance. Regardless of whether the basic number of lanes and lane balance are maintained, lane drops at exit ramps are not typical and are a source of relatively frequent erratic maneuvers (Taylor and McGee, 1973).

Chen et al. (2009) examined crash data for 326 freeway segments in Florida. Each segment had an exit ramp. The collective set of segments represented right-side exit ramps with four different geometric designs, of which three designs had a lane drop. The analysis unit was a freeway segment with a speed-change lane. Hence, the database included both freeway segment crashes and speed-change-related crashes.

The crash rates computed by Chen et al. for each of the four designs are reproduced in Table 4. The last column provides a ratio that can be used to make some judgment about the possible influence of a lane drop. The basis of comparison for this ratio is the first ramp listed in the table. This ramp represents the typical design with a single lane ramp, no lane drop, and freeway lane balance. The crash-rate ratio indicates that the exits with a lane drop have more crashes, for the same traffic volume.

TABLE 4. Comparison of total crash rates for exit ramps with a lane drop

Type	Ramp Lanes	Exit Ramp Design		Crash Rate crash/mvm	Crash Rate Ratio ¹
		Speed-Change Lane Design	Lane Drop? Lane Balance?		
1	1		No Yes	0.34	--
2	1		Yes No	0.57	1.68
3	2		Yes Yes	0.46	1.35
4	2		Yes No	0.86	2.53

Note:

1 - Ratio uses the crash rate for the type 1 ramp as the basis of comparison.

Freeway Segments

This subsection describes the findings from a review of the safety literature related to freeway segments. Topics of discussion include freeway segments that are distant from interchange ramps as well as segments in the vicinity of ramp entrances or exits. Unless specifically noted otherwise, the segment is defined to include both travel directions.

Basic Descriptors

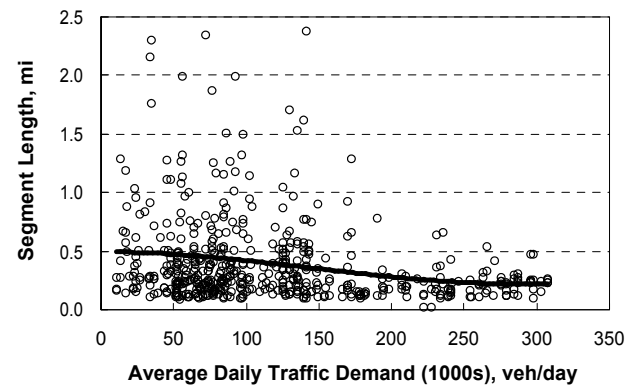
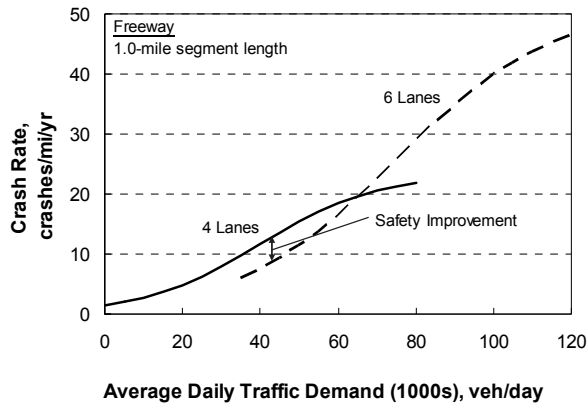
This subsection describes various fundamental descriptors of freeway segment design and operation. Topics addressed include number of lanes and area type.

Number of Through Lanes. The relationship between number of lanes and safety is complex such that generalization is difficult. It is generally believed that an additional lane effectively increases the separation between vehicles and that this separation reduces the potential for conflict. Evidence to support this belief is reported by McCasland and Biggs (1980) in their examination of the change in safety associated with a change in cross section at 15 freeway segments in seven states. In each instance, a lane was added within the existing cross section by reducing the lane or shoulder widths. Each site experienced a reduction in its total crash rate, with an average reduction of 29 percent.

More recent research that has examined the relationship between number of lanes and safety indicates that cross sections with more lanes are associated with more crashes, for the same traffic volume. Milton and Mannering (1998) used a cross-sectional study to examine crash trends on principal arterial highways in Washington. They found that crashes were more frequent on those highways with more lanes. They rationalized that this trend may be due to an increase in lane changing that occurs on cross sections with more lanes. A similar finding was described by Abdel-Aty and Radwan (2000) in their examination of urban roadway sections.

Kononov et al. (2008) examined crash data for urban freeways in three states in an effort to understand the relationship between number of lanes and safety. Based on their examination of the data for a wide range of traffic volumes, they found that number of lanes had a unique influence on the relationship between traffic demand and crash rate. A series of regression analyses resulted in the consistent trend for an ogive shape in the calibrated SPF, as shown in Figure 14a. Separate SPFs were calibrated for differing numbers of lanes.

Each trend line in Figure 14a illustrates the observed relationship between traffic demand and crash rate for a given number of lanes. Each trend line is shown to “flatten” (or converge) to a specific large number of crashes at higher traffic demand. Kononov et al. attribute this convergence to a high-density, congested freeway operation where speed and movement is constrained.



a. Relationship between crash rate and lanes. b. Correlation between volume and length.

Figure 14. Relationship between crash rate, traffic demand, and number of lanes.

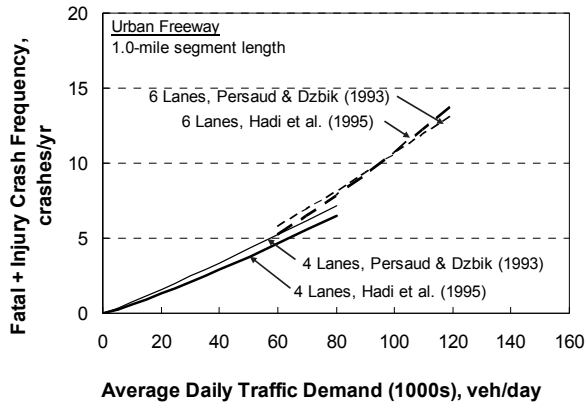
The effect of number of lanes is observed by comparing the two trend lines shown in Figure 14a. The six-lane trend line is shown to have a steeper slope than that for four lanes. Kononov et al. rationalize that the steeper slope is a consequence of the increased number of opportunities for lane changes, which is associated with an increased number of lanes.

The regression analysis by Kononov et al. is based on “crashes per mile per year” as the dependent variable, as opposed to “crashes per year.” An examination of the relationship between AADT volume and segment length for freeways in several states indicates that there is a consistent negative correlation between segment length and AADT volume. This trend is shown in Figure 14b for freeway segments in California. Segment length and AADT volume have a correlation of -0.24 in this figure. This correlation was found to partially explain the flattening of the trend lines in Figure 14a. The flattening is not evident when using “crashes per year” as the dependent variable.

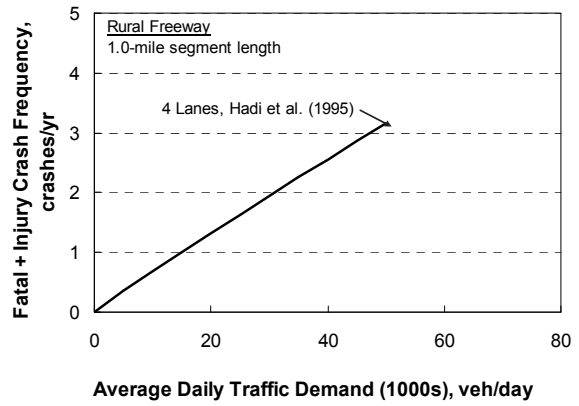
Several researchers have developed SPFs for freeway segments with a specified number of lanes. These SPFs are compared in Figure 15. They are based on fatal-and-injury (FI) crashes.

The SPFs shown in Figures 15c and 15d were developed by Torbic et al. (2007) for the ISAT software. The SPFs shown in Figures 15e and 15f were developed by Bonneson and Pratt (2008) using data for Texas freeways. The SPFs shown in these four figures are based on freeway segments that are distant from interchanges, such that there is negligible effect of lane changes associated with ramp entry or exit. It was not possible to verify this “isolation” of interchange influence in the SPFs represented in Figures 15a and 15b.

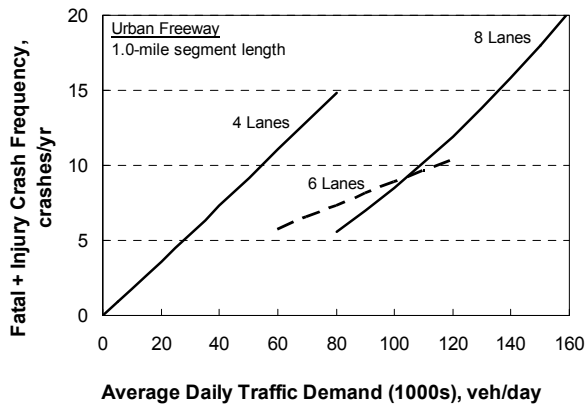
An examination of the trends in Figure 15 indicates that there is little agreement among researchers on the association between number of lanes and crash frequency.



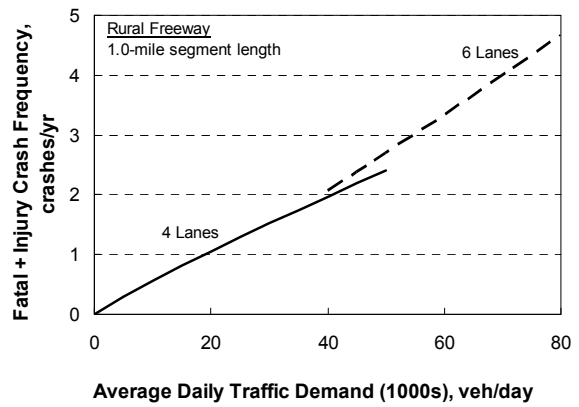
a. Two urban freeway SPFs.



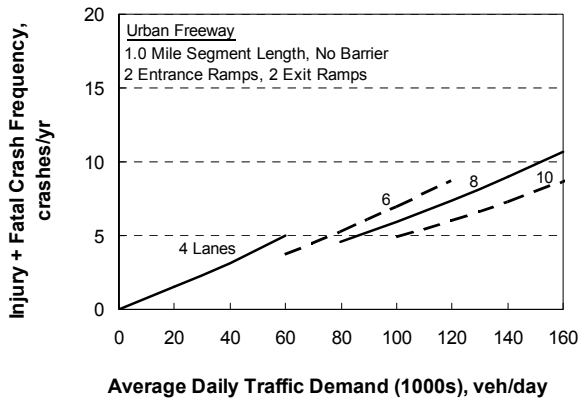
b. One rural freeway SPF.



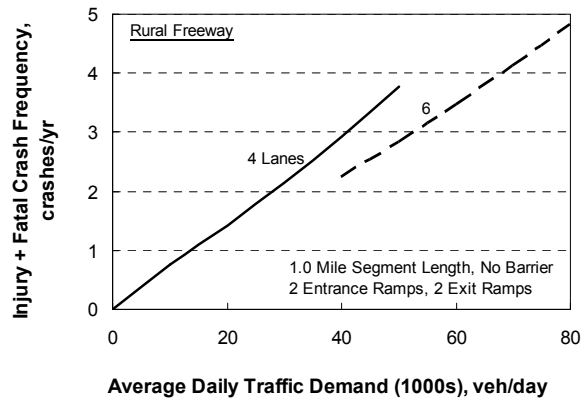
c. ISAT urban freeway SPFs.



d. ISAT rural freeway SPFs.



e. Texas urban freeway SPFs.



f. Texas rural freeway SPFs.

Figure 15. Freeway segment SPFs based on FI crashes.

During the development of the SPFs shown in Figures 15e and 15f, Bonneson and Pratt (2008) noted that an examination of crash rates for freeway segments revealed that crash rate

tended to increase as the number of lanes increased, similar to the finding by Milton and Mannering (1998). However, the reverse trend is shown in Figures 15e and 15f, similar to the finding by McCasland and Biggs (1980). This reversal stemmed from the use of a regression model that included factors to account for the effect of barrier presence, median width, and horizontal clearance. They found that a greater portion of the segment length was protected by a barrier (in both the median and along the roadside) on freeways with more lanes. Similarly, they found that the horizontal clearance and median width was smaller on freeways with more lanes. Both of these trends were rationalized to explain the observed increase in crash rate, as opposed to the increase in number of lanes.

Area Type. This descriptor indicates the population density in the vicinity of the freeway segment. The categories used are urban and rural. The trends shown in Figure 15 indicate that urban freeway segments have a higher crash frequency than rural segments, for a given traffic volume.

Elements with Quantified Relationship

This subsection describes various associations between safety and freeway segment design or operation that have been quantified through an analysis of crash data. Topics addressed include horizontal curve radius, grade, lane width, outside shoulder width, inside shoulder width, median width, shoulder rumble strips, horizontal clearance, and ramp meter operation.

Horizontal Curve Radius. The correlation between curve radius and freeway segment crash frequency has not received considerable attention in the research literature. One examination of this relationship was undertaken by Raff (1953). He examined total crash data for curves on undivided, divided, and controlled-access rural highways in 15 states. The data cited for controlled-access highways were re-analyzed for this report for the purpose of deriving a CMF. The relationship found is shown in Figure 16.

Also shown in Figure 16 is a horizontal curve CMF developed by Bonneson and Pratt (2008) for FI crashes on highway curves. This CMF includes a sensitivity to speed limit. When used with a speed limit of 50 mi/h (which was the average highway speed in the early 1950s), it compares favorably with the trend attributed to the Raff data.

A third horizontal curve CMF is also shown in Figure 16. This CMF is documented by Harwood et al. (2000) and is applicable to total crashes on two-lane highway curves. It is shown only to illustrate the trend. It was derived using data from the mid-1980s for curves in Washington. The national speed limit at this time was 55 mi/h.

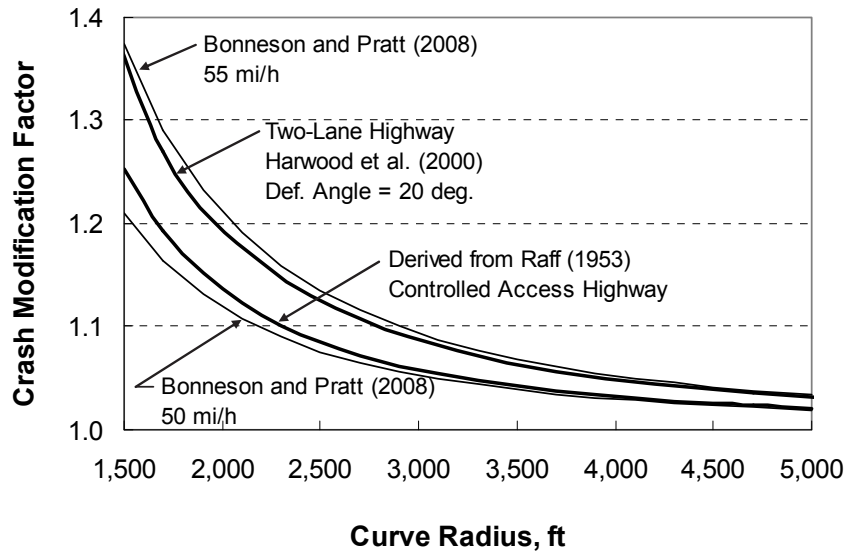


Figure 16. Relationship between CMF value and curve radius.

Grade. As with horizontal curvature, research on the relationship between grade and freeway crash frequency is relatively limited. Dunlap et al. (1978) examined the relationship between grade and crash rate on turnpikes in Ohio and Pennsylvania. They found that crash rates increased on downgrade segments, relative to level or upgrade segments.

Milton and Mannering (1998) calibrated a regression model that predicted total crash frequency as a function of grade and other geometric and traffic variables. It was calibrated using data for 2,700 miles of urban and rural multilane highways in Washington. The highways were classified as principal arterials. For highways in eastern Washington, they found that when the grade exceeds 2.5 percent (uphill or downhill) crash frequency increases by 2 percent. For highways in western Washington, they found a 6 percent higher crash frequency for segments with a grade in excess of 1.0 percent.

Lane Width. Hadi et al. (1995) calibrated a series of regression models for predicting crash frequency on Florida streets and highways. The models were developed using four years of crash data. The model developed for total crashes on freeway segments included a variable for lane width. The associated regression coefficient was used to derive a CMF for this report. It is shown in Figure 17. The slope of the trend line suggests that a 1-ft reduction in lane width results in a 35 to 40 percent increase in crashes. This increase is unrealistically large and is probably a result of lane width being correlated with other influential variables that are not in the safety prediction model developed by Hadi et al.

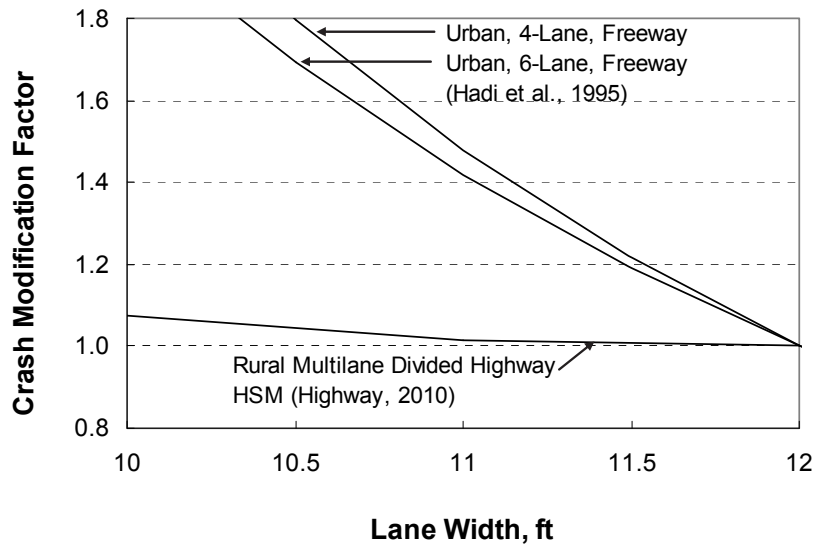


Figure 17. Relationship between CMF value and lane width based on total crashes.

In Figure 17, the CMF that is attributed to the *HSM* (Highway, 2010) was developed for rural multilane divided highways. It illustrates a more likely relationship between lane width and freeway safety, as compared to that attributed to Hadi et al. (1995). It is rationalized that the design and operational differences between a freeway and a divided highway (as related solely to the correlation between lane width and crash frequency) are not so distinct as to invalidate this comparison.

Research by Bonneson et al. (2007a) and by Gross et al. (2009) documents an interaction between lane width and shoulder width on rural two-lane highways. As a result of this interaction, the relationship between crash risk and a change in lane width is influenced by the width of the adjacent shoulder (and vice versa). The combined lane-width and shoulder-width CMF developed by Bonneson et al. is shown in Figure 18. The relationship identified by Gross et al. is very similar. Research investigating a similar interaction for freeways was not found during the literature review.

Outside Shoulder Width. Several researchers have developed regression models relating freeway-segment crash frequency with outside shoulder width (among other variables). A CMF for shoulder width was derived from each of these models for this report. They are shown in Figure 19.

The data used by Knuiman et al. (1993) represent a mixture of freeway and highway segments in Ohio and Illinois. Three years of crash data were assembled for Illinois segments and four years of data were assembled for the Ohio segments. The segments total 3,055 miles, with about two-thirds of the miles in Illinois. Collectively, the segments represent both urban and rural areas. The data assembled by Harkey et al. (2008) represent access-controlled highways in California. Ten years of crash data were assembled for 993 miles of rural segments and 501 miles of urban segments.

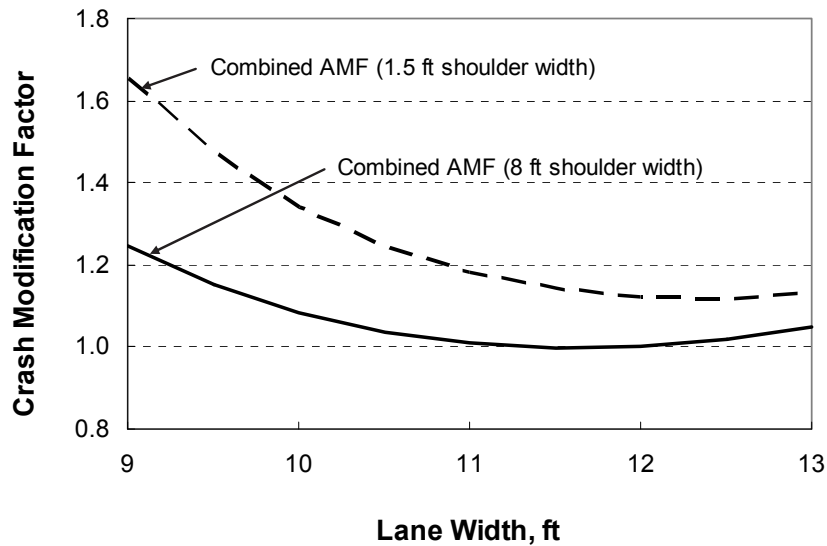


Figure 18. Illustrative interaction between shoulder width and lane width.

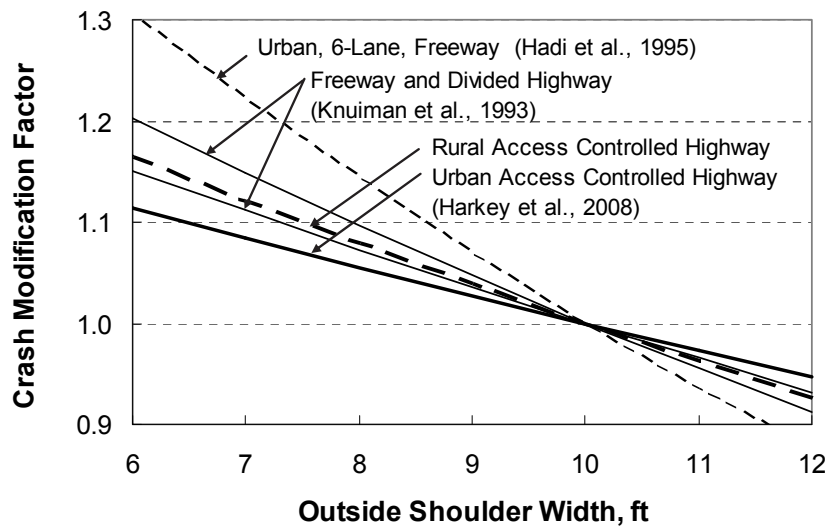


Figure 19. Relationship between CMF value and outside shoulder width based on total crashes.

The trend lines shown in Figure 19 indicate a general agreement among the various alternative CMFs. However, the slopes are sufficiently different among sources as to suggest that other factors may be exerting some influence. For example, it is possible that the CMFs with steeper slopes are associated with roadways with narrower traffic lanes. They may also reflect roadways with more frequent roadside barrier sections, shorter offset to roadside barrier, or both.

Inside Shoulder Width. A review of the literature revealed two independent efforts to quantify the relationship between inside shoulder width and freeway crash frequency. Both research projects calibrated a regression model that included a variable for inside shoulder width on a freeway segment. A CMF was derived from each model and is shown in Figure 20. A visual

comparison of the trends in Figures 19 and 20 suggests that a change in inside shoulder width has slightly smaller influence on the CMF value than a similar change in outside shoulder width.

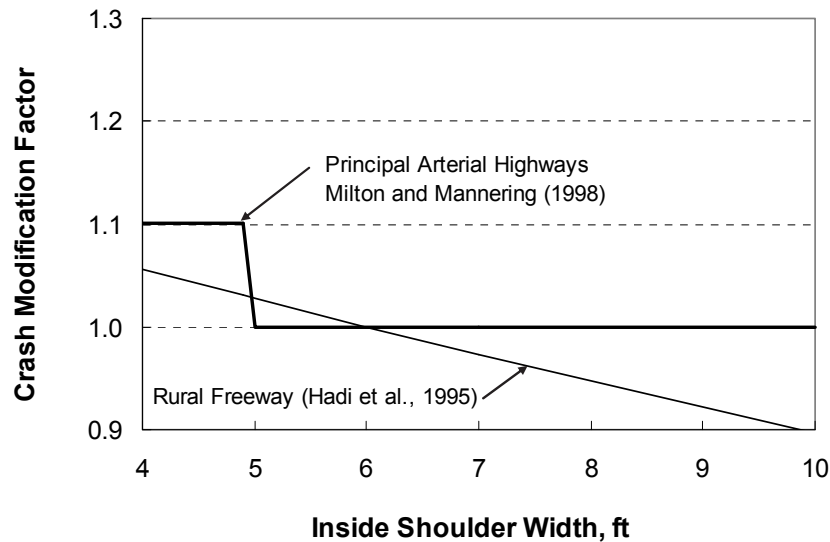
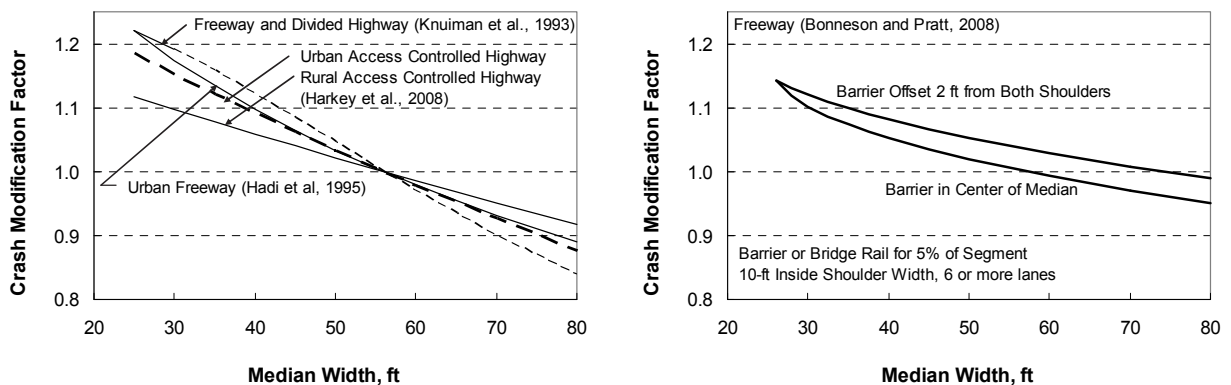


Figure 20. Relationship between CMF value and inside shoulder width based on total crashes.

Median Width. CMFs for median width were derived from regression models developed by Hadi et al. (1995), Knuiman et al. (1993), Harkey et al. (2008), and Bonneson and Pratt (2008). The CMFs derived from the Hadi and Bonneson models were calibrated using freeway crash data. The Knuiman model was based on crash data for a mixture of freeways and major highways in Illinois. The Harkey model was based on crash data for controlled-access highways. The derived CMFs are shown in Figure 21.



a. CMFs for three researchers - total crashes.

b. CMFs with barrier influence - FI crashes.

Figure 21. Relationship between CMF value and median width.

The trend lines in Figure 21a apply to total crashes. They show general agreement that narrower medians are associated with more frequent crashes. However, the slopes of the trend

lines vary among sources and may be a consequence of other, unexplained factors such as inside shoulder width or barrier presence. For example, Figure 21b illustrates the influence of barrier presence on median width. The trend lines shown are applicable when a barrier is present in the median for 5 percent of the segment length. The lines shift upward with increasing barrier percentage.

The effect of median barrier presence on crash frequency and severity was examined by Tarko et al. (2008). They found that the conversion of a depressed median to a flush median with a rigid barrier increased total single-vehicle crashes by 120 percent, while reducing total same-direction crashes only 20 percent. This trend was also found in by Bonneson and Pratt (2008) and is reflected in the CMF shown in Figure 21b. Tarko et al. also found that the inclusion of a barrier in the median increased the likelihood of severe crashes (although it nearly eliminated fatal crashes).

For all of the CMFs shown in Figure 21, the median width is measured from the near edges of the travel way of the opposing roadbeds. Thus, this width includes the width of the inside shoulder. The CMFs shown in Figure 21a do not account for the effect of inside shoulder width. Thus, the same factor value is obtained when median width is reduced by two feet and there is either a one-foot reduction of both inside shoulders or a two-foot reduction of the area between shoulders. Logically, a reduction in the inside shoulder width should be accompanied by a larger median-width factor value than a reduction of width between the inside shoulders.

Shoulder Rumble Strips. Griffith (1999) investigated the correlation between the presence of continuous, rolled-in rumble strips and crash frequency on urban and rural freeways in California and Illinois. The focus of his examination was single-vehicle run-off-road crashes. The reported crash data were used to calculate rumble strip CMFs. These calculations and the resulting CMFs are shown in Table 5.

TABLE 5. CMFs for shoulder rumble strips

Data Source	State	Severity Level	Treated Site Crashes ¹		Comparison Site Crashes		CMF (f_{rs}) ²	Standard Deviation ³
			After	Before	After	Before		
Griffith (1993)	Illinois	Total/all	1895	2801	1833	2288	0.84	0.036
	California	Total/all	469	579	364	417	0.93	0.088
	Combined	Total/all	2364	3380	2197	2705	0.86	0.034
	Illinois	Injury	877	1135	765	874	0.88	0.059

Notes:

1 - Analysis applies to single-vehicle run-off-road crashes.

2 - $f_{rs} = \text{After}_{treated} \times \text{Before}_{comp} / (\text{Before}_{treated} \times \text{After}_{comp})$.

3 - Standard deviation = $f_{rs} \times (1/\text{After}_{treated} + 1/\text{Before}_{comp} + 1/\text{Before}_{treated} + 1/\text{After}_{comp})^{0.5}$.

Horizontal Clearance. The clear zone concept is based on the rationale that crash frequency and severity will be reduced by increasing the lateral offset to vertical obstructions (or non-traversable ditch cross sections) along the roadside. Objects that cannot be relocated or removed from the clear zone are protected by barrier or made to operate in a break-away manner

in the event of a collision. Research on the relationship between horizontal clearance and FI crash frequency was examined by Bonneson and Pratt (2008). The CMF that they derived is illustrated in Figure 22.

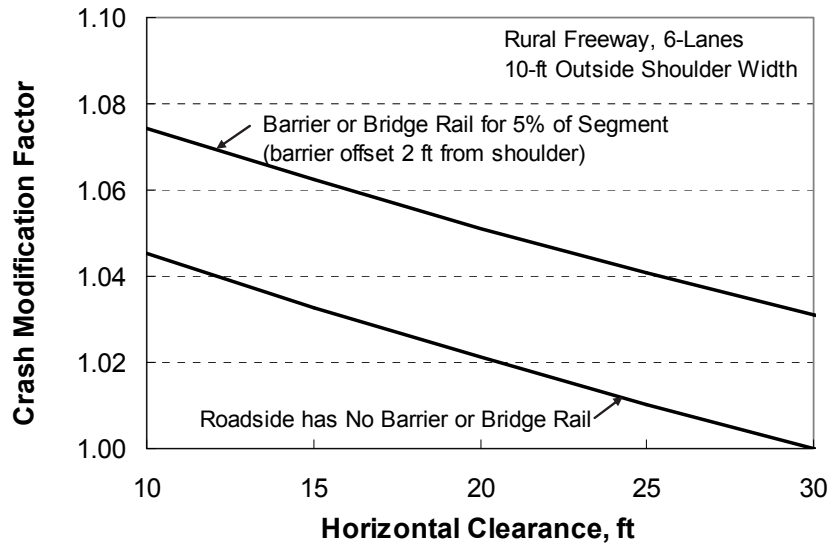


Figure 22. Relationship between CMF value and horizontal clearance based on FI crashes.

The trend lines in Figure 22 indicate that barrier presence along the roadside has some influence on crash risk. The barrier itself is a fixed object, but one that is designed to reduce fatalities associated with roadside crashes. This CMF is applicable when there is a barrier or bridge rail on the roadside (it can consist of several short barrier sections on a portion of the segment or one barrier that extends the length of the segment). The barrier can be rigid or semi-rigid. It can be located adjacent to one roadbed, both roadbeds, or at a specified distance from the edge of traveled way.

Ramp Meter Operation. Ramp metering is a freeway traffic-management strategy that is generally recognized to improve freeway operation and safety. Research is cited by Everall (1972) of reductions in total crashes that range from 40 to 70 percent following the introduction of ramp meters on freeway sections in Atlanta, Chicago, and Houston.

More recently, Upchurch and Cleavenger (1999) examined the effect of ramp metering on freeway crash frequency. They conducted a before-after study using the non-metered hours as a comparison group. They examined freeway crashes during a period of three years before and three years after ramp meters were installed on nine ramps of an Arizona freeway. A log-odds analysis of the reported data was conducted for this report. This analysis indicates that total crashes on the freeway were reduced by 40 percent when ramp metering was operational.

In 2000, Minnesota DOT disabled ramp meters on its freeways at the direction of the State Legislature. A subsequent analysis of total crash data indicated that freeway crash frequency increased 26 percent as a result of the cessation of the ramp meter operation (Cambridge 2001).

Illumination. The presence of lighting along a freeway segment has been found to improve safety. Griffith (1994) compared daytime and nighttime crash rates on urban freeway segments with and without continuous lighting. The database contained 54.6 mi of data for segments with continuous lighting and 35.5 mi of data for segments with lighting only at the interchanges. He found that segments without continuous lighting had 12 percent larger nighttime crash rates (based on total crashes).

Elvik and Vaa (2004) conducted a meta analysis of several published studies focused on the effect of illumination on safety. They found that injury crash frequency increased 17 percent when lighting level was reduced. More recently, Monsere and Fischer (2008) found that injury crash frequency increased 39 percent when freeway segment lighting was reduced (i.e., lighting fixtures eliminated) along 5.5 mi of interstate highway in Oregon.

Related Topics

This subsection describes various topics related to the safety of the freeway segment. The focus is on freeway design and operational elements. The topics addressed in this section include ramp entrance/exit-related lane changing, weaving, interchange spacing, truck lane restrictions, and volume-to-capacity ratio. The first three topics relate to lane changing that occurs on the freeway segment in the vicinity of interchange ramps, but not at the speed-change lane. This lane changing is a result of drivers maneuvering from an inside lane to an outside lane to access an exit ramp, or maneuvering from an outside lane to an inside lane to avoid vehicles entering the freeway from an entrance ramp.

Ramp Entrance/Exit-Related Lane Changing. The presence of a ramp entrance or exit creates a large number of lane changes on the freeway and a notable variation in lane volume. SPFs were developed by Kiattikomol et al. (2008) in part to examine the influence of interchange ramp presence on freeway crash frequency. They collected three years of crash data for urban freeway segments in North Carolina and Tennessee. A total of 377 miles were represented in the database, with slightly more of the miles (204) on Tennessee freeways. Segments located more than 1,500 ft from the middle of the interchange were considered to be “non-interchange” segments. Total crash rates of 42 and 82 crashes per 100 million vehicle-miles (100 mvm) were found for non-interchange segments in North Carolina and Tennessee, respectively. These rates were found to increase by about 200 percent on interchange segments.

Torbic et al. (2007) also developed separate SPFs for freeway segments that were located either within or outside of an interchange area. Segments located more than 0.3 mi from the nearest ramp gore were considered to be “outside” interchange segments. A comparison of the SPFs for both segment types indicates that “within” interchange segments have more crashes than “outside” interchange segments. The amount of increase varies from 0 percent at low volume to more than 100 percent at high volume. Torbic et al. rationalized that this increase is due to the weaving and lane-changing associated with the interchange ramps.

Research by Goswami and Bham (2006) was examined to determine the extent of lane-changing activity in the vicinity of an interchange ramp terminal. They used vehicle trajectory data for a segment of I-80 in California for this purpose. They decomposed the freeway segment passing through the interchange into 200-ft zones, with separate zones for each lane. They

counted the lane volume and the lane changes that occurred within each zone. The lane-change frequency for entrance and exit ramps is shown in Figure 23. It is expressed as a percentage of freeway lane volume. The trend lines in this figure represent a regression model fit to the data points shown. The trend lines suggest a gradual reduction in lane change activity with distance from the ramp gore.

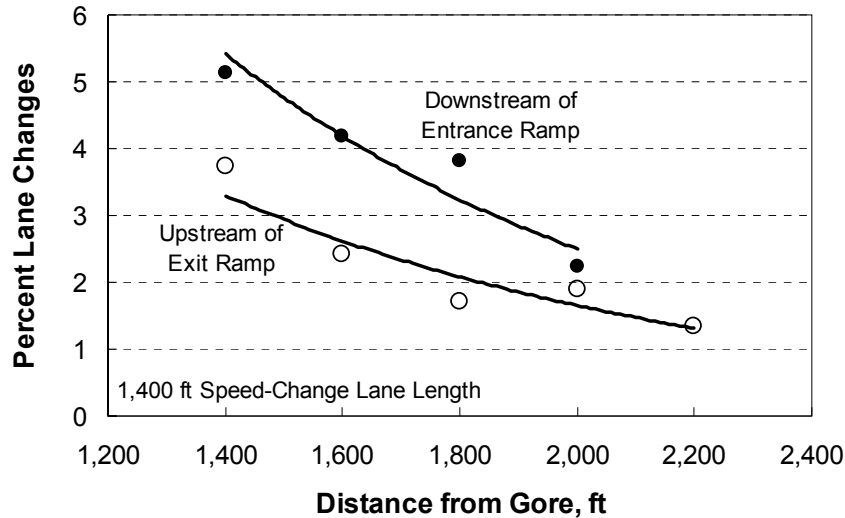


Figure 23. Percent of lane changes as a function of distance from ramp gore.

Cirillo (1968) examined total crash rates for segments of the Interstate Highway System that were in the vicinity of an interchange. Several years of crash data were obtained from 20 state DOTs. The database represented more than 9,000 mile-years of data. Crash rates were computed for segments that were located within these distances from the ramp gore: 0.2 mi, 0.2 to 0.4 mi, 0.5 to 0.9 mi, 1.0 to 1.9 mi, 2.0 to 3.9 mi, and 4.0 to 7.9 mi. Crashes on the freeway in the vicinity of the speed-change lane were excluded. Crash rates were separately calculated for entrance and exit ramps in urban and rural areas. These crash rates for the urban segments are shown in Figure 24. The trend line shows that crash rate gradually reduces as distance from the ramp gore increases.

It is likely that the lane-change activity associated with the ramp has a direct influence on the trends in crash rate shown in Figure 24. This influence is reflected in a CMF of the following form.

$$CMF_x = 1.0 + (0.001 AADT_{ramp})^{b_0} e^{-b_1 x} \quad (3)$$

where,

CMF_x = crash modification factor for lane changes at a distance x from the ramp gore;

b_0, b_1 = regression coefficients; and

x = distance from ramp gore, mi.

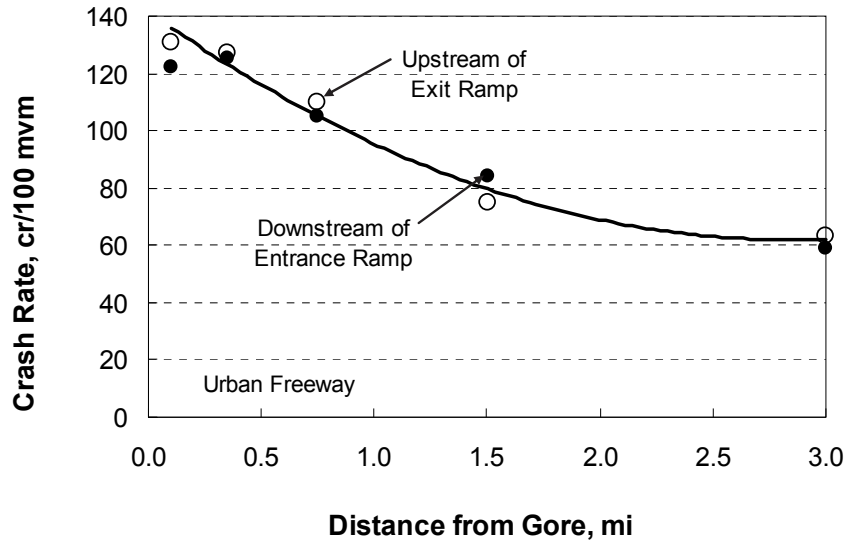


Figure 24. Total crash rate as a function of distance from ramp gore.

Equation 3 can be integrated to obtain an average CMF value for a segment that extends a distance x_b to x_e from the ramp gore. The result of this integration is shown in Equation 4. The CMF value converges to 1.0 as the subject segment length or location approaches infinity.

$$CMF_{lc} = \frac{\int_{x_b}^{x_e} CMF_x dx}{\int_{x_b}^{x_e} dx} \quad (4)$$

$$= 1.0 + \frac{(0.001 AADT_{ramp})^{b_0}}{b_1 (x_e - x_b)} (e^{-b_1 x_b} - e^{-b_1 x_e})$$

where,

- CMF_{lc} = crash modification factor for ramp-related lane changes;
- x_b = distance from ramp gore to start of segment, mi; and
- x_e = distance from ramp gore to end of segment ($x_e > x_b$), mi.

Nonlinear regression was used to fit Equation 4 (using a simple SPF) to the data reported by Cirillo (1968). A factor was included in the SPF to account for differences between urban and rural segments. The b_1 regression coefficient was allowed to have a unique value for exit ramps and for entrance ramps. The calibrated CMF is shown in Figure 25 for a freeway segment that starts 2,000 ft from the ramp terminal. Other trend lines can be computed for other starting locations.

If the subject freeway segment starts 2,000 ft from the gore, then Figure 25 can be used to obtain a factor value for any specified segment length. For example, if the segment is 1,500 ft long and downstream of an entrance ramp, then the end of the segment is at 3,500 ft and the factor value is 1.65. This value can also be obtained by inspection of the trends in Figure 24.

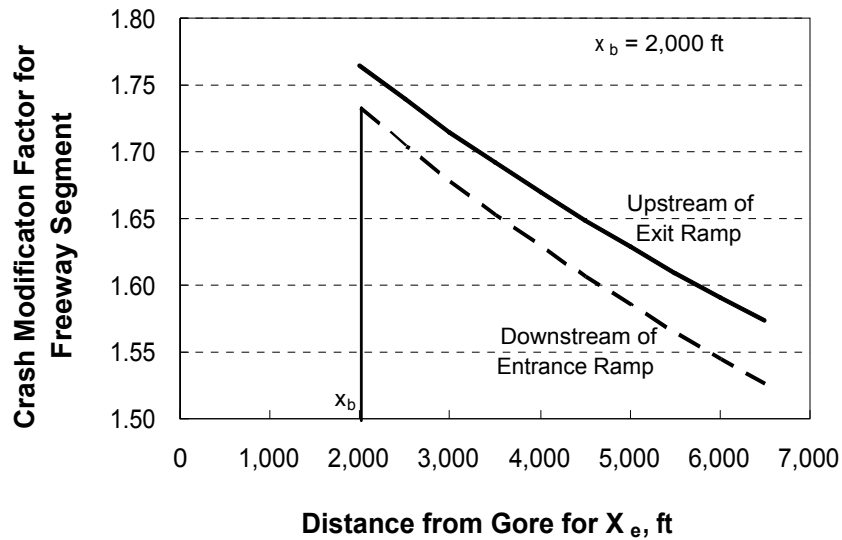


Figure 25. Relationship between CMF value and distance from gore.

Weaving Section. A weaving section presents a combination of merging and diverging maneuvers along a relatively short length of the freeway. Speed differentials between weaving and non-weaving vehicles can be significant. During heavy traffic demand periods, a weaving section often becomes a bottleneck and increases the potential for rear-end crashes.

Cirillo (1970) examined weaving sections at 646 full cloverleaf interchanges on the Interstate Highway System. The weaving sections ranged from 400 to 800 ft in length and included all freeway lanes. An examination of the data indicated that the crash rate for the weaving section decreased as weaving length increased. The amount of decrease was found to vary with freeway traffic demand, with a larger percent decrease associated with lower volume. The data were used to develop a CMF for this report. This equation is shown in Figure 26. It is based on total crashes.

Bonneson and Pratt (2008) collected crash data for 588 freeway segments in Texas. The database included freeway segments with and without weaving sections. All weaving sections were between interchanges, included one auxiliary lane, and required one lane change for both the entering and exiting vehicles. The regression model included a variable to account for weaving length. Ramp traffic demand was not available, so it was not included in the model. They derived the CMF that is shown in Figure 26. It yields a factor value of 1.0 as weaving length increases. It is based on FI crashes.

Some weaving sections require two or more lane changes for one or more of the weaving movements. These weaving sections are not as common as those that require one lane change for both weaving movements. Research cited in the *HSM* (Highway, 2010) indicates that the conversion of “two-lane-change” weaving sections to “one-lane-change” sections reduces total crashes in the merging lanes by 32 percent.

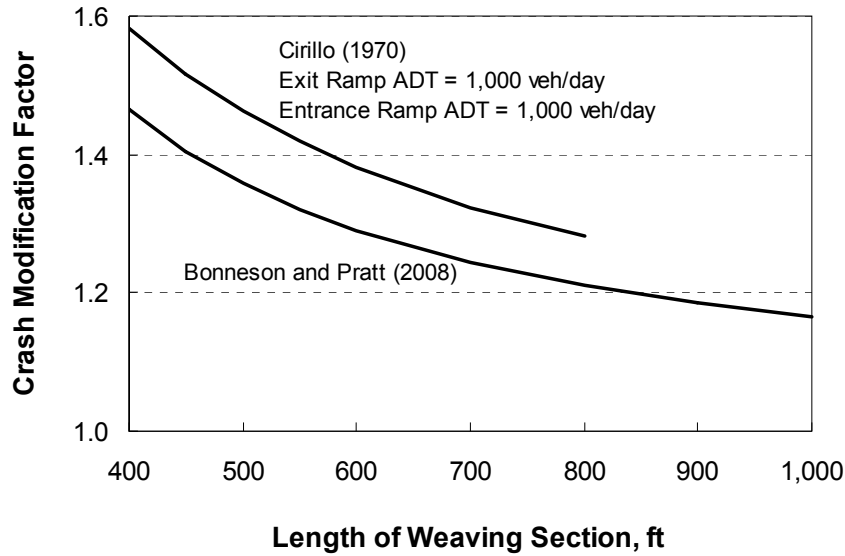


Figure 26. Relationship between CMF value and weaving length.

Interchange Spacing. Bared et al. (2006) evaluated the relationship between total crash frequency and interchange spacing using a regression model. They found that segment crash frequency, when expressed on a “per mile” basis, declined with increasing interchange spacing. The following CMF for interchange spacing was derived from this model.

$$CMF_{sp} = \left(\frac{L_{sp}}{3.0} \right)^{-0.361} \left(\frac{AADT_r}{34,200} \right)^{0.221} \quad (5)$$

where,

CMF_{sp} = crash modification factor for interchange spacing;

$AADT_r$ = sum of the AADT volumes for all four ramps (two entrance ramps, two exit ramps), veh/day; and

L_{sp} = spacing between ramp terminals of adjacent interchanges (see Figure 27), mi.

Equation 5 is shown in Figure 27 using a thick trend line. The $AADT_{ramp}$ for the trend line shown is equal to 34,200 veh/day. Equation 5 is derived to yield a CMF of 1.0 at a spacing of 3.0 mi.

Two CMFs were derived from other sources and are also shown in Figure 27. The CMF attributed to Bonneson and Pratt (2008) is derived from the safety prediction methodology they developed for TxDOT. The derivation of this CMF was more complicated given the formulation of the models. It has the following form. It is based on FI crashes.

$$CMF_{sp} = \left(1.0 + \frac{\sum [C_{enr} + C_{exr}]}{C_{mv} + C_{sv}} \right) CMF_{ocsb} CMF_{wev|agg} CMF_{enr|agg} \quad (6)$$

where,

C_{enr} = ramp entrance crash frequency;

C_{exr} = ramp exit crash frequency;

C_{mv} = multiple-vehicle non-ramp crash frequency;

C_{sv} = single-vehicle crash frequency;
 CMF_{ocsb} = outside clearance (some barrier) crash modification factor;
 $CMF_{wev|agg}$ = aggregated weaving section crash modification factor; and
 $CMF_{enr|agg}$ = aggregated ramp entrance crash modification factor.

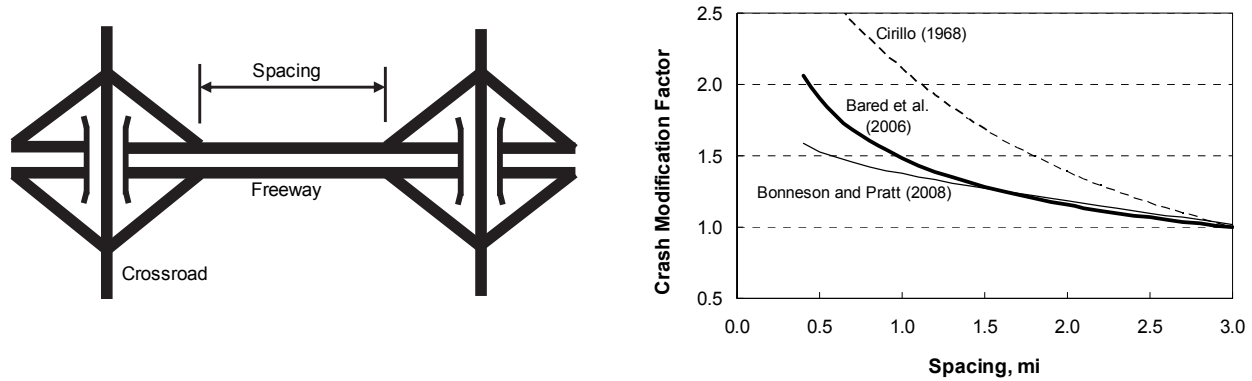


Figure 27. Relationship between CMF value and interchange spacing.

The outside clearance CMF shown in Equation 6 was incorporated after an analysis of Texas data indicated a trend toward more roadside barrier and reduced horizontal clearance with decreasing interchange spacing. Spacings of less than 0.6 mi were assumed to have a weaving section; those greater than 0.6 mi had ramp entrance lengths of 0.3 mi. An urban eight-lane cross section with an AADT volume of 188,000 veh/day was used for the analysis. The CMF from Equation 6 was normalized to yield a value of 1.0 at a spacing of 3.0 miles for consistency with Equation 5.

The CMF attributed to Cirillo (1968) is based on the ramp-related lane-change CMF shown previously as Equation 4. The distance from the ramp gore to the start of the segment x_b was set to 0.0 mi. A ramp AADT volume of 1,000 veh/day was assumed. One CMF was calibrated for lane changes that occurred upstream of the exit ramp and a second CMF was calibrated for lane changes that occurred downstream of the entrance ramp. Both were adjusted to yield a value of 1.0 at a spacing of 3.0 mi to facilitate comparison with the other CMFs. The two lane-change CMFs were then multiplied together (since there is both a downstream ramp and an upstream ramp in the weaving section between interchanges) to obtain the trend shown in Figure 27.

Truck Lane Restriction. Many states have implemented truck lane restrictions on selected freeways. The typical restriction prohibits trucks from using the inside (left-most) lane of a freeway with three or more lanes in the subject travel direction. The goal is to improve the overall operation and safety of the traffic stream.

Research was undertaken by Cate and Urbanik (2004) to examine the safety and operational benefits of truck lane restrictions. They cite a 1997 survey that found 40 percent of state DOTs used truck lane restrictions on Interstate Highway System. They used simulation to investigate the effect of truck lane restrictions. They found that truck lane restrictions

substantially reduce lane changes, which they speculate may provide “significant gains in the area of safety and driver comfort.”

Kobelo et al. (2008) examined crashes on limited-access highways in Florida. A total of 1,216 mi of highways were represented in the database. At total of 430 mi had a truck lane restriction. The average AADT volume per lane was 18,417 veh/day. One year of crash data were gathered and analyzed in a cross-sectional manner using a regression model. The researchers found that total crash frequency was 4 percent lower on highways with a truck lane restriction, relative to those with no restrictions.

Fontaine et al. (2009) examined crashes on interstate highways in Virginia. Six years of crash data were obtained for a time period that spanned the point in time that truck restrictions were implemented. The segments with a truck restriction totaled 237 directional miles. Highway segments for which there was no truck restriction were used as a reference sample to facilitate an empirical Bayes analysis of the before-after data. The reference sample included 154 directional miles. The researchers found that total crash frequency was reduced by 13 percent when the AADT volume per lane was less than 10,000 veh/day. When the AADT volume per lane was higher than 10,000 veh/day, total crash frequency increased by 28 percent. They attributed this trend to the increased difficulty of a lane change with higher lane volume.

Volume-to-Capacity Ratio. The volume-to-capacity ratio relates the demand volume to the capacity of a roadway. As the volume nears capacity, average speed tends to decrease and headway is reduced. Logically, these changes have some influence on crash frequency, as well as the crash type (i.e., single vehicle versus multiple vehicle) and crash severity distributions.

Some research has been undertaken to examine the relationship between volume-to-capacity ratio and crash character. This research typically compares average hourly volume estimates with the crashes that occur during the same hour for one or more years. In this manner, the analysis is often structured by time of day. There are issues of sample size, day versus night, and autocorrelation that complicate this type of analysis.

Hall and Pendleton (1989) gathered data for 41, ten-mile segments on the New Mexico State Highway System. Each segment was selected primarily because it included one of the 50 permanent count stations maintained by the New Mexico DOT. About one-half of the segments had a two-lane cross section and the other one-half had a four-lane cross section. All of the segments were verified to be free of “significant” access points. Three years of crash data were assembled for each segment. The relationship between total crash rate and volume-to-capacity ratio for the “high-volume” segments (which were primarily four-lane highways) is shown in Figure 28. Each data point represents one hour of the average day.

As noted by Hall and Pendleton, the segments included in the study did not have sufficient volume to allow the examination of high volume-to-capacity ratios and crash frequency. The trend lines in Figure 28 indicate that there is an increase in crash risk with lower volume-to-capacity ratios. In fact, the trend takes a sharp upward slope during nighttime hours. Further examination of the nighttime data points indicates that those with the highest crash rates occurred between midnight and 5:00 a.m. This finding suggests that lighting level or a lack of

driver alertness may be the reason for the higher rates during late-night hours (as opposed to a low volume-to-capacity ratio).

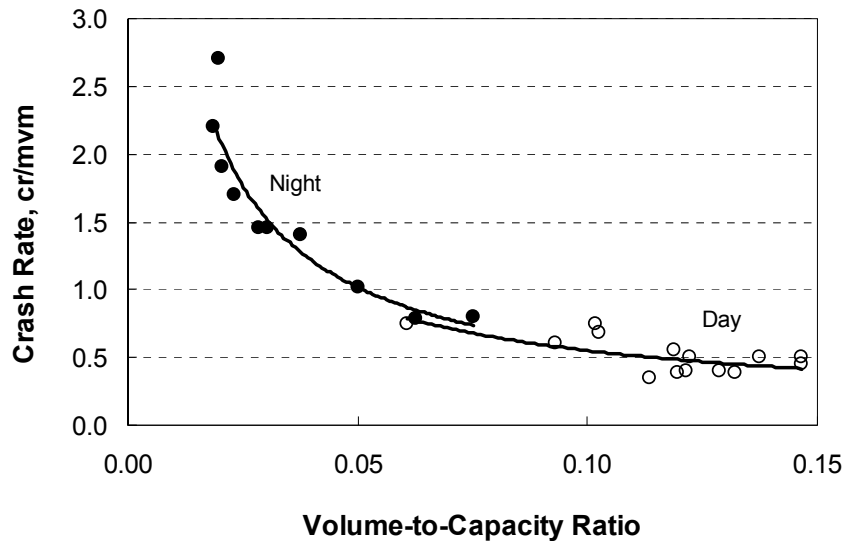


Figure 28. Relationship between total crash rate and volume-to-capacity ratio for highways.

Zhou and Sisiopiku (1997) examined the relationship between volume-to-capacity ratio and total crash rate for three segments of I-94 in Detroit, Michigan. The three segments total 16 miles and experienced 5,047 crashes during a two-year period. The relationship between crash rate and volume-to-capacity ratio in this data is shown in Figure 29. Each data point represents one hour of the average day.

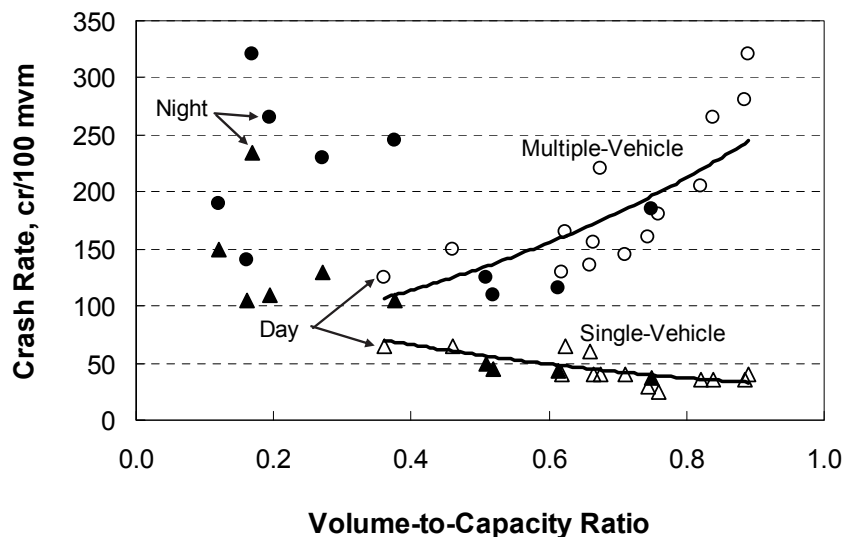


Figure 29. Relationship between total crash rate and volume-to-capacity ratio for freeways.

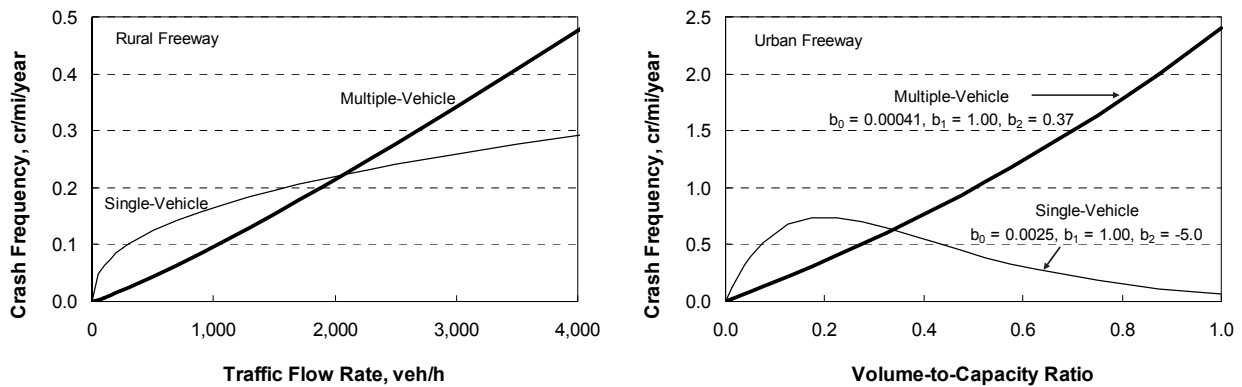
The triangle symbols in Figure 29 represent single-vehicle crash rates. The circular symbols represent multiple-vehicle crash rates. The dark (or solid) symbols represent nighttime

hours. The open symbols represent daytime hours. The trend lines shown represent the relationships found for the daytime crash rates. Similar trends were not as clear in the nighttime data. However, if the trend lines are extrapolated to the lower ratios, then the nighttime crash rates would appear to be above those for the daytime (suggesting that crash risk is higher during nighttime hours).

In Figure 29, there does not appear to be a difference between nighttime and daytime crash rates for volume-to-capacity ratios above 0.4. These nighttime rates correspond to the hours from 8:00 p.m. to 11:00 p.m. This trend is similar to that for rates of 0.06 or more in Figure 28. It suggests that a lack of driver alertness is the likely reason for the higher rates during late-night hours.

Trends similar to those shown in Figure 29 for multiple-vehicle and single-vehicle crashes were also found by Martin (2002). He examined crash rates on interurban motorways in France (primarily tollways). He did not find a significant difference between day and night crash rates. However, he did find that crashes are 1.17 times more severe at night; reflecting frequent high-speed single-vehicle crashes resulting from drowsiness.

An analysis of freeway crash data by Lord et al. (2005) also indicates that both crash frequency and crash type vary with volume-to-capacity ratio. Both relationships are shown in Figure 30. The two trend lines shown in each figure indicate that the safety influence of volume-to-capacity ratio varies with crash type. The trends shown in Figure 30a were noted previously in Figure 10 for ramps and have been found by Persaud and Mucsi (1995) for two-lane rural roads.



a. Traffic demand and crash frequency.

b. Volume-to-capacity ratio and crash frequency.

Figure 30. Relationship between traffic demand, crash type, and total crash frequency.

The predictive model used by Lord et al. (2005) to fit the trends shown in Figure 30 is represented by the following equation.

$$N = b_o Y L V_h^{b_1} CMF_{v/c} \quad (7)$$

with,

$$CMF_{v/c} = e^{b_2 \frac{V_h}{c}} \quad (8)$$

where,

- N = estimate of expected crash frequency, cr;
- b_i = regression coefficients, $i = 0, 1, 2$;
- L = segment length, mi;
- Y = time period of crash estimate, yr;
- V_h = traffic volume, veh/h;
- $CMF_{v/c}$ = crash modification factor for volume-to-capacity ratio; and
- c = capacity, veh/h.

In application, Equation 7 is calibrated using volume and crash data representing a common time period (say one year), where the volume is a specified hourly volume for the average day of the year and the crash data represent the count of crashes during the same hour for the entire year. Equation 7 is separately calibrated for single-vehicle crashes and for multiple-vehicle crashes.

The use of the exponential relationship in Equation 8 is supported by the trends lines shown in Figures 28 and 29. A review of the values of b_2 that provide a best fit to the data in these figures indicates that b_2 typically has a value between -0.5 and -5.0 for single-vehicle crashes. In contrast, it has a value between 0.4 and 1.0 for multiple-vehicle crashes. These ranges are consistent with the models calibrated by Lord et al. (2005). The sensitivity of the factor value to the typical range of values for b_2 is shown in Figure 31.

The structure of Equations 7 and 8 suggests that the regression coefficients associated with the traffic-volume variable will be correlated. This condition requires the thoughtful assembly of calibration data to ensure that b_1 and b_2 are accurately quantified. Specifically, it requires multiple observations for each hourly volume level, where the capacity varies among sites at each volume level.

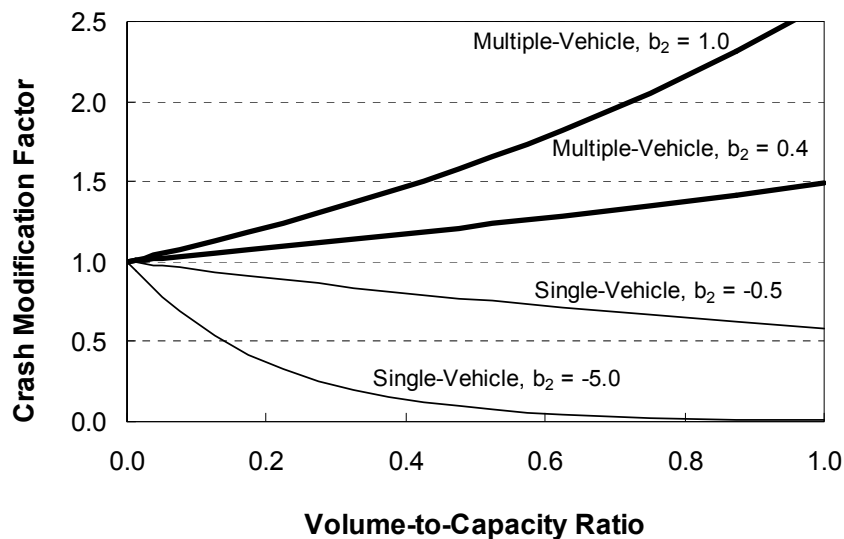


Figure 31. Relationship between CMF value and volume-to-capacity ratio.

HOV Facilities

This subsection describes the findings from a review of the safety literature related to high-occupancy vehicle (HOV) facilities on freeways. The focus of the discussion is on HOV facilities that are integral to the freeway cross section.

A review of national trends in HOV facility development was undertaken by Fuhs and Obenberger (2002). They found that over 130 HOV facilities were operating on freeways in 23 metropolitan areas as of 2001. About 85 percent of the facilities used a “2+” eligibility policy and 50 percent of the HOV facilities operated on a part-time or time-of-day basis.

Fuhs and Obenberger (2002) estimate that HOV facilities represent 1,200 route-miles of freeway (the cumulative lane mileage is twice this amount). Their examination of trends over a 30-year period prior to 2001 indicates that HOV route-miles are growing at a rate of 10 percent per year, with a forecast of 1,800 route-miles for 2009. This forecast mileage would constitute 3 percent of the freeway mileage identified in Table 1.

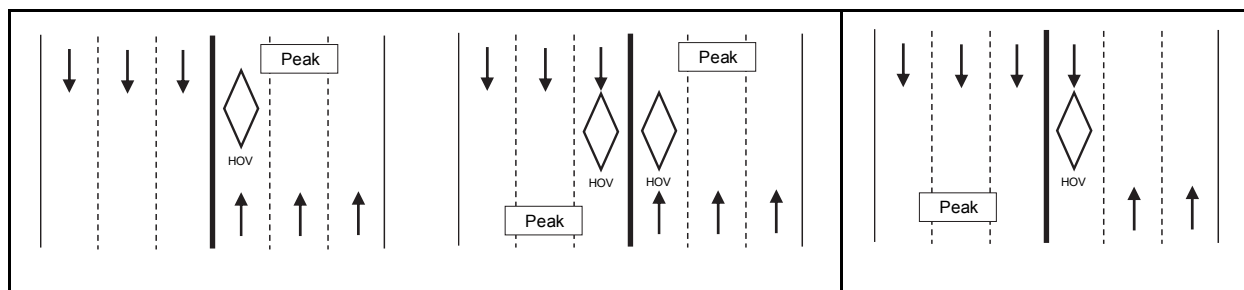
In 2007, the U.S. DOT’s Research and Innovative Technology Administration (Research, 2007) conducted a survey of 94 metropolitan areas. The survey results indicate that 14 metropolitan areas (15 percent) have HOV facilities. These facilities constitute 4 percent of the total freeway mileage that exists in the 94 metropolitan areas.

Basic Descriptors

This subsection describes various descriptors of HOV lane design and operation. Topics addressed include travel direction (relative to the adjacent general purpose lane), HOV access type, and lateral separation.

Travel Direction. HOV lanes can be described as having concurrent flow operation or contra-flow operation. The distinction between these two types is determined by the nature of the travel direction in the HOV lane relative to that in the adjacent general purpose lane. Figure 32 illustrates each type of travel direction. The concurrent flow operation has the vehicles in the adjacent lane and the HOV lane traveling in the same direction. The contra-flow operation has vehicles in the HOV lane and the adjacent lane (on the same side of the median) traveling in opposing directions. A review of HOV operation by Fuhs and Obenberger (2002) indicates that about 95 percent of all HOV facilities use concurrent flow operation.

Cothron et al. (2004) evaluated crash data for a 5.6-mile contra-flow HOV lane on I-30 in Dallas, Texas. A movable concrete barrier is provided on both sides of the HOV lane. Fatal and injury (FI) crash data were gathered for six years before the HOV lane was opened. It was also collected for nine years after the lane was opened. One year of before data and five years of after data were excluded from the analysis due to major reconstruction projects that occurred in the corridor during those years. The remaining data were analyzed for this report using a regression-based before-after analysis. A 14-percent reduction in FI crashes was found to occur after the HOV lane was opened. Details of the reconstruction projects were not provided, so it is difficult to determine whether these projects contributed to the noted safety improvement.



a. Concurrent flow operation.

b. Contra-flow operation.

Figure 32. High-occupancy vehicle travel direction types.

Cothron et al. (2004) also evaluated crash data for two freeway segments with concurrent flow HOV lanes in Dallas, Texas. Both segments were 6.5 miles in length, had a three-foot “painted” (i.e., marked) buffer, and one HOV lane in each travel direction. FI crash data were gathered for five years before the HOV lanes were opened and for four years after they were opened. A re-analysis of these data indicate that crashes increased by about 50 percent on each of the two freeway segments. The speed differential between the HOV lane and the adjacent general purpose lane was cited by Cothron et al. as a contributor to the observed degradation in safety. The reduced lane and shoulder width introduced in the freeway cross section to accommodate the HOV lane was also cited as a possible cause for the crash-rate increase.

HOV Access Type. Access to the HOV lane can be described as “continuous” or “limited.” Continuous access is provided when vehicles can enter or exit the HOV facility continuously along the freeway segment. Limited access is provided when vehicles can enter or exit the HOV facility only at designated entrance or exit points, as may be defined by pavement markings or physical barriers. A review of national trends in HOV facility design by Fuhs and Obenberger (2002) indicates that 28 percent of HOV facilities have continuous access and 72 percent have limited access.

Jang et al. (2009) examined the relative safety of the two HOV access types. They examined crash rates for four freeway segments with continuous access (40.7 mi) and four segments with limited access (50.9 mi). The segments represent six freeways in California. The limited access segments have a buffer width that ranges from 1 to 5 ft. The reported crash rates for FI crashes indicate that facilities with continuous HOV access have 16 percent fewer crashes than facilities with limited HOV access.

Lateral Separation. When an HOV lane has limited access, the separation between it and the adjacent general purpose lane can be described as “barrier” or “buffer.” Barrier separation denotes the use of some type of physical object between the two lanes to discourage or prevent vehicles from entering or exiting the HOV lane. The barrier is usually a concrete safety-shaped barrier. A review of national trends in HOV facility design by Fuhs and Obenberger (2002) indicates that 48 percent of HOV facilities have barrier separation. Some type of barrier separation is provided for another 24 percent and the remaining 28 percent have no buffer (i.e., continuous access).

The relative safety of the two HOV access types was examined by Newman et al. (1988). They compared crash rates for three access/separation combinations:

- 15 freeway segments with continuous access (i.e., no buffer),
- 13 segments with limited access and 2-ft buffer, and
- 6 segments with limited access and a 13-ft buffer.

The segments collectively represent eight freeways in California. All segments had concurrent operation. The first two combinations were noted to have no inside shoulder.

The analysis by Newman et al. (1988) revealed that there was no difference in crash rate between the first two types identified in the previous bullet list. In contrast, the analysis revealed that the segments with a 13-ft buffer had a lower crash rate than the other two types. A re-analysis of these crash rates for this report indicates that the 13-ft buffer reduced total crash rate by 30 percent. The contribution of the inside shoulder width to these findings was not evaluated by Newman et al.

Elements with Quantified Relationship

This subsection describes various associations between safety and HOV facility design or operation that have been quantified through an analysis of crash data. Topics addressed include speed differential, lane or shoulder width reduction to add an HOV lane, inside shoulder width, HOV access location, and HOV access length.

Speed Differential. Speed differential represents the difference between the speed in the HOV lane and that in the adjacent general-purpose lane. Where such differentials exist, the speed in the HOV lane is higher than that of the adjacent lane. Cothron et al. (2004) found that freeway crash rates increased following the opening of two limited access, buffer-separated HOV lane facilities. They rationalized that the increase may be due to the speed differential that was observed to range from 21 to 35 mi/h.

Newman et al. (1988) examined crash rates for several freeway segments with HOV facilities, as described previously. One element of the database was speed differential. A regression model was fit to these data for this report. The relationship between speed differential and FI crash rate was statistically significant. It is shown in Figure 33. The trend line suggests that a 25-mi/h speed differential is associated with a 130 percent increase in crash rate.

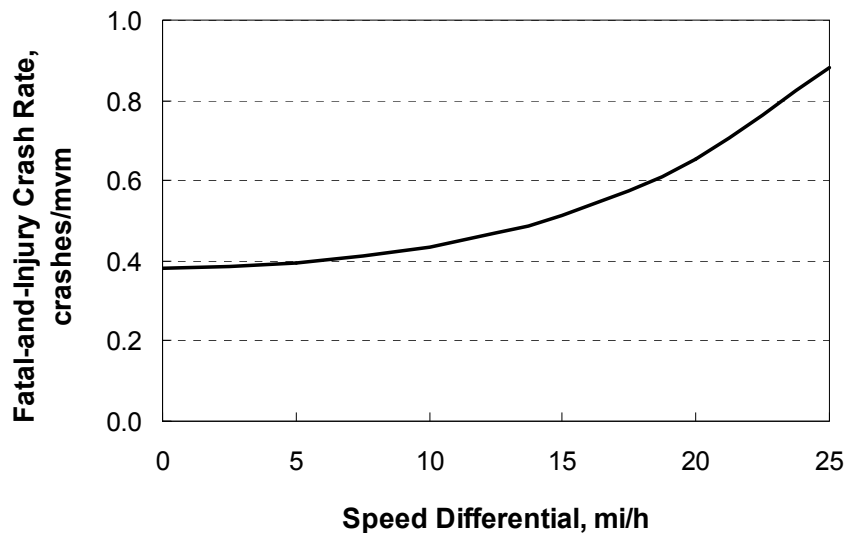


Figure 33. Relationship between FI crash rate and speed differential.

Reducing Lane and Shoulder Width to Add HOV Lanes. HOV lanes are sometimes added to the freeway cross section by reducing the width of the existing lanes or shoulders. This practice was used at two HOV facilities in Dallas, Texas and was cited by Cothron et al. (2004) as possibly contributing to the increase in crash rate following the opening of the facilities.

Bauer et al. (2004) examined crash data for 124 freeway segments in southern California that underwent a reduction in lane or shoulder width to add a lane (typically an HOV lane). The treated sites were located on four freeways and totaled 48.9 mi. They found that projects that added one lane to a four-lane (per direction) cross section experienced an 11 percent increase in FI crash frequency. Those projects that added one lane to a five-lane cross section experienced a 7 percent increase in FI crash frequency.

Inside Shoulder Width. Jang et al. (2009) examined the relationship between inside shoulder width and crash rate in the HOV lane. They found that, for a common access type, those HOV facilities with a shoulder width of 5 ft or less tended to have a total crash rate that was 100 percent larger than those with a shoulder width of 8 ft or more.

HOV Access Location. The location of an HOV lane entrance or exit, relative to the nearest interchange ramp has been speculated to have some influence on crash frequency. This issue of access location is applicable only to HOV lanes with limited access.

Jang et al. (2009) examined the relationship between HOV lane access location and freeway segment crash rate. They computed crash rates for 24 different freeway segments having either an HOV lane entrance or exit. When examined in the context of the distance to the nearest ramp, they found that HOV access points within 0.3 mi of the nearest ramp were often associated with a relatively large crash rate. These access points often had a high traffic volume in the HOV lane during the peak demand hours.

HOV Access Length. The length of an HOV lane entrance or exit has also been thought to have some influence on crash frequency. This issue of access length is applicable only to HOV lanes with limited access.

Jang et al. (2009) computed crash rates for 24 different freeway segments with either an HOV lane entrance or exit. One characteristic of those segments with a relatively large crash rate was the presence of an HOV access length that is characterized as “short” (i.e., less than 0.25 mi long).

Crossroad Ramp Terminal

This subsection describes the findings from a review of the safety literature related to the crossroad ramp terminal. The discussion in this section is focused on the terminals at service interchanges, as opposed to system interchanges.

With a couple of exceptions, the literature review did not identify research that is specific to the safety of crossroad ramp terminals. As a result, the discussion is broadened to include all types of intersections (not just those at interchanges). This discussion is intended to identify the various design and operational elements that have been found to have some safety influence on intersection safety—elements that are likely to have some influence on the safety of crossroad ramps terminals. This type of discussion helped to guide the development of a framework for safety evaluation (as documented in Chapter 3). However, an in-depth discussion of the reported influence of each element on safety is not provided given that its influence at a ramp terminal is unknown.

Basic Descriptors

This subsection describes various fundamental descriptors of crossroad ramp terminal design and operation. Topics addressed include area type, terminal configuration, and control mode.

Area Type. This descriptor indicates the population density in the vicinity of the crossroad ramp terminal. The categories used are urban and rural. A comparison of crash rates for urban and rural intersections in Texas indicates that rural intersections typically have more crashes for common volume levels (Bonneson and Pratt, 2008; Bonneson et al., 2007). In recognition of the different type of highway environment found in urban areas, relative to rural areas, Part C of the *HSM* (Highway, 2010) describes separate safety predictive methods for urban and rural intersections.

Terminal Configuration. The right-hand side of Figure 5 illustrates the configuration of six typical ramp terminals. Also shown are the left-turn and through movements at each terminal. The diamond interchange terminals typically have four legs and the parclo interchange terminals typically have three legs. The number and type of turn movements at each terminal tend to vary among the configurations. They translate into a different number of conflicting travel paths and conflicting volumes for each configuration. These characteristics suggest the possible need for different SPFs for each configuration; however, no research has been identified that confirms this speculation.

Bared et al. (2005) developed an SPF for 27 diamond interchanges in Washington. The ramp terminal spacing varied among these interchanges such that conventional, compressed, and tight urban diamonds were represented in the database. The database also was noted to include a mixture of urban and rural interchanges and a mixture of signalized and unsignalized interchanges. Bared et al. indicated that variables reflecting area type and control mode were included in the regression analysis but were found to not have statistical significance. The calibrated SPF for total crashes at diamond interchanges is shown in Figure 34.

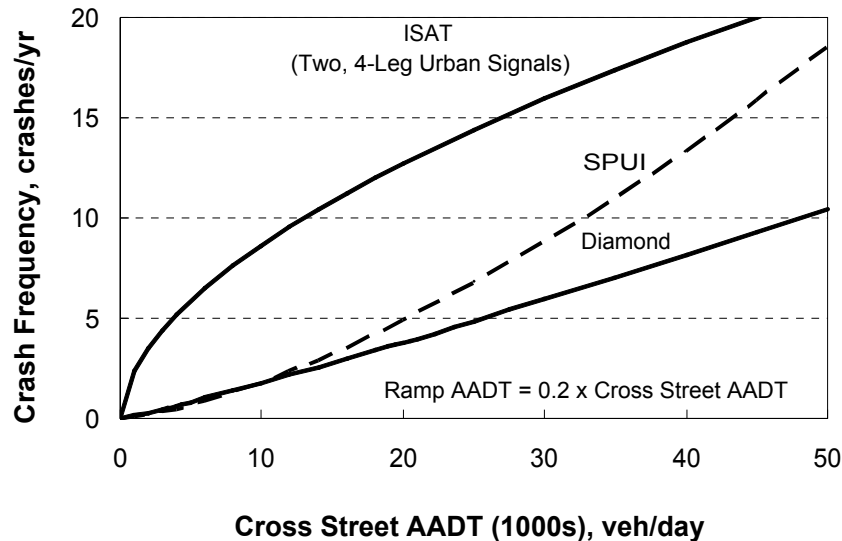


Figure 34. SPF for two interchange types based on total crashes.

Bared et al. (2005) also reported crash data for 13 SPUIs that collectively represent five states. An SPF was fit to the data for this report. The form of the SPF is similar to that used for the diamond interchanges; however, an indicator variable was used to identify the SPUIs from Maryland. The five SPUIs in Maryland had less than half of the crashes that were reported for the other SPUIs, after the effect of traffic volume and crash years were removed. The resulting SPF is shown in Figure 34 for the “non-Maryland” SPUIs. The trends indicate that the SPUI may experience more crashes than does the diamond interchange at higher volume levels.

Also shown in Figure 34 is the expected total crash frequency for an interchange with two, signalized four-leg ramp terminals in an urban setting. This estimate was obtained using the SPFs in ISAT. It was rationalized that this combination of conditions was most comparable to the other two interchange SPFs shown. Crashes that occur on the segment between ramp terminals were not included in the estimated expected crash frequency. It is noted that the SPFs provided in ISAT were calibrated using data for conventional intersections (as opposed to crossroad ramp terminals). The ISAT trend line shown in Figure 34 is notably different from the other two trend lines and is evidence of a likely difference in the safety of ramp terminals, relative to conventional intersections.

Number of Legs. The number of legs at an intersection has been found to have some correlation with crash frequency. More precisely, the influence of leg count is a reflection of the likelihood that each leg facilitates arrival movements, departure movements, or both at the intersection. The number of times each movement crosses the path of another intersection movement represents a conflict, as well as exposure to the possibility of a collision. The number of conflicts for all movement combinations increases exponentially with the number of intersection movements and, thus, with the number of legs that support these movements.

A comparison of FI crash rates for three-leg and four-leg intersections in Texas indicates that four-leg intersections typically have 50 to 100 percent more crashes than three-leg intersections for common volume levels (Bonneson and Pratt, 2008; Bonneson et al., 2007). In recognition of this influence, SPFs in Part C of the *HSM* (Highway, 2010) have been derived separately for three-leg and four-leg intersections.

Control Mode. The control mode used at an intersection is generally characterized as two-way stop, all-way stop, and signalized. The control mode can vary among movements on each approach. Of particular note is the use of free or yielding right-turn movements on an approach for which the left-turn and through movements are stop or signal controlled. Research has shown that control mode influences crash frequency, crash severity, and collision type.

A comparison of crash rates for two-way-stop-controlled and signalized intersections in Texas indicates that signalized intersections tend to have slightly fewer crashes than two-way-stop intersections in rural areas and for common volume levels (Bonneson et al., 2007). A similar comparison of crash rates for urban intersections indicates that the number of intersection legs has some interaction with control mode such that crash rates were found to be higher at signalized intersections with many lanes than two-way-stop intersections (Bonneson and Pratt, 2008). In contrast, crash rates were lower at signalized intersections with few lanes. In recognition of the influence of control mode, SPFs in Part C of the *HSM* (Highway, 2010) have been derived separately for signalized and two-way stop-controlled intersections.

Elements with Quantified Relationship

This subsection describes possible associations between safety and crossroad ramp terminal design or operation. Given the limited amount of information on crossroad ramp terminal safety, the discussion in this section is intended only to identify the design and operational elements that have been found to have an influence on the safety of a conventional intersection. Table 6 provides a summary of these elements and their relationships to safety. The table content is based on a review of the *HSM* (Highway, 2010) and the reported findings from a previous review by Bonneson et al. (2005).

TABLE 6. Elements that may influence the safety of crossroad ramp terminals

Category	Element	Safety Relationship
Geometric design	Left-turn lane or bay presence	Addition of bay correlated with a reduction in crash frequency.
	Right-turn lane or bay presence	Addition of a bay correlated with a reduction in crash frequency.
	Number of lanes on the major or minor road	Additional lanes at a signalized intersections are correlated with a larger crash frequency. The reverse trend applies to two-way stop-controlled intersections.
	Skew angle	Smaller skew angle is correlated with a smaller crash frequency.
	Median presence and width	Wider median at two-way stop-controlled intersections is correlated with a smaller crash frequency.
	Outside shoulder width	Narrow shoulders are correlated with a larger crash frequency.
	Lane width	Narrow lanes are correlated with a larger crash frequency at urban intersections.
	Right-turn channelization (free right)	Urban intersections with right-turn channelization are associated with a larger crash frequency.
Access	Driveway presence	Driveway presence is correlated with an increase in crash frequency.
Operation	Left-turn signal phasing	Intersections with protected or protected-permissive left-turn phasing are correlated with smaller crash frequency.
	Right turn on red	Urban intersection approaches for which right turn on red is prohibited have a smaller crash frequency.
Other	Truck percentage	Rural two-way stop-controlled intersections with a higher percentage of trucks are associated with fewer crashes. The reverse trend applies to signalized intersections.
	Lighting presence	Addition of lighting is correlated with a reduction in nighttime crash frequency.
	Red light camera operation	Use of red light enforcement cameras is associated with a decrease in right-angle crashes and an increase in rear-end crashes.

Related Topics

This subsection describes wrong-way traffic movements at crossroad ramp terminals and explores possible configurations and design elements that may influence the frequency of these maneuvers.

A problem inherent to service interchanges is the potential for wrong-way entry into an exit ramp (Policy, 2004). While the maneuver is not frequent, it has the potential to result in a severe crash. A study by Cirillo et al. (1969) indicates that about 5 percent of all fatalities on the Interstate Highway System in the 1960s were attributable to crashes resulting from wrong-way movements.

The problem of wrong-way driving on freeways was examined by several researchers in the 1970s and the findings were summarized by Leisch et al. (1982). The parclo A (2-quad) and parclo B (2-quad) interchange types (see Figure 3) were noted to be particularly susceptible to

wrong-way movements because the ramp approach and departure legs are located on the same side of the crossroad and are typically located very close to one another. A “half-diamond” (with one missing entrance ramp and one missing exit ramp) and other “incomplete” (or partial) interchanges were also noted to be associated with a large number of wrong-way maneuvers.

Leisch et al. (1982) noted that about 75 percent of all wrong-way movements occurred at night, during periods of low volume with little traffic on the crossroad to light the roadway and cue other drivers. Countermeasures that were identified include “Do Not Enter,” “Wrong Way,” “No Left Turn,” and “No Right Turn” signs posted at the crossroad ramp terminal. Also identified as a countermeasure was the use of large pavement arrows on the ramp approaches.

Design-related techniques identified in the *Green Book* (Policy, 2004) that have been used to minimize wrong-way maneuvers include channelization and curb return modifications. Figure 35 illustrates how median channelization on the crossroad can be extended slightly into the intersection to provide shadowing of the approach leg to discourage improper left turns into the exit ramp.

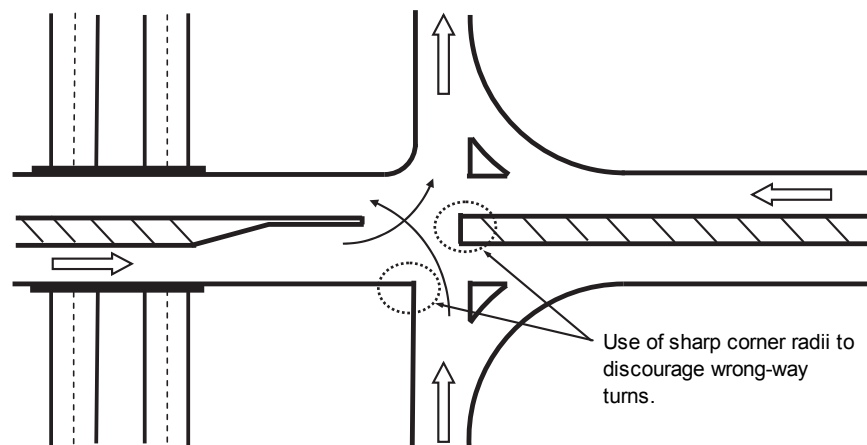


Figure 35. Designs to discourage wrong-way maneuvers.

Another technique to prevent wrong-way maneuvers is to use a short-radius curve, or angular break, at the intersection of the left-edge of the exit ramp approach with the right edge of the crossroad approach. This technique is also shown in Figure 35. It should discourage improper right-turns into the exit ramp.

A more recent examination of U.S. fatal crash data for the late 1990s by Moler (2002) indicates that about 0.8 percent of all fatalities (i.e., 350 persons/yr) are attributable to wrong-way maneuvers. This percentage represents a significant reduction in wrong-way fatalities since the 1960s and likely reflects agency use of the aforementioned countermeasures.

CHAPTER 3: FRAMEWORK FOR SAFETY PREDICTION

This chapter describes a framework for freeway and interchange safety prediction. The framework includes the safety performance functions (SPFs) and crash modification factors (CMFs). These SPFs and CMFs are needed to support safety-based decision making for the planning and designing of freeways and interchanges.

The chapter consists of two parts. The first part provides an overview of the safety prediction methodology in the *Highway Safety Manual (HSM)* (Highway, 2010). The second part describes the prioritized lists of recommended SPFs and CMFs.

OVERVIEW OF *HSM* METHODOLOGY

The methodology for evaluating freeway or interchange safety is envisioned to mirror the chapters described in Part C of the *HSM* (Highway, 2010). Each chapter is considered to describe a *methodology* for safety evaluation that is focused on describing a safety predictive method but also describes the scope, limitations, and applications of the method. A safety *predictive method* represents a process for evaluating the safety of a road facility for a specified time period. A *facility* is defined to consist of two or more contiguous sites and *site* is defined as either a homogeneous road segment or an intersection.

HSM Predictive Method

The *HSM* predictive method consists of 18 procedural steps. These steps are shown in Figure 36. The method is generic enough to be applied to the evaluation of rural highways and urban streets. With slight modification, it may also be tailored to the evaluation of freeway segments and interchanges. The key attributes of the *HSM* method are summarized in the following paragraphs.

Basic Safety Estimate. In one procedural step, a predictive model is used to estimate the expected crash frequency of a site. A *predictive model* combines the SPF with CMFs and a calibration factor. The expected crash frequency can be estimated as a total for all crash types and severities, or separately by crash type and severity, if desired.

Enhanced Safety Estimate. An optional procedural step can be used to incorporate reported crash data into the evaluation of an existing site. This procedure uses the empirical Bayes (EB) approach to combine the expected crash frequency from the predictive model with the reported crash data to obtain a more-reliable estimate of the site's expected crash frequency.

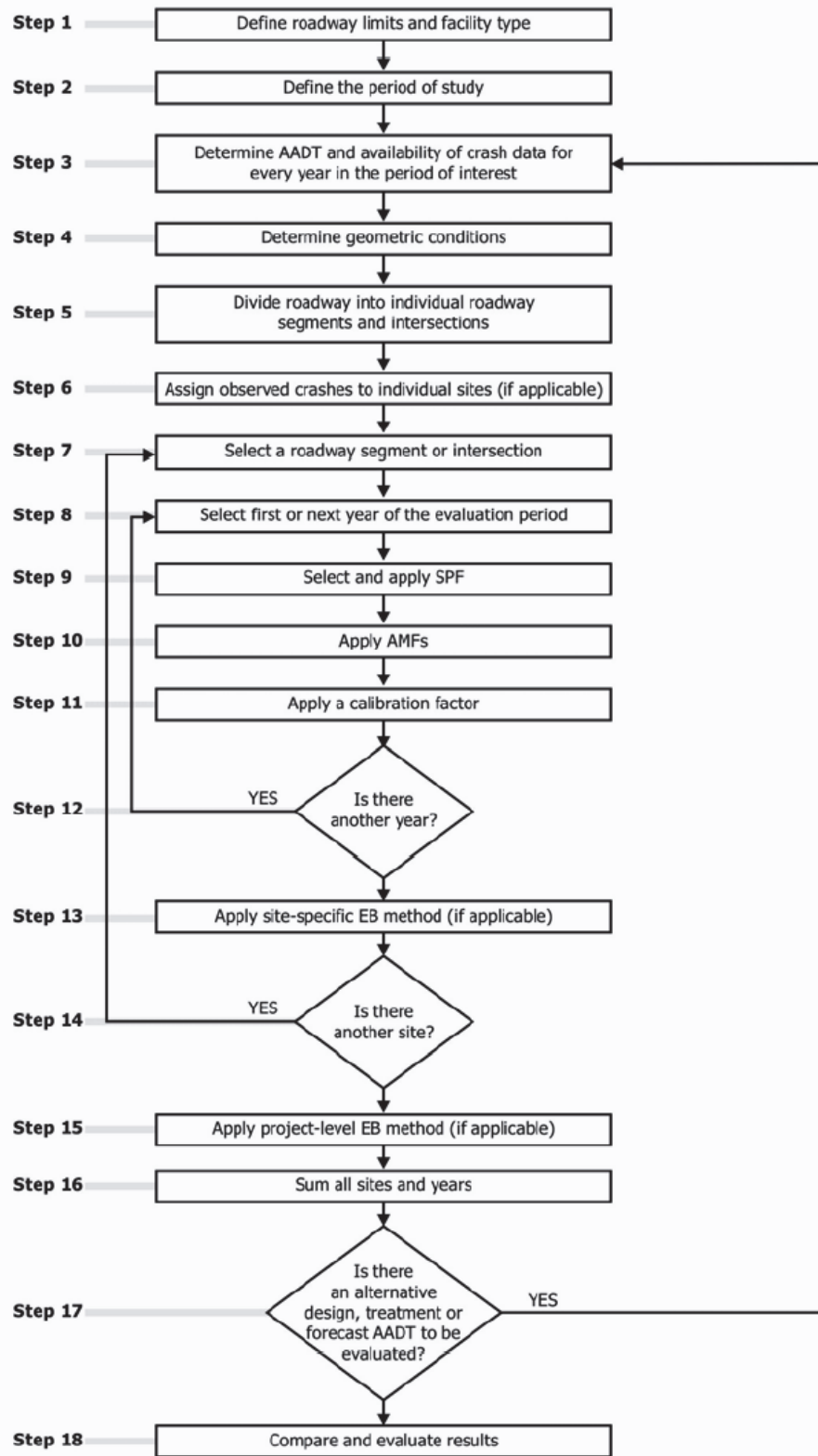


Figure 36. Highway Safety Manual predictive method.

Scalable Evaluation. The predictive method is scalable such that it can be used to evaluate an individual site or a facility. If the analyst desires to evaluate a facility, then the road is divided into individual sites and each site is separately evaluated using a single application of the method. The results for each site are then added to obtain an estimate of the expected crash frequency for the facility.

Multiple-Year Evaluation. If it is desired to evaluate a site (or facility) for multiple years (e.g., for a facility's design life), then the analysis period is divided into one-year increments and each year is separately evaluated using a single application of the method. The results for each year are then added to obtain an estimate of the expected crash frequency for the analysis period.

Freeway and Interchange Methodology

The methodology for freeway and interchange evaluation will consist of two separate predictive methods. One method will describe the evaluation of freeway sections and one method will describe the evaluation of interchanges. Collectively, the two methods can be used to evaluate a freeway facility. Each method will include predictive models that can be used to estimate the expected crash frequency for a segment or ramp terminal. An overview of each method is provided in the following subsections.

Freeway Predictive Method

The freeway predictive method will include predictive models for evaluating the following freeway components.

- freeway segment, and
- freeway speed-change lane.

These predictive models will be developed to support freeway safety evaluation, as may be influenced by road geometry, roadside features, traffic volume, and lane-change-related traffic maneuvers. The models will be calibrated using site-based observations that include the AADT volume and crash counts for one or more years. The segment-based observations will represent both travel directions combined.

Interchange Predictive Method

The interchange predictive method will include predictive models for the following interchange components on a site-by-site basis.

- interchange ramp, and
- crossroad ramp terminal.

These predictive models will be developed to support interchange safety evaluation, as may be influenced by ramp configuration, ramp terminal configuration, and ramp-crossroad interaction. Ramp configuration influences are likely to be sensitive to ramp cross section and alignment. Ramp terminal configuration influences are likely to be sensitive to intersection

control mode, number of legs, and turn movement accommodation. The influence of ramp-crossroad interaction is likely to be reflected in the travel path orientation through the interchange and the spacing between ramps (as measured along the crossroad).

All predictive models will be calibrated using AADT volume and crash counts for one or more years. The ramp model will be calibrated using ramp segments or entire ramps, the choice depending on their representation in the state DOT database. The ramp model will be described in the predictive method in a manner that will allow it to be used to evaluate specific ramp segments if desired.

It is envisioned that some CMFs in the *HSM* will be applicable to crossroad ramp terminals. Specifically, some CMFs applicable to conventional intersections should also be applicable to ramp terminals.

Role of SPFs and CMFs

The SPFs are intended to quantify the relationship between exposure and crash frequency, where exposure is represented by traffic count, segment length, and possibly other events that combine to form a chance set up for a crash (i.e., the necessary conditions). The crash frequency estimate from the SPF is intended to represent typical design and operating conditions.

The CMFs are intended to quantify the relative association between one or more design or operational elements and crash frequency. They are typically described as functions. However, the simplest CMFs can be represented using a constant. CMFs are used in a multiplicative manner with the SPFs to adjust the estimate from the SPF to account for elements whose dimensions, conditions, or presence at the subject site are not consistent with those sites represented by the SPF.

PRIORITIZED LIST OF SPFS AND CMFS

This part of the chapter summarizes the candidate SPFs and CMFs for the freeway and interchange methodology. It also describes of their estimated relative priority, as related to the objectives and scope of this research. The first section describes the procedure used to prioritize the SPFs and CMFs. The second section provides the prioritized list for each freeway facility component.

Prioritization Process

Several SPFs and CMFs are needed for the freeway and interchange methodology. These SPFs and CMFs were identified using the ranked list of safety information needs obtained from the practitioner interviews (as summarized in Appendix A). A separate set of SPFs and CMFs are planned for each of the following freeway and interchange components:

- freeway segment,
- interchange ramp,
- crossroad ramp terminal, and
- freeway speed-change lane.

The SPF and CMF identification process was intentionally broad to ensure that a wide range of safety influences were fairly considered.

The prioritization process was undertaken because of the large number of candidate SPFs and CMFs that were identified and the realization that sufficient project resources would not be available to adequately address each potential influence through statistical analysis.

The prioritization process focused on consideration of four criteria. One criterion used represents the “importance” of the SPF or CMF. This determination was based on input provided during a survey of practitioners. It reflects consideration of (1) the frequency that a topic is considered by practitioners in the design or operation of a facility, and (2) the perceived influence that a topic has on safety. A ranking of “high,” “medium,” or “low” was used to indicate the importance of each SPF or CMF.

A second criterion used is the level of effort required to obtain the raw data needed to define the key (or only) input variables for a given SPF or CMF. The effort was considered to have a low resource cost if the data were directly available from a state DOT database. The effort was considered to have a medium cost if the data had to be obtained by making a measurement from on an aerial photograph. It was considered to have a high cost if the data required multiple measurements from an aerial photograph, consultation of a video log, or submission of a special data request to a DOT.

A third criterion addresses the case where an SPF or CMF is associated with multiple input variables. The data collection effort was considered to be significant when multiple variables were needed for an SPF or CMF and each variable required multiple measurements. For example, the horizontal curvature CMF requires curve length and radius input variables, each of which are based on multiple measurements from an aerial photograph. Thus, this CMF will require more resources to calibrate.

A fourth criterion used is the relative need of the SPFs or CMFs for each of the freeway or interchange components. The goal of this criterion was to equalize the priorities among the components such that the relative need for each SPF or CMF was comparable among components. The relative need was determined to be higher for SPFs associated with the more commonly found facility types. In contrast, SPFs and CMFs for less common facility types (e.g., HOV facilities) were judged to have lower relative need. Of particular note in this regard was the finding that there are several variations of HOV facility that are each sufficiently unique as to require the development of a separate set of predictive models, yet no one HOV facility type exists with sufficient frequency as to be used on more than 2 percent of the freeway mileage in the U.S.

A priority index was computed for each SPF and CMF. It represents the weighed sum of the four criteria. This process yields larger index values for higher priority SPFs and CMFs. The weight for each criterion and the value for each criterion level are identified in the following list.

- Importance: weight = 3
 - high = 3, medium = 2, and low = 1.
- Level of effort: weight = 2

- high = 1, medium = 2, and low = 3.
- Number of attributes: weight = -1
 - value equal to the number of attributes associated with a variable.
- Relative need: weight = 1
 - value varies (see discussion below).

The value for the “relative need” criterion is 1 for many SPFs and CMFs; however, higher or lower values are used in some instances, based partly on guidance from the project panel. The specific values used as a basis for the prioritization are documented in the tables described in the next section.

Based on the aforementioned weights and values, the priority index was calculated for each SPF and CMF. For example, the index for a basic freeway segment is based on its high importance (= 3), a low level of effort (= 3), a relative-need value of 1, and a number-of-attributes value of 0.8 (this value is less than 1.0 because this SPF’s variables are shared with other SPFs). The index is computed as $15.2 (= 3 \times 3 + 3 \times 2 + 0.8 \times [-1] + 1 \times 1)$.

As a last step, the collective set of indices was used to determine the priority group for each SPF or CMF. Those SPFs and CMFs with an index value that ranks in the top one-third of all values are assigned “high” priority. Those in the bottom one-third are assigned a “low” priority. Those in the middle one-third are assigned a “medium” priority.

Prioritized Lists

This section provides the prioritized list of SPFs and CMFs for each freeway or interchange component. Separate subsections are provided for each component.

Freeway Segment

This subsection describes the prioritized list of SPFs and CMFs for the evaluation of basic freeway segment safety. The freeway segment predictive model is envisioned to be capable of evaluating the following scenarios:

- interchange or ramp spacing,
- changes in lane continuity (e.g., outside lane drop and inside lane add), and
- changes in cross section to add capacity.

Table 7 identifies the prioritized list of SPFs and CMFs for freeway segments. The table has two sections. The first section identifies the different types of freeway segment analysis units that were identified. Each unique combination of segment type and basic descriptor is considered to represent a separate SPF.

TABLE 7. Prioritized list of SPFs and CMFs for freeway segments

Category	Topic ¹	Importance	Level of Effort	Number Attrib.	Relative Need	Priority
Different Analysis Units						
Segment types	Basic segment	High	Low	0.8	1	High
	Basic segment with HOV lane present	Medium	Medium	2.8	0	Medium
	Basic segment with ramp meter operation	Low	Medium	1.8	1	Low
	Basic segment with truck lane restriction	Low	High	1.8	4	Medium
	Basic segment with shoulder use by time of day	Low	High	1.8	1	Low
Basic descriptors	Area type (urban, rural)	High	Low	1	1	High
	Number of lanes	High	Low	1	1	High
Design or Operation Elements						
Operation elements	Effect of lane-changing downstream of entrance ramp (after speed-change lane)	High	High	3.3	3	High
	Effect of lane-changing upstream of exit ramp (before speed-change lane)	High	High	3.3	3	High
	Effect of recurring congestion (percent hours per day that are congested)	High	High	1	1	High
Roadway elements	Combined effect of lane and shoulder width	Medium	Medium	3	1	Medium
	Effect of lane drop (with and without horizontal curvature)	Medium	Medium	1.5	1	Medium
	Effect of lane add	Low	Medium	1	1	Low
Roadside elements and barrier	Combined effect of median width and barrier (incl. barrier length and offset)	High	High	4	4	High
	Combined effect of clear zone width and barrier (incl. barrier length and offset)	High	High	4	4	High
	Effect of side slope (traversable or not)	Medium	High	1	4	High
	Effect of crash cushion presence at roadside features	Medium	High	2	1	Low
	Effect of median crossover	Low	Medium	1	1	Low
Alignment elements	Effect of horizontal curvature (including tangent length before curve)	High	High	3.5	1	Medium
	Effect of superelevation rate of horizontal curve	Low	High	1	1	Low
	Effect of grade (including length of grade)	Low	High	2	1	Low
Other elements	Effect of continuous shoulder rumble strips	Low	High	1	1	Low
	Effect of highway illumination between interchanges	Medium	High	1	1	Medium

Note:

1 - High and medium priority topics are identified by bold font.

The second section of Table 7 lists the various design or operation elements that were identified during the literature search or interview process. Each element listed is considered to represent a CMF.

The “clear zone width” listed in Table 7 is specific to vertical objects in the clear zone, and does not include non-traversable slopes. This limitation reflects the type of information that can be discerned from aerial photographs (which was the primary source of supplemental data for this project, as described in Chapter 4). The clear zone width is measured from the edge of traveled way to the nearest continuous line of vertical objects that are roughly parallel to the road centerline. This line is typically indicated as a tree line, fence line, or utility poles.

The third through sixth columns of Table 7 indicate the importance, level of effort, number of attributes, and relative need, respectively, for each analysis unit or element. These descriptors were described in the previous section and used to estimate the priority for each unit and element. The number of attributes associated with a given topic is sometimes represented as a decimal value. In these instances, one or more of the attributes needed to calibrate the associated topic is shared with other topics such that the “cost” of acquiring the attribute is spread among topics. It is important to note that the use of the “relative need” criterion is intended to yield priorities that can be compared among the subsequent tables of freeway and interchange components.

The proposed priority associated with each SPF or CMF topic is shown in the last column of Table 7. This priority is an indication of which topics should be considered first during the development of safety predictive models. Every effort will be made to ensure that the SPF or CMF associated with a high-priority topic is calibrated. Remaining resources will be used to calibrate medium priority topics. The low priority topics will be considered after the higher priority topics have been addressed.

HOV facilities have a unique influence on freeway operation—to the extent that the presence of an HOV lane on a freeway segment requires treatment of the segment as a separate facility type. The literature review indicated that HOV facilities constitute only about 3 percent of the freeway mileage in the U.S. For this reason, safety predictive models for HOV facilities are not believed to be highly important in achieving the project objectives. Moreover, there are many different types of HOV facilities, as distinguished by flow direction (contra flow, or concurrent flow) and lane separation (i.e., barrier, buffer, and continuous access). For this reason, a comprehensive set of safety predictive models for HOV facility analysis would likely require a large amount of effort to develop.

Interchange Ramp

This subsection describes the prioritized list of SPFs and CMFs for the evaluation of interchange ramp safety. The ramp predictive model is envisioned to be capable of evaluating both individual ramp segments and entire ramp configurations.

Table 8 identifies the prioritized list of SPFs and CMFs for interchange ramps. The proposed priority associated with each SPF or CMF topic is shown in the last column. This priority is an indication of which topics deserve first consideration during the development of safety predictive models.

TABLE 8. Prioritized list of SPFs and CMFs for interchange ramp

Category	Topic ¹	Importance	Level of Effort	Number Attrib.	Relative Need	Priority
Different Analysis Units						
Segment types	Basic segment	High	Low	2.3	1	High
	Basic segment with ramp meter operation	Low	Medium	1.8	1	Low
	Basic seg. with ramp meter and HOV bypass lane	Low	Medium	2.8	0	Low
Basic descriptors	Area type (urban, rural)	High	Low	1	1	High
	Ramp type (exit, entrance)	Low	Low	1	2	High
	Number of lanes	Medium	Low	1	1	High
Design or Operation Elements						
Operation elements	Effect of combined merge, diverge, and lane-changing in coll.-distributor weaving section	Low	High	7	8	Medium
Roadway elements	Effect of lane width	Low	Medium	1	1	Low
	Effect of inside and outside shoulder width	Medium	Medium	2	1	Medium
Roadside elements and barrier	Effect of roadside barrier (barrier length and offset)	High	High	4	1	Medium
	Effect of side slope (traversable or not)	Medium	High	1	1	Medium
	Effect of crash cushion presence at roadside features	High	High	2	1	Medium
Alignment elements	Effect of horiz. curvature (including distance to freeway ramp terminal and crossroad ramp terminal as surrogates for curve operating speed)	High	High	5	1	Medium
	Effect of superelevation rate of horizontal curve	Medium	High	1	1	Low
	Effect of compound curve or spiral transition	Medium	High	1	1	Medium
Other elements	Effect of ramp illumination	Low	Medium	1	1	Low
	Effect of ramp-to-ramp merge point presence	Medium	Medium	1	1	Medium
	Effect of ramp-to-ramp diverge point presence	Medium	Medium	1	1	Medium

Note:

1 - High and medium priority topics are identified by bold font.

A segment-based predictive model for ramps should be developed, as opposed to an entire-ramp-based model that is characterized by its configuration (e.g., diamond, free-flow parclo, etc.). As documented in Chapter 2, previous attempts at developing the latter type of SPF have not demonstrated a consistent trend among configurations. It is likely that differences in cross section and alignment at the segment level are causing this inconsistency.

Crossroad Ramp Terminal

This subsection describes the prioritized list of SPFs and CMFs for the evaluation of crossroad ramp terminal safety. The ramp terminal predictive model is envisioned to be capable of evaluating alternative interchange type comparisons and ramp terminal spacing.

Table 9 identifies the prioritized list of SPFs and CMFs for crossroad ramp terminals. The proposed priority associated with each SPF or CMF topic is shown in the last column. This priority is an indication of which topics deserve first consideration during the development of safety predictive models.

TABLE 9. Prioritized list of SPFs and CMFs for crossroad ramp terminals

Category	Topic ¹	Importance	Level of Effort	Number Attrib.	Relative Need	Priority
Different Analysis Units						
Terminal types	Basic ramp terminal	High	Low	2	1	High
	Ramp terminal with frontage road movements	Low	Medium	2	0	Low
	Roundabout ramp terminal	Low	High	1	0	Low
Basic descriptors	Area type (urban, rural)	High	Low	1	1	High
	Terminal configuration (number of legs and movements)	High	Medium	1	1	High
	Control mode (signalized, two-way stop)	High	Medium	1	1	High
Design or Operation Elements						
Roadway elements	Effect of left-turn bay provision on crossroad	High	Medium	1	1	High
	Effect of right-turn bay provision on crossroad	Low	Medium	1	1	Low
	Effect of channelized (free) right-turn lane on crossroad	Medium	Medium	1	1	Medium
	Effect of channelized (free) right-turn lane on ramp	Medium	Medium	1	1	Medium
	Effect of lane width	Low	Medium	1	1	Low
	Effect of outside shoulder width	Low	Medium	1	1	Low
	Effect of median presence and width	Medium	Medium	3	1	Low
	Effect of number of lanes on crossroad	High	Low	1	1	High
	Effect of number of lanes on ramp approach	High	Low	2	1	High
Alignment elements	Effect of intersection skew angle	Medium	Medium	1	1	Medium
	Effect of approach grade	Low	High	2	1	Low
Other elements	Effect of distance between ramps	Medium	Medium	1	1	Medium
	Effect of sight distance restrictions (due to crossroad crest curve)	Medium	High	1	1	Medium
	Effect of driveway presence on the approach	Low	Medium	1	1	Low
	Effect of illumination at terminal	Low	Medium	1	1	Low
	Effect of innovative signing and marking to prevent wrong-way ramp entry	Low	High	1	1	Low
	Effect of protected left-turn phasing (if signal)	Medium	High	1	4	High
	Effect of right-turn on red (if signal)	Low	High	1	1	Low

Note:

1 - High and medium priority topics are identified by bold font.

The findings from the review of the literature and several state DOT databases indicated that only about 1 percent of all interchanges have the SPUI form. Thus, the challenge to developing an SPF for the single-point urban interchange (SPUI) is to find a sufficient number of these interchanges to quantify statistically valid relationships.

Freeway Speed-Change Lanes

This subsection describes the prioritized list of SPFs and CMFs for the evaluation of freeway speed-change lane safety. The speed-change lane predictive model is envisioned to be capable of evaluating ramp entrance length, ramp exit length, ramp entrance/exit side (i.e., left or right-hand side of freeway), and weaving section length and type.

Table 10 identifies the prioritized list of SPFs and CMFs for freeway speed-change lanes. The proposed priority associated with each SPF or CMF topic is shown in the last column. This priority is an indication of which topics deserve first consideration during the development of safety predictive models.

TABLE 10. Prioritized list of SPFs and CMFs for freeway speed-change lanes

Category	Topic ¹	Importance	Level of Effort	Number Attrib.	Relative Need	Priority
Different Analysis Units						
Terminal types	Basic speed-change lane	High	Low	2	1	High
Basic descriptors	Area type (urban, rural)	High	Low	1	1	High
	Ramp type (exit, entrance)	High	Low	1	1	High
	Lane design (parallel, tapered)	Medium	Medium	1	1	High
Design or Operation Elements						
Operation elements	Effect of combined merge, diverge, and lane-changing in weaving section	High	High	4.3	4	High
Roadway elements	Effect of number of lanes on ramp	Medium	Medium	1	1	Medium
Alignment elements	Effect of ramp entrance (or exit) length	High	Medium	1	1	High
	Effect of horizontal curvature on ramp entrance (or exit)	Low	High	1	1	Low
Other elements	Effect of illumination at terminal	Low	Medium	1	1	Low
	Effect of entrance/exit side (left or right side)	Medium	Medium	2	1	Medium
	Effect of lane drop at exit ramp	High	Medium	1	1	High

Note:

1 - High and medium priority topics are identified by bold font.

Desirably, separate predictive models would be developed for the speed-change lane and for the basic freeway segment. This approach is used successfully in the *HSM* to describe predictive methods for intersections and segments. However, unlike intersection-related crashes,

speed-change-related crashes are difficult to accurately identify using the attributes provided in highway crash databases. For this reason, the SPFs and CMFs described in this subsection are envisioned to be based on the combined speed-change lane and freeway segment adjacent to the speed-change lane. In this manner, the SPFs and CMFs for speed-change lanes may be functionally similar to those for freeway segments.

CHAPTER 4: DATABASE DEVELOPMENT

This chapter describes a summary of the data assembled for safety prediction model development and calibration. The database is founded on the road inventory data obtained from the Highway Safety Information System (HSIS). These data were enhanced through the inclusion of road inventory data extracted from aerial photographs. The enhanced database was then combined with crash data (also obtained from HSIS) to form the highway safety database needed for model development and calibration.

This chapter consists of two parts. The first part summarizes the procedures used to assemble the database. The second part summarizes the database contents using categorical descriptions and various statistics. It also provides a discussion about some trends observed in the data.

DATA COLLECTION PROCEDURES

The data collection process consisted of a series of activities that culminated in the assembly of a highway safety database suitable for the development of a comprehensive safety prediction methodology for freeways and interchanges. It consisted of the following activities:

- Develop data reduction procedures guide.
- Develop enhanced data collection process and software.
- Assemble road inventory database from HSIS data.
- Enhance safety database.
- Merge road inventory and crash data.

Each of these activities is described briefly in the following sections.

Develop Data Reduction Procedures Guide

It was determined that a robust safety prediction methodology would require the use of a cross-sectional study approach and that the data would need to be attribute-rich and of high quality. To facilitate the development of this database, supplemental road inventory data were added to the HSIS databases. A series of data reduction procedures guides were developed to ensure consistency in the collection of supplemental road inventory data. One guide was developed for freeway segments and speed-change lanes. A second guide was developed for interchange ramp segments. A third guide was developed for crossroad ramp terminals.

Each guide described the variables obtained from supplemental data sources (i.e., aerial photographs and interchange diagrams). These data were collected as part of the database enhancement activity, described in the next section. Each guide included a definition for each variable as well as the technique for measuring it. The technicians that comprise the data-collection team were trained from this document to ensure consistency in the data collection process.

Develop Enhanced Data Collection Process and Software

Data enhancement consisted of using supplemental data sources to acquire additional data for each freeway segment, ramp segment, and crossroad ramp terminal in the state database. A key element of this process is the use of aerial photography to extract additional road inventory data for each segment or terminal. These photographs are available from several Internet sources. The data being collected include the width of key cross section elements, barrier location, horizontal curvature, ramp configuration, turn bay presence, median type, etc.

Data extraction proceeded on a segment-by-segment basis. The database is represented in a spreadsheet. One row of the spreadsheet represents one segment or crossroad ramp terminal. Each variable is assigned to a column. The supplemental data for each segment or intersection are extracted from an aerial photograph or a road-level photograph. The aerial photographs were obtained from Google Earth and the road-level photographs were obtained from its companion tool, Street View. Google Earth is software available from Google ©.

Two procedures were developed for the collection of supplemental data. One procedure was used for data that required the technician to make a determination of presence or condition (e.g., presence of rumble strips, intersection control type, presence of an HOV lane, presence of a channelizing right-turn lane). This data is typically categorical. This procedure is referred to as the “manual” procedure.

The other procedure is based on the digitization of key roadway design elements using aerial photographs and software tools. Using this process, the road alignments, cross sections, barrier pieces, and speed-change lanes were manually “digitized” such that relevant points are located using geodetic coordinates. The digitized points were saved to an electronic file and then processed by software to produce the desired widths, lengths, and radii. The data is typically continuous. This procedure is referred to as the “semi-automatic” procedure. It is described more fully in Appendix B.

Assemble Road Inventory Database from HSIS Data

The database assembly activities consist of three tasks. The first task involved processing the HSIS data to construct a road inventory database with a wide range of variables. The second task involved subsetting the processed data such that the resulting database included a wide range of segment representation (e.g., number of lanes, urban/rural). The need to subset the data was motivated by the recognition that project resources would limit the subsequent collection of supplemental data to only a subset of the full database. The third task involved digitizing the road alignments for the purpose of defining the geodetic coordinates of each segment’s begin milepost.

Database Construction

There were several steps associated with the database construction task. It produced nine separate databases. Each database represents one combination of state (California, Maine, Washington) and roadway component (freeway segment, interchange ramp proper, crossroad

ramp terminal). Speed-change lane data were included in the freeway segment database. This task included the following steps:

- Merge the roadlog, curve, grade, special-use-lane, and other road- or traffic-volume-related files to form a unified file that fully describes each road segment.
- Rename variables for consistency across state databases.
- Convert data for common variables to a common format for consistency across databases.
- Verify that there were no changes in geometry during the analysis years.
- Convert, combine, or manipulate database variables to compute the variables identified in Chapter 3 as being associated with a desired SPF or CMF.
- Identify freeway segments, ramp segments, and ramp terminals for which all data are complete.
- Identify freeway segments and ramp segments that have special-use lanes.
- Identify freeway segments adjacent to ramps and link relevant ramp attributes.
- Identify crossroad ramp terminals by manually linking the intersecting ramps and crossroad segment.
- Confirm that all selected segments satisfy the criteria for minimum length, minimum exposure, and maximum length (described in the following paragraphs).

Analysis Period. A three-year analysis period was established for the freeway segment and the crossroad ramp terminal databases. A five-year period was established for the interchange ramp segments. In general, a three-year duration is preferred because it minimizes the potential for changes in geometry, traffic, or environment over the analysis period. However, the frequent occurrence of segments with zero crashes can degrade the accuracy of the statistical analysis. For this reason, a longer, five-year period was used for ramps because of their low volume and shorter length.

Site Selection Criteria. The freeway and ramp segments were selected in part based on a minimum-length and a maximum-length criterion. Specifically, each segment had to have a length that equaled or exceeded the precision of their crash location variables. Based on this consideration, the minimum segment length for California and Washington data was 0.01 miles. For the Maine data, the minimum length was 0.10 miles.

It was rationalized that the geometric homogeneity of a segment would become more suspect with increasing segment length. For this reason, a maximum length criterion was somewhat subjectively established at 1.6 miles. This length was established based on experience gained by evaluating the homogeneity of many segments using aerial photographs.

The presence of managed lanes was used as a site selection criterion. Freeway segments with managed lanes were not included in the database. This action was taken to provide a focus on basic freeway segments with general-purpose lanes. The entrances, exits, and separation elements associated with managed lane facilities was reasoned to provide a complicated safety influence that would justify the separate development of a managed-lane safety prediction method.

A minimum exposure criterion was also established for freeway segments. Segments with low exposure (i.e., short length or low traffic volume) have a large residual value when they are

associated with one or more crashes. This residual often exerts undue leverage on the regression model coefficients and increases the error variance beyond that explained by the negative binomial distribution. To avoid these issues, all candidate segments were screened such that only those segments with a minimum level of exposure were included in the regression database. Equation 9 was used to compute the minimum segment exposure.

$$E_{\min} = \frac{PR^2 + 2 - \sqrt{(PR^2 + 2)^2 - 4}}{2 \text{ Base } y} \quad (9)$$

where,

E_{\min} = minimum segment exposure, million-vehicle-miles (mvm/yr);

PR = prediction ratio (= 3.0);

y = analysis period duration, yr; and

Base = fatal-and-injury crash rate, crashes/mvm.

The prediction ratio PR is the standardized residual for an observation. It is set to 3.0 in Equation 9. This value corresponds to a 99.7th percentile confidence interval. Segments with low exposure and one or more crashes will have a prediction ratio in excess of 3.0—a condition that should occur less than 0.3 percent of the segments that satisfy this criterion. The crash rate used in this equation represents fatal-and-injury (FI) crashes for typical freeway segments, as determined during the literature review documented in Chapter 2. These rates and the corresponding minimum exposure values are listed in Table 11.

TABLE 11. Base FI crash rates for minimum exposure criteria

Area Type	Number of Lanes	Analysis Period Duration, yr	FI Crash Rate, cr/mvm ¹	Minimum Exposure, mvm/yr
Urban	4	3	0.24	0.13
	6	3	0.36	0.08
	8	3	0.54	0.06
	10	3	0.56	0.05
Rural	4	3	0.14	0.22
	6	3	0.21	0.15
	8	3	0.27	0.11

Note:

1 - mvm: million vehicle-miles.

Manual Assembly Elements. The HSIS data for Maine describes the roadway using a link-node system. Each link for a divided roadway represents one travel direction. In contrast, the HSIS data for California and Washington describe the roadway using two-directional road segments uniquely identified by the state-established milepost referencing system. To facilitate the calibration of models using a common segment definition, the data for Maine had to be manually processed on a link-by-link basis. The manual process was used to convert each link into a set of two-directional road segments with an artificially established milepost referencing system. Once this segment-based file was assembled, the construction of the road inventory database for Maine proceeded in accordance with the steps outlined in the previous bullet list.

A manual assembly process was necessary to assemble the crossroad ramp terminal database for each state. The “intersection” files provided in HSIS for these states was inadequate for this purpose because it was tailored to typical intersections of two state routes. With the manual process, candidate ramp terminals were initially identified in the HSIS ramp data. Interchange maps provided by Maine and by Washington were used to locate the individual ramps that comprise a crossroad ramp terminal. Descriptive variables in the ramp data were used with Google Earth to locate ramp terminals with the California data. Then, once the ramps were located, the HSIS data were interrogated to identify the crossroad segment at the point of intersection with the ramps. As a final step, the road inventory data for the intersecting ramps and crossroad segment were extracted from the HSIS database and combined into a common intersection database. At this point, the construction of the road inventory database proceeded in accordance with the steps outlined in the previous bullet list.

Level of Effort Indicators. The construction process outlined in the previous bullet list was facilitated using Statistical Analysis Software (SAS) data manipulation and merge procedures. A separate SAS processing code was developed for each of nine databases (i.e., three states and three components for each state). The code reflects the unique nature of each state’s data and its treatment of each roadway component. The lines of code developed for this activity are identified in Table 12. They provide an indication of the magnitude of the development effort.

TABLE 12. SAS Processing Effort

Roadway Component	Task	Lines of SAS Code by State		
		California	Maine	Washington
Freeway segment and freeway speed-change lane	Identify segments for manual file assembly	0	510	0
	Construct road inventory database	1,560	1,590	1,890
	Merge crash data and categorize	540	910	760
	Total:	2,100	3,010	2,650
Ramp proper (including collector-distributor ramps)	Identify segments for manual file assembly	0	0	0
	Construct road inventory database	750	470	630
	Merge crash data and categorize	560	550	580
	Total:	1,310	1,020	1,210
Crossroad ramp terminal	Identify intersections for manual file assembly	510	500	970
	Construct road inventory database	1,200	1,320	940
	Merge crash data and categorize	570	620	530
	Total:	2,280	2,440	2,440

Table 12 also lists the lines of SAS code needed for the “merge crash data and categorize” task. This code and related effort is separate from the assembly and construction process described in this section. The crash data merging activity is described in a subsequent section.

Database Attributes. Table 13 indicates the number of database variables in each of the nine databases that were assembled. The first row for each roadway component identifies the number of variables obtained from the HSIS database that are considered to be useful to the development of safety prediction models. Examination of Table 13 indicates that relatively few of the HSIS variables for crossroad ramp terminals and for Maine freeways were found to be directly useful for model development.

TABLE 13. Database attributes

Roadway Component	Attribute	Attribute Value by State		
		California	Maine	Washington
Freeway segment and freeway speed-change lane	Variables from state database	48	4	76
	Variables created from state database	31	56	48
	Variables added to database	95	109	95
	Total:	174	169	219
Ramp proper (including collector-distributor ramps)	Variables from state database	26	33	48
	Variables created from state database	5	8	5
	Variables added to database	53	52	49
	Total:	84	93	102
Crossroad ramp terminal	Variables from state database	4	2	1
	Variables created from state database	47	84	39
	Variables added to database	32	75	46
	Total:	83	161	86

The second row for each roadway component in Table 13 identifies the number of HSIS variables that were combined using SAS code to create new variables. For example, the horizontal curve database available from HSIS for Washington was used to link curves to segments and to determine the proportion of the curve on each segment. Also, the ramp databases from HSIS for both California and Washington were used to link ramps to freeway segments, such that a variable was added to the freeway segment database that relates the distance between the ramp and segment.

The third row for each roadway component identifies the number of variables that were obtained from supplemental sources as part of the data enhancement activity. The details of this activity are described in the next section. The numbers provided in Table 13 indicate that the variables from supplemental sources tended to account for about one-half of the variables in each database.

Sampling Technique

There are several thousand freeway segments in the HSIS databases for California and Washington. There are also many ramp segments represented in these two databases. However, project resources limited the collection of supplemental data to only a subset of the full database.

Thus, a sampling technique was developed to select a cross section of freeway (and ramp) segments, such that a uniform distribution of values for several key variables was obtained.

Separate sampling techniques were developed for freeway segments and ramp segments. For freeway segments, the key variables included area type (i.e., urban or rural), number of lanes, right shoulder width, and median type. For ramps, the key variables included area type, ramp type (i.e., entrance, exit), and ramp configuration.

A sampling technique was not required for several of the databases. Specifically, the number of freeway and ramp segments in the HSIS database for Maine was sufficiently limited that all segments that satisfied the site selection criteria were included in the assembled databases.

No sampling was used for the selection of target crossroad ramp terminals. The need for full representation in the HSIS database tended to limit the number of available ramp terminals such that the entire database for each state had to be examined to maximize the potential for exceeding the minimum sample size. The most limiting requirements for ramp terminal selection were: (1) the adjacent crossroad segment had to be on the state highway system, (2) traffic volume was available for the intersecting ramp terminals, and (3) the ramp terminal was more than 500 ft from the nearest, non-ramp signalized intersection. The first criterion ensured that a complete crash history was available for the terminal. The third criterion reasonably ensured that ramp-terminal-related crashes could be isolated and assigned to the ramp terminal of interest. All of the ramp terminals that satisfied these criteria were considered “target” intersections.

Table 14 indicates the number of target segments and crossroad ramp terminals that were assembled. The sample size for Maine represents all available segments in the HSIS database. Similarly, the sample size for crossroad ramp terminals represents all available terminals in the HSIS database.

TABLE 14. Database target sample size

Category	Roadway Component	Sample Size by State ¹			
		Calif.	Maine	Wash.	Total
Number of segments or ramp terminals	Freeway segment and freeway speed-change lane	<u>613</u>	213	<u>1,428</u>	2,254
	Ramp proper (including collector-distributor ramps)	<u>412</u>	209	<u>1,292</u>	1,913
	Crossroad ramp terminal	223	62	412	697
	Total:	1,248	484	3,132	4,864
Total segment length, miles	Freeway segment and freeway speed-change lane	254	107	241	602
	Ramp proper (including collector-distributor ramps)	66	49	143	258
	Total:	320	156	384	860
Average segment length, miles	Freeway segment and freeway speed-change lane	0.41	0.50	0.17	0.27
	Ramp proper (including collector-distributor ramps)	0.16	0.23	0.11	0.13

Note:

1 - Underlined values represent a subset sample of the HSIS data. All other “sample size” values represent all of the segments or intersections found in the HSIS data that satisfy the site selection criteria.

Geo-Location of Segments

The third task of the database assembly activity was the geo-location of each segment and ramp terminal in the database. The location process was based on the use of Google Earth and Earth Tools software. Earth Tools software is described in Appendix B.

Google Earth was used to digitize the road alignment for a group of adjacent segments. The digitized alignment was then submitted to Earth Tools software along with the segment milepost data. The software used this information computed the geodetic coordinates of each segment begin milepost. The suitability of each segment for subsequent supplemental data collection was also evaluated at this time. Specifically, a segment was considered to be “suitable” if the aerial photograph’s resolution was sufficient to discern the pavement markings and if there was no evidence of construction activity during the analysis period.

The geo-location process was needed to facilitate the collection of supplemental data. The coordinates for each segment or intersection were subsequently used by the technicians to “return” to the location using Google Earth so they could collect their assigned data. An added benefit of the digitized alignments is that they could be used (with Earth Tools) to compute horizontal curve geometry for no additional time investment.

Enhance Safety Database

Database enhancement consisted of using supplemental data sources to acquire additional data for each target segment or crossroad ramp terminal. The data enhancement activity focused on two tasks. One task was the development of data describing for each segment the proportion of hours per day that are congested. Supplemental data were collected and used to derive this proportion for freeway segments. Automatic traffic recorder (ATR) data for the station nearest to each freeway segment were used for this purpose. These ATR data were acquired from the appropriate state agencies.

The second task of the data enhancement activity was the use of aerial photography to collect additional data for each segment or ramp terminal. These photographs were obtained from Google Earth. The data collected include the width of key road cross section elements, barrier presence and location, horizontal curvature, ramp configuration, turn bay presence, and median type. The number of variables added to each database is identified in Table 13.

Data reduction guidelines and software tools were used to make the collection of supplemental data as consistent and efficient as possible. The development of these guides and tools was described in a previous section.

Some of the cross section data and curvature data that were collected using the semi-automated procedure were compared with the equivalent variables provided in the HSIS data. The findings from these comparisons were documented in Appendix B. For the cross section data, the findings indicated that there was a weak correlation between the HSIS data and the measured data. For the curvature data, there was fairly good agreement between the HSIS data and measured data.

The extraction and processing of supplemental data was the most time-consuming of all the data collection activities. Technicians were used for most of the extraction activities. Some of the more complicated activities (e.g., developing alignment files for segment location and curvature measurement) were completed by an engineer. It is estimated that the data extraction effort required about 0.45 h (= 0.30 h of technician time and 0.15 h of engineer time) for each target segment or crossroad ramp terminal in the database. It is estimated that the processing and management efforts required about 0.15 h of engineer time for each target segment or crossroad ramp terminal.

Merge Road Inventory and Crash Data

This activity involved merging the crash data with the enhanced road inventory databases. The crash data were obtained from HSIS. The objective was to assemble the highway safety database that included all of the relevant data for model calibration. A separate safety database was assembled for each combination of state and roadway component.

File Merge Issues

A key component of this activity was the association of each crash with a roadway component. There were three main issues related to this effort. They are described in the following paragraphs.

Link-Node Conversions. One issue that was encountered related to the link-node system in the Maine HSIS data. This system assigns crashes to links and nodes, where a link represents one direction of travel on divided roadways and a node represents the endpoint of a link (often an intersection or ramp terminal). A link is identified by the numbers of the two nodes that bound it. Crash location along a link is identified by its distance from the lowest node number. The node numbers were found to be randomly assigned by Maine DOT to a node and have no relationship to each other, the direction of travel, or distance along the highway. Furthermore, the distance identified in the HSIS data for a given link often disagreed with the actual length measured on road maps or aerial photographs. These issues were compounded by Maine DOT's conversion to a new node numbering system in 2007. The interchange maps provided by Maine DOT used the 2007 node numbers and the HSIS data used the pre-2007 node numbers. This issue was overcome through the development of additional SAS algorithms and link distance scaling techniques.

Speed-Change Crash Identification. A second issue that was encountered related to the identification of freeway speed-change-related crashes. None of the HSIS databases includes crash attributes that could be used to identify with certainty whether a crash was related to the speed-change lane. This issue was resolved by assuming that all crashes located (by milepost) on the freeway segment between the mileposts that define the speed-change lane are speed-change-lane-related crashes. The location of a speed-change lane was defined to match the "ramp entrance length" and the "ramp exit length" dimensions shown in Figure 11.

Crossroad-Ramp-Terminal-Related Crash Identification. A third issue that was encountered related to the identification of crossroad-ramp-terminal-related crashes. The Washington HSIS database includes a variable that indicates whether a crash is related to the

intersection's activity, behavior, or control. This variable was evaluated using various cross-variable tabulations and found to be reasonably accurate in identifying crossroad-ramp-terminal-related crashes. In contrast, the HSIS databases for California and Maine do not include a variable that identifies intersection-related crashes.

When developing robust safety prediction models, it is important to have criteria for identifying intersection-related crashes that is uniform from state to state. Vogt (1999) examined this issue in some detail and developed the following criteria for identifying intersection-related crashes:

1. The crash must occur within 250 ft of the intersection center, and
2. The crash must have one or more of the following attributes:
 - a. involve a pedestrian;
 - b. one vehicle involved in the crash is making a left turn, right turn, or U turn; or
 - c. if two or more vehicles are involved, manner of collision is sideswipe, rear end, or angle.

The criteria developed by Vogt have a logical dependence on the distance between the crash and the intersection. It is defensible when applied to typical highway intersections; however, it may not be adequate for identifying ramp-terminal-related crashes on ramp segments. In fact, many rear-end crashes on exit ramps are related to the ramp terminal even when they occur more than 250 ft from the terminal because of extensive terminal-related queuing that occurs on some exit ramps. Bauer and Harwood (1998) evaluated 100 reports for rear-end crashes on exit ramps and found that 95 percent of these crashes were related to the operation of the crossroad ramp terminal, regardless of the distance between the crash and the terminal.

Based on these findings, the criteria in Table 15 were developed and used to identify crossroad-ramp-terminal-related crashes. It is noted that crash location, in terms of its distance to the subject crossroad ramp terminal, is available in both the California and Maine HSIS databases.

Level of Effort Indicators

The merging of the road inventory and crash databases was facilitated using SAS data manipulation and merge procedures. A separate SAS processing code was developed for each of the nine databases. Each code reflects the unique nature of each state's data and its treatment of crash records. The lines of code developed for this activity are identified in Table 12. They illustrate the magnitude of the development effort.

TABLE 15. Criteria for defining crossroad-ramp-terminal-related crashes

State	Leg	Criteria
Washington	Crossroad	1. The crash must occur within 250 ft of the terminal and have one of the following attributes: a. intersection related; b. at intersection; c. at driveway, or d. driveway related.
	Ramp	1. The crash must have one or more of the following attributes: a. intersection related; or b. at intersection. OR 2. The ramp is an exit ramp and the manner of collision is rear end.
California and Maine	Crossroad	1. The crash must occur within 250 ft of the terminal and have the following attribute: a. at intersection. OR 2. The crash must occur within 250 ft of the terminal and have one or more of the following attributes: a. involve a pedestrian; b. one vehicle involved in the crash is making a left turn, right turn, or U turn; or c. if two or more vehicles are involved, the manner of collision is sideswipe, rear end, or angle.
	Ramp	1. The crash must satisfy the same criteria as specified for the crossroad. OR 2. The ramp is an exit ramp and the manner of collision is rear end.

DATABASE SUMMARY

This part of the chapter summarizes the data assembled for the purpose of calibrating the predictive models needed to evaluate the safety of freeways and interchanges. The discussion herein is organized in terms of the freeway and interchange components that comprise the freeway system. They are:

- freeway segment,
- interchange ramp,
- crossroad ramp terminal, and
- freeway speed-change lane.

A separate section is devoted to the discussion associated with each component.

The discussion of in this part of the chapter focuses on fatal-and-injury (FI) crashes. This focus is intended to minimize differences in reporting threshold (both formal and informal) that may vary among the states represented in the database. FI crash data are more consistently reported throughout the U.S. and thus, they provide a more uniform basis for comparing crash trends among different jurisdictions.

Evidence of the variability encountered when using property-damage-only (PDO) crashes for comparison is provided by Zegeer et al. (1998). Their examination of rural freeway crashes in four states found that the percentage of PDO crashes varies from 60 to 77 percent. Slightly

smaller variation was found for urban freeways. They speculated that this variation is due to differences in reporting threshold, as opposed to differences in freeway safety.

Table 16 lists the final sample size for each of the nine databases that were assembled. The numbers in this table can be compared with the target sample sizes identified in Table 14. In many instances, the final sample size is lower than the target sample size. This reduction reflects decisions made during the database enhancement activity. In some cases, Street View photographs were not available during the enhancement activity such that barrier could not be accurately located. In other instances, road construction activities missed during the database assembly activity were discovered during the enhancement activity. For a variety of reasons, about 18 percent of the target segments or intersections were eliminated during the enhancement activity.

TABLE 16. Database sample size

Category	Roadway Component	Sample Size by State			
		Calif.	Maine	Wash.	Total
Number of segments or ramp terminals	Freeway segment and freeway speed-change lane	533	203	1,144	1,880
	Ramp proper (including collector-distributor ramps)	405	209	923	1,537
	Crossroad ramp terminal	216	62	291	569
	Total:	1,154	474	2,358	3,986
Total segment length, miles	Freeway segment and freeway speed-change lane	209	101	200	510
	Ramp proper (including collector-distributor ramps)	65	49	114	228
	Total:	274	150	314	738
Average segment length, miles	Freeway segment and freeway speed-change lane	0.39	0.50	0.17	0.27
	Ramp proper (including collector-distributor ramps)	0.16	0.23	0.12	0.15

Freeway Segment

This section describes the freeway segments represented in the safety database. Initially, the traffic and geometric characteristics of each segment are presented. Then, the segment crash data are examined. The data presented for freeway segments includes segments with speed-change lanes. This approach is taken to provide a “complete” picture of freeway segment elements; it recognizes the difficulty of accurately isolating speed-change-related crashes. A subsequent section provides a more detailed examination of the crash characteristics of freeway speed-change lanes.

Segment Characteristics

A total of 1,880 freeway segments are represented in the combined freeway segment database. These segments represent about 209, 101, and 200 miles of freeway in California, Maine, and Washington, respectively. Selected segment characteristics are provided in Table 17.

TABLE 17. Summary characteristics for freeway segments

State	Area Type	Through Lanes	Total Segments	Total Length, mi	Seg. Length Range, mi		Volume Range, veh/day	
					Minimum	Maximum	Minimum	Maximum
California	Rural	4	83	42.1	0.13	1.3	17,000	74,000
		6	56	31.9	0.13	1.6	45,300	139,000
		8	64	32.8	0.13	1.5	71,700	143,000
	Urban	4	86	28.4	0.11	1.1	26,000	97,700
		6	111	40.2	0.11	0.8	55,000	194,000
		8	80	20.2	0.11	0.8	104,000	270,000
		10	53	13.2	0.12	0.5	198,000	308,000
	Overall:		533	208.8	0.11	1.6	17,000	308,000
Maine	Rural	4	116	66.4	0.12	1.2	11,300	62,000
		6	17	7.9	0.12	1.3	42,600	58,000
		8						
	Urban	4	67	25.7	0.12	1.1	11,400	69,500
		6	2	0.5	0.18	0.3	56,200	62,000
		8	1	0.2	0.19	0.2	83,700	83,700
		10						
	Overall:		203	100.6	0.12	1.3	11,300	83,700
Washington	Rural	4	179	81.0	0.03	1.6	9,600	55,800
		6	312	49.6	0.01	0.5	44,000	110,000
		8						
	Urban	4	266	28.5	0.01	0.4	18,400	98,300
		6	272	27.6	0.01	0.3	38,800	121,000
		8	115	13.7	0.01	0.4	89,300	197,000
		10						
	Overall:		1,144	200.4	0.01	1.6	9,600	197,000

The number of segments for each combination of area type and through lanes is indicated in column four of Table 17. The numbers shown for California and Washington are relatively uniform among rows and reflect the sampling technique described in a previous section. Sampling was not used for the Maine data because of the limited number of freeway miles available in that state. As a result, the distribution of segment count for the Maine data roughly reflects the mileage of each combination on the Maine freeway system.

The barrier and ramp characteristics for freeway segments are listed in Table 18. This table lists the average proportion of the segment length that has barrier. This proportion is separately tabulated for the inside (i.e., median) and outside (i.e., roadside) of the roadway. The proportion of the segment length with barrier is shown to increase with the number of through lanes and tends to be higher in urban areas. These trends likely reflect situations where through

lanes were added to the alignment without taking additional right-of-way. In these situations, the clear zone or the median width is reduced and barrier is needed to protect motorists from the resulting hazards.

TABLE 18. Barrier and ramp characteristics for freeway segments

State	Area Type	Through Lanes	Proportion Barrier		Proportion Ramp		Number of Ramps		
			Inside ¹	Outside ¹	Entrance ²	Weave ²	Entrance	Exit	
California	Rural	4	0.649	0.118	0.080	0.017	53	48	
		6	0.997	0.130	0.061	0.000	22	25	
		8	0.949	0.098	0.067	0.015	25	24	
	Urban	4	0.734	0.178	0.089	0.013	47	41	
		6	0.964	0.188	0.112	0.060	87	65	
		8	0.988	0.327	0.106	0.236	39	38	
		10	1.000	0.624	0.104	0.118	31	30	
	Overall:		0.887	0.223	0.091	0.066	304	271	
	Maine	Rural	4	0.650	0.242	0.032	0.000	21	21
			6	0.985	0.149	0.071	0.000	4	3
8									
Urban		4	0.806	0.370	0.067	0.051	24	20	
		6	0.727	0.750	0.161	0.493	1	1	
		8	1.000	0.998	0.000	0.997	0	1	
		10							
Overall:		0.733	0.285	0.048	0.027	50	46		
Washington		Rural	4	0.563	0.146	0.085	0.007	19	19
			6	0.584	0.257	0.096	0.016	40	40
	8								
	Urban	4	0.631	0.334	0.068	0.327	44	42	
		6	0.550	0.417	0.048	0.256	44	36	
		8	0.921	0.343	0.136	0.133	20	20	
		10							
	Overall:		0.618	0.304	0.080	0.156	167	157	

Notes:

1 - Proportion of segment length with rigid barrier. Inside barrier is in the median. Outside barrier is on the roadside.

2 - Proportion of segment length associated with total ramp entrance length or total weave length.

The data in Table 18 also indicate that entrance-ramp-related speed-change lanes constitute about 5 to 9 percent of the segment length. For this statistic, the speed-change lane length is computed as the ramp entrance length or the ramp exit length, as shown in Figure 11. Although not shown in the table, ramp exits tended to account for an additional 6 percent of the segment length.

The proportion of the total segment length that is located in a weaving section varies widely among the states. Maine has the least mileage in the database with weaving. In contrast, the Washington data has the largest amount of mileage with weaving. Many weaving sections in California were coincident with managed lane facilities, which were explicitly excluded from the database assembled for this project.

Crash Characteristics

Crash data were identified for each segment using the most recently available data from the HSIS. Three years of crash data were identified for each segment. The analysis period is 2005, 2006, and 2007 for the California and Washington segments. It is 2004, 2005, and 2006 for the Maine segments.

The crash records associated with each segment were categorized in terms of whether they described a multiple-vehicle non-ramp-related crash, single-vehicle crash, ramp-entrance-related crash, or ramp-exit-related crash. The latter two crash types crashes are referred to herein as speed-change-related crashes. Ramp-entrance- and ramp-exit-related crashes do include some crashes that occur on the ramp proper, near the speed-change lane. Crashes of each severity level (i.e., K, A, B, C, or PDO) were included in the database. However, only those associated with injury or fatality are summarized in this subsection.

The crash data for the freeway segments are summarized in Table 19. These segments were collectively associated with 8,381 injury or fatal crashes (= 5,492 + 661 + 2,228). The trends in crash rate are provided in the last column of the table. These rates indicate that urban freeway segments experience more crashes than rural freeway segments, for the same volume and length. They also indicate that urban segments with more lanes tend to experience more crashes than urban segments with few lanes. Given that the proportion of barrier was also observed to increase with the number of lanes, it is likely that the increase in urban freeway crash rate with increasing lanes is reflective of the reduced horizontal clearance to barrier and other obstructions. In other words, the addition of lanes to a freeway is not likely causing the observed increase in crashes. Rather, it is the reduced clearance (that often associates with the addition of lanes) that is causing the crashes. These trends were observed in a previous analysis of Texas crash data (Bonneson and Pratt, 2008).

Although not shown in the table, the total number of crashes for each state was also computed. This total includes the FI crashes listed in Table 19 plus the PDO crashes that were reported. The total number of crashes for the segments is 26,426. The distribution by state is 17,548, 2,495, and 6,383 for California, Maine, and Washington, respectively. Overall, the FI crashes represent 32 percent of the total crashes. However, this percentage varies among the three states. Specifically, it is 31 percent, 26 percent, and 35 percent for California, Maine, and Washington, respectively. The variation in these percentages is consistent with the variation among states found by Zegeer et al. (1998) and reaffirms the benefit of focusing on FI crashes when comparing crash trends among different jurisdictions.

Multiple-vehicle crashes in California and Washington tend to be nearly twice as frequent as single-vehicle crashes. This trend is not maintained in the Maine data. It is likely due to the lower traffic density on the Maine segments.

TABLE 19. Crash data summary for freeway segments

State	Area Type	Through Lanes	Exposure, ¹ mvm	FI Crashes / 3 years ⁴					Crash Rate, cr/mvm
				Multiple-Vehicle ²	Single-Vehicle	Ramp Entrance ³	Ramp Exit ³	Total	
California	Rural	4	1,927	108	165	33	20	326	0.17
		6	3,271	223	229	22	25	499	0.15
		8	4,004	222	269	21	15	527	0.13
	Urban	4	1,819	193	128	48	8	377	0.21
		6	4,560	641	428	141	54	1,264	0.28
		8	4,057	782	274	125	44	1,225	0.30
		10	3,873	888	235	112	39	1,274	0.33
Overall:		23,511	3,057	1,728	502	205	5,492	0.23	
Maine	Rural	4	2,506	154	229	10	8	401	0.16
		6	446	25	16	2	0	43	0.10
		8							
	Urban	4	1,050	88	80	14	11	193	0.18
		6	31	5	3	3	2	13	0.42
		8	17	6	4	0	1	11	0.63
		10							
Overall:		4,051	278	332	29	22	661	0.16	
Washington	Rural	4	1,954	64	179	4	2	249	0.13
		6	3,332	184	189	15	6	394	0.12
		8							
	Urban	4	1,358	175	108	17	9	309	0.23
		6	2,259	301	136	15	10	462	0.20
		8	2,301	594	115	83	22	814	0.35
		10							
Overall:		11,203	1,318	727	134	49	2,228	0.20	
All states	Rural	4	6,387	326	573	47	30	976	0.15
		6	7,050	432	434	39	31	936	0.13
		8	4,004	222	269	21	15	527	0.13
	Urban	4	4,227	456	316	79	28	879	0.21
		6	6,850	947	567	159	66	1,739	0.25
		8	6,375	1,382	393	208	67	2,050	0.32
		10	3,873	888	235	112	39	1,274	0.33
Overall:		38,765	4,653	2,787	665	276	8,381	0.22	
All states, excluding speed-change lane-related crashes	Rural	4	6,387	326	573			899	0.14
		6	7,050	432	434			866	0.12
		8	4,004	222	269			491	0.12
	Urban	4	4,227	456	316			772	0.18
		6	6,850	947	567			1,514	0.22
		8	6,375	1,382	393			1,775	0.28
		10	3,873	888	235			1,123	0.29
Overall:		38,765	4,653	2,787			7,440	0.19	

Notes:

1 - mvm: million vehicle-miles.

2 - Multiple-vehicle crashes do not include speed-change-related crashes.

3 - Referred to herein as speed-change-related crashes.

4 - FI: fatal-and-injury crashes.

Interchange Ramp

This section describes the ramp segments represented in the safety database. Initially, the traffic and geometric characteristics of each segment are presented. Then, the segment crash data are examined. A ramp segment is defined as a portion of the entire ramp. An entire ramp is defined to extend from the gore point at the freeway speed-change lane to either (1) the gore point at a crossroad speed-change lane or (2) the near edge of the crossroad traveled way at the crossroad ramp terminal. For the California and Maine databases, all of the ramp segments extend for the length of the entire ramp. For the Washington database, the ramp segments are typically only a small portion of the entire ramp.

Segment Characteristics

A total of 1,537 ramp segments are represented in the combined ramp segment database. These segments represent about 65, 49, and 114 miles of ramps in California, Maine, and Washington, respectively. Selected segment characteristics are provided in Table 20. The ramp configurations identified in this table are shown in Figure 4.

The number of segments for each combination of ramp type and configuration is indicated in column four of Table 20. The numbers shown for California are relatively uniform among rows and reflect the sampling technique described in a previous section. Sampling was also applied to the Washington data; however, it was not possible to make the distribution more uniform among ramp configurations given the relatively limited number of viable loop and buttonhook ramps represented in the data. Sampling was not used for the Maine data because all of ramps available in that state were considered for inclusion in the database.

Collector-distributor road segments were included in the database for Maine and Washington. These segments could not be accurately located using the HSIS data for California because interchange maps were not available for this state.

TABLE 20. Summary characteristics for ramp segments

State	Ramp Type ¹	Ramp Config.	Total Segments	Total Length, mi	Seg. Length Range, mi		Volume Range, veh/day		
					Minimum	Maximum	Minimum	Maximum	
California	C-D road	Segment							
	Exit	Connector	39	8.4	0.08	0.43	440	21,600	
		Diagonal	65	12.1	0.12	0.29	400	13,200	
		Button hook	43	4.8	0.05	0.24	780	15,000	
		Loop	63	11.0	0.08	0.25	960	12,400	
	Entrance	Connector	40	8.1	0.07	0.65	1,500	18,100	
		Diagonal	57	9.6	0.10	0.25	520	13,300	
		Button hook	33	2.7	0.05	0.14	740	8,800	
		Loop	65	8.6	0.09	0.22	530	11,800	
	Overall:			405	65.3	0.05	0.65	400	21,600
	Maine	C-D road	Segment	7	1.0	0.09	0.20	3,200	11,100
Exit		Connector	39	11.1	0.12	0.76	1,100	9,800	
		Diagonal	43	10.2	0.15	0.38	400	7,100	
		Button hook	1	0.1	0.09	0.09	1,800	1,800	
		Loop	21	3.7	0.10	0.30	1,400	6,400	
Entrance		Connector	34	7.8	0.11	0.40	750	8,800	
		Diagonal	40	10.4	0.14	0.42	720	8,500	
		Button hook	1	0.1	0.08	0.08	2,500	2,500	
		Loop	23	5.1	0.11	0.38	560	6,600	
Overall:			209	49.5	0.08	0.76	400	11,100	
Washington		C-D road	Segment	195	17.1	0.02	0.21	2,200	29,500
	Exit	Connector	79	12.2	0.02	0.40	1,400	33,000	
		Diagonal	239	30.6	0.02	0.26	140	10,900	
		Button hook	13	1.7	0.05	0.41	450	11,000	
		Loop	34	5.3	0.02	0.42	160	11,400	
	Entrance	Connector	103	12.6	0.02	0.36	1,800	23,800	
		Diagonal	229	30.1	0.02	0.27	140	9,800	
		Button hook	2	0.1	0.04	0.06	5,000	5,000	
		Loop	29	4.2	0.01	0.35	740	15,300	
	Overall:			923	113.9	0.01	0.42	140	33,000

Note:

1 - C-D road: collector-distributor ramp roadway.

The barrier and ramp characteristics for ramp segments are listed in Table 21. This table lists the average proportion of the segment length that has barrier. This proportion is separately tabulated for the inside (i.e., left side) and outside (i.e., right side) of the ramp roadway. The

proportion of the segment with barrier for Maine ramps is about twice that of the Washington and California ramps.

TABLE 21. Barrier and cross section characteristics for ramp segments

State	Ramp Type	Ramp Config.	Proportion Barrier		Proportion Curve ²	Average Width, ft			
			Inside ¹	Outside ¹		Left Shldr.	Lane	Right Shldr.	
California	C-D road	Segment							
	Exit	Connector	0.203	0.328	0.524	3.6	12.7	7.0	
		Diagonal	0.047	0.136	0.441	3.4	12.6	5.8	
		Button hook	0.163	0.159	0.477	3.0	12.6	5.5	
		Loop	0.204	0.116	0.651	3.4	13.4	5.8	
	Entrance	Connector	0.070	0.078	0.556	3.6	13.1	6.5	
		Diagonal	0.041	0.047	0.417	3.2	13.1	6.5	
		Button hook	0.042	0.078	0.707	3.3	15.5	5.6	
		Loop	0.118	0.027	0.822	3.4	14.4	6.1	
	Overall:			0.111	0.121	0.574	3.4	13.4	6.1
	Maine	C-D road	Segment	0.124	0.416	0.126	4.0	12.0	10.0
Exit		Connector	0.303	0.476	0.612	5.4	15.5	6.4	
		Diagonal	0.237	0.229	0.438	5.2	15.3	6.6	
		Button hook	0.422	0.433	0.731	0.0	19.0	0.0	
		Loop	0.321	0.186	0.844	4.6	18.3	5.0	
Entrance		Connector	0.266	0.391	0.516	5.1	16.7	5.9	
		Diagonal	0.150	0.253	0.343	5.5	15.2	6.6	
		Button hook	0.543	0.364	0.658	4.0	18.0	4.0	
		Loop	0.426	0.390	0.792	4.3	17.7	4.6	
Overall:			0.310	0.349	0.562	4.2	16.4	5.5	
Washington		C-D road	Segment	0.740	0.416	0.353	6.0	13.8	8.3
	Exit	Connector	0.376	0.567	0.589	5.3	13.8	7.7	
		Diagonal	0.079	0.221	0.470	5.2	14.3	7.9	
		Button hook	0.000	0.000	0.380	5.1	13.4	6.4	
		Loop	0.000	0.000	0.749	5.4	16.2	7.6	
	Entrance	Connector	0.225	0.197	0.609	5.6	14.0	8.7	
		Diagonal	0.137	0.283	0.458	5.2	14.1	8.1	
		Button hook	0.000	0.000	0.348	6.4	13.9	8.6	
		Loop	0.000	0.000	0.855	5.0	15.7	7.4	
	Overall:			0.173	0.187	0.535	5.5	14.4	7.9

Notes:

1 - Proportion of segment length with rigid barrier. Inside barrier is in the median. Outside barrier is on the roadside.

2 - Proportion of segment length on horizontal curve.

The sixth column of Table 21 indicates the average proportion of the ramp segment length that has curvature. This proportion is highest for the loop ramp configurations, which is logical given their design. All of the ramp configurations tend to have curvature for 40 percent or more of their length.

The last three columns of Table 21 list the average width of the shoulders and lanes on the ramp segments. It is noteworthy that the average lane width on the Maine ramps is two feet wider than the Washington ramps and three feet wider than the California ramps. It is also noteworthy that the combined cross section of the California ramps is several feet narrower than the ramps in either Maine or Washington.

Crash Characteristics

Crash data were identified for each ramp segment using the most recently available data from the HSIS. Five years of crash data were identified for each segment. The analysis period is 2003, 2004, 2005, 2006, and 2007 for the California and Washington segments. It is 2002, 2003, 2004, 2005, and 2006 for the Maine segments.

The crash records associated with each segment were categorized in terms of whether they described a multiple-vehicle crash or a single-vehicle crash. Crashes of each severity level (i.e., K, A, B, C, or PDO) were included in the database. However, only those associated with injury or fatality are summarized in this subsection.

The crash data for the ramp segments are summarized in Table 22. These segments were collectively associated with 1,178 injury or fatal crashes (= 382 + 89 + 707). The trends in crash rate are provided in the last column of the table. These rates suggest that crash risk on a ramp is about twice that on a freeway segment. This trend is likely due to the sharper curves on ramps, relative to freeways and the significant speed change associated with ramp driving.

A closer examination of the crash rates in Table 22 indicates that most ramp crashes are single-vehicle crashes, which is logical given the typical lack of adjacent or oncoming lanes and the frequent presence of sharp curves on ramps.

The crash rates for the Maine ramps are notably smaller than that found for the California and Washington ramps. This trend may reflect the longer length of the Maine ramps, their wider cross section, or both, relative to the California and Washington ramps. The longer length may provide a more accommodating distance for the speed change that occurs on the ramp. Wider lane and shoulder widths have been found to reduce crashes on street and highway segments (as noted in Chapter 2).

Although not shown in the table, the total number of crashes for each state was also computed. This total includes the FI crashes listed in Table 22 plus the PDO crashes that were reported. The total number of crashes for the segments is 3,541. The distribution by state is 1,120, 324, and 2,097 for California, Maine, and Washington, respectively. The FI crashes represent 33 percent of the total crashes. However, this percentage varies among the three states. Specifically, it is 34 percent, 27 percent, and 34 percent for California, Maine, and Washington,

respectively. The variation in these percentages is consistent with the variation among the states found in the freeway segment crash data.

TABLE 22. Crash data summary for ramp segments

State	Ramp Type	Ramp Config.	Exposure, ¹ mvm	FI Crashes / 5 years			Crash Rate, cr/mvm
				Multiple-Vehicle ²	Single-Vehicle	Total	
California	C-D road	Segment					
	Exit	Connector	145.1	3	62	65	0.45
		Diagonal	137.9	0	36	36	0.26
		Button hook	50.7	1	45	46	0.91
		Loop	126.9	3	96	99	0.78
	Entrance	Connector	120.9	6	40	46	0.38
		Diagonal	89.5	3	36	39	0.44
		Button hook	22.5	0	5	5	0.22
		Loop	62.5	7	39	46	0.74
	Overall:			756.0	23	359	382
Maine	C-D road	Segment	12.9	0	1	1	0.08
	Exit	Connector	101.9	0	20	20	0.20
		Diagonal	47.0	3	15	18	0.38
		Button hook	0.3	0	0	0	0.00
		Loop	22.6	0	9	9	0.40
	Entrance	Connector	65.2	8	17	25	0.38
		Diagonal	56.0	4	3	7	0.13
		Button hook	0.4	0	0	0	0.00
		Loop	32.0	5	4	9	0.28
	Overall:			338.2	20	69	89
Washington	C-D road	Segment	366.8	114	44	158	0.43
	Exit	Connector	202.4	17	169	186	0.92
		Diagonal	172.3	6	73	79	0.46
		Button hook	18.7	2	21	23	1.23
		Loop	39.2	2	27	29	0.74
	Entrance	Connector	231.8	37	102	139	0.60
		Diagonal	149.3	12	44	56	0.38
		Button hook	0.9	1	5	6	6.57
		Loop	32.8	1	30	31	0.95
	Overall:			1,214.2	192	515	707

Notes:

1 - mvm: million vehicle-miles.

2 - Multiple-vehicle crashes do not include speed-change-related crashes.

The data in Table 22 are summarized by ramp type and configuration in Table 23 to facilitate some preliminary examination of trend. The crash rates shown indicate that button hook exit ramps tend to have the highest crash rate, which is intuitive given their inherently short length and sharp curvature. In contrast, the diagonal entrance ramp has the lowest crash rate. A pair-wise comparison of exit and entrance ramps by configuration indicates that the exit ramps tend to have a higher crash rate than entrance ramps.

TABLE 23. Crash data summary by ramp configuration

Ramp Type	Ramp Config.	Exposure, ¹ mvm	FI Crashes / 5 years	Crash Rate, cr/mvm
C-D road	Segment	379.7	159	0.42
Exit	Connector	449.4	271	0.60
	Diagonal	357.2	133	0.37
	Button hook	69.7	69	0.99
	Loop	188.7	137	0.73
Entrance	Connector	417.9	210	0.50
	Diagonal	294.8	102	0.35
	Button hook	23.8	11	0.46
	Loop	127.3	86	0.68
Overall:		2,308.5	1,178	0.51

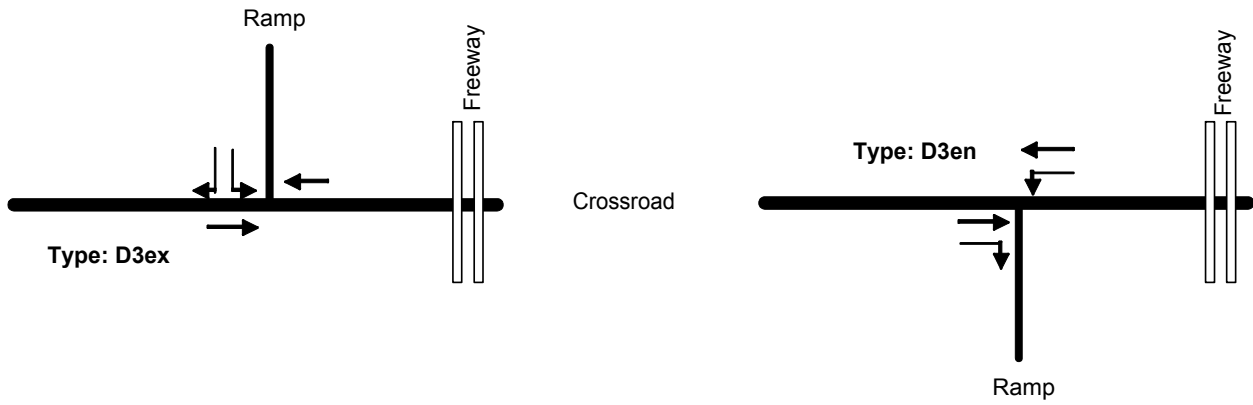
Note:

1 - mvm: million vehicle-miles.

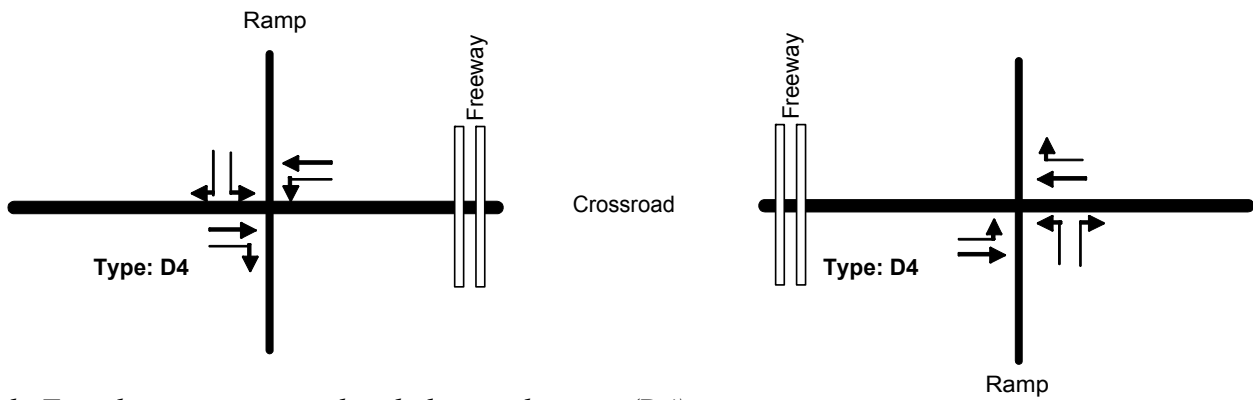
Crossroad Ramp Terminal

This section describes the crossroad ramp terminals represented in the safety database. Initially, the traffic and geometric characteristics of each ramp terminal are presented. Then, the ramp terminal crash data are examined.

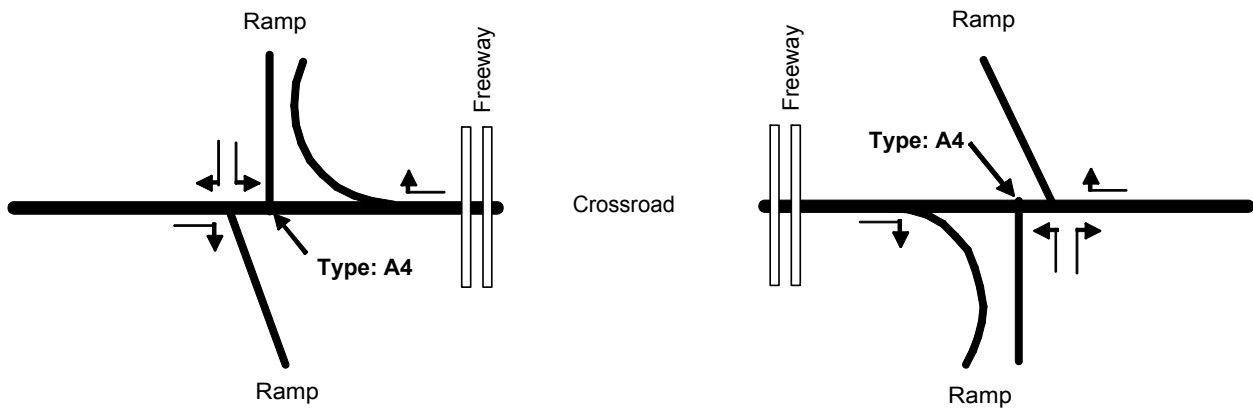
There are many different ramp configurations found at interchanges. The more common ones are identified in Figure 37. Differences among ramp terminals are shown to reflect the number of ramp legs, ramp configuration, number of left-turn movements, and location of crossroad left-turn storage (i.e., internal or external to interchange). Although not shown, control type (i.e., signalized or unsignalized) is also an important factor in characterizing ramp terminal safety and operation.



a. Three-leg ramp terminal with diagonal exit ramp or entrance ramp (D3ex and D3en).

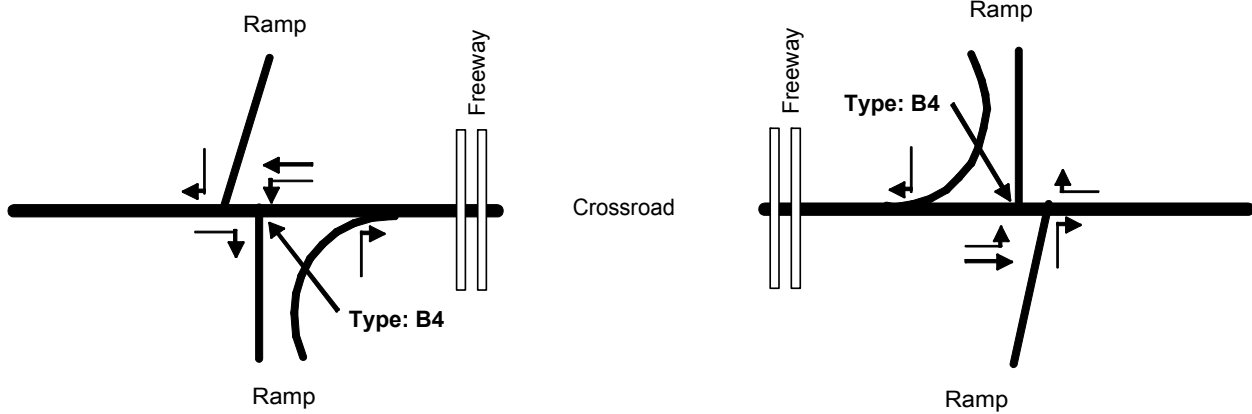


b. Four-leg ramp terminal with diagonal ramps (D4).

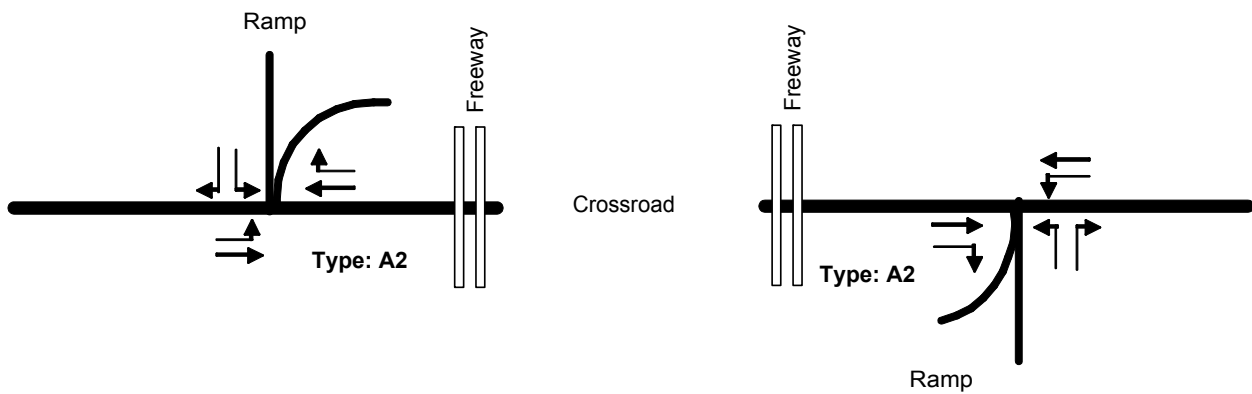


c. Ramp terminal at four-quadrant parclo A (A4).

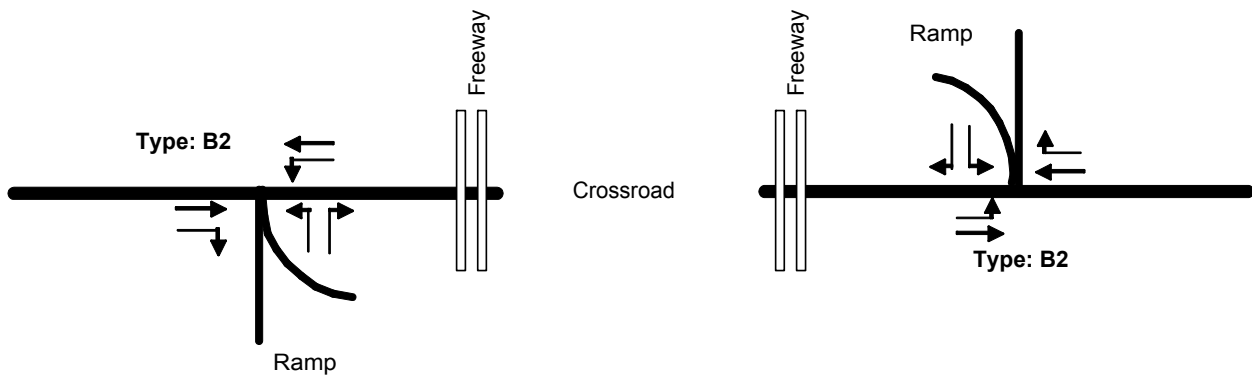
Figure 37. Ramp terminal configurations.



d. Ramp terminal at four-quadrant parclo B (B4).



e. Ramp terminal at two-quadrant parclo A (A2).



f. Ramp terminal at two-quadrant parclo B (B2).

Figure 37. Ramp terminal configurations (continued).

Ramp Terminal Characteristics

All total, 569 ramp terminals are represented in the combined database. More specifically, the database includes 216, 62, and 291 ramp terminals in California, Maine, and Washington, respectively. Selected ramp terminal characteristics are provided in Table 24.

The number of ramp terminals for each combination of control type and configuration is indicated in column 4 of Table 24. When distributed among the 13 combinations shown, there are several combinations with a small number of ramp terminals. Most notable is the small number of “parclo B4” and “diagonal 3-leg” configurations. As noted previously, this sample represents all of the ramp terminals that are fully represented in the HSIS databases. Sample size issues are discussed at the end of this section.

Crash Characteristics

Crash data were identified for each ramp terminal using the most recently available data from the HSIS. Three years of crash data were identified for each ramp terminal. The analysis period is 2005, 2006, and 2007 for the California and Washington segments. It is 2004, 2005, and 2006 for the Maine segments.

Crashes of each severity level (i.e., K, A, B, C, or PDO) were included in the database. Those crashes associated with an injury or fatality are summarized separately from those associated with property damage only (PDO).

The crash data for the ramp terminals are summarized in Table 25. These ramp terminals were collectively associated with 2,177 injury or fatal crashes (= 810 + 171 + 1,196). The trends in crash rate are provided in the last column of the table. Typical FI crash rates for three-leg intersections are 0.14 and 0.20 cr/mev for unsignalized and signalized control, respectively (Bonneson and Pratt, 2008). The rates shown in Table 25 are consistent with these typical values.

The overall crash rates for the California ramp terminals (i.e., 0.13 and 0.42 cr/mvm) are notably lower than those for the Maine and Washington ramp terminals. However, the average exposure per ramp terminal for the California sites is 26 mev (= 6123.4 / 216), which is much larger than that for Maine (13 mev) and Washington (19 mev). Thus, the noted trend in crash rate is likely a reflection of the non-linear relationship between ramp terminal volume and crash frequency.

TABLE 24. Summary characteristics for crossroad ramp terminals

State	Control Type	Terminal Configuration	Total Terminals	Crossroad Volume, veh/day		Ramp Volume, veh/day	
				Minimum	Maximum	Minimum	Maximum
California	Signal	Parclo A2	11	7,700	48,700	2,900	15,100
		Parclo A4	41	13,100	68,700	1,900	22,000
		Parclo B2	6	7,300	45,700	2,000	11,700
		Parclo B4	0				
		Diagonal 3 leg	4	12,100	30,000	1,000	10,500
		Diagonal 4 leg	55	6,800	46,400	3,000	15,500
	Unsignalized ¹	Parclo A2	8	700	10,500	500	4,400
		Parclo A4	16	4,000	17,300	340	10,200
		Parclo B2	6	745	23,000	310	7,200
		Parclo B4	1	13,600	13,600	4,300	4,300
		Diagonal 3 leg	5	11,800	40,900	1,000	6,100
		Diagonal 4 leg	63	1,900	18,900	320	4,700
		Speed-change	0				
	Overall:			216	700	68,700	310
Maine	Signal	Parclo A2	0				
		Parclo A4	1	15,200	15,200	4,700	4,700
		Parclo B2	2	14,700	15,600	3,200	3,400
		Parclo B4	0				
		Diagonal 3 leg	1	34,000	34,000	10,800	10,800
		Diagonal 4 leg	4	13,300	17,800	4,000	6,000
	Unsignalized ¹	Parclo A2	7	3,400	17,300	1,700	14,700
		Parclo A4	0				
		Parclo B2	9	4,600	12,100	1,200	4,600
		Parclo B4	1	18,300	18,300	3,100	3,100
		Diagonal 3 leg	7	4,700	11,100	590	2,400
		Diagonal 4 leg	24	1,900	12,700	510	4,400
		Speed-change	6	8,270	20,530	373	7,300
	Overall:			62	1,900	34,000	373
Washington	Signal	Parclo A2	11	8,100	42,000	1,800	13,100
		Parclo A4	8	11,900	42,800	1,200	7,900
		Parclo B2	6	10,400	25,300	3,600	8,500
		Parclo B4	2	31,700	38,300	5,300	14,700
		Diagonal 3 leg	6	2,900	33,400	4,700	21,600
		Diagonal 4 leg	87	9,400	43,300	3,500	11,700
	Unsignalized ¹	Parclo A2	11	3,000	17,200	860	7,000
		Parclo A4	2	12,900	22,700	590	5,000
		Parclo B2	7	1,200	26,800	380	5,400
		Parclo B4	4	8,800	24,800	940	9,900
		Diagonal 3 leg	19	1,200	22,400	270	17,700
		Diagonal 4 leg	127	370	10,400	180	4,200
		Speed-change	1	24,200	24,200	4,700	4,700
	Overall:			291	370	43,300	180

Note:

1 - Unsignalized intersections have an uncontrolled major street and a stop-controlled minor street.

TABLE 25. Crash data summary for crossroad ramp terminals

State	Control Type	Terminal Configuration	Exposure, ¹ mev	Crashes / 3 years			Crash Rate, cr/mev	
				PDO ²	FI ³	Total	FI ³	Total
California	Signal	Parclo A2	442.1	111	41	152	0.09	0.34
		Parclo A4	2,252.2	552	287	839	0.13	0.37
		Parclo B2	253.6	47	19	66	0.07	0.26
		Parclo B4						
		Diagonal 3 leg	125.3	16	14	30	0.11	0.24
		Diagonal 4 leg	1,900.5	742	298	1,040	0.16	0.55
	Unsignalized ¹	Parclo A2	57.6	15	8	23	0.14	0.40
		Parclo A4	208.4	89	43	132	0.21	0.63
		Parclo B2	73.1	16	8	24	0.11	0.33
		Parclo B4	19.5	0	1	1	0.05	0.05
		Diagonal 3 leg	143.1	36	19	55	0.13	0.38
		Diagonal 4 leg	648.0	144	72	216	0.11	0.33
		Speed-change						
	Overall:			6,123.4	1,768	810	2,578	0.13
Maine	Signal	Parclo A2						
		Parclo A4	21.8	8	4	12	0.18	0.55
		Parclo B2	40.5	19	16	35	0.40	0.86
		Parclo B4						
		Diagonal 3 leg	49.0	41	15	56	0.31	1.14
		Diagonal 4 leg	90.2	87	45	132	0.50	1.46
	Unsignalized ¹	Parclo A2	114.7	56	26	82	0.23	0.71
		Parclo A4						
		Parclo B2	105.6	29	10	39	0.09	0.37
		Parclo B4	23.4	12	4	16	0.17	0.68
		Diagonal 3 leg	73.3	10	9	19	0.12	0.26
		Diagonal 4 leg	203.0	63	28	91	0.14	0.45
		Speed-change	107.0	34	14	48	0.13	0.45
	Overall:			828.5	359	171	530	0.21
Washington	Signal	Parclo A2	320.9	125	82	207	0.26	0.65
		Parclo A4	227.8	92	43	135	0.19	0.59
		Parclo B2	169.0	78	46	124	0.27	0.73
		Parclo B4	98.5	48	24	72	0.24	0.73
		Diagonal 3 leg	231.1	73	36	109	0.16	0.47
		Diagonal 4 leg	2,883.9	1,310	770	2,080	0.27	0.72
	Unsignalized ¹	Parclo A2	133.6	14	15	29	0.11	0.22
		Parclo A4	45.1	2	3	5	0.07	0.11
		Parclo B2	90.5	21	13	34	0.14	0.38
		Parclo B4	88.1	22	14	36	0.16	0.41
		Diagonal 3 leg	252.2	46	26	72	0.10	0.29
		Diagonal 4 leg	870.5	211	121	332	0.14	0.38
		Speed-change	31.7	3	3	6	0.09	0.19
	Overall:			5,442.8	2,045	1,196	3,241	0.22

Notes:

1 - mev: million-entering-vehicles per year.

2 - PDO: property-damage-only crashes.

3 - FI: fatal-and-injury crashes.

The data in Table 25 are summarized by control type and terminal configuration in Table 26 to facilitate some preliminary examination of trend. The crash rates shown indicate that the signalized “parclo B4” configuration has the highest crash rate. However, these statistics are based on only two ramp terminals and may not be representative of similar terminals at other locations.

The signalized “diagonal 4 leg” has the second highest crash rate shown in Table 26. This trend may be related to the fact that this configuration is the only one that has four legs (all other configurations typically have three legs). In contrast, the unsignalized “parclo B2” and “diagonal 3 leg” terminals have lowest crash rate. A pair-wise comparison of signalized and unsignalized terminals by configuration indicates that the signalized terminals tend to have a higher crash rate than the unsignalized terminals.

Sample Size Considerations

Sample size considerations are complex and involve many factors. However, it is considered desirable to have at least 25 ramp terminals for each combination of control type and configuration to ensure reasonable representation of that type of facility. Also, statistical considerations indicate a desirable minimum of 150 crashes in the database for each combination.

Table 27 indicates the total number of ramp terminals for each configuration across all three states represented in the combined database. An examination of columns 3 and 4 indicates that only 3 of the 13 configurations satisfy both criteria. However, 5 of 13 configurations have more than 25 ramp terminals.

Several options are available to address these concerns. The option chosen was to aggregate selected terminal configurations with similar turn movement patterns. For example, consultation of Figure 37 indicates that the “parclo A4” has movements that are very similar to a “diagonal 3 leg” where the ramp leg is associated with an exit ramp. Similarly, the “parclo B4” has movements that are very similar to a “diagonal 3 leg” where the ramp leg is associated with an entrance ramp. Also, the “parclo B2” and “parclo A2” have very similar movements. These configurations were combined to examine their impact on the sample size considerations. The results are shown in the last three columns of Table 27. With this option, 4 of the 9 configurations satisfy both minimum criteria. Moreover, 6 of 9 configurations have more than 25 ramp terminals.

TABLE 26. Crash data summary by ramp terminal configuration

Control Type	Terminal Configuration	Exposure, mev	Crashes / 3 years			Crash Rate, cr/mev	
			PDO	FI	Total	FI	Total
Signal	Parclo A2	763.0	236	123	359	0.16	0.47
	Parclo A4	2,501.8	652	334	986	0.13	0.39
	Parclo B2	463.1	144	81	225	0.17	0.49
	Parclo B4	98.5	48	24	72	0.24	0.73
	Diagonal 3 leg	405.4	130	65	195	0.16	0.48
	Diagonal 4 leg	4,874.6	2,139	1,113	3,252	0.23	0.67
Unsignalized	Parclo A2	305.9	85	49	134	0.16	0.44
	Parclo A4	253.5	91	46	137	0.18	0.54
	Parclo B2	269.2	66	31	97	0.12	0.36
	Parclo B4	131.0	34	19	53	0.15	0.40
	Diagonal 3 leg	468.6	92	54	146	0.12	0.31
	Diagonal 4 leg	1,721.5	418	221	639	0.13	0.37
	Speed-change	138.7	37	17	54	0.12	0.39
Overall:		12,394.8	4,172	2,177	6,349	0.18	0.51

TABLE 27. Sample size considerations for crossroad ramp terminals

Control Type	Terminal Configuration	Total Terminals ¹	FI Crashes / 3 years ¹	Possible Combinations		
				Terminal Configuration	Total Terminals ¹	FI Crashes / 3 years ¹
Signal	Parclo A2	22	123			
	Parclo A4	<u>50</u>	<u>334</u>	Parclo A4 and Diagonal 3 leg exit ramps	<u>55</u>	<u>367</u>
	Parclo B2	14	81	Parclo B2 and Parclo A2	<u>36</u>	<u>204</u>
	Parclo B4	2	24	Parclo B4 and Diagonal 3 leg entrance ramps	8	56
	Diagonal 3 leg	11	65			
	Diagonal 4 leg	<u>146</u>	<u>1,113</u>	Diagonal 4 leg	<u>146</u>	<u>1,113</u>
Unsignalized	Parclo A2	<u>26</u>	49			
	Parclo A4	18	46	Parclo A4 and Diagonal 3 leg exit ramps	<u>33</u>	73
	Parclo B2	22	31	Parclo B2 and Parclo A2	<u>48</u>	80
	Parclo B4	6	19	Parclo B4 and Diagonal 3 leg entrance ramps	22	46
	Diagonal 3 leg	<u>31</u>	54			
	Diagonal 4 leg	<u>214</u>	<u>221</u>	Diagonal 4 leg	<u>214</u>	<u>221</u>
	Speed-change	7	17	Speed-change	7	17
Overall:		569	2,177		569	2,177

Note:

1 - Underlined values identify configurations that meet or exceed desired sample sizes.

Freeway Speed-Change Lane

This section describes the freeway speed-change lanes represented in the safety database. As described previously, all crashes located (by milepost) on the freeway segment between the mileposts that define the speed-change lane are speed-change-lane-related crashes. The location of a speed-change lane is defined by the mileposts of its taper and gore points.

The crash data for speed-change lanes are summarized in Table 28. The data are categorized by state, ramp type, and number of speed-change lanes per freeway segment. Almost all of the segments with speed-change lanes have one entrance speed-change lane and one exit speed-change lane. A few of the longer segments have as many as three entrance speed-change lanes and two exit speed-change lanes. The exposure statistic in Table 28 is based on the length of the speed-change lane and the freeway segment AADT volume. The ramp AADT volume is not factored into the calculation of exposure.

The last column of Table 28 lists the crash rate associated with the speed-change lanes. A comparison of these rates with those in Table 19 indicates that the crash rate in a speed-change lane exceeds that of a basic freeway segment (i.e., with speed-change-related crashes excluded). This trend is logical and likely reflects the increased risk of crash associated with frequent lane changes in the speed-change lane. An examination of the crash rates for entrance- and exit-related speed-change lanes does not indicate that there is any correlation between ramp type and crash rate.

TABLE 28. Summary characteristics for freeway speed-change lane segments

State	Ramp Type	No. S-C Lanes/Seg	Total Segments	S-C Lane Length, mi	Exposure, ¹ mvm	FI Crashes / 3years	Crash Rate, cr/mvm
California	Entrance	1	231	20.7	1,352.7	369	0.27
		2	54	9.7	574.2	127	0.22
		3	3	0.5	19.2	6	0.31
	Exit	1	222	9.8	593.4	177	0.30
		2	23	2.4	139.8	28	0.20
		3	0				
	Overall:		533	43.1	2,679.3	707	0.26
Maine	Entrance	1	52	5.8	129.1	22	0.17
		2	3	0.7	25.2	7	0.28
		3	0				
	Exit	1	58	5.3	106.4	18	0.17
		2	3	0.5	12.7	3	0.24
		3	0				
	Overall:		116	12.3	273.4	50	0.18
Washington	Entrance	1	239	17.1	624.6	129	0.21
		2	6	0.9	25.5	5	0.20
		3	0				
	Exit	1	197	7.3	285.8	49	0.17
		2	0				
		3	0				
	Overall:		442	25.2	935.9	183	0.20
All States	Entrance	1	522	43.6	2,106.4	520	0.25
		2	63	11.3	624.9	139	0.22
		3	3	0.5	19.2	6	0.31
	Exit	1	477	22.4	985.6	244	0.25
		2	26	2.9	152.5	31	0.20
		3	0				
	Overall:		1,091	80.7	3,888.6	940	0.24

Note:

1 - mev: million-entering-vehicles per year.

CHAPTER 5: PREDICTIVE MODEL FOR FREEWAY SEGMENTS

This chapter describes the activities undertaken to calibrate and validate safety predictive models for freeway segments and for freeway speed-change lanes. Each model consists of a safety performance function (SPF) and a family of crash modification factors (CMFs). The SPF is derived to estimate the crash frequency for segments and speed-change lanes with specified design elements and operating conditions. The CMFs are used to adjust the SPF estimate whenever one or more elements or conditions deviate from those that are specified.

The calibrated safety predictive models were used to develop a freeway safety predictive method. This method describes how to use the models to evaluate freeway safety, as may be influenced by road geometry, roadside features, traffic volume, and lane-change-related traffic maneuvers. The predictive method for freeways is documented in Appendix C.

The predictive method includes predictive models for freeway segments and for speed-change lanes. The freeway segment models are used to evaluate both freeway travel directions combined. In contrast, the speed-change lane models are used to evaluate the one travel direction associated with a speed-change lane.

Collectively, the predictive models for freeway segments address the following area type and lane combinations.

- rural freeway with four through lanes,
- rural freeway with six through lanes,
- rural freeway with eight through lanes,
- urban freeway with four through lanes,
- urban freeway with six through lanes,
- urban freeway with eight through lanes, and
- urban freeway with ten through lanes.

The speed-change models address ramp entrances and ramp exits for freeways with the area types and lane combinations identified in the preceding list.

This chapter is divided into six parts. The first part provides some background information on the topic of predictive models for freeway segments. The second part describes the theoretic development of selected CMFs. The third part describes the method used to calibrate the proposed models. The fourth part describes the calibration of the models to predict fatal-and-injury (FI) crash frequency. The fifth part describes the calibration of the models to predict property-damage-only crash (PDO) frequency. The sixth part provides a list of the variables defined in this chapter.

BACKGROUND

This part of the chapter consists of three sections. The first section describes the decomposition of a freeway facility into analysis units (i.e., sites). The second section provides a brief overview of the predictive model structure. The third section reviews the highway safety data assembled for model calibration.

Roadway Segments, Ramp Segments, and Ramp Terminals

For analysis purposes, a freeway facility is considered to include a freeway section and, possibly, one or more interchanges. The freeway section includes a contiguous set of freeway segments and, possibly, one or more speed-change lanes. An interchange is considered to consist of a set of ramp segments, crossroad ramp terminals, and, possibly, one or more C-D road segments. These components are also referred to as “sites.”

Figure 38 illustrates the sites associated with a short section of freeway near an interchange. The arrangement shown is intended to illustrate the types of sites used for freeway facility safety evaluation—it is not a typical interchange and many freeway segments are not likely to include speed-change lanes.

As indicated in the *HSM* (Highway, 2010), road segment boundaries are typically defined by intersections or by a change in the cross section. This guidance applies to crossroad segments and to freeway segments. Specifically, freeway segment boundaries are defined by the presence of a gore point associated with a ramp. However, the length of the freeway segment is reduced by the length of the speed-change lane. This distinction stems from: (1) the lack of a clear and consistent designation of speed-change-related crashes in state DOT crash databases and (2) the presence of a speed-change lane on only one side of the freeway. For these reasons, a speed-change-related crash was identified as any crash that occurred: (1) between the marked gore point and taper points of a ramp merge or diverge area and (2) on the same side of the freeway as the merge or diverge area. This approach requires a reduction in the effective length of the freeway segment to account for the crashes re-assigned to any speed-change lanes that are located on the segment. This reduction is shown in the bottom of Figure 38 for a freeway section with one ramp entrance and one ramp exit.

Safety Predictive Models

The predicted average crash frequency for a freeway section is computed as the sum of the predicted average crash frequency of all sites that comprise the section. This calculation is described by Equation 10.

$$N_{section} = \sum_{all\ segments} (N_{mv} + N_{sv}) + \sum_{all\ entrances} (N_{en}) + \sum_{all\ exits} (N_{ex}) \quad (10)$$

where,

- $N_{section}$ = predicted average crash frequency within the limits of a freeway section, crashes/yr;
- N_{mv} = predicted average multiple-vehicle non-entrance/exit crash frequency, crashes/yr;
- N_{sv} = predicted average single-vehicle non-entrance/exit crash frequency, crashes/yr;
- N_{en} = predicted average ramp-entrance-related crash frequency, crashes/yr; and
- N_{ex} = predicted average ramp-exit-related crash frequency, crashes/yr.

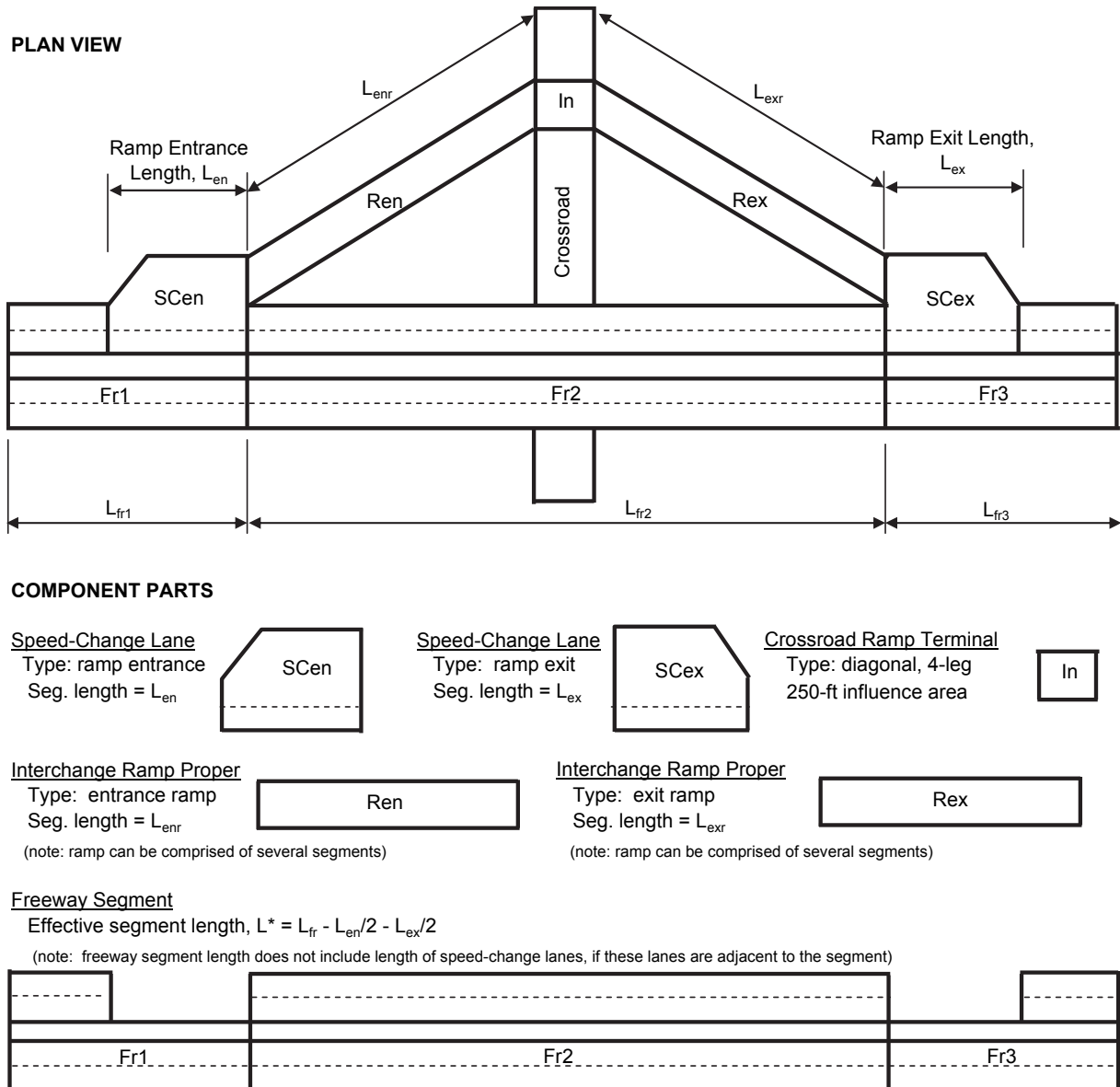


Figure 38. Illustrative freeway facility analysis sites.

The predicted average crash frequency for each site is computed using a predictive model. Each model represents the combination of an SPF and several CMFs. The SPF is used to estimate the average crash frequency for a generic site whose attributes are consistent with the SPF's stated base conditions. The CMFs are used to adjust the SPF estimate when the attributes of the subject site are not consistent with the base conditions. The general form of the four safety predictive models developed in this research is shown below as Equation 11 to Equation 14.

$$N_{mv} = C_{mv} \times N_{spf, mv} \times (CMF_{mv,1} \times \dots \times CMF_{mv,w}) \times (CMF_1 \times \dots \times CMF_k) \quad (11)$$

$$N_{sv} = C_{sv} \times N_{spf, sv} \times (CMF_{sv,1} \times \dots \times CMF_{sv,x}) \times (CMF_1 \times \dots \times CMF_k) \quad (12)$$

$$N_{en} = C_{en} \times N_{spf, en} \times (CMF_{en,1} \times \dots \times CMF_{en,y}) \times (CMF_1 \times \dots \times CMF_k) \quad (13)$$

$$N_{ex} = C_{ex} \times N_{spf, ex} \times (CMF_{ex,1} \times \dots \times CMF_{ex,z}) \times (CMF_1 \times \dots \times CMF_k) \quad (14)$$

where,

- $N_{spf, mv}$ = predicted average multiple-vehicle non-entrance/exit crash frequency for base conditions, crashes/yr;
- $N_{spf, sv}$ = predicted average single-vehicle non-entrance/exit crash frequency for base conditions, crashes/yr;
- $N_{spf, en}$ = predicted average ramp-entrance-related crash frequency for base conditions, crashes/yr;
- $N_{spf, ex}$ = predicted average ramp-exit-related crash frequency for base conditions, crashes/yr;
- C_{mv} = local calibration factor for multiple-vehicle non-entrance/exit crashes;
- C_{sv} = local calibration factor for single-vehicle non-entrance/exit crashes;
- C_{en} = local calibration factor for ramp-entrance-related crashes;
- C_{ex} = local calibration factor for ramp-exit-related crashes;
- $CMF_{mv, 1} \dots CMF_{mv, w}$ = crash modification factors for multiple-vehicle crashes at a site with specific geometric design features w ;
- $CMF_{sv, 1} \dots CMF_{sv, x}$ = crash modification factors for single-vehicle crashes at a site with specific geometric design features x ;
- $CMF_{en, 1} \dots CMF_{en, y}$ = crash modification factors for ramp-entrance-related crashes at a site with specific geometric design features y ;
- $CMF_{ex, 1} \dots CMF_{ex, z}$ = crash modification factors for ramp-exit-related crashes at a site with specific geometric design features z ; and
- $CMF_1 \dots CMF_k$ = crash modification factors for freeway segment crashes at a site with specific geometric design features k .

The first term in parentheses in Equations 11 to 14 recognizes that the influence of some geometric factors is unique to each crash type. In contrast, the second term in parentheses in these equations recognizes that some geometric factors have a similar influence on all crash types.

Highway Safety Database

The Highway Safety Information System (HSIS) was used as the primary source of data for model calibration and validation. The “HSIS” states California, Maine, and Washington were identified as including ramp volume data, which was of fundamental importance to all aspects of the project. These data were not available from the other HSIS states. Hence, the database assembly focused on these three states. They are called the “study states” in this report.

In addition to ramp volume data, each study state database included a range of data describing the location, area type, traffic characteristics, geometry, and lane use for freeway segments. The data acquired from these databases is summarized in Table 29.

TABLE 29. Freeway variables from HSIS database

Category	Variable	Description
Descriptive	state	Source of data (CA, ME, WA)
	rte_nbr	State route number
	rte_suf	State route suffix
	county	County number (established by state DOT)
	begmp	Begin milepost (established by state DOT in CA, WA; by researchers for ME)
	endmp	End milepost (established by state DOT in CA, WA; by researchers for ME)
	seg_lng	Segment length, miles
	rodwycls	Road functional classification (established by HSIS staff)
	rururb	Area type (urban, rural)
Traffic	ave_adt	Segment AADT averaged for a three-year period
	entr_to_begmp_adt	AADT of ramp located at entr_begmp (see Table 30)
	exit_to_begmp_adt	AADT of ramp located at exit_begmp (see Table 30)
	entr_to_endmp_adt	AADT of ramp located at entr_endmp (see Table 30)
	exit_to_endmp_adt	AADT of ramp located at exit_endmp (see Table 30)
	weav_aadt_inc_ent	AADT of ramp entering weaving section for travel in increasing direction
	weav_aadt_inc_ext	AADT of ramp exiting weaving section for travel in increasing direction
	weav_aadt_dec_ent	AADT of ramp entering weaving section for travel in decreasing direction
	weav_aadt_dec_ext	AADT of ramp exiting weaving section for travel in decreasing direction
	ramp_aadt	AADT of ramp associated with speed-change lane 1
	:	repeat variable above for each of up to four speed-change lanes on segment
Crash	nk_mv	Count of reported fatal, multiple-vehicle non-entrance/exit crashes during three-year period
	na_mv	Count of reported incapacitating-injury, multiple-vehicle non-entrance/exit crashes during three-year period
	nb_mv	Count of reported non-incapacitating-injury, multiple-vehicle non-entrance/exit crashes during three-year period
	nc_mv	Count of reported possible-injury, multiple-vehicle non-entrance/exit crashes during three-year period
	no_mv	Count of reported property-damage-only, multiple-vehicle non-entrance/exit crashes during three-year period
	:	repeat five variables above for single-vehicle non-entrance/exit crashes, crashes in ramp entrance area, and crashes in ramp exit area

The data identified as “Descriptive” in Table 29 were obtained directly from the HSIS database for each study state. The data identified as “Traffic” or “Crash Data” were derived from the HSIS data. SAS software was used to manipulate the HSIS data to compute the desired variables. The ramp data identified in the table required that each ramp be visually located first (using aerial photography) using the freeway milepost reference system.

As discussed in Appendix B, several of the geometry and lane use variables in the study state databases were of unknown accuracy. Also, several variables often had subtly different definitions among states. Moreover, the study state databases often did not include variables that

describe road-related factors known to be associated with crash frequency. To overcome these limitations, the study-state databases were enhanced using data from other sources. These variables are listed in Table 30. The collection of these data required the location of each ramp using geographic coordinates and aerial photography, based on the freeway milepost reference system in HSIS.

TABLE 30. Freeway variables from supplemental data sources

Category	Variable	Description
Descriptive	lat_lon_coord	Latitude and longitude of begin milepost
	inc_lane_use	Special lane use for travel in increasing milepost
	dec_lane_use	Special lane use for travel in decreasing milepost
	inc_shldr_use	Use of shoulder by time of day for travel in increasing milepost
	dec_shldr_use	Use of shoulder by time of day for travel in decreasing milepost
Traffic	pct_hrs	Proportion of hours in average day that volume exceeds 1,000 veh/h/ln
	pct_veh	Proportion of AADT during hours where volume exceeds 1,000 veh/h/ln
Roadway	inc_lanes	Number of lanes for travel in increasing milepost
	dec_lanes	Number of lanes for travel in decreasing milepost
	inc_drop-add_lanes	Number of lane drops or adds on seg. for travel in increasing milepost
	dec_drop-add_lanes	Number of lane drops or adds on seg. for travel in decreasing milepost
	out_shld_meas	Outside shoulder width (average of both directions)
	lane_meas	Lane width (average for all lanes in both directions)
	in_meas	Width of inside shoulders and non-shoulder median (= median width)
	in_shld_meas	Inside shoulder width (average of both directions)
	med_width_meas	Width of median measured between near edges of inside shoulder
med_nontrav_meas	Width of median barrier, if present	
Roadside or median	med_type_meas	Median type (1 = raised curb, 2 - barrier, 3 = depressed or unsurfaced)
	in_barrier_off	Average offset to barrier in median, measured from face of barrier to near edge of inside shoulder
	in_barrier_len	Total length of barrier in median
	out_barrier_off	Average offset to barrier on roadside, measured from face of barrier to near edge of outside shoulder
	out_barrier_len	Total length of barrier on roadside
	inc_clear_zone	Average clear zone width for travel in increasing milepost
	dec_clear_zone	Average clear zone width for travel in decreasing milepost
Alignment	nbr_curves	Count of curves on segment
	curv_rad	Radius of curve 1
	curv_ang_deg	Deflection angle of curve 1
	curv_lgt_ft	Length of curve 1
	curv_begmp	Begin milepost for curve 1
	curv_lgt_on_seg	Length of curve 1 on segment
	:	repeat five variables above for each of up to three curves on segment

TABLE 30. Freeway variables from supplemental data sources (continued)

Category	Variable	Description
Speed-change lane	n_sc_lanes	Count of speed-change lanes adjacent to segment (in whole or part)
	sc_design	Design for speed-change lane 1 (e.g., P=parallel, T=taper, etc.)
	sc_lane_use	Lane use for speed-change lane 1 (e.g., N = normal, R=meter)
	sc_type	Orientation of speed-change lane 1 (e.g., entrance/exit, left/right side)
	sc_mrk_begmp	Freeway begin milepost at start of speed-change lane1 pavement marking
	sc_mrk_endmp	Freeway end milepost at end of speed-change lane 1 pavement marking
	sc_lgt_on_seg	Length of speed-change lane 1
	sc_ramp_lanes	Number of lanes in speed-change lane 1 at gore point
	sc_trav_dir	Freeway travel direction adjacent to speed-change lane 1
	:	repeat eight variables above for each of up to four speed-change lanes on segment
Weaving section	inc_A_lanes	Number of lanes on freeway and ramps before the weaving section
	inc_B_lanes	Number of lanes on freeway (including auxiliary lanes) in the weaving section
	inc_C_lanes	Number of lanes on freeway and ramps after weaving section
	inc_D_lanes	Number of lanes on <u>right-side</u> entrance ramp before weaving section
	inc_E_lanes	Number of lanes on <u>right-side</u> exit ramp after weaving section
	inc_Lw	Length of weaving section (gore to gore)
	inc_wev_lgt_on_seg	Length of weaving section on segment
	dec_A_lanes	Number of lanes on freeway and ramps before the weaving section
	dec_B_lanes	Number of lanes on freeway (including auxiliary lanes) in the weaving section
	dec_C_lanes	Number of lanes on freeway and ramps after weaving section
	dec_D_lanes	Number of lanes on <u>right-side</u> entrance ramp before weaving section
	dec_E_lanes	Number of lanes on <u>right-side</u> exit ramp after weaving section
	dec_Lw	Length of weaving section (gore to gore)
	dec_wev_lgt_on_seg	Length of weaving section on segment
Other	ramp_exit_cnt	Count of ramp exit gore points adjacent to segment
	ramp_ent_cnt	Count of ramp entrance gore points adjacent to segment
	in_rumble	Proportion of segment length with rumble strips on inside shoulders
	out_rumble	Proportion of segment length with rumble strips on outside shoulders
	entr_begmp	Milepost for ramp entrance marked gore point. Ramp is located on side of road where travel is in increasing milepost and upstream of segment begin milepost (Q ramp)
	exit_begmp	Milepost for ramp exit marked gore point. ramp is located on side of road where travel is in decreasing milepost and downstream of segment begin milepost (R ramp)
	entr_endmp	Milepost for ramp entrance marked gore point. Ramp is located on side of road where travel is in decreasing milepost and upstream of segment end milepost (S ramp)
	exit_endmp	Milepost for ramp exit marked gore point. Ramp is located on side of road where travel is in increasing milepost and downstream of segment end milepost (P ramp)

One source of enhanced data was the continuous traffic counting station data routinely collected by each state DOT. The freeway station nearest to each segment in the study state database was identified and used to compute the proportion of hours per day that are considered

to have “high volume” and the proportion of daily traffic using the segment during these high-volume hours.

Aerial photography was used as a second source of enhanced data. These photographs were obtained from the Internet using Google Earth software. The data collected include the width of road cross section elements, barrier presence and location, horizontal curvature, ramp configuration, ramp entrance location, and median type. A description of the variables acquired from aerial photography is provided in Table 30.

The “inc_lane_use” and “dec_lane_use” variables were used to identify the type of lane use that exists on a segment. Lane uses considered include: bus-only lane, reversible lane, truck-only lane, and HOV lane. These uses were not ranked high in the prioritization process, as documented in Chapter 3. Hence, only “normal” lane use is represented in the freeway and speed-change lane database. For similar reasons, segments with “shoulder use by time of day” are not represented in the database.

CMF DEVELOPMENT

This part of the chapter describes the development of three CMFs. The first section describes the development of a CMF that predicts the effect of lane-change frequency on crash frequency. The second section describes the development of a CMF that predicts the effect of high-volume conditions on crash frequency. The last section describes the development of a CMF that predicts the effect of horizontal curvature on crash frequency.

Lane-Change CMF

The lane-change CMF is intended to reflect the effect of lane-changing activity on crash frequency. A review of the literature (documented in Chapter 2) indicated that lane-change frequency is highest in the vicinity of ramp entrances and ramp exits. It then declines with increasing distance from the ramp. It also increases in proportion to the ramp volume. Equation 4 (in Chapter 2) was derived to describe these influences in the form of a crash modification factor.

High-Volume CMF

The volume-to-capacity ratio relates the demand volume to the capacity of a roadway segment. As volume nears capacity, average speed tends to decrease and headway is reduced. Logically, these changes have some influence on crash characteristics, including crash frequency, crash type distribution (i.e., single vehicle versus multiple vehicle), and crash severity distribution.

Some research has been undertaken to examine the relationship between volume-to-capacity ratio and crash character. This research typically compares average hourly volume estimates with the crashes that occur during the same hour for one or more years. In this manner, the analysis is often structured by time of day. There are issues of sample size, day versus night, and autocorrelation that complicate this type of analysis.

A review of the literature (documented in Chapter 2) confirmed an association between time of day and crash frequency, as well as between volume-to-capacity ratio and crash

frequency. It also highlights some of the aforementioned issues. Based on the findings from the literature review, it was rationalized that a “complete” safety evaluation (and models that support this evaluation) should consider all of the crashes that occur during a 24-hour period; not just those crashes that occur during a particular hour (e.g., the peak hour). Treatments that improve safety during one hour of the day may degrade safety during other hours. Moreover, given that crashes are rare events, the safety evaluation should be based on annual crash frequency; not just those crashes occurring during a peak hour, day, or month. Finally, the safety predictive models should include variables that reflect a sensitivity to the fact that high-volume conditions tend to last for only a few peak hours, and sometimes only during a peak season.

Two statistics were developed to support a complete safety evaluation and provide the sensitivity to recurring high-volume conditions. These statistics were derived from a pragmatic perspective. That is, it was determined that they had to be quantifiable by practitioners that use the predictive method. The first statistic developed is the “proportion of hours in the average day that volume exceeds 1,000 veh/h/ln” (i.e., proportion of hours). The second statistic developed is the “proportion of AADT during hours where volume exceeds 1,000 veh/h/ln” (i.e., “proportion of volume”). Both statistics are defined to have a value of zero if the volume on the associated segment does not exceed the threshold value for any hour of the day.

Both statistics were quantified using the continuous traffic counting station data routinely collected by each state DOT. The freeway station nearest to each segment in the study state database was identified and the hourly volume distribution for the average day acquired. This distribution was then used to compute the hourly traffic volume for each hour of the average day for each segment.

The threshold value of 1,000 veh/h/ln was used to define “high-volume” conditions. It was selected after considering several values. The volume of 1,000 veh/h/ln corresponds to an average vehicle headway of 3.6 s. The freeway speed-volume relationship shown in Chapter 23 of the *Highway Capacity Manual* (Highway, 2000) suggests that the average speed tends to drop as flow rates increase beyond 1,000 veh/h/ln. This trend suggests that drivers are reducing speed to improve their comfort and safety as their headway gets shorter than 3.6 s.

Higher threshold values were considered because they would reflect the presence of a more congested condition. However, with a threshold of 1,000 veh/h/ln, only 44 percent of the segments were found to have a non-zero value for either statistic. With a higher threshold, this percentage decreased significantly, leaving a large majority of segments with no information about the extent of traffic congestion they experience.

The value of both statistics increases with an increase in the number of hours that exceed the threshold value. If the volume during each hour of the day exceeds the threshold value, then both statistics equal 1.0. In general, the proportion-of-hours statistic is large when hourly volumes are continuously high throughout the day (i.e., the hourly volume distribution is relatively flat during daylight hours). In contrast, the proportion-of-volume statistic is large when hourly volumes are continuously high *or* when there are a few peak hours with an exceptionally large volume.

The hourly distribution of traffic volume on two freeway segments is shown in Figure 39. Figure 39a shows the distribution as a proportion of the AADT volume. Route 51 is shown to have a “flatter” distribution during the daylight hours than Route 5. Figure 39b shows the distribution in terms of hourly volume per lane. Route 51 is shown to have 16 hours that exceed the threshold value (proportion of hours = 0.67) and 87 percent of its volume served during these hours (proportion of volume = 0.87). Route 5 has 2 hours that exceed the threshold value (proportion of hours = 0.08) and 15 percent of its volume served during these hours (proportion of volume = 0.15).

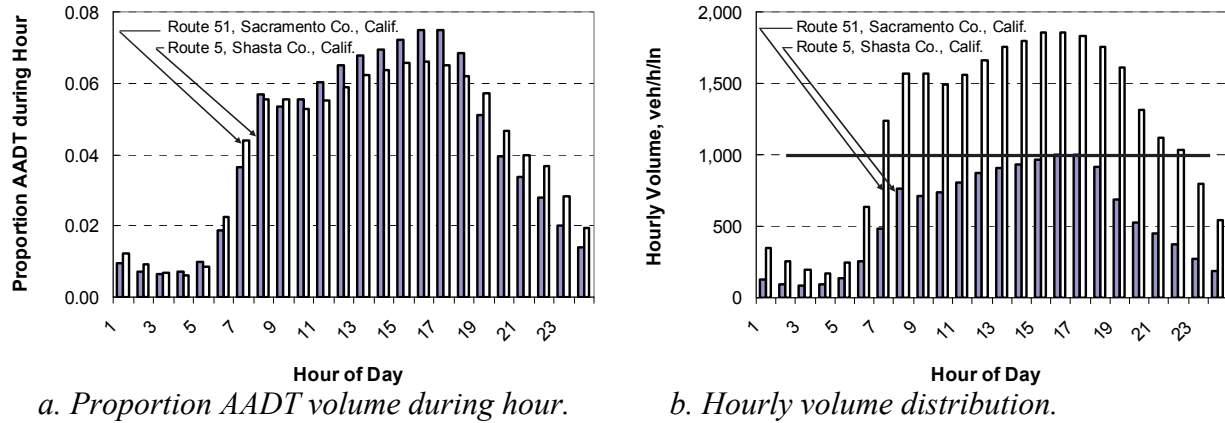


Figure 39. Hourly volume distribution for two freeway segments.

The trend in the proportion-of-volume statistic for several hundred freeway segments is shown in Figure 40. A similar trend is found for the proportion-of-hours statistic. There are many segments with a statistic value of 0.0 because these segments do not experience an hourly volume in excess of 1,000 veh/h/ln during the average day.

The trend in the data in Figure 40 indicates that the statistic value increases with increasing daily volume per lane. However, there is considerable variability in this variable value for segments with a volume in the range of 10,000 to 25,000 veh/day/ln. The variability declines for higher volumes, which indicates that these segments consistently operate at high volume for most, or all, of the day. The variability in this statistic suggests that it may contain information about segment conditions, beyond that provided by the *AADT* and number-of-lanes variables.

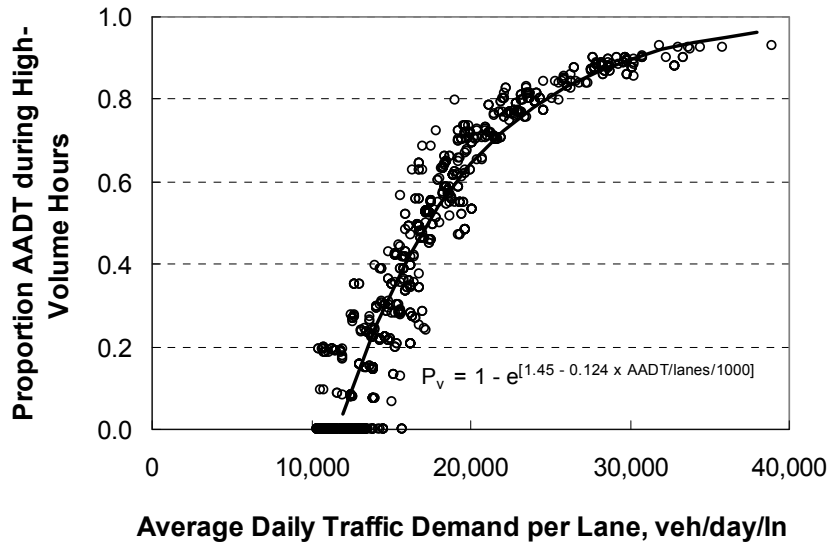


Figure 40. Proportion-of-volume statistic for freeway segments in three states.

The CMF used to represent the effect of high-volume conditions is described using the following equation.

$$CMF_{hv} = e^{b_{hv} P_{hv}} \quad (15)$$

where,

CMF_{hv} = high volume crash modification factor;

b_{hv} = calibration coefficient; and

P_{hv} = proportion of AADT during hours where volume exceeds 1,000 veh/h/ln.

The CMF is shown using the proportion-of-volume statistic. A similar CMF can be derived using the proportion-of-hours statistic. However, only one of these CMFs is used in the model given that they are highly correlated.

Horizontal Curve CMF

The horizontal curve CMF is defined by the following equation.

$$CMF_{hc} = \frac{N_{seg} + N_{curve}}{N_{seg}} \quad (16)$$

where,

CMF_{hc} = horizontal curve crash modification factor;

N_{seg} = predicted average crash frequency on segment (regardless of curvature), crashes/yr; and

N_{curve} = predicted average additional crashes due to curvature; crashes/yr.

The following equations are rationalized to represent the components of Equation 16.

$$N_{seg} = a AADT^b L_c CMF_i \quad (17)$$

$$N_{curve} = a AADT^b I_c f_d CMF_i \quad (18)$$

$$f_d = \frac{(1.47 V_c)^2}{32.2 R} - e \quad (19)$$

where,

CMF_i = crash modification factor for element i (i = lane width, shoulder width, etc.);

L_c = length of horizontal curve ($= I_c \times R / 5280 / 57.3$), mi;

I_c = curve deflection angle, degrees;

f_d = side friction demand factor;

V_c = average curve speed, mi/h;

e = superelevation rate, ft/ft; and

R = curve radius, ft.

Equation 18 does not include curve length L_c as a measure of exposure. Rather, curve deflection angle I_c is rationalized as the appropriate measure of exposure for crashes that occur because the segment is curved. Just as segment length L represents the product of forward velocity and travel time, deflection angle represents the product of angular velocity and travel time.

Side friction demand is included in Equation 18 as being logically correlated with crash frequency. As side friction demand reaches the roll threshold for tall vehicles, the propensity for a roll-over crash increases. Also, as side friction demand reaches the limit of available friction, the propensity for sliding off the road increases. The relationship between crash rate and side friction demand derived by Bonneson et al. (2007b) is shown in Figure 41.

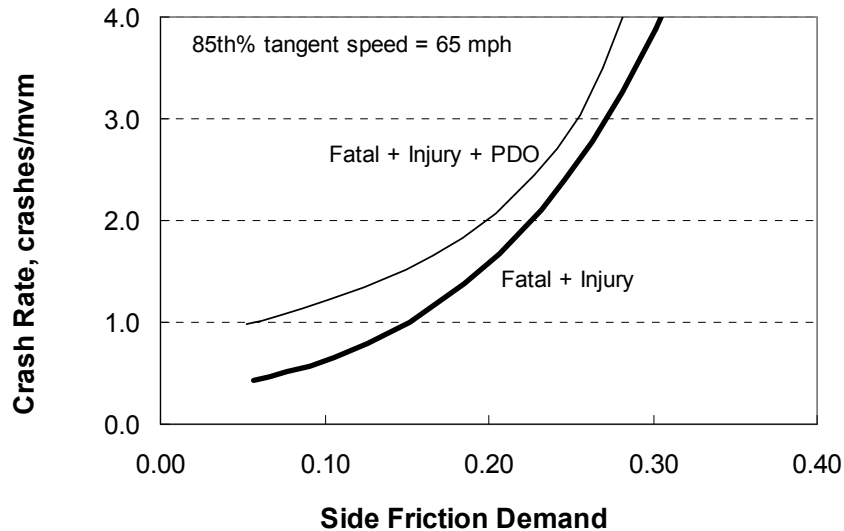


Figure 41. Relationship between crash rate and side friction demand.

Equations 16 through 19 can be combined to yield the following horizontal curve CMF.

$$CMF_{hc} = 1.0 + b_0 \frac{(1.47 V_c)^2}{32.2 R^2} \quad (20)$$

where,

b_0 = calibration coefficient.

The contribution of the superelevation term (i.e., $e/100$) in Equation 19 is small and is removed for mathematical convenience. This CMF is compared in Figure 16 with similar CMFs for several highway types.

The speed variable in Equation 20 is not available in the study state databases. However, the typical freeway speed limit is similar among the three states. In rural areas, it is 70, 65, and 70 mi/h for California, Maine, and Washington, respectively. In urban areas, it is 65, 55, and 60 mi/h in California, Maine, and Washington, respectively.

METHODOLOGY

This part of the chapter describes the methodology used to calibrate the freeway segment and speed-change lane safety predictive models. It is divided into three sections. The first section describes several supplemental variables used to calibrate the predictive models. The second section describes several analytic relationships used to calibrate non-homogeneous segments. The last section provides an overview of the approach used to calibrate the predictive models.

Supplemental Variables

As noted in a previous part of this chapter, several variables in the database were obtained from aerial photographs of the freeway segments and speed-change lanes represented in the study state databases. Of these variables, some of the more complex ones are defined in this section.

Ramp Entrance/Exit Length and Type

Ideally, the defined location of a speed-change lane for use in a predictive model would coincide with that used in the *Green Book* (Policy, 2004). However, crash location attributes in most state DOT databases are not sufficiently refined as to allow the accurate identification of crashes associated with the speed-change lane definitions in the *Green Book*, as shown in Figure 11. More importantly, these databases do not explicitly identify speed-change-related crashes.

Given the challenges in identifying crashes associated with speed-change lane operation, a revised definition of speed-change lane location was developed. The revised definition was dictated primarily by the desire to identify all speed-change-related crashes. To this end, the entrance ramp speed-change lane is considered to coincide with the “ramp entrance length” shown in Figure 11, and include all lanes associated with the freeway and ramp for a common travel direction. Similarly, the exit ramp speed-change lane is considered to coincide with the “ramp exit length” shown in Figure 11, and include all lanes associated with the freeway and

ramp for a common travel direction. These definitions are consistent with the ramp entrance and exit sites identified in Figure 38.

By applying the aforementioned definition, a speed-change-related crash is identified as a crash that is located between the taper point and the gore point and on the same side of the freeway as the ramp. This definition is likely to identify most speed-change-related crashes, but it may also identify some freeway crashes that are not associated with the speed-change lane. For this reason, some factors that influence crash frequency on freeway segments (e.g., lane width) may also influence crashes in the speed-change lane.

Weaving Length and Type

Entrance-exit ramp pairs that form a weaving section were identified in the database. In all cases, these ramp pairs were on the right-hand side of the freeway. The type of weaving section was also identified using the definitions in Chapter 13 of the *Highway Capacity Manual* (Highway, 2000). Figure 42 illustrates the three weaving section types defined in this manual. There are 17 mi of Type A weaving section in the database and 19 mi of Type B weaving section in the database. In contrast, there are only 1.3 mi of Type C weaving section in the database. There were no two-sided Type C weaving sections in the database (this configuration is not shown in Figure 42).

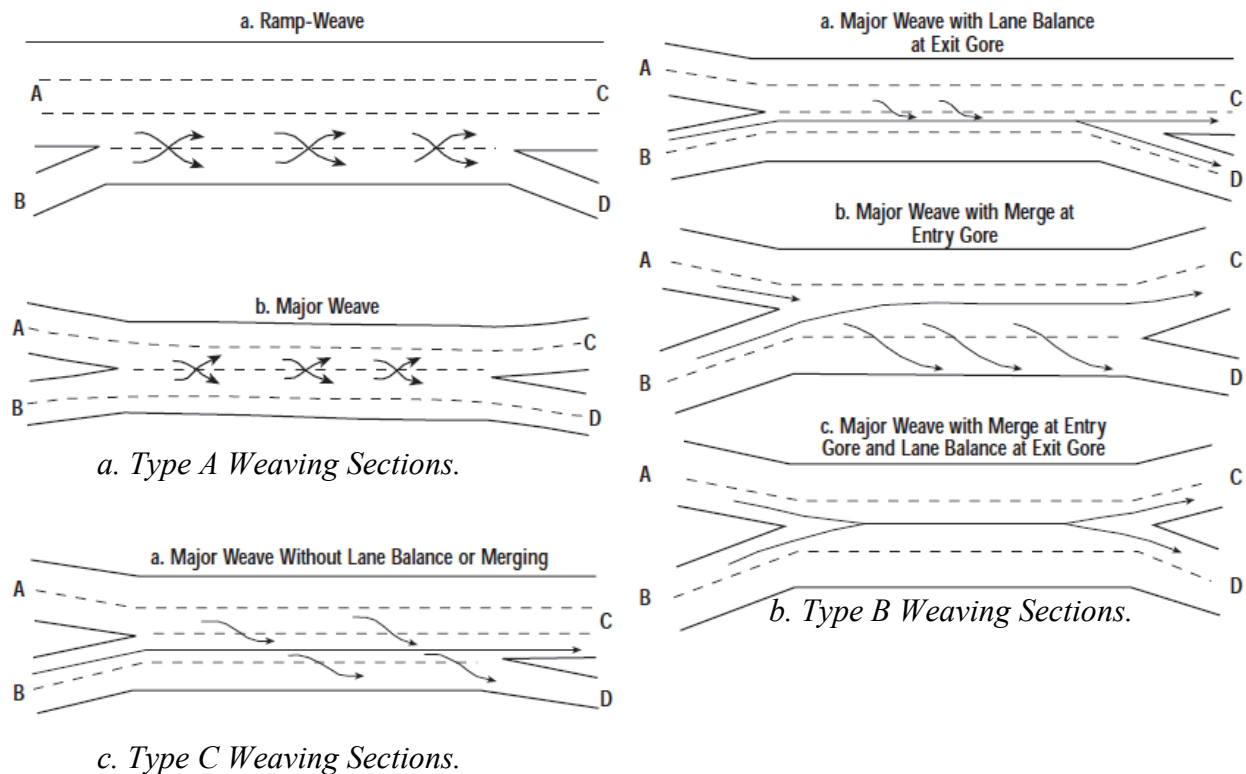


Figure 42. Weaving section types.

It is generally recognized that the length of the weaving section has an important influence on the operation of the freeway segment. This influence relates to the degree to which

the weaving activity is concentrated along the freeway. In recognition of a possible correlation between weaving section concentration and crash frequency, the length of the weaving section was also included in the database. The convention used to measure this length is shown in Figure 43.

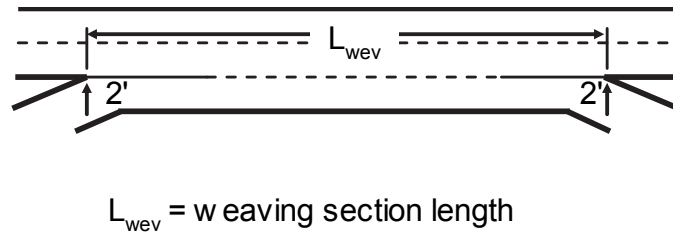


Figure 43. Weaving section length measurement.

Horizontal Clearance Distance

The clear zone distance was measured from the outside edge of the traveled way to either the nearest continuous obstruction (e.g., fence line, utility poles, etc.) or the near edge of the frontage road traveled way, whichever is closer to the freeway. If a barrier was present on the roadside for only a portion of the segment, the clear zone distance was measured only for that portion of the segment without the barrier.

Longitudinal Barriers

Longitudinal barriers (i.e., cable barrier, concrete barrier, guardrail, or bridge rail) were noted when present on a segment. Attributes used to quantify barrier presence include barrier offset, length, and width. Barrier offset, length, and width were each measured separately for inside and outside locations (e.g., inside barrier offset, outside barrier offset, etc.).

Barrier offset represents a lateral distance measured from the near edge of the shoulder to the face of the barrier (i.e., it does not include the width of the shoulder). Barrier length represents the length of lane paralleled by a barrier; it is a total for both travel directions. For example, if the outside barrier extends for the length of the roadway on both sides of the roadway, then the outside barrier length equals twice the segment length.

Median barrier width represents either the physical width of the barrier if only one barrier is used, or the lateral distance between barrier “faces” if two parallel barriers are provided in the median area. A barrier face is the side of the barrier that is exposed to vehicle traffic.

Analytic Relationships for Non-Homogeneous Segments

In most instances, the segments in the study state databases were not homogeneous in terms of the variables of interest. One or more geometric elements were often found to start or end at some point along the length of a segment. When this occurs, the length of the segment associated with the element’s initial condition and the length associated with its changed

condition were recorded in the database. Geometric elements that were sometimes only partially located on a segment are identified in the following list.

- horizontal curve presence,
- weaving section presence,
- ramp entrance presence,
- ramp exit presence,
- rumble strip presence on inside shoulder,
- rumble strip presence on outside shoulder,
- median barrier presence, and
- roadside barrier presence.

CMFs are typically developed for application to homogeneous segments. Thus, they do not include variables that allow them to be modified for application to segments on which they only partially apply. However, the following equation was used to convert a CMF for homogeneous segments into one that could be used for non-homogeneous segments.

$$CMF_{i|agg} = (1.0 - P_{L,i})1.0 + P_{L,i} CMF_i \quad (21)$$

where,

- $CMF_{i|agg}$ = aggregated CMF for element i ;
- $P_{L,i}$ = proportion of the segment length with element i ; and
- CMF_i = crash modification factor for element i .

To illustrate the use of Equation 21, it can be combined with Equation 20 to compute the aggregate CMF for segments with combined curve and tangent portions. The result is shown in the following equation.

$$CMF_{hc|agg} = 1.0 + b_0 \frac{(1.47 V)^2}{32.2 R^2} P_c \quad (22)$$

where,

- $CMF_{hc|agg}$ = aggregated horizontal curve CMF for a segment with both tangent and curved portions;
- P_c = proportion of the segment length with curvature; and
- CMF_{hc} = horizontal curve crash modification factor.

Modeling Approach

Combined Regression Models

The calibration activity used statistical analysis software that employs maximum likelihood methods and a negative binomial distribution of crash frequency. Four models were calibrated. The form of each model is shown in the following equations.

$$N_{mv} = N_{spf,mv} \times (CMF_{mv,1} \times \dots \times CMF_{mv,w}) \times (CMF_1 \times \dots \times CMF_k) \quad (23)$$

$$N_{sv} = N_{spf,sv} \times (CMF_{sv,1} \times \dots \times CMF_{sv,x}) \times (CMF_1 \times \dots \times CMF_k) \quad (24)$$

$$N_{en} = N_{spf,en} \times (CMF_{en,1} \times \dots \times CMF_{en,y}) \times (CMF_1 \times \dots \times CMF_k) \quad (25)$$

$$N_{ex} = N_{spf,ex} \times (CMF_{ex,1} \times \dots \times CMF_{ex,z}) \times (CMF_1 \times \dots \times CMF_k) \quad (26)$$

The SPFs associated with these models are defined using the following equations.

$$N_{spf,mv} = \left(L - 0.5 \sum L_{en,seg,i} - 0.5 \sum L_{ex,seg,i} \right) e^{b_{mv,0} + b_{mv,1} \ln(AADT/1,000)} \quad (27)$$

$$N_{spf,sv} = \left(L - 0.5 \sum L_{en,seg,i} - 0.5 \sum L_{ex,seg,i} \right) e^{b_{sv,0} + b_{sv,1} \ln(AADT/1,000)} \quad (28)$$

$$N_{spf,en} = \left(\sum L_{en,seg,i} \right) e^{b_{en,0} + b_{en,1} \ln(AADT/2,000)} \quad (29)$$

$$N_{spf,ex} = \left(\sum L_{ex,seg,i} \right) e^{b_{ex,0} + b_{ex,1} \ln(AADT/2,000)} \quad (30)$$

where,

- L = length of segment, mi;
- $L_{en,seg,i}$ = length of ramp entrance i on segment, mi;
- $L_{ex,seg,i}$ = length of ramp exit i on segment, mi;
- $AADT$ = AADT volume on segment, veh/day; and
- $b_{j,i}$ = calibration coefficients for model j ($j = mv, sv, en, ex$), $i = 0, 1$.

The second term of Equations 23 to 26 recognizes that the influence of some geometric factors is unique to each crash type. In contrast, the third term of these equations recognizes that some geometric factors have a similar influence on all crash types.

The use of common CMFs in multiple models required the use of a combined-model approach. With this approach, the regression analysis evaluated all four models simultaneously and used the total log-likelihood statistic for all four models to determine the best fit calibration coefficients. A simulation analysis was undertaken to determine if this type of regression would bias the calibration coefficients or their standard error. The results of this analysis indicated that: (1) the coefficients were not biased and (2) that the standard error of those coefficients associated with a variable were not biased. The regression analysis is described in more detail in the next part of this chapter.

Cross-Sectional Database

The database is described as cross sectional (as opposed to panel). It represents a common three-year study period for all observations. Study duration in “years” is represented as an offset variable in the regression model.

One reason for using cross-sectional data for model calibration relates to the accuracy of the AADT values in most highway safety databases. Examination of the AADT volume in the assembled database (and examination of associated database and state DOT documentation) indicated that segment AADT volume is frequently extrapolated by the state DOT from partial-year counts taken at temporary count stations located several miles from the subject segment. Thus, there are accuracy implications associated with this temporal and spatial extrapolation. Moreover, State DOT practice when a current count is not available for a segment is sometimes to adjust the AADT volume from the last year it was counted (which could be several years

previous); sometimes it is to leave the variable as missing. In fact, it is common for a segment's AADT volume to be missing for one or more years. In these cases, the researchers for this project have had to estimate a value using the AADT volume trends for adjacent years and adjacent segments. Thus, averaging each segment's AADT volume over years minimizes the variability in AADT volume which, based on the aforementioned observations, is considered largely random. More generally, cross-sectional data provide a more robust predictive model than panel data when the year-to-year variability in the independent variables is largely random.

A second reason for using cross-sectional data for model calibration is to minimize the problems associated with over-representation of segments or intersections with zero crashes. Statistical methods have been developed to improve the fit of a model to this "zero-inflated" data. However, Lord et al. (2007) indicate that when these methods have been applied to highway crash data, they have (1) an inherent tendency to over-fit the data, (2) a theoretic explanation of dual state highway safety that is problematic, and (3) the potential to obfuscate the interpretation of predictive model trend and coefficient meaning. Thus, summing each segment's crashes over years minimizes the proportion of segments or intersections with zero crashes in the database and precludes the need for a dual state distribution.

It was assumed that segment crash frequency is Poisson distributed, and that the distribution of the mean crash frequency for a group of similar segments is gamma distributed. In this manner, the distribution of crashes for a group of similar segments can be described by the negative binomial distribution. The variance of this distribution is described by the following equation.

$$V[X] = y N + \frac{(y N)^2}{K L} \quad (31)$$

where,

$V[X]$ = crash frequency variance for a group of similar locations, crashes²;

N = predicted average crash frequency, crashes/yr;

X = reported crash count for y years, crashes;

y = time interval during which X crashes were reported, yr; and

K = inverse dispersion parameter (= $1/k$, where k = overdispersion parameter), mi^{-1} .

Prediction of PDO Crash Frequency

Experience with regression-based calibration of SPFs and CMFs using total crashes and using only FI crashes indicates that the calibration coefficients often vary among model types for common variables. Some of this variation is likely due to the fact that geometric elements often have a different effect on FI crashes than on PDO crashes. As a result, the search for correlation and possible causation is challenged when using total crash data to build total crash prediction models because total crashes combine FI and PDO crashes. The presence of barrier is one example of a geometric component that has a different effect on FI crash frequency than it has on PDO crash frequency. These observations suggest that PDO-based models are preferable to total-crash models.

It is widely-recognized that PDO crash counts vary widely on a regional basis due to significant variation in the reporting threshold. This issue was discussed in Chapter 4 where it

was noted that there was wide variation in the representation of PDO crashes in the study-state databases. When crash frequency varies systematically from county to county, district to district, and state to state because of formal and informal differences in the reporting threshold, the use of PDO crash data to build PDO crash prediction models is problematic. This observation suggests that PDO-based and total-crash models are likely to include regional biases and added uncertainty due to variation in reporting thresholds.

Based on these issues, the following model-building process was developed. It was rationalized that (1) FI crash data are likely to provide the most accurate insight into regression model structure and factors influencing safety and (2) PDO-based models are preferred to total-crash models. However, the development of PDO regression models is problematic because of under-reporting. Therefore, the FI regression model structure was developed first and then used as a “starting point” for the development of the PDO regression model.

To minimize the influence of reporting threshold variability among counties, districts, and states, the “county” and “state” variables were treated as both fixed and random effects in separate versions of the PDO regression model. The Hausman test (Hausman, 1978) was used to determine when the fixed-effect treatment was appropriate. The fixed-effect treatment of county and state required that the PDO regression model include an indicator variable for each county and state combination represented in the database.

Regardless of whether a fixed- or random-effect model is used, significant county and state differences often emerged through this process. As a result, some geometric variables that were significant in the FI model were less significant in the PDO model. Specifically, the standard error was increased for those geometric variables that varied more among counties than within counties. Unfortunately, it is not known whether the among-county variation is due to differences in reporting threshold (as may be informally applied at different levels within a state) or because of differences in geometry. This approach often resulted in the PDO model having fewer geometric variables than the FI model. However, the benefit of this approach is that the remaining calibration coefficients in the PDO model are less likely to be biased by differences in the reporting threshold.

MODEL CALIBRATION FOR FI CRASHES

This part of the chapter describes the calibration and validation of the combined freeway segment and speed-change lane predictive models based on FI crashes. The first section identifies the data used for model calibration. The second section describes the structure of each of the four predictive models, as used in the regression analysis. The third section summarizes statistical analysis methods used for model calibration. The fourth section describes the regression statistics for each of the calibrated models. The fifth section describes a validation of the calibrated models. The sixth section describes the proposed predictive models and calibrated CMFs. The seventh section provides a sensitivity analysis of the predictive models over a range of traffic demands. The last section describes some techniques for extending the models to address atypical freeway conditions.

Calibration Data

The data collection process consisted of a series of activities that culminated in the assembly of a highway safety database suitable for the development of a comprehensive safety prediction methodology for freeways and speed-change lanes. These activities are described Chapter 4.

Crash data were identified for each segment and speed-change lane using the most recently available data from the HSIS. Three years of crash data were identified for each segment. The analysis period is 2005, 2006, and 2007 for the California and Washington segments. It is 2004, 2005, and 2006 for the Maine segments. The AADT volume for each year was merged into the assembled database. A total of 8,381 FI crashes and 18,045 PDO crashes are represented in the database. Additional information about the database is provided in Chapter 4.

Model Development

This section describes the proposed predictive models and the methods used to calibrate them. The following regression model form was used to facilitate the analysis of the combined models.

$$N_j = (N_{mv}I_{mv} + N_{sv}I_{sv} + N_{en}I_{en} + N_{ex}I_{ex}) \times CMF_{lw} \times CMF_{isw} \times CMF_{mb|agg} \quad (32)$$

with,

$$CMF_{lw} = \begin{cases} e^{b_{lw}(W_l - 12)} & : \text{If } W_l < 13 \text{ ft} \\ e^{b_{lw}(1.0)} & : \text{If } W_l \geq 13 \text{ ft} \end{cases} \quad (33)$$

$$CMF_{isw} = e^{b_{is}(W_{is} - 6)} \quad (34)$$

$$CMF_{mb|agg} = (1.0 - P_{ib})1.0 + P_{ib} e^{b_{bar}/W_{icb}} \quad (35)$$

where,

- N_j = predicted average crash frequency for model j ($j = mv$ if $I_{mv} = 1.0$; $j = sv$ if $I_{sv} = 1.0$; $j = en$ if $I_{en} = 1.0$; $j = ex$ if $I_{ex} = 1.0$); crashes/yr;
- N_{mv} = predicted average multiple-vehicle non-entrance/exit crash frequency, crashes/yr;
- N_{sv} = predicted average single-vehicle non-entrance/exit crash frequency, crashes/yr;
- N_{en} = predicted average ramp-entrance-related crash frequency, crashes/yr;
- N_{ex} = predicted average ramp-exit-related crash frequency, crashes/yr.
- I_{mv} = crash indicator variable (= 1.0 if multiple-vehicle non-entrance/exit crash data, 0.0 otherwise);
- I_{sv} = crash indicator variable (= 1.0 if single-vehicle non-entrance/exit crash data, 0.0 otherwise);
- I_{en} = crash indicator variable (= 1.0 if ramp-entrance-related crash data, 0.0 otherwise);
- I_{ex} = crash indicator variable (= 1.0 if ramp-exit-related crash data, 0.0 otherwise);
- CMF_{lw} = lane width crash modification factor;
- W_l = lane width, ft;
- CMF_{isw} = inside shoulder width crash modification factor;
- W_{is} = inside shoulder width, ft;
- $CMF_{mb|agg}$ = aggregated median barrier crash modification factor;

P_{ib} = proportion of segment length with a barrier present in the median (i.e., inside);
 W_{icb} = distance from edge of inside shoulder to barrier face, ft;
 b_i = calibration coefficient for condition i (see Table 31); and
 other variables are previously defined.

The final form of the regression model is described here, before the discussion of regression analysis results. However, this form reflects the findings from several preliminary regression analyses where alternative model forms were examined. The form that is described represents that which provided the best fit to the data, while also having coefficient values that are logical and constructs that are theoretically defensible and properly bounded.

Equation 32 combines four “component” models. The multiple-vehicle and single-vehicle models apply to basic freeway segments. The two ramp-related models apply to freeway segments with a speed-change lane. The regression model form of each model is described in the following subsections. The CMFs in Equation 32 apply to all component models. The other CMFs that were developed were found to provide a better fit to the data when applied to just one or two of the component models.

Freeway Segment - Multiple-Vehicle Non-Entrance/Exit Crash Frequency

$$N_{mv} = (N_{spf,mv,4}I_4 + N_{spf,mv,6}I_6 + N_{spf,mv,8}I_8 + N_{spf,mv,10}I_{10}) \times (CMF_{mv,lc|agg} \times CMF_{mv,mw|agg} \times CMF_{mv,hc|agg} \times CMF_{mv,hv}) \quad (36)$$

with,

$$N_{spf,mv,4} = (L - 0.5 \sum L_{en,seg,i} - 0.5 \sum L_{ex,seg,i}) e^{b_{mv,4} + b_{mv,1} \ln(AADT/1,000) + b_{mv,rural} I_{rural}} \quad (37)$$

$$N_{spf,mv,6} = (L - 0.5 \sum L_{en,seg,i} - 0.5 \sum L_{ex,seg,i}) e^{b_{mv,6} + b_{mv,1} \ln(AADT/1,000) + b_{mv,rural} I_{rural}} \quad (38)$$

$$N_{spf,mv,8} = (L - 0.5 \sum L_{en,seg,i} - 0.5 \sum L_{ex,seg,i}) e^{b_{mv,8} + b_{mv,1} \ln(AADT/1,000) + b_{mv,rural} I_{rural}} \quad (39)$$

$$N_{spf,mv,10} = (L - 0.5 \sum L_{en,seg,i} - 0.5 \sum L_{ex,seg,i}) e^{b_{mv,10} + b_{mv,1} \ln(AADT/1,000) + b_{mv,rural} I_{rural}} \quad (40)$$

$$CMF_{mv,lc|agg} = (0.5 f_{wev,inc} f_{lc,inc}) + (0.5 f_{wev,dec} f_{lc,dec}) \quad (41)$$

$$f_{wev,inc} = (1.0 - P_{wevB,inc}) 1.0 + P_{wevB,inc} e^{b_{wev}/L_{wev,inc}} \quad (42)$$

$$f_{wev,dec} = (1.0 - P_{wevB,dec}) 1.0 + P_{wevB,dec} e^{b_{wev}/L_{wev,dec}} \quad (43)$$

$$f_{lc,inc} = \left(1.0 + \frac{e^{-b_x X_{b,ent} + b_v \ln(AADT_{b,ent}/1,000)}}{b_x L} [1.0 - e^{-b_x L}] \right) \times \left(1.0 + \frac{e^{-b_x X_{e,ext} + b_v \ln(AADT_{e,ext}/1,000)}}{b_x L} [1.0 - e^{-b_x L}] \right) \quad (44)$$

$$f_{lc,dec} = \left(1.0 + \frac{e^{-b_x X_{e,ent} + b_v \ln(AADT_{e,ent}/1,000)}}{b_x L} [1.0 - e^{-b_x L}] \right) \times \left(1.0 + \frac{e^{-b_x X_{b,ext} + b_v \ln(AADT_{b,ext}/1,000)}}{b_x L} [1.0 - e^{-b_x L}] \right) \quad (45)$$

$$CMF_{mv,mw|agg} = (1.0 - P_{ib}) e^{b_{mv,mw}(W_m - 2W_{is} - 48)} + P_{ib} e^{b_{mv,mw}(2W_{icb} - 48)} \quad (46)$$

$$CMF_{mv,hc|agg} = 1.0 + b_{mv,cr} \sum_{i=1}^3 \left(\frac{5,730}{R_i} \right)^2 P_{c,i} \quad (47)$$

$$CMF_{mv,hv} = e^{b_{mv,hv} P_{hv}} \quad (48)$$

where,

- $N_{spf, mv, n}$ = predicted average multiple-vehicle non-entrance/exit crash frequency for number of through lanes n ($n = 4, 6, 8, 10$); crashes/yr;
- I_n = cross section indicator variable (= 1.0 if cross section has n lanes, 0.0 otherwise);
- $CMF_{mv, lc|agg}$ = aggregated lane change crash modification factor for multiple-vehicle crashes;
- $CMF_{mv, mw|agg}$ = aggregated median width crash modification factor for multiple-vehicle crashes;
- $CMF_{mv, hc|agg}$ = aggregated horizontal curve crash modification factor for multiple-vehicle crashes;
- $CMF_{mv, hv}$ = high-volume crash modification factor for multiple-vehicle crashes;
- I_{rural} = area type indicator variable (= 1.0 if area is rural, 0.0 if it is urban);
- $f_{wev, inc}$ = weaving section adjustment factor for travel in increasing milepost direction;
- $f_{wev, dec}$ = weaving section adjustment factor for travel in decreasing milepost direction;
- $f_{lc, inc}$ = lane change adjustment factor for travel in increasing milepost direction;
- $f_{lc, dec}$ = lane change adjustment factor for travel in decreasing milepost direction;
- $P_{wevB, inc}$ = proportion of segment length within a Type B weaving section for travel in increasing milepost direction;
- $P_{wevB, dec}$ = proportion of segment length within a Type B weaving section for travel in decreasing milepost direction;
- $L_{wev, inc}$ = weaving section length for travel in increasing milepost direction (may extend beyond segment boundaries), mi;
- $L_{wev, dec}$ = weaving section length for travel in decreasing milepost direction (may extend beyond segment boundaries), mi;
- $X_{b, ent}$ = distance from segment begin milepost to nearest upstream entrance ramp gore point, for travel in increasing milepost direction, mi;
- $X_{b, ext}$ = distance from segment begin milepost to nearest downstream exit ramp gore point, for travel in decreasing milepost direction, mi;
- $X_{e, ent}$ = distance from segment end milepost to nearest upstream entrance ramp gore point, for travel in decreasing milepost direction, mi;
- $X_{e, ext}$ = distance from segment end milepost to nearest downstream exit ramp gore point, for travel in increasing milepost direction, mi;
- $AADT_{b, ent}$ = AADT volume of entrance ramp located at distance $X_{b, ent}$, veh/day;

- $AADT_{b, ext}$ = AADT volume of exit ramp located at distance $X_{b, ext}$, veh/day;
 $AADT_{e, ent}$ = AADT volume of entrance ramp located at distance $X_{e, ent}$, veh/day;
 $AADT_{e, ext}$ = AADT volume of exit ramp located at distance $X_{e, ext}$, veh/day;
 W_m = median width (measured from near edges of traveled way in both travel directions), ft;
 R_i = radius of curve i , ft;
 $P_{c,i}$ = proportion of segment length with curve i ;
 P_{hv} = proportion of AADT during hours where volume exceeds 1,000 veh/h/ln;
 b_i = calibration coefficient for condition i (see Table 31) and other variables are previously defined.

The lane change CMF, as described in Equations 41 to 45, is a directional CMF because its terms are derived to apply to specific travel directions along the segment. The constant “0.5” in Equation 41 is used to compute an average of the CMF value for each direction. The weaving section adjustment factor provides a sensitivity to weaving section type. The preliminary regression analysis indicated that the Type B weaving sections were correlated with crash frequency, so the CMF is derived to include this sensitivity. The constant “48” in Equation 46 represents a base median width of 60 ft and a base inside shoulder width of 6 ft (i.e., 48 = 60 - 2×6).

Freeway Segment - Single-Vehicle Non-Entrance/Exit Crash Frequency

$$\begin{aligned}
 N_{sv} = & \left(L - 0.5 \sum L_{en, seg, i} - 0.5 \sum L_{ex, seg, i} \right) e^{b_{sv, 0} + b_{sv, 1} \ln(AADT/1,000) + b_{sv, 2} n} \\
 & \times \left(CMF_{sv, osw|agg} \times CMF_{sv, mw|agg} \times CMF_{sv, oc|agg} \times CMF_{sv, ob|agg} \right) \\
 & \times \left(CMF_{sv, hc|agg} \times CMF_{sv, hv} \times CMF_{sv, rs|agg} \right)
 \end{aligned} \quad (49)$$

with,

$$CMF_{sv, osw|agg} = \left(1.0 - \sum P_{c,i} \right) e^{b_{s, tan} (W_s - 10)} + \left(\sum P_{c,i} \right) e^{b_{s, cur} (W_s - 10)} \quad (50)$$

$$CMF_{sv, mw|agg} = \left(1.0 - P_{ib} \right) e^{b_{sv, mw} (W_m - 2W_{is} - 48)} + P_{ib} e^{b_{sv, mw} (2W_{icb} - 48)} \quad (51)$$

$$CMF_{sv, oc|agg} = \left(1.0 - P_{ob} \right) e^{b_{oc} (W_{hc} - W_s - 20)} + P_{ob} e^{b_{oc} (W_{ocb} - 20)} \quad (52)$$

$$CMF_{sv, ob|agg} = \left(1.0 - P_{ob} \right) 1.0 + P_{ob} e^{b_{bar} / W_{ocb}} \quad (53)$$

$$CMF_{sv, hc|agg} = 1.0 + b_{sv, cr} \sum_{i=1}^3 \left(\frac{5,730}{R_i} \right)^2 P_{c,i} \quad (54)$$

$$CMF_{sv, hv} = e^{b_{sv, hv} P_{hv}} \quad (55)$$

$$CMF_{sv, rs|agg} = \left(1.0 - \sum P_{c,i} \right) f_{tan} + \left(\sum P_{c,i} \right) f_{cur} \quad (56)$$

$$f_{tan} = 0.5 \left([1.0 - P_{ir}] 1.0 + P_{ir} e^{b_{rs, tan}} \right) + 0.5 \left([1.0 - P_{or}] 1.0 + P_{or} e^{b_{rs, tan}} \right) \quad (57)$$

$$f_{cur} = 0.5 \left([1.0 - P_{ir}] 1.0 + P_{ir} e^{b_{rs,cur}} \right) + 0.5 \left([1.0 - P_{or}] 1.0 + P_{or} e^{b_{rs,cur}} \right) \quad (58)$$

where,

- n = number of through lanes on segment ($n = 4, 6, 8, 10$);
- $CMF_{sv,osw|agg}$ = aggregated outside shoulder width crash modification factor for single-vehicle crashes;
- $CMF_{sv,mw|agg}$ = aggregated median width crash modification factor for single-vehicle crashes;
- $CMF_{sv,oc|agg}$ = aggregated outside clearance crash modification factor for single-vehicle crashes;
- $CMF_{sv,ob|agg}$ = aggregated outside barrier crash modification factor for single-vehicle crashes;
- $CMF_{sv,hc|agg}$ = aggregated horizontal curve crash modification factor for single-vehicle crashes;
- $CMF_{sv,hv}$ = high-volume crash modification factor for single-vehicle crashes;
- $CMF_{sv,rs|agg}$ = aggregated shoulder rumble strip crash modification factor for single-vehicle crashes;
- W_s = outside shoulder width, ft;
- W_{hc} = clear zone width, ft;
- P_{ob} = proportion of segment length with a barrier present on the roadside (i.e., outside);
- W_{ocb} = distance from edge of outside shoulder to barrier face, ft;
- f_{tan} = factor for rumble strip presence on tangent portions of the segment;
- f_{cur} = factor for rumble strip presence on curved portions of the segment;
- P_{ir} = proportion of segment length with rumble strips present on the inside shoulders;
- P_{or} = proportion of segment length with rumble strips present on the outside shoulders;
- b_i = calibration coefficient for condition i (see Table 31) and other variables are previously defined.

The shoulder rumble strip CMF, as described in Equations 56 to 58, is sensitive to rumble strip location in terms of their use on the outside shoulders, inside shoulders, or both. The constant “0.5” in Equations 57 and 58 is used to compute an average of the CMF value for both locations. The constant “20” in Equation 52 represents a base clear zone width of 30 ft and a base outside shoulder width of 10 ft (i.e., $20 = 30 - 10$).

Speed-Change Lane - Ramp Entrance Crash Frequency

$$N_{en} = \left(\sum L_{en,seg,i} \right) e^{b_{en,0} + b_{en,1} \ln(AADT/2,000) + b_{en,2} n + b_{en,rural} I_{rural}} \times \left(CMF_{mv,mw|agg} \times CMF_{mv,hc|agg} \times CMF_{mv,hv|agg} \times CMF_{en|agg} \right) \quad (59)$$

with,

$$CMF_{en|agg} = \frac{\sum \left(L_{en,seg,i} e^{b_{left} I_{left,i} + b_{en,len} / L_{en,i} + b_{en,adt} \ln(AADT_{r,i} / 1,000)} \right)}{\sum \left(L_{en,seg,i} \right)} \quad (60)$$

where,

- $CMF_{en|agg}$ = aggregated ramp entrance crash modification factor;
- $I_{left,i}$ = ramp side indicator variable for ramp i ($= 1.0$ if entrance or exit is on left side of through lanes, 0.0 if it is on right side);
- $L_{en,i}$ = length of ramp entrance for ramp i (may extend beyond segment boundaries), mi;
- $AADT_{r,i}$ = AADT volume of ramp i , veh/day;
- b_i = calibration coefficient for condition i (see Table 31) and other variables are previously defined.

This model is derived to predict the total number of ramp-entrance-related crashes on a segment with one or more ramp entrances. This form is dictated by the non-homogeneous character of most freeway segments in the database. Specifically, many segments include only a portion of a speed-change lane. The calibrated version of this model can be algebraically re-written such that it can be applied separately to individual ramp entrance speed-change lanes.

Speed-Change Lane - Ramp Exit Crash Frequency

$$N_{ex} = \left(\sum L_{ex,seg,i} \right) e^{b_{ex,0} + b_{ex,1} \ln(AADT/2,000)} \times \left(CMF_{mv,mw|agg} \times CMF_{mv,hc|agg} \times CMF_{mv,hv|agg} \times CMF_{en|agg} \right) \quad (61)$$

with,

$$CMF_{ex|agg} = \frac{\sum \left(L_{ex,seg,i} e^{b_{left} L_{left,i} + b_{ex,len} L_{ex,i}} \right)}{\sum \left(L_{ex,seg,i} \right)} \quad (62)$$

where,

- $CMF_{ex|agg}$ = aggregated ramp exit crash modification factor;
- $L_{ex,i}$ = length of ramp exit for ramp i (may extend beyond segment boundaries), mi;
- b_i = calibration coefficient for condition i (see Table 31); and
- other variables are previously defined.

This model is derived to predict the total number of ramp-exit-related crashes on a segment with one or more ramp exits. This form is dictated by the non-homogeneous character of most freeway segments in the database. Specifically, many segments include only a portion of a speed-change lane. The calibrated version of this model can be algebraically re-written such that it can be applied separately to individual ramp exit speed-change lanes.

Barrier Variable Calculations

Two key variables that are needed for the evaluation of barrier presence are the inside barrier distance W_{icb} and the outside barrier distance W_{ocb} . As indicated in Equations 35 and 53, this distance is included as a divisor in the exponential term. This relationship implies that the correlation between distance and crash frequency is an inverse one (i.e., crash frequency decreases with increasing distance). When multiple sections of barrier exist along the segment, a length-weighted average of the *reciprocal* of the individual distances is needed to properly reflect this inverse relationship. The length used to weight the average is the barrier length.

Additional key variables include the proportion of segment length with a barrier present in the median P_{ib} and the proportion of segment length with a barrier present on the roadside P_{ob} . Equations for calculating these proportions and the aforementioned distances are described in the following paragraphs.

For segments with a continuous barrier centered in the median (i.e., symmetric median barrier), the following equations are used to estimate W_{icb} and P_{ib} .

$$W_{icb} = \frac{2L}{\sum \frac{L_{ib,i}}{W_{off,in,i} - W_{is}} + \frac{2L - \sum L_{ib,i}}{0.5(W_m - 2W_{is} - W_{ib})}} \quad (63)$$

$$P_{ib} = 1.0 \quad (64)$$

where,

$L_{ib,i}$ = length of lane paralleled by inside barrier i (include both travel directions), mi;

W_{ib} = inside barrier width (measured from barrier face to barrier face), ft; and

$W_{off,in,i}$ = horizontal clearance from the edge of the traveled way to the face of inside barrier i , ft.

The first summation term “ \sum ” in Equation 63 applies to short lengths of barrier in the median. It indicates that the ratio of barrier length L_{ib} to clearance distance $W_{off,in,i} - W_{is}$ should be computed for each individual length of barrier that is found in the median along the segment (e.g., a barrier protecting a sign support). The continuous median barrier is not included in this summation.

For segments with a continuous barrier adjacent to one roadbed (i.e., asymmetric median barrier), the following equations should be used to estimate W_{icb} and P_{ib} .

$$W_{icb} = \frac{2L}{\frac{L}{W_{near} - W_{is}} + \sum \frac{L_{ib,i}}{W_{off,in,i} - W_{is}} + \frac{L - \sum L_{ib,i}}{W_m - 2W_{is} - W_{ib} - W_{near}}} \quad (65)$$

$$P_{ib} = 1.0 \quad (66)$$

where,

W_{near} = “near” horizontal clearance from the edge of the traveled way to the continuous median barrier (measure for both travel directions and use the smaller distance), ft.

Similar to the previous guidance, the first summation term “ \sum ” in Equation 65 applies to short lengths of barrier in the median. The ratio of barrier length L_{ib} to the distance $W_{off,in,i} - W_{is}$ should be computed for each individual length of barrier that is found in the median along the segment. The continuous median barrier is not included in this summation.

For segments with a depressed median and some short sections of barrier in the median (e.g., bridge rail), the following equations should be used to estimate W_{icb} and P_{ib} .

$$W_{icb} = \frac{\sum L_{ib,i}}{\sum \frac{L_{ib,i}}{W_{off,in,i} - W_{is}}} \quad (67)$$

$$P_{ib} = \frac{\sum L_{ib,i}}{2L} \quad (68)$$

For segments with depressed medians without a continuous barrier or short sections of barrier in the median, the following equation should be used to estimate P_{ib} .

$$P_{ib} = 0.0 \quad (69)$$

As suggested by Equation 35, the calculation of W_{icb} is not required when $P_{ib} = 0.0$.

For segments with barrier on the roadside, the following equations should be used to estimate W_{ocb} and P_{ob} .

$$W_{ocb} = \frac{\sum L_{ob,i}}{\sum \frac{L_{ob,i}}{W_{off,o,i} - W_s}} \quad (70)$$

$$P_{ob} = \frac{\sum L_{ob,i}}{2L} \quad (71)$$

where,

$L_{ob,i}$ = length of lane paralleled by outside barrier i (include both travel directions), mi; and
 $W_{off,o,i}$ = horizontal clearance from the edge of the traveled way to the face of outside barrier i , ft.

For segments without barrier on the roadside, the following equation should be used to estimate P_{ob} .

$$P_{ob} = 0.0 \quad (72)$$

As suggested by Equation 53, the calculation of W_{ocb} is not required when $P_{ob} = 0.0$.

Statistical Analysis Methods

The nonlinear regression procedure (NLMIXED) in the SAS software was used to estimate the proposed model coefficients. This procedure was used because the proposed predictive model is both nonlinear and discontinuous. The log-likelihood function for the negative binomial distribution was used to determine the best-fit model coefficients. Equation 31 was used to define the variance function for all models. The variable L in this equation was adjusted to account for the presence of one or more speed-change lanes on a segment. The procedure was set up to estimate model coefficients based on maximum-likelihood methods.

Several statistics were used to assess model fit to the data. One measure of model fit is the Pearson χ^2 statistic. This statistic is calculated using the following equation.

$$\chi^2 = \sum_{i=1}^n \frac{(X_i - y N_i)^2}{V[X]_i} \quad (73)$$

where,

n = number of observations.

This statistic follows the χ^2 distribution with $n-p$ degrees of freedom, where n is the number of observations (i.e., segments) and p is the number of model variables (McCullagh and Nelder, 1983). This statistic is asymptotic to the χ^2 distribution for larger sample sizes.

The root mean square error s_e is a useful statistic for describing the precision of the model estimate. It represents the standard deviation of the estimate when each independent variable is at its mean value. This statistic is computed using the following equation.

$$s_e = \frac{1.0}{y} \sqrt{\frac{\sum_{i=1}^n (X_i - y N_i)^2}{n-p}} \quad (74)$$

where,

s_e = root mean square error of the model estimate, crashes/yr.

The scale parameter ϕ is used to assess the amount of variation in the observed data, relative to the specified distribution. This statistic is calculated by dividing Equation 73 by the quantity $n-p$. A scale parameter near 1.0 indicates that the assumed distribution of the dependent variable is approximately equivalent to that found in the data (i.e., negative binomial).

Another measure of model fit is the coefficient of determination R^2 . This statistic is commonly used for normally distributed data. However, it has some useful interpretation when applied to data from other distributions when computed in the following manner (Kvalseth, 1985). It is computed using the following equation.

$$R^2 = 1.0 + \frac{SSE}{SST} \quad (75)$$

with,

$$SSE = \sum_{i=1}^n (X_i - y N_i)^2 \quad (76)$$

$$SST = \sum_{i=1}^n (X_i - \bar{X})^2 \quad (77)$$

where,

\bar{X} = average crash frequency for all n observations.

The last measure of model fit is the dispersion-parameter-based coefficient of determination R_k^2 . This statistic was developed by Miaou (1996) for use with data that exhibit a negative binomial distribution. It is computed using the following equation.

$$R_k^2 = 1.0 - \frac{k}{k_{null}} \quad (78)$$

where,

k_{null} = overdispersion parameter based on the variance in the observed crash frequency.

The null overdispersion parameter k_{null} represents the dispersion in the reported crash frequency, relative to the overall average crash frequency for all segments. This parameter can be

obtained using a null model formulation (i.e., a model with no independent variables but with the same error distribution, link function, and offset in years y).

Model Calibration

The predictive model calibration process was based on regression analysis using combined models, as discussed in the section titled Modeling Approach. With this approach, the component models and CMFs (represented by Equations 32 to 58) are calibrated using a database of common sites. This approach is needed because several CMFs were common to two or more component models. The database assembled for calibration included four replications of the original database. The dependent variable in the first replication was set equal to the multiple-vehicle crashes. The dependent variable in the second replication was set equal to the single-vehicle crashes. That for the third replication was set equal to the ramp-entrance-related crashes and that for the fourth replication was set equal to the ramp-exit-related crashes.

The predicted crash frequency from each of the four component models was computed for each segment. The four values were then totaled for each segment and compared with the total reported crash frequency for the segment. The difference between the two totals was then summed for all segments. This sum was found to be very small (i.e., less than 0.5 percent of the total reported crash frequency), so it was concluded that there was no bias in the component models in terms of their ability to predict total crash frequency.

The models were calibrated using the California and Washington data. The Maine data were reserved for model validation. The discussion in this section focuses on the findings from the model calibration. The findings from model validation are provided in the next section.

The results of the regression model calibration are presented in Table 31. The Pearson χ^2 statistic for the model is 4,069, and the degrees of freedom are 4036 ($= n - p = 4,076 - 40$). As this statistic is less than $\chi^2_{0.05, 4036} (= 4,185)$, the hypothesis that the model fits the data cannot be rejected.

The t-statistic for each coefficient is listed in the last column of Table 31. These statistics describe a test of the hypothesis that the coefficient value is equal to 0.0. Those t-statistics with an absolute value that is larger than 2.0 indicate that the hypothesis can be rejected with the probability of error in this conclusion being less than 0.05. For those few variables where the absolute value of the t-statistic is smaller than 2.0, it was decided that the variable was important to the model and its trend was found to be intuitive and, where available, consistent with previous research findings (even if the specific value was not known with a great deal of certainty as applied to this database).

TABLE 31. Freeway FI model statistical description–combined model–two states

Model Statistics		Value		
R^2 :		0.66		
Scale parameter ϕ :		1.01		
Pearson χ^2 :		4,069 ($\chi^2_{0.05, 4036} = 4,185$)		
Observations n_o :		1,644 seg. (7,379 injury or fatal crashes in 3 years) 584 ramp entrances, 462 ramp exits		
Calibrated Coefficient Values				
Variable	Inferred Effect of...	Value	Std. Dev.	t-statistic
$b_{mv, cr}$	Horizontal curvature on 2+ veh. crashes	0.0187	0.0069	2.7
$b_{sv, cr}$	Horizontal curvature on 1 veh. crashes	0.0847	0.0162	5.2
b_{hw}	Lane width	-0.0147	0.0374	-0.4
$b_{s, tan}$	Outside shoulder width on 1 veh. crashes, tangents	-0.0618	0.0175	-3.5
$b_{s, cur}$	Outside shoulder width on 1 veh. crashes, curves	-0.0850	0.0249	-3.4
b_{is}	Inside shoulder width	-0.0161	0.0062	-2.6
$b_{rs, tan}$	Shoulder rumble strip on 1 veh. crashes, tangents	-0.168	0.0782	-2.1
$b_{rs, cur}$	Shoulder rumble strip on 1 veh. crashes, curves	0.293	0.1185	2.5
$b_{mv, mw}$	Median width on 2+ veh. crashes	-0.00335	0.0009	-3.6
$b_{sv, mw}$	Median width on 1 veh. crashes	0.00042	0.0007	0.6
b_{bar}	Barrier presence	0.1023	0.0496	2.1
b_{oc}	Outside clearance on 1 veh. crashes	-0.00197	0.0054	-0.4
b_{wev}	Type B weaving section presence on 2+ veh. crashes	0.179	0.0549	3.3
b_v	Ramp AADT on lane-change-related crashes	-0.294	0.1507	-2.0
b_x	Distance from ramp on lane-change-related crashes	13.876	4.8850	2.8
b_{left}	Left side entrance or exit on speed-change lane crashes	0.487	0.5610	0.9
$b_{en, adt}$	Ramp AADT on ramp-entrance-related crashes	0.202	0.0754	2.7
$b_{en, len}$	Ramp entrance length on related crashes	0.0283	0.0150	1.9
$b_{ex, len}$	Ramp exit length on related crashes	0.0103	0.0108	1.0
$b_{mv, hv}$	High-volume conditions on 2+ veh. crashes	0.238	0.1515	1.6
$b_{sv, hv}$	High-volume conditions on 1 veh. crashes	-0.0804	0.1179	-0.7
$b_{mv, 4}$	4 lanes on 2+ vehicle crashes in urban areas	-6.000	0.536	-11.2
$b_{mv, 6}$	6 lanes on 2+ vehicle crashes in urban areas	-6.103	0.600	-10.2
$b_{mv, 8}$	8 lanes on 2+ vehicle crashes in urban areas	-6.192	0.649	-9.5
$b_{mv, 10}$	10 lanes on 2+ vehicle crashes in urban areas	-6.416	0.692	-9.3
$b_{mv, 1}$	AADT on 2+ vehicle crashes	1.620	0.141	11.5
$b_{mv, rural}$	Added effect of rural area type on 2+ veh. crashes	-0.582	0.062	-9.3
$b_{sv, 0}$	1 veh. crashes	-2.499	0.248	-10.1
$b_{sv, 2}$	Number of lanes on 1 veh. crashes	0.0328	0.023	1.4
$b_{sv, 1}$	AADT on 1 veh. crashes	0.700	0.080	8.7
$b_{en, 0}$	Ramp-entrance crashes in urban areas	-3.331	0.556	-6.0
$b_{en, 2}$	Number of lanes on ramp-ent. crashes in urban areas	-0.142	0.052	-2.7
$b_{en, 1}$	AADT on ramp-entrance crashes	1.248	0.202	6.2
$b_{en, rural}$	Added effect of rural area type on ramp-ent. crashes	-0.191	0.154	-1.2
$b_{ex, 0}$	Ramp-exit crashes	-3.017	0.626	-4.8
$b_{ex, 1}$	AADT on ramp-exit crashes	1.010	0.157	6.4

The findings from an examination of the coefficient values on the corresponding CMF or SPF predictions are documented in a subsequent section. In general, the sign and magnitude of the calibration coefficients in Table 31 are logical and consistent with previous research findings.

An indicator variable for the state of California was included in an initial version of the regression model. The coefficient for this variable was very small and not statistically significant. This finding is evidence that the combined model form is able to explain differences in crash occurrence among the two states.

Model Validation

Model validation was a two-step process. The first step required using the calibrated models to predict the crash frequency for sites from a third state (i.e., Maine). The objective of this step was to demonstrate the robustness of the model structure and its transferability to another state.

The second step required comparing the calibrated CMFs with similar CMFs reported in the literature, where such information was available. The objective of this step was to demonstrate that the calibrated CMFs were consistent with previous research findings.

The findings from the first step of the validation process are described in this section. Those from the second step are described in the next section.

The first step of the validation process consisted of several tasks. The first task was to quantify the local calibration factor for each of the four models (i.e., C_{mv} , C_{sv} , C_{en} , C_{ex}), which would be the first step for any agency using the *HSM* methodology. This produced a “re-calibrated” set of four models (i.e., the models with the coefficients from Table 31 plus the local calibration factors). The local calibration factor values for the Maine data are provided in the list below:

- Calibration factor for multiple-vehicle non-entrance/exit crashes, $C_{mv} = 1.27$
- Calibration factor for single-vehicle non-entrance/exit crashes, $C_{sv} = 1.08$
- Calibration factor for ramp-entrance-related crashes, $C_{en} = 0.89$
- Calibration factor for ramp-exit-related crashes, $C_{ex} = 0.95$

The second task was to apply the re-calibrated models to the Maine data to compute the predicted average crash frequency for each segment or speed-change lane (i.e., N_{mv} , N_{sv} , N_{en} , N_{ex}). The predicted crash frequency was then compared to the reported crash frequency for each site.

The third task was to compute the fit statistics and assess the robustness of the calibrated model. These statistics are listed in Table 32. The Pearson χ^2 statistic for each component model, and for the overall model, is less than $\chi^2_{0.05}$ so the hypothesis that the model fits the validation data cannot be rejected.

TABLE 32. Freeway model validation statistics

Component Model	R^2	R_k^2	Scale Parameter ϕ	Pearson χ^2	Deg. of Freedom	$\chi^2_{0.05, n-1}$
Multiple-veh. non-entrance/exit	0.57	0.89	1.14	228.4	201	235.1
Single-veh. non-entrance/exit	0.35	0.92	1.11	224.9	202	236.2
Ramp entrance related	0.28	0.97	1.20	68.3	57	75.6
Ramp exit related	0.41	0.70	0.60	38.3	64	83.7
Overall:	0.45		1.06	559.8	527	581.5

The findings from this validation step indicate that the trends in the Maine data are not significantly different from those in the California and Washington data. These findings also suggest that the model structure is transferable to other states (when locally calibrated) for the prediction of FI crash frequency. Based on these findings, the data for the three states were combined and used in a second regression model calibration. The larger sample size associated with the combined database reduced the standard error of several calibration coefficients. Bared and Zhang (2007) also used this approach in their development of predictive models for urban freeways.

Combined Model

The data from the three study states were combined and the predictive models were calibrated a second time using the combined data. The calibration coefficients for the four models are described in the next subsection. The subsequent four subsections describe the fit of each component model. The fit statistics were separately computed using the calibrated component model and an analysis of its residuals.

Aggregate Model

The results of the regression model calibration are presented in Table 33. The Pearson χ^2 statistic for the model is 4,574, and the degrees of freedom are 4,568 ($= n - p = 4,604 - 36$). As this statistic is less than $\chi^2_{0.05, 4568} (= 4,726)$, the hypothesis that the model fits the data cannot be rejected. Several segments were removed as a result of outlier analysis such that the calibration database included only 8,038 of the 8,381 crashes identified in Chapter 4.

The t-statistic for each coefficient is listed in the last column of Table 33. These statistics have generally increased, relative to their counterparts in Table 31, as a result of the increased sample size. With a few exceptions, these statistics have an absolute value that is larger than 2.0, which indicates that the null hypothesis can be rejected with the probability of error in this conclusion being less than 0.05. For those few variables where the absolute value of the t-statistic is smaller than 2.0, it was decided that the variable was important to the model and its trend was found to be intuitive and, where available, consistent with previous research findings (even if the specific value was not known with a great deal of certainty as applied to this database). This consistency is demonstrated in a subsequent section.

TABLE 33. Freeway FI model statistical description–combined model–three states

Model Statistics		Value		
R^2 :		0.65		
Scale parameter ϕ :		1.00		
Pearson χ^2 :		4,574 ($\chi^2_{0.05, 4568} = 4,726$)		
Observations n_o :		1,850 seg. (8,038 injury or fatal crashes in 3 years) 642 ramp entrances, 527 ramp exits		
Calibrated Coefficient Values				
Variable	Inferred Effect of...	Value	Std. Dev.	t-statistic
$b_{mv, cr}$	Horizontal curvature on 2+ veh. crashes	0.0172	0.0064	2.7
$b_{sv, cr}$	Horizontal curvature on 1 veh. crashes	0.0719	0.0144	5.0
b_{hw}	Lane width	-0.0376	0.0358	-1.1
$b_{s, tan}$	Outside shoulder width on 1 veh. crashes, tangents	-0.0647	0.0163	-4.0
$b_{s, cur}$	Outside shoulder width on 1 veh. crashes, curves	-0.0897	0.0248	-3.6
b_{is}	Inside shoulder width	-0.0172	0.0060	-2.9
$b_{rs, tan}$	Shoulder rumble strip on 1 veh. crashes, tangents	-0.209	0.0724	-2.9
$b_{rs, cur}$	Shoulder rumble strip on 1 veh. crashes, curves	0.274	0.1039	2.6
$b_{mv, mw}$	Median width on 2+ veh. crashes	-0.00302	0.0009	-3.5
$b_{sv, mw}$	Median width on 1 veh. crashes	0.00102	0.0006	1.6
b_{bar}	Barrier presence	0.131	0.0478	2.7
b_{oc}	Outside clearance on 1 veh. crashes	-0.00451	0.0052	-0.9
b_{wev}	Type B weaving section presence on 2+ veh. crashes	0.175	0.0519	3.4
b_v	Ramp AADT on lane-change-related crashes	-0.272	0.1421	-1.9
b_x	Distance from ramp on lane-change-related crashes	12.561	3.5232	3.6
b_{left}	Left side entrance or exit on speed-change lane crashes	0.594	0.5440	1.1
$b_{en, adt}$	Ramp AADT on ramp-entrance-related crashes	0.198	0.0730	2.7
$b_{en, len}$	Ramp entrance length on related crashes	0.0318	0.0147	2.2
$b_{ex, len}$	Ramp exit length on related crashes	0.0116	0.0095	1.2
$b_{mv, hv}$	High-volume conditions on 2+ veh. crashes	0.350	0.1350	2.6
$b_{sv, hv}$	High-volume conditions on 1 veh. crashes	-0.0675	0.1135	-0.6
$b_{mv, 4}$	4 lanes on 2+ vehicle crashes in urban areas	-5.470	0.426	-12.9
$b_{mv, 6}$	6 lanes on 2+ vehicle crashes in urban areas	-5.587	0.484	-11.5
$b_{mv, 8}$	8 lanes on 2+ vehicle crashes in urban areas	-5.635	0.525	-10.7
$b_{mv, 10}$	10 lanes on 2+ vehicle crashes in urban areas	-5.842	0.562	-10.4
$b_{mv, 1}$	AADT on 2+ vehicle crashes	1.492	0.115	13.0
$b_{mv, rural}$	Added effect of rural area type on 2+ veh. crashes	-0.505	0.058	-8.7
$b_{sv, 0}$	1 veh. crashes	-2.266	0.219	-10.4
$b_{sv, 2}$	Number of lanes on 1 veh. crashes	0.0351	0.022	1.6
$b_{sv, 1}$	AADT on 1 veh. crashes	0.646	0.071	9.1
$b_{en, 0}$	Ramp-entrance crashes in urban areas	-3.194	0.500	-6.4
$b_{en, 2}$	Number of lanes on ramp-ent. crashes in urban areas	-0.130	0.050	-2.6
$b_{en, 1}$	AADT on ramp-entrance crashes	1.173	0.187	6.3
$b_{en, rural}$	Added effect of rural area type on ramp-ent. crashes	-0.180	0.146	-1.2
$b_{ex, 0}$	Ramp-exit crashes	-2.679	0.488	-5.5
$b_{ex, 1}$	AADT on ramp-exit crashes	0.903	0.132	6.8

Indicator variables were included for the states of California and Maine in the regression model. The coefficient for each variable was very small and not statistically significant. This finding is evidence that the combined model form is able to explain differences in crash occurrence among states.

Model for Predicting Multiple-Vehicle Non-Ramp-Related Crash Frequency

The results of the multiple-vehicle model calibration are presented in Table 34. The Pearson χ^2 statistic for the model is 1,659, and the degrees of freedom are 1,577 ($= n - p = 1,591 - 14$). As this statistic is less than $\chi^2_{0.05, 1577} (= 1,670)$, the hypothesis that the model fits the data cannot be rejected. The R^2 for the model is 0.66. An alternative measure of model fit that is better suited to the negative binomial distribution is R_k^2 . The R_k^2 for the calibrated model is 0.92.

TABLE 34. Freeway FI model statistical description—multiple-vehicle model—three states

Model Statistics	Value
$R^2 (R_k^2)$:	0.66 (0.92)
Scale parameter ϕ :	1.05
Pearson χ^2 :	1,659 ($\chi^2_{0.05, 1577} = 1,670$)
Inverse dispersion parameter K :	17.6 mi^{-1}
Observations n_o :	1,591 segments (4,392 injury or fatal crashes in 3 years)
Standard deviation s_e :	± 1.07 crashes/yr

The inverse dispersion parameter is relatively large when compared to that for other models reported in the literature. This trend implies that there is less unexplained site-to-site variability in the predicted mean crash frequency for groups of similar sites. There are several reasons for this trend. Those reasons that tend to reduce the overall variability in the database include:

- The data is cross sectional such that each independent variable value is averaged for each site over the analysis period. In contrast, with panel data, each independent variable value is measured for each site for each year in the analysis period. Thus, cross-sectional data inherently have less variability than panel data when the year-to-year variability in the independent variables is largely random (Lord and Park, 2008). Of particular note is the random variability in the AADT data found in most highway safety databases, as discussed previously in the section titled Modeling Approach.
- The manual collection of geometric variables using aerial photographs for this project was found to significantly reduce the variability of these variables, relative to that found in the equivalent variables in highway safety databases obtained from state agencies. For example, the standard deviation of lane width in one state database is 2.0 ft while that in the manually assembled data for the same segments is 0.6 ft.
- The researchers that assembled the database for this project intentionally removed exceptionally short and exceptionally long segments for reasons of statistical control. This approach results in less variability in the database.

An additional reason for the relatively large inverse dispersion parameter value stems from this project’s development of a “full” model (i.e., one with multiple variables). This type of model inherently explains more variability than a simple model (e.g., an AADT-to-a-power model), and results in a larger inverse dispersion parameter (Mitra and Washington, 2007).

The coefficients in Table 33 were combined with Equations 37 to 40 to obtain the calibrated SPFs for multiple-vehicle non-entrance/exit crashes. The form of each model is described in the following equations.

$$N_{spf,mv,4} = \left(L - 0.5 \sum L_{en,seg,i} - 0.5 \sum L_{ex,seg,i} \right) e^{-5.470 + 1.492 \ln(AADT/1,000) - 0.505 I_{rural}} \quad (79)$$

$$N_{spf,mv,6} = \left(L - 0.5 \sum L_{en,seg,i} - 0.5 \sum L_{ex,seg,i} \right) e^{-5.587 + 1.492 \ln(AADT/1,000) - 0.505 I_{rural}} \quad (80)$$

$$N_{spf,mv,8} = \left(L - 0.5 \sum L_{en,seg,i} - 0.5 \sum L_{ex,seg,i} \right) e^{-5.635 + 1.492 \ln(AADT/1,000) - 0.505 I_{rural}} \quad (81)$$

$$N_{spf,mv,10} = \left(L - 0.5 \sum L_{en,seg,i} - 0.5 \sum L_{ex,seg,i} \right) e^{-5.842 + 1.492 \ln(AADT/1,000) - 0.505 I_{rural}} \quad (82)$$

The calibrated CMFs used with these SPFs are described in a subsequent section.

The fit of the calibrated models is shown in Figure 44. This figure compares the predicted and reported crash frequency in the calibration database. The trend line shown represents a “y = x” line. A data point would lie on this line if its predicted and reported crash frequency were equal. The data points shown represent the reported multiple-vehicle non-entrance/exit crash frequency for the segments used to calibrate the corresponding component model.

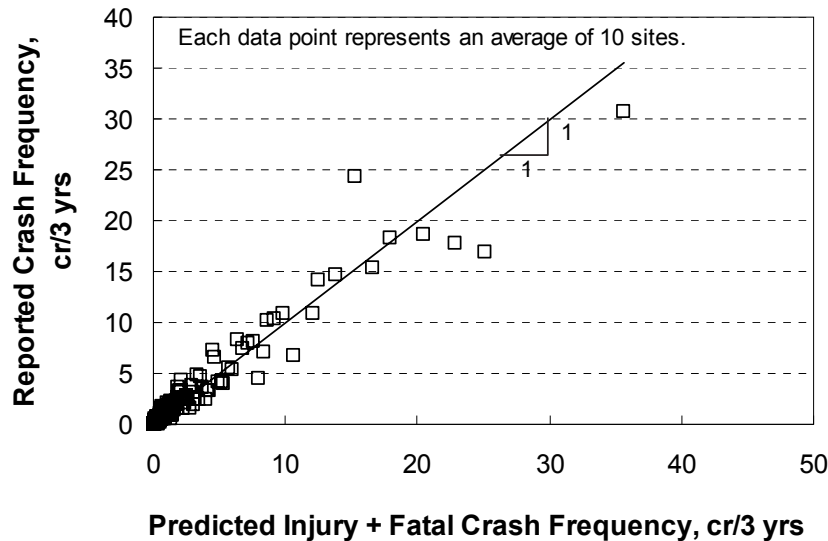


Figure 44. Predicted vs. reported multiple-vehicle freeway FI crashes.

Each data point shown in Figure 44 represents the average predicted and average reported crash frequency for a group of 10 segments. The data were sorted by predicted crash frequency

to form groups of segments with similar crash frequency. The purpose of this grouping was to reduce the number of data points shown in the figure and, thereby, to facilitate an examination of trends in the data. The individual segment observations were used for model calibration. In general, the data shown in the figure indicate that the model provides an unbiased estimate of expected crash frequency for segments experiencing up to 40 multiple-vehicle crashes in a three-year period.

Model for Predicting Single-Vehicle Non-Ramp-Related Crash Frequency

The results of the single-vehicle model calibration are presented in Table 35. The Pearson χ^2 statistic for the model is 1,836, and the degrees of freedom are 1,837 ($= n - p = 1,850 - 13$). As this statistic is less than $\chi^2_{0.05, 1837} (= 1,938)$, the hypothesis that the model fits the data cannot be rejected. The R^2 for the model is 0.65. The R_k^2 for the calibrated model is 0.93.

TABLE 35. Freeway FI model statistical description—single-vehicle model—three states

Model Statistics	Value
R^2 (R_k^2):	0.65 (0.93)
Scale parameter ϕ :	0.99
Pearson χ^2 :	1,836 ($\chi^2_{0.05, 1837} = 1,938$)
Inverse dispersion parameter K :	30.1 mi ⁻¹
Observations n_o :	1,850 segments (2,762 injury or fatal crashes in 3 years)
Standard deviation s_e :	± 0.51 crashes/yr

The inverse dispersion parameter is relatively large when compared to that for other models reported in the literature. The reasons for this trend were identified in the discussion associated with Table 34.

The coefficients in Table 33 were combined with Equation 49 to obtain the calibrated SPF for single-vehicle non-entrance/exit crashes. The form of this model is described in the following equation.

$$N_{spf,sv} = \left(L - 0.5 \sum L_{en,seg,i} - 0.5 \sum L_{ex,seg,i} \right) e^{-2.266 + 0.646 \ln(AADT/1,000) + 0.0351 n} \quad (83)$$

The calibrated CMFs used with this SPF are described in a subsequent section.

The fit of the calibrated model is shown in Figure 45. This figure compares the predicted and reported crash frequency in the calibration database. Each data point shown represents the average predicted and average reported crash frequency for a group of 10 segments. In general, the data shown in the figure indicate that the model provides an unbiased estimate of expected crash frequency for segments experiencing up to 15 single-vehicle crashes in a three-year period.

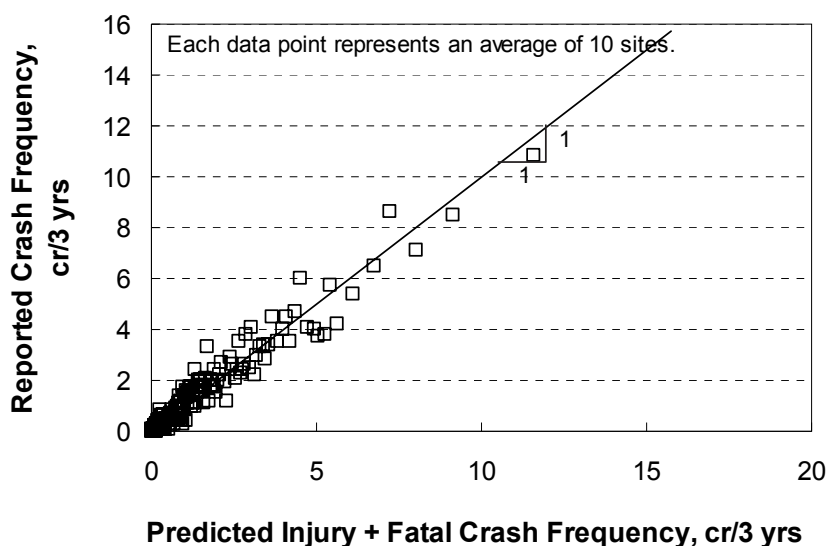


Figure 45. Predicted vs. reported single-vehicle freeway FI crashes.

Model for Predicting Ramp-Entrance-Related Crash Frequency

The results of the ramp-entrance-related model calibration are presented in Table 36. The Pearson χ^2 statistic for the model is 597, and the degrees of freedom are 630 ($= n - p = 642 - 12$). As this statistic is less than $\chi^2_{0.05, 630}$ ($= 690$), the hypothesis that the model fits the data cannot be rejected. The R^2 for the model is 0.50. The R_k^2 for the calibrated model is 0.96.

TABLE 36. Freeway FI model statistical description—ramp entrance model—three states

Model Statistics	Value
R^2 (R_k^2):	0.50 (0.96)
Scale parameter ϕ :	0.93
Pearson χ^2 :	597 ($\chi^2_{0.05, 630} = 690$)
Inverse dispersion parameter K :	26.1 mi^{-1}
Observations n_o :	642 ramp entrances (624 injury or fatal crashes in 3 years)
Standard deviation s_e :	± 0.47 crashes/yr

The coefficients in Table 33 were combined with Equation 59 to obtain the calibrated SPF for ramp-entrance-related crashes. The form of this model is described in the following equation.

$$N_{spf, en} = (L_{en}) e^{-3.194 + 1.173 \ln(AADT / 2,000) - 0.130 n - 0.180 I_{rural}} \quad (84)$$

The calibrated CMFs used with this SPF are described in a subsequent section. This SPF is applied to a ramp entrance speed-change lane, as shown in Figure 38. The “segment” length is equal to the ramp entrance length L_{en} , which is measured using the gore and taper points identified in Figure 11.

The fit of the calibrated model is shown in Figure 46. This figure compares the predicted and reported crash frequency in the calibration database. Each data point shown represents the average predicted and average reported crash frequency for a group of 10 segments. In general, the data shown in the figure indicate that the model provides an unbiased estimate of expected crash frequency for segments experiencing up to 8.0 ramp-entrance-related crashes in a three-year period.

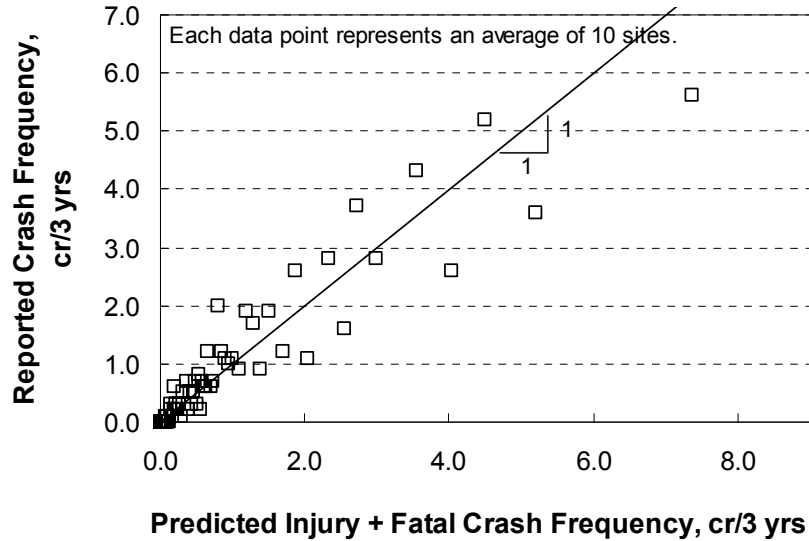


Figure 46. Predicted vs. reported ramp-entrance-related FI crashes.

Model for Predicting Ramp-Exit-Related Crash Frequency

The results of the ramp-exit-related model calibration are presented in Table 37. The Pearson χ^2 statistic for the model is 481, and the degrees of freedom are 518 ($= n - p = 527 - 9$). As this statistic is less than $\chi^2_{0.05, 518}$ ($= 572$), the hypothesis that the model fits the data cannot be rejected. The R^2 for the model is 0.41. The R_k^2 for the calibrated model is 0.95. The inverse dispersion parameter for this model is dimensionless because crash frequency variance was found to be insensitive to ramp exit length (i.e., the variable L was removed from Equation 31).

TABLE 37. Freeway FI model statistical description—ramp exit model—three states

Model Statistics	Value
R^2 (R_k^2):	0.41 (0.95)
Scale parameter ϕ :	0.91
Pearson χ^2 :	481 ($\chi^2_{0.05, 518} = 572$)
Inverse dispersion parameter K :	1.78
Observations n_o :	527 ramp exits (624 injury or fatal crashes in 3 years)
Standard deviation s_e :	± 0.47 crashes/yr

The coefficients in Table 33 were combined with Equation 61 to obtain the calibrated SPF for ramp-exit-related crashes. The form of this model is described in the following equation.

$$N_{spf,ex} = (L_{ex}) e^{-2.679 + 0.903 \ln(AADT/2,000)} \quad (85)$$

The calibrated CMFs used with this SPF are described in a subsequent section. This SPF is applied to a ramp exit speed-change lane, as shown in Figure 38. The “segment” length is equal to the ramp exit length L_{ex} , which is measured using the gore and taper points identified in Figure 11.

The fit of the calibrated models is shown in Figure 47. This figure compares the predicted and reported crash frequency in the calibration database. Each data point shown represents the average predicted and average reported crash frequency for a group of 10 segments. In general, the data shown in the figure indicate that the model provides an unbiased estimate of expected crash frequency for segments experiencing up to 4.0 ramp-exit-related crashes in a three-year period.

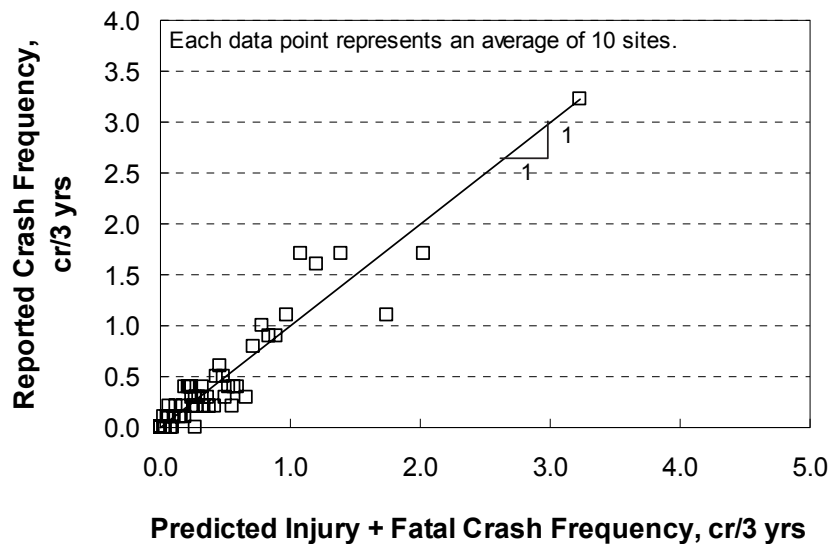


Figure 47. Predicted vs. reported ramp-exit-related FI crashes.

Calibrated CMFs

Several CMFs were calibrated in conjunction with the SPFs. All of them were calibrated using FI crash data. Collectively, they describe the relationship between various geometric factors and crash frequency. These CMFs are described in this section and, where possible, compared with the findings from previous research as means of model validation.

Many of the CMFs found in the literature are typically derived from (and applied to) the combination of multiple-vehicle and single-vehicle crashes. That is, one CMF is used to indicate the influence of a specified geometric feature on total crashes. In contrast, the models developed for this project include several CMFs that are calibrated for a specific crash type. In these instances, Equation 86 is used to facilitate a comparison of the CMFs reported in the literature

with those developed for this project. Specifically, this equation is used to convert the CMFs developed for a specific crash type to one that applies to total crashes.

$$CMF_{iagg} = (1.0 - P_{mv}) CMF_{sv,i} + P_{mv} CMF_{mv,i} \quad (86)$$

where,

CMF_{iagg} = aggregated CMF for element i ;

P_{mv} = proportion of multiple-vehicle crashes; and

$CMF_{j,i}$ = crash modification factor for element i and crash type j ($j = mv, sv$).

The proportion of multiple-vehicle crashes used in this equation is obtained from Table 38. The data in this table were obtained from the study state databases.

TABLE 38. Distribution of FI crashes on freeways

Area Type	Number of Through Lanes	Multiple-Vehicle Non-Entrance/Exit FI Crashes (MV)	Single-Vehicle Non-Entrance/Exit FI Crashes	Proportion MV Crashes
Rural	4	326	573	0.363
	6	432	434	0.499
	8	222	269	0.452
Urban	4	456	316	0.591
	6	947	567	0.625
	8	1,382	393	0.779
	10	888	235	0.791

Horizontal Curve CMF. The calibrated horizontal curve CMF has two forms, depending on which component model is being used. The CMF for multiple-vehicle non-entrance/exit crashes, ramp-entrance-related crashes, and ramp-exit related crashes is described using the following equation.

$$CMF_{mv,hc|agg} = 1.0 + 0.0172 \sum_{i=1}^m \left(\frac{5,730}{R_i} \right)^2 P_{c,i} \quad (87)$$

The CMF for single-vehicle crashes is described using the following equation.

$$CMF_{sv,hc|agg} = 1.0 + 0.0719 \sum_{i=1}^m \left(\frac{5,730}{R_i} \right)^2 P_{c,i} \quad (88)$$

These two CMFs are derived to be applicable to a segment that has a mixture of uncurved and curved lengths. The variable $P_{c,i}$ is computed as the ratio of the length of curve i on the segment to the length of the segment. For example, consider a segment that is 0.5 mi long and a curve that is 0.2 mi long. If one-half of the curve is on the segment, then $P_{c,i} = 0.20$ ($= 0.1/0.5$). In fact, this proportion is the same regardless of the curve's length (provided that it is 0.1 mi or longer and 0.1 mi of this curve is located on the segment).

The combined horizontal curve CMF is shown in Figure 48 using a series of thick, solid trend lines. Equation 86 was used to create these trend lines. They represent different

combinations of area type and through lanes through their association with the different proportions of multiple-vehicle crashes in Table 38. The radii used to calibrate this CMF range from 1,500 to 12,000 ft. The base condition for this CMF is an uncurved (i.e., tangent) segment.

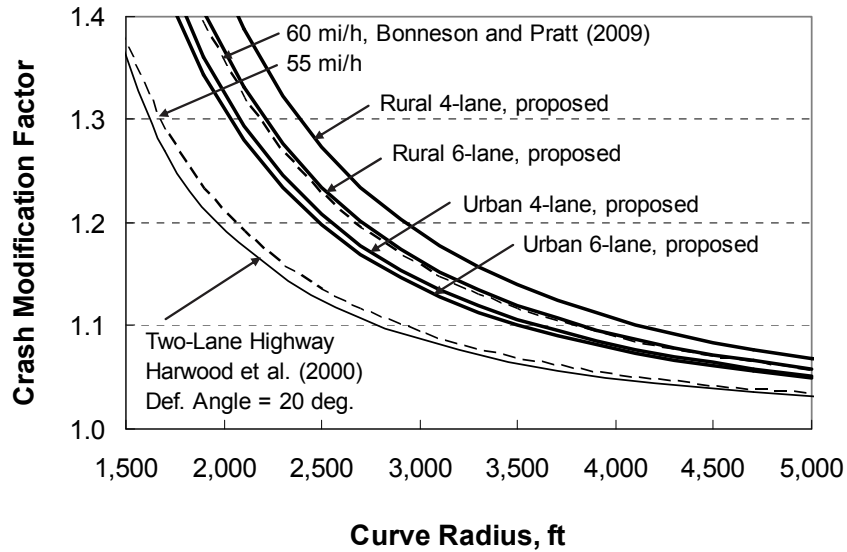


Figure 48. Calibrated freeway horizontal curve CMF for FI crashes.

Also shown in Figure 48 are CMFs developed by other researchers. Thin lines are used to differentiate these CMFs from those developed for this research project. The correlation between curve radius and crash frequency is consistent among all CMFs. The sensitivity to speed found in the model by Bonneson and Pratt (2009) suggests that the CMFs developed for this project reflect speeds of 60 to 65 mi/h. Speed data were not available in the study state databases.

Lane Width CMF. The lane width CMF is described using the following equation.

$$CMF_{lw} = \begin{cases} e^{-0.0376(W_l-12)} & : \text{If } W_l < 13 \text{ ft} \\ 0.963 & : \text{If } W_l \geq 13 \text{ ft} \end{cases} \quad (89)$$

The lane width used in this CMF is an average for all through lanes on the segment. The CMF is discontinuous, breaking at a lane width of 13 ft. Widths of 13 ft to 14 ft were not found to have a correlation with crash frequency. Collectively, the crash data for segments with lane widths in excess of 13 ft tended to be insensitive to lane width. These segments represent about 4.5 percent of the freeway segments evaluated.

The lane width CMF is shown in Figure 49 using a thick, solid trend line. The lane widths used to calibrate this CMF range from 10.5 to 14 ft. The base condition for this CMF is a 12-ft lane width.

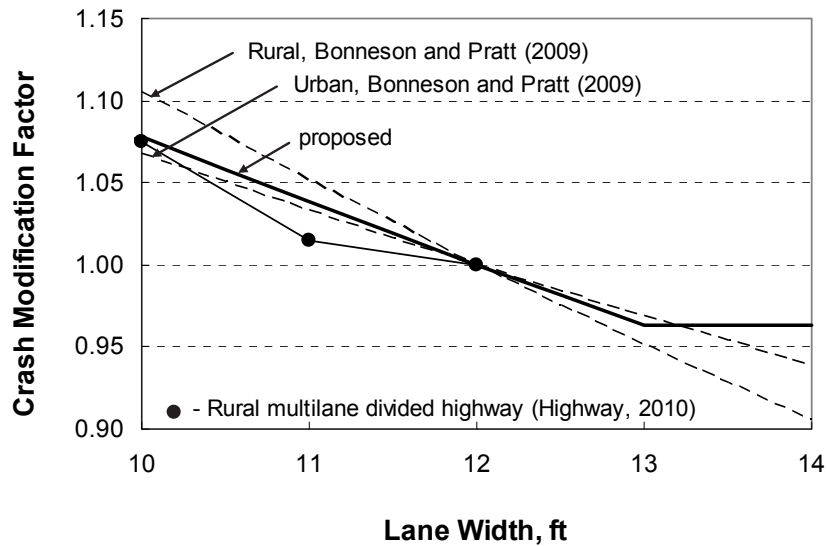


Figure 49. Calibrated freeway lane width CMF for FI crashes.

Also shown in Figure 49 are CMFs developed by other researchers. Thin lines or data points are used to differentiate these CMFs from those developed for this research project. The correlation between lane width and crash frequency is consistent among all CMFs.

Outside Shoulder Width CMF. The outside shoulder width CMF is described using the following equation.

$$CMF_{sv,osw|agg} = (1.0 - \sum P_{c,i})e^{-0.0647(W_s-10)} + (\sum P_{c,i})e^{-0.0897(W_s-10)} \quad (90)$$

This CMF is applicable to single-vehicle crashes. The regression analysis indicated that the outside shoulder width had an insignificant correlation with multiple-vehicle crashes. The shoulder width used in this CMF is an average for both directions of travel. The variable $P_{c,i}$ is computed as the ratio of the length of curve i on the segment to the length of the segment.

The combined outside shoulder width CMF for uncurved segments is shown in Figure 50 using a series of thick, solid trend lines. Equation 86 was used to create this CMF (with $CMF_{mv,osw} = 1.0$). It represents the likely correlation between outside shoulder width and total crash frequency. The trend lines represent different combinations of area type and through lanes through their association with the different proportions of multiple-vehicle crashes in Table 38. The shoulder widths used to calibrate this CMF range from 6 to 14 ft. The base condition for this CMF is a 10-ft shoulder width.

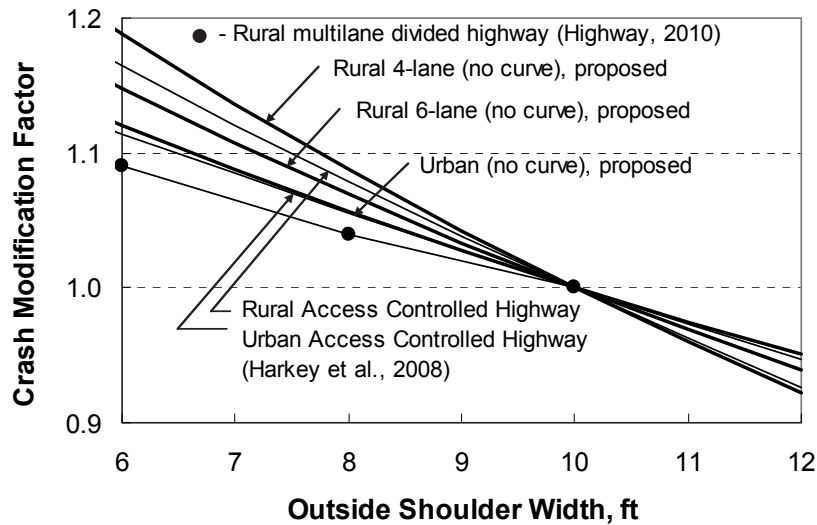


Figure 50. Calibrated freeway outside shoulder width CMF for FI crashes.

Also shown in Figure 50 are CMFs developed by other researchers. Thin lines or data points are used to differentiate these CMFs from those developed for this research project. The correlation between outside shoulder width and crash frequency is consistent among all CMFs.

Inside Shoulder Width CMF. The inside shoulder width CMF is described using the following equation.

$$CMF_{isw} = e^{-0.0172(w_{is}-6)} \quad (91)$$

The shoulder width used in this CMF is an average for both directions of travel.

The inside shoulder width CMF is shown in Figure 51 using a thick, solid trend line. The shoulder widths used to calibrate this CMF range from 2 to 11 ft. The base condition for this CMF is a 6-ft shoulder width.

Also shown in Figure 51 are CMFs developed by other researchers. Thin lines are used to differentiate these CMFs from those developed for this research project. The correlation between inside shoulder width and crash frequency is consistent among all CMFs.

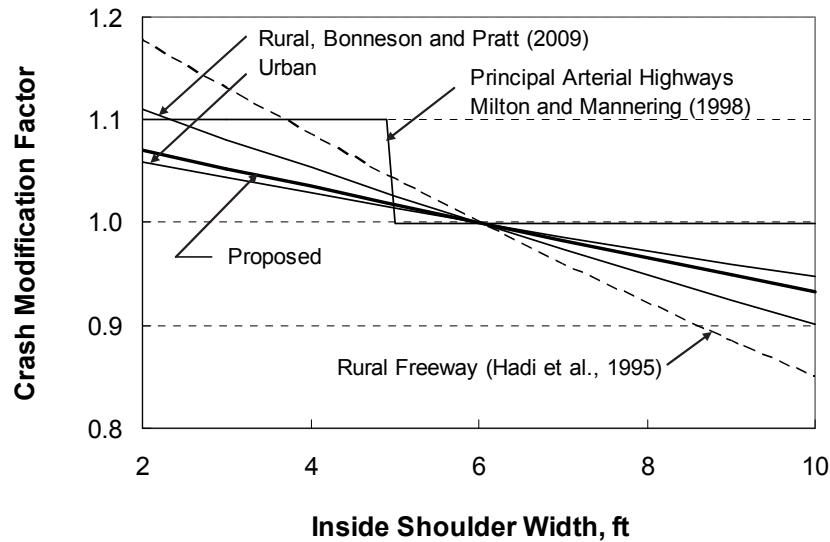


Figure 51. Calibrated freeway inside shoulder width CMF for FI crashes.

Median Width CMF. The calibrated median width CMF has two forms, depending on which component model is being used. The CMF for multiple-vehicle non-entrance/exit crashes, ramp-entrance-related crashes, and ramp-exit related crashes is described using the following equation.

$$CMF_{mv,mv|agg} = (1.0 - P_{ib}) e^{-0.00302(W_m - 2W_{is} - 48)} + P_{ib} e^{-0.00302(2W_{icb} - 48)} \quad (92)$$

The CMF for single-vehicle crashes is described using the following equation.

$$CMF_{sv,mv|agg} = (1.0 - P_{ib}) e^{0.00102(W_m - 2W_{is} - 48)} + P_{ib} e^{0.00102(2W_{icb} - 48)} \quad (93)$$

The median width used in either CMF is an average for the segment. These two CMFs are derived to be applicable to a segment that has median barrier present along some portion of the segment. Guidance for computing the variables P_{ib} and W_{icb} was provided previously in the subsection titled Barrier Variable Calculations.

The sign of the calibration coefficients in Equation 92 indicates that multiple-vehicle crash frequency decreases with an increase in median width. However, the coefficients in Equation 93 indicate that single-vehicle crash frequency *increases* slightly with an increase in median width. This latter trend reflects the fact an errant vehicle is more likely to have a single-vehicle crash with a wide median and a multiple-vehicle crash with a narrow median. Considering both single-vehicle and multiple-vehicle crashes together, the combined CMF indicates that the total number of FI crashes decreases with an increase in median width.

The combined median width CMF is shown in Figure 52 using the thick, solid trend line labeled “No barrier, proposed.” Equation 86 was used to create this CMF. The trend line shown represents an urban freeway. The slope of the line is slightly flatter for a rural freeway. The median widths used to calibrate this CMF range from 9 to 140 ft. The base condition for this

CMF is a 60-ft median width and an inside shoulder width of 6.0 ft. The trend lines labeled “Barrier in center...” are discussed with the next CMF.

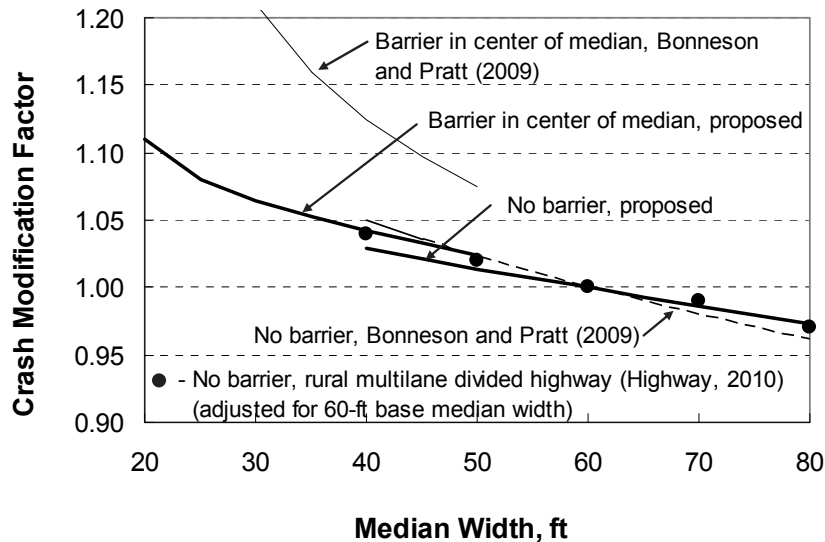


Figure 52. Calibrated freeway median width CMF for FI crashes.

Also shown in Figure 52 are CMFs developed by other researchers. Thin lines or data points are used to differentiate these CMFs from those developed for this research project. The correlation between median width and crash frequency is consistent among all CMFs.

Median Barrier CMF. The median barrier CMF is described using the following equation.

$$CMF_{mb|agg} = (1.0 - P_{ib})1.0 + P_{ib} e^{0.131/W_{icb}} \quad (94)$$

Guidance for computing the variables P_{ib} and W_{icb} was provided previously in the subsection titled Barrier Variable Calculations. The variable W_{icb} (representing the distance from the edge of inside shoulder to median barrier face) ranges in value from 1.0 to 17 ft in the database. The base condition for this CMF is no barrier.

This median barrier CMF is shown in Figure 52. The relevant trend lines are labeled “Barrier in center...”. The values shown represent the median barrier CMF multiplied by the median width CMF because both CMFs are sensitive to the variable W_{icb} . The trend line shown is for urban freeways. It drops slightly for rural freeways.

The calibration coefficient in Table 33 for this CMF is 0.131. However, research by Bonneson and Pratt (2008) using Texas data found a coefficient value of 0.890 for an identical CMF. There is a significant difference between these two coefficients, where the smaller value suggests that barrier presence produces a smaller CMF value. This difference can also be seen in Figure 52 by comparing the two trend lines associated with barrier in the center of the median. The trend line attributed to Bonneson and Pratt (2009) is based on rigid and semi-rigid barrier on

Texas freeways. In contrast, the other barrier-related trend line is based on a mixture of rigid, semi-rigid, and cable barrier types in the study states. It is possible that some of the difference between the two trend lines reflects differences in barrier design between Texas and the study states.

Shoulder Rumble Strip CMF. The shoulder rumble strip CMF is described using the following equation.

$$CMF_{sv,rs|agg} = (1.0 - \sum P_{c,i}) f_{tan} + (\sum P_{c,i}) f_{cur} \quad (95)$$

$$f_{tan} = 0.5 ([1.0 - P_{ir}] 1.0 + P_{ir} 0.811) + 0.5 ([1.0 - P_{or}] 1.0 + P_{or} 0.811) \quad (96)$$

$$f_{cur} = 0.5 ([1.0 - P_{ir}] 1.0 + P_{ir} 1.32) + 0.5 ([1.0 - P_{or}] 1.0 + P_{or} 1.32) \quad (97)$$

This CMF is applicable to single-vehicle crashes. The regression analysis indicated that shoulder rumble strip presence had an insignificant correlation with multiple-vehicle crashes. The proportion P_{ir} represents the proportion of the segment length with rumble strips present on the inside shoulders. It is computed by summing the length of roadway with rumble strips on the inside shoulder in *both* travel directions and dividing by twice the segment length. The proportion P_{or} represents the proportion of the segment length with rumble strips present on the outside shoulders. It is computed by summing the length of roadway with rumble strips on the outside shoulder in *both* travel directions and dividing by twice the segment length.

The constant “0.811” in Equation 96 represents the calibration coefficient after conversion. It corresponds to a CMF value of 0.811 for FI single-vehicle crashes on uncurved (i.e., tangent) road segments when shoulder rumble strips are continuously present. This value compares favorably with the CMF value of 0.84 recommended by Torbic et al. (2009) for crashes of the same type and severity on rural freeways.

The constant “1.32” in Equation 97 represents the calibration coefficient after conversion. It corresponds to a CMF value of 1.32 for FI single-vehicle crashes on curved road segments when shoulder rumble strips are continuously present. It suggests that there are 32 percent more crashes on curved road segments when rumble strips are present. A review of the literature on the safety effect of shoulder rumble strips on curves did not reveal any evidence that could support or refute this finding. In related research, Torbic et al. (2009) examined the safety effect of centerline rumble strips on rural two-lane highways in three states. They found that centerline rumble strips increased total crashes 3.5 percent on curved segments (although this result was not statistically significant). Their examination of FI crash frequency for the same curves showed a range of results—crashes were reduced by 36.7 percent in one state but increased 9.8 percent in another state.

Outside Clearance CMF. The calibrated outside clearance CMF is described using the following equation.

$$CMF_{sv,oc|agg} = (1.0 - P_{ob}) e^{-0.00451(W_{nc} - W_s - 20)} + P_{ob} e^{-0.00451(W_{ocb} - 20)} \quad (98)$$

This CMF is applicable to single-vehicle crashes. The regression analysis indicated that outside clearance had an insignificant correlation with multiple-vehicle crashes. The clear zone width used in this CMF is an average for both directions of travel. This CMF is derived to be

applicable to a segment that has roadside barrier present along some portion of the segment. Guidance for computing the variables P_{ob} and W_{ocb} was provided previously in the subsection titled Barrier Variable Calculations.

The combined outside clearance CMF is shown in Figure 53 using a series of thick, solid trend lines. Equation 86 was used to create this CMF (with $CMF_{mv, oc} = 1.0$). The trend lines represent different combinations of area type and through lanes through their association with the different proportions of multiple-vehicle crashes in Table 38. The clear zone widths used to calibrate this CMF range from 0 to 30 ft. The base condition for this CMF is a 30-ft clear zone and a 10-ft outside shoulder width. The trend lines labeled “Roadside has barrier...” are discussed with the next CMF.

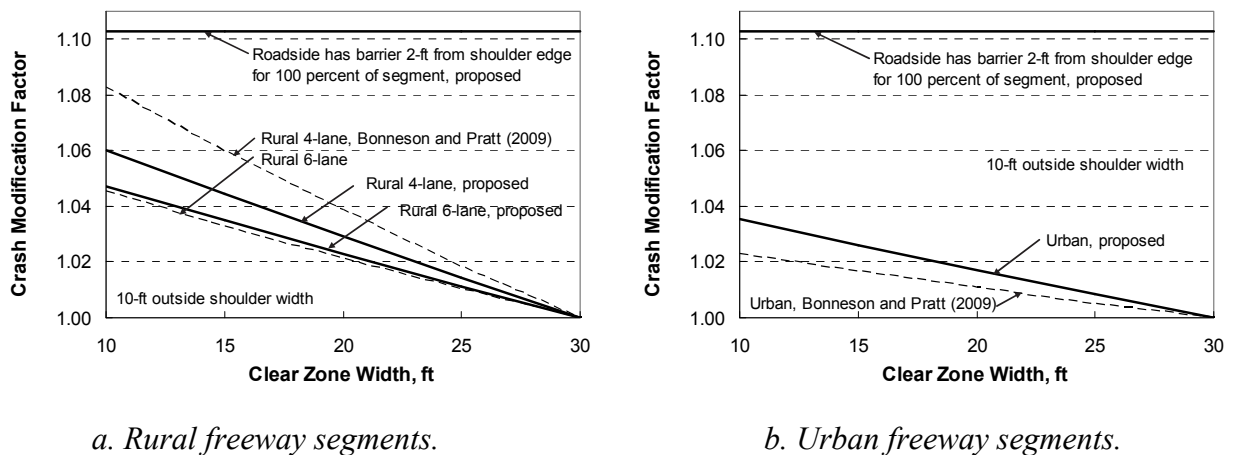


Figure 53. Calibrated freeway outside clearance CMF for FI crashes.

Also shown in Figure 53 are CMFs developed by other researchers. Thin lines are used to differentiate these CMFs from those developed for this research project. The correlation between clear zone width and crash frequency is consistent among all CMFs.

Outside Barrier CMF. The calibrated outside barrier CMF is described using the following equation.

$$CMF_{sv, ob|agg} = (1.0 - P_{ob})1.0 + P_{ob} e^{0.131/W_{ocb}} \quad (99)$$

This CMF is applicable to single-vehicle crashes. The regression analysis indicated that outside barrier presence had an insignificant correlation with multiple-vehicle crashes. Guidance for computing the variables P_{ob} and W_{ocb} was provided previously in the subsection titled Barrier Variable Calculations. The variable W_{ocb} (representing the distance from the edge of outside shoulder to median barrier face) ranges in value from 1.0 to 17 ft in the database. The base condition for this CMF is no barrier.

The combined outside barrier CMF is shown in Figure 53. The relevant trend lines are labeled “Roadside has barrier...”. Equation 86 was used to create this CMF (with $CMF_{mv, ob} =$

1.0). The values shown represent the outside barrier CMF multiplied by the outside clearance CMF because both are sensitive to the variable W_{ocb} . The trend lines represent different combinations of area type and through lanes; however, the sensitivity to these influences is very small.

Lane Change CMF. The calibrated lane change CMF is described using the following equations.

$$CMF_{mv,lc|agg} = (0.5 f_{wev,inc} f_{lc,inc}) + (0.5 f_{wev,dec} f_{lc,dec}) \quad (100)$$

$$f_{wev,inc} = (1.0 - P_{wevB,inc}) 1.0 + P_{wevB,inc} e^{0.175/L_{wev,inc}} \quad (101)$$

$$f_{wev,dec} = (1.0 - P_{wevB,dec}) 1.0 + P_{wevB,dec} e^{0.175/L_{wev,dec}} \quad (102)$$

$$f_{lc,inc} = \left(1.0 + \frac{e^{-12.56 X_{b,ent} - 0.272 \ln(AADT_{b,ent}/1,000)}}{12.56 L} [1.0 - e^{-12.56 L}] \right) \times \left(1.0 + \frac{e^{-12.56 X_{e,ext} - 0.272 \ln(AADT_{e,ext}/1,000)}}{12.56 L} [1.0 - e^{-12.56 L}] \right) \quad (103)$$

$$f_{lc,dec} = \left(1.0 + \frac{e^{-12.56 X_{e,ent} - 0.272 \ln(AADT_{e,ent}/1,000)}}{12.56 L} [1.0 - e^{-12.56 L}] \right) \times \left(1.0 + \frac{e^{-12.56 X_{b,ext} - 0.272 \ln(AADT_{b,ext}/1,000)}}{12.56 L} [1.0 - e^{-12.56 L}] \right) \quad (104)$$

The variables for weaving section length (i.e., $L_{wev,inc}$, $L_{wev,dec}$) in Equations 101 and 102 are intended to reflect the degree to which the weaving activity is concentrated along the freeway. This variable has negligible correlation with segment length L .

The variables $P_{wevB,inc}$ and $P_{wevB,dec}$ in Equations 101 and 102, respectively, are computed as the ratio of the length of the weaving section on the segment to the length of the segment. If the segment is wholly located in the weaving section, then this variable is equal to 1.0. The calibration coefficient in these two equations indicates that lane change CMF value will increase if the segment is in a Type B weaving section. The amount of this increase is inversely related to the length of the weaving section.

This CMF consists of several component equations but only requires a few input variables. These variables describe the distance to (and volume of) the four nearest ramps to the subject segment. Two of the ramps of interest are on side of the freeway with travel in the increasing milepost direction. One ramp on this side of the freeway is upstream of the segment and one ramp is downstream of the segment. Similarly, one ramp on the other side of the freeway is upstream of the segment and one ramp is downstream. Only those entrance ramps that contribute volume to the subject segment are of interest. Hence a downstream entrance ramp is

not of interest. For similar reasons, an upstream exit ramp is not of interest. If the segment is in a Type B weaving section, then the length of the weaving section is also an input.

To illustrate this CMF, consider a 0.5-mi section of rural six-lane freeway. It consists of five segments that are each 0.1 mi in length. There is an interchange at one end of the section. The distance to the next interchange is sufficiently large that its ramp traffic has no influence on segment lane change activity. No weaving section is present. Under this scenario, $f_{wev, inc}$ equals 1.0, $f_{wev, dec}$ equals 1.0, the second term of Equation 103 equals 1.0, and the first term of Equation 104 equals 1.0. The CMF for each of the five segments is plotted in Figure 54. The example 0.5-mi freeway section is shown in plan view in the upper left corner of this figure.

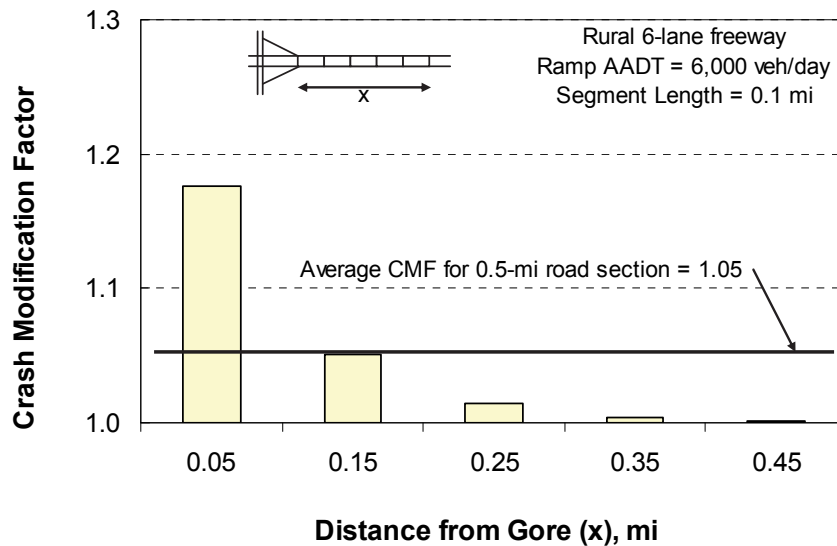


Figure 54. Lane change CMF as a function of distance from ramp gore.

The CMF is 1.18 for the segment that starts at the ramp gore and extends 0.1 mi (i.e., segment center is $x = 0.05$ mi). The CMF value for the next segment is 1.05. CMF values continue to decrease for each subsequent segment. This decline in CMF value reflects the decreasing number of lane changes with increasing distance from the ramp gore. The overall average CMF for all five segments is 1.05.

Consider a 0.5-mi section of rural six-lane freeway that is bounded on each end by an interchange. It consists of five segments that are each 0.1 mi in length. A Type A weaving section exists in each travel direction. Under this scenario, $f_{wev, inc}$ equals 1.0 and $f_{wev, dec}$ equals 1.0. The CMF for each of the five segments is plotted in Figure 55. The example 0.5-mi freeway section is shown in the upper left corner of this figure.

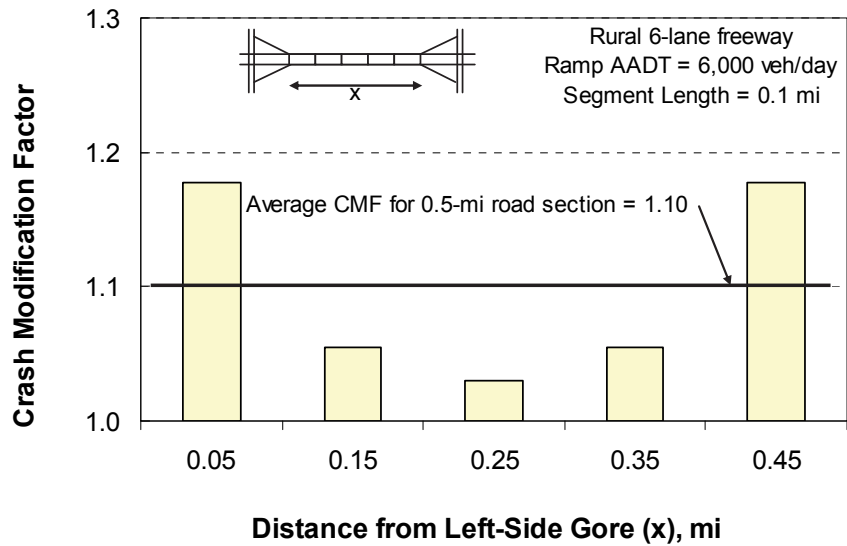


Figure 55. Lane change CMF for segments between a pair of interchanges.

As before, the CMF is 1.18 for the segment that starts at the ramp gore on the left and extends 0.1 mi (i.e., segment center is $x = 0.05$ mi). The CMF value for the next segment is 1.06. The CMF continues to decrease until the middle segment is reached and then starts to increase as the segments get closer to the next interchange. The overall average CMF for all five segments is 1.10.

The lane-change CMF was applied to other weaving section lengths and the average CMF was computed for each length. This process was undertaken to facilitate a comparison of the lane-change CMF with two weaving-section CMFs shown previously in Figure 26. The results of this process are plotted in Figure 56. The trends shown indicate relatively good agreement between the lane-change CMF and these other CMFs.

Weaving sections associated with a full cloverleaf interchange typically have a length of 0.10 to 0.18 miles. Figure 56 suggests that weaving sections with a length in this range will be associated with a relatively high CMF value and high crash rate. In fact, interchange design practice in the last few decades has been to relocate the weaving section associated with a full cloverleaf interchange to a collector-distributor roadway to improve freeway safety and operation.

The lane-change CMF is applicable to any segment in the vicinity of one or more ramps. It is equally applicable to segments in a weaving section and segments in a non-weaving section (i.e., segments between an entrance ramp and an exit ramp where both ramps have a speed-change lane).

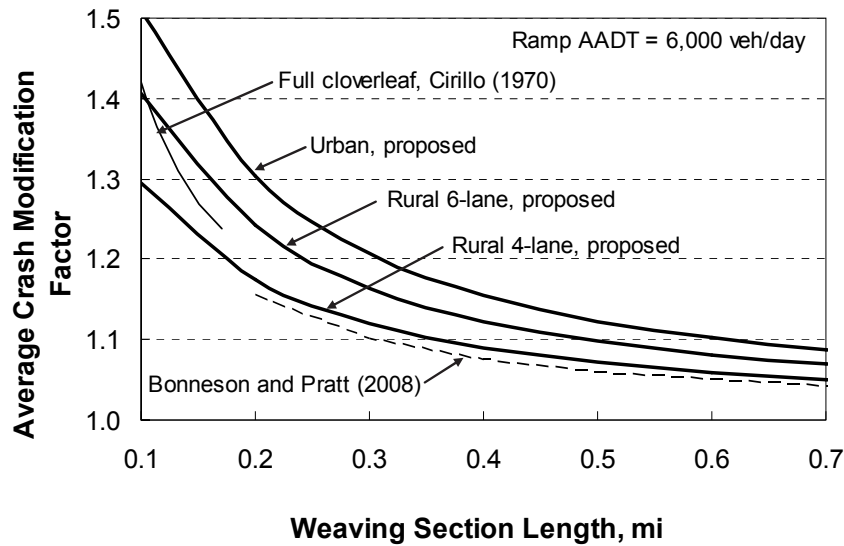


Figure 56. Average CMF value for FI crashes as a function of weaving section length.

The two component models for predicting speed-change-related crash frequency (i.e., Equations 84 and 85) are not used when evaluating a weaving section because the ramps that form the weaving section do not have a speed-change lane. As a result, the predicted crash frequency for the set of segments that comprise a weaving section will tend to be smaller than that predicted for a similar set of segments located in a non-weaving section. This generalization will always be true for the Type A and Type C weaving sections. It may or may not hold for the Type B weaving section, depending on the length of the weaving section.

The calibration coefficient associated with the ramp AADT term in Equations 103 and 104 is negative which is counterintuitive at first glance. It indicates that the lane change CMF is larger for segments associated with lower volume ramps. This trend may be explained by the fact that high-volume ramp flows tend to dominate the traffic stream such that a large portion of the traffic stream is changing lanes and all drivers are more aware of these maneuvers. Regardless, the entering ramp volumes are also included in the segment AADT volume and the coefficient associated with the segment AADT variable in the SPF is positive and relatively large. As a result, when all relevant SPFs and CMFs are combined, the predicted average crash frequency for a freeway segment increases with an increase in the AADT volume of nearby ramps. This trend is logical and intuitive.

Ramp Entrance CMF. The ramp entrance CMF is described using the following equation.

$$CMF_{en} = e^{0.594 I_{left} + 0.0318 / L_{en} + 0.198 \ln(AADT_r / 1,000)} \quad (105)$$

This CMF is applied to a ramp entrance speed-change lane, as shown in Figure 38. The “segment” length is equal to the ramp entrance length L_{en} , which is measured using the gore and taper points identified in Figure 11. This CMF applies only to the side of the freeway with the subject speed-change lane.

The variable for ramp entrance length L_{en} in Equation 105 is intended to reflect the degree to which the lane-changing activity is concentrated along the ramp entrance. This variable has negligible correlation with segment length L .

The indicator variable for ramp side I_{left} is associated with a positive calibration coefficient. It suggests that a ramp entrance on the left side of the through lanes is associated with an 81 percent increase in crashes, relative to one on the right side. This finding is consistent with that of Moon and Hummer (2009), and with that from the re-analysis of the data reported by Lundy (1966), as documented in Chapter 2.

The ramp entrance CMF for right-side ramps is shown in Figure 57 using a thick, solid trend line. It has been adjusted using Equation 106 to facilitate a comparison with the CMFs reported by other researchers because they apply to entire segments (i.e., both sides of the freeway). The ramp entrance lengths used to calibrate this CMF range from 0.07 to 0.22 mi (370 to 1,200 ft).

$$CMF_i = 0.5 + 0.5 CMF_{en} \quad (106)$$

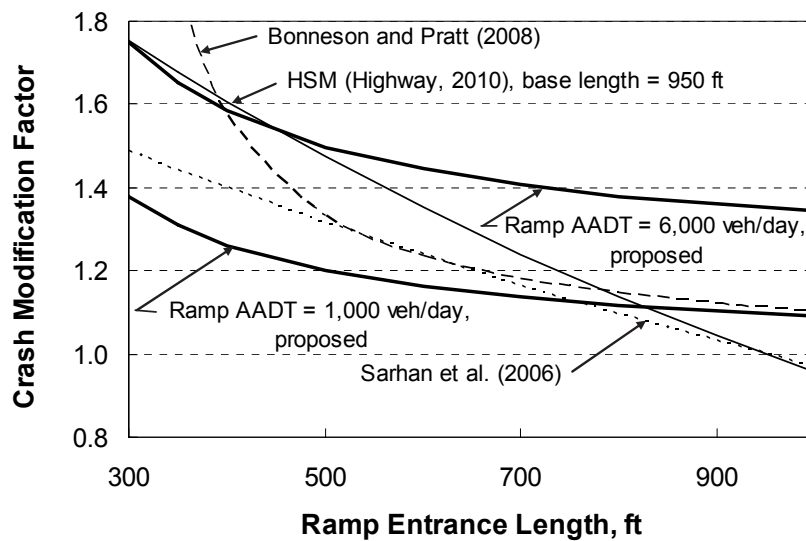


Figure 57. Calibrated freeway ramp entrance CMF for right-side ramps and FI crashes.

Also shown in Figure 57 are CMFs developed by other researchers. Thin lines are used to differentiate these CMFs from those developed for this research project. The correlation between ramp entrance length and crash frequency is consistent among all CMFs.

Ramp Exit CMF. The ramp exit CMF is described using the following equation.

$$CMF_{ex} = e^{0.594I_{left} + 0.0116/L_{ex}} \quad (107)$$

This CMF is applied to a ramp exit speed-change lane, as shown in Figure 38. The “segment” length is equal to the ramp exit length L_{ex} , which is measured using the gore and taper

points identified in Figure 11. This CMF applies only to the side of the freeway with the subject speed-change lane.

The variable for ramp exit length L_{ex} in Equation 107 is intended to reflect the degree to which the lane-changing activity is concentrated along the ramp exit. This variable has negligible correlation with segment length L .

The interpretation of the indicator variable for ramp side I_{left} is provided with the previous CMF discussion.

The ramp exit CMF for right-side ramps is shown in Figure 58 using a thick, solid trend line. It has been adjusted using Equation 106 to facilitate a comparison with the CMFs reported by other researchers, which apply to entire segments (i.e., both sides of the freeway). The ramp exit lengths used to calibrate this CMF range from 0.03 to 0.21 mi (160 to 1,100 ft).

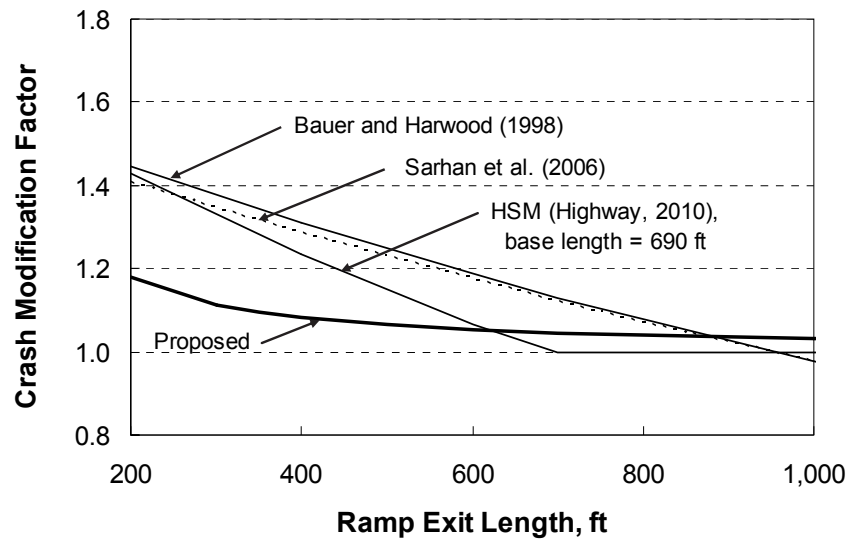


Figure 58. Calibrated freeway ramp exit CMF for right-side ramps and FI crashes.

Also shown in Figure 58 are CMFs developed by other researchers. Thin lines are used to differentiate these CMFs from those developed for this research project. The correlation between ramp exit length and crash frequency is similar, but not consistent among CMFs. The calibrated CMF value is smaller than that obtained from the other CMFs for lengths less than 600 ft.

High-Volume CMF. The calibrated high-volume CMF has two forms, depending on which component model is being used. The CMF for multiple-vehicle non-entrance/exit crashes, ramp-entrance-related crashes, and ramp-exit related crashes is described using the following equation.

$$CMF_{mv,hv} = e^{0.350 P_{hv}} \quad (108)$$

The CMF for single-vehicle crashes is described using the following equation.

$$CMF_{sv,hv} = e^{-0.0675 P_{hv}} \quad (109)$$

The proportion of AADT during hours where volume exceeds 1,000 veh/h/ln P_{hv} is computed using the average hourly volume distribution associated with the subject segment. This distribution will typically be computed using the data obtained from the nearest continuous traffic counting station (on a freeway of similar character). The variable P_{hv} is positively correlated with the volume-to-capacity ratio experienced by the segment on an hourly basis.

The high-volume CMF is shown in Figure 59 using a thick, solid trend line. The trend lines represent different combinations of area type and through lanes through their association with the different proportions of multiple-vehicle crashes in Table 38. The base condition for this CMF is a proportion P_{hv} equal to 0.0. The trends shown in both figures are consistent with those developed by Lord et al. (2005) for multiple-vehicle and single-vehicle crashes as a function of volume-to-capacity ratio.

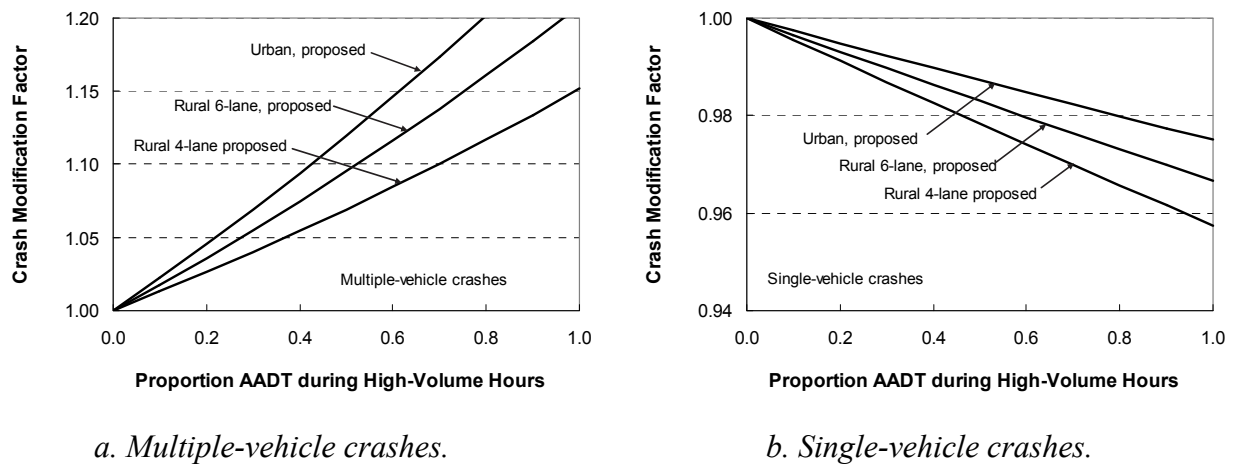


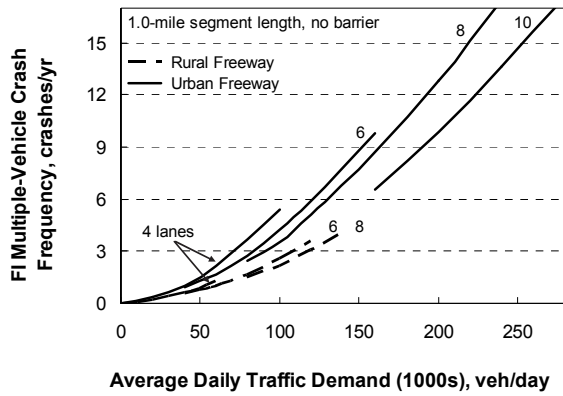
Figure 59. Calibrated freeway high-volume CMF for FI crashes.

Sensitivity Analysis

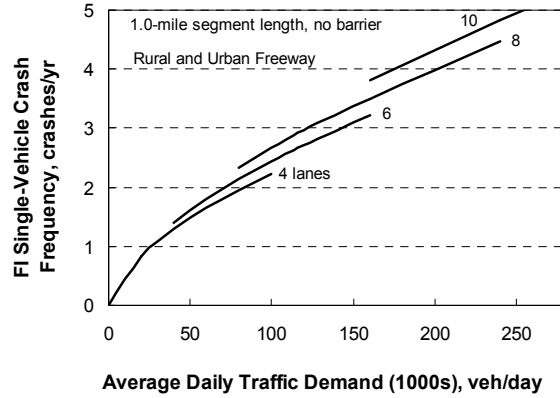
The relationship between crash frequency and traffic demand, as obtained from the combined calibrated models, is illustrated in Figure 60 for a 1-mile freeway segment with two ramp entrances, two ramp exits, no curvature, and no barrier. The individual component models are illustrated in Figures 60a, 60b, 60c, and 60d. The sum of the individual component crash frequencies is illustrated in Figure 61. The length of the trend lines in Figures 60 and 61 reflect the range of AADT volume in the data. The trends in Figure 61 are comparable to those in Figure 15e and 15f.

The trend lines shown in Figure 61 indicate that urban freeways have about 20 to 30 percent more crashes than rural freeways. By comparison, the crash rates listed in Table 19 indicate that urban freeways have 50 to 250 percent more crashes than rural freeways. It is likely that this latter trend reflects the influence of barrier length, ramp entrances, ramp exits, and weaving section length. As shown in Table 18, these influences are more prevalent on urban freeway segments. In contrast, these influences have been explicitly quantified in the proposed model such that they do not influence the trends shown in Figure 61. The proposed model

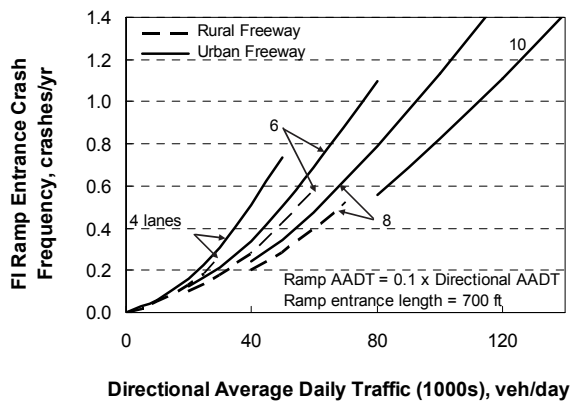
provides a more accurate indication of differences between freeway segments in rural versus urban areas, when the segments have the same barrier proportion, ramp entrance length, and weaving section length.



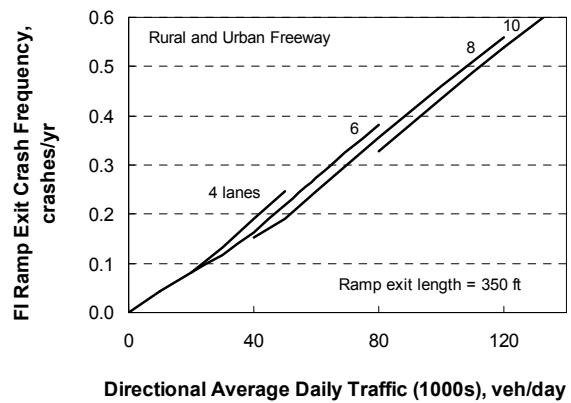
a. Multiple-vehicle crashes.



b. Single-vehicle crashes.



c. Ramp-entrance-related crashes.



d. Ramp-exit-related crashes.

Figure 60. Freeway FI model components.

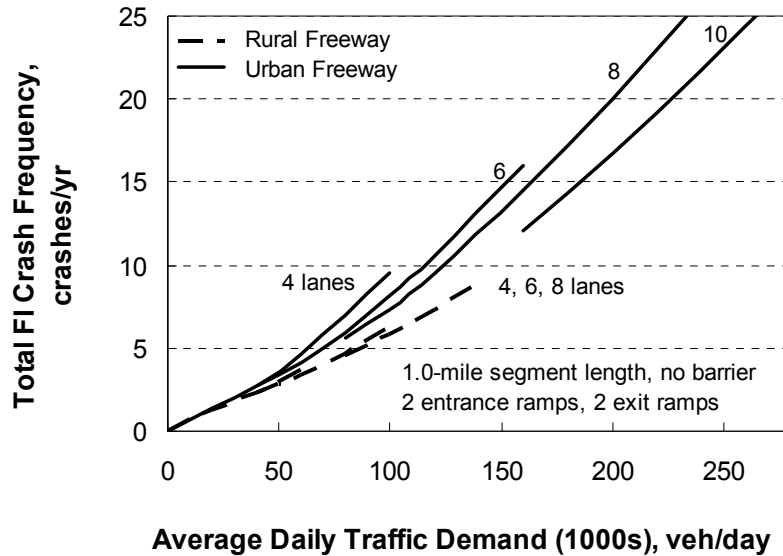


Figure 61. Freeway FI model.

The trend lines shown in Figure 61 also indicate that crash frequency is *lower* on freeways with many lanes than it is on freeways with few lanes. In fact, the models indicate that an urban six-lane freeway segment has about 7 percent fewer crashes than an urban four-lane segment and that a rural six-lane segment has about 3 percent fewer crashes than an urban four-lane segment. These trends are counter to those found when comparing the crash rates in Table 19, which indicate that crash rate is *higher* on freeways with many lanes. It is likely that these trends in crash rate reflect the fact that the proportion of barrier along a freeway segment typically increases (and the lateral clearance decreases) with an increase in the number of lanes. The proposed predictive models account for the influence of barrier presence and lateral clearance and, therefore, provide a more accurate indication of the relationship between number-of-lanes and crash frequency.

Model Extensions

This section describes two extensions to the predictive models described in the previous sections. The models were developed to be applicable to a wide range of geometric conditions. However, limitations of the data did not allow model calibration for some situations. These situations are addressed in this section as model extensions.

AADT Volume Varies by Direction

The speed-change models and several of the CMFs are sensitive to geometric elements and ramp volumes that exist in only one travel direction on the segment (e.g., weaving section). These features make the safety evaluation more adaptive to segment geometry on a directional basis and the results more accurate.

One situation that could not be addressed in the SPF development was a segment with an unbalanced daily traffic demand. The AADT volumes in the study state database represent both

travel directions and it is commonly assumed that the daily directional distribution is balanced (i.e., the same in each direction). If the daily directional distribution is known, then the calibrated SPFs are revised as shown in the following equations.

$$N_{spf,mv,4} = \left(\frac{1.406}{1.0 + 1.468 \sigma_p^2} \right) \left(L - 0.5 \sum L_{en,seg,i} - 0.5 \sum L_{ex,seg,i} \right) \times \left(e^{-5.470 - 0.505 I_{rural}} \right) \times \left(e^{1.492 \ln(P_1 AADT/1,000)} + e^{1.492 \ln(P_2 AADT/1,000)} \right) \quad (110)$$

$$N_{spf,sv} = \left(\frac{0.782}{1.0 - 0.457 \sigma_p^2} \right) \left(L - 0.5 \sum L_{en,seg,i} - 0.5 \sum L_{ex,seg,i} \right) \times \left(e^{-2.266 + 0.0351 n} \right) \times \left(e^{0.646 \ln(P_1 AADT/1,000)} + e^{0.646 \ln(P_2 AADT/1,000)} \right) \quad (111)$$

$$N_{spf,en} = (L_{en}) e^{-3.194 + 1.173 \ln(P_i AADT/1,000) - 0.130 n - 0.180 I_{rural}} \quad (112)$$

$$N_{spf,ex} = (L_{ex}) e^{-2.679 + 0.903 \ln(P_i AADT/1,000)} \quad (113)$$

with,

$$\sigma_p^2 = (0.5 - P_1)^2 \quad (114)$$

where,

- P_1 = proportion of AADT in travel direction 1;
- P_2 = proportion of AADT in travel direction 2 (= 1.0 - P_1);
- σ_p = standard deviation of P_i ; and
- P_i = proportion of AADT in travel direction i that corresponds to subject speed-change lane.

The first term in Equations 110 and 111 represents a correction factor for using directional traffic demand in the SPF. Equation 110 is the SPF for multiple-vehicle crashes on four-lane freeway segments. The other multiple-vehicle-crash SPFs can be similarly converted using the same correction factor. It is noted that both correction factors have a value in the range of 0.97 to 1.02 for most conditions. The AADT divisor in Equations 112 and 113 is “1,000,” rather than the “2,000” used in the calibrated versions of these equations. The value “2,000” was intentionally used for calibration because it corresponds to a value of P_i equal to 0.5.

Number-of-Lanes Varies by Direction

There are few freeway segments with an unequal number of lanes in opposing directions from the standpoint of statistically valid sample sizes. However, there are a sufficient number of these segments encountered during a safety evaluation that an extension is needed to provide reasonable estimates of average crash frequency.

If a freeway segment has X total lanes that represent Y lanes in one direction and Z lanes in the opposite direction (i.e., $X = Y + Z$) and Y is not equal to Z , then it recommended that the segment be evaluated twice. One evaluation would be conducted where the number of lanes is equal to $2Y$ and one evaluation would be conducted where the number of lanes is equal to $2Z$. All

other inputs to the models would be unchanged between evaluations. The two estimates of average crash frequency obtained in this manner are then averaged to obtain the best estimate of the predicted average crash frequency for the subject segment.

MODEL CALIBRATION FOR PDO CRASHES

This part of the chapter describes the calibration of the combined freeway segment and speed-change lane predictive models based on PDO crashes. The methodology used to calibrate the models is described in the part titled Methodology. The calibration data, model development, and statistical analysis methods are described in the part titled Model Calibration for FI Crashes.

An initial regression analysis was undertaken with county and state variable combinations treated as fixed effects and as random effects. The Hausman test was performed using the covariance matrix to determine whether the fixed effect model was appropriate (Hausman, 1978). The null hypothesis is that the regression coefficients from the two model treatments are consistent. This hypothesis was rejected ($p = 0.0001$) indicating that the coefficients are different (i.e., inconsistent) among the two treatments. In this case, it is concluded that the regression coefficient values are influenced by county so a fixed-effect treatment is needed to remove the county effect.

Model Calibration

The results of the regression model calibration are presented in Table 39. The Pearson χ^2 statistic for the model is 4,888, and the degrees of freedom are 4,557 ($= n - p = 4,587 - 30$). This statistic is greater than the $\chi^2_{0.05, 4577}$ ($= 4,715$) so the hypothesis that the model fits the data is rejected by this test. Several segments were removed as a result of outlier analysis such that the calibration database included only 17,265 of the 18,045 crashes identified in Chapter 4.

Closer examination of the data indicates that a small number of sites with a length less than 0.10 mi and many crashes were causing the lack of fit. A test of the scaled deviance was also conducted. This statistic is also chi-square distributed but is less sensitive to sites with short length and many crashes. The scaled deviance for this model is 4,532, which is less than 4,715 so the hypothesis that the model fits the data cannot be rejected by this test. An examination of the other fit statistics in Table 39 indicates the model provides a relatively good fit, and supports the conclusion reached by the scaled deviance test.

The t-statistic for each coefficient is listed in the last column of Table 39. These statistics describe a test of the hypothesis that the coefficient value is equal to 0.0. Those t-statistics with an absolute value that is larger than 2.0 indicate that the hypothesis can be rejected with the probability of error in this conclusion being less than 0.05. For those few variables where the absolute value of the t-statistic is smaller than 2.0, it was decided that the variable was important to the model and its trend was found to be intuitive and, where available, consistent with previous research findings (even if the specific value was not known with a great deal of certainty as applied to this database).

TABLE 39. Freeway PDO model statistical description–combined model –three states

Model Statistics		Value		
R^2 :		0.66		
Scale parameter ϕ :		1.07		
Pearson χ^2 :		4,888 ($\chi^2_{0.05, 4557} = 4,715$)		
Observations n_o :		1,848 segments (17,265 PDO crashes in 3 years) 637 ramp entrances, 513 ramp exits		
Calibrated Coefficient Values				
Variable	Inferred Effect of...	Value	Std. Dev.	t-statistic
$b_{mv, cr}$	Horizontal curvature on 2+ veh. crashes	0.0340	0.0071	4.8
$b_{sv, cr}$	Horizontal curvature on 1 veh. crashes	0.0626	0.0116	5.4
$b_{s, cur}$	Outside shoulder width on 1 veh. crashes, curves	-0.0840	0.0224	-3.7
b_{is}	Inside shoulder width	-0.0153	0.0056	-2.7
$b_{rs, cur}$	Shoulder rumble strip on 1 veh. crashes, curves	0.186	0.0934	2.0
$b_{mv, mw}$	Median width on 2+ veh. crashes	-0.00291	0.0007	-4.3
$b_{sv, mw}$	Median width on 1 veh. crashes	-0.00289	0.0006	-4.7
b_{bar}	Barrier presence	0.169	0.0424	4.0
b_{wev}	Type B weaving section presence on 2+ veh. crashes	0.123	0.0503	2.5
b_v	Ramp AADT on lane-change-related crashes	-0.283	0.1551	-1.8
b_x	Distance from ramp on lane-change-related crashes	13.461	3.5160	3.8
b_{left}	Left side entrance or exit on speed-change lane crashes	0.824	0.4888	1.7
$b_{en, len}$	Ramp entrance length on related crashes	0.0252	0.0130	1.9
$b_{mv, hv}$	High-volume conditions on 2+ veh. crashes	0.283	0.1218	2.3
$b_{sv, hv}$	High-volume conditions on 1 veh. crashes	-0.611	0.1142	-5.3
$b_{mv, 4}$	4 lanes on 2+ vehicle crashes in urban areas	-6.355	0.369	-17.2
$b_{mv, 6}$	6 lanes on 2+vehicle crashes in urban areas	-6.616	0.415	-15.9
$b_{mv, 8}$	8 lanes on 2+ vehicle crashes in urban areas	-6.804	0.451	-15.1
$b_{mv, 10}$	10 lanes on 2+ vehicle crashes in urban areas	-7.067	0.478	-14.8
$b_{mv, 1}$	AADT on 2+ vehicle crashes	1.936	0.101	19.2
$b_{mv, rural}$	Added effect of rural area type on 2+ veh. crashes	-0.332	0.050	-6.7
$b_{sv, 0}$	1 veh. crashes	-1.955	0.204	-9.6
$b_{sv, 2}$	Number of lanes on 1 veh. crashes	-0.0193	0.022	-0.9
$b_{sv, 1}$	AADT on 1 veh. crashes	0.876	0.073	11.9
$b_{en, 0}$	Ramp-entrance crashes in urban areas	-2.180	0.386	-5.6
$b_{en, 2}$	Number of lanes on ramp-ent. crashes in urban areas	-0.101	0.041	-2.5
$b_{en, 1}$	AADT on ramp-entrance crashes	1.215	0.140	8.7
$b_{en, rural}$	Added effect of rural area type on ramp-ent. crashes	-0.0989	0.108	-0.9
$b_{ex, 0}$	Ramp-exit crashes	-1.575	0.381	-4.1
$b_{ex, 1}$	AADT on ramp-exit crashes	0.932	0.107	8.7

The coefficients for forty-three county indicator variables are not shown in Table 39 because their individual significance is not directly relevant to model fit assessment or its application. However, it is recognized that the “intercept” variables in Table 39 (i.e., $b_{mv, 4}$, $b_{mv, 6}$, $b_{mv, 8}$, $b_{mv, 10}$, $b_{sv, 0}$, $b_{en, 0}$, $b_{ex, 0}$) correspond to only one state and county combination. Desirably, the intercept would represent an average value for all states and counties in the database. To this

end, the predicted crash frequencies from the model described by Table 39 were submitted to a second regression analysis using Equation 115.

$$X_i = \frac{y N_i}{e^{I_{co,i} b_{co,i}}} e^{c_o} \quad (115)$$

where,

- X_i = reported crash count for y years in county i , crashes;
- y = time interval during which X crashes were reported, yr;
- N_i = predicted average crash frequency for county i , crashes/yr;
- $I_{co,i}$ = county indicator variable (= 1.0 if county i , 0.0 otherwise);
- $b_{co,i}$ = county i regression coefficient; and
- c_o = regression coefficient.

The regression coefficient c_o was determined to be -0.193 for multiple-vehicle crashes, -0.203 for single-vehicle crashes, -0.212 for ramp-entrance-related crashes, and -0.223 for ramp-exit-related crashes. Each of these values is added to the appropriate intercept variables to compute an average intercept value for the overall database. This addition is shown in each of the next four sections.

Model for Predicting Multiple-Vehicle Non-Ramp-Related Crash Frequency

The results of the multiple-vehicle model calibration are presented in Table 40. The Pearson χ^2 statistic for the model is 1,743, the scaled deviance is 1,580, and the degrees of freedom are 1,576 ($= n - p = 1,589 - 13$). The Pearson χ^2 statistic is greater than $\chi^2_{0.05, 1576}$ (= 1,669) but the scaled deviance is less than 1,669. For reasons cited previously with regard to the full model, the hypothesis that the model fits the data is not rejected. The R^2 for the model is 0.66. An alternative measure of model fit that is better suited to the negative binomial distribution is R_k^2 . The R_k^2 for the calibrated model is 0.93.

TABLE 40. Freeway PDO model statistical description—multiple-vehicle model—three states

Model Statistics	Value
R^2 (R_k^2):	0.66 (0.93)
Scale parameter ϕ :	1.10
Pearson χ^2 :	1,743 ($\chi^2_{0.05, 1576} = 1,669$)
Inverse dispersion parameter K :	18.8 mi^{-1}
Observations n_o :	1,589 segments (9,960 PDO crashes in 3 years)
Standard deviation s_e :	± 2.59 crashes/yr

The coefficients in Table 39 were combined with Equations 37 to 40 to obtain the calibrated SPFs for multiple-vehicle non-entrance/exit crashes. The form of each model is described in the following equations.

$$N_{spf,mv,4} = \left(L - 0.5 \sum L_{en,seg,i} - 0.5 \sum L_{ex,seg,i} \right) e^{-6.355 - 0.193 + 1.936 \ln(AADT/1,000) - 0.332 I_{rural}} \quad (116)$$

$$N_{spf,mv,6} = \left(L - 0.5 \sum L_{en,seg,i} - 0.5 \sum L_{ex,seg,i} \right) e^{-6.616 - 0.193 + 1.936 \ln(AADT/1,000) - 0.332 I_{rural}} \quad (117)$$

$$N_{spf,mv,8} = \left(L - 0.5 \sum L_{en,seg,i} - 0.5 \sum L_{ex,seg,i} \right) e^{-6.804 - 0.193 + 1.936 \ln(AADT/1,000) - 0.332 I_{rural}} \quad (118)$$

$$N_{spf,mv,10} = \left(L - 0.5 \sum L_{en,seg,i} - 0.5 \sum L_{ex,seg,i} \right) e^{-7.067 - 0.193 + 1.936 \ln(AADT/1,000) - 0.332 I_{rural}} \quad (119)$$

The calibrated CMFs used with these SPFs are described in a subsequent section.

The fit of the calibrated models is shown in Figure 62. This figure compares the predicted and reported crash frequency in the calibration database. The trend line shown represents a “y = x” line. A data point would lie on this line if its predicted and reported crash frequency were equal. The data points shown represent the reported multiple-vehicle non-entrance/exit crash frequency for the segments used to calibrate the corresponding component model.

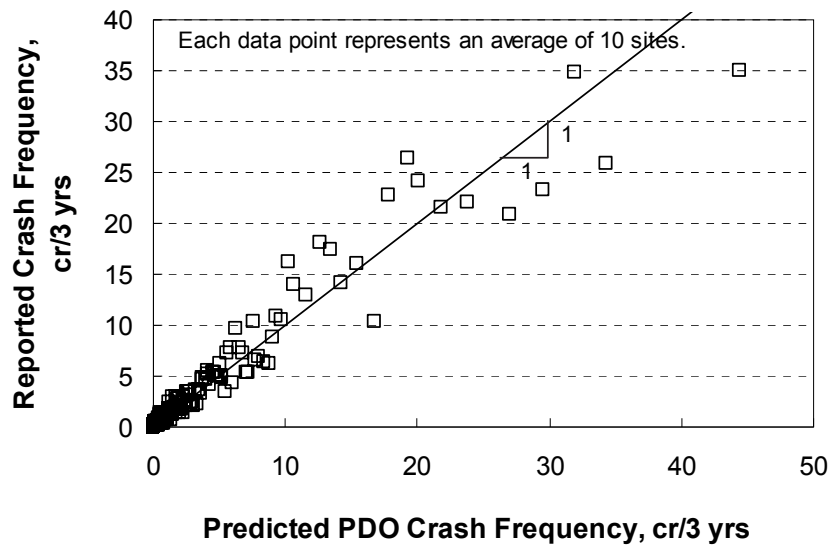


Figure 62. Predicted vs. reported multiple-vehicle freeway PDO crashes.

Each data point shown in Figure 62 represents the average predicted and average reported crash frequency for a group of 10 segments. The data were sorted by predicted crash frequency to form groups of segments with similar crash frequency. The purpose of this grouping was to reduce the number of data points shown in the figure and, thereby, to facilitate an examination of trends in the data. The individual segment observations were used for model calibration. In general, the data shown in the figure indicate that the model provides an unbiased estimate of expected crash frequency for segments experiencing up to 50 multiple-vehicle crashes in a three-year period.

Model for Predicting Single-Vehicle Non-Ramp-Related Crash Frequency

The results of the single-vehicle model calibration are presented in Table 41. The Pearson χ^2 statistic for the model is 2,036, the scaled deviance is 1,927, and the degrees of freedom are 1,838 ($= n - p = 1,848 - 10$). The Pearson χ^2 is greater than $\chi^2_{0.05, 1838} (= 1,939)$ but the scaled deviance is less than 1,939. For reasons cited previously with regard to the full model, the

hypothesis that the model fits the data is not rejected. The R^2 for the model is 0.65. The R_k^2 for the calibrated model is 0.89.

TABLE 41. Freeway PDO model statistical description—single-vehicle model—three states

Model Statistics	Value
R^2 (R_k^2):	0.65 (0.89)
Scale parameter ϕ :	1.10
Pearson χ^2 :	2,036 ($\chi^2_{0.05, 1838} = 1,939$)
Inverse dispersion parameter K :	20.7 mi ⁻¹
Observations n_o :	1,848 segments (5,372 PDO crashes in 3 years)
Standard deviation s_e :	±0.88 crashes/yr

The coefficients in Table 39 were combined with Equation 49 to obtain the calibrated SPF for single-vehicle non-entrance/exit crashes. The form of this model is described in the following equation.

$$N_{spf,sv} = \left(L - 0.5 \sum L_{en,seg,i} - 0.5 \sum L_{ex,seg,i} \right) e^{-1.955 - 0.203 + 0.876 \ln(AADT/1,000) - 0.0193 n} \quad (120)$$

The calibrated CMFs used with this SPF are described in a subsequent section.

The fit of the calibrated model is shown in Figure 63. This figure compares the predicted and reported crash frequency in the calibration database. Each data point shown represents the average predicted and average reported crash frequency for a group of 10 segments. In general, the data shown in the figure indicate that the model provides an unbiased estimate of expected crash frequency for segments experiencing up to 20 single-vehicle crashes in a three-year period.

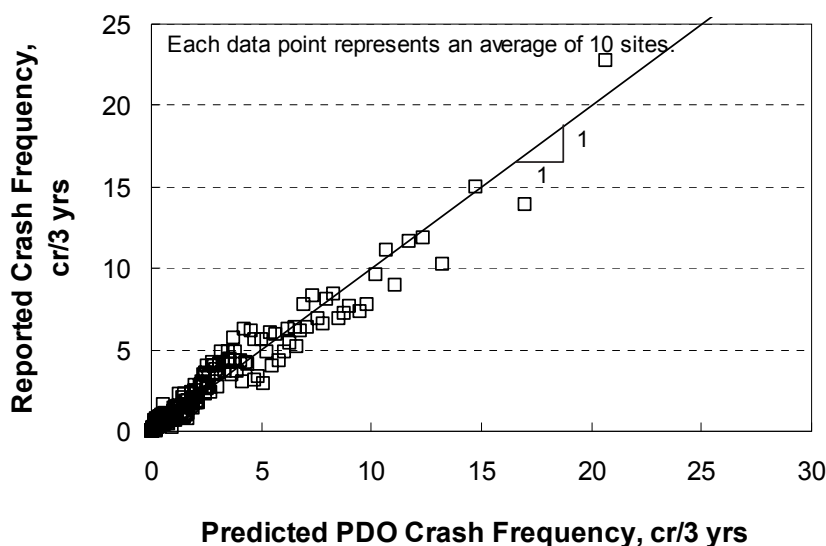


Figure 63. Predicted vs. reported single-vehicle freeway PDO crashes.

Model for Predicting Ramp-Entrance-Related Crash Frequency

The results of the ramp-entrance-related model calibration are presented in Table 42. The Pearson χ^2 statistic for the model is 623, and the degrees of freedom are 627 ($= n - p = 637 - 10$). As this statistic is less than $\chi^2_{0.05, 627} (= 686)$, the hypothesis that the model fits the data cannot be rejected. The R^2 for the model is 0.57. The R_k^2 for the calibrated model is 0.96.

TABLE 42. Freeway PDO model statistical description—ramp entrance model—three states

Model Statistics	Value
$R^2 (R_k^2)$:	0.57 (0.96)
Scale parameter ϕ :	0.93
Pearson χ^2 :	623 ($\chi^2_{0.05, 627} = 686$)
Inverse dispersion parameter K :	24.8 mi^{-1}
Observations n_o :	637 ramp entrances (1,369 PDO crashes in 3 years)
Standard deviation s_e :	± 0.96 crashes/yr

The coefficients in Table 39 were combined with Equation 59 to obtain the calibrated SPF for ramp-entrance-related crashes. The form of this model is described in the following equation.

$$N_{spf, en} = (L_{en}) e^{-2.180 - 0.212 + 1.215 \ln(AADT / 2,000) - 0.101 n - 0.0989 I_{rural}} \quad (121)$$

The calibrated CMFs used with this SPF are described in a subsequent section. This SPF is applied to a ramp entrance speed-change lane, as shown in Figure 38. The “segment” length is equal to the ramp entrance length L_{en} , which is measured using the gore and taper points identified in Figure 11.

The fit of the calibrated model is shown in Figure 64. This figure compares the predicted and reported crash frequency in the calibration database. Each data point shown represents the average predicted and average reported crash frequency for a group of 10 segments. In general, the data shown in the figure indicate that the model provides an unbiased estimate of expected crash frequency for segments experiencing up to 9.0 ramp-entrance-related crashes in a three-year period.

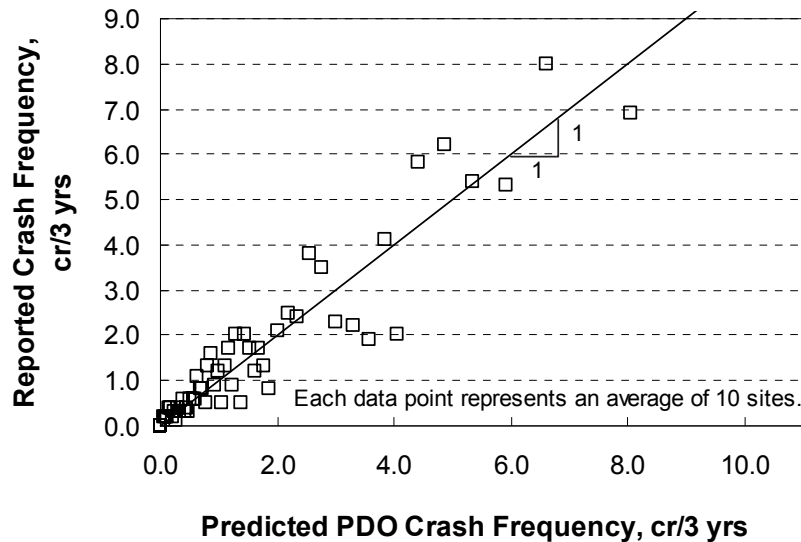


Figure 64. Predicted vs. reported ramp-entrance-related PDO crashes.

Model for Predicting Ramp-Exit-Related Crash Frequency

The results of the ramp-exit-related model calibration are presented in Table 43. The Pearson χ^2 statistic for the model is 487, and the degrees of freedom are 504 ($= n - p = 513 - 9$). As this statistic is less than $\chi^2_{0.05, 504} (= 557)$, the hypothesis that the model fits the data cannot be rejected. The R^2 for the model is 0.53. The R_k^2 for the calibrated model is 0.95. The inverse dispersion parameter for this model is dimensionless because crash frequency variance was found to be insensitive to ramp exit length.

TABLE 43. Freeway PDO model statistical description—ramp exit model—three states

Model Statistics	Value
R^2 (R_k^2):	0.53 (0.95)
Scale parameter ϕ :	0.95
Pearson χ^2 :	487 ($\chi^2_{0.05, 504} = 557$)
Inverse dispersion parameter K :	1.58
Observations n_o :	513 ramp exits (564 PDO crashes in 3 years)
Standard deviation s_e :	± 0.58 crashes/yr

The coefficients in Table 39 were combined with Equation 61 to obtain the calibrated SPF for ramp-exit-related crashes. The form of this model is described in the following equation.

$$N_{spf,ex} = (L_{ex}) e^{-1.575 - 0.223 + 0.932 \ln(AADT/2,000)} \quad (122)$$

The calibrated CMFs used with this SPF are described in a subsequent section. This SPF is applied to a ramp exit speed-change lane, as shown in Figure 38. The “segment” length is equal to the ramp exit length L_{ex} , which is measured using the gore and taper points identified in Figure 11.

The fit of the calibrated models is shown in Figure 65. This figure compares the predicted and reported crash frequency in the calibration database. Each data point shown represents the average predicted and average reported crash frequency for a group of 10 segments. In general, the data shown in the figure indicate that the model provides an unbiased estimate of expected crash frequency for segments experiencing up to 4.0 ramp-exit-related crashes in a three-year period.

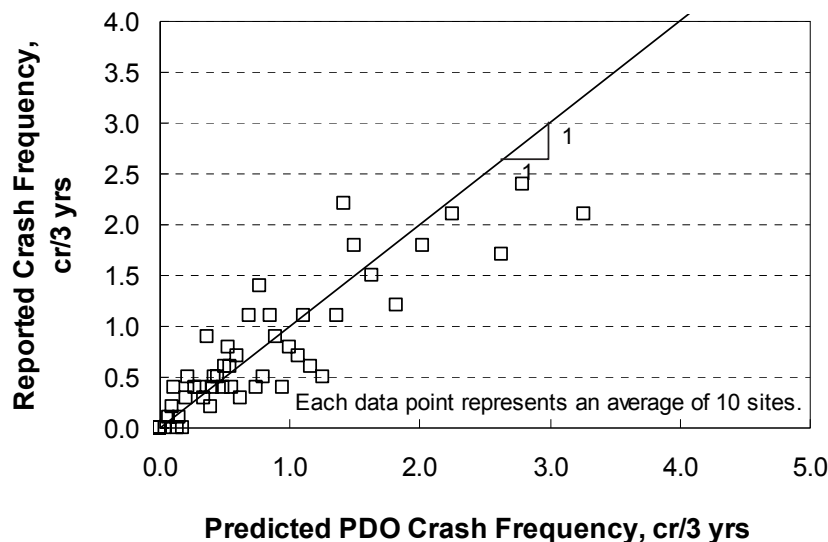


Figure 65. Predicted vs. reported ramp-exit-related PDO crashes.

Calibrated CMFs

Several CMFs were calibrated in conjunction with the SPFs. All of them were calibrated using PDO crash data. Collectively, they describe the relationship between various geometric factors and PDO crash frequency.

Many of the CMFs found in the literature are typically derived from (and applied to) the combination of multiple-vehicle and single-vehicle crashes. That is, one CMF is used to indicate the influence of a specified geometric factor on total crashes. In contrast, the models developed for this research project include several CMFs that are calibrated for a specific crash type. In

these instances, Equation 86 is used to convert the CMFs developed for this project into equivalent total-crash CMFs for the purpose of illustrating the overall trend. The proportion of multiple-vehicle crashes used in this equation is obtained from Table 44. The data in this table were obtained from the study state databases.

TABLE 44. Distribution of PDO crashes on freeways

Area Type	Number of Through Lanes	Multiple-Vehicle Non-Entrance/Exit PDO Crashes (MV)	Single-Vehicle Non-Entrance/Exit PDO Crashes	Proportion MV Crashes
Rural	4	628	1,162	0.351
	6	926	1,131	0.450
	8	388	346	0.529
Urban	4	906	662	0.578
	6	2,280	1,110	0.673
	8	2,868	635	0.819
	10	2,198	326	0.871

Horizontal Curve CMF. The calibrated horizontal curve CMF has two forms, depending on which component model is being used. The CMF for multiple-vehicle non-entrance/exit crashes, ramp-entrance-related crashes, and ramp-exit related crashes is described using the following equation.

$$CMF_{mv, hc|agg} = 1.0 + 0.0340 \sum_{i=1}^m \left(\frac{5,730}{R_i} \right)^2 P_{c,i} \quad (123)$$

The CMF for single-vehicle crashes is described using the following equation.

$$CMF_{sv, hc|agg} = 1.0 + 0.0626 \sum_{i=1}^m \left(\frac{5,730}{R_i} \right)^2 P_{c,i} \quad (124)$$

These two CMFs are derived to be applicable to a segment that has a mixture of uncurved and curved lengths. The variable $P_{c,i}$ is computed as the ratio of the length of curve i on the segment to the length of the segment.

The combined horizontal curve CMF is shown in Figure 66 using a series of thick, solid trend lines. Equation 86 was used to create these trend lines. They represent different combinations of area type and through lanes through their association with the different proportions of multiple-vehicle crashes in Table 44. The radii used to calibrate this CMF range from 1,500 to 12,000 ft. The base condition for this CMF is an uncurved (i.e., tangent) segment.

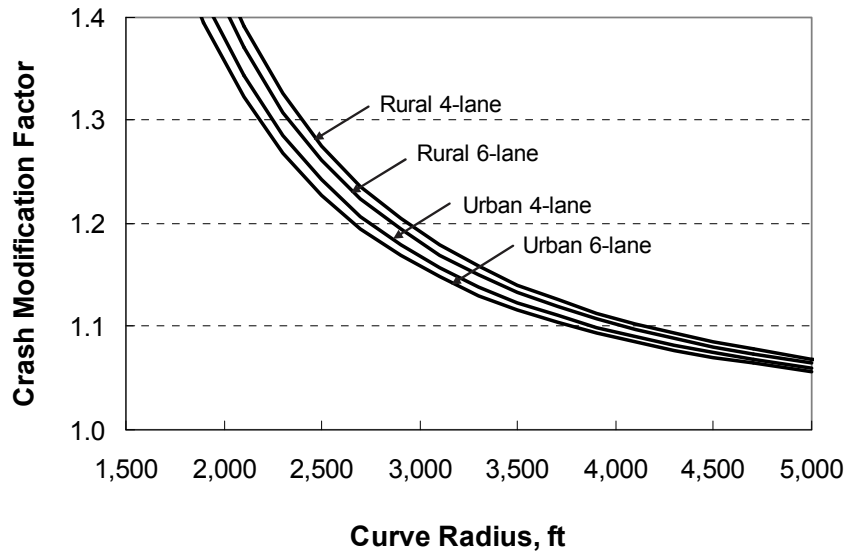


Figure 66. Calibrated freeway horizontal curve CMF for PDO crashes.

Outside Shoulder Width CMF. The outside shoulder width CMF is described using the following equation.

$$CMF_{sv,osw|agg} = (1.0 - \sum P_{c,i})1.0 + (\sum P_{c,i})e^{-0.0840(w_s-10)} \quad (125)$$

This CMF is applicable to single-vehicle crashes. The regression analysis indicated that the outside shoulder width had an insignificant correlation with multiple-vehicle crashes. The shoulder width used in this CMF is an average for both directions of travel. The variable $P_{c,i}$ is computed as the ratio of the length of curve i on the segment to the length of the segment. The CMF value is 1.0 when applied to a segment that is straight (i.e., no curves).

The combined outside shoulder width CMF for curved segments is shown in Figure 67. Equation 86 was used to create this CMF (with $CMF_{mv,osw} = 1.0$). It represents the likely correlation between outside shoulder width and total crash frequency. The trend lines represent different combinations of area type and through lanes through their association with the different proportions of multiple-vehicle crashes in Table 44. The shoulder widths used to calibrate this CMF range from 6 to 14 ft. The base condition for this CMF is a 10-ft shoulder width.

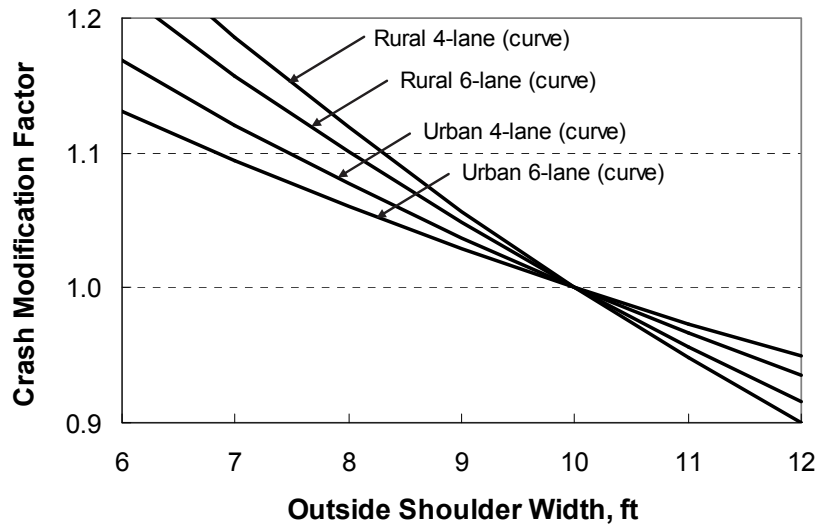


Figure 67. Calibrated freeway outside shoulder width CMF for PDO crashes.

Inside Shoulder Width CMF. The inside shoulder width CMF is described using the following equation.

$$CMF_{isw} = e^{-0.0153(W_{is}-6)} \quad (126)$$

The shoulder width used in this CMF is an average for both directions of travel. The inside shoulder width CMF is shown in Figure 68. The shoulder widths used to calibrate this CMF range from 2 to 11 ft. The base condition for this CMF is a 6-ft shoulder width.

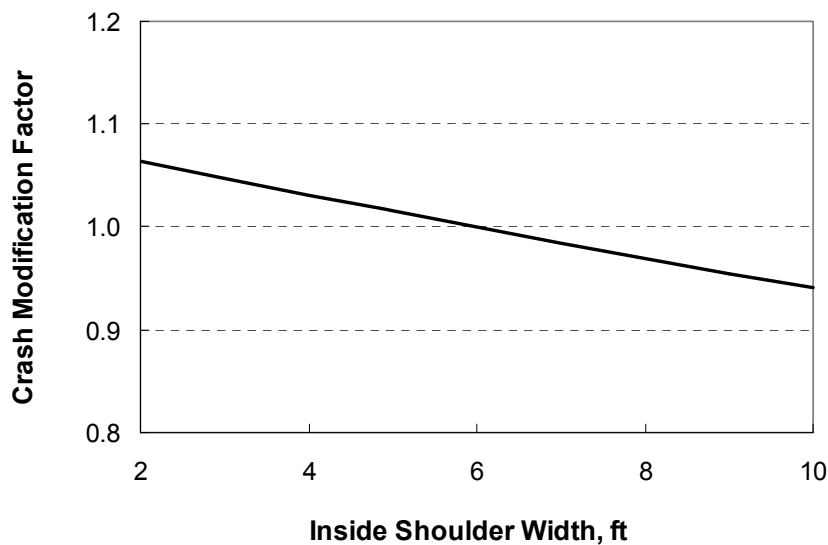


Figure 68. Calibrated freeway inside shoulder width CMF for PDO crashes.

Median Width CMF. The calibrated median width CMF has two forms, depending on which component model is being used. The CMF for multiple-vehicle non-entrance/exit crashes,

ramp-entrance-related crashes, and ramp-exit related crashes is described using the following equation.

$$CMF_{mv,mv|agg} = (1.0 - P_{ib}) e^{-0.00291(W_m - 2W_{is} - 48)} + P_{ib} e^{-0.00291(2W_{icb} - 48)} \quad (127)$$

The CMF for single-vehicle crashes is described using the following equation.

$$CMF_{sv,mv|agg} = (1.0 - P_{ib}) e^{-0.00289(W_m - 2W_{is} - 48)} + P_{ib} e^{-0.00289(2W_{icb} - 48)} \quad (128)$$

The median width used in either CMF is an average for the segment. These two CMFs are derived to be applicable to a segment that has median barrier present along some portion of the segment. Guidance for computing the variables P_{ib} and W_{icb} was provided previously in the subsection titled Barrier Variable Calculations.

The combined median width CMF is shown in Figure 69 using the line labeled “No barrier.” Equation 86 was used to create this CMF. The trend line shown represents an urban freeway. The slope of the line is slightly flatter for a rural freeway. The median widths used to calibrate this CMF range from 9 to 140 ft. The base condition for this CMF is a 60-ft median width and an inside shoulder width of 6.0 ft. The trend line labeled “Barrier in center...” is discussed with the next CMF.

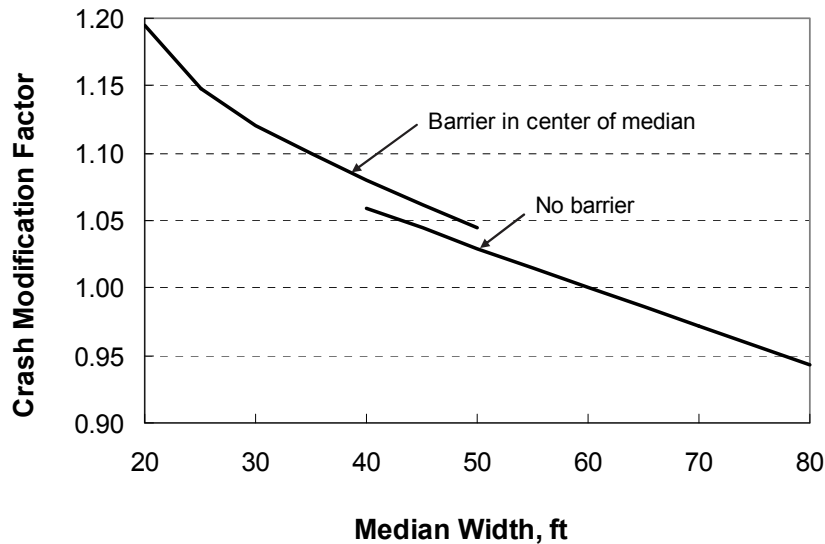


Figure 69. Calibrated freeway median width CMF for PDO crashes.

Median Barrier CMF. The median barrier CMF is described using the following equation.

$$CMF_{mb|agg} = (1.0 - P_{ib}) 1.0 + P_{ib} e^{0.169/W_{icb}} \quad (129)$$

Guidance for computing the variables P_{ib} and W_{icb} was provided previously in the subsection titled Barrier Variable Calculations. The variable W_{icb} (representing the distance from the edge of inside shoulder to median barrier face) ranges in value from 1.0 to 17 ft in the database. The base condition for this CMF is no barrier.

This median barrier CMF is shown in Figure 69 using the line labeled “Barrier in center...”. The values shown represent the median barrier CMF multiplied by the median width CMF because both CMFs are sensitive to the variable W_{icb} . The trend line shown is for urban freeways. It drops slightly for rural freeways.

Shoulder Rumble Strip CMF. The shoulder rumble strip CMF is described using the following equation.

$$CMF_{sv,rs|agg} = (1.0 - \sum P_{c,i})1.0 + (\sum P_{c,i})f_{cur} \quad (130)$$

$$f_{cur} = 0.5 ([1.0 - P_{ir}]1.0 + P_{ir} 1.20) + 0.5 ([1.0 - P_{or}]1.0 + P_{or} 1.20) \quad (131)$$

This CMF is applicable to single-vehicle crashes. The regression analysis indicated that shoulder rumble strip presence had an insignificant correlation with multiple-vehicle crashes. The proportion P_{ir} represents the proportion of the segment length with rumble strips present on the inside shoulders. It is computed by summing the length of roadway with rumble strips on the inside shoulder in *both* travel directions and dividing by twice the segment length. The proportion P_{or} represents the proportion of the segment length with rumble strips present on the outside shoulders. It is computed by summing the length of roadway with rumble strips on the outside shoulder in *both* travel directions and dividing by twice the segment length.

The constant “1.20” in Equation 131 represents the calibration coefficient after conversion. It corresponds to a CMF value of 1.20 for PDO crashes on curved road segments when shoulder rumble strips are continuously present. It suggests that there are 20 percent more crashes on curved road segments when rumble strips are present. A review of the literature on the safety effect of shoulder rumble strips on curves did not reveal any evidence that could support or refute this finding. In related research, Torbic et al. (2009) examined the safety effect of centerline rumble strips on rural two-lane highways in three states. They found that centerline rumble strips increased total crashes 3.5 percent on curved segments (although this result was not statistically significant).

Outside Barrier CMF. The calibrated outside barrier CMF is described using the following equation.

$$CMF_{sv,ob|agg} = (1.0 - P_{ob})1.0 + P_{ob} e^{0.169/W_{ocb}} \quad (132)$$

This CMF is applicable to single-vehicle crashes. The regression analysis indicated that outside barrier presence had an insignificant correlation with multiple-vehicle crashes. Guidance for computing the variables P_{ob} and W_{ocb} was provided previously in the subsection titled Barrier Variable Calculations. The variable W_{ocb} (representing the distance from the edge of outside shoulder to median barrier face) ranges in value from 1.0 to 17 ft in the database. The base condition for this CMF is no barrier.

The combined outside barrier CMF is shown in Figure 70. Equation 86 was used to create this CMF (with $CMF_{mv,ob} = 1.0$). It represents the likely correlation between outside barrier offset distance and crash frequency for total crashes. The trend lines represent different combinations of area type and through lanes through their association with the different proportions of multiple-vehicle crashes in Table 44.

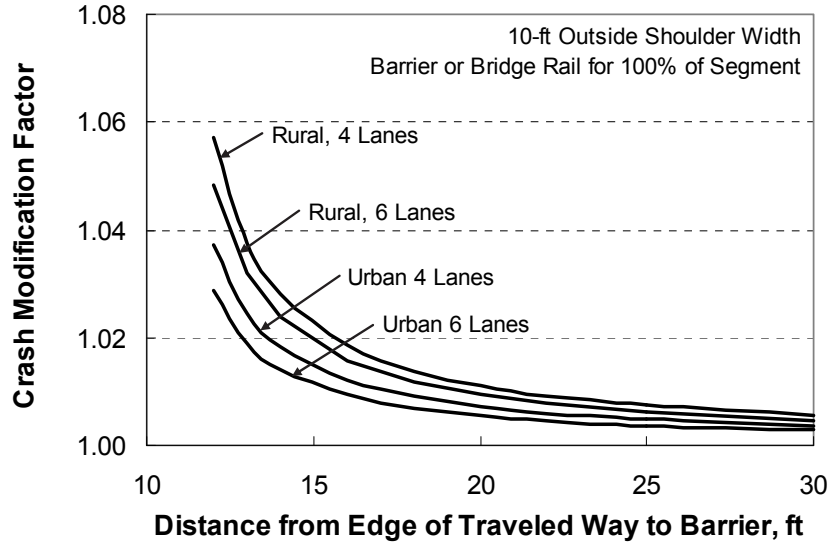


Figure 70. Calibrated freeway outside barrier CMF for PDO crashes.

Lane Change CMF. The calibrated lane change CMF is described using the following equations.

$$CMF_{mv,lc|agg} = (0.5 f_{wev,inc} f_{lc,inc}) + (0.5 f_{wev,dec} f_{lc,dec}) \quad (133)$$

$$f_{wev,inc} = (1.0 - P_{wevB,inc}) 1.0 + P_{wevB,inc} e^{0.123/L_{wev,inc}} \quad (134)$$

$$f_{wev,dec} = (1.0 - P_{wevB,dec}) 1.0 + P_{wevB,dec} e^{0.123/L_{wev,dec}} \quad (135)$$

$$f_{lc,inc} = \left(1.0 + \frac{e^{-13.46 X_{b,ent} - 0.283 \ln(AADT_{b,ent}/1,000)}}{13.46 L} [1.0 - e^{-13.46 L}] \right) \times \left(1.0 + \frac{e^{-13.46 X_{e,ext} - 0.283 \ln(AADT_{e,ext}/1,000)}}{13.46 L} [1.0 - e^{-13.46 L}] \right) \quad (136)$$

$$f_{lc,dec} = \left(1.0 + \frac{e^{-13.46 X_{e,ent} - 0.283 \ln(AADT_{e,ent}/1,000)}}{13.46 L} [1.0 - e^{-13.46 L}] \right) \times \left(1.0 + \frac{e^{-13.46 X_{b,ext} - 0.283 \ln(AADT_{b,ext}/1,000)}}{13.46 L} [1.0 - e^{-13.46 L}] \right) \quad (137)$$

The variables for weaving section length (i.e., $L_{wev,inc}$, $L_{wev,dec}$) in Equations 134 and 135 are intended to reflect the degree to which the weaving activity is concentrated along the freeway. This variable has negligible correlation with segment length L .

The variables $P_{wevB, inc}$ and $P_{wevB, dec}$ in Equations 134 and 135, respectively, are computed as the ratio of the length of the weaving section on the segment to the length of the segment. If the segment is wholly located in the weaving section, then this variable is equal to 1.0. The calibration coefficient in these two equations indicates that lane change CMF value will increase if the segment is in a Type B weaving section. The amount of this increase is inversely related to the length of the weaving section.

This CMF consists of several component equations but only requires a few input variables. These variables describe the distance to (and volume of) the four nearest ramps to the subject segment. Two of the ramps of interest are on side of the freeway with travel in the increasing milepost direction. One ramp on this side of the freeway is upstream of the segment and one ramp is downstream of the segment. Similarly, one ramp on the other side of the freeway is upstream of the segment and one ramp is downstream. Only those entrance ramps that contribute volume to the subject segment are of interest. Hence a downstream entrance ramp is not of interest. For similar reasons, an upstream exit ramp is not of interest. If the segment is in a Type B weaving section, then the length of the weaving section is also an input.

The lane-change CMF was applied to a range of weaving section lengths and the average CMF was computed for each length. The results of this process are plotted in Figure 71.

The lane-change CMF is applicable to any segment in the vicinity of one or more ramps. It is equally applicable to segments in a weaving section and segments in a non-weaving section (i.e., segments between an entrance ramp and an exit ramp where both ramps have a speed-change lane).

The two component models for predicting speed-change-related crash frequency (i.e., Equations 121 and 122) are not used when evaluating a weaving section because the ramps that form the weaving section do not have a speed-change lane. As a result, the predicted crash frequency for the set of segments that comprise a weaving section will tend to be smaller than that predicted for a similar set of segments located in a non-weaving section. This generalization will always be true for the Type A and Type C weaving sections. It may or may not hold for the Type B weaving section, depending on the length of the weaving section.

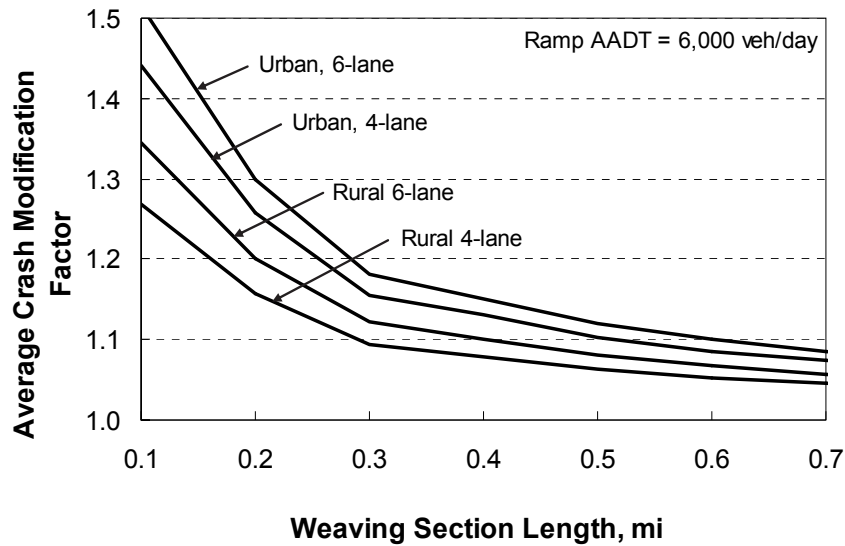


Figure 71. Average CMF value for PDO crashes as a function of weaving section length.

The calibration coefficient associated with the ramp AADT term in Equations 136 and 137 is negative which is counterintuitive at first glance. It indicates that the lane change CMF is larger for segments associated with lower volume ramps. This trend may be explained by the fact that high-volume ramp flows tend to dominate the traffic stream such that a large portion of the traffic stream is changing lanes and all drivers are more aware of these maneuvers. Regardless, the entering ramp volumes are also included in the segment AADT volume and the coefficient associated with the segment AADT variable in the SPF is positive and relatively large. As a result, when all relevant SPFs and CMFs are combined, the predicted average crash frequency for a freeway segment increases with an increase in the AADT volume of nearby ramps. This trend is logical and intuitive.

Ramp Entrance CMF. The ramp entrance CMF is described using the following equation.

$$CMF_{en} = e^{0.824 I_{left} + 0.0252 / L_{en}} \quad (138)$$

This CMF is applied to a ramp entrance speed-change lane, as shown in Figure 38. The “segment” length is equal to the ramp entrance length L_{en} , which is measured using the gore and taper points identified in Figure 11. This CMF applies only to the side of the freeway with the subject speed-change lane.

The variable for ramp entrance length L_{en} in Equation 138 is intended to reflect the degree to which the lane-changing activity is concentrated along the ramp entrance. This variable has negligible correlation with segment length L .

The indicator variable for ramp side I_{left} is associated with a positive calibration coefficient. It suggests that a ramp entrance on the left side of the through lanes is associated with a 128 percent increase in crashes, relative to one on the right side. This finding is consistent

with that of Moon and Hummer (2009), and with that from the re-analysis of the data reported by Lundy (1966), as documented in Chapter 2.

The ramp entrance CMF for right-side ramps is shown in Figure 72. It has been adjusted using Equation 106 to convert it into a CMF that is applicable to the entire segment (i.e., both sides of the freeway). The ramp entrance lengths used to calibrate this CMF range from 0.07 to 0.22 mi (370 to 1,200 ft).

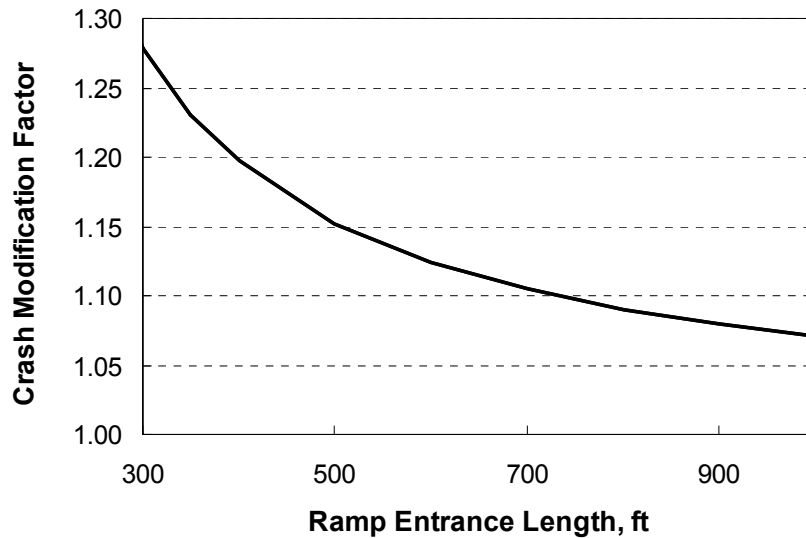


Figure 72. Calibrated freeway ramp entrance CMF for right-side ramps and PDO crashes.

Ramp Exit CMF. The ramp exit CMF is described using the following equation.

$$CMF_{ex} = e^{0.824 I_{left}} \quad (139)$$

This CMF is applied to a ramp exit speed-change lane, as shown in Figure 38. The “segment” length is equal to the ramp exit length L_{ex} , which is measured using the gore and taper points identified in Figure 11. This CMF applies only to the side of the freeway with the subject speed-change lane.

The interpretation of the indicator variable for ramp side I_{left} is provided with the previous CMF discussion.

High-Volume CMF. The calibrated high-volume CMF has two forms, depending on which component model is being used. The CMF for multiple-vehicle non-entrance/exit crashes, ramp-entrance-related crashes, and ramp-exit related crashes is described using the following equation.

$$CMF_{mv,hv} = e^{0.283 P_{hv}} \quad (140)$$

The CMF for single-vehicle crashes is described using the following equation.

$$CMF_{sv,hv} = e^{-0.611P_{hv}} \quad (141)$$

The proportion of AADT during hours where volume exceeds 1,000 veh/h/ $\ln P_{hv}$ is computed using the average hourly volume distribution associated with the subject segment. This distribution will typically be computed using the data obtained from the nearest continuous traffic counting station (on a freeway of similar character). The variable P_{hv} is positively correlated with the volume-to-capacity ratio experienced by the segment on an hourly basis.

The high-volume CMF is shown in Figure 73. The trend lines represent different combinations of area type and through lanes through their association with the different proportions of multiple-vehicle crashes in Table 44. The base condition for this CMF is a proportion P_{hv} equal to 0.0. The trends shown in both figures are consistent with those developed by Lord et al. (2005) for multiple-vehicle and single-vehicle crashes as a function of volume-to-capacity ratio.

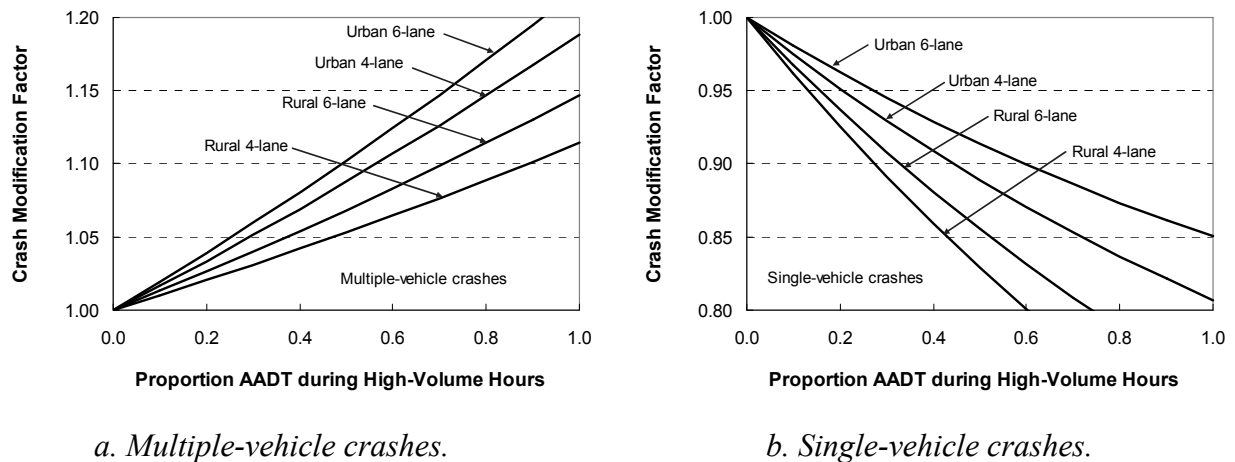
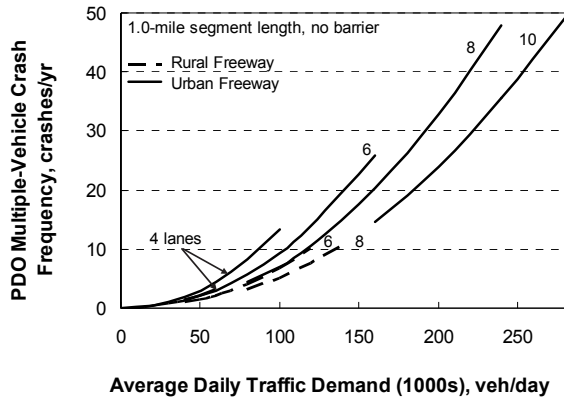


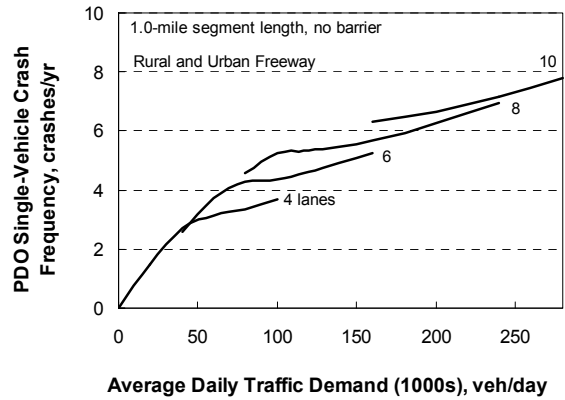
Figure 73. Calibrated freeway high-volume CMF for PDO crashes.

Sensitivity Analysis

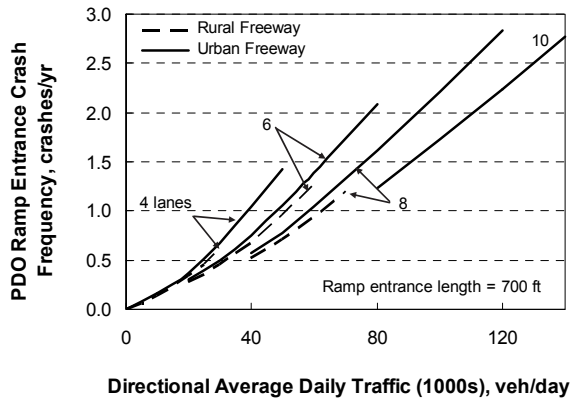
The relationship between crash frequency and traffic demand, as obtained from the combined calibrated models, is illustrated in Figure 74 for a 1-mile freeway segment with two ramp entrances, two ramp exits, no curvature, and no barrier. The individual component models are illustrated in Figures 74a, 74b, 74c, and 74d. The sum of the individual component crash frequencies is illustrated in Figure 75. The length of the trend lines in Figures 74 and 75 reflect the range of AADT volume in the data.



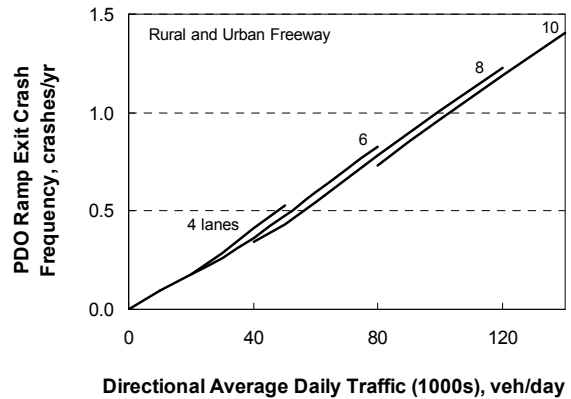
a. Multiple-vehicle crashes.



b. Single-vehicle crashes.



c. Ramp-entrance-related crashes.



d. Ramp-exit-related crashes.

Figure 74. Freeway PDO model components.

The trend lines shown in Figure 75 indicate that urban freeways have about 15 percent more crashes than rural freeways. By comparison, the crash rates listed in Table 19 indicate that urban freeways have 50 to 250 percent more crashes than rural freeways. It is likely that this latter trend reflects the influence of barrier length, ramp entrances, ramp exits, and weaving section length. As shown in Table 18, these influences are more prevalent on urban freeway segments. In contrast, these influences have been explicitly quantified in the proposed model such that they do not influence the trends shown in Figure 75. The proposed model provides a more accurate indication of differences between freeway segments in rural versus urban areas, when the segments have the same barrier proportion, ramp entrance length, and weaving section length.

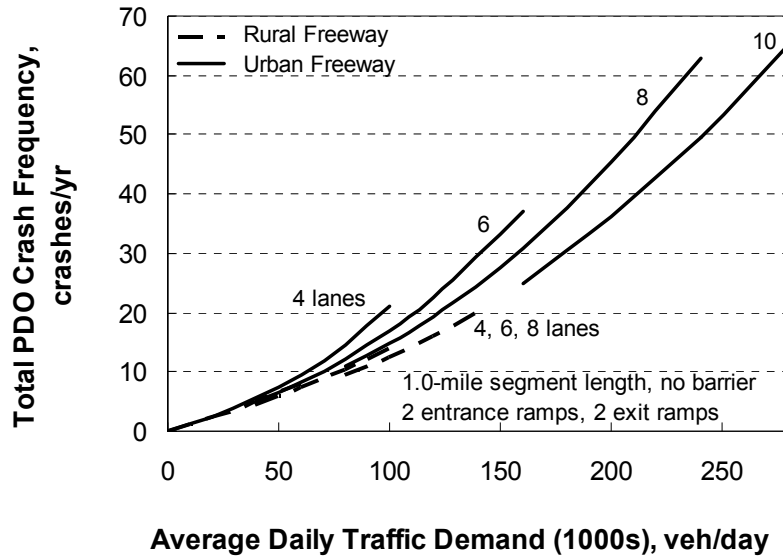


Figure 75. Freeway PDO model.

The trend lines shown in Figure 75 also indicate that crash frequency is *lower* on freeways with many lanes than it is on freeways with few lanes. In fact, the models indicate that an urban six-lane freeway segment has about 15 percent fewer crashes than an urban four-lane segment and that a rural six-lane segment has about 10 percent fewer crashes than an urban four-lane segment. These trends are counter to those found when comparing the crash rates in Table 19, which indicate that crash rate is *higher* on freeways with many lanes. It is likely that these trends in crash rate reflect the fact that the proportion of barrier along a freeway segment typically increases (and the lateral clearance decreases) with an increase in the number of lanes. The proposed predictive models account for the influence of barrier presence and lateral clearance and, therefore, provide a more accurate indication of the relationship between number-of-lanes and crash frequency.

NOMENCLATURE

- σ_p = standard deviation of P_i ;
- $AADT$ = AADT volume on segment, veh/day;
- $AADT_{b, ent}$ = AADT volume of entrance ramp located at distance $X_{b, ent}$, veh/day;
- $AADT_{b, ext}$ = AADT volume of exit ramp located at distance $X_{b, ext}$, veh/day;
- $AADT_{e, ent}$ = AADT volume of entrance ramp located at distance $X_{e, ent}$, veh/day;
- $AADT_{e, ext}$ = AADT volume of exit ramp located at distance $X_{e, ext}$, veh/day;
- $AADT_r$ = AADT volume of ramp, veh/day;
- $AADT_{r, i}$ = AADT volume of ramp i , veh/day;
- b_0 = calibration coefficient;
- b_i = calibration coefficient for condition i
- $b_{j, i}$ = calibration coefficients for model j ($j = mv, sv, en, ex$), $i = 0, 1$;
- C_{en} = local calibration factor for ramp-entrance-related crashes;
- C_{ex} = local calibration factor for ramp-exit-related crashes;
- $CMF_1 \dots CMF_k$ = crash modification factors for freeway segment crashes at a site with specific geometric design features k ;

CMF_{en} = ramp entrance crash modification factor;
 $CMF_{en|agg}$ = aggregated ramp entrance crash modification factor;
 $CMF_{en,1} \dots CMF_{en,y}$ = crash modification factors for ramp-entrance-related crashes at a site with specific geometric design features y ;
 $CMF_{ex,1} \dots CMF_{ex,z}$ = crash modification factors for ramp-exit-related crashes at a site with specific geometric design features z ;
 $CMF_{ex|agg}$ = aggregated ramp exit crash modification factor;
 CMF_{hc} = horizontal curve crash modification factor;
 $CMF_{hc|agg}$ = aggregated horizontal curve CMF for a segment with both tangent and curved portions;
 CMF_{hv} = high volume crash modification factor;
 CMF_i = crash modification factor for element i ;
 $CMF_{i|agg}$ = aggregated CMF for element i ;
 CMF_{isw} = inside shoulder width crash modification factor;
 $CMF_{j,i}$ = crash modification factor for element i and crash type j ($j = mv, sv$);
 CMF_{lc} = lane change crash modification factor;
 CMF_{lw} = lane width crash modification factor;
 $CMF_{mb|agg}$ = aggregated median barrier crash modification factor;
 $CMF_{mv,1} \dots CMF_{mv,w}$ = crash modification factors for multiple-vehicle crashes at a site with specific geometric design features w ;
 $CMF_{mv,hc|agg}$ = aggregated horizontal curve crash modification factor for multiple-vehicle crashes;
 $CMF_{mv,hv}$ = high-volume crash modification factor for multiple-vehicle crashes;
 $CMF_{mv,lc|agg}$ = aggregated lane change crash modification factor for multiple-vehicle crashes;
 $CMF_{mv,mw|agg}$ = aggregated median width crash modification factor for multiple-vehicle crashes;
 $CMF_{sv,1} \dots CMF_{sv,x}$ = crash modification factors for single-vehicle crashes at a site with specific geometric design features x ;
 $CMF_{sv,hc|agg}$ = aggregated horizontal curve crash modification factor for single-vehicle crashes;
 $CMF_{sv,hv}$ = high-volume crash modification factor for single-vehicle crashes;
 $CMF_{sv,mw|agg}$ = aggregated median width crash modification factor for single-vehicle crashes;
 $CMF_{sv,ob|agg}$ = aggregated outside barrier crash modification factor for single-vehicle crashes;
 $CMF_{sv,oc|agg}$ = aggregated outside clearance crash modification factor for single-vehicle crashes;
 $CMF_{sv,osw|agg}$ = aggregated outside shoulder width crash modification factor for single-vehicle crashes;
 $CMF_{sv,rs|agg}$ = aggregated shoulder rumble strip crash modification factor for single-vehicle crashes;
 C_{mv} = local calibration factor for multiple-vehicle non-entrance/exit crashes;
 C_{sv} = local calibration factor for single-vehicle non-entrance/exit crashes;
 e = superelevation rate, ft/ft;
 f_{cur} = factor for rumble strip presence on curved portions of the segment;
 f_d = side friction demand factor;
 $f_{lc,dec}$ = lane change adjustment factor for travel in decreasing milepost direction;
 $f_{lc,inc}$ = lane change adjustment factor for travel in increasing milepost direction;
 f_{tan} = factor for rumble strip presence on tangent portions of the segment;
 $f_{wev,dec}$ = weaving section adjustment factor for travel in decreasing milepost direction;
 $f_{wev,inc}$ = weaving section adjustment factor for travel in increasing milepost direction;

I_c = curve deflection angle, degrees;
 I_{en} = crash indicator variable (= 1.0 if ramp-entrance-related crash data, 0.0 otherwise);
 I_{ex} = crash indicator variable (= 1.0 if ramp-exit-related crash data, 0.0 otherwise);
 $I_{left,i}$ = ramp side indicator variable for ramp i (= 1.0 if entrance or exit is on left side of through lanes, 0.0 if it is on right side);
 I_{mv} = crash indicator variable (= 1.0 if multiple-vehicle non-entrance/exit crash data, 0.0 otherwise);
 I_n = cross section indicator variable (= 1.0 if cross section has n lanes, 0.0 otherwise);
 I_{rural} = area type indicator variable (= 1.0 if area is rural, 0.0 if it is urban);
 I_{sv} = crash indicator variable (= 1.0 if single-vehicle non-entrance/exit crash data, 0.0 otherwise);
 k = overdispersion parameter, mi;
 K = inverse dispersion parameter (= $1/k$), mi^{-1} ;
 k_{null} = overdispersion parameter based on the variance in the observed crash frequency;
 L = length of segment, mi;
 L_c = length of horizontal curve (= $I_c \times R / 5280 / 57.3$), mi;
 $L_{en,i}$ = length of ramp entrance for ramp i (may extend beyond segment boundaries), mi;
 $L_{en,seg,i}$ = length of ramp entrance i on segment, mi;
 $L_{ex,i}$ = length of ramp exit for ramp i (may extend beyond segment boundaries), mi;
 $L_{ex,seg,i}$ = length of ramp exit i on segment, mi;
 $L_{ib,i}$ = length of lane paralleled by inside barrier i (include both travel directions), mi;
 $L_{ob,i}$ = length of lane paralleled by outside barrier i (include both travel directions), mi; and
 $L_{wev,dec}$ = weaving section length for travel in decreasing milepost direction (may extend beyond segment boundaries), mi;
 $L_{wev,inc}$ = weaving section length for travel in increasing milepost direction (may extend beyond segment boundaries), mi;
 n = number of observations;
 n = number of through lanes on segment;
 N = predicted average crash frequency, crashes/yr;
 N_{curve} = predicted average additional crashes due to curvature; crashes/yr;
 N_{en} = predicted average ramp-entrance-related crash frequency, crashes/yr;
 N_{ex} = predicted average ramp-exit-related crash frequency, crashes/yr;
 N_j = predicted average crash frequency for model j ($j = mv, sv, en, ex$); crashes/yr;
 N_{mv} = predicted average multiple-vehicle non-entrance/exit crash frequency, crashes/yr;
 $N_{section}$ = predicted average crash frequency within the limits of a freeway section, crashes/yr;
 N_{seg} = predicted average crash frequency on segment (regardless of curvature), crashes/yr;
 $N_{spf,en}$ = predicted average ramp-entrance-related crash frequency for base conditions, crashes/yr;
 $N_{spf,ex}$ = predicted average ramp-exit-related crash frequency for base conditions, crashes/yr;
 $N_{spf,mv,n}$ = predicted average multiple-vehicle non-entrance/exit crash frequency for base conditions for number of through lanes n ($n = 4, 6, 8, 10$); crashes/yr;
 $N_{spf,mv}$ = predicted average multiple-vehicle non-entrance/exit crash frequency for base conditions, crashes/yr;
 $N_{spf,sv}$ = predicted average single-vehicle non-entrance/exit crash frequency for base conditions, crashes/yr;

N_{sv} = predicted average single-vehicle non-entrance/exit crash frequency, crashes/yr;
 P_1 = proportion of AADT in travel direction 1;
 P_2 = proportion of AADT in travel direction 2 (= 1.0 - P_1);
 P_c = proportion of the segment length with curvature;
 $P_{c,i}$ = proportion of segment length with curve i ;
 P_{hv} = proportion of AADT during hours where volume exceeds 1,000 veh/h/ln;
 P_i = proportion of AADT in travel direction i that corresponds to subject speed-change lane;
 P_{ib} = proportion of segment length with a barrier present in the median (i.e., inside);
 P_{ir} = proportion of segment length with rumble strips present on the inside shoulders;
 $P_{L,i}$ = proportion of the segment length with element i ;
 P_{mv} = proportion of multiple-vehicle crashes;
 P_{ob} = proportion of segment length with a barrier present on the roadside (i.e., outside);
 P_{or} = proportion of segment length with rumble strips present on the outside shoulders;
 $P_{wevB, dec}$ = proportion of segment length within a Type B weaving section for travel in decreasing milepost direction;
 $P_{wevB, inc}$ = proportion of segment length within a Type B weaving section for travel in increasing milepost direction;
 R = curve radius, ft;
 R_i = radius of curve i , ft;
 s_e = root mean square error of the model estimate, crashes/yr;
 V_c = average curve speed, mi/h;
 $V[X]$ = crash frequency variance for a group of similar locations, crashes²;
 W_{hc} = clear zone width, ft;
 W_{ib} = inside barrier width (measured from barrier face to barrier face), ft;
 W_{icb} = distance from edge of inside shoulder to barrier face, ft;
 W_{is} = inside shoulder width, ft;
 W_l = lane width, ft;
 W_m = median width (measured from near edges of traveled way in both travel directions), ft;
 W_{near} = “near” horizontal clearance from the edge of the traveled way to the continuous median barrier (measure for both travel directions and use the smaller distance), ft;
 W_{ocb} = distance from edge of outside shoulder to barrier face, ft;
 $W_{off, in, i}$ = horizontal clearance from the edge of the traveled way to the face of inside barrier i , ft.
 $W_{off, o, i}$ = horizontal clearance from the edge of the traveled way to the face of outside barrier i , ft.
 W_s = outside shoulder width, ft;
 X = reported crash count for y years, crashes;
 \bar{X} = average crash frequency for all n observations;
 $X_{b, ent}$ = distance from segment begin milepost to nearest upstream entrance ramp gore point, for travel in increasing milepost direction, mi;
 $X_{b, ext}$ = distance from segment begin milepost to nearest downstream exit ramp gore point, for travel in decreasing milepost direction, mi;
 x_b = distance from ramp gore to start of segment, mi;
 $X_{e, ent}$ = distance from segment end milepost to nearest upstream entrance ramp gore point, for travel in decreasing milepost direction, mi;
 $X_{e, ext}$ = distance from segment end milepost to nearest downstream exit ramp gore point, for travel in increasing milepost direction, mi;

$x_e =$ distance from ramp gore to end of segment ($x_e > x_b$), mi;
 $y =$ time interval during which X crashes were reported, yr;

CHAPTER 6: PREDICTIVE MODEL FOR RAMP SEGMENTS

This chapter describes the activities undertaken to calibrate and validate safety predictive models for ramp segments and collector-distributor (C-D) road segments. Each model consists of a safety performance function (SPF) and a family of crash modification factors (CMFs). The SPF is derived to estimate the crash frequency for ramp and C-D road segments with specified design elements and operating conditions. The CMFs are used to adjust the SPF estimate whenever one or more elements or conditions deviate from those that are specified.

The calibrated safety predictive models were used to develop a safety predictive method for ramps and C-D roads. This method describes how to use the models to evaluate ramp and C-D road safety, as may be influenced by road geometry, roadside features, traffic volume, and lane-change-related traffic maneuvers. This predictive method is documented in Appendix D.

Collectively, the predictive models for ramp and C-D road segments address the following area type and lane combinations.

- rural entrance ramp with one lane,
- rural exit ramp with one lane,
- rural C-D road with one lane
- urban C-D road with one lane,
- urban C-D road with two lanes,
- urban entrance ramp with one lane,
- urban entrance ramp with two lanes,
- urban exit ramp with one lane, and
- urban exit ramp with two lanes.

Eight typical ramp configurations were identified in Figure 4. In reality, there are many variations of each configuration and no two ramps are identical. In recognition of this variability in ramp configuration, it was rationalized that a predictive model should include CMFs to account for the differences in ramp geometry that underlie ramp configuration. To ensure adequate sensitivity to geometric differences among configurations, the calibration database was assembled to include a wide range of ramp configurations.

This chapter is divided into six parts. The first part provides some background information on the topic of predictive models for ramp and C-D road segments. The second part describes the theoretic development of selected CMFs. The third part describes the method used to calibrate the proposed models. The fourth part describes the calibration of the models to predict fatal-and-injury (FI) crash frequency. The fifth part describes the calibration of the models to predict property-damage-only crash (PDO) frequency. The sixth part provides a list of the variables defined in this chapter.

BACKGROUND

This part of the chapter consists of three sections. The first section describes the decomposition of an interchange into analysis units (i.e., sites). The second section provides a brief overview of the safety predictive model structure. The third section reviews the highway safety data assembled for model calibration.

Ramp Segments, C-D Road Segments, and Ramp Terminals

For analysis purposes, an interchange is considered to consist of a set of ramp segments, crossroad ramp terminals, and, possibly, one or more C-D road segments. These components are also referred to as “sites.”

Figure 76 illustrates these sites in the context of four ramps and a C-D road at an interchange. The arrangement shown is intended to illustrate the types of sites used for interchange safety evaluation—it is not necessarily a typical interchange and many interchanges are not likely to include a C-D road.

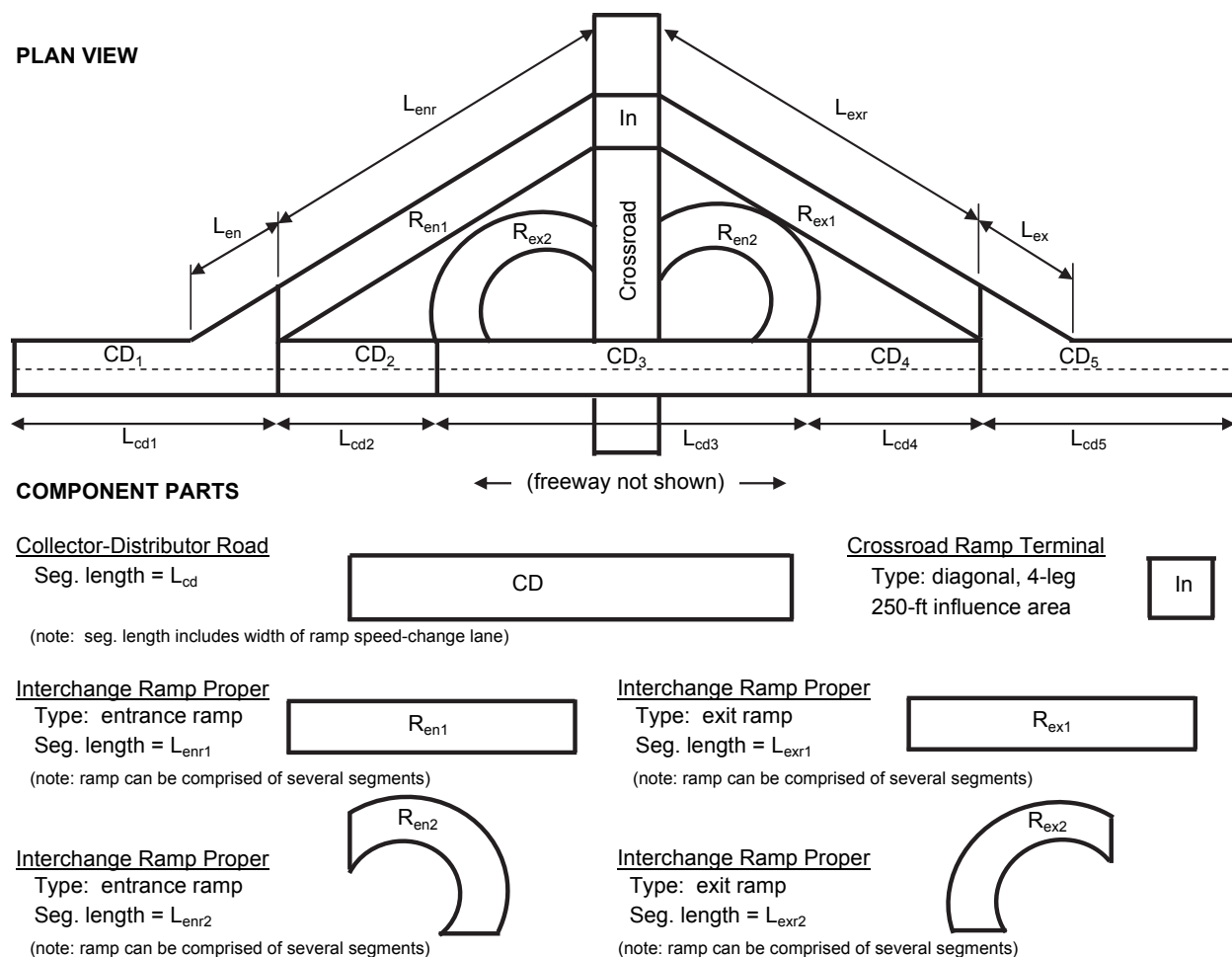


Figure 76. Illustrative interchange analysis sites.

As indicated in the *HSM*, road segment boundaries are typically defined by intersections or by a change in the cross section. This guidance also applies to ramp, C-D road, and crossroad segments.

Unlike freeways, speed-change lanes on ramps and on crossroads are not explicitly represented by a predictive model. However, a CMF was developed to recognize their presence on a ramp or C-D road segment.

Safety Predictive Models

The predicted average crash frequency for an interchange is computed as the sum of the predicted average crash frequency of all sites that comprise the facility. This calculation is described by Equation 142.

$$N_{interchange} = \sum_{all\ segments} (N_{mv} + N_{sv}) + \sum_{all\ terminals} (N_{rt}) \quad (142)$$

where,

$N_{interchange}$ = predicted average crash frequency within the limits of an interchange, crashes/yr;

N_{mv} = predicted average multiple-vehicle crash frequency, crashes/yr;

N_{sv} = predicted average single-vehicle crash frequency, crashes/yr; and

N_{rt} = predicted average crossroad ramp terminal crash frequency, crashes/yr.

The predicted average crash frequency for each site is computed using a predictive model. Each model represents the combination of an SPF and several CMFs. The SPF is used to estimate the average crash frequency for a generic site whose attributes are consistent with the SPF's stated base conditions. The CMFs are used to adjust the SPF estimate when the attributes of the subject site are not consistent with the base conditions. The general form of the safety predictive models for segments is shown as Equation 143 and Equation 144. The general form of the model for crossroad ramp terminals is described in Chapter 7.

$$N_{mv} = C_{mv} \times N_{spf, mv} \times (CMF_{mv,1} \times \dots \times CMF_{mv,w}) \times (CMF_1 \times \dots \times CMF_k) \quad (143)$$

$$N_{sv} = C_{sv} \times N_{spf, sv} \times (CMF_{sv,1} \times \dots \times CMF_{sv,x}) \times (CMF_1 \times \dots \times CMF_k) \quad (144)$$

where,

$N_{spf, mv}$ = predicted average multiple-vehicle crash frequency for base conditions, crashes/yr;

$N_{spf, sv}$ = predicted average single-vehicle crash frequency for base conditions, crashes/yr;

C_{mv} = local calibration factor for multiple-vehicle crashes;

C_{sv} = local calibration factor for single-vehicle crashes;

$CMF_{mv, 1} \dots CMF_{mv, w}$ = crash modification factors for multiple-vehicle crashes at a site with specific geometric design features w ;

$CMF_{sv, 1} \dots CMF_{sv, x}$ = crash modification factors for single-vehicle crashes at a site with specific geometric design features x ; and

$CMF_1 \dots CMF_k$ = crash modification factors for ramp and C-D road segment crashes at a site with specific geometric design features k .

The first term in parentheses in Equations 143 and 144 recognizes that the influence of some geometric factors is unique to each crash type. In contrast, the second term in parentheses in these equations recognizes that some geometric factors have a similar influence on all crash types.

Highway Safety Database

The Highway Safety Information System (HSIS) was used as the primary source of data for model calibration and validation. The “HSIS” states California, Maine, and Washington were identified as including ramp volume data, which is of fundamental importance to all aspects of this project. These data were not available from the other HSIS states. Hence, the database assembly focused on these three states. They are called the “study states” in this report.

In addition to ramp volume data, each study state database included a range of data describing the location, area type, traffic characteristics, geometry, and lane use for ramp and C-D road segments. The data acquired from these databases is summarized in Table 45.

TABLE 45. Ramp variables from HSIS database

Category	Variable	Description
Descriptive	state	Source of data (CA, ME, WA)
	rte_nbr	State route number
	rte_suf	State route suffix
	county	County number (established by state DOT)
	begmp	Begin milepost (established by state DOT in CA, WA; by researchers for ME)
	endmp	End milepost (established by state DOT in CA, WA; by researchers for ME)
	seg_lng	Segment length, mi
	rururb	Area type (urban, rural)
Traffic	ave_adt	Segment AADT averaged for a five-year period
Crash	nk_mv	Count of reported fatal, multiple-vehicle crashes during five-year period
	na_mv	Count of reported incapacitating-injury, multiple-vehicle crashes during five-year period
	nb_mv	Count of reported non-incapacitating-injury, multiple-vehicle crashes during five-year period
	nc_mv	Count of reported possible-injury, multiple-vehicle crashes during five-year period
	no_mv	Count of reported property-damage-only, multiple-vehicle crashes during five-year period
	:	Repeat five variables above for single-vehicle crashes

The data identified as “Descriptive” in Table 45 were obtained directly from the HSIS database for each study state. The data identified as “Traffic” or “Crash Data” were derived from the HSIS data. SAS software was used to manipulate the HSIS data to compute the desired variables.

As discussed in Appendix B, several of the geometry and lane use variables in the study state databases were of unknown accuracy. Also, several variables often had subtly different definitions among states. Moreover, the study state databases often did not include variables that describe road-related factors known to be associated with crash frequency. To overcome these limitations, the study-state databases were enhanced using data from other sources. These variables are listed in Table 46. The collection of these data required the location of each ramp using geographic coordinates and aerial photography, based on the freeway milepost reference system in HSIS.

TABLE 46. Ramp variables from supplemental data sources

Category	Variable	Description
Descriptive	lat_lon_coord	Latitude and longitude of begin milepost
	shape	Configuration of ramp (e.g., diagonal, loop, C-D road, etc.)
	start_location	Quadrant in which segment is located
	start_side	Indicates whether ramp diverges from freeway on left or right side
	end_side	Indicates whether ramp merges with freeway on left or right side
	meter	Indicates whether ramp has a meter on it
	HOV_bypass	Indicates whether ramp has an HOV bypass lane on it
Roadway	lanes_1	Number of lanes at the start of the segment
	lanes_2	Number of lanes at the end of the segment
	r_shld_width	Width of paved right shoulder
	lane_width	Lane width (average for all lanes)
	l_shld_width	Width of paved left shoulder
	opp_traf_len	Length of segment that is adjacent to another segment with vehicles traveling in an opposing direction (no restrictive median)
Roadside	r_barrier_off	Average offset to barrier on the right side of the segment, measured from the face of barrier to the near edge of right shoulder
	r_barrier_len	Total length of barrier on the right side of the segment
	l_barrier_off	Average offset to barrier on the left side of the segment, measured from the face of barrier to the near edge of left shoulder
	l_barrier_len	Total length of barrier on the left side of the segment
Alignment	grade	Indication of whether segment is on downgrade or upgrade
	nbr_curves	Count of curves on segment
	curv_rad1	Radius of curve 1
	curv_ang_deg1	Deflection angle of curve 1
	curv_lgt_ft1	Length of curve 1
	curv_begmp1	Begin milepost for curve 1
	curv_lgt_on_seg1	Length of curve 1 on segment
	:	repeat five variables above for each of up to three curves on segment
Other	splits	Count of splits that occur on the segment
	CD_md_len	Length of the merge-diverge (weaving) section on a C-D road
	CD_md_lgt_on_seg	Length of the merge-diverge section on the subject segment

Aerial photography was used as the source of the enhanced data. These photographs were obtained from the Internet using Google Earth software. The data collected include the width of road cross section elements, barrier presence and location, and horizontal curvature. A description of the variables acquired from aerial photography is provided in Table 46.

The “meter” and “HOV_bypass” variables were used to identify entrance ramps with a meter or an HOV bypass lane. These ramp features were not ranked high in the prioritization process, as documented in Chapter 3. Hence, these variables were used to screen ramps with either attribute from the database.

CMF DEVELOPMENT

This part of the chapter describes the development of a ramp curve speed prediction procedure. The need for this procedure stems from the realization that curve speed is likely to be highly correlated with curve crash frequency. This relationship between speed and crash risk is described in the horizontal curve CMF that was developed in Chapter 5.

The speed prediction procedure consists of a sequence of steps that lead to a prediction of average entry speed for each curve on the subject ramp or C-D road. Each curve is addressed by the procedure in the same sequence as they are encountered when traveling along the ramp or C-D road. In this manner, the speed for all previous curves encountered must be calculated first, before the speed on the subject curve can be calculated. The steps used will vary depending on whether the segment is part of an entrance ramp, exit ramp, connector ramp, or C-D road.

The horizontal curves are located along the ramp or C-D road using a linear referencing system. For exit ramps, the “0.0” milepost is located at the gore point. This point is defined as the point in the gore area where the distance between the near edge of the freeway traveled way and the ramp traveled way is equal to 2 ft. The gore point is also used to define the “0.0” milepost for C-D roads and for entrance ramps that diverge from the crossroad using a speed-change lane. For entrance ramps that intersect the crossroad, the “0.0” milepost is located at the point where the ramp reference line intersects with the near edge of traveled way of the crossroad. The ramp reference line is defined as the right edge of ramp traveled way. The location of the “0.0” milepost is shown in Figure 77.

Factors Influencing Ramp Speed

This section examines the factors that influence vehicle speed on ramp curves. It consists of two subsections. The first subsection describes the development of separate models for predicting speed as a function of acceleration and deceleration distance. The second subsection describes the development of a model relating curve speed to curve radius.

Speed Change with Distance

This subsection describes the models used to predict average vehicle speed as a function of travel distance. Separate models are described for the case of acceleration and deceleration, as found on entrance and exit ramps, respectively.

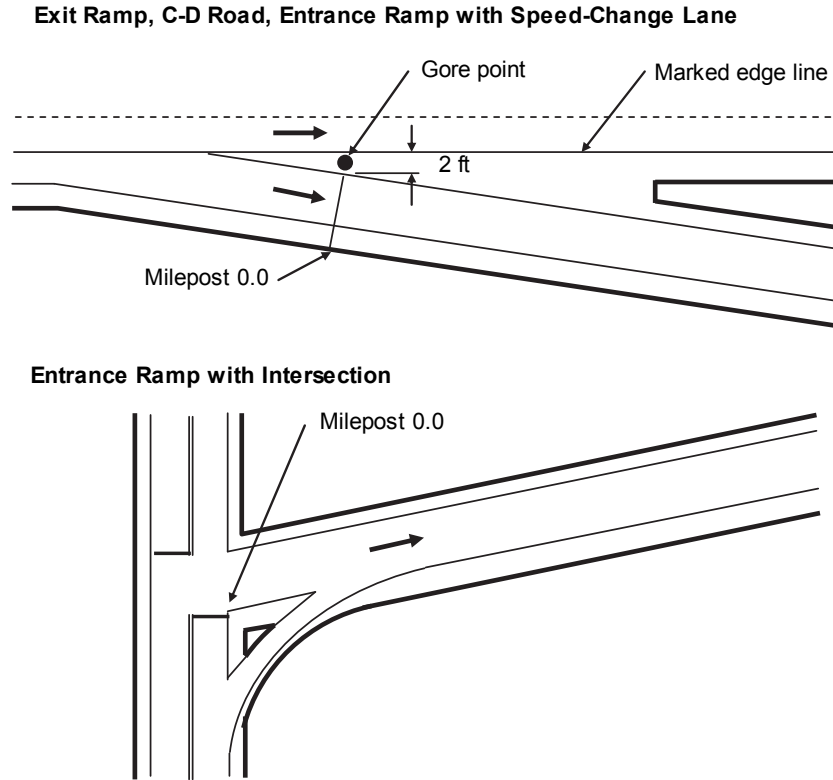


Figure 77. Starting milepost location on ramps and C-D roads.

The vehicle acceleration trend lines shown in Exhibit 2-24 of the *Green Book* (Policy, 2004) were used to define the relationship between acceleration and speed. An examination of the trends shown in the exhibit indicated that acceleration was a function of speed. The best-fit relationship to the trends shown ($R^2 = 0.99$) is described using the following relationship: $a = b_0 / v$, with b_0 equal to 165. Combining this relationship with the fundamental differential of distance and speed (i.e., $dx = v/a dv$) and integrating yields the following speed prediction model for entrance ramps.

$$v_f = (v_i^3 + 3 \times X \times b_0)^{1/3} \quad (145)$$

where,

- v_f = speed reached after traveling distance X , ft/s;
- v_i = initial speed, ft/s;
- X = distance traveled, ft; and
- b_0 = calibration coefficient (= 165), ft^2/s^3 .

The vehicle deceleration distance trend lines in Exhibit 2-25 of the *Green Book* were used to define the relationship between deceleration and speed. Examination of the trends shown in the exhibit indicated that deceleration was a function of speed. The best-fit relationship to the trends shown ($R^2 = 0.97$) is described using the following relationship: $a = (a_m/v_m) v$, with a_m equal to 12.4 ft/s^2 and $v_m = 102.9 \text{ ft/s}$. Combining this relationship with the fundamental differential of distance and speed (i.e., $dx = v/a dv$) and integrating yields the following speed prediction model for exit ramps.

$$v_f = v_i - X \times \frac{a_m}{v_m} \quad (146)$$

where,

a_m = instantaneous deceleration rate at speed m (= 3.5), ft/s²; and
 v_m = speed associated with acceleration rate a_m (= 102.9), ft/s.

Exhibit 2-25 of the *Green Book* describes deceleration with steady braking. Livneh et al. (1988) found that deceleration with steady braking is only applied just prior to the ramp curve. They found that a majority of the ramp traversal takes place using deceleration in gear, which is associated with a deceleration rate that is about 28 percent of that used for steady braking (i.e., $a_m = 3.5 \text{ ft/s}^2$ [= 0.28×12.4]). Deceleration in gear is used herein to predict ramp speed for safety evaluation.

Curve Speed

The curve speed prediction model is based on data collected by Bonneson (2000). These data were collected at five interchange loop ramp curves and 20 rural two-lane highway curves. The best-fit relationship ($R^2 = 0.82$) is described using the following equation.

$$v_c = 3.24 (32.2 R)^{0.30} \quad (147)$$

where,

v_c = average curve speed, ft/s; and
 R = radius of curve, ft.

Ramp Speed Predictive Model

This section describes the procedure for predicting vehicle speed upon entry to a ramp or C-D road curve. The procedure is separately described for entrance ramps, exit ramps, and C-D Roads.

This procedure is developed for use with the safety predictive models described in this chapter. It is not intended to be used for other applications, or to predict vehicle speed at points other than the start of a curve.

Input Data

The input data needed for this procedure are identified in Table 47. The first three variables listed represent required input data. The default values listed in the table can be used for the remaining variables.

TABLE 47. Input data for ramp curve speed prediction

Variable	Description	Default Value	Applicable Procedure
X_i	Milepost of the point of change from tangent to curve (PC) for curve i^1 , mi	none	All
R_i	Radius of curve i^2 , ft	none	All
$L_{c,i}$	Length of horizontal curve i , mi	none	All
V_{frwy}	Average traffic speed on freeway during off-peak periods of the typical day, mi/h	Estimate as equal to the speed limit	All
V_{xroad}	Average speed at point where ramp connects to crossroad, mi/h	15 - ramps with stop-, yield-, or signal-controlled crossroad ramp terminals 30 - all other ramps at service interchanges	Entrance ramp, exit ramp, connector ramp at service interchange
V_{cdroad}	Average speed on C-D road or connector ramp (measured at the mid-point of the C-D road or ramp), mi/h	40	C-D road, connector ramp at system interchange

Notes:

- 1 - If the curve is preceded by a spiral transition, then X_i is computed as equal to the average of the TS and SC mileposts, where TS is the milepost of the point of change from tangent to spiral and SC is the milepost of the point of change from spiral to curve.
- 2 - If the curve has spiral transitions, then R_i is equal to the radius of the central circular portion of the curve.

Entrance Ramp Procedure

This procedure is applicable to entrance ramps and connector ramps at service interchanges that serve motorists traveling from the crossroad to the freeway.

Step 1 - Gather Input Data. The input data needed for this procedure are identified in Table 47.

Step 2 - Compute Limiting Curve Speed. The limiting curve speed is computed for each curve on the ramp using the following equation.

$$v_{max,i} = 3.24 (32.2 R_i)^{0.30} \quad (148)$$

where, $v_{max,i}$ equals the limiting speed for curve i , ft/s.

The analysis proceeds in the direction of travel. The first curve encountered is curve 1 ($i=1$). The value of v_{max} is computed for all curves prior to, and including, the curve of interest. The value obtained from Equation 148 represents an upper limit on the curve speed. The vehicle may reach this speed if the distance between curves is lengthy or the crossroad speed is high.

Step 3 - Calculate Curve 1 Entry Speed. The average entry speed at curve 1 is computed using the following equation.

$$v_{ent,1} = \left([1.47 V_{xroad}]^3 + 495 \times 5280 X_1 \right)^{1/3} \leq 1.47 V_{frwy} \quad (149)$$

where, $v_{ent,1}$ equals the average entry speed for curve 1, ft/s.

The boundary condition on the right side of the equation indicates that the value computed cannot exceed the average freeway speed.

Step 4 - Calculate Curve 1 Exit Speed. The average exit speed at curve 1 is equal to the value obtained from the following equation.

$$v_{ext,1} = \left(V_{ent,1}^3 + 495 \times 5280 L_{c,1} \right)^{1/3} \leq v_{max,1} \text{ and } \leq 1.47 V_{frwy} \quad (150)$$

where, $v_{ext,1}$ equals the average exit speed for curve 1, ft/s.

The boundary condition indicates that the value computed should not exceed the limiting curve speed or the average freeway speed.

Step 5 - Calculate Curve i Entry Speed. The average entry speed at curve 2 (and all subsequent curves) is computed using the following equation.

$$v_{ent,i} = \left(V_{ext,i-1}^3 + 495 \times 5280 [X_i - X_{i-1} - L_{c,i-1}] \right)^{1/3} \leq 1.47 V_{frwy} \quad (151)$$

where, $v_{ent,i}$ equals the average entry speed for curve i ($i = 2, 3, \dots$), ft/s; and $v_{ext,i}$ equals the average exit speed for curve i , ft/s.

Step 6 - Calculate Curve i Exit Speed. The average exit speed at curve 2 (and all subsequent curves) is computed using the following equation.

$$v_{ext,i} = \left(V_{ent,i}^3 + 495 \times 5280 L_{c,i} \right)^{1/3} \leq v_{max,i} \text{ and } \leq 1.47 V_{frwy} \quad (152)$$

Step 7 - Calculate Speed on Successive Curves. The entry and exit speeds for curve 3 and higher are computed by applying steps 5 and 6 for each curve. Step 6 does not need to be applied for the last curve because only the entry speed is used in the safety evaluation.

Exit Ramp Procedure

This procedure is applicable to exit ramps and connector ramps at service interchanges that serve motorists traveling from the freeway to the crossroad.

Step 1 - Gather Input Data. The input data needed for this procedure are identified in Table 47.

Step 2 - Compute Limiting Curve Speed. This step is the same as step 2 for the entrance ramp procedure. A lower curve speed than that obtained from Equation 148 is possible due to the deceleration that occurs along the ramp as the driver transitions from the freeway speed to the crossroad speed.

Step 3 - Calculate Curve 1 Entry Speed. The average entry speed at curve 1 is computed using the following equation.

$$v_{ent,1} = 1.47 V_{frwy} - 0.034 \times 5280 X_1 \geq 1.47 V_{xroad} \quad (153)$$

The boundary condition on the right side of the equation indicates that the value computed cannot be less than the average speed at the point where the ramp connects to the crossroad.

Step 4 - Calculate Curve 1 Exit Speed. The average exit speed at curve 1 is equal to the value obtained from the following equation.

$$v_{ext,1} = v_{ent,1} - 0.034 \times 5280 L_{c,1} \leq v_{max,1} \text{ and } \geq 1.47 V_{xroad} \quad (154)$$

The boundary condition indicates that the value computed should not exceed the limiting curve speed and should not be less than the average speed at the point where the ramp connects to the crossroad.

Step 5 - Calculate Curve *i* Entry Speed. The average entry speed at curve 2 (and all subsequent curves) is computed using the following equation.

$$v_{ent,i} = v_{ext,i-1} - 0.034 \times 5280 (X_1 - X_{i-1} - L_{c,i-1}) \geq 1.47 V_{xroad} \quad (155)$$

Step 6 - Calculate Curve *i* Exit Speed. The average exit speed at curve 2 (and all subsequent curves) is computed using the following equation.

$$v_{ext,i} = v_{ent,i} - 0.034 \times 5280 L_{c,i} \leq v_{max,i} \text{ and } \geq 1.47 V_{xroad} \quad (156)$$

Step 7 - Calculate Speed on Successive Curves. This step is the same as step 7 for the entrance ramp procedure.

C-D Road Procedure

This procedure is applicable to C-D roads and connector ramps at system interchanges.

Step 1 - Gather Input Data. The input data needed for this procedure are identified in Table 47.

Step 2 - Compute Limiting Curve Speed. This step is the same as step 2 for the entrance ramp procedure.

Step 3 - Calculate Curve 1 Entry Speed. The average entry speed at curve 1 is computed using Equation 157 or 158, depending on the following two conditions.

If $1.47 \times V_{frwy} \leq v_{max, 1}$ then:

$$v_{ent,1} = 1.47 V_{frwy} \quad (157)$$

If $1.47 \times V_{frwy} > v_{max, 1}$ then:

$$v_{ent,1} = 1.47 V_{frwy} - 0.034 \times 5280 X_1 \geq 1.47 V_{cdroad} \quad (158)$$

The boundary condition for Equation 158 indicates that the value computed cannot be less than the average speed on the C-D road.

Step 4 - Calculate Curve 1 Exit Speed. The average exit speed at curve 1 is equal to the entrance speed, provided that it does not exceed the limiting curve speed. The following rule is used to make this determination.

$$v_{ext,1} = v_{ent,1} \leq v_{max,1} \quad (159)$$

Step 5 - Calculate Curve i Entry Speed. The average entry speed at curve 2 (and all subsequent curves) is computed using Equation 160 or 161, depending on the following conditions.

If $v_{ext, i-1} \leq v_{max, i}$ then:

$$v_{ent,i} = \left(V_{ext,i-1}^3 + 495 \times 5280 [X_i - X_{i-1} - L_{c,i-1}] \right)^{1/3} \leq 1.47 V_{frwy} \quad (160)$$

If $v_{ext, i-1} > v_{max, i}$ then:

$$v_{ent,i} = v_{ext,i-1} - 0.034 \times 5280 (X_i - X_{i-1} - L_{c,i-1}) \geq 1.47 V_{cdroad} \quad (161)$$

Step 6 - Calculate Curve i Exit Speed. The average exit speed at curve 2 (and all subsequent curves) is computed using the following equation.

$$v_{ext,i} = v_{ent,i} \leq v_{max,i} \quad (162)$$

Step 7 - Calculate Speed on Successive Curves. This step is the same as step 7 for the entrance ramp procedure.

Example Application

The section provides an application of the ramp entrance and ramp exit procedures described in previous sections. These two procedures will be applied to the diagonal ramps shown in Figure 78. The input data that describe these ramps is listed in Table 48. Default values are used for all variables not listed in Table 48.

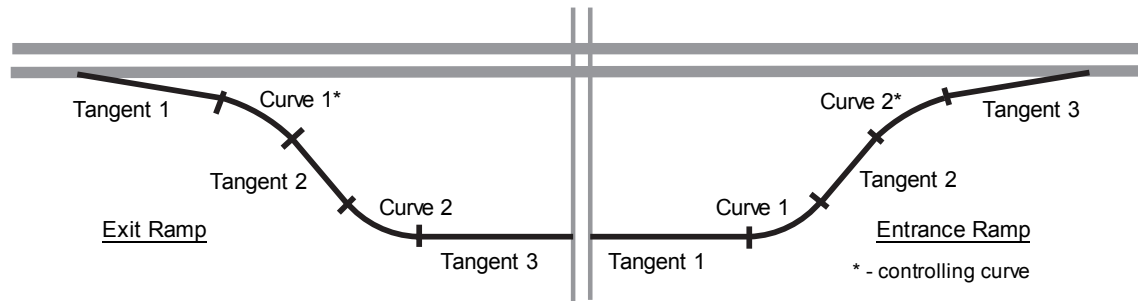


Figure 78. Diagonal ramp configuration for example application.

TABLE 48. Input data for example application

Variable	Description	Exit Ramp	Entrance Ramp
X_1	Milepost of the PC for curve 1, mi	0.12	0.02
R_1	Radius of curve 1, ft	1,000	500
$L_{c,1}$	Length of horizontal curve 1, mi	0.10	0.05
X_2	Milepost of the PC for curve 2, mi	0.25	0.10
R_2	Radius of curve 2, ft	500	1,000
$L_{c,2}$	Length of horizontal curve 2, mi	0.05	0.10
V_{frwy}	Average speed on freeway, mi/h	70	70
V_{xroad}	Average speed at point where ramp connects to crossroad, mi/h	15	15

The results of the calculations are shown in Table 49. For the exit ramp, the average vehicle enters the speed-change lane at the freeway speed of 70 mi/h (102.9 ft/s). After traveling 0.12 mi, Equation 153 predicts that the vehicle will slow to 81.3 ft/s as it enters the first curve. This speed is in excess of the limiting curve speed of 72.9 ft/s so the vehicle will likely decelerate to at least this speed. Using Equation 154, the exit curve speed is computed as 63.5 ft/s. The vehicle then decelerates to 58.0 ft/s as it enters the second curve. This speed is not in excess of the limiting curve speed of 59.2 ft/s. The two entry speeds v_{ent} are subsequently used in the safety predictive method to estimate the CMF for these two curves.

For the entrance ramp, the average vehicle enters the ramp at a speed of 15 mi/h (22.1 ft/s). After traveling 0.02 mi, Equation 149 predicts that the vehicle will accelerate to 39.8 ft/s as it enters the first curve. This speed is not in excess of the limiting curve speed of 59.2 ft/s so the vehicle continues to accelerate. Using Equation 150, the exit curve speed is computed as 57.8 ft/s. The vehicle then accelerates to 64.8 ft/s as it enters the second curve. This speed is not in excess of the limiting curve speed of 72.9 ft/s. The two entry speeds v_{ent} are subsequently used in the safety predictive method to estimate the CMF for these two curves.

TABLE 49. Results for example application

Ramp	Location	X, mi	R, ft	L_c , mi	v_{max} , ft/s	v_{ent} , ft/s	v_{ext} , ft/s
Exit	Freeway	--	--	--	--	--	102.9
	Curve 1 PC	0.12	1,000	0.10	72.9	81.3	63.5
	Curve 2 PC	0.25	500	0.05	59.2	58.0	
Entrance	Begin	0.00	--	--	--	--	22.1
	Curve 1 PC	0.02	500	0.05	59.2	39.8	57.8
	Curve 2 PC	0.10	1,000	0.10	72.9	64.8	

METHODOLOGY

This part of the chapter describes the methodology used to calibrate the ramp and C-D road predictive models. It is divided into three sections. The first section describes several supplemental variables used to calibrate the predictive models. The second section describes several analytic relationships used to model non-homogeneous segments. The last section provides an overview of the approach used to calibrate the predictive models.

Supplemental Variables

As noted in a previous part of this chapter, several variables in the database were obtained from aerial photographs of the ramp and C-D road segments represented in the study state databases. Of these variables, some of the more complex ones are defined in this section.

Ramp Entrance/Exit Length and Type

Speed-change lanes have two design types, the parallel design and the taper design. Both designs are shown in Figure 79. The ramp entrance length begins at the gore point and ends at the taper point. The ramp exit length begins at the taper point and ends at the gore point. As shown in Figure 11, these two lengths are not the same as the ramp acceleration (or deceleration) length that is defined in the *Green Book* (Policy, 2004). The lengths shown in Figure 79 include the taper and are believed to more realistically describe the speed-change length for safety modeling.

Weaving Length

Ramp pairs that form a weaving section on a C-D road were identified in the database. In all cases, these ramp pairs were on the right-hand side of the C-D road. There are 3.3 mi of weaving section in the database.

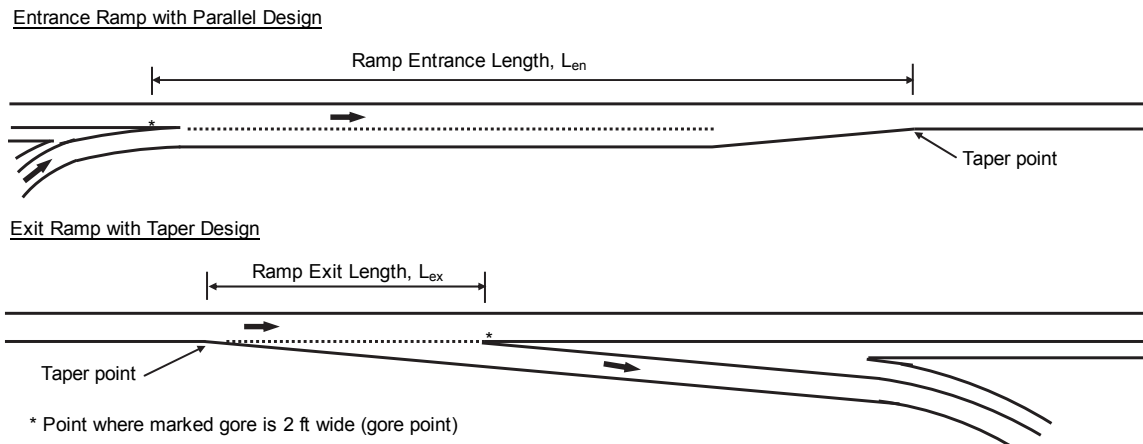


Figure 79. Speed-change lane location on ramps and C-D roads.

It is generally recognized that the length of the weaving section has an important influence on the operation of the C-D road segment. This influence relates to the degree to which the weaving activity is concentrated along the C-D road. In recognition of a possible correlation between weaving section concentration and crash frequency, the length of the weaving section was also included in the database. The convention used to measure this length is the same as that used for freeway weaving sections, and is shown in Figure 43.

Longitudinal Barriers

Longitudinal barriers (i.e., cable barrier, concrete barrier, guardrail, or bridge rail) were noted when present on a segment. Attributes used to quantify barrier presence includes barrier offset and length. Barrier offset and length were each measured separately for the left side and right side locations (e.g., left barrier offset, right barrier offset, etc.).

Barrier offset represents a lateral distance measured from the near edge of the shoulder to the face of the barrier (i.e., it does not include the width of the shoulder). Barrier length represents the length of lane paralleled by a barrier. For example, if the left side barrier extends for the length of the ramp segment, then the left side barrier length equals the segment length.

Analytic Relationships for Non-Homogeneous Segments

In most instances, the segments in the study state databases were not homogeneous in terms of the variables of interest. One or more geometric elements often start or end at some point along the length of a segment. When this occurs, the length of the segment associated with the element's initial condition and its changed condition is recorded in the database. Geometric elements that are sometimes only partially located on a segment are identified in the following list.

- horizontal curve presence,
- weaving section presence, and
- barrier presence.

CMFs are typically developed for application to homogeneous segments. Thus, they do not include variables that allow them to be modified for application to segments on which they only partially apply. However, the following equation can be used to convert a CMF for homogeneous segments into one that can be used for non-homogeneous segments.

$$CMF_{i|agg} = (1.0 - P_{L,i})1.0 + P_{L,i} CMF_i \quad (163)$$

where,

$CMF_{i|agg}$ = aggregated CMF for element i ;

$P_{L,i}$ = proportion of the segment length with element i ; and

CMF_i = crash modification factor for element i .

Modeling Approach

This section describes the regression modeling approach and the rationale for using a cross-sectional database. Details of the methods used for PDO model calibration are provided in Chapter 5 in the subsection titled Prediction of PDO Crash Frequency.

Combined Regression Models

The calibration activity used statistical analysis software that employs maximum likelihood methods and a negative binomial distribution of crash frequency. Two models were calibrated. The form of each model is shown in the following equations.

$$N_{mv} = N_{spf,mv} \times (CMF_{mv,1} \times \dots \times CMF_{mv,w}) \times (CMF_1 \times \dots \times CMF_k) \quad (164)$$

$$N_{sv} = N_{spf,sv} \times (CMF_{sv,1} \times \dots \times CMF_{sv,x}) \times (CMF_1 \times \dots \times CMF_k) \quad (165)$$

where all variables were defined previously.

The SPFs associated with these models are defined using the following equations.

$$N_{spf,mv} = L e^{b_{mv,0} + b_{mv,1} \ln(AADT/1,000)} \quad (166)$$

$$N_{spf,sv} = L e^{b_{sv,0} + b_{sv,1} \ln(AADT/1,000)} \quad (167)$$

where,

L = length of segment, mi;

$AADT$ = AADT volume on segment, veh/day; and

$b_{j,i}$ = calibration coefficients for model j ($j = mv, sv$), $i = 0, 1$.

The second term of Equations 164 and 165 recognizes that the influence of some geometric factors is unique to each crash type. In contrast, the third term of Equations 164 and 165 recognizes that some geometric factors have a similar influence on all crash types.

The use of common CMFs in multiple models required the use of a combined-model approach. With this approach, the regression analysis evaluated both models simultaneously and used the total log-likelihood statistic for both models to determine the best fit calibration coefficients. A simulation analysis was undertaken to determine if this type of regression would bias the calibration coefficients or their standard error. The results of this analysis indicated that: (1) the coefficients were not biased and (2) that the standard error of those coefficients associated with a variable were not biased. The regression analysis is described in more detail in the next part of this chapter.

Cross-Sectional Database

The database is described as cross sectional (as opposed to panel). It represents a common five-year study period for all observations. Study duration in “years” is represented as an offset variable in the regression model. The rationale for using this type of database is provided in Chapter 5 in the section titled Cross-Sectional Database.

It was assumed that segment crash frequency is Poisson distributed, and that the distribution of the mean crash frequency for a group of similar segments is gamma distributed. In this manner, the distribution of crashes for a group of similar segments can be described by the negative binomial distribution. The variance of this distribution is described by the following equation.

$$V[X] = y N + \frac{(y N)^2}{K L} \quad (168)$$

where,

$V[X]$ = crash frequency variance for a group of similar locations, crashes²;

N = predicted average crash frequency, crashes/yr;

X = reported crash count for y years, crashes;

y = time interval during which X crashes were reported, yr; and

K = inverse dispersion parameter ($= 1/k$, where k = overdispersion parameter), mi^{-1} .

MODEL CALIBRATION FOR FI CRASHES

This part of the chapter describes the calibration and validation of the combined ramp and C-D road segment predictive model. The first section identifies the data used for model calibration. The second section describes the structure of both predictive models as used in the regression analysis. The third section summarizes statistical analysis methods used for model calibration. The fourth section describes the regression statistics for each of the calibrated models. The fifth section describes a validation of the calibrated models. The sixth section describes the proposed predictive models and calibrated CMFs. The last section provides a sensitivity analysis of the predictive models over a range of traffic demands.

Calibration Data

The data collection process consisted of a series of activities that culminated in the assembly of a highway safety database suitable for the development of a comprehensive safety prediction methodology for ramp and C-D road segments. These activities are described in Chapter 4.

Crash data were identified for each ramp and C-D road segment using the most recently available data from the HSIS. Five years of crash data were identified for each segment. The analysis period is 2003, 2004, 2005, 2006, and 2007 for the California and Washington segments. It is 2002, 2004, 2004, 2005, and 2006 for the Maine segments. The AADT volume for each year was merged into the assembled database. A total of 1,178 FI crashes and 2,363 PDO crashes are represented in the database. Additional information about the database is provided in Chapter 4.

Model Development

This section describes the proposed safety predictive models and the methods used to calibrate them. The following regression model form was used to facilitate the regression analysis of the combined models.

$$N_j = C_{ca} \times (N_{mv} I_{mv} + N_{sv} I_{sv}) \times CMF_{lw} \times CMF_{rsw} \times CMF_{lsw} \times CMF_{rb|agg} \times CMF_{lb|agg} \times CMF_{a-d|agg} \times CMF_{wev|agg} \quad (169)$$

with,

$$CMF_{lw} = e^{b_{lw}(W_l - 14)} \quad (170)$$

$$CMF_{rsw} = e^{b_{rsw}(W_{rs} - 8)} \quad (171)$$

$$CMF_{lsw} = \begin{cases} e^{b_{sw}(W_{ls} - 4)} & : \text{If urban with } W_{ls} \leq b_{lsw}, \text{ or rural} \\ e^{b_{sw2}(W_{ls} - 4)} & : \text{If urban with } W_{ls} > b_{lsw} \end{cases} \quad (172)$$

$$CMF_{rb|agg} = (1.0 - P_{rb})1.0 + P_{rb} e^{b_{bar}/W_{rcb}} \quad (173)$$

$$CMF_{lb|agg} = (1.0 - P_{lb})1.0 + P_{lb} e^{b_{bar}/W_{lcb}} \quad (174)$$

$$CMF_{a-d|agg} = (1.0 - P_{tpr})1.0 + P_{tpr} e^{b_{lanes}(I_{add} - I_{drop})} \quad (175)$$

$$CMF_{wev|agg} = (1.0 - P_{wev})1.0 + P_{wev} e^{[b_{wev} + b_v \ln(AADT/1,000)]/L_{wev}} \quad (176)$$

$$C_{ca} = e^{b_{ca} I_{ca}} \quad (177)$$

where,

N_j = predicted average crash frequency for model j ($j = mv$ if $I_{mv} = 1.0$; $j = sv$ if $I_{sv} = 1.0$); crashes/yr;

N_{mv} = predicted average multiple-vehicle crash frequency, crashes/yr;

N_{sv} = predicted average single-vehicle crash frequency, crashes/yr;
 I_{mv} = crash indicator variable (= 1.0 if multiple-vehicle crash data, 0.0 otherwise);
 I_{sv} = crash indicator variable (= 1.0 if single-vehicle crash data, 0.0 otherwise);
 C_{ca} = calibration factor for California;
 CMF_{lw} = lane width crash modification factor;
 W_l = lane width, ft;
 CMF_{rsw} = right shoulder width crash modification factor;
 W_{rs} = right shoulder width, ft;
 CMF_{lsw} = left shoulder width crash modification factor;
 W_{ls} = left shoulder width, ft;
 $CMF_{rb|agg}$ = aggregated right barrier crash modification factor;
 P_{rb} = proportion of segment length with a barrier present on the right side;
 W_{rcb} = distance from edge of right shoulder to barrier face, ft;
 $CMF_{lb|agg}$ = aggregated left barrier crash modification factor;
 P_{lb} = proportion of segment length with a barrier present on the left side;
 W_{lcb} = distance from edge of left shoulder to barrier face, ft;
 $CMF_{a-d|agg}$ = aggregated lane add or drop crash modification factor;
 P_{tpr} = proportion of segment length adjacent to the taper associated with a lane add or drop;
 I_{add} = lane add indicator variable (= 1.0 if one or more lanes are added, 0.0 otherwise);
 I_{drop} = lane drop indicator variable (= 1.0 if one or more lanes are dropped, 0.0 otherwise);
 $CMF_{wev|agg}$ = aggregated weaving section crash modification factor;
 P_{wev} = proportion of segment length within a weaving section;
 L_{wev} = weaving section length (may extend beyond segment boundaries), mi;
 I_{ca} = California indicator variable (= 1.0 if segment in California, 0.0 otherwise);
 b_i = calibration coefficient for condition i (see Table 50); and
 other variables are previously defined.

The final form of the regression model is described here, before the discussion of regression analysis results. However, this form reflects the findings from several preliminary regression analyses where alternative model forms were examined. The form that is described represents that which provided the best fit to the data, while also having coefficient values that are logical and constructs that are theoretically defensible and properly bounded.

Equation 169 combines two “component” models. One model predicts multiple-vehicle crash frequency. The second model predicts single-vehicle crash frequency. The regression model form of each model is described in the following subsections. The CMFs in Equation 169 apply to all component models. The other CMFs that were developed were found to provide a better fit to the data when applied to just one of the component models.

Multiple-Vehicle Crash Frequency

$$N_{mv} = (N_{spf,mv,1}I_1 + N_{spf,mv,2}I_2) \times CMF_{mv,hc|agg} \times CMF_{mv,sc|agg} \quad (178)$$

with,

$$N_{spf,mv,1} = L e^{b_{mv,0,1} + b_{mv,1} \ln(AADT/1,000) + b_{mv,2} (AADT/1,000) + b_{mv,env}I_{env} + b_{mv,exc}I_{exc} + b_{mv,rural}I_{rural}} \quad (179)$$

$$N_{spf,mv,2} = L e^{b_{mv,0,2} + b_{mv,1} \ln(AADT/1,000) + b_{mv,2} (AADT/1,000) + b_{mv,entr} I_{entr} + b_{mv,exr} I_{exr} + b_{mv,rural} I_{rural}} \quad (180)$$

$$CMF_{mv,hc|agg} = 1.0 + b_{mv,cr} \frac{1,000}{32.2} \sum_{i=1}^3 \left(\frac{v_{ent,i}}{R_i} \right)^2 P_{c,i} \quad (181)$$

$$CMF_{mv,sc|agg} = (1.0 - P_{en-ex}) 1.0 + P_{en-ex} e^{b_{mv,en-ex}} \quad (182)$$

where,

- $N_{spf, mv, n}$ = predicted average multiple-vehicle crash frequency for base conditions for number of through lanes n ($n = 1, 2$); crashes/yr;
- I_n = cross section indicator variable (= 1.0 if cross section has n lanes, 0.0 otherwise);
- $CMF_{mv, hc|agg}$ = aggregated horizontal curve crash modification factor for multiple-vehicle crashes;
- $CMF_{mv, sc|agg}$ = aggregated ramp speed-change lane crash modification factor for multiple-vehicle crashes;
- I_{entr} = entrance ramp indicator variable (= 1.0 if segment is an entrance ramp, 0.0 otherwise);
- I_{exr} = exit ramp indicator variable (= 1.0 if segment is an exit ramp, 0.0 otherwise);
- I_{rural} = area type indicator variable (= 1.0 if area is rural, 0.0 if it is urban);
- $v_{ent,i}$ = average entry speed for curve i , ft/s;
- R_i = radius of curve i , ft;
- $P_{c,i}$ = proportion of segment length with curve i ;
- P_{en-ex} = proportion of segment length that is adjacent to the speed-change lane for a connecting ramp;
- b_i = calibration coefficient for condition i (see Table 50); and other variables are previously defined.

Equations 179 and 180 include two terms for AADT volume. The first term is the traditional AADT term in this type of model. The second term was added to obtain a better fit to the data. The two terms together provide for a point of inflection in the relationship between crash frequency and AADT volume. An examination of the residual errors of a single-term model indicated that the two-term form was needed to provide a relatively unbiased fit over the range of AADT volumes in the database.

Equation 178 is applicable to entrance ramp, exit ramp, and C-D road segments. Indicator variables (i.e., I_{entr} and I_{exr}) in Equations 179 and 180 are used to adapt the set of models to the specific segment type being evaluated. Both variables are set to 0.0 to apply the models to C-D road segments.

The horizontal curve CMF includes variables for curve speed and radius. The development of this model is described in Chapter 5. The constant “1,000” in Equation 181 is a scale factor used for convenience (i.e., so the value of the calibration coefficient will be near 1.0).

Single-Vehicle Crash Frequency

$$N_{sv} = (N_{spf,sv,1}I_1 + N_{spf,sv,2}I_2) \times CMF_{mv, hc|agg} \quad (183)$$

with,

$$N_{spf,sv,1} = L e^{b_{sv,0,1} + b_{sv,1} \ln(AADT/1,000) + b_{sv,env}I_{env} + b_{sv,exr}I_{exr} + b_{sv,rural}I_{rural}} \quad (184)$$

$$N_{spf,sv,2} = L e^{b_{sv,0,2} + b_{sv,1} \ln(AADT/1,000) + b_{sv,env}I_{env} + b_{sv,exr}I_{exr} + b_{sv,rural}I_{rural}} \quad (185)$$

$$CMF_{sv, hc|agg} = 1.0 + b_{sv,cr} \frac{1,000}{32.2} \sum_{i=1}^3 \left(\frac{v_{ent,i}}{R_i} \right)^2 P_{c,i} \quad (186)$$

where,

$N_{spf,sv,n}$ = predicted average single-vehicle crash frequency for base conditions for number of through lanes n ($n = 1, 2$); crashes/yr;

$CMF_{sv, hc|agg}$ = aggregated horizontal curve crash modification factor for single-vehicle crashes;

b_i = calibration coefficient for condition i (see Table 50); and
other variables are previously defined.

Barrier Variable Calculations

Two key variables that are needed for the evaluation of barrier presence are the right side barrier distance W_{rcb} and the left side barrier distance W_{lcb} . As indicated in Equations 173 and 174, this distance is included as a divisor in the exponential term. This relationship implies that the correlation between distance and crash frequency is an inverse one (i.e., crash frequency decreases with increasing distance to the barrier). When multiple sections of barrier exist along the segment, a length-weighted average of the *reciprocal* of the individual distances is needed to properly reflect this inverse relationship. The length used to weight the average is the barrier length.

The following equations should be used to estimate W_{rcb} and P_{rb} .

$$W_{rcb} = \frac{\sum L_{rb,i}}{\sum \frac{L_{rb,i}}{W_{off,r,i} - W_{rs}}} \quad (187)$$

$$P_{rb} = \frac{\sum L_{rb,i}}{L} \quad (188)$$

where,

$L_{rb,i}$ = length of right side lane paralleled by barrier i , mi; and

$W_{off,r,i}$ = horizontal clearance from the edge of the traveled way to the face of barrier i on right side of segment, ft.

The following equations should be used to estimate W_{lcb} and P_{lb} .

$$W_{lcb} = \frac{\sum L_{lb,i}}{\sum \frac{L_{lb,i}}{W_{off,l,i} - W_{ls}}} \quad (189)$$

$$P_{lb} = \frac{\sum L_{lb,i}}{L} \quad (190)$$

where,

- $L_{lb,i}$ = length of left side lane paralleled by barrier i , mi; and
- $W_{off,l,i}$ = horizontal clearance from the edge of the traveled way to the face of barrier i on left side of segment, ft.

Statistical Analysis Methods

The nonlinear regression procedure (NLMIXED) in the SAS software was used to estimate the proposed model coefficients. This procedure was used because the proposed predictive model is both nonlinear and discontinuous. The log-likelihood function for the negative binomial distribution was used to determine the best-fit model coefficients. Equation 168 was used to define the variance function for all models. The procedure was set up to estimate model coefficients based on maximum-likelihood methods. The statistics used to assess model fit to the data are described in Chapter 5.

Model Calibration

The predictive model calibration process was based on a combined-model approach, as discussed in the section titled Modeling Approach. With this approach, the component models and CMFs (represented by Equations 169 to 186) are calibrated using a database of common sites. This approach is needed because several CMFs are common to both component models. The database assembled for calibration included two replications of the original database. The dependent variable in the first replication was set equal to the multiple-vehicle crashes. The dependent variable in the second replication was set equal to the single-vehicle crashes.

The predicted crash frequency from both of the component models was computed for each segment. Both values were then totaled for each segment and compared with the total reported crash frequency for the segment. The difference between the two totals was then summed for all segments. This sum was found to be very small (i.e., less than 0.5 percent of the total reported crash frequency), so it was concluded that there was no bias in the component models in terms of their ability to predict total crash frequency.

The models were calibrated using the California and Washington data. The Maine data were reserved for model validation. The discussion in this section focuses on the findings from the model calibration. The findings from model validation are provided in the next section.

The results of the regression model calibration are presented in Table 50. The Pearson χ^2 statistic for the model is 2,557, and the degrees of freedom are 2,603 ($= n - p = 2,628 - 25$). As this statistic is less than $\chi^2_{0.05, 2603} (= 2,723)$, the hypothesis that the model fits the data cannot be rejected.

TABLE 50. Ramp FI model statistical description—combined model—two states

Model Statistics		Value		
R^2 :		0.17		
Scale parameter ϕ :		0.98		
Pearson χ^2 :		2,557 ($\chi^2_{0.05, 2603} = 2,723$)		
Observations n_o :		1,314 seg. (938 injury or fatal crashes in 5 years)		
Calibrated Coefficient Values				
Variable	Inferred Effect of...	Value	Std. Dev.	t-statistic
b_{lw}	Lane width	-0.056	0.0298	-1.9
b_{sw}	Shoulder width (left and right side, except case below)	-0.067	0.0214	-3.1
$b_{sw, 2}$	Left shoulder width on urban seg. with width $> b_{lsw}$	0.038	0.0388	1.0
b_{lsw}	Threshold left shoulder width	4.048	1.2640	3.2
b_{bar}	Barrier presence	0.146	0.0786	1.9
$b_{mv, cr}$	Horizontal curvature on 2+ veh. crashes	0.732	0.4828	1.5
$b_{sv, cr}$	Horizontal curvature on 1 veh. crashes	2.352	0.5785	4.1
b_{lanes}	Change in lane count (i.e., lane add or drop)	-0.259	0.0948	-2.7
b_{wev}	Weaving section presence	0.209	0.1014	2.1
b_v	AADT on weaving-related crashes	-0.080	0.0438	-1.8
$b_{mv, en-ex}$	Ramp speed-change lane presence on 2+ veh. crashes	0.262	0.3178	0.8
$b_{mv, enr}$	Added effect of entrance ramp on 2+ vehicle crashes	-0.696	0.250	-2.8
$b_{mv, exr}$	Added effect of exit ramp on 2+ vehicle crashes	-1.905	0.311	-6.1
$b_{mv, 0, 1}$	1 lane on 2+ veh. crashes for C-D roads in urban areas	-3.020	0.544	-5.5
$b_{mv, 0, 2}$	2 lanes on 2+ veh. crashes for C-D roads in urban areas	-2.598	0.589	-4.4
$b_{mv, 1}$	AADT on 2+ vehicle crashes	0.541	0.326	1.7
$b_{mv, 2}$	AADT on 2+ vehicle crashes	0.076	0.026	2.9
$b_{mv, rural}$	Added effect of rural area type on 2+ veh. crashes	-2.064	1.114	-1.9
$b_{sv, enr}$	Added effect of entrance ramp on 1 veh. crashes	0.933	0.233	4.0
$b_{sv, exr}$	Added effect of exit ramp on 1 veh. crashes	1.228	0.234	5.2
$b_{sv, 0, 1}$	1 lane on 1 veh. crashes for C-D roads in urban areas	-2.820	0.273	-10.3
$b_{sv, 0, 2}$	2 lanes on 1 veh. crashes for C-D roads in urban areas	-2.886	0.322	-9.0
$b_{sv, 1}$	AADT on 1 veh. crashes	0.739	0.070	10.6
$b_{sv, rural}$	Added effect of rural area type on 1 veh. crashes	-0.197	0.186	-1.1
b_{ca}	Location in California	-0.376	0.130	-2.9

The t-statistic for each coefficient is listed in the last column of Table 50. These statistics describe a test of the hypothesis that the coefficient value is equal to 0.0. Those t-statistics with an absolute value that is larger than 2.0 indicate that the hypothesis can be rejected with the probability of error in this conclusion being less than 0.05. For those few variables where the absolute value of the t-statistic is smaller than 2.0, it was decided that the variable was important to the model and its trend was found to be intuitive and, where available, consistent with previous research findings (even if the specific value was not known with a great deal of certainty as applied to this database).

The findings from an examination of the coefficient values and the corresponding CMF or SPF predictions are documented in a subsequent section. In general, the sign and magnitude of the calibration coefficients in Table 50 are logical and consistent with previous research findings.

An indicator variable for the state of California was included in the regression model. The coefficient for this variable is shown in the last row of Table 50. It is statistically significant. Its value indicates that the ramps in California have about 30 percent fewer crashes than those in Washington. This trend is consistent with that found in the comparison of summary crash rates for these two states in Table 22. The trend could not be explained by differences in ramp design among the two states. It is likely due to differences between states that are due to unobserved variables such as ramp grade, signing, pavement condition, weather, and speed limit.

Model Validation

Model validation was a two-step process. The first step required using the calibrated models to predict the crash frequency for sites from a third state (i.e., Maine). The objective of this step was to demonstrate the robustness of the model structure and its transferability to another state.

The second step required comparing the calibrated CMFs with similar CMFs reported in the literature, where such information was available. The objective of this step was to demonstrate that the calibrated CMFs were consistent with previous research findings.

The findings from the first step of the validation process are described in this section. Those from the second step are described in the next section.

The first step of the validation process consisted of several tasks. The first task was to quantify the local calibration factor for both models (i.e., C_{mv} , C_{sv}), which would be the first step for any agency using the *HSM* methodology. This produced a “re-calibrated” set of models (i.e., the models with the coefficients from Table 50 plus the local calibration factors). The local calibration factor values for the Maine data are provided in the list below:

- Calibration factor for multiple-vehicle crashes, $C_{mv} = 1.46$
- Calibration factor for single-vehicle crashes, $C_{sv} = 0.43$

The second task was to apply the re-calibrated models to the Maine data to compute the predicted average crash frequency for each segment (i.e., N_{mv} , N_{sv}). The predicted crash frequency was then compared to the reported crash frequency for each site.

The third task was to compute the fit statistics and assess the robustness of the calibrated model. These statistics are listed in Table 51. The Pearson χ^2 statistic for each component model, and for the overall model, is less than $\chi^2_{0.05}$ so the hypothesis that the model fits the validation data cannot be rejected.

TABLE 51. Ramp model validation statistics

Component Model	R^2	R_k^2	Scale Parameter ϕ	Pearson χ^2	Deg. of Freedom	$\chi^2_{0.05, n-1}$
Multiple-vehicle	0.25	0.98	0.54	107.2	197	230.7
Single-vehicle	0.04	0.65	1.09	214.6	197	230.7
Overall:	0.08		0.81	321.8	395	441.3

The findings from this validation step indicate that the trends in the Maine data are not significantly different from those in the California and Washington data. These findings also suggest that the model structure is transferable to other states (when locally calibrated) for the prediction of FI crash frequency. Based on these findings, the data for the three states were combined and used in a second regression model calibration. The larger sample size associated with the combined database reduced the standard error of several calibration coefficients. Bared and Zhang (2007) also used this approach in their development of predictive models for urban freeways.

Combined Model

The data from the three study states were combined and the predictive models were calibrated a second time using the combined data. The calibration coefficients for the two models are described in the next subsection. The subsequent two subsections describe the fit of each component model. The fit statistics were separately computed using the calibrated component model and an analysis of its residuals.

Aggregate Model

The results of the regression model calibration are presented in Table 52. The Pearson χ^2 statistic for the model is 2,833, and the degrees of freedom are 2,998 ($= n - p = 3,024 - 26$). As this statistic is less than $\chi^2_{0.05, 2998}$ ($= 3,126$), the hypothesis that the model fits the data cannot be rejected. Several segments were removed as a result of outlier analysis such that the calibration database included only 1,021 of the 1,178 crashes identified in Chapter 4.

The t-statistics for each coefficient are listed in the last column of Table 52. These statistics have generally increased, relative to their counterparts in Table 50, as a result of the increased sample size. With a few exceptions, these statistics have an absolute value that is larger than 2.0, which indicates that the null hypothesis can be rejected with the probability of error in this conclusion being less than 0.05. For those few variables where the absolute value of the t-statistic is smaller than 2.0, it was decided that the variable was important to the model and its trend was found to be intuitive and, where available, consistent with previous research findings (even if the specific value was not known with a great deal of certainty as applied to this database). This consistency is demonstrated in a subsequent section.

Indicator variables were included for the states of California and Maine in the regression model. These coefficients are shown in the last two rows of Table 52. Both are statistically significant. Their values indicate that the ramps in California and Maine have fewer crashes than

those in Washington. This trend is consistent with that found in the comparison of summary crash rates for these states in Table 22. The trend could not be explained by differences in ramp design among the two states. It is likely due to differences between states that are due to unobserved variables such as ramp grade, signing, pavement condition, weather, and speed limit.

TABLE 52. Ramp FI model statistical description—combined model—three states

Model Statistics		Value		
R^2 :		0.17		
Scale parameter ϕ :		0.95		
Pearson χ^2 :		2,833 ($\chi^2_{0.05, 2998} = 3,126$)		
Observations n_o :		1,512 segments (1,021 injury or fatal crashes in 5 yrs)		
Calibrated Coefficient Values				
Variable	Inferred Effect of...	Value	Std. Dev.	t-statistic
b_{lw}	Lane width	-0.0458	0.0273	-1.7
b_{sw}	Shoulder width (left and right side, except case below)	-0.0539	0.0195	-2.8
$b_{sw, 2}$	Left shoulder width on urban seg. with width $> b_{lsw}$	0.0479	0.0381	1.3
b_{lsw}	Threshold left shoulder width	4.130	1.2507	3.3
b_{bar}	Barrier presence	0.210	0.0748	2.8
$b_{mv, cr}$	Horizontal curvature on 2+ veh. crashes	0.779	0.4695	1.7
$b_{sv, cr}$	Horizontal curvature on 1 veh. crashes	2.406	0.5487	4.4
b_{lanes}	Change in lane count (i.e., lane add or drop)	-0.231	0.0929	-2.5
b_{wev}	Weaving section presence	0.191	0.1046	1.8
b_v	AADT on weaving-related crashes	-0.0715	0.0453	-1.6
$b_{mv, en-ex}$	Ramp speed-change lane presence on 2+ veh. crashes	0.310	0.3265	1.0
$b_{mv, enr}$	Added effect of entrance ramp on 2+ vehicle crashes	-0.508	0.247	-2.1
$b_{mv, exr}$	Added effect of exit ramp on 2+ vehicle crashes	-1.974	0.310	-6.4
$b_{mv, 0, 1}$	1 lane on 2+veh. crashes for C-D roads in urban areas	-2.997	0.486	-6.2
$b_{mv, 0, 2}$	2 lanes on 2+ veh. crashes for C-D roads in urban areas	-2.515	0.533	-4.7
$b_{mv, 1}$	AADT on 2+ vehicle crashes	0.524	0.291	1.8
$b_{mv, 2}$	AADT on 2+ vehicle crashes	0.0699	0.025	2.8
$b_{mv, rural}$	Added effect of rural area type on 2+ veh. crashes	-1.721	0.761	-2.3
$b_{sv, enr}$	Added effect of entrance ramp on 1 veh. crashes	0.882	0.230	3.8
$b_{sv, exr}$	Added effect of exit ramp on 1 veh. crashes	1.203	0.231	5.2
$b_{sv, 0, 1}$	1 lane on 1 veh. crashes for C-D roads in urban areas	-2.848	0.265	-10.8
$b_{sv, 0, 2}$	2 lanes on 1 veh. crashes for C-D roads in urban areas	-2.881	0.313	-9.2
$b_{sv, 1}$	AADT on 1 veh. crashes	0.718	0.066	10.9
$b_{sv, rural}$	Added effect of rural area type on 1 veh. crashes	-0.154	0.166	-0.9
b_{me}	Location in Maine	-0.658	0.145	-4.5
b_{ca}	Location in California	-0.295	0.126	-2.3

Model for Predicting Multiple-Vehicle Non-Ramp-Related Crash Frequency

The results of the multiple-vehicle model calibration are presented in Table 53. The Pearson χ^2 statistic for the model is 1,327, and the degrees of freedom are 1,494 ($= n - p = 1,512 - 18$). As this statistic is less than $\chi^2_{0.05,1494}$ ($= 1,585$), the hypothesis that the model fits the data cannot be rejected. The R^2 for the model is 0.24. An alternative measure of model fit that is better suited to the negative binomial distribution is R_k^2 . The R_k^2 for the calibrated model is 0.95.

TABLE 53. Ramp FI model statistical description—multiple-vehicle model—three states

Model Statistics	Value
R^2 (R_k^2):	0.24 (0.95)
Scale parameter ϕ :	0.88
Pearson χ^2 :	1,327 ($\chi^2_{0.05,1494} = 1,585$)
Inverse dispersion parameter K :	14.6 mi^{-1}
Observations n_o :	1,512 segments (191 injury or fatal crashes in 5 years)
Standard deviation s_e :	± 0.10 crashes/yr

The inverse dispersion parameter is relatively large when compared to that for other models reported in the literature. This trend implies that there is less unexplained site-to-site variability in the predicted mean crash frequency for groups of similar sites. There are several reasons for this trend. Those reasons are documented in Chapter 5 in the discussion associated with Table 34.

The coefficients in Table 52 were combined with Equations 179 and 180 to obtain the calibrated SPFs for multiple-vehicle crashes. The form of each model is described in the following equations.

$$N_{spf,mv,1} = L e^{-2.997 + 0.524 \ln(AADT/1,000) + 0.0699 (AADT/1,000) - 0.508 I_{enr} - 1.974 I_{exr} - 1.721 I_{rural}} \quad (191)$$

$$N_{spf,mv,2} = L e^{-2.515 + 0.524 \ln(AADT/1,000) + 0.0699 (AADT/1,000) - 0.508 I_{enr} - 1.974 I_{exr} - 1.721 I_{rural}} \quad (192)$$

The calibrated CMFs used with these SPFs are described in a subsequent section. The number of lanes present at the start of the ramp segment (in the direction of travel) defines which SPF to use.

The fit of the calibrated models is shown in Figure 80. This figure compares the predicted and reported crash frequency in the calibration database. The trend line shown represents a “ $y = x$ ” line. A data point would lie on this line if its predicted and reported crash frequency were equal. The data points shown represent the reported multiple-vehicle crash frequency for the segments used to calibrate the corresponding component model.

Each data point shown in Figure 80 represents the average predicted and average reported crash frequency for a group of 10 segments. The data were sorted by predicted crash frequency

to form groups of segments with similar crash frequency. The purpose of this grouping was to reduce the number of data points shown in the figure and, thereby, to facilitate an examination of trends in the data. The individual segment observations were used for model calibration. In general, the data shown in the figure indicate that the model provides an unbiased estimate of expected crash frequency for segments experiencing up to 2 multiple-vehicle crashes in a five-year period.

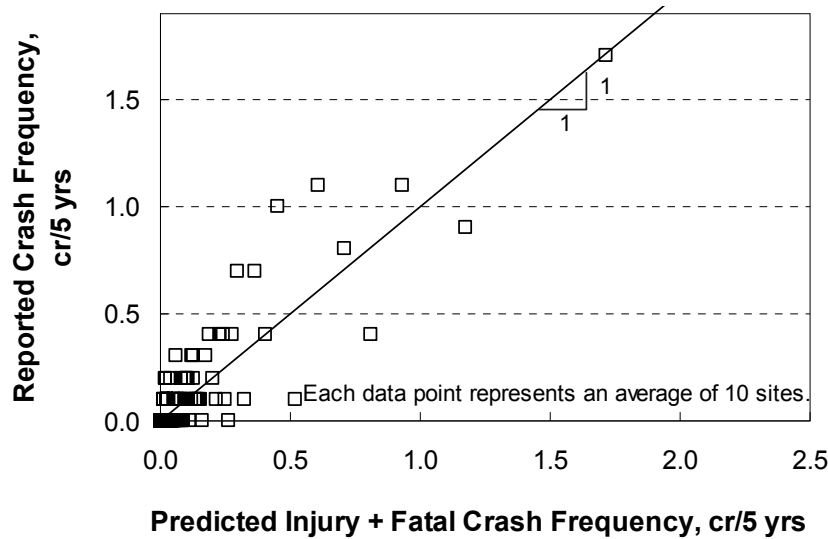


Figure 80. Predicted vs. reported multiple-vehicle ramp FI crashes.

Model for Predicting Single-Vehicle Crash Frequency

The results of the single-vehicle model calibration are presented in Table 54. The Pearson χ^2 statistic for the model is 1,506, and the degrees of freedom are 1,496 ($= n - p = 1,512 - 16$). As this statistic is less than $\chi^2_{0.05,1496} (= 1,587)$, the hypothesis that the model fits the data cannot be rejected. The R^2 for the model is 0.15. The R_k^2 for the calibrated model is 0.70.

TABLE 54. Ramp FI model statistical description—single-vehicle model—three states

Model Statistics	Value
$R^2 (R_k^2)$:	0.15 (0.70)
Scale parameter ϕ :	1.00
Pearson χ^2 :	1,506 ($\chi^2_{0.05,1496} = 1,587$)
Inverse dispersion parameter K :	7.91 mi^{-1}
Observations n_o :	1,512 segments (830 injury or fatal crashes in 5 years)
Standard deviation s_e :	± 0.23 crashes/yr

The inverse dispersion parameter is relatively large when compared to that for other models reported in the literature. The reasons for this trend were identified in the discussion associated with Table 34.

The coefficients in Table 52 were combined with Equations 184 and 185 to obtain the calibrated SPF for single-vehicle crashes. The form of each model is described in the following equations.

$$N_{spf,sv,1} = L e^{-2.848 + 0.718 \ln(AADT/1,000) + 0.882 I_{enr} + 1.203 I_{exr} - 0.154 I_{rural}} \quad (193)$$

$$N_{spf,sv,2} = L e^{-2.881 + 0.718 \ln(AADT/1,000) + 0.882 I_{enr} + 1.203 I_{exr} - 0.154 I_{rural}} \quad (194)$$

The calibrated CMFs used with this SPF are described in a subsequent section. The number of lanes present at the start of the ramp segment (in the direction of travel) defines which SPF to use.

The fit of the calibrated model is shown in Figure 81. This figure compares the predicted and reported crash frequency in the calibration database. Each data point shown represents the average predicted and average reported crash frequency for a group of 10 segments. In general, the data shown in the figure indicate that the model provides an unbiased estimate of expected crash frequency for segments experiencing up to 4 single-vehicle crashes in a five-year period.

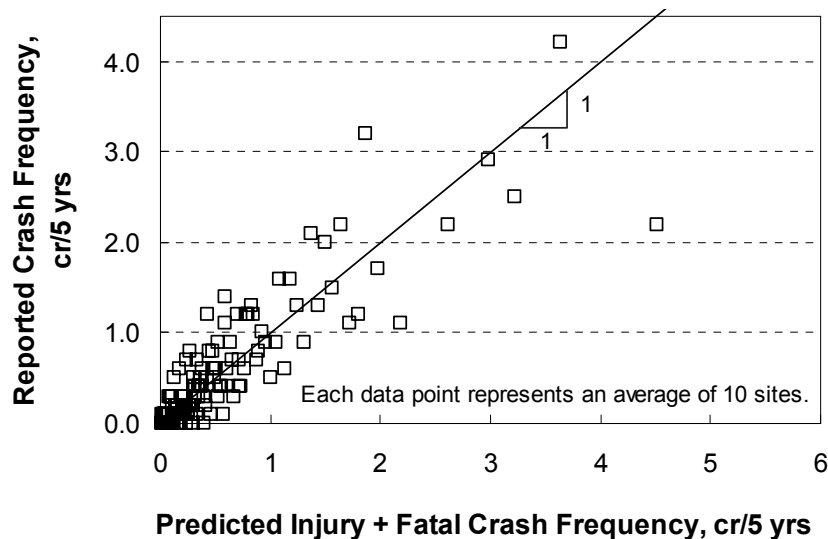


Figure 81. Predicted vs. reported single-vehicle ramp FI crashes.

Calibrated CMFs

Several CMFs were calibrated in conjunction with the SPFs. All of them were calibrated using FI crash data. Collectively, they describe the relationship between various geometric factors and crash frequency. These CMFs are described in this section and, where possible, compared with the findings from previous research as means of model validation.

Many of the CMFs found in the literature are typically derived from (and applied to) the combination of multiple-vehicle and single-vehicle crashes. That is, one CMF is used to indicate

the influence of a specified geometric factor on total crashes. In contrast, the models developed for this research project include several CMFs that are calibrated for a specific crash type. In these instances, Equation 195 is used to facilitate a comparison of the CMFs reported in the literature with those developed for this project. Specifically, this equation is used to convert the CMFs developed for a specific crash type to one that applies to total crashes.

$$CMF_{i|agg} = (1.0 - P_{mv}) CMF_{sv,i} + P_{mv} CMF_{mv,i} \quad (195)$$

where,

$CMF_{i|agg}$ = aggregated CMF for element i ;

P_{mv} = proportion of multiple-vehicle crashes; and

$CMF_{j,i}$ = crash modification factor for element i and crash type j ($j = mv, sv$).

The proportion of multiple-vehicle crashes used in this equation is obtained from Table 55. The data in this table were obtained from the study state databases.

TABLE 55. Distribution of FI crashes on ramps

Area Type	Number of Through Lanes	Multiple-Vehicle FI Crashes (MV)	Single-Vehicle FI Crashes (SV)	Proportion MV Crashes
Rural	1	2	94	0.021
Urban	1	82	529	0.134
	2	107	207	0.341

Horizontal Curve CMF. The calibrated horizontal curve CMF has two forms, depending on which component model is being used. The CMF for multiple-vehicle crashes is described using the following equation.

$$CMF_{mv,hc|agg} = 1.0 + 0.779 \frac{1,000}{32.2} \sum_{i=1}^m \left(\frac{v_{ent,i}}{R_i} \right)^2 P_{c,i} \quad (196)$$

The CMF for single-vehicle crashes is described using the following equation.

$$CMF_{sv,hc|agg} = 1.0 + 2.406 \frac{1,000}{32.2} \sum_{i=1}^m \left(\frac{v_{ent,i}}{R_i} \right)^2 P_{c,i} \quad (197)$$

These two CMFs are derived to be applicable to a segment that has a mixture of uncurved and curved lengths. The variable $P_{c,i}$ is computed as the ratio of the length of curve i on the segment to the length of the segment. For example, consider a segment that is 0.5 mi long and a curve that is 0.2 mi long. If one-half of the curve is on the segment, then $P_{c,i} = 0.20$ ($= 0.1/0.5$). In fact, this proportion is the same regardless of the curve's length (provided that it is 0.1 mi or longer and 0.1 mi of this curve is located on the segment).

The combined horizontal curve CMF is shown in Figure 82 using a series of thick, solid trend lines. Equation 195 was used to create these trend lines. They represent urban ramps with one through lane using the corresponding proportion of multiple-vehicle crashes in Table 55. The

radii used to calibrate this CMF range from 100 to 3,500 ft. The base condition for this CMF is an uncurved (i.e., tangent) segment.

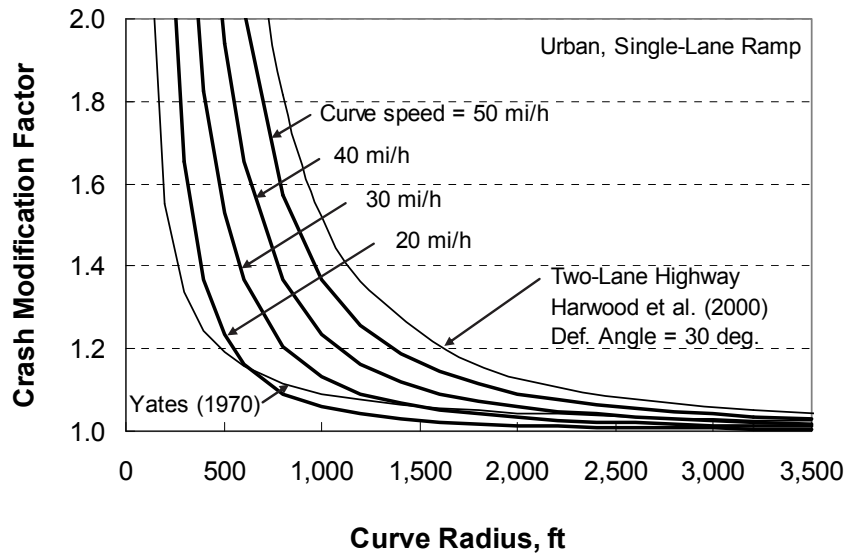


Figure 82. Calibrated ramp horizontal curve CMF for FI crashes.

Also shown in Figure 82 are CMFs developed by other researchers. Thin lines are used to differentiate these CMFs from those developed for this research project. The correlation between curve radius and crash frequency is consistent among all CMFs. Both of the trends attributed to other researchers were discussed previously in Chapter 2. The trend attributed to Yates (1970) is based on data for loop and connector ramps at full-cloverleaf interchanges.

Lane Width CMF. The lane width CMF is described using the following equation.

$$CMF_{lw} = e^{-0.0458 (W_l - 14)} \quad (198)$$

This CMF is applicable to both multiple- and single-vehicle crashes. The lane width used in the CMF is an average for all through lanes on the segment.

The lane width CMF is shown in Figure 83 using a thick, solid trend line. The lane widths used to calibrate this CMF range from 11 to 18 ft. The base condition for this CMF is a 14-ft lane width.

Also shown in Figure 83 is a CMF derived from a regression model reported by Bauer and Harwood (1998). The model was calibrated for ramp proper segments using all crashes, except those identified as rear end. They rationalized that rear-end crashes on exit ramps were more likely related to the crossroad ramp terminal than the ramp proper geometry. The correlation between lane width and crash frequency in their model is consistent with that described by Equation 198.

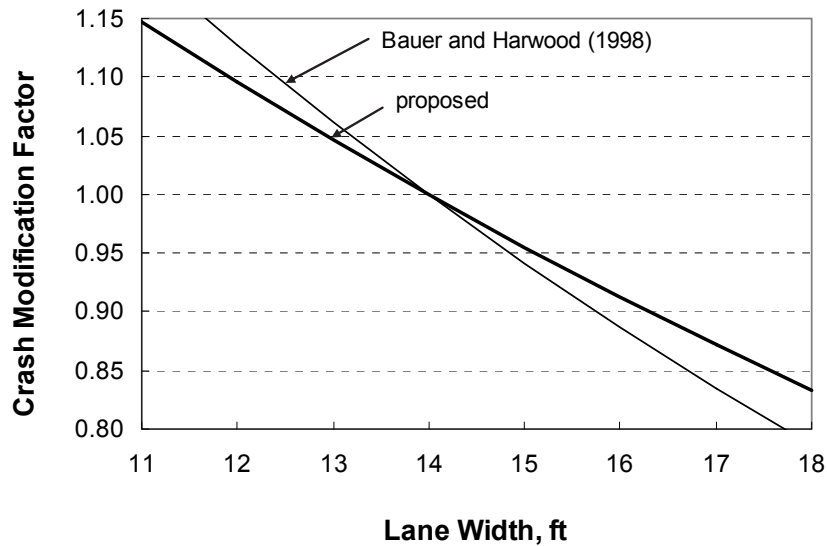


Figure 83. Calibrated ramp lane width CMF for FI crashes.

Right Shoulder Width CMF. The right shoulder width CMF is described using the following equation.

$$CMF_{rsw} = e^{-0.0539(W_{rs}-8)} \quad (199)$$

This CMF is applicable to multiple- and single-vehicle crashes. The shoulder width used in this CMF is an average for the length of the segment.

The right shoulder width CMF is shown in Figure 84 using a thick, solid trend line. The shoulder widths used to calibrate this CMF range from 3 to 11 ft. The base condition for this CMF is an 8-ft shoulder width.

Also shown in Figure 84 are similar CMFs developed by other researchers. A CMF for ramp right shoulder width was not found in a review of the literature. The trends attributed to other researchers are for frontage roads and highways. Thin lines are used to differentiate these CMFs from those developed for this research project. The correlation between right shoulder width and crash frequency is consistent among all CMFs.

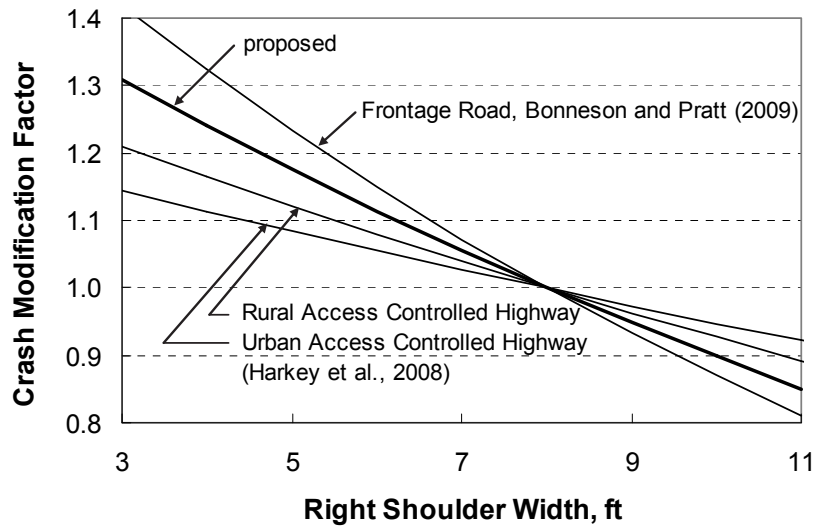


Figure 84. Calibrated ramp right shoulder width CMF for FI crashes.

Left Shoulder Width CMF. The left shoulder width CMF is described using the following equation.

$$CMF_{lsw} = \begin{cases} e^{-0.0539(W_{ls}-4)} & : \text{If urban with } W_{ls} \leq 4.13, \text{ or rural} \\ e^{0.0479(W_{ls}-4)} & : \text{If urban with } W_{ls} > 4.13 \end{cases} \quad (200)$$

This CMF is applicable to multiple- and single-vehicle crashes. The shoulder width used in this CMF is an average for the length of the segment. The value “4.13” in this CMF is a regression coefficient from Table 52.

The inside shoulder width CMF is shown in Figure 85 using a thick trend line. The shoulder widths used to calibrate this CMF range from 2 to 9 ft. The base condition for this CMF is a 4-ft shoulder width.

The thick solid trend line indicates that the relationship between left shoulder width and crash frequency for rural ramps has the same slope as for right shoulder width. The same slope was found for urban ramps when the left shoulder width is less than 4.13 ft. However, urban ramps were found to have an increase in crash frequency as the left shoulder width increased beyond 4.13 ft. A review of the literature on the safety effect of ramp shoulder width did not reveal any evidence that could support or refute this finding. It is possible that disabled vehicles are frequently parked on the left shoulders of urban ramps when the shoulder width is sufficiently wide as to provide some refuge. Collisions between these vehicles and ramp drivers (or collisions indirectly related to the presence of these vehicles) may explain the trend in Figure 85. Nevertheless, it is recommended that this portion of Equation 200 not be used until additional research can confirm its validity.

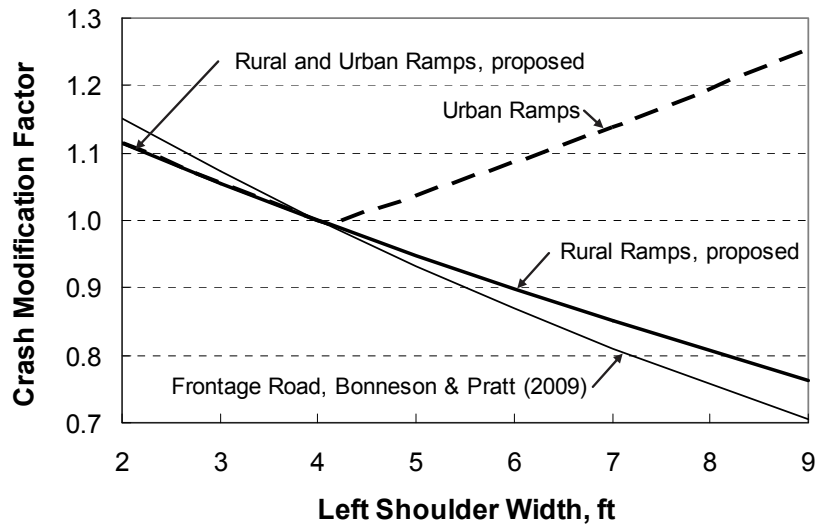


Figure 85. Calibrated ramp left shoulder width CMF for FI crashes.

Also shown in Figure 85 is a CMF developed by other researchers for frontage roads. A CMF for ramp left shoulder width was not found in a review of the literature. A thin line is used to differentiate this CMF from that developed for this research project. The correlation between left shoulder width and crash frequency is consistent among the two CMFs for rural ramps and for urban ramps with a shoulder width less than 4.13 ft.

Right Side Barrier CMF. The calibrated right side barrier CMF is described using the following equation.

$$CMF_{rb|agg} = (1.0 - P_{rb})1.0 + P_{rb} e^{0.210/W_{rcb}} \quad (201)$$

This CMF is applicable to multiple- and single-vehicle crashes.

Guidance for computing the variables P_{rb} and W_{rcb} was provided previously in the subsection titled Barrier Variable Calculations. The variable W_{rcb} (representing the distance from the edge of right shoulder to the barrier face) ranges in value from 1.0 to 25 ft in the database. The base condition for this CMF is no barrier.

The right side barrier CMF is shown in Figure 86. The trend lines are based on the use of Equation 187 and a right shoulder width of 8 ft. One trend line applies when right side barrier exists for the length of the segment. The other trend line applies when barrier exists for only one-half of the segment length.

No research was found in the literature that describes the association between ramp barrier presence and crash frequency. However, the trends shown in Figure 86 are very similar to those found for freeway median barrier and roadside barrier, as documented in Chapter 5.

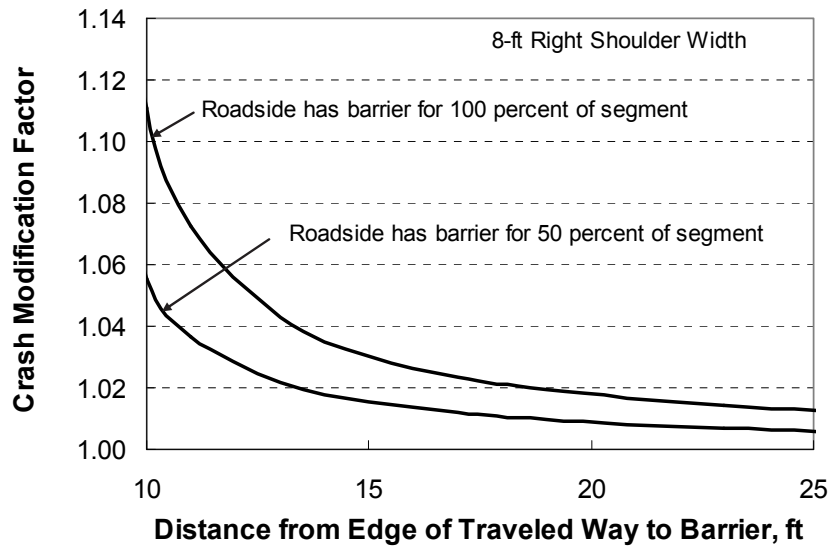


Figure 86. Calibrated ramp right side barrier CMF for FI crashes.

Left Side Barrier CMF. The calibrated left side barrier CMF is described using the following equation.

$$CMF_{lb|agg} = (1.0 - P_{lb})1.0 + P_{lb} e^{0.210/W_{lcb}} \quad (202)$$

This CMF is applicable to multiple- and single-vehicle crashes.

Guidance for computing the variables P_{lb} and W_{lcb} was provided previously in the subsection titled Barrier Variable Calculations. The variable W_{lcb} (representing the distance from the edge of left shoulder to the barrier face) ranges in value from 1.0 to 24 ft in the database. The base condition for this CMF is no barrier.

The left side barrier CMF is shown in Figure 87. The trend lines are based on the use of Equation 189 and a left shoulder width of 4 ft. One trend line applies when left side barrier exists for the length of the segment. The other trend line applies when barrier exists for only one-half of the segment length.

No research was found in the literature that describes the association between ramp barrier presence and crash frequency. However, the trends shown in Figure 87 are very similar to those found for freeway median barrier and roadside barrier, as documented in Chapter 5.

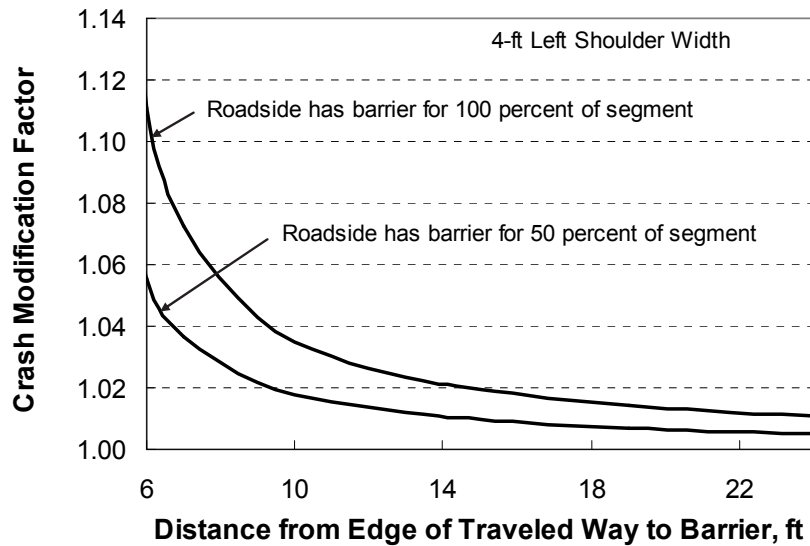


Figure 87. Calibrated ramp left side barrier CMF for FI crashes.

Weaving Section CMF. The calibrated weaving section CMF is described using the following equation.

$$CMF_{wev|agg} = (1.0 - P_{wev})1.0 + P_{wev} e^{[0.191 - 0.0715 \ln(AADT/1,000)]/L_{wev}} \quad (203)$$

This CMF is applicable to multiple- and single-vehicle crashes. It is used to evaluate C-D road segments that have some or all of their length in a weaving section. This CMF is not used with the ramp speed-change lane CMF or the lane add or drop CMF.

The variable P_{wev} in Equation 203 is computed as the ratio of the length of the weaving section on the segment to the length of the segment. If the segment is wholly located in the weaving section, then this variable is equal to 1.0.

The variable for weaving section length L_{wev} in Equation 203 is intended to reflect the degree to which the weaving activity is concentrated along the C-D road. This variable has negligible correlation with segment length L .

The weaving section CMF is shown in Figure 88 using a thick trend line. The weaving section lengths used to calibrate this CMF range from 0.07 to 0.25 mi. The base condition for this CMF is no weaving section present.

The calibration coefficient associated with the AADT term in Equation 203 is negative which is counterintuitive at first glance. It indicates that the weaving section CMF is larger for segments associated with lower AADT volumes. This trend may be explained by the fact that the portion of the traffic stream that is weaving increases with AADT volume and drivers are more aware of weaving maneuvers as these maneuvers become more frequent. Regardless, the coefficient associated with the segment AADT variable in the SPF is positive and relatively large

and, when the SPF is combined with Equation 203, the predicted average crash frequency for the C-D road segment increases with an increase in AADT volume. This trend is logical and intuitive.

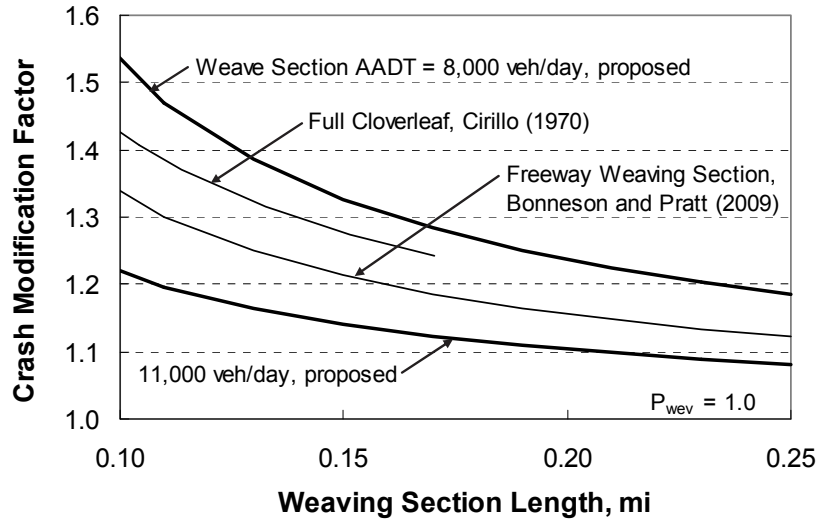


Figure 88. Calibrated ramp weaving section CMF for FI crashes.

Ramp Speed-Change Lane CMF. The ramp speed-change lane CMF is described using the following equation.

$$CMF_{mv,sc|agg} = (1.0 - P_{en-ex})1.0 + P_{en-ex} e^{0.310} \quad (204)$$

This CMF is applicable to multiple-vehicle crashes. It is used to evaluate a ramp or C-D road segment that is being joined by another ramp by way of a speed-change lane. The speed-change lane can be either an acceleration lane or a deceleration lane. This CMF is not used with the weaving section CMF because the ramps in a weaving section are joined by an auxiliary lane (i.e., they do not have a speed-change lane).

The ramp speed-change lane CMF is shown in Figure 89. The trends shown are based on the use of Equation 195 and the proportion of multiple-vehicle crashes in Table 55. No other research was found in the literature that describes the association between ramp speed-change lane presence and ramp crash frequency.

The variable P_{en-ex} in Equation 204 is computed as the ratio of the length of the ramp speed-change lane on the segment to the length of the segment. If the segment is wholly located along the speed-change lane, then this variable is equal to 1.0.

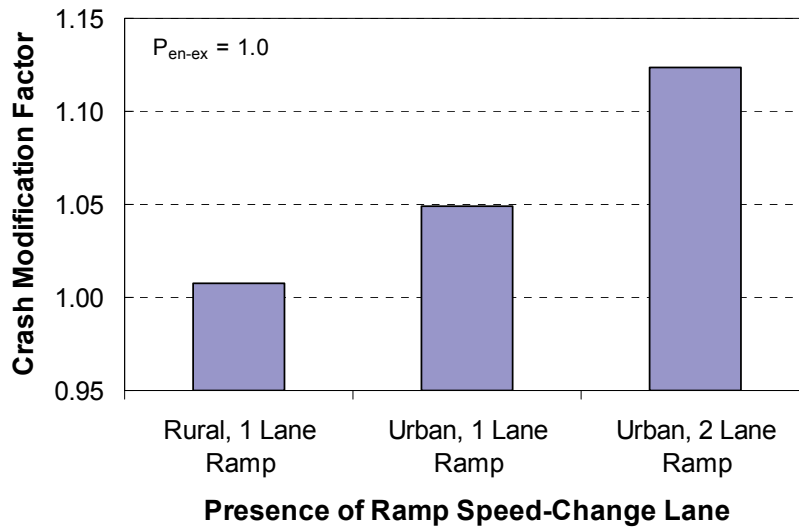


Figure 89. Calibrated ramp speed-change lane CMF for FI crashes.

Lane Add or Drop CMF. The lane add or drop CMF is described using the following equation.

$$CMF_{a-d|agg} = (1.0 - P_{tpr})1.0 + P_{tpr} e^{-0.231(I_{add} - I_{drop})} \quad (205)$$

This CMF is applicable to both multiple- and single-vehicle crashes. It is used to evaluate a ramp or C-D road segment that has a lane added to it, or dropped from it. This CMF is not used with the weaving section CMF.

The variable P_{tpr} in Equation 205 is computed as the ratio of the length of the lane add (or drop) taper on the segment to the length of the segment. If the segment is wholly located in the taper, then this variable is equal to 1.0.

The lane add or drop CMF is shown in Figure 90. No other research was found in the literature that describes the association between ramp lane add or drop presence and ramp crash frequency.

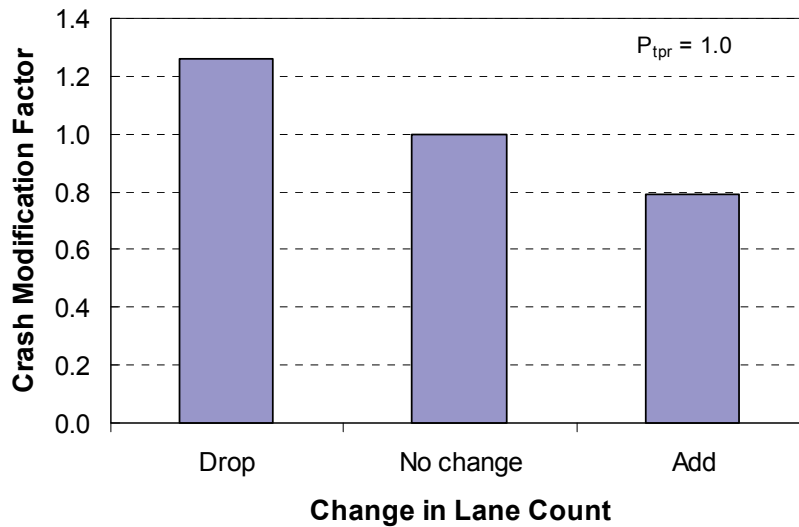


Figure 90. Calibrated ramp lane add or drop CMF for FI crashes.

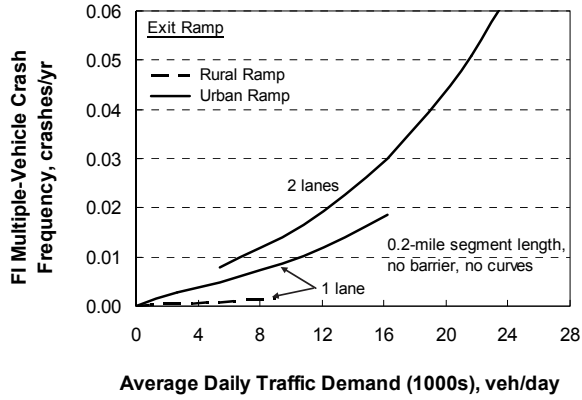
Sensitivity Analysis

The relationship between crash frequency and traffic demand, as obtained from the combined calibrated models, is illustrated in Figure 91 for a 0.2-mile ramp or C-D road segment with no barrier or curvature. The individual component models are illustrated in Figures 91a, 91b, 91c, and 91d. The sum of the individual component crash frequencies is illustrated in Figure 92. The length of the trend lines in Figures 91 and 92 reflect the range of AADT volume in the data.

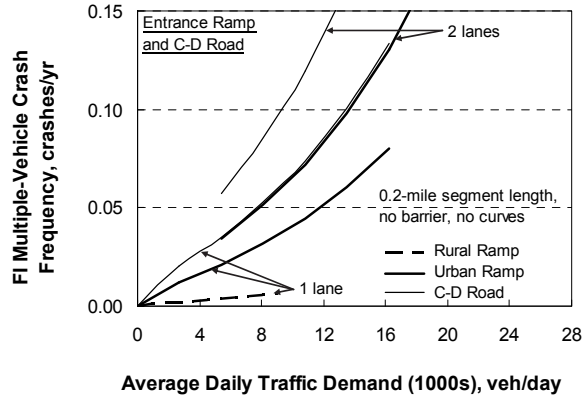
The trends in Figure 92 are not directly comparable to those in Figure 7 because those in Figure 7 are based on total crashes (i.e., all severities) by ramp configuration and likely include barrier and curvature influences. However, as indicated in Chapter 4, FI crashes represent 33 percent of all ramp crashes. This ratio was used to confirm that the general trends among the figures are consistent.

The trend lines shown in Figure 92 indicate that urban ramps have about 20 to 30 percent more crashes than rural ramps, which is consistent with the finding for freeway segments.

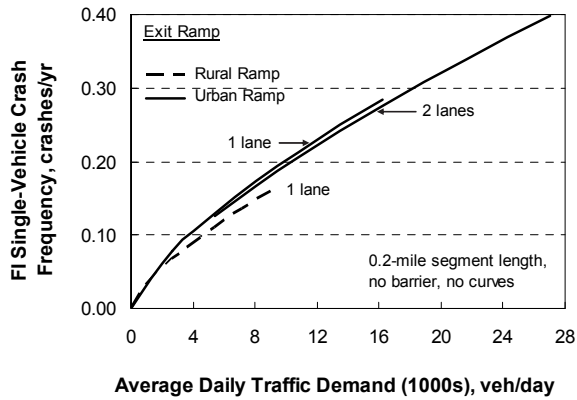
The crash rates listed in Table 23 indicate that crash rates vary widely by ramp configuration. It is likely that this variation is actually a reflection of differences in barrier length and curvature commonly associated with these configurations. These differences are shown in Table 21. In contrast, these influences have been explicitly quantified in the proposed model such that they do not influence the trends shown in Figure 92. The proposed model provides a more accurate indication of differences between ramp and C-D road segments in rural versus urban areas, when the segments have the same barrier proportion and curvature.



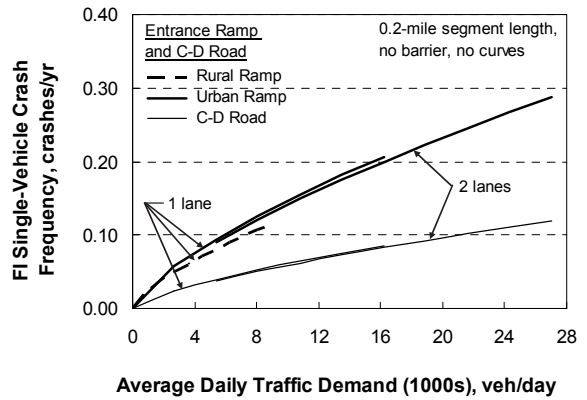
a. Multiple-vehicle crashes on exit ramps.



b. Multiple-vehicle crashes on entrance ramps and C-D roads.

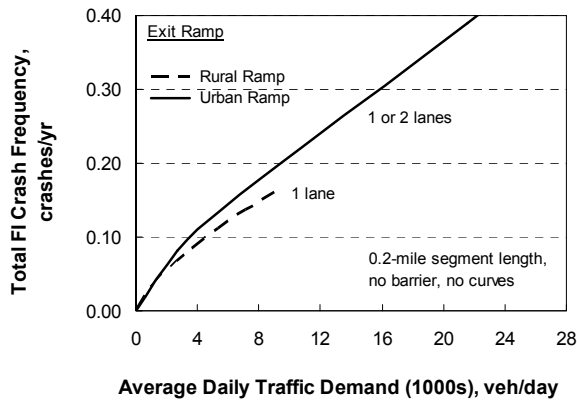


c. Single-vehicle crashes on exit ramps.

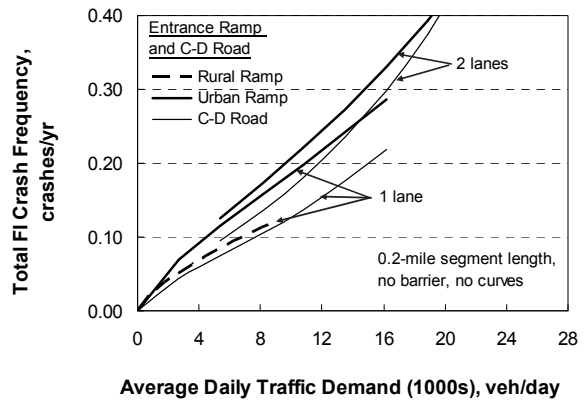


d. Single-vehicle crashes on entrance ramps and C-D roads.

Figure 91. Ramp FI model components.



a. Exit ramps.



b. Entrance ramps and C-D roads.

Figure 92. Ramp FI model.

The trend lines shown in Figure 92 also indicate that crash frequency is *lower* on urban entrance ramps and C-D roads with one lane, relative to those with two lanes. In fact, the models indicate that single-lane urban entrance ramp segments have about 10 percent fewer crashes than two-lane urban entrance ramp segments. They also indicate that a single-lane urban C-D road segment has about 25 percent fewer crashes than a two-lane urban C-D road segment. Examination of Figures 91b and 91d indicates that this trend is due to a significant increase in multiple-vehicle crashes on two-lane entrance ramps and C-D roads, relative to those on single-lane ramps and C-D roads. It is likely that these trends reflect the fact that the second lane represents an added exposure to same-direction sideswipe and other lane-change-related crashes.

MODEL CALIBRATION FOR PDO CRASHES

This part of the chapter describes the calibration of the ramp and C-D road segment predictive models based on PDO crashes. The methodology used to calibrate the models is described in the part titled Methodology. The calibration data, model development, and statistical analysis methods are described in the part titled Model Calibration for FI Crashes.

An initial regression analysis was undertaken with county and state variable combinations treated as fixed effects and as random effects. The Hausman test was performed using the covariance matrix to determine whether the fixed effect model was appropriate. The null hypothesis is that the regression coefficients from the two model treatments are consistent. This hypothesis could not be rejected ($p = 0.99$) indicating that the coefficients are not different among the two treatments. In this case, it is concluded that the random effects treatment is appropriate because it provides more efficient coefficient estimates.

Model Calibration

The results of the regression model calibration are presented in Table 56. The Pearson χ^2 statistic for the model is 3,044, and the degrees of freedom are 3,031 ($= n - p = 3,050 - 19$). As this statistic is less than $\chi^2_{0.05, 3031} (= 3,160)$, the hypothesis that the model fits the data cannot be rejected. Several segments were removed as a result of outlier analysis such that the calibration database included only 2,017 of the 2,363 crashes identified in Chapter 4.

The t-statistic for each coefficient is listed in the last column of Table 56. These statistics describe a test of the hypothesis that the coefficient value is equal to 0.0. Those t-statistics with an absolute value that is larger than 2.0 indicate that the hypothesis can be rejected with the probability of error in this conclusion being less than 0.05. For those few variables where the absolute value of the t-statistic is smaller than 2.0, it was decided that the variable was important to the model and its trend was found to be intuitive and, where available, consistent with previous research findings (even if the specific value was not known with a great deal of certainty as applied to this database).

TABLE 56. Ramp PDO model statistical description–combined model–three states

Model Statistics		Value		
R^2 :		0.29		
Scale parameter ϕ :		1.0		
Pearson χ^2 :		3,044 ($\chi^2_{0.05, 3031} = 3,160$)		
Observations n_o :		1,525 segments (2,017 PDO crashes in 5 years)		
Calibrated Coefficient Values				
Variable	Inferred Effect of..	Value	Std. Dev.	t-statistic
b_{sw}	Shoulder width (left and right side, except case below)	-0.0259	0.0151	-1.7
$b_{sw, 2}$	Left shoulder width on urban seg. with width $> b_{lsw}$	0.0195	0.0342	0.6
b_{lsw}	Threshold left shoulder width	4.243	2.2341	1.9
b_{bar}	Barrier presence	0.193	0.0620	3.1
$b_{mv, cr}$	Horizontal curvature on 2+ veh. crashes	0.545	0.2792	2.0
$b_{sv, cr}$	Horizontal curvature on 1 veh. crashes	3.136	0.5715	5.5
b_{wev}	Weaving section presence	0.187	0.0777	2.4
b_v	AADT on weaving-related crashes	-0.0580	0.0347	-1.7
$b_{mv, enr}$	Added effect of entrance ramp on 2+ vehicle crashes	-0.508	0.250	-2.0
$b_{mv, exr}$	Added effect of exit ramp on 2+ vehicle crashes	-1.540	0.260	-5.9
$b_{mv, 0, 1}$	1 lane on 2+veh. crashes for C-D roads in urban areas	-3.311	0.334	-9.9
$b_{mv, 0, 2}$	2 lanes on 2+ veh. crashes for C-D roads in urban areas	-2.475	0.380	-6.5
$b_{mv, l}$	AADT on 2+ vehicle crashes	1.256	0.108	11.6
$b_{sv, enr}$	Added effect of entrance ramp on 1 veh. crashes	0.944	0.263	3.6
$b_{sv, exr}$	Added effect of exit ramp on 1 veh. crashes	1.151	0.261	4.4
$b_{sv, 0, 1}$	1 lane on 1 veh. crashes for C-D roads in urban areas	-2.659	0.282	-9.4
$b_{sv, 0, 2}$	2 lanes on 1 veh. crashes for C-D roads in urban areas	-2.344	0.304	-7.7
$b_{sv, l}$	AADT on 1 veh. crashes	0.689	0.057	12.1
$b_{sv, rural}$	Added effect of rural area type on 1 veh. crashes	-0.231	0.143	-1.6

Model for Predicting Multiple-Vehicle Non-Ramp-Related Crash Frequency

The results of the multiple-vehicle model calibration are presented in Table 57. The Pearson χ^2 statistic for the model is 1,528, and the degrees of freedom are 1,514 ($= n - p = 1,525 - 11$). As this statistic is less than $\chi^2_{0.05, 1514} (= 1,606)$, the hypothesis that the model fits the data cannot be rejected. The R^2 for the model is 0.50. An alternative measure of model fit that is better suited to the negative binomial distribution is R_k^2 . The R_k^2 for the calibrated model is 0.93.

TABLE 57. Ramp PDO model statistical description–multiple-vehicle model–three states

Model Statistics		Value		
R^2 (R_k^2):		0.50 (0.93)		
Scale parameter ϕ :		1.00		
Pearson χ^2 :		1,528 ($\chi^2_{0.05, 1514} = 1,606$)		
Inverse dispersion parameter K :		12.7 mi ⁻¹		
Observations n_o :		1,525 segments (490 PDO crashes in 5 years)		
Standard deviation s_e :		±0.18 crashes/yr		

The coefficients in Table 56 were combined with the regression model to obtain the calibrated SPFs for multiple-vehicle crashes. The form of each model is described in the following equations.

$$N_{spf,mv,1} = L e^{-3.311 + 1.256 \ln(AADT/1,000) - 0.508 I_{enr} - 1.540 I_{exr}} \quad (206)$$

$$N_{spf,mv,2} = L e^{-2.475 + 1.256 \ln(AADT/1,000) - 0.508 I_{enr} - 1.540 I_{exr}} \quad (207)$$

The calibrated CMFs used with these SPFs are described in a subsequent section. The number of lanes present at the start of the ramp segment (in the direction of travel) defines which SPF to use.

The fit of the calibrated models is shown in Figure 93. This figure compares the predicted and reported crash frequency in the calibration database. Each data point shown represents the average predicted and average reported crash frequency for a group of 10 segments. In general, the data shown in the figure indicate that the model provides an unbiased estimate of expected crash frequency for segments experiencing up to 3 multiple-vehicle crashes in a five-year period.

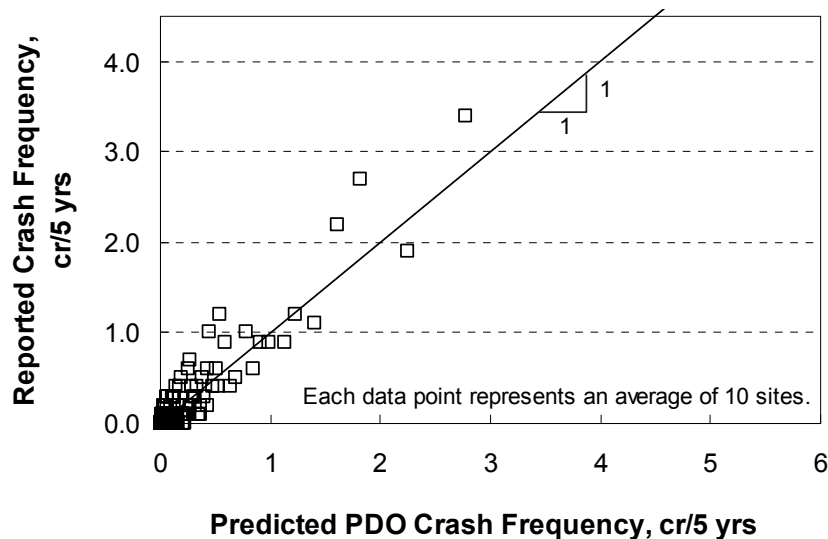


Figure 93. Predicted vs. reported multiple-vehicle ramp PDO crashes.

Model for Predicting Single-Vehicle Crash Frequency

The results of the single-vehicle model calibration are presented in Table 58. The Pearson χ^2 statistic for the model is 1,516, and the degrees of freedom are 1,513 ($= n - p = 1,525 - 12$). As this statistic is less than $\chi^2_{0.05,1513} (= 1,605)$, the hypothesis that the model fits the data cannot be rejected. The R^2 for the model is 0.21. The R_k^2 for the calibrated model is 0.72.

TABLE 58. Ramp PDO model statistical description—single-vehicle model—three states

Model Statistics	Value
R^2 (R_k^2):	0.21 (0.72)
Scale parameter ϕ :	0.99
Pearson χ^2 :	1,516 ($\chi^2_{0.05, 1513} = 1,605$)
Inverse dispersion parameter K :	9.77 mi ⁻¹
Observations n_o :	1,525 segments (1,527 PDO crashes in 5 years)
Standard deviation s_e :	±0.39 crashes/yr

The coefficients in Table 56 were combined with the regression model to obtain the calibrated SPF for single-vehicle crashes. The form of each model is described in the following equations.

$$N_{spf,sv,1} = L e^{-2.659 + 0.689 \ln(AADT/1,000) + 0.944 I_{enr} + 1.151 I_{exr} - 0.231 I_{rural}} \quad (208)$$

$$N_{spf,sv,1} = L e^{-2.344 + 0.689 \ln(AADT/1,000) + 0.944 I_{enr} + 1.151 I_{exr} - 0.231 I_{rural}} \quad (209)$$

The calibrated CMFs used with this SPF are described in a subsequent section. The number of lanes present at the start of the ramp segment (in the direction of travel) defines which SPF to use.

The fit of the calibrated model is shown in Figure 94. This figure compares the predicted and reported crash frequency in the calibration database. Each data point shown represents the average predicted and average reported crash frequency for a group of 10 segments. In general, the data shown in the figure indicate that the model provides an unbiased estimate of expected crash frequency for segments experiencing up to 7 single-vehicle crashes in a five-year period.

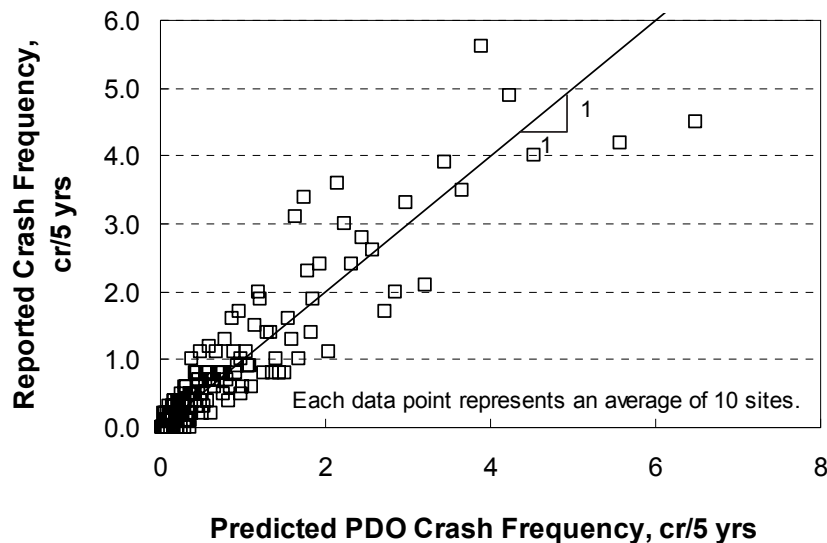


Figure 94. Predicted vs. reported single-vehicle ramp PDO crashes.

Calibrated CMFs

Several CMFs were calibrated in conjunction with the SPFs. All of them were calibrated using PDO crash data. Collectively, they describe the relationship between various geometric factors and PDO crash frequency.

Many of the CMFs found in the literature are typically derived from (and applied to) the combination of multiple-vehicle and single-vehicle crashes. That is, one CMF is used to indicate the influence of a specified geometric factor on total crashes. In contrast, the models developed for this research project include several CMFs that are calibrated for a specific crash type. In these instances, Equation 195 is used to convert the CMFs developed for this project into equivalent total-crash CMFs for the purpose of illustrating the overall trend. The proportion of multiple-vehicle crashes used in Equation 195 is obtained from Table 59. The data in this table were obtained from the study state databases.

TABLE 59. Distribution of PDO crashes on ramps

Area Type	Number of Through Lanes	Multiple-Vehicle PDO Crashes (MV)	Single-Vehicle PDO Crashes (SV)	Proportion MV Crashes
Rural	1	21	157	0.118
Urban	1	172	973	0.150
	2	297	379	0.428

Horizontal Curve CMF. The calibrated horizontal curve CMF has two forms, depending on which component model is being used. The CMF for multiple-vehicle crashes is described using the following equation.

$$CMF_{mv, hc|agg} = 1.0 + 0.545 \frac{1,000}{32.2} \sum_{i=1}^m \left(\frac{v_{ent,i}}{R_i} \right)^2 P_{c,i} \quad (210)$$

The CMF for single-vehicle crashes is described using the following equation.

$$CMF_{sv, hc|agg} = 1.0 + 3.136 \frac{1,000}{32.2} \sum_{i=1}^m \left(\frac{v_{ent,i}}{R_i} \right)^2 P_{c,i} \quad (211)$$

These two CMFs are derived to be applicable to a segment that has a mixture of uncurved and curved lengths. The variable $P_{c,i}$ is computed as the ratio of the length of curve i on the segment to the length of the segment.

The combined horizontal curve CMF is shown in Figure 95 using a series of thick, solid trend lines. Equation 195 was used to create these trend lines. They represent urban ramps with one through lane using the corresponding proportion of multiple-vehicle crashes in Table 59. The radii used to calibrate this CMF range from 100 to 3,500 ft. The base condition for this CMF is an uncurved (i.e., tangent) segment.

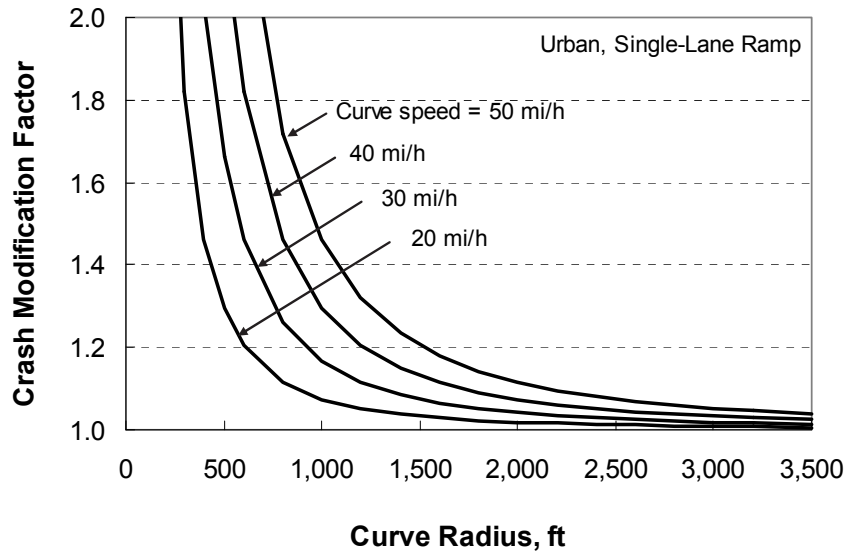


Figure 95. Calibrated ramp horizontal curve CMF for PDO crashes.

Right Shoulder Width CMF. The right shoulder width CMF is described using the following equation.

$$CMF_{rsw} = e^{-0.0259(W_{rs} - 8)} \quad (212)$$

This CMF is applicable to multiple- and single-vehicle crashes. The shoulder width used in this CMF is an average for the length of the segment.

The right shoulder width CMF is shown in Figure 96. The shoulder widths used to calibrate this CMF range from 3 to 11 ft. The base condition for this CMF is an 8-ft shoulder width.



Figure 96. Calibrated ramp right shoulder width CMF for PDO crashes.

Left Shoulder Width CMF. The left shoulder width CMF is described using the following equation.

$$CMF_{lsw} = \begin{cases} e^{-0.0259(W_{ls} - 4)} & : \text{If urban with } W_{ls} \leq 4.24, \text{ or rural} \\ e^{0.0195(W_{ls} - 4)} & : \text{If urban with } W_{ls} > 4.24 \end{cases} \quad (213)$$

This CMF is applicable to multiple- and single-vehicle crashes. The shoulder width used in this CMF is an average for the length of the segment.

The inside shoulder width CMF is shown in Figure 97. The shoulder widths used to calibrate this CMF range from 2 to 9 ft. The base condition for this CMF is a 4-ft shoulder width.

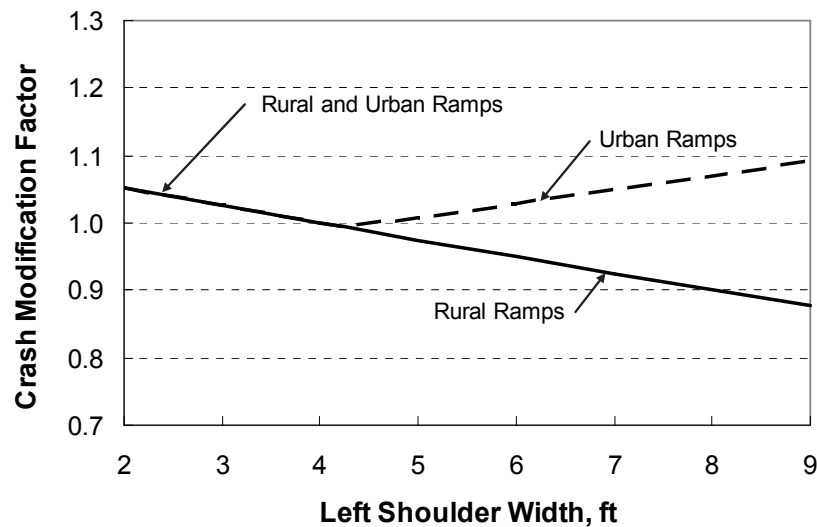


Figure 97. Calibrated ramp left shoulder width CMF for PDO crashes.

The thick solid trend line indicates that the relationship between left shoulder width and crash frequency for rural ramps has the same slope as for right shoulder width. The same slope was found for urban ramps when the left shoulder width is less than 4.24 ft. However, urban ramps were found to have an increase in crash frequency as the left shoulder width increased beyond 4.24 ft. A review of the literature on the safety effect of ramp shoulder width did not reveal any evidence that could support or refute this finding. It is possible that disabled vehicles are frequently parked on the left shoulders of urban ramps when the shoulder width is sufficiently wide as to provide some refuge. Collisions between these vehicles and ramp drivers (or collisions indirectly related to the presence of these vehicles) may explain the trend in Figure 97. Nevertheless, it is recommended that this portion of Equation 213 not be used until additional research can confirm its validity.

Right Side Barrier CMF. The calibrated right side barrier CMF is described using the following equation.

$$CMF_{rb|agg} = (1.0 - P_{rb})1.0 + P_{rb} e^{0.193/W_{rcb}} \quad (214)$$

This CMF is applicable to multiple- and single-vehicle crashes. Guidance for computing the variables P_{rb} and W_{rcb} was provided previously in the subsection titled Barrier Variable Calculations. The variable W_{rcb} (representing the distance from the edge of right shoulder to the barrier face) ranges in value from 1.0 to 25 ft in the database. The base condition for this CMF is no barrier.

The right side barrier CMF is shown in Figure 98. The trend lines are based on the use of Equation 187 and a right shoulder width of 8 ft. One trend line applies when right side barrier exists for the length of the segment. The other trend line applies when barrier exists for only one-half of the segment length.

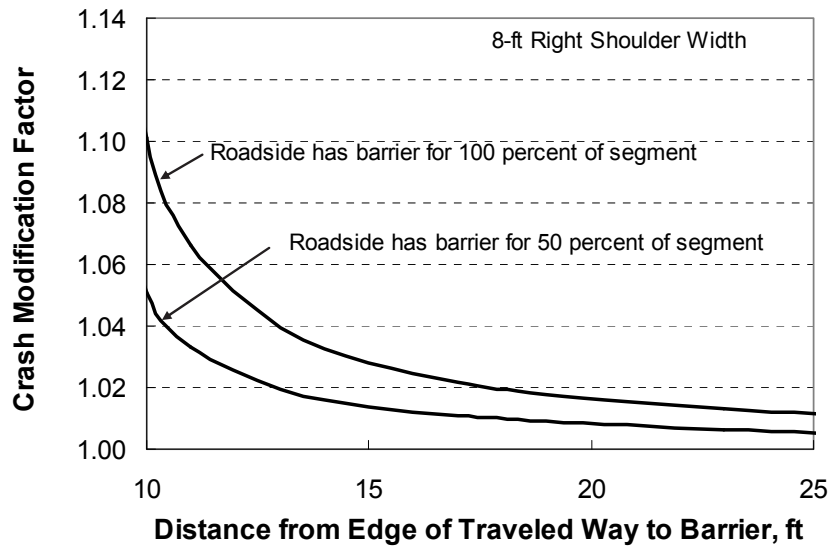


Figure 98. Calibrated ramp right side barrier CMF for PDO crashes.

Left Side Barrier CMF. The calibrated left side barrier CMF is described using the following equation.

$$CMF_{lb|agg} = (1.0 - P_{lb})1.0 + P_{lb} e^{0.193/W_{lcb}} \quad (215)$$

This CMF is applicable to multiple- and single-vehicle crashes.

Guidance for computing the variables P_{lb} and W_{lcb} was provided previously in the subsection titled Barrier Variable Calculations. The variable W_{lcb} (representing the distance from the edge of left shoulder to the barrier face) ranges in value from 1.0 to 24 ft in the database. The base condition for this CMF is no barrier.

The left side barrier CMF is shown in Figure 99. The trend lines are based on the use of a left shoulder width of 4 ft. One trend line applies when left side barrier exists for the length of the segment. The other trend line applies when barrier exists for only one-half of the segment length.

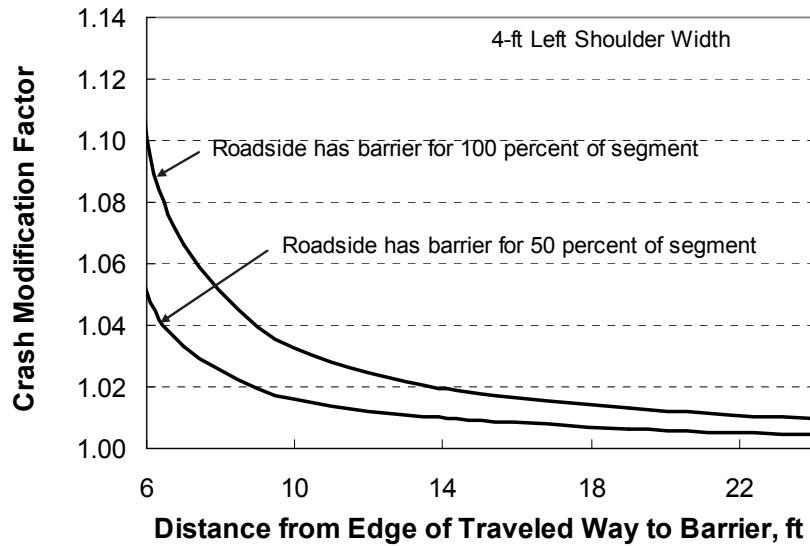


Figure 99. Calibrated ramp left side barrier CMF for PDO crashes.

Weaving Section CMF. The calibrated weaving section CMF is described using the following equation.

$$CMF_{wev|agg} = (1.0 - P_{wev})1.0 + P_{wev} e^{[0.187 - 0.0580 \ln(AADT/1,000)]/L_{wev}} \quad (216)$$

This CMF is applicable to multiple- and single-vehicle crashes. It is used to evaluate C-D road segments that have some or all of their length in a weaving section. This CMF is not used with the ramp speed-change lane CMF or the lane add or drop CMF.

The variable P_{wev} in Equation 216 is computed as the ratio of the length of the weaving section on the segment to the length of the segment. If the segment is wholly located in the weaving section, then this variable is equal to 1.0.

The variable for weaving section length L_{wev} in Equation 216 is intended to reflect the degree to which the weaving activity is concentrated along the C-D road. This variable has negligible correlation with segment length L .

The weaving section CMF is shown in Figure 100 using a thick trend line. The weaving section lengths used to calibrate this CMF range from 0.07 to 0.25 mi. The base condition for this CMF is no weaving section present.

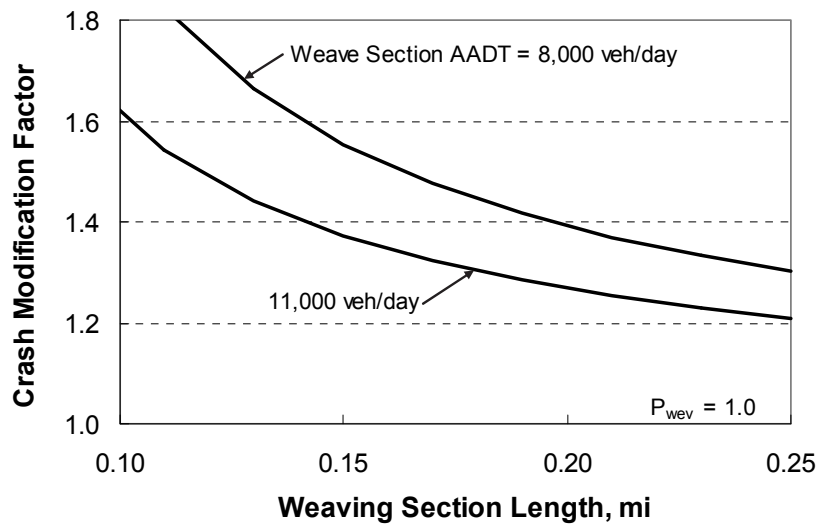


Figure 100. Calibrated ramp weaving section CMF for PDO crashes.

The calibration coefficient associated with the AADT term in Equation 216 is negative which is counterintuitive at first glance. It indicates that the weaving section CMF is larger for segments associated with lower AADT volumes. This trend may be explained by the fact that the portion of the traffic stream that is weaving increases with AADT volume and drivers are more aware of weaving maneuvers as these maneuvers become more frequent. Regardless, the coefficient associated with the segment AADT variable in the SPF is positive and relatively large and, when the SPF is combined with Equation 216, the predicted average crash frequency for the C-D road segment increases with an increase in AADT volume. This trend is logical and intuitive.

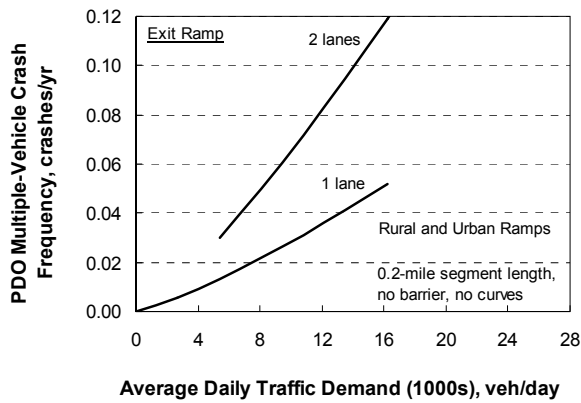
Sensitivity Analysis

The relationship between crash frequency and traffic demand, as obtained from the combined calibrated models, is illustrated in Figure 101 for a 0.2-mile ramp or C-D road segment with no barrier or curvature. The individual component models are illustrated in Figures 101a, 101b, 101c, and 101d. The sum of the individual component crash frequencies is illustrated in Figure 102. The length of the trend lines in Figures 101 and 102 reflect the range of AADT volume in the data.

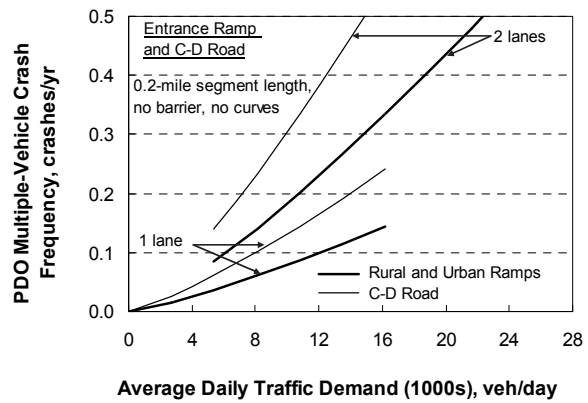
The trend lines shown in Figure 102 indicate that urban ramps have about 20 percent more crashes than rural ramps, which is consistent with the finding for freeway segments.

The crash rates listed in Table 23 indicate that crash rates vary widely by ramp configuration. It is likely that this variation is actually a reflection of differences in barrier length and curvature commonly associated with these configurations. These differences are shown in Table 21. In contrast, these influences have been explicitly quantified in the proposed model such that they do not influence the trends shown in Figure 102. The proposed model provides a

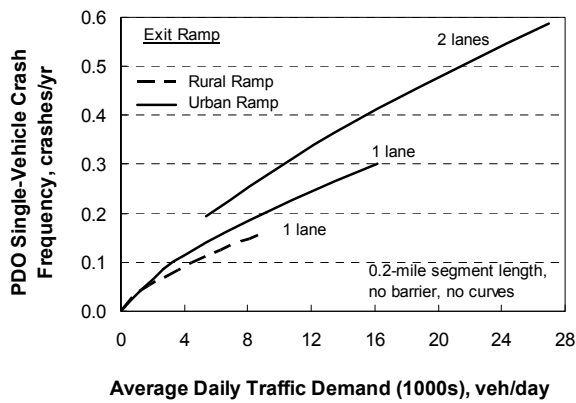
more accurate indication of differences between ramp and C-D road segments in rural versus urban areas, when the segments have the same barrier proportion and curvature.



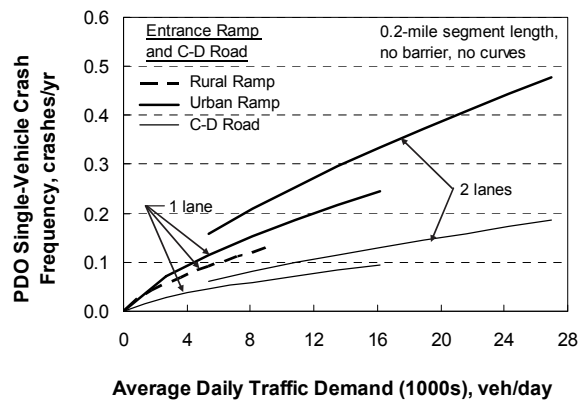
a. Multiple-vehicle crashes on exit ramps.



b. Multiple-vehicle crashes on entrance ramps and C-D roads.



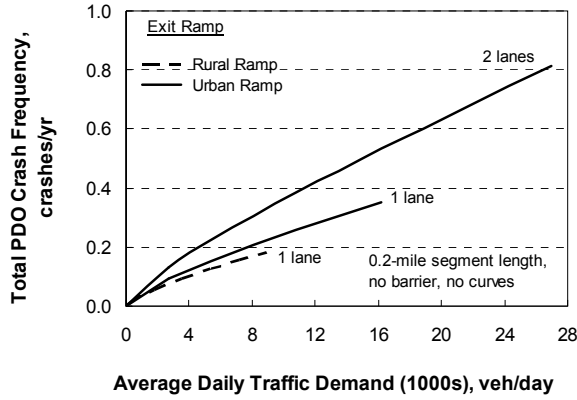
c. Single-vehicle crashes on exit ramps.



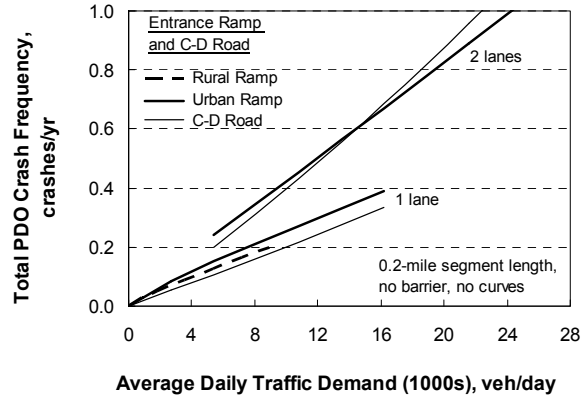
d. Single-vehicle crashes on entrance ramps and C-D roads.

Figure 101. Ramp PDO model components.

The trend lines shown in Figure 102 also indicate that crash frequency is *lower* on urban ramps and C-D roads with one lane, relative to those with two lanes. In fact, the models indicate that single-lane urban ramp segments have about 35 percent fewer crashes than two-lane urban entrance ramp segments. They also indicate that a single-lane urban C-D road segment has about 50 percent fewer crashes than a two-lane urban C-D road segment. Examination of Figure 101 indicates that this trend is due to a significant increase in multiple-vehicle crashes on two-lane entrance ramps and C-D roads, relative to those on single-lane ramps and C-D roads. It is likely that these trends reflect the fact that the second lane represents an added exposure to same-direction sideswipe and other lane-change-related crashes.



a. Exit ramps.



b. Entrance ramps and C-D roads.

Figure 102. Ramp PDO model.

NOMENCLATURE

- $AADT$ = AADT volume on segment, veh/day;
- a_m = instantaneous deceleration rate at speed m , ft/s^2 ;
- b_i = calibration coefficient for condition i
- $b_{j,i}$ = calibration coefficients for model j ($j = mv, sv$), $i = 0, 1$;
- C_{ca} = calibration factor for California;
- $CMF_1 \dots CMF_k$ = crash modification factors for ramp and C-D road segment crashes at a site with specific geometric design features k ;
- $CMF_{a-d|agg}$ = aggregated lane add or drop crash modification factor;
- CMF_i = crash modification factor for element i ;
- $CMF_{i|agg}$ = aggregated CMF for element i ;
- $CMF_{j,i}$ = crash modification factor for element i and crash type j ($j = mv, sv$);
- $CMF_{lb|agg}$ = aggregated left barrier crash modification factor;
- CMF_{lsw} = left shoulder width crash modification factor;
- CMF_{lw} = lane width crash modification factor;
- $CMF_{mv,1} \dots CMF_{mv,w}$ = crash modification factors for multiple-vehicle crashes at a site with specific geometric design features w ;
- $CMF_{mv,hc|agg}$ = aggregated horizontal curve crash modification factor for multiple-vehicle crashes;
- $CMF_{mv,sc|agg}$ = aggregated ramp speed-change lane crash modification factor for multiple-vehicle crashes;
- $CMF_{rb|agg}$ = aggregated right barrier crash modification factor;
- CMF_{rsw} = right shoulder width crash modification factor;
- $CMF_{sv,1} \dots CMF_{sv,x}$ = crash modification factors for single-vehicle crashes at a site with specific geometric design features x ;
- $CMF_{sv,hc|agg}$ = aggregated horizontal curve crash modification factor for single-vehicle crashes;
- $CMF_{wev|agg}$ = aggregated weaving section crash modification factor;
- C_{mv} = local calibration factor for multiple-vehicle crashes;
- C_{sv} = local calibration factor for single-vehicle crashes;
- I_{add} = lane add indicator variable (= 1.0 if one or more lanes are added, 0.0 otherwise);

I_{ca} = California indicator variable (= 1.0 if segment in California, 0.0 otherwise);
 I_{drop} = lane drop indicator variable (= 1.0 if one or more lanes are dropped, 0.0 otherwise);
 I_{enr} = entrance ramp indicator variable (= 1.0 if segment is an entrance ramp, 0.0 otherwise);
 I_{exr} = exit ramp indicator variable (= 1.0 if segment is an exit ramp, 0.0 otherwise);
 I_{mv} = crash indicator variable (= 1.0 if multiple-vehicle crash data, 0.0 otherwise);
 I_n = cross section indicator variable (= 1.0 if cross section has n lanes, 0.0 otherwise);
 I_{rural} = area type indicator variable (= 1.0 if area is rural, 0.0 if it is urban);
 I_{sv} = crash indicator variable (= 1.0 if single-vehicle crash data, 0.0 otherwise);
 k = overdispersion parameter, mi
 K = inverse dispersion parameter (= $1/k$), mi^{-1} ;
 L = length of segment, mi;
 $L_{c,i}$ = length of horizontal curve i , mi;
 $L_{lb,i}$ = length of left side lane paralleled by barrier i , mi;
 $L_{rb,i}$ = length of right side lane paralleled by barrier i , mi;
 L_{wev} = weaving section length (may extend beyond segment boundaries), mi;
 N = predicted average crash frequency, crashes/yr;
 $N_{interchange}$ = predicted average crash frequency within the limits of an interchange, crashes/yr;
 N_j = predicted average crash frequency for model j ($j = mv, sv$); crashes/yr;
 N_{mv} = predicted average multiple-vehicle crash frequency, crashes/yr;
 N_{mv} = predicted average multiple-vehicle crash frequency, crashes/yr;
 N_{rt} = predicted average crossroad ramp terminal crash frequency, crashes/yr;
 $N_{spf, mv, n}$ = predicted average multiple-vehicle crash frequency for base conditions for number of through lanes n ($n = 1, 2$); crashes/yr;
 $N_{spf, mv}$ = predicted average multiple-vehicle crash frequency for base conditions, crashes/yr;
 $N_{spf, sv, n}$ = predicted average single-vehicle crash frequency for base conditions for number of through lanes n ($n = 1, 2$); crashes/yr;
 $N_{spf, sv}$ = predicted average single-vehicle crash frequency for base conditions, crashes/yr;
 N_{sv} = predicted average single-vehicle crash frequency, crashes/yr;
 $P_{c, i}$ = proportion of segment length with curve i ;
 P_{en-ex} = proportion of segment length that is adjacent to the speed-change lane for a connecting ramp;
 $P_{L, i}$ = proportion of the segment length with element i ;
 P_{lb} = proportion of segment length with a barrier present on the left side;
 P_{mv} = proportion of multiple-vehicle crashes;
 P_{rb} = proportion of segment length with a barrier present on the right side;
 P_{tpr} = proportion of segment length adjacent to the taper associated with a lane add or drop;
 P_{wev} = proportion of segment length within a weaving section;
 R_i = radius of curve i , ft;
 v_c = average curve speed, ft/s;
 V_{cdroad} = average speed on collector-distributor road, mi/h;
 $v_{ent, i}$ = average entry speed for curve i , ft/s;
 $v_{ext, i}$ = average exit speed for curve i , ft/s;
 v_f = speed reached after traveling distance X , ft/s;
 V_{frwy} = average speed on freeway, mi/h;
 v_i = initial speed, ft/s;
 v_m = speed associated with acceleration rate a_m , ft/s

$v_{max,i}$ = limiting speed for curve i , ft/s;
 V_{xroad} = average speed at point where ramp connects to crossroad, mi/h;
 $V[X]$ = crash frequency variance for a group of similar locations, crashes²;
 W_l = lane width, ft;
 W_{lcb} = distance from edge of left shoulder to barrier face, ft;
 W_{ls} = left shoulder width, ft;
 $W_{off, l,i}$ = horizontal clearance from the edge of the traveled way to the face of barrier i on left side of segment, ft;
 $W_{off, r,i}$ = horizontal clearance from the edge of the traveled way to the face of barrier i on right side of segment, ft;
 W_{rcb} = distance from edge of right shoulder to barrier face, ft;
 W_{rs} = right shoulder width, ft;
 X = distance traveled, ft;
 X = reported crash count for y years, crashes;
 X_i = milepost of the point of change from tangent to curve (PC) for curve i , mi;
 y = time interval during which X crashes were reported, yr;

CHAPTER 7: PREDICTIVE MODEL FOR CROSSROAD RAMP TERMINALS

This chapter describes the activities undertaken to calibrate and validate safety predictive models for both signalized and unsignalized crossroad ramp terminals. Each model consists of a safety performance function (SPF) and a family of crash modification factors (CMFs). The SPF is derived to estimate the crash frequency for crossroad ramp terminals with specified design elements and operating conditions. The CMFs are used to adjust the SPF estimate whenever one or more elements or conditions deviate from those that are specified.

The calibrated safety predictive models were used to develop a safety predictive method for crossroad ramp terminals. This method will describe how to use the models to evaluate terminal safety, as may be influenced by road geometry, roadside features, and traffic volume. This method is documented in Appendix D.

Collectively, the predictive models for crossroad ramp terminals address the following area type and traffic control modes:

- rural ramp terminal with stop control
- rural ramp terminal with signal control,
- urban ramp terminal with stop control, and
- urban ramp terminal with signal control.

Several typical ramp terminal configurations were identified in Figure 37. Other configurations exist but they are less common than those shown in the figure. Based on the conclusions reached during the prioritization process (as described in Chapter 3), it was determined that the predictive model would address the configurations shown in Figure 37.

This chapter is divided into six parts. The first part provides some background information on the topic of predictive models for crossroad ramp terminals. The second part describes the theoretic development of selected CMFs. The third part describes the method used to calibrate the proposed models. The fourth part describes the calibration of the models to predict fatal-and-injury (FI) crash frequency. The fifth part describes the calibration of the models to predict property-damage-only crash (PDO) frequency. The sixth part provides a list of the variables defined in this chapter.

BACKGROUND

This part of the chapter consists of three sections. The first section describes the crossroad ramp terminal analysis units (i.e., sites). The second section provides a brief overview of the predictive model structure. The last part reviews the highway safety data assembled for model calibration.

Crossroad Ramp Terminals

For analysis purposes, an interchange is considered to consist of a set of ramp segments, crossroad ramp terminals, and, possibly, one or more C-D road segments. These components are also referred to as “sites.”

The more common crossroad ramp terminal configurations are identified in the list below; they are illustrated in Figure 37.

- three-leg ramp terminal with diagonal exit ramp (D3ex),
- three-leg ramp terminal with diagonal entrance ramp (D3en),
- four-leg ramp terminal with diagonal ramps (D4),
- four-leg ramp terminal at four-quadrant parclo A (A4),
- four-leg ramp terminal at four-quadrant parclo B (B4),
- three-leg ramp terminal at two-quadrant parclo A (A2), and
- three-leg ramp terminal at two-quadrant parclo B (B2).

Figure 103 illustrates two crossroad ramp terminals with the D4 configuration. Each terminal represents a separate site. The two terminals are shown in the context of a diamond interchange. The arrangement shown is intended to illustrate the ramp terminal boundaries used for safety evaluation—it is not necessarily typical ramp terminal geometry.

In the context of the predictive method, the free-flow loop ramp associated with the four-quadrant parclos (i.e., the A4 and B4 configurations) is not considered to be part of the ramp terminal. All subsequent discussions where “ramp AADT” is identified for these two configurations are referring to the volume of the diagonal entrance ramp or the diagonal exit ramp. With one exception, the loop ramp of the A4 and B4 configuration is not explicitly addressed by the models described in this chapter. The one exception is that the right-turn channelization that serves traffic entering the loop ramp at the A4 configuration can be part of the ramp terminal design, and its associated crashes are addressed by the predictive models.

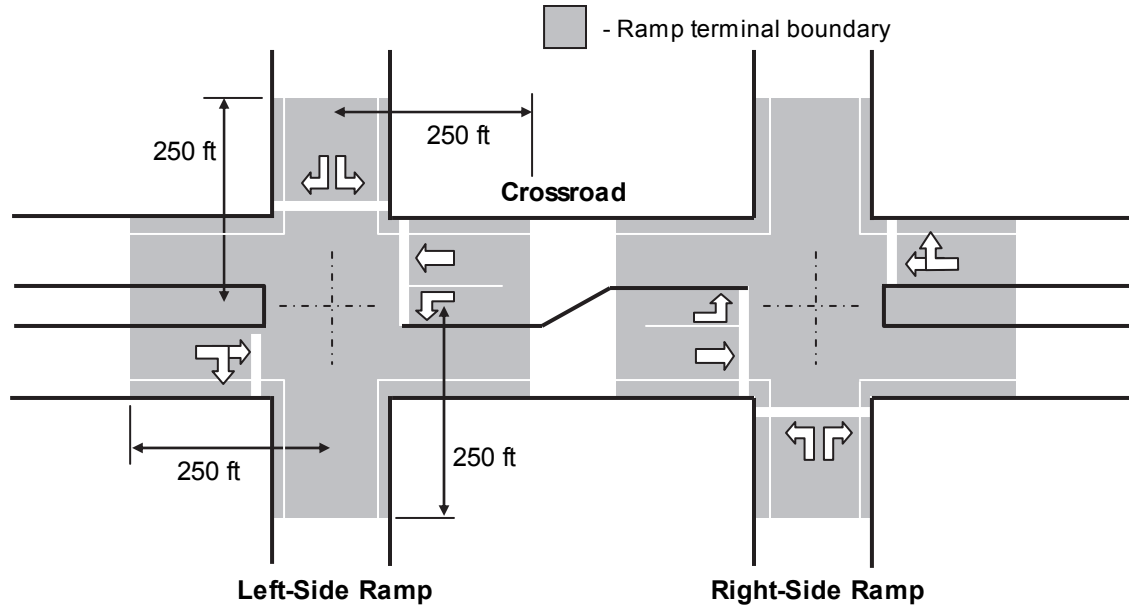


Figure 103. Illustrative crossroad ramp terminal boundary.

Safety Predictive Models

The predicted average crash frequency for an interchange is computed as the sum of the predicted average crash frequency of all sites that comprise the facility. This calculation is described by Equation 217.

$$N_{interchange} = \sum_{all\ segments} (N_{mv} + N_{sv}) + \sum_{all\ terminals} (N_{rt}) \quad (217)$$

where,

$N_{interchange}$ = predicted average crash frequency within the limits of an interchange, crashes/yr;

N_{mv} = predicted average multiple-vehicle crash frequency, crashes/yr;

N_{sv} = predicted average single-vehicle crash frequency, crashes/yr; and

N_{rt} = predicted average crossroad ramp terminal crash frequency, crashes/yr.

The predicted average crash frequency for each site is computed using a predictive model. Each model represents the combination of an SPF and several CMFs. The SPF is used to estimate the average crash frequency for a generic site whose attributes are consistent with the SPF's stated base conditions. The CMFs are used to adjust the SPF estimate when the attributes of the subject site are not consistent with the base conditions. The general form of the safety predictive models for crossroad ramp terminals is shown as Equations 218 to 221. The general form of the model for ramp and C-D road segments is described in Chapter 6.

$$N_{rt,A2B2} = C_{A2B2} \times N_{spf,A2B2} \times (CMF_{A2B2,1} \times \dots \times CMF_{A2B2,w}) \times (CMF_1 \times \dots \times CMF_k) \quad (218)$$

$$N_{rt,A4D3ex} = C_{A4D3ex} \times N_{spf,A4D3ex} \times (CMF_{A4D3ex,1} \times \dots \times CMF_{A4D3ex,x}) \times (CMF_1 \times \dots \times CMF_k) \quad (219)$$

$$N_{rt,B4D3en} = C_{B4D3en} \times N_{spf,B4D3en} \times (CMF_{B4D3en,1} \times \dots \times CMF_{B4D3en,y}) \times (CMF_1 \times \dots \times CMF_k) \quad (220)$$

$$N_{rt,D4} = C_{D4} \times N_{spf,D4} \times (CMF_{D4,1} \times \dots \times CMF_{D4,z}) \times (CMF_1 \times \dots \times CMF_k) \quad (221)$$

where,

$N_{spf,A2B2}$ = predicted average crash frequency for A2 and B2 configurations for base conditions, crashes/yr;

$N_{spf,A4D3ex}$ = predicted average crash frequency for A4 and D3ex configurations for base conditions, crashes/yr;

$N_{spf,B4D3en}$ = predicted average crash frequency for B4 and D3en configurations for base conditions, crashes/yr;

$N_{spf,D4}$ = predicted average crash frequency for D4 configuration for base conditions, crashes/yr;

C_{A2B2} = local calibration factor for A2 and B2 configurations;

C_{A4D3ex} = local calibration factor for A4 and D3ex configurations;

C_{B4D3en} = local calibration factor for B4 and D3en configurations;

C_{D4} = local calibration factor for D4 configuration;

$CMF_{A2B2,1} \dots CMF_{A2B2,w}$ = crash modification factors for crashes at an A2 or B2 site with specific geometric design features w ;

$CMF_{A4D3ex,1} \dots CMF_{A4D3ex,x}$ = crash modification factors for crashes at an A4 or D3ex site with specific geometric design features x ;

$CMF_{B4D3en,1} \dots CMF_{B4D3en,y}$ = crash modification factors for crashes at a B4 or D3en site with specific geometric design features y ;

$CMF_{D4,1} \dots CMF_{D4,z}$ = crash modification factors for crashes at a D4 site with specific geometric design features z ; and

$CMF_1 \dots CMF_k$ = crash modification factors for ramp terminal crashes at a site with specific geometric design features k .

The subscript for the dependent variables indicates the ramp terminal configuration to which the predictive model applies. Four configuration groups are identified using this nomenclature. The four groups were developed to overcome limitations in the sample size for the component ramp terminal configurations. Three of the four groups include two configurations. The configurations that were paired for each group have the same turn movement orientation and very similar conflicting movements. For these reasons, they are rationalized to have a similar relationship between traffic volume and crash frequency.

The first term in parentheses in Equations 218 to 221 recognizes the influence of some geometric factors is unique to each ramp terminal configuration group. In contrast, the second term in parentheses in these equations recognizes that some geometric factors have a similar influence on all groups.

Highway Safety Database

The Highway Safety Information System (HSIS) was used as the primary source of data for model calibration and validation. The “HSIS” states California, Maine, and Washington were identified as including ramp volume data, which is of fundamental importance to all aspects of

this project. These data were not available from the other HSIS states. Hence, the database assembly focused on these three states. They are called the “study states” in this report.

In addition to ramp volume data, each study state database included a range of data describing the location, area type, traffic characteristics, geometry, and lane use for crossroad ramp terminals. The data acquired from these databases is summarized in Table 60.

TABLE 60. Terminal variables from HSIS database

Category	Variable	Description
Descriptive	state	Source of data (CA, ME, WA)
	rte_nbr	State route number
	rte_suf	State route suffix
	county	County number (established by state DOT)
	begmp	Begin milepost (established by state DOT in CA, WA; by researchers for ME)
	endmp	End milepost (established by state DOT in CA, WA; by researchers for ME)
	rururb	Area type (urban, rural)
Traffic	ave_adt_xrd	Crossroad segment AADT volume averaged for a three-year period
	ave_adt_ramp1	Ramp segment AADT volume averaged for a three-year period
	ave_adt_ramp2	Ramp segment AADT volume averaged for a three-year period
Crash	nk_mv	Count of reported fatal during three-year period
	na_mv	Count of reported incapacitating-injury crashes during three-year period
	nb_mv	Count of reported non-incapacitating-injury crashes during three-year period
	nc_mv	Count of reported possible-injury crashes during three-year period
	no_mv	Count of reported property-damage-only crashes during three-year period

The data identified as “Descriptive” in Table 60 were obtained directly from the HSIS database for each study state. The data identified as “Traffic” or “Crash Data” were derived from the HSIS data. SAS software was used to manipulate the HSIS data to compute the desired variables.

As discussed in Appendix B, several of the geometry and lane use variables in the study state databases were of unknown accuracy. Also, several variables often had subtly different definitions among states. Moreover, the study state databases often did not include variables that describe road-related factors known to be associated with crash frequency. To overcome these limitations, the study-state databases were enhanced using data from other sources. These variables are listed in Table 61. The collection of these data required the location of each ramp using geographic coordinates and aerial photography, based on the freeway milepost reference system in HSIS.

Aerial photography was used as the source of the enhanced data. These photographs were obtained from the Internet using Google Earth software. The data collected include the ramp terminal configuration, number of lanes, bay presence, type of control, and median width. A description of the variables acquired from aerial photography is provided in Table 61.

TABLE 61. Variables from supplemental data sources

Category	Variable	Description
Descriptive	problem_flag	Code to identify issues that make segment unsuitable for analysis
	lat_lon_coord	Latitude and longitude of ramp terminal center
	term_type	Terminal configuration (diamond, spui, parclo A, etc.; see discussion)
	frontage	Presence of frontage road movement
	RR_crossing	Presence of a railroad crossing on one or more ramp terminal legs
	offsys_legs	Number of intersecting legs that are “off-system”
	skew	Skew angle of the exit ramp at the ramp terminal
Roadway	xrd_th_lanes	Number of through lanes on the crossroad
	xrd_lt_bays	Number of crossroad legs with a left-turn bay (or lane)
	xrd_rt_bays	Number of crossroad legs with a right-turn bay (or lane)
	xrd_rt_chan	Number of crossroad approaches with a right-turn channelizing island
	xrd_med_width	Width of crossroad median (excluding width of left-turn bays)
	ent_lanes	Number of lanes on the ramp leg serving as a freeway entrance ramp
	exit_lanes	Number of lanes on the ramp leg serving as a freeway exit ramp
	exit_rt_bay	Presence of a right-turn bay (or lane) on the exit ramp approach
	exit_rt_chan	Presence of right-turn channelizing island on the exit ramp approach
Traffic control	control_type	Type of control for conflicting movements at the ramp terminal
	xrd_prot_lt	Presence of protected left-turn phasing on crossroad (if signal)
	xrd_rt_cntl	Type of control for right turn entering ramp from crossroad
	exit_rt_cntl	Type of control for right turn entering crossroad from ramp
	adj_ramp_cntl	Type of control for nearest ramp terminal
	nonramp_cntl	Type of control for nearest non-ramp intersection
Other	xrd_int_dist	Distance between centers of subject and nearest ramp intersections
	xrd_ext_dist	Distance between centers of subject and nearest non-ramp intersections
	xrd_dway	Number of driveways on the crossroad within 250 ft of stop line
	offsys_st	Presence of public street approach on the crossroad within 250 ft of stop line

The “frontage” and “RR_crossing” variables were used to identify ramp terminals with a frontage road approach or a railroad crossing in the ramp terminal boundary. Quantifying the safety influence of these conditions was not ranked high in the prioritization process, as documented in Chapter 3. Hence, these variables were used to screen ramp terminals having either attribute from the database.

CMF DEVELOPMENT

This part of the chapter describes the development of several CMFs. The first section describes the development of a general CMF model for quantifying the relationship between intersection safety and some geometric characteristic of one of the intersecting roads. This model was developed because most of the CMFs in the literature that address a road-specific treatment (e.g., widen major road median) are used to adjust the prediction of *total* intersection crashes, as opposed to just that portion that occur on the treated road.

The second section describes the development of a general CMF model for quantifying the relationship between safety and some geometric characteristic of an intersection leg. Most of the CMFs in the literature that address a leg-specific treatment (e.g., add turn bay) are used to adjust the prediction of total intersection crashes, as opposed to just that portion that occur on the treated leg.

The third and subsequent sections describe the development of a CMF for specific geometric elements at intersections. These elements include: add turn bay, widen median, change exit ramp capacity, and change intersection skew angle.

General CMF Model for Street Treatments

The general CMF model is developed for the situation where a CMF is developed to estimate the relationship between “intersection crash frequency” and a change that is made to one of the two intersecting streets. In this context, “intersection crash frequency” is meant to include all crashes that occur at the intersection plus those that occur in the immediate vicinity of the intersection and which are identified as “intersection related.” Intuitively, a treatment applied to one street (e.g., increase lane width) should not have an influence on crashes associated with the intersecting street.

Consider the situation where a treatment is applied to one intersecting street at an intersection. The magnitude of its safety effect can be quantified using a CMF that is based on just the crashes associated with the treated street (i.e., CMF_{str}). This effect can then be extended to an estimate of the CMF for total intersection crashes (i.e., CMF_{int}) using the following equation.

$$CMF_{int,i} = CMF_{str} R_i + 1.0 (1.0 - R_i) \quad (222)$$

where,

$CMF_{int,i}$ = CMF for a specified treatment to street i , quantified in terms of intersection crashes ($i = 1$ for major street or 2 for minor street);

CMF_{str} = CMF for a specified treatment to any street, quantified in terms of the crashes that occur on the subject street; and

R_i = proportion of intersection crashes that occur on treated street i .

By using a simple crash rate relationship, Bonneson and Pratt (2008) suggest that the value of $R_{str,i}$ can be estimated as the ratio of traffic volume on the subject street to that on both intersecting streets. The following equation can be used to compute this estimate.

$$R_i \approx P_i = \frac{AADT_i}{AADT_1 + AADT_2} \quad (223)$$

where,

P_i = proportion of total leg AADT on street i ; and

$AADT_i$ = AADT volume for street i ($i = 1$ for major street or 2 for minor street), veh/day.

If Equation 223 is applied to a crossroad ramp terminal then the word “crossroad” is substituted for “major-street” in the variable definitions (with $i = xrd$ or rmp , as appropriate), and the minor street AADT volume is computed using Equation 224.

$$AADT_2 = AADT_{rmp} = 0.5 AADT_{en} + 0.5 AADT_{ex} \quad (224)$$

where,

$AADT_{ex}$ = AADT volume for the exit ramp, veh/day (= 0 if ramp does not exist); and

$AADT_{en}$ = AADT volume for the entrance ramp, veh/day (= 0 if ramp does not exist).

Equation 222 (with Equation 223) represents the “General CMF Model for Street Treatments.” It recognizes that the effect of a treatment on intersection crashes is a function of the AADT volume on the treated street. If both streets are treated, then the intersection CMF for the combined treatment (i.e., $CMF_{int,1,2}$) is computed using the following equation.

$$CMF_{int,1,2} = [CMF_{str} P_1 + 1.0 (1.0 - P_1)] \times [CMF_{str} P_2 + 1.0 (1.0 - P_2)] \quad (225)$$

The general model is appropriate for treatments that occur along an intersecting street, on both sides of the intersection. Changes in lane width or shoulder width are examples of such treatments. A model is described in the next section that is applicable to treatments that occur on a specific intersection leg.

General CMF Model for Leg Treatments

The framework developed in the previous section is extended in this section to the development of a general CMF model when the treatment is specific to an intersection leg (as opposed to one of the intersecting streets). The form of this model is described in the following equation.

$$CMF_{int,k} = CMF_{leg} R_k + 1.0 (1.0 - R_k) \quad (226)$$

with,

$$R_k \approx P_k = \frac{AADT_k}{AADT_1 + AADT_2 + AADT_3 + AADT_4} \quad (227)$$

where,

$CMF_{int,k}$ = CMF for a specified treatment to leg k , quantified in terms of intersection crashes ($k = 1$ for one major-street leg, 2 for the other major-street leg, 3 for one minor-street leg, and 4 for the other minor-street leg);

CMF_{leg} = CMF for a specified treatment to any leg, quantified in terms of the crashes that occur on the subject leg;

R_k = proportion of intersection crashes that occur on treated leg k ;

P_k = proportion of total leg AADT on leg k ; and

$AADT_k$ = AADT volume for leg k , veh/day.

Equations 226 and 227 are equally applicable to three- or four-leg intersections. However, if applied to a three-leg intersection, $AADT_4$ is set equal to zero. If these equations are applied to a ramp terminal, then $AADT_3$ is set equal to $AADT_{ex}$, $AADT_4$ is set equal to $AADT_{en}$, and the word “crossroad” is substituted for “major-street” in the variable definitions (with $k = in, out, ex, or en$, as appropriate). The subscript “in” corresponds to the crossroad leg is that located between the two ramp terminals of the interchange. The subscript “out” is the other crossroad leg.

Equation 226 is used in a multiplicative manner to address treatments made to any number of legs. For example, if two legs are treated, then the intersection CMF (i.e., $CMF_{int,k,l}$) is computed using the following equation.

$$CMF_{int,k,l} = [CMF_{leg} P_k + 1.0 (1.0 - P_k)] \times [CMF_{leg} P_l + 1.0 (1.0 - P_l)] \quad (228)$$

The general model is appropriate for treatments that occur on an intersection leg. The installation of a turn lane, a channelized right-turn, or the addition of a driveway are examples of such treatments.

Turn Lane CMF - Total Crashes

This section describes the development of the leg-specific turn lane CMFs using the intersection- and street-specific turn lane CMFs developed by Harwood et al. (2002). They developed CMFs for left-turn lanes and right-turn lanes installed individually and in pairs at signalized and unsignalized intersections. The intersections were located in urban and rural areas. Some intersections had three legs and others had four legs. Finally, some intersections had signal control installed at the time of the lane installation (they were referred to as “newly signalized” intersections).

The database assembled by Harwood et al. (2002) represents 280 treated intersections (143 rural and 137 urban intersections) collectively located in eight states. At these intersections, 392 left-turn lanes were added and 182 right-turn lanes were added. They used the crash data for these intersections to develop FI-crash CMFs and total-crash CMFs. The total-crash CMFs are the focus of this section.

The objective of the analysis described in the remainder of this section is to quantify leg-specific total-crash CMFs for the left-turn lane and right-turn lane treatments at signalized, newly signalized, and unsignalized intersections in urban and rural settings using the data reported by Harwood et al. (2002). These combinations represent a maximum of 12 CMFs ($= 2 \times 3 \times 2$).

A series of regression equations were developed that related the CMFs reported by Harwood et al. (2002) to leg-specific CMFs. In each equation, the leg-specific CMF represented the regression coefficient. The regression model structure is described in the report by Bonneson and Pratt (2008).

The regression equations were calibrated using the crash reduction factors (CRFs) for total crashes provided in Appendix C of the report by Harwood et al. (2002). The crash reduction factors were converted into CMFs using the following equation.

$$CMF = 1.0 + \frac{CRF}{100} \quad (229)$$

The CMFs obtained from Equation 229 were used as the dependent variable in the regression analysis. A search algorithm was used to simultaneously evaluate all of the regression equations and find the value of the leg-specific CMFs (i.e., $CMF_{leg,m,n}$) that minimized the sum of the squared error. This algorithm was automated using the Nonlinear Regression (NLIN) procedure in the SAS software (SAS, 2009). The SAS procedure was coded to minimize the

weighted squared error, where the weight for each CMF observation was equal to the reciprocal of its squared standard error.

The results of the model calibration are presented in Table 62. Calibration of this model focused on CMFs for total crash frequency. The R^2 for the model is 0.45.

TABLE 62. Turn lane CMF model statistical description - total crashes

Model Statistics		Value		
R^2 :		0.45		
Observations n_o :		78 CMFs (from 248 intersections and 440 legs)		
Standard deviation s_e :		±0.083		
Calibrated Coefficient Values				
Variable	Definition	Value	Std. Dev.	t-statistic ¹
b_0	Rural CMF exponent	1.397	0.136	-2.9
$CMF_{leg,sig,left}$	Leg-specific CMF for left-turn lane installation at signalized urban intersection	0.672	0.007	47.0
$CMF_{leg,sig,right}$	Leg-specific CMF for right-turn lane installation at signalized urban intersection	0.868	0.015	8.7
$CMF_{leg,new,left}$	Leg-specific CMF for left-turn lane installation at newly signalized urban intersection	0.694	0.021	14.6
$CMF_{leg,new,right}$	Leg-specific CMF for right-turn lane installation at newly signalized urban intersection	0.941	0.067	0.9
$CMF_{leg,unsig,left}$	Leg-specific CMF for left-turn lane installation at unsignalized urban intersection (uncontrolled)	0.586	0.028	14.8
$CMF_{leg,unsig,right}$	Leg-specific CMF for right-turn lane installation at unsignalized urban intersection (uncontrolled)	0.758	0.035	6.9

Note:

1 - Test of null hypothesis that coefficient value is equal to 1.0.

Figure 104 provides a graphical indication of the fit of the model to the reported CMFs. The figure compares the residual error of the predicted CMF over the range of predicted CMFs. Each residual error was “standardized” by dividing it by its standard error. Each data point represents one of the 78 CMFs reported by Harwood et al. (2002). The data are centered on “0” which indicates that there is no bias in the predicted CMFs. The scatter in the data indicates that almost all observations are within three standard deviations.

The CMFs reported in Table 62 for urban intersections are repeated in Table 63. The rural CMF exponent was used to compute the CMFs for rural intersections, as described in the footnote to the table. The CMFs in this table are applicable to leg-specific total crashes. They can be used with Equation 226 to estimate the relationship between turn lane presence on a leg and overall intersection crash frequency.

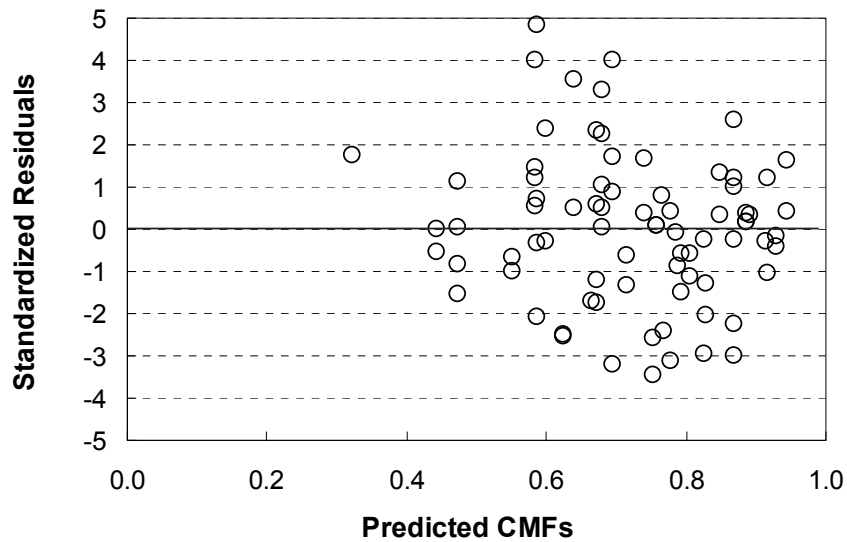


Figure 104. Comparison of predicted turn lane CMFs with standardized residuals - total crashes.

TABLE 63. Leg-specific turn lane CMFs - total crashes

Area Type	Control Type	Left-Turn Lane	Right-Turn Lane
Rural ¹	Unsignalized ²	0.47	0.68
	Signalized	0.57	0.82
	Newly signalized	0.60	0.92
Urban (and suburban)	Unsignalized ²	0.59	0.76
	Signalized	0.67	0.87
	Newly signalized	0.69	0.94

Notes:

1 - Rural CMFs computed from urban CMFs for common control type and turn lane configuration using the following equation $CMF_{rural} = (CMF_{urban})^{1.397}$.

2 - CMFs listed are for the uncontrolled approach at an unsignalized intersection.

To illustrate the use of the CMFs in Table 63, consider the installation of a left-turn lane on one approach of a four-leg urban intersection with the same AADT volume on all legs. The intersection is signal controlled. Table 63 indicates the CMF for leg-specific crashes is 0.67. Thus, if there are 10 crashes/yr on the leg before the lane is installed, the expected crash frequency after installation is 6.7 crashes/yr ($= 10 \times 0.67$), which corresponds to a reduction of 3.3 crashes/yr.

Continuing with the same example, the leg-specific CMF of 0.67 can be converted into an equivalent CMF for intersection crashes using Equation 226. Based on Equation 227, the proportion of intersection crashes for the treated leg P_k is equal to 0.25 because each leg has the same AADT volume in this example. This calculation yields a CMF of 0.91 ($= 0.67 \times 0.25 + 1.0$

[1 - 0.25]). Thus, if the intersection experiences 40 crashes/yr, the expected crash frequency after installation is 36.5 crashes/yr ($= 40 \times 0.91$), which corresponds to a reduction of 3.5 crashes/yr.

Consider the installation of a left-turn lane and a right-turn lane on one approach of a four-leg urban intersection with the same AADT volume on all legs. The intersection is signal controlled. Table 63 indicates the CMF for leg-specific crashes is 0.67 and 0.87 for left-turn and right-turn lanes, respectively. The combined CMF for both lanes is equal to the product of these two CMFs, or 0.58. Thus, if there are 10 crashes/yr on the leg before the lanes are installed, the expected crash frequency after installation is 5.8 crashes/yr ($= 10 \times 0.58$), which corresponds to a reduction of 4.2 crashes/yr.

Continuing with the same example, the leg-specific CMFs of 0.67 and 0.87 can be converted into an equivalent CMF for intersection crashes using Equation 228. Based on Equation 227, the proportion of intersection crashes for the treated leg P_k is equal to 0.25 because each leg has the same AADT volume in this example. This calculation yields a CMF of 0.88 ($= \{0.67 \times 0.25 + 1.0 [1 - 0.25]\} \times \{0.87 \times 0.25 + 1.0 [1 - 0.25]\}$). Thus, if the intersection experiences 40 crashes/yr, the expected crash frequency after installation is 35.3 crashes/yr ($= 40 \times 0.88$), which corresponds to a reduction of 4.7 crashes/yr. This same result would be realized if the lanes were implemented on opposing approaches, provided that the leg AADT volumes were the same. If they are not the same, then Equation 227 would be used to compute P_k for each leg, and these two proportions would be used in Equation 228 to obtain the combined CMF.

Turn Lane CMF - FI Crashes

This section describes the development of leg-specific turn lane CMFs for FI crashes. The development process is the same as that described in the previous section. However, it is based on a regression analysis of the FI-based CMFs reported by Harwood et al. (2002). Details of the statistical analysis are reported by Bonneson and Pratt (2008). The R^2 for the model is 0.53.

The converted CMFs are listed in Table 64. The CMFs in this table are applicable to leg-specific, FI crashes. They can be used with Equations 226 or 227 to estimate the relationship between turn lane presence and intersection crash frequency.

TABLE 64. Leg-specific turn lane CMFs - FI crashes

Area Type	Control Type	Left-Turn Lane CMF	Right-Turn Lane CMF
Rural	Unsignalized ¹	0.36	0.76
	Signalized	0.44	0.59
	Newly signalized	0.34	0.62
Urban (and suburban)	Unsignalized ¹	0.59	0.87
	Signalized	0.65	0.76
	Newly signalized	0.57	0.78

Note:

1 - CMFs listed are for the uncontrolled approach at an unsignalized intersection.

Turn Lane CMF - PDO Crashes

This section describes the development of leg-specific turn lane CMFs for PDO crashes. The total-crash CMFs in Table 63 and the FI-crash CMFs in Table 64 were combined for this purpose. Specifically, they were used with Equation 230 to compute the equivalent PDO CMFs for each combination of area type, control type, and turn movement.

$$CMF_{tot} = CMF_{FI} P_{FI} + CMF_{PDO} (1.0 - P_{FI}) \quad (230)$$

where,

- CMF_{tot} = CMF for total crashes;
- CMF_{FI} = CMF for fatal-and-injury crashes;
- CMF_{PDO} = CMF for property-damage-only crashes; and
- P_{FI} = proportion of intersection crashes that have a fatal or injury severity.

The average proportion of FI crashes in the database assembled by Harwood et al. (2002) is 0.40. This proportion was used in Equation 230 to compute the leg-specific PDO crash CMFs for turn lane treatments. The computed CMFs are listed in Table 65.

TABLE 65. Leg-specific turn lane CMFs - PDO crashes

Area Type	Control Type	Left-Turn Lane	Right-Turn Lane
Rural ¹	Unsignalized ¹	0.55	0.63
	Signalized	0.66	0.97
Urban (and suburban)	Unsignalized ¹	0.58	0.69
	Signalized	0.68	0.94

Note:

1 - CMFs listed are for the uncontrolled approach at an unsignalized intersection.

Median Width CMF

Chapter 14 of the *HSM* indicates that median presence at an intersection can influence crash frequency, provided that its width is 14 ft or more (Highway, 2010). The *HSM* indicates that, at rural unsignalized intersections, an increase in median width is associated with a decrease in crash frequency. In contrast, at urban intersections (unsignalized and signalized), an increase in median width is associated with an *increase* in crash frequency. This latter trend is contrary to segment-based safety research that shows crash frequency decreases with an increase in median width. Although this trend is not discussed in the *HSM*, the referenced sources describe conflict studies that confirm a tendency for improper use of wide median areas within intersections that, when complicated by high traffic volume, results in an increased propensity for multiple-vehicle crashes (Harwood et al., 1995).

Based on the discussion in the previous paragraph, the median width CMF is defined using the following equation.

$$CMF_{mw} = \left[e^{(b_{me} + b_{AADT,me}AADT_{in}/1,000)W_{me,in}} P_{in} + 1.0(1.0 - P_{in}) \right] \times \left[e^{(b_{me} + b_{AADT,me}AADT_{out}/1,000)W_{me,out}} P_{out} + 1.0(1.0 - P_{out}) \right] \quad (231)$$

with,

$$P_{in} = \frac{AADT_{in}}{AADT_{in} + AADT_{out} + AADT_{en} + AADT_{ex}} \quad (232)$$

$$W_{me,k} = W_m - W_{mb,k} \geq 0.0 \quad (233)$$

$$W_{mb,k} = \text{Max}(W_{b,k}; 14) \quad (234)$$

where,

- CMF_{mw} = median width crash modification factor;
- $AADT_{in}$ = AADT volume for crossroad leg between ramps, veh/day;
- P_{in} = proportion of total leg AADT on crossroad leg between ramps;
- $AADT_{out}$ = AADT volume for crossroad leg outside of interchange, veh/day;
- P_{out} = proportion of total leg AADT on crossroad leg outside of interchange;
- $AADT_{en}$ = AADT volume for the entrance ramp, veh/day (= 0 if ramp does not exist);
- $AADT_{ex}$ = AADT volume for the exit ramp, veh/day (= 0 if ramp does not exist);
- $W_{b,k}$ = left-turn lane (or bay) width for crossroad leg k ($k = in$ or out) (= 0.0 if no lane present on leg), ft;
- $W_{mb,k}$ = base median width for crossroad leg k ($k = in$ or out), ft;
- $W_{me,k}$ = width of median adjacent to turn lane (or bay) for crossroad leg k ($k = in$ or out), ft;
- W_m = median width, ft; and
- b_i = calibration coefficient for condition i

The base median width represents the larger of the left-turn lane (or bay) width or 14 ft. It will typically have a value of 14 ft, but it could be larger if there are two or more lanes to serve left-turning traffic. Guidelines for measuring median width and left-turn lane width are provided in the next part of this chapter. The AADT volume of the loop exit ramp at a B4 terminal configuration is not included in $AADT_{ex}$. Similarly, the AADT volume of the loop entrance ramp at an A4 configuration is not included in $AADT_{en}$.

Equation 231 is applicable to ramp terminals with 0, 1, or 2 left-turn lanes (or bays) present on the crossroad. The two exponential terms in Equation 231 represent the leg-specific CMFs for median width on the two crossroad approaches. The proportions P_{in} and P_{out} are based on Equation 227; its application to the calculation of P_{in} is shown in Equation 232.

The CMF described by Equation 231 yields a value of 1.0 when the median width is 14 ft, which is consistent with the guidance described in the *HSM*. If the regression coefficient b_{me} is negative and $b_{AADT,me}$ is positive, then the trend described in the *HSM* can be replicated for urban and rural unsignalized intersections. This trend is shown in Figure 105 using hypothetical coefficients and values of P_{in} and P_{out} equal to 0.39. The thick solid lines correspond to the CMFs described in the *HSM*. The thin dashed lines illustrate Equation 231 using the hypothetical coefficients. These coefficients suggest that a major-road AADT volume of about 9,000 veh/day yields a CMF value of 1.0, regardless of median width.

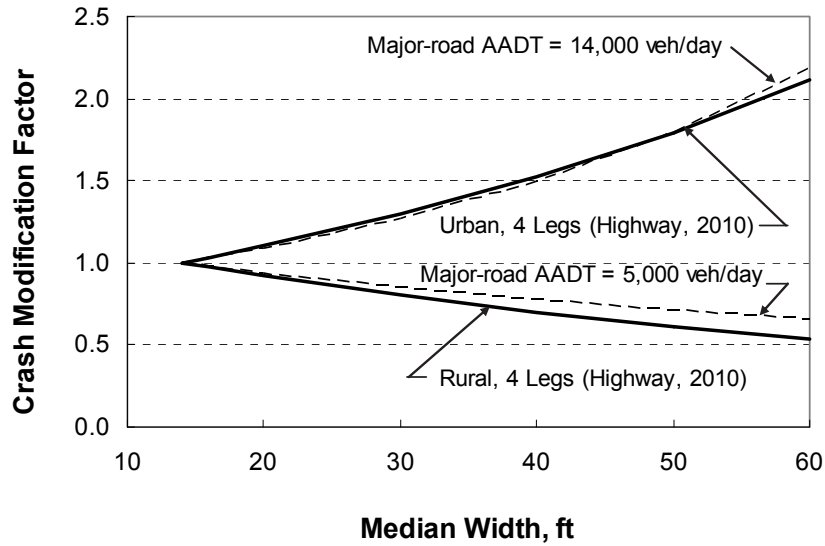


Figure 105. Relationship between median width and CMF value at unsignalized intersections.

Exit Ramp Capacity CMF

Excessively long queues on exit ramps are recognized as sometimes creating unsafe operating conditions. Crash risk tends to increase as the length of ramp available for deceleration to the back of queue is reduced due to long queues from the downstream ramp terminal. The exit ramp capacity CMF is derived to capture this trend. It is described using the following equation.

$$CMF_{rc} = e^{\frac{b_{rc} AADT_{ex}}{1,000 n_{ex,eff}}} P_{ex} + 1.0 (1.0 - P_{ex}) \quad (235)$$

with,

$$n_{ex,eff} = \begin{cases} 0.5 (n_{ex} - 1.0) + 1.0 & : \text{merge or free-flow right turn} \\ 0.5 n_{ex} & : \text{signal, stop, or yield-controlled right turn} \end{cases} \quad (236)$$

$$P_{ex} = \frac{AADT_{ex}}{AADT_{in} + AADT_{out} + AADT_{en} + AADT_{ex}} \quad (237)$$

where,

- CMF_{rc} = exit ramp capacity crash modification factor;
- P_{ex} = proportion of total leg AADT on exit ramp leg;
- $n_{ex,eff}$ = effective number of lanes serving exit ramp traffic, lanes; and
- n_{ex} = number of lanes serving exit ramp traffic; lanes.

The number of lanes serving the exit ramp is based on the count of lanes taken at the last point where all exiting movements are joined (i.e., at the channelization gore point if right-turn channelization is provided). All lanes counted need to be fully developed for 100 ft or more upstream from the point at which their respective movement intersects with the crossroad. The lane (or lanes) associated with the loop exit ramp at a B4 terminal configuration are not included

in this count. Similarly, the AADT volume of the loop exit ramp is not included in $AADT_{ex}$ and the AADT volume of the loop entrance ramp at an A4 configuration is not included in $AADT_{en}$.

This CMF is applicable to any ramp terminal with an exit ramp. The exponential term in Equation 235 represents the leg-specific CMF for ramp capacity. The proportion P_{ex} is based on Equation 227; its application to the calculation of P_{ex} is shown in Equation 237. It is likely the calibration coefficient will vary, depending on whether the intersection is signalized or unsignalized.

The effective number of lanes is based on the number of lanes on the exit ramp and the type of control used for the exit ramp right-turn movement. The constant “0.5” in Equation 236 approximately represents the ratio of capacity for a signal, stop, or yield controlled lane to the capacity of a free-flow lane. Figure 106 illustrates the use of Equation 236 to calculate the effective number of lanes for various exit ramp configurations.

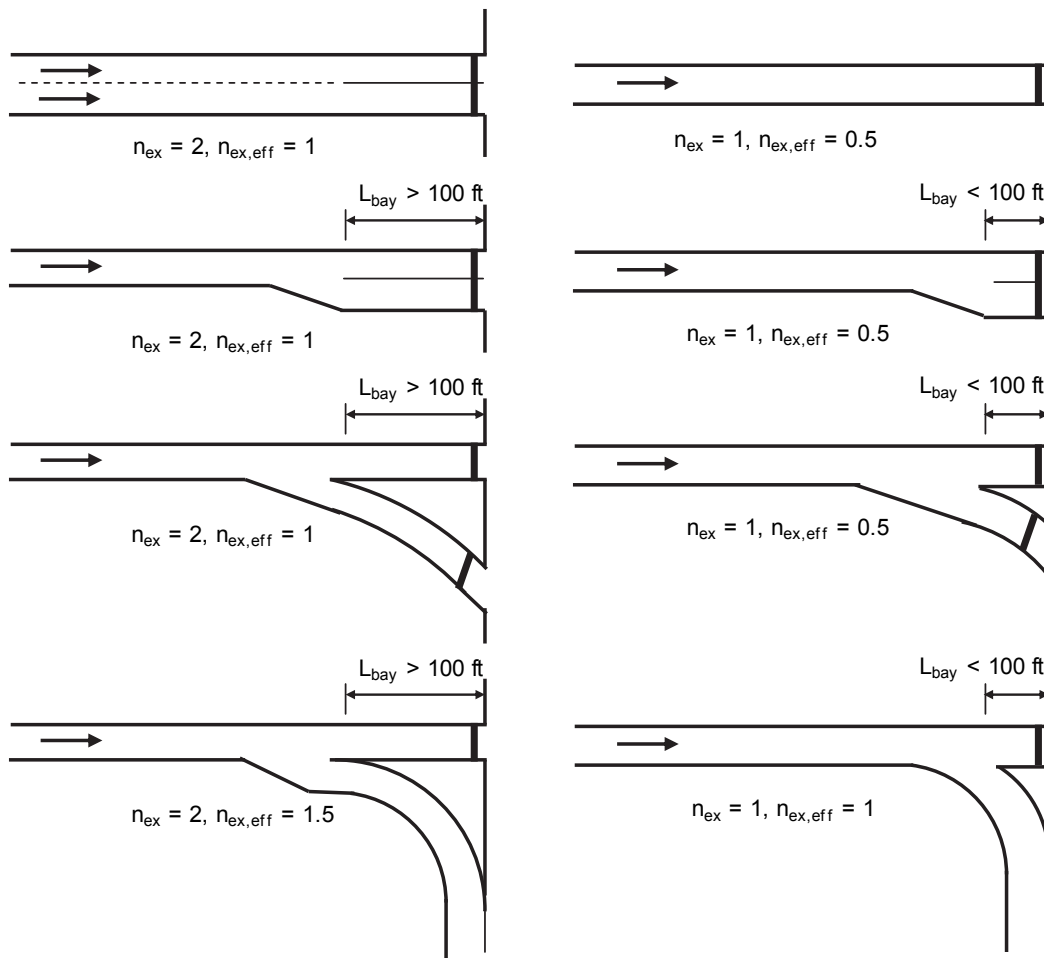


Figure 106. Effective number of lanes for various exit ramp configurations.

The trend in CMF values suggested by Equation 235 is shown in Figure 107 using a hypothetical coefficient and a value of P_{ex} equal to 0.12. The trend lines correspond to three

relatively common combinations of ramp lanes and right-turn control for exit ramps. They suggest that, for a given ramp AADT volume, crash risk increases as ramp capacity decreases. The inference from this trend is that the associated ramp queues are reducing the length of ramp available for deceleration.

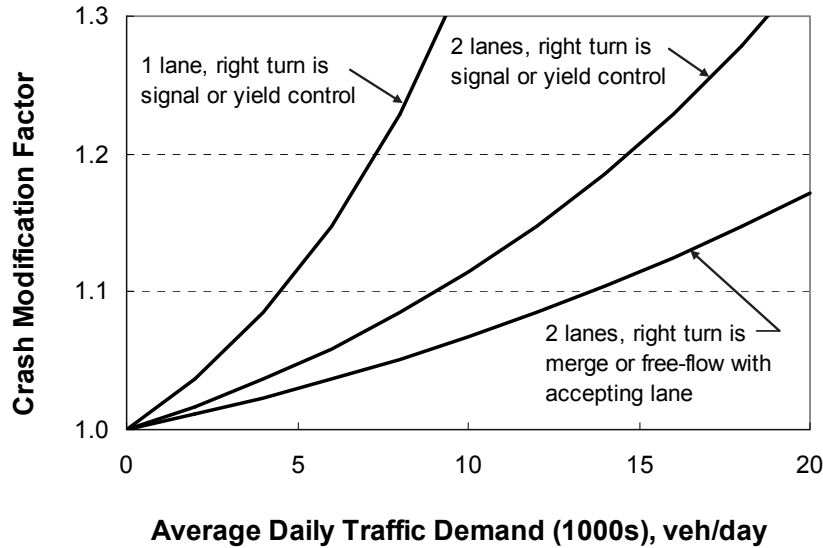


Figure 107. Relationship between exit ramp volume, control, and CMF value at signalized terminals.

Skew Angle CMF

Chapter 14 of the *HSM* describes several CMFs for skew angle at rural unsignalized intersections (Highway, 2010). All of the CMFs are continuous functions of the skew angle. The CMF value increases above 1.0 as the skew angle increases above 0.0 degrees. Intersection skew angle is defined as 0.0 degrees when the two roadways intersect at a right angle (i.e., are perpendicular). The *HSM* does not provide a similar CMF for signalized intersections and suggests that this angle may have little influence on signalized intersection safety.

The CMFs in the *HSM* provide much larger CMF values for multilane highway intersections, relative to two-lane highway intersections. This difference is not acknowledged or discussed. It is likely a reflection of the volume differences that exist among the two intersection types.

Based on the discussion in the previous paragraph, the skew angle CMF is defined using the following equation.

$$CMF_{sk} = e^{b_{sk} \sin(I_{sk}) AADT_{ex}/1,000} P_{ex} + 1.0 (1.0 - P_{ex}) \quad (238)$$

where,

CMF_{sk} = skew angle crash modification factor;

I_{sk} = skew angle between exit ramp and crossroad, degrees; and

$\sin(x)$ = sine of angle x .

The sine function is added to Equation 238 in recognition of the trends observed in the *HSM* CMFs. The sine of an angle has a relatively small change in value for angle changes in the range of 0 to 10 degrees and 80 to 90 degrees. In contrast, it has a relatively large change for angle changes between 30 and 60 degrees. These trends are logical when extended to the relationship between safety and skew angle.

This CMF is applicable to any unsignalized ramp terminal with an exit ramp. The exponential term in Equation 238 represents the leg-specific CMF for skew angle. At a B4 ramp terminal, the skew angle represents that for the diagonal exit ramp (not the loop exit ramp). The AADT volume of the loop exit ramp at a B4 terminal configuration is not included in $AAADT_{ex}$.

The CMF described by Equation 238 yields a value of 1.0 when the skew angle is 0.0 degrees, which is consistent with the guidance described in the *HSM*. If the regression coefficient b_{sk} is positive, then the trend described in the *HSM* relative to multilane and two-lane highway intersections can be replicated. This trend is shown in Figure 108 using a hypothetical coefficient. The thick solid lines correspond to the CMFs described in the *HSM*. The thin dashed lines illustrate Equation 238 using a hypothetical coefficient and a value of P_{ex} equal to 0.12.

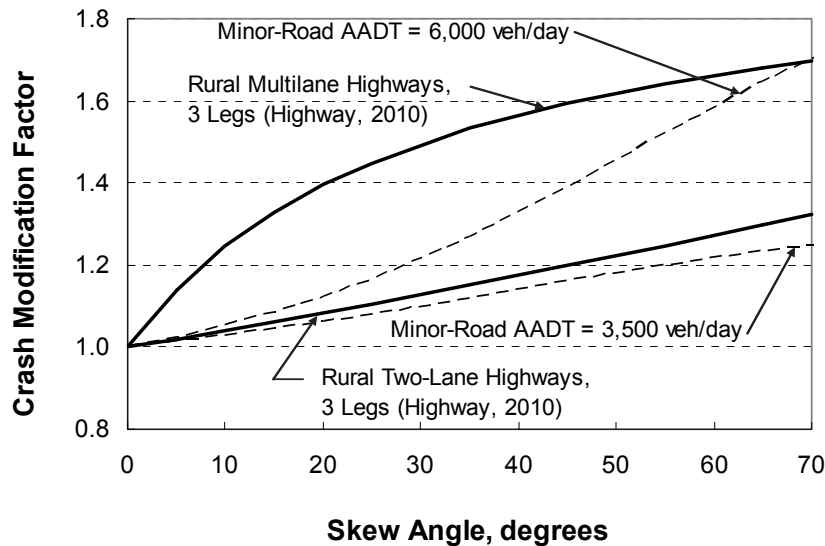


Figure 108. Relationship between skew angle and CMF value at unsignalized intersections.

METHODOLOGY

This part of the chapter describes the methodology used to calibrate the crossroad ramp terminal predictive models. It is divided into two sections. The first section describes several supplemental variables used to calibrate the predictive models. The second section provides an overview of the approach used to calibrate the predictive models.

Supplemental Variables

As noted in a previous part of this chapter, several variables in the database were obtained from aerial photographs of the ramp terminals represented in the study state databases. Of these variables, two of the more complex ones are defined in this section.

Right-Turn Channelization Length

Channelizing islands are frequently provided for the right-turn movements at crossroad ramp terminals. This treatment provides a larger radius for the right-turn movement which accommodates the swept path of large trucks that frequently use these terminals.

A useful characteristic that describes the geometry of the channelization is the length of the channelizing island, as measured along the side of the island adjacent to the non-turning traffic stream. This length is measured from the gore point (i.e., the point where the painted gore, or its equivalent, is 2.0 ft wide) to the point where the non-turning traffic stream intersects with the near edge of the crossing traffic stream's traveled way. This length is shown in Figure 109 for two ramp terminals with the D4 configuration. The length of interest is identified by the variables $L_{ch,ex}$ and $L_{ch,en}$.

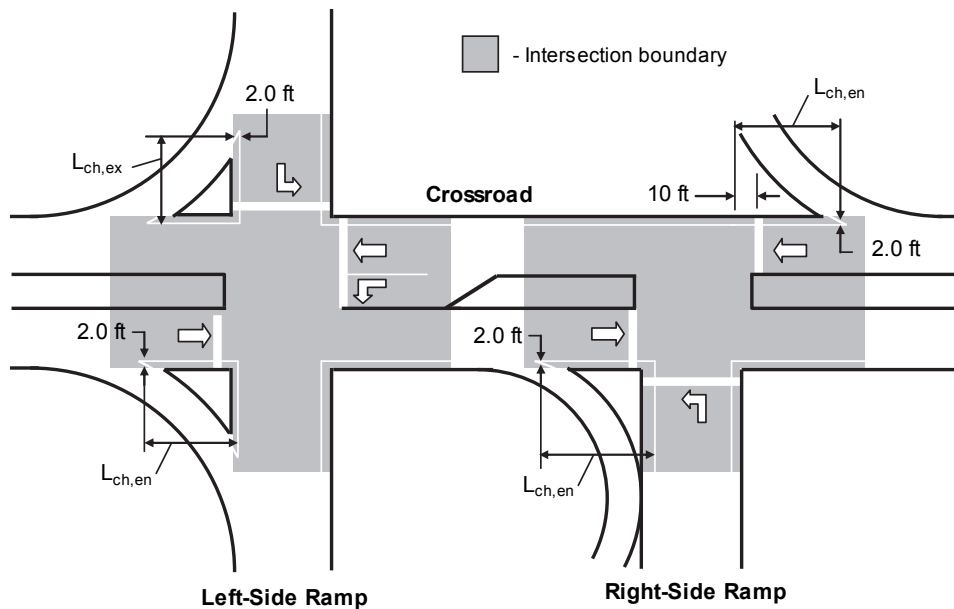


Figure 109. Right-turn channelization length.

Median Width

The crossroad median width at an intersection is measured between the near edges of the traveled way associated with the opposing through traffic streams. It includes the width of the left shoulder and any left-turn lanes that are present. It is measured in an identical manner for road segments. The median width at a ramp terminal is shown in Figure 110.

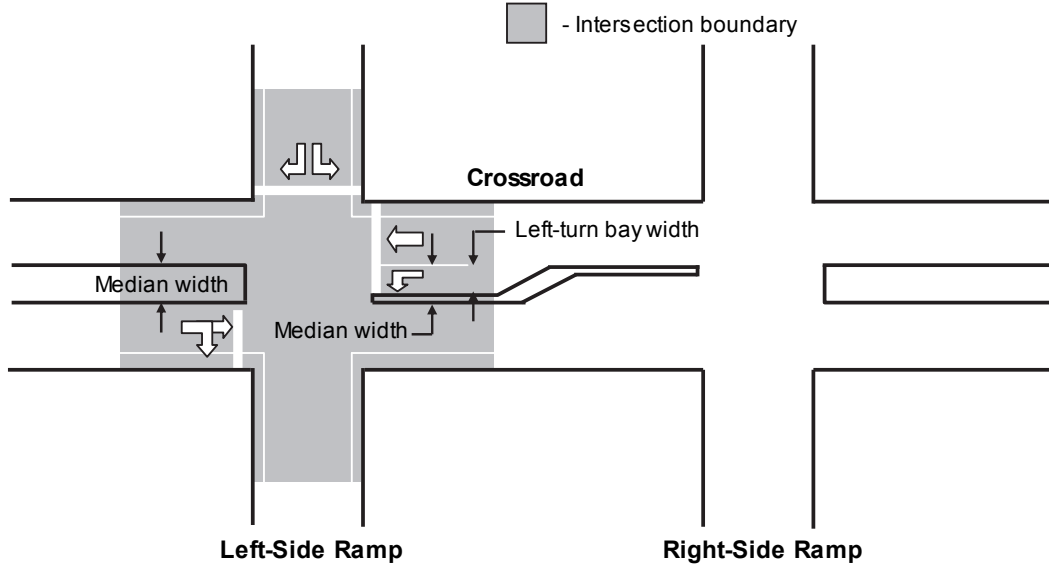


Figure 110. Crossroad median width.

The left-turn bay width is also shown in Figure 110 for the one approach with a left-turn bay. This width is measured from the near edge of the traveled way of the adjacent through lane to the lane marking (or curb face) that delineates the median.

Modeling Approach

This section describes the regression modeling approach and the rationale for using a cross-sectional database. Details of the methods used for PDO model calibration are provided in Chapter 5 in the subsection titled Prediction of PDO Crash Frequency.

Combined Regression Models

The calibration activity used statistical analysis software that employs maximum likelihood methods and a negative binomial distribution of crash frequency. Four models were calibrated. The form of each model is shown in the following equations.

$$N_{rt,A2B2} = N_{spf,A2B2} \times (CMF_{A2B2,1} \times \dots \times CMF_{A2B2,w}) \times (CMF_1 \times \dots \times CMF_k) \quad (239)$$

$$N_{rt,A4D3ex} = N_{spf,A4D3ex} \times (CMF_{A4D3ex,1} \times \dots \times CMF_{A4D3ex,x}) \times (CMF_1 \times \dots \times CMF_k) \quad (240)$$

$$N_{rt,B4D3en} = N_{spf,B4D3en} \times (CMF_{B4D3en,1} \times \dots \times CMF_{B4D3en,y}) \times (CMF_1 \times \dots \times CMF_k) \quad (241)$$

$$N_{rt,D4} = N_{spf,D4} \times (CMF_{D4,1} \times \dots \times CMF_{D4,z}) \times (CMF_1 \times \dots \times CMF_k) \quad (242)$$

where all variables were defined previously.

The SPFs associated with these models are defined as:

$$N_{spf,A2B2} = e^{b_{0,A2B2} + b_{xrd,A2B2} \ln(AADT_{xrd}/1,000) + b_{rmp,A2B2} \ln(AADT_{ex}/1,000 + AADT_{en}/1,000)} \quad (243)$$

$$N_{spf,A4D3ex} = e^{b_{0,A4D3ex} + b_{xrd,A4D3ex} \ln(AADT_{xrd}/1,000) + b_{rmp,A4D3ex} \ln(AADT_{ex}/1,000 + AADT_{en}/1,000)} \quad (244)$$

$$N_{spf,B4D3en} = e^{b_{0,B4D3en} + b_{xrd,B4D3en} \ln(AADT_{xrd}/1,000) + b_{rmp,B4D3en} \ln(AADT_{ex}/1,000 + AADT_{en}/1,000)} \quad (245)$$

$$N_{spf,D4} = e^{b_{0,D4} + b_{xrd,D4} \ln(AADT_{xrd}/1,000) + b_{rmp,D4} \ln(AADT_{ex}/1,000 + AADT_{en}/1,000)} \quad (246)$$

where all variables were defined previously.

The second term of Equations 239 to 242 recognizes that the influence of some geometric factors is unique to each crash type. In contrast, the third term of Equations 239 to 242 recognizes that some geometric factors have a similar influence on all crash types.

The use of common CMFs in multiple models required the use of a combined-model approach. With this approach, the regression analysis evaluated all four models simultaneously and used the total log-likelihood statistic for all models to determine the best fit calibration coefficients. The regression analysis is described in more detail in the next part of this chapter.

Cross-Sectional Database

The database is described as cross sectional (as opposed to panel). It represents a common three-year study period for all observations. Study duration in “years” is represented as an offset variable in the regression model. The rationale for using this type of database is provided in Chapter 5 in the section titled Cross-Sectional Database.

Inverse Dispersion Parameter

It was assumed that ramp terminal crash frequency is Poisson distributed, and that the distribution of the mean crash frequency for a group of similar ramp terminals is gamma distributed. In this manner, the distribution of crashes for a group of similar terminals can be described by the negative binomial distribution. The variance of this distribution is computed using the following equation.

$$V[X] = y N + \frac{(y N)^2}{K} \quad (247)$$

where,

$V[X]$ = crash frequency variance for a group of similar locations, crashes²;
 N = predicted average crash frequency, crashes/yr;
 X = reported crash count for y years, crashes;
 y = time interval during which X crashes were reported, yr; and
 K = inverse dispersion parameter ($= 1/k$, where k = overdispersion parameter).

Research by Lord (2006) has indicated that databases with low sample mean values and small sample size may not exhibit the variability associated with crash data of similar sites, as described by Equation 247. Rather, the regression model may “over-explain” some of the random variability in a small database, or the low sample mean may introduce an instability in the model coefficients.

Lord (2006) explored the effect of sample size on the variability of crash data through the use of simulation. Specifically, he simulated the crash frequency for three database sizes (i.e., 50, 100, and 1,000 sites), each with three different average crash frequencies (i.e., 0.5, 1.0, and 10 crashes per site), and three inverse dispersion parameters (i.e., 0.5, 1, and 2). One complete set of simulations consisted of the nine combinations of average crash frequency and dispersion parameter, each simulated once for each site yielding a total of 10,350 ($= 3 \times 3 \times [50 + 100 + 1,000]$) site crash frequency estimates. A total of 30 replications was conducted yielding 310,500 site estimates. A maximum likelihood technique was used to estimate the dispersion parameter for each of the 27 combinations. This process was repeated 30 times to yield 30 estimates of K for each of the 27 combinations. The average value of K for each combination is shown in Figure 111.

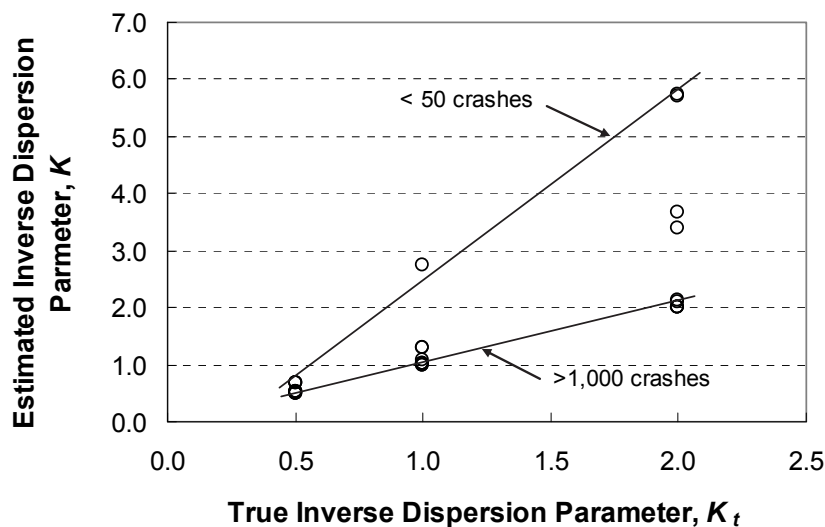


Figure 111. Simulation results for the inverse dispersion parameter.

As shown in Figure 111, the estimated inverse dispersion parameter for a given database was about equal to the specified (i.e., true) over-dispersion parameter, *provided* that there were 1,000 or more crashes in the database. However, the estimated dispersion parameter was larger than the true value when the number of crashes was less than 1,000. The following relationship

was derived to relate the estimated and true dispersion parameters based on observed trends in the data:

$$K_r = K_t + \frac{17.2 K_t^2}{(n - p) m} \quad (248)$$

where,

K_r = estimated inverse dispersion parameter obtained from database analysis;

K_t = true inverse dispersion parameter;

n = number of observations (i.e., segments or intersections in database);

p = number of model variables; and

m = average number of crashes per observation (= total crashes in database / n).

The constant “17.2” in Equation 248 represents an empirical adjustment derived through weighted regression analysis ($s_k = 2.45$, $p = 0.0001$). Equation 248 was algebraically manipulated to yield the following relationship for estimating the true inverse dispersion parameter, given the other variables as input values.

$$K_t = \frac{\sqrt{(n - p)^2 m^2 + 68.8 K_r (n - p) m} - (n - p) m}{34.5} \quad (249)$$

Equation 249 was used to estimate the true inverse dispersion parameter for each of the ramp terminal models described in this chapter. The ramp terminal databases tend to have a relatively small sample size. In contrast, the freeway and ramp segment databases were relatively large and did not require adjustment using Equation 249. All subsequent references to the inverse dispersion parameter K for ramp terminals show the estimated true parameter obtained from Equation 249 (i.e., hereafter, $K = K_t$ for ramp terminals).

MODEL CALIBRATION FOR FI CRASHES

This part of the chapter describes the calibration and validation of the crossroad ramp terminal predictive models based on FI crashes. The first section identifies the data used for model calibration. The second section summarizes statistical analysis methods used for model calibration. The third section describes the results leading to the development of predictive models for signalized ramp terminals. The last section describes the results leading to the development of predictive models for unsignalized ramp terminals.

Calibration Data

The data collection process consisted of a series of activities that culminated in the assembly of a highway safety database suitable for the development of a comprehensive safety prediction methodology for crossroad ramp terminals. These activities are described in Chapter 4.

Crash data were identified for each crossroad ramp terminal using the most recently available data from the HSIS. Three years of crash data were identified for each ramp terminal. The analysis period is 2005, 2006, and 2007 for the California and Washington segments. It is 2004, 2005, and 2006 for the Maine segments. The AADT volume for each year was merged

into the assembled database. A total of 2,177 FI crashes and 4,172 PDO crashes are represented in the database. Additional information about the database is provided in Chapter 4.

Statistical Analysis Methods

The nonlinear regression procedure (NLMIXED) in the SAS software was used to estimate the proposed model coefficients. This procedure was used because the proposed predictive model is both nonlinear and discontinuous. The log-likelihood function for the negative binomial distribution was used to determine the best-fit model coefficients. Equation 247 was used to define the variance function for all models. The procedure was set up to estimate model coefficients based on maximum-likelihood methods. The statistics used to assess model fit to the data are described in Chapter 5.

Signalized Ramp Terminal Models

This section describes the development of predictive models for signalized ramp terminals. The first subsection describes the structure of the predictive models as used in the regression analysis. The second subsection describes the regression statistics for each of the calibrated models. The third subsection describes a validation of the calibrated models. The fourth subsection describes the proposed predictive models. The fifth section describes the calibrated CMFs. The last subsection provides a sensitivity analysis of the predictive models over a range of traffic demands.

Model Development

This subsection describes the proposed predictive models and the methods used to calibrate them. The regression models are generalized to accommodate a wide range of ramp terminal geometry and right-turn control modes. The generalized form shows all the CMFs in the model, even though some CMFs are applicable only to some ramp terminal configurations. Indicator variables are used to determine which CMFs are applicable to each ramp terminal observation in the database. Those CMFs that are not applicable to a given ramp terminal are set to 1.0 using an indicator variable.

The generalized form includes intersection CMFs that include leg-specific terms for both crossroad legs, even when the associated treatment is only applicable to one leg. For example, a left-turn lane is typically added to the “inside” crossroad leg for a D4 configuration, where the inside leg is that leg located between the two ramp terminals of the interchange. In contrast, a left-turn lane is typically added to the outside crossroad leg for an A2 configuration. The generalized form of the left-turn lane CMF includes terms for both left-turn bays, where indicator variables are used to determine which terms are applicable (and which should be set to 1.0) for each observation.

The following regression model form was used to facilitate the combined regression analysis of the four models for signalized ramp terminals.

$$N_{rt,j} = C_{ca} \times (N_{spf,A2B2} I_{A2B2} + N_{spf,A4D3ex} I_{A4D3ex} + N_{spf,B4D3en} I_{B4D3en} + N_{spf,D4} I_{D4}) \quad (250)$$

$$\times CMF_{p,lt} \times CMF_{ch,xrd} \times CMF_{ch,ex} \times CMF_{ps} \times CMF_{rc} \times CMF_{bay,lt} \times CMF_{bay,rt}$$

$$\times CMF_{nd} \times CMF_{sl} \times CMF_{mw}$$

with,

$$N_{spf,A2B2} = e^{b_{0,A2B2} + b_{ln} n_{th} + b_{xrd,A2B2} \ln(AADT_{xrd}/1,000) + b_{rmp,A2B2} \ln(AADT_{ex}/1,000 + AADT_{en}/1,000)} \quad (251)$$

$$N_{spf,A4D3ex} = e^{b_{0,A4D3ex} + b_{ln} n_{th} + b_{xrd,A4D3ex} \ln(AADT_{xrd}/1,000) + b_{rmp,A4D3ex} \ln(AADT_{ex}/1,000 + AADT_{en}/1,000)} \quad (252)$$

$$N_{spf,B4D3en} = e^{b_{0,B4D3en} + b_{ln} n_{th} + b_{xrd,B4D3en} \ln(AADT_{xrd}/1,000) + b_{rmp,B4D3en} \ln(AADT_{ex}/1,000 + AADT_{en}/1,000)} \quad (253)$$

$$N_{spf,D4} = e^{b_{0,D4} + b_{ln} n_{th} + b_{xrd,D4} \ln(AADT_{xrd}/1,000) + b_{rmp,D4} \ln(AADT_{ex}/1,000 + AADT_{en}/1,000)} \quad (254)$$

$$CMF_{p,lt} = \left[e^{b_{p,lt} n_{o,in}} P_{xrd} + 1.0 (1.0 - P_{xrd}) \right]^{I_{p,lt,in}} \times \quad (255)$$

$$\left[e^{b_{p,lt} n_{o,out}} P_{xrd} + 1.0 (1.0 - P_{xrd}) \right]^{I_{p,lt,out}}$$

$$P_{xrd} = \frac{AADT_{in} + AADT_{out}}{AADT_{in} + AADT_{out} + AADT_{en} + AADT_{ex}} \quad (256)$$

$$CMF_{ch,xrd} = \left[e^{b_{ch,xrd}} P_{in} + 1.0 (1.0 - P_{in}) \right]^{I_{ch,in}} \times \quad (257)$$

$$\left[e^{b_{ch,xrd}} P_{out} + 1.0 (1.0 - P_{out}) \right]^{I_{ch,out}}$$

$$CMF_{ch,ex} = \left[e^{b_{ch,ex}} P_{ex} + 1.0 (1.0 - P_{ex}) \right]^{I_{ch,ex}} \quad (258)$$

$$CMF_{ps} = e^{b_{ps} I_{ps}} \quad (259)$$

$$CMF_{bay,lt} = \left[(0.44 I_{rural} + 0.65 [1.0 - I_{rural}]) P_{in} + 1.0 (1.0 - P_{in}) \right]^{I_{bay,lt,in}} \times \quad (260)$$

$$\left[(0.44 I_{rural} + 0.65 [1.0 - I_{rural}]) P_{out} + 1.0 (1.0 - P_{out}) \right]^{I_{bay,lt,out}}$$

$$CMF_{bay,rt} = \left[(0.59 I_{rural} + 0.76 [1.0 - I_{rural}]) P_{in} + 1.0 (1.0 - P_{in}) \right]^{I_{bay,rt,in}} \times \quad (261)$$

$$\left[(0.59 I_{rural} + 0.76 [1.0 - I_{rural}]) P_{out} + 1.0 (1.0 - P_{out}) \right]^{I_{bay,rt,out}}$$

$$CMF_{ap} = e^{b_{nd} (n_{dw} + n_{ps})} P_{out} + 1.0 (1.0 - P_{out}) \quad (262)$$

$$CMF_{sl} = e^{b_{sl} (1.0/L_{rmp} + 1.0/L_{str} - 0.333)} \quad (263)$$

$$C_{ca} = e^{b_{ca} I_{ca}} \quad (264)$$

where,

- $N_{rt,j}$ = predicted average crossroad ramp terminal crash frequency for model j ($j = A2B2$ if $I_{A2B2} = 1.0$; $j = A4D3ex$ if $I_{A4D3ex} = 1.0$; $j = B4D3en$ if $I_{B4D3en} = 1.0$; $j = D4$ if $I_{D4} = 1.0$); crashes/yr;
- $N_{rt,A2B2}$ = predicted average crash frequency for A2 and B2 configurations, crashes/yr;
- $N_{rt,A4D3ex}$ = predicted average crash frequency for A4 and D3ex configurations, crashes/yr;
- $N_{rt,B4D3en}$ = predicted average crash frequency for B4 and D3en configurations, crashes/yr;
- $N_{rt,D4}$ = predicted average crash frequency for D4 configuration, crashes/yr;
- $AADT_{xrd}$ = AADT volume for crossroad (= $0.5 AADT_{in} + 0.5 AADT_{out}$), veh/day;
- I_{A2B2} = crash indicator variable (= 1.0 if A2 or B2 crash data, 0.0 otherwise);
- I_{A4D3ex} = crash indicator variable (= 1.0 if A4 or D3ex crash data, 0.0 otherwise);
- I_{B4D3en} = crash indicator variable (= 1.0 if B4 or D3en crash data, 0.0 otherwise);
- I_{D4} = crash indicator variable (= 1.0 if D4 crash data, 0.0 otherwise);
- C_{ca} = calibration factor for California;
- $CMF_{p,lt}$ = protected left-turn operation crash modification factor;
- $CMF_{ch,xrd}$ = channelized right turn from crossroad crash modification factor;
- $CMF_{ch,ex}$ = channelized right turn from exit ramp crash modification factor;
- CMF_{ps} = non-ramp public street leg crash modification factor;
- $CMF_{bay,lt}$ = crossroad left-turn lane crash modification factor;
- $CMF_{bay,rt}$ = crossroad right-turn lane crash modification factor;
- CMF_{ap} = access point frequency crash modification factor;
- CMF_{sl} = segment length crash modification factor;
- n_{th} = number of through traffic lanes on the crossroad at the ramp terminal (total of both directions), lanes;
- $n_{o,k}$ = number of through traffic lanes that oppose the left-turn movement on crossroad leg k ($k = in$ or out), lanes;
- P_{xrd} = proportion of total leg AADT on the crossroad;
- $I_{p,lt,k}$ = protected left-turn operation indicator variable for crossroad leg k ($k = in$ or out) (= 1.0 if protected operation exists, 0.0 otherwise);
- P_{in} = proportion of total leg AADT on crossroad leg between ramps;
- P_{out} = proportion of total leg AADT on crossroad leg outside of interchange;
- $I_{ch,k}$ = right-turn channelization indicator variable for leg k ($k = in, out, or ex$) (= 1.0 if right-turn channelization exists, 0.0 otherwise);
- I_{ps} = non-ramp public street leg indicator variable (= 1.0 if leg is present, 0.0 otherwise);
- I_{rural} = area type indicator variable (= 1.0 if area is rural, 0.0 if it is urban);
- $I_{bay,lt,k}$ = left-turn lane (or bay) indicator variable for crossroad leg k ($k = in$ or out) (= 1.0 if left-turn lane (or bay) present, 0.0 otherwise);
- $I_{bay,rt,k}$ = right-turn lane (or bay) indicator variable for crossroad leg k ($k = in$ or out) (= 1.0 if right-turn lane (or bay) present, 0.0 otherwise);
- n_{dw} = number of unsignalized driveways on the crossroad leg outside of the interchange and within 250 ft of the ramp terminal;
- n_{ps} = number of unsignalized public street approaches to the crossroad leg outside of the interchange and within 250 ft of the ramp terminal;
- L_{rmp} = distance between subject ramp terminal and adjacent ramp terminal (measured along the crossroad from terminal center to terminal center), mi;

L_{str} = distance between subject ramp terminal and nearest public road intersection in a direction away from freeway (measured along the crossroad from terminal center to intersection center), mi; and

b_i = calibration coefficient for condition i

The final form of the regression model is described here, before the discussion of regression analysis results. However, this form reflects the findings from several preliminary regression analyses where alternative model forms were examined. The form that is described represents that which provided the best fit to the data, while also having coefficient values that are logical and constructs that are theoretically defensible and properly bounded.

Equation 255 describes a CMF that quantifies the relationship between left-turn control mode and crash frequency. The CMF is specific to protected left-turn operation. If a ramp terminal has permissive or protected-permissive operation then it does not have protected operation. This focus on protected operation is based partly on the guidance in Chapter 14 of the *HSM* that indicates a change from permissive to protected-permissive operation has a negligible effect on safety. The number of opposing through traffic lanes is included in this CMF because most traffic engineering guidelines for left-turn mode selection indicate that protected operation is more effective when there are many opposing lanes.

Equations 260 and 261 describe CMFs for left- and right-turn lane (or bay) presence, respectively. These CMFs are not associated with a regression coefficient. Rather, these CMFs are considered to be fairly definitive based on the extensive nature of the research that produced them (Harwood et al., 2002). The derivation of the leg-specific CMF values that are used in Equations 260 and 261 is described in the discussion associated with Table 64.

Equation 263 describes the relationship between ramp terminal crash frequency and the distance to the adjacent ramp and nearest public street intersection. The preliminary examination of the data indicated that crash frequency tends to increase as this distance increases.

The CMF for median width CMF_{mw} was described previously using Equation 231. Similarly, the CMF for exit ramp capacity CMF_{rc} was described using Equation 235.

The indicator variables used in several of the CMFs are identified in Table 66 for typical ramp terminal configurations. A value of 1.0 is shown in the table to indicate that the associated CMF *can* apply to the configuration, approach, and movement; whether the CMF *does* apply at a specific ramp terminal is based on whether the condition the CMF defines is present at that terminal.

TABLE 66. Indicator variable values for typical ramp terminal configurations

CMF	Indicator Variable Value by Ramp Terminal Configuration ¹						
	D3ex	A4	D3en	B4	A2	B2	D4
Protected left turn operation	$I_{p,lt,in} = 0.0$ $I_{p,lt,out} = 0.0$	$I_{p,lt,in} = 0.0$ $I_{p,lt,out} = 0.0$	$I_{p,lt,in} = 1.0$ $I_{p,lt,out} = 0.0$	$I_{p,lt,in} = 1.0$ $I_{p,lt,out} = 0.0$	$I_{p,lt,in} = 0.0$ $I_{p,lt,out} = 1.0$	$I_{p,lt,in} = 1.0$ $I_{p,lt,out} = 0.0$	$I_{p,lt,in} = 1.0$ $I_{p,lt,out} = 0.0$
Chan. right turn from crossroad	$I_{ch,in} = 0.0$ $I_{ch,out} = 0.0$	$I_{ch,in} = 1.0$ $I_{ch,out} = 1.0$	$I_{ch,in} = 0.0$ $I_{ch,out} = 1.0$	$I_{ch,in} = 0.0$ $I_{ch,out} = 1.0$	$I_{ch,in} = 1.0$ $I_{ch,out} = 0.0$	$I_{ch,in} = 0.0$ $I_{ch,out} = 1.0$	$I_{ch,in} = 0.0$ $I_{ch,out} = 1.0$
Chan. right turn from exit ramp	$I_{ch,ex} = 1.0$	$I_{ch,ex} = 1.0$	$I_{ch,ex} = 0.0$	$I_{ch,ex} = 0.0$	$I_{ch,ex} = 1.0$	$I_{ch,ex} = 1.0$	$I_{ch,ex} = 1.0$
Crossroad left-turn lane	$I_{bay,lt,in} = 0.0$ $I_{bay,lt,out} = 0.0$	$I_{bay,lt,in} = 0.0$ $I_{bay,lt,out} = 0.0$	$I_{bay,lt,in} = 1.0$ $I_{bay,lt,out} = 0.0$	$I_{bay,lt,in} = 1.0$ $I_{bay,lt,out} = 0.0$	$I_{bay,lt,in} = 0.0$ $I_{bay,lt,out} = 1.0$	$I_{bay,lt,in} = 1.0$ $I_{bay,lt,out} = 0.0$	$I_{bay,lt,in} = 1.0$ $I_{bay,lt,out} = 0.0$
Crossroad right-turn lane	$I_{bay,rt,in} = 0.0$ $I_{bay,rt,out} = 0.0$	$I_{bay,rt,in} = 1.0$ $I_{bay,rt,out} = 1.0$	$I_{bay,rt,in} = 0.0$ $I_{bay,rt,out} = 1.0$	$I_{bay,rt,in} = 0.0$ $I_{bay,rt,out} = 1.0$	$I_{bay,rt,in} = 1.0$ $I_{bay,rt,out} = 0.0$	$I_{bay,rt,in} = 0.0$ $I_{bay,rt,out} = 1.0$	$I_{bay,rt,in} = 0.0$ $I_{bay,rt,out} = 1.0$

Note:

1 - An indicator value of 1.0 in this table only indicates that such a value is *possible* for the associated configuration. The actual indicator value can still be 0.0 if the condition it defines is not satisfied at the subject terminal (e.g., a left-turn lane is not provided). Values indicated as “0.0” can, in fact, be 1.0 if there is a non-ramp public street leg present at the ramp terminal.

Model Calibration

The predictive model calibration process was based on a combined-model approach, as discussed in the section titled Modeling Approach. With this approach, the combined ramp terminal models and the CMFs (represented by Equations 250 to 264) are calibrated using a common database. This approach is needed because several CMFs are common to two or more of the ramp terminal models.

The models were calibrated using the California and Washington data. The Maine data were reserved for model validation. The discussion in this section focuses on the findings from the model calibration. The findings from model validation are provided in the next section.

The results of the combined regression model calibration are presented in Table 67. The Pearson χ^2 statistic for the model is 226, and the degrees of freedom are 202 ($= n - p = 225 - 23$). As this statistic is less than $\chi^2_{0.05, 202}$ ($= 236$), the hypothesis that the model fits the data cannot be rejected.

The t-statistic for each coefficient is listed in the last column of Table 67. These statistics describe a test of the hypothesis that the coefficient value is equal to 0.0. Those t-statistics with an absolute value that is larger than 2.0 indicate that the hypothesis can be rejected with the probability of error in this conclusion being less than 0.05. For those few variables where the absolute value of the t-statistic is smaller than 2.0, it was decided that the variable was important to the model and its trend was found to be intuitive and, where available, consistent with previous research findings (even if the specific value was not known with a great deal of certainty as applied to this database).

TABLE 67. Terminal FI model statistical description—combined model—two states—signalized

Model Statistics		Value		
R^2 :		0.56		
Scale parameter ϕ :		1.01		
Pearson χ^2 :		226 ($\chi^2_{0.05, 202} = 236$)		
Observations n_o :		225 terminals (1,615 injury or fatal crashes in 3 years)		
Calibrated Coefficient Values				
Variable	Inferred Effect of...	Value	Std. Dev.	t-statistic
$b_{p, lt}$	Protected left-turn operation	-0.414	0.093	-4.5
$b_{ch, xrd}$	Right-turn channelization on crossroad	0.524	0.191	2.7
$b_{ch, ex}$	Right-turn channelization on exit ramp	1.014	0.278	3.6
b_{nd}	Driveways or unsignalized public street approaches	0.133	0.081	1.6
b_{ps}	Public street leg at ramp terminal	0.663	0.289	2.3
b_{sl}	Distance to adjacent ramp terminal and intersection	-0.0211	0.0048	-4.4
b_{rc}	Exit ramp capacity	0.0684	0.0277	2.5
b_{me}	Width of median adjacent to left-turn lane (or bay)	0.0283	0.0104	2.7
$b_{AADT, me}$	AADT on median width	-0.00072	0.0004	-1.8
$b_{0, A2B2}$	A2 and B2 ramp terminal configuration	-0.623	0.664	-0.9
$b_{xrd, A2B2}$	Crossroad AADT	0.320	0.267	1.2
$b_{rmp, A2B2}$	Ramp AADT	0.195	0.243	0.8
$b_{0, A4D3ex}$	A4 and D3ex ramp terminal configuration	-1.538	0.595	-2.6
$b_{xrd, A4D3ex}$	Crossroad AADT	0.355	0.185	1.9
$b_{rmp, A4D3ex}$	Ramp AADT	0.385	0.132	2.9
$b_{0, B4D3en}$	B4 and D3en ramp terminal configuration	-2.331	1.578	-1.5
$b_{xrd, B4D3en}$	Crossroad AADT	0.257	0.344	0.7
$b_{rmp, B4D3en}$	Ramp AADT	0.922	0.675	1.4
$b_{0, D4}$	D4 ramp terminal configuration	-3.044	0.421	-7.2
$b_{xrd, D4}$	Crossroad AADT	1.255	0.177	7.1
$b_{rmp, D4}$	Ramp AADT	0.114	0.162	0.7
b_{ln}	Number of through lanes	0.156	0.044	3.6
b_{ca}	Location in California	-0.438	0.095	-4.6

The findings from an examination of the coefficient values and the corresponding CMF or SPF predictions are documented in a subsequent section. In general, the sign and magnitude of the calibration coefficients in Table 67 are logical and consistent with previous research findings.

An indicator variable for the state of California was included in the regression model. The coefficient for this variable is shown in the last row of Table 67. It is statistically significant. Its value indicates that the ramp terminals in California have about 35 percent fewer crashes than those in Washington. This trend is consistent with that found in the comparison of summary crash rates for these two states in Table 25. The trend could not be explained by differences in ramp terminal design among the two states. It is likely due to differences between states that are due to unobserved variables such as approach grade, signing, pavement condition, weather, and speed limit.

Model Validation

Model validation was a two-step process. The first step required using the calibrated models to predict the crash frequency for sites from a third state (i.e., Maine). The objective of this step was to demonstrate the robustness of the model structure and its transferability to another state. The second step required comparing the calibrated CMFs with similar CMFs reported in the literature, where such information was available. The objective of this step was to demonstrate that the calibrated CMFs were consistent with previous research findings.

The findings from the first step of the validation process are described in this section. Those from the second step are described in the next section.

The first step of the validation process consisted of several tasks. The first task was to quantify the local calibration factor for each of the four ramp terminal models, which would be the first step for any agency using the *HSM* methodology. However, only a single, overall calibration factor could be computed because there are only 11 signalized ramp terminals in the Maine database. This overall calibration factor was used to produce a “re-calibrated” set of models (i.e., the models with the coefficients from Table 67 plus the local calibration factors). The local calibration factor value for the Maine data C_{me} was computed as 1.30.

The second task was to apply the re-calibrated models to the Maine data to compute the predicted average crash frequency for each ramp terminal. The predicted crash frequency was then compared to the reported crash frequency for each site.

The third task was to compute the fit statistics and assess the robustness of the calibrated model. These statistics are listed in Table 68. The Pearson χ^2 statistic for combined model is less than $\chi^2_{0.05, n-1}$ so the hypothesis that the model fits the validation data cannot be rejected.

TABLE 68. Terminal model validation statistics—signalized

R^2	R_k^2	Scale Parameter ϕ	Pearson χ^2	Deg. of Freedom	$\chi^2_{0.05, n-1}$
0.40	0.53	1.46	14.6	10	18.3

The findings from this validation step indicate that the trends in the Maine data are not significantly different from those in the California and Washington data. These findings also suggest that the model structure is transferable to other states (when locally calibrated) for the prediction of FI crash frequency. Based on these findings, the data for the three states were combined and used in a second regression model calibration. The larger sample size associated with the combined database reduced the standard error of several calibration coefficients. Bared and Zhang (2007) also used this approach in their development of predictive models for urban freeways.

Combined Model

The data from the three study states were combined and the predictive models were calibrated a second time using the combined data. The calibration coefficients for the combined

ramp terminal models are described first. Then, the fit statistics and inverse dispersion parameter for each ramp terminal model are described.

The results of the combined regression model calibration are presented in Table 69. The Pearson χ^2 statistic for the model is 239, and the degrees of freedom are 212 ($= n - p = 236 - 24$). As this statistic is less than $\chi^2_{0.05, 212} (= 247)$, the hypothesis that the model fits the data cannot be rejected. Several terminals were removed as a result of outlier analysis such that the calibration database included only 1,708 of the 1,740 crashes identified in Chapter 4.

TABLE 69. Terminal FI model statistical description—combined model—three states—signalized

Model Statistics		Value		
R^2 :		0.56		
Scale parameter ϕ :		1.02		
Pearson χ^2 :		239 ($\chi^2_{0.05, 212} = 247$)		
Observations n_o :		236 terminals (1,708 injury or fatal crashes in 3 years)		
Calibrated Coefficient Values				
Variable	Inferred Effect of...	Value	Std. Dev.	t-statistic
$b_{p, lt}$	Protected left-turn operation	-0.363	0.084	-4.3
$b_{ch, xrd}$	Right-turn channelization on crossroad	0.466	0.190	2.5
$b_{ch, ex}$	Right-turn channelization on exit ramp	0.992	0.270	3.7
b_{nd}	Driveways or unsignalized public street approaches	0.158	0.076	2.1
b_{ps}	Public street leg at ramp terminal	0.592	0.285	2.1
b_{sl}	Distance to adjacent ramp terminal and intersection	-0.0185	0.0046	-4.0
b_{rc}	Exit ramp capacity	0.0668	0.0276	2.4
b_{me}	Width of median adjacent to left-turn lane (or bay)	0.0287	0.0102	2.8
$b_{AADT, me}$	AADT on median width	-0.00074	0.0004	-1.9
$b_{0, A2B2}$	A2 and B2 ramp terminal configuration	-0.778	0.643	-1.2
$b_{xrd, A2B2}$	Crossroad AADT	0.325	0.263	1.2
$b_{rmp, A2B2}$	Ramp AADT	0.212	0.242	0.9
$b_{0, A4D3ex}$	A4 and D3ex ramp terminal configuration	-1.672	0.580	-2.9
$b_{xrd, A4D3ex}$	Crossroad AADT	0.379	0.182	2.1
$b_{rmp, A4D3ex}$	Ramp AADT	0.394	0.131	3.0
$b_{0, B4D3en}$	B4 and D3en ramp terminal configuration	-2.388	1.577	-1.5
$b_{xrd, B4D3en}$	Crossroad AADT	0.265	0.345	0.8
$b_{rmp, B4D3en}$	Ramp AADT	0.905	0.674	1.3
$b_{0, D4}$	D4 ramp terminal configuration	-2.975	0.405	-7.4
$b_{xrd, D4}$	Crossroad AADT	1.191	0.172	6.9
$b_{rmp, D4}$	Ramp AADT	0.131	0.158	0.8
b_{ln}	Number of through lanes	0.160	0.043	3.7
b_{me}	Location in Maine	0.305	0.160	1.9
b_{ca}	Location in California	-0.477	0.093	-5.1

The t-statistic for each coefficient is listed in the last column of Table 69. These statistics have generally increased, relative to their counterparts in Table 67, as a result of the increased sample size. With a few exceptions, these statistics have an absolute value that is larger than 2.0, which indicates that the null hypothesis can be rejected with the probability of error in this conclusion being less than 0.05. For those few variables where the absolute value of the t-statistic is smaller than 2.0, it was decided that the variable was important to the model and its trend was found to be intuitive and, where available, consistent with previous research findings (even if the specific value was not known with a great deal of certainty as applied to this database). This consistency is demonstrated in a subsequent section.

Indicator variables were included for the states of California and Maine in the regression model. These coefficients are shown in the last two rows of Table 69. The value for California is statistically significant. The value for California indicates that the ramp terminals in California have fewer crashes than those in Washington. The opposite trend is suggested for Maine ramp terminals. This trend is consistent with that found in the comparison of summary crash rates for these states in Table 25. The trend could not be explained by differences in ramp terminal design among the two states. It is likely due to differences between states that are due to unobserved variables such as approach grade, signing, pavement condition, weather, and speed limit.

Model for A2 and B2 Configurations. The statistics describing the calibrated model for A2 and B2 ramp terminal configurations are presented in Table 70. The Pearson χ^2 statistic for the model is 33.2, and the degrees of freedom are 31 ($= n - p = 32 - 1$). As this statistic is less than $\chi^2_{0.05,31}$ ($= 45$), the hypothesis that the model fits the data cannot be rejected. The R^2 for the model is 0.43. The R_k^2 for the calibrated model is 0.63. The inverse dispersion parameter was adjusted using Equation 249.

TABLE 70. Terminal FI model statistical description—A2 and B2 configuration—signalized

Model Statistics	Value
R^2 (R_k^2):	0.43 (0.63)
Scale parameter ϕ :	1.07
Pearson χ^2 :	33.2 ($\chi^2_{0.05,31} = 45$)
Inverse dispersion parameter K :	2.17
Observations n_o :	32 terminals (168 injury or fatal crashes in 3 years)
Standard deviation s_e :	± 1.37 crashes/yr

The coefficients in Table 69 were combined with Equation 251 to obtain the calibrated SPF for the A2 and B2 configuration. The form of the model is described in the following equation.

$$N_{spf, A2B2} = e^{-0.778 + 0.160 n_{th} + 0.325 \ln(AADT_{rd}/1,000) + 0.212 \ln(AADT_{ex}/1,000 + AADT_{en}/1,000)} \quad (265)$$

The calibrated CMFs used with this SPF are described in a subsequent section.

The fit of the calibrated model is shown in Figure 112. This figure compares the predicted and reported crash frequency in the calibration database. The trend line shown represents a “ $y = x$ ” line. A data point would lie on this line if its predicted and reported crash frequency were equal. The data points shown represent the reported crash frequency for the ramp terminals used to calibrate the corresponding component model. In general, the data shown in the figure indicate that the model provides an unbiased estimate of expected crash frequency for ramp terminals experiencing up to 12 crashes in a three-year period.

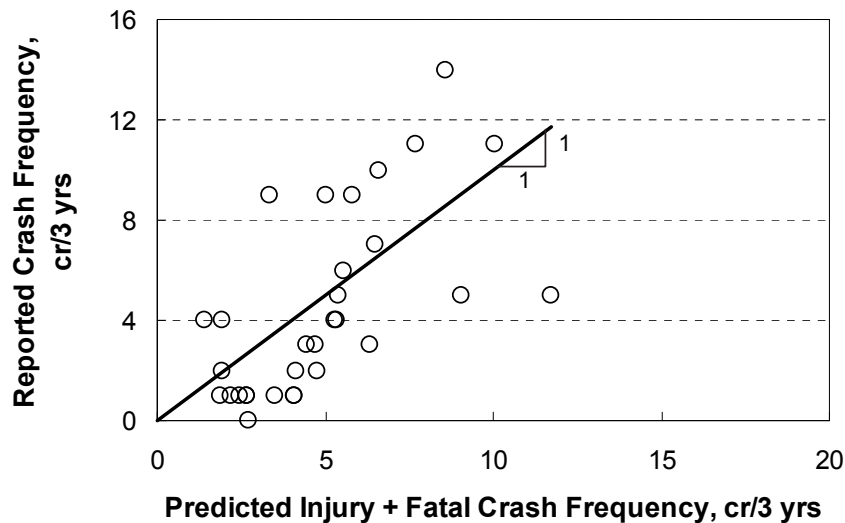


Figure 112. Predicted vs. reported FI crashes at signalized A2 and B2 configurations.

Model for A4 and D3ex Configurations. The statistics describing the calibrated model for A4 and D3ex ramp terminal configurations are presented in Table 71. The Pearson χ^2 statistic for the model is 67.1, and the degrees of freedom are 59 ($= n - p = 60 - 1$). As this statistic is less than $\chi^2_{0.05,59}$ ($= 78$), the hypothesis that the model fits the data cannot be rejected. The R^2 for the model is 0.45. The R_k^2 for the calibrated model is 0.73. The inverse dispersion parameter was adjusted using Equation 249.

TABLE 71. Terminal FI model statistical description—A4 and D3ex configuration—signalized

Model Statistics	Value
R^2 (R_k^2):	0.45 (0.73)
Scale parameter ϕ :	1.14
Pearson χ^2 :	67.1 ($\chi^2_{0.05, 59} = 78$)
Inverse dispersion parameter K :	8.72
Observations n_o :	60 terminals (422 injury or fatal crashes in 3 years)
Standard deviation s_e :	± 1.13 crashes/yr

The coefficients in Table 69 were combined with Equation 252 to obtain the calibrated SPF for the A4 and D3ex configuration. The form of the model is described in the following equation.

$$N_{spf, A4D3ex} = e^{-1.672 + 0.160 n_{th} + 0.379 \ln(AADT_{xrd}/1,000) + 0.394 \ln(AADT_{ex}/1,000 + AADT_{en}/1,000)} \quad (266)$$

The calibrated CMFs used with this SPF are described in a subsequent section. The AADT volume of the loop entrance ramp at an A4 configuration is not included in $AADT_{en}$. Also, $AADT_{en}$ equals 0.0 when the SPF is applied to a D3ex configuration.

The fit of the calibrated model is shown in Figure 113. In general, the data shown in the figure indicate that the model provides an unbiased estimate of expected crash frequency for ramp terminals experiencing up to 17 crashes in a three-year period.

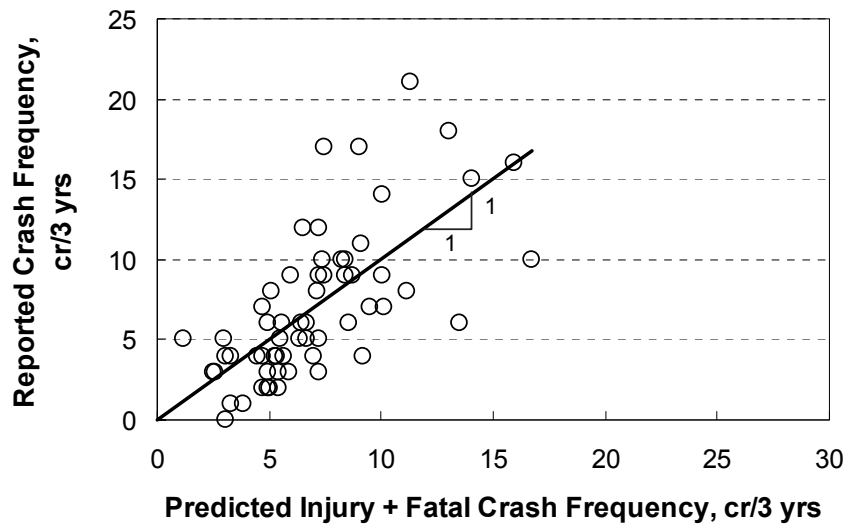


Figure 113. Predicted vs. reported FI crashes at signalized A4 and D3ex configurations.

Model for B4 and D3en Configurations. The statistics describing the calibrated model for B4 and D3en ramp terminal configurations are presented in Table 72. The Pearson χ^2 statistic for the model is 2.67, and the degrees of freedom are 3 ($= n - p = 4 - 1$). As this statistic is less than $\chi^2_{0.05,3} (= 7.8)$, the hypothesis that the model fits the data cannot be rejected. The R^2 for the model is 0.51. The R_k^2 for the calibrated model is 0.57. The inverse dispersion parameter was adjusted using Equation 249.

TABLE 72. Terminal FI model statistical description—B4 and D3en configuration—signalized

Model Statistics	Value
$R^2 (R_k^2)$:	0.51 (0.57)
Scale parameter ϕ :	0.88
Pearson χ^2 :	2.67 ($\chi^2_{0.05,3} = 7.8$)
Inverse dispersion parameter K :	5.37
Observations n_o :	4 terminals (34 injury or fatal crashes in 3 years)
Standard deviation s_e :	± 1.58 crashes/yr

The coefficients in Table 69 were combined with Equation 253 to obtain the calibrated SPF for the B4 and D3en configuration. The form of the model is described in the following equation.

$$N_{spf, B4D3en} = e^{-2.388 + 0.160 n_{th} + 0.265 \ln(AADT_{xrd} / 1,000) + 0.905 \ln(AADT_{ex} / 1,000 + AADT_{en} / 1,000)} \quad (267)$$

The calibrated CMFs used with this SPF are described in a subsequent section. The AADT volume of the loop exit ramp at a B4 configuration is not included in $AADT_{ex}$. Also, $AADT_{ex}$ equals 0.0 when the SPF is applied to a D3en configuration.

The fit of the calibrated SPF is shown in Figure 114. The small number of observations for this configuration limits the ability to make broad claims about the transferability of the SPF. The fit is adequate and the SPF predictions compare favorably with the other SPFs (see Figure 118). Local calibration will be very important for this SPF to ensure that it provides an acceptable level of accuracy.

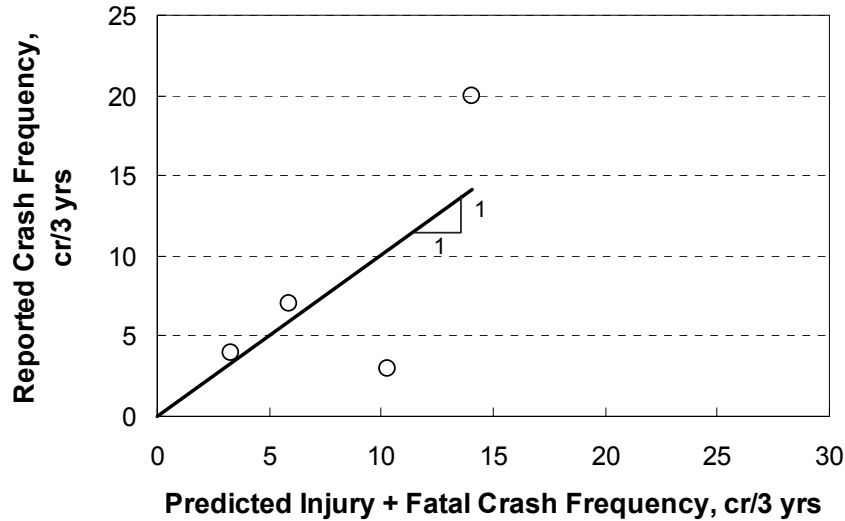


Figure 114. Predicted vs. reported FI crashes at signalized B4 and D3en configurations.

Model for D4 Configuration. The statistics describing the calibrated model for D4 ramp terminal configuration are presented in Table 73. The Pearson χ^2 statistic for the model is 139, and the degrees of freedom are 139 ($= n - p = 140 - 1$). As this statistic is less than $\chi^2_{0.05,139}$ ($= 167$), the hypothesis that the model fits the data cannot be rejected. The R^2 for the model is 0.60. The R_k^2 for the calibrated model is 0.82. The inverse dispersion parameter was adjusted using Equation 249.

TABLE 73. Terminal FI model statistical description–D4 configuration–signalized

Model Statistics	Value
$R^2 (R_k^2)$:	0.60 (0.82)
Scale parameter ϕ :	1.00
Pearson χ^2 :	139 ($\chi^2_{0.05, 139} = 167$)
Inverse dispersion parameter K :	11.5
Observations n_o :	140 terminals (1,084 injury or fatal crashes in 3 years)
Standard deviation s_e :	± 1.28 crashes/yr

The coefficients in Table 69 were combined with Equation 254 to obtain the calibrated SPF for the D4 configuration. The form of the model is described in the following equation.

$$N_{spf, D4} = e^{-2.975 + 0.160 n_m + 1.191 \ln(AADT_{rd} / 1,000) + 0.131 \ln(AADT_{ex} / 1,000 + AADT_{en} / 1,000)} \quad (268)$$

The calibrated CMFs used with this SPF are described in a subsequent section.

The fit of the calibrated model is shown in Figure 115. In general, the data shown in the figure indicate that the model provides an unbiased estimate of expected crash frequency for ramp terminals experiencing up to 30 crashes in a three-year period.

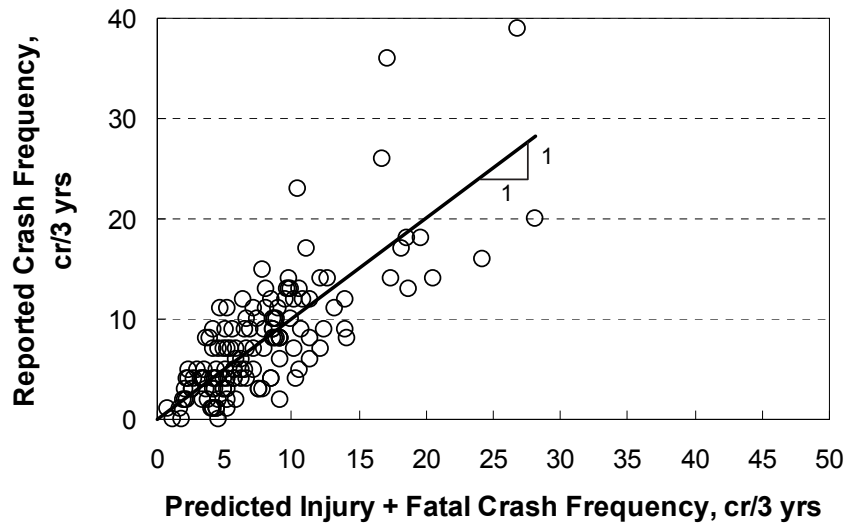


Figure 115. Predicted vs. reported FI crashes at signalized D4 configurations.

Calibrated CMFs

Several CMFs were calibrated in conjunction with the SPFs. All of them were calibrated using FI crash data. Collectively, they describe the relationship between various geometric factors and crash frequency. These CMFs are described in this section and, where possible, compared with the findings from previous research as means of model validation.

Many of the CMFs found in the literature are typically derived from (and applied to) “intersection” crashes. That is, one CMF is used to indicate the influence of a leg-specific geometric factor on total crashes. In contrast, the models developed for this research project include several CMFs that are calibrated for leg-specific conditions. In these instances, Equations 222 and 226 were used to convert the leg-specific CMF to an intersection CMF. The converted CMFs are compared in this subsection with the intersection CMFs reported in the literature using typical values for the leg AADT distribution at intersections (as opposed to that found at ramp terminals).

The following CMFs were described previously in this chapter and are not discussed in this section. The figure provided for the last CMF listed is based on the calibration coefficients in Table 69.

- crossroad left-turn lane CMF (Equation 260, Table 64);
- crossroad right-turn lane CMF (Equation 261, Table 64); and
- exit ramp capacity CMF (Equation 235, Figure 107).

Protected Left-Turn Operation CMF. The protected left-turn operation CMF is described using the following equation.

$$CMF_{p,lt} = \left[e^{-0.363 n_{o,in}} P_{xrd} + 1.0 (1.0 - P_{xrd}) \right]^{I_{p,lt,in}} \times \left[e^{-0.363 n_{o,out}} P_{xrd} + 1.0 (1.0 - P_{xrd}) \right]^{I_{p,lt,out}} \quad (269)$$

This CMF is applicable to any crossroad leg with protected left-turn operation. It is not applicable to any leg that has permissive or protected-permissive operation.

The values obtained from this CMF are listed in Table 74 for both ramp terminals and for intersections. The CMF values for ramp terminals reflect a proportion of total leg AADT on the crossroad P_{xrd} of 0.78, which is a typical value for ramp terminals. The CMF values for intersections are based on AADT proportions that are more consistent with those found at the intersection of a major and minor street.

Chapter 14 of the *HSM* recommends a CMF value of 0.94 for the conversion from permissive or protected-permissive left-turn operation to protected operation on one intersection leg (Highway, 2010). This value compares with the values of 0.91 and 0.79 in Table 74 for minor and major street legs, respectively. One of the references cited in the *HSM* as a source of the recommended value is a report by Davis and Aul (2007). Consultation of this report indicates that they derived a CMF value of 0.82 for intersections where both minor street legs were converted. This value compares favorably with the value of 0.83 in Table 74 (second row from bottom). Davis and Aul reported a CMF value of 0.58 for an intersection where both major street legs were converted. This value compares favorably with the values of 0.41 and 0.62 in Table 74 (last row).

TABLE 74. Calibrated protected left-turn operation CMF for FI crashes

Junction Location	Legs with Protected Operation	Leg Location	Proportion AADT	CMF Value by Number of Opposing Lanes	
				1 lane	2 lanes
Ramp terminal	1	Crossroad	0.78	0.76	0.60
	2	Crossroad	0.78	0.58	0.36
Intersection	1	Minor street ¹	0.30	0.91	0.85
		Major street ¹	0.70	0.79	0.64
	2	Minor street ¹	0.30	0.83	0.71
		Major street ¹	0.70	0.62	0.41

Note:

1 - Intersection CMFs are computed using Equation 269 and the AADT proportion shown in the table.

Channelized Right-Turn CMFs. Two CMFs are discussed in this section. One is the CMF for channelized right turns from the crossroad and the other is the CMF for right turns from the exit ramp. These two CMFs are described using the following equations.

$$CMF_{ch,xrd} = \left[e^{0.466 P_{in}} + 1.0 (1.0 - P_{in}) \right]^{I_{ch,in}} \times \left[e^{0.466 P_{out}} + 1.0 (1.0 - P_{out}) \right]^{I_{ch,out}} \quad (270)$$

$$CMF_{ch,ex} = \left[e^{0.992 P_{ex}} + 1.0 (1.0 - P_{ex}) \right]^{I_{ch,ex}} \quad (271)$$

The first CMF listed is applicable to any ramp terminal with right-turn channelization on one or both crossroad legs, where the associated right-turn movement is turning from the crossroad. This CMF can be applied to channelization associated with the loop entrance ramp of the A4 configuration.

The second CMF listed is applicable to any ramp terminal with a diagonal exit ramp that has right-turn channelization, where the associated right-turn movement is turning from the exit ramp. This CMF is not applicable to the loop exit ramp of the B4 configuration.

The values obtained from these CMFs are listed in Table 75 for both ramp terminals and intersections. The values for ramp terminals reflect the proportion of total leg AADT on the subject legs that are typical for ramp terminals. The values for intersections are based on leg AADT proportions that are more consistent with those found at the intersection of a major and minor street.

A channelized right-turn CMF derived by Bonneson and Pratt (2008) for four-leg urban signalized intersections indicates a value of 1.04 when one minor leg has channelization. This value compares with the value of 1.09 in Table 75 (second row from bottom). Similarly, this source indicates a value of 1.10 with one major leg has channelization. This value compares with the value of 1.21 in Table 75 (last row).

TABLE 75. Calibrated right-turn channelization CMF for FI crashes—signalized

Junction Location	Leg Location	Proportion AADT on Leg	CMF Value by Number of Legs with Channelization	
			1 leg	2 legs
Ramp terminal	Exit ramp	0.12	1.20	1.45
	Crossroad ¹	0.39	1.23	1.52
Intersection	Minor street ^{1,2}	0.15	1.09	1.19
	Major street ^{1,2}	0.35	1.21	1.46

Notes:

1 - For Equation 270, P_{in} is assumed to equal P_{out} .

2 - Intersection CMFs are computed using Equation 270 and the AADT proportion shown in the table.

The value of this CMF implies that channelized right turns are less safe than right turns made at the intersection (without channelization). This finding is consistent with that of Dixon et al.(2000) (and later confirmed by Fitzpatrick et al. [2006]) who found a higher right-turn-related crash frequency for channelized right turns than for right turns made at the intersection (without channelization). It likely reflects the fact that the channelized-right-turn driver’s check of the merge gap requires a relatively large head rotation coupled with a lengthy diversion of attention from the road ahead. Sometimes this gap check occurs while the vehicle is still moving forward, all of which can be problematic if the right-turning driver just ahead decides to yield.

Non-Ramp Public Street Leg CMF. The non-ramp public street CMF is described using the following equation.

$$CMF_{ps} = e^{0.592 I_{ps}} \tag{272}$$

This CMF is applicable to any ramp terminal that has a fourth leg that: (1) is a public street serving two-way traffic and (2) intersects with the crossroad at the terminal. Public street legs are fairly rare (i.e., they were found at about 2 percent of the terminals in the database). At most ramp terminals, the public street leg will be on the opposite side of the crossroad from the exit ramp. At the B4 and A4 ramp terminals, the public street leg will be opposite from the diagonal exit ramp (the diagonal entrance ramp will intersect with the crossroad at some distance from the ramp terminal such that it is not part of the ramp terminal). At the D3en configuration, the public street leg will be on the opposite side of the crossroad from the entrance ramp.

This CMF has a value of 1.81 when a public street approach is present at a ramp terminal. The corresponding increase in the predicted number of crashes is likely a reflection of the increased number of conflicting movements created at the ramp terminal by a two-way traffic leg.

Access Point Frequency CMF. The access point frequency CMF is described using the following equation.

$$CMF_{ap} = e^{0.158(n_{dw}+n_{ps})} P_{out} + 1.0(1.0 - P_{out}) \tag{273}$$

This CMF applies to any ramp terminal with unsignalized driveways or unsignalized public street approaches on the crossroad leg that is outside of the interchange. Driveways and

approaches on both sides of the leg should be counted when they are within 250 ft of the ramp terminal. The count of driveways should only include *active* driveways (i.e., those driveways with an average daily volume of 10 veh/day or more).

The values obtained from this CMF are listed in Table 76 for ramp terminals and for intersections. The CMF values for ramp terminals reflect the proportion of total leg AADT on crossroad legs that are typical for ramp terminals. The CMF values for intersections are based on leg AADT proportions that are more consistent with those found on the major street at the intersection of a major and minor street.

TABLE 76. Calibrated access point frequency CMF for FI crashes—signalized

Junction Location	Proportion AADT on Leg	CMF Value by Number of Driveways or Public Street Approaches			
		1	2	3	4
Ramp terminal	0.39	1.07	1.14	1.24	1.34
Intersection ¹	0.35	1.06	1.13	1.21	1.31

Note:

1 - Intersection CMFs are computed using Equation 273 and the AADT proportion shown in the table.

A driveway frequency CMF derived by Bonneson et al. (2005) for rural signalized intersections indicates a value of 1.05 when one driveway is present. This value compares with the value of 1.06 in Table 76 (last row). Similarly, this source indicates a value of 1.20 when four driveways are present. This value compares with the value of 1.31 in Table 76 (last row).

Segment Length CMF. The segment length CMF is described using the following equation.

$$CMF_{sl} = e^{-0.0185(1.0/L_{rmp} + 1.0/L_{str} - 0.333)} \quad (274)$$

This CMF is applicable to all ramp configurations. It describes the relationship between ramp terminal crash frequency and the distance to the adjacent ramp or nearest public street intersection. The adjacent ramp or intersection can be signalized or unsignalized.

The distances used to calibrate this CMF were as small as 100 ft. The base condition for this CMF is no adjacent ramp or public street intersection (i.e., $L_{rmp} = L_{str} = 6.0$ mi).

The segment length CMF is shown in Figure 116. The trend line shown indicates that the CMF value increases with increasing distance. It is rationalized that the distance between the subject ramp and its adjacent ramp and intersection is correlated with crossroad operating speed. This speed is likely to increase as distance increases, and an increase in speed is likely to increase the risk of a crash.

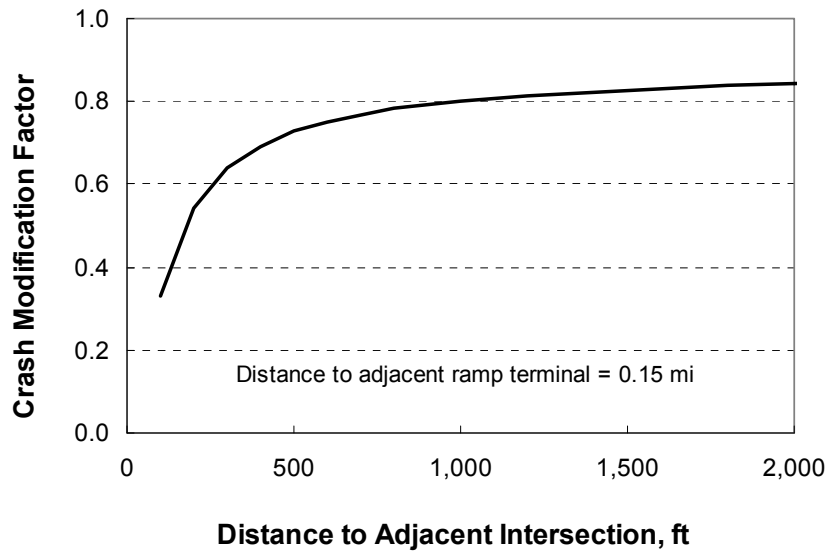


Figure 116. Calibrated segment length CMF for FI crashes—signalized.

Median Width CMF. The median width CMF is described using the following equation.

$$CMF_{mw} = \left[e^{(0.0287 - 0.00074 AADT_{in}/1,000) W_{me,in}} P_{in} + 1.0 (1.0 - P_{in}) \right] \times \left[e^{(0.0287 - 0.00074 AADT_{out}/1,000) W_{me,out}} P_{out} + 1.0 (1.0 - P_{out}) \right] \quad (275)$$

with,

$$W_{me,k} = W_m - W_{mb,k} \geq 0.0 \quad (276)$$

$$W_{mb,k} = \text{Max}(W_{b,k}; 12) \quad (277)$$

Guidance for using this CMF was provided in the CMF Development part of this chapter (in the section titled Median Width CMF). The constant “12” represents the minimum median width below which the CMF value is 1.0. This value is decreased from the 14 ft value stated in the *HSM* based on the trends found in the ramp terminal safety database. The applicable AADT volumes range from 14,000 to 60,000 veh/day. AADT volumes smaller than 14,000 should be set to 14,000 in Equation 275.

The median width CMF is shown in Figure 117. The trend line shown indicates that the CMF value increases with increasing median width. This trend is consistent with the CMF described in the *HSM* for urban four-leg signalized intersections. By interpolation, the *HSM* CMF is consistent with a crossroad AADT volume of about 23,000 veh/day. Other CMF values are obtained for other AADT volumes. A CMF value of about 1.0 is obtained for an AADT volume of 40,000 veh/day.

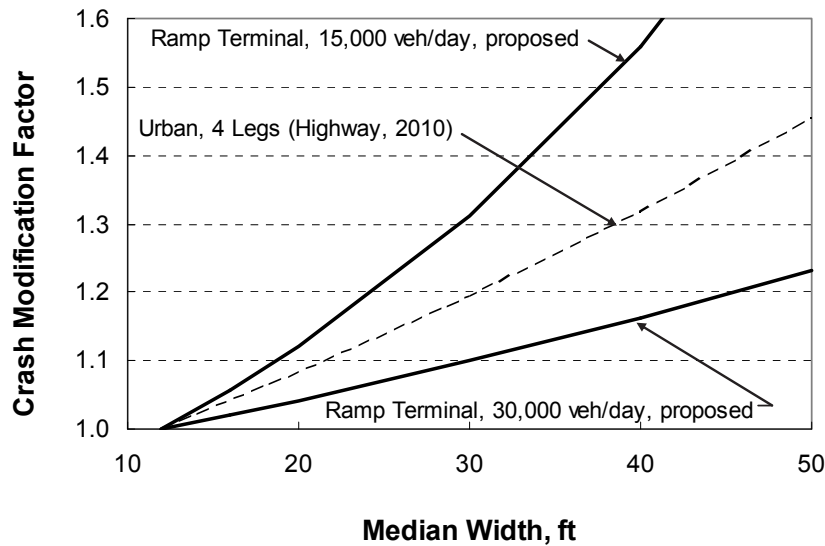


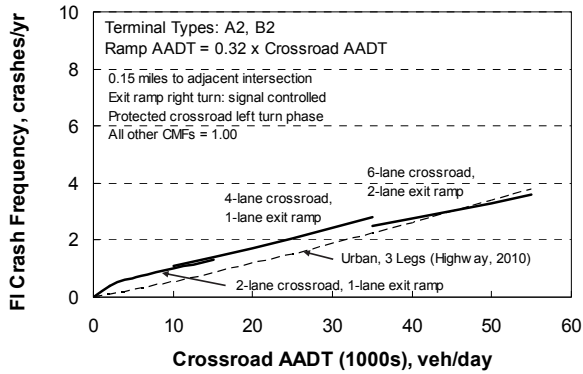
Figure 117. Calibrated median width CMF for FI crashes—signalized.

The AADT coefficient is negative indicating that the CMF value decreases with increasing AADT volume. This trend is opposite to that for unsignalized intersections, as suggested previously by the trends in Figure 105. For AADT volumes in the range of 14,000 to 15,000, Equation 275 yields about the same CMF value as that shown in Figure 105 for unsignalized intersections. This trend suggests that the CMF value is largest for AADT volumes in this range and lower for larger or smaller AADT volumes. It is likely that the negative AADT coefficient value in Equation 275 reflects a tendency for drivers to be more cautious as the intersection becomes busier. Also, busier intersections may have long queues present for more cycles, which could reduce the likelihood of errant vehicles in middle or outside lanes that have sufficient speed to cross the median.

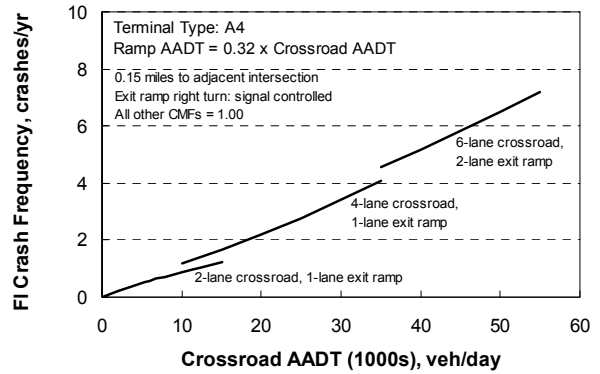
Sensitivity Analysis

The relationship between crash frequency and traffic demand, as obtained from the combined calibrated models, is shown in Figure 118 for signalized ramp terminals. The distance between ramps is 0.15 mi and the distance to the nearest public street intersection is also 0.15 mi. The ramp terminal has protected left-turn operation for the crossroad left-turn movement. All other geometric and control conditions are such that the associated CMF has a value of 1.0. The axis scale for each graph in Figure 118 is the same. This technique is used to facilitate comparison among ramp configurations.

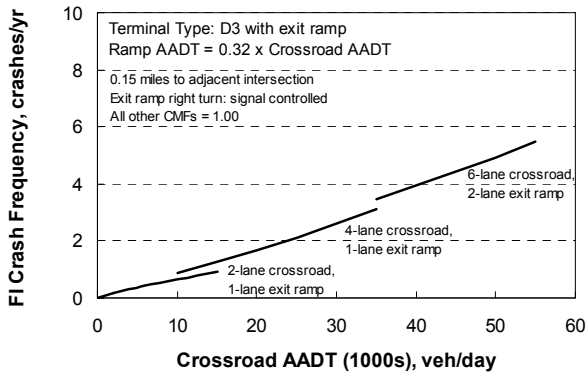
Figure 118a shows the SPF for urban three-leg signalized intersections that is described in the *HSM*. Similarly, Figure 118f shows the SPF for urban four-leg signalized intersections that is described in the *HSM*. The trend lines in Figure 118a indicate that three-leg ramp terminals have about the same number of crashes as three-leg intersections. In contrast, the trend lines in Figure 118f suggest that four-leg ramp terminals have up to 30 percent more crashes than four-leg intersections.



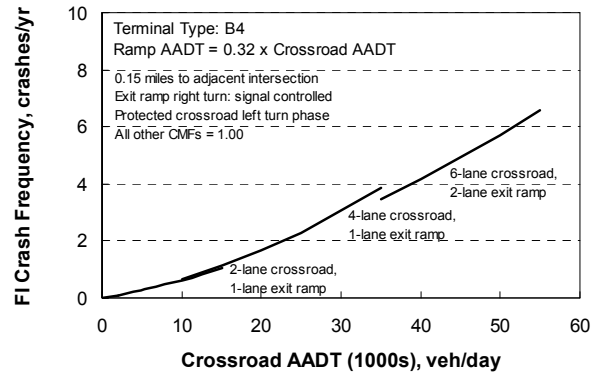
a. Terminal types A2 and B2.



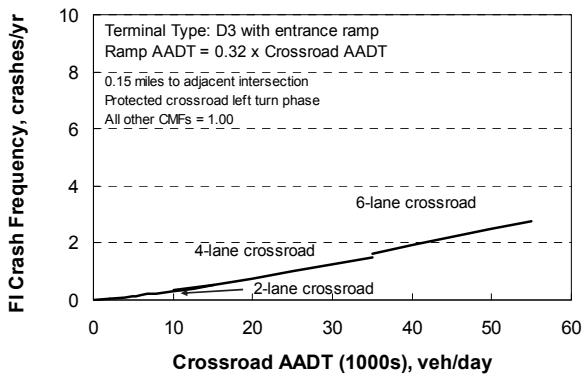
b. Terminal type A4.



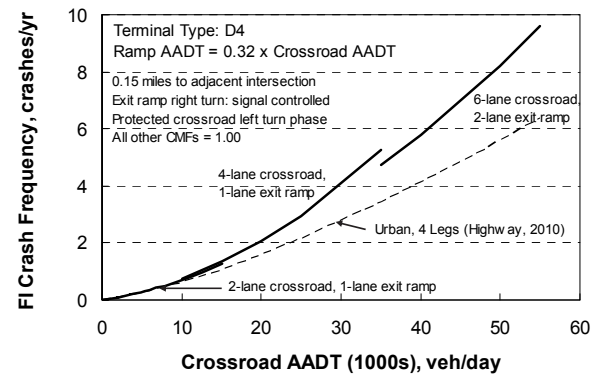
c. Terminal Type D3 with exit ramp.



d. Terminal type B4.



e. Terminal Type D3 with entrance ramp.



f. Terminal type D4.

Figure 118. Terminal FI models—signalized.

The A2, B2, and D3 configurations are shown in Figure 118 to have fewer crashes than the other configurations, for a given AADT volume. This trend is likely due to the fact that these

configurations have only three legs, while the other configurations have four legs. The number of conflict points increases significantly with the number of legs. The D4 configuration is shown in Figure 118f to have more crashes for a given AADT volume than the other configurations. This trend is likely a reflection of the fact that it has four legs, two left-turn movements, and a higher “sum of conflicting volumes” than the other configurations. Although the D3en and B4 configurations are represented collectively by only four observations, the trends shown in Figure 118d and 118e are consistent with those of the other configurations shown and provide some evidence of the validity of the associated SPF.

Unsignalized Ramp Terminal Models

This section describes the development of predictive models for unsignalized ramp terminals. An unsignalized ramp terminal has either one-way stop control (with stop control for the exit ramp) or all-way stop control.

The first subsection describes the structure of the predictive models as used in the regression analysis. The second subsection describes the regression statistics for each of the calibrated models. The third subsection describes a validation of the calibrated models. The fourth subsection describes the proposed predictive models. The fifth section describes the calibrated CMFs. The last subsection provides a sensitivity analysis of the predictive models over a range of traffic demands.

Model Development

This subsection describes the proposed predictive models and the methods used to calibrate them. The regression models are generalized to accommodate a wide range of ramp terminal geometry and right-turn control modes. The generalized form shows all the CMFs in the model, even though some CMFs are applicable only to some ramp terminal configurations. Indicator variables are used to determine which CMFs are applicable to each ramp terminal observation in the database. Those CMFs that are not applicable to a given ramp terminal are set to 1.0 using an indicator variable.

The generalized form includes intersection CMFs that include leg-specific terms for both crossroad legs, even when the associated treatment is only applicable to one leg. For example, a left-turn lane is typically added to the “inside” crossroad leg for a D4 configuration, where the inside leg is that leg located between the two ramp terminals of the interchange. In contrast, a left-turn lane is typically added to the outside crossroad leg for an A2 configuration. The generalized form of the left-turn lane CMF includes terms for both left-turn bays, where indicator variables are used to determine which terms are applicable (and which should be set to 1.0) for each observation.

The following regression model form was used to facilitate the combined regression analysis of the four models for unsignalized ramp terminals.

$$N_{rt,j} = (N_{spf,A2B2} I_{A2B2} + N_{spf,A4D3ex} I_{A4D3ex} + N_{spf,B4D3en} I_{B4D3en} + N_{spf,D4} I_{D4}) \quad (278)$$

$$\times CMF_{sk} \times CMF_{rc} \times CMF_{bay,lt} \times CMF_{bay,rt}$$

$$\times CMF_{ns} \times CMF_{sl} \times CMF_{mw} \times CMF_{awsc}$$

with,

$$N_{spf,A2B2} = e^{b_{0,A2B2} + b_{rural} I_{rural} + b_{xrd,A2B2} \ln(AADT_{xrd}/1,000) + b_{rmp,A2B2} \ln(AADT_{ex}/1,000 + AADT_{en}/1,000)} \quad (279)$$

$$N_{spf,A4D3ex} = e^{b_{0,A4D3ex} + b_{rural} I_{rural} + b_{xrd,A4D3ex} \ln(AADT_{xrd}/1,000) + b_{rmp,A4D3ex} \ln(AADT_{ex}/1,000 + AADT_{en}/1,000)} \quad (280)$$

$$N_{spf,B4D3en} = e^{b_{0,B4D3en} + b_{rural} I_{rural} + b_{xrd,B4D3en} \ln(AADT_{xrd}/1,000) + b_{rmp,B4D3en} \ln(AADT_{ex}/1,000 + AADT_{en}/1,000)} \quad (281)$$

$$N_{spf,D4} = e^{b_{0,D4} + b_{rural} I_{rural} + b_{xrd,D4} \ln(AADT_{xrd}/1,000) + b_{rmp,D4} \ln(AADT_{ex}/1,000 + AADT_{en}/1,000)} \quad (282)$$

$$CMF_{bay,lt} = [(0.36 I_{rural} + 0.59 [1.0 - I_{rural}]) P_{in} + 1.0 (1.0 - P_{in})]^{I_{bay,lt,in}} \times \quad (283)$$

$$[(0.36 I_{rural} + 0.59 [1.0 - I_{rural}]) P_{out} + 1.0 (1.0 - P_{out})]^{I_{bay,lt,out}}$$

$$CMF_{bay,rt} = [(0.76 I_{rural} + 0.87 [1.0 - I_{rural}]) P_{in} + 1.0 (1.0 - P_{in})]^{I_{bay,rt,in}} \times \quad (284)$$

$$[(0.76 I_{rural} + 0.87 [1.0 - I_{rural}]) P_{out} + 1.0 (1.0 - P_{out})]^{I_{bay,rt,out}}$$

$$CMF_{ap} = e^{b_{ns} n_{ps} P_{out}} + 1.0 (1.0 - P_{out}) \quad (285)$$

$$CMF_{sl} = e^{b_{sl} (1.0/L_{rmp} + 1.0/L_{str} - 0.333)} \quad (286)$$

$$CMF_{awsc} = e^{b_{awsc} I_{awsc}} \quad (287)$$

where,

CMF_{ap} = access point frequency crash modification factor;

CMF_{awsc} = all-way stop control crash modification factor; and

I_{awsc} = all-way stop control indicator variable (= 1.0 if ramp terminal has all-way stop controlled, 0.0 if it has one-way stop control for the exit ramp).

All other variables are defined previously.

The final form of the regression model is described here, before the discussion of regression analysis results. However, this form reflects the findings from several preliminary regression analyses where alternative model forms were examined. The form that is described represents that which provided the best fit to the data, while also having coefficient values that are logical and constructs that are theoretically defensible and properly bounded.

Equations 283 and 284 describe CMFs for left- and right-turn lane (or bay) presence, respectively. These CMFs are not associated with a regression coefficient. Rather, these CMFs are considered to be fairly definitive based on the extensive nature of the research that produced them (Harwood et al., 2002). The derivation of the leg-specific CMF values that are used in Equations 283 and 284 is described in the discussion associated with Table 64.

Equation 286 describes the relationship between ramp terminal crash frequency and the distance to the adjacent ramp and nearest public street intersection. The preliminary examination of the data indicated that crash frequency tends to increase as this distance increases.

Equation 287 describes the relationship between ramp terminal crash frequency and the presence of all-way stop control. If the ramp terminal has one-way stop control (with stop control for the exit ramp), then this CMF equals 1.0.

The CMF for median width CMF_{mw} was described previously using Equation 231. Similarly, the CMF for exit ramp capacity CMF_{rc} was described using Equation 235 and the CMF for skew was described using Equation 238. The indicator variables used in several of the CMFs were previously identified in Table 66 for typical ramp terminal configurations.

Model Calibration

The predictive model calibration process was based on a combined-model approach, as discussed in the section titled Modeling Approach. With this approach, the combined ramp terminal models and the CMFs (represented by Equations 278 to 287) are calibrated using a common database. This approach is needed because several CMFs are common to two or more of the ramp terminal models.

The models were calibrated using the California and Washington data. The Maine data were reserved for model validation. The discussion in this section focuses on the findings from the model calibration. The findings from model validation are provided in the next section.

The results of the combined regression model calibration are presented in Table 77. The Pearson χ^2 statistic for the model is 273, and the degrees of freedom are 240 ($= n - p = 260 - 20$). As this statistic is less than $\chi^2_{0.05, 240} (= 277)$, the hypothesis that the model fits the data cannot be rejected.

The t-statistic for each coefficient is listed in the last column of Table 77. These statistics describe a test of the hypothesis that the coefficient value is equal to 0.0. Those t-statistics with an absolute value that is larger than 2.0 indicate that the hypothesis can be rejected with the probability of error in this conclusion being less than 0.05. For those few variables where the absolute value of the t-statistic is smaller than 2.0, it was decided that the variable was important to the model and its trend was found to be intuitive and, where available, consistent with previous research findings (even if the specific value was not known with a great deal of certainty as applied to this database).

TABLE 77. Terminal FI model statistical description—combined model—two states—unsignalized

Model Statistics		Value		
R^2 :		0.41		
Scale parameter ϕ :		1.05		
Pearson χ^2 :		273 ($\chi^2_{0.05, 240} = 277$)		
Observations n_o :		260 terminals (325 injury or fatal crashes in 3 years)		
Calibrated Coefficient Values				
Variable	Inferred Effect of...	Value	Std. Dev.	t-statistic
b_{sk}	Skew angle between exit ramp and crossroad	0.487	0.333	1.5
b_{ns}	Unsignalized public street approaches	0.588	0.304	1.9
b_{sl}	Distance to adjacent ramp terminal and intersection	-0.0178	0.0079	-2.3
b_{rc}	Exit ramp capacity	0.162	0.046	3.5
b_{me}	Width of median adjacent to left-turn lane (or bay)	-0.0410	0.040	-1.0
$b_{AADT, me}$	AADT on median width	0.00411	0.0029	1.4
b_{awsc}	All-way stop control	-0.422	0.300	-1.4
$b_{0, A2B2}$	A2 and B2 ramp terminal configuration	-2.410	0.597	-4.0
$b_{xrd, A2B2}$	Crossroad AADT	0.232	0.389	0.6
$b_{rmp, A2B2}$	Ramp AADT	0.876	0.384	2.3
$b_{0, A4D3ex}$	A4 and D3ex ramp terminal configuration	-2.545	0.842	-3.0
$b_{xrd, A4D3ex}$	Crossroad AADT	0.369	0.374	1.0
$b_{rmp, A4D3ex}$	Ramp AADT	0.854	0.239	3.6
$b_{0, B4D3en}$	B4 and D3en ramp terminal configuration	-4.202	1.731	-2.4
$b_{xrd, B4D3en}$	Crossroad AADT	0.805	0.532	1.5
$b_{rmp, B4D3en}$	Ramp AADT	1.111	0.456	2.4
$b_{0, D4}$	D4 ramp terminal configuration	-3.049	0.355	-8.6
$b_{xrd, D4}$	Crossroad AADT	1.054	0.178	5.9
$b_{rmp, D4}$	Ramp AADT	0.140	0.157	0.9
b_{ln}	Rural area type	0.355	0.161	2.2

The findings from an examination of the coefficient values and the corresponding CMF or SPF predictions are documented in a subsequent section. In general, the sign and magnitude of the calibration coefficients in Table 77 are logical and consistent with previous research findings.

Model Validation

Model validation was a two-step process. The first step required using the calibrated models to predict the crash frequency for sites from a third state (i.e., Maine). The objective of this step was to demonstrate the robustness of the model structure and its transferability to another state.

The second step required comparing the calibrated CMFs with similar CMFs reported in the literature, where such information was available. The objective of this step was to demonstrate that the calibrated CMFs were consistent with previous research findings.

The findings from the first step of the validation process are described in this section. Those from the second step are described in the next section.

The first step of the validation process consisted of several tasks. The first task was to quantify the local calibration factor for each of the four ramp terminal models, which would be the first step for any agency using the *HSM* methodology. However, only a single, overall calibration factor could be computed because there are only 41 unsignalized ramp terminals in the Maine database. This overall calibration factor was used to produce a “re-calibrated” set of models (i.e., the models with the coefficients from Table 77 plus the local calibration factors). The local calibration factor value for the Maine data C_{me} was computed as 0.81.

The second task was to apply the re-calibrated models to the Maine data to compute the predicted average crash frequency for each ramp terminal. The predicted crash frequency was then compared to the reported crash frequency for each site.

The third task was to compute the fit statistics and assess the robustness of the combined calibrated model. These statistics are listed in Table 78. The Pearson χ^2 statistic for combined model is less than $\chi^2_{0.05}$ so the hypothesis that the model fits the validation data cannot be rejected.

TABLE 78. Terminal model validation statistics—unsignalized

R^2	R_k^2	Scale Parameter ϕ	Pearson χ^2	Deg. of Freedom	$\chi^2_{0.05, n-1}$
0.28	0.39	1.14	45.7	40	55.8

The findings from this validation step indicate that the trends in the Maine data are not significantly different from those in the California and Washington data. These findings also suggest that the model structure is transferable to other states (when locally calibrated) for the prediction of FI crash frequency. Based on these findings, the data for the three states were combined and used in a second regression model calibration. The larger sample size associated with the combined database reduced the standard error of several calibration coefficients. Bared and Zhang (2007) also used this approach in their development of predictive models for urban freeways.

Combined Model

The data from the three study states were combined and the predictive models were calibrated a second time using the combined data. The calibration coefficients for the combined ramp terminal models are described first. Then, the fit statistics and inverse dispersion parameter for each ramp terminal model are described.

The results of the combined regression model calibration are presented in Table 79. The Pearson χ^2 statistic for the model is 311, and the degrees of freedom are 281 ($= n - p = 301 - 20$). As this statistic is less than $\chi^2_{0.05, 281}$ ($= 321$), the hypothesis that the model fits the data cannot be rejected. Several terminals were removed as a result of outlier analysis such that the calibration database included only 365 of the 420 crashes identified in Chapter 4.

TABLE 79. Terminal FI model statistical description—combined model—three states—unsignalized

Model Statistics		Value		
R^2 :		0.40		
Scale parameter ϕ :		1.04		
Pearson χ^2 :		311 ($\chi^2_{0.05, 281} = 321$)		
Observations n_o :		301 terminals (365 injury or fatal crashes in 3 years)		
Calibrated Coefficient Values				
Variable	Inferred Effect of...	Value	Std. Dev.	t-statistic
b_{sk}	Skew angle between exit ramp and crossroad	0.341	0.404	0.8
b_{ns}	Unsignalized public street approaches	0.522	0.309	1.7
b_{sl}	Distance to adjacent ramp terminal and intersection	-0.0141	0.0075	-1.9
b_{rc}	Exit ramp capacity	0.151	0.046	3.3
b_{me}	Width of median adjacent to left-turn lane (or bay)	-0.0322	0.036	-0.9
$b_{AADT, me}$	AADT on median width	0.00354	0.0027	1.3
b_{awsc}	All-way stop control	-0.377	0.295	-1.3
$b_{0, A2B2}$	A2 and B2 ramp terminal configuration	-2.687	0.588	-4.6
$b_{xrd, A2B2}$	Crossroad AADT	0.260	0.357	0.7
$b_{rmp, A2B2}$	Ramp AADT	0.947	0.348	2.7
$b_{0, A4D3ex}$	A4 and D3ex ramp terminal configuration	-3.223	0.847	-3.8
$b_{xrd, A4D3ex}$	Crossroad AADT	0.582	0.376	1.5
$b_{rmp, A4D3ex}$	Ramp AADT	0.899	0.228	4.0
$b_{0, B4D3en}$	B4 and D3en ramp terminal configuration	-3.141	0.992	-3.2
$b_{xrd, B4D3en}$	Crossroad AADT	0.709	0.384	1.8
$b_{rmp, B4D3en}$	Ramp AADT	0.730	0.323	2.3
$b_{0, D4}$	D4 ramp terminal configuration	-3.064	0.331	-9.2
$b_{xrd, D4}$	Crossroad AADT	1.008	0.171	5.9
$b_{rmp, D4}$	Ramp AADT	0.177	0.149	1.2
b_{ln}	Rural area type	0.324	0.147	2.2

The t-statistic for each coefficient is listed in the last column of Table 79. These statistics have generally increased, relative to their counterparts in Table 77, as a result of the increased sample size. With a few exceptions, these statistics have an absolute value that is larger than 2.0, which indicates that the null hypothesis can be rejected with the probability of error in this conclusion being less than 0.05. For those few variables where the absolute value of the t-statistic is smaller than 2.0, it was decided that the variable was important to the model and its trend was found to be intuitive and, where available, consistent with previous research findings (even if the specific value was not known with a great deal of certainty as applied to this database). This consistency is demonstrated in a subsequent section.

Model for A2 and B2 Configurations. The statistics describing the calibrated model for A2 and B2 ramp terminal configurations are presented in Table 80. The Pearson χ^2 statistic for the model is 32.9, and the degrees of freedom are 39 ($= n - p = 40 - 1$). As this statistic is less than $\chi^2_{0.05, 39} (= 55)$, the hypothesis that the model fits the data cannot be rejected. The R^2 for the model is 0.55. The R_k^2 for the calibrated model is 1.00.

TABLE 80. Terminal FI model statistical description—A2 and B2 configuration—unsignalized

Model Statistics	Value
$R^2 (R_k^2)$:	0.55 (1.00)
Scale parameter ϕ :	0.84
Pearson χ^2 :	32.9 ($\chi^2_{0.05, 39} = 55$)
Inverse dispersion parameter K :	99 (3.40 recommended for empirical Bayes applications)
Observations n_o :	40 terminals (61 injury or fatal crashes in 3 years)
Standard deviation s_e :	± 0.34 crashes/yr

The fit of the model to the data was sufficiently good that the inverse overdispersion factor was infinitely large such that the error distribution converged to a Poisson distribution. However, this result is likely an aberration of the data (i.e., relatively small sample coupled with too much similarity among ramp terminals). The true error distribution for these configurations is undoubtedly negative binomial and the inverse dispersion parameter is likely to be much lower than 99.

It is desirable to have an estimate of the inverse dispersion parameter K for empirical Bayes applications of the predictive method. A lower bound on this parameter was obtained by conducting a regression analysis using the null model (i.e., $N = b_0$) with a negative binomial distribution. The parameter for this model K_{null} was 3.40. The true value of K for the calibrated model is likely to be larger than 3.40 but less than 99. Hence, for the empirical Bayes application a conservatively small value of K equal to 3.40 is recommended.

The coefficients in Table 79 were combined with Equation 279 to obtain the calibrated SPF for the A2 and B2 configuration. The form of the model is described in the following equation.

$$N_{spf, A2B2} = e^{-2.687 + 0.324 I_{rural} + 0.260 \ln(AADT_{srd}/1,000) + 0.947 \ln(AADT_{ca}/1,000 + AADT_{cm}/1,000)} \quad (288)$$

The calibrated CMFs used with this SPF are described in a subsequent section.

The fit of the calibrated model is shown in Figure 119. This figure compares the predicted and reported crash frequency in the calibration database. In general, the data shown in the figure indicate that the model provides an unbiased estimate of expected crash frequency for ramp terminals experiencing up to 5 crashes in a three-year period.

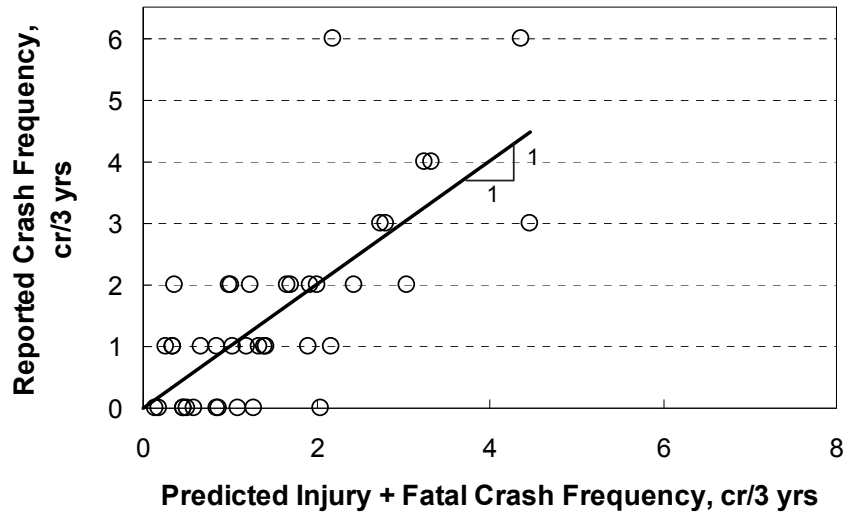


Figure 119. Predicted vs. reported FI crashes at unsignalized A2 and B2 configurations.

Model for A4 and D3ex Configurations. The statistics describing the calibrated model for A4 and D3ex ramp terminal configurations are presented in Table 81. The Pearson χ^2 statistic for the model is 35.1, and the degrees of freedom are 36 ($= n - p = 37 - 1$). As this statistic is less than $\chi^2_{0.05,36}$ ($= 51$), the hypothesis that the model fits the data cannot be rejected. The R^2 for the model is 0.55. The R_k^2 for the calibrated model is 0.88. The inverse dispersion parameter was adjusted using Equation 249.

TABLE 81. Terminal FI model statistical description—A4 and D3ex configuration—unsignalized

Model Statistics	Value
R^2 (R_k^2):	0.55 (0.88)
Scale parameter ϕ :	0.88
Pearson χ^2 :	31.5 ($\chi^2_{0.05,36} = 51$)
Inverse dispersion parameter K :	2.16
Observations n_o :	37 terminals (58 injury or fatal crashes in 3 years)
Standard deviation s_e :	± 0.51 crashes/yr

The coefficients in Table 79 were combined with Equation 280 to obtain the calibrated SPF for the A4 and D3ex configuration. The form of the model is described in the following equation.

$$N_{spf, A4D3ex} = e^{-3.223 + 0.324 I_{rural} + 0.582 \ln(AADT_{rd}/1,000) + 0.899 \ln(AADT_{ex}/1,000 + AADT_{en}/1,000)} \quad (289)$$

The calibrated CMFs used with this SPF are described in a subsequent section. The AADT volume of the loop entrance ramp at an A4 configuration is not included in $AADT_{en}$. Also, $AADT_{en}$ equals 0.0 when the SPF is applied to a D3ex configuration.

The fit of the calibrated model is shown in Figure 120. In general, the data shown in the figure indicate that the model provides an unbiased estimate of expected crash frequency for ramp terminals experiencing up to 8 crashes in a three-year period.

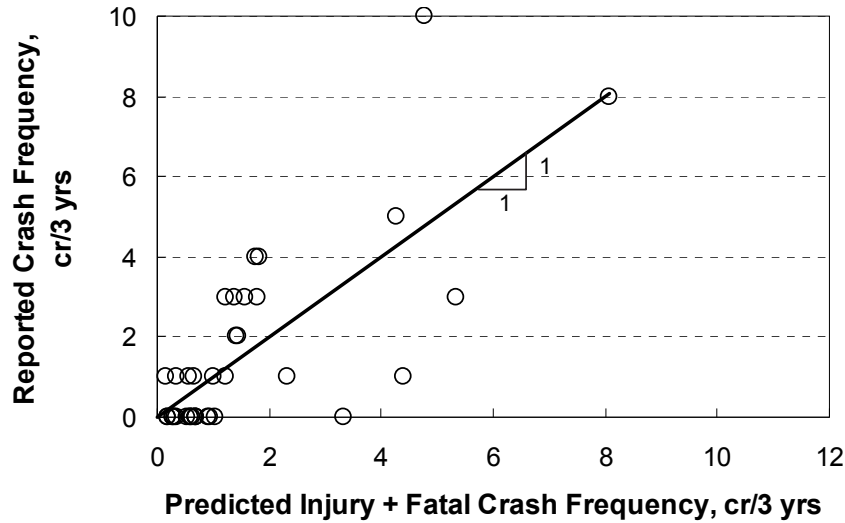


Figure 120. Predicted vs. reported FI crashes at unsignalized A4 and D3ex configurations.

Model for B4 and D3en Configurations. The statistics describing the calibrated model for B4 and D3en ramp terminal configurations are presented in Table 82. The Pearson χ^2 statistic for the model is 17.8, and the degrees of freedom are 21 ($= n - p = 22 - 1$). As this statistic is less than $\chi^2_{0.05,21}$ ($= 33$), the hypothesis that the model fits the data cannot be rejected. The R^2 for the model is 0.22. The R_k^2 for the calibrated model is 0.81. The inverse dispersion parameter was adjusted using Equation 249.

TABLE 82. Terminal FI model statistical description—B4 and D3en configuration—unsignalized

Model Statistics	Value
R^2 (R_k^2):	0.22 (0.81)
Scale parameter ϕ :	0.85
Pearson χ^2 :	17.8 ($\chi^2_{0.05,21} = 33$)
Inverse dispersion parameter K :	0.918
Observations n_o :	22 terminals (40 injury or fatal crashes in 3 years)
Standard deviation s_e :	± 0.61 crashes/yr

The coefficients in Table 79 were combined with Equation 281 to obtain the calibrated SPF for the B4 and D3en configuration. The form of the model is described by the following equation.

$$N_{spf, B4D3en} = e^{-3.141 + 0.324 I_{rural} + 0.709 \ln(AADT_{xrd} / 1,000) + 0.730 \ln(AADT_{ex} / 1,000 + AADT_{en} / 1,000)} \quad (290)$$

The calibrated CMFs used with this SPF are described in a subsequent section. The AADT volume of the loop exit ramp at a B4 configuration is not included in $AADT_{ex}$. Also, $AADT_{ex}$ equals 0.0 when the SPF is applied to a D3en configuration.

The fit of the calibrated model is shown in Figure 121. In general, the data shown in the figure indicate that the model provides an unbiased estimate of expected crash frequency for ramp terminals experiencing up to 8 crashes in a three-year period.

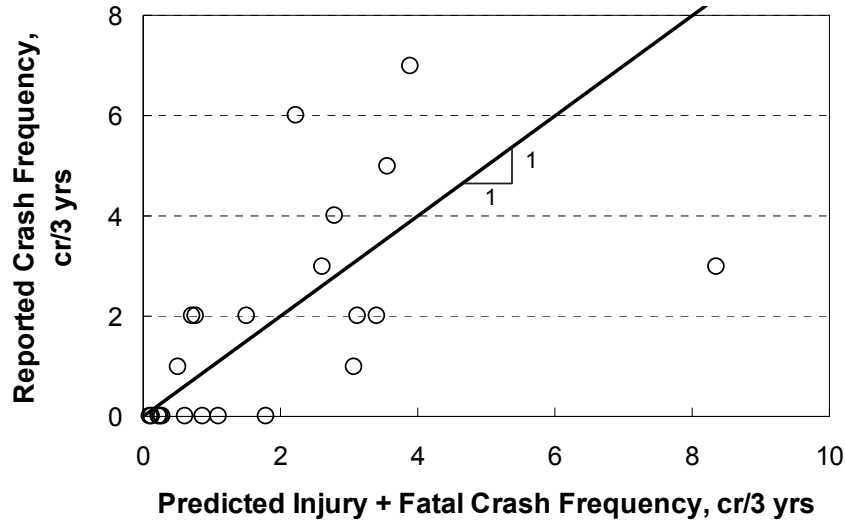


Figure 121. Predicted vs. reported FI crashes at unsignalized B4 and D3en configurations.

Model for D4 Configuration. The statistics describing the calibrated model for D4 ramp terminal configuration are presented in Table 83. The Pearson χ^2 statistic for the model is 214, and the degrees of freedom are 201 ($= n - p = 202 - 1$). As this statistic is less than $\chi^2_{0.05,201}$ ($= 235$), the hypothesis that the model fits the data cannot be rejected. The R^2 for the model is 0.31. The R_k^2 for the calibrated model is 0.74. The inverse dispersion parameter was adjusted using Equation 249.

TABLE 83. Terminal FI model statistical description—D4 configuration—unsignalized

Model Statistics	Value
R^2 (R_k^2):	0.31 (0.74)
Scale parameter ϕ :	1.06
Pearson χ^2 :	214 ($\chi^2_{0.05,201} = 235$)
Inverse dispersion parameter K :	2.58
Observations n_o :	202 terminals (206 injury or fatal crashes in 3 years)
Standard deviation s_e :	± 0.41 crashes/yr

The coefficients in Table 79 were combined with Equation 282 to obtain the calibrated SPF for the D4 configuration. The form of the model is described in the following equation.

$$N_{spf,D4} = e^{-3.064 + 0.324 I_{rural} + 1.008 \ln(AADT_{3rd}/1,000) + 0.177 \ln(AADT_{ex}/1,000 + AADT_{en}/1,000)} \quad (291)$$

The calibrated CMFs used with this SPF are described in a subsequent section.

The fit of the calibrated model is shown in Figure 122. In general, the data shown in the figure indicate that the model provides an unbiased estimate of expected crash frequency for ramp terminals experiencing up to 4 crashes in a three-year period.

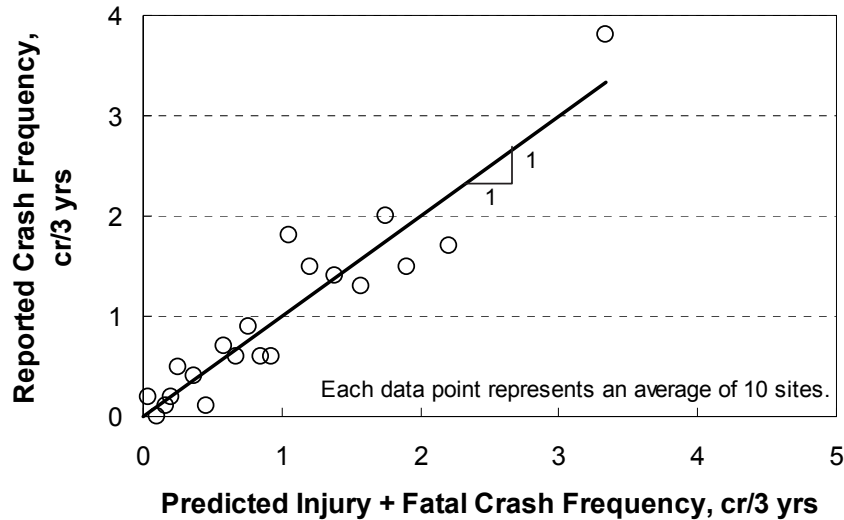


Figure 122. Predicted vs. reported FI crashes at unsignalized D4 configurations.

Each data point shown in Figure 122 represents the average predicted and average reported crash frequency for a group of 10 ramp terminals. The data were sorted by predicted crash frequency to form groups of terminals with similar crash frequency. The purpose of this grouping was to reduce the number of data points shown in the figure and, thereby, to facilitate an examination of trends in the data. The individual terminal observations were used for model calibration.

Calibrated CMFs

Several CMFs were calibrated in conjunction with the SPFs. All of them were calibrated using FI crash data. Collectively, they describe the relationship between various geometric factors and crash frequency. These CMFs are described in this section and, where possible, compared with the findings from previous research as means of model validation.

Many of the CMFs found in the literature are typically derived from (and applied to) “intersection” crashes. That is, one CMF is used to indicate the influence of a leg-specific geometric factor on total crashes. In contrast, the models developed for this research project include several CMFs that are calibrated for leg-specific conditions. In these instances,

Equations 222 and 226 were used to convert the leg-specific CMF to an intersection CMF. The converted CMFs are compared in this subsection with the intersection CMFs reported in the literature using typical values for the leg AADT distribution at intersections (as opposed to that found at ramp terminals).

The following CMFs were described previously in this chapter and are not discussed in this section. The figure provided for the last CMF listed is based on the calibration coefficients in Table 79.

- crossroad left-turn lane CMF (Equation 283, Table 64);
- crossroad right-turn lane CMF (Equation 284, Table 64); and
- skew angle CMF (Equation 238, Figure 108).

Exit Ramp Capacity CMF. The exit ramp capacity CMF is described using the following equation.

$$CMF_{rc} = e^{0.151 \frac{AADT_{ex}}{1,000 n_{ex,eff}}} P_{ex} + 1.0 (1.0 - P_{ex}) \quad (292)$$

Guidance for using this CMF was provided in the CMF Development part of this chapter (in the section titled Exit Ramp Capacity CMF).

The exit ramp capacity CMF is shown in Figure 123. The trend line shown indicates that the CMF value increases with increasing exit ramp AADT volume. For a given AADT volume, the CMF value is lower with a two-lane ramp than a one-lane ramp. For a given AADT volume on a two-lane ramp, the CMF value is lower for the ramp with right-turn merge operation than the ramp with right-turn stop control. This trend is consistent with the Exit Ramp Capacity CMF described previously for signalized ramp terminals.

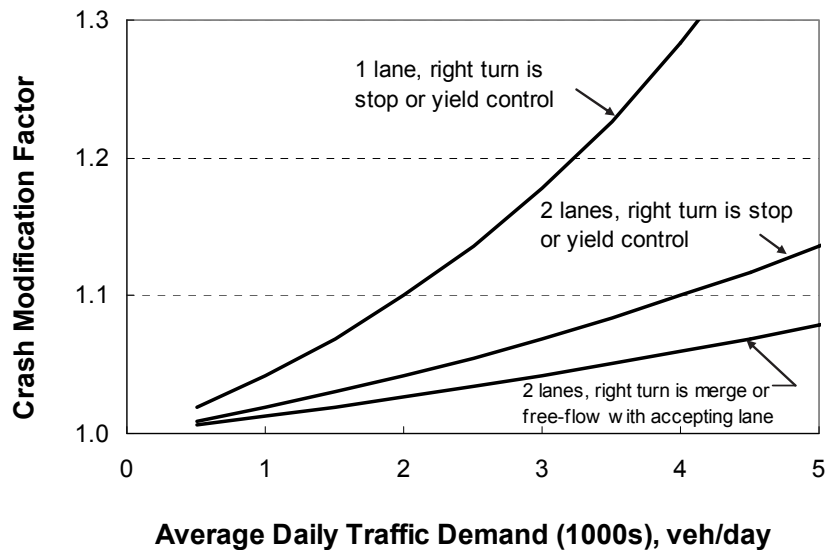


Figure 123. Calibrated exit ramp capacity CMF for FI crashes—unsignalized.

Access Point Frequency CMF. The access point frequency CMF is described using the following equation.

$$CMF_{ap} = e^{0.522 n_{ps} P_{out}} + 1.0 (1.0 - P_{out}) \quad (293)$$

This CMF applies to any ramp terminal with one or more unsignalized public street approaches on the crossroad leg that is outside of the interchange. Approaches on both sides of the leg should be counted when they are within 250 ft of the ramp terminal.

The values obtained from this CMF are listed in Table 84 for ramp terminals and for intersections. The CMF values for ramp terminals reflect the proportion of total leg AADT on crossroad legs that are typical for ramp terminals. The CMF values for intersections are based on leg AADT proportions that are more consistent with those found on the major street at the intersection of a major and minor street.

TABLE 84. Calibrated access point frequency CMF for FI crashes—unsignalized

Junction Location	Proportion AADT on Leg	CMF Value by Number of Public Street Approaches	
		1	2
Ramp terminal	0.39	1.26	1.71
Intersection ¹	0.35	1.24	1.64

Note:

1 - Intersection CMFs are computed using Equation 293 and the AADT proportion shown in the table.

Segment Length CMF. The segment length CMF is described using the following equation.

$$CMF_{sl} = e^{-0.0141(1.0/L_{rmp} + 1.0/L_{str} - 0.333)} \quad (294)$$

This CMF is applicable to all ramp configurations. It describes the relationship between ramp terminal crash frequency and the distance to the adjacent ramp or nearest public street intersection. The adjacent ramp or intersection can be signalized or unsignalized.

The distances used to calibrate this CMF were as small as 100 ft. The base condition for this CMF is no adjacent ramp or public street intersection (i.e., $L_{rmp} = L_{str} = 6.0$ mi).

The segment length CMF is shown in Figure 124. The trend line shown indicates that the CMF value increases with increasing distance. It is rationalized that the distance between the subject ramp and its adjacent ramp and intersection is correlated with crossroad operating speed. This speed is likely to increase as distance increases, and an increase in speed is likely to increase the risk of a crash.

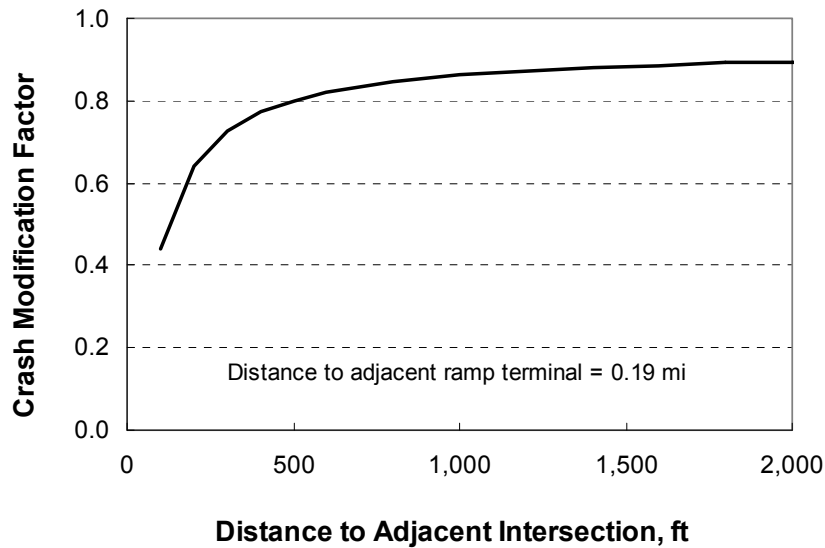


Figure 124. Calibrated segment length CMF for FI crashes—unsignalized.

All-Way Stop Control CMF. The all-way stop control CMF is described using the following equation.

$$CMF_{awsc} = e^{-0.377 I_{awsc}} \quad (295)$$

This CMF is applicable to any ramp terminal where an engineering study has determined that all-way stop control is appropriate. The base condition is one-way stop control for the ramp terminal with stop control for the exit ramp left-turn movement.

The regression coefficient indicates that the CMF has a value of 0.686 when applied to all-way stop-controlled ramp terminals. Chapter 14 of the *HSM* identifies a CMF value of 0.30 for urban intersections converted from minor-road stop control to all-way stop control. It identifies a CMF value of 0.52 for rural intersections undergoing this conversion.

Median Width CMF. The median width CMF is described using the following equation.

$$CMF_{mw} = \left[e^{(-0.0322 + 0.00354 AADT_{in}/1,000) W_{me,in}} P_{in} + 1.0 (1.0 - P_{in}) \right] \times \left[e^{(-0.0322 + 0.00354 AADT_{out}/1,000) W_{me,out}} P_{out} + 1.0 (1.0 - P_{out}) \right] \quad (296)$$

with,

$$W_{me,k} = W_m - W_{mb,k} \geq 0.0 \quad (297)$$

$$W_{mb,k} = \text{Max}(W_{b,k}; 12) \quad (298)$$

Guidance for using this CMF was provided in the CMF Development part of this chapter (in the section titled Median Width CMF). The constant “12” represents the minimum median width below which the CMF value is 1.0. This value is decreased from the 14 ft value stated in

the *HSM* based on the trends found in the ramp terminal safety database. The applicable AADTs range from 0 to 14,000 veh/day. AADT volumes larger than 14,000 should be set to 14,000 in Equation 296. The median width CMF is shown in Figure 105.

Sensitivity Analysis

The relationship between crash frequency and traffic demand, as obtained from the combined calibrated models, is illustrated in Figure 125 for unsignalized ramp terminals. The distance between ramps is 0.19 mi and the distance to the nearest public street intersection is also 0.19 mi. The ramp terminal is located in an urban area. All other geometric and control conditions are such that the associated CMF has a value of 1.0. The axis scale for each graph in Figure 125 is the same. This technique is used to facilitate comparison among ramp configurations.

Figure 125a also shows the SPF for urban three-leg unsignalized intersections that is described in the *HSM*. Similarly, Figure 125f shows the SPF for urban four-leg unsignalized intersections that is described in the *HSM*. The trend lines shown in Figure 125a indicate that three-leg ramp terminals have about the same number of crashes as three-leg intersections. In contrast, the trend lines in Figure 125f suggest that four-leg ramp terminals can have up to 25 percent fewer crashes than four-leg intersections.

The A2, B2, and D3 configurations are shown in Figure 125 to have fewer crashes than the other configurations, for a given AADT volume. This trend is likely due to the fact that these configurations have only three legs, while the other configurations have four legs. The number of conflict points increases significantly with the number of legs.

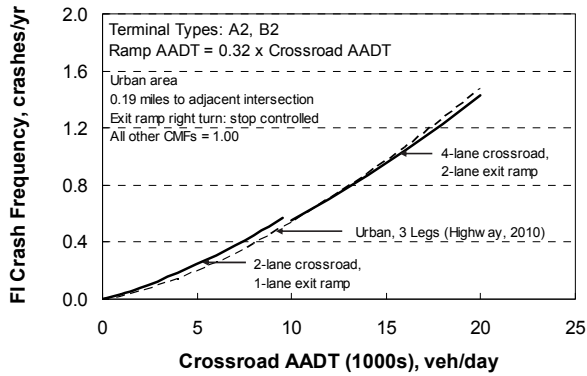
MODEL CALIBRATION FOR PDO CRASHES

This part of the chapter describes the calibration of the crossroad ramp terminal predictive models based on PDO crashes. The methodology used to calibrate the models is described in the part titled Methodology. The calibration data, model development, and statistical analysis methods are described in the part titled Model Calibration for FI Crashes.

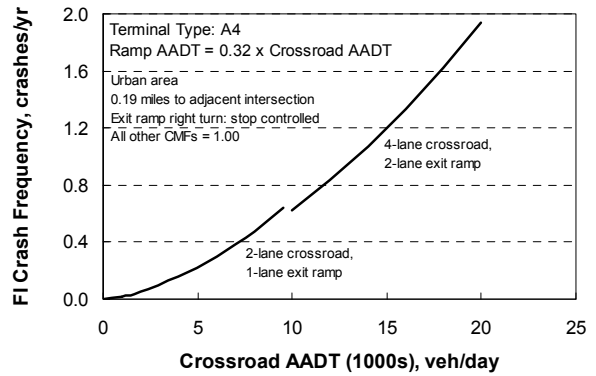
Signalized Ramp Terminal Models

This section describes the calibrated PDO crash prediction models for signalized ramp terminals. The regression model used had the same form as used to develop the FI crash prediction model (i.e., Equation 250). The turn bay CMFs were obtained from Table 65.

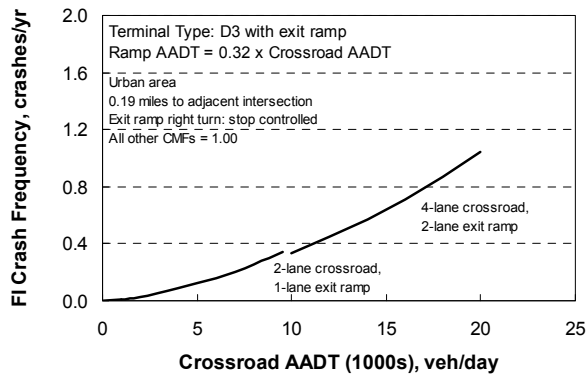
An initial regression analysis was undertaken with county and state variable combinations treated as fixed effects and as random effects. The Hausman test was performed using the covariance matrix to determine whether the fixed effect model was appropriate. The null hypothesis is that the regression coefficients from the two model treatments are consistent. This hypothesis was rejected ($p = 0.0001$) indicating that the coefficients are different (i.e., inconsistent) among the two treatments. In this case, it is concluded that the regression coefficient values are influenced by county so a fixed-effect treatment is needed to remove the county effect.



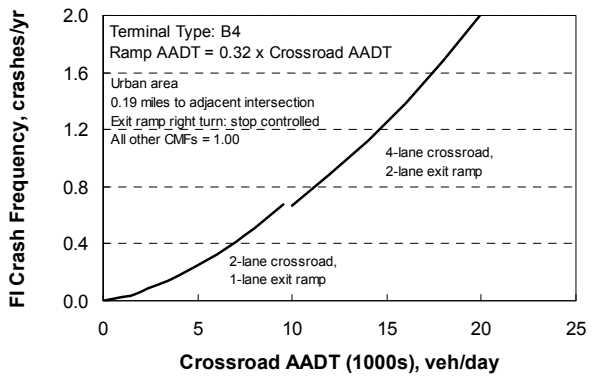
a. Terminal types A2 and B2.



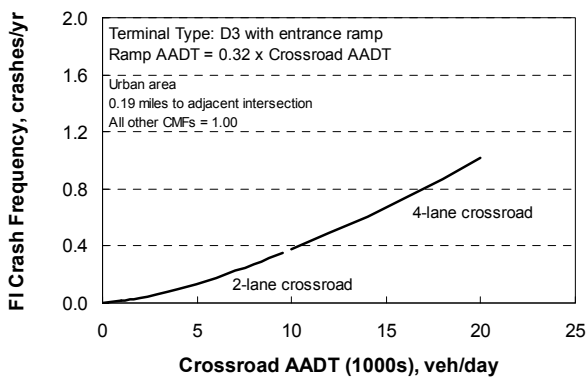
b. Terminal type A4.



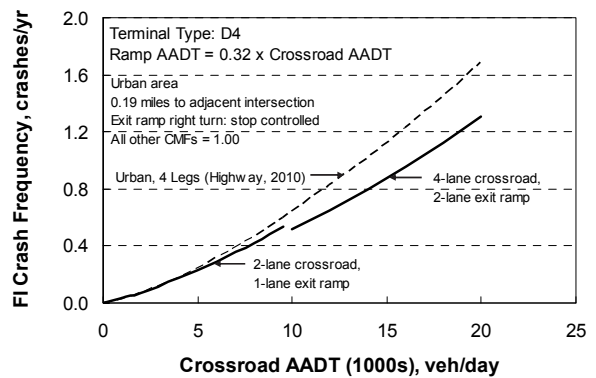
c. Terminal Type D3 with exit ramp.



d. Terminal type B4.



e. Terminal Type D3 with entrance ramp.



f. Terminal type D4.

Figure 125. Terminal FI models—unsignalized.

Model Calibration

The results of the regression model calibration are presented in Table 85. The Pearson χ^2 statistic for the model is 219, and the degrees of freedom are 215 ($= n - p = 236 - 21$). As this statistic is less than $\chi^2_{0.05, 215}$ ($= 250$), the hypothesis that the model fits the data cannot be rejected. Several segments were removed as a result of outlier analysis such that the calibration database included only 3,245 of the 3,349 crashes identified in Chapter 4.

TABLE 85. Terminal PDO model statistical description—combined model—three states—signalized

Model Statistics		Value		
R^2 :		0.53		
Scale parameter ϕ :		0.93		
Pearson χ^2 :		219 ($\chi^2_{0.05, 215} = 250$)		
Observations n_o :		236 terminals (3,245 PDO crashes in 3 years)		
Calibrated Coefficient Values				
Variable	Inferred Effect of...	Value	Std. Dev.	t-statistic
$b_{p, lt}$	Protected left-turn operation	-0.223	0.089	-2.5
$b_{ch, xrd}$	Right-turn channelization on crossroad	0.465	0.210	2.2
$b_{ch, ex}$	Right-turn channelization on exit ramp	1.429	0.231	6.2
b_{nd}	Driveways or unsignalized public street approaches	0.203	0.079	2.6
b_{ps}	Public street leg at ramp terminal	0.520	0.277	1.9
b_{sl}	Distance to adjacent ramp terminal and intersection	-0.0186	0.0049	-3.8
b_{me}	Width of median adjacent to left-turn lane (or bay)	0.0610	0.0242	2.5
$b_{AADT, me}$	AADT on median width	-0.00246	0.0010	-2.4
$b_{0, A2B2}$	A2 and B2 ramp terminal configuration	-2.309	0.886	-2.6
$b_{xrd, A2B2}$	Crossroad AADT	0.592	0.304	1.9
$b_{rmp, A2B2}$	Ramp AADT	0.516	0.217	2.4
$b_{0, A4D3ex}$	A4 and D3ex ramp terminal configuration	-2.755	0.801	-3.4
$b_{xrd, A4D3ex}$	Crossroad AADT	0.797	0.227	3.5
$b_{rmp, A4D3ex}$	Ramp AADT	0.384	0.119	3.2
$b_{0, B4D3en}$	B4 and D3en ramp terminal configuration	-3.543	1.725	-2.1
$b_{xrd, B4D3en}$	Crossroad AADT	0.741	0.411	1.8
$b_{rmp, B4D3en}$	Ramp AADT	0.845	0.655	1.3
$b_{0, D4}$	D4 ramp terminal configuration	-3.058	0.522	-5.9
$b_{xrd, D4}$	Crossroad AADT	0.879	0.186	4.7
$b_{rmp, D4}$	Ramp AADT	0.545	0.182	3.0
b_{ln}	Number of through lanes	0.0879	0.055	1.6

The t-statistic for each coefficient is listed in the last column of Table 85. These statistics describe a test of the hypothesis that the coefficient value is equal to 0.0. Those t-statistics with an absolute value that is larger than 2.0 indicate that the hypothesis can be rejected with the probability of error in this conclusion being less than 0.05. For those few variables where the absolute value of the t-statistic is smaller than 2.0, it was decided that the variable was important to the model and its trend was found to be intuitive and, where available, consistent with

previous research findings (even if the specific value was not known with a great deal of certainty as applied to this database).

The coefficients for forty-three county indicator variables are not shown in Table 85 because their individual significance is not directly relevant to model fit assessment or its application. However, it is recognized that the “intercept” variables in Table 85 (i.e., $b_{0, A2B2}$, $b_{0, A4D3ex}$, $b_{0, B4D3en}$, $b_{0, D4}$) correspond to only one state and county combination. Desirably, the intercept would represent an average value for all states and counties in the database. To this end, the predicted crash frequencies from the model described by Table 85 were submitted to a second regression analysis using Equation 115 (in Chapter 5).

The regression coefficient c_o was determined to be 0.596 for the A2B2 intercept, 0.332 for the A4D3ex intercept, 0.436 for the B4D3en intercept, and 0.634 for the D4 intercept. Each of these values is added to the appropriate intercept variables to compute an average intercept value for the overall database. This addition is shown in the models described in the next section.

Calibrated Models

This section describes the fit statistics and inverse dispersion parameter for each of the four ramp terminal models. It also shows the model form with the calibration coefficients from Table 85.

Model for A2 and B2 Configurations. The statistics describing the calibrated model for A2 and B2 ramp terminal configurations are presented in Table 86. The Pearson χ^2 statistic for the model is 27.0, and the degrees of freedom are 31 ($= n - p = 32 - 1$). As this statistic is less than $\chi^2_{0.05,31} (= 45.0)$, the hypothesis that the model fits the data cannot be rejected. The R^2 for the model is 0.62. The R_k^2 for the calibrated model is 0.77. The inverse dispersion parameter was adjusted using Equation 249.

TABLE 86. Terminal PDO model statistical description—A2 and B2 configuration—signalized

Model Statistics	Value
$R^2 (R_k^2)$:	0.62 (0.77)
Scale parameter ϕ :	0.87
Pearson χ^2 :	27.0 ($\chi^2_{0.05,31} = 45$)
Inverse dispersion parameter K :	4.27
Observations n_o :	32 terminals (321 PDO crashes in 3 years)
Standard deviation s_e :	± 2.12 crashes/yr

The coefficients in Table 85 were combined with the regression model to obtain the calibrated SPF for the A2 and B2 configuration. The form of the model is described in the following equation.

$$N_{spf, A2B2} = e^{-2.309 + 0.596 + 0.0879 n_{th} + 0.592 \ln(AADT_{rd}/1,000) + 0.516 \ln(AADT_{ex}/1,000 + AADT_{en}/1,000)} \quad (299)$$

The calibrated CMFs used with this SPF are described in a subsequent section.

The fit of the calibrated model is shown in Figure 126. This figure compares the predicted and reported crash frequency in the calibration database. In general, the data shown in the figure indicate that the model provides an unbiased estimate of expected crash frequency for ramp terminals experiencing up to 20 crashes in a three-year period.

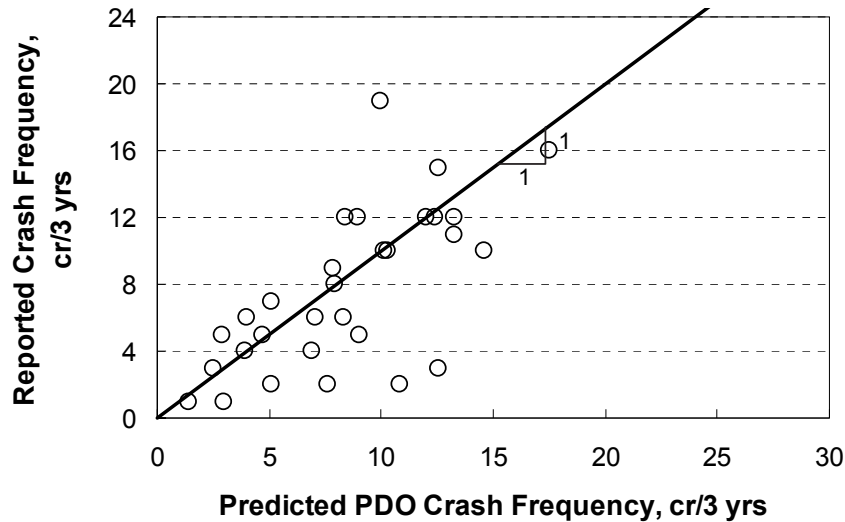


Figure 126. Predicted vs. reported PDO crashes at signalized A2 and B2 configurations.

Model for A4 and D3ex Configurations. The statistics describing the calibrated model for A4 and D3ex ramp terminal configurations are presented in Table 87. The Pearson χ^2 statistic for the model is 55.1, and the degrees of freedom are 59 ($= n - p = 60 - 1$). As this statistic is less than $\chi^2_{0.05,59}$ ($= 78$), the hypothesis that the model fits the data cannot be rejected. The R^2 for the model is 0.48. The R_k^2 for the calibrated model is 0.56. The inverse dispersion parameter was adjusted using Equation 249.

TABLE 87. Terminal PDO model statistical description—A4 and D3ex configuration—signalized

Model Statistics	Value
R^2 (R_k^2):	0.48 (0.56)
Scale parameter ϕ :	0.93
Pearson χ^2 :	55.1 ($\chi^2_{0.05,59} = 78$)
Inverse dispersion parameter K :	4.05
Observations n_o :	60 terminals (814 PDO crashes in 3 years)
Standard deviation s_e :	± 2.48 crashes/yr

The coefficients in Table 85 were combined with the regression model to obtain the calibrated SPF for the A4 and D3ex configuration. The form of the model is:

$$N_{spf, A4D3ex} = e^{-2.755 + 0.332 + 0.0879 n_{th} + 0.797 \ln(AADT_{xrd} / 1,000) + 0.384 \ln(AADT_{ex} / 1,000 + AADT_{en} / 1,000)} \quad (300)$$

The calibrated CMFs used with this SPF are described in a subsequent section. The AADT volume of the loop entrance ramp at an A4 configuration is not included in $AADT_{en}$. Also, $AADT_{en}$ equals 0.0 when the SPF is applied to a D3ex configuration.

The fit of the calibrated model is shown in Figure 127. In general, the data shown in the figure indicate that the model provides an unbiased estimate of expected crash frequency for ramp terminals experiencing up to 30 crashes in a three-year period.

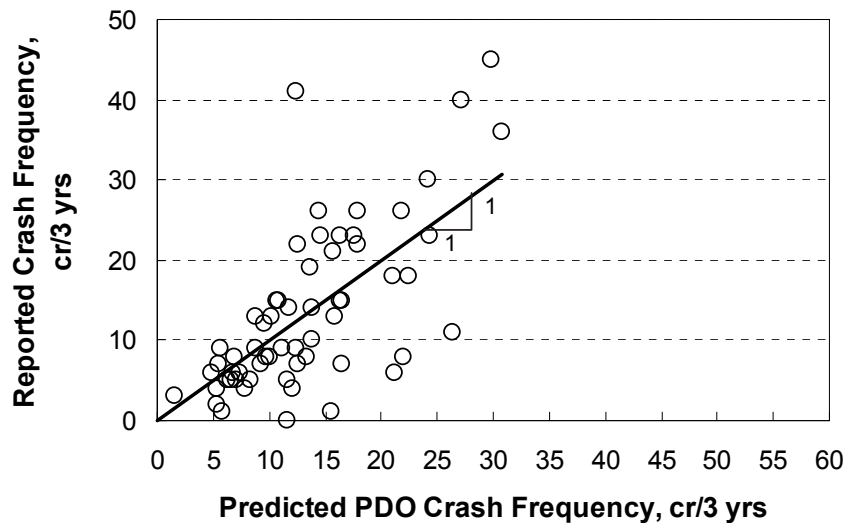


Figure 127. Predicted vs. reported PDO crashes at signalized A4 and D3ex configurations.

Model for B4 and D3en Configurations. The statistics describing the calibrated model for B4 and D3en ramp terminal configurations are presented in Table 88. The Pearson χ^2 statistic for the model is 2.50, and the degrees of freedom are 3 ($= n - p = 4 - 1$). As this statistic is less than $\chi^2_{0.05,3} (= 7.8)$, the hypothesis that the model fits the data cannot be rejected. The R^2 for the model is 0.27. The R_k^2 for the calibrated model is 0.63. The inverse dispersion parameter was adjusted using Equation 249.

TABLE 88. Terminal PDO model statistical description—B4 and D3en configuration—signalized

Model Statistics	Value
$R^2 (R_k^2)$:	0.27 (0.63)
Scale parameter ϕ :	0.83
Pearson χ^2 :	2.50 ($\chi^2_{0.05,3} = 7.8$)
Inverse dispersion parameter K :	3.72
Observations n_o :	4 terminals (61 PDO crashes in 3 years)
Standard deviation s_e :	± 3.75 crashes/yr

The coefficients in Table 85 were combined with the regression model to obtain the calibrated SPF for the B4 and D3en configuration. The form of the model is described in the following equation.

$$N_{spf, B4D3en} = e^{-3.543 + 0.436 n_{th} + 0.0879 \ln(AADT_{xrd}/1,000) + 0.845 \ln(AADT_{ex}/1,000 + AADT_{en}/1,000)} \quad (301)$$

The calibrated CMFs used with this SPF are described in a subsequent section. The AADT volume of the loop exit ramp at a B4 configuration is not included in $AADT_{ex}$. Also, $AADT_{ex}$ equals 0.0 when the SPF is applied to a D3en configuration.

The fit of the calibrated SPF is shown in Figure 128. The small number of observations for this configuration limits the ability to make broad claims about the transferability of the SPF. The fit is adequate and the SPF predictions compare favorably with the other SPFs (see Figure 132). Local calibration will be very important for this SPF to ensure that it provides an acceptable level of accuracy.

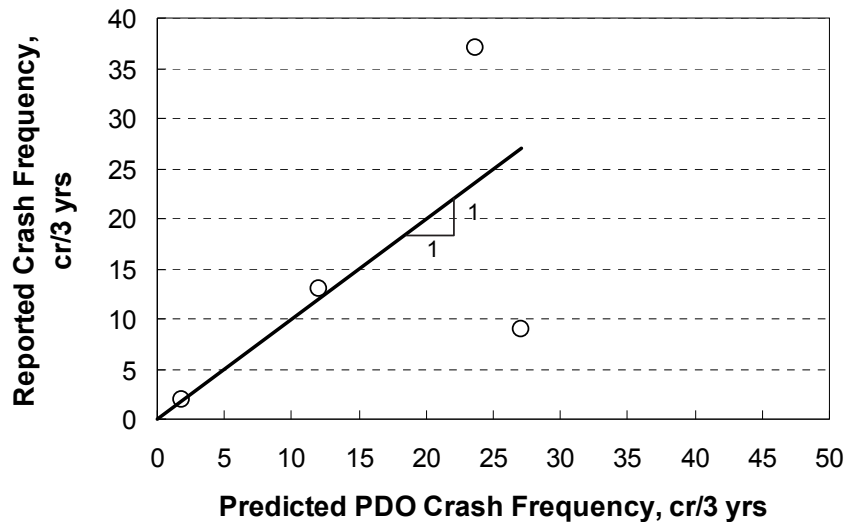


Figure 128. Predicted vs. reported PDO crashes at signalized B4 and D3en configurations.

Model for D4 Configuration. The statistics describing the calibrated model for D4 ramp terminal configuration are presented in Table 89. The Pearson χ^2 statistic for the model is 135, and the degrees of freedom are 139 ($= n - p = 140 - 1$). As this statistic is less than $\chi^2_{0.05,139}$ ($= 167$), the hypothesis that the model fits the data cannot be rejected. The R^2 for the model is 0.53. The R_k^2 for the calibrated model is 0.69. The inverse dispersion parameter was adjusted using Equation 249.

TABLE 89. Terminal PDO model statistical description–D4 configuration–signalized

Model Statistics	Value
$R^2 (R_k^2)$:	0.53 (0.69)
Scale parameter ϕ :	0.97
Pearson χ^2 :	135 ($\chi^2_{0.05, 139} = 167$)
Inverse dispersion parameter K :	7.21
Observations n_o :	140 terminals (2,049 PDO crashes in 3 years)
Standard deviation s_e :	± 2.47 crashes/yr

The coefficients in Table 85 were combined with the regression model to obtain the calibrated SPF for the D4 configuration. The form of the model is described by the following equation.

$$N_{spf, D4} = e^{-3.058 + 0.634 + 0.0879 n_{th} + 0.879 \ln(AADT_{xrd}/1,000) + 0.545 \ln(AADT_{ex}/1,000 + AADT_{en}/1,000)} \quad (302)$$

The calibrated CMFs used with this SPF are described in a subsequent section.

The fit of the calibrated model is shown in Figure 129. In general, the data shown in the figure indicate that the model provides an unbiased estimate of expected crash frequency for ramp terminals experiencing up to 55 crashes in a three-year period.

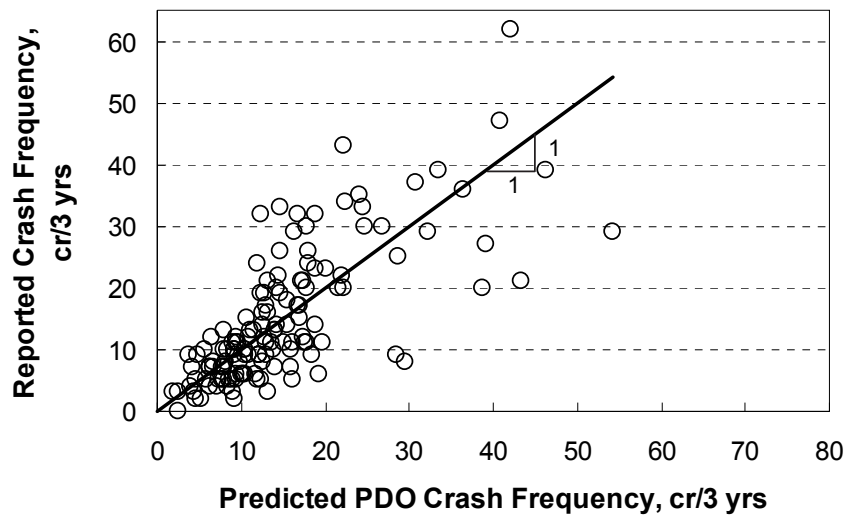


Figure 129. Predicted vs. reported PDO crashes at signalized D4 configurations.

Calibrated CMFs

Several CMFs were calibrated in conjunction with the SPFs. All of them were calibrated using PDO crash data. Collectively, they describe the relationship between various geometric factors and crash frequency.

Many of the CMFs found in the literature are typically derived from (and applied to) “intersection” crashes. That is, one CMF is used to indicate the influence of a leg-specific geometric factor on total crashes. In contrast, the models developed for this research project include several CMFs that are calibrated for leg-specific conditions. In these instances, Equations 222 and 226 were used to convert the leg-specific CMF to an intersection CMF for the purpose of illustrating the overall trend.

Left-Turn Lane CMF. The left-turn lane CMF is described using the following equation.

$$CMF_{bay,lt} = [(0.66 I_{rural} + 0.68 [1.0 - I_{rural}])P_{in} + 1.0 (1.0 - P_{in})]^{I_{bay,lt,in}} \times [(0.66 I_{rural} + 0.68 [1.0 - I_{rural}])P_{out} + 1.0 (1.0 - P_{out})]^{I_{bay,lt,out}} \quad (303)$$

Equation 303 is not associated with one of the regression coefficients in Table 85. Rather, it is based on a fairly definitive set of CMFs developed by Harwood et al. 2002. The derivation of the leg-specific CMF values that are used in Equation 303 is described in the discussion associated with Table 65. This CMF is applicable to turn bay presence on one or both of the crossroad legs at the ramp terminal.

The values obtained from this CMF are listed in Table 90. The CMF values reflect a proportion of total leg AADT on the crossroad P_{in} and P_{out} of 0.39, which is a typical value for ramp terminals.

TABLE 90. Calibrated left-turn CMF for PDO crashes—signalized

Junction Location	Legs with Turn Lane	Leg Location	Proportion AADT on Leg	CMF Value by Area Type	
				Urban	Rural
Ramp terminal	1	Crossroad ¹	0.39	0.88	0.87
	2	Crossroad ¹	0.39	0.77	0.75

Note:

1 - For Equation 303, P_{in} is assumed to equal P_{out} .

Right-Turn Lane CMF. The right-turn lane CMF is described using the following equation.

$$CMF_{bay,rt} = [(0.97 I_{rural} + 0.94 [1.0 - I_{rural}])P_{in} + 1.0 (1.0 - P_{in})]^{I_{bay,rt,in}} \times [(0.97 I_{rural} + 0.94 [1.0 - I_{rural}])P_{out} + 1.0 (1.0 - P_{out})]^{I_{bay,rt,out}} \quad (304)$$

Equation 304 is not associated with one of the regression coefficients in Table 85. Rather, it is based on a fairly definitive set of CMFs developed by Harwood et al. (2002). The derivation of the leg-specific CMF values that are used in Equation 304 is described in the discussion associated with Table 65. This CMF is applicable to turn bay presence on one or both of the crossroad legs at the ramp terminal.

The values obtained from this CMF are listed in Table 91. The CMF values reflect a proportion of total leg AADT on the crossroad P_{in} and P_{out} of 0.39, which is a typical value for ramp terminals.

TABLE 91. Calibrated right-turn CMF for PDO crashes—signalized

Junction Location	Legs with Turn Lane	Leg Location	Proportion AADT on Leg	CMF Value by Area Type	
				Urban	Rural
Ramp terminal	1	Crossroad ¹	0.39	0.98	0.99
	2	Crossroad ¹	0.39	0.95	0.98

Note:

1 - For Equation 304, P_{in} is assumed to equal P_{out} .

Protected Left-Turn Operation CMF. The protected left-turn operation CMF is described using the following equation.

$$CMF_{p,lt} = \left[e^{-0.223 n_{o,in}} P_{xrd} + 1.0 (1.0 - P_{xrd}) \right]^{I_{p,lt,in}} \times \left[e^{-0.223 n_{o,out}} P_{xrd} + 1.0 (1.0 - P_{xrd}) \right]^{I_{p,lt,out}} \quad (305)$$

This CMF is applicable to any crossroad leg with protected left-turn operation. It is not applicable to any leg that has permissive or protected-permissive operation.

The values obtained from this CMF are listed in Table 92. The CMF values reflect a proportion of total leg AADT on the crossroad P_{xrd} of 0.78, which is a typical value for ramp terminals.

TABLE 92. Calibrated protected left-turn operation CMF for PDO crashes

Junction Location	Legs with Protected Operation	Leg Location	Proportion AADT	CMF Value by Number of Opposing Lanes	
				1 lane	2 lanes
Ramp terminal	1	Crossroad	0.78	0.84	0.72
	2	Crossroad	0.78	0.71	0.52

Channelized Right-Turn CMFs. Two CMFs are discussed in this section. One is the CMF for channelized right turns from the crossroad and the other is the CMF for right turns from the exit ramp. These two CMFs are described using the following equations.

$$CMF_{ch,xrd} = \left[e^{0.465 P_{in}} + 1.0 (1.0 - P_{in}) \right]^{I_{ch,in}} \times \left[e^{0.465 P_{out}} + 1.0 (1.0 - P_{out}) \right]^{I_{ch,out}} \quad (306)$$

$$CMF_{ch,ex} = \left[e^{1.429 P_{ex}} + 1.0 (1.0 - P_{ex}) \right]^{I_{ch,ex}} \quad (307)$$

The first CMF listed is applicable to any ramp terminal with right-turn channelization on one or both crossroad legs, where the associated right-turn movement is turning from the crossroad. This CMF can be applied to channelization associated with the loop entrance ramp of the A4 configuration.

The second CMF listed is applicable to any ramp terminal with a diagonal exit ramp that has right-turn channelization, where the associated right-turn movement is turning from the exit ramp. This CMF is not applicable to the loop exit ramp of the B4 configuration.

The values obtained from these CMFs are listed in Table 93. The values reflect the proportion of total leg AADT on the subject legs that are typical for ramp terminals.

TABLE 93. Calibrated right-turn channelization CMF for PDO crashes—signalized

Junction Location	Leg Location	Proportion AADT on Leg	CMF Value by Number of Legs with Channelization	
			1 leg	2 legs
Ramp terminal	Exit ramp	0.12	1.38	1.91
	Crossroad ¹	0.39	1.23	1.52

Note:

1 - For Equation 306, P_{in} is assumed to equal P_{out} .

The value of this CMF implies that channelized right turns are less safe than right turns made at the intersection (without channelization). This finding is consistent with that of Dixon et al. (2000) (and later confirmed by Fitzpatrick et al. [2006]) who found a higher right-turn-related crash frequency for channelized right turns than for right turns made at the intersection (without channelization). It likely reflects the fact that the channelized-right-turn driver's check of the merge gap requires a relatively large head rotation coupled with a lengthy diversion of attention from the road ahead. Sometimes this gap check occurs while the vehicle is still moving forward, all of which can be problematic if the right-turning driver just ahead decides to yield.

Non-Ramp Public Street Leg CMF. The non-ramp public street CMF is described using the following equation.

$$CMF_{ps} = e^{0.520 I_{ps}} \quad (308)$$

This CMF is applicable to any ramp terminal that has a fourth leg that: (1) is a public street serving two-way traffic and (2) intersects with the crossroad at the terminal. Public street legs are fairly rare (i.e., they were found at about 2 percent of the terminals in the database). At most ramp terminals, the public street leg will be on the opposite side of the crossroad from the exit ramp. At the B4 and A4 ramp terminals, the public street leg will be opposite from the

diagonal exit ramp (the diagonal entrance ramp will intersect with the crossroad at some distance from the ramp terminal such that it is not part of the ramp terminal). At the D3en configuration, the public street leg will be on the opposite side of the crossroad from the entrance ramp.

This CMF has a value of 1.68 when a public street approach is present at a ramp terminal. The corresponding increase in the predicted number of crashes is likely a reflection of the increased number of conflicting movements created at the ramp terminal by a two-way traffic leg.

Access Point Frequency CMF. The access point frequency CMF is described using the following equation.

$$CMF_{ap} = e^{0.203(n_{dw} + n_{ps})} P_{out} + 1.0(1.0 - P_{out}) \quad (309)$$

This CMF applies to any ramp terminal with unsignalized driveways or unsignalized public street approaches on the crossroad leg that is outside of the interchange. Driveways and approaches on both sides of the leg should be counted when they are within 250 ft of the ramp terminal. The count of driveways should only include *active* driveways (i.e., those driveways with an average daily volume of 10 veh/day or more).

The values obtained from this CMF are listed in Table 94. The CMF values reflect the proportion of total leg AADT on crossroad legs that are typical for ramp terminals.

TABLE 94. Calibrated access point frequency CMF for PDO crashes—signalized

Junction Location	Proportion AADT on Leg	CMF Value by Number of Driveways or Public Street Approaches			
		1	2	3	4
Ramp terminal	0.39	1.09	1.19	1.33	1.49

Segment Length CMF. The segment length CMF is described using the following equation.

$$CMF_{sl} = e^{-0.0186(1.0/L_{rmp} + 1.0/L_{str} - 0.333)} \quad (310)$$

This CMF is applicable to all ramp configurations. It describes the relationship between ramp terminal crash frequency and the distance to the adjacent ramp or nearest public street intersection. The adjacent ramp or intersection can be signalized or unsignalized.

The distances used to calibrate this CMF were as small as 100 ft. The base condition for this CMF is no adjacent ramp or public street intersection (i.e., $L_{rmp} = L_{str} = 6.0$ mi).

The segment length CMF is shown in Figure 130. The trend line shown indicates that the CMF value increases with increasing distance. It is rationalized that the distance between the subject ramp and its adjacent ramp and intersection is correlated with crossroad operating speed. This speed is likely to increase as distance increases, and an increase in speed is likely to increase the risk of a crash.

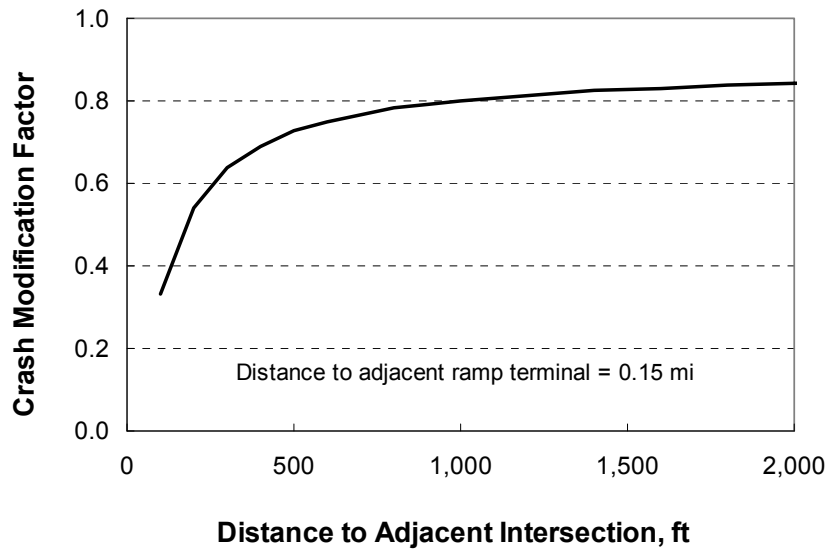


Figure 130. Calibrated segment length CMF for PDO crashes—signalized.

Median Width CMF. The median width CMF is described using the following equation.

$$CMF_{mw} = \left[e^{(0.0610 - 0.00246 AADT_{in}/1,000) W_{me,in}} P_{in} + 1.0 (1.0 - P_{in}) \right] \times \left[e^{(0.0610 - 0.00246 AADT_{out}/1,000) W_{me,out}} P_{out} + 1.0 (1.0 - P_{out}) \right] \quad (311)$$

with,

$$W_{me,k} = W_m - W_{mb,k} \geq 0.0 \quad (312)$$

$$W_{mb,k} = \text{Max}(W_{b,k}; 12) \quad (313)$$

Guidance for using this CMF was provided in the CMF Development part of this chapter (in the section titled Median Width CMF). The constant “12” represents the minimum median width below which the CMF value is 1.0. This value is decreased from the 14 ft value stated in the *HSM* based on the trends found in the ramp terminal safety database. The applicable AADT volumes range from 14,000 to 60,000 veh/day. AADT volumes smaller than 14,000 should be set to 14,000 in Equation 311.

The median width CMF is shown in Figure 131. The trend line shown indicates that the CMF value increases with increasing median width, provided that the AADT volume is less than 25,000 veh/day. The reverse trend occurs for AADT volumes in excess of about 25,000 veh/day. A CMF value of about 1.0 is obtained for an AADT volume of 25,000 veh/day.

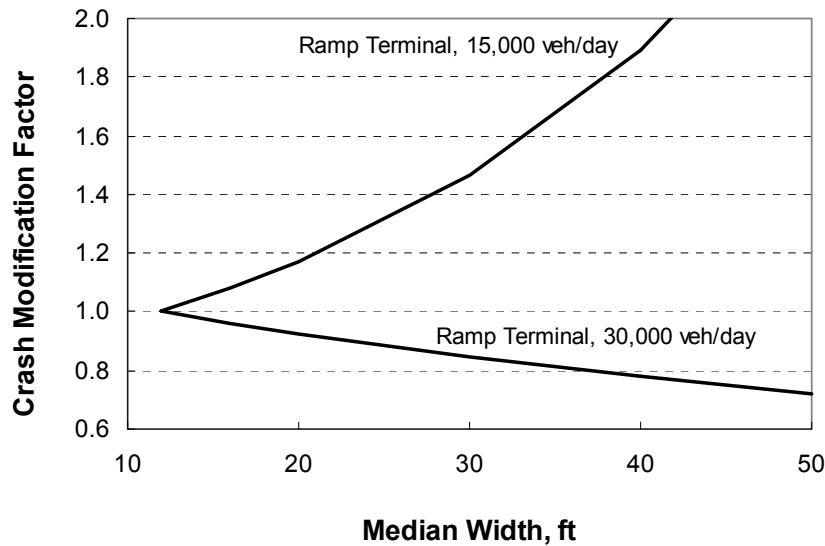


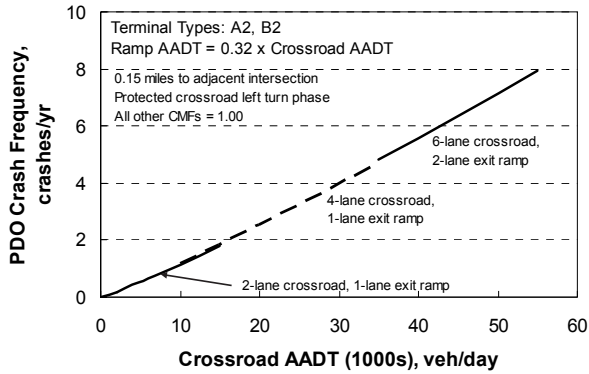
Figure 131. Calibrated median width CMF for PDO crashes—signalized.

The AADT coefficient is negative indicating that the CMF value decreases with increasing AADT volume. It is likely that the negative AADT coefficient value in Equation 311 reflects a tendency for drivers to be more cautious as the intersection becomes busier. Also, busier intersections may have long queues present for more cycles, which could reduce the likelihood of errant vehicles in middle or outside lanes that have sufficient speed to cross the median.

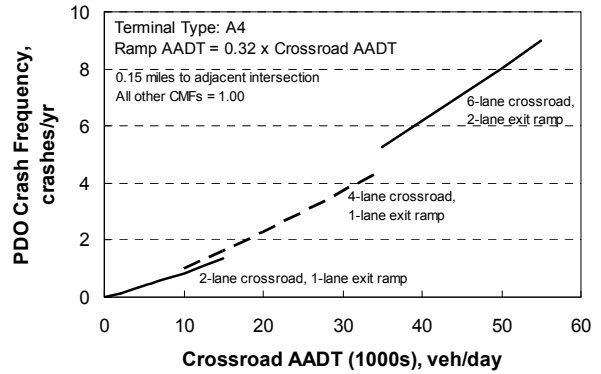
Sensitivity Analysis

The relationship between crash frequency and traffic demand, as obtained from the combined calibrated models, is shown in Figure 132 for signalized ramp terminals. The distance between ramps is 0.15 mi and the distance to the nearest public street intersection is also 0.15 mi. The ramp terminal has protected left-turn operation for the crossroad left-turn movement. All other geometric and control conditions are such that the associated CMF has a value of 1.0. The axis scale for each graph in Figure 132 is the same. This technique is used to facilitate comparison among ramp configurations.

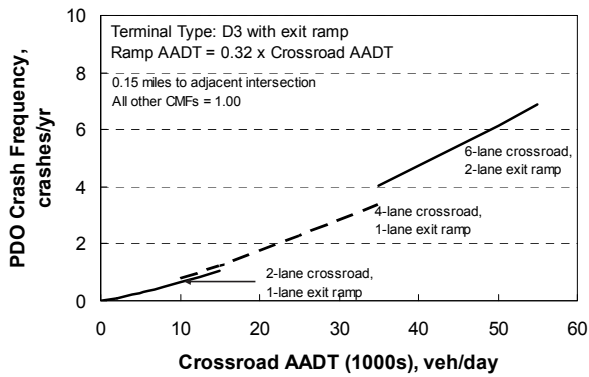
The A2, B2, and D3 configurations are shown in Figure 132 to have fewer crashes than the other configurations, for a given AADT volume. This trend is likely due to the fact that these configurations have only three legs, while the other configurations have four legs. The number of conflict points increases significantly with the number of legs. The D4 configuration is shown in Figure 132f to have more crashes for a given AADT volume than the other configurations. This trend is likely a reflection of the fact that it has four legs, two left-turn movements, and a higher “sum of conflicting volumes” than the other configurations. Although the D3en and B4 configurations are represented collectively by only four observations, the trends shown in Figure 132d and 132e are consistent with those of the other configurations shown and provide some evidence of the validity of the associated SPF.



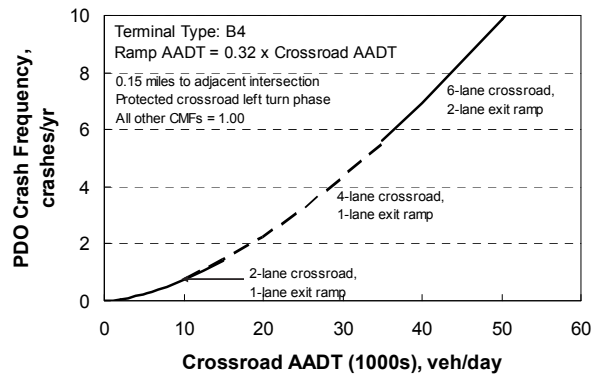
a. Terminal types A2 and B2.



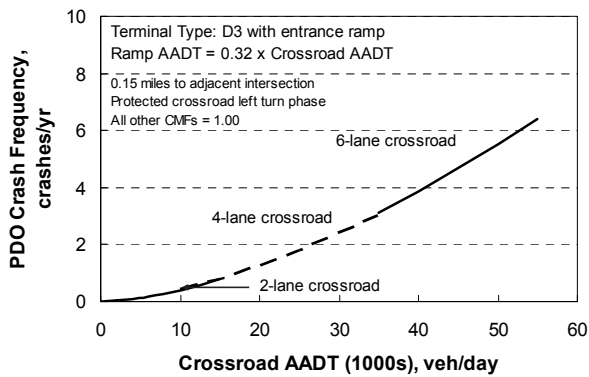
b. Terminal type A4.



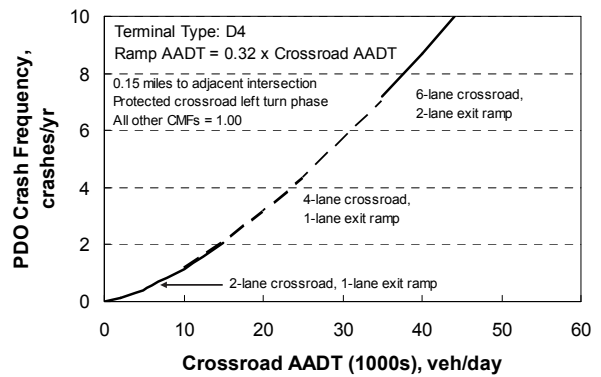
c. Terminal Type D3 with exit ramp.



d. Terminal type B4.



e. Terminal Type D3 with entrance ramp.



f. Terminal type D4.

Figure 132. Terminal PDO models—signalized.

Unsignalized Ramp Terminal Models

This section describes the calibrated PDO crash prediction models for signalized ramp terminals. The regression model used had the same form as used to develop the FI crash prediction model (i.e., Equation 278). The turn bay CMFs were obtained from Table 65.

An initial regression analysis was undertaken with county and state variable combinations treated as fixed effects and as random effects. The Hausman test was performed using the covariance matrix to determine whether the fixed effect model was appropriate. The null hypothesis is that the regression coefficients from the two model treatments are consistent. This hypothesis was rejected ($p = 0.02$) indicating that the coefficients are different (i.e., inconsistent) among the two treatments. In this case, it is concluded that the regression coefficient values are influenced by county so a fixed-effect treatment is needed to remove the county effect.

Model Calibration

The results of the combined regression model calibration are presented in Table 95. The Pearson χ^2 statistic for the model is 297, and the degrees of freedom are 289 ($= n - p = 301 - 12$). As this statistic is less than $\chi^2_{0.05, 289} (= 330)$, the hypothesis that the model fits the data cannot be rejected. Several terminals were removed as a result of outlier analysis such that the calibration database included only 656 of the 786 crashes identified in Chapter 4.

TABLE 95. Terminal PDO model statistical description—combined model—three states—unsignalized

Model Statistics		Value		
R^2 :		0.61		
Scale parameter ϕ :		0.99		
Pearson χ^2 :		297 ($\chi^2_{0.05, 289} = 330$)		
Observations n_o :		301 terminals (656 PDO crashes in 3 years)		
Calibrated Coefficient Values				
Variable	Inferred Effect of...	Value	Std. Dev.	t-statistic
$b_{0, A2B2}$	A2 and B2 ramp terminal configuration	-3.595	0.652	-5.5
$b_{xrd, A2B2}$	Crossroad AADT	0.773	0.350	2.2
$b_{rmp, A2B2}$	Ramp AADT	0.878	0.331	2.7
$b_{0, A4D3ex}$	A4 and D3ex ramp terminal configuration	-3.164	0.704	-4.5
$b_{xrd, A4D3ex}$	Crossroad AADT	0.595	0.309	1.9
$b_{rmp, A4D3ex}$	Ramp AADT	0.937	0.199	4.7
$b_{0, B4D3en}$	B4 and D3en ramp terminal configuration	-2.961	0.706	-4.2
$b_{xrd, B4D3en}$	Crossroad AADT	0.885	0.302	2.9
$b_{rmp, B4D3en}$	Ramp AADT	0.350	0.264	1.3
$b_{0, D4}$	D4 ramp terminal configuration	-2.953	0.309	-9.6
$b_{xrd, D4}$	Crossroad AADT	0.845	0.144	5.9
$b_{rmp, D4}$	Ramp AADT	0.476	0.133	3.6

The t-statistic for each coefficient is listed in the last column of Table 95. These statistics describe a test of the hypothesis that the coefficient value is equal to 0.0. Those t-statistics with an absolute value that is larger than 2.0 indicate that the hypothesis can be rejected with the probability of error in this conclusion being less than 0.05. For those few variables where the absolute value of the t-statistic is smaller than 2.0, it was decided that the variable was important to the model and its trend was found to be intuitive and, where available, consistent with previous research findings (even if the specific value was not known with a great deal of certainty as applied to this database).

The coefficients for forty-three county indicator variables are not shown in Table 95 because their individual significance is not directly relevant to model fit assessment or its application. However, it is recognized that the “intercept” variables in Table 95 (i.e., $b_{0, A2B2}$, $b_{0, A4D3ex}$, $b_{0, B4D3en}$, $b_{0, D4}$) correspond to only one state and county combination. Desirably, the intercept would represent an average value for all states and counties in the database. To this end, the predicted crash frequencies from the model described by Table 95 were submitted to a second regression analysis using Equation 115 (in Chapter 5).

The regression coefficient c_o was determined to be 0.540 for the A2B2 intercept, 0.494 for the A4D3ex intercept, 0.603 for the B4D3en intercept, and 0.521 for the D4 intercept. Each of these values is added to the appropriate intercept variables to compute an average intercept value for the overall database. This addition is shown in the models described in the next section.

Table 95 includes only coefficients associated with the SPF models. It does not include any coefficients associated with geometric elements. Coefficients for several geometric variables were found to be significant in the examination of FI crash data (as documented in Table 79). However, none of the coefficients for these variables were significant in the examination of PDO crash data. This result is partially due to the inclusion of county indicator variables and likely a reflection of correlation between county and geometric design. The potential for this result was discussed in a previous section titled Prediction of PDO Crash Frequency.

Calibrated Models

This section describes the fit statistics and inverse dispersion parameter for each of the four ramp terminal models. It also shows the model form with the calibration coefficients from Table 95.

Model for A2 and B2 Configurations. The statistics describing the calibrated model for A2 and B2 ramp terminal configurations are presented in Table 96. The Pearson χ^2 statistic for the model is 45.5, and the degrees of freedom are 39 ($= n - p = 40 - 1$). As this statistic is less than $\chi^2_{0.05,39} (= 55)$, the hypothesis that the model fits the data cannot be rejected. The R^2 for the model is 0.69. The R_k^2 for the calibrated model is 0.93. The inverse dispersion parameter was adjusted using Equation 249.

The coefficients in Table 95 were combined with the regression model to obtain the calibrated SPF for the A2 and B2 configuration. The form of the model is described in the following equation.

$$N_{spf, A2B2} = e^{-3.595 + 0.540 + 0.773 \ln(AADT_{xrd} / 1,000) + 0.878 \ln(AADT_{ex} / 1,000 + AADT_{en} / 1,000)} \quad (314)$$

The calibrated CMFs used with this SPF are described in a subsequent section.

TABLE 96. Terminal PDO model statistical description—A2 and B2 configuration—unsignalized

Model Statistics	Value
$R^2 (R_k^2)$:	0.69 (0.93)
Scale parameter ϕ :	1.17
Pearson χ^2 :	45.5 ($\chi^2_{0.05, 39} = 55$)
Inverse dispersion parameter K :	5.49
Observations n_o :	40 terminals (109 PDO crashes in 3 years)
Standard deviation s_e :	± 0.60 crashes/yr

The fit of the calibrated model is shown in Figure 133. This figure compares the predicted and reported crash frequency in the calibration database. In general, the data shown in the figure indicate that the model provides an unbiased estimate of expected crash frequency for ramp terminals experiencing up to 11 crashes in a three-year period.

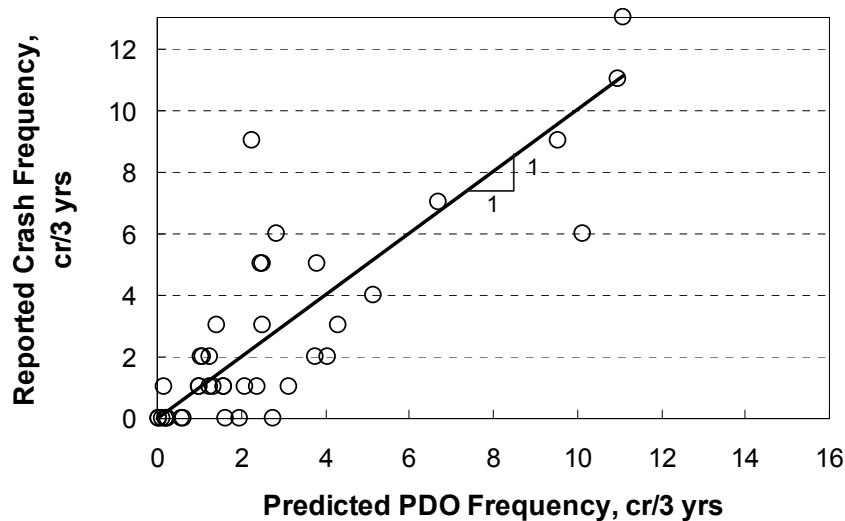


Figure 133. Predicted vs. reported PDO crashes at unsignalized A2 and B2 configurations.

Model for A4 and D3ex Configurations. The statistics describing the calibrated model for A4 and D3ex ramp terminal configurations are presented in Table 97. The Pearson χ^2 statistic for the model is 28.9, and the degrees of freedom are 36 ($= n - p = 37 - 1$). As this statistic is less than $\chi^2_{0.05, 36} (= 51)$, the hypothesis that the model fits the data cannot be rejected. The R^2 for the model is 0.78. The R_k^2 for the calibrated model is 0.96. The inverse dispersion parameter was adjusted using Equation 249.

TABLE 97. Terminal PDO model statistical description—A4 and D3ex configuration—unsignalized

Model Statistics	Value
$R^2 (R_k^2)$:	0.78 (0.96)
Scale parameter ϕ :	0.80
Pearson χ^2 :	28.9 ($\chi^2_{0.05, 36} = 51$)
Inverse dispersion parameter K :	6.57
Observations n_o :	37 terminals (91 PDO crashes in 3 years)
Standard deviation s_e :	± 0.61 crashes/yr

The coefficients in Table 95 were combined with the regression model to obtain the calibrated SPF for the A4 and D3ex configuration. The form of the model is described in the following equation.

$$N_{spf, A4D3ex} = e^{-3.164 + 0.494 + 0.595 \ln(AADT_{rd}/1,000) + 0.937 \ln(AADT_{ex}/1,000 + AADT_{en}/1,000)} \quad (315)$$

The calibrated CMFs used with this SPF are described in a subsequent section. The AADT volume of the loop entrance ramp at an A4 configuration is not included in $AADT_{en}$. Also, $AADT_{en}$ equals 0.0 when the SPF is applied to a D3ex configuration.

The fit of the calibrated model is shown in Figure 134. In general, the data shown in the figure indicate that the model provides an unbiased estimate of expected crash frequency for ramp terminals experiencing up to 10 crashes in a three-year period.

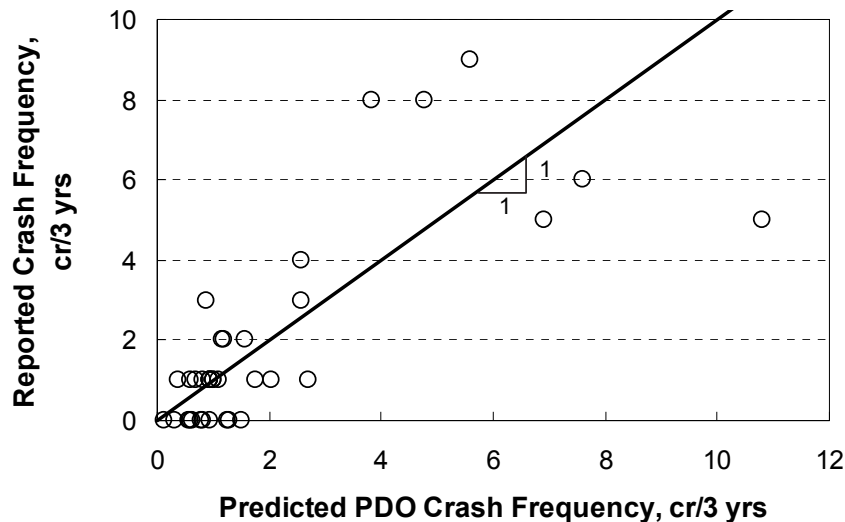


Figure 134. Predicted vs. reported PDO crashes at unsignalized A4 and D3ex configurations.

Model for B4 and D3en Configurations. The statistics describing the calibrated model for B4 and D3en ramp terminal configurations are presented in Table 98. The Pearson χ^2 statistic

for the model is 20.5, and the degrees of freedom are 21 ($= n - p = 22 - 1$). As this statistic is less than $\chi^2_{0.05,21}$ ($= 33$), the hypothesis that the model fits the data cannot be rejected. The R^2 for the model is 0.65. The R_k^2 for the calibrated model is 0.92. The inverse dispersion parameter was adjusted using Equation 249.

TABLE 98. Terminal PDO model statistical description—B4 and D3en configuration—unsignalized

Model Statistics	Value
R^2 (R_k^2):	0.65 (0.92)
Scale parameter ϕ :	0.98
Pearson χ^2 :	20.5 ($\chi^2_{0.05,21} = 33$)
Inverse dispersion parameter K :	3.90
Observations n_o :	22 terminals (68 PDO crashes in 3 years)
Standard deviation s_e :	± 0.71 crashes/yr

The coefficients in Table 95 were combined with the regression model to obtain the calibrated SPF for the B4 and D3en configuration. The form of the model is described by the following equation.

$$N_{spf, B4D3en} = e^{-2.961 + 0.603 + 0.885 \ln(AADT_{rd}/1,000) + 0.350 \ln(AADT_{ex}/1,000 + AADT_{en}/1,000)} \quad (316)$$

The calibrated CMFs used with this SPF are described in a subsequent section. The AADT volume of the loop exit ramp at a B4 configuration is not included in $AADT_{ex}$. Also, $AADT_{ex}$ equals 0.0 when the SPF is applied to a D3en configuration.

The fit of the calibrated model is shown in Figure 135. In general, the data shown in the figure indicate that the model provides an unbiased estimate of expected crash frequency for ramp terminals experiencing up to 12 crashes in a three-year period.

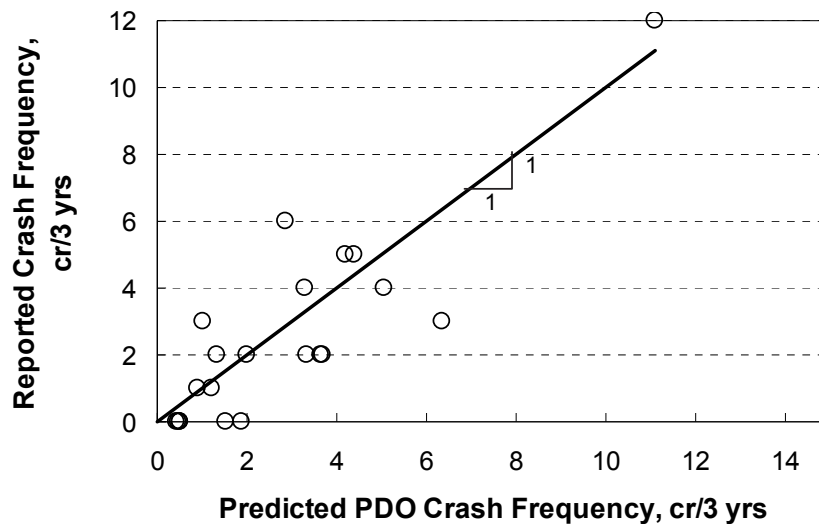


Figure 135. Predicted vs. reported PDO crashes at unsignalized B4 and D3en configurations.

Model for D4 Configuration. The statistics describing the calibrated model for D4 ramp terminal configuration are presented in Table 99. The Pearson χ^2 statistic for the model is 200, and the degrees of freedom are 201 ($= n - p = 202 - 1$). As this statistic is less than $\chi^2_{0.05,201}$ ($= 235$), the hypothesis that the model fits the data cannot be rejected. The R^2 for the model is 0.48. The R_k^2 for the calibrated model is 0.85. The inverse dispersion parameter was adjusted using Equation 249.

TABLE 99. Terminal PDO model statistical description—D4 configuration—unsignalized

Model Statistics	Value
$R^2 (R_k^2)$:	0.48 (0.85)
Scale parameter ϕ :	0.99
Pearson χ^2 :	200 ($\chi^2_{0.05,201} = 235$)
Inverse dispersion parameter K :	4.27
Observations n_o :	202 terminals (388 PDO crashes in 3 years)
Standard deviation s_e :	± 0.62 crashes/yr

The coefficients in Table 95 were combined with the regression model to obtain the calibrated SPF for the D4 configuration. The form of the model is described in the following equation.

$$N_{spf,D4} = e^{-2.953 + 0.521 + 0.845 \ln(AADT_{xrd}/1,000) + 0.476 \ln(AADT_{ex}/1,000 + AADT_{en}/1,000)} \quad (317)$$

The calibrated CMFs used with this SPF are described in a subsequent section.

The fit of the calibrated model is shown in Figure 136. In general, the data shown in the figure indicate that the model provides an unbiased estimate of expected crash frequency for ramp terminals experiencing up to 5 crashes in a three-year period.

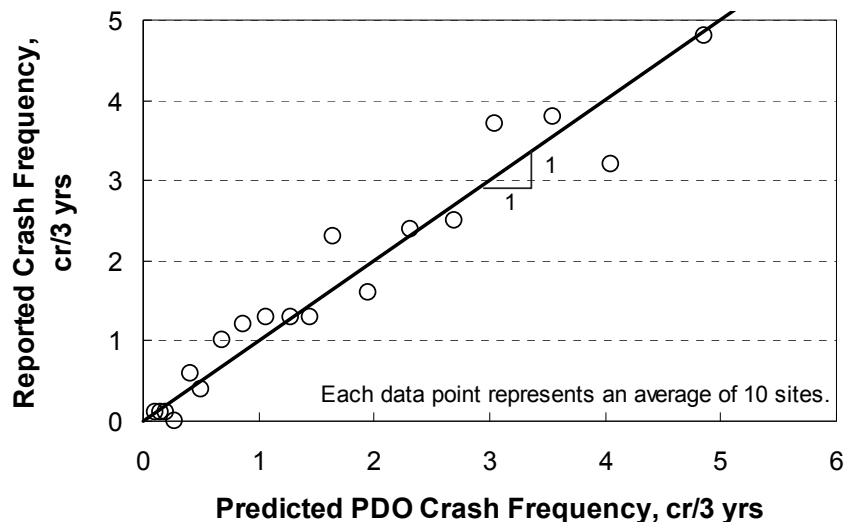


Figure 136. Predicted vs. reported PDO crashes at unsignalized D4 configurations.

Each data point shown in Figure 136 represents the average predicted and average reported crash frequency for a group of 10 ramp terminals. The data were sorted by predicted crash frequency to form groups of terminals with similar crash frequency. The purpose of this grouping was to reduce the number of data points shown in the figure and, thereby, to facilitate an examination of trends in the data. The individual terminal observations were used for model calibration.

Calibrated CMFs

This section describes two CMFs that were derived from the literature. Both CMFs relate to turn bay presence on the crossroad legs of the ramp terminal. Their derivation was previously described in the discussion associated with Table 65.

Left-Turn Lane CMF. The left-turn lane CMF is described using the following equation.

$$CMF_{bay,lt} = [(0.55 I_{rural} + 0.58 [1.0 - I_{rural}])P_{in} + 1.0 (1.0 - P_{in})]^{I_{bay,lt,in}} \times [(0.55 I_{rural} + 0.58 [1.0 - I_{rural}])P_{out} + 1.0 (1.0 - P_{out})]^{I_{bay,lt,out}} \quad (318)$$

Equation 318 is not associated with one of the regression coefficients in Table 95. Rather, it is based on a fairly definitive set of CMFs developed by Harwood et al. (2002). The derivation of the leg-specific CMF values that are used in Equation 318 is described in the discussion associated with Table 65. This CMF is applicable to turn bay presence on one or both of the crossroad legs at the ramp terminal, provided that the leg is uncontrolled. If the leg is stop-controlled, then this CMF is not applicable.

The values obtained from this CMF are listed in Table 100. The CMF values reflect a proportion of total leg AADT on the crossroad P_{in} and P_{out} of 0.39, which is a typical value for ramp terminals.

TABLE 100. Calibrated left-turn CMF for PDO crashes—unsignalized

Junction Location	Legs with Turn Lane	Leg Location	Proportion AADT on Leg	CMF Value by Area Type	
				Urban	Rural
Ramp terminal	1	Crossroad ¹	0.39	0.84	0.82
	2	Crossroad ¹	0.39	0.70	0.68

Note:

1 - For Equation 318, P_{in} is assumed to equal P_{out} .

Right-Turn Lane CMF. The right-turn lane CMF is described using the following equation.

$$CMF_{bay,rt} = [(0.63 I_{rural} + 0.69 [1.0 - I_{rural}])P_{in} + 1.0 (1.0 - P_{in})]^{I_{bay,rt,in}} \times [(0.63 I_{rural} + 0.69 [1.0 - I_{rural}])P_{out} + 1.0 (1.0 - P_{out})]^{I_{bay,rt,out}} \quad (319)$$

Equation 319 is not associated with one of the regression coefficients in Table 95. Rather, it is based on a fairly definitive set of CMFs developed by Harwood et al. (2002). The derivation of the leg-specific CMF values that are used in Equation 319 is described in the discussion associated with Table 65. This CMF is applicable to turn bay presence on one or both of the crossroad legs at the ramp terminal, provided that the leg is uncontrolled. If the leg is stop-controlled, then this CMF is not applicable.

The values obtained from this CMF are listed in Table 101. The CMF values reflect a proportion of total leg AADT on the crossroad P_{in} and P_{out} of 0.39, which is a typical value for ramp terminals.

TABLE 101. Calibrated right-turn CMF for PDO crashes—unsignalized

Junction Location	Legs with Turn Lane	Leg Location	Proportion AADT on Leg	CMF Value by Area Type	
				Urban	Rural
Ramp terminal	1	Crossroad ¹	0.39	0.88	0.86
	2	Crossroad ¹	0.39	0.77	0.73

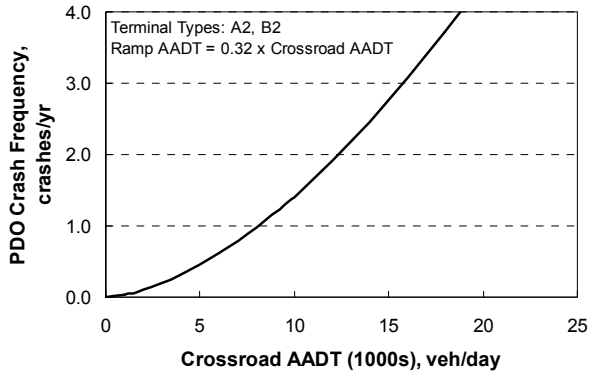
Note:

1 - For Equation 319, P_{in} is assumed to equal P_{out} .

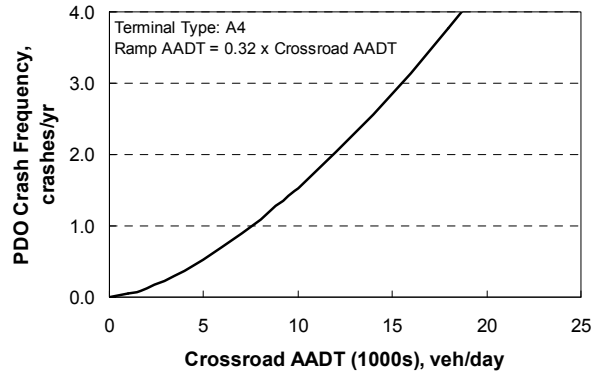
Sensitivity Analysis

The relationship between crash frequency and traffic demand, as obtained from the combined calibrated models, is illustrated in Figure 137 for unsignalized ramp terminals. The axis scale for each graph in Figure 137 is the same. This technique is used to facilitate comparison among ramp configurations.

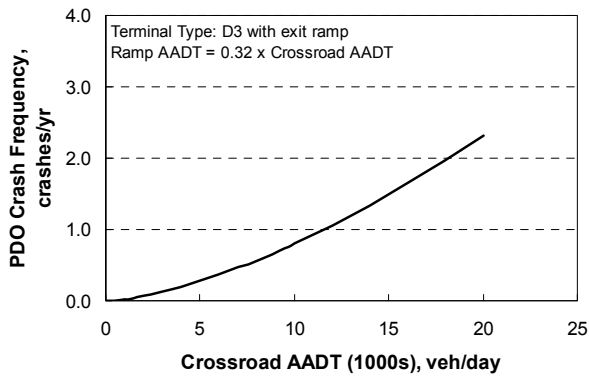
The D3 configurations are shown in Figure 137 to have fewer crashes than the other configurations, for a given AADT volume. This trend is likely due to the fact that these configurations have only three legs, while the other configurations have four legs. The number of conflict points increases significantly with the number of legs.



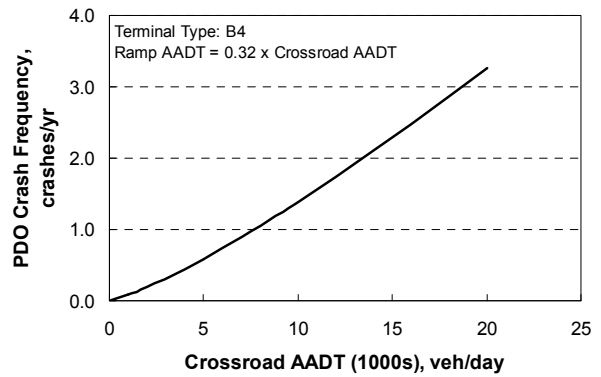
a. Terminal types A2 and B2.



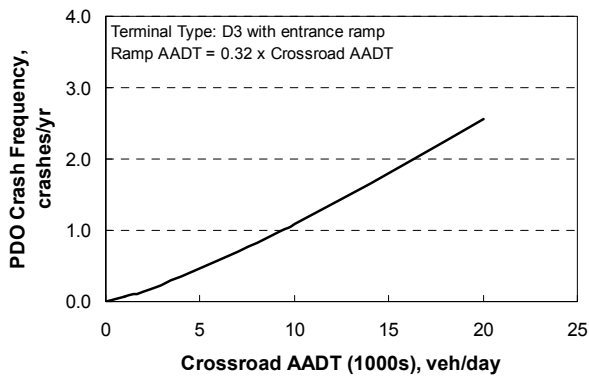
b. Terminal type A4.



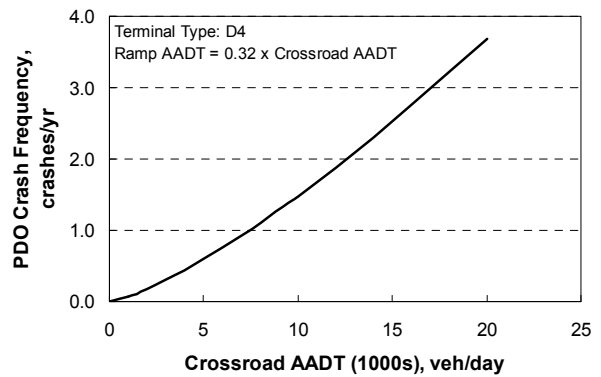
c. Terminal Type D3 with exit ramp.



d. Terminal type B4.



e. Terminal Type D3 with entrance ramp.



f. Terminal type D4.

Figure 137. Terminal PDO models—unsignalized.

NOMENCLATURE

$AADT_{en}$	AADT volume for the entrance ramp, veh/day (= 0 if ramp does not exist);
$AADT_{ex}$	AADT volume for the exit ramp, veh/day (= 0 if ramp does not exist);
$AADT_i$	AADT volume for street i , veh/day;
$AADT_{in}$	AADT volume for crossroad leg between ramps, veh/day;
$AADT_k$	AADT volume for leg k , veh/day.
$AADT_{out}$	AADT volume for crossroad leg outside of interchange, veh/day;
$AADT_{xrd}$	AADT volume for crossroad (= $0.5 AADT_{in} + 0.5 AADT_{out}$), veh/day;
C_{A2B2}	local calibration factor for A2 and B2 configurations;
C_{A4D3ex}	local calibration factor for A4 and D3ex configurations;
C_{B4D3en}	local calibration factor for B4 and D3en configurations;
C_{ca}	calibration factor for California;
C_{D4}	local calibration factor for D4 configuration;
$CMF_1 \dots CMF_k$	crash modification factors for ramp terminal crashes at a site with specific geometric design features k ;
$CMF_{A2B2, 1} \dots CMF_{A2B2, w}$	crash modification factors for crashes at an A2 or B2 site with specific geometric design features w ;
$CMF_{A4D3ex, 1} \dots CMF_{A4D3ex, x}$	crash modification factors for crashes at an A4 or D3ex site with specific geometric design features x ;
CMF_{ap}	access point frequency crash modification factor;
CMF_{awsc}	all-way stop control crash modification factor;
$CMF_{B4D3en, 1} \dots CMF_{B4D3en, y}$	crash modification factors for crashes at a B4 or D3en site with specific geometric design features y ;
$CMF_{bay, rt}$	crossroad right-turn lane crash modification factor;
$CMF_{bay, lt}$	crossroad left-turn lane crash modification factor;
$CMF_{ch, xrd}$	channelized right turn from crossroad crash modification factor;
$CMF_{ch, ex}$	channelized right turn from exit ramp crash modification factor;
$CMF_{D4, 1} \dots CMF_{D4, z}$	crash modification factors for crashes at a D4 site with specific geometric design features z ;
$CMF_{int, k}$	CMF for a specified treatment to leg k , quantified in terms of intersection crashes ($k = 1$ for one major-street leg, 2 for the other major-street leg, 3 for one minor-street leg, and 4 for the other minor-street leg);
$CMF_{int, i}$	CMF for a specified treatment to street i , quantified in terms of intersection crashes ($i = 1$ for major street or 2 for minor street);
CMF_{leg}	CMF for a specified treatment to any leg, quantified in terms of the crashes that occur on the subject leg;
CMF_{mw}	median width crash modification factor;
$CMF_{p, lt}$	protected left-turn operation crash modification factor;
CMF_{ps}	non-ramp public street leg crash modification factor;
CMF_{rc}	exit ramp capacity crash modification factor;
CMF_{sk}	skew angle crash modification factor;
CMF_{sl}	segment length crash modification factor;
CMF_{str}	CMF for a specified treatment to any street, quantified in terms of the crashes that occur on the subject street;
I_{A2B2}	crash indicator variable (= 1.0 if A2 or B2 crash data, 0.0 otherwise);
I_{A4D3ex}	crash indicator variable (= 1.0 if A4 or D3ex crash data, 0.0 otherwise);

I_{awsc} = all-way stop control indicator variable (= 1.0 if ramp terminal has all-way stop controlled, 0.0 if it has one-way stop control for the exit ramp); and
 I_{B4D3en} = crash indicator variable (= 1.0 if B4 or D3en crash data, 0.0 otherwise);
 $I_{bay, rt, k}$ = right-turn lane (or bay) indicator variable for crossroad leg k ($k = in$ or out) (= 1.0 if right-turn lane (or bay) present, 0.0 otherwise);
 $I_{bay, lt, k}$ = left-turn lane (or bay) indicator variable for crossroad leg k ($k = in$ or out) (= 1.0 if left-turn lane (or bay) present, 0.0 otherwise);
 $I_{ch, k}$ = right-turn channelization indicator variable for leg k ($k = in, out, or ex$) (= 1.0 if right-turn channelization exists, 0.0 otherwise);
 I_{D4} = crash indicator variable (= 1.0 if D4 crash data, 0.0 otherwise);
 $I_{p, lt, k}$ = protected left-turn operation indicator variable for crossroad leg k ($k = in$ or out) (= 1.0 if protected operation exists, 0.0 otherwise);
 I_{ps} = non-ramp public street leg indicator variable (= 1.0 if leg is present, 0.0 otherwise);
 I_{rural} = area type indicator variable (= 1.0 if area is rural, 0.0 if it is urban);
 I_{sk} = skew angle between exit ramp and crossroad, degrees;
 K = inverse dispersion parameter (= $1/k$, where k = overdispersion parameter).
 L_{rmp} = distance between subject ramp terminal and adjacent ramp terminal (measured along the crossroad from terminal center to terminal center), mi;
 L_{str} = distance between subject ramp terminal and nearest public road intersection in a direction away from freeway (measured along the crossroad from terminal center to intersection center), mi;
 N = predicted average crash frequency, crashes/yr;
 n_{dw} = number of unsignalized driveways on the crossroad leg outside of the interchange and within 250 ft of the ramp terminal;
 n_{ex} = number of lanes serving exit ramp traffic; lanes;
 $n_{ex, eff}$ = effective number of lanes serving exit ramp traffic, lanes;
 $N_{interchange}$ = predicted average crash frequency within the limits of an interchange, crashes/yr;
 N_{mv} = predicted average multiple-vehicle crash frequency, crashes/yr;
 $n_{o, k}$ = number of through traffic lanes that oppose the left-turn movement on crossroad leg k ($k = in$ or out), lanes;
 n_{ps} = number of unsignalized public street approaches to the crossroad leg outside of the interchange and within 250 ft of the ramp terminal;
 $N_{rt, D4}$ = predicted average crash frequency for D4 configuration, crashes/yr;
 N_{rt} = predicted average crossroad ramp terminal crash frequency, crashes/yr;
 $N_{rt, j}$ = predicted average crossroad ramp terminal crash frequency for model j ; crashes/yr;
 $N_{rt, A4D3ex}$ = predicted average crash frequency for A4 and D3ex configurations, crashes/yr;
 $N_{rt, A2B2}$ = predicted average crash frequency for A2 and B2 configurations, crashes/yr;
 $N_{rt, j}$ = predicted average crossroad ramp terminal crash frequency for model j ($j = A2B2$ if $I_{A2B2} = 1.0$; $j = A4D3ex$ if $I_{A4D3ex} = 1.0$; $j = B4D3en$ if $I_{B4D3en} = 1.0$; $j = D4$ if $I_{D4} = 1.0$); crashes/yr;
 $N_{rt, B4D3en}$ = predicted average crash frequency for B4 and D3en configurations, crashes/yr;
 $N_{spf, A2B2}$ = predicted average crash frequency for A2 and B2 configurations for base conditions, crashes/yr;
 $N_{spf, B4D3en}$ = predicted average crash frequency for B4 and D3en configurations for base conditions, crashes/yr;
 $N_{spf, A4D3ex}$ = predicted average crash frequency for A4 and D3ex configurations for base conditions, crashes/yr;

- $N_{spf, D4}$ = predicted average crash frequency for D4 configuration for base conditions, crashes/yr;
- N_{sv} = predicted average single-vehicle crash frequency, crashes/yr;
- n_{th} = number of through traffic lanes on the crossroad at the ramp terminal (total of both directions), lanes;
- P_{ex} = proportion of total leg AADT on exit ramp leg;
- P_i = proportion of total leg AADT on street i ;
- P_{in} = proportion of total leg AADT on crossroad leg between ramps;
- P_k = proportion of total leg AADT on leg k ;
- P_{out} = proportion of total leg AADT on crossroad leg outside of interchange;
- P_{xrd} = proportion of total leg AADT on the crossroad;
- R_k = proportion of intersection crashes that occur on treated leg k ;
- R_i = proportion of intersection crashes that occur on treated street i ;
- $Sin(x)$ = sine of angle x ;
- $V[X]$ = crash frequency variance for a group of similar locations, crashes²;
- $W_{b, k}$ = left-turn lane (or bay) width for crossroad leg k ($k = in$ or out) (= 0.0 if no lane present on leg), ft;
- W_m = median width, ft;
- $W_{mb, k}$ = base median width for crossroad leg k ($k = in$ or out), ft;
- $W_{me, k}$ = width of median adjacent to turn lane (or bay) for crossroad leg k ($k = in$ or out), ft;
- X = reported crash count for y years, crashes;
- y = time interval during which X crashes were reported, yr.

CHAPTER 8: SEVERITY DISTRIBUTION FUNCTIONS

This chapter describes the activities undertaken to calibrate severity distribution functions (SDFs) for various components of the freeway system. A SDF is a discrete choice model that includes variables describing a site's geometric design, traffic control features, traffic characteristics, and a calibration factor. It is used to predict for each site the proportion of crashes associated with each of the following severity levels.

- Fatal (K).
- Incapacitating injury (A).
- Non-incapacitating injury (B).
- Possible injury (C).

The SDFs were developed to be used with a predictive model to estimate the expected crash frequency for each severity level. They were calibrated using a highway safety database that combines crash data with road inventory data. The procedure used to assemble the highway safety database is described in Chapter 4. The application of SDFs is described in Appendices C and D.

This chapter consists of four parts. The first part gives a brief background on SDFs used in highway safety evaluation. The second part describes the development of a SDF for freeway segments. The third part describes the development of a SDF for ramp and C-D road segments. The fourth part describes the development of a SDF for crossroad ramp terminals.

LITERATURE REVIEW

Previous studies have documented models for estimating crash frequency for each severity level by jointly modeling the frequency of crashes by severity level using multivariate Poisson and mixed-Poisson models (Ma and Kockelman, 2006; Park and Lord, 2007). In contrast, a recent study used a two-stage frequency-severity model that linked the SDF with a safety performance function to estimate the frequency of crashes by severity level (Wang et al., 2011).

Several statistical models are available to develop SDFs. The models that are more commonly used by safety analysts include the ordered logit or probit, partially-ordered logit, ordered mixed logit, multinomial logit, nested logit, and random parameters (mixed) logit. Each of these statistical models is briefly described in the following paragraphs.

Due to the ordinal nature of crash severities, an ordered logit or probit model is the logical choice for SDF development. This kind of model recognizes the natural order of increasing severity among the response alternatives (i.e., C, B, A, K) by fitting one function for all severity levels, with a unique cut-off value for each severity level. In this manner, the ordinal structure is well suited to modeling factors that have the same effect across all severity levels. The ordered logit and ordered probit models have been extensively used for crash severity analysis (Kweon and Kockelman, 2003; Donnell and Mason, 2004; Wang and Abdel-Aty, 2008).

Two important limitations exist when an ordinal model is used (Savolainen and Mannering, 2007). The first limitation relates to under-reporting issues associated with PDO and C severity crashes. When under-reporting occurs, the ordered probability model yields biased and inconsistent coefficient estimates (Ye and Lord, 2011).

The second limitation of the ordinal model corresponds to the implied influence of each model variable. Ordered models constrain each variable's effect such that a variable that increases the probability of the most severe outcome decreases the probability of the less severe outcomes. Similarly, a variable that increases the probability of the least severe outcome decreases the probability of the more severe outcomes. This limitation is problematic when the influence of a variable does not follow this trend. For example, an increase in barrier offset is likely to decrease both fatal crash frequency and PDO crash frequency.

The partially-ordered logit model can be used to overcome the aforementioned disadvantage of the ordered logit model. This model allows the coefficient of some variables to vary across severity levels, while the effect of other variables will be fixed across severity levels. Wang and Abdel-Aty (2008) used this model to examine the severity of left-turn-related crashes. They found that partial proportional odds models consistently perform better than ordered probability models. Wang et al. (2009) used this model to evaluate the effect of geometric and environmental conditions on crash severity in freeway diverge areas.

An ordered mixed (i.e., random effects) logit model represents an extension of the ordered logit. It quantifies that portion of the response variability that represents unobserved heterogeneity among sites (i.e., variation among sites that is likely explainable by missing variables). The response variability is reduced by this technique, with the result being more efficient regression coefficient estimates. Srinivasan (2002) used this model structure to evaluate the driver and vehicle factors that influence crash severity on highways.

The multinomial logit model (MNL) has also been used to analyze crash severities (Shankar and Mannering, 1996). It offers flexibility of constraining some variables to have the same effect on each severity level, while allowing the effect of other variables to vary among severity levels. As a result, the MNL model has the advantage of greater flexibility in modeling variable influence.

The MNL model was derived assuming that the error components are extreme value distributed (i.e., Gumbel). Though this assumption simplifies the probability equation, it adds the "independence from irrelevant alternatives" (IIA) property in the MNL model. The IIA property of the MNL restricts the ratio of probabilities for any pair of crash severities to be independent of the existence and characteristics of other crash severities in the set of severities considered in the model. This restriction implies that the introduction of a new crash severity level in the set will affect all other severities proportionately (Koppelman and Bhat, 2006).

The nested logit overcomes the IIA limitation of MNL model. The nested logit model groups crash severities that share unobserved attributes at different levels of a nest. This technique allows error terms within a nest to be correlated. Several studies have used the nested logit model for crash severity analysis (Shankar et al., 1996; Savolainen and Mannering, 2007).

The (multinomial) random parameters logit model (i.e., mixed logit model) represents a more generalized version of the ordered mixed logit model. This type of model has also been used by researchers to examine crash severity (Milton et al., 2008; Anastasopoulos and Mannering, 2011). This model overcomes the aforementioned disadvantage of the ordered logit structure by allowing a more flexible formulation that calibrates separate functions to each severity level. The “random parameters” element of this model quantifies for each model variable the portion of the response variability that is due to site-to-site variation. One disadvantage of this model structure is that it requires simulation-based methods to estimate the model regression coefficients, which leads to an increase in model development time. Another disadvantage is that it does not consider the hierarchy of severity levels (Savolainen et al., 2011).

FREEWAY SEGMENTS

This part of the chapter consists of four sections. The first section describes the data used to calibrate the SDF for freeway segments. The second section describes the methodology used for calibrating the models. The third section presents the modeling results. The last section describes the procedure for local calibration of a SDF.

Highway Safety Database

The Highway Safety Information System (HSIS) was used as the primary source of data for model calibration. The “HSIS” states California, Maine, and Washington were identified as including ramp volume data, which is of fundamental importance to all aspects of this project. These data were not available from the other HSIS states. Hence, the database assembly focused on these three states. They are called the “study states” in this report. The data acquired from the HSIS is summarized in Table 29.

As discussed in Appendix B, several of the geometry and lane use variables in the study state databases were of unknown accuracy. Also, several variables often had subtly different definitions among states. Moreover, the study state databases often did not include variables that describe road-related factors known to be associated with crash severity. To overcome these limitations, the study-state databases were enhanced using data from other sources. The data collected include the width of various cross section elements, barrier presence and location, horizontal curvature, ramp configuration, ramp entrance location, and median type. A complete list of the supplemental data is provided in Table 30.

Methodology

This section describes the methodology used to calibrate the SDF for freeway segments. The first subsection describes the discrete choice model used for SDF development. The second subsection describes the approach used to develop the SDF model form.

Discrete Choice Model

Based on a review of the literature, it was concluded that the prediction of crash frequency by severity level can be accomplished by using a SDF with a safety prediction model. For freeway safety evaluation, the SDF would be used with the safety prediction models in Chapter 5. This approach is intended to minimize the frequency-severity indeterminacy problem

described by Hauer (2006). The SDF model considers all severity levels together and, therefore, can be used to predict the shift in crashes among levels due to a change in roadway conditions. The discrete choice model includes only infrastructure-specific variables (such as geometric design, traffic control, and traffic characteristic data). It ignores post-crash variables (such as driver behavior and environmental data). This approach results in some loss in forecasting accuracy, relative to models that include these variables (Anastasopoulos and Mannering, 2011), but is appropriate for the intended application.

The MNL model was selected as the basis for SDF development. Nested logit models were developed to evaluate the IIA limitation of the MNL model for this application. A test comparing the two models showed that the inclusive value parameters (for nesting) for these models were not significantly different from 1.0. For an acceptable nesting structure, the inclusive values need to be between 0.0 and 1.0. An inclusive value parameter equal to 1.0 indicates that there is no correlation in the unobserved factors within the nest and, therefore, the nested logit model is not different from the standard MNL model. A linear function was used to relate the crash severity with the geometric design features, traffic control features, and traffic characteristics.

Modeling Approach

For highway safety applications, the MNL model is used to predict the probability of each crash severity level. An individual crash's severity among the given severities was considered to be predicted if the crash severity likelihood function was maximum for that particular severity.

The MNL model was derived assuming that the error components are extreme value distributed (McFadden, 1981). The probability of outcome j is defined by the following equation.

$$P_j = \frac{e^{V_j}}{\sum_{i=1}^J e^{V_i}} \quad (320)$$

where,

- P_j = probability of the outcome j ;
- V_j = deterministic component of outcome j ; and
- J = total number of possible outcomes modeled.

When applied to crash severity, the outcomes for severe crashes can be represented by three severity levels (i.e., K, A, and B), with severity level C used as the base scenario. This application is shown in the following equations.

$$P_K = \frac{e^{V_K}}{\frac{1.0}{C} + e^{V_K} + e^{V_A} + e^{V_B}} \quad (321)$$

$$P_A = \frac{e^{V_A}}{\frac{1.0}{C} + e^{V_K} + e^{V_A} + e^{V_B}} \quad (322)$$

$$P_B = \frac{e^{V_B}}{\frac{1.0}{C} + e^{V_K} + e^{V_A} + e^{V_B}} \quad (323)$$

$$P_C = 1.0 - (P_K + P_A + P_B) \quad (324)$$

where,

- P_K = probability of severity level K (fatal);
- P_A = probability of severity level A (incapacitating injury);
- P_B = probability of severity level B (non-incapacitating injury);
- P_C = probability of severity level C (possible injury); and
- C = local calibration factor.

The likelihood function for the MNL model is considered to have a deterministic component and a random error component. While the deterministic part is assumed to contain variables that can be measured; the random part corresponds to the unaccounted factors that impact crash severity. The deterministic part of the crash severity model was designated as a linear function of roadway conditions. The following equation is used to describe the deterministic component.

$$V_j = ASC_j + \sum_{n=1}^N b_{n,j} X_n \quad (325)$$

where,

- V_j = deterministic component for severity level j ($j = K, A, B$);
- ASC_j = alternative specific constant for crash severity level j ;
- $b_{n,j}$ = calibration coefficient for crash severity level j and variable n ;
- X_n = independent variable n , $n = 1, 2, \dots, N$; and
- N = total number of independent variables included in the model.

The SAS (2009) non-linear mixed modeling procedure (NLMIXED) was used for model calibration.

Modeling Results

This section describes the modeling results. It is divided into four subsections. The first subsection describes the calibration data. The second subsection describes the formulation of the calibration model. The third subsection describes the calibrated model and estimation results. The last subsection examines the sensitivity of the model prediction to selected variable values.

Calibration Data

The database assembled for calibration included crash severity level as the dependent variable. Geometric design features, traffic control features, and traffic characteristics were included as independent variables.

The highway safety database required modification to be used for SDF calibration. Each observation in the highway safety database represents one site with known geometric features,

traffic control features, traffic characteristics, and crash frequency (by severity level). To convert this database to the form needed for SDF calibration, each observation is repeated once for each fatal or injury crash associated with it. An attribute indicating the severity of the crash is added to the newly-created SDF database. In this manner, sites that experience only PDO crashes are excluded from the SDF database. The total sample size of the SDF database is equal to total number of injury and fatal crashes in the highway safety database. During the model calibration, the “possible injury” level is set as the base scenario with coefficients restricted to 0.0.

Table 102 presents a brief summary of the variables used for SDF development. The variables listed were those found to have an important influence on the crash severity level. A complete list of all variables in the database is given in Chapter 5.

TABLE 102. Summary statistics for freeway SDF development

Variable	Type	Mean	Standard Deviation	Minimum	Maximum	Crash Count
Proportion of segment with barrier		0.58	0.24	0.00	1.00	8,249
Proportion of AADT during high-volume hours		0.49	0.35	0.00	0.93	8,249
Proportion of segment with rumble strips		0.20	0.38	0.00	1.00	8,249
Proportion of segment with horizontal curve		0.28	0.33	0.00	1.00	8,249
Lane width, ft		11.99	0.59	10.1	14.9	8,249
Area type	Rural					2,417
	Urban					5,832
Severity level	K					171
	A					445
	B					2,550
	C					5,083

Model Development

The following model form was used for the deterministic component of the SDF during the regression analysis.

$$V_K = ASC_K + (b_{bar,K} \times 0.5 \times [P_{ib} + P_{ob}]) + (b_{hv,K} \times P_{hv}) + (b_{rs,K} \times 0.5 \times [P_{ir} + P_{or}]) + (b_{hc,K} \times P_c) + (b_{l,K} \times W_l) + (b_{rural,K} \times I_{rural}) \quad (326)$$

$$V_A = ASC_A + (b_{bar,A} \times 0.5 \times [P_{ib} + P_{ob}]) + (b_{hv,A} \times P_{hv}) + (b_{rs,A} \times 0.5 \times [P_{ir} + P_{or}]) + (b_{hc,A} \times P_c) + (b_{rural,A} \times I_{rural}) \quad (327)$$

$$V_B = ASC_B + (b_{bar,B} \times 0.5 \times [P_{ib} + P_{ob}]) + (b_{hv,B} \times P_{hv}) + (b_{rs,B} \times 0.5 \times [P_{ir} + P_{or}]) + (b_{hc,B} \times P_c) + (b_{l,B} \times W_l) + (b_{rural,B} \times I_{rural}) \quad (328)$$

$$C = e^{b_{ca} I_{ca}} \quad (329)$$

where,

- P_{ib} = proportion of segment length with a barrier present in the median (i.e., inside);
 P_{ob} = proportion of segment length with a barrier present on the roadside (i.e., outside);
 P_{hv} = proportion of AADT during hours where volume exceeds 1,000 veh/h/ln;
 P_{ir} = proportion of segment length with rumble strips present on the inside shoulders;
 P_{or} = proportion of segment length with rumble strips present on the outside shoulders;
 P_c = proportion of the segment length with curvature;
 W_l = lane width, ft;
 I_{rural} = area type indicator variable (= 1.0 if area is rural, 0.0 if it is urban); and
 I_{ca} = California indicator variable (= 1.0 if segment in California, 0.0 otherwise).

The final form of the regression model is described by the preceding equations. This form reflects the findings from several preliminary regression analyses where alternative model forms were examined. The form that is described represents that which provided the best fit to the data, while also having coefficient values that are logical and constructs that are theoretically defensible and properly bounded.

Model Calibration

Table 103 summarizes the estimation results of model calibration. An examination of the coefficient values and their implication on the corresponding crash severity levels are documented in a subsequent section. In general, the sign and magnitude of the regression coefficients in Table 103 are logical and consistent with previous research findings.

The t-statistic for each coefficient in Table 103 indicates a test of the hypothesis that the coefficient value is equal to 0.0. Those t-statistics with an absolute value that is larger than 2.0 indicate that the hypothesis can be rejected with the probability of error in this conclusion being less than 0.05. For those few variables where the absolute value of the t-statistic is smaller than 2.0, it was decided that the variable was important to the model and its trend was found to be intuitive and, where available, consistent with previous research findings (even if the specific value was not known with a great deal of certainty as applied to this database).

TABLE 103. Parameter estimation for freeway SDF

Variable	Inferred Effect of...	Fatal (K)		Incapacitating Injury (A)		Non-Incapacitating Injury (B)	
		Value	t-statistic	Value	t-statistic	Value	t-statistic
ASC	Alternative specific constant	-0.1705	-0.09	-2.3929	-13.49	0.0732	0.13
b_{bar}	Proportion of barrier	-0.3883	-1.06	-0.3253	-1.41	-0.2499	-2.08
b_{hv}	Proportion volume during high-volume hours	-0.9239	-3.03	-0.8528	-4.42	-0.8720	-8.96
b_{rs}	Proportion of rumble strips	0.3868	1.67	0.3906	2.63	0.1347	1.63
b_{hc}	Proportion of horiz. curves	0.2079	0.88	0.2427	1.62	0.1312	1.75
b_l	Lane width	-0.2608	-1.72			-0.0464	-1.03
b_{rural}	Added effect of rural area type	0.4919	2.47	0.4302	3.42	0.2079	3.14
b_{ca}	Location in California	0.3490	6.45	0.3490	6.45	0.3490	6.45

Indicator variables were included for the states of California and Maine. However, only the coefficient for California was statistically significant. The coefficient for this variable is shown in the last row of Table 103. Its value indicates that a crash on a freeway in California is likely to be more severe than a crash on a freeway in Maine and Washington. The trend could not be explained by differences in road design among the states. A more detailed discussion of this variable is given in the subsequent section.

The coefficients in Table 103 were combined with Equations 326 to 328 to obtain the deterministic component of each crash severity level for freeway crashes. The form of each model is described by the following equations.

$$V_K = -0.1705 - (0.3883 \times 0.5 \times [P_{ib} + P_{ob}]) - (0.9239 \times P_{hv}) + (0.3868 \times 0.5 \times [P_{ir} + P_{or}]) + (0.2079 \times P_c) - (0.2608 \times W_l) + (0.4919 \times I_{rural}) \quad (330)$$

$$V_A = -2.3929 - (0.3253 \times 0.5 \times [P_{ib} + P_{ob}]) - (0.8528 \times P_{hv}) + (0.3906 \times 0.5 \times [P_{ir} + P_{or}]) + (0.2427 \times P_c) + (0.4302 \times I_{rural}) \quad (331)$$

$$V_B = 0.0732 - (0.2499 \times 0.5 \times [P_{ib} + P_{ob}]) - (0.8720 \times P_{hv}) + (0.1347 \times 0.5 \times [P_{ir} + P_{or}]) + (0.1312 \times P_c) - (0.0464 \times W_l) + (0.2079 \times I_{rural}) \quad (332)$$

The probability of each severity level is obtained by combining Equations 321 to 324 with Equations 330 to 332. The procedure for estimating the local calibration factor is described in the next section.

Predicted Probabilities

Barrier Presence. Two variables that define the existence of barrier include the proportion of segment length with a barrier present in the median P_{ib} , and the proportion of segment length with a barrier present on the roadside P_{ob} . These variables are calculated using Equations 68 and 71 (in Chapter 5), respectively. The proportion-of-median-barrier and proportion-of-roadside-barrier variables were considered separately during the model calibration. However, both variables showed similar effect and, thus, the average of these two variables is represented in the final model. Barrier is defined herein to be any combination of cable barrier, concrete barrier, guardrail, or bridge rail.

The relationship between the proportion-of-segment-with-barrier variable and severity level is shown in Figure 138. The negative value of the associated coefficient (in Table 103) indicates that, as the proportion of barrier increases, the likelihood of severity levels K, A, and B decreases. The trends in Figure 138 indicate that the fatal crash percentage changes from 7.1 percent without a barrier, to 5.7 percent with a continuous barrier. A similar trend is shown for severity levels A and B.

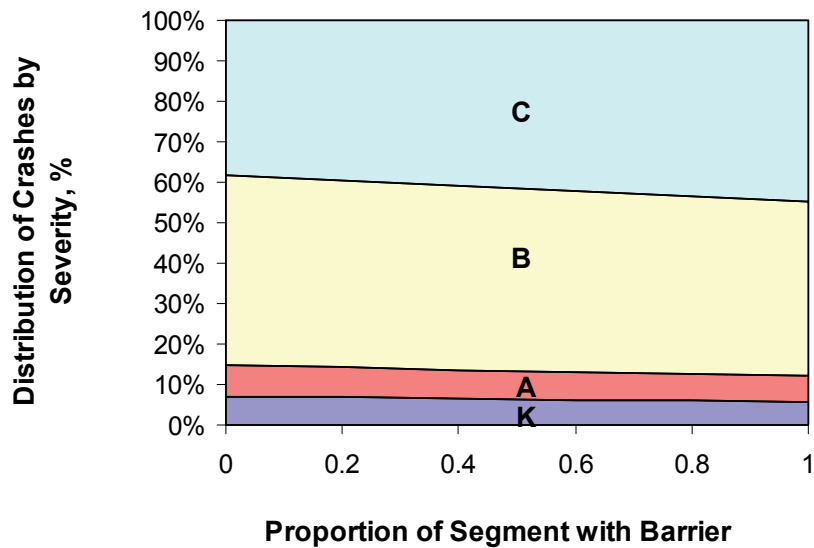


Figure 138. Freeway severity distribution based on the proportion of segment with barrier.

The trends shown in Figure 138 are consistent with the findings of other researchers. For example, Bligh et al. (2006) found that locations where barrier was not present had cross-median and other median-related crashes that were more likely to be of the K, A, or B severity, relative to locations with longitudinal barrier. Donnell and Mason (2006) found that the installation of median barriers decreases the probability of fatal and injury crashes. In another study, Tarko et al. (2008) noted that installing a concrete barrier decreased the most severe head-on crashes but increased the other non-severe crash types.

High-Volume. This variable indicates the proportion of AADT during hours where volume exceeds 1,000 veh/h/ln. It is computed using the average hourly volume distribution associated with the subject segment. This distribution will typically be computed using the data obtained from the nearest continuous traffic counting station (on a freeway of similar character). The variable is positively correlated with the volume to-capacity ratio experienced by the segment on an hourly basis. A more detailed explanation of this variable is provided in Chapter 5.

The relationship between the proportion of AADT during high-volume hours and severity level is shown in Figure 139. The negative value of the associated coefficient (in Table 103) indicates that, as the proportion of high-volume hours increases, the likelihood of severity levels K, A, and B decreases. The trends in Figure 139 indicate that the fatal crash percentage changes from 7.1 percent when the proportion equals 0.0, to 4.4 percent when the proportion equals 1.0. A similar trend is shown for severity levels A and B.

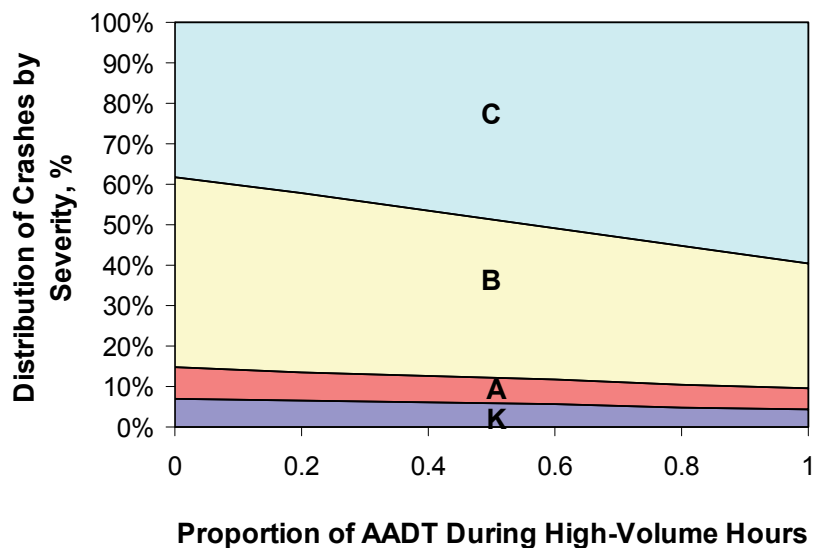


Figure 139. Freeway severity distribution based on the proportion of AADT during high-volume hours.

It is rationalized that the trends in Figure 139 are due to the correlation between the proportion variable and speed. During high-volume conditions, the running speed of the vehicles decreases and, thus, the chance to be involved in a severe crash decreases. Martin (2002) investigated the relationship of traffic flow and crash severity on French motorways and concluded that lower traffic flow is associated with an increase in crash severity. In a study of London highways, Noland and Quddus (2005) found that congestion is less likely to be associated with severe crashes in urban conditions. The authors stated that the mobility benefits of reduced traffic congestion might be offset by the occurrence of more severe crashes. In another study, Quddus et al. (2010) explored the relationship between crash severity and congestion. They found that the level of traffic congestion does not affect crash severity, which contradicts the 2005 study.

Rumble Strips. The presence of shoulder rumble strips was found to have some association with the crash severity distribution. This presence is quantified as the proportion of the segment with rumble strips. It is computed separately for the outside shoulders and the inside shoulders. For the inside shoulders, this proportion is computed by summing the length of roadway with rumble strips on the inside shoulder in *both* travel directions and dividing by twice the segment length. For the outside shoulders, this proportion is computed by summing the length of roadway with rumble strips on the outside shoulder in *both* travel directions and dividing by twice the segment length. An initial regression model form contained both the inside and outside rumble strip proportions. However, the two variables yielded a similar relationship with crash severity level and, thus, the average of these two variables is represented in the final model.

The relationship between the proportion-of-segment-with-rumble-strips variable and severity level is shown in Figure 140. The positive value of the associated coefficient (in Table 103) indicates that, as the proportion of rumble strips increases, the likelihood of severity levels K, A, and B also increases. The trends in Figure 140 indicate that the fatal crash

percentage changes from 7.1 percent when the proportion equals 0.0, to 9.2 percent when the proportion equals 1.0. A similar trend is shown for severity levels A and B.

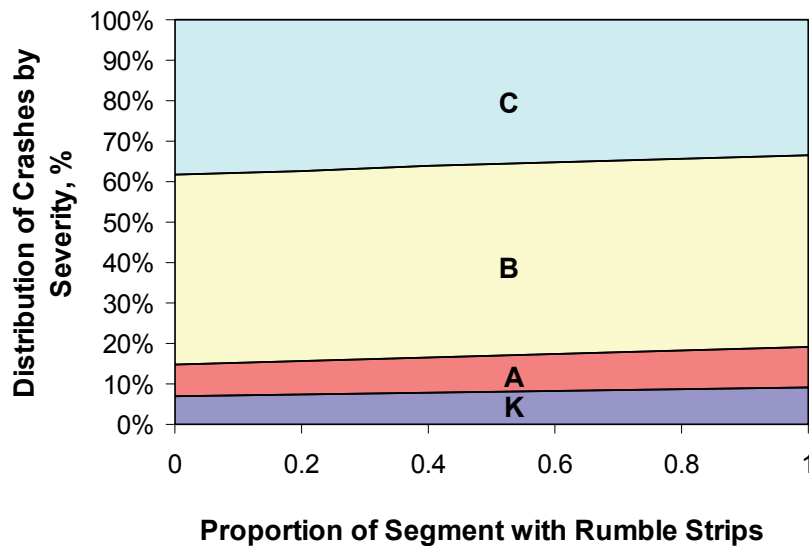


Figure 140. Freeway severity distribution based on the proportion of segment with rumble strips.

The trends shown in Figure 140 are consistent with the findings of other researchers. For example, Griffith (1999) found this trend in his before-after study of the effect of continuous shoulder rumble strips on freeways. He concluded that, for impaired drivers, there could be a possible transfer from single-vehicle run-off-the-road crashes to multiple-vehicle crashes, the latter crash type being more severe. Hu and Donnell (2010) concluded that an increase in severity could be caused by over-steering, which results in the driver leaving the traveled-way in order to avoid possible multi-vehicle rear-end or sideswipe crashes with vehicles in adjacent lanes. It is possible that some drivers who encounter rumble strips on curves may respond by over steering.

Marvin and Clark (2003) conducted a before-after study to evaluate the safety effectiveness of shoulder rumble strips. They concluded that, in certain situations, rumble strips increased the severity of rollover crashes. They hypothesized that the increase could be through rumble strip deployment or other undefined factors. Smith and Ivan (2005) observed an increase in the proportion of multiple-vehicle crashes with the addition of rumble strips. They stated that a possible reason for the increase in the multiple-vehicle crashes is because of a driver hitting the rumble strip and subsequently panicking, which causes the driver to swerve and hit another vehicle. In contrast, Sayed et al. (2010) reported a reduction in crash severity after the installation of shoulder rumble strips.

The association of rumble strip treatment with increased crash severity could be the result of confounding variables. That is, it is possible that rumble strips are being installed at locations where crash severity is relatively high. However, the application of rumble strips on freeways is a fairly routine practice among state transportation agencies, such that rumble strips tend to be installed as a matter of policy rather than as a problem-site treatment. Moreover, at least two of

the studies cited in the previous paragraphs used a before-after design, which would control for some confounding elements.

Horizontal Curve. The “proportion of segment with horizontal curve” variable P_c is computed as the ratio of the length of all curves on the segment to the length of the segment. For example, consider a segment that is 0.5 mi long and has only one curve that is 0.2 mi long. If one-half of the curve is on the segment, then $P_c = 0.20 (= 0.1/0.5)$. In fact, this proportion is the same regardless of the curve’s length (provided that it is 0.1 mi or longer and 0.1 mi of this curve is located on the segment). In addition to P_c , different combinations of curve radius and length were considered during model calibration. However, the proportion-of-segment-with-curve variable was the only one found to be correlated with crash severity.

The relationship between the proportion-of-segment-with-horizontal-curve and severity level is shown in Figure 141. The positive value of the associated coefficient (in Table 103) indicates that, as the proportion of the segment with horizontal curvature increases, the likelihood of severity levels K, A, and B also increases. The trends in Figure 141 indicate that the fatal crash percentage increases from 7.1 percent for a segment with no curve to 8.0 percent for a segment located fully on a horizontal curve. A similar trend is shown for severity levels A and B.

Hu and Donnell (2010) found a similar result when analyzing median barrier crashes on curved and uncurved freeway segments. They concluded that the trend is likely due to the fact that vehicles on horizontal curves impact longitudinal barriers at higher impact angles, relative to those on tangent segments. Shankar et al. (1996) found that road sections with frequent horizontal curves tend to have a larger proportion of injury crashes, relative to road sections with infrequent curves. Abdel-Aty (2003) also found that roadway curves contribute to higher probability of injuries on roadway sections. Donnell and Mason (2006) analyzed the effect of curved sections on crash severity. They found the likelihood that a crash is designated as fatal or injury is higher for curved sections than for tangent sections.

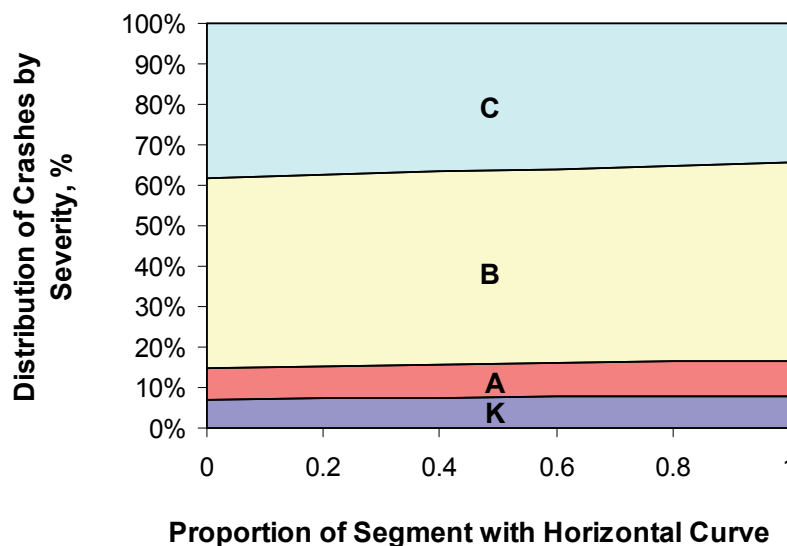


Figure 141. Freeway severity distribution based on the proportion of segment with horizontal curve.

Lane Width. The lane width used in this research is an average for all through lanes on the segment. Shoulder width was also considered during model calibration, but it was not found to have a correlation with crash severity.

The relationship between lane width and severity level is shown in Figure 142. The negative value of the associated coefficient (in Table 103) indicates that, as the lane width increases, the likelihood of severity levels K, A, and B decreases. The trends in Figure 142 indicate that the fatal crash percentage decreases from 5.7 percent at 10-ft lane width, to 2.3 percent for a 14-ft lane width. A similar trend is shown for severity levels A and B.

Previous studies have shown that an increase in lane width decreases head-on collisions, which are typically severe (Al-Senan et al., 1987; Zegeer et al., 1981). Geedipally et al. (2010) found that if a crash occurs on rural two-lane highways with a wider lane width, it is less likely to be classified as a rear-end collision. With wider lane widths, it is possible that drivers have more opportunity to avoid rear-end and head-on collisions, which in turn reduces the likelihood of high crash severity.

Area Type. The relationship between area type and crash severity level was also considered during model calibration. Previous studies have documented differences in crash severity between urban and rural roadways (Lee and Mannering, 2002; Khorashadi et al., 2005). It is generally recognized that probabilistic models should be developed separately for urban and rural crashes. However, separate models were not developed in this project due to the limited sample size.

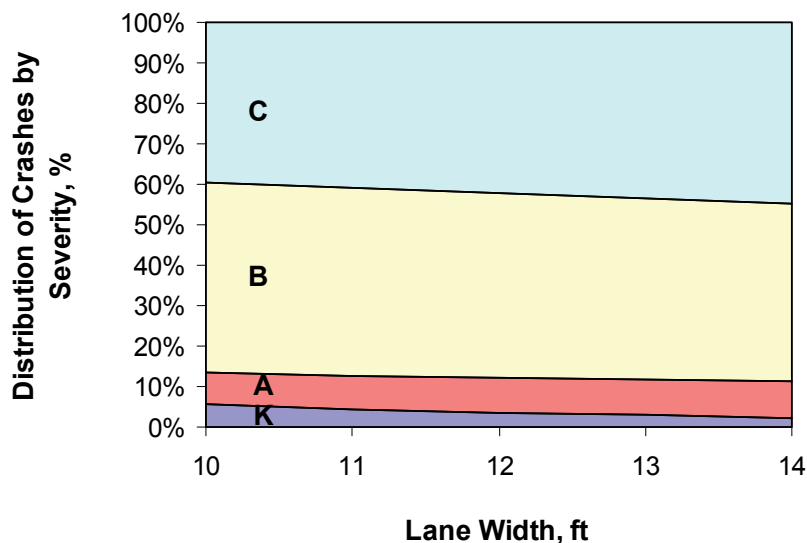


Figure 142. Freeway severity distribution based on lane width.

The relationship between area type and severity level is shown in Table 104. The positive value of the associated coefficient (in Table 103) indicates that a crash in a rural area is likely to be more severe than a crash in an urban area, when all other variables are controlled. The percentages in Table 104 indicate that the fatal crash percentage on a rural freeway is

7.1 percent, and it is 5.1 percent on an urban freeway. A similar trend is shown for severity levels A and B.

TABLE 104. Freeway severity distribution based on area type and state

Variable	Type	Severity Level Distribution, percent			
		Fatal (K)	Incapacitating Injury (A)	Non-Incapacitating Injury (B)	Possible Injury (C)
Area type	Rural	7.1	7.6	47.2	38.1
	Urban	5.1	5.8	44.7	44.5
State	Calif.	7.1	7.6	47.2	38.1
	Other	6.1	6.5	40.7	46.6

The trend with area type in Table 104 can be attributed to higher operating speeds on rural freeways. A crash that occurs at higher speed typically has higher severity than a crash at lower speed.

State. In addition to the roadway variables, an indicator variable for each state was included in the calibrated model to account for differences between states that could not be explained with the other variables in the model. Indicator variables for the states of California and Maine were initially included in the regression model. However, the coefficient for Maine was very small and not statistically significant. This finding suggests that the state effect is very similar between Maine and Washington. The Maine indicator variable was removed as a result.

The coefficient for California is relatively large and statistically significant. Its positive sign indicates that a crash on freeways in California is more severe than a crash on freeways in Washington or Maine, when all other variables are controlled. This difference may be explained by different crash reporting practices, highway design practices (e.g., use of different roadside design features, etc.), terrain, and weather for the various states. The severity distribution for California is compared with that of the other states in Table 104.

Local Calibration Procedure

This section describes the procedure for calibrating the SDF to local conditions. At least 30 sites should be randomly selected as calibration sites. They should have geometric design and traffic control features that are representative of facilities in the region, and similar to those to which the calibrated SDF will be applied. If the calibration site is a segment (as opposed to an intersection), then it should be between 0.1 and 1.0 mi in length to ensure statistical validity and site homogeneity.

The calibration data should represent reported crashes for each calibration site for a period of at least one year, and no more than three years. Each year represented in the calibration period should have a duration of 12 consecutive months to avoid seasonal effects in the data.

The calibration database should include at least 300 fatal or injury crashes for the calibration period. If this minimum is not realized for the sites selected, then (1) additional sites should be added to the database or (2) the calibration period should be expanded to include more years (but no more than three years).

The procedure consists of three steps. During the first step, the count of injury or fatal crashes during the calibration period $N_{o, K+A+B+C}$ is determined for each site. Also, the count of crashes with a severity level of K, A, or B during the calibration period $N_{o, K+A+B}$ is also determined for each site. These two counts are then separately summed for all sites and used to compute the observed probability of a K, A, or B crash $P_{o, K+A+B}$ ($= N_{o, K+A+B} / N_{o, K+A+B+C}$), given that the crash involves an injury or fatality. In this manner, one average observed probability is obtained for all sites combined.

In the second step, the uncalibrated SDF model (i.e., $C = 1.0$) is used with the predictive method described in a previous chapter to estimate the predicted number of fatal-and-injury crashes during the calibration period $N_{p, K+A+B+C}$ is determined for each site. Also, the predicted number of crashes with a severity level of K, A, or B during the calibration period $N_{p, K+A+B}$ is also determined for each site. These two estimates are then separately summed for all sites and used to compute the predicted probability of a K, A, or B crash $P_{p, K+A+B}$ ($= N_{p, K+A+B} / N_{p, K+A+B+C}$), given that the crash involves an injury or fatality. In this manner, one average predicted probability is obtained for all sites combined.

In the third step, Equation 333 is used to estimate the local calibration factor using the probabilities computed in steps 1 and 2.

$$C = \frac{P_{o, K+A+B}}{1.0 - P_{o, K+A+B}} \times \frac{1.0 - P_{p, K+A+B}}{P_{p, K+A+B}} \quad (333)$$

where,

- C = local calibration factor;
- $P_{o, K+A+B}$ = probability of a crash having a K, A, or B severity, given that it is an injury or fatal crash, and based on reported crash data; and
- $P_{p, K+A+B}$ = probability of a crash having a K, A, or B severity, given that it is an injury or fatal crash, and based on predicted crashes.

Table 105 illustrates the local calibration procedure using sample data from 50 freeway segments. The reported crash data are listed in columns 2 through 5 and the predicted crashes are listed in columns 6 through 9. The value of $P_{o, K+A+B}$ is computed as 0.431 ($= [8 + 15 + 95] / [8 + 15 + 95 + 156]$). In a similar manner, the value of $P_{p, K+A+B}$ is computed as 0.373 using the predicted crash data. Substitution of these two proportions in Equation 333 yields a calibration factor of 1.27.

TABLE 105. Example application of SDF local calibration procedure

Site Number	Reported Crashes by Severity Level (N_o)				Predicted Crashes by Severity Level (N_p)			
	K	A	B	C	K	A	B	C
1	1	3	17	25	1.1	2.4	16.0	26.6
2	1	2	6	7	0.2	0.7	4.5	10.6
3	0	0	1	1	0.0	0.1	0.5	1.4
:	:	:	:	:	:	:	:	:
50	0	1	3	18	0.2	0.6	4.4	16.7
Total:	8	15	95	156	5.8	15.0	81.3	171.8

RAMP SEGMENTS

This part of the chapter describes the activities undertaken to calibrate a SDF for ramp and C-D road segments. It consists of three sections. The first section describes the data used to calibrate the SDF. The second section provides an overview of the approach used to develop the SDF model form. The third section presents the modeling results.

Highway Safety Database

The Highway Safety Information System (HSIS) was used as the primary source of data for model calibration. The “HSIS” states California, Maine, and Washington were identified as including ramp volume data, which is of fundamental importance to all aspects of this project. These data were not available from the other HSIS states. Hence, the database assembly focused on these three states. They are called the “study states” in this report. The data acquired from the HSIS is summarized in Table 45.

As discussed in Appendix B, several of the geometry and lane use variables in the study state databases were of unknown accuracy. Also, several variables often had subtly different definitions among states. Moreover, the study state databases often did not include variables that describe road-related factors known to be associated with crash severity. To overcome these limitations, the study-state databases were enhanced using data from other sources. The data collected include the width of various cross section elements, barrier presence and location, horizontal curvature, and ramp entrance location. A complete list of the supplemental data is provided in Table 46.

Modeling Approach

For highway safety applications, the multinomial logit (MNL) model is used to predict the probability of each crash severity level. A brief description of the MNL model and other discrete choice models was given in the part titled Literature Review. This model is shown in Equations 320 to 325. The deterministic component of the model is used to relate the crash severity with the site’s geometric design features, traffic control features, and traffic characteristics. The SAS (2009) non-linear mixed modeling procedure (NLMIXED) was used for the evaluation of MNL model.

Initially, the SDF was developed to predict the proportion of crashes in each severity level. However, the model was not able to quantify statistically significant coefficients for most variables due to a small number of reported fatal crashes. Thus, the fatal and incapacitating injury crashes are combined into one level for model calibration. The probability for each crash severity level is given by the following equations.

$$P_{K+A} = \frac{e^{V_{K+A}}}{\frac{1.0}{C} + e^{V_{K+A}} + e^{V_B}} \quad (334)$$

$$P_B = \frac{e^{V_B}}{\frac{1.0}{C} + e^{V_{K+A}} + e^{V_B}} \quad (335)$$

$$P_C = 1.0 - (P_{K+A} + P_B) \quad (336)$$

where P_{K+A} is the probability of severity level K or A (fatal or incapacitating injury) and the other variables are defined previously.

Modeling Results

This section describes the modeling results. It is divided into four subsections. The first subsection describes the calibration data. The second subsection describes the formulation of the calibration model. The third subsection describes the calibrated model and estimation results. The last subsection examines the sensitivity of the model prediction to selected variable values.

Calibration Data

The database assembled for calibration included crash severity level as the dependent variable. Geometric design features, traffic control features, and traffic characteristics were included as independent variables.

The highway safety database required modification to be used for SDF calibration. Each observation in the highway safety database represents one site with known geometric features, traffic control features, traffic characteristics, and crash frequency (by severity level). To convert this database to the form needed for SDF calibration, each observation is repeated once for each fatal or injury crash associated with it. An attribute indicating the severity of the crash is added to the newly-created SDF database. The total sample size of the SDF database is equal to total number of injury and fatal crashes in the highway safety database. During the model calibration, the “possible injury” level is set as the base scenario with coefficients restricted to 0.0.

Table 106 presents a brief summary of the variables used for SDF development. The variables listed were those found to have an important influence on the crash severity level. A complete list of all variables in the database is given in Chapter 6.

TABLE 106. Summary statistics for ramp SDF development

Variable	Type	Mean	Standard Deviation	Minimum	Maximum	Crash Count
Proportion of segment with barrier		0.34	0.34	0.00	1.00	1,034
Number of lanes		1.31	0.16	1	2	1,034
Area type	Rural					109
	Urban					925
Ramp type ¹	Exit					502
	Other					532
Severity level	K					27
	A					81
	B					415
	C					511

Note:

1 - "Other" includes entrance ramps, connector ramps at system interchanges, and C-D roads.

Model Development

The following model form was used for the deterministic component of the SDF during the regression analysis.

$$V_{K+A} = ASC_{K+A} + (b_{bar,K+A} \times 0.5 \times [P_{lb} + P_{rb}]) + (b_{n,K+A} \times n) + (b_{rural,K+A} \times I_{rural}) + (b_{exr,K+A} \times I_{exr}) \quad (337)$$

$$V_B = ASC_B + (b_{bar,B} \times 0.5 \times [P_{lb} + P_{rb}]) + (b_{n,B} \times n) + (b_{rural,B} \times I_{rural}) \quad (338)$$

$$C = e^{b_{ca} I_{ca}} \quad (339)$$

where,

- P_{lb} = proportion of segment length with a barrier present on the left side;
- P_{rb} = proportion of segment length with a barrier present on the right side;
- n = number of through lanes on segment;
- I_{rural} = area type indicator variable (= 1.0 if area is rural, 0.0 if it is urban);
- I_{exr} = exit ramp indicator variable (= 1.0 if segment is an exit ramp, 0.0 otherwise); and
- I_{ca} = California indicator variable (= 1.0 if segment in California, 0.0 otherwise).

The final form of the regression model is described by the preceding equations. This form reflects the findings from several preliminary regression analyses where alternative model forms were examined. The form that is described represents that which provided the best fit to the data, while also having coefficient values that are logical and constructs that are theoretically defensible and properly bounded.

Model Calibration

Table 107 summarizes the estimation results of model calibration. An examination of the coefficient values and their implication on the corresponding crash severity levels are documented in a subsequent section. In general, the sign and magnitude of the regression coefficients in Table 107 are logical and consistent with previous research findings.

TABLE 107. Parameter estimation for ramp SDF

Variable	Inferred Effect of...	Fatal (K) or Incapacitating Injury (A)		Non-Incapacitating Injury (B)	
		Value	t-statistic	Value	t-statistic
ASC	Alternative specific constant	-1.5373	-3.85	0.2355	0.92
b_{bar}	Proportion of barrier	-0.4813	-1.34	-0.4312	-1.92
b_n	Number of lanes	-0.2280	-0.87	-0.4350	-2.68
b_{rural}	Added effect of rural area type	0.6681	1.93	0.6963	2.91
b_{exr}	Added effect of exit ramp	0.4260	1.92		
b_{ca}	Location in California	0.4487	3.04	0.4487	3.04

The t-statistics describe a test of the hypothesis that the coefficient value is equal to 0.0. Those t-statistics with an absolute value that is larger than 2.0 indicate that the hypothesis can be rejected with the probability of error in this conclusion being less than 0.05. For those few variables where the absolute value of the t-statistic is smaller than 2.0, it was decided that the variable was important to the model and its trend was found to be consistent with previous research findings (even if the specific value was not known with a great deal of certainty as applied to this database).

Indicator variables were included for the states of California and Maine. However, only the coefficient for California was statistically significant. The coefficient for this variable is shown in the last row of Table 107. Its value indicates that a crash on a ramp in California is likely to be more severe than a crash on a ramp in Maine and Washington. The difference may be explained by different crash reporting practices, highway design practices, terrain, and weather for the various states.

The coefficients in Table 107 were combined with Equations 337 and 338 to obtain the deterministic component of each crash severity level for ramp and C-D road crashes. The form of each model is described by the following equations.

$$V_{K+A} = -1.5373 - (0.4813 \times 0.5 \times [P_{lb} + P_{rb}]) - (0.2280 \times n) + (0.6681 \times I_{rural}) + (0.4260 \times I_{exr}) \quad (340)$$

$$V_B = 0.2355 - (0.4312 \times 0.5 \times [P_{lb} + P_{rb}]) - (0.4350 \times n) + (0.6963 \times I_{rural}) \quad (341)$$

The probability of each severity level is obtained by combining Equations 334 to 336 with Equations 340 and 341. A procedure for local calibration was described previously in the discussion associated with Table 105.

Predicted Probabilities

Barrier Presence. Two variables that define the existence of barrier include the proportion of segment length with a barrier present on the right side P_{rb} , and the proportion of segment length with a barrier present on the left side P_{lb} . These variables are calculated using Equations 188 and 190 (in Chapter 6), respectively. The proportion of right side barrier and left side barrier variables were considered separately during the model calibration. However, both variables showed similar effect and, thus, the average of these two variables is represented in the final model. Barrier is defined herein to be any combination of cable barrier, concrete barrier, guardrail, or bridge rail.

The relationship between the proportion-of-segment-with-barrier variable and severity level is shown in Figure 143. The negative value of the associated coefficient (in Table 107) indicates that, as the proportion of barrier increases, the likelihood of severity levels K+A and B decreases. The trends in Figure 143 indicate that the K+A crash percentage changes from 17.8 percent without a barrier, to 13.8 percent with a continuous barrier. A similar trend is shown for severity level B.

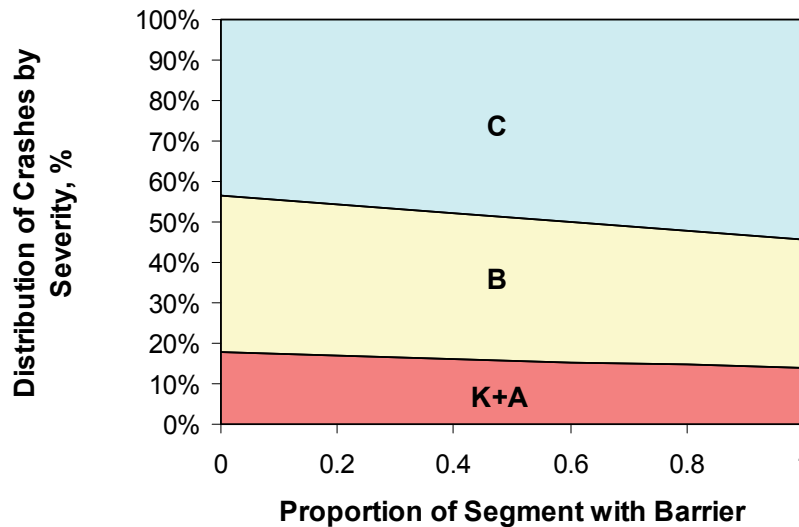


Figure 143. Ramp severity distribution based on the proportion of segment with barrier.

Barriers are installed on the sides of a ramp to prevent a vehicle from leaving the roadway and striking a fixed object or rolling over. For some ramp configurations, a barrier is installed along the left side of the ramp to prevent crashes with vehicles traveling on an adjacent ramp or the main lanes. Previous studies have shown that a significant percentage of severe crashes involve a vehicle that has run off the road and either struck a fixed object or rolled over

(Zegeer et al., 1981; Neuman et al., 2003). Roll-over crashes are more likely to be severe than other crashes (Viano and Parenteau, 2004).

Number of Lanes. This variable represents the count of through lanes at the start of the ramp or C-D road segment, relative to the direction of travel. It does not include speed-change lanes or the auxiliary lane in a C-D road weaving section.

The relationship between number of lanes and severity level is shown in Table 108. The negative value of the associated coefficient (in Table 107) indicates that a crash on a one-lane segment is likely to be more severe than a crash on a two-lane segment, when all other variables are controlled. The percentages in Table 108 indicate that the K+A crash percentage on a one-lane segment is 16.4 percent, and it is 15.6 percent on a two-lane segment.

The trends in Table 108 for number of lanes may be partly explained by the fact that segments with more lanes have increased likelihood of less-severe same direction sideswipe crashes and reduced likelihood of more-severe rear-end crashes (Jonsson et al., 2007). Also, two-lane ramps are more common in urban areas and, thus, are more likely to be associated with lower speed than ramps in rural areas. Abdel-Aty and Keller (2005) analyzed crash severity at signalized intersections and found that intersections with more lanes on the major road have less severe crashes.

TABLE 108. Ramp severity distribution based on lanes, area type, and ramp type

Variable	Type	Severity Level Distribution, percent		
		Fatal (K) or Incapacitating Injury (A)	Non-Incapacitating Injury (B)	Possible Injury (C)
Number of lanes	1	16.4	36.4	47.2
	2	15.6	28.1	56.3
Area type	Rural	21.1	47.9	31.0
	Urban	16.4	36.4	47.2
Ramp type ¹	Exit	16.4	36.4	47.2
	Other	11.8	36.6	51.7

Note:

1 - "Other" includes entrance ramps, connector ramps at system interchanges, and C-D roads.

Area Type. The relationship between area type and crash severity level was also considered during model calibration. It is generally recognized that probabilistic models should be developed separately for urban and rural crashes. However, separate models were not developed in this project due to the limited sample size.

The relationship between area type and severity level is shown in Table 108. The positive value of the associated coefficient (in Table 107) indicates that a crash in a rural area is likely to be more severe than a crash in an urban area, when all other variables are controlled. The percentages in Table 108 indicate that the K+A crash percentage on a rural ramp is 21.1 percent, and it is 16.4 percent on an urban ramp.

The trend with area type in Table 108 can be attributed to higher operating speeds on rural freeways and associated ramps. A crash that occurs at higher speed typically has higher severity than a crash at lower speed.

Ramp Type. The relationship between ramp type and severity level is shown in Table 108. The positive value of the associated coefficient (in Table 107) indicates that a crash on an exit ramp is likely to be more severe than a crash on another type of ramp or on a C-D road, when all other variables are controlled. The percentages in Table 108 indicate that the K+A crash percentage on an exit ramp is 16.4 percent, and it is 11.8 percent on other ramp types.

The increased likelihood of severe crashes on exit ramps can be attributed to driver speed adaption. Drivers on exit ramps tend to have difficulty reducing speed and complying with ramp advisory speeds after a long period of driving on a freeway (Highway, 2010). Jason et al. (1998) found that rear-end crashes involving trucks are more likely to occur in freeway sections with exit ramps than in sections with entrance ramps.

CROSSROAD RAMP TERMINALS

This part of the chapter describes the activities undertaken to calibrate a SDF for crossroad ramp terminals. It consists of three sections. The first section describes the data used to calibrate the SDFs. The second section provides an overview of the approach used to develop the SDF model form. The third section presents the modeling results.

Highway Safety Database

The Highway Safety Information System (HSIS) was used as the primary source of data for model calibration. The “HSIS” states California, Maine, and Washington were identified as including ramp volume data, which is of fundamental importance to all aspects of this project. These data were not available from the other HSIS states. Hence, the database assembly focused on these three states. They are called the “study states” in this report. The data acquired from the HSIS is summarized in Table 60.

As discussed in Appendix B, several of the geometry and lane use variables in the study state databases were of unknown accuracy. Also, several variables often had subtly different definitions among states. Moreover, the study state databases often did not include variables that describe road-related factors known to be associated with crash severity. To overcome these limitations, the study-state databases were enhanced using data from other sources. The data collected include the ramp terminal configuration, number of lanes, bay presence, type of control, and median width. A complete list of the supplemental data is provided in Table 61.

Modeling Approach

For highway safety applications, the multinomial logit (MNL) model is used to predict the probability of each crash severity level. A brief description of the MNL model and other discrete choice models was given in the part titled Literature Review. This model is shown in Equations 320 to 325. The deterministic component of the model is used to relate the crash severity with the site’s geometric design features, traffic control features, and traffic

characteristics. The SAS (2009) non-linear mixed modeling procedure (NLMIXED) was used for the evaluation of MNL model.

Initially, the SDF was developed to predict the proportion of crashes in each severity level. However, the model was not able to quantify statistically significant coefficients for most variables due to a small number of reported fatal crashes. Thus, the fatal and incapacitating injury crashes are combined into one level for model calibration. The probability for each crash severity level is given by Equations 334 to 336, as shown in the part of this chapter addressing ramp segments.

Modeling Results

This section describes the modeling results. It is divided into five subsections. The first subsection describes the calibration data. The second subsection describes the formulation of the calibration model. The third subsection describes the calibrated model and estimation results. The fourth subsection examines the sensitivity of the model for signalized crossroad ramp terminals. The last subsection examines the sensitivity of the model for unsignalized crossroad ramp terminals.

Calibration Data

The database assembled for calibration included crash severity level as a dependent variable. Geometric design features, traffic control features, and traffic characteristics were included as independent variables.

The highway safety database required modification to be used for SDF calibration. Each observation in the highway safety database represents one site with known geometric features, traffic control features, traffic characteristics, and crash frequency (by severity level). To convert this database to the form needed for SDF calibration, each observation is repeated once for each fatal or injury crash associated with it. An attribute indicating the severity of the crash is added to the newly-created SDF database. The total sample size of the SDF database is equal to total number of injury and fatal crashes in the highway safety database. During the model calibration, the “possible injury” level is set as the base scenario with coefficients restricted to 0.0.

Table 109 presents a brief summary of the data variables used for SDF development. The variables listed were those found to have an important influence on crash severity level. A complete list of all variables in the database is given in Chapter 7.

Model Development

The following model form was used for the deterministic component of the SDF during the regression analysis.

$$V_{K+A} = ASC_{K+A} + (b_{p,K+A} \times I_{p,lt}) + (b_{nd,K+A} \times [n_{dw} + n_{ps}]) + (b_{ps,K+A} \times I_{ps}) + (b_{rural,K+A} \times I_{rural}) \quad (342)$$

$$V_B = ASC_B + (b_{p,B} \times I_{p,lt}) + (b_{nd,B} \times [n_{dw} + n_{ps}]) + (b_{ps,B} \times I_{ps}) + (b_{rural,B} \times I_{rural}) \quad (343)$$

$$C = e^{b_{ca} I_{ca} + b_{me} I_{me}} \quad (344)$$

where,

- $I_{p,lt}$ = protected left-turn operation indicator variable for crossroad (= 1.0 if protected operation exists, 0.0 otherwise);
- n_{dw} = number of unsignalized driveways on the crossroad leg outside of the interchange and within 250 ft of the ramp terminal;
- n_{ps} = number of unsignalized public street approaches to the crossroad leg outside of the interchange and within 250 ft of the ramp terminal;
- I_{ps} = non-ramp public street leg indicator variable (= 1.0 if leg is present, 0.0 otherwise);
- I_{rural} = area type indicator variable (= 1.0 if area is rural, 0.0 if it is urban);
- I_{me} = Maine indicator variable (= 1.0 if segment in Maine, 0.0 otherwise); and
- I_{ca} = California indicator variable (= 1.0 if segment in California, 0.0 otherwise).

TABLE 109. Summary statistics for crossroad ramp terminal SDF development

Control Type	Variable	Type	Mean	Standard Deviation	Minimum	Maximum	Crash Count
Signalized	Driveway + public street approach freq.		0.63	0.99	0	4	1,708
	Left-turn operation	Protected					908
		Other					800
	Non-ramp public street leg	Present					1,679
		Not present					29
	Area type	Rural					69
		Urban					1,639
	Severity level	K					2
		A					50
		B					316
C						1,340	
Unsig-nalized	Area type	Rural					176
		Urban					189
	Severity level	K					4
		A					21
		B					88
		C					252

The final form of the regression model is described by the preceding equations. This form reflects the findings from several preliminary regression analyses where alternative model forms were examined. The form that is described represents that which provided the best fit to the data, while also having coefficient values that are logical and constructs that are theoretically defensible and properly bounded.

Model Calibration

Table 110 summarizes the estimation results of model calibration. An examination of the coefficient values and their implication on the corresponding crash severity levels are documented in a subsequent section. In general, the sign and magnitude of the regression coefficients in Table 110 are logical and consistent with previous research findings.

The t-statistics describe a test of the hypothesis that the coefficient value is equal to 0.0. Those t-statistics with an absolute value that is larger than 2.0 indicate that the hypothesis can be rejected with the probability of error in this conclusion being less than 0.05. For those few variables where the absolute value of the t-statistic is smaller than 2.0, it was decided that the variable was important to the model and its trend was found to be consistent with previous research findings (even if the specific value was not known with a great deal of certainty as applied to this database).

TABLE 110. Parameter estimation for crossroad ramp terminal SDF

Control Type	Variable	Inferred Effect of...	Fatal (K) or Incapacitating Injury (A)		Non-Incapacitating Injury (B)	
			Value	t-statistic	Value	t-statistic
Signalized	<i>ASC</i>	Alternative specific constant	-3.2571	-14.78	-1.5107	-14.79
	<i>b_p</i>	Protected left-turn operation	-0.2884	-0.99	-0.1933	-1.5
	<i>b_{nd}</i>	Driveways or pub. st. approaches	0.09905	0.71	0.1487	2.44
	<i>b_{ps}</i>	Public street leg at ramp terminal	1.171	1.48	0.7410	1.74
	<i>b_{rural}</i>	Added effect of area type	0.6191	0.99	0.4160	1.36
	<i>b_{me}</i>	Location in Maine	0.5248	2.24	0.5248	2.24
Unsignalized	<i>ASC</i>	Alternative specific constant	-3.167	-7.96	-1.476	-7.22
	<i>b_{rural}</i>	Added effect of area type	0.8907	1.91	0.2207	0.86
	<i>b_{ca}</i>	Location in California	0.7327	3.11	0.7327	3.11

Indicator variables were included for the states of California and Maine. For signalized terminals, only the coefficient for Maine was statistically significant. The coefficient for this variable is shown in row 6 of Table 110. Its value indicates that a crash at a signalized terminal in Maine is likely to be more severe than a crash at a signalized terminal in California and Washington. For unsignalized terminals, only the coefficient for California was significant. Its value indicates that a crash at an unsignalized terminal in California is likely to be more severe than a crash at an unsignalized terminal in Maine or Washington. The difference may be explained by different crash reporting practices, highway design practices, terrain, and weather for the various states.

The coefficients in Table 110 were combined with Equations 342 and 343 to obtain the deterministic component of each crash severity level for crossroad ramp terminal crashes. The form of each model for signalized ramp terminals is described by the following equations.

$$\begin{aligned}
 V_{K+A} = & -3.2571 - (0.2884 \times I_{p,lt}) + (0.09905 \times [n_{dw} + n_{ps}]) \\
 & + (1.171 \times I_{ps}) + (0.6191 \times I_{rural})
 \end{aligned}
 \tag{345}$$

$$V_B = -1.5107 - (0.1933 \times I_{p,lt}) + (0.1487 \times [n_{dw} + n_{ps}]) + (0.7410 \times I_{ps}) + (0.4160 \times I_{rural}) \quad (346)$$

The probability of each severity level is obtained by combining Equations 334 to 336 with Equations 345 and 346. A procedure for local calibration was described previously in the discussion associated with Table 105.

Although several variables are considered during the calibration of the SDF for unsignalized terminal, only the rural indicator variable was found to be significant. The insignificance of other variables is partially attributed to small sample size. The form of each model for unsignalized ramp terminals is described by the following equations.

$$V_{K+A} = -3.1676 + (0.8907 \times I_{rural}) \quad (347)$$

$$V_B = -1.476 + (0.2207 \times I_{rural}) \quad (348)$$

The probability of each severity level is obtained by combining Equations 334 to 336 with Equations 347 and 348.

Predicted Probabilities for Signalized Crossroad Ramp Terminals

Access Point Frequency. The access point frequency at a crossroad ramp terminal represents the total number of driveways and unsignalized public street approaches on the crossroad leg that is outside of the interchange. Driveways and approaches on both sides of the leg should be counted when they are within 250 ft of the ramp terminal. The count of driveways should only include active driveways (i.e., those driveways with an average daily volume of 10 veh/day or more).

The relationship between access point frequency and severity level is shown in Figure 144. The positive value of the associated coefficient (in Table 110) indicates that, as the number of access points increases, the likelihood of severity levels K, A, and B also increases. The trends in Figure 144 indicate that the K+A crash percentage changes from 6.7 percent with no access points, to 8.4 percent with four access points. A similar trend is shown for severity level B.

It is rationalized that crashes associated with driveway traffic tend to be of the right-angle type, which tend to be more severe than other crashes that occur on intersection approaches. Kim et al. (2006) found that the number of driveways within 250 ft of intersection center have a positive association with angle, rear-end, and sideswipe crash types, with angle crashes being the most severe among the three crash types. Oh et al. (2004) stated that driveways at intersections provide additional conflict points that increase the chance of driveway-related crashes. A study of the safety impacts of access management techniques in Utah found that the driveway consolidation decreased crash severity (Schultz et al., 2007).

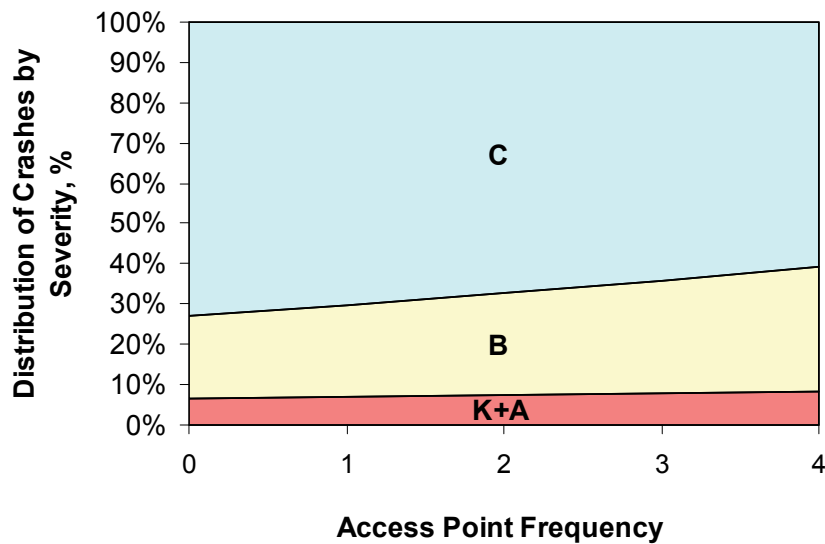


Figure 144. Crossroad ramp terminal severity distribution based on access point frequency.

Left-turn Operation. This variable reflects the presence of protected-only left-turn operation on *either* crossroad approach (if signalized). If a ramp terminal has permissive or protected-permissive operation then it does not have protected operation. This focus on protected operation is based partly on the guidance in Chapter 14 of the *HSM* that indicates a change from permissive to protected-permissive operation has a negligible effect on safety.

The relationship between left-turn operation and severity level is shown in Table 111. The negative value of the associated coefficient (in Table 110) indicates that a crash at a terminal without protected-only left-turn operation is likely to be more severe than a crash at a terminal with protected-only operation, when all other variables are controlled. The percentages in Table 111 indicate that the K+A crash percentage at a terminal with protected-only operation is 7.0 percent, and it is 8.7 percent at a terminal without protected-only operation.

TABLE 111. Crossroad ramp terminal severity distribution—signalized

Variable	Type	Severity Level Distribution, percent		
		Fatal (K) or Incapacitating Injury (A)	Non-Incapacitating Injury (B)	Possible Injury (C)
Left-turn operation	Protected only	7.0	21.8	71.2
	Other	8.7	24.8	66.5
Non-ramp public st. leg	Present	16.0	32.7	51.4
	Not present	6.9	21.6	71.5
Area type	Rural	7.0	21.8	71.2
	Urban	4.2	16.1	79.7

It is rationalized that intersections without protected left-turn operation are more likely to have crashes between left-turn vehicles turning permissively through gaps in oncoming traffic. The collisions that result from permissive operation tend to involve oncoming traffic that is moving with high speed, relative to the vehicles involved in collisions associated with protected-only operation. Research by Wang and Abdel-Aty (2008) indicates that a protected left-turn phase is associated with less severe crashes.

Non-Ramp Public Street Leg. This variable is applicable to any ramp terminal that has a fourth leg that: (1) is a public street serving two-way traffic and (2) intersects with the crossroad at the terminal. Public street legs are fairly rare (i.e., they were found at about 2 percent of the terminals in the database). At most ramp terminals, the public street leg will be on the opposite side of the crossroad from the exit ramp.

The relationship between public street leg presence and severity level is shown in Table 111. The positive value of the associated coefficient (in Table 110) indicates that a crash at a terminal with a public street leg is likely to be more severe than a crash at a terminal without a public street leg, when all other variables are controlled. The percentages in Table 111 indicate that the K+A crash percentage at a terminal with a public street leg is 16.0 percent, and it is 6.9 percent at a terminal without a public street leg.

It is rationalized that when a public street leg is present, there is an increased opportunity of head-on, angle and side-swipe-opposite-direction crashes, which are typically severe. The presence of a public street leg effectively converts a three-leg terminal into a four-leg terminal. Thus, the effect of public street leg presence on crash severity should be similar to that found when comparing three-leg and four-leg intersections. Jonsson et al. (2007) showed that three-leg intersections typically experience a higher percentage of less-severe same direction crashes. Similarly, Vogt and Bared (1998) noted that the percentage of K, A, and B crashes at four-leg intersection is much larger than at three-leg intersections.

Area Type. The relationship between area type and crash severity level was also considered during model calibration. It is generally recognized that probabilistic models should be developed separately for urban and rural crashes. However, separate models were not developed in this project due to the limited sample size.

The relationship between area type and severity level is shown in Table 111. The positive value of the associated coefficient (in Table 110) indicates that a crash in a rural area is likely to be more severe than a crash in an urban area, when all other variables are controlled. This trend can be attributed to higher operating speeds on rural crossroads. A crash that occurs at higher speed typically has higher severity than a crash at lower speed. The percentages in Table 111 indicate that the K+A crash percentage at a rural ramp terminal is 7.0 percent, and it is 4.2 percent at an urban ramp terminal.

Predicted Probabilities for Unsignalized Crossroad Ramp Terminals

Unsignalized ramp terminals are fairly common in rural areas. Of 301 ramp terminals in the database, about 65 percent are located in a rural area. However, only about 50 percent of the crashes in the database occurred at rural ramp terminals.

The relationship between area type and severity level for unsignalized terminals is shown in Table 112. The positive value of the associated coefficient (in Table 110) indicates that a crash in a rural area is likely to be more severe than a crash in an urban area, when all other variables are controlled. This trend is similar to that found for signalized ramp terminals and can be attributed to higher operating speeds on rural crossroads. A comparison of the percentages in Tables 111 and 112 indicates that a crash is more likely to have severity level K or A if it occurs at an unsignalized ramp terminal, than if it occurs at a signalized terminal.

TABLE 112. Crossroad ramp terminal severity distribution—unsignalized

Variable	Type	Severity Level Distribution, percent		
		Fatal (K) or Incapacitating Injury (A)	Non-Incapacitating Injury (B)	Possible Injury (C)
Area type	Rural	14.2	19.0	66.7
	Urban	6.7	17.4	76.0

CHAPTER 9: CONCLUSIONS AND RECOMMENDATIONS

The following conclusions have been developed based on the research conducted for this project.

- This report documents a safety prediction method for freeways that is suitable for incorporation in the *HSM*. The method addresses freeway segments and freeway speed-change lanes. It includes crash modification factors that describe the observed relationship between crash frequency and horizontal curvature, lane width, shoulder width, median width, barrier length and offset, ramp-related lane changes, rumble strip presence, clear zone width, and the extent of recurring congestion.
- This report documents a safety prediction method for ramps that is suitable for incorporation in the *HSM*. The method addresses ramp segments, C-D road segments, and crossroad ramp terminals. For segments, it includes crash modification factors that describe the observed relationship between crash frequency and horizontal curvature, lane width, shoulder width, barrier length and offset, a change in the number of basic lanes, presence of a ramp-to-ramp merge or diverge point, and ramp-related lane changes on a C-D road.

For crossroad ramp terminals, the method includes crash modification factors that describe the observed relationship between crash frequency and exit ramp control, exit ramp lanes, presence of turn lanes on the crossroad, presence of driveway access points, distance to the adjacent ramp terminal, median width, presence of protected-only left-turn operation, presence of right-turn channelization, and skew angle.

- The aforementioned safety prediction methods use a disaggregate approach for evaluating freeway sections, ramps, C-D roads, or entire freeway facilities within the limits of a project. The roadway of interest is initially separated into individual segments and intersections. Each segment has similar geometry and traffic conditions along its length. Each segment and intersection is then evaluated using the prediction method. The results for each segment and intersection are then combined to yield safety information for the overall project. For each segment or intersection, the method can be used to produce an estimate of the expected crash frequency by crash severity, crash type, or both.
- The safety prediction method was developed using data for California, Maine, and Washington. It includes a procedure for calibrating the models to local conditions. The data from the state of Maine was used to validate the models after they were calibrated using data for the other two states.

The following recommendations have been developed based on the research conducted for this project.

- The safety prediction methods developed in this research should be incorporated into the *HSM*.

- The safety prediction method for freeways is believed to be sufficiently complete that it can be used to address all rural freeways and most urban freeways. However, its coverage could be broadened through the conduct of future research to incorporate models that quantify the safety effect of the following geometric design and traffic control features.
 - Freeways with 11 or more through lanes in urban areas.
 - Freeways with 9 or more through lanes in rural areas.
 - Freeways with continuous access high-occupancy vehicle (HOV) lanes.
 - Freeways with limited access managed lanes that are buffer-separated from the general purpose lanes.
 - Freeways with ramp metering.
 - Use of safety shoulders as travel lanes.

- The analysis of freeway crash data indicated that crashes on curved freeway segments with shoulder rumble strips were more frequent than on curved segments without shoulder rumble strips. This finding is partially supported by other research documented in the literature. Additional research is needed to quantify the safety effect of shoulder rumble strips on freeway curves.

- The safety prediction method for ramps is believed to be sufficiently complete that it can be used to address all rural ramps and most urban ramps. However, its coverage could be broadened through the conduct of future research to incorporate models that quantify the safety effect of the following geometric design and traffic control features.
 - Ramp or C-D road segments in rural areas with 2 or more lanes.
 - Ramp or C-D road segments in urban areas with 3 or more lanes.
 - Ramps and C-D roads providing two-way travel.
 - Ramps with ramp metering.
 - A high-occupancy-vehicle (HOV) bypass lane on a ramp or C-D road.
 - A crossroad speed-change lane.
 - A crossroad ramp terminal with 3 or more left-turn lanes on a crossroad approach.
 - A crossroad ramp terminal where the crossroad provides one-way travel.
 - The crossroad ramp terminal formed by a single-point urban interchange or roundabout.

- The safety prediction method for ramps does not address frontage roads. Frontage roads are sufficiently unique in their design and operation that a separate safety prediction method should be developed to specifically address them. This method would include predictive models that separately address one-way frontage-road segments, two-way frontage-road segments, frontage-road ramp terminals, and frontage-road crossroad terminals.

- An interim predictive method for all-way stop control is included in the safety predictive method for crossroad ramp terminals. It is based on the use of an adjustment factor with the predictive model for one-way stop-controlled terminals. Additional research is needed to develop a more robust predictive model for terminals with this control mode.

REFERENCES

- Abdel-Aty, R., and A. Radwan. (2000). "Modeling Traffic Accident Occurrence and Involvement." *Accident Analysis and Prevention*. Vol. 32, No. 5. Elsevier Ltd., Oxford, Great Britain, pp. 633-642.
- Abdel-Aty, M. (2003). "Analysis of Driver Injury Severity Levels at Multiple Locations Using Ordered Probit Models." *Journal of Safety Research*. Vol. 34, No. 5. Elsevier Ltd., Oxford, Great Britain, pp. 597-603.
- Abdel-Aty, M., and J. Keller. (2005). "Exploring the Overall and Specific Crash Severity Levels at Signalized Intersections." *Accident Analysis and Prevention*, Vol. 37, No. 3. Elsevier Ltd., Oxford, Great Britain, pp. 417-425.
- Al-Senan, S., and P. Wright. (1987). "Prediction of Head-On Accident Sites." *Transportation Research Record 1122*. Transportation Research Board, Washington, D.C., pp. 79-85.
- Anastasopoulos, P., and F. Mannering. (2011). "An Empirical Assessment Of Fixed And Random Parameter Logit Models Using Crash- and Non-Crash-Specific Injury Data." *Accident Analysis and Prevention*. Vol. 43. Elsevier Ltd., Oxford, Great Britain, pp. 1140-1147.
- Bahar, G., T. DiLorenzo, J. Munro, and B. Persaud. (2001). "Prioritization of Interchanges and Ramps Based on Potential for Safety Improvements." *Proceedings of 2001 Spring ITE Conference*. Institute of Transportation Engineers, Washington, D.C.
- Bahar, G., M. Parkhill, E. Hauer, F. Council, B. Persaud, C. Zegeer, R. Elvik, A. Smiley, and B. Scott. (2007). *Prepare Parts I and II of the Highway Safety Manual - Final Report*. NCHRP Project 17-27. National Cooperative Highway Research Association, Transportation Research Board, Washington, D.C.
- Bared, J., A. Powell, E. Kaiser, and R. Jagannathan. (2005). "Crash Comparison of Single Point and Tight Diamond Interchanges." *Journal of Transportation Engineering*. Vol. 131, No. 5. American Society of Civil Engineers, Reston, Virginia, pp. 379-381.
- Bared, J., P. Edara, and T. Kim. (2006). "Safety Impact of Interchange Spacing on Urban Freeways." Paper presented at the Annual Meeting of the Transportation Research Board, Washington, D.C.
- Bared, J., and W. Zhang. (2007). *Safety Assessment of Interchange Spacing on Urban Freeways*. FHWA-HRT-07-031. Federal Highway Administration, Washington, D.C.
- Bauer, K., and D. Harwood. (1998). *Statistical Models of Accidents on Interchange Ramps and Speed-Change Lanes*. FHWA-RD-97-106. Federal Highway Administration, Washington, D.C.

- Bauer, K., D. Harwood, W. Hughes, and K. Richard. (2004). "Safety Effects of Narrow Lanes and Shoulder-Use Lanes to Increase Capacity of Urban Freeways." *Transportation Research Record 1897*. Transportation Research Board, Washington, D.C., pp. 71-80.
- Bissell, H., G. Pilkington, J. Mason, and D. Woods. (1982). *Synthesis of Safety Research Related to Traffic Control and Roadway Elements - Volume 1*. Chapter 1 - Roadway Cross Section and Alignment. FHWA-TS-82-232. Federal Highway Administration, Washington, D.C.
- Bligh, R., S-P. Miaou, D. Lord, and S. Cooner. (2006). *Median Barrier Guidelines for Texas*. Report No. FHWA/TX-06/0-4254-1. Texas Transportation Institute, College Station, Texas.
- Bonneson, J. (2000). *NCHRP Report 439: Superelevation Distribution Methods and Transition Designs*. National Cooperative Highway Research Association, Transportation Research Board, Washington, D.C.
- Bonneson, J., K. Zimmerman, and K. Fitzpatrick. (2005). *Roadway Safety Design Synthesis*. FHWA/TX-05/0-4703-P1. Texas Transportation Institute, College Station, Texas.
- Bonneson, J., D. Lord, K. Zimmerman, K. Fitzpatrick, and M. Pratt. (2007a). *Development of Tools for Evaluating the Safety Implications of Highway Design Decisions*. FHWA/TX-07/0-4703-4. Texas Transportation Institute, College Station, Texas.
- Bonneson, J., M. Pratt, J. Miles, and P. Carlson. (2007b). *Development of Guidelines for Establishing Effective Curve Advisory Speeds*. FHWA/TX-07/0-5439-1. Texas Transportation Institute, College Station, Texas.
- Bonneson, J., and M. Pratt. (2008). *Calibration Factors Handbook: Safety Prediction Models Calibrated with Texas Highway System Data*. FHWA/TX-08/0-4703-5. Texas Transportation Institute, College Station, Texas.
- Bonneson, J., and M. Pratt. (2009). *Roadway Safety Design Workbook*. FHWA/TX-09/0-4703-P2. Texas Transportation Institute, College Station, Texas.
- Cambridge Systematics. (2001). *Twin Cities Ramp Meter Evaluation: Final Report*. Cambridge Systematics, Inc., Oakland, California.
- Cate, M., and T. Urbanik, II. (2004). "Another View of Truck Lane Restrictions." *Transportation Research Record 1867*. Transportation Research Board, Washington, D.C., pp. 19-24.
- Chen, H., P. Liu, J. Lu, and B. Behzadi. (2009). "Evaluating the Safety Impacts of the Number and Arrangements of Lanes on Freeway Exit Ramps." *Accident Analysis and Prevention*. Vol. 41. Elsevier Ltd., Oxford, Great Britain, pp. 543-551.
- Cirillo, J. (1968). "Interstate System Accident Research Study II, Interim Report II." *Public Roads*, Vol. 35, No. 3. U.S. Department of Transportation, Washington, D.C.

Cirillo, J., S. Dietz, and R. Beatty. (1969). *Analysis and Modeling of Relationships Between Accidents and the Geometric and Traffic Characteristics of the Interstate System*. Bureau of Public Roads, Washington, D.C.

Cirillo, J. (1970). "The Relationship of Accidents to Length of Speed-Change Lanes and Weaving Areas on Interstate Highways." *Highway Research Record 312*. Highway Research Board, Washington, D.C., pp. 17-32.

Cothron, A., S. Ranft, C. Walters, D. Fenno, and D. Lord. (2004). *Crash Analysis of Selected High-Occupancy Vehicle Facilities in Texas: Methodology, Findings, and Recommendations*. FHWA/TX-04/0-4431-1. Texas Department of Transportation, Austin, Texas.

Davis, G., and N. Aul. (2007). *Safety Effects of Left-Turn Phasing Schemes at High-Speed Intersections*. Report No. MN/RC-2007-03. University of Minnesota, Minneapolis, Minnesota.

Dixon, K., J. Hibbard, and H. Nyman. (2000). "Right-Turn Treatment for Signalized Intersections." *TRB Circular E-C019: Urban Street Symposium*. Transportation Research Board, Washington, D.C..

Donnell, E., and J. Mason. (2004). "Predicting the Severity of Median-Related Crashes in Pennsylvania by Using Logistic Regression." *Transportation Research Record 1897*. Transportation Research Board, Washington, D.C., pp. 55-63.

Donnell, E., and J. Mason. (2006). "Methodology to Develop Median Barrier Warrant Criteria." *Journal of Transportation Engineering*. Vol. 132, No. 4, American Society of Civil Engineers, Reston, Virginia, pp. 269-281.

Dunlap, D., P. Fancher, R. Scott, C. MacAdam, and L. Segel. (1978). *NCHRP Report 184: Influence of Combined Highway Grade and Horizontal Alignment on Skidding*. National Cooperative Highway Research Association, Transportation Research Board, Washington, D.C.

Elvik R., and T. Vaa. (2004). *Handbook of Road Safety Measures*. Elsevier Ltd., Oxford, Great Britain.

Everall, P. (1972). *Urban Freeway Surveillance and Control*. Federal Highway Administration, Washington, D.C.

Federal Highway Administration. (2009). *Highway Statistics Series*. U.S. Department of Transportation, Washington, D.C., <http://www.fhwa.dot.gov/policy/ohpi/hss/index.cfm>. Accessed July 2009.

Fitzpatrick, K., W. Schneider IV, and E-S. Park. (2006). "Operation and Safety of Right-Turn Lane Designs." *Transportation Research Record 1961*. Transportation Research Board, Washington, D.C., pp. 55-64.

- Fontaine, M., C. Bhamidipati, and L. Dougald. (2009). "Safety Impact of Truck Lane Restrictions on Multilane Freeways." In *Transportation Research Record 2096*. Transportation Research Board, Washington, D.C., pp. 25-32.
- Fuhs, C., and J. Obenberger. (2002). "HOV Facility Development: A Review of National Trends." *Transportation Research Record 1781*. Transportation Research Board, Washington, D.C., pp. 1-9.
- Garber, N., M. Chowdhury, and R. Kalaputapu. (1992) *Accident Characteristics of Large Trucks on Highway Ramps*. AAA Foundation for Traffic Safety. Washington, D.C.
- Garber, N., and M. Fontaine. (1999). *Guidelines for Preliminary Selection of the Optimum Interchange Type for a Specific Location. Final Report*. Virginia Transportation Research Council.
- Geedipally, S., S. Patil, and D. Lord. (2010). "Examination of Methods for Estimating Crash Counts According to their Collision Type." *Transportation Research Record 2165*. Transportation Research Board, Washington, D.C., pp 12-20.
- Goswami, V., and G. Bham. (2006). "A Study of Lane Change Frequency on a Multilane Freeway." *Proceedings of the 9th International Conference of Applications in Advanced Technology in Transportation*. American Society of Civil Engineers, Reston, Virginia.
- Griffith, M. (1994). "Comparison of the Safety of Lighting Options on Urban Freeways." Vol. 58, No. 2. *Public Roads*. Federal Highway Administration, Washington, D.C.
- Griffith, M. (1999). "Safety Evaluation of Rolled-In Continuous Shoulder Rumble Strips Installed on Freeways." *Transportation Research Record 1665*. Transportation Research Board, Washington, D.C., pp. 28-34.
- Gross, F., P. Jovanis, K. Eccles, and K. Chen. (2009). *Safety Evaluation of Lane and Shoulder Width Combinations on Rural, Two-Lane, Undivided Roads*. FHWA-HRT-09-031. Federal Highway Administration, Washington, D.C.
- Hadi, M.A., J. Aruldas, L-F. Chow, and J. Wattleworth. (1995). "Estimating Safety Effects of Cross-Section Design for Various Highway Types Using Negative Binomial Regression." *Transportation Research Record 1500*. Transportation Research Board, Washington, D.C., pp. 169-177.
- Hall, J., and O. Pendleton. (1989). *Relationship between v/c Ratios and Accident Rates*. FHWA-HPR-NM-88-02. University of New Mexico, Albuquerque, New Mexico.
- Harkey, D., R. Srinivasan, J. Baek, F. Council, K. Eccles, N. Lefler, F. Gross, B. Persaud, C. Lyon, E. Hauer, and J. Bonneson. (2008). *NCHRP Report 617: Accident Modification Factors for Traffic Engineering and ITS Improvements*. National Cooperative Highway Research Association, Transportation Research Board, Washington, D.C.

Harwood, D. W., M. Pietrucha, M. Wooldridge, R. Brydia, and K. Fitzpatrick. (1995). *NCHRP Report 375: Median Intersection Design*. National Cooperative Highway Research Association, Transportation Research Board, Washington, D.C.

Harwood, D., F. Council, E. Hauer, W. Hughes, and A. Vogt. (2000). *Prediction of the Expected Safety Performance of Rural Two-Lane Highways*. FHWA-RD-99-207. Federal Highway Administration, Washington, D.C.

Harwood, D., K. Bauer, I. Potts, D. Torbic, K. Richard, E. Kohlman Rabbani, E. Hauer, and L. Elefteriadou. (2002). *Safety Effectiveness of Intersection Left- and Right-Turn Lanes*. Report No. FHWA-RD-02-089. Federal Highway Administration, Washington, D.C.

Harwood, D., D. Torbic, K. Richard, and M. Meyer. (July 2010). *Safety Analyst: Software Tools for Safety Management of Specific Highway Sites*. Report No. FHWA-HRT-10-063. U.S. Department of Transportation, Federal Highway Administration, Washington, D.C.

Hauer, E. (2006). "The Frequency-Severity Indeterminacy." *Accident Analysis and Prevention*. Vol. 38. Elsevier Ltd., Oxford, Great Britain, pp. 78-83.

Hausman, J. (1978). "Specification Tests in Econometrics." *Econometrica*. Vol. 46, No. 6. pp 1251-1271.

Highway Safety Manual, First Edition. (2010). American Association of State Highway and Transportation Officials, Washington, D.C.

Highway Capacity Manual. (2000). Transportation Research Board, Washington, D.C.

Hu, W., and E. Donnell. (2010). "Median barrier crash severity: Some new insights." *Accident Analysis and Prevention*. Vol. 42. Elsevier Ltd., Oxford, Great Britain, pp. 1697-1704.

Jang, K., K. Chung, D. Ragland, and C-Y. Chan. (2009). "Safety Performance of High-Occupancy Vehicle Facilities: Evaluation of HOV Lane Configurations in California." *Transportation Research Record 2099*. Transportation Research Board, Washington, D.C., pp. 132-140.

Jason, B., W. Awed, J. Robles, J. Kononov, and B. Pinkerton. (1998). "Truck accidents at freeway ramps: Data analysis and high-risk site identification." *Journal of Transportation Statistics*. Vol. 1, No. 1. Bureau of Transportation Statistics, U.S. Department of Transportation, Washington, D.C. pp. 76-92.

Jonsson, T., J. Ivan, and C. Zhang. (2007). "Crash Prediction Models for Intersections on Rural Multilane Highways: Differences by Collision Type." *Transportation Research Record 2019*. Transportation Research Board, Washington, D.C., pp. 91-98.

Khorashadi, A. (1998). *Effect of Ramp Type and Geometry on Accidents*. FHWA/CA/TE-98-13. California Department of Transportation, Sacramento, California.

- Khorashadi, A., D. Niemeier, V. Shankar, and F. Mannering. (2005). "Differences in Rural and Urban Driver Injury Severities in Accidents Involving Large Trucks: An Explanatory Analysis." *Accident Analysis and Prevention*. Vol. 37, No. 5. Elsevier Ltd., Oxford, Great Britain, pp.910-921.
- Kiattikomol, V., A. Chatterjee, J. Hummer, and M. Younger. (2008). "Planning Level Regression Models for Prediction of Crashes on Interchange and Noninterchange Segments of Urban Freeways." *Journal of Transportation Engineering*. Vol. 134, No. 1. American Society of Civil Engineers, Reston, Virginia, pp. 111-117.
- Kim, D., S. Washington, and J. Oh. (2006). "Modeling Crash Outcomes: New Insights into the Effects of Covariates on Crashes at Rural Intersections." Vol. 132, No. 4. *Journal of Transportation Engineering*. American Society of Civil Engineers, Reston, Virginia, pp. 505-513.
- Knuiman, M., F. Council, and D. Reinfurt. (1993). "Association of Median Width and Highway Accident Rates." *Transportation Research Record 1401*. Transportation Research Board, Washington, D.C., pp. 70-82.
- Kobelo, D., V. Patrangenu, and R. Mussa. (2008). "Safety Analysis of Florida Urban Limited Access Highways with Special Focus on the Influence of Truck Lane Restriction Policy." *Journal of Transportation Engineering*. Vol. 134, No. 7. American Society of Civil Engineers, Reston, Virginia, pp. 297-306.
- Koepke, F. (1993). "Ramp Exit/Entrance Design—Taper Versus Parallel and Critical Dimensions." *Transportation Research Record 1385*. Transportation Research Board, Washington, D.C., pp. 126-132.
- Kononov, B. Bailey, and B. Allery. (2008). "Relationships between Safety and Both Congestion and Number of Lanes on Urban Freeways." *Transportation Research Record 2083*. Transportation Research Board, Washington, D.C., pp. 26-39.
- Koppelman, F., and C. Bhat. (2006). *A Self Instructing Course in Mode Choice Modeling: Multinomial and Nested Logit Models*. U.S. Department of Transportation, Federal Transit Administration, Washington, D.C. pp. 79-80.
- Kvalseth, T. (1985). "Cautionary Note About R^2 ." *The American Statistician*. Vol. 39, No. 4, (Part 1), American Statistical Association, November, pp. 279-285.
- Kweon, Y., and K. Kockelman. (2003). "Overall Injury Risk to Different Drivers: Combining Exposure, Frequency, and Severity Models." *Accident Analysis and Prevention*. Vol. 35, No.4. Elsevier Ltd., Oxford, Great Britain, pp. 441-450.
- Lee, J., and F. Mannering. (2002). "Impact of Roadside Features on the Frequency and Severity of Run-Off Roadway Accidents: An Empirical Analysis." *Accident Analysis and Prevention*. Vol. 34. Elsevier Ltd., Oxford, Great Britain, pp.149-61.

- Leisch, J.E., T. Neuman, J.P. Leisch, J. Hess, M. Rosenbaum.. (1982). *Synthesis of Safety Research Related to Traffic Control and Roadway Elements - Volume 1*. Chapter 6 - Interchanges. FHWA-TS-82-232. Federal Highway Administration, Washington, D.C.
- Livneh, M., A. Polus, and J. Factor. (1988). "Vehicle Behavior on Deceleration Lanes." Vol. 114, No. 6. *Journal of Transportation Engineering*. American Association of Civil Engineers, Reston, Virginia, pp. 706-717.
- Lord, D., A. Manar, and A. Vizioli. (2005). "Modeling Crash-Flow-Density and Crash-Flow-V/C Ratio Relationships for Rural and Urban Freeway Segments." *Accident Analysis and Prevention*. Vol. 37. Elsevier Ltd., Oxford, Great Britain, pp. 422-423.
- Lord, D. (2006). "Modeling Motor Vehicle Crashes using Poisson-Gamma Models: Examining the Effects of Low Sample Mean Values and Small Sample Size on the Estimation of the Fixed Dispersion Parameter." *Accident Analysis and Prevention*, Vol. 38, No. 4. Elsevier Ltd., Oxford, Great Britain, pp. 751-766.
- Lord, D., S. Washington, and J. Ivan. (2007). "Further Notes on the Application of Zero-Inflated Models in Highway Safety." Vol. 39. *Accident Analysis and Prevention*. Vol. 39. Elsevier Ltd., Oxford, Great Britain, pp. 53-57.
- Lord, D., and P. Park. (2008). "Investigating the Effects of the Fixed and Varying Dispersion Parameters of Poisson-Gamma Models on Empirical Bayes Estimates." *Accident Analysis and Prevention*. Vol. 40. Elsevier Ltd., Oxford, Great Britain, pp. 1441-1457.
- Lundy, R. (1966). *The Effect of Ramp Type and Geometry on Accidents*. 2nd edition. Traffic Department, Division of Highways, Department of Public Works, Sacramento, California. As reported by Twomey, J.M., M.L. Heckman, and J.C. Hayward. (1992).
- Ma, J., and K. Kockelman. (2006). "Bayesian Multivariate Poisson Regression for Models of Injury Count by Severity." *Transportation Research Record 1950*. Transportation Research Board, Washington, D.C., pp. 24-34.
- Martin, J-L. (2002). "Relationship between Crash Rate and Hourly Traffic Flow on Interurban Motorways." *Accident Analysis and Prevention*. Vol. 34. Elsevier Ltd., Oxford, Great Britain, pp. 619-629.
- Marvin, R., and D. Clark. (2003). *An Evaluation of Shoulder Rumble Strips In Montana*. Montana Department of Transportation, Helena, Montana.
- McCasland, D., and R. Biggs. (1980). *Freeway Modifications to Increase Traffic Flow*. FHWA-TS-80-203. Federal Highway Administration, Washington, D.C. As reported by Bissell et al. (1982).
- McCullagh, P., and J. Nelder. (1983). *Generalized Linear Models*. Chapman and Hall, New York, N.Y.

McFadden, D (1981). "Econometric Models of Probabilistic Choice." In Manski and McFadden (Eds.), *Structural Analysis of Discrete Data with Econometric Applications*. The MIT Press, Cambridge, Massachusetts.

Miaou, S-P. (1996). *Measuring the Goodness-of-Fit of Accident Prediction Models*. FHWA-RD-96-040. Federal Highway Administration, Washington, D.C.

Milton, J. and F. Mannering. (1998). "The Relationship Among Highway Geometrics, Traffic-Related Elements, and Motor-Vehicle Accident Frequencies." *Transportation*, Vol. 25, No. 4. pp. 395-413.

Milton, J., V. Shankar, and F. Mannering. (2008). "Highway Accident Severities and the Mixed Logit Model: An Exploratory Empirical Analysis." *Accident Analysis and Prevention*. Vol. 40. Elsevier Ltd., Oxford, Great Britain, pp. 260-266.

Mitra, S., and S. Washington. (2007). "On the Nature of Over-Dispersion in Motor Vehicle Crash Prediction Models." *Accident Analysis and Prevention*. Vol. 39. Elsevier Ltd., Oxford, Great Britain, pp. 459-468.

Moler, S. "Stop. You are Going the Wrong Way!" (2002). Vol. 66, No. 2. *Public Roads*. Federal Highway Administration, Washington, D.C.

Monsere, C., and E. Fischer. (2008). "Safety Effects of Reducing Freeway Illumination for Energy Conservation." *Accident Analysis and Prevention*. Vol. 40. Elsevier Ltd., Oxford, Great Britain, pp. 1773-1780.

Moon, J-P. and J. Hummer. (2009) "Development of Safety Prediction Models for Influence Areas of Ramps in Freeways." *Journal of Transportation Safety & Security*. Vol. 1, No. 1. Francis and Taylor Group, LLC, United Kingdom, pp. 1-17.

Neuman, T., R. Pfefer, K. Slack, K. Hardy, F. Council, H. McGee, L. Prothe, and K. Eccles. (2003) *NCHRP Report 500: Guidance for Implementation of the AASHTO Strategic Highway Safety Plan. Volume 6: A Guide for Addressing Run-Off-Road Collisions*. National Cooperative Highway Research Association, Transportation Research Board, Washington, D.C.

Newman, L., C. Nuworsoo, and A. May. (1988). "Operational and Safety Experience with Freeway HOV Facilities in California." *Transportation Research Record 1173*. Transportation Research Board, Washington, D.C., pp. 18-24.

Noland, R. , and M. Quddus. (2005). "Congestion and Safety: A Spatial Analysis of London." *Transportation Research, Part A: Policy and Practice*. Vol. 39. Elsevier Ltd., Oxford, Great Britain, pp. 737-754.

Oh, J., S. Washington, and K. Choi. (2004). "Development of Accident Prediction Models for Rural Highway Intersections." *Transportation Research Record 1897*. Transportation Research Board, Washington, D.C., pp. 18-27.

Park, E-S., and D. Lord. (2007). "Multivariate Poisson-Lognormal Models for Jointly Modeling Crash Frequency by Severity." *Transportation Research Record 2019*. Transportation Research Board, Washington, D.C., pp.1-6.

Persaud, B., and K. Mucsi. (1995). "Microscopic Accident Potential Models for Two-Lane Rural Roads." *Transportation Research Record 1485*. Transportation Research Board, Washington, D.C., pp. 134-139.

Persaud, B., and L. Dzbik. (1993). "Accident Prediction Models for Freeways." *Transportation Research Record 1401*. Transportation Research Board, Washington, D.C., pp. 55-60.

A Policy on Geometric Design of Highways and Streets. (2004). American Association of State Highway and Transportation Officials, Washington, D.C.

Quddus, M., C., Wang, and S. Ison. (2010). "Road Traffic Congestion and Crash Severity: An Econometric Analysis Using Ordered Response Models." *Journal of Transportation Engineering*. Vol. 136. No. 5, American Society of Civil Engineers, Reston, Virginia, pp. 424-435.

Raff, M. (1953). "Interstate Highway-Accident Study." *Highway Research Board Bulletin 74*. Highway Research Board, Washington, D.C. As reported by Bissell et al. (1982).

Research and Innovative Technology Administration. (2007). *ITS Deployment Statistics Database - Freeway Management*. U.S. Department of Transportation, Washington, D.C. <http://www.itsdeployment.its.dot.gov/>. Accessed September 2009.

Sarhan, M., Y. Hassan, and A. Halim. (2006). "Design of Freeway Speed-Change Lanes: Safety Explicit Approach." *Proceedings of the 2006 TRB Annual Meeting*. Paper No. 06-1937. Transportation Research Board, Washington, D.C.

SAS/STAT User's Guide, Version 9.2. (2009). Second edition, SAS Institute, Inc., Cary, North Carolina.

Savolainen, P., and F. Mannering. (2007). "Probabilistic Models of Motorcyclists' Injury Severities in Single- and Multi-Vehicle Crashes." *Accident Analysis and Prevention*. No. 39. Elsevier Ltd., Oxford, Great Britain, pp. 955-963.

Savolainen, P., F. Mannering, D. Lord, and M. Quddus (2011) "The Statistical Analysis of Highway Crash-Injury Severities: A Review and Assessment of Methodological Alternatives." *Accident Analysis and Prevention*. Vol. 43, No. 5. Elsevier Ltd., Oxford, Great Britain, pp. 1666-1676.

Sayed, T., P. deLeur, and J. Pump. (2010). "Impact of Rumble Strips on Collision Reduction on Highways in British Columbia, Canada." *Transportation Research Record 2148*. Transportation Research Board, Washington, D.C., pp. 9-15.

Schultz, G., J. Lewis, and T. Boschert. (2007). "Safety Impacts of Access Management Techniques in Utah." *Transportation Research Record 1994*. Transportation Research Board, Washington, D.C., pp. 35-42.

Shankar, V., and F. Mannering. (1996). "An Exploratory Multinomial Logit Analysis of Single-Vehicle Motorcycle Accident Severity." *Journal of Safety Research*. Vol. 27 No. 3. Elsevier Ltd., Oxford, Great Britain, pp. 183-194.

Shankar, V., F. Mannering, and W. Barfield. (1996). "Statistical Analysis of Accident Severity on Rural Freeways." *Accident Analysis and Prevention*. Vol. 28, No. 3. Elsevier Ltd., Oxford, Great Britain, pp. 391-401.

Smith, E., and J. Ivan. (2005). "Evaluation of Safety Benefits and Potential Crash Migration Due to Shoulder Rumble Strip Installation on Connecticut Freeways." *Transportation Research Record 1908*. Transportation Research Board, Washington, D.C., pp. 104-113.

Srinivasan, K. (2002). "Injury and Severity Analysis with Variable and Correlated Thresholds." *Transportation Research Record 1784*. Transportation Research Board, Washington, D.C., pp. 132-142.

Tarko, A., N. Villwock, and N. Blond. (2008). "Effect of Median Design on Rural Freeway Safety." *Transportation Research Record 2060*. Transportation Research Board, Washington, D.C., pp. 29-37.

Taylor, J. and H. McGee. (1973). *NCHRP Report 145: Improving Traffic Operations and Safety at Exit Gore Areas*. National Cooperative Highway Research Association, Transportation Research Board, Washington, D.C.

Torbic, D., D. Harwood, D. Gilmore, and K. Richard. (2007). *Safety Analysis of Interchanges*. Final Report. Federal Highway Administration, Washington, D.C.

Torbic, D., J. Hutton, C., Brokenkroger, K. Bauer, D. Harwood, D. Gilmore, J. Dunn, J. Ronchetto, E. Donnell, H. Sommer, P. Garvey, B. Persaud, and C. Lyon. (2009). *NCHRP Report 641 - Guidance for the Design and Application of Shoulder and Centerline Rumble Strips*. National Cooperative Highway Research Association, Transportation Research Board, Washington, D.C.

Twomey, J., M. Heckman, and J. Hayward. (1992). *Safety Effectiveness of Highway Design Features – Volume IV: Interchanges*. FHWA-RD-91-047. Federal Highway Administration, Washington, D.C.

Upchurch, J. and D. Cleavenger. (1999). "Freeway Ramp Metering's Effect on Accidents: Recent Arizona Experience." *Proceedings of the 69th Annual Meeting of the ITE*. Institute of Transportation Engineers, Washington, D.C.

Viano, D., and C. Parenteau. (2004). "Rollover crash sensing and safety overview." *Proceedings of SAE World Congress, March 8 to 11, 2004*. SAE International, Detroit, Michigan.

Vogt, A. (1999). *Crash Models for Rural Intersections: Four-Lane by Two-Lane Stop-Controlled and Two-Lane by Two-Lane Signalized*. Report No. FHWA-RD-99-128. Federal Highway Administration, McLean, Virginia.

Vogt, A., and J. Bared. (1998). "Accident Models for Two-Lane Rural Segments and Intersections." *Transportation Research Record 1635*. Transportation Research Board, Washington, D.C., pp. 18-29.

Wang, C., M. Quddus, and S. Ison. (2011). "Prediction of Accident Frequency at Their Severity Levels and Its Application in Site Ranking Using Two-Stage Mixed Multivariate Model." *Proceedings of the 2011 TRB Annual Meeting*. Paper No. 11-2510. Transportation Research Board, Washington, D.C.

Wang, X., and M. Abdel-Aty. (2008). "Analysis of Left-Turn Crash Injury Severity by Conflicting Pattern Using Partial Proportional Odds Models." *Accident Analysis and Prevention*. Vol. 40, No. 5. Elsevier Ltd., Oxford, Great Britain, pp. 1674-1682.

Wang, Z., H. Chen, and J. Lu. (2009). "Exploring Impacts of Factors Contributing to Injury Severity at Freeway Diverge Areas." *Transportation Research Record 2102*. Transportation Research Board, Washington, D.C., pp. 43-52.

Worrall, R. (1969). *The Suitability of Left-Hand Entrance and Exit Ramps for Freeways and Expressways*. Final Report, Project IHR 61. Northwestern University, Department of Civil Engineering, Evanston, Illinois.

Yates, J. (1970). "Relationship Between Curvature and Accident Experience on Loop and Outer Connection Ramps." *Highway Research Record 312*. Highway Research Board, Washington, D.C., pp. 64-75.

Ye, F., and D. Lord. (2011). "Investigating the Effects of Underreporting of Crash Data on Three Commonly Used Traffic Crash Severity Models: Multinomial Logit, Ordered Probit and Mixed Logit Models." *Proceedings of the 2011 TRB Annual Meeting*. Paper No. 11-1930. Transportation Research Board, Washington, D.C.

Zegeer, C., H. Huang, J. R. Stewart, R. Pfefer, and J. Wang. (1998) "Effects of a Towaway Reporting Threshold on Crash Analysis Results." *Transportation Research Record 1635*. Transportation Research Board, Washington, D.C., pp. 49-57.

Zegeer, C., R. Deen, and J. Mayes. (1981). "Effect of Lane and Shoulder Widths on Accident Reduction on Rural Two-Lane Roads." *Transportation Research Record 806*. Transportation Research Board, Washington, D.C., pp. 33-43.

Zhao, J. and H Zhou. (2009). "A Study on the Safety of Left-Side Off-Ramps on Freeways." *Proceedings of the 2009 Transport Chicago Conference*. Chicago, Illinois.
<http://www.transportchicago.org>. Accessed August 8, 2009.

Zhou, M. and S. Sisiopiku. (1997). "On the Relationship between Volume-to-Capacity Ratios and Accident Rates." *Transportation Research Record 1581*. Transportation Research Board, Washington, D.C., pp. 47-52.

APPENDIX A: PRACTITIONER INTERVIEWS

This appendix describes the findings from interviews with practitioners on the topic of freeway and interchange safety. The findings were used to identify design and operational elements that have a significant effect on safety and knowledge gaps. This information was used to develop a methodological framework for a freeway and interchange safety prediction methodology and analysis tool. The framework is described in Chapter 3.

OVERVIEW

The primary objectives of the interviews were to: (1) obtain a sense of the type of issues encountered in the design and operation of freeways and interchanges and (2) identify the safety-related information needed by practitioners during the project planning and development processes.

Three different groups were included in the interviews. One group included planners and engineers that were interviewed using a common set of questions. A second group included engineers at FHWA responsible for the review of interchange justification reports. A third group included engineers that have used ISAT to conduct an engineering analysis of interchange safety. The information obtained from each group is described in the next three subsections.

The interviews revealed that a key motivation for the development of ISAT was the request for an interchange safety evaluation tool by several FHWA division offices. These offices (notably the Illinois office) indicated that tools were needed to support the safety evaluation for interchange and access justification reports. These reports are required for all proposed changes in access to the Interstate Highway System and must be approved by FHWA.

INTERVIEWS WITH PLANNERS AND ENGINEERS

A primary source of safety information was the interviews with engineering and planning professionals. Both in-person and telephone interviews were conducted. In-person interviews were held with state DOT engineers in Alabama, Illinois, Maryland, and Washington. Telephone interviews were conducted with eighteen agencies representing FHWA field offices, state DOTs, and metropolitan planning organizations (MPO). The demographics of the agencies contacted for telephone interviews are listed in Table A-1. Collectively, 40 persons were interviewed in person and 22 persons were interviewed by telephone.

The in-person interviews typically took place over several hours and included engineers involved in freeway concept planning, preliminary design, final design, traffic operation, and safety programs. The telephone interviews were intentionally kept to about 30 minutes and typically included only one or two individuals. To adhere to this time limit, only a subset of the questions used in the in-person interviews were used for the telephone interviews. In a few instances, the interviewees opted to conduct the interview by e-mail.

TABLE A-1. Demographics of telephone interview groups

Expertise	Agency Representation		
	FHWA Field Offices	State DOT	MPO
Engineering	4	8	1
Planning	1	1	3

Each interview typically consisted of three parts. The duration of each part was adjusted depending on whether the interview was in-person or via telephone. Initially, a presentation was made by the researchers to provide background information. An overview of the project was provided and ISAT was described. Then, the questions in Figure A-1 were posed in sequence and the responses recorded. Most of these questions were intentionally broad to encourage discussion and a free flow of ideas. A subset of the questions was used for the telephone interviews. The specific questions asked during each telephone interview were varied in a predetermined manner to ensure an equal number of responses were received for each question.

<p>Operational Issues</p> <ol style="list-style-type: none"> 1. a. What are some common design problems or operational issues encountered in <u>freeway</u> projects? b. What are the safety concerns related to these problems or issues? 2. a. What are some common design problems or operational issues encountered in <u>interchange</u> projects? b. What are the safety concerns related to these problems or issues? 3. Are HOV or HOT lanes used? If yes, what are some common problems or issues encountered? <p>Decision-Making Process</p> <ol style="list-style-type: none"> 4. Is there some official guidance that... <ol style="list-style-type: none"> a. Describes how to evaluate safety? or, b. How to determine when there is a safety problem? 5. How does crash severity influence decisions? <p>Level of Analysis Detail</p> <ol style="list-style-type: none"> 6. For the <u>planning</u> stage of the project development process... <ol style="list-style-type: none"> a. Is it important to quantify the performance of the entire project? or b. Is it sufficient to evaluate a few select segments, ramps, or ramp terminals that are suspected of having issues? 7. For the <u>design</u> stage of the project development process... <ol style="list-style-type: none"> a. Is it important to quantify the performance of the entire project? or b. Is it sufficient to evaluate a few select segments, ramps, or ramp terminals that are suspected of having issues? <p>Evaluation Tools or Techniques</p> <ol style="list-style-type: none"> 8. What simulation models are used to evaluate traffic operation? 9. Were you aware of ISAT before today? <ol style="list-style-type: none"> a. If yes, are you having it used on your projects? b. What is the best thing about it? c. What could make it more useful?
--

Figure A-1. Questions posed during the interviews.

A final element of the interview was an interactive session where specific design or operational elements were posed and the interviewees were asked to provide a number indicating the importance of each element. The responses to the questions in Figure A-1 are summarized in the following sections.

Interview Questions

Operational Issues

The most commonly mentioned operational issue was freeway congestion. Its impact on crash frequency, manner of collision, and crash severity are issues for many of the interviewees. The long-standing belief that capacity improvements lead to safety improvements was cited by some. However, a more quantitative understanding of this relationship appears to be desired. Another issue that was frequently cited was bringing an alignment into compliance with the latest design criteria through reconstruction. By implication, this process should improve safety; however, a few interviewees indicated a desire for information that can be used to quantify this improvement.

Topics that were mentioned often enough to be noteworthy include weaving section design and periodic maintenance pull-outs on urban freeways. Both elements are believed to have an influence on safety, but the relationship is undocumented.

About one-half of the interviewed agencies indicate that high-occupancy-vehicle (HOV) lanes are used in their state. Most of these agencies also have some high-occupancy-toll (HOT) mileage. A range of issues was cited but with little commonality among them. This trend appears to reflect the wide range of HOV lane designs that are being used in the various states. A couple of interviewees noted that the speed differential between the HOV and adjacent lanes was a safety issue, especially when trucks were allowed in the HOV lane. Another issue cited by more than one interviewee was the lack of a shoulder of sufficient width to protect a stalled vehicle or facilitate enforcement in many barrier-separated HOV lanes.

Decision-Making Process

This question was answered by the state DOT interviewees. The tools for safety evaluation and safety problem identification vary among the states. Some use a site's crash rate for evaluation and compare it to statewide averages for similar facilities to determine problem locations. Other states use an index value for safety evaluation, where the index represents a mathematical combination of crash frequency, severity, and rate. A couple of states noted that they were using (or planning to use) safety performance functions instead of statewide crash rates or indices as a basis for identifying problem locations.

The severity of crashes is recognized as an important factor in evaluating the safety of a project or highway facility. Examples illustrating the consideration of severity typically focused on fatal crashes, or fatal crash rates. A couple of states indicated the use of a weighting system to compute a site's severity index, where the weight given to each of the severity classes (K, A, B, C, PDO) decreases in an exponential manner, with fatality (K) weighted highest and property-damage-only (PDO) given negligible or no weight.

Level of Analysis Detail

The planners and the engineers involved in concept planning described a need to evaluate the entirety of the project, regardless of whether the focus is cost, operations, or safety. Some interviewees indicated that the evaluation should reflect performance of the project over its design life. A similar sentiment was expressed by some engineers involved in preliminary design and final design; however, other engineers tended to have interest only in evaluating specific intersections, segments, or ramps.

Evaluation Tools or Techniques

Three simulation models were identified as being used to evaluate freeway segments or interchanges; they include: CORSIM, VISSIM, and SimTraffic. No one of these tools was mentioned notably more often than the other.

Fourteen of the 18 telephone interviewees were not aware of ISAT prior to the interview. Similarly, three of the four state DOTs participating in the in-person interviews were not aware of ISAT. Of those that were aware of ISAT, only one interviewee was aware of it having been used for an engineering project.

Given the limited prior awareness of ISAT, comments about its strengths and weaknesses were limited primarily to the participants of the in-person interviews (who had the benefit of a 30-minute ISAT presentation and demonstration). In this regard, it was offered that ISAT looked easy to use. There was some concern about the need for local calibration of the many safety performance functions in ISAT. Also, its ability to model only four ramp configurations (i.e., diamond, parclo, free-flow loop, and directional) was seen as a limitation. A lack of sensitivity to many geometric and operational design elements on the freeway, crossroad, and ramp (e.g., curve radius, weave section) was also seen as a limitation.

Interactive Session Results

During the interactive session, specific freeway and interchange elements were posed and the interviewees were asked to provide a number indicating the importance of each element. Specifically, they were asked to indicate: (1) the frequency with which an element was discussed during the planning or project development processes and (2) the perceived influence of the element on safety. The response to each question was one of three numbers based on the following scale: 0 - never/none; 1 - sometimes/some; 2 - often/high. Thus, two “scores” were recorded for each element, one score for frequency and one score for influence.

The results of this session are shown in Tables A-2, A-3, and A-4 for freeway segments, interchange ramps, and interchange ramp terminals, respectively. The last column of each table indicates how the element ranked, relative to the other elements in the same table. The ranking is based on the product of the two scores. An element that ranks with a “1” is considered most frequently and is believed to have the most influence on safety, relative to the other elements listed.

TABLE A-2. Safety information needs for freeway segments

Category	Element ¹	Rank ²
Roadway	Lane width	12
	Inside or outside shoulder width	2
	Median width	9
Roadside and Safety devices in median	Clear recovery distance	13
	Side slope	4
	Barrier length along embankments	3
	Barrier type (say, to less rigid)	10
	Median barrier	7
	Crash cushions at roadside features	5
Alignment	Horizontal curve radius	6
	Superelevation of horizontal curve	8
	Vertical grade	15
Other elements	Continuous shoulder rumble strips	11
	Highway illumination between interchanges	14
	Distance between two ramps (e.g., weaving section)	1
	HOV lane(s)	16
	Use buffer-separation or barrier-separation for HOV lane	18
	HOV lane entrance or exit frequency or location	17
Any	Other: Interchange spacing Lane drop (lane drop in curve) Congestion extent or duration Truck-only facilities Lane continuity along segment Ramp meter operation Tangent length between curves Crest vertical curvature Lane add Median crossover Lane balance at ramp ent. and exit Signing consistency Barrier on curve (block sight lines) Shoulder use by bicyclists	

Notes:

1- Top ranking elements are identified by bold font.

2- 1 = most frequently considered and believed to have most influence on safety.

TABLE A-3. Safety information needs for interchange ramps

Category	Element ¹	Rank ²
Roadway	Ramp configuration (diamond, loop; direct, semidirect)	2
	Lane width	13
	Inside or outside shoulder width	12
	Number of lanes	9
Roadside	Clear recovery distance	10
	Side slopes	8
	Crash cushions at roadside features	1
Alignment	Horizontal curve radius	3
	Superelevation of horizontal curve	5
	Vertical grade	4
Other elements	Ramp illumination	10
	Use of collector-distributor road	6
	Weaving length on collector-distributor road	7
	Ramp meter	14
Any	Other: HOV bypass lane on entrance ramps	

Notes:

1- Top ranking elements are identified by bold font.

2- 1 = most frequently considered and believed to have most influence on safety.

The number of responses that underlie a rank ranges from seven to ten, with nine being the most common. There was some variability in the responses for each element that reflects differences in opinion among the interviewees. Nevertheless, those elements in the top one-third of the rankings are consistently in the “more important” category for almost all interviewees. These elements have been identified in the table by bold font. Similarly, those elements in the bottom one-third of the rankings are consistently in the “less important” category for almost all interviewees.

The last row in each of the three tables lists other elements that were identified during the interviews. In each instance, one or more interviewees felt that safety information about the element listed would be helpful in their work.

TABLE A-4. Safety information needs for interchange ramp terminal

Category	Element ¹	Rank ²
Freeway speed-change lane	Left-hand or right-hand ramp	11
	Lane length (sensitivity to truck percent, grade, no. of ramp lanes)	2
	Ramp illumination	12
Crossroad speed-change lane	Provide (or not)	16
Crossroad ramp terminal	Interchange type (SPUI, diamond, parclo)	1
	Intersection skew angle	8
	Left-turn lane or bay	5
	Right-turn lane or bay	10
	Left-turn lane length	6
	Right-turn lane length	9
	Outside shoulder width	15
	Intersection median width	12
	Sight distance restrictions	4
	Driveway presence on crossroad approaches to intersection	3
	Lane width	17
	Channelized (free) right-turn lane	14
	Illumination at terminal	7
Any	Other: Ramp entrance or exit on freeway curve Design or signing treatments to reduce wrong-way maneuvers Roundabout crossroad ramp terminal Taper versus parallel entrance ramp Various (unnamed) pedestrian accommodations at terminals Ramp storage size to minimize queue spillback onto freeway Grade of terminal approach	

Notes:

1- Top ranking elements are identified by bold font.

2- 1 = most frequently considered and believed to have most influence on safety.

MEETING WITH FHWA ENGINEERS

The researchers met with engineers in FHWA’s Office of Infrastructure. This office has the responsibility of approving interchange justification reports and access justification reports. These reports have been required by FHWA since about the mid-1980s. In the early 1990s, FHWA’s policy for modifications to access to the Interstate Highway System was updated to require adherence to eight specific elements. The third element states that the proposed access point should “...not have a significant adverse impact on the safety and operation of the Interstate facility based on an analysis of current and future traffic.” This element provides the motivation for documenting the findings from a formal safety evaluation in the preparation of these reports.

Experience in reviewing justification reports indicates that the safety impacts of a proposed access point are often addressed through an assessment of its compliance with approved design criteria. In many instances, capacity improvements made in conjunction with the new access are cited as having an indirect safety benefit through the alleviation of queue spillback or bottleneck. It was noted that some interchange or access justification reports are prepared at a time in the project development process where some design details have not been determined. This situation can limit the level of analysis detail.

Specific evaluation tools (e.g., ISAT or CORSIM) are not required for the safety or operations evaluation. The operations evaluation is only required when the freeway facility will experience congested flow conditions. The FHWA engineers estimated that these conditions are encountered in about one-half of the reports that they review. VISSIM is the most commonly used simulation tool used for operational evaluation. However, CORSIM is also often used and the *Highway Capacity Manual* methods are used in some situations.

There are three ingredients that FHWA desires in the safety evaluation for an interchange or access justification report. First, the evaluation should address the entire project, as opposed to just selected locations or components. Second, the evaluation should reflect consideration of the crash history in the most recent three-year period for which crash data are available. These data would be used to identify locations in the project area at which crashes are relatively frequent. Third, the report should describe the proposed changes such that the project will not have a significant adverse effect on safety.

The presence of HOV lanes on the freeway in the project vicinity is rarely a point of concern in the interchange or access justification report. Issues that have come up when reviewing these reports include: (1) the distance between the HOV entrance (or exit) and the nearest ramp terminal and (2) the speed differential between the HOV lane and adjacent through lane during peak traffic periods.

The FHWA engineers have not found many reports where ISAT has been used in the safety evaluation. They believe that this trend may be a result of its limited ability to model complicated ramps and interchanges. They suggested that its capability should be broadened so that it could be used to evaluate ramp-to-ramp junctions, combined system and service interchanges, and complicated ramp alignments (e.g., braided ramps).

INTERVIEWS WITH ISAT USERS

The purpose of the interviews with ISAT users was to determine the types of applications for which ISAT is being used and to identify any useful improvements that could be made to it. Eleven professionals were identified as potential ISAT users. They were identified in a variety of ways, including information provided by FHWA's Office of Safety R&D and leads provided during the interviews with planners and engineers. Each potential user was contacted by e-mail and asked to provide some feedback on their ISAT experience. Only three persons indicated that they had experience using ISAT (a few did not reply and a few others indicated that they had ISAT but have not had an occasion to use it).

One of the respondents used ISAT in preparation of an interchange justification report. The other respondents used it for environmental evaluations and planning studies. The stated benefits of using ISAT were:

- it can be used to evaluate a range of alternative interchange types, and
- it can predict crash frequency by severity.

Identified areas of potential technical improvement for ISAT include the ability to evaluate the following design elements and components:

- weaving section design,
- left-hand versus right-hand ramps,
- the length of the marked gore area,
- auxiliary lane addition, and
- sensitivity to level of service or volume-to-capacity ratio.

Identified areas of potential user-interface improvement for ISAT include:

- improved guidelines for model calibration, and
- ability to generate a user-friendly report of computed safety measures.

APPENDIX B: DATABASE ENHANCEMENT

As described in Chapter 4, the data maintained by three state DOTs provide the foundation for the database used for model calibration. These data describe road inventory information for the state highway system in each state. The highways are represented as a series of consecutive road segments with a homogenous cross section and a length ranging from 0.05 to 1.0 mi. The state data were acquired from the Highway Safety Information System (HSIS).

This appendix describes the process used to enhance the state data. Data enhancement consisted of using supplemental data sources to acquire additional data for each segment in the database.

This appendix consists of two parts. The first part describes the procedural steps of the enhancement process. The second part summarizes the findings from a data verification activity that was undertaken to assess the consistency between data in a state database and that acquired from aerial photographs.

DATA ENHANCEMENT ACTIVITIES

The data enhancement activities focused on two tasks. One task was the development of data to describe for each segment the proportion of hours per day that are congested. Supplemental data were collected and used to derive this proportion for freeway segments. Automatic traffic recorder (ATR) data for the station nearest to each freeway segment were used for this purpose. These ATR data were acquired from the appropriate state agencies.

The second task of the data enhancement activity was the use of aerial photography to collect additional data for each segment or ramp terminal. These photographs were obtained from Google Earth. The data collected include the width of key cross section elements, barrier presence and location, horizontal curvature, ramp configuration, turn bay presence, and median type.

Data Extraction Process

A process was developed to partially automate the extraction of data from aerial photographs. The process is based on the digitization of roadway design elements using aerial photographs that are keyed to a geodetic coordinate system. Using this process, the road alignments, the road cross sections, the barrier pieces, and the speed-change lanes are all manually digitized. Software is used to process the digitized locations and compute the desired quantities.

Using this process, a technician digitizes the photograph of each segment, saves the measurement locations in a file, and submits the file to a computer program for error checking. At a later time, an engineer reviews the technician's measurement locations by viewing them on the digitized photo. He or she then submits the file to a second computer program that computes the desired variable values. This process is described in more detail in the following sections.

This process is used to digitize cross sections and alignments. When applied to alignments, the engineer digitizes the horizontal alignment of a length of roadway and saves the file of digitized locations. He or she then submits the file to a computer program that computes (1) the coordinates of each segment begin milepost and (2) the geometry of each horizontal curve.

Digitized locations along an alignment are saved in an “alignment file.” Digitized locations along a cross section are saved in a “segment file.” Details of these two files and the process by which they are assembled are provided in the next two sections.

Digitized Alignment File

Google Earth is used to develop the digitized alignment file. The start and end of an alignment is predetermined to include one or more target road segments, as well as the nearest interchange. Figure B-1 illustrates a digitized alignment for a 2.2-mile section of Interstate 5 in California.

The alignment shown in Figure B-1 consists of 29 “placemarks” located along the alignment. A placemark represents a point of known latitude and longitude. Each placemark is shown using a push-pin symbol. For this reason, placemarks are hereafter referred to as “pins.”

The digitizing process consists of three steps. During the first step, pins are located along the roadway reference line in the direction of increasing milepost. For freeway segments, this line is defined by the inside edge of traveled way for the increasing milepost direction. The pins are placed at the start of the alignment, the end of the alignment, and at a short spacing along each horizontal curve located between the start and end points. The maximum distance between pins along a curve is intentionally short such that errors in length measurement are negligible.

When the alignment file is complete, it is saved in keyhole markup language (kml) format (Wikipedia, 2010b). This format is an xml-based, standardized file structure for describing geographic annotation in Internet-based Earth browsers. A more complete description of this language is provided at the Google Earth website (KML, 2010).

During the second step, additional pins are placed along the alignment and saved in a second kml file. These pins correspond to known interchange gore points or intersections that are defined in the state database by milepost. Multiple gore points and intersections are located in this manner and then used to determine the milepost that corresponds to the start of the alignment file.

During the third step, additional pins are placed along the alignment and saved in the kml file established in the second step. These pins correspond to the begin milepost of each road segment in the roadlog database provided by HSIS. The location of a segment begin milepost is determined by computing the difference between it and that determined to correspond to the start of the alignment file. Each begin milepost pin is located at the computed distance, as measured along the alignment reference line.

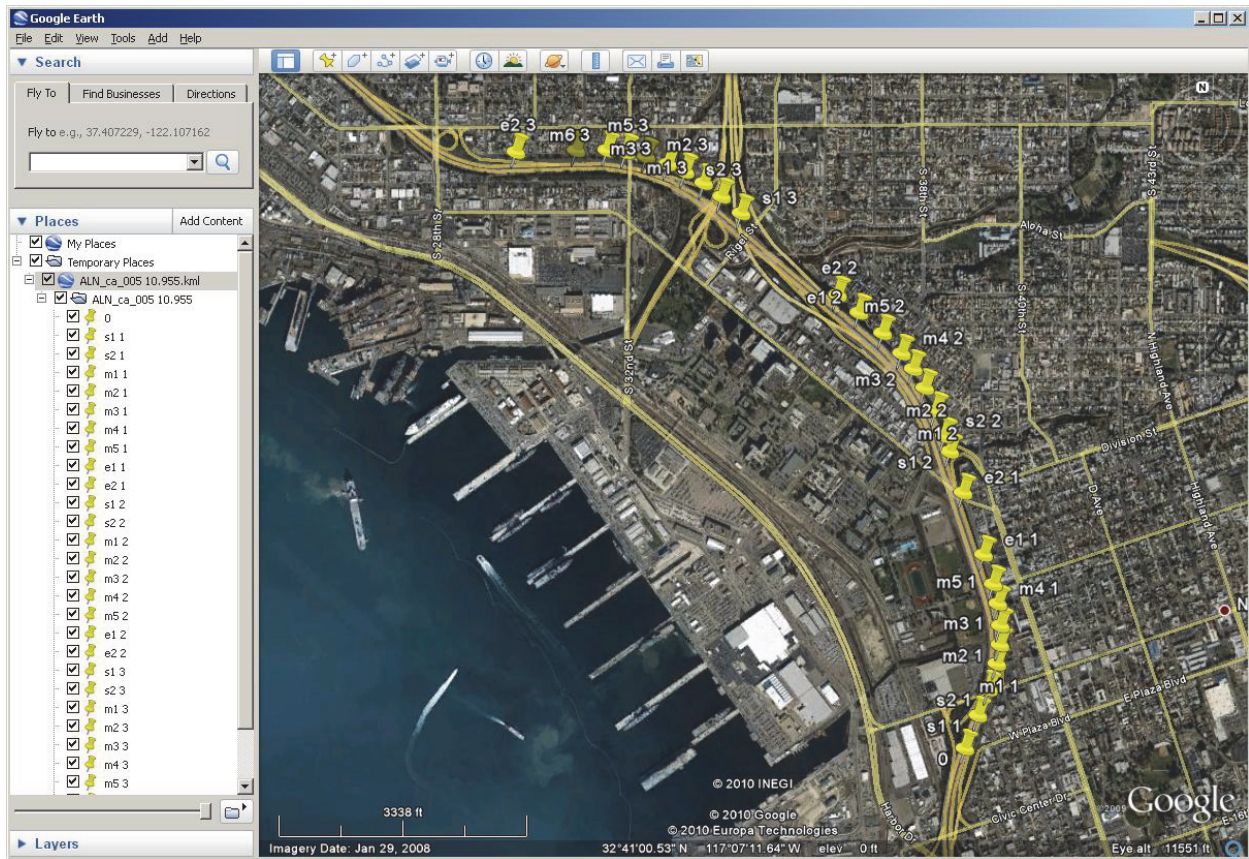


Figure B-1. Example digitized alignment.

Steps two and three are automated using Earth Tools software developed for this project and described in a subsequent section.

The geodetic coordinates (i.e., latitude and longitude) of each segment begin (and end) milepost are determined through this process. In terms of defining a feature's relative location on a common photograph, the standard error of these coordinates is about ± 0.1 ft. Thus, the standard error for a lane width or curve length measurement is about ± 0.14 ft. In terms of defining a feature's true earth location, the standard error is about ± 30 ft.

Digitized Segment File

Google Earth is used to develop the digitized segment file. The segment file is used to describe the cross section, barrier, and speed-change lanes on a given segment. One file is created for each segment. Figure B-2 illustrates a digitized 0.273-mile segment on Interstate 5 in California.

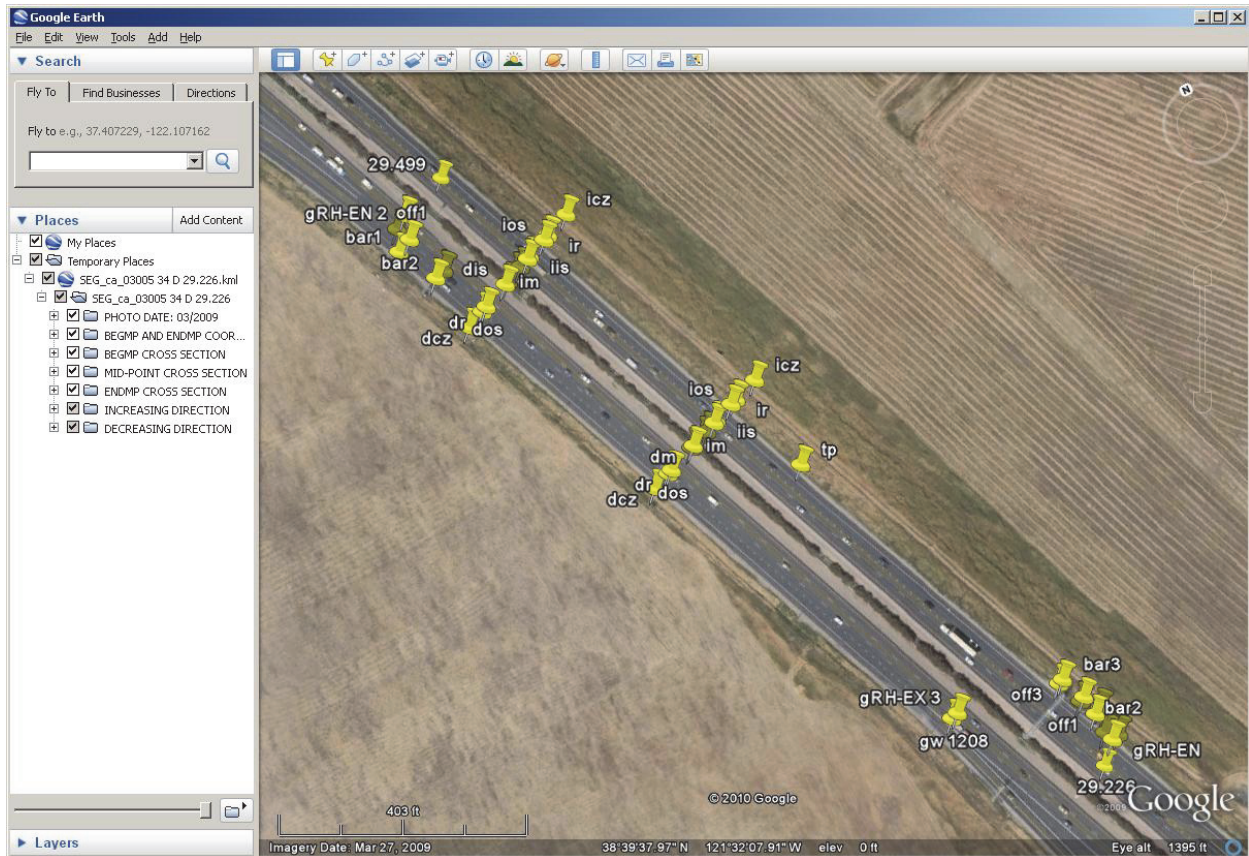


Figure B-2. Example digitized segment.

The segment shown in Figure B-2 consists of 59 pins located at key points along the alignment. One pin is used to define the begin milepost (i.e., 29.226) and one pin is used to define the end milepost (i.e., 29.499). One set of 14 pins are used to define the cross section elements (i.e., clear zone, outside shoulder, lane, inside shoulder, median, and median barrier widths) near the middle of the segment and another set of 14 pins are used to define the cross section at the end of the segment. A third set of pins are used to define the roadside barrier near the start of the segment (right roadbed) and that near the end of the segment (left roadbed). A fourth set of pins are used to define the gore points associated with the weaving section (left roadbed). A fifth set of pins are used to define the speed-change lane near the start of the segment (right roadbed).

The digitizing process consists of locating the pins for each design element present on the segment. In practice, one technician is tasked with locating the cross section pins. Another technician is tasked with locating the barrier pins. An engineer is tasked with locating the pins for speed-change lanes (and weaving sections) due to their greater complication.

All pins for a segment are saved in one kml file. The geodetic coordinates of each design feature are determined through this process. In terms of defining a feature's relative location or length, the standard error of these coordinates is about ± 0.1 ft.

Processing Software

Computer software was developed to process both the alignment and segment files. This processing included reading the kml file, diagnosing the pin placements, and computing the desired database variables. The software was written as a Visual Basic for Applications (VBA) macro in an Excel® spreadsheet. It is called Earth Tools. The welcome screen for Earth Tools is shown in Figure B-3.

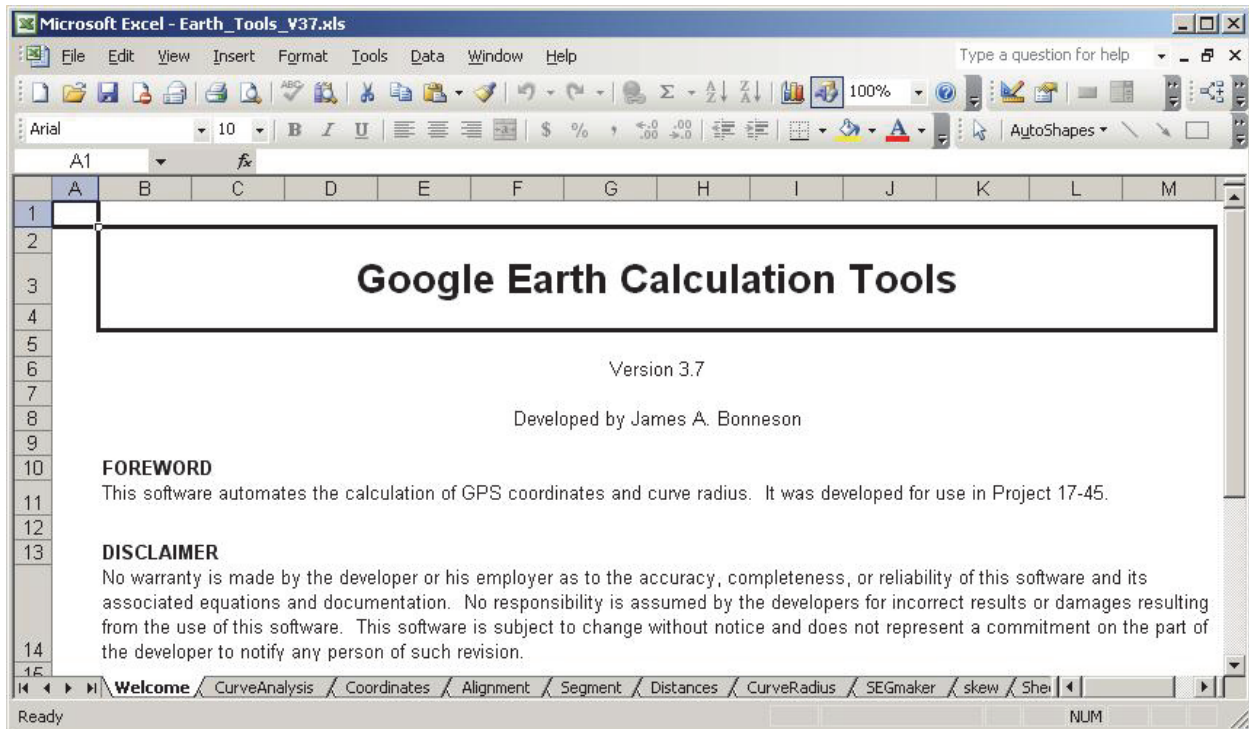


Figure B-3. Google Earth Calculation Tools welcome screen.

The software includes a variety of tools useful to the researchers in developing or evaluating kml files. Each tool is provided its own spreadsheet, as accessed by the corresponding tab identified along the bottom of Figure B-3. Of particular note are the following tools:

- Curve Analysis
- Alignment
- Segment

The purpose of each of these tools is described in the following subsections.

Curve Analysis Tool

The Curve Analysis tool is used to compute the geometry of each horizontal curve represented in an alignment file. The tool computes the radius, deflection angle, chord, length of curve on a specified segment, curve begin milepost, and curve end milepost.

The tool converts the geodetic coordinates associated with each pin into earth-centered-earth-fixed (ECEF) Cartesian coordinates, and then into east-north-up (ENU) Cartesian coordinates (Wikipedia, 2010a). The ENU coordinates are desirable because they place the roadway in an x - y plane where x is east, y is north, and z represents elevation. The distance between any two pins is then computed using their x - y coordinates (the error caused by ignoring the elevation change is negligible for the distances being measured). The relationship between the ECEF and ENU coordinate systems is shown in Figure B-4.

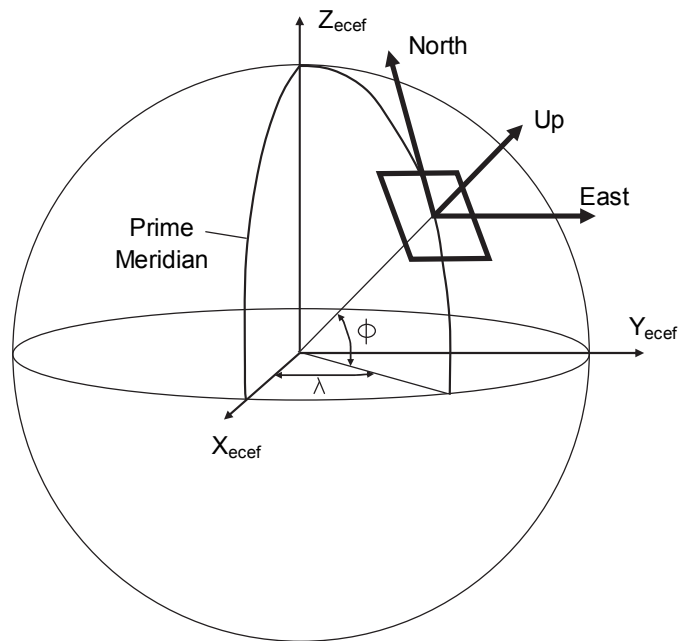


Figure B-4. Earth-Centered-Earth-Fixed and East-North-Up coordinate systems.

Curve radius is computed using an algorithm developed by Imram et al. (2006). This algorithm incorporates a non-linear regression procedure derived by Manthey (2010). The algorithm was adapted to use the pins in an alignment file (see Figure B-1). It can be used to compute the geometry of simple curves, two-centered compound curves, and three-centered compound curves. Geometric data are provided for each curve in a compound curve. A circular curve with spiral transitions is approximated as a compound curve and an average radius is computed for the spiral transition.

The accuracy of the computed curve geometry was evaluated using data from one state database. The computed radii were found to be within 4 percent of the reported radii. The computed deflection angles were found to be within 5 percent of the reported deflection angles.

Further inspection of the data indicates that the larger deviations in either range occurs when the photograph quality is poor or when the curve can be characterized as having a short length and small deflection angle. Additional information about this evaluation is provided in the second part of this appendix.

Alignment Tool

The Alignment tool is used to compute the coordinates of user-specified mileposts. Typically, the mileposts of interest are those representing the begin milepost of a segment. The computations require an alignment file (as described previously) that includes the segment of interest. They also require the user to input the milepost of the starting point of the alignment. The Alignment tool then reads the file and defines the coordinates of the user-specified mileposts based on their distance along the reference line.

Once computed, the coordinates for each user-specified milepost are exported to a new kml file. This file can be loaded into Google Earth and the computed points displayed on an aerial photograph of the roadway. This type of display is shown in Figure B-5 for a section of road comprised of five segments.

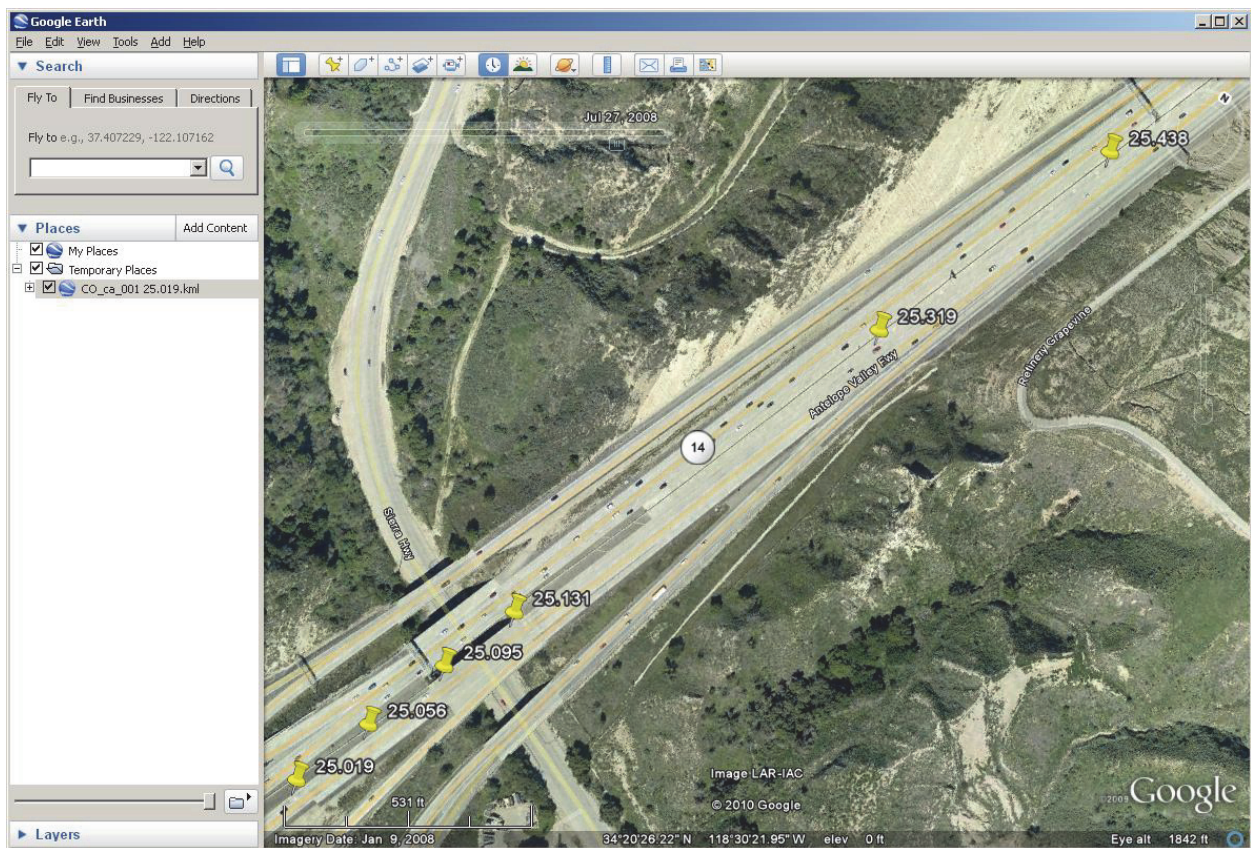


Figure B-5. Display of computed begin mileposts for five segments.

Segment Tool

The Segment tool is used to diagnose the segment file and compute the desired database variables. It includes an extensive set of routines that check the completeness and logic of the pins placed in the segment file. If a file is determined to have missing pins or illogical pin placements, then an error message is displayed indicating the nature of the error and a suggested means of correction. If a file is determined to be error-free, then the computed values for specified variables are displayed in a manner suitable for inclusion in the safety database.

Table B-1 lists the variables computed from the segment files. The speed-change lane variables listed in the table are provided for up to four speed-change lanes per segment.

VERIFICATION OF SELECTED VARIABLES

Some of the data collected during the enhancement process were redundant to the data in the state databases. These data were used to verify the accuracy of the extracted data. The findings from this activity are described in this section. The objective of the verification process was to provide justification for using the enhancement process. It is not intended to suggest that state highway databases are inaccurate for their intended purposes.

The verification process is based on the graphical and statistical comparison of selected variables. For each variable, data were extracted from aerial photographs and checked following the process described in the previous part of this appendix. These variables are referred to as “measured” variables. They are then compared to identically defined data provided in the state database. These variables are referred to as “reported” variables.

Separate verification activities were undertaken for the cross section measurements and the alignment measurements. The findings from these two activities are described separately in the following two sections.

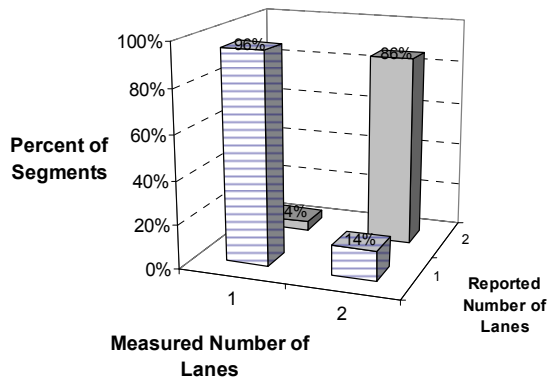
TABLE B-1. Variables computed from segment file

Category	Variable	Description
Roadway	inc_drop-add_lanes	Number of lane drops or adds on seg. for travel in increasing milepost
	dec_drop-add_lanes	Number of lane drops or adds on seg. for travel in decreasing milepost
	out_shld_meas	Outside shoulder width (average of both directions)
	lane_meas	Lane width (average for all lanes in both directions)
	in_meas	Width of both shoulders and median
	in_shld_meas	Inside shoulder width (average of both directions)
	med_width_meas	Width of median
	med_nontrav_meas	Width of median barrier, if present
Roadside	med_type_meas	Median type (1 = raised curb, 2 - barrier, 3 = depressed or unsurfaced)
	in_lane_barrier_len	Total length of barrier adjacent to the lane in median
	in_shld_barrier_len	Total length of barrier adjacent to the shoulder in median
	in_off_barrier_len	Total length of barrier offset from the shoulder in median
	out_lane_barrier_len	Total length of barrier adjacent to the lane on roadside
	out_shld_barrier_len	Total length of barrier adjacent to the shoulder on roadside
	out_off_barrier_len	Total length of barrier offset from the shoulder on roadside
	inc_clear_zone	Average clear zone width for travel in increasing milepost
	dec_clear_zone	Average clear zone width for travel in decreasing milepost
Speed-Change Lane	sc_design	Design for speed-change lane (e.g., P=parallel, T=taper, etc.)
	sc_type	Orientation of speed-change lane (e.g., entrance/exit, left/right side)
	sc_lgt_on_seg	Length of speed-change lane on subject segment
	sc_ramp_lanes	Number of lanes in the speed-change lane
Weaving Section	inc_A_lanes ^a	Number of lanes on freeway and ramps before weaving section
	inc_C_lanes ^a	Number of lanes on freeway and ramps after weaving section
	inc_D_lanes ^a	Number of lanes on <u>right-side</u> entrance ramp before weaving section
	inc_E_lanes ^a	Number of lanes on <u>right-side</u> exit ramp after weaving section
	inc_Lw ^a	Length of weaving section (gore to gore)
	inc_wev_lgt_on_seg ^a	Length of weaving section on segment
	dec_A_lanes ^b	Number of lanes on freeway and ramps before weaving section
	dec_C_lanes ^b	Number of lanes on freeway and ramps after weaving section
	dec_D_lanes ^b	Number of lanes on <u>right-side</u> entrance ramp before weaving section
	dec_E_lanes ^b	Number of lanes on <u>right-side</u> exit ramp after weaving section
	dec_Lw ^b	Length of weaving section (gore to gore)
	dec_wev_lgt_on_seg ^b	Length of weaving section on segment
Other	ramp_exit_cnt	Count of ramp exit gore points adjacent to segment
	ramp_ent_cnt	Count of ramp entrance gore points adjacent to segment

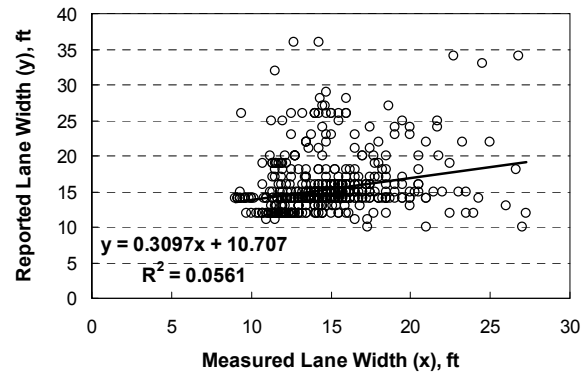
Cross Section Elements

The findings for selected ramp cross section variables are described first. Then, the findings for selected freeway segment cross section variables are described. Data associated with

ramp lane count and lane width are shown in Figure B-6. Figure B-6a indicates that ramps with one lane were correctly identified in the database as having one lane for 96 percent of the segments (4 percent of these segments were reported as having two lanes). Similarly, ramps with two lanes were correctly identified in the database as having two lanes for 86 percent of the segments (14 percent of these segments were reported as having one lane).



a. Number of lanes.



b. Lane width.

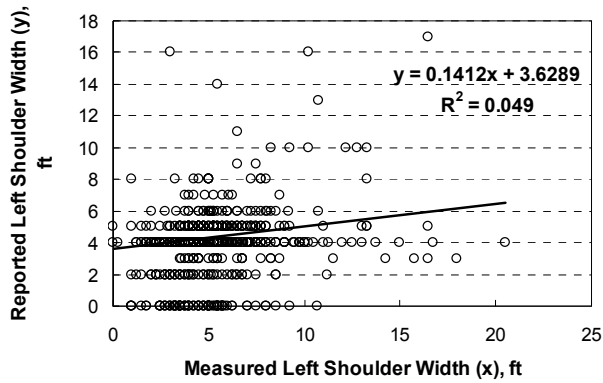
Figure B-6. Ramp lane data comparison.

Figure B-6b indicates a weak correlation between the measured ramp lane width and the lane width reported in the database. The figure indicates that there is considerable random variation in the error, and the “best fit” trend line suggests that there is some bias (e.g., ramps measured to have 10-ft lane width, tend to be reported as having a 14-ft lane width). This type of bias is particularly problematic because it translates into biased regression coefficients.

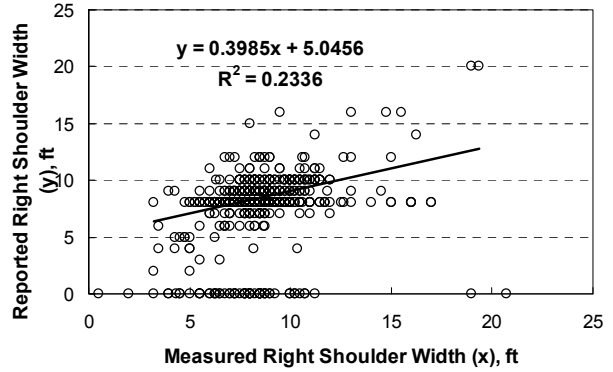
From a statistical standpoint, random error in a variable can be overcome by increasing the sample size. Thus, it could be argued that using the entire state database (instead of just those segments that can be manually verified using data from aerial photographs or similar) would overcome the random variation shown in Figure B-6b. However, random variation in the independent variable of a regression model will bias the regression coefficients. Through simulation experiments, Weed and Barros (1987) found that significant variability in the independent variable causes bias in the regression model coefficients. This variability also increases the model’s residual error and makes the t-tests of model coefficients less efficient.

The findings from a comparison of ramp shoulder width are shown in Figure B-7. The random error is notable, as is the bias in the data.

The findings from a comparison of freeway median width and left (inside) shoulder width are shown in Figure B-8. Again, the random error and bias in the shoulder width data is notable. The median width does not appear to exhibit significant bias but the random error is large.

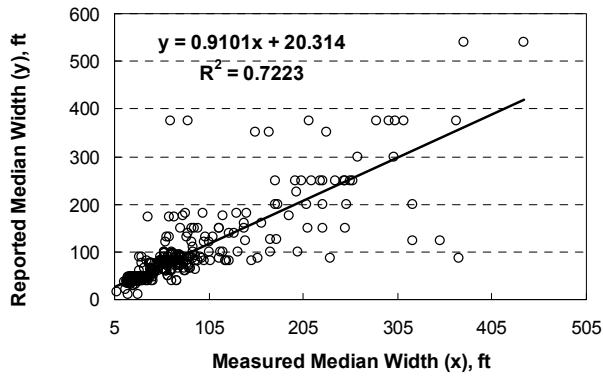


a. Left shoulder width.

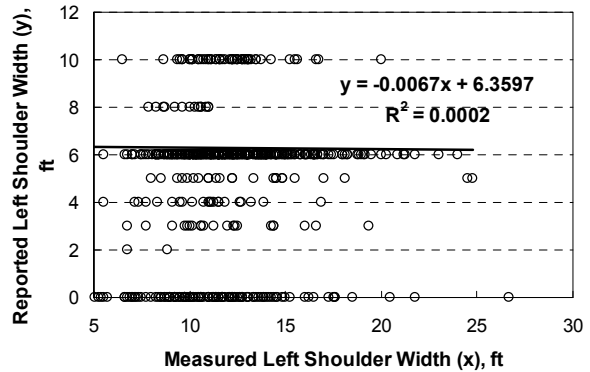


b. Right shoulder width.

Figure B-7. Ramp shoulder data comparison.



a. Median width.



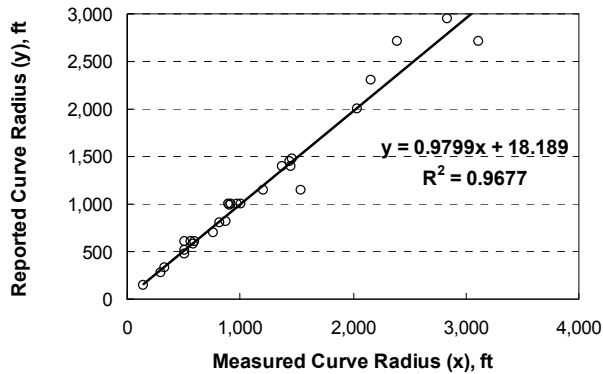
b. Left (inside) shoulder width.

Figure B-8. Freeway shoulder and median data comparison.

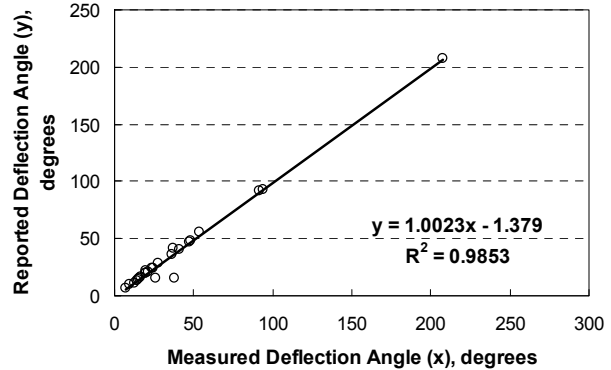
Horizontal Curve Geometry

Curve data for ramp and freeway segments in one state database were computed using the Curve Analysis tool and alignment files. The findings from the evaluation of the ramp curve data are shown in Figure B-9. Each data point shown represents one curve. The 28 curves included in this evaluation were randomly selected and rationalized to be representative.

The graphs shown (and statistics cited) in Figure B-9 indicate that there is good agreement between the measured and reported curve radius and deflection angle on ramps. The trend line shown in each graph is a line of “best fit” based on a linear regression analysis. The t-statistic for the slope of the regression line in Figure B-9a indicates that the slope is not significantly different from 1.0. Also, the intercept for this line is not significantly different from 0.0. Similar results were found for the regression line coefficients shown in Figure B-9b.



a. Curve radius.



b. Deflection angle.

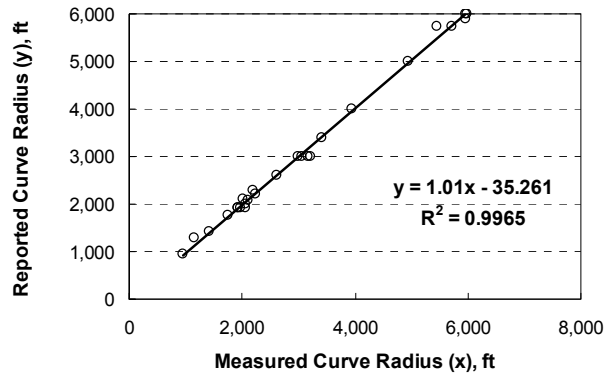
Figure B-9. Ramp curve geometry data comparison.

A small number of data points in Figure B-9a indicate a notable difference of several hundred feet between the measured and reported radius values. A closer inspection of these points indicated that the difference may be due to the inclusion of short spiral transitions (or compound transition curvature with a short, large-radius curve) prior to a sharp curve on the ramp. Transition curves are difficult to visually detect from photographs, especially if they have a short length and small deflection angle. If they were not detected, the measured radius would represent an average value for the combined circular curve and transition curve.

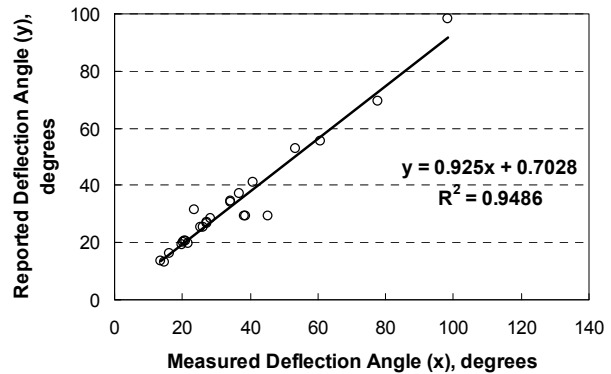
A couple of the deflection angles shown in Figure B-9b indicate a notable difference of several degrees between the measured and reported values. An examination of the data indicated that the measured values from Curve Analysis Tool were in agreement with manually measured deflections taken directly from the aerial photograph with a protractor. It is recognized that photograph quality could explain a few degrees of deviation in extreme cases, but not the several degrees found for a couple of curves. It is believed that these curves have spiral transitions and that the deflection angle reported in the state database is for the circular portion of the curve, rather than the total deflection in the alignment.

The findings from the evaluation of the freeway curve data are shown in Figure B-10. Each data point shown represents one curve. The 26 curves included in this evaluation were randomly selected and rationalized to be representative.

The graphs shown (and statistics cited) in Figure B-10 indicate that there is good agreement between the measured and reported curve radius and deflection angle on freeway segments. The trend line shown in each graph is a line of “best fit” based on a linear regression analysis. The t-statistic for the slope of the regression line in Figure B-10a indicates that the slope is not significantly different from 1.0. Also, the intercept for this line is not significantly different from 0.0. Similar results were found for the regression line coefficients shown in Figure B-10b.



a. Curve radius.



b. Deflection angle.

Figure B-10. Freeway curve geometry data comparison.

A few of the deflection angles shown in Figure B-10b indicate a difference of several degrees between the measured and reported values. The reasons for these deviations are the same as offered in the discussion of Figure B-9b.

REFERENCES

Imran, M., Y. Hassan, and D. Patterson. (2006). "GPS-GIS-Based Procedure for Tracking Vehicle Path on Horizontal Alignments." *Computer-Aided Civil and Infrastructure Engineering*. Vol. 21. Blackwell Publishing, Malden, Massachusetts, pp. 383-394.

KML Documentation Information. (2010). Google Earth.
<http://code.google.com/apis/kml/documentation/>. Accessed June 10, 2010.

Manthey, David. (2010). "General Least-Squares - Direct Solutions and Bundle Adjustments."
<http://www.orbitals.com/self/least/least.htm>. Accessed June 10, 2010.

Weed, R.M., and R.T. Barros. (1987). "Demonstration of Regression Analysis with Error in the Independent Variable." *Transportation Research Record 1111*. Transportation Research Board, National Research Council, Washington, D.C., pp. 48-54.

Wikipedia. (2010a). "Geodetic System." Wikipedia Foundation, Inc.
http://en.wikipedia.org/wiki/Geodetic_system. Accessed June 10, 2010.

Wikipedia. (2010b). "Keyhole Markup Language." Wikipedia Foundation, Inc.
http://en.wikipedia.org/wiki/Keyhole_Markup_Language. Accessed June 10, 2010.

APPENDIX C

PROPOSED HSM FREEWAYS CHAPTER

CHAPTER 18—PREDICTIVE METHOD FOR FREEWAYS

TABLE OF CONTENTS

List of Figures.....	iii
List of Tables.....	iv
18.1. Introduction.....	1
18.2. Overview of the Predictive Method.....	1
18.3. Freeways—Definitions and Predictive Models.....	2
18.3.1. Definition of Freeway Facility and Site Types.....	2
18.3.2. Predictive Model for Freeway Segments.....	5
18.3.3. Predictive Model for Freeway Speed-Change Lanes.....	6
18.4. Predictive Method for Freeways.....	7
18.4.1. Step-by-Step Description of the Predictive Method.....	7
18.4.2. Data Needed to Apply the Predictive Method.....	15
18.5. Roadway Segments and Speed-Change Lanes.....	21
18.5.1. Definition of Freeway Segment and Speed-Change Lane.....	21
18.5.2 Segmentation Process.....	22
18.5.3. Crash Assignment to Sites.....	24
18.6. Safety Performance Functions.....	24
18.6.1. Safety Performance Functions for Roadway Segments.....	25
18.6.2. Safety Performance Functions for Speed-Change Lanes.....	31
18.7. Crash Modification Factors.....	38
18.7.1. Crash Modification Factors for Roadway Segments.....	39

18.7.2. Crash Modification Factors for Speed-Change Lanes	50
18.7.3. Supplemental Calculations to Apply Crash Modification Factors	56
18.8. Severity Distribution Functions	59
18.9. Calibration of the SPFs and SDFs to Local Conditions	61
18.10. Limitations of Predictive Method	62
18.11. Application of Predictive Method	62
18.11.1. Freeways with Barrier-Separated Managed Lanes	63
18.11.2. Freeways with Toll Facilities	63
18.12. Summary	63
18.13. Sample Problems	64
18.13.1. Sample Problem 1	64
18.13.2. Sample Problem 2	75
18.13.3. Sample Problem 3	88
18.13.4. Sample Problem 4	97
18.13.5. Sample Problem 5	106
18.13.6. Sample Problem 6	113
18.14. References	119
Appendix 18A—Worksheets for Predictive Method for Freeways	120

LIST OF FIGURES

Figure 18-1. The HSM Predictive Method	8
Figure 18-2. Through Lane Count in Segments with Lane Add or Lane Drop	15
Figure 18-3. Freeway Speed-Change Lane Length	16
Figure 18-4. Curve Length and Radius Measurements.....	17
Figure 18-5. Measurement of Cross Section Data Elements	18
Figure 18-6. Barrier Variables	19
Figure 18-7. Type B Weaving Section and Length.....	19
Figure 18-8. Distance to Nearest Ramp	20
Figure 18-9. Clear Zone Width Considerations	21
Figure 18-10. Illustrative Freeway Segments and Speed-Change Lanes	22
Figure 18-11. Segmentation for Varying Median Width	24
Figure 18-12. Graphical Form of the SPFs for Multiple-Vehicle Crashes on Freeway Segments...	27
Figure 18-13. Graphical Form of the SPFs for Single-Vehicle Crashes on Freeway Segments.....	30
Figure 18-14. Graphical Form of the SPFs for Ramp Entrance Speed-Change Lanes	33
Figure 18-15. Graphical Form of the SPFs for Ramp Exit Speed-Change Lanes.....	35

LIST OF TABLES

Table 18-1. Freeway Segment SPFs	3
Table 18-2. Freeway Speed-Change Lane SPFs	4
Table 18-3. Freeway Safety Performance Functions	24
Table 18-4. Applicable AADT Volume Ranges for SPFs.....	25
Table 18-5. SPF Coefficients for Multiple-Vehicle Crashes on Freeway Segments	27
Table 18-6. Default Distribution of Multiple-Vehicle Crashes by Crash Type for Freeway Segments	28
Table 18-7. SPF Coefficients for Single-Vehicle Crashes on Freeway Segments.....	29
Table 18-8. Default Distribution of Single-Vehicle Crashes by Crash Type for Freeway Segments	31
Table 18-9. SPF Coefficients for Ramp-Entrance-Related Crashes in Speed-Change Lanes	32
Table 18-10. Default Distribution of Ramp-Entrance-Related Crashes by Crash Type	34
Table 18-11. SPF Coefficients for Ramp-Exit-Related Crashes in Speed-Change Lanes.....	35
Table 18-12. Default Distribution of Ramp-Exit-Related Crashes by Crash Type.....	37
Table 18-13. Freeway Crash Modification Factors and their Corresponding SPFs	38
Table 18-14. Coefficients for Horizontal Curve CMF–Freeway Segments.....	40
Table 18-15. Coefficients for Lane Width CMF–Freeway Segments	41
Table 18-16. Coefficients for Inside Shoulder Width CMF–Freeway Segments	41
Table 18-17. Coefficients for Median Width CMF–Freeway Segments	42
Table 18-18. Coefficients for Median Barrier CMF–Freeway Segments.....	43
Table 18-19. Coefficients for High Volume CMF–Freeway Segments.....	44
Table 18-20. Coefficients for Lane Change CMF–Freeway Segments.....	46
Table 18-21. Coefficients for Outside Shoulder Width CMF–Freeway Segments	47
Table 18-22. Coefficients for Outside Barrier CMF–Freeway Segments	49
Table 18-23. Coefficients for Horizontal Curve CMF–Speed-Change Lanes.....	50
Table 18-24. Coefficients for Inside Shoulder Width CMF–Speed-Change Lanes	52

Table 18-25. Coefficients for Median Width CMF—Speed-Change Lanes	52
Table 18-26. Coefficients for Median Barrier CMF—Speed-Change Lanes	53
Table 18-27. Coefficients for High Volume CMF—Speed-Change Lanes	54
Table 18-28. Coefficients for Ramp Entrance CMF—Speed-Change Lanes	55
Table 18-29. Coefficients for Ramp Exit CMF—Speed-Change Lanes	56
Table 18-30. SDF Coefficients for Freeway Segments and Speed-Change Lanes	61
Table 18-31. List of Sample Problems	64
Table 18-32. Freeway Segment Worksheet (1 of 4)—Sample Problem 1	72
Table 18-33. Freeway Segment Worksheet (2 of 4)—Sample Problem 1	73
Table 18-34. Freeway Segment Worksheet (3 of 4)—Sample Problem 1	74
Table 18-35. Freeway Segment Worksheet (4 of 4)—Sample Problem 1	75
Table 18-36. Freeway Segment Worksheet (1 of 4)—Sample Problem 2	85
Table 18-37. Freeway Segment Worksheet (2 of 4)—Sample Problem 2	86
Table 18-38. Freeway Segment Worksheet (3 of 4)—Sample Problem 2	87
Table 18-39. Freeway Segment Worksheet (4 of 4)—Sample Problem 2	88
Table 18-40. Freeway Speed-Change Lane Worksheet (1 of 3)—Sample Problem 3	95
Table 18-41. Freeway Speed-Change Lane Worksheet (2 of 3)—Sample Problem 3	96
Table 18-42. Freeway Speed-Change Lane Worksheet (3 of 3)—Sample Problem 3	97
Table 18-43. Freeway Speed-Change Lane Worksheet (1 of 3)—Sample Problem 4	104
Table 18-44. Freeway Speed-Change Lane Worksheet (2 of 3)—Sample Problem 4	105
Table 18-45. Freeway Speed-Change Lane Worksheet (3 of 3)—Sample Problem 4	106
Table 18-46. Freeway Segment Worksheet (1 of 4)—Sample Problem 5	110
Table 18-47. Freeway Segment Worksheet (2 of 4)—Sample Problem 5	111
Table 18-48. Freeway Segment Worksheet (3 of 4)—Sample Problem 5	112
Table 18-49. Freeway Segment Worksheet (4 of 4)—Sample Problem 5	113
Table 18-50. Project-Level EB Method Worksheet (1 of 2)—Sample Problem 6	118
Table 18-51. Project-Level EB Method Worksheet (2 of 2)—Sample Problem 6	119

Chapter 18—Predictive Method for Freeways

18.1. INTRODUCTION

This chapter presents the predictive method for freeways. A general introduction to the *Highway Safety Manual* (HSM) predictive method is provided in Part C—Introduction and Applications Guidance.

The predictive method for freeways provides a structured methodology to estimate the expected average crash frequency (in total, or by crash type or severity) for a freeway with known characteristics. Crashes involving vehicles of all types are included in the estimate. The predictive method can be applied to an existing freeway, a design alternative for an existing freeway, a new freeway, or for alternative traffic volume projections. An estimate can be made of expected average crash frequency for a prior time period (i.e., what did or would have occurred) or a future time period (i.e., what is expected to occur). The development of the predictive method in this chapter is documented by Bonneson et al. (1).

This chapter presents the following information about the predictive method for freeways:

- A concise overview of the predictive method.
- Definitions of the facility types and site types addressed by the predictive method.
- A step-by-step description of the predictive method.
- Details for dividing a freeway facility into individual evaluation sites.
- Safety performance functions (SPFs) for freeways.
- Crash modification factors (CMFs) for freeways.
- Severity distribution functions (SDFs) for freeways.
- Limitations of the predictive method.
- Sample problems illustrating the application of the predictive method.

18.2. OVERVIEW OF THE PREDICTIVE METHOD

The predictive method provides an 18-step procedure to estimate the expected average crash frequency (in total, or by crash type or severity) for a roadway network, facility, or site. A site is a freeway segment or a freeway speed-change lane. A freeway speed-change lane is an uncontrolled terminal between a ramp and a freeway. It has a length along the freeway that is measured between the marked gore point and the taper point of the speed-change lane. The freeway lanes adjacent to the speed-change lane are considered part of the terminal area because of challenges in identifying (a) crashes in the lane associated with the ramp entrance or exit and (b) crashes specifically related to speed-change lane operation.

A facility consists of a contiguous set of individual sites. Different facilities are determined by the surrounding land use, roadway cross section, and degree of access. A roadway network consists of a number of contiguous facilities.

The predictive method is used to estimate the expected number of crashes for an individual site. This estimate can be summed for all sites to compute the expected number of crashes for the entire facility or network. The estimate represents a given time period of interest (in years) during which the geometric design and traffic control features are unchanged and traffic volumes are known or forecasted. The expected average crash frequency is obtained by dividing the expected number of crashes by the time period of interest.

The predictive models used in this chapter are described in detail in Section 18.3. The predicted average crash frequency from a predictive model can be used as an estimate of the expected average crash frequency, or it can be combined with observed crash data (using the empirical Bayes [EB] Method) to obtain a more reliable estimate of the expected average crash frequency.

The predictive models used in this chapter to determine the predicted average crash frequency are of the general form shown in Equation 18-1.

$$N_{p,w,x,y,z} = N_{spf,w,x,y,z} \times (CMF_{1,w,x,y,z} \times CMF_{2,w,x,y,z} \times \dots \times CMF_{m,w,x,y,z}) \times C_{w,x,y,z} \quad \text{Equation 18-1}$$

Where:

$N_{p,w,x,y,z}$ = predicted average crash frequency for a specific year for site type w , cross section or control type x , crash type y , and severity z (crashes/yr);

$N_{spf,w,x,y,z}$ = predicted average crash frequency determined for base conditions of the SPF developed for site type w , cross section or control type x , crash type y , and severity z (crashes/yr);

$CMF_{m,w,x,y,z}$ = crash modification factors specific to site type w , cross section or control type x , crash type y , and severity z for specific geometric design and traffic control features m ; and

$C_{w,x,y,z}$ = calibration factor to adjust SPF for local conditions for site type w , cross section or control type x , crash type y , and severity z .

The predictive models provide estimates of the predicted average crash frequency in total, or by crash type or severity. A default distribution of crash type is included in the predictive method. It is used with the predictive models to quantify the crash frequency for each of ten crash types. The models predict fatal-and-injury crash frequency and property-damage-only crash frequency. A severity distribution function is available to further quantify the crash frequency by the following severity levels: fatal, incapacitating injury, non-incapacitating injury, and possible injury.

18.3. FREEWAYS—DEFINITIONS AND PREDICTIVE MODELS

This section provides the definitions of the facility and site types discussed in this chapter. It also describes the predictive models for each of the site types.

18.3.1. Definition of Freeway Facility and Site Types

The predictive method in this chapter applies to the following freeway facilities: rural freeway segment with four to eight lanes, urban freeway segment with four to ten lanes, and freeway speed-change lanes associated with entrance ramps and exit ramps. Freeways have fully-restricted access control and grade separation with all intersecting roadways. Freeways are accessed only through grade-separated interchanges. Roads having at-grade access should be analyzed as rural highways or urban or suburban arterials. These facility types are addressed in Chapters 10, 11, and 12.

The terms “freeway,” “roadway,” and “road” are used interchangeably in this chapter and apply to all freeways independent of official state designation or local highway designation.

Classifying an area as urban, suburban, or rural is subject to the roadway characteristics, surrounding population, and surrounding land uses, and is at the analyst’s discretion. In the HSM, the definition of “urban” and “rural” areas is based on Federal Highway Administration (FHWA) guidelines which classify “urban” areas as places inside urban boundaries where the population is greater than 5,000 persons. “Rural” areas are defined as places outside urban areas where the population is less than 5,000 persons. The HSM uses the term “suburban” to refer to outlying portions of an urban area; the predictive method does not distinguish between urban and suburban portions of a developed area.

Table 18-1 identifies the freeway segment site types for which SPFs have been developed. These SPFs are used to estimate the predicted average crash frequency by crash type and crash severity. These estimates are added to yield the total predicted average crash frequency for an individual site. The freeway segment SPFs are used to evaluate both freeway travel directions combined. One set of SPFs is developed for urban areas and a second set is developed for rural areas.

Table 18-1. Freeway Segment SPFs

Site Type (<i>w</i>)	Cross Section (<i>x</i>)	Crash Type (<i>y</i>)	Crash Severity (<i>z</i>)	SPF	
Freeway segments (<i>fs</i>)	Four-lane divided (<i>4</i>)	Multiple vehicle (<i>mv</i>)	Fatal and injury (<i>fi</i>)	$N_{spf, fs, 4, mv, fi}$	
			Property damage only (<i>pdo</i>)	$N_{spf, fs, 4, mv, pdo}$	
		Single vehicle (<i>sv</i>)	Fatal and injury (<i>fi</i>)	$N_{spf, fs, 4, sv, fi}$	
			Property damage only (<i>pdo</i>)	$N_{spf, fs, 4, sv, pdo}$	
		Six-lane divided (<i>6</i>)	Multiple vehicle (<i>mv</i>)	Fatal and injury (<i>fi</i>)	$N_{spf, fs, 6, mv, fi}$
				Property damage only (<i>pdo</i>)	$N_{spf, fs, 6, mv, pdo}$
	Single vehicle (<i>sv</i>)		Fatal and injury (<i>fi</i>)	$N_{spf, fs, 6, sv, fi}$	
			Property damage only (<i>pdo</i>)	$N_{spf, fs, 6, sv, pdo}$	
	Eight-lane divided (<i>8</i>)		Multiple vehicle (<i>mv</i>)	Fatal and injury (<i>fi</i>)	$N_{spf, fs, 8, mv, fi}$
				Property damage only (<i>pdo</i>)	$N_{spf, fs, 8, mv, pdo}$
		Single vehicle (<i>sv</i>)	Fatal and injury (<i>fi</i>)	$N_{spf, fs, 8, sv, fi}$	
			Property damage only (<i>pdo</i>)	$N_{spf, fs, 8, sv, pdo}$	
Ten-lane divided (<i>10</i>) (urban areas only)		Multiple vehicle (<i>mv</i>)	Fatal and injury (<i>fi</i>)	$N_{spf, fs, 10, mv, fi}$	
			Property damage only (<i>pdo</i>)	$N_{spf, fs, 10, mv, pdo}$	
	Single vehicle (<i>sv</i>)	Fatal and injury (<i>fi</i>)	$N_{spf, fs, 10, sv, fi}$		
		Property damage only (<i>pdo</i>)	$N_{spf, fs, 10, sv, pdo}$		

The freeway segment is defined as follows:

- *Four-lane freeway segment (4)*—a length of roadway consisting of four through lanes with a constant cross section providing two directions of travel in which the opposing travel lanes are physically separated by a median.

- *Six-lane freeway segment (6)*— a length of roadway consisting of six through lanes with a constant cross section providing two directions of travel in which the opposing travel lanes are physically separated by a median.
- *Eight-lane freeway segment (8)*— a length of roadway consisting of eight through lanes with a constant cross section providing two directions of travel in which the opposing travel lanes are physically separated by a median.
- *Ten-lane freeway segment (10)*— a length of roadway consisting of ten through lanes with a constant cross section providing two directions of travel in which the opposing travel lanes are physically separated by a median.

Table 18-2 identifies the speed-change lane site types for which SPFs have been developed. These SPFs are used to estimate the predicted average crash frequency by crash severity. These estimates are added to yield the total predicted average crash frequency for an individual site. The speed-change lane SPFs are used to evaluate the speed-change lane together with the adjacent freeway lanes (i.e., those lanes on the same side of the freeway as the speed-change lane). One set of SPFs is developed for urban areas and a second set is developed for rural areas.

Table 18-2. Freeway Speed-Change Lane SPFs

Site Type (<i>w</i>)	Cross Section (<i>x</i>)	Crash Type (<i>y</i>)	Crash Severity (<i>z</i>)	SPF
Speed-change lanes (<i>sc</i>)	Ramp entrance to four-lane divided (<i>4EN</i>)	All types (<i>at</i>)	Fatal and injury (<i>fi</i>)	$N_{spf, sc, 4EN, at, fi}$
			Property damage only (<i>pdo</i>)	$N_{spf, sc, 4EN, at, pdo}$
	Ramp entrance to six-lane divided (<i>6EN</i>)	All types (<i>at</i>)	Fatal and injury (<i>fi</i>)	$N_{spf, sc, 6EN, at, fi}$
			Property damage only (<i>pdo</i>)	$N_{spf, sc, 6EN, at, pdo}$
	Ramp entrance to eight-lane divided (<i>8EN</i>)	All types (<i>at</i>)	Fatal and injury (<i>fi</i>)	$N_{spf, sc, 8EN, at, fi}$
			Property damage only (<i>pdo</i>)	$N_{spf, sc, 8EN, at, pdo}$
	Ramp entrance to ten-lane divided (<i>10EN</i>) (urban areas only)	All types (<i>at</i>)	Fatal and injury (<i>fi</i>)	$N_{spf, sc, 10EN, at, fi}$
			Property damage only (<i>pdo</i>)	$N_{spf, sc, 10EN, at, pdo}$
	Ramp exit from four-lane divided (<i>4EX</i>)	All types (<i>at</i>)	Fatal and injury (<i>fi</i>)	$N_{spf, sc, 4EX, at, fi}$
			Property damage only (<i>pdo</i>)	$N_{spf, sc, 4EX, at, pdo}$
	Ramp exit from six-lane divided (<i>6EX</i>)	All types (<i>at</i>)	Fatal and injury (<i>fi</i>)	$N_{spf, sc, 6EX, at, fi}$
			Property damage only (<i>pdo</i>)	$N_{spf, sc, 6EX, at, pdo}$
	Ramp exit from eight-lane divided (<i>8EX</i>)	All types (<i>at</i>)	Fatal and injury (<i>fi</i>)	$N_{spf, sc, 8EX, at, fi}$
			Property damage only (<i>pdo</i>)	$N_{spf, sc, 8EX, at, pdo}$
	Ramp exit from ten-lane divided (<i>10EX</i>) (urban areas only)	All types (<i>at</i>)	Fatal and injury (<i>fi</i>)	$N_{spf, sc, 10EX, at, fi}$
			Property damage only (<i>pdo</i>)	$N_{spf, sc, 10EX, at, pdo}$

The speed-change lane cross section is defined as a ramp entrance (*nEN*) or ramp exit (*nEX*) with *n* lanes. The variable *n* is used to describe the number of through lanes in the portion of freeway adjacent to the speed-change lane *plus* those freeway lanes in the opposing travel direction. This approach to describing the speed-change lane cross section is used for consistency with that used for freeway segment SPFs. The variable *n* is not intended to describe the number of lanes in the speed-change lane.

18.3.2. Predictive Model for Freeway Segments

In general, a predictive model is used to compute the predicted average crash frequency for a site. It combines the SPF, CMFs, and a calibration factor. The predicted quantity can describe crash frequency in total, or by crash type or severity. This section describes the predictive model for freeway segments. The next section describes the predictive model for speed-change lanes.

The predictive model for freeway segments is used to estimate the predicted average frequency of segment crashes (i.e., the estimate does not include speed-change-lane-related crashes). Speed-change-related crashes are defined in Section 18.3.3 and estimated using the predictive method described in that section.

The predictive model for freeway segments is presented in Equation 18-2 through Equation 18-6.

$$N_{p, fs, n, at, as} = N_{p, fs, n, mv, fi} + N_{p, fs, n, sv, fi} + N_{p, fs, n, mv, pdo} + N_{p, fs, n, sv, pdo} \quad \text{Equation 18-2}$$

$$N_{p, fs, n, mv, fi} = C_{fs, ac, mv, fi} \times N_{spf, fs, n, mv, fi} \times \left(CMF_{1, fs, ac, mv, fi} \times \dots \times CMF_{m, fs, ac, mv, fi} \right) \times \left(CMF_{1, fs, ac, at, fi} \times \dots \times CMF_{m, fs, ac, at, fi} \right) \quad \text{Equation 18-3}$$

$$N_{p, fs, n, sv, fi} = C_{fs, ac, sv, fi} \times N_{spf, fs, n, sv, fi} \times \left(CMF_{1, fs, ac, sv, fi} \times \dots \times CMF_{m, fs, ac, sv, fi} \right) \times \left(CMF_{1, fs, ac, at, fi} \times \dots \times CMF_{m, fs, ac, at, fi} \right) \quad \text{Equation 18-4}$$

$$N_{p, fs, n, mv, pdo} = C_{fs, ac, mv, pdo} \times N_{spf, fs, n, mv, pdo} \times \left(CMF_{1, fs, ac, mv, pdo} \times \dots \times CMF_{m, fs, ac, mv, pdo} \right) \times \left(CMF_{1, fs, ac, at, pdo} \times \dots \times CMF_{m, fs, ac, at, pdo} \right) \quad \text{Equation 18-5}$$

$$N_{p, fs, n, sv, pdo} = C_{fs, ac, sv, pdo} \times N_{spf, fs, n, sv, pdo} \times \left(CMF_{1, fs, ac, sv, pdo} \times \dots \times CMF_{m, fs, ac, sv, pdo} \right) \times \left(CMF_{1, fs, ac, at, pdo} \times \dots \times CMF_{m, fs, ac, at, pdo} \right) \quad \text{Equation 18-6}$$

Where:

$N_{p, fs, n, y, z}$ = predicted average crash frequency of a freeway segment with *n* lanes, crash type *y* (*y* = *sv*: single vehicle, *mv*: multiple vehicle, *at*: all types), and severity *z* (*z* = *fi*: fatal and injury, *pdo*: property damage only, *as*: all severities) (crashes/yr);

$N_{spf, fs, n, y, z}$ = predicted average crash frequency of a freeway segment with base conditions, *n* lanes, crash type *y* (*y* = *sv*: single vehicle, *mv*: multiple vehicle, *at*: all types), and severity *z* (*z* = *fi*: fatal and injury, *pdo*: property damage only) (crashes/yr);

$CMF_{m, fs, ac, y, z}$ = crash modification factor for a freeway segment with any cross section *ac*, features *m*, crash type *y* (*y* = *sv*: single vehicle, *mv*: multiple vehicle, *at*: all types), and severity *z* (*z* = *fi*: fatal and injury, *pdo*: property damage only); and

$C_{fs, ac, y, z}$ = calibration factor for freeway segments with any cross section ac , crash type y ($y = sv$: single vehicle, mv : multiple vehicle, at : all types), and severity z ($z = fi$: fatal and injury, pdo : property damage only).

Equation 18-2 shows that freeway segment crash frequency is estimated as the sum of four components: fatal-and-injury multiple-vehicle crash frequency, fatal-and-injury single-vehicle crash frequency, property-damage-only multiple-vehicle crash frequency, and property-damage-only single-vehicle crash frequency.

Different CMFs are used in Equation 18-3 to Equation 18-6. The first term in parentheses in each equation recognizes that the influence of some geometric features is unique to each crash type. In contrast, the second term in parentheses in these equations recognizes that some geometric features have a similar influence on all crash types. All CMFs are unique to crash severity.

Equation 18-3 and Equation 18-4 are used to estimate the fatal-and-injury crash frequency. Equation 18-5 and Equation 18-6 are used to estimate the property-damage-only crash frequency.

The SPFs for freeway segments are presented in Section 18.6.1. The associated CMFs are presented in Section 18.7.1. Similarly, the associated SDFs are presented in Section 18.8. A procedure for establishing the value of the calibration factor is described in Section B.1 of Appendix B to Part C.

18.3.3. Predictive Model for Freeway Speed-Change Lanes

The predictive model for speed-change lanes is used to compute the predicted average crash frequency for a speed-change lane. Speed-change-related crashes include all crashes that are located between the gore point and the taper point of a speed-change lane and that involve vehicles (a) in the speed-change lane or (b) in the freeway lanes on the same side of the freeway as the speed-change lane.

The predictive model for ramp entrance speed-change lanes is presented in Equation 18-7 to Equation 18-9.

$$N_{p, sc, nEN, at, as} = N_{p, sc, nEN, at, fi} + N_{p, sc, nEN, at, pdo} \quad \text{Equation 18-7}$$

$$N_{p, sc, nEN, at, fi} = C_{sc, EN, at, fi} \times N_{spf, sc, nEN, at, fi} \times (CMF_{1, sc, nEN, at, fi} \times \dots \times CMF_{m, sc, nEN, at, fi}) \times (CMF_{1, sc, ac, at, fi} \times \dots \times CMF_{m, sc, ac, at, fi}) \quad \text{Equation 18-8}$$

$$N_{p, sc, nEN, at, pdo} = C_{sc, EN, at, pdo} \times N_{spf, sc, nEN, at, pdo} \times (CMF_{1, sc, nEN, at, pdo} \times \dots \times CMF_{m, sc, nEN, at, pdo}) \times (CMF_{1, sc, ac, at, pdo} \times \dots \times CMF_{m, sc, ac, at, pdo}) \quad \text{Equation 18-9}$$

Where:

$N_{p, sc, nEN, at, z}$ = predicted average crash frequency of ramp entrance speed-change lane on a freeway with n lanes, all crash types at , and severity z ($z = fi$: fatal and injury, pdo : property damage only, as : all severities) (crashes/yr);

$N_{spf, sc, nEN, at, z}$ = predicted average crash frequency of a ramp entrance speed-change lane on a freeway with base conditions, n lanes, all crash types at , and severity z ($z = fi$: fatal and injury, pdo : property damage only) (crashes/yr);

$CMF_{m, sc, x, at, z}$ = crash modification factor for a speed-change lane with features m , cross section x ($x = nEN$: ramp entrance adjacent to a freeway with n lanes, nEX : ramp exit adjacent to a freeway with n lanes, ac : any cross section), all crash types at , and severity z ($z = fi$: fatal and injury, pdo : property damage only); and

$C_{sc, EN, at, z}$ = calibration factor for a ramp entrance speed-change lane with all crash types at and severity z ($z = fi$: fatal and injury, pdo : property damage only).

The predictive model for ramp exit speed-change lanes is presented in Equation 18-10 and Equation 18-12.

$$N_{p, sc, nEX, at, as} = N_{p, sc, nEX, at, fi} + N_{p, sc, nEX, at, pdo} \quad \text{Equation 18-10}$$

$$N_{p, sc, nEX, at, fi} = C_{sc, EX, at, fi} \times N_{spf, sc, nEX, at, fi} \times \left(CMF_{1, sc, nEX, at, fi} \times \dots \times CMF_{m, sc, nEX, at, fi} \right) \times \left(CMF_{1, sc, ac, at, fi} \times \dots \times CMF_{m, sc, ac, at, fi} \right) \quad \text{Equation 18-11}$$

$$N_{p, sc, nEX, at, pdo} = C_{sc, EX, at, pdo} \times N_{spf, sc, nEX, at, pdo} \times \left(CMF_{1, sc, nEX, at, pdo} \times \dots \times CMF_{m, sc, nEX, at, pdo} \right) \times \left(CMF_{1, sc, ac, at, pdo} \times \dots \times CMF_{m, sc, ac, at, pdo} \right) \quad \text{Equation 18-12}$$

Where:

$N_{p, sc, nEX, at, z}$ = predicted average crash frequency of ramp exit speed-change lane on a freeway with n lanes, all crash types at , and severity z ($z = fi$: fatal and injury, pdo : property damage only, as : all severities) (crashes/yr);

$N_{spf, sc, nEX, at, z}$ = predicted average crash frequency of a ramp exit speed-change lane on a freeway with base conditions, n lanes, all crash types at , and severity z ($z = fi$: fatal and injury, pdo : property damage only) (crashes/yr); and

$C_{sc, EX, at, z}$ = calibration factor for a ramp exit speed-change lane with all crash types at and severity z ($z = fi$: fatal and injury, pdo : property damage only).

Equation 18-7 and Equation 18-10 show that speed-change lane crash frequency is estimated as the sum of two components: predicted average fatal-and-injury crash frequency and predicted average property-damage-only crash frequency.

Different CMFs are used in Equation 18-8, Equation 18-9, Equation 18-11, and Equation 18-12. The first term in parentheses in each equation recognizes that the influence of some geometric features is unique to each speed-change lane type. In contrast, the second term in parentheses in these equations recognizes that some geometric features have a similar influence on both speed-change lane types. All CMFs are unique to crash severity.

The SPFs for speed-change lanes are presented in Section 18.6.2. The associated CMFs are presented in Section 18.7.2. Similarly, the associated SDFs are presented in Section 18.8. A procedure for establishing the value of the calibration factor is described in Section B.1 of Appendix B to Part C.

18.4. PREDICTIVE METHOD FOR FREEWAYS

This section describes the predictive method for freeways. It consists of two sections. The first section provides a step-by-step description of the predictive method. The second section describes the geometric design features, traffic control features, and traffic volume data needed to apply the predictive method.

18.4.1. Step-by-Step Description of the Predictive Method

The predictive method for freeways is shown in Figure 18-1. Applying the predictive method yields an estimate of the expected average crash frequency (in total, or by crash type or severity) for a freeway facility or network. The predictive models described in this chapter are applied in Steps 9, 10, and 11 of the predictive method. The information needed to apply each step is provided in this section.

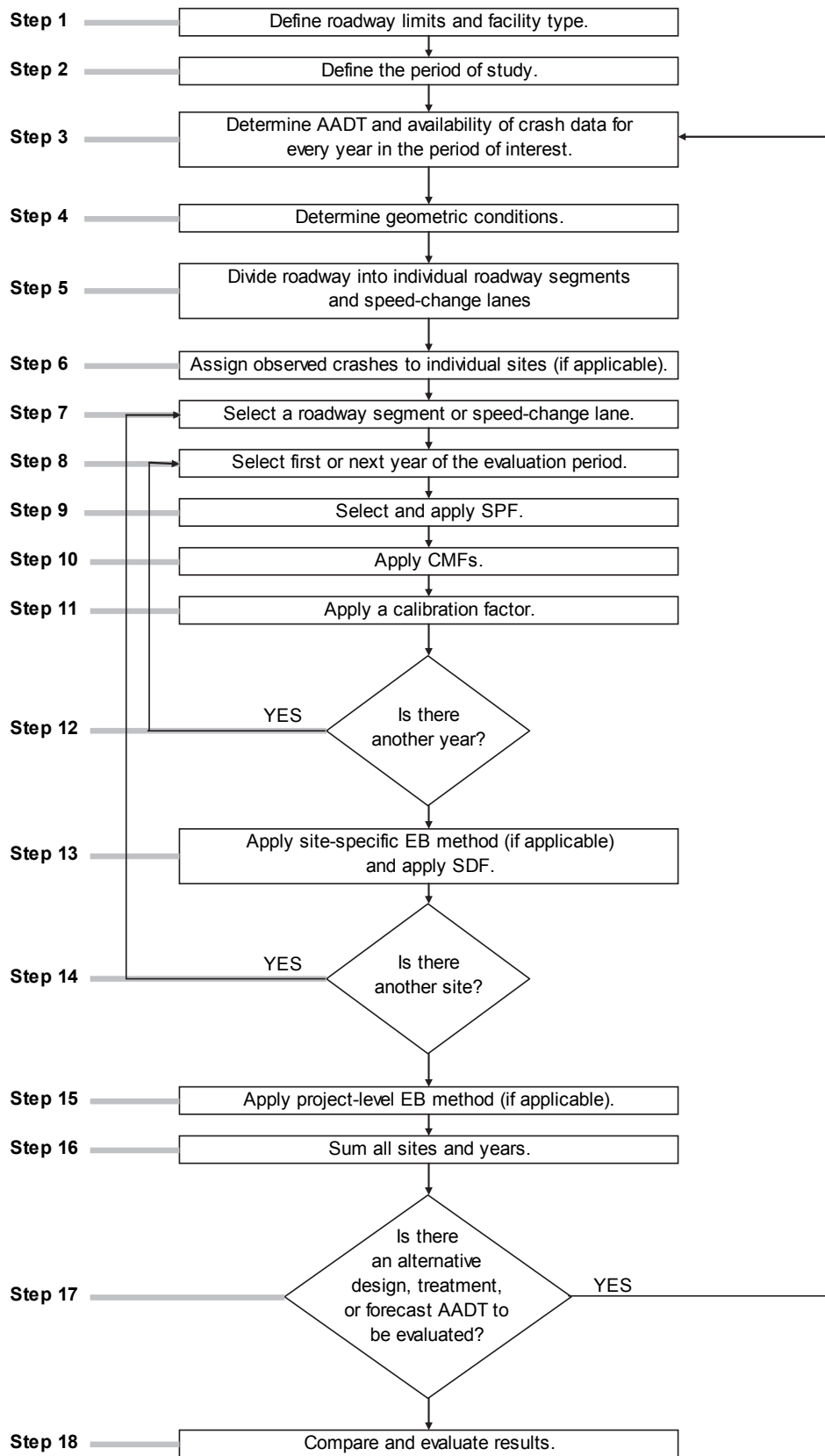


Figure 18-1. The HSM Predictive Method

There are 18 steps in the predictive method. In some situations, certain steps will not be needed because data are not available or the step is not applicable to the situation at hand. In other situations, steps may be repeated if an estimate is desired for several sites or for a period of several years. In addition, the predictive method can be repeated as necessary to undertake crash estimation for each alternative design, traffic volume scenario, or proposed treatment option (within the same time period to allow for comparison).

The following discussion explains the details of each step of the method, as applied to freeways.

Step 1—Define the limits of the project.

A project can be a freeway network, a freeway facility, or a site. A site is either a speed-change lane or a homogeneous freeway segment. A site is further categorized by its cross section. A description of the specific site types is provided in Section 18.3.

The project limits are defined in this step. They will depend on the purpose of the study. The study may be limited to one specific site or, to a group of contiguous sites. Alternatively, the limits can be expanded to include a very long corridor for the purposes of network screening (as discussed in Chapter 4). For comparative analysis of design alternatives, the project limits should be the same for all alternatives.

The analyst should identify (or establish) the reference line for the freeway. This line is defined as the inside edge of traveled way in the increasing milepost direction of travel. All lengths along the roadway are determined using this line.

Step 2—Define the period of interest.

The *study period* is defined as the consecutive years for which an estimate of the expected average crash frequency is desired. The *crash period* is defined as the consecutive years for which observed crash data are available. The *evaluation period* is defined as the combined set of years represented by the study period and crash period. Every year in the evaluation period is evaluated using the predictive method. All periods are measured in years.

If the EB Method is not used, then the study period is the same as the evaluation period. The EB Method is discussed in more detail in Step 3.

If the EB Method is used and the crash period is not fully included in the study period, then the predictive models need to be applied to the study years *plus* each year of the crash period not represented in the study period. In this situation, the evaluation period includes the study period and any additional years represented by the crash data but not in the study period. For example, let the study period be defined as the years 2010, 2011, and 2012. If crash data are available for 2008, 2009, and 2010, then the evaluation period is 2008, 2009, 2010, 2011, and 2012.

The study period can represent either a past time period or a future time period. Whether the predictive method is used for a past or future period depends upon the purpose of the study. The study period may be:

- A past period for:
 - An existing roadway network, facility, or site. If observed crash data are available, the study period is the period of time for which the observed crash data are available and for which (during that period) the site geometric design features, traffic control features, and traffic volumes are known.
 - An existing roadway network, facility, or site for which alternative geometric design or traffic control features are proposed (for near-term conditions) and site traffic volumes are known.
- A future period for:

- An existing roadway network, facility, or site for a future period where forecast traffic volumes are available.
- An existing roadway network, facility, or site for which alternative geometric design or traffic control features are proposed and forecast traffic volumes are available.
- A new freeway network, facility, or site that does not currently exist but is proposed for construction and for which forecast traffic volumes are available.

Step 3—For the study period, determine the availability of AADT volumes and, for an existing project, the availability of observed crash data (to determine whether the EB Method is applicable).

Traffic volume data are acquired in this step. Also, a decision is made whether the EB Method will be applied. If it will be applied, then it must also be decided whether the site-specific or project-level EB Method will be applied. If the EB Method will be applied, then the observed crash data are also acquired in this step.

Determining Traffic Volumes

The SPFs used in Step 9 (and some CMFs in Step 10) include annual average daily traffic (AADT) volume as a variable. For a past period, the AADT volume may be determined by using automated recorder data, or estimated from a sample survey. For a future period, the AADT volume may be a forecast estimate based on appropriate land use planning and traffic volume forecasting models.

For each freeway segment, five AADT values are required. They include the AADT volume of the freeway segment, AADT volume of the nearest entrance ramp upstream of (or in) the segment for both travel directions, and AADT volume of the nearest exit ramp downstream of (or in) the segment for both travel directions.

For each ramp entrance speed-change lane, two values are required. They include the AADT volume of the freeway segment and the AADT volume of the ramp.

For each ramp exit speed-change lane, only the AADT volume of the freeway segment is required. The AADT volume of the ramp is not needed.

The AADT volumes are needed for each year of the evaluation period. The AADT volume for a given year represents an annual average daily 24-hour traffic volume. The freeway segment AADT volume is a two-way volume (i.e., total of both travel directions). Each ramp AADT volume represents a one-way volume.

In many cases, it is expected that AADT data will not be available for all years of the evaluation period. In that case, an estimate of AADT volume for each year is interpolated or extrapolated, as appropriate. If there is not an established procedure for doing this, the following rules may be applied within the predictive method to estimate the AADT volumes for years in which no data are available.

- If AADT volume is available for only a single year, that same volume is assumed to apply to all years of the evaluation period.
- If two or more years of AADT data are available, the AADT volumes for intervening years are computed by interpolation.
- The AADT volumes for years before the first year for which data are available are assumed to be equal to the AADT volume for that first year.

- The AADT volumes for years after the last year for which data are available are assumed to be equal to the AADT volume for that last year.

Determining Availability of Observed Crash Data

Where an existing site (or alternative conditions for an existing site) is being considered, the EB Method can be used to obtain a more reliable estimate of the expected average crash frequency. The EB Method is applicable when crash data are available for the entire project, or for its individual sites. Crash data may be obtained directly from the jurisdiction's crash report system. At least two years of crash data are desirable to apply the EB Method. The EB Method (and criteria to determine whether the EB Method is applicable) is presented in Section B.2 in Appendix B to Part C.

The EB Method can be applied at the site-specific level or at the project level. At the site-specific level, crash data are assigned to specific sites in Step 6. The site-specific EB Method is applied in Step 13. At the project level, crash data are assigned to a group of sites (typically because they cannot be assigned to individual sites). The project-level EB Method is applied in Step 15. In general, the best results will be obtained if the site-specific EB Method is used. Guidance to determine whether the site-specific or project-level EB Method is applicable is presented in Section B.2.2 in Appendix B to Part C.

Step 4—Determine geometric design features, traffic control features, and site characteristics for all sites in the project limits.

A range of data is needed to apply a predictive model. These data are used in the SPFs and CMFs to estimate the predicted average crash frequency for the selected site and year. These data represent the geometric design features, traffic control features, and traffic demand characteristics that have been found to have some relationship to safety. These data are needed for each site in the project limits. They are needed for the study period and, if applicable, the crash period. The specific data, and means by which they are measured or obtained, is described in Section 18.4.2.

Step 5—Divide the roadway into sites.

Using the information from Step 1 and Step 4, the freeway is divided into individual sites, consisting of individual homogeneous freeway segments and speed-change lanes. The procedure for dividing the freeway into individual segments is provided in Section 18.5.

Step 6—Assign observed crashes to the individual sites (if applicable).

Step 6 applies if it was determined in Step 3 that the site-specific EB Method is applicable. If the site-specific EB Method is not applicable, then proceed to Step 7. In this step, the observed crash data are assigned to the individual sites using the criteria outlined in the next paragraph. Specific criteria for assigning crashes to individual sites are presented in Section B.2.3 in Appendix B to Part C.

Step 7—Select the first or next individual site in the project limits. If there are no more sites to be evaluated, proceed to Step 15.

Steps 7 through 14 are repeated for each site within the project limits identified in Step 1.

Any site can be selected for evaluation because each site is considered to be independent of the other sites. However, good practice is to select the sites in an orderly manner, such as in the order of their physical occurrence in the direction of increasing milepost.

Step 8—For the selected site, select the first or next year in the period of interest. If there are no more years to be evaluated for that site, proceed to Step 13.

Steps 8 through 12 are repeated for each year in the evaluation period for the selected site.

The individual years of the evaluation period are analyzed one year at a time because the SPFs and some CMFs are dependent on AADT volume, which may change from year to year.

Step 9—For the selected site, determine and apply the appropriate SPF.

The SPF determines the predicted average crash frequency for a site whose features match the SPF's base conditions. The SPFs (and their base conditions) are described in Section 18.6.

Determine the appropriate SPF for the selected site based on its site type and cross section (or traffic control). This SPF is then used to compute the crash frequency for the selected year using the AADT volume for that year, as determined in Step 3.

Step 10—Multiply the result obtained in Step 9 by the appropriate CMFs.

Collectively, the CMFs are used in the predictive model to adjust the SPF estimate from Step 9 such that the resulting predicted average crash frequency accurately reflects the geometric design and traffic control features of the selected site. The available CMFs are described in Section 18.7.

All CMFs presented in this chapter have the same base conditions as the SPFs in this chapter. Only the CMFs presented in Section 18.7 may be used as part of the predictive method described in this chapter.

For the selected site, determine the appropriate CMFs for the site type, geometric design features, and traffic control features present. The CMF's designation by crash type and severity must match that of the SPF with which it is used (unless indicated otherwise in the CMF description). The CMFs for the selected site are calculated using (a) the AADT volume determined in Step 3 for the selected year and (b) the geometric design and traffic control features determined in Step 4.

Multiply the result from Step 9 by the appropriate CMFs.

Step 11—Multiply the result obtained in Step 10 by the appropriate calibration factor.

The SPFs and CMFs in this chapter have each been developed with data from specific jurisdictions and time periods. Calibration to local conditions will account for any differences between these conditions and those present at the selected sites. A calibration factor is applied to each SPF in the predictive method. Detailed guidance for the development of calibration factors is included in Section B.1 of Appendix B to Part C.

Multiply the result from Step 10 by the calibration factor to obtain the predicted average crash frequency.

Step 12—If there is another year to be evaluated in the evaluation period for the selected site, return to Step 8. Otherwise, proceed to Step 13.

This step creates a loop from Step 8 through Step 12 that is repeated for each year of the evaluation period for the selected site.

Step 13—Apply site-specific EB Method (if applicable) and apply SDFs.

The site-specific EB Method combines the predicted average crash frequency computed in Step 11 with the observed crash frequency of the selected site. It produces a more statistically reliable estimate of the site's expected average crash frequency. The procedure for applying the site-specific EB Method is provided in Section B.2.4 of Appendix B to Part C.

The decision to apply the site-specific EB Method was determined in Step 3. If the EB Method is not used, then the expected average crash frequency for each year of the study period is limited to the predicted average crash frequency for that year, as computed in Step 11.

If the EB Method is used, then the expected average crash frequency is equal to the estimate obtained from the EB Method. An estimate is obtained for each year of the crash period (i.e., the period for which the observed crash data are available). The individual years of the crash period are analyzed one year at a time because the SPFs and some CMFs are dependent on AADT volume, which may change from year to year.

Apply the site-specific EB Method to a future time period, if appropriate.

Section B.2.6 in Appendix B to Part C provides a procedure for converting the estimates from the EB Method to any years in the study period that are not represented in the crash period (e.g., future years). This approach gives consideration to any differences in traffic volume, geometry, or traffic control between the study period and the crash period. This procedure yields the expected average crash frequency for each year of the study period.

Apply the severity distribution functions (SDFs), if desired.

The SDFs can be used to compute the expected average crash frequency for each of the following severity levels: fatal, incapacitating injury, non-incapacitating injury, and possible injury. Each SDF includes variables that describe the geometric design and traffic control features of a site. In this manner, the computed distribution gives consideration to the features present at the selected site. The SDFs are described in Section 18.8. They can benefit from being updated based on local data as part of the calibration process. Detailed guidance for the development of the SDF calibration factor is included in Section B.1.4 of Appendix B to Part C.

Apply the crash type distribution, if desired.

Each predictive model includes a default distribution of crash type. This distribution can be used to compute the expected average crash frequency for each of ten crash types (e.g., head-on, fixed object). The distribution is presented in Section 18.6. It can benefit from being updated based on local data as part of the calibration process.

Step 14—If there is another site to be evaluated, return to Step 7; otherwise, proceed to Step 15.

This step creates a loop from Step 7 through Step 14 that is repeated for each site of interest.

Step 15—Apply the project-level EB Method (if applicable) and apply SDFs.

The activities undertaken during this step are the same as undertaken for Step 13 but they occur at the project level (i.e., network or facility). They are based on estimating the project-level predicted average crash frequency. This crash frequency is computed for each year during the crash period. It is computed as the sum of the predicted average crash frequency for all sites (as computed in Step 11).

The project-level EB Method combines the project-level predicted average crash frequency with the observed crash frequency for all sites within the project limits. It produces a more statistically reliable estimate of the project-level expected average crash frequency. The procedure for applying the project-level EB Method is provided in Section B.2.5 of Appendix B to Part C.

The decision to apply the project-level EB Method was determined in Step 3. If this method is not used, then the project-level expected average crash frequency for each year of the study period is limited to the project-level predicted average crash frequency for that year, as computed in Step 11.

If the EB Method is used, then the project-level expected average crash frequency is equal to the estimate obtained from the EB Method. An estimate is obtained for each year of the crash period (i.e., the period for which the observed crash data are available). The individual years of the crash period are analyzed one year at a time because the SPFs and some CMFs are dependent on AADT volume, which may change from year to year.

Apply the project-level EB Method to a future time period, if appropriate.

Follow the same guidance as provided in Step 13 using the estimate from the project-level EB Method.

Apply the severity distribution functions, if desired.

Follow the same guidance as provided in Step 13 using the estimate from the project-level EB Method.

Apply the crash type distribution, if desired.

Follow the same guidance as provided in Step 13 using the estimate from the project-level EB Method.

Step 16—Sum all sites and years in the study to estimate the total crash frequency.

One outcome of the predictive method is the total expected average crash frequency. The term “total” indicates that the estimate includes all crash types and severities. It is computed from an estimate of the total expected number of crashes, which represents the sum of the total expected average crash frequency for each site and for each year in the study period. The total expected number of crashes during the study period is calculated using Equation 18-13:

$$N_{e, aS, ac, at, as}^* = \sum_{j=1}^{n_s} \left(\sum_{i=1}^{all\ sites} N_{e, fs(i), n, at, as, j} + \sum_{i=1}^{all\ sites} N_{e, sc(i), nEN, at, as, j} + \sum_{i=1}^{all\ sites} N_{e, sc(i), nEX, at, as, j} \right) \quad \text{Equation 18-13}$$

Where:

$N_{e, aS, ac, at, as}^*$ = total expected number of crashes for all sites aS and all years in the study period (includes all cross sections ac , all crash types at , and all severities as) (crashes);

$N_{e, fs(i), n, at, as, j}$ = expected average crash frequency of freeway segment i with n lanes for year j (includes all crash types at and all severities as) (crashes/yr);

$N_{e, sc(i), nEN, at, as, j}$ = expected average crash frequency of ramp entrance speed-change lane i on a freeway with n lanes for year j (includes all crash types at and all severities as) (crashes/yr);

$N_{e, sc(i), nEX, at, as, j}$ = expected average crash frequency of ramp exit speed-change lane i on a freeway with n lanes for year j (includes all crash types at and all severities as) (crashes/yr); and

n_s = number of years in the study period (yr).

Equation 18-13 is used to compute the total expected number of crashes estimated to occur in the project limits during the study period. The summation of crashes by type and severity for each site and year is not shown in mathematic terms (but it is implied by the subscripts at and as).

Equation 18-14 is used to estimate the overall expected average crash frequency within the project limits during the study period.

$$N_{e, aS, ac, at, as} = \frac{N_{e, aS, ac, at, as}^*}{n_s} \quad \text{Equation 18-14}$$

Where:

$N_{e, aS, ac, at, as}$ = overall expected average crash frequency for all sites aS and all years in the study period (includes all cross sections ac , all crash types at , and all severities as) (crashes/yr).

Step 17—Determine if there is an alternative design, treatment, or forecast AADT to be evaluated.

Steps 3 through 17 are repeated as appropriate for the same project limits but for alternative conditions, treatments, periods of interest, or forecast AADT volumes.

Step 18—Evaluate and compare results.

The predictive method is used to provide a statistically reliable estimate of the expected average crash frequency (in total, or by crash type and severity) for the specified project limits, study period, geometric design and traffic control features, and known or estimated AADT volume.

18.4.2. Data Needed to Apply the Predictive Method

The input data needed for the predictive models are identified in this section. These data represent the geometric design features, traffic control features, and traffic demand characteristics that have been found to have some relationship to safety. The data are needed for each site in the project limits. Criteria for defining site boundaries are described in Section 18.5.

There are several data identified in this section that describe a length along the roadway (e.g., segment length, curve length, weaving section length, etc.). *All of these lengths are measured along the reference line*, which is the inside edge of traveled way in the increasing milepost direction of travel. Points that do not lie on the reference line must be projected onto the reference line (along a perpendicular line if the alignment is straight, or along a radial line if the alignment is curved) to facilitate length determination.

- Number of through lanes. For a freeway segment, use the total number of through lanes (in both directions of travel). For a speed-change lane, use the number of through lanes in the portion of freeway adjacent to the speed-change lane *plus* those freeway lanes in the opposing travel direction. Rural freeways are limited to eight lanes. Urban freeways are limited to ten lanes. A segment with a lane-add (or lane-drop) taper is considered to have the same number of through lanes as the roadway just downstream of the lane-add (or lane-drop) taper. This guidance is shown in Figure 18-2.
- Do not include any high-occupancy vehicle (HOV) lanes or managed lanes.
- Do not include any auxiliary lanes that are associated with a weaving section, unless the weaving section length exceeds 0.85 mi (4,500 ft). If this length is exceeded, then the auxiliary lane is counted as a through lane that starts as a lane-add ramp entrance and ends as a lane-drop ramp exit.
- Do not include the speed-change lane that is associated with a ramp that merges with (or diverges from) the freeway, unless its length exceeds 0.30 mi (1,600 ft). If this length is exceeded, then the speed-change lane is counted as a through lane that starts as a lane-add ramp entrance and ends as a lane drop by taper (or starts as a lane add by taper and ends as a lane-drop ramp exit).

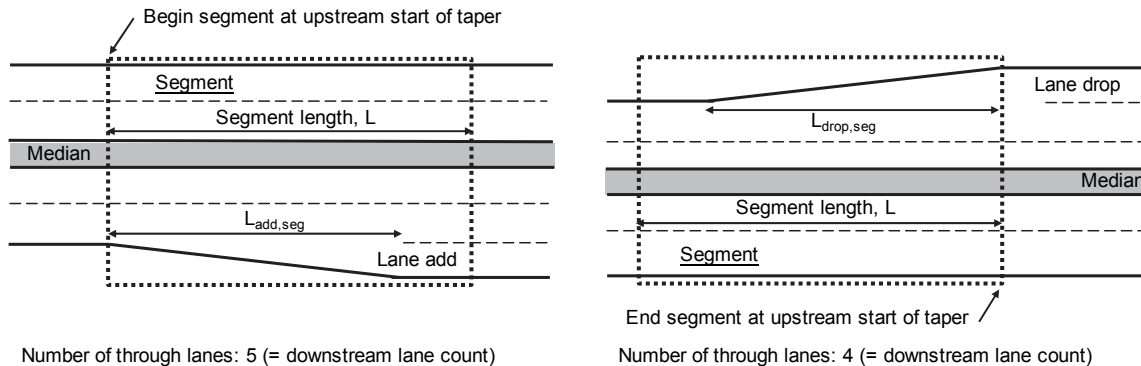


Figure 18-2. Through Lane Count in Segments with Lane Add or Lane Drop

- Length of freeway segment, and length of speed-change lane (if present). Speed-change lane length is measured from the gore point to the taper point. Figure 18-3 illustrates these measurement points for a ramp entrance and a ramp exit speed-change lane with the parallel and taper design, respectively.

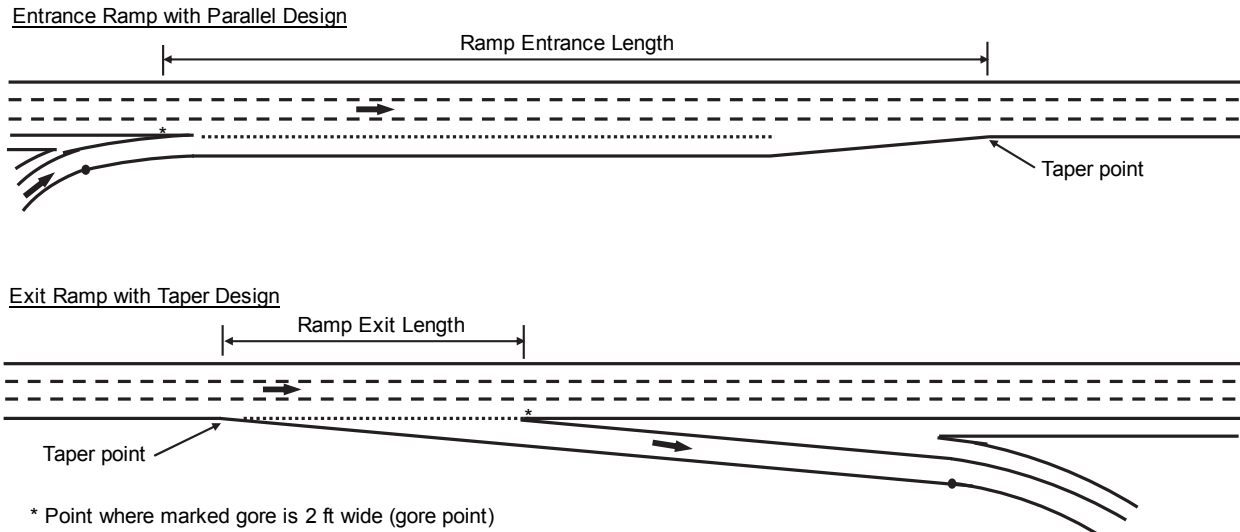
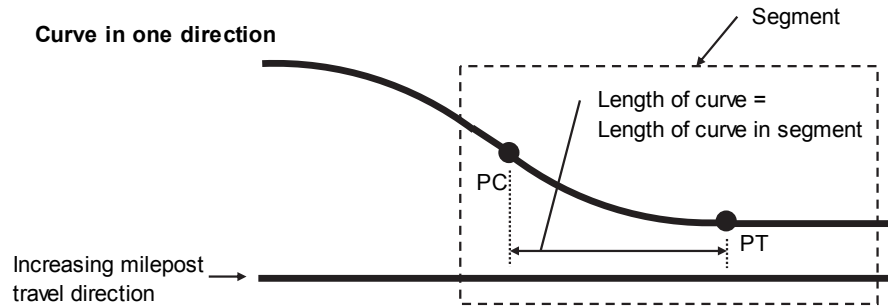


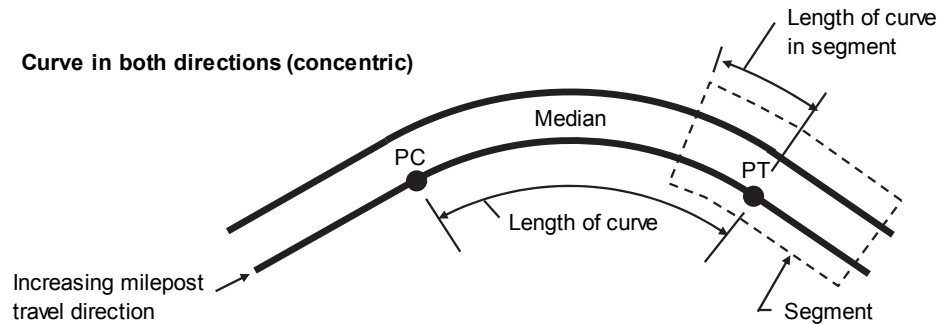
Figure 18-3. Freeway Speed-Change Lane Length

- Presence of a horizontal curve on one or both roadbeds. If a curve is present, then the three data elements in the following list are needed. Guidelines for obtaining these data are provided in Figure 18-4.
 - Length of curve.
 - Curve length is measured along the reference line from the point where the tangent ends and the curve begins (i.e., the PC) to the point where the curve ends and the tangent begins (PT). If the curve PC and PT do not lie on the reference line, then they must be projected onto this line and the curve length measured between these projected points along the reference line.
 - If the curve has spiral transitions, then measure from the “effective” PC point to the “effective” PT point. The effective PC point is located midway between the TS and SC mileposts, where the TS is the point of change from tangent to spiral and the SC is the point of change from spiral to circular curve. The effective PT is located midway between the CS and ST.
 - Radius of curve. If the curve has spiral transitions, then use the radius of the central circular portion of the curve. The line used to define curve radius is dependent on whether one or both roadbeds have curves, as follows:
 - One Direction. Radius is defined by the inside edge of the traveled way of the roadbed associated with the curve.
 - Both Directions. Measure radius for each curve. For a given curve, radius is defined by the inside edge of the traveled way of the roadbed associated with the curve.
 - Length of curve in segment. The length of the curve within the boundaries of the segment (or speed-change lane). This length cannot exceed the segment length or the curve length.



Rules

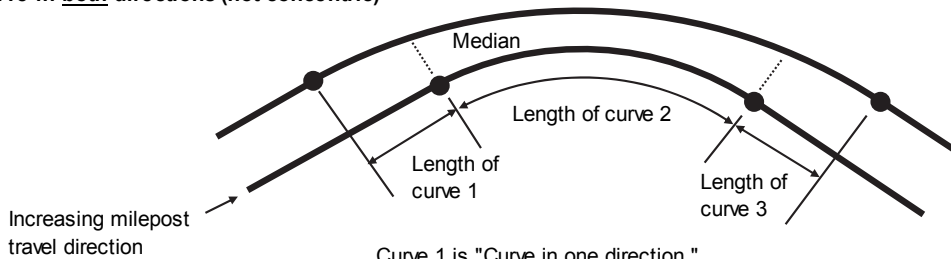
1. Roadbed in increasing milepost travel direction is basis of curve length measurement.
 2. Curve length is measured along the inside edge of traveled way.
 3. Radius is measured for curved roadbed.
 4. Radius is measured to inside edge of traveled way.
- Note: curve is shown to be fully in segment, but could also be only partially in segment.



Rules

1. Roadbed in increasing milepost travel direction is basis of curve length measurement.
 2. Curve length is measured along the inside edge of traveled way.
 3. Radius is measured for both roadbeds.
 4. Radius is measured to inside edge of traveled way.
- Note: curve is shown to be only partially in segment, but could also be fully in segment.

Curve in both directions (not concentric)



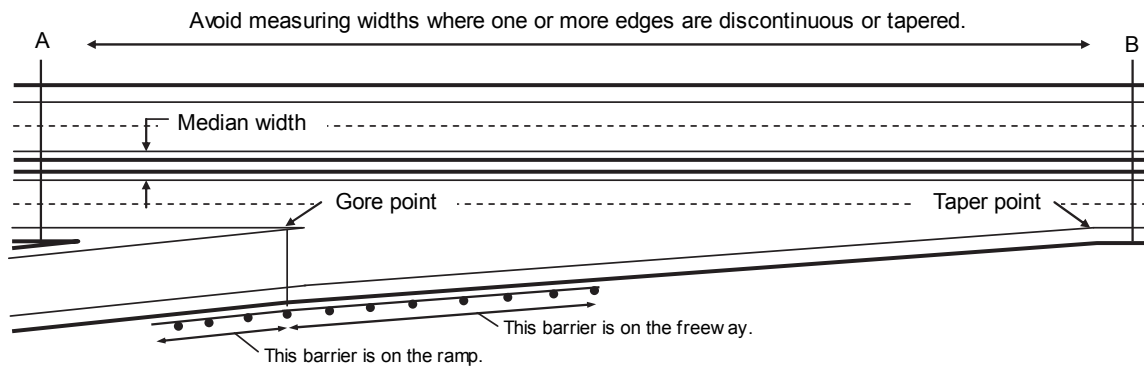
Curve 1 is "Curve in one direction."
 Curve 2 is "Curve in both directions."
 Curve 3 is "Curve in one direction."

Rules

1. Disaggregate into multiple curved pieces, where one or both roadbeds are curved in each piece.
 2. If one roadbed is curved, use rules for "Curve in one direction."
 3. If both roadbeds are curved, use rules for "Curve in both directions (concentric)."
- Note: roadbeds are shown to curve in same direction; however, these rules also apply when curves are in the opposite direction.

Figure 18-4. Curve Length and Radius Measurements

- Widths of lanes, outside shoulders, inside shoulders, and median. The first three elements represent an average for both roadbeds. These widths should be measured where the cross section is constant, such as along line A or B shown in Figure 18-5. They should not be measured where one or more edges are discontinuous or tapered. If a width varies along the segment or speed-change lane (but not enough to justify beginning a new segment), then compute the length-weighted average width. Rules for defining segment boundaries are provided in Section 18.5.2.
- Lane width is an average for all through lanes.
- Shoulder width represents the paved width.
- Median width is measured between the edges of the traveled way for the two roadways in the opposite direction of travel, including the width of the inside shoulders, if they are present.



Measure lane, shoulder, and median widths in areas with constant cross section. Measure along a line such as line A or line B. If necessary, move the line off the subject segment to the nearest point with constant cross section.

Figure 18-5. Measurement of Cross Section Data Elements

- Length of rumble strips on the inside (or median) shoulder and on the outside (or roadside) shoulder. Measured separately for each shoulder type and travel direction.
- Length of (and offset to) the barrier in the median and the barrier on the roadside. Measured for each short piece of barrier. Offset is also measured for barrier that continues for the length of the segment or speed-change lane (and beyond). Each piece is represented once for a site. Barrier length is measured along the reference line. Offset is measured to the near edge of traveled way.
- Figure 18-6 illustrates these measurements for two barrier elements protecting a sign support in a median with width W_m and adjacent to shoulders with width W_{is} . Each barrier element has a portion of its length that is parallel to the roadway and a portion of its length that is tapered from the roadway. One way to evaluate these elements is to separate them into four pieces, as shown in Figure 18-6. Each piece is represented by its average offset $W_{off, in, i}$ and length $L_{ib, i}$. Alternatively, the analyst may recognize that the offset is the same for pieces 1 and 4 and for pieces 2 and 3. In this case, each pair can be combined by adding the two lengths (e.g., $L_{ib, 1} + L_{ib, 4}$) and using the common offset.
- A barrier is associated with the freeway if the offset from the near edge of traveled way is 30 ft or less. Barrier adjacent to a ramp but also within 30 ft of the freeway traveled way should also be associated with the freeway. The determination of whether a barrier is adjacent to a speed-change lane or a ramp is based on the gore and taper points, as shown in Figure 18-5.

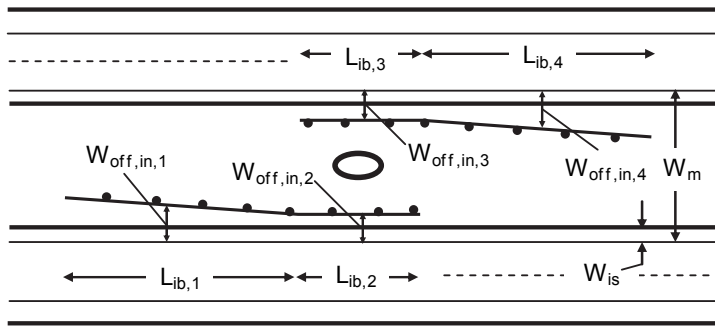


Figure 18-6. Barrier Variables

- Width of continuous median barrier, if present.
- Presence and length of a Type B weaving section.
 - A Type B weaving section has the following characteristics: (a) one of the two weaving movements can be made without making any lane changes, (b) the other weaving movement requires at most one lane change, and (c) both the ramp entrance and ramp exit associated with the weaving section are located on the right side of the freeway. Typical Type B weaving sections are shown in Figure 18-7.
 - Weaving section length. This length is measured along the edge of the freeway traveled way from the gore point of the ramp entrance to the gore point of the next ramp exit, as shown in Figure 18-7. The gore point is located where the pair of solid white pavement edge markings that separate the ramp from the freeway main lanes are 2.0 ft apart. If the markings do not extend to a point where they are 2.0 ft apart, then the gore point is found by extrapolating both markings until the extrapolated portion is 2.0 ft apart. If the measured gore-to-gore distance exceeds 0.85 mi (4,500 ft), then a weaving section is not considered to exist. Rather, the entrance ramp is a “lane add” and the exit ramp is a “lane drop.”

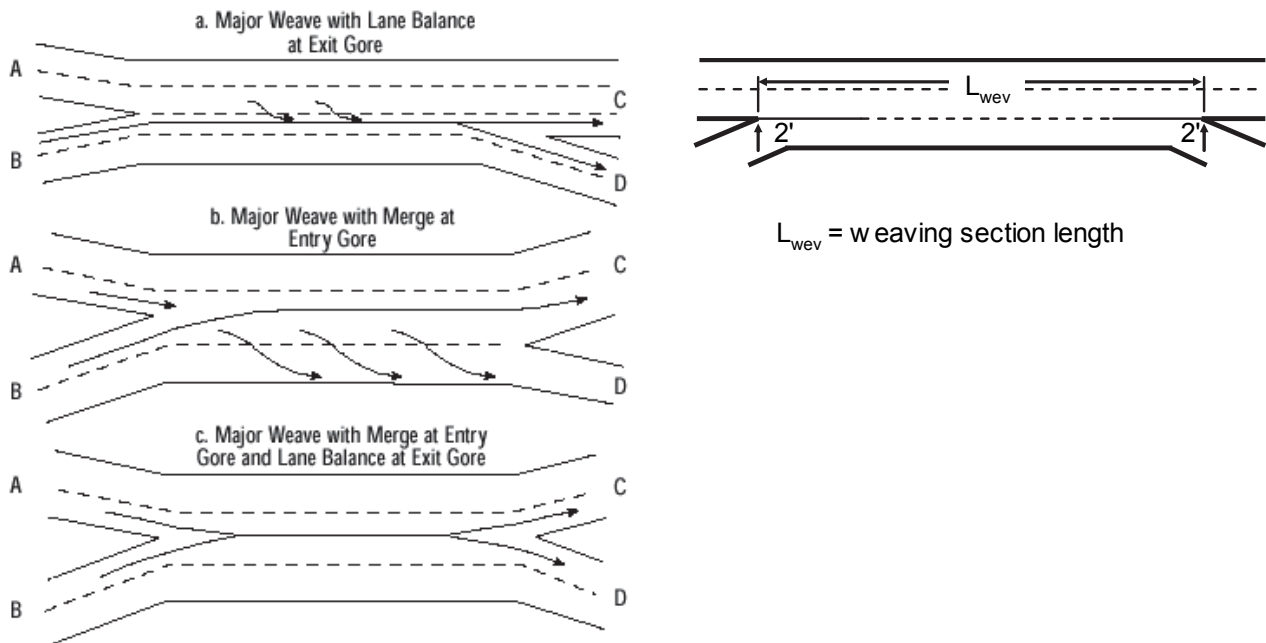
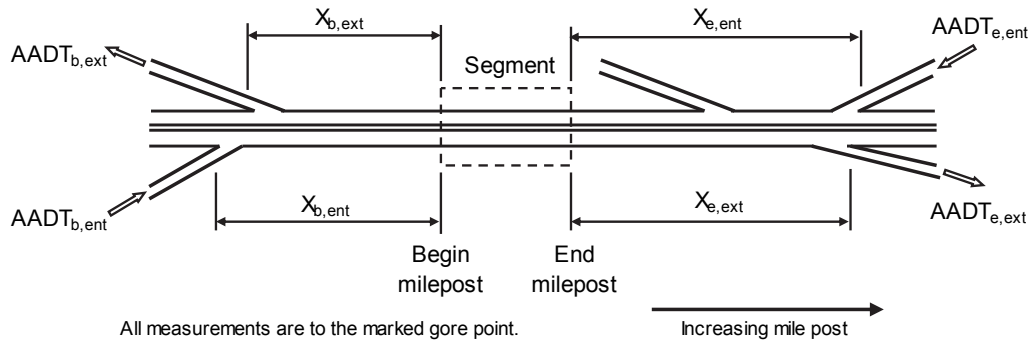
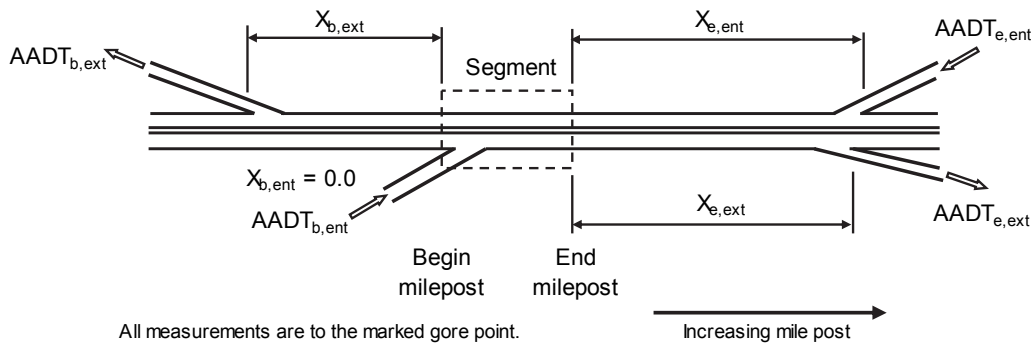


Figure 18-7. Type B Weaving Section and Length

- Distance to nearest upstream entrance ramp in each travel direction.
 - Measure this distance from the segment boundary to the ramp gore point, along the freeway’s solid white pavement edge marking that intersects the gore point. The distance to the nearest upstream entrance ramp in each travel direction is shown in Figure 18-8 using the two variables $X_{b, ent}$ and $X_{e, ent}$. If the ramp entrance is located in the segment, then the corresponding distance is equal to 0.0 mi. If the ramp does not exist or is located more than 0.5 mi from the segment, then this distance can be set to a large value (i.e., 999) in the predictive method to obtain the correct results.
 - The gore point is located where the pair of solid white pavement edge markings that separate the ramp from the freeway main lanes are 2.0 ft apart. If the markings do not extend to a point where they are 2.0 ft apart, then the gore point is found by extrapolating both markings until the extrapolated portion is 2.0 ft apart.
 - Upstream *exit* ramps are not of direct interest, and data are not needed for them if they exist in the vicinity of the segment. Figure 18-8a shows an upstream exit ramp serving travel in the decreasing milepost direction. This ramp is not of interest to the evaluation of the subject segment.
- Distance to nearest downstream exit ramp in each travel direction. The measurement technique is the same as for upstream entrance ramps. This distance is shown in Figure 18-8 using the two variables $X_{b, ext}$ and $X_{e, ext}$. Downstream *entrance* ramps are not of direct interest, and their data are not needed.



a. All Ramps External to the Segment



b. Three Ramps External to the Segment and One Ramp in the Segment

Figure 18-8. Distance to Nearest Ramp

- Clear zone width. This width is measured from the edge of traveled way to typical limits of vertical obstruction (e.g., ditch, fence line, utility poles) along the roadway. It includes the width of the outside shoulder. It is measured for both travel directions. If this width varies along the segment, then use the estimated length-weighted average clear zone width (excluding the portion of the segment with barrier). Do not consider roadside barrier when determining the clear zone width for the predictive method. Barrier location and influence is addressed in other CMFs. If the segment has roadside barrier on both sides for its entire length, then the clear zone width will not influence the model prediction and any value can be used as a model input (e.g., 30 ft).

This guidance is illustrated in Figure 18-9 where the clear zone is shown to be established by a fence line that varies in offset from the edge of traveled way. A length-weighted width is appropriate for this situation. The lone tree and the guardrail are not considered in the determination of clear zone width.

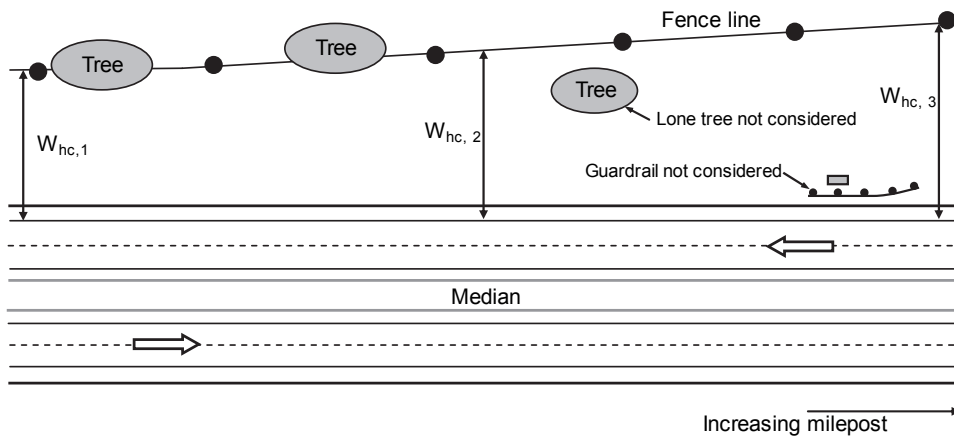


Figure 18-9. Clear Zone Width Considerations

- Proportion of freeway AADT volume that occurs during hours where the lane volume exceeds 1,000 vehicles per hour per lane (veh/h/ln). The lane volume for hour i LV_i is computed as $LV_i = HV_i/n$ where HV_i is the volume during hour i ($i = 1, 2, 3, \dots, 24$) and n is the number of through lanes. The desired proportion P_{hv} is computed as $P_{hv} = (\sum HV_i^*)/AADT$ where $\sum HV_i^*$ is the sum of the volume during each hour where the lane volume exceeds 1,000 veh/h/ln. The $AADT$, HV , and n variables include both freeway travel directions. These data will typically be obtained from the continuous traffic counting station that (1) is nearest to the subject freeway and (2) has similar traffic demand and peaking characteristics. A default value can be computed as $P_{hv} = 1.0 - \exp(1.45 - 0.000124 \times AADT/n)$. If the value computed is less than 0.0, then it is set to 0.0.
- Freeway AADT volume, upstream entrance ramp AADT volume, downstream exit ramp AADT volume.

18.5. ROADWAY SEGMENTS AND SPEED-CHANGE LANES

This section consists of three subsections. The first subsection defines freeway segments and speed-change lanes. The second subsection provides guidelines for segmenting the freeway facility. The assignment of crashes to sites is discussed in the last subsection.

18.5.1. Definition of Freeway Segment and Speed-Change Lane

When using the predictive method, the freeway within the defined project limits is divided into individual sites. A site is either a homogeneous freeway segment or a speed-change lane. A facility consists of a contiguous set of individual sites. A roadway network consists of a number of contiguous facilities.

A speed-change lane site is defined as the section of roadway area located (a) between the marked gore and taper points of a ramp merge or diverge area, and (b) on the same side of the freeway as the merge or diverge area. The location of the gore and taper points is identified in Figure 18-3.

Three freeway segments are shown schematically in Figure 18-10. They are labeled *Fr* in the figure. The presence of a speed-change lane adjacent to a freeway segment requires a reduction in the effective length of the freeway segment. This reduction is used to account for the crashes assigned to the speed-change lane. The equation for computing the “effective” segment length is shown in the bottom of Figure 18-10 for a freeway segment with one ramp entrance and one ramp exit.

Two speed-change lanes are shown schematically in Figure 18-10. The speed-change lane associated with an entrance ramp is labeled *SCen* and that associated with an exit ramp exit is labeled *SCex*.

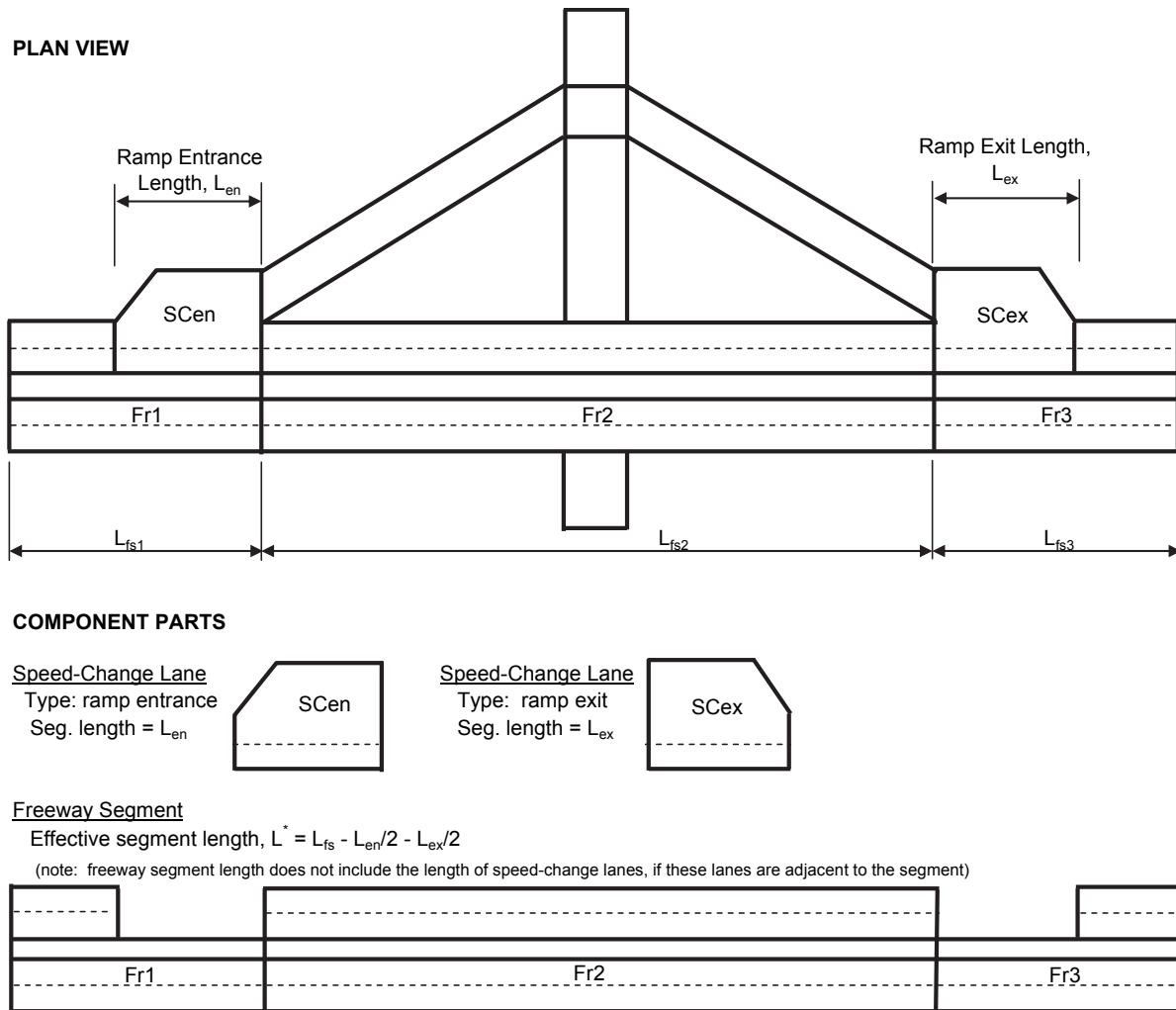


Figure 18-10. Illustrative Freeway Segments and Speed-Change Lanes

18.5.2 Segmentation Process

A speed-change lane site begins at the gore (or taper) point and ends at the associated taper (or gore) point. These points are shown in Figure 18-3.

The segmentation process produces a set of segments of varying length, each of which is homogeneous with respect to characteristics such as traffic volumes, key geometric design features, and traffic control features. A new homogeneous freeway segment begins where there is a change in at least one of the following characteristics of the freeway:

- Number of through lanes. Begin segment at the gore point if the lane is added or dropped at a ramp or C-D road. Begin segment at the upstream start of taper if the lane is added or dropped by taper. This guidance is shown in Figure 18-2.
- Lane width. Measure the lane width at successive points along the roadway. Compute an average lane width for each point and round this average to the nearest 0.5 ft. Begin a new segment if the rounded value for the current point changes from that of the previous point (e.g., from 11.5 to 12.0 ft).
- Outside shoulder width. Measure the outside shoulder width at successive points along the roadway. Compute an average shoulder width for each point and round this average to the nearest 1.0 ft. Begin a new segment if the rounded value for the current point changes from that of the previous point (e.g., from 6 to 7 ft).
- Inside shoulder width. Measure the inside shoulder width at successive points along the roadway. Compute an average shoulder width for each point and round this average to the nearest 1.0 ft. Begin a new segment if the rounded value for the current point changes from that of the previous point (e.g., from 6 to 5 ft).
- Median width. Measure the median width at successive points along the roadway. Round the measured median width at each point to the nearest 10 ft. If the rounded value exceeds 90 ft, then set it to 90 ft. Begin a new segment if the rounded value for the current point changes from that of the previous point (e.g., from 30 to 20 ft).
- Ramp presence. Begin segment at the ramp gore point.
- Clear zone width. Measure the clear zone width at successive points along the roadway. Compute an average clear zone width for each point and round this average to the nearest 5 ft. Begin a new segment if the rounded value for the current point changes from that of the previous point (e.g., from 25 to 30 ft).

The presence of a horizontal curve does not necessarily define segment boundaries.

Application of the “median width” segmentation criterion is shown in Figure 18-11. The freeway section in this figure is shown to consist of five segments. Segment 1 has a rounded median width of 70 ft. Segment 2 starts where the rounded median width first changes to 80 ft. Segment 3 begins at the point where the rounded median width first changes to 90 ft. Segment 4 begins where the rounded median width first changes to 80 ft. Segment 5 begins where the rounded median width first changes to 70 ft.

Guidance regarding the location of the lane, shoulder, median, and clear zone width measurement points is provided in Figure 18-5. The rounded lane, shoulder, median, and clear zone width values are used solely to determine segment boundaries. Once these boundaries are determined, the guidance in the text associated with Figure 18-5 is used to determine the average lane, shoulder, median, and clear zone width for the segment. The unrounded average for the segment is then used for all subsequent calculations in the predictive method.

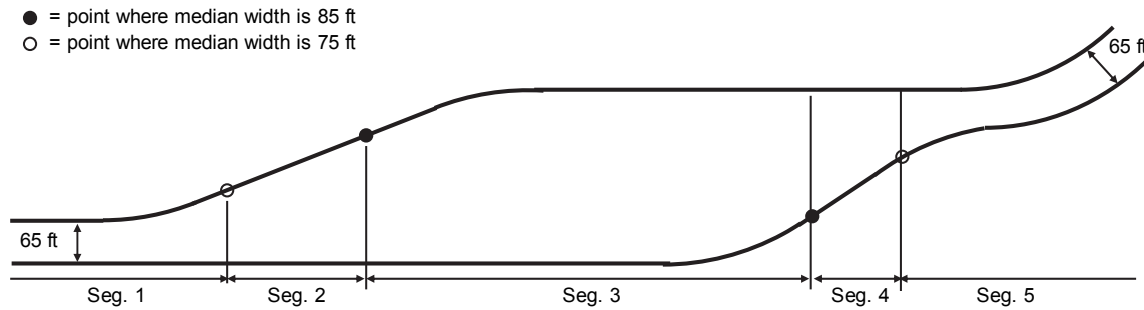


Figure 18-11. Segmentation for Varying Median Width

18.5.3. Crash Assignment to Sites

Observed crash counts are assigned to the individual sites to apply the site-specific EB Method. Any crashes that occur on the freeway are classified as speed-change-lane-related or segment-related crashes. The speed-change-lane-related crashes are assigned to the corresponding speed-change lane. The speed-change lane predictive model estimates the frequency of these crashes. The segment-related crashes are assigned to the corresponding freeway segment. The freeway segment predictive model estimates the frequency of these crashes. The procedure for assignment of crashes to individual sites is presented in Section B.2.3 in Appendix B to Part C.

18.6. SAFETY PERFORMANCE FUNCTIONS

When using the predictive method, the appropriate safety performance functions (SPFs) are used to estimate the predicted average crash frequency of a site with base conditions. Each SPF was developed as a regression model using observed crash data for a set of similar sites as the dependent variable. The SPFs, like all regression models, estimate the value of the dependent variable as a function of a set of independent variables. The independent variables for the freeway segment SPFs include the segment AADT volume, segment length, and area type (i.e., rural or urban). The independent variables for the speed-change lane SPFs include the AADT volume of the freeway, speed-change lane length, and area type. The SPFs in this chapter are summarized in Table 18-3.

Table 18-3. Freeway Safety Performance Functions

Site Type (w)	Cross Section (x)	Crash Type (y)	SPF Equations
Freeway segments (fs)	n lanes (n)	Multiple vehicle (mv)	Equation 18-15
		Single vehicle (sv)	Equation 18-18
Speed-change lanes (sc)	Ramp entrance, n lanes (nEN)	All types (at)	Equation 18-20
	Ramp exit, n lanes (nEX)	All types (at)	Equation 18-22

A detailed discussion of SPFs and their use in the HSM is presented in Section 3.5.2 of Chapter 3, and in Section C.6.3 of Part C.

Some highway agencies may have performed statistically-sound studies to develop their own jurisdiction-specific SPFs. These SPFs may be substituted for the SPFs presented in this chapter. Criteria for the development of SPFs for use in the predictive method are addressed in the calibration procedure presented in Section B.1.2 in Appendix B to Part C.

Each SPF has an associated overdispersion parameter k . The overdispersion parameter provides an indication of the statistical reliability of the SPF. The closer the overdispersion parameter is to zero, the more statistically reliable the SPF. This parameter is used in the EB Method that is discussed in Section B.2 in Appendix B to Part C.

18.6.1. Safety Performance Functions for Roadway Segments

The SPFs for freeway segments are presented in this section. Specifically, SPFs are provided for freeway segments with 4, 6, 8, or 10 through lanes (total of both travel directions). The range of AADT volume for which these SPFs are applicable is shown in Table 18-4. Application of the SPFs to sites with AADT volumes substantially outside these ranges may not provide reliable results.

Table 18-4. Applicable AADT Volume Ranges for SPFs

Area Type	Cross Section (Through Lanes) (x)	Applicable AADT Volume Range (veh/day)
Rural	4	0 to 73,000
	6	0 to 130,000
	8	0 to 190,000
Urban	4	0 to 110,000
	6	0 to 180,000
	8	0 to 270,000
	10	0 to 310,000

The SPFs described in this section are directly applicable to segments with an even number of through lanes. They can be extended to the evaluation of segments with 5, 7, or 9 lanes using the following procedure. If a freeway segment has X total lanes that represent Y lanes in one direction and Z lanes in the opposite direction (i.e., $X = Y + Z$) and Y is not equal to Z , then it is recommended that the segment be evaluated twice. One evaluation would be conducted where the number of lanes is equal to $2 \times Y$ and one evaluation would be conducted where the number of lanes is equal to $2 \times Z$. All other inputs to the SPFs would be unchanged between evaluations. The two estimates of predicted average crash frequency obtained in this manner are then averaged to obtain the best estimate of the predicted average crash frequency for the subject segment.

Other types of freeway segments may be found on freeways but are not addressed by the predictive model described in this chapter.

Multiple-Vehicle Crashes

The base conditions for the SPFs for multiple-vehicle crashes on freeway segments are:

- Horizontal curve Not present
- Lane width 12 ft
- Inside shoulder width 6 ft
- Median width 60 ft
- Median barrier Not present

- | | |
|--|-------------------------------|
| ■ Hours where volume exceeds 1000 vehicles per hour per lane | None |
| ■ Upstream ramp entrances and downstream ramp exits | More than 0.5 mi from segment |
| ■ Type B weaving section | Not present |

The SPFs for multiple-vehicle crashes on freeway segments are represented using the following equation.

$$N_{spf, fs, n, mv, z} = L^* \times \exp(a + b \times \ln[c \times AADT_{fs}]) \quad \text{Equation 18-15}$$

with,

$$L^* = L_{fs} - \left(0.5 \times \sum_{i=1}^2 L_{en, seg, i} \right) - \left(0.5 \times \sum_{i=1}^2 L_{ex, seg, i} \right) \quad \text{Equation 18-16}$$

Where:

$N_{spf, fs, n, mv, z}$ = predicted average multiple-vehicle crash frequency of a freeway segment with base conditions, n lanes, and severity z ($z = \hat{f}i$: fatal and injury, pdo : property damage only) (crashes/yr);

L^* = effective length of freeway segment (mi);

L_{fs} = length of freeway segment (mi);

$L_{en, seg, i}$ = length of ramp entrance i adjacent to subject freeway segment (mi);

$L_{ex, seg, i}$ = length of ramp exit i adjacent to subject freeway segment (mi);

$AADT_{fs}$ = AADT volume of freeway segment (veh/day); and

a, b, c = regression coefficients.

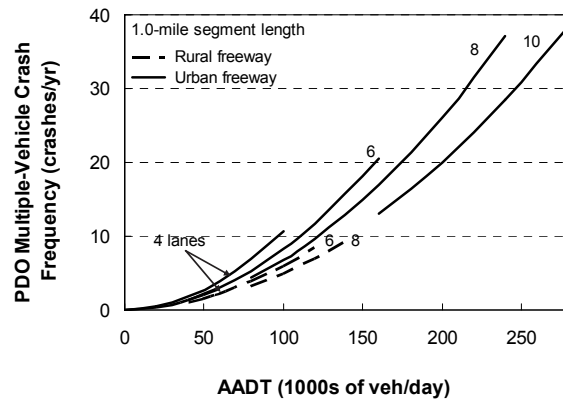
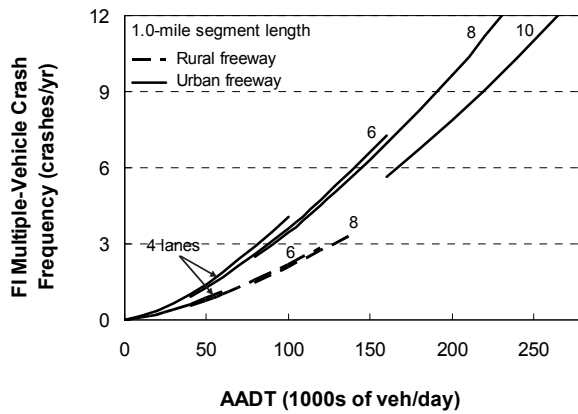
The calculation of the “effective length of freeway segment” was discussed in the text associated with Figure 18-10. The variable $L_{en, seg, i}$ represents the length of the speed-change lane located between the start and end points of the adjacent freeway segment. This length cannot exceed the length of the segment or the length of the ramp entrance speed-change lane. Similarly, the variable $L_{ex, seg, i}$ represents the length of the speed-change lane located between the start and end points of the adjacent freeway segment.

The summation terms in Equation 18-16 recognize the potential for there to be as many as two ramp entrances (and two ramp exits) adjacent to a freeway segment. If there are two ramp entrances, then they will be serving opposing directions of travel. If there are two ramp exits, then they will be serving opposing directions of travel.

The SPF regression coefficients and the inverse dispersion parameter are provided in Table 18-5. The SPFs are illustrated in Figure 18-12.

Table 18-5. SPF Coefficients for Multiple-Vehicle Crashes on Freeway Segments

Crash Severity (<i>z</i>)	Area Type	Number of Through Lanes (<i>n</i>)	SPF Coefficient			Inverse Dispersion Parameter $K_{fs, n, mv, z}$ (mi^{-1})
			<i>a</i>	<i>b</i>	<i>c</i>	
Fatal and injury (<i>fi</i>)	Rural	4	-5.975	1.492	0.001	17.6
		6	-6.092	1.492	0.001	17.6
		8	-6.140	1.492	0.001	17.6
	Urban	4	-5.470	1.492	0.001	17.6
		6	-5.587	1.492	0.001	17.6
		8	-5.635	1.492	0.001	17.6
		10	-5.842	1.492	0.001	17.6
Property damage only (<i>pdo</i>)	Rural	4	-6.880	1.936	0.001	18.8
		6	-7.141	1.936	0.001	18.8
		8	-7.329	1.936	0.001	18.8
	Urban	4	-6.548	1.936	0.001	18.8
		6	-6.809	1.936	0.001	18.8
		8	-6.997	1.936	0.001	18.8
		10	-7.260	1.936	0.001	18.8



a. Fatal-and-Injury Crash Frequency

b. Property-Damage-Only Crash Frequency

Figure 18-12. Graphical Form of the SPFs for Multiple-Vehicle Crashes on Freeway Segments

The value of the overdispersion parameter associated with the SPFs for freeway segments is determined as a function of the segment length. This value is computed using Equation 18-17.

- Hours where volume exceeds 1000 vehicles per hour per lane None
- Outside shoulder width 10 ft
- Shoulder rumble strip Not present
- Outside clearance 30-ft clear zone
- Outside barrier Not present

The SPFs for single-vehicle crashes on freeway segments are represented with the following equation.

$$N_{spf, fs, n, sv, z} = L^* \times \exp(a + b \times \ln[c \times AADT_{fs}]) \tag{Equation 18-18}$$

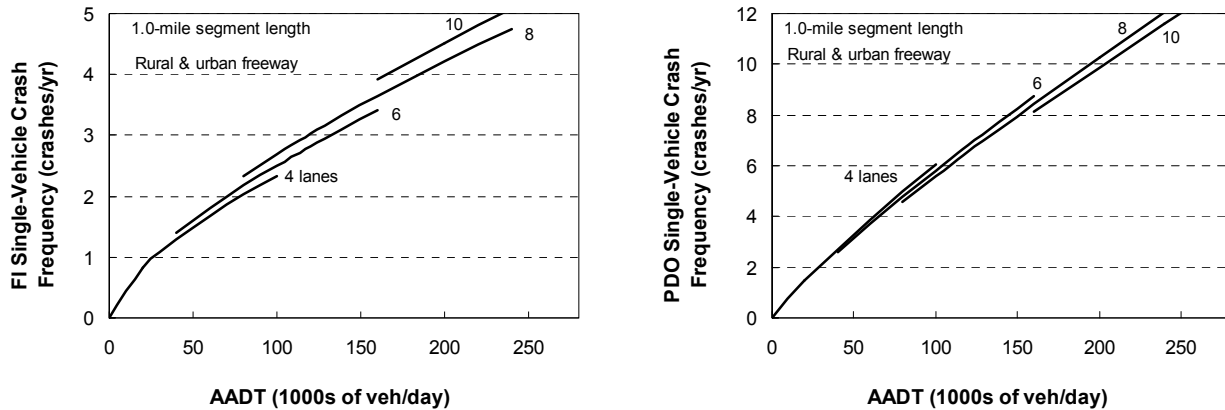
Where:

$N_{spf, fs, n, sv, z}$ = predicted average single-vehicle crash frequency of a freeway segment with base conditions, n lanes, and severity z ($z = fi$: fatal and injury, pdo : property damage only) (crashes/yr).

The SPF regression coefficients and the inverse dispersion parameter are provided in Table 18-7. The SPFs are illustrated in Figure 18-13.

Table 18-7. SPF Coefficients for Single-Vehicle Crashes on Freeway Segments

Crash Severity (z)	Area Type	Number of Through Lanes (n)	SPF Coefficient			Inverse Dispersion Parameter $K_{fs, n, sv, z}$ (mi^{-1})
			a	b	c	
Fatal and injury (fi)	Rural	4	-2.126	0.646	0.001	30.1
		6	-2.055	0.646	0.001	30.1
		8	-1.985	0.646	0.001	30.1
	Urban	4	-2.126	0.646	0.001	30.1
		6	-2.055	0.646	0.001	30.1
		8	-1.985	0.646	0.001	30.1
		10	-1.915	0.646	0.001	30.1
Property damage only (pdo)	Rural	4	-2.235	0.876	0.001	20.7
		6	-2.274	0.876	0.001	20.7
		8	-2.312	0.876	0.001	20.7
	Urban	4	-2.235	0.876	0.001	20.7
		6	-2.274	0.876	0.001	20.7
		8	-2.312	0.876	0.001	20.7
		10	-2.351	0.876	0.001	20.7



a. Fatal-and-Injury Crash Frequency

b. Property-Damage-Only Crash Frequency

Figure 18-13. Graphical Form of the SPFs for Single-Vehicle Crashes on Freeway Segments

The value of the overdispersion parameter associated with the SPFs for freeway segments is determined as a function of the segment length. This value is computed using Equation 18-19.

$$k_{fs,n,sv,z} = \frac{1}{K_{fs,n,sv,z} \times L^*} \tag{Equation 18-19}$$

Where:

$k_{fs,n,sv,z}$ = overdispersion parameter for freeway segments with n lanes, single-vehicle crashes sv and severity z ; and

$K_{fs,n,sv,z}$ = inverse dispersion parameter for freeway segments with n lanes, single-vehicle crashes sv and severity z (mi^{-1}).

The inverse dispersion parameter for segments with even numbers of lanes is provided in Table 18-7. A procedure is described in Section B.2.7 in Appendix B to Part C for using these parameters to estimate the overdispersion parameter for segments with odd numbers of lanes.

The crash frequency obtained from Equation 18-18 can be multiplied by the proportions in Table 18-8 to estimate the predicted average single-vehicle crash frequency by crash type category.

Table 18-8. Default Distribution of Single-Vehicle Crashes by Crash Type for Freeway Segments

Area Type	Crash Type Category	Proportion of Crashes by Severity	
		Fatal and Injury	Property Damage Only
Rural	Crash with animal	0.010	0.065
	Crash with fixed object	0.567	0.625
	Crash with other object	0.031	0.125
	Crash with parked vehicle	0.024	0.023
	Other single-vehicle crashes	0.368	0.162
Urban	Crash with animal	0.004	0.022
	Crash with fixed object	0.722	0.716
	Crash with other object	0.051	0.139
	Crash with parked vehicle	0.015	0.016
	Other single-vehicle crashes	0.208	0.107

18.6.2. Safety Performance Functions for Speed-Change Lanes

The SPFs for freeway speed-change lanes are presented in this section. SPFs are provided for ramp entrances and ramp exits adjacent to freeways with 4, 6, 8, or 10 through lanes. The SPFs for speed-change lanes are applicable to the same freeway AADT volume ranges that are listed in Table 18-4. Application to sites with AADT volumes substantially outside these ranges may not provide reliable results.

The SPFs described in this section are directly applicable to speed-change lanes adjacent to freeways with an even number of through lanes. They can be extended to the evaluation of speed-change lanes adjacent to freeways with 5, 7, and 9 lanes using the procedure described in Section 18.6.1.

Ramp Entrance Speed-Change Lanes

The base conditions for the SPFs for ramp-entrance speed-change lanes are:

- Horizontal curve Not present
- Lane width 12 ft
- Inside shoulder width 6 ft
- Median width 60 ft
- Median barrier Not present
- Hours where volume exceeds 1,000 vehicles per hour per lane None

The SPFs for ramp entrance speed-change lanes are represented using the following equation.

$$N_{spf, sc, nEN, at, z} = L_{en} \times \exp(a + b \times \ln[c \times AADT_{fs}]) \quad \text{Equation 18-20}$$

Where:

$N_{spf, sc, nEN, at, z}$ = predicted average crash frequency of a ramp entrance speed-change lane on a freeway with base conditions, n lanes, all crash types at , and severity z ($z = fi$: fatal and injury, pdo : property damage only) (crashes/yr); and

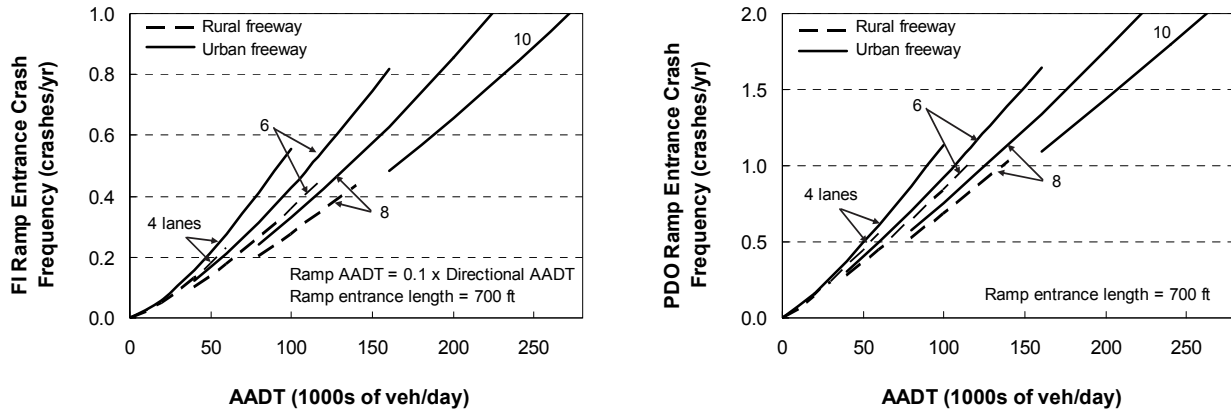
L_{en} = length of ramp entrance (mi).

The SPF regression coefficients and the inverse dispersion parameter are provided in Table 18-9. The variable n is used in this table to describe the number of through lanes in the portion of freeway adjacent to the speed-change lane *plus* those freeway lanes in the opposing travel direction. This approach to describing the speed-change lane cross section is used for consistency with that used for freeway segment SPFs. The variable n is not intended to describe the number of lanes in the speed-change lane.

Table 18-9. SPF Coefficients for Ramp-Entrance-Related Crashes in Speed-Change Lanes

Crash Severity (z)	Area Type	Number of Through Lanes (n)	SPF Coefficient			Inverse Dispersion Parameter $K_{sc, nEN, at, z}$ (mi^{-1})
			a	b	c	
Fatal and injury (fi)	Rural	4	-3.894	1.173	0.0005	26.1
		6	-4.154	1.173	0.0005	26.1
		8	-4.414	1.173	0.0005	26.1
	Urban	4	-3.714	1.173	0.0005	26.1
		6	-3.974	1.173	0.0005	26.1
		8	-4.234	1.173	0.0005	26.1
		10	-4.494	1.173	0.0005	26.1
Property damage only (pdo)	Rural	4	-2.895	1.215	0.0005	24.8
		6	-3.097	1.215	0.0005	24.8
		8	-3.299	1.215	0.0005	24.8
	Urban	4	-2.796	1.215	0.0005	24.8
		6	-2.998	1.215	0.0005	24.8
		8	-3.200	1.215	0.0005	24.8
		10	-3.402	1.215	0.0005	24.8

The SPFs are illustrated in Figure 18-14. The Ramp entrance CMF is combined with this SPF to create the trend lines shown in the figure. This CMF is a function of entrance ramp volume and the speed-change lane length. These variables in combination do not readily lend themselves to the specification of a representative base condition. For this reason, the CMF is combined with the SPF for the graphical presentation. The Ramp entrance CMF is described in Section 18.7.2.



a. Fatal-and-Injury Crash Frequency

b. Property-Damage-Only Crash Frequency

Figure 18-14. Graphical Form of the SPFs for Ramp Entrance Speed-Change Lanes

The value of the overdispersion parameter associated with the SPFs for ramp-entrance speed-change lanes is determined as a function of the speed-change lane length. This value is computed as:

$$k_{sc, nEN, at, z} = \frac{1}{K_{sc, nEN, at, z} \times L_{en}} \tag{Equation 18-21}$$

Where:

$k_{sc, nEN, at, z}$ = overdispersion parameter for ramp entrance speed-change lane on a freeway with n lanes, all crash types at , and severity z ; and

$K_{sc, nEN, at, z}$ = inverse dispersion parameter for ramp entrance speed-change lane on a freeway with n lanes, all crash types at , and severity z (mi^{-1}).

The inverse dispersion parameter for speed-change lanes adjacent to freeways with 4, 6, 8, or 10 through lanes is provided in Table 18-9. A procedure is described in Section B.2.7 in Appendix B to Part C for using these parameters to estimate the overdispersion parameter for speed-change lanes adjacent to freeways with 5, 7, or 9 lanes.

The crash frequency obtained from Equation 18-20 can be multiplied by the proportions in Table 18-10 to estimate the predicted average ramp-entrance-related crash frequency by crash type or crash type category. These proportions are based on ramp-entrance speed-change lane crashes. They do not include crashes associated with a ramp entrance that adds a lane to the cross section.

Table 18-10. Default Distribution of Ramp-Entrance-Related Crashes by Crash Type

Area Type	Crash Type	Crash Type Category	Proportion of Crashes by Severity	
			Fatal and Injury	Property Damage Only
Rural	Multiple vehicle	Head-on	0.021	0.004
		Right-angle	0.032	0.013
		Rear-end	0.351	0.260
		Sideswipe	0.128	0.242
		Other multiple-vehicle crash	0.011	0.040
	Single vehicle	Crash with animal	0.000	0.009
		Crash with fixed object	0.245	0.296
		Crash with other object	0.021	0.070
		Crash with parked vehicle	0.021	0.000
		Other single-vehicle crashes	0.170	0.066
Urban	Multiple vehicle	Head-on	0.004	0.001
		Right-angle	0.019	0.016
		Rear-end	0.543	0.530
		Sideswipe	0.133	0.252
		Other multiple-vehicle crash	0.017	0.015
	Single vehicle	Crash with animal	0.000	0.002
		Crash with fixed object	0.194	0.129
		Crash with other object	0.019	0.036
		Crash with parked vehicle	0.004	0.003
		Other single-vehicle crashes	0.067	0.016

Ramp Exit Speed-Change Lanes

The base conditions for the SPFs for ramp exit speed-change lanes are the same as those for ramp entrance speed-change lanes, as described in the preceding subsection.

The SPFs for ramp exit speed-change lanes are represented using the following equation.

$$N_{spf, sc, nEX, at, z} = L_{ex} \times \exp(a + b \times \ln[c \times AADT_{fs}]) \quad \text{Equation 18-22}$$

Where:

$N_{spf, sc, nEX, at, z}$ = predicted average crash frequency of a ramp exit speed-change lane on a freeway with base conditions, n lanes, all crash types at , and severity z ($z = fi$: fatal and injury, pdo : property damage only) (crashes/yr); and

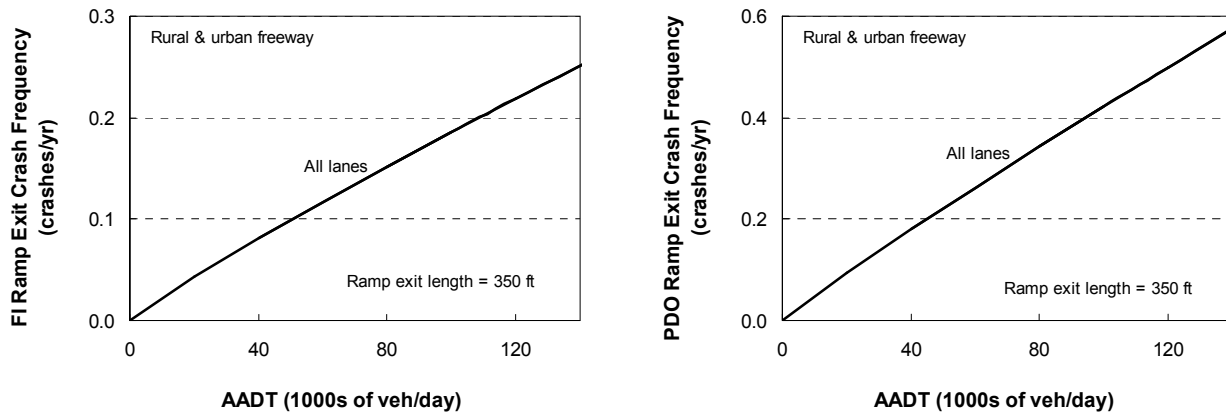
L_{ex} = length of ramp exit (mi).

The SPF regression coefficients and the inverse dispersion parameter are provided in Table 18-11. The variable n is used in this table to describe the number of through lanes in the portion of freeway adjacent to the speed-change lane *plus* those freeway lanes in the opposing travel direction.

Table 18-11. SPF Coefficients for Ramp-Exit-Related Crashes in Speed-Change Lanes

Crash Severity (z)	Area Type	Number of Through Lanes (n)	SPF Coefficient			Inverse Dispersion Parameter $K_{sc, nEX, at, z}$
			a	b	c	
Fatal and injury (fi)	Rural	4, 6, 8	-2.679	0.903	0.0005	1.78
	Urban	4, 6, 8, 10	-2.679	0.903	0.0005	1.78
Property damage only (pdo)	Rural	4, 6, 8	-1.798	0.932	0.0005	1.58
	Urban	4, 6, 8, 10	-1.798	0.932	0.0005	1.58

The SPFs are illustrated in Figure 18-15. The Ramp exit CMF is combined with the fatal-and-injury SPF to create the trend lines shown in the figure for fatal-and-injury crashes. This CMF is a function of the speed-change lane length. This variable (in combination with the SPF length variable) does not readily lend itself to the specification of a representative base condition. For this reason, the CMF is combined with the SPF for the graphical presentation. The Ramp exit CMF is described in Section 18.7.2



a. Fatal-and-Injury Crash Frequency

b. Property-Damage-Only Crash Frequency

Figure 18-15. Graphical Form of the SPFs for Ramp Exit Speed-Change Lanes

The overdispersion parameter associated with the SPFs for ramp exit speed-change lanes is computed as:

$$k_{sc,nEX,at,z} = \frac{1}{K_{sc,nEX,at,z}}$$

Equation 18-23

Where:

$k_{sc,nEX,at,z}$ = overdispersion parameter for ramp exit speed-change lane on a freeway with n lanes, all crash types at , and severity z ; and

$K_{sc,nEX,at,z}$ = inverse dispersion parameter for ramp exit speed-change lane on a freeway with n lanes, all crash types at , and severity z .

The inverse dispersion parameter for speed-change lanes adjacent to freeways with 4, 6, 8, or 10 through lanes is provided in Table 18-11. A procedure is described in Section B.2.7 in Appendix B to Part C for using these parameters to estimate the overdispersion parameter for speed-change lanes adjacent to freeways with 5, 7, or 9 lanes.

The crash frequency obtained from Equation 18-22 can be multiplied by the proportions in Table 18-12 to estimate the predicted average ramp-exit-related crash frequency by crash type or crash type category. These proportions are based on ramp-exit speed-change lane crashes. They do not include crashes associated with a ramp exit that drops a lane from the cross section.

Table 18-12. Default Distribution of Ramp-Exit-Related Crashes by Crash Type

Area Type	Crash Type	Crash Type Category	Proportion of Crashes by Severity	
			Fatal and Injury	Property Damage Only
Rural	Multiple vehicle	Head-on	0.000	0.000
		Right-angle	0.015	0.000
		Rear-end	0.463	0.304
		Sideswipe	0.104	0.243
		Other multiple-vehicle crash	0.000	0.009
	Single vehicle	Crash with animal	0.000	0.061
		Crash with fixed object	0.224	0.235
		Crash with other object	0.030	0.061
		Crash with parked vehicle	0.000	0.017
		Other single-vehicle crashes	0.164	0.070
Urban	Multiple vehicle	Head-on	0.005	0.002
		Right-angle	0.011	0.012
		Rear-end	0.549	0.565
		Sideswipe	0.158	0.138
		Other multiple-vehicle crash	0.016	0.016
	Single vehicle	Crash with animal	0.000	0.007
		Crash with fixed object	0.196	0.207
		Crash with other object	0.016	0.030
		Crash with parked vehicle	0.000	0.000
		Other single-vehicle crashes	0.049	0.023

18.7. CRASH MODIFICATION FACTORS

This section describes the CMFs applicable to the SPFs presented in Section 18.6. These CMFs were calibrated along with the SPFs. They are summarized in Table 18-13.

Table 18-13. Freeway Crash Modification Factors and their Corresponding SPFs

Applicable SPF(s)	CMF Variable	CMF Description	CMF Equations
Freeway segments or speed-change lanes	$CMF_{1, w, x, y, z}$	Horizontal curve	Equation 18-24, Equation 18-40
	$CMF_{2, w, x, y, fi}$	Lane width	Equation 18-25, Equation 18-41
	$CMF_{3, w, x, y, z}$	Inside shoulder width	Equation 18-26, Equation 18-42
	$CMF_{4, w, x, y, z}$	Median width	Equation 18-27, Equation 18-43
	$CMF_{5, w, x, y, z}$	Median barrier	Equation 18-28, Equation 18-44
	$CMF_{6, w, x, y, z}$	High volume	Equation 18-29, Equation 18-45
Multiple-vehicle crashes on freeway segments	$CMF_{7, fs, ac, mv, z}$	Lane change	Equation 18-30
Single-vehicle crashes on freeway segments	$CMF_{8, fs, ac, sv, z}$	Outside shoulder width	Equation 18-35
	$CMF_{9, fs, ac, sv, fi}$	Shoulder rumble strip	Equation 18-36
	$CMF_{10, fs, ac, sv, fi}$	Outside clearance	Equation 18-38
	$CMF_{11, fs, ac, sv, z}$	Outside barrier	Equation 18-39
Ramp entrances	$CMF_{12, sc, nEN, at, z}$	Ramp entrance	Equation 18-46
Ramp exits	$CMF_{13, sc, nEX, at, z}$	Ramp exit	Equation 18-47

Note: Subscripts to the CMF variables use the following notation:

- Site type w ($w = fs$: freeway segment, sc : speed-change lane),
- Cross section x ($x = n$: n -lane freeway, nEN : ramp entrance speed-change lane adjacent to a freeway with n lanes, nEX : ramp exit speed-change lane adjacent to a freeway with n lanes, ac : any cross section),
- Crash type y ($y = sv$: single vehicle, mv : multiple vehicle, at : all types), and
- Severity z ($z = fi$: fatal and injury, pdo : property damage only, as : all severities).

Many of the CMFs in Table 18-13 are developed for specific site types, cross sections, crash types, or crash severities. This approach was undertaken to make the predictive model sensitive to the geometric design and traffic control features of specific sites with specific cross sections, in terms of their influence on specific crash types and severities. The subscripts for each CMF variable indicate the sites, cross sections, crash types, and severities to which each CMF is applicable. The subscript definitions are provided in the table footnote. In some cases, a CMF is applicable to several site types, cross sections, crash types, or severities. In these cases, the subscript retains the generic letter w , x , y , or z , as appropriate. The discussion of these CMFs in Section 18.7.1 or 18.7.2 identifies the specific site types, cross sections, crash types, or severities to which they apply.

As indicated in Table 18-13, some of the CMFs apply to both freeway segments and speed-change lanes. These CMFs are presented in Section 18.7.1 and referenced in Section 18.7.2. For some of the CMFs, supplemental calculations must be performed before the CMF value can be computed. For example, to apply the Median width CMF, the proportion of the segment length having inside barrier and the length-weighted

average barrier offset (as measured from the edge of the inside shoulder) must be computed. Procedures for supplemental calculations are described in Section 18.7.3.

18.7.1. Crash Modification Factors for Roadway Segments

The CMFs for geometric design and traffic control features of freeway segments are presented in this section.

CMF_{1, w, x, y, z}—Horizontal Curve

Four CMFs are used to describe the relationship between horizontal curve geometry and predicted crash frequency. The SPFs to which they apply are identified in the following list:

- SPF for fatal-and-injury multiple-vehicle crashes, specified number of lanes (fs, n, mv, fi);
- SPF for property-damage-only multiple-vehicle crashes, specified number of lanes (fs, n, mv, pdo);
- SPF for fatal-and-injury single-vehicle crashes, specified number of lanes (fs, n, sv, fi); and
- SPF for property-damage-only single-vehicle crashes, specified number of lanes (fs, n, sv, pdo).

The base condition is an uncurved (i.e., tangent) segment. The CMFs are described using the following equation.

$$CMF_{1, fs, ac, y, z} = 1.0 + a \times \left[\sum_{i=1}^m \left(\frac{5,730}{R_i^*} \right)^2 \times P_{c,i} \times f_{c,i} \right] \quad \text{Equation 18-24}$$

Where:

$CMF_{1, fs, ac, y, z}$ = crash modification factor for horizontal curvature in a freeway segment with any cross section ac , crash type y , and severity z ;

R_i^* = equivalent radius of curve i ($= [0.5/R_{a,i}^2 + 0.5/R_{b,i}^2]^{-0.5}$ if both roadbeds are curved, $R_{a,i}$ if only one roadbed is curved) (ft);

$R_{a,i}$ = radius of curve i in one roadbed (ft);

$R_{b,i}$ = radius of curve i in second roadbed (used if both roadbeds are curved) (ft);

$P_{c,i}$ = proportion of segment length with curve i ;

$f_{c,i}$ = roadbed adjustment factor for curve i ($= 1.0$ if both roadbeds are curved, 0.5 if only one roadbed is curved); and

m = number of horizontal curves in the segment.

The regression coefficient for Equation 18-24 is provided in Table 18-14. Equation 18-24 is derived to recognize that more than one curve may exist in a segment and that a curve may be located only partially in the segment (and partially on an adjacent segment). The variable $P_{c,i}$ is computed as the ratio of the length of curve i in the segment to the length of the freeway segment L_{fs} . For example, consider a segment that is 0.5 mi long and a curve that is 0.2 mi long. If one-half of the curve is in the segment, then $P_{c,i} = 0.20$ ($= 0.1/0.5$). In fact, this proportion is the same regardless of the curve's length (provided that it is 0.1 mi or longer and 0.1 mi of this curve is located in the segment).

The roadbed adjustment factor $f_{c,i}$ is used to modify the CMF so that it can be applied to freeway segments where only one roadbed is curved (and the other roadbed is tangent). This situation occurs on some freeway segments in rural areas (although, it can also occur in urban areas).

Table 18-14. Coefficients for Horizontal Curve CMF—Freeway Segments

Cross Section (<i>x</i>)	Crash Type (<i>y</i>)	Crash Severity (<i>z</i>)	CMF Variable	Regression Coefficient (<i>a</i>)
Any cross section (<i>ac</i>)	Multiple vehicle (<i>mv</i>)	Fatal and injury (<i>fi</i>)	$CMF_{1,fs,ac,mv,fi}$	0.0172
		Property damage only (<i>pdo</i>)	$CMF_{1,fs,ac,mv,pdo}$	0.0340
	Single vehicle (<i>sv</i>)	Fatal and injury (<i>fi</i>)	$CMF_{1,fs,ac,sv,fi}$	0.0719
		Property damage only (<i>pdo</i>)	$CMF_{1,fs,ac,sv,pdo}$	0.0626

Details regarding the measurement of radius, curve length, and other variables associated with this CMF are provided in Section 18.4.2. The CMF is applicable to curves with a radius of 1,000 ft or larger.

CMF_{2,w,x,y,fi}—Lane Width

Two CMFs are used to describe the relationship between average lane width and predicted crash frequency. The SPFs to which they apply are identified in the following list:

- SPF for fatal-and-injury multiple-vehicle crashes, specified number of lanes (*fs, n, mv, fi*); and
- SPF for fatal-and-injury single-vehicle crashes, specified number of lanes (*fs, n, sv, fi*).

The base condition is a 12-ft lane width. The CMFs are described using the following equation.

$$CMF_{2,fs,ac,y,fi} = \begin{cases} \exp(a \times [W_l - 12]) & : \text{If } W_l < 13 \text{ ft} \\ b & : \text{If } W_l \geq 13 \text{ ft} \end{cases} \quad \text{Equation 18-25}$$

Where:

$CMF_{2,fs,ac,y,fi}$ = crash modification factor for lane width in a freeway segment with any cross section *ac*, crash type *y*, and fatal-and-injury crashes *fi*; and

W_l = lane width (ft).

The regression coefficients for Equation 18-25 are provided in Table 18-15. In fact, the coefficient values are the same for both crash types listed in the table, which indicates that the CMF value is the same for the corresponding SPFs. The CMF is discontinuous, breaking at a lane width of 13 ft. The CMF is applicable to lane widths in the range of 10.5 to 14 ft.

Table 18-15. Coefficients for Lane Width CMF–Freeway Segments

Cross Section (x)	Crash Type (y)	Crash Severity (z)	CMF Variable	Regression Coefficients	
				a	b
Any cross section (ac)	Multiple vehicle (mv)	Fatal and injury (fi)	$CMF_{2,fs,ac,mv,fi}$	-0.0376	0.963
	Single vehicle (sv)	Fatal and injury (fi)	$CMF_{2,fs,ac,sv,fi}$	-0.0376	0.963

CMF_{3,w,x,y,z}—Inside Shoulder Width

Four CMFs are used to describe the relationship between average inside shoulder width and predicted crash frequency. The SPFs to which they apply are identified in the following list:

- SPF for fatal-and-injury multiple-vehicle crashes, specified number of lanes (fs, n, mv, fi);
- SPF for property-damage-only multiple-vehicle crashes, specified number of lanes (fs, n, mv, pdo);
- SPF for fatal-and-injury single-vehicle crashes, specified number of lanes (fs, n, sv, fi); and
- SPF for property-damage-only single-vehicle crashes, specified number of lanes (fs, n, sv, pdo).

The base condition is a 6-ft inside shoulder width. The CMFs are described using the following equation.

$$CMF_{3,fs,ac,y,z} = \exp(a \times [W_{is} - 6]) \quad \text{Equation 18-26}$$

Where:

$CMF_{3,fs,ac,y,z}$ = crash modification factor for inside shoulder width in a freeway segment with any cross section ac , crash type y , and severity z ; and

W_{is} = inside shoulder width (ft).

The regression coefficient for Equation 18-26 is provided in Table 18-16. For a given severity, the coefficient values are the same for both crash types listed in the table, which indicates that the CMF value is the same for the corresponding SPFs. The CMF is applicable to shoulder widths in the range of 2 to 12 ft.

Table 18-16. Coefficients for Inside Shoulder Width CMF–Freeway Segments

Cross Section (x)	Crash Type (y)	Crash Severity (z)	CMF Variable	Regression Coefficient (a)
Any cross section (ac)	Multiple vehicle (mv)	Fatal and injury (fi)	$CMF_{3,fs,ac,mv,fi}$	-0.0172
		Property damage only (pdo)	$CMF_{3,fs,ac,mv,pdo}$	-0.0153
	Single vehicle (sv)	Fatal and injury (fi)	$CMF_{3,fs,ac,sv,fi}$	-0.0172
		Property damage only (pdo)	$CMF_{3,fs,ac,sv,pdo}$	-0.0153

CMF_{4, w, x, y, z}—Median Width

Four CMFs are used to describe the relationship between median width and predicted crash frequency. The SPFs to which they apply are identified in the following list:

- SPF for fatal-and-injury multiple-vehicle crashes, specified number of lanes (fs, n, mv, fi);
- SPF for property-damage-only multiple-vehicle crashes, specified number of lanes (fs, n, mv, pdo);
- SPF for fatal-and-injury single-vehicle crashes, specified number of lanes (fs, n, sv, fi); and
- SPF for property-damage-only single-vehicle crashes, specified number of lanes (fs, n, sv, pdo).

The base condition is a 60-ft median width, a 6-ft inside shoulder width, and no barrier present in the median. The CMFs are described using the following equation.

$$CMF_{4, fs, ac, y, z} = (1.0 - P_{ib}) \times \exp(a \times [W_m - 2 \times W_{is} - 48]) + P_{ib} \times \exp(a \times [2 \times W_{icb} - 48]) \quad \text{Equation 18-27}$$

Where:

$CMF_{4, fs, ac, y, z}$ = crash modification factor for median width in a freeway segment with any cross section ac , crash type y , and severity z ;

P_{ib} = proportion of segment length with a barrier present in the median (i.e., inside);

W_m = median width (measured from near edges of traveled way in both directions) (ft); and

W_{icb} = distance from edge of inside shoulder to barrier face (ft).

The regression coefficient for Equation 18-27 is provided in Table 18-17. These CMFs are derived to be applicable to a segment that has median barrier present along some portion of the segment. Guidance for computing the variables P_{ib} and W_{icb} is provided in Section 18.7.3.

Table 18-17. Coefficients for Median Width CMF—Freeway Segments

Cross Section (x)	Crash Type (y)	Crash Severity (z)	CMF Variable	Regression Coefficient (a)
Any cross section (ac)	Multiple vehicle (mv)	Fatal and injury (fi)	$CMF_{4, fs, ac, mv, fi}$	-0.00302
		Property damage only (pdo)	$CMF_{4, fs, ac, mv, pdo}$	-0.00291
	Single vehicle (sv)	Fatal and injury (fi)	$CMF_{4, fs, ac, sv, fi}$	0.00102
		Property damage only (pdo)	$CMF_{4, fs, ac, sv, pdo}$	-0.00289

The CMF is applicable to median widths of 9 ft or more, W_{icb} values in the range of 0.75 to 17 ft, and shoulder widths in the range of 2 to 12 ft. If the median width exceeds 90 ft, then 90 ft should be used for W_m in Equation 18-27.

CMF_{5, w, x, y, z}—Median Barrier

Four CMFs are used to describe the relationship between median barrier presence and predicted crash frequency. The SPFs to which they apply are identified in the following list:

- SPF for fatal-and-injury multiple-vehicle crashes, specified number of lanes (fs, n, mv, fi);
- SPF for property-damage-only multiple-vehicle crashes, specified number of lanes (fs, n, mv, pdo);
- SPF for fatal-and-injury single-vehicle crashes, specified number of lanes (fs, n, sv, fi); and
- SPF for property-damage-only single-vehicle crashes, specified number of lanes (fs, n, sv, pdo).

The base condition is no barrier present in the median. The CMFs are described using the following equation.

$$CMF_{5, fs, ac, y, z} = (1.0 - P_{ib}) \times 1.0 + P_{ib} \times \exp\left(\frac{a}{W_{icb}}\right) \tag{Equation 18-28}$$

Where:

$CMF_{5, fs, ac, y, z}$ = crash modification factor for median barrier in a freeway segment with any cross section ac , crash type y , and severity z .

The regression coefficient for Equation 18-28 is provided in Table 18-18. For a given severity, the coefficient values are the same for both crash types listed in the table, which indicates that the CMF value is the same for the corresponding SPFs. Guidance for computing the variables P_{ib} and W_{icb} is provided in Section 18.7.3.

Table 18-18. Coefficients for Median Barrier CMF–Freeway Segments

Cross Section (x)	Crash Type (y)	Crash Severity (z)	CMF Variable	Regression Coefficient (a)
Any cross section (ac)	Multiple vehicle (mv)	Fatal and injury (fi)	$CMF_{5, fs, ac, mv, fi}$	0.131
		Property damage only (pdo)	$CMF_{5, fs, ac, mv, pdo}$	0.169
	Single vehicle (sv)	Fatal and injury (fi)	$CMF_{5, fs, ac, sv, fi}$	0.131
		Property damage only (pdo)	$CMF_{5, fs, ac, sv, pdo}$	0.169

The CMF is applicable to W_{icb} values in the range of 0.75 to 17 ft. This CMF is applicable to cable barrier, concrete barrier, guardrail, and bridge rail.

CMF_{6, w, x, y, z}—High Volume

As volume nears capacity, average freeway speed tends to decrease and headway is reduced. Logically, these changes have some influence on crash characteristics, including crash frequency, crash type, and crash severity. This CMF was developed to provide some sensitivity to volume variation during the average day and specifically to those peak hours where traffic volume is likely to be near (or in excess of) capacity.

A statistic was developed to describe the degree of volume concentration during peak hours of the average day. It represents the proportion of the AADT that occurs during hours where the volume exceeds 1,000 vehicles per hour per lane (veh/h/ln). It has a value of zero if the volume on the associated segment does not exceed the threshold value for any hour of the day. It has a value of one if the volume during each hour of the average day exceeds the threshold value. In general, its value is large when hourly volumes are continuously high or when there is a peak few hours with an exceptionally large volume.

Typical freeway speed-volume relationships show that the average speed tends to drop as flow rates increase beyond 1,000 veh/h/ln. This trend suggests that drivers reduce their speed to improve their comfort and safety as their headway gets shorter than 3.6 s/veh (= 3,600/1,000).

Four CMFs are used to describe the relationship between volume concentration and predicted crash frequency. The SPFs to which they apply are identified in the following list:

- SPF for fatal-and-injury multiple-vehicle crashes, specified number of lanes (fs, n, mv, fi);
- SPF for property-damage-only multiple-vehicle crashes, specified number of lanes (fs, n, mv, pdo);
- SPF for fatal-and-injury single-vehicle crashes, specified number of lanes (fs, n, sv, fi); and
- SPF for property-damage-only single-vehicle crashes, specified number of lanes (fs, n, sv, pdo).

The base condition is no hours having a volume that exceeds 1,000 veh/h/ln. The CMFs are described using the following equation.

$$CMF_{6, fs, ac, y, z} = \exp(a \times P_{hv}) \quad \text{Equation 18-29}$$

Where:

$CMF_{6, fs, ac, y, z}$ = crash modification factor for high volume in a freeway segment with any cross section ac , crash type y , and severity z ; and

P_{hv} = proportion of AADT during hours where volume exceeds 1,000 veh/h/ln.

The regression coefficient for Equation 18-29 is provided in Table 18-19. The CMF is applicable to P_{hv} values in the range of 0.0 to 1.0.

Table 18-19. Coefficients for High Volume CMF–Freeway Segments

Cross Section (x)	Crash Type (y)	Crash Severity (z)	CMF Variable	Regression Coefficient (a)
Any cross section (ac)	Multiple vehicle (mv)	Fatal and injury (fi)	$CMF_{6, fs, ac, mv, fi}$	0.350
		Property damage only (pdo)	$CMF_{6, fs, ac, mv, pdo}$	0.283
	Single vehicle (sv)	Fatal and injury (fi)	$CMF_{6, fs, ac, sv, fi}$	-0.0675
		Property damage only (pdo)	$CMF_{6, fs, ac, sv, pdo}$	-0.611

CMF_{7, fs, ac, mv, z}—Lane Change

Two CMFs are used to describe the relationship between lane change activity and predicted crash frequency. The SPFs to which they apply are identified in the following list:

- SPF for fatal-and-injury multiple-vehicle crashes, specified number of lanes (fs, n, mv, fi); and
- SPF for property-damage-only multiple-vehicle crashes, specified number of lanes (fs, n, mv, pdo).

The base condition is no significant lane changing due to ramp entry or exit. More specifically, the base condition is no ramp entrance or ramp exit within 0.5 mi of the segment. The CMFs are described using the following equations:

$$CMF_{7, fs, ac, mv, z} = (0.5 \times f_{wev, inc} \times f_{lc, inc}) + (0.5 \times f_{wev, dec} \times f_{lc, dec}) \quad \text{Equation 18-30}$$

with,

$$f_{wev, inc} = (1.0 - P_{wevB, inc}) \times 1.0 + P_{wevB, inc} \times \exp\left(\frac{a}{L_{wev, inc}}\right) \quad \text{Equation 18-31}$$

$$f_{wev, dec} = (1.0 - P_{wevB, dec}) \times 1.0 + P_{wevB, dec} \times \exp\left(\frac{a}{L_{wev, dec}}\right) \quad \text{Equation 18-32}$$

$$f_{lc, inc} = \left(1.0 + \frac{\exp(-b \times X_{b, ent} + d \times \ln[c \times AADT_{b, ent}])}{b \times L_{fs}}\right) \times [1.0 - \exp(-b \times L_{fs})] \times \left(1.0 + \frac{\exp(-b \times X_{e, ext} + d \times \ln[c \times AADT_{e, ext}])}{b \times L_{fs}}\right) \times [1.0 - \exp(-b \times L_{fs})] \quad \text{Equation 18-33}$$

$$f_{lc, dec} = \left(1.0 + \frac{\exp(-b \times X_{e, ent} + d \times \ln[c \times AADT_{e, ent}])}{b \times L_{fs}}\right) \times [1.0 - \exp(-b \times L_{fs})] \times \left(1.0 + \frac{\exp(-b \times X_{b, ext} + d \times \ln[c \times AADT_{b, ext}])}{b \times L_{fs}}\right) \times [1.0 - \exp(-b \times L_{fs})] \quad \text{Equation 18-34}$$

Where:

$CMF_{7, fs, ac, mv, z}$ = crash modification factor for lane changes in a freeway segment with any cross section ac , multiple-vehicle crashes mv , and severity z ;

$f_{lc, inc}$ = lane change adjustment factor for travel in increasing milepost direction;

$f_{lc, dec}$ = lane change adjustment factor for travel in decreasing milepost direction;

$f_{wev, inc}$ = weaving section adjustment factor for travel in increasing milepost direction;

$f_{wev, dec}$ = weaving section adjustment factor for travel in decreasing milepost direction;

$P_{wevB, inc}$ = proportion of segment length within a Type B weaving section for travel in increasing milepost direction;

$P_{wevB, dec}$ = proportion of segment length within a Type B weaving section for travel in decreasing milepost direction;

$L_{wev, inc}$ = weaving section length for travel in increasing milepost direction (may extend beyond segment boundaries) (mi);

$L_{wev, dec}$	= weaving section length for travel in decreasing milepost direction (may extend beyond segment boundaries) (mi);
$X_{b, ent}$	= distance from segment begin milepost to nearest upstream entrance ramp gore point, for travel in increasing milepost direction (mi);
$X_{b, ext}$	= distance from segment begin milepost to nearest downstream exit ramp gore point, for travel in decreasing milepost direction (mi);
$X_{e, ent}$	= distance from segment end milepost to nearest upstream entrance ramp gore point, for travel in decreasing milepost direction (mi);
$X_{e, ext}$	= distance from segment end milepost to nearest downstream exit ramp gore point, for travel in increasing milepost direction (miles);
$AADT_{b, ent}$	= AADT volume of entrance ramp located at distance $X_{b, ent}$ (veh/day);
$AADT_{b, ext}$	= AADT volume of exit ramp located at distance $X_{b, ext}$ (veh/day);
$AADT_{e, ent}$	= AADT volume of entrance ramp located at distance $X_{e, ent}$ (veh/day); and
$AADT_{e, ext}$	= AADT volume of exit ramp located at distance $X_{e, ext}$ (veh/day).

The regression coefficients for Equation 18-31 to Equation 18-34 are provided in Table 18-20.

Table 18-20. Coefficients for Lane Change CMF–Freeway Segments

Cross Section (x)	Crash Type (y)	Crash Severity (z)	CMF Variable	Regression Coefficients			
				a	b	c	d
Any cross section (ac)	Multiple vehicle (mv)	Fatal and injury (fi)	$CMF_{7, fs, ac, mv, fi}$	0.175	12.56	0.001	-0.272
		Property damage only (pdo)	$CMF_{7, fs, ac, mv, pdo}$	0.123	13.46	0.001	-0.283

If the segment is in a Type B weaving section, then the length of the weaving section is an input to the CMF. The variables for weaving section length (i.e., $L_{wev, inc}$, $L_{wev, dec}$) in Equation 18-31 and Equation 18-32 are intended to reflect the degree to which the weaving activity is concentrated along the freeway. The sign of the regression coefficient in these two equations indicates that the lane change CMF value will increase if the segment is in a Type B weaving section. The amount of this increase is inversely related to the length of the weaving section. Guidance for determining if a weaving section is Type B is provided in Section 18.4.

The variables $P_{wevB, inc}$ and $P_{wevB, dec}$ in Equation 18-31 and Equation 18-32, respectively, are computed as the ratio of the length of the weaving section in the segment to the length of the freeway segment L_{fs} . If the segment is wholly located in the weaving section, then this variable is equal to 1.0.

The X and $AADT$ variables describe the distance to (and volume of) the four nearest ramps to the subject segment. Two of the ramps of interest are on the side of the freeway with travel in the increasing milepost direction. One ramp on this side of the freeway is upstream of the segment, and one ramp is downstream of the segment. Similarly, one ramp on the other side of the freeway is upstream of the segment and one ramp is downstream. Only those entrance ramps that contribute volume to the subject segment are of interest. Hence, a downstream entrance ramp is not of interest. For similar reasons, an upstream exit ramp is not of interest.

The Lane change CMF is applicable to any segment in the vicinity of one or more ramps. It is equally applicable to segments in a weaving section (regardless of the weaving section type) and segments in a non-weaving section (i.e., segments between an entrance ramp and an exit ramp where both ramps have a speed-change lane). If the weaving section is Type B, then an additional adjustment is made using Equation 18-31 and Equation 18-32. The CMF is applicable to weaving section lengths between 0.10 and 0.85 mi. It is applicable to any value for the distance variable X and to the range of ramp AADTs in Table 19-4 of Chapter 19.

The two SPFs for predicting speed-change-related crash frequency (i.e., Equation 18-20 and Equation 18-22) are not used when evaluating a weaving section because the ramps that form the weaving section do not have a speed-change lane. As a result, the predicted crash frequency for the set of segments that comprise a weaving section will tend to be smaller than that predicted for a similar set of segments located in a non-weaving section but having entrance and exit ramps. This generalization will always be true for weaving sections that are not Type B. It may or may not hold for the Type B weaving section, depending on the length of the weaving section.

CMF_{8, fs, ac, sv, z}—Outside Shoulder Width

Two CMFs are used to describe the relationship between average outside shoulder width and predicted crash frequency. The SPFs to which they apply are identified in the following list:

- SPF for fatal-and-injury single-vehicle crashes, specified number of lanes (fs, n, sv, fi); and
- SPF for property-damage-only single-vehicle crashes, specified number of lanes (fs, n, sv, pdo).

The base condition is a 10-ft outside shoulder width. The CMFs are described using the following equation.

$$CMF_{8, fs, ac, sv, z} = \left(1.0 - \sum_{i=1}^m P_{c,i}\right) \times \exp(a \times [W_s - 10]) + \left(\sum_{i=1}^m P_{c,i}\right) \times \exp(b \times [W_s - 10]) \tag{Equation 18-35}$$

Where:

$CMF_{8, fs, ac, sv, z}$ = crash modification factor for outside shoulder width in a freeway segment with any cross section ac , single-vehicle crashes sv , and severity z ; and

W_s = outside shoulder width (ft).

The regression coefficients for Equation 18-35 are provided in Table 18-21. The variable $P_{c,i}$ is computed as the ratio of the length of curve i in the segment to the length of the freeway segment L_{fs} . The CMF is applicable to shoulder widths in the range of 4 to 14 ft.

Table 18-21. Coefficients for Outside Shoulder Width CMF—Freeway Segments

Cross Section (x)	Crash Type (y)	Crash Severity (z)	CMF Variable	Regression Coefficients	
				a	b
Any cross section (ac)	Single vehicle (sv)	Fatal and injury (fi)	$CMF_{8, fs, ac, sv, fi}$	-0.0647	-0.0897
		Property damage only (pdo)	$CMF_{8, fs, ac, sv, pdo}$	0.00	-0.0840

CMF_{9, fs, ac, sv, fi}—Shoulder Rumble Strips

One CMF is used to describe the relationship between shoulder rumble strip presence and predicted crash frequency. The SPF to which it applies is identified in the following list:

- SPF for fatal-and-injury single-vehicle crashes, specified number of lanes (*fs, n, sv, fi*).

The base condition is no shoulder rumble strips present. The CMF is described using the following equation.

$$CMF_{9, fs, ac, sv, fi} = \left(1.0 - \sum_{i=1}^m P_{c,i}\right) \times f_{tan} + \left(\sum_{i=1}^m P_{c,i}\right) \times 1.0 \quad \text{Equation 18-36}$$

$$f_{tan} = 0.5 \times ([1.0 - P_{ir}] \times 1.0 + P_{ir} \times 0.811) + 0.5 \times ([1.0 - P_{or}] \times 1.0 + P_{or} \times 0.811) \quad \text{Equation 18-37}$$

Where:

$CMF_{9, fs, ac, sv, fi}$ = crash modification factor for shoulder rumble strips in a freeway segment with any cross section *ac* and fatal-and-injury *fi* single-vehicle crashes *sv*;

f_{tan} = factor for rumble strip presence on tangent portions of the segment;

P_{ir} = proportion of segment length with rumble strips present on the inside shoulders; and

P_{or} = proportion of segment length with rumble strips present on the outside shoulders.

The proportion P_{ir} represents the proportion of the segment length with rumble strips present on the inside shoulders. It is computed by summing the length of roadway with rumble strips on the inside shoulder in *both* travel directions and dividing by twice the freeway segment length L_{fs} . The proportion P_{or} represents the proportion of the segment length with rumble strips present on the outside shoulders. It is computed by summing the length of roadway with rumble strips on the outside shoulder in *both* travel directions and dividing by twice the freeway segment length L_{fs} .

This CMF addresses shoulder rumble strip placement on uncurved (i.e., tangent) segments. It has a value less than 1.0 on tangent segments with shoulder rumble strips suggesting that crash frequency is lowered by the presence of rumble strips. This trend was not found in the calibration data for curved segments.

CMF_{10, fs, ac, sv, fi}—Outside Clearance

One CMF is used to describe the relationship between average outside clearance and predicted crash frequency. The SPF to which it applies is identified in the following list:

- SPF for fatal-and-injury single-vehicle crashes, specified number of lanes (*fs, n, sv, fi*).

The base condition is a 30-ft clear zone, a 10-ft outside shoulder width, and no barrier present in the clear zone. The CMF is described using the following equation.

$$CMF_{10, fs, ac, sv, fi} = (1.0 - P_{ob}) \times \exp(-0.00451 \times [W_{hc} - W_s - 20]) + P_{ob} \times \exp(-0.00451 \times [W_{ocb} - 20]) \quad \text{Equation 18-38}$$

Where:

$CMF_{10, fs, ac, sv, fi}$ = crash modification factor for outside clearance in a freeway segment with any cross section ac , single-vehicle sv , fatal-and-injury fi crashes;

P_{ob} = proportion of segment length with a barrier present on the roadside (i.e., outside);

W_{hc} = clear zone width (ft); and

W_{ocb} = distance from edge of outside shoulder to barrier face (ft).

This CMF is derived to be applicable to a segment that has roadside barrier present along some portion of the segment. Guidance for computing the variables P_{ob} and W_{ocb} is provided in Section 18.7.3. The CMF is applicable to clear zone widths of 30 ft or less, W_{ocb} values in the range of 0.75 to 17 ft, and to shoulder widths in the range of 4 to 14 ft.

CMF_{11, fs, ac, sv, z}—Outside Barrier

Two CMFs are used to describe the relationship between outside barrier presence and predicted crash frequency. The SPFs to which they apply are identified in the following list:

- SPF for fatal-and-injury single-vehicle crashes, specified number of lanes (fs, n, sv, fi); and
- SPF for property-damage-only single-vehicle crashes, specified number of lanes (fs, n, sv, pdo).

The base condition is no barrier present in the clear zone. The CMFs are described using the following equation.

$$CMF_{11, fs, ac, sv, z} = (1.0 - P_{ob}) \times 1.0 + P_{ob} \times \exp\left(\frac{a}{W_{ocb}}\right) \quad \text{Equation 18-39}$$

Where:

$CMF_{11, fs, ac, sv, z}$ = crash modification factor for roadside barrier in a freeway segment with any cross section ac , single-vehicle crashes sv , and severity z .

The regression coefficient for Equation 18-39 is provided in Table 18-22. Guidance for computing the variables P_{ob} and W_{ocb} is provided in Section 18.7.3.

Table 18-22. Coefficients for Outside Barrier CMF—Freeway Segments

Cross Section (x)	Crash Type (y)	Crash Severity (z)	CMF Variable	Regression Coefficient (a)
Any cross section (ac)	Single vehicle (sv)	Fatal and injury (fi)	$CMF_{11, fs, ac, sv, fi}$	0.131
		Property damage only (pdo)	$CMF_{11, fs, ac, sv, pdo}$	0.169

The variable W_{ocb} represents the distance from the edge of outside shoulder to roadside barrier face. The value used for this variable in Equation 18-39 is an average for the segment. The CMF is applicable to W_{ocb} values in the range of 0.75 to 17 ft. This CMF is applicable to cable barrier, concrete barrier, guardrail, and bridge rail.

18.7.2. Crash Modification Factors for Speed-Change Lanes

The CMFs for geometric design and traffic control features of speed-change lanes are presented in this section.

CMF_{1, w, x, y, z}—Horizontal Curve

Two CMFs are used to describe the relationship between horizontal curve geometry and predicted crash frequency. The SPFs to which they apply are identified in the following list:

- SPF for fatal-and-injury crashes, ramp entrance, freeway lanes n (sc, nEN, at, fi);
- SPF for property-damage-only crashes, ramp entrance, freeway lanes n (sc, nEN, at, pdo);
- SPF for fatal-and-injury crashes, ramp exit, freeway lanes n (sc, nEX, at, fi); and
- SPF for property-damage-only crashes, ramp exit, freeway lanes n (sc, nEX, at, pdo).

The base condition is an uncurved (i.e., tangent) alignment through the speed-change lane. The CMFs are described using the following equation.

$$CMF_{1, sc, ac, at, z} = 1.0 + a \times \left[\sum_{i=1}^m \left(\frac{5,730}{R_i} \right)^2 \times P_{c,i} \right] \quad \text{Equation 18-40}$$

Where:

$CMF_{1, sc, ac, at, z}$ = crash modification factor for horizontal curvature at a speed-change lane with any cross section ac , all crash types at , and severity z ;

R_i = radius of curve i (ft);

$P_{c,i}$ = proportion of speed-change lane length with curve i ; and

m = number of horizontal curves in the speed-change lane.

The regression coefficient for Equation 18-40 is provided in Table 18-23. The variable $P_{c,i}$ is computed as the ratio of the length of curve i in the speed-change lane to the length of the speed-change lane L_{en} or L_{ex} . Additional discussion of this CMF is provided in Section 18.7.1.

Table 18-23. Coefficients for Horizontal Curve CMF—Speed-Change Lanes

Cross Section (x)	Crash Type (y)	Crash Severity (z)	CMF Variable	Regression Coefficient (a)
Any cross section (ac)	All types (at)	Fatal and injury (fi)	$CMF_{1, sc, ac, at, fi}$	0.0172
		Property damage only (pdo)	$CMF_{1, sc, ac, at, pdo}$	0.0340

CMF_{2, w, x, y, fi}—Lane Width

One CMF is used to describe the relationship between average lane width and predicted crash frequency. The SPFs to which it applies are identified in the following list:

- SPF for fatal-and-injury crashes, ramp entrance, freeway lanes n (sc, nEN, at, fi); and
- SPF for fatal-and-injury crashes, ramp exit, freeway lanes n (sc, nEX, at, fi).

The base condition is a 12-ft lane width. The CMF is described using the following equation.

$$CMF_{2,sc,ac,at,fi} = \begin{cases} \exp(-0.0376 \times [W_l - 12]) & : \text{If } W_l < 13 \text{ ft} \\ 0.963 & : \text{If } W_l \geq 13 \text{ ft} \end{cases} \quad \text{Equation 18-41}$$

Where:

$CMF_{2,sc,ac,at,fi}$ = crash modification factor for lane width at a speed-change lane with any cross section ac , all crash types at , and fatal-and-injury crashes fi ; and

W_l = lane width (ft).

The CMF is applicable to lane widths in the range of 10.5 to 14 ft.

$CMF_{3,w,x,y,z}$ —Inside Shoulder Width

Two CMFs are used to describe the relationship between average inside shoulder width and predicted crash frequency. The SPFs to which they apply are identified in the following list:

- SPF for fatal-and-injury crashes, ramp entrance, freeway lanes n (sc, nEN, at, fi);
- SPF for property-damage-only crashes, ramp entrance, freeway lanes n (sc, nEN, at, pdo);
- SPF for fatal-and-injury crashes, ramp exit, freeway lanes n (sc, nEX, at, fi); and
- SPF for property-damage-only crashes, ramp exit, freeway lanes n (sc, nEX, at, pdo).

The base condition is a 6-ft inside shoulder width. The CMFs are described using the following equation.

$$CMF_{3,sc,ac,at,z} = \exp(a \times [W_{is} - 6]) \quad \text{Equation 18-42}$$

Where:

$CMF_{3,sc,ac,at,z}$ = crash modification factor for inside shoulder width at a speed-change lane with any cross section ac , all crash types at , and severity z ; and

W_{is} = inside shoulder width (ft).

The regression coefficient for Equation 18-42 is provided in Table 18-24. The CMF is applicable to shoulder widths in the range of 2 to 12 ft.

Table 18-24. Coefficients for Inside Shoulder Width CMF–Speed-Change Lanes

Cross Section (<i>x</i>)	Crash Type (<i>y</i>)	Crash Severity (<i>z</i>)	CMF Variable	Regression Coefficient (<i>a</i>)
Any cross section (<i>ac</i>)	All types (<i>at</i>)	Fatal and injury (<i>fi</i>)	$CMF_{3, sc, ac, at, fi}$	-0.0172
		Property damage only (<i>pdo</i>)	$CMF_{3, sc, ac, at, pdo}$	-0.0153

CMF_{4, w, x, y, z}—Median Width

Two CMFs are used to describe the relationship between median width and predicted crash frequency. The SPFs to which they apply are identified in the following list:

- SPF for fatal-and-injury crashes, ramp entrance, freeway lanes *n* (*sc, nEN, at, fi*);
- SPF for property-damage-only crashes, ramp entrance, freeway lanes *n* (*sc, nEN, at, pdo*);
- SPF for fatal-and-injury crashes, ramp exit, freeway lanes *n* (*sc, nEX, at, fi*); and
- SPF for property-damage-only crashes, ramp exit, freeway lanes *n* (*sc, nEX, at, pdo*).

The base condition is a 60-ft median width, a 6-ft inside shoulder width, and no barrier present in the median. The CMFs are described using the following equation.

$$CMF_{4, sc, ac, at, z} = (1.0 - P_{ib}) \times \exp(a \times [W_m - 2 \times W_{is} - 48]) + P_{ib} \times \exp(a \times [2 \times W_{icb} - 48]) \quad \text{Equation 18-43}$$

Where:

$CMF_{4, sc, ac, at, z}$ = crash modification factor for median width at a speed-change lane with any cross section *ac*, all crash types *at*, and severity *z*;

P_{ib} = proportion of speed-change lane length with a barrier present in the median (i.e., inside);

W_m = median width (measured from near edges of traveled way in both directions) (ft); and

W_{icb} = distance from edge of inside shoulder to barrier face (ft).

The regression coefficient for Equation 18-43 is provided in Table 18-25. These CMFs are derived to be applicable to a speed-change lane that has median barrier present along some portion of its length. Guidance for computing the variables P_{ib} and W_{icb} is provided in Section 18.7.3.

Table 18-25. Coefficients for Median Width CMF–Speed-Change Lanes

Cross Section (<i>x</i>)	Crash Type (<i>y</i>)	Crash Severity (<i>z</i>)	CMF Variable	Regression Coefficient (<i>a</i>)
Any cross section (<i>ac</i>)	All types (<i>at</i>)	Fatal and injury (<i>fi</i>)	$CMF_{4, sc, ac, at, fi}$	-0.00302
		Property damage only (<i>pdo</i>)	$CMF_{4, sc, ac, at, pdo}$	-0.00291

The CMF is applicable to median widths 9 ft or more, W_{icb} values in the range of 0.75 to 17 ft, and shoulder widths in the range of 2 to 12 ft. If the median width exceeds 90 ft, then 90 ft should be used for W_m in Equation 18-43.

CMF_{5,w,x,y,z}—Median Barrier

Two CMFs are used to describe the relationship between median barrier presence and predicted crash frequency. The SPFs to which they apply are identified in the following list:

- SPF for fatal-and-injury crashes, ramp entrance, freeway lanes n (sc, nEN, at, fi);
- SPF for property-damage-only crashes, ramp entrance, freeway lanes n (sc, nEN, at, pdo);
- SPF for fatal-and-injury crashes, ramp exit, freeway lanes n (sc, nEX, at, fi); and
- SPF for property-damage-only crashes, ramp exit, freeway lanes n (sc, nEX, at, pdo).

The base condition is no barrier present in the median. The CMFs are described using the following equation.

$$CMF_{5,sc,ac,at,z} = (1.0 - P_{ib}) \times 1.0 + P_{ib} \times \exp\left(\frac{a}{W_{icb}}\right) \quad \text{Equation 18-44}$$

Where:

$CMF_{5,sc,ac,at,z}$ = crash modification factor for median barrier at a speed-change lane with any cross section ac , all crash types at , and severity z .

The regression coefficient for Equation 18-44 is provided in Table 18-26. Guidance for computing the variables P_{ib} and W_{icb} is provided in Section 18.7.3.

Table 18-26. Coefficients for Median Barrier CMF–Speed-Change Lanes

Cross Section (x)	Crash Type (y)	Crash Severity (z)	CMF Variable	Regression Coefficient (a)
Any cross section (ac)	All types (at)	Fatal and injury (fi)	$CMF_{5,sc,ac,at,fi}$	0.131
		Property damage only (pdo)	$CMF_{5,sc,ac,at,pdo}$	0.169

The CMF is applicable to W_{icb} values in the range of 0.75 to 17 ft. This CMF is applicable to cable barrier, concrete barrier, guardrail, and bridge rail.

CMF_{6,w,x,y,z}—High Volume

Two CMFs are used to describe the relationship between volume concentration and predicted crash frequency. The SPFs to which they apply are identified in the following list:

- SPF for fatal-and-injury crashes, ramp entrance, freeway lanes n (sc, nEN, at, fi);
- SPF for property-damage-only crashes, ramp entrance, freeway lanes n (sc, nEN, at, pdo);
- SPF for fatal-and-injury crashes, ramp exit, freeway lanes n (sc, nEX, at, fi); and

- SPF for property-damage-only crashes, ramp exit, freeway lanes n (sc, nEX, at, pdo).

The base condition is no hours having a volume that exceeds 1,000 veh/h/ln. The CMFs are described using the following equation.

$$CMF_{6,sc,ac,at,z} = \exp(a \times P_{hv}) \quad \text{Equation 18-45}$$

Where:

$CMF_{6,sc,ac,at,z}$ = crash modification factor for high volume at a speed-change lane with any cross section ac , all crash types at , and severity z ; and

P_{hv} = proportion of AADT during hours where volume exceeds 1,000 veh/h/ln.

The regression coefficient for Equation 18-45 is provided in Table 18-27. Additional discussion of this CMF is provided in Section 18.7.1.

Table 18-27. Coefficients for High Volume CMF–Speed-Change Lanes

Cross Section (x)	Crash Type (y)	Crash Severity (z)	CMF Variable	Regression Coefficient (a)
Any cross section (ac)	All types (at)	Fatal and injury (fi)	$CMF_{6,sc,ac,at,fi}$	0.350
		Property damage only (pdo)	$CMF_{6,sc,ac,at,pdo}$	0.283

$CMF_{12,sc,nEN,at,z}$ —Ramp Entrance

Two CMFs are used to describe the relationship between ramp entrance geometry and predicted crash frequency. The SPFs to which they apply are identified in the following list:

- SPF for fatal-and-injury crashes, ramp entrance, freeway lanes n (sc, nEN, at, fi); and
- SPF for property-damage-only crashes, ramp entrance, freeway lanes n (sc, nEN, at, pdo).

The CMFs are described using the following equation.

$$CMF_{12,sc,nEN,at,z} = \exp\left(a \times I_{left} + \frac{b}{L_{en}} + d \times \ln[c \times AADT_r]\right) \quad \text{Equation 18-46}$$

Where:

$CMF_{12,sc,nEN,at,z}$ = crash modification factor for ramp entrance geometry on a freeway with n lanes with all crash types at and severity z ;

L_{en} = length of ramp entrance (mi);

I_{left} = ramp side indicator variable (= 1.0 if entrance or exit is on left side of through lanes, 0.0 if it is on right side); and

$AADT_r$ = AADT volume of ramp (veh/day).

The regression coefficients for Equation 18-46 are provided in Table 18-28.

Table 18-28. Coefficients for Ramp Entrance CMF–Speed-Change Lanes

Cross Section (x)	Crash Type (y)	Crash Severity (z)	CMF Variable	Regression Coefficients			
				a	b	c	d
Ramp entrance, n lanes (nEN)	All types (at)	Fatal and injury (fi)	$CMF_{12, sc, nEN, at, fi}$	0.594	0.0318	0.001	0.198
		Property damage only (pdo)	$CMF_{12, sc, nEN, at, pdo}$	0.824	0.0252	0.001	0.00

This CMF is applicable to a ramp entrance speed-change lane, as shown in Figure 18-10. The ramp entrance length is measured using the reference points identified in Figure 18-3.

The variable for ramp entrance length L_{en} in Equation 18-46 is intended to reflect the degree to which the lane-changing activity is concentrated along the ramp entrance. The CMF is applicable to ramp entrance lengths in the range of 0.04 to 0.30 mi (210 to 1,600 ft). It is applicable to the range of ramp AADTs in Table 19-4 of Chapter 19.

The indicator variable for ramp side I_{left} is associated with a positive regression coefficient. This sign indicates that a ramp entrance on the left side of the through lanes is associated with an increase in crash frequency, relative to one on the right side. The data used to calibrate this CMF represent freeways where ramp entrances are typically located on the right side.

CMF_{13, sc, nEX, at, z}—Ramp Exit

Two CMFs are used to describe the relationship between ramp exit geometry and predicted crash frequency. The SPFs to which they apply are identified in the following list:

- SPF for fatal-and-injury crashes, ramp exit, freeway lanes n (sc, nEX, at, fi); and
- SPF for property-damage-only crashes, ramp exit, freeway lanes n (sc, nEX, at, pdo).

The CMFs are described using the following equation.

$$CMF_{13, sc, nEX, at, z} = \exp\left(a \times I_{left} + \frac{b}{L_{ex}}\right) \quad \text{Equation 18-47}$$

Where:

$CMF_{13, sc, nEX, at, z}$ = crash modification factor for ramp exit geometry on a freeway with n lanes with all crash types at and severity z ;

L_{ex} = length of ramp exit (mi); and

I_{left} = ramp side indicator variable (= 1.0 if entrance or exit is on left side of through lanes, 0.0 if it is on right side).

The regression coefficients for Equation 18-47 are provided in Table 18-29.

Table 18-29. Coefficients for Ramp Exit CMF–Speed-Change Lanes

Cross Section (x)	Crash Type (y)	Crash Severity (z)	CMF Variable	Regression Coefficients	
				a	b
Ramp exit, <i>n</i> lanes (<i>nEX</i>)	All types (<i>at</i>)	Fatal and injury (<i>fi</i>)	$CMF_{13, sc, nEX, at, fi}$	0.594	0.0116
		Property damage only (<i>pdo</i>)	$CMF_{13, sc, nEX, at, pdo}$	0.824	0.00

This CMF is applied to a ramp exit speed-change lane, as shown in Figure 18-10. The ramp exit length is measured using the reference points identified in Figure 18-3.

The variable for ramp exit length L_{ex} in Equation 18-47 is intended to reflect the degree to which the lane-changing activity is concentrated along the ramp exit. The CMF is applicable to ramp exit lengths in the range of 0.02 to 0.30 mi (106 to 1600 ft).

The indicator variable for ramp side I_{left} is associated with a positive regression coefficient. This sign indicates that a ramp exit on the left side of the through lanes is associated with an increase in crash frequency, relative to one on the right side. The data used to calibrate this CMF represent freeways where ramp exits are typically located on the right side.

18.7.3. Supplemental Calculations to Apply Crash Modification Factors

Some of the CMFs in Section 18.7.1 and Section 18.7.2 require the completion of supplemental calculations before they can be applied to the SPFs in Section 18.6. These CMFs are:

- Median width.
- Median barrier.
- Outside clearance.
- Outside barrier.

These four CMFs include variables that describe the presence of barrier in the median or on the roadside. These variables include barrier offset, length, and width.

Barrier offset represents a lateral distance measured from the near edge of the shoulder to the face of the barrier (i.e., it does not include the width of the shoulder). Barrier length represents the length of lane paralleled by a barrier; it is a total for both travel directions. For example, if the outside barrier extends for the length of the roadway on both sides of the roadway, then the outside barrier length equals twice the segment length.

Median barrier width represents either (a) the physical width of the barrier if only one barrier is used or (b) the lateral distance between barrier “faces” if two parallel barriers are provided in the median area. A barrier face is the side of the barrier that is exposed to traffic.

Two key variables that are needed for the evaluation of barrier presence are the inside barrier offset distance W_{icb} and the outside barrier offset distance W_{ocb} . As indicated in Equation 18-28 and Equation 18-39, this distance is included as a divisor in the exponential term. This relationship implies that the correlation between barrier distance and crash frequency is an inverse one (i.e., crash frequency decreases with increasing distance to the barrier). When multiple sections of barrier exist along the segment, a length-

weighted average of the *reciprocal* of the individual distances is needed to properly reflect this inverse relationship. The length used to weight the average is the barrier length.

Additional key variables include the proportion of segment length with a barrier present in the median P_{ib} and the proportion of segment length with a barrier present on the roadside P_{ob} . Equations for calculating these proportions and the aforementioned distances are described in the following paragraphs.

The length of segment L used in the following equations is equal to that of the freeway segment L_{fs} or speed-change lane L_{ex} , L_{en} , as appropriate for the CMF to which the calculated value will be applied. If the median width exceeds 90 ft, then 90 ft should be used for W_m in the following equations.

For segments or speed-change lanes with a continuous barrier centered in the median (i.e., symmetric median barrier), the following equations are used to estimate W_{icb} and P_{ib} .

$$W_{icb} = \frac{2 \times L}{\sum \frac{L_{ib,i}}{W_{off,in,i} - W_{is}} + \frac{2 \times L - \sum L_{ib,i}}{0.5 \times (W_m - 2 \times W_{is} - W_{ib})}} \quad \text{Equation 18-48}$$

$$P_{ib} = 1.0 \quad \text{Equation 18-49}$$

Where:

W_{icb} = distance from edge of inside shoulder to barrier face (ft);

P_{ib} = proportion of segment length with a barrier present in the median (i.e., inside);

L = length of segment (mi);

$L_{ib,i}$ = length of lane paralleled by inside barrier i (include both travel directions) (mi);

W_{ib} = inside barrier width (measured from barrier face to barrier face) (ft);

W_{is} = inside shoulder width (ft);

W_m = median width (measured from near edges of traveled way in both directions) (ft); and

$W_{off,in,i}$ = horizontal clearance from the edge of the traveled way to the face of inside barrier i (ft).

The first summation term “ \sum ” in Equation 18-48 applies to short lengths of barrier in the median. It indicates that the ratio of barrier length $L_{ib,i}$ to clearance distance ($= W_{off,in,i} - W_{is}$) should be computed for each individual length of barrier that is found in the median along the segment (e.g., a barrier protecting a sign support). The continuous median barrier is not considered in this summation. Any clearance distance that is less than 0.75 ft should be set to 0.75 ft. Similarly, if the distance “ $0.5 \times (W_m - 2 \times W_{is} - W_{ib})$ ” is less than 0.75 ft, then it should be set to 0.75 ft.

For segments or speed-change lanes with a continuous barrier adjacent to one roadbed (i.e., asymmetric median barrier), the following equations should be used to estimate W_{icb} and P_{ib} .

$$W_{icb} = \frac{2 \times L}{\frac{L}{W_{near} - W_{is}} + \sum \frac{L_{ib,i}}{W_{off,in,i} - W_{is}} + \frac{L - \sum L_{ib,i}}{W_m - 2 \times W_{is} - W_{ib} - W_{near}}} \quad \text{Equation 18-50}$$

$$P_{ib} = 1.0 \quad \text{Equation 18-51}$$

Where:

W_{near} = “near” horizontal clearance from the edge of the traveled way to the continuous median barrier (measure for both travel directions and use the smaller distance) (ft).

Similar to the previous guidance, the first summation term “ \sum ” in Equation 18-50 applies to short lengths of barrier in the median. The ratio of barrier length L_{ib} to the clearance distance ($= W_{off,in,i} - W_{is}$) should be computed for each individual length of barrier that is found in the median along the segment. The continuous median barrier is not considered in this summation. Any clearance distance that is less than 0.75 ft should be set to 0.75 ft. Similarly, if the distance “ $W_{near} - W_{is}$ ” or the distance “ $W_m - 2 \times W_{is} - W_{ib} - W_{near}$ ” is less than 0.75 ft, then it should be set to 0.75 ft.

For segments or speed-change lanes with a depressed median and some short sections of barrier in the median (e.g., bridge rail), the following equations should be used to estimate W_{icb} and P_{ib} .

$$W_{icb} = \frac{\sum L_{ib,i}}{\sum \frac{L_{ib,i}}{W_{off,in,i} - W_{is}}} \quad \text{Equation 18-52}$$

$$P_{ib} = \frac{\sum L_{ib,i}}{2 \times L} \quad \text{Equation 18-53}$$

Any clearance distance ($= W_{off,in,i} - W_{is}$) that is less than 0.75 ft should be set to 0.75 ft.

For segments or speed-change lanes with depressed medians without a continuous barrier or short sections of barrier in the median, the following equation should be used to estimate P_{ib} .

$$P_{ib} = 0.0 \quad \text{Equation 18-54}$$

As suggested by Equation 18-28, the calculation of W_{icb} is not required when $P_{ib} = 0.0$.

For segments or speed-change lanes with barrier on the roadside, the following equations should be used to estimate W_{ocb} and P_{ob} .

$$W_{ocb} = \frac{\sum L_{ob,i}}{\sum \frac{L_{ob,i}}{W_{off,o,i} - W_s}} \quad \text{Equation 18-55}$$

$$P_{ob} = \frac{\sum L_{ob,i}}{2 \times L} \quad \text{Equation 18-56}$$

Where:

$L_{ob, i}$ = length of lane paralleled by outside barrier i (include both travel directions) (mi);

P_{ob} = proportion of segment length with a barrier present on the roadside (i.e., outside);

W_{ocb} = distance from edge of outside shoulder to barrier face (ft);

W_s = outside shoulder width (ft); and

$W_{off, o, i}$ = horizontal clearance from the edge of the traveled way to the face of outside barrier i (ft).

Any clearance distance ($= W_{off, o, i} - W_s$) that is less than 0.75 ft should be set to 0.75 ft.

For segments or speed-change lanes without barrier on the roadside, the following equation should be used to estimate P_{ob} .

$$P_{ob} = 0.0 \quad \text{Equation 18-57}$$

As suggested by Equation 18-39, the calculation of W_{ocb} is not required when $P_{ob} = 0.0$.

18.8. SEVERITY DISTRIBUTION FUNCTIONS

The severity distribution functions (SDFs) are presented in this section. They are used in the predictive model to estimate the expected average crash frequency for the following severity levels: fatal K , incapacitating injury A , non-incapacitating injury B , and possible injury C . Each SDF was developed as a regression model using observed crash data for a set of similar sites as the dependent variable. The SDF, like all regression models, estimates the value of the dependent variable as a function of a set of independent variables. The independent variables include various geometric features, traffic control features, and area type (i.e., rural or urban). The SDFs described in this section are equally applicable to freeway segments and speed-change lanes.

The general model form for the severity distribution prediction is shown in the following equation.

$$N_{e, w, x, y, j} = N_{e, w, x, y, fi} \times P_{w, ac, at, j} \quad \text{Equation 18-58}$$

Where:

$N_{e, w, x, y, j}$ = expected average crash frequency for site type w , cross section or control type x , crash type y , and severity level j ($j = K$: fatal, A : incapacitating injury, B : non-incapacitating injury, C : possible injury) (crashes/yr);

$N_{e, w, x, y, fi}$ = expected average crash frequency for site type w , cross section or control type x , crash type y , and fatal-and-injury crashes fi (crashes/yr); and

$P_{w, x, at, j}$ = probability of the occurrence of severity level j ($j = K$: fatal, A : incapacitating injury, B : non-incapacitating injury, C : possible injury) for all crash types at at site type w with cross section or control type x .

There is one SDF associated with each probability level j in the predictive model. An SDF predicts the probability of occurrence of severity level j for a crash based on various geometric design and traffic control features at the subject site. Each SDF also contains a calibration factor that is used to calibrate it to local conditions.

The SDFs for freeway segments and speed-change lanes are described by the following equations.

$$P_{fs+sc,ac,at,K} = \frac{\exp(V_K)}{\frac{1.0}{C_{sdf,fs+sc}} + \exp(V_K) + \exp(V_A) + \exp(V_B)} \quad \text{Equation 18-59}$$

$$P_{fs+sc,ac,at,A} = \frac{\exp(V_A)}{\frac{1.0}{C_{sdf,fs+sc}} + \exp(V_K) + \exp(V_A) + \exp(V_B)} \quad \text{Equation 18-60}$$

$$P_{fs+sc,ac,at,B} = \frac{\exp(V_B)}{\frac{1.0}{C_{sdf,fs+sc}} + \exp(V_K) + \exp(V_A) + \exp(V_B)} \quad \text{Equation 18-61}$$

$$P_{fs+sc,ac,at,C} = 1.0 - (P_K + P_A + P_B) \quad \text{Equation 18-62}$$

with,

$$V_j = a + \left(b \times \frac{P_{ib} + P_{ob}}{2} \right) + (c \times P_{hv}) + \left(d \times \frac{P_{ir} + P_{or}}{2} \right) + \left(e \times \sum P_{c,i} \right) + (f \times W_l) + (g \times I_{rural}) \quad \text{Equation 18-63}$$

Where:

- V_j = systematic component of crash severity likelihood for severity level j ;
- $C_{sdf,fs+sc}$ = calibration factor to adjust SDF for local conditions for freeway segments and speed-change lanes;
- P_{ib} = proportion of segment length with a barrier present in the median (i.e., inside);
- P_{ob} = proportion of segment length with a barrier present on the roadside (i.e., outside);
- P_{hv} = proportion of AADT during hours where volume exceeds 1,000 veh/h/ln;
- P_{ir} = proportion of segment length with rumble strips present on the inside shoulders;
- P_{or} = proportion of segment length with rumble strips present on the outside shoulders;
- $P_{c,i}$ = proportion of segment length with curve i ;
- W_l = lane width (ft);
- I_{rural} = area type indicator variable (= 1.0 if area is rural, 0.0 if it is urban); and

a, b, c, d, e, f, g = regression coefficients.

The SDF regression coefficients in Equation 18-63 are provided in Table 18-30. Guidance for computing the variables P_{ib} and P_{ob} is provided in Section 18.7.3.

Table 18-30. SDF Coefficients for Freeway Segments and Speed-Change Lanes

Severity Level (<i>j</i>)	Variable	Regression Coefficients						
		<i>a</i>	<i>b</i>	<i>c</i>	<i>d</i>	<i>e</i>	<i>f</i>	<i>g</i>
Fatal (<i>K</i>)	V_K	-0.171	-0.388	-0.924	0.387	0.208	-0.261	0.492
Incapacitating injury (<i>A</i>)	V_A	-2.393	-0.325	-0.853	0.391	0.243	0.00	0.430
Non-incapacitating inj. (<i>B</i>)	V_B	0.0732	-0.250	-0.872	0.135	0.131	-0.0464	0.208

The proportion of AADT during hours where the volume exceeds 1,000 veh/h/ln is computed using the average hourly volume distribution associated with the subject segment. This distribution will typically be computed using the data obtained from the continuous traffic counting station that (1) is nearest to the subject freeway and (2) has similar traffic demand and peaking characteristics. The SDF is applicable to P_{hw} values in the range of 0.0 to 1.0. Additional discussion of this variable is provided in Section 18.7.1 for the High Volume CMF.

The proportion P_{ir} is computed by summing the length of roadway with rumble strips on the inside shoulder in *both* travel directions and dividing by twice the freeway segment length L_{fs} . The proportion P_{or} is computed by summing the length of roadway with rumble strips on the outside shoulder in *both* travel directions and dividing by twice the freeway segment length L_{fs} .

The variable $P_{c,i}$ is computed as the ratio of the length of curve *i* in the segment to the length of the freeway segment L_{fs} . For example, consider a segment that is 0.5 mi long and a curve that is 0.2 mi long. If one-half of the curve is in the segment, then $P_{c,i} = 0.20$ ($= 0.1/0.5$). In fact, this proportion is the same regardless of the curve's length (provided that it is 0.1 mi or longer and 0.1 mi of this curve is located in the segment). When the SDF is applied to a speed-change lane, the variable $P_{c,i}$ is computed as the ratio of the length of curve *i* in the speed-change lane to the length of the speed-change lane L_{en} or L_{ex} .

The SDF is applicable to lane widths in the range of 10.5 to 14 ft.

The sign of a regression coefficient in Table 18-30 indicates the change in the proportion of crashes associated with a change in the corresponding variable. For example, the negative coefficient associated with barrier presence indicates that the proportion of fatal *K* crashes decreases with an increase in the proportion of barrier present in the segment. A similar trend is indicated for barrier presence on incapacitating injury *A* crashes and non-incapacitating injury *B* crashes. By inference, the proportion of possible injury *C* crashes *increases* with an increase in the proportion of barrier present.

18.9. CALIBRATION OF THE SPFS AND SDFS TO LOCAL CONDITIONS

Crash frequencies, even for nominally similar freeway segments or speed-change lanes, can vary widely from one jurisdiction to another. Geographic regions differ markedly in climate, animal population, driver populations, crash-reporting threshold, and crash-reporting practices. These variations may result in some jurisdictions experiencing a different number of traffic crashes on freeways than others. Calibration factors are included in the methodology to allow highway agencies to adjust the SPFs and SDFs to match actual local conditions.

The SPF calibration factors will have values greater than 1.0 for segments or speed-change lanes that, on average, experience more crashes than those used in the development of the SPFs. Similarly, the calibration factors for segments or speed-change lanes that experience fewer crashes on average than those used in the

development of the SPFs will have values less than 1.0. The calibration procedures for SPFs are presented in Section B.1.1 of Appendix B to Part C.

The SDF calibration factors will have values greater than 1.0 for segments or speed-change lanes that, on average, experience more severe crashes than those used in the development of the SDFs. Similarly, the calibration factors for segments or speed-change lanes that experience fewer severe crashes on average than those used in the development of the SDFs will have values less than 1.0. The calibration procedures for SDFs are presented in Section B.1.4 of Appendix B to Part C.

Default values are also provided for the crash type distributions used in the methodology. These values can also be replaced with locally derived values. The derivation of these values is addressed in Section B.1.3 of Appendix B to Part C.

18.10. LIMITATIONS OF PREDICTIVE METHOD

The limitations of the predictive method which apply generally across all of the Part C chapters are discussed in Section C.14 of Part C. This section discusses limitations of the predictive models described in this chapter.

The predictive method described in this chapter can be applied to the combinations of area type (rural or urban) and number of lanes that are listed in Section 18.6. The method can be extended to freeway segments with unequal number of lanes in opposing directions, but only if the number of lanes is within the ranges listed in Section 18.6.1 and varies by no more than one lane between the two travel directions.

The predictive method does not account for the influence of the following conditions on freeway safety:

- Freeways with 11 or more through lanes in urban areas.
- Freeways with 9 or more through lanes in rural areas.
- Freeways with continuous access high-occupancy vehicle (HOV) lanes.
- Freeways with limited access managed lanes that are buffer-separated from the general purpose lanes.
- Ramp metering.
- Use of safety shoulders as travel lanes.
- Toll plazas.
- Reversible lanes.

The predictive method does not distinguish between barrier types (i.e., cable barrier, concrete barrier, guardrail, and bridge rail) in terms of their possible different influence on crash severity.

18.11. APPLICATION OF PREDICTIVE METHOD

The predictive method presented in this chapter is applied to a freeway facility by following the 18 steps presented in Section 18.4. Worksheets are provided in Appendix 13A for applying calculations in the predictive method. All computations of crash frequencies within these worksheets are conducted with values expressed to three decimal places. This level of precision is needed only for consistency in computations. In the last stage of computations, rounding the final estimates of expected average crash frequency to one decimal place is appropriate.

18.11.1. Freeways with Barrier-Separated Managed Lanes

The predictive method can be used to evaluate freeways with barrier-separated managed lanes. The managed lanes are considered to be part of the median (i.e., the median width is measured between the near edges of the traveled way for the general purpose lanes) and the managed lane's entry or exit points are treated as entrance or exit ramps, respectively, on the adjacent freeway. The average lane width is based on the general purpose lanes (i.e., the managed lanes are not considered). The shoulder width is measured from the edge of the general-purpose-lanes traveled way. The barrier between the general purpose lanes and managed lanes is treated as median barrier.

The safety of the managed lanes is not addressed by this technique. The estimate of expected average crash frequency only includes crashes that occur in the general purpose lanes.

18.11.2. Freeways with Toll Facilities

The predictive method can be used to evaluate a freeway section that is part of toll facility provided that the section is sufficiently distant from the toll facility that the facility does not influence vehicle operation. The predictive method is not directly applicable to any portion of the freeway that (a) is in the immediate vicinity of a toll plaza, (b) is widened to accommodate vehicle movements through the toll plaza, (c) experiences toll-related traffic queues, or (d) experiences toll-related speed changes.

18.12. SUMMARY

The predictive method for freeways is applied by following the 18 steps of the predictive method presented in Section 18.4. It is used to estimate the expected average crash frequency for a series of contiguous sites, or a single individual site. If a freeway facility is being evaluated, then it is divided into a series of sites in Step 5 of the predictive method. Predictive models are applied in Steps 9, 10, and 11 of the method to estimate the expected average crash frequency of each site.

Each predictive model consists of a safety performance function (SPF), crash modification factors (CMFs), a severity distribution function (SDF), and calibration factors. The SPF is selected in Step 9. It is used to estimate the predicted average crash frequency for a site with base conditions. CMFs are selected in Step 10. They are combined with the estimate from the SPF to produce the expected average crash frequency for the subject site. Optionally, the SDFs are selected in Step 13. They can be used to estimate the expected average crash frequency for one or more crash severity levels (i.e., fatal, incapacitating injury, non-incapacitating injury, or possible injury crash). Optionally, the crash type distribution can be used in Step 13 to estimate the expected crash frequency for one or more crash types (e.g., head-on, fixed object).

When observed crash data are available, the EB Method is applied in Step 13 or 15 of the predictive method to improve the reliability of the estimated expected average crash frequency. The EB Method can be applied at the site-specific level in Step 13, or at the project level in Step 15. The choice of level will depend on (a) the required reliability of the estimate and (b) the accuracy with which each observed crash can be associated with an individual site. The EB Method is described in Section B.2 of Appendix B to Part C.

The SPF is calibrated to the specific state or geographic region in which the project is located. Calibration accounts for differences in state or regional crash frequencies, relative to the states and regions represented in the data used to define the predictive models described in this chapter. The process for determining calibration factors for the predictive models is described in Section B.1 of Appendix B to Part C.

Section 18.13 presents several sample problems that detail the application of the predictive method. A series of worksheets are used to guide the method application and document the calculations. The use of these worksheets is illustrated in the sample problems. Appendix 18A contains blank worksheets that can be copied to document future method applications.

18.13. SAMPLE PROBLEMS

In this section, six sample problems are presented using the predictive method steps for freeway facilities. Sample Problems 1 and 2 illustrate how to calculate the predicted average crash frequency for freeway segments. Sample Problem 3 illustrates how to calculate the predicted average crash frequency for an entrance-ramp speed-change lane. Sample Problem 4 illustrates a similar calculation for an exit-ramp speed-change lane. Sample Problem 5 illustrates how to combine the results from Sample Problems 1 and 2 in a case where site-specific observed crash data are available (i.e., using the site-specific EB Method). Sample Problem 6 illustrates how to combine the results from Sample Problems 1 and 2 in a case where crash data are available but cannot be assigned to specific segments (i.e., using the project-level EB Method).

Table 18-31. List of Sample Problems

Problem No.	Description
1	Predicted average crash frequency for a tangent six-lane urban freeway segment
2	Predicted average crash frequency for a six-lane urban freeway segment with a curve
3	Predicted average crash frequency for a urban freeway entrance-ramp speed-change lane
4	Predicted average crash frequency for a urban freeway exit-ramp speed-change lane
5	Expected average crash frequency for a facility when site-specific observed crash data are available
6	Expected average crash frequency for a facility when crash data are available, but cannot be assigned to specific segments

18.13.1. Sample Problem 1

The Site/Facility

A tangent six-lane urban freeway segment.

The Question

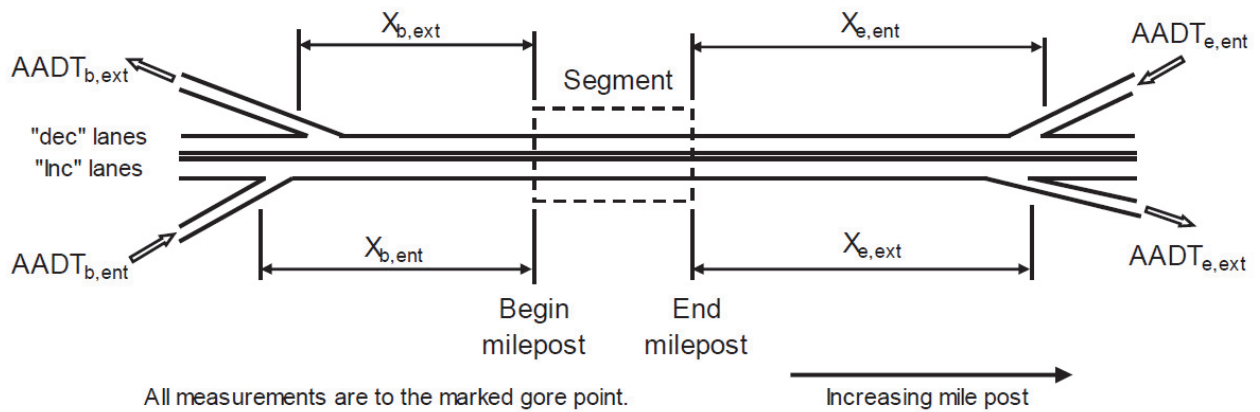
What is the predicted average crash frequency of the freeway segment for a one-year period?

The Facts

The study year is 2011. The conditions present during this year are provided in the following list.

- 0.75-mi length
- 120,000 veh/day
- 10 percent of AADT volume occurs during high-volume hours
- No horizontal curvature
- 12-ft lane width
- 10-ft outside shoulder width
- 6-ft inside shoulder width
- 40-ft median width

- No rumble strips on inside or outside shoulders
- No median or roadside barrier
- 30-ft clear zone width
- No Type B weaving sections
- Data to describe four ramps in the vicinity of the segment



Variable Subscript (a,b)	Distance from Segment, $X_{a,b}$ (mi)	Ramp Volume, $AADT_{a,b}$ (veh/day)
b, ent	0.5	8,000
e, ext	0.85	7,150
e, ent	0.85	6,750
b, ext	0.5	7,675

Assumptions

- Crash type distributions used are the default values presented in Table 18-6 and Table 18-8.
- The calibration factor is 1.00.

Results

Using the predictive method steps as outlined below, the predicted average fatal-and-injury crash frequency for the roadway segment in Sample Problem 1 is determined to be 6.0 crashes per year, and the predicted average property-damage-only crash frequency is determined to be 14.7 crashes per year (rounded to one decimal place).

Steps

Step 1 through 8

To determine the predicted average crash frequency of the freeway segment in Sample Problem 1, only Steps 9 through 13 are conducted. No other steps are necessary because only one freeway segment is analyzed for one year, and the EB Method is not applied.

Step 9 – For the selected site, determine and apply the appropriate SPF.

For a six-lane urban freeway segment, SPF values for multiple-vehicle and single-vehicle crashes are determined.

Multiple-Vehicle Crashes

The SPF for multiple-vehicle fatal-and-injury crashes is calculated from Equation 18-15 and Table 18-5 as follows:

$$\begin{aligned} N_{spf, fs, 6, mv, fi} &= L^* \times \exp(a + b \times \ln[c \times AADT_{fs}]) \\ &= 0.75 \times \exp(-5.587 + 1.492 \times \ln[0.001 \times 120,000]) \\ &= 3.555 \text{ crashes/year} \end{aligned}$$

Similarly, the SPF for multiple-vehicle property-damage-only crashes is calculated from Equation 18-15 and Table 18-5 to yield the following result:

$$N_{spf, fs, 6, mv, pdo} = 8.775 \text{ crashes/year}$$

Single-Vehicle Crashes

The SPF for single-vehicle fatal-and-injury crashes is calculated from Equation 18-18 and Table 18-7 as follows:

$$\begin{aligned} N_{spf, fs, 6, sv, fi} &= L^* \times \exp(a + b \times \ln[c \times AADT_{fs}]) \\ &= 0.75 \times \exp(-2.055 + 0.646 \times \ln[0.001 \times 120,000]) \\ &= 2.117 \text{ crashes/year} \end{aligned}$$

Similarly, the SPF for single-vehicle property-damage-only crashes is calculated from Equation 18-18 and Table 18-7 to yield the following result:

$$N_{spf, fs, 6, sv, pdo} = 5.115 \text{ crashes/year}$$

Step 10 – Multiply the result obtained in Step 9 by the appropriate CMFs.

Each CMF used in the calculation of the predicted average crash frequency of the freeway segment is calculated in this step.

Horizontal Curve (CMF_{1, fs, 6, y, z})

The segment does not have horizontal curvature. Hence, $CMF_{1, fs, 6, y, fi}$ and $CMF_{1, fs, 6, y, pdo}$ are equal to 1.000.

Lane Width (CMF_{2, fs, 6, y, z})

The segment has 12-ft lanes, which is the base condition for the lane width CMF. Hence, $CMF_{2, fs, 6, y, fi}$ and $CMF_{2, fs, 6, y, pdo}$ are equal to 1.000.

Inside Shoulder Width ($CMF_{3,fs,6,y,z}$)

The segment has 6-ft inside shoulders, which is the base condition for the inside shoulder width CMF. Hence, $CMF_{3,fs,6,y,fi}$ and $CMF_{3,fs,6,y,pdo}$ are equal to 1.000.

Median Width ($CMF_{4,fs,6,y,z}$)

$CMF_{4,fs,6,y,fi}$ is calculated from Equation 18-27 as follows:

$$CMF_{4,fs,6,y,fi} = (1.0 - P_{ib}) \times \exp(a \times [W_m - 2 \times W_{is} - 48]) + P_{ib} \times \exp(a \times [2 \times W_{icb} - 48])$$

The segment does not have inside barrier, so $P_{ib} = 0.0$ and the calculation of W_{icb} does not apply. From Table 18-17, $a = -0.00302$ for multiple-vehicle fatal-and-injury crashes. $CMF_{4,fs,6,mv,fi}$ is calculated as follows:

$$\begin{aligned} CMF_{4,fs,6,mv,fi} &= (1.0 - 0.0) \times \exp(-0.00302 \times [40 - 2 \times 6 - 48]) + 0.0 \times \exp(-0.00302 \times [2 \times W_{icb} - 48]) \\ &= 1.062 \end{aligned}$$

Calculations using the other coefficients from Table 18-17 yield the following results:

$$CMF_{4,fs,6,sv,fi} = 0.980$$

$$CMF_{4,fs,6,mv,pdo} = 1.060$$

$$CMF_{4,fs,6,sv,pdo} = 1.060$$

Median Barrier ($CMF_{5,fs,6,y,z}$)

The segment does not have inside barrier. Hence, $CMF_{5,fs,6,y,fi}$ and $CMF_{5,fs,6,y,pdo}$ are equal to 1.000.

High Volume ($CMF_{6,fs,6,y,z}$)

$CMF_{6,fs,6,mv,fi}$ is calculated from Equation 18-29 and the coefficient $a = 0.350$ from Table 18-19 as follows:

$$\begin{aligned} CMF_{6,fs,6,mv,fi} &= \exp(a \times P_{hv}) \\ &= \exp(0.350 \times 0.1) \\ &= 1.036 \end{aligned}$$

Calculations using the other coefficients from Table 18-19 yield the following results:

$$CMF_{6,fs,6,sv,fi} = 0.993$$

$$CMF_{6,fs,6,mv,pdo} = 1.029$$

$$CMF_{6,fs,6,sv,pdo} = 0.941$$

Lane Change ($CMF_{7,fs,6,mv,z}$)

The segment does not have a ramp entrance or a ramp exit within 0.5 mi, which is the base condition for the lane change CMF. Hence, $CMF_{7,fs,6,mv,fi}$ and $CMF_{7,fs,6,mv,pdo}$ are equal to 1.000.

Outside Shoulder Width ($CMF_{8,fs,6,sv,z}$)

The segment has 10-ft outside shoulders, which is the base condition for the outside shoulder width CMF. Hence, $CMF_{8,fs,6,sv,fi}$ and $CMF_{8,fs,6,sv,pdo}$ are equal to 1.000.

Shoulder Rumble Strip ($CMF_{9,fs,6,sv,z}$)

The segment does not have shoulder rumble strips. Hence, $CMF_{9,fs,6,sv,fi}$ and $CMF_{9,fs,6,sv,pdo}$ are equal to 1.000.

Outside Clearance ($CMF_{10,fs,6,sv,z}$)

The segment has 30-ft clear zones and no outside barrier, which are the base conditions for the outside clearance CMF. Hence, $CMF_{10,fs,6,sv,fi}$ and $CMF_{10,fs,6,sv,pdo}$ are equal to 1.000.

Outside Barrier ($CMF_{11,fs,6,sv,z}$)

The segment does not have outside barrier. Hence, $CMF_{11,fs,6,sv,fi}$ and $CMF_{11,fs,6,sv,pdo}$ are equal to 1.000.

Multiple-Vehicle Crashes

The CMFs are applied to the multiple-vehicle fatal-and-injury SPF as follows:

$$\begin{aligned} N_{p^*,fs,6,mv,fi} &= N_{spf,fs,6,mv,fi} \times (CMF_{1,fs,6,mv,fi} \times \dots \times CMF_{7,fs,6,mv,fi}) \\ &= 3.555 \times (1.000 \times 1.000 \times 1.000 \times 1.062 \times 1.000 \times 1.036 \times 1.000) \\ &= 3.555 \times 1.100 \\ &= 3.911 \text{ crashes/year} \end{aligned}$$

The CMFs are applied to the multiple-vehicle property-damage-only SPF as follows:

$$\begin{aligned} N_{p^*,fs,6,mv,pdo} &= N_{spf,fs,6,mv,pdo} \times (CMF_{1,fs,6,mv,pdo} \times \dots \times CMF_{7,fs,6,mv,pdo}) \\ &= 8.775 \times (1.000 \times 1.000 \times 1.000 \times 1.060 \times 1.000 \times 1.029 \times 1.000) \\ &= 8.775 \times 1.091 \\ &= 9.569 \text{ crashes/year} \end{aligned}$$

Single-Vehicle Crashes

The CMFs are applied to the single-vehicle fatal-and-injury SPF as follows:

$$\begin{aligned} N_{p^*,fs,6,sv,fi} &= N_{spf,fs,6,sv,fi} \times (CMF_{1,fs,6,sv,fi} \times \dots \times CMF_{6,fs,6,sv,fi} \times CMF_{8,fs,6,sv,fi} \times \dots \times CMF_{11,fs,6,sv,fi}) \\ &= 2.117 \times (1.000 \times 1.000 \times 1.000 \times 0.980 \times 1.000 \times 0.993 \times 1.000 \times 1.000 \times 1.000 \times 1.000) \\ &= 2.117 \times 0.973 \\ &= 2.060 \text{ crashes/year} \end{aligned}$$

The CMFs are applied to the single-vehicle property-damage-only SPF as follows:

$$\begin{aligned} N_{p^*,fs,6,sv,pdo} &= N_{spf,fs,6,sv,pdo} \times (CMF_{1,fs,6,sv,pdo} \times \dots \times CMF_{6,fs,6,sv,pdo} \times CMF_{8,fs,6,sv,pdo} \times \dots \times CMF_{11,fs,6,sv,pdo}) \\ &= 5.115 \times (1.000 \times 1.000 \times 1.000 \times 1.060 \times 1.000 \times 0.941 \times 1.000 \times 1.000 \times 1.000 \times 1.000) \\ &= 5.115 \times 0.997 \\ &= 5.099 \text{ crashes/year} \end{aligned}$$

Step 11 – Multiply the result obtained in Step 10 by the appropriate calibration factor.

It is assumed that a calibration factor of 1.00 has been determined for local conditions. As a result, $N_{p,fs,6,y,z} = N_{p^*,fs,6,y,z}$ for both crash types y ($y = mv$: multiple-vehicle, sv : single-vehicle) and both crash severities z ($z = fi$: fatal-and-injury, pdo : property-damage-only). See Section B.1 of Appendix B to Part C for further discussion on calibration of the predicted models.

Calculation of Predicted Average Crash Frequency

The predicted average crash frequency is calculated using Equation 18-2 based on the results obtained in Steps 9 through 11 as follows.

Fatal-and-injury crashes:

$$\begin{aligned} N_{p,fs,6,at,fi} &= N_{p,fs,6,mv,fi} + N_{p,fs,6,sv,fi} \\ &= 3.911 + 2.060 \\ &= 5.971 \text{ crashes/year} \end{aligned}$$

Property-damage-only crashes:

$$\begin{aligned} N_{p,fs,6,at,pdo} &= N_{p,fs,6,mv,pdo} + N_{p,fs,6,sv,pdo} \\ &= 9.569 + 5.099 \\ &= 14.668 \text{ crashes/year} \end{aligned}$$

Step 12—If there is another year to be evaluated in the evaluation period for the selected site, return to Step 8. Otherwise, proceed to Step 13.

The study period is one year (2011), so steps 8 through 11 need not be repeated.

Step 13—Apply site-specific EB Method (if applicable) and apply SDFs.

This step consists of three optional sets of calculations—site-specific EB Method, severity distribution functions, and crash type distribution.

Apply the site-specific EB Method to a future time period, if appropriate.

The site-specific EB Method is not applied in this sample problem because crash data are not available.

Apply the severity distribution functions (SDFs), if desired.

To apply the SDFs, the systematic component of crash severity likelihood V_j is computed for each severity level j using Equation 18-63 as follows:

$$V_j = a + \left(b \times \frac{P_{ib} + P_{ob}}{2} \right) + (c \times P_{hv}) + \left(d \times \frac{P_{ir} + P_{or}}{2} \right) + (e \times \sum P_{c,i}) + (f \times W_l) + (g \times I_{rural})$$

The coefficients a , b , c , d , e , f , and g are obtained from Table 18-30 for each severity level j . The segment does not have barrier, rumble strips, or horizontal curvature, so P_{ib} , P_{ob} , P_{ir} , P_{or} , and $P_{c,i}$ are equal to 0.0. V_j is computed for fatal crashes as follows:

$$\begin{aligned} V_K &= -0.171 + \left(-0.388 \times \frac{0.0 + 0.0}{2} \right) + (-0.924 \times 0.1) + \left(0.387 \times \frac{0.0 + 0.0}{2} \right) \\ &\quad + (0.208 \times 0.0) + (-0.261 \times 12) + (0.492 \times 0.0) \\ &= -3.392 \end{aligned}$$

Calculations using the coefficients for incapacitating injury crashes and non-incapacitating injury crashes from Table 18-30 yield the following results:

$$V_A = -2.478$$

$$V_B = -0.571$$

Using these computed V_K , V_A , and V_B values, and assuming a calibration factor $C_{sdf,fs+sc}$ of 1.0, the probability of occurrence of a fatal crash is computed using Equation 18-59 as follows:

$$\begin{aligned} P_{fs+sc,ac,at,K} &= \frac{\exp(V_K)}{\frac{1.0}{C_{sdf,fs+sc}} + \exp(V_K) + \exp(V_A) + \exp(V_B)} \\ &= \frac{\exp(-3.392)}{\frac{1.0}{1.0} + \exp(-3.392) + \exp(-2.478) + \exp(-0.571)} \\ &= 0.020 \end{aligned}$$

Similar calculations using Equation 18-60 and Equation 18-61 yield the following results:

$$P_{fs+sc,ac,at,A} = 0.050$$

$$P_{fs+sc,ac,at,B} = 0.336$$

The probability of occurrence of a possible-injury crash is computed using Equation 18-62 as follows:

$$\begin{aligned} P_{fs+sc,ac,at,C} &= 1.0 - (P_{fs+sc,ac,at,K} + P_{fs+sc,ac,at,A} + P_{fs+sc,ac,at,B}) \\ &= 1.0 - (0.020 + 0.050 + 0.336) \\ &= 0.594 \end{aligned}$$

The probability of occurrence of a fatal crash is multiplied by the fatal-and-injury crash frequency obtained in Step 11 using Equation 18-58 as follows:

$$\begin{aligned} N_{e,fs,6,at,K} &= N_{e,fs,6,at,fi} \times P_{fs+sc,ac,at,K} \\ &= 5.971 \times 0.020 \\ &= 0.119 \text{ crashes/year} \end{aligned}$$

Similar calculations using Equation 18-58 and the probabilities of occurrences of the other crash severities yield the following results:

$$N_{e,fs,6,at,A} = 0.298 \text{ crashes/year}$$

$$N_{e,fs,6,at,B} = 2.005 \text{ crashes/year}$$

$$N_{e,fs,6,at,C} = 3.549 \text{ crashes/year}$$

Note that the sum of the estimates by severity equals the total fatal-and-injury crash frequency (i.e., $5.971 = 0.119 + 0.298 + 2.005 + 3.549$).

Apply the crash type distribution, if desired.

The crash type distributions are applied by multiplying the default crash type distribution proportions in Table 18-6 and Table 18-8 by the predicted average crash frequencies obtained in Step 11.

Worksheets

The step-by-step instructions are provided to illustrate the predictive method for calculating the predicted average crash frequency for a freeway segment. To apply the predictive method steps to multiple segments, a series of worksheets are provided for determining the predicted average crash frequency. The worksheets include:

- Table 18-32. Freeway Segment Worksheet (1 of 4)—Sample Problem 1
- Table 18-33. Freeway Segment Worksheet (2 of 4)—Sample Problem 1
- Table 18-34. Freeway Segment Worksheet (3 of 4)—Sample Problem 1
- Table 18-35. Freeway Segment Worksheet (4 of 4)—Sample Problem 1

Filled versions of these worksheets are provided below. Blank versions of worksheets used in the Sample Problems are provided in Appendix 18A.

Table 18-32 is a summary of general information about the freeway segment, analysis, input data (i.e., “The Facts”), and assumptions for Sample Problem 1. The input data include area type, crash data, basic roadway data, alignment data, and cross section data.

Table 18-33 is a summary of general information about the freeway segment, analysis, input data (i.e., “The Facts”), and assumptions for Sample Problem 1. The input data include roadside data, ramp access data, and traffic data.

Table 18-34 is a tabulation of the CMF and SPF computations for Sample Problem 1.

Table 18-35 is a tabulation of the crash severity and crash type distributions for Sample Problem 1.

Table 18-32. Freeway Segment Worksheet (1 of 4)—Sample Problem 1

General Information					Location Information				
Analyst					Roadway				
Agency or company					Roadway section				
Date performed					Study year				
Area type		X	Urban		Rural				
Input Data									
Crash Data				Crash Period	Study Year	Complete the study year column. Complete the crash period column if the EB Method is used.			
Crash data time period						First year	--	Last year	--
Count of multiple-vehicle FI crashes $N_{o,fs,n,mv,fi}^*$				--					
Count of single-vehicle FI crashes $N_{o,fs,n,sv,fi}^*$				--					
Count of multiple-vehicle PDO crashes $N_{o,fs,n,mv,pdo}^*$				--					
Count of single-vehicle PDO crashes $N_{o,fs,n,sv,pdo}^*$				--					
Basic Roadway Data									
Number of through lanes n				6		Same value for crash period and study year.			
Segment length L (mi)				--	0.75				
Alignment Data									
Horizontal Curve Data									
1	Presence of horizontal curve 1			--	Y/N	N	Y/N	If Yes, then enter data in the next three rows.	
	Equivalent curve radius R_1^* (ft)			--		--			
	Length of curve L_{c1} (mi)			--		--			
	Length of curve in segment $L_{c1,seg}$ (mi)			--		--			
2	Presence of horizontal curve 2			--	Y/N	N	Y/N	If Yes, then enter data in the next three rows.	
	Equivalent curve radius R_2^* (ft)			--		--			
	Length of curve L_{c2} (mi)			--		--			
	Length of curve in segment $L_{c2,seg}$ (mi)			--		--			
Cross Section Data									
Lane width W_l (ft)				--		12			
Outside shoulder width W_s (ft)				--		10			
Inside shoulder width W_{is} (ft)				--		6			
Median width W_m (ft)				--		40			
Presence of rumble strips on outside shoulder				--	Y/N	N	Y/N	If Yes, then enter data in the next two rows.	
Length of rumble strip in increasing milepost dir. (mi)				--		--			
Length of rumble strip in decreasing milepost dir. (mi)				--		--			
Presence of rumble strips on inside shoulder				--	Y/N	N	Y/N	If Yes, then enter data in the next two rows.	
Length of rumble strip in increasing milepost dir. (mi)				--		--			
Length of rumble strip in decreasing milepost dir. (mi)				--		--			
Presence of barrier in median				--	Y/N	N	Y/N	If Yes, then use the freeway barrier worksheet.	

Table 18-33. Freeway Segment Worksheet (2 of 4)—Sample Problem 1

Input Data						
Roadside Data		Crash Period		Study Year		Complete the study year column. Complete the crash period column if the EB Method is used.
Clear zone width W_{hc} (ft)		--		30		
Presence of barrier on roadside		--	Y/N	N	Y/N	If Yes, then use the freeway barrier worksheet.
Ramp Access Data						
Travel in Increasing Milepost Direction						
Ent. ramp	Distance from begin milepost to upstream entrance ramp gore $X_{b, ent}$ (mi)	--		0.5		If ramp entrance is in the segment, enter 0.0.
	Presence of speed-change lane in segment	--	Y/N	N	Y/N	If Yes, then enter data in the next row.
	Length of s-c lane in segment $L_{en, seg, inc}$ (mi)	--		--		
Exit ramp	Distance from end milepost to upstream exit ramp gore $X_{e, ext}$ (mi)	--		0.85		If ramp exit is in the segment, enter 0.0.
	Presence of speed-change lane in segment	--	Y/N	N	Y/N	If Yes, then enter data in the next row.
	Length of s-c lane in segment $L_{ex, seg, inc}$ (mi)	--		--		
Weave	Presence of a Type B weave in segment	--	Y/N	N	Y/N	If Yes, then enter data in the next two rows.
	Length of weaving section $L_{wev, inc}$ (mi)	--		--		
	Length of weaving section in seg. $L_{wev, seg, inc}$ (mi)	--		--		
Travel in Decreasing Milepost Direction						
Ent. ramp	Distance from end milepost to upstream entrance ramp gore $X_{e, ent}$ (mi)	--		0.85		If ramp entrance is in the segment, enter 0.0.
	Presence of speed-change lane in segment	--	Y/N	N	Y/N	If Yes, then enter data in the next row.
	Length of s-c lane in segment $L_{en, seg, dec}$ (mi)	--		--		
Exit ramp	Distance from begin milepost to downstream exit ramp gore $X_{b, ext}$ (mi)	--		0.5		If ramp exit is in the segment, enter 0.0.
	Presence of speed-change lane in segment	--	Y/N	N	Y/N	If Yes, then enter data in the next row.
	Length of s-c lane in segment $L_{ex, seg, dec}$ (mi)	--		--		
Weave	Presence of a Type B weave in segment	--	Y/N	N	Y/N	If Yes, then enter data in the next two rows.
	Length of weaving section $L_{wev, dec}$ (mi)	--		--		
	Length of weaving section in seg. $L_{wev, seg, dec}$ (mi)	--		--		
Traffic Data						
Proportion of AADT during high-volume hours P_{hv}		--		0.1		
Freeway segment AADT $AADT_{fs}$ (veh/day)		--		120,000		
AADT of entrance ramp for travel in increasing milepost direction $AADT_{b, ent}$ (veh/day)		--		8,000		
AADT of exit ramp for travel in increasing milepost direction $AADT_{e, ext}$ (veh/day)		--		7,150		
AADT of entrance ramp for travel in decreasing milepost direction $AADT_{e, ent}$ (veh/day)		--		6,750		
AADT of exit ramp for travel in decreasing milepost direction $AADT_{b, ext}$ (veh/day)		--		7,675		

Table 18-34. Freeway Segment Worksheet (3 of 4)—Sample Problem 1

Crash Modification Factors

Complete the study year column. Complete the crash period column if the EB Method is used. Equation	Fatal and Injury				Property Damage Only				
	Multiple Vehicle		Single Vehicle		Multiple Vehicle		Single Vehicle		
	Crash Period	Study Year	Crash Period	Study Year	Crash Period	Study Year	Crash Period	Study Year	
Horizontal curve $CMF_{1,fs,ac,y,z}$	18-24	--	1.000	--	1.000	--	1.000	--	1.000
Lane width $CMF_{2,fs,ac,y,fi}$	18-25	--	1.000	--	1.000				
Inside shoulder width $CMF_{3,fs,ac,y,z}$	18-26	--	1.000	--	1.000	--	1.000	--	1.000
Median width $CMF_{4,fs,ac,y,z}$	18-27	--	1.062	--	0.980	--	1.060	--	1.060
Median barrier $CMF_{5,fs,ac,y,z}$	18-28	--	1.000	--	1.000	--	1.000	--	1.000
High volume $CMF_{6,fs,ac,y,z}$	18-29	--	1.036	--	0.993	--	1.029	--	0.941
Lane change $CMF_{7,fs,ac,mv,z}$	18-30	--	1.000			--	1.000		
Outside shoulder width $CMF_{8,fs,ac,sv,z}$	18-35			--	1.000			--	1.000
Shoulder rumble strip $CMF_{9,fs,ac,sv,fi}$	18-36			--	1.000				
Outside clearance $CMF_{10,fs,ac,sv,fi}$	18-38			--	1.000				
Outside barrier $CMF_{11,fs,ac,sv,z}$	18-39			--	1.000			--	1.000
Combined CMF (multiply all CMFs evaluated)		--	1.100	--	0.973	--	1.091	--	0.997

Expected Average Crash Frequency^a

Complete the study year column. Complete the crash period column if the <i>site-specific</i> EB Method is used.	Fatal and Injury				Property Damage Only			
	Multiple Vehicle		Single Vehicle		Multiple Vehicle		Single Vehicle	
	Crash Period	Study Year	Crash Period	Study Year	Crash Period	Study Year	Crash Period	Study Year
Calibration factor $C_{fs,ac,y,z}$	1.00		1.00		1.00		1.00	
Overdispersion parameter $k_{fs,n,y,z}$	--		--		--		--	
Observed crash count $N_{a,fs,n,y,z}^*$ (cr)	--		--		--		--	
Reference year r	--		--		--		--	
Predicted average crash freq. for reference year $N_{p,fs,n,y,z,r}$ (cr/yr)	--		--		--		--	
Predicted number of crashes for crash period (sum all years) $N_{p,fs,n,y,z}^*$ (cr)	--		--		--		--	
Equivalent years associated with crash count $C_{b,fs,n,y,z,r}$ (yr)	--		--		--		--	
Adjusted average crash freq. for ref. year given $N_{os}^*, N_{a,fs,n,y,z,r}$ (cr/yr)	--		--		--		--	
Study year s		2011		2011		2011		2011
Predicted average crash freq. for study year $N_{p,fs,n,y,z,s}$ (cr/yr)		3.911		2.060		9.568		5.099
Expected average crash freq. for study year $N_{e,fs,n,y,z,s}$ (cr/yr)		3.911		2.060		9.568		5.099
Expected average crash freq. for study year (all crash types) $N_{e,fs,n,at,z,s}$ (cr/yr)				5.971				14.668

Note:

a – If the EB Method is not used, then substitute the word “predicted” for the word “expected” and substitute the subscript “p” for the subscript “e”.

Table 18-35. Freeway Segment Worksheet (4 of 4)—Sample Problem 1

Expected Average Crash Frequency ^a							
Crash Severity Distribution							
	K	A	B	C	Total FI	PDO	Total FI + PDO
Proportion by injury level	0.020	0.050	0.336	0.594	1.000		
Expected average crash freq. for study year (all crash types) $N_{e, fs, n, at, z, s}$ (cr/yr)	0.119	0.298	2.005	3.548	5.971	14.668	20.638
Crash Type Distribution							
Crash Type Category	Table	Fatal and Injury		Property Damage Only		Total	
		Proportion	Expected Average Crash Frequency for Study Year $N_{e, fs, n, y, fi, s}$ (cr/yr)	Proportion	Expected Average Crash Frequency for Study Year $N_{e, fs, n, y, pdo, s}$ (cr/yr)	Expected Average Crash Frequency for Study Year $N_{e, fs, n, y, as, s}$ (cr/yr)	Expected Average Crash Frequency for Study Year $N_{e, fs, n, y, as, s}$ (cr/yr)
Multiple-Vehicle Crashes	18-6						
Head-on		0.008	0.031	0.002	0.019	0.050	
Right-angle		0.031	0.121	0.018	0.172	0.293	
Rear-end		0.750	2.933	0.690	6.602	9.535	
Sideswipe		0.180	0.704	0.266	2.545	3.249	
Other multiple-vehicle crashes		0.031	0.121	0.024	0.230	0.351	
Total		1.000	3.911	1.000	9.568	13.479	
Single-Vehicle Crashes	18-8						
Crash with animal		0.004	0.008	0.022	0.112	0.120	
Crash with fixed object		0.722	1.487	0.716	3.651	5.138	
Crash with other object		0.051	0.105	0.139	0.709	0.814	
Crash with parked vehicle		0.015	0.031	0.016	0.082	0.112	
Other single-vehicle crashes		0.208	0.428	0.107	0.546	0.974	
Total		1.000	2.060	1.000	5.099	7.159	

Note:

a – If the EB Method is not used, then substitute the word “predicted” for the word “expected” and substitute the subscript “p” for the subscript “e”.

18.13.2. Sample Problem 2

The Site/Facility

A six-lane urban freeway segment with a horizontal curve.

The Question

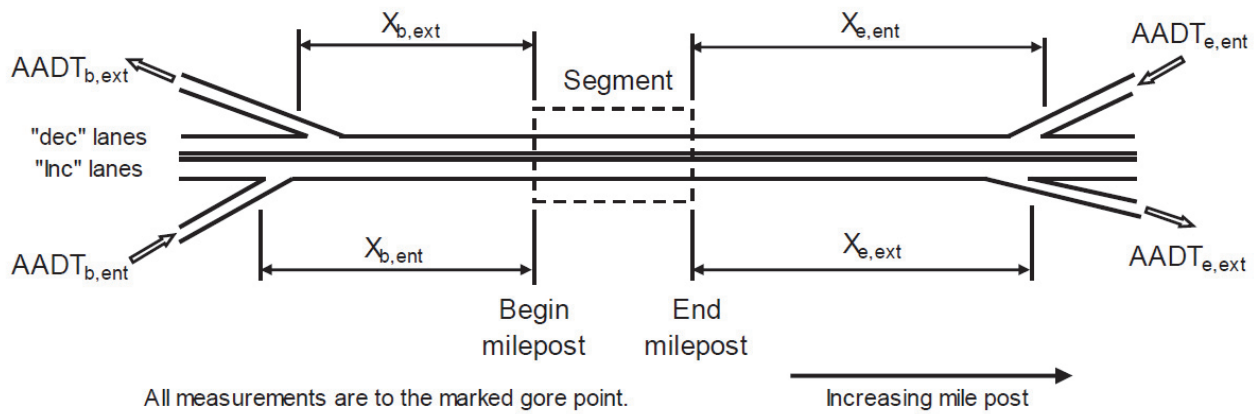
What is the predicted average crash frequency of the freeway segment for a one-year period?

The Facts

The study year is 2011. The conditions present during this year are provided in the following list.

- 0.75-mi length
- 120,000 veh/day

- 10 percent of AADT volume occurs during high-volume hours
- One horizontal curve
 - 2,100-ft equivalent radius
 - 0.25-mi length, entirely in the segment
 - Curve exists on both roadbeds
- 12-ft lane width
- 7-ft outside shoulder width
- 6-ft inside shoulder width
- 40-ft median width
- 0.25 mi of rumble strips on outside shoulders in both travel directions
- 0.25 mi of rumble strips on inside shoulders in both travel directions
- No median or roadside barrier
- 30-ft clear zone width
- No Type B weaving sections
- Data to describe four ramps in the vicinity of the segment



Variable Subscript (a,b)	Distance from Segment, $X_{a,b}$ (mi)	Ramp Volume, $AADT_{a,b}$ (veh/day)
b, ent	1.25	8,000
e, ext	0.1	7,150
e, ent	0.1	6,750
b, ext	1.25	7,675

Assumptions

- Crash type distributions used are the default values presented in Table 18-6 and Table 18-8.
- The calibration factor is 1.00.

Results

Using the predictive method steps as outlined below, the predicted average fatal-and-injury crash frequency for the freeway segment in Sample Problem 2 is determined to be 7.8 crashes per year, and the predicted average property-damage-only crash frequency is determined to be 17.0 crashes per year (rounded to one decimal place).

Steps**Step 1 through 8**

To determine the predicted average crash frequency of the freeway segment in Sample Problem 2, only Steps 9 through 13 are conducted. No other steps are necessary because only one freeway segment is analyzed for one year, and the EB Method is not applied.

Step 9 – For the selected site, determine and apply the appropriate SPF.

For a six-lane urban freeway segment, SPF values for multiple-vehicle and single-vehicle crashes are determined.

Multiple-Vehicle Crashes

The SPF for multiple-vehicle fatal-and-injury crashes is calculated from Equation 18-15 and Table 18-5 as follows:

$$\begin{aligned} N_{spf, fs, 6, mv, fi} &= L^* \times \exp(a + b \times \ln[c \times AADT_{fs}]) \\ &= 0.75 \times \exp(-5.587 + 1.492 \times \ln[0.001 \times 120,000]) \\ &= 3.555 \text{ crashes/year} \end{aligned}$$

Similarly, the SPF for multiple-vehicle property-damage-only crashes is calculated from Equation 18-15 and Table 18-5 to yield the following result:

$$N_{spf, fs, 6, mv, pdo} = 8.775 \text{ crashes/year}$$

Single-Vehicle Crashes

The SPF for single-vehicle fatal-and-injury crashes is calculated from Equation 18-18 and Table 18-7 as follows:

$$\begin{aligned} N_{spf, fs, 6, sv, fi} &= L^* \times \exp(a + b \times \ln[c \times AADT_{fs}]) \\ &= 0.75 \times \exp(-2.055 + 0.646 \times \ln[0.001 \times 120,000]) \\ &= 2.117 \text{ crashes/year} \end{aligned}$$

Similarly, the SPF for single-vehicle property-damage-only crashes is calculated from Equation 18-18 and Table 18-7 to yield the following result:

$$N_{spf, fs, 6, sv, pdo} = 5.115 \text{ crashes/year}$$

Step 10 – Multiply the result obtained in Step 9 by the appropriate CMFs.

Each CMF used in the calculation of the predicted average crash frequency of the freeway segment is calculated in this step.

Horizontal Curve (CMF_{1,fs,6,y,z})

CMF_{1,fs,6,y,fi} is calculated from Equation 18-24 as follows:

$$CMF_{1,fs,6,y,fi} = 1.0 + a \times \left[\sum_{i=1}^m \left(\frac{5,730}{R_i^*} \right)^2 \times P_{c,i} \times f_{c,i} \right]$$

The segment is 0.75 mi long, the curve is 0.25 mi long, and its entire length is in the segment. Hence, $P_{c,i} = 0.33$. The curve exists on both roadbeds, so $f_{c,i} = 1.0$. From Table 18-14, $a = 0.0172$ for multiple-vehicle fatal-and-injury crashes. CMF_{1,fs,6,mv,fi} is calculated as follows:

$$\begin{aligned} CMF_{1,fs,6,mv,fi} &= 1.0 + 0.0172 \times \left[\sum_{i=1}^m \left(\frac{5,730}{2,100} \right)^2 \times 0.33 \times 1.0 \right] \\ &= 1.043 \end{aligned}$$

Calculations using the other coefficients from Table 18-14 yield the following results:

$$CMF_{1,fs,6,sv,fi} = 1.178$$

$$CMF_{1,fs,6,mv,pdo} = 1.084$$

$$CMF_{1,fs,6,sv,pdo} = 1.155$$

Lane Width (CMF_{2,fs,6,y,z})

The segment has 12-ft lanes, which is the base condition for the lane width CMF. Hence, CMF_{2,fs,6,y,fi} and CMF_{2,fs,6,y,pdo} are equal to 1.000.

Inside Shoulder Width (CMF_{3,fs,6,y,z})

The segment has 6-ft inside shoulders, which is the base condition for the inside shoulder width CMF. Hence, CMF_{3,fs,6,y,fi} and CMF_{3,fs,6,y,pdo} are equal to 1.000.

Median Width (CMF_{4,fs,6,y,z})

CMF_{4,fs,6,y,fi} is calculated from Equation 18-27 as follows:

$$CMF_{4,fs,6,y,z} = (1.0 - P_{ib}) \times \exp(a \times [W_m - 2 \times W_{is} - 48]) + P_{ib} \times \exp(a \times [2 \times W_{icb} - 48])$$

The segment does not have inside barrier, so $P_{ib} = 0.0$ and the calculation of W_{icb} does not apply. From Table 18-17, $a = -0.00302$ for multiple-vehicle fatal-and-injury crashes. CMF_{4,fs,6,mv,fi} is calculated as follows:

$$\begin{aligned} CMF_{4,fs,6,mv,fi} &= (1.0 - 0.0) \times \exp(-0.00302 \times [40 - 2 \times 6 - 48]) + 0.0 \times \exp(-0.00302 \times [2 \times W_{icb} - 48]) \\ &= 1.062 \end{aligned}$$

Calculations using the other coefficients from Table 18-17 yield the following results:

$$CMF_{4, fs, 6, sv, fi} = 0.980$$

$$CMF_{4, fs, 6, mv, pdo} = 1.060$$

$$CMF_{4, fs, 6, sv, pdo} = 1.060$$

Median Barrier ($CMF_{5, fs, 6, y, z}$)

The segment does not have inside barrier. Hence, $CMF_{5, fs, 6, y, fi}$ and $CMF_{5, fs, 6, y, pdo}$ are equal to 1.000.

High Volume ($CMF_{6, fs, 6, y, z}$)

$CMF_{6, fs, 6, mv, fi}$ is calculated from Equation 18-29 and the coefficient $a = 0.350$ from Table 18-19 as follows:

$$\begin{aligned} CMF_{6, fs, 6, mv, fi} &= \exp(a \times P_{hv}) \\ &= \exp(0.350 \times 0.1) \\ &= 1.036 \end{aligned}$$

Calculations using the other coefficients from Table 18-19 yield the following results:

$$CMF_{6, fs, 6, sv, fi} = 0.993$$

$$CMF_{6, fs, 6, mv, pdo} = 1.029$$

$$CMF_{6, fs, 6, sv, pdo} = 0.941$$

Lane Change ($CMF_{7, fs, 6, mv, z}$)

$CMF_{7, fs, 6, mv, fi}$ is calculated from Equation 18-30 as follows:

$$CMF_{7, fs, 6, mv, fi} = (0.5 \times f_{inc, wev} \times f_{inc, lc}) + (0.5 \times f_{dec, wev} \times f_{dec, lc})$$

The segment does not have Type B weaving sections, so the weaving section adjustment factors $f_{inc, wev}$ and $f_{dec, wev}$ are equal to 1.00. The lane change adjustment factors $f_{inc, lc}$ and $f_{dec, lc}$ are calculated from Equation 18-33 and Equation 18-34 as follows:

$$\begin{aligned} f_{inc, lc} &= \left(1.0 + \frac{\exp(-b \times X_{b, ent} + d \times \ln[c \times AADT_{b, ent}])}{b \times L_{fs}} \right) \times [1.0 - \exp(-b \times L_{fs})] \\ &\times \left(1.0 + \frac{\exp(-b \times X_{e, ext} + d \times \ln[c \times AADT_{e, ext}])}{b \times L_{fs}} \right) \times [1.0 - \exp(-b \times L_{fs})] \end{aligned}$$

$$\begin{aligned} f_{dec, lc} &= \left(1.0 + \frac{\exp(-b \times X_{e, ent} + d \times \ln[c \times AADT_{e, ent}])}{b \times L_{fs}} \right) \times [1.0 - \exp(-b \times L_{fs})] \\ &\times \left(1.0 + \frac{\exp(-b \times X_{b, ext} + d \times \ln[c \times AADT_{b, ext}])}{b \times L_{fs}} \right) \times [1.0 - \exp(-b \times L_{fs})] \end{aligned}$$

From Table 18-20, the coefficients b , c , and d for fatal-and-injury crashes are 12.56, 0.001, and -0.272, respectively. The lane change adjustment factors are calculated as follows:

$$f_{inc,lc} = \left(1.0 + \frac{\exp(-12.56 \times 1.25 - 0.272 \times \ln[0.001 \times 8,000])}{12.56 \times 0.75} \right) \times [1.0 - \exp(-12.56 \times 0.75)] \\ \times \left(1.0 + \frac{\exp(-12.56 \times 0.1 - 0.272 \times \ln[0.001 \times 7,150])}{12.56 \times 0.75} \right) \times [1.0 - \exp(-12.56 \times 0.75)] \\ = 1.018$$

$$f_{dec,lc} = \left(1.0 + \frac{\exp(-12.56 \times 0.1 - 0.272 \times \ln[0.001 \times 6,750])}{12.56 \times 0.75} \right) \times [1.0 - \exp(-12.56 \times 0.75)] \\ \times \left(1.0 + \frac{\exp(-12.56 \times 1.25 - 0.272 \times \ln[0.001 \times 7,675])}{12.56 \times 0.75} \right) \times [1.0 - \exp(-12.56 \times 0.75)] \\ = 1.018$$

$CMF_{7,fs,6,mv,fi}$ is calculated using the weaving section and lane change adjustment factors as follows:

$$CMF_{7,fs,6,mv,fi} = (0.5 \times 1.00 \times 1.018) + (0.5 \times 1.00 \times 1.018) \\ = 1.018$$

Similar calculations using the property-damage-only coefficients from Table 18-20 yield the following results:

$$CMF_{7,fs,6,mv,pdo} = 1.015$$

Outside Shoulder Width ($CMF_{8,fs,6,sv,z}$)

$CMF_{8,fs,6,sv,fi}$ is calculated from Equation 18-35 as follows:

$$CMF_{8,fs,ac,sv,z} = (1.0 - \sum P_{c,i}) \times \exp(a \times [W_s - 10]) + (\sum P_{c,i}) \times \exp(b \times [W_s - 10])$$

The segment is 0.75 mi long, the curve is 0.25 mi long, and its entire length is in the segment. Hence, $P_{c,i} = 0.33$. From Table 18-21, $a = -0.0647$ and $b = -0.0897$. $CMF_{8,fs,6,sv,fi}$ is calculated as follows:

$$CMF_{8,fs,6,sv,fi} = (1.0 - 0.33) \times \exp(-0.0647 \times [7 - 10]) + (0.33) \times \exp(-0.0897 \times [7 - 10]) \\ = 1.246$$

Similar calculations using the property-damage-only coefficients from Table 18-21 yield the following results:

$$CMF_{8,fs,6,sv,pdo} = 1.096$$

Shoulder Rumble Strip ($CMF_{9,fs,6,sv,z}$)

$CMF_{9,fs,6,sv,fi}$ is calculated from Equation 18-36 as follows:

$$CMF_{9,fs,6,sv,fi} = (1.0 - \sum P_{c,i}) \times f_{tan} + (\sum P_{c,i}) \times 1.0$$

The factor f_{lan} is calculated from Equation 18-37 as follows:

$$\begin{aligned} f_{lan} &= 0.5 \times ([1.0 - P_{ir}] \times 1.0 + P_{ir} \times 0.811) + 0.5 \times ([1.0 - P_{or}] \times 1.0 + P_{or} \times 0.811) \\ &= 0.5 \times ([1.0 - 0.33] \times 1.0 + 0.33 \times 0.811) + 0.5 \times ([1.0 - 0.33] \times 1.0 + 0.33 \times 0.811) \\ &= 0.906 \end{aligned}$$

$CMF_{9,fs,6,sv,fi}$ is calculated as follows:

$$\begin{aligned} CMF_{9,fs,6,sv,fi} &= (1.0 - 0.33) \times 0.906 + (0.33) \times 1.0 \\ &= 0.958 \end{aligned}$$

Outside Clearance ($CMF_{10,fs,6,sv,z}$)

The segment has 30-ft clear zones and no outside barrier, which are the base conditions for the outside clearance CMF. Hence, $CMF_{10,fs,6,sv,fi}$ and $CMF_{10,fs,6,sv,pdo}$ are equal to 1.000.

Outside Barrier ($CMF_{11,fs,6,sv,z}$)

The segment does not have outside barrier. Hence, $CMF_{11,fs,6,sv,fi}$ and $CMF_{11,fs,6,sv,pdo}$ are equal to 1.000.

Multiple-Vehicle Crashes

The CMFs are applied to the multiple-vehicle fatal-and-injury SPF as follows:

$$\begin{aligned} N_{p^*,fs,6,mv,fi} &= N_{spf,fs,6,mv,fi} \times (CMF_{1,fs,6,mv,fi} \times \dots \times CMF_{7,fs,6,mv,fi}) \\ &= 3.555 \times (1.043 \times 1.000 \times 1.000 \times 1.062 \times 1.000 \times 1.036 \times 1.018) \\ &= 3.555 \times 1.168 \\ &= 4.150 \text{ crashes/year} \end{aligned}$$

The CMFs are applied to the multiple-vehicle property-damage-only SPF as follows:

$$\begin{aligned} N_{p^*,fs,6,mv,pdo} &= N_{spf,fs,6,mv,pdo} \times (CMF_{1,fs,6,mv,pdo} \times \dots \times CMF_{7,fs,6,mv,pdo}) \\ &= 8.775 \times (1.084 \times 1.000 \times 1.000 \times 1.060 \times 1.000 \times 1.029 \times 1.015) \\ &= 8.775 \times 1.200 \\ &= 10.530 \text{ crashes/year} \end{aligned}$$

Single-Vehicle Crashes

The CMFs are applied to the single-vehicle fatal-and-injury SPF as follows:

$$\begin{aligned} N_{p^*,fs,6,sv,fi} &= N_{spf,fs,6,sv,fi} \times (CMF_{1,fs,6,sv,fi} \times \dots \times CMF_{6,fs,6,sv,fi} \times CMF_{8,fs,6,sv,fi} \times \dots \times CMF_{11,fs,6,sv,fi}) \\ &= 2.117 \times (1.178 \times 1.000 \times 1.000 \times 0.980 \times 1.000 \times 0.993 \times 1.246 \times 0.958 \times 0.987 \times 1.000) \\ &= 2.117 \times 1.351 \\ &= 2.858 \text{ crashes/year} \end{aligned}$$

The CMFs are applied to the single-vehicle property-damage-only SPF as follows:

$$\begin{aligned}
 N_{p^*, fs, 6, sv, pdo} &= N_{spf, fs, 6, sv, pdo} \times (CMF_{1, fs, 6, sv, pdo} \times \dots \times CMF_{6, fs, 6, sv, pdo} \times CMF_{8, fs, 6, sv, pdo} \times \dots \times CMF_{11, fs, 6, sv, pdo}) \\
 &= 5.115 \times (1.155 \times 1.000 \times 1.000 \times 1.060 \times 1.000 \times 0.941 \times 1.096 \times 1.000 \times 1.000 \times 1.000) \\
 &= 5.115 \times 1.263 \\
 &= 6.454 \text{ crashes/year}
 \end{aligned}$$

Step 11 – Multiply the result obtained in Step 10 by the appropriate calibration factor.

It is assumed that a calibration factor of 1.00 has been determined for local conditions. As a result, $N_{p, fs, 6, y, z} = N_{p^*, fs, 6, y, z}$ for both crash types y ($y = mv$: multiple-vehicle, sv : single-vehicle) and both crash severities z ($z = fi$: fatal-and-injury, pdo : property-damage-only). See Section B.1 of Appendix B to Part C for further discussion on calibration of the predicted models.

Calculation of Predicted Average Crash Frequency

The predicted average crash frequency is calculated using Equation 18-2 based on the results obtained in Steps 9 through 11 as follows.

Fatal-and-injury crashes:

$$\begin{aligned}
 N_{p, fs, 6, at, fi} &= N_{p, fs, 6, mv, fi} + N_{p, fs, 6, sv, fi} \\
 &= 4.150 + 2.858 \\
 &= 7.008 \text{ crashes/year}
 \end{aligned}$$

Property-damage-only crashes:

$$\begin{aligned}
 N_{p, fs, 6, at, pdo} &= N_{p, fs, 6, mv, pdo} + N_{p, fs, 6, sv, pdo} \\
 &= 10.530 + 6.454 \\
 &= 16.984 \text{ crashes/year}
 \end{aligned}$$

Step 12—If there is another year to be evaluated in the evaluation period for the selected site, return to Step 8. Otherwise, proceed to Step 13.

The study period is one year (2011), so steps 8 through 11 need not be repeated.

Step 13—Apply site-specific EB Method (if applicable) and apply SDFs.

This step consists of three optional sets of calculations—site-specific EB Method, severity distribution functions, and crash type distribution.

Apply the site-specific EB Method to a future time period, if appropriate.

The site-specific EB Method is not applied in this sample problem because crash data are not available.

Apply the severity distribution functions (SDFs), if desired.

To apply the SDFs, the systematic component of crash severity likelihood V_j is computed for each severity level j using Equation 18-63 as follows:

$$V_j = a + \left(b \times \frac{P_{ib} + P_{ob}}{2} \right) + (c \times P_{hv}) + \left(d \times \frac{P_{ir} + P_{or}}{2} \right) + (e \times \sum P_{c,i}) + (f \times W_l) + (g \times I_{rural})$$

The coefficients a , b , c , d , e , f , and g are obtained from Table 18-30 for each severity level j . The segment does not have barrier, so P_{ib} and P_{ob} are equal to 0.0. V_j is computed for fatal crashes as follows:

$$\begin{aligned}
 V_K &= -0.171 + \left(-0.388 \times \frac{0.0 + 0.0}{2} \right) + (-0.924 \times 0.1) + \left(0.387 \times \frac{0.33 + 0.33}{2} \right) \\
 &\quad + (0.208 \times 0.33) + (-0.261 \times 12) + (0.492 \times 0.0) \\
 &= -3.194
 \end{aligned}$$

Calculations using the coefficients for incapacitating injury crashes and non-incapacitating injury crashes from Table 18-30 yield the following results:

$$V_A = -2.267$$

$$V_B = -0.482$$

Using these computed V_K , V_A , and V_B values, and assuming a calibration factor $C_{sdf,fs+sc}$ of 1.0, the probability of occurrence of a fatal crash is computed using Equation 18-59 as follows:

$$\begin{aligned}
 P_{fs+sc,ac,at,K} &= \frac{\exp(V_K)}{\frac{1.0}{C_{sdf,fs+sc}} + \exp(V_K) + \exp(V_A) + \exp(V_B)} \\
 &= \frac{\exp(-3.194)}{\frac{1.0}{1.0} + \exp(-3.194) + \exp(-2.267) + \exp(-0.482)} \\
 &= 0.023
 \end{aligned}$$

Similar calculations using Equation 18-60 and Equation 18-61 yield the following results:

$$P_{fs+sc,ac,at,A} = 0.059$$

$$P_{fs+sc,ac,at,B} = 0.350$$

The probability of occurrence of a possible-injury crash is computed using Equation 18-62 as follows:

$$\begin{aligned}
 P_{fs+sc,ac,at,C} &= 1.0 - (P_{fs+sc,ac,at,K} + P_{fs+sc,ac,at,A} + P_{fs+sc,ac,at,B}) \\
 &= 1.0 - (0.020 + 0.050 + 0.336) \\
 &= 0.567
 \end{aligned}$$

The probability of occurrence of a fatal crash is multiplied by the fatal-and-injury crash frequency obtained in Step 11 using Equation 18-58 as follows:

$$\begin{aligned}
 N_{e,fs,6,at,K} &= N_{e,fs,6,at,fi} \times P_{fs+sc,ac,at,K} \\
 &= 7.008 \times 0.023 \\
 &= 0.163 \text{ crashes/year}
 \end{aligned}$$

Similar calculations using Equation 18-58 and the probabilities of occurrences of the other crash severities yield the following results:

$$N_{e,fs,6,at,A} = 0.412 \text{ crashes/year}$$

$$N_{e,fs,6,at,B} = 2.456 \text{ crashes/year}$$

$$N_{e,fs,6,at,C} = 3.977 \text{ crashes/year}$$

Apply the crash type distribution, if desired.

The crash type distributions are applied by multiplying the default crash type distribution proportions in Table 18-6 and Table 18-8 by the predicted average crash frequencies obtained in Step 11.

Worksheets

The step-by-step instructions are provided to illustrate the predictive method for calculating the predicted average crash frequency for a freeway segment. To apply the predictive method steps to multiple segments, a series of worksheets are provided for determining the predicted average crash frequency. The worksheets include:

- Table 18-36. Freeway Segment Worksheet (1 of 4)—Sample Problem 2
- Table 18-37. Freeway Segment Worksheet (2 of 4)—Sample Problem 2
- Table 18-38. Freeway Segment Worksheet (3 of 4)—Sample Problem 2
- Table 18-39. Freeway Segment Worksheet (4 of 4)—Sample Problem 2

Filled versions of these worksheets are provided below. Blank versions of worksheets used in the Sample Problems are provided in Appendix 18A.

Table 18-36 is a summary of general information about the freeway segment, analysis, input data (i.e., “The Facts”), and assumptions for Sample Problem 2. The input data include area type, crash data, basic roadway data, alignment data, and cross section data.

Table 18-37 is a summary of general information about the freeway segment, analysis, input data (i.e., “The Facts”), and assumptions for Sample Problem 2. The input data include roadside data, ramp access data, and traffic data.

Table 18-38 is a tabulation of the CMF and SPF computations for Sample Problem 2.

Table 18-39 is a tabulation of the crash severity and crash type distributions for Sample Problem 2.

Table 18-36. Freeway Segment Worksheet (1 of 4)—Sample Problem 2

General Information					Location Information				
Analyst					Roadway				
Agency or company					Roadway section				
Date performed					Study year				
Area type		X	Urban		Rural				
Input Data									
Crash Data				Crash Period	Study Year	Complete the study year column. Complete the crash period column if the EB Method is used.			
Crash data time period						First year	--	Last year	--
Count of multiple-vehicle FI crashes $N_{o,fs,n,mv,fi}^*$				--					
Count of single-vehicle FI crashes $N_{o,fs,n,sv,fi}^*$				--					
Count of multiple-vehicle PDO crashes $N_{o,fs,n,mv,pdo}^*$				--					
Count of single-vehicle PDO crashes $N_{o,fs,n,sv,pdo}^*$				--					
Basic Roadway Data									
Number of through lanes n				6		Same value for crash period and study year.			
Segment length L (mi)				--	0.75				
Alignment Data									
Horizontal Curve Data									
1	Presence of horizontal curve 1			--	Y/N	Y	Y/N	If Yes, then enter data in the next three rows.	
	Equivalent curve radius R_1^* (ft)			--		2,100			
	Length of curve L_{c1} (mi)			--		0.25			
	Length of curve in segment $L_{c1,seg}$ (mi)			--		0.25			
2	Presence of horizontal curve 2			--	Y/N	N	Y/N	If Yes, then enter data in the next three rows.	
	Equivalent curve radius R_2^* (ft)			--		--			
	Length of curve L_{c2} (mi)			--		--			
	Length of curve in segment $L_{c2,seg}$ (mi)			--		--			
Cross Section Data									
Lane width W_l (ft)				--		12			
Outside shoulder width W_s (ft)				--		7			
Inside shoulder width W_{is} (ft)				--		6			
Median width W_m (ft)				--		40			
Presence of rumble strips on outside shoulder				--	Y/N	Y	Y/N	If Yes, then enter data in the next two rows.	
Length of rumble strip in increasing milepost dir. (mi)				--		0.25			
Length of rumble strip in decreasing milepost dir. (mi)				--		0.25			
Presence of rumble strips on inside shoulder				--	Y/N	Y	Y/N	If Yes, then enter data in the next two rows.	
Length of rumble strip in increasing milepost dir. (mi)				--		0.25			
Length of rumble strip in decreasing milepost dir. (mi)				--		0.25			
Presence of barrier in median				--	Y/N	N	Y/N	If Yes, then use the freeway barrier worksheet.	

Table 18-37. Freeway Segment Worksheet (2 of 4)—Sample Problem 2

Input Data						
Roadside Data		Crash Period		Study Year		Complete the study year column. Complete the crash period column if the EB Method is used.
Clear zone width W_{hc} (ft)		--		30		
Presence of barrier on roadside		--	Y/N	N	Y/N	If Yes, then use the freeway barrier worksheet.
Ramp Access Data						
Travel in Increasing Milepost Direction						
Ent. ramp	Distance from begin milepost to upstream entrance ramp gore $X_{b, ent}$ (mi)	--		1.25		If ramp entrance is in the segment, enter 0.0.
	Presence of speed-change lane in segment	--	Y/N	N	Y/N	If Yes, then enter data in the next row.
	Length of s-c lane in segment $L_{en, seg, inc}$ (mi)	--		--		
Exit ramp	Distance from end milepost to upstream exit ramp gore $X_{e, ext}$ (mi)	--		0.1		If ramp exit is in the segment, enter 0.0.
	Presence of speed-change lane in segment	--	Y/N	N	Y/N	If Yes, then enter data in the next row.
	Length of s-c lane in segment $L_{ex, seg, inc}$ (mi)	--		--		
Weave	Presence of a Type B weave in segment	--	Y/N	N	Y/N	If Yes, then enter data in the next two rows.
	Length of weaving section $L_{wev, inc}$ (mi)	--		--		
	Length of weaving section in seg. $L_{wev, seg, inc}$ (mi)	--		--		
Travel in Decreasing Milepost Direction						
Ent. ramp	Distance from end milepost to upstream entrance ramp gore $X_{e, ent}$ (mi)	--		0.1		If ramp entrance is in the segment, enter 0.0.
	Presence of speed-change lane in segment	--	Y/N	N	Y/N	If Yes, then enter data in the next row.
	Length of s-c lane in segment $L_{en, seg, dec}$ (mi)	--		--		
Exit ramp	Distance from begin milepost to downstream exit ramp gore $X_{b, ext}$ (mi)	--		1.25		If ramp exit is in the segment, enter 0.0.
	Presence of speed-change lane in segment	--	Y/N	N	Y/N	If Yes, then enter data in the next row.
	Length of s-c lane in segment $L_{ex, seg, dec}$ (mi)	--		--		
Weave	Presence of a Type B weave in segment	--	Y/N	N	Y/N	If Yes, then enter data in the next two rows.
	Length of weaving section $L_{wev, dec}$ (mi)	--		--		
	Length of weaving section in seg. $L_{wev, seg, dec}$ (mi)	--		--		
Traffic Data						
Proportion of AADT during high-volume hours P_{hv}		--		0.1		
Freeway segment AADT $AADT_{fs}$ (veh/day)		--		120,000		
AADT of entrance ramp for travel in increasing milepost direction $AADT_{b, ent}$ (veh/day)		--		8,000		
AADT of exit ramp for travel in increasing milepost direction $AADT_{e, ext}$ (veh/day)		--		7,150		
AADT of entrance ramp for travel in decreasing milepost direction $AADT_{e, ent}$ (veh/day)		--		6,750		
AADT of exit ramp for travel in decreasing milepost direction $AADT_{b, ext}$ (veh/day)		--		7,675		

Table 18-38. Freeway Segment Worksheet (3 of 4)—Sample Problem 2

Crash Modification Factors									
Complete the study year column. Complete the crash period column if the EB Method is used. Equation	Fatal and Injury				Property Damage Only				
	Multiple Vehicle		Single Vehicle		Multiple Vehicle		Single Vehicle		
	Crash Period	Study Year	Crash Period	Study Year	Crash Period	Study Year	Crash Period	Study Year	
Horizontal curve $CMF_{1,fs,ac,y,z}$	18-24	--	1.043	--	1.178	--	1.084	--	1.155
Lane width $CMF_{2,fs,ac,y,fi}$	18-25	--	1.000	--	1.000				
Inside shoulder width $CMF_{3,fs,ac,y,z}$	18-26	--	1.000	--	1.000	--	1.000	--	1.000
Median width $CMF_{4,fs,ac,y,z}$	18-27	--	1.062	--	0.980	--	1.060	--	1.060
Median barrier $CMF_{5,fs,ac,y,z}$	18-28	--	1.000	--	1.000	--	1.000	--	1.000
High volume $CMF_{6,fs,ac,y,z}$	18-29	--	1.036	--	0.993	--	1.029	--	0.941
Lane change $CMF_{7,fs,ac,mv,z}$	18-30	--	1.018			--	1.015		
Outside shoulder width $CMF_{8,fs,ac,sv,z}$	18-35			--	1.246			--	1.096
Shoulder rumble strip $CMF_{9,fs,ac,sv,fi}$	18-36			--	0.958				
Outside clearance $CMF_{10,fs,ac,sv,fi}$	18-38			--	0.987				
Outside barrier $CMF_{11,fs,ac,sv,z}$	18-39			--	1.000			--	1.000
Combined CMF (multiply all CMFs evaluated)		--	1.168	--	1.351	--	1.200	--	1.263

Expected Average Crash Frequency^a									
Complete the study year column. Complete the crash period column if the <i>site-specific</i> EB Method is used.	Fatal and Injury				Property Damage Only				
	Multiple Vehicle		Single Vehicle		Multiple Vehicle		Single Vehicle		
	Crash Period	Study Year	Crash Period	Study Year	Crash Period	Study Year	Crash Period	Study Year	
Calibration factor $C_{fs,ac,y,z}$	1.00		1.00		1.00		1.00		
Overdispersion parameter $k_{fs,n,y,z}$	--		--		--		--		
Observed crash count $N_{a,fs,n,y,z}^*$ (cr)	--		--		--		--		
Reference year r	--		--		--		--		
Predicted average crash freq. for reference year $N_{p,fs,n,y,z,r}$ (cr/yr)	--		--		--		--		
Predicted number of crashes for crash period (sum all years) $N_{p,fs,n,y,z}^*$ (cr)	--		--		--		--		
Equivalent years associated with crash count $C_{b,fs,n,y,z,r}$ (yr)	--		--		--		--		
Adjusted average crash freq. for ref. year given $N_{os}^*, N_{a,fs,n,y,z,r}$ (cr/yr)	--		--		--		--		
Study year s		2011		2011		2011		2011	
Predicted average crash freq. for study year $N_{p,fs,n,y,z,s}$ (cr/yr)		4.150		2.858		10.530		6.454	
Expected average crash freq. for study year $N_{e,fs,n,y,z,s}$ (cr/yr)		4.150		2.858		10.530		6.454	
Expected average crash freq. for study year (all crash types) $N_{e,fs,n,at,z,s}$ (cr/yr)				7.008				16.984	

Note:

a – If the EB Method is not used, then substitute the word “predicted” for the word “expected” and substitute the subscript “p” for the subscript “e”.

Table 18-39. Freeway Segment Worksheet (4 of 4)—Sample Problem 2

Expected Average Crash Frequency ^a							
Crash Severity Distribution							
	K	A	B	C	Total FI	PDO	Total FI + PDO
Proportion by injury level	0.023	0.059	0.350	0.567	1.000		
Expected average crash freq. for study year (all crash types) $N_{e, fs, n, at, z, s}$ (cr/yr)	0.163	0.412	2.456	3.977	7.008	16.984	23.992
Crash Type Distribution							
Crash Type Category	Table	Fatal and Injury		Property Damage Only		Total	
		Proportion	Expected Average Crash Frequency for Study Year $N_{e, fs, n, y, fi, s}$ (cr/yr)	Proportion	Expected Average Crash Frequency for Study Year $N_{e, fs, n, y, pdo, s}$ (cr/yr)	Expected Average Crash Frequency for Study Year $N_{e, fs, n, y, as, s}$ (cr/yr)	Expected Average Crash Frequency for Study Year $N_{e, fs, n, y, as, s}$ (cr/yr)
Multiple-Vehicle Crashes 18-6							
Head-on		0.008	0.033	0.002	0.021	0.054	
Right-angle		0.031	0.129	0.018	0.190	0.318	
Rear-end		0.750	3.113	0.690	7.265	10.378	
Sideswipe		0.180	0.747	0.266	2.801	3.548	
Other multiple-vehicle crashes		0.031	0.129	0.024	0.253	0.381	
Total		1.000	4.150	1.000	10.530	14.680	
Single-Vehicle Crashes 18-8							
Crash with animal		0.004	0.011	0.022	0.142	0.153	
Crash with fixed object		0.722	2.063	0.716	4.621	6.685	
Crash with other object		0.051	0.146	0.139	0.897	1.043	
Crash with parked vehicle		0.015	0.043	0.016	0.103	0.146	
Other single-vehicle crashes		0.208	0.594	0.107	0.691	1.285	
Total		1.000	2.858	1.000	6.454	9.312	

Note:

a – If the EB Method is not used, then substitute the word “predicted” for the word “expected” and substitute the subscript “p” for the subscript “e”.

18.13.3. Sample Problem 3

The Site/Facility

A ramp-entrance speed-change lane on a six-lane urban freeway.

The Question

What is the predicted average crash frequency of the speed-change lane for a one-year period?

The Facts

The study year is 2011. The conditions present during this year are provided in the following list.

- 0.1-mi length

- Freeway mainline data
 - 120,000 veh/day
 - 10 percent of AADT volume occurs during high-volume hours
 - No horizontal curvature
 - 12-ft lane width
 - 6-ft inside shoulder width
 - 40-ft median width
 - No median barrier
- Ramp entrance data
 - 6,750 veh/day
 - On right side of mainline

Assumptions

- Crash type distributions used are the default values presented in Table 18-10.
- The calibration factor is 1.00.

Results

Using the predictive method steps as outlined below, the predicted average fatal-and-injury crash frequency for the speed-change lane in Sample Problem 3 is determined to be 0.5 crashes per year, and the predicted average property-damage-only crash frequency is determined to be 1.0 crashes per year (rounded to one decimal place).

Steps

Step 1 through 8

To determine the predicted average crash frequency of the speed-change lane in Sample Problem 3, only Steps 9 through 11 are conducted. No other steps are necessary because only one speed-change lane is analyzed for one year, and the EB Method is not applied.

Step 9 – For the selected site, determine and apply the appropriate SPF.

For a ramp-entrance speed-change lane on a six-lane urban freeway, an SPF value for ramp entrance crashes is determined.

Ramp Entrance Crashes

The SPF for fatal-and-injury ramp entrance crashes is calculated from Equation 18-20 and Table 18-9 as follows:

$$\begin{aligned}
 N_{spf,sc,6EN,at,fi} &= L_{en} \times \exp(a + b \times \ln[c \times AADT_{fs}]) \\
 &= 0.10 \times \exp(-3.974 + 1.173 \times \ln[0.0005 \times 120,000]) \\
 &= 0.229 \text{ crashes/year}
 \end{aligned}$$

Similarly, the SPF for property-damage-only ramp entrance crashes is calculated from Equation 18-20 and Table 18-9 to yield the following result:

$$N_{spf,sc,6EN,at,pdo} = 0.722 \text{ crashes/year}$$

Step 10 – Multiply the result obtained in Step 9 by the appropriate CMFs.

Each CMF used in the calculation of the predicted average crash frequency of the speed-change lane is calculated below:

Horizontal Curve ($CMF_{1,sc,6EN,at,z}$)

The speed-change lane does not have horizontal curvature. Hence, $CMF_{1,sc,6EN,at,fi}$ and $CMF_{1,sc,6EN,at,pdo}$ are equal to 1.000.

Lane Width ($CMF_{2,sc,6EN,at,z}$)

The segment has 12-ft lanes, which is the base condition for the lane width CMF. Hence, $CMF_{2,sc,6EN,at,fi}$ and $CMF_{2,sc,6EN,at,pdo}$ are equal to 1.000.

Inside Shoulder Width ($CMF_{3,sc,6EN,at,z}$)

The segment has 6-ft inside shoulders, which is the base condition for the inside shoulder width CMF. Hence, $CMF_{3,sc,6EN,at,fi}$ and $CMF_{3,sc,6EN,at,pdo}$ are equal to 1.000.

Median Width ($CMF_{4,sc,6EN,at,z}$)

$CMF_{4,sc,6EN,at,fi}$ is calculated from Equation 18-43 as follows:

$$CMF_{4,sc,6EN,at,fi} = (1.0 - P_{ib}) \times \exp(a \times [W_m - 2 \times W_{is} - 48]) + P_{ib} \times \exp(a \times [2 \times W_{icb} - 48])$$

The segment does not have inside barrier, so $P_{ib} = 0.0$ and the calculation of W_{icb} does not apply. From Table 18-25, $a = -0.00302$. $CMF_{4,sc,6EN,at,fi}$ is calculated as follows:

$$\begin{aligned}
 CMF_{4,sc,6EN,at,fi} &= (1.0 - 0.0) \times \exp(-0.00302 \times [40 - 2 \times 6 - 48]) + 0.0 \times \exp(-0.00302 \times [2 \times W_{icb} - 48]) \\
 &= 1.062
 \end{aligned}$$

Similar calculations using the property-damage-only coefficient from Table 18-25 yield the following results:

$$CMF_{4,sc,6EN,at,pdo} = 1.060$$

Median Barrier ($CMF_{5,sc,6EN,at,z}$)

The segment does not have inside barrier. Hence, $CMF_{5,sc,6EN,at,fi}$ and $CMF_{5,sc,6EN,at,pdo}$ are equal to 1.000.

High Volume ($CMF_{6,sc,6EN,at,z}$)

$CMF_{6,sc,6EN,at,fi}$ is calculated from Equation 18-45 and the coefficient $a = 0.350$ from Table 18-27 as follows:

$$\begin{aligned}
 CMF_{6,fs,6,mv,fi} &= \exp(a \times P_{hv}) \\
 &= \exp(0.350 \times 0.1) \\
 &= 1.036
 \end{aligned}$$

Similar calculations using the property-damage-only coefficients from Table 18-27 yield the following results:

$$CMF_{6,sc,6EN,at,pdo} = 1.029$$

Ramp Entrance ($CMF_{12,sc,6EN,at,z}$)

$CMF_{12,sc,6EN,at,fi}$ is calculated from Equation 18-46 as follows:

$$CMF_{12,sc,6EN,at,fi} = \exp\left(a \times I_{left} + \frac{b}{L_{en}} + d \times \ln[c \times AADT_r]\right)$$

The ramp entrance connects to the right side of the freeway mainline. Hence, $I_{left} = 0.0$. From Table 18-28, the coefficients a , b , c , and d for fatal-and-injury crashes are 0.594, 0.0318, 0.001, and 0.198, respectively. $CMF_{12,sc,6EN,at,fi}$ is calculated as follows:

$$CMF_{12,sc,6EN,at,fi} = \exp\left(0.594 \times 0.0 + \frac{0.0318}{0.1} + 0.198 \times \ln[0.001 \times 6,750]\right) = 2.006$$

Similar calculations using the property-damage-only coefficients from Table 18-28 yield the following results:

$$CMF_{12,sc,6EN,at,pdo} = 1.287$$

Ramp Entrance Crashes

The CMFs are applied to the ramp entrance fatal-and-injury SPF as follows:

$$\begin{aligned}
 N_{p^*,sc,6EN,at,fi} &= N_{spf,sc,6EN,at,fi} \times (CMF_{1,sc,6EN,at,fi} \times \dots \times CMF_{6,sc,6EN,at,fi} \times CMF_{12,sc,6EN,at,fi}) \\
 &= 0.229 \times (1.000 \times 1.000 \times 1.000 \times 1.062 \times 1.000 \times 1.036 \times 2.006) \\
 &= 0.229 \times 2.207 \\
 &= 0.505 \text{ crashes/year}
 \end{aligned}$$

The CMFs are applied to the ramp entrance property-damage-only SPF as follows:

$$\begin{aligned}
 N_{p^*,sc,6EN,at,pdo} &= N_{spf,sc,6EN,at,pdo} \times (CMF_{1,sc,6EN,at,pdo} \times \dots \times CMF_{6,sc,6EN,at,pdo} \times CMF_{12,sc,6EN,at,pdo}) \\
 &= 0.722 \times (1.000 \times 1.000 \times 1.000 \times 1.060 \times 1.000 \times 1.029 \times 1.287) \\
 &= 0.722 \times 1.403 \\
 &= 1.013 \text{ crashes/year}
 \end{aligned}$$

Step 11 – Multiply the result obtained in Step 10 by the appropriate calibration factor.

It is assumed that a calibration factor of 1.00 has been determined for local conditions. See Section B.1 of Appendix B to Part C for further discussion on calibration of the predicted models.

Calculation of Predicted Average Crash Frequency

The predicted average crash frequency is calculated using Equation 18-2 based on the results obtained in Steps 9 through 11 as follows.

Fatal-and-injury crashes:

$$\begin{aligned} N_{p, sc, 6EN, at, fi} &= N_{spf^*, sc, 6EN, at, fi} \times C_{fs, sc, 6EN, at, fi} \\ &= 0.505 \times 1.00 \\ &= 0.505 \text{ crashes/year} \end{aligned}$$

Property-damage-only crashes:

$$\begin{aligned} N_{p, sc, 6EN, at, pdo} &= N_{spf^*, sc, 6EN, at, pdo} \times C_{fs, sc, 6EN, at, pdo} \\ &= 1.013 \times 1.00 \\ &= 1.013 \text{ crashes/year} \end{aligned}$$

Step 12—If there is another year to be evaluated in the evaluation period for the selected site, return to Step 8. Otherwise, proceed to Step 13.

The study period is one year (2011), so steps 8 through 11 need not be repeated.

Step 13—Apply site-specific EB Method (if applicable) and apply SDFs.

This step consists of three optional sets of calculations—site-specific EB Method, severity distribution functions, and crash type distribution.

Apply the site-specific EB Method to a future time period, if appropriate.

The site-specific EB Method is not applied in this sample problem because crash data are not available.

Apply the severity distribution functions (SDFs), if desired.

To apply the SDFs, the systematic component of crash severity likelihood V_j is computed for each severity level j using Equation 18-63 as follows:

$$V_j = a + \left(b \times \frac{P_{ib} + P_{ob}}{2} \right) + (c \times P_{hv}) + \left(d \times \frac{P_{ir} + P_{or}}{2} \right) + (e \times \sum P_{c,i}) + (f \times W_l) + (g \times I_{rural})$$

The coefficients a , b , c , d , e , f , and g are obtained from Table 18-30 for each severity level j . The segment does not have barrier, rumble strips, or horizontal curvature, so P_{ib} , P_{ob} , P_{ir} , P_{or} , and $P_{c,i}$ are equal to 0.0. V_j is computed for fatal crashes as follows:

$$\begin{aligned} V_K &= -0.171 + \left(-0.388 \times \frac{0.0 + 0.0}{2} \right) + (-0.924 \times 0.1) + \left(0.387 \times \frac{0.0 + 0.0}{2} \right) \\ &\quad + (0.208 \times 0.0) + (-0.261 \times 12) + (0.492 \times 0.0) \\ &= -3.392 \end{aligned}$$

Calculations using the coefficients for incapacitating injury crashes and non-incapacitating injury crashes from Table 18-30 yield the following results:

$$V_A = -2.478$$

$$V_B = -0.571$$

Using these computed V_K , V_A , and V_B values, and assuming a calibration factor $C_{sdf,fs+sc}$ of 1.0, the probability of occurrence of a fatal crash is computed using Equation 18-59 as follows:

$$\begin{aligned} P_{fs+sc,ac,at,K} &= \frac{\exp(V_K)}{\frac{1.0}{C_{sdf,fs+sc}} + \exp(V_K) + \exp(V_A) + \exp(V_B)} \\ &= \frac{\exp(-3.392)}{\frac{1.0}{1.0} + \exp(-3.392) + \exp(-2.478) + \exp(-0.571)} \\ &= 0.020 \end{aligned}$$

Similar calculations using Equation 18-60 and Equation 18-61 yield the following results:

$$P_{fs+sc,ac,at,A} = 0.050$$

$$P_{fs+sc,ac,at,B} = 0.336$$

The probability of occurrence of a possible-injury crash is computed using Equation 18-62 as follows:

$$\begin{aligned} P_{fs+sc,ac,at,C} &= 1.0 - (P_{fs+sc,ac,at,K} + P_{fs+sc,ac,at,A} + P_{fs+sc,ac,at,B}) \\ &= 1.0 - (0.020 + 0.050 + 0.336) \\ &= 0.594 \end{aligned}$$

The probability of occurrence of a fatal crash is multiplied by the fatal-and-injury crash frequency obtained in Step 11 using Equation 18-58 as follows:

$$\begin{aligned} N_{e,sc,6EN,at,K} &= N_{e,sc,6EN,at,fi} \times P_{fs+sc,ac,at,K} \\ &= 0.505 \times 0.020 \\ &= 0.010 \text{ crashes/year} \end{aligned}$$

Similar calculations using Equation 18-58 and the probabilities of occurrences of the other crash severities yield the following results:

$$N_{e,sc,6EN,at,A} = 0.025 \text{ crashes/year}$$

$$N_{e,sc,6EN,at,B} = 0.170 \text{ crashes/year}$$

$$N_{e,sc,6EN,at,C} = 0.300 \text{ crashes/year}$$

Apply the crash type distribution, if desired.

The crash type distributions are applied by multiplying the default crash type distribution proportions in Table 18-10 by the predicted average crash frequencies obtained in Step 11.

Worksheets

The step-by-step instructions are provided to illustrate the predictive method for calculating the predicted average crash frequency for a freeway segment. To apply the predictive method steps to multiple segments, a series of worksheets are provided for determining the predicted average crash frequency. The worksheets include:

- Table 18-40. Freeway Speed-Change Lane Worksheet (1 of 3)—Sample Problem 3
- Table 18-41. Freeway Speed-Change Lane Worksheet (2 of 3)—Sample Problem 3
- Table 18-42. Freeway Speed-Change Lane Worksheet (3 of 3)—Sample Problem 3

Filled versions of these worksheets are provided below. Blank versions of worksheets used in the Sample Problems are provided in Appendix 18A.

Table 18-40 is a summary of general information about the freeway speed-change lane, analysis, input data (i.e., “The Facts”), and assumptions for Sample Problem 3. The input data include area type, crash data, basic roadway data, alignment data, cross section data, and traffic data.

Table 18-41 is a tabulation of the CMF and SPF computations for Sample Problem 3.

Table 18-42 is a tabulation of the crash severity and crash type distributions for Sample Problem 3.

Table 18-40. Freeway Speed-Change Lane Worksheet (1 of 3)—Sample Problem 3

General Information					Location Information					
Analyst					Roadway					
Agency or company					Roadway section					
Date performed					Study year					
Area type		X	Urban		Rural					
Input Data										
Crash Data					Crash Period	Study Year	Complete the study year column. Complete the crash period column if the EB Method is used.			
Crash data time period							First year	--	Last year	--
Count of speed-change-related FI crashes $N_{o,sc,x,at,fi}^*$					--					
Count of speed-change-related PDO crashes $N_{o,sc,x,at,pdo}^*$					--					
Basic Roadway Data										
Number of through lanes n					6		Same value for crash period and study year.			
Segment length L (mi)					--	0.1	Equals the length of the speed-change lane.			
Configuration					Entrance		Choices: Entrance, Exit			
Alignment Data										
Horizontal Curve Data										
1	Presence of horizontal curve 1				--	Y/N	N	Y/N	If Yes, then enter data in the next three rows.	
	Curve radius R_1 (ft)				--		--			
	Length of curve L_{c1} (mi)				--		--			
	Length of curve in segment $L_{c1,seg}$ (mi)				--		--			
2	Presence of horizontal curve 2				--	Y/N	N	Y/N	If Yes, then enter data in the next three rows.	
	Curve radius R_2 (ft)				--		--			
	Length of curve L_{c2} (mi)				--		--			
	Length of curve in segment $L_{c2,seg}$ (mi)				--		--			
Cross Section Data										
Lane width W_l (ft)					--	12				
Inside shoulder width W_{is} (ft)					--	6				
Median width W_m (ft)					--	40				
Presence of barrier in median					--	Y/N	N	Y/N	If Yes, then use the freeway barrier worksheet.	
Entrance or exit side (left- or right-hand side)					--	L/R	R	L/R		
Traffic Data										
Proportion of AADT during high-volume hours P_{hv}					--	0.1				
Freeway segment AADT $AADT_f$ (veh/day)					--	120,000				
AADT of ramp $AADT_r$ (veh/day)					--	6,750	Only needed for entrance ramp.			

Table 18-41. Freeway Speed-Change Lane Worksheet (2 of 3)—Sample Problem 3

Crash Modification Factors

Complete the study year column. Complete the crash period column if the EB Method is used.	Equation	Fatal and Injury		Property Damage Only	
		Crash Period	Study Year	Crash Period	Study Year
Horizontal curve $CMF_{1, sc, ac, at, z}$	18-40	--	1.000	--	1.000
Lane width $CMF_{2, sc, ac, at, fi}$	18-41	--	1.000		
Inside shoulder width $CMF_{3, sc, ac, at, z}$	18-42	--	1.000	--	1.000
Median width $CMF_{4, sc, ac, at, z}$	18-43	--	1.062	--	1.060
Median barrier $CMF_{5, sc, ac, at, z}$	18-44	--	1.000	--	1.000
High volume $CMF_{6, sc, ac, at, z}$	18-45	--	1.036	--	1.029
Ramp entrance $CMF_{12, sc, nEN, at, z}$	18-46	--	2.006	--	1.287
Ramp exit $CMF_{13, sc, nEX, at, z}$	18-47	--	1.000	--	1.000
Combined CMF (multiply all CMFs evaluated)		--	2.207	--	1.403

Expected Average Crash Frequency^a

Complete the study year column. Complete the crash period column if the <i>site-specific</i> EB Method is used.	Fatal and Injury		Property Damage Only	
	Crash Period	Study Year	Crash Period	Study Year
Calibration factor $C_{sc, x, at, z}$	1.00		1.00	
Overdispersion parameter $k_{sc, x, at, z}$	--		--	
Observed crash count $N_{o, sc, x, at, z}^*$ (cr)	--		--	
Reference year r	--		--	
Predicted average crash freq. for reference year $N_{p, sc, x, at, z, r}$ (cr/yr)	--		--	
Predicted number of crashes for crash period (sum all years) $N_{p, sc, x, at, z}^*$ (cr)	--		--	
Equivalent years associated with crash count $C_{b, sc, x, at, z, r}$ (yr)	--		--	
Adjusted average crash freq. for ref. year given $N_{o, sc, x, at, z, r}^*$ (cr/yr)	--		--	
Study year s		2011		2011
Predicted average crash freq. for study year $N_{p, sc, x, at, z, s}$ (cr/yr)		0.505		1.013
Expected average crash freq. for study year $N_{e, sc, x, at, z, s}$ (cr/yr)		0.505		1.013

Note:

a – If the EB Method is not used, then substitute the word “predicted” for the word “expected” and substitute the subscript “p” for the subscript “e”.

Table 18-42. Freeway Speed-Change Lane Worksheet (3 of 3)—Sample Problem 3**Expected Average Crash Frequency^a****Crash Severity Distribution**

	K	A	B	C	Total FI	PDO	Total FI + PDO
Proportion by injury level	0.020	0.050	0.336	0.594	1.000		
Expected average crash freq. for study year $N_{e, sc, x, at, z, s}$ (cr/yr)	0.010	0.025	0.170	0.300	0.505	1.013	1.518

Crash Type Distribution

Crash Type Category	Table 18-10 or 18-12	Fatal and Injury		Property Damage Only		Total
		Proportion	Expected Average Crash Frequency for Study Year $N_{e, sc, x, at, fi, s}$ (cr/yr)	Proportion	Expected Average Crash Frequency for Study Year $N_{e, sc, x, at, pdo, s}$ (cr/yr)	Expected Average Crash Frequency for Study Year $N_{e, sc, x, at, as, s}$ (cr/yr)
Multiple-Vehicle Crashes						
Head-on		0.004	0.002	0.001	0.001	0.003
Right-angle		0.019	0.010	0.016	0.016	0.026
Rear-end		0.543	0.274	0.530	0.537	0.811
Sideswipe		0.133	0.067	0.252	0.255	0.322
Other multiple-vehicle crashes		0.017	0.009	0.015	0.015	0.024
Single-Vehicle Crashes						
Crash with animal		0.000	0.000	0.002	0.002	0.002
Crash with fixed object		0.194	0.098	0.129	0.131	0.229
Crash with other object		0.019	0.010	0.036	0.036	0.046
Crash with parked vehicle		0.004	0.002	0.003	0.003	0.005
Other single-vehicle crashes		0.067	0.034	0.016	0.016	0.050
Total		1.000	0.505	1.000	1.013	1.518

Note:

a – If the EB Method is not used, then substitute the word “predicted” for the word “expected” and substitute the subscript “p” for the subscript “e”.

18.13.4. Sample Problem 4**The Site/Facility**

A ramp-exit speed-change lane on a six-lane urban freeway.

The Question

What is the predicted average crash frequency of the speed-change lane for a one-year period?

The Facts

The study year is 2011. The conditions present during this year are provided in the following list.

- 0.1-mi length
- Freeway mainline data

- 120,000 veh/day
- 10 percent of AADT volume occurs during high-volume hours
- No horizontal curvature
- 12-ft lane width
- 6-ft inside shoulder width
- 40-ft median width
- No median barrier
- Ramp exit data
 - On right side of mainline

Assumptions

- Crash type distributions used are the default values presented in Table 18-12.
- The calibration factor is 1.00.

Results

Using the predictive method steps as outlined below, the predicted average fatal-and-injury crash frequency for the speed-change lane in Sample Problem 4 is determined to be 0.3 crashes per year, and the predicted average property-damage-only crash frequency is determined to be 0.8 crashes per year (rounded to one decimal place).

Steps

Step 1 through 8

To determine the predicted average crash frequency of the speed-change lane in Sample Problem 4, only Steps 9 through 11 are conducted. No other steps are necessary because only one speed-change lane is analyzed for one year, and the EB Method is not applied.

Step 9 – For the selected site, determine and apply the appropriate SPF.

For a ramp-exit speed-change lane on a six-lane urban freeway, SPF values for ramp exit crashes are determined.

Ramp Exit Crashes

The SPF for fatal-and-injury ramp exit crashes is calculated from Equation 18-22 and Table 18-11 as follows:

$$\begin{aligned}
 N_{spf,sc,6EX,at,fi} &= L_{ex} \times \exp(a + b \times \ln[c \times AADT_{fs}]) \\
 &= 0.10 \times \exp(-2.679 + 0.903 \times \ln[0.0005 \times 120,000]) \\
 &= 0.277 \text{ crashes/year}
 \end{aligned}$$

Similarly, the SPF for property-damage-only ramp exit crashes is calculated from Equation 18-22 and Table 18-11 to yield the following result:

$$N_{spf,sc,6EX,at,pdo} = 0.752 \text{ crashes/year}$$

Step 10 – Multiply the result obtained in Step 9 by the appropriate CMFs.

Each CMF used in the calculation of the predicted average crash frequency of the speed-change lane is calculated in this step.

Horizontal Curve ($CMF_{1,sc,6EX,at,z}$)

The segment does not have horizontal curvature. Hence, $CMF_{1,sc,6EX,at,fi}$ and $CMF_{1,sc,6EX,at,pdo}$ are equal to 1.000.

Lane Width ($CMF_{2,sc,6EX,at,fi}$)

The segment has 12-ft lanes, which is the base condition for the lane width CMF. Hence, $CMF_{2,sc,6EX,at,fi}$ is equal to 1.000.

Inside Shoulder Width ($CMF_{3,sc,6EX,at,z}$)

The segment has 6-ft inside shoulders, which is the base condition for the inside shoulder width CMF. Hence, $CMF_{3,sc,6EX,at,fi}$ and $CMF_{3,sc,6EX,at,pdo}$ are equal to 1.000.

Median Width ($CMF_{4,sc,6EX,at,z}$)

$CMF_{4,sc,6EX,at,fi}$ is calculated from Equation 18-43 as follows:

$$CMF_{4,sc,6EX,at,fi} = (1.0 - P_{ib}) \times \exp(a \times [W_m - 2 \times W_{is} - 48]) + P_{ib} \times \exp(a \times [2 \times W_{icb} - 48])$$

The segment does not have inside barrier, so $P_{ib} = 0.0$ and the calculation of W_{icb} does not apply. From Table 18-25, $a = -0.00302$ for fatal-and-injury crashes. $CMF_{4,sc,6EX,at,fi}$ is calculated as follows:

$$\begin{aligned} CMF_{4,sc,6EX,at,fi} &= (1.0 - 0.0) \times \exp(-0.00302 \times [40 - 2 \times 6 - 48]) + 0.0 \times \exp(-0.00302 \times [2 \times W_{icb} - 48]) \\ &= 1.062 \end{aligned}$$

Similar calculations using the property-damage-only coefficients from Table 18-25 yield the following results:

$$CMF_{4,sc,6EX,at,pdo} = 1.060$$

Median Barrier ($CMF_{5,sc,6EX,at,z}$)

The segment does not have inside barrier. Hence, $CMF_{5,sc,6EX,at,fi}$ and $CMF_{5,sc,6EX,at,pdo}$ are equal to 1.000.

High Volume ($CMF_{6,sc,6EX,at,z}$)

$CMF_{6,sc,6EX,at,fi}$ is calculated from Equation 18-45 and the coefficient $a = 0.350$ from Table 18-27 as follows:

$$\begin{aligned} CMF_{6,fs,6,mv,fi} &= \exp(a \times P_{hv}) \\ &= \exp(0.350 \times 0.1) \\ &= 1.036 \end{aligned}$$

Similar calculations using the property-damage-only coefficients from Table 18-27 yield the following results:

$$CMF_{6,sc,6EX,at,pdo} = 1.029$$

Ramp Exit ($CMF_{13,sc,6EX,at,z}$)

$CMF_{13,sc,6EX,at,fi}$ is calculated from Equation 18-47 as follows:

$$CMF_{13,sc,6EX,at,fi} = \exp\left(a \times I_{left} + \frac{b}{L_{ex}}\right)$$

The ramp entrance connects to the right side of the freeway mainline. Hence, $I_{left} = 0.0$. From Table 18-29, the coefficients a and b for fatal-and-injury crashes are 0.594 and 0.0116, respectively. $CMF_{13,sc,6EX,at,fi}$ is calculated as follows:

$$CMF_{13,sc,6EX,at,fi} = \exp\left(0.594 \times 0.0 + \frac{0.0116}{0.1}\right) = 1.123$$

Similar calculations using the property-damage-only coefficients from Table 18-29 yield the following results:

$$CMF_{13,sc,6EX,at,pdo} = 1.000$$

Ramp Exit Crashes

The CMFs are applied to the ramp exit fatal-and-injury SPF as follows:

$$\begin{aligned} N_{p^*,sc,6EX,at,fi} &= N_{spf,sc,6EX,at,fi} \times (CMF_{1,sc,6EX,at,fi} \times \dots \times CMF_{6,sc,6EX,at,fi} \times CMF_{13,sc,6EX,at,fi}) \\ &= 0.277 \times (1.000 \times 1.000 \times 1.000 \times 1.062 \times 1.000 \times 1.036 \times 1.123) \\ &= 0.277 \times 1.235 \\ &= 0.342 \text{ crashes/year} \end{aligned}$$

The CMFs are applied to the ramp exit property-damage-only SPF as follows:

$$\begin{aligned} N_{p^*,sc,6EX,at,pdo} &= N_{spf,sc,6EX,at,pdo} \times (CMF_{1,sc,6EX,at,pdo} \times \dots \times CMF_{6,sc,6EX,at,pdo} \times CMF_{13,sc,6EX,at,pdo}) \\ &= 0.752 \times (1.000 \times 1.000 \times 1.000 \times 1.060 \times 1.000 \times 1.029 \times 1.000) \\ &= 0.752 \times 1.090 \\ &= 0.820 \text{ crashes/year} \end{aligned}$$

Step 11 – Multiply the result obtained in Step 10 by the appropriate calibration factor.

It is assumed that a calibration factor of 1.00 has been determined for local conditions. See Section B.1 of Appendix B to Part C for further discussion on calibration of the predicted models.

Calculation of Predicted Average Crash Frequency

The predicted average crash frequency is calculated using Equation 18-2 based on the results obtained in Steps 9 through 11 as follows.

Fatal-and-injury crashes:

$$\begin{aligned} N_{p, sc, 6EX, at, fi} &= N_{spf^*, sc, 6EX, at, fi} \times C_{fs, sc, 6EX, at, fi} \\ &= 0.342 \times 1.00 \\ &= 0.342 \text{ crashes/year} \end{aligned}$$

Property-damage-only crashes:

$$\begin{aligned} N_{p, sc, 6EX, at, pdo} &= N_{spf^*, sc, 6EX, at, pdo} \times C_{fs, sc, 6EX, at, pdo} \\ &= 0.820 \times 1.00 \\ &= 0.820 \text{ crashes/year} \end{aligned}$$

Step 12—If there is another year to be evaluated in the evaluation period for the selected site, return to Step 8. Otherwise, proceed to Step 13.

The study period is one year (2011), so steps 8 through 11 need not be repeated.

Step 13—Apply site-specific EB Method (if applicable) and apply SDFs.

This step consists of three optional sets of calculations—site-specific EB Method, severity distribution functions, and crash type distribution.

Apply the site-specific EB Method to a future time period, if appropriate.

The site-specific EB Method is not applied in this sample problem because crash data are not available.

Apply the severity distribution functions (SDFs), if desired.

To apply the SDFs, the systematic component of crash severity likelihood V_j is computed for each severity level j using Equation 18-63 as follows:

$$V_j = a + \left(b \times \frac{P_{ib} + P_{ob}}{2} \right) + (c \times P_{hv}) + \left(d \times \frac{P_{ir} + P_{or}}{2} \right) + (e \times \sum P_{c,i}) + (f \times W_l) + (g \times I_{rural})$$

The coefficients a , b , c , d , e , f , and g are obtained from Table 18-30 for each severity level j . The segment does not have barrier, rumble strips, or horizontal curvature, so P_{ib} , P_{ob} , P_{ir} , P_{or} , and $P_{c,i}$ are equal to 0.0. V_j is computed for fatal crashes as follows:

$$\begin{aligned} V_K &= -0.171 + \left(-0.388 \times \frac{0.0 + 0.0}{2} \right) + (-0.924 \times 0.1) + \left(0.387 \times \frac{0.0 + 0.0}{2} \right) \\ &\quad + (0.208 \times 0.0) + (-0.261 \times 12) + (0.492 \times 0.0) \\ &= -3.392 \end{aligned}$$

Calculations using the coefficients for incapacitating injury crashes and non-incapacitating injury crashes from Table 18-30 yield the following results:

$$V_A = -2.478$$

$$V_B = -0.571$$

Using these computed V_K , V_A , and V_B values, and assuming a calibration factor $C_{sdf,fs+sc}$ of 1.0, the probability of occurrence of a fatal crash is computed using Equation 18-59 as follows:

$$\begin{aligned} P_{fs+sc,ac,at,K} &= \frac{\exp(V_K)}{\frac{1.0}{C_{sdf,fs+sc}} + \exp(V_K) + \exp(V_A) + \exp(V_B)} \\ &= \frac{\exp(-3.392)}{\frac{1.0}{1.0} + \exp(-3.392) + \exp(-2.478) + \exp(-0.571)} \\ &= 0.020 \end{aligned}$$

Similar calculations using Equation 18-60 and Equation 18-61 yield the following results:

$$P_{fs+sc,ac,at,A} = 0.050$$

$$P_{fs+sc,ac,at,B} = 0.336$$

The probability of occurrence of a possible-injury crash is computed using Equation 18-62 as follows:

$$\begin{aligned} P_{fs+sc,ac,at,C} &= 1.0 - (P_{fs+sc,ac,at,K} + P_{fs+sc,ac,at,A} + P_{fs+sc,ac,at,B}) \\ &= 1.0 - (0.020 + 0.050 + 0.336) \\ &= 0.594 \end{aligned}$$

The probability of occurrence of a fatal crash is multiplied by the fatal-and-injury crash frequency obtained in Step 11 using Equation 18-58 as follows:

$$\begin{aligned} N_{e,sc,6EX,at,K} &= N_{e,sc,6EX,at,fi} \times P_{fs+sc,ac,at,K} \\ &= 0.342 \times 0.020 \\ &= 0.007 \text{ crashes/year} \end{aligned}$$

Similar calculations using Equation 18-58 and the probabilities of occurrences of the other crash severities yield the following results:

$$N_{e,sc,6EX,at,A} = 0.017 \text{ crashes/year}$$

$$N_{e,sc,6EX,at,B} = 0.115 \text{ crashes/year}$$

$$N_{e,sc,6EX,at,C} = 0.203 \text{ crashes/year}$$

Apply the crash type distribution, if desired.

The crash type distributions are applied by multiplying the default crash type distribution proportions in Table 18-12 by the predicted average crash frequencies obtained in Step 11.

Worksheets

The step-by-step instructions are provided to illustrate the predictive method for calculating the predicted average crash frequency for a freeway segment. To apply the predictive method steps to multiple segments, a

series of worksheets are provided for determining the predicted average crash frequency. The worksheets include:

- Table 18-43. Freeway Speed-Change Lane Worksheet (1 of 3)—Sample Problem 4
- Table 18-44. Freeway Speed-Change Lane Worksheet (2 of 3)—Sample Problem 4
- Table 18-45. Freeway Speed-Change Lane Worksheet (3 of 3)—Sample Problem 4

Filled versions of these worksheets are provided below. Blank versions of worksheets used in the Sample Problems are provided in Appendix 18A.

Table 18-43 is a summary of general information about the freeway speed-change lane, analysis, input data (i.e., “The Facts”), and assumptions for Sample Problem 4. The input data include area type, crash data, basic roadway data, alignment data, cross section data, and traffic data.

Table 18-44 is a tabulation of the CMF and SPF computations for Sample Problem 4.

Table 18-45 is a tabulation of the crash severity and crash type distributions for Sample Problem 4.

Table 18-43. Freeway Speed-Change Lane Worksheet (1 of 3)—Sample Problem 4

General Information					Location Information					
Analyst					Roadway					
Agency or company					Roadway section					
Date performed					Study year					
Area type		X	Urban		Rural					
Input Data										
Crash Data					Crash Period	Study Year	Complete the study year column. Complete the crash period column if the EB Method is used.			
Crash data time period							First year	--	Last year	--
Count of speed-change-related FI crashes $N_{o,sc,x,at,fi}^*$					--					
Count of speed-change-related PDO crashes $N_{o,sc,x,at,pdo}^*$					--					
Basic Roadway Data										
Number of through lanes n					6		Same value for crash period and study year.			
Segment length L (mi)					--	0.1	Equals the length of the speed-change lane.			
Configuration					Exit		Choices: Entrance, Exit			
Alignment Data										
Horizontal Curve Data										
1	Presence of horizontal curve 1				--	Y/N	N	Y/N	If Yes, then enter data in the next three rows.	
	Curve radius R_1 (ft)				--		--			
	Length of curve L_{c1} (mi)				--		--			
	Length of curve in segment $L_{c1,seg}$ (mi)				--		--			
2	Presence of horizontal curve 2				--	Y/N	N	Y/N	If Yes, then enter data in the next three rows.	
	Curve radius R_2 (ft)				--		--			
	Length of curve L_{c2} (mi)				--		--			
	Length of curve in segment $L_{c2,seg}$ (mi)				--		--			
Cross Section Data										
Lane width W_l (ft)					--		12			
Inside shoulder width W_{is} (ft)					--		6			
Median width W_m (ft)					--		40			
Presence of barrier in median					--	Y/N	N	Y/N	If Yes, then use the freeway barrier worksheet.	
Entrance or exit side (left- or right-hand side)					--	L/R	R	L/R		
Traffic Data										
Proportion of AADT during high-volume hours P_{hv}					--		0.1			
Freeway segment AADT $AADT_{fs}$ (veh/day)					--		120,000			
AADT of ramp $AADT_r$ (veh/day)					--		--	Only needed for entrance ramp.		

Table 18-44. Freeway Speed-Change Lane Worksheet (2 of 3)—Sample Problem 4

Crash Modification Factors		Fatal and Injury		Property Damage Only	
Complete the study year column. Complete the crash period column if the EB Method is used.	Equation	Crash Period	Study Year	Crash Period	Study Year
		Horizontal curve $CMF_{1, sc, ac, at, z}$	18-40	--	1.000
Lane width $CMF_{2, sc, ac, at, fi}$	18-41	--	1.000		
Inside shoulder width $CMF_{3, sc, ac, at, z}$	18-42	--	1.000	--	1.000
Median width $CMF_{4, sc, ac, at, z}$	18-43	--	1.062	--	1.060
Median barrier $CMF_{5, sc, ac, at, z}$	18-44	--	1.000	--	1.000
High volume $CMF_{6, sc, ac, at, z}$	18-45	--	1.036	--	1.029
Ramp entrance $CMF_{12, sc, nEN, at, z}$	18-46	--	1.000	--	1.000
Ramp exit $CMF_{13, sc, nEX, at, z}$	18-47	--	1.123	--	1.000
Combined CMF (multiply all CMFs evaluated)		--	1.235	--	1.090

Expected Average Crash Frequency^a		Fatal and Injury		Property Damage Only	
Complete the study year column. Complete the crash period column if the <i>site-specific</i> EB Method is used.		Crash Period	Study Year	Crash Period	Study Year
		Calibration factor $C_{sc, x, at, z}$		1.00	
Overdispersion parameter $k_{sc, x, at, z}$		--		--	
Observed crash count $N_{o, sc, x, at, z}^*$ (cr)		--		--	
Reference year r		--		--	
Predicted average crash freq. for reference year $N_{p, sc, x, at, z, r}$ (cr/yr)		--		--	
Predicted number of crashes for crash period (sum all years) $N_{p, sc, x, at, z}^*$ (cr)		--		--	
Equivalent years associated with crash count $C_{b, sc, x, at, z, r}$ (yr)		--		--	
Adjusted average crash freq. for ref. year given $N_{o, sc, x, at, z, r}^*$ (cr/yr)		--		--	
Study year s			2011		2011
Predicted average crash freq. for study year $N_{p, sc, x, at, z, s}$ (cr/yr)			0.342		0.820
Expected average crash freq. for study year $N_{e, sc, x, at, z, s}$ (cr/yr)			0.342		0.820

Note:

a – If the EB Method is not used, then substitute the word “predicted” for the word “expected” and substitute the subscript “p” for the subscript “e”.

Table 18-45. Freeway Speed-Change Lane Worksheet (3 of 3)—Sample Problem 4**Expected Average Crash Frequency^a****Crash Severity Distribution**

	K	A	B	C	Total FI	PDO	Total FI + PDO
Proportion by injury level	0.020	0.050	0.336	0.594	1.000		
Expected average crash freq. for study year $N_{e, sc, x, at, z, s}$ (cr/yr)	0.007	0.017	0.115	0.203	0.342	0.820	1.162

Crash Type Distribution

Crash Type Category	Table 18-10 or 18-12	Fatal and Injury		Property Damage Only		Total
		Proportion	Expected Average Crash Frequency for Study Year $N_{e, sc, x, at, fi, s}$ (cr/yr)	Proportion	Expected Average Crash Frequency for Study Year $N_{e, sc, x, at, pdo, s}$ (cr/yr)	Expected Average Crash Frequency for Study Year $N_{e, sc, x, at, as, s}$ (cr/yr)
Multiple-Vehicle Crashes						
Head-on		0.004	0.001	0.001	0.001	0.002
Right-angle		0.019	0.006	0.016	0.013	0.020
Rear-end		0.543	0.186	0.530	0.435	0.620
Sideswipe		0.133	0.045	0.252	0.207	0.252
Other multiple-vehicle crashes		0.017	0.006	0.015	0.012	0.018
Single-Vehicle Crashes						
Crash with animal		0.000	0.000	0.002	0.002	0.002
Crash with fixed object		0.194	0.066	0.129	0.106	0.172
Crash with other object		0.019	0.006	0.036	0.030	0.036
Crash with parked vehicle		0.004	0.001	0.003	0.002	0.004
Other single-vehicle crashes		0.067	0.023	0.016	0.013	0.036
Total		1.000	0.342	1.000	0.820	1.162

Note:

a – If the EB Method is not used, then substitute the word “predicted” for the word “expected” and substitute the subscript “p” for the subscript “e”.

18.13.5. Sample Problem 5**The Project**

A project of interest consists of two sites located on a six-lane urban freeway: a tangent segment and a segment with a horizontal curve. (This project is a compilation of the freeway segments from Sample Problems 1 and 2.)

The Question

What is the expected crash frequency of the project for a particular year incorporating both the predicted crash frequencies from Sample Problems 1 and 2 and the observed crash frequencies using the *site-specific EB Method*?

The Facts

The study year is 2011. The conditions present during this year are provided in the following list.

- 2 freeway segments—segment 1 (tangent), segment 2 (curved)
- Crash period is 2009 and 2010
- Use the same AADT volumes for 2009 to 2011
- 30 observed fatal-and-injury crashes
 - Segment 1: 10 multiple-vehicle, 4 single-vehicle
 - Segment 2: 8 multiple-vehicle, 8 single-vehicle
- 50 observed property-damage-only crashes
 - Segment 1: 14 multiple-vehicle, 12 single-vehicle
 - Segment 2: 10 multiple-vehicle, 14 single-vehicle

Outline of Solution

To calculate the expected crash frequency, observed crash frequencies are combined with predicted crash frequencies on a site-by-site basis for the project. Observed crashes are assigned to specific speed-change lanes or freeway segments. The site-specific EB Method presented in Section B.2.4 of Appendix B to Part C is used for this purpose.

Results

The expected average crash frequency for the project is 13.5 fatal-and-injury crashes per year and 27.5 property-damage-only crashes per year (rounded to one decimal place).

Steps

The expected average crash frequency for reference year r at a site i with type $w(i)$ and cross section or control type $x(i)$ for a specified crash type y and severity z is computed using Equation B-5 through Equation B-7 as follows:

$$N_{e, w(i), x(i), y, z, r} = w_{w(i), x(i), y, z} \times N_{p, w(i), x(i), y, z, r} + (1.0 - w_{w(i), x(i), y, z}) \times \frac{N_{o, w(i), x(i), y, z, r}^*}{C_{b, w(i), x(i), y, z, r}}$$

$$w_{w(i), x(i), y, z} = \frac{1.0}{1.0 + \left(k_{w(i), x(i), y, z} \times \sum_{j=1}^{n_c} N_{p, w(i), x(i), y, z, r} \right)}$$

$$C_{b, w(i), x(i), y, z, r} = \frac{1.0}{N_{p, w(i), x(i), y, z, r}} \times \sum_{j=1}^{n_c} N_{p, w(i), x(i), y, z, j}$$

$C_{b, w(i), x(i), y, z, r} = 2.0$ because the same AADT volumes are used for all years in the analysis period. The overdispersion parameter for segment 1 for fatal-and-injury multiple-vehicle crashes $k_{fs, 6, mv, ft}$ is computed using Equation 18-17 with the segment length and the inverse dispersion parameter from Table 18-5.

$$k_{fs, 6, mv, ft} = \frac{1.0}{17.6 \times 0.75} = 0.076$$

The predicted average fatal-and-injury multiple-vehicle crash frequency $N_{p, fs, 6, mv, fi}$ was computed as 3.911 crashes/year in Sample Problem 1. The weighted adjustment factor $w_{fs, 6, mv, fi}$ is computed as follows:

$$w_{fs, 6, mv, fi} = \frac{1.0}{1.0 + (0.076 \times [3.911 + 3.911])} = 0.627$$

Then, the expected average crash frequency $N_{e, fs, 6, mv, fi}$ is computed as follows:

$$N_{e, fs, 6, mv, fi, r} = 0.627 \times 3.911 + (1.0 - 0.627) \times \frac{10}{2} = 4.316 \text{ crashes/year}$$

This process is repeated for fatal-and-injury single-vehicle crashes, property-damage-only multiple-vehicle crashes, and property-damage-only single-vehicle crashes for segment 1, and for all crashes for segment 2, to obtain the following results:

- Segment 1
 - $N_{e, fs, 6, mv, fi, r} = 4.316$ crashes/year
 - $N_{e, fs, 6, sv, fi, r} = 2.050$ crashes/year
 - $N_{e, fs, 6, mv, pdo, r} = 8.090$ crashes/year
 - $N_{e, fs, 6, sv, pdo, r} = 5.456$ crashes/year
- Segment 2
 - $N_{e, fs, 6, mv, fi, r} = 4.092$ crashes/year
 - $N_{e, fs, 6, sv, fi, r} = 3.089$ crashes/year
 - $N_{e, fs, 6, mv, pdo, r} = 7.218$ crashes/year
 - $N_{e, fs, 6, sv, pdo, r} = 6.702$ crashes/year

Worksheets

The step-by-step instructions are provided to illustrate the predictive method for calculating the predicted average crash frequency for a freeway segment. To apply the predictive method steps to multiple segments, a series of worksheets are provided for determining the predicted average crash frequency. The worksheets include:

- Table 18-46. Freeway Segment Worksheet (1 of 4)—Sample Problem 5
- Table 18-47. Freeway Segment Worksheet (2 of 4)—Sample Problem 5
- Table 18-48. Freeway Segment Worksheet (3 of 4)—Sample Problem 5
- Table 18-49. Freeway Segment Worksheet (4 of 4)—Sample Problem 5

Filled versions of these worksheets are provided below for segment 1. The same worksheets would be used for segment 2, but are not shown. Blank versions of worksheets used in the Sample Problems are provided in Appendix 18A.

Table 18-46 is a summary of general information about the freeway segment, analysis, input data (i.e., “The Facts”), and assumptions for segment 1. The input data include area type, crash data, basic roadway data, alignment data, and cross section data.

Table 18-47 is a summary of general information about the freeway segment, analysis, input data (i.e., “The Facts”), and assumptions for segment 1. The input data include roadside data, ramp access data, and traffic data.

Table 18-48 is a tabulation of the CMF and SPF computations for segment 1.

Table 18-49 is a tabulation of the crash severity and crash type distributions for segment 1.

Table 18-46. Freeway Segment Worksheet (1 of 4)—Sample Problem 5

General Information					Location Information				
Analyst					Roadway				
Agency or company					Roadway section				
Date performed					Study year				
Area type		X	Urban		Rural				
Input Data									
Crash Data				Crash Period	Study Year	Complete the study year column. Complete the crash period column if the EB Method is used.			
Crash data time period						First year	2009	Last year	2010
Count of multiple-vehicle FI crashes $N_{o,fs,n,mv,fi}^*$				5					
Count of single-vehicle FI crashes $N_{o,fs,n,sv,fi}^*$				2					
Count of multiple-vehicle PDO crashes $N_{o,fs,n,mv,pdo}^*$				7					
Count of single-vehicle PDO crashes $N_{o,fs,n,sv,pdo}^*$				6					
Basic Roadway Data									
Number of through lanes n				6		Same value for crash period and study year.			
Segment length L (mi)				0.75	0.75				
Alignment Data									
Horizontal Curve Data									
1	Presence of horizontal curve 1			N	Y/N	N	Y/N	If Yes, then enter data in the next three rows.	
	Equivalent curve radius R_1^* (ft)			--	--				
	Length of curve L_{c1} (mi)			--	--				
	Length of curve in segment $L_{c1,seg}$ (mi)			--	--				
2	Presence of horizontal curve 2			N	Y/N	N	Y/N	If Yes, then enter data in the next three rows.	
	Equivalent curve radius R_2^* (ft)			--	--				
	Length of curve L_{c2} (mi)			--	--				
	Length of curve in segment $L_{c2,seg}$ (mi)			--	--				
Cross Section Data									
Lane width W_l (ft)				12	12				
Outside shoulder width W_s (ft)				10	10				
Inside shoulder width W_{is} (ft)				6	6				
Median width W_m (ft)				40	40				
Presence of rumble strips on outside shoulder				N	Y/N	N	Y/N	If Yes, then enter data in the next two rows.	
Length of rumble strip in increasing milepost dir. (mi)				--	--				
Length of rumble strip in decreasing milepost dir. (mi)				--	--				
Presence of rumble strips on inside shoulder				N	Y/N	N	Y/N	If Yes, then enter data in the next two rows.	
Length of rumble strip in increasing milepost dir. (mi)				--	--				
Length of rumble strip in decreasing milepost dir. (mi)				--	--				
Presence of barrier in median				N	Y/N	N	Y/N	If Yes, then use the freeway barrier worksheet.	

Table 18-47. Freeway Segment Worksheet (2 of 4)—Sample Problem 5

Input Data						
Roadside Data		Crash Period		Study Year		Complete the study year column. Complete the crash period column if the EB Method is used.
Clear zone width W_{hc} (ft)		30		30		
Presence of barrier on roadside		N	Y/N	N	Y/N	If Yes, then use the freeway barrier worksheet.
Ramp Access Data						
Travel in Increasing Milepost Direction						
Ent. ramp	Distance from begin milepost to upstream entrance ramp gore $X_{b, ent}$ (mi)	0.5		0.5		If ramp entrance is in the segment, enter 0.0.
	Presence of speed-change lane in segment	N	Y/N	N	Y/N	If Yes, then enter data in the next row.
	Length of s-c lane in segment $L_{en, seg, inc}$ (mi)	--		--		
Exit ramp	Distance from end milepost to upstream exit ramp gore $X_{e, ext}$ (mi)	0.85		0.85		If ramp exit is in the segment, enter 0.0.
	Presence of speed-change lane in segment	N	Y/N	N	Y/N	If Yes, then enter data in the next row.
	Length of s-c lane in segment $L_{ex, seg, inc}$ (mi)	--		--		
Weave	Presence of a Type B weave in segment	N	Y/N	N	Y/N	If Yes, then enter data in the next two rows.
	Length of weaving section $L_{wev, inc}$ (mi)	--		--		
	Length of weaving section in seg. $L_{wev, seg, inc}$ (mi)	--		--		
Travel in Decreasing Milepost Direction						
Ent. ramp	Distance from end milepost to upstream entrance ramp gore $X_{e, ent}$ (mi)	0.85		0.85		If ramp entrance is in the segment, enter 0.0.
	Presence of speed-change lane in segment	N	Y/N	N	Y/N	If Yes, then enter data in the next row.
	Length of s-c lane in segment $L_{en, seg, dec}$ (mi)	--		--		
Exit ramp	Distance from begin milepost to downstream exit ramp gore $X_{b, ext}$ (mi)	0.5		0.5		If ramp exit is in the segment, enter 0.0.
	Presence of speed-change lane in segment	N	Y/N	N	Y/N	If Yes, then enter data in the next row.
	Length of s-c lane in segment $L_{ex, seg, dec}$ (mi)	--		--		
Weave	Presence of a Type B weave in segment	N	Y/N	N	Y/N	If Yes, then enter data in the next two rows.
	Length of weaving section $L_{wev, dec}$ (mi)	--		--		
	Length of weaving section in seg. $L_{wev, seg, dec}$ (mi)	--		--		
Traffic Data						
Proportion of AADT during high-volume hours P_{hv}		0.1		0.1		
Freeway segment AADT $AADT_{fs}$ (veh/day)		120,000		120,000		
AADT of entrance ramp for travel in increasing milepost direction $AADT_{b, ent}$ (veh/day)		8,000		8,000		
AADT of exit ramp for travel in increasing milepost direction $AADT_{e, ext}$ (veh/day)		7,150		7,150		
AADT of entrance ramp for travel in decreasing milepost direction $AADT_{e, ent}$ (veh/day)		6,750		6,750		
AADT of exit ramp for travel in decreasing milepost direction $AADT_{b, ext}$ (veh/day)		7,675		7,675		

Table 18-48. Freeway Segment Worksheet (3 of 4)—Sample Problem 5

Crash Modification Factors

Complete the study year column. Complete the crash period column if the EB Method is used. Equation	Fatal and Injury				Property Damage Only			
	Multiple Vehicle		Single Vehicle		Multiple Vehicle		Single Vehicle	
	Crash Period	Study Year	Crash Period	Study Year	Crash Period	Study Year	Crash Period	Study Year
Horizontal curve $CMF_{1,fs,ac,y,z}$ 18-24	1.000	1.000	1.000	1.000	1.000	1.000	1.000	1.000
Lane width $CMF_{2,fs,ac,y,fi}$ 18-25	1.000	1.000	1.000	1.000				
Inside shoulder width $CMF_{3,fs,ac,y,z}$ 18-26	1.000	1.000	1.000	1.000	1.000	1.000	1.000	1.000
Median width $CMF_{4,fs,ac,y,z}$ 18-27	1.062	1.062	0.980	0.980	1.060	1.060	1.060	1.060
Median barrier $CMF_{5,fs,ac,y,z}$ 18-28	1.000	1.000	1.000	1.000	1.000	1.000	1.000	1.000
High volume $CMF_{6,fs,ac,y,z}$ 18-29	1.036	1.036	0.993	0.993	1.029	1.029	0.941	0.941
Lane change $CMF_{7,fs,ac,mv,z}$ 18-30	1.000	1.000			1.000	1.000		
Outside shoulder width $CMF_{8,fs,ac,sv,z}$ 18-35			1.000	1.000			1.000	1.000
Shoulder rumble strip $CMF_{9,fs,ac,sv,fi}$ 18-36			1.000	1.000				
Outside clearance $CMF_{10,fs,ac,sv,fi}$ 18-38			1.000	1.000				
Outside barrier $CMF_{11,fs,ac,sv,z}$ 18-39			1.000	1.000			1.000	1.000
Combined CMF (multiply all CMFs evaluated)	1.100	1.100	0.973	0.973	1.091	1.091	0.997	0.997

Expected Average Crash Frequency^a

Complete the study year column. Complete the crash period column if the <i>site-specific</i> EB Method is used.	Fatal and Injury				Property Damage Only			
	Multiple Vehicle		Single Vehicle		Multiple Vehicle		Single Vehicle	
	Crash Period	Study Year	Crash Period	Study Year	Crash Period	Study Year	Crash Period	Study Year
Calibration factor $C_{fs,ac,y,z}$	1.00		1.00		1.00		1.00	
Overdispersion parameter $k_{fs,n,y,z}$	0.076		0.044		0.071		0.064	
Observed crash count $N_{a,fs,n,y,z}^*$ (cr)	10		4		14		12	
Reference year r	2009		2009		2009		2009	
Predicted average crash freq. for reference year $N_{p,fs,n,y,z,r}$ (cr/yr)	3.911		2.060		9.568		5.099	
Predicted number of crashes for crash period (sum all years) $N_{p,fs,n,y,z}^*$ (cr)	3.911		2.060		9.568		5.099	
Equivalent years associated with crash count $C_{b,fs,n,y,z,r}$ (yr)	2		2		2		2	
Adjusted average crash freq. for ref. year given $N_{os}^*, N_{a,fs,n,y,z,r}$ (cr/yr)	4.316		2.050		8.090		5.456	
Study year s	2011		2011		2011		2011	
Predicted average crash freq. for study year $N_{p,fs,n,y,z,s}$ (cr/yr)	3.911		2.060		9.568		5.099	
Expected average crash freq. for study year $N_{e,fs,n,y,z,s}$ (cr/yr)	4.316		2.050		8.090		5.456	
Expected average crash freq. for study year (all crash types) $N_{e,fs,n,at,z,s}$ (cr/yr)			6.367				13.546	

Note:

a – If the EB Method is not used, then substitute the word “predicted” for the word “expected” and substitute the subscript “p” for the subscript “e”.

Table 18-49. Freeway Segment Worksheet (4 of 4)—Sample Problem 5**Expected Average Crash Frequency^a****Crash Severity Distribution**

	K	A	B	C	Total FI	PDO	Total FI + PDO
Proportion by injury level	0.020	0.050	0.336	0.594	1.000		
Expected average crash freq. for study year (all crash types) $N_{e, fs, n, at, z, s}$ (cr/yr)	0.127	0.317	2.138	3.784	6.367	13.546	19.912

Crash Type Distribution

Crash Type Category	Table	Fatal and Injury		Property Damage Only		Total
		Proportion	Expected Average Crash Frequency for Study Year $N_{e, fs, n, y, fi, s}$ (cr/yr)	Proportion	Expected Average Crash Frequency for Study Year $N_{e, fs, n, y, pdo, s}$ (cr/yr)	Expected Average Crash Frequency for Study Year $N_{e, fs, n, y, as, s}$ (cr/yr)
Multiple-Vehicle Crashes	18-6					
Head-on		0.008	0.035	0.002	0.016	0.051
Right-angle		0.031	0.134	0.018	0.146	0.279
Rear-end		0.750	3.237	0.690	5.582	8.819
Sideswipe		0.180	0.777	0.266	2.152	2.929
Other multiple-vehicle crashes		0.031	0.134	0.024	0.194	0.328
Total		1.000	4.316	1.000	8.090	12.406
Single-Vehicle Crashes	18-8					
Crash with animal		0.004	0.008	0.022	0.120	0.128
Crash with fixed object		0.722	1.480	0.716	3.907	5.387
Crash with other object		0.051	0.105	0.139	0.758	0.863
Crash with parked vehicle		0.015	0.031	0.016	0.087	0.118
Other single-vehicle crashes		0.208	0.427	0.107	0.584	1.010
Total		1.000	2.050	1.000	5.456	7.507

Note:

a – If the EB Method is not used, then substitute the word “predicted” for the word “expected” and substitute the subscript “p” for the subscript “e”.

18.13.6. Sample Problem 6**The Project**

A project of interest consists of two sites located on a six-lane urban freeway: a tangent segment and a segment with a horizontal curve. (This project is a compilation of freeway segments from Sample Problems 1 and 2.)

The Question

What is the expected crash frequency of the project for a particular year incorporating both the predicted crash frequencies from Sample Problems 1 and 2 and the observed crash frequencies using the *project-level EB Method*?

The Facts

The study year is 2011. The conditions present during this year are provided in the following list.

- 2 freeway segments—segment 1 (tangent), segment 2 (curved)
- Crash period is 2009 and 2010
- Use the same AADT volumes for 2009 to 2011
- 30 observed fatal-and-injury crashes and 50 observed property-damage-only crashes (but no information is available to attribute specific crashes to specific sites)

Outline of Solution

To calculate the expected crash frequency, the observed crash frequency for the project as a whole is combined with predicted crash frequency for the project. The predicted crash frequency for the project is based on the sum of the predicted crash frequency for each site within the project. The project-level EB Method presented in Section B.2.5 of Appendix B to Part C is used for this purpose.

Results

The expected average crash frequency for the project is 13.9 fatal-and-injury crashes per year and 27.1 property-damage-only crashes per year (rounded to one decimal place).

Steps

Step 1—Sum the predicted average crash frequency and observed crash counts.

The predicted average crash frequencies for segments 1 and 2 were computed in Sample Problems 1 and 2, respectively. For freeway segments, separate values are obtained for multiple-vehicle and single-vehicle crashes, and for fatal-and-injury and property-damage-only crashes. The following values were obtained:

- Segment 1
 - $N_{p, fs, 6, mv, fi, r} = 3.911$ crashes/year
 - $N_{p, fs, 6, sv, fi, r} = 2.060$ crashes/year
 - $N_{p, fs, 6, mv, pdo, r} = 9.568$ crashes/year
 - $N_{p, fs, 6, sv, pdo, r} = 5.099$ crashes/year
- Segment 2
 - $N_{p, fs, 6, mv, fi, r} = 4.150$ crashes/year
 - $N_{p, fs, 6, sv, fi, r} = 2.858$ crashes/year
 - $N_{p, fs, 6, mv, pdo, r} = 10.530$ crashes/year
 - $N_{p, fs, 6, sv, pdo, r} = 6.454$ crashes/year
- All fatal-and-injury crashes: $N_{p, aS, ac, at, fi, r} = 12.979$ crashes/year
- All property-damage-only crashes: $N_{p, aS, ac, at, pdo, r} = 31.651$ crashes/year

The crash period is two years, and the same AADT volumes were used for the two years. Hence, the predicted numbers of crashes in the crash period are simply double the predicted average crash frequency. That is:

- All fatal-and-injury crashes: $N_{p, aS, ac, at, fi}^* = 25.958$ crashes/year
- All property-damage-only crashes: $N_{p, aS, ac, at, pdo}^* = 63.302$ crashes/year

The observed crash counts were given as 30 fatal-and-injury crashes and 50 property-damage-only crashes in the years 2009 and 2010. That is:

- $N_{o, aS, ac, at, fi}^* = 30$ crashes/year
- $N_{o, aS, ac, at, pdo}^* = 50$ crashes/year

Step 2—Compute the variance of the predicted average crash frequency.

Two variance estimates are computed in this step. One estimate is based on the assumption that the sites are independent and the other estimate is based on the assumption that the sites are perfectly correlated.

Equation B-11 and Equation B-12 are used for these computations. The overdispersion parameters $k_{fs, 6, mv, fi}$ and $k_{fs, 6, sv, fi}$ were computed in Sample Problem 5 as 0.076 and 0.044, respectively. The two variance estimates for fatal-and-injury crashes are computed as follows.

Assuming independence:

$$\begin{aligned}
 V_{0, fs, ac, at, fi} &= \sum_i^{\text{all sites}} \sum_k^{\text{all crash types}} k_{fs, 6, at, fi} \times \left[\sum_j^{n_c} N_{p, fs, 6, at, fi} \right]^2 \\
 &= 0.076 \times (2 \times 3.911)^2 + 0.044 \times (2 \times 2.060)^2 + 0.076 \times (2 \times 4.150)^2 + 0.044 \times (2 \times 2.858)^2 \\
 &= 12.053
 \end{aligned}$$

Assuming perfect correlation:

$$\begin{aligned}
 V_{1, fs, ac, at, fi} &= \left(\sum_i^{\text{all sites}} \sum_k^{\text{all crash types}} \sqrt{k_{fs, 6, at, fi} \times \left[\sum_j^{n_c} N_{p, fs, 6, at, fi} \right]^2} \right)^2 \\
 &= \left(\sqrt{0.076 \times (2 \times 3.911)^2} + \sqrt{0.044 \times (2 \times 2.060)^2} \right. \\
 &\quad \left. + \sqrt{0.076 \times (2 \times 4.150)^2} + \sqrt{0.044 \times (2 \times 2.858)^2} \right)^2 \\
 &= 42.346
 \end{aligned}$$

Similar calculations using the property-damage-only crash frequencies and counts yield the following results.

Assuming independence:

$$V_{0, fs, ac, at, pdo} = 74.858$$

Assuming perfect correlation:

$$V_{1, fs, ac, at, pdo} = 274.531$$

Step 3—Compute the weighted adjustment factor.

Two weighted adjustment factors are computed in this step. One estimate is based on the assumption that the sites are independent and the other estimate is based on the assumption that the sites are perfectly correlated. Equation B-13 and Equation B-14 are used for these computations. The two weighted adjustment factor estimates for fatal-and-injury crashes are computed as follows.

Assuming independence:

$$\begin{aligned} w_{0, fs, ac, at, fi} &= \frac{1.0}{1.0 + \frac{V_{0, fs, ac, at, fi}}{N_{p, fs, ac, at, fi}^*}} \\ &= \frac{1.0}{1.0 + \frac{12.053}{25.958}} \\ &= 0.683 \end{aligned}$$

Assuming perfect correlation:

$$\begin{aligned} w_{1, fs, ac, at, fi} &= \frac{1.0}{1.0 + \frac{V_{1, fs, ac, at, fi}}{N_{p, fs, ac, at, fi}^*}} \\ &= \frac{1.0}{1.0 + \frac{42.346}{25.958}} \\ &= 0.380 \end{aligned}$$

Similar calculations using the property-damage-only variances yield the following results.

Assuming independence:

$$w_{0, fs, ac, at, pdo} = 0.458$$

Assuming perfect correlation:

$$w_{1, fs, ac, at, pdo} = 0.187$$

Step 4—Compute the equivalent years in the crash period.

The crash period is two years, and the same AADT volumes were used for the two years. Hence, the number of equivalent years in the crash period is 2.000.

Step 5—Compute the expected average crash frequency.

The expected average fatal-and-injury crash frequency for the reference year (2009) is computed as follows.

Assuming independence:

$$\begin{aligned}
 N_{0, fs, ac, at, fi, r} &= w_{0, fs, ac, at, fi} \times N_{p, fs, ac, at, fi, r} + (1.0 - w_{0, fs, ac, at, fi}) \times \frac{N_{o, fs, ac, at, fi, r}^*}{C_{b, fs, ac, at, fi, r}} \\
 &= 0.683 \times 12.979 + (1.0 - 0.683) \times \frac{30}{2} \\
 &= 13.619 \text{ crashes/year}
 \end{aligned}$$

Assuming perfect correlation:

$$\begin{aligned}
 N_{1, fs, ac, at, fi, r} &= w_{1, fs, ac, at, fi} \times N_{p, fs, ac, at, fi, r} + (1.0 - w_{1, fs, ac, at, fi}) \times \frac{N_{o, fs, ac, at, fi, r}^*}{C_{b, fs, ac, at, fi, r}} \\
 &= 0.380 \times 12.979 + (1.0 - 0.380) \times \frac{30}{2} \\
 &= 14.232 \text{ crashes/year}
 \end{aligned}$$

Expected average fatal-and-injury crash frequency:

$$\begin{aligned}
 N_{e, fs, ac, at, fi, r} &= \frac{N_{0, fs, ac, at, fi, r} + N_{1, fs, ac, at, fi, r}}{2} \\
 &= \frac{13.619 + 14.232}{2} \\
 &= 13.926 \text{ crashes/year}
 \end{aligned}$$

Similar calculations yield the expected average property-damage-only crash frequency:

$$N_{e, fs, ac, at, pdo, r} = 27.147 \text{ crashes/year}$$

Worksheets

To apply the project-level EB Method to multiple freeway segments and speed-change lanes on a freeway combined, two worksheets are provided for determining the expected average crash frequency. The two worksheets include:

- Table 18-50. Project-Level EB Method Worksheet (1 of 2)—Sample Problem 6
- Table 18-51. Project-Level EB Method Worksheet (2 of 2)—Sample Problem 6

Filled versions of these worksheets are provided below for fatal-and-injury crashes. The same worksheets would be used for property-damage-only crashes, but are not shown. Blank versions of worksheets used in the Sample Problems are provided in Appendix 18A.

Table 18-50 is a summary of the predicted average crash frequencies for segments 1 and 2 that were obtained in Sample Problems 1 and 2. It also contains calculations of the variances of the predicted average crash frequencies.

Table 18-51 is a summary of the expected average crash frequency calculations. These calculations involve applying weights to the predicted average crash frequencies (based on their variances) and their observed crash counts to obtain a refined estimate of expected average crash frequency.

Table 18-50. Project-Level EB Method Worksheet (1 of 2)—Sample Problem 6

Calculations by Site

Crash severity category addressed <i>z</i>	X	FI		PDO																
	Site Summary^b																Total			
Site type and number ^a	F1	F2																		
Overdispersion Parameter^c																				
(1) Multiple-vehicle crashes $k_{w,x,mv,z}$	0.076	0.076																		
(2) Single-vehicle crashes $k_{w,x,sv,z}$	0.044	0.044																		
(3) All crash types $k_{w,x,at,z}$																				
Predicted Number of Crashes during the Crash Period^c																				
(4) Multiple-vehicle crashes $N_{p,w,x,mv,z}^*$ (cr)	7.8	8.3																		16.1
(5) Single-vehicle crashes $N_{p,w,x,sv,z}^*$ (cr)	4.1	5.7																		9.8
(6) All crash types $N_{p,w,x,at,z}^*$ (cr)																				
Predicted number of crashes $N_{p,aS,ac,at,z}^*$ (cr)	= (4) + (5) + (6)																26.0			
Predicted Average Crash Frequency for Reference Year^c																				
(7) Multiple-vehicle crashes $N_{p,w,x,mv,z,r}$ (cr/yr)	3.9	4.2																		8.1
(8) Single-vehicle crashes $N_{p,w,x,sv,z,r}$ (cr/yr)	2.1	2.9																		4.9
(9) All crash types $N_{p,w,x,at,z,r}$ (cr/yr)																				
Predicted freq. for reference year $N_{p,aS,ac,at,z,r}$ (cr/yr)	= (7) + (8) + (9)																13.0			
Predicted Average Crash Frequency for Study Year^c																				
(10) Multiple-vehicle crashes $N_{p,w,x,mv,z,s}$ (cr/yr)	3.9	4.2																		8.1
(11) Single-vehicle crashes $N_{p,w,x,sv,z,s}$ (cr/yr)	2.1	2.9																		4.9
(12) All crash types $N_{p,w,x,at,z,s}$ (cr/yr)																				
Predicted freq. for study year $N_{p,aS,ac,at,z,s}$ (cr/yr)	= (10) + (11) + (12)																13.0			
Variance of Predicted Average Crash Frequency^c																				
(13) Multiple-vehicle product [= (1) × (4) ²]	4.7	5.2																		
(14) Single-vehicle product [= (2) × (5) ²]	0.7	1.4																		
(15) All crash types [= (3) × (6) ²]																				
Variance if independent $V_{0,aS,ac,at,z}$	= (13) + (14) + (15)																12.1			
(16) Multiple-vehicle product [= (1) ^{0.5} × (4)]	2.15	2.29																		
(17) Single-vehicle product [= (2) ^{0.5} × (5)]	0.86	1.20																		
(18) All crash types [= (3) ^{0.5} × (6)]																				
Variance if correlated $V_{1,aS,ac,at,z}$	= [(16) + (17) + (18)] ²																42.3			

Notes:

- a. Site numbering convention: X,y. X: site type; F = freeway segment, R = ramp segment, C = C-D road segment, T = crossroad ramp terminal. y: site number; 1, 2, 3, ...
- b. Use additional sheets if there are more than nine sites in the project limits.
- c. Use the "multiple-vehicle" and "single-vehicle" rows for segments. Use the "all crash types" rows for speed-change lanes and crossroad ramp terminals.

Table 18-51. Project-Level EB Method Worksheet (2 of 2)—Sample Problem 6

Calculations for Project			
	Crash Period	Study Year	
Observed crash count during the crash period $N_{o, aS, ac, at, z}^*$ (cr)	30		Include crashes of all types at all sites during the crash period.
Reference year r	2009		Choose the first year of the crash period.
Predicted average crash freq. for reference year $N_{p, aS, ac, at, z, r}$ (cr/yr)	12.979		
Predicted number of crashes for crash period (sum all years) $N_{p, aS, ac, at, z}^*$ (cr)	25.958		
Equivalent years associated with crash count $C_{b, aS, ac, at, z, r}$ (yr)	2.000		$= N_{p, aS, ac, at, z}^* / N_{p, aS, ac, at, z, r}$
Independent Sites Crash Analysis			
Variance if independent $V_{0, aS, ac, at, z}$	12.053		
Weight associated with $N_{p, \dots, r}$ $w_{0, aS, ac, at, z}$	0.683		$= 1.0 / (1.0 + V_{0, aS, ac, at, z} / N_{p, aS, ac, at, z}^*)$
Adjusted average crash freq. for reference year given $N_{o, aS, ac, at, z, r}^*$	13.619		$= w_{0, aS, ac, at, z} \times N_{p, aS, ac, at, z, r} + (1.0 - w_{0, aS, ac, at, z}) \times N_{o, aS, ac, at, z}^* / C_{b, aS, ac, at, z, r}$
Correlated Sites Crash Analysis			
Variance if correlated $V_{1, aS, ac, at, z}$	42.346		
Weight associated with $N_{p, \dots, r}$ $w_{1, aS, ac, at, z}$	0.380		$= 1.0 / (1.0 + V_{1, aS, ac, at, z} / N_{p, aS, ac, at, z}^*)$
Adjusted average crash freq. for reference year given $N_{o, aS, ac, at, z, r}^*$	14.232		$= w_{1, aS, ac, at, z} \times N_{p, aS, ac, at, z, r} + (1.0 - w_{1, aS, ac, at, z}) \times N_{o, aS, ac, at, z}^* / C_{b, aS, ac, at, z, r}$
Expected Average Crash Frequency			
Adjusted average crash freq. for reference year given $N_{o, aS, ac, at, z, r}^*$	13.926		$= (N_{o, aS, ac, at, z, r} + N_{I, aS, ac, at, z, r}) / 2.0$
Study year s		2011	
Predicted average crash freq. for study year $N_{p, aS, ac, at, z, s}$ (cr/yr)		12.979	
Expected average crash freq. for study year $N_{e, aS, ac, at, z, s}$ (cr/yr)		13.926	$= N_{a, aS, ac, at, z, r} \times N_{p, aS, ac, at, z, s} / N_{p, aS, ac, at, z, r}$

18.14. REFERENCES

- (1) Bonneson, J., S. Geedipally, M. Pratt, and D. Lord. *National Cooperative Highway Research Program Document XXX, Safety Prediction Methodology and Analysis Tool for Freeways and Interchanges*. (Web-Only). NCHRP, Transportation Research Board, Washington, D.C., 2012.

APPENDIX 18A—WORKSHEETS FOR PREDICTIVE METHOD FOR FREEWAYS

Freeway Segment Worksheet (1 of 4)

General Information					Location Information				
Analyst					Roadway				
Agency or company					Roadway section				
Date performed					Study year				
Area type		Urban		Rural					
Input Data									
Crash Data				Crash Period	Study Year	Complete the study year column. Complete the crash period column if the EB Method is used.			
Crash data time period						First year		Last year	
Count of multiple-vehicle FI crashes $N_{o,fs,n,mv,fi}^*$									
Count of single-vehicle FI crashes $N_{o,fs,n,sv,fi}^*$									
Count of multiple-vehicle PDO crashes $N_{o,fs,n,mv,pdo}^*$									
Count of single-vehicle PDO crashes $N_{o,fs,n,sv,pdo}^*$									
Basic Roadway Data									
Number of through lanes n						Same value for crash period and study year.			
Segment length L (mi)									
Alignment Data									
Horizontal Curve Data									
1	Presence of horizontal curve 1				Y/N		Y/N	If Yes, then enter data in the next three rows.	
	Equivalent curve radius R_1^* (ft)								
	Length of curve L_{c1} (mi)								
	Length of curve in segment $L_{c1,seg}$ (mi)								
2	Presence of horizontal curve 2				Y/N		Y/N	If Yes, then enter data in the next three rows.	
	Equivalent curve radius R_2^* (ft)								
	Length of curve L_{c2} (mi)								
	Length of curve in segment $L_{c2,seg}$ (mi)								
Cross Section Data									
Lane width W_l (ft)									
Outside shoulder width W_s (ft)									
Inside shoulder width W_{is} (ft)									
Median width W_m (ft)									
Presence of rumble strips on outside shoulder					Y/N		Y/N	If Yes, then enter data in the next two rows.	
Length of rumble strip in increasing milepost dir. (mi)									
Length of rumble strip in decreasing milepost dir. (mi)									
Presence of rumble strips on inside shoulder					Y/N		Y/N	If Yes, then enter data in the next two rows.	
Length of rumble strip in increasing milepost dir. (mi)									
Length of rumble strip in decreasing milepost dir. (mi)									
Presence of barrier in median					Y/N		Y/N	If Yes, then use the freeway barrier worksheet.	

Freeway Segment Worksheet (2 of 4)

Input Data					
Roadside Data		Crash Period	Study Year	Complete the study year column. Complete the crash period column if the EB Method is used.	
Clear zone width W_{hc} (ft)					
Presence of barrier on roadside			Y/N	Y/N	If Yes, then use the freeway barrier worksheet.
Ramp Access Data					
Travel in Increasing Milepost Direction					
Ent. ramp	Distance from begin milepost to upstream entrance ramp gore $X_{b, ent}$ (mi)				If ramp entrance is in the segment, enter 0.0.
	Presence of speed-change lane in segment		Y/N	Y/N	If Yes, then enter data in the next row.
	Length of s-c lane in segment $L_{en, seg, inc}$ (mi)				
Exit ramp	Distance from end milepost to upstream exit ramp gore $X_{e, ext}$ (mi)				If ramp exit is in the segment, enter 0.0.
	Presence of speed-change lane in segment		Y/N	Y/N	If Yes, then enter data in the next row.
	Length of s-c lane in segment $L_{ex, seg, inc}$ (mi)				
Weave	Presence of a Type B weave in segment		Y/N	Y/N	If Yes, then enter data in the next two rows.
	Length of weaving section $L_{wev, inc}$ (mi)				
	Length of weaving section in seg. $L_{wev, seg, inc}$ (mi)				
Travel in Decreasing Milepost Direction					
Ent. ramp	Distance from end milepost to upstream entrance ramp gore $X_{e, ent}$ (mi)				If ramp entrance is in the segment, enter 0.0.
	Presence of speed-change lane in segment		Y/N	Y/N	If Yes, then enter data in the next row.
	Length of s-c lane in segment $L_{en, seg, dec}$ (mi)				
Exit ramp	Distance from begin milepost to downstream exit ramp gore $X_{b, ext}$ (mi)				If ramp exit is in the segment, enter 0.0.
	Presence of speed-change lane in segment		Y/N	Y/N	If Yes, then enter data in the next row.
	Length of s-c lane in segment $L_{ex, seg, dec}$ (mi)				
Weave	Presence of a Type B weave in segment		Y/N	Y/N	If Yes, then enter data in the next two rows.
	Length of weaving section $L_{wev, dec}$ (mi)				
	Length of weaving section in seg. $L_{wev, seg, dec}$ (mi)				
Traffic Data					
Proportion of AADT during high-volume hours P_{hv}					
Freeway segment AADT $AADT_{fs}$ (veh/day)					
AADT of entrance ramp for travel in increasing milepost direction $AADT_{b, ent}$ (veh/day)					
AADT of exit ramp for travel in increasing milepost direction $AADT_{e, ext}$ (veh/day)					
AADT of entrance ramp for travel in decreasing milepost direction $AADT_{e, ent}$ (veh/day)					
AADT of exit ramp for travel in decreasing milepost direction $AADT_{b, ext}$ (veh/day)					

Freeway Segment Worksheet (3 of 4)

Crash Modification Factors

Complete the study year column. Complete the crash period column if the EB Method is used.	Equation	Fatal and Injury				Property Damage Only			
		Multiple Vehicle		Single Vehicle		Multiple Vehicle		Single Vehicle	
		Crash Period	Study Year	Crash Period	Study Year	Crash Period	Study Year	Crash Period	Study Year
Horizontal curve $CMF_{1,fs,ac,y,z}$	13-24								
Lane width $CMF_{2,fs,ac,y,fi}$	13-25								
Inside shoulder width $CMF_{3,fs,ac,y,z}$	13-26								
Median width $CMF_{4,fs,ac,y,z}$	13-27								
Median barrier $CMF_{5,fs,ac,y,z}$	13-28								
High volume $CMF_{6,fs,ac,y,z}$	13-29								
Lane change $CMF_{7,fs,ac,mv,z}$	13-30								
Outside shoulder width $CMF_{8,fs,ac,sv,z}$	13-35								
Shoulder rumble strip $CMF_{9,fs,ac,sv,fi}$	13-36								
Outside clearance $CMF_{10,fs,ac,sv,fi}$	13-38								
Outside barrier $CMF_{11,fs,ac,sv,z}$	13-39								
Combined CMF (multiply all CMFs evaluated)									

Expected Average Crash Frequency^a

Complete the study year column. Complete the crash period column if the <i>site-specific</i> EB Method is used.	Fatal and Injury				Property Damage Only			
	Multiple Vehicle		Single Vehicle		Multiple Vehicle		Single Vehicle	
	Crash Period	Study Year	Crash Period	Study Year	Crash Period	Study Year	Crash Period	Study Year
Calibration factor $C_{fs,ac,y,z}$								
Overdispersion parameter $k_{fs,n,y,z}$								
Observed crash count $N_{o,fs,n,y,z}^*$ (cr)								
Reference year r								
Predicted average crash freq. for reference year $N_{p,fs,n,y,z,r}$ (cr/yr)								
Predicted number of crashes for crash period (sum all years) $N_{p,fs,n,y,z}^*$ (cr)								
Equivalent years associated with crash count $C_{b,fs,n,y,z,r}$ (yr)								
Adjusted average crash freq. for ref. year given $N_{o, N_{a,fs,n,y,z,r}}^*$ (cr/yr)								
Study year s								
Predicted average crash freq. for study year $N_{p,fs,n,y,z,s}$ (cr/yr)								
Expected average crash freq. for study year $N_{e,fs,n,y,z,s}$ (cr/yr)								
Expected average crash freq. for study year (all crash types) $N_{e,fs,n,at,z,s}$ (cr/yr)								

Note:

a – If the EB Method is not used, then substitute the word “predicted” for the word “expected” and substitute the subscript “p” for the subscript “e”.

Freeway Segment Worksheet (4 of 4)

Expected Average Crash Frequency^a

Crash Severity Distribution

	K	A	B	C	Total FI	PDO	Total FI + PDO
Proportion by injury level					1.000		
Expected average crash freq. for study year (all crash types) $N_{e,fs,n,at,z,s}$ (cr/yr)							

Crash Type Distribution

Crash Type Category	Table	Fatal and Injury		Property Damage Only		Total
		Proportion	Expected Average Crash Frequency for Study Year $N_{e,fs,n,y,fi,s}$ (cr/yr)	Proportion	Expected Average Crash Frequency for Study Year $N_{e,fs,n,y,pdo,s}$ (cr/yr)	Expected Average Crash Frequency for Study Year $N_{e,fs,n,y,as,s}$ (cr/yr)
Multiple-Vehicle Crashes	13-6					
Head-on						
Right-angle						
Rear-end						
Sideswipe						
Other multiple-vehicle crashes						
Total		1.000		1.000		
Single-Vehicle Crashes	13-8					
Crash with animal						
Crash with fixed object						
Crash with other object						
Crash with parked vehicle						
Other single-vehicle crashes						
Total		1.000		1.000		

Note:

a – If the EB Method is not used, then substitute the word “predicted” for the word “expected” and substitute the subscript “p” for the subscript “e”.

Freeway Speed-Change Lane Worksheet (1 of 3)

General Information				Location Information			
Analyst				Roadway			
Agency or company				Roadway section			
Date performed				Study year			
Area type		Urban		Rural			

Input Data

<i>Crash Data</i>	Crash Period	Study Year	Complete the study year column. Complete the crash period column if the EB Method is used.			
Crash data time period			First year		Last year	
Count of speed-change-related FI crashes $N_{o,sc,x,at,fi}^*$						
Count of speed-change-related PDO crashes $N_{o,sc,x,at,pdo}^*$						

Basic Roadway Data

Number of through lanes n		Same value for crash period and study year.
Segment length L (mi)		Equals the length of the speed-change lane.
Configuration		Choices: Entrance, Exit

Alignment Data

Horizontal Curve Data

1	Presence of horizontal curve 1		Y/N		Y/N	If Yes, then enter data in the next three rows.
	Curve radius R_1 (ft)					
	Length of curve L_{c1} (mi)					
	Length of curve in segment $L_{c1,seg}$ (mi)					
2	Presence of horizontal curve 2		Y/N		Y/N	If Yes, then enter data in the next three rows.
	Curve radius R_2 (ft)					
	Length of curve L_{c2} (mi)					
	Length of curve in segment $L_{c2,seg}$ (mi)					

Cross Section Data

Lane width W_l (ft)					
Inside shoulder width W_{is} (ft)					
Median width W_m (ft)					
Presence of barrier in median		Y/N		Y/N	If Yes, then use the freeway barrier worksheet.
Entrance or exit side (left- or right-hand side)		L/R		L/R	

Traffic Data

Proportion of AADT during high-volume hours P_{hv}				
Freeway segment AADT $AADT_{fs}$ (veh/day)				
AADT of ramp $AADT_r$ (veh/day)				Only needed for entrance ramp.

Freeway Speed-Change Lane Worksheet (2 of 3)

Crash Modification Factors					
Complete the study year column. Complete the crash period column if the EB Method is used.	Equation	Fatal and Injury		Property Damage Only	
		Crash Period	Study Year	Crash Period	Study Year
Horizontal curve $CMF_{1,sc,ac,at,z}$	13-40				
Lane width $CMF_{2,sc,ac,at,fi}$	13-41				
Inside shoulder width $CMF_{3,sc,ac,at,z}$	13-42				
Median width $CMF_{4,sc,ac,at,z}$	13-43				
Median barrier $CMF_{5,sc,ac,at,z}$	13-44				
High volume $CMF_{6,sc,ac,at,z}$	13-45				
Ramp entrance $CMF_{12,sc,nEN,at,z}$	13-46				
Ramp exit $CMF_{13,sc,nEX,at,z}$	13-47				
Combined CMF (multiply all CMFs evaluated)					

Expected Average Crash Frequency^a					
Complete the study year column. Complete the crash period column if the <i>site-specific</i> EB Method is used.		Fatal and Injury		Property Damage Only	
		Crash Period	Study Year	Crash Period	Study Year
Calibration factor $C_{sc,x,at,z}$					
Overdispersion parameter $k_{sc,x,at,z}$					
Observed crash count $N_{o,sc,x,at,z}^*$ (cr)					
Reference year r					
Predicted average crash freq. for reference year $N_{p,sc,x,at,z,r}$ (cr/yr)					
Predicted number of crashes for crash period (sum all years) $N_{p,sc,x,at,z}^*$ (cr)					
Equivalent years associated with crash count $C_{b,sc,x,at,z,r}$ (yr)					
Adjusted average crash freq. for ref. year given $N_{o,sc,x,at,z,r}^*$ (cr/yr)					
Study year s					
Predicted average crash freq. for study year $N_{p,sc,x,at,z,s}$ (cr/yr)					
Expected average crash freq. for study year $N_{e,sc,x,at,z,s}$ (cr/yr)					

Note:

a – If the EB Method is not used, then substitute the word “predicted” for the word “expected” and substitute the subscript “p” for the subscript “e”.

Freeway Speed-Change Lane Worksheet (3 of 3)

Expected Average Crash Frequency^a

Crash Severity Distribution

	K	A	B	C	Total FI	PDO	Total FI + PDO
Proportion by injury level					1.000		
Expected average crash freq. for study year $N_{e, sc, x, at, z, s}$ (cr/yr)							

Crash Type Distribution

Crash Type Category	Table 13-10 or 13-12	Fatal and Injury		Property Damage Only		Total
		Proportion	Expected Average Crash Frequency for Study Year $N_{e, sc, x, at, fi, s}$ (cr/yr)	Proportion	Expected Average Crash Frequency for Study Year $N_{e, sc, x, at, pdo, s}$ (cr/yr)	Expected Average Crash Frequency for Study Year $N_{e, sc, x, at, as, s}$ (cr/yr)
Multiple-Vehicle Crashes						
Head-on						
Right-angle						
Rear-end						
Sideswipe						
Other multiple-vehicle crashes						
Single-Vehicle Crashes						
Crash with animal						
Crash with fixed object						
Crash with other object						
Crash with parked vehicle						
Other single-vehicle crashes						
Total		1.000		1.000		

Note:

a – If the EB Method is not used, then substitute the word “predicted” for the word “expected” and substitute the subscript “p” for the subscript “e”.

Freeway Barrier Worksheet

Input Data			
Segment length L (mi)		Crash period	Study year
Inside shoulder width W_{is} (ft)		Outside shoulder width W_s (ft)	
Nearest distance from edge of traveled way to median barrier face (only needed when continuous barrier present and adjacent to one roadbed) W_{near} (ft)		Inside barrier width W_{ib} (ft)	
		Median width W_m (ft)	
Distance from edge of traveled way to outside barrier face, <i>increasing</i> milepost direction (only needed when continuous barrier is present) $W_{off, inc}$ (ft)		Distance from edge of traveled way to outside barrier face, <i>decreasing</i> milepost (only needed when continuous barrier is present) $W_{off, dec}$ (ft)	
Individual Median Barrier Element Data			
Barrier Location	Length $L_{ib, i}$ (mi)	Width from Edge of Traveled Way to Face of Barrier $W_{off, in, i}$ (ft)	Ratio $L_{ib, i} / (W_{off, in, i} - W_{is})$
1.			
2.			
3.			
4.			
5.			
6.			
7.			
	Sum1	Sum2	
Individual Outside Barrier Element Data			
Barrier Location	Length $L_{ob, i}$ (mi)	Width from Edge of Traveled Way to Face of Barrier $W_{off, o, i}$ (ft)	Ratio $L_{ob, i} / (W_{off, o, i} - W_s)$
1.			
2.			
3.			
4.			
5.			
6.			
7.			
	Sum3	Sum4	
Median Barrier Calculations			
Inside Clearance - Some Barrier Present			
Proportion of segment length with barrier in median $P_{ib} = \text{Sum1} / [2 \times L]$		Width from edge of shoulder to barrier face $W_{icb} = \text{Sum1} / \text{Sum2}$ (ft)	
Inside Clearance - Full Barrier Present			
Width from edge of shoulder to barrier face W_{icb} (ft) For barrier in center of median $W_{ocb} = [2 \times L] / [\text{Sum2} + 2 \times (2 \times L - \text{Sum1}) / (W_m - 2 \times W_{is} - W_{ib})]$ For barrier adjacent to one roadbed $W_{ocb} = [2 \times L] / [L / (W_{near} - W_{is}) + \text{Sum2} + (L - \text{Sum1}) / (W_m - 2 \times W_{is} - W_{ib} - W_{near})]$			
Outside Barrier Calculations			
Outside Clearance - Some Barrier Present			
Proportion of segment length with barrier in median $P_{ob} = \text{Sum3} / [2 \times L]$		Width from edge of shoulder to barrier face $W_{ocb} = \text{Sum3} / \text{Sum4}$ (ft)	
Outside Clearance - Full Barrier Present			
Width from edge of shoulder to barrier face $W_{ocb} = [2 \times L] / [1.0 / (W_{off, inc} - W_s) + 1.0 / (W_{off, dec} - W_s)]$ (ft)			

Project-Level EB Method Worksheet (1 of 2)

Calculations by Site										
Crash severity category addressed z		FI		PDO						
	Site Summary ^b									Total
Site type and number ^a										
Overdispersion Parameter^c										
(1) Multiple-vehicle crashes $k_{w,x,mv,z}$										
(2) Single-vehicle crashes $k_{w,x,sv,z}$										
(3) All crash types $k_{w,x,at,z}$										
Predicted Number of Crashes during the Crash Period^c										
(4) Multiple-vehicle crashes $N_{p,w,x,mv,z}^*$ (cr)										
(5) Single-vehicle crashes $N_{p,w,x,sv,z}^*$ (cr)										
(6) All crash types $N_{p,w,x,at,z}^*$ (cr)										
Predicted number of crashes $N_{p,aS,ac,at,z}^*$ (cr)	= (4) + (5) + (6)									
Predicted Average Crash Frequency for Reference Year^c										
(7) Multiple-vehicle crashes $N_{p,w,x,mv,z,r}$ (cr/yr)										
(8) Single-vehicle crashes $N_{p,w,x,sv,z,r}$ (cr/yr)										
(9) All crash types $N_{p,w,x,at,z,r}$ (cr/yr)										
Predicted freq. for reference year $N_{p,aS,ac,at,z,r}$ (cr/yr)	= (7) + (8) + (9)									
Predicted Average Crash Frequency for Study Year^c										
(10) Multiple-vehicle crashes $N_{p,w,x,mv,z,s}$ (cr/yr)										
(11) Single-vehicle crashes $N_{p,w,x,sv,z,s}$ (cr/yr)										
(12) All crash types $N_{p,w,x,at,z,s}$ (cr/yr)										
Predicted freq. for study year $N_{p,aS,ac,at,z,s}$ (cr/yr)	= (10) + (11) + (12)									
Variance of Predicted Average Crash Frequency^c										
(13) Multiple-vehicle product [= (1) × (4) ²]										
(14) Single-vehicle product [= (2) × (5) ²]										
(15) All crash types [= (3) × (6) ²]										
Variance if independent $V_{0,aS,ac,at,z}$	= (13) + (14) + (15)									
(16) Multiple-vehicle product [= (1) ^{0.5} × (4)]										
(17) Single-vehicle product [= (2) ^{0.5} × (5)]										
(18) All crash types [= (3) ^{0.5} × (6)]										
Variance if correlated $V_{1,aS,ac,at,z}$	= [(16) + (17) + (18)] ²									

Notes:

- a. Site numbering convention: X,y. X: site type; F = freeway segment, R = ramp segment, C = C-D road segment, T = crossroad ramp terminal. y: site number; 1, 2, 3, ...
- b. Use additional sheets if there are more than nine sites in the project limits.
- c. Use the "multiple-vehicle" and "single-vehicle" rows for segments. Use the "all crash types" rows for speed-change lanes and crossroad ramp terminals.

Project-Level EB Method Worksheet (2 of 2)

Calculations for Project			
	Crash Period	Study Year	
Observed crash count during the crash period $N_{o, aS, ac, at, z}^*$ (cr)			Include crashes of all types at all sites during the crash period.
Reference year r			Choose the first year of the crash period.
Predicted average crash freq. for reference year $N_{p, aS, ac, at, z, r}$ (cr/yr)			
Predicted number of crashes for crash period (sum all years) $N_{p, aS, ac, at, z}^*$ (cr)			
Equivalent years associated with crash count $C_{b, aS, ac, at, z, r}$ (yr)			$= N_{p, aS, ac, at, z}^* / N_{p, aS, ac, at, z, r}$
Independent Sites Crash Analysis			
Variance if independent $V_{0, aS, ac, at, z}$			
Weight associated with $N_{p, \dots, r}$ $w_{0, aS, ac, at, z}$			$= 1.0 / (1.0 + V_{0, aS, ac, at, z} / N_{p, aS, ac, at, z}^*)$
Adjusted average crash freq. for reference year given $N_{o, aS, ac, at, z, r}^*$			$= w_{0, aS, ac, at, z} \times N_{p, aS, ac, at, z, r} + (1.0 - w_{0, aS, ac, at, z}) \times N_{o, aS, ac, at, z}^* / C_{b, aS, ac, at, z, r}$
Correlated Sites Crash Analysis			
Variance if correlated $V_{1, aS, ac, at, z}$			
Weight associated with $N_{p, \dots, r}$ $w_{1, aS, ac, at, z}$			$= 1.0 / (1.0 + V_{1, aS, ac, at, z} / N_{p, aS, ac, at, z}^*)$
Adjusted average crash freq. for reference year given $N_{o, aS, ac, at, z, r}^*$			$= w_{1, aS, ac, at, z} \times N_{p, aS, ac, at, z, r} + (1.0 - w_{1, aS, ac, at, z}) \times N_{o, aS, ac, at, z}^* / C_{b, aS, ac, at, z, r}$
Expected Average Crash Frequency			
Adjusted average crash freq. for reference year given $N_{o, aS, ac, at, z, r}^*$			$= (N_{0, aS, ac, at, z, r} + N_{1, aS, ac, at, z, r}) / 2.0$
Study year s			
Predicted average crash freq. for study year $N_{p, aS, ac, at, z, s}$ (cr/yr)			
Expected average crash freq. for study year $N_{e, aS, ac, at, z, s}$ (cr/yr)			$= N_{a, aS, ac, at, z, r} \times N_{p, aS, ac, at, z, s} / N_{p, aS, ac, at, z, r}$

APPENDIX D

PROPOSED HSM RAMPS CHAPTER

CHAPTER 19—PREDICTIVE METHOD FOR RAMPS

TABLE OF CONTENTS

List of Figures.....	iii
List of Tables.....	v
19.1. Introduction.....	1
19.2. Overview of the Predictive Method.....	1
19.3. Ramps—Definitions and Predictive Models	2
19.3.1. Definition of Ramp Site Types	3
19.3.2. Predictive Model for Ramp Segments	6
19.3.3. Predictive Model for Ramp Terminals.....	9
19.4. Predictive Method for Ramps and Ramp Terminals.....	10
19.4.1. Step-by-Step Description of the Predictive Method	10
19.4.2. Data Needed to Apply the Predictive Method.....	18
19.5. Ramp Segments and Ramp Terminals	27
19.5.1. Definition of Ramp Segment and Ramp Terminal	27
19.5.2 Segmentation Process.....	28
19.5.3. Crash Assignment to Sites	29
19.6. Safety Performance Functions	29
19.6.1. Safety Performance Functions for Ramp Segments	30
19.6.2. Safety Performance Functions for Ramp Terminals.....	38
19.7. Crash Modification Factors.....	51
19.7.1. Crash Modification Factors for Ramp Segments	52

19.7.2. Crash Modification Factors for Ramp Terminals	61
19.7.3. Supplemental Calculations to Apply Crash Modification Factors	73
19.8. Severity Distribution Functions	79
19.8.1. Severity Distribution Functions for Ramp Segments	80
19.8.2. Severity Distribution Functions for Ramp Terminals.....	81
19.9. Calibration of the SPFs and SDFs to Local Conditions.....	83
19.10. Interim Predictive Method for All-Way Stop Control.....	84
19.11. Limitations of Predictive Method	85
19.12. Application of Predictive Method	86
19.13. Summary	86
19.14. Sample Problems.....	87
19.14.1. Sample Problem 1	87
19.14.2. Sample Problem 2	98
19.14.3. Sample Problem 3	108
19.14.4. Sample Problem 4	121
19.14.5. Sample Problem 5	132
19.14.6. Sample Problem 6	142
19.15. References.....	151
Appendix 19A—Worksheets for Predictive Method for Ramps.....	152

LIST OF FIGURES

Figure 19-1. Ramp Terminal Configurations	3
Figure 19-2. The HSM Predictive Method	11
Figure 19-3. Number-of-Lanes Determination for Ramp Segments.....	19
Figure 19-4. Starting Milepost Location on Ramps and C-D Roads	20
Figure 19-5. Barrier Variables	21
Figure 19-6. Speed-Change Lane Location on Ramps and C-D Roads	22
Figure 19-7. C-D Road Weaving Section Length.....	23
Figure 19-8. Illustrative Ramp Terminals	23
Figure 19-9. Exit Ramp Skew Angle	25
Figure 19-10. Illustrative Ramp Segments and Ramp Terminals.....	28
Figure 19-11. Graphical Form of the SPFs for Multiple-Vehicle Crashes on Entrance Ramp Segments	32
Figure 19-12. Graphical Form of the SPFs for Multiple-Vehicle Crashes on Exit Ramp Segments	33
Figure 19-13. Graphical Form of the SPFs for Single-Vehicle Crashes on Entrance Ramp Segments	36
Figure 19-14. Graphical Form of the SPFs for Single-Vehicle Crashes on Exit Ramp Segments ..	36
Figure 19-15. Graphical Form of the SPF for Crashes at Signalized Ramp Terminals–Three-Leg Terminal at Two-Quadrant Parclo A or B (<i>A2, B2</i>).....	43
Figure 19-16. Graphical Form of the SPF for Crashes at Signalized Ramp Terminals–Three-Leg Terminal with Diagonal Exit Ramp or Four-Leg Terminal at Four-Quadrant Parclo A (<i>D3ex, A4</i>) ..	43
Figure 19-17. Graphical Form of the SPF for Crashes at Signalized Ramp Terminals–Three-Leg Terminal with Diagonal Entrance Ramp or Four-Leg Terminal at Four-Quadrant Parclo B (<i>D3en, B4</i>).....	44
Figure 19-18. Graphical Form of the SPF for Crashes at Signalized Ramp Terminals–Four-Leg Terminal with Diagonal Ramps (<i>D4</i>)	44
Figure 19-19. Graphical Form of the SPF Crashes at One-Way Stop-Controlled Ramp Terminals– Three-Leg Terminal at Two-Quadrant Parclo A or B (<i>A2, B2</i>)	48

Figure 19-20. Graphical Form of the SPF Crashes at One-Way Stop-Controlled Ramp Terminals– Three-Leg Terminal with Diagonal Exit Ramp or Four-Leg Terminal at Four-Quadrant Parclo A (<i>D3ex, A4</i>)	48
Figure 19-21. Graphical Form of the SPF Crashes at One-Way Stop-Controlled Ramp Terminals– Three-Leg Terminal with Diagonal Entrance Ramp or Four-Leg Terminal at Four-Quadrant Parclo B (<i>D3en, B4</i>).....	49
Figure 19-22. Graphical Form of the SPF Crashes at One-Way Stop-Controlled Ramp Terminals– Four-Leg Terminal with Diagonal Ramps (<i>D4</i>).....	49
Figure 19-23. Effective Number of Lanes for Various Exit Ramp Configurations	63
Figure 19-24. Starting Milepost Location for Ramp and C-D Road Combinations	74

LIST OF TABLES

Table 19-1. Ramp and Collector-Distributor Road SPFs	5
Table 19-2. Crossroad Ramp Terminal SPFs	6
Table 19-3. Ramp Safety Performance Functions	30
Table 19-4. Applicable AADT Volume Ranges for Ramp SPFs	31
Table 19-5. SPF Coefficients for Multiple-Vehicle Crashes on Ramp Segments.....	32
Table 19-6. Default Distribution of Multiple-Vehicle Crashes by Crash Type for Ramp and C-D Road Segments.....	33
Table 19-7. SPF Coefficients for Multiple-Vehicle Crashes on C-D Road Segments	34
Table 19-8. SPF Coefficients for Single-Vehicle Crashes on Ramp Segments	35
Table 19-9. Default Distribution of Single-Vehicle Crashes by Crash Type for Ramp and C-D Road Segments	37
Table 19-10. SPF Coefficients for Single-Vehicle Crashes on C-D Road Segments.....	38
Table 19-11. Applicable AADT Volume Ranges for Crossroad Ramp Terminal SPFs	39
Table 19-12. SPF Coefficients for Crashes at Signalized Ramp Terminals—Three-Leg Terminal at Two-Quadrant Parclo A or B (<i>A2, B2</i>)	41
Table 19-13. SPF Coefficients for Crashes at Signalized Ramp Terminals—Three-Leg Terminal with Diagonal Exit Ramp or Four-Leg Terminal at Four-Quadrant Parclo A (<i>D3ex, A4</i>)	41
Table 19-14. SPF Coefficients for Crashes at Signalized Ramp Terminals—Three-Leg Terminal with Diagonal Entrance Ramp or Four-Leg Terminal at Four-Quadrant Parclo B (<i>D3en, B4</i>).....	42
Table 19-15. SPF Coefficients for Crashes at Signalized Ramp Terminals—Four-Leg Terminal with Diagonal Ramps (<i>D4</i>).....	42
Table 19-16. Default Distribution of Signal-Controlled Ramp Terminal Crashes by Crash Type	45
Table 19-17. SPF Coefficients for Crashes at One-Way Stop-Controlled Ramp Terminals—Three-Leg Terminal at Two-Quadrant Parclo A or B (<i>A2, B2</i>)	46
Table 19-18. SPF Coefficients for Crashes at One-Way Stop-Controlled Ramp Terminals—Three-Leg Terminal with Diagonal Exit Ramp or Four-Leg Terminal at Four-Quadrant Parclo A (<i>D3ex, A4</i>)	47

Table 19-19. SPF Coefficients for Crashes at One-Way Stop-Controlled Ramp Terminals–Three-Leg Terminal with Diagonal Entrance Ramp or Four-Leg Terminal at Four-Quadrant Parclo B (<i>D3en, B4</i>)	47
Table 19-20. SPF Coefficients for Crashes at One-Way Stop-Controlled Ramp Terminals–Four-Leg Terminal with Diagonal Ramps (<i>D4</i>)	47
Table 19-21. Default Distribution of One-Way Stop-Controlled Ramp Terminal Crashes by Crash Type	50
Table 19-22. Ramp Segment Crash Modification Factors and their Corresponding SPFs	51
Table 19-23. Crossroad Ramp Terminal Crash Modification Factors and their Corresponding SPFs	52
Table 19-24. Coefficients for Horizontal Curve CMF–Ramp and C-D Road Segments	53
Table 19-25. Coefficients for Lane Width CMF–Ramp and C-D Road Segments	54
Table 19-26. Coefficients for Right Shoulder Width CMF–Ramp and C-D Road Segments.....	55
Table 19-27. Coefficients for Left Shoulder Width CMF–Ramp and C-D Road Segments	56
Table 19-28. Coefficients for Right Side Barrier CMF–Ramp and C-D Road Segments	57
Table 19-29. Coefficients for Left Side Barrier CMF–Ramp and C-D Road Segments.....	58
Table 19-30. Coefficients for Lane Add or Drop CMF–Ramp and C-D Road Segments	59
Table 19-31. Coefficients for Weaving Section CMF–C-D Road Segments	60
Table 19-32. Coefficients for Exit Ramp Capacity CMF–Crossroad Ramp Terminals	62
Table 19-33. Coefficients for Crossroad Left-Turn Lane CMF–Crossroad Ramp Terminals	64
Table 19-34. Coefficients for Crossroad Right-Turn Lane CMF–Crossroad Ramp Terminals.....	65
Table 19-35. Coefficients for Access Point Frequency CMF–Crossroad Ramp Terminals.....	66
Table 19-36. Coefficients for Segment Length CMF–Crossroad Ramp Terminals	67
Table 19-37. Coefficients for Median Width CMF–Crossroad Ramp Terminals	69
Table 19-38. Coefficients for Protected Left-Turn Operation CMF–Crossroad Ramp Terminals....	70
Table 19-39. Coefficients for Channelized Right Turn on Crossroad CMF–Crossroad Ramp Terminals.....	71
Table 19-40. Coefficients for Channelized Right Turn on Exit Ramp CMF–Crossroad Ramp Terminals.....	71
Table 19-41. Coefficients for Non-Ramp Public Street Leg CMF–Crossroad Ramp Terminals.....	72

Table 19-42. Input Data for Ramp Curve Speed Prediction.....	75
Table 19-43. SDF Coefficients for Ramp Segments	81
Table 19-44. SDF Coefficients for Crossroad Ramp Terminals	83
Table 19-45. Default Distribution of All-Way Stop-Controlled Ramp Terminal Crashes by Crash Type	85
Table 19-46. List of Sample Problems	87
Table 19-47. Ramp Segment Worksheet (1 of 4)—Sample Problem 1	95
Table 19-48. Ramp Segment Worksheet (2 of 4)—Sample Problem 1	96
Table 19-49. Ramp Segment Worksheet (3 of 4)—Sample Problem 1	97
Table 19-50. Ramp Segment Worksheet (4 of 4)—Sample Problem 1	98
Table 19-51. Ramp Segment Worksheet (1 of 4)—Sample Problem 2	105
Table 19-52. Ramp Segment Worksheet (2 of 4)—Sample Problem 2	106
Table 19-53. Ramp Segment Worksheet (3 of 4)—Sample Problem 2	107
Table 19-54. Ramp Segment Worksheet (4 of 4)—Sample Problem 2	108
Table 19-55. Ramp Segment Worksheet (1 of 4)—Sample Problem 3	117
Table 19-56. Ramp Segment Worksheet (2 of 4)—Sample Problem 3	118
Table 19-57. Ramp Segment Worksheet (3 of 4)—Sample Problem 3	119
Table 19-58. Ramp Segment Worksheet (4 of 4)—Sample Problem 3	120
Table 19-59. Ramp Barrier Worksheet—Sample Problem 3	121
Table 19-60. Ramp Terminal Worksheet (1 of 4)—Sample Problem 4	129
Table 19-61. Ramp Terminal Worksheet (2 of 4)—Sample Problem 4	130
Table 19-62. Ramp Terminal Worksheet (3 of 4)—Sample Problem 4	131
Table 19-63. Ramp Terminal Worksheet (4 of 4)—Sample Problem 4	132
Table 19-64. Ramp Terminal Worksheet (1 of 4)—Sample Problem 5.....	139
Table 19-65. Ramp Terminal Worksheet (2 of 4)—Sample Problem 5.....	140
Table 19-66. Ramp Terminal Worksheet (3 of 4)—Sample Problem 5.....	141
Table 19-67. Ramp Terminal Worksheet (4 of 4)—Sample Problem 5.....	142

Table 19-68. Ramp Terminal Worksheet (1 of 4)—Sample Problem 6	148
Table 19-69. Ramp Terminal Worksheet (2 of 4)—Sample Problem 6	149
Table 19-70. Ramp Terminal Worksheet (3 of 4)—Sample Problem 6	150
Table 19-71. Ramp Terminal Worksheet (4 of 4)—Sample Problem 6	151

Chapter 19—Predictive Method for Ramps

19.1. INTRODUCTION

This chapter presents the predictive method for ramps, as used to connect two or more highway legs at an interchange. The method is also applicable to collector-distributor (C-D) roadways that connect with ramps and one or more highway legs at an interchange. A general introduction to the *Highway Safety Manual* (HSM) predictive method is provided in Part C—Introduction and Applications Guidance.

The predictive methodology for ramps provides a structured methodology to estimate the expected average crash frequency (in total, or by crash type or severity) for a ramp with known characteristics. Crashes involving vehicles of all types are included in the estimate. The predictive method can be applied to an existing ramp, a design alternative for an existing ramp, a new ramp, or for alternative traffic volume projections. An estimate can be made of expected average crash frequency for a prior time period (i.e., what did or would have occurred) or a future time period (i.e., what is expected to occur). The development of the predictive method in this chapter is documented in Bonneson et al. (1).

This chapter presents the following information about the predictive method for ramps:

- A concise overview of the predictive method.
- The definitions of the site types addressed by the predictive method.
- A step-by-step description of the predictive method.
- Details for dividing a ramp into individual evaluation sites.
- Safety performance functions (SPFs) for ramps.
- Crash modification factors (CMFs) for ramps.
- Severity distribution functions (SDFs) for ramps.
- Limitations of the predictive method.
- Sample problems illustrating the application of the predictive method.

19.2. OVERVIEW OF THE PREDICTIVE METHOD

The predictive method provides an 18-step procedure to estimate the expected average crash frequency (in total, or by crash type or severity) for an entire ramp or C-D road. The gore point of the speed-change lane is used to define the beginning (or ending) point of a ramp or C-D road.

The predictive method is used to evaluate an entire ramp, C-D road, or site. A site is a ramp segment, a C-D road segment, or crossroad ramp terminal. A crossroad ramp terminal is a controlled terminal between a ramp and a crossroad. A crossroad speed-change lane (i.e., an uncontrolled terminal between a ramp and a crossroad) is not addressed by the method.

The predictive method is applicable to ramps or C-D roads in the vicinity of an interchange. The interchange may connect a freeway and a crossroad (service interchange) or two freeways (system interchange). The method is applicable to ramps and C-D roads that are one-way roadways.

The predictive method is used to estimate the expected number of crashes for an individual site. This estimate can be summed for all sites to compute the expected number of crashes for the entire ramp or C-D road. The estimate represents a given time period of interest (in years) during which the geometric design and traffic control features are unchanged and traffic volumes are known or forecasted. The expected average crash frequency is obtained by dividing the expected number of crashes by the time period of interest.

The predictive models used in this chapter are described in detail in Section 19.3. The predicted average crash frequency from a predictive model can be used as an estimate of the expected average crash frequency, or it can be combined with observed crash data (using the empirical Bayes [EB] Method) to obtain a more reliable estimate of the expected average crash frequency.

The predictive models used in this chapter to determine the predicted average crash frequency are of the general form shown in Equation 19-1.

$$N_{p,w,x,y,z} = N_{spf,w,x,y,z} \times (CMF_{1,w,x,y,z} \times CMF_{2,w,x,y,z} \times \dots \times CMF_{m,w,x,y,z}) \times C_{w,x,y,z} \quad \text{Equation 19-1}$$

Where:

$N_{p,w,x,y,z}$ = predicted average crash frequency for a specific year for site type w , cross section or control type x , crash type y , and severity z (crashes/yr);

$N_{spf,w,x,y,z}$ = predicted average crash frequency determined for base conditions of the SPF developed for site type w , cross section or control type x , crash type y , and severity z (crashes/yr);

$CMF_{m,w,x,y,z}$ = crash modification factors specific to site type w , cross section or control type x , crash type y , and severity z for specific geometric design and traffic control features m ; and

$C_{w,x,y,z}$ = calibration factor to adjust SPF for local conditions for site type w , cross section or control type x , crash type y , and severity z .

The predictive models provide estimates of the predicted average crash frequency in total, or by crash type or severity. A default distribution of crash type is included in the predictive method. It is used with the predictive models to quantify the crash frequency for each of ten crash types. The models predict fatal-and-injury crash frequency and property-damage-only crash frequency. A severity distribution function is available to further quantify the crash frequency by the following severity levels: fatal, incapacitating injury, non-incapacitating injury, and possible injury.

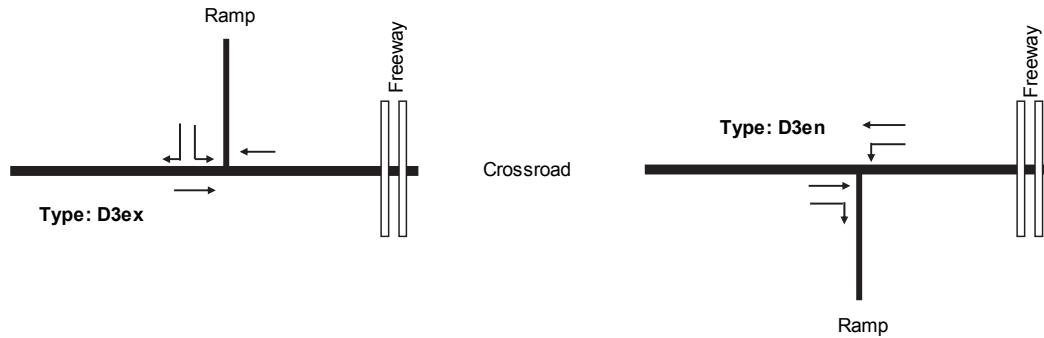
19.3. RAMPS—DEFINITIONS AND PREDICTIVE MODELS

This section provides the definitions of the site types discussed in this chapter. It also describes the predictive models for each of the site types.

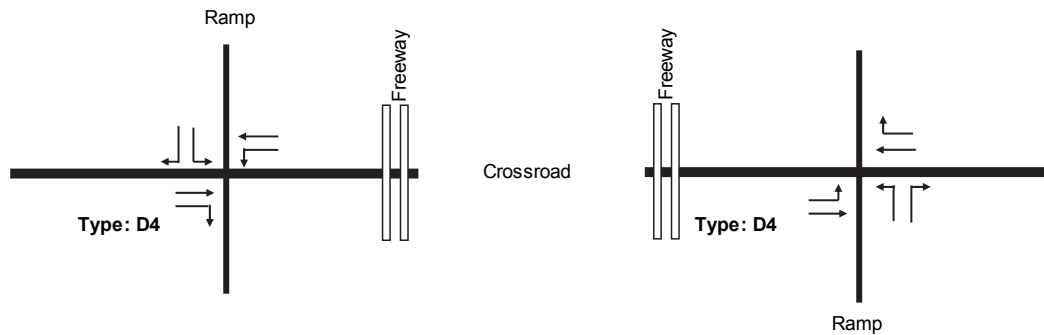
19.3.1. Definition of Ramp Site Types

The predictive method in this chapter applies to the following site types: entrance ramp segment with one or two lanes, exit ramp segment with one or two lanes, C-D road segment with one or two lanes, and crossroad ramp terminal. Connector ramp segments are represented using one of these site types.

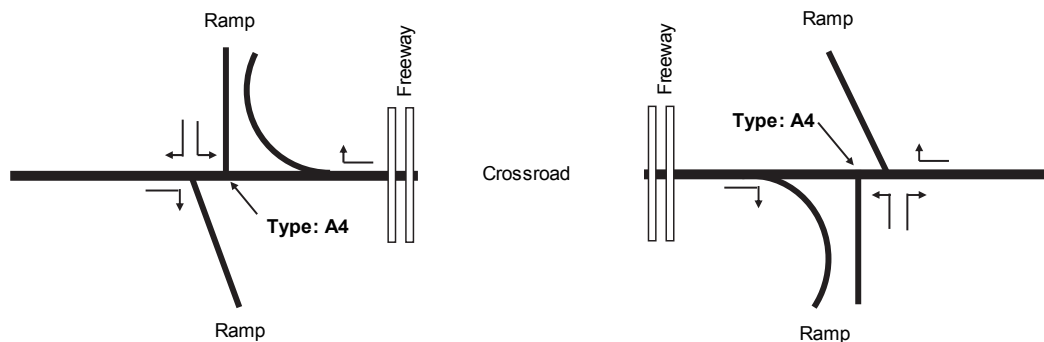
There are many different configurations of crossroad ramp terminal used at interchanges. For this reason, the definition of “site type” is broadened when applied to crossroad ramp terminals to be specific to each configuration. The more common configurations are identified in Figure 19-1.



a. Three-Leg Ramp Terminal With Diagonal Exit or Entrance Ramp (*D3ex* and *D3en*)

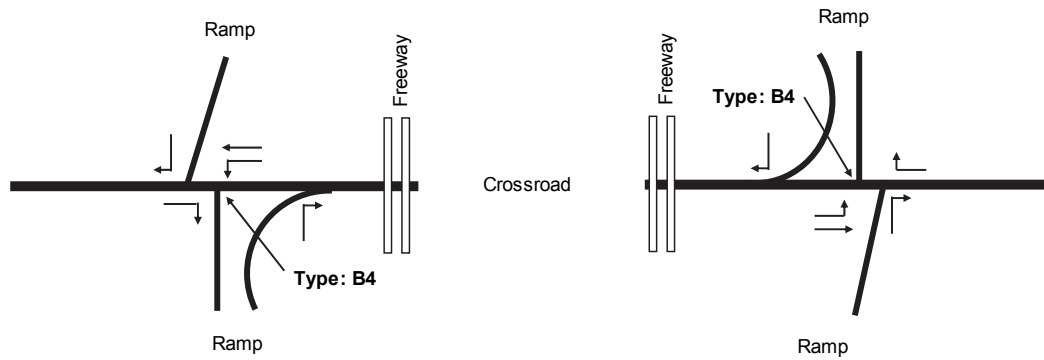


b. Four-Leg Ramp Terminal With Diagonal Ramps (*D4*)

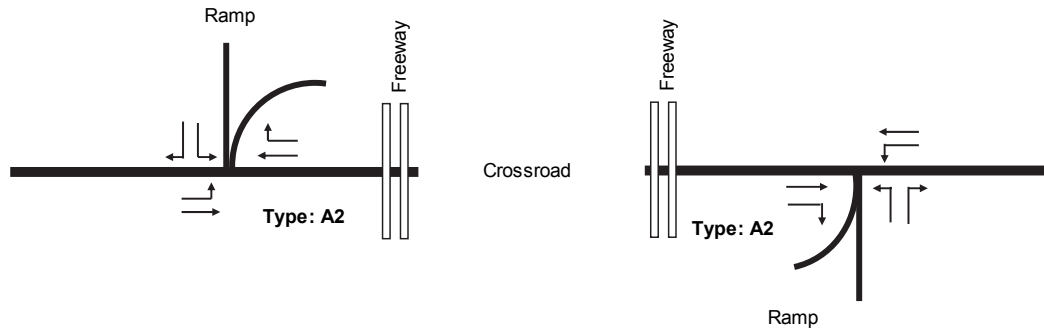


c. Four-Leg Ramp Terminal at Four-Quadrant Parclo A (*A4*)

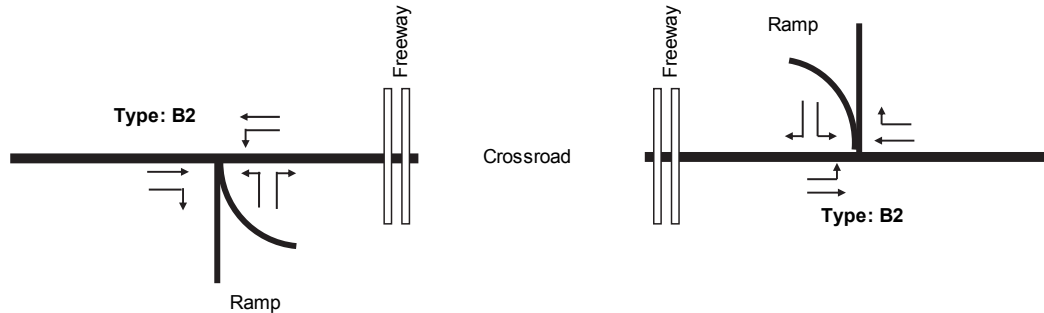
Figure 19-1. Ramp Terminal Configurations



d. Four-Leg Ramp Terminal at Four-Quadrant Parclo B (B4)



e. Three-Leg Ramp Terminal at Two-Quadrant Parclo A (A2)



f. Three-Leg Ramp Terminal at Two-Quadrant Parclo B (B2)

Figure 19-1. Ramp Terminal Configurations *continued*

Differences among the terminals shown Figure 19-1 reflect the number of ramp legs, number of left-turn movements, and location of crossroad left-turn storage (i.e., inside or outside of the interchange). Although not shown, control type (i.e., signalized or stop controlled) is also an important factor in characterizing a crossroad ramp terminal.

The terms “highway,” “roadway,” and “road” are used interchangeably in this chapter and apply to all freeways and crossroads independent of official state designation or local highway designation.

Classifying an area as urban, suburban, or rural is subject to the roadway characteristics, surrounding population, and surrounding land uses, and is at the analyst's discretion. In the HSM, the definition of "urban" and "rural" areas is based on Federal Highway Administration (FHWA) guidelines which classify "urban" areas as places inside urban boundaries where the population is greater than 5,000 persons. "Rural" areas are defined as places outside urban areas where the population is less than 5,000 persons. The HSM uses the term "suburban" to refer to outlying portions of an urban area; the predictive method does not distinguish between urban and suburban portions of a developed area.

Table 19-1 identifies the ramp and C-D road segment site types for which SPFs have been developed. These SPFs are used to estimate the predicted average crash frequency by crash type and crash severity. These estimates are added to yield the total predicted average crash frequency for an individual site. One set of SPFs is developed for urban areas and a second set is developed for rural areas.

Table 19-1. Ramp and Collector-Distributor Road SPFs

Site Type (w)	Cross Section (x)	Crash Type (y)	Crash Severity (z)	SPF
Ramp segments (rps)	One-lane entrance ramp ($1EN$)	Multiple vehicle (mv)	Fatal and injury (fi)	$N_{spf, rps, 1EN, mv, fi}$
			Property damage only (pdo)	$N_{spf, rps, 1EN, mv, pdo}$
		Single vehicle (sv)	Fatal and injury (fi)	$N_{spf, rps, 1EN, sv, fi}$
			Property damage only (pdo)	$N_{spf, rps, 1EN, sv, pdo}$
	Two-lane entrance ramp ($2EN$) (urban areas only)	Multiple vehicle (mv)	Fatal and injury (fi)	$N_{spf, rps, 2EN, mv, fi}$
			Property damage only (pdo)	$N_{spf, rps, 2EN, mv, pdo}$
		Single vehicle (sv)	Fatal and injury (fi)	$N_{spf, rps, 2EN, sv, fi}$
			Property damage only (pdo)	$N_{spf, rps, 2EN, sv, pdo}$
	One-lane exit ramp ($1EX$)	Multiple vehicle (mv)	Fatal and injury (fi)	$N_{spf, rps, 1EX, mv, fi}$
			Property damage only (pdo)	$N_{spf, rps, 1EX, mv, pdo}$
		Single vehicle (sv)	Fatal and injury (fi)	$N_{spf, rps, 1EX, sv, fi}$
			Property damage only (pdo)	$N_{spf, rps, 1EX, sv, pdo}$
Two-lane exit ramp ($2EX$) (urban areas only)	Multiple vehicle (mv)	Fatal and injury (fi)	$N_{spf, rps, 2EX, mv, fi}$	
		Property damage only (pdo)	$N_{spf, rps, 2EX, mv, pdo}$	
	Single vehicle (sv)	Fatal and injury (fi)	$N_{spf, rps, 2EX, sv, fi}$	
		Property damage only (pdo)	$N_{spf, rps, 2EX, sv, pdo}$	
C-D road segments (cds)	One-lane C-D road (1)	Multiple vehicle (mv)	Fatal and injury (fi)	$N_{spf, cds, 1, mv, fi}$
			Property damage only (pdo)	$N_{spf, cds, 1, mv, pdo}$
		Single vehicle (sv)	Fatal and injury (fi)	$N_{spf, cds, 1, sv, fi}$
			Property damage only (pdo)	$N_{spf, cds, 1, sv, pdo}$
	Two-lane C-D road (2) (urban areas only)	Multiple vehicle (mv)	Fatal and injury (fi)	$N_{spf, cds, 2, mv, fi}$
			Property damage only (pdo)	$N_{spf, cds, 2, mv, pdo}$
		Single vehicle (sv)	Fatal and injury (fi)	$N_{spf, cds, 2, sv, fi}$
			Property damage only (pdo)	$N_{spf, cds, 2, sv, pdo}$

The ramp segment and C-D road segment are defined as follows:

- *One-lane segment*—a length of roadway consisting of one lane with a constant cross section providing one direction of travel.
- *Two-lane segment*—a length of roadway consisting of two lanes with a constant cross section providing one direction of travel.

Table 19-2 identifies the crossroad ramp terminal site types for which SPFs have been developed. These SPFs are used to estimate the predicted average crash frequency by crash severity. These estimates are added to yield the total predicted average crash frequency for an individual site. One set of SPFs is developed for urban areas and a second set is developed for rural areas.

Table 19-2. Crossroad Ramp Terminal SPFs

Site Type (<i>w</i>)	Cross Section and Control Type (<i>x</i>)	Crash Type (<i>y</i>)	Crash Severity (<i>z</i>)	SPF
Three-leg terminals with diagonal exit ramp (<i>D3ex</i>),	One-way stop control; 2, 3, or 4 lane crossroad (<i>ST</i>)	All types (<i>at</i>)	Fatal and injury (<i>fi</i>)	$N_{spf, w, ST, at, fi}$
Three-leg terminals with diagonal entrance ramp (<i>D3en</i>),			Property damage only (<i>pdo</i>)	$N_{spf, w, ST, at, pdo}$
Four-leg terminals with diagonal ramps (<i>D4</i>),	Signal control, 2-lane crossroad (<i>SG2</i>)	All types (<i>at</i>)	Fatal and injury (<i>fi</i>)	$N_{spf, w, SG2, at, fi}$
Four-leg terminals at four-quadrant parcel A (<i>A4</i>),	Signal control, 3-lane crossroad (<i>SG3</i>)		Property damage only (<i>pdo</i>)	$N_{spf, w, SG2, at, pdo}$
Four-leg terminals at four-quadrant parcel B (<i>B4</i>),	Signal control, 4-lane crossroad (<i>SG4</i>)	All types (<i>at</i>)	Fatal and injury (<i>fi</i>)	$N_{spf, w, SG3, at, fi}$
Three-leg terminals at two-quadrant parcel A (<i>A2</i>),			Property damage only (<i>pdo</i>)	$N_{spf, w, SG3, at, pdo}$
Three-leg terminals at two-quadrant parcel B (<i>B2</i>),	Signal control, 5-lane crossroad (<i>SG5</i>) (urban areas only)	All types (<i>at</i>)	Fatal and injury (<i>fi</i>)	$N_{spf, w, SG4, at, fi}$
			Property damage only (<i>pdo</i>)	$N_{spf, w, SG4, at, pdo}$
	Signal control, 6-lane crossroad (<i>SG6</i>) (urban areas only)	All types (<i>at</i>)	Fatal and injury (<i>fi</i>)	$N_{spf, w, SG5, at, fi}$
			Property damage only (<i>pdo</i>)	$N_{spf, w, SG5, at, pdo}$
	Signal control, 6-lane crossroad (<i>SG6</i>) (urban areas only)	All types (<i>at</i>)	Fatal and injury (<i>fi</i>)	$N_{spf, w, SG6, at, fi}$
			Property damage only (<i>pdo</i>)	$N_{spf, w, SG6, at, pdo}$

For the purposes of evaluation, a crossroad ramp terminal’s “site type” is defined in terms of its configuration. The terminal configurations addressed in the predictive method are shown in Figure 19-1. These terminals are further categorized by crossroad cross section and the type of traffic control used at the terminal. Stop-controlled terminals have a stop sign on the ramp approach to the intersection, and no stop or yield sign on the crossroad approaches. Signal-controlled terminals have traffic signals on the ramp and crossroad approaches.

19.3.2. Predictive Model for Ramp Segments

In general, a predictive model is used to compute the predicted average crash frequency for a site. It combines with the SPF, CMFs, and a calibration factor. The predicted quantity can describe crash frequency in total, or by crash type or severity. This section describes the predictive model for ramp and C-D road segments. The next section describes the predictive model for crossroad ramp terminals.

The predictive model for ramp and C-D road segments is used to estimate the predicted average crash frequency of segment crashes (i.e., the estimate does not include ramp-terminal-related crashes). Segment crashes include crashes that occur in the segment and either (a) away from the crossroad ramp terminal or (b) within the limits of the crossroad ramp terminal but not related to the terminal. That is, the predictive model estimate includes crashes that would occur regardless of whether the crossroad ramp terminal is present.

The predictive model for entrance ramps (and connector ramps at service interchanges that serve motorists traveling from the crossroad to the freeway) is presented in Equation 19-2 through Equation 19-6.

$$N_{p, rps, nEN, at, as} = N_{p, rps, nEN, mv, fi} + N_{p, rps, nEN, sv, fi} + N_{p, rps, nEN, mv, pdo} + N_{p, rps, nEN, sv, pdo} \quad \text{Equation 19-2}$$

$$N_{p, rps, nEN, mv, fi} = C_{rps, EN, mv, fi} \times N_{spf, rps, nEN, mv, fi} \times \left(CMF_{1, rps, ac, mv, fi} \times \dots \times CMF_{m, rps, ac, mv, fi} \right) \times \left(CMF_{1, rps, ac, at, fi} \times \dots \times CMF_{m, rps, ac, at, fi} \right) \quad \text{Equation 19-3}$$

$$N_{p, rps, nEN, sv, fi} = C_{rps, EN, sv, fi} \times N_{spf, rps, nEN, sv, fi} \times \left(CMF_{1, rps, ac, sv, fi} \times \dots \times CMF_{m, rps, ac, sv, fi} \right) \times \left(CMF_{1, rps, ac, at, fi} \times \dots \times CMF_{m, rps, ac, at, fi} \right) \quad \text{Equation 19-4}$$

$$N_{p, rps, nEN, mv, pdo} = C_{rps, EN, mv, pdo} \times N_{spf, rps, nEN, mv, pdo} \times \left(CMF_{1, rps, ac, mv, pdo} \times \dots \times CMF_{m, rps, ac, mv, pdo} \right) \times \left(CMF_{1, rps, ac, at, pdo} \times \dots \times CMF_{m, rps, ac, at, pdo} \right) \quad \text{Equation 19-5}$$

$$N_{p, rps, nEN, sv, pdo} = C_{rps, EN, sv, pdo} \times N_{spf, rps, nEN, sv, pdo} \times \left(CMF_{1, rps, ac, sv, pdo} \times \dots \times CMF_{m, rps, ac, sv, pdo} \right) \times \left(CMF_{1, rps, ac, at, pdo} \times \dots \times CMF_{m, rps, ac, at, pdo} \right) \quad \text{Equation 19-6}$$

Where:

$N_{p, rps, nEN, y, z}$ = predicted average crash frequency of an entrance ramp segment with n lanes, crash type y ($y = sv$: single vehicle, mv : multiple vehicle, at : all types), and severity z ($z = fi$: fatal and injury, pdo : property damage only, as : all severities) (crashes/yr);

$N_{spf, rps, nEN, y, z}$ = predicted average crash frequency of an entrance ramp segment with base conditions, n lanes, crash type y ($y = sv$: single vehicle, mv : multiple vehicle, at : all types), and severity z ($z = fi$: fatal and injury, pdo : property damage only) (crashes/yr);

$CMF_{m, rps, ac, y, z}$ = crash modification factor for a ramp segment with any cross section ac , features m , crash type y ($y = sv$: single vehicle, mv : multiple vehicle, at : all types), and severity z ($z = fi$: fatal and injury, pdo : property damage only); and

$C_{rps, EN, y, z}$ = calibration factor for entrance ramp segments with any lanes, crash type y ($y = sv$: single vehicle, mv : multiple vehicle, at : all types), and severity z ($z = fi$: fatal and injury, pdo : property damage only).

The predictive model for exit ramps (and connector ramps at service interchanges that serve motorists traveling from the freeway to the crossroad) is identical to that for entrance ramps except that the subscript “EX” is substituted for “EN” in Equation 19-2 to Equation 19-6.

Equation 19-2 shows that entrance ramp segment crash frequency is estimated as the sum of four components: fatal-and-injury multiple-vehicle crash frequency, fatal-and-injury single-vehicle crash

frequency, property-damage-only multiple-vehicle crash frequency, and property-damage-only single-vehicle crash frequency.

Different CMFs are used in Equation 19-3 to Equation 19-6. The first terms in parentheses in each equation recognizes that the influence of some geometric factors is unique to each crash type. In contrast, the second term in parentheses in these equations recognizes that some geometric features have a similar influence on all crash types. All CMFs are unique to crash severity.

Equation 19-3 and Equation 19-4 are used to estimate the fatal-and-injury crash frequency. Equation 19-5 and Equation 19-6 are used to estimate the property-damage-only crash frequency.

The predictive model for C-D roads (and connector ramps at system interchanges) is presented in Equation 19-7 through Equation 19-11.

$$N_{p, cds, n, at, as} = N_{p, cds, n, mv, fi} + N_{p, cds, n, sv, fi} + N_{p, cds, n, mv, pdo} + N_{p, cds, n, sv, pdo} \quad \text{Equation 19-7}$$

$$N_{p, cds, n, mv, fi} = C_{cds, ac, mv, fi} \times N_{spf, cds, n, mv, fi} \times \left(CMF_{1, cds, ac, mv, fi} \times \dots \times CMF_{m, cds, ac, mv, fi} \right) \times \left(CMF_{1, cds, ac, at, fi} \times \dots \times CMF_{m, cds, ac, at, fi} \right) \quad \text{Equation 19-8}$$

$$N_{p, cds, n, sv, fi} = C_{cds, ac, sv, fi} \times N_{spf, cds, n, sv, fi} \times \left(CMF_{1, cds, ac, sv, fi} \times \dots \times CMF_{m, cds, ac, sv, fi} \right) \times \left(CMF_{1, rps, ac, at, fi} \times \dots \times CMF_{m, rps, ac, at, fi} \right) \quad \text{Equation 19-9}$$

$$N_{p, cds, n, mv, pdo} = C_{cds, ac, mv, pdo} \times N_{spf, cds, n, mv, pdo} \times \left(CMF_{1, cds, ac, mv, pdo} \times \dots \times CMF_{m, cds, ac, mv, pdo} \right) \times \left(CMF_{1, cds, ac, at, pdo} \times \dots \times CMF_{m, cds, ac, at, pdo} \right) \quad \text{Equation 19-10}$$

$$N_{p, cds, n, sv, pdo} = C_{cds, ac, sv, pdo} \times N_{spf, cds, n, sv, pdo} \times \left(CMF_{1, cds, ac, sv, pdo} \times \dots \times CMF_{m, cds, ac, sv, pdo} \right) \times \left(CMF_{1, cds, ac, at, pdo} \times \dots \times CMF_{m, cds, ac, at, pdo} \right) \quad \text{Equation 19-11}$$

Where:

$N_{p, cds, n, y, z}$ = predicted average crash frequency of a C-D road segment with n lanes, crash type y ($y = sv$: single vehicle, mv : multiple vehicle, at : all types), and severity z ($z = fi$: fatal and injury, pdo : property damage only, as : all severities) (crashes/yr);

$N_{spf, cds, n, y, z}$ = predicted average crash frequency of a C-D road segment with base conditions, n lanes, crash type y ($y = sv$: single vehicle, mv : multiple vehicle, at : all types), and severity z ($z = fi$: fatal and injury, pdo : property damage only) (crashes/yr);

$CMF_{m, cds, ac, y, z}$ = crash modification factor for a C-D road segment with any cross section ac , features m , crash type y ($y = sv$: single vehicle, mv : multiple vehicle, at : all types), and severity z ($z = fi$: fatal and injury, pdo : property damage only); and

$C_{cds, ac, y, z}$ = calibration factor for C-D road segments with any cross section ac , crash type y ($y = sv$: single vehicle, mv : multiple vehicle, at : all types), and severity z ($z = fi$: fatal and injury, pdo : property damage only).

The interpretation of these equations is similar to that described previously for ramp entrance segments.

The SPFs for ramp and C-D road segments are presented in Section 19.6.1. The associated CMFs are presented in Section 19.7.1. Similarly, the associated SDFs are presented in Section 19.8.1. A procedure for establishing the value of the calibration factor is described in Section B.1 of Appendix B to Part C.

19.3.3. Predictive Model for Ramp Terminals

The predictive model for crossroad ramp terminals is used to compute the predicted average crash frequency for a crossroad ramp terminal. Terminal-related crashes include (a) all crashes that occur within the limits of the intersection (i.e., at-intersection crashes) and (b) crashes that occur on the ramp or crossroad legs and are attributed to the presence of an intersection (i.e., intersection-related crashes).

The predictive model for one-way stop-controlled crossroad ramp terminals is presented in Equation 19-12 to Equation 19-14.

$$N_{p,w,ST,at,as} = N_{p,w,ST,at,fi} + N_{p,w,ST,at,pdo} \quad \text{Equation 19-12}$$

$$N_{p,w,ST,at,fi} = C_{aS,ST,at,fi} \times N_{spf,w,ST,at,fi} \times (CMF_{1,aS,ST,at,fi} \times \dots \times CMF_{m,aS,ST,at,fi}) \quad \text{Equation 19-13}$$

$$N_{p,w,ST,at,pdo} = C_{aS,ST,at,pdo} \times N_{spf,w,ST,at,pdo} \times (CMF_{1,aS,ST,at,pdo} \times \dots \times CMF_{m,aS,ST,at,pdo}) \quad \text{Equation 19-14}$$

Where:

$N_{p,w,ST,at,z}$ = predicted average crash frequency of a stop-controlled crossroad ramp terminal of site type w ($w = D3ex, D3en, D4, A4, B4, A2, B2$), all crash types at , and severity z ($z = fi$: fatal and injury, pdo : property damage only, as : all severities) (crashes/yr);

$N_{spf,w,ST,at,z}$ = predicted average crash frequency of a one-way stop-controlled crossroad ramp terminal of site type w ($w = D3ex, D3en, D4, A4, B4, A2, B2$) with base conditions, all crash types at , and severity z ($z = fi$: fatal and injury, pdo : property damage only) (crashes/yr);

$CMF_{m,aS,ST,at,z}$ = crash modification factor for a stop-controlled crossroad ramp terminal (any site type aS) with features m , all crash types at , and severity z ($z = fi$: fatal and injury, pdo : property damage only); and

$C_{aS,ST,at,z}$ = calibration factor for a stop-controlled crossroad ramp terminal (any site type aS) with all crash types at and severity z ($z = fi$: fatal and injury, pdo : property damage only).

The seven site types (i.e., $D3ex, D3en, D4, A4, B4, A2, B2$) are shown in Figure 19-1.

Equation 19-12 shows that crossroad ramp terminal crash frequency is estimated as the sum of two components: predicted average fatal-and-injury crash frequency and predicted average property-damage-only crash frequency.

Different CMFs are used in Equation 19-13 and Equation 19-14. The term in parentheses in each equation recognizes that the influence of some geometric features is unique to type of control used at the terminal. All CMFs are unique to crash severity.

The predictive model for signal-controlled crossroad ramp terminals is presented in Equation 19-15 to Equation 19-17.

$$N_{p,w,SGn,at,as} = N_{p,w,SGn,at,fi} + N_{p,w,SGn,at,pdo} \quad \text{Equation 19-15}$$

$$N_{p,w,SGn,at,fi} = C_{aS,SG,at,fi} \times N_{spf,w,SGn,at,fi} \times (CMF_{1,aS,SGn,at,fi} \times \dots \times CMF_{m,aS,SGn,at,fi}) \quad \text{Equation 19-16}$$

$$N_{p,w,SGn,at,pdo} = C_{aS,SG,at,pdo} \times N_{spf,w,SGn,at,pdo} \times (CMF_{1,aS,SGn,at,pdo} \times \dots \times CMF_{m,aS,SGn,at,pdo}) \quad \text{Equation 19-17}$$

Where:

$N_{p,w,SGn,at,z}$ = predicted average crash frequency of a signal-controlled crossroad ramp terminal of site type w ($w = D3ex, D3en, D4, A4, B4, A2, B2$) with n crossroad lanes, all crash types at , and severity z ($z = fi$: fatal and injury, pdo : property damage only, as : all severities) (crashes/yr);

$N_{spf,w,SGn,at,z}$ = predicted average crash frequency of a signal-controlled crossroad ramp terminal of site type w ($w = D3ex, D3en, D4, A4, B4, A2, B2$) with base conditions, n crossroad lanes, all crash types at , and severity z ($z = fi$: fatal and injury, pdo : property damage only) (crashes/yr);

$CMF_{m,aS,SGn,at,z}$ = crash modification factor for a signal-controlled crossroad ramp terminal (any site type aS) on a crossroad with n lanes, features m , all crash types at , and severity z ($z = fi$: fatal and injury, pdo : property damage only); and

$C_{aS,SG,at,z}$ = calibration factor for a signal-controlled crossroad ramp terminal (any site type aS) with all crash types at and severity z ($z = fi$: fatal and injury, pdo : property damage only).

The SPFs for crossroad ramp terminals are presented in Section 19.6.2. The associated CMFs are presented in Section 19.7.2. Similarly, the associated SDFs are presented in Section 19.8.2. A procedure for establishing the value of the calibration factor is described in Section B.1 of Appendix B to Part C.

19.4. PREDICTIVE METHOD FOR RAMPS AND RAMP TERMINALS

This section describes the predictive method for ramps, C-D roads, and ramp terminals. It consists of two sections. The first section provides a step-by-step description of the predictive method. The second section describes the geometric design features, traffic control features, and traffic volume data needed to apply the predictive method.

19.4.1. Step-by-Step Description of the Predictive Method

The predictive method for ramps is shown in Figure 19-2. Applying the predictive method yields an estimate of the expected average crash frequency (in total, or by crash type or severity) for an entire ramp or C-D road. The predictive models described in this chapter are applied in Steps 9, 10, and 11 of the predictive method. The information needed to apply each step is provided in this section.

There are 18 steps in the predictive method. In some situations certain steps will not be needed because data are not available or the step is not applicable to the situation at hand. In other situations, steps may be repeated if an estimate is desired for several sites or for a period of several years. In addition, the predictive method can be repeated as necessary to undertake crash estimation for each alternative design, traffic volume scenario, or proposed treatment option (within the same time period to allow for comparison).

The following discussion explains the details of each step of the method as applied to ramps.

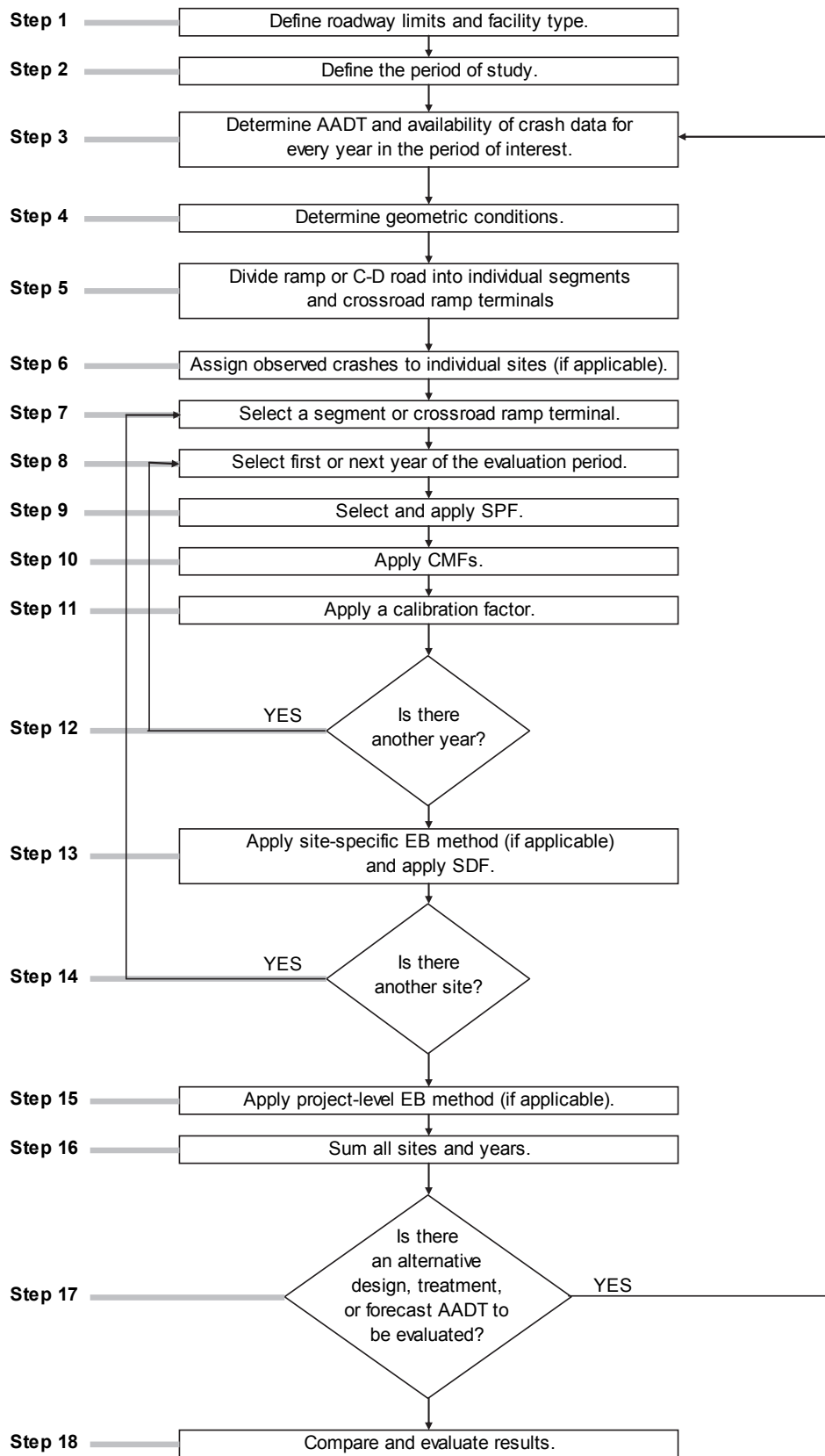


Figure 19-2. The HSM Predictive Method

Step 1—Define the limits of the project.

A project can be all of the ramps and C-D roads in the vicinity of an interchange, an entire ramp, an entire C-D road, or an individual site. A site is a crossroad ramp terminal, a homogeneous ramp segment, or a homogeneous C-D road segment. A site is further categorized by its cross section or control type. A description of the specific site types is provided in Section 19.3.

The project limits are defined in this step. They will depend on the purpose of the study. The study may be limited to one specific site, or to a group of contiguous sites. Alternatively, the limits can be expanded to include all of the ramps, C-D roads, and crossroad ramp terminals in the vicinity of an interchange. For comparative analysis of design alternatives, the project limits should be the same for all alternatives.

The analyst should identify (or establish) the reference line for each ramp and C-D road. This line is defined as the right edge of traveled way in the direction of travel. All lengths along the roadway are determined using this line.

Step 2—Define the period of interest.

The *study period* is defined as the consecutive years for which an estimate of the expected average crash frequency is desired. The *crash period* is defined as the consecutive years for which observed crash data are available. The *evaluation period* is defined as the combined set of years represented by the study period and crash period. Every year in the evaluation period is evaluated using the predictive method. All periods are measured in years.

If the EB Method is not used, then the study period is the same as the evaluation period. The EB Method is discussed in more detail in Step 3.

If the EB Method is used and the crash period is not fully included in the study period, then the predictive models need to be applied to the study years *plus* each year of the crash period not represented in the study period. In this situation, the evaluation period includes the study period and any additional years represented by the crash data but not in the study period. For example, let the study period be defined as the years 2010, 2011, and 2012. If crash data are available for 2008, 2009, and 2010, then the evaluation period is 2008, 2009, 2010, 2011, and 2012.

The study period can represent either a past time period or a future time period. Whether the predictive method is used for a past or future period depends upon the purpose of the study. The study period may be:

- A past period for:
 - An existing ramp or C-D road. If observed crash data are available, the study period is the period of time for which the observed crash data are available and for which (during that period) the site geometric design features, traffic control features, and traffic volumes are known.
 - An existing ramp or C-D road for which alternative geometric design or traffic control features are proposed (for near-term conditions) and site traffic volumes are known.
- A future period for:
 - An existing ramp or C-D road for a future period where forecast traffic volumes are available.
 - An existing ramp or C-D road for which alternative geometric design or traffic control features are proposed and forecast traffic volumes are available.

- A new ramp or C-D road that does not currently exist but is proposed for construction and for which forecast traffic volumes are available.

Step 3—For the study period, determine the availability of AADT volumes and, for an existing project, the availability of observed crash data (to determine whether the EB Method is applicable).

Traffic volume data are acquired in this step. Also, a decision is made whether the EB Method will be applied. If it will be applied, then it must also be decided whether the site-specific or project-level EB Method will be applied. If the EB Method will be applied, then the observed crash data are also acquired in this step.

Determining Traffic Volumes

The SPFs used in Step 9 (and some CMFs in Step 10) include annual average daily traffic (AADT) volume as a variable. For a past period, the AADT volume may be determined by using automated recorder data, or estimated by a sample survey. For a future period, the AADT volume may be a forecast estimate based on appropriate land use planning and traffic volume forecasting models.

The AADT volume of the ramp is needed for the evaluation of one or more ramp segments. The AADT volume of the C-D road is needed for the evaluation of one or more C-D road segments.

For each crossroad ramp terminal, one AADT value is needed for each intersecting leg. Thus, for a four-leg ramp terminal, the following values are needed: AADT volume of the crossroad leg “inside” the interchange, AADT volume of the crossroad leg “outside” of the interchange, AADT volume of the exit ramp, and AADT volume of the entrance ramp. The inside crossroad leg is the leg that is on the side of the ramp terminal nearest to the freeway. The outside crossroad leg is on the other side of the ramp terminal.

The AADT volumes are needed for each year of the evaluation period. The AADT volume for a given year represents an annual average daily 24-hour traffic volume. The ramp and C-D road segment AADT volume is a one-way volume. The crossroad segment AADT volume is a two-way volume (i.e., total of both travel directions).

In many cases, it is expected that AADT data will not be available for all years of the evaluation period. In that case, an estimate of AADT volume for each year is interpolated or extrapolated, as appropriate. If there is not an established procedure for doing this, the following rules may be applied within the predictive method to estimate the AADT volumes for years in which no data are available.

- If AADT volume is available for only a single year, that same volume is assumed to apply to all years of the evaluation period.
- If two or more years of AADT data are available, the AADT volumes for intervening years are computed by interpolation.
- The AADT volumes for years before the first year for which data are available are assumed to be equal to the AADT volume for that first year.
- The AADT volumes for years after the last year for which data are available are assumed to be equal to the AADT volume for that last year.

Determining Availability of Observed Crash Data

Where an existing site (or alternative conditions for an existing site) is being considered, the EB Method can be used to obtain a more reliable estimate of the expected average crash frequency. The EB Method is

applicable when crash data are available for the entire project, or for its individual sites. Crash data may be obtained directly from the jurisdiction's crash report system. At least two years of crash data are desirable to apply the EB Method. The EB Method (and criteria to determine whether the EB Method is applicable) is presented in Section B.2 in Appendix B to Part C.

The EB Method can be applied at the site-specific level or at the project level. At the site-specific level, crash data are assigned to specific sites in Step 6. The site-specific EB Method is applied in Step 13. At the project level, crash data are assigned to a group of sites (typically because they cannot be assigned to individual sites). The project-level EB Method is applied in Step 15. In general, the best results will be obtained if the site-specific EB Method is used. Guidance to determine whether the site-specific or project-level EB Method is applicable is presented in Section B.2.2 in Appendix B to Part C.

Step 4—Determine geometric design features, traffic control features, and site characteristics for all sites in the project limits.

A range of data is needed to apply a predictive model. These data are used in the SPFs and CMFs to estimate the predicted average crash frequency for the selected site and year. These data represent the geometric design features, traffic control features, and traffic demand characteristics that have been found to have some relationship to safety. These data are needed for each site in the project limits. They are needed for the study period and, if applicable, the crash period. The specific data, and means by which they are measured or obtained, is described in Section 19.4.2.

Step 5—Divide the roadway into sites.

Using the information from Step 1 and Step 4, the ramp or C-D road is divided into individual sites, consisting of individual homogeneous segments and ramp terminals. The procedure for dividing the ramp or C-D road into individual segments is provided in Section 19.5.

Step 6—Assign observed crashes to the individual sites (if applicable).

Step 6 applies if it was determined in Step 3 that the site-specific EB Method is applicable. If the site-specific EB Method is not applicable, then proceed to Step 7. In this step, the observed crash data are assigned to the individual sites using the criteria outlined in the next paragraph. Specific criteria for assigning crashes to individual sites are presented in Section B.2.3 in Appendix B to Part C.

Step 7—Select the first or next individual site in the project limits. If there are no more sites to be evaluated, proceed to Step 15.

Steps 7 through 14 are repeated for each site within the project limits identified in Step 1.

Any site can be selected for evaluation because each site is considered to be independent of the other sites. However, good practice is to select the sites in an orderly manner, such as in the order of their physical occurrence in the direction of increasing milepost.

Step 8—For the selected site, select the first or next year in the period of interest. If there are no more years to be evaluated for that site, proceed to Step 13.

Steps 8 through 12 are repeated for each year in the evaluation period for the selected site.

The individual years of the evaluation period are analyzed one year at a time because the SPFs and some CMFs are dependent on AADT volume, which may change from year to year.

Step 9—For the selected site, determine and apply the appropriate SPF.

The SPF determines the predicted average crash frequency for a site whose features match the SPF's base conditions. The SPFs (and their base conditions) are described in Section 19.6.

Determine the appropriate SPF for the selected site based on its site type and cross section (or traffic control). This SPF is then used to compute the crash frequency for the selected year using the AADT volume for that year, as determined in Step 3.

Step 10—Multiply the result obtained in Step 9 by the appropriate CMFs.

Collectively, the CMFs are used in the predictive model to adjust the SPF estimate from Step 9 such that the resulting predicted average crash frequency accurately reflects the geometric design and traffic control features of the selected site. The available CMFs are described in Section 19.7.

All CMFs presented in this chapter have the same base conditions as the SPFs in this chapter. Only the CMFs presented in Section 19.7 may be used as part of the predictive method described in this chapter.

For the selected site, determine the appropriate CMFs for the site type, geometric design features, and traffic control features present. The CMF's designation by crash type and severity must match that of the SPF with which it is used (unless indicated otherwise in the CMF description). The CMFs for the selected site are calculated using (a) the AADT volume determined in Step 3 for the selected year and (b) the geometric design and traffic control features determined in Step 4.

Multiply the result from Step 9 by the appropriate CMFs.

Step 11—Multiply the result obtained in Step 10 by the appropriate calibration factor.

The SPFs and CMFs in this chapter have each been developed with data from specific jurisdictions and time periods. Calibration to local conditions will account for any differences between these conditions and those present at the selected sites. A calibration factor is applied to each SPF in the predictive method. Detailed guidance for the development of calibration factors is included in Section B.1 of Appendix B to Part C.

Multiply the result from Step 10 by the calibration factor to obtain the predicted average crash frequency.

Step 12—If there is another year to be evaluated in the evaluation period for the selected site, return to Step 8. Otherwise, proceed to Step 13.

This step creates a loop from Step 8 through Step 12 that is repeated for each year of the evaluation period for the selected site.

Step 13—Apply site-specific EB Method (if applicable) and apply SDFs.

The site-specific EB Method combines the predicted average crash frequency computed in Step 11 with the observed crash frequency of the selected site. It produces a more statistically reliable estimate of the site's expected average crash frequency. The procedure for applying the site-specific EB Method is provided in Section B.2.4 of Appendix B to Part C.

The decision to apply the site-specific EB Method was determined in Step 3. If the EB Method is not used, then the expected average crash frequency for each year of the study period is limited to the predicted average crash frequency for that year, as computed in Step 11.

If the EB Method is used, then the expected average crash frequency is equal to the estimate obtained from the EB Method. An estimate is obtained for each year of the crash period (i.e., the period for which the observed crash data are available). The individual years of the crash period are analyzed one year at a time because the SPFs and some CMFs are dependent on AADT volume, which may change from year to year.

Apply the site-specific EB Method to a future time period, if appropriate.

Section B.2.6 in Appendix B to Part C provides a procedure for converting the estimates from the EB Method to any years in the study period that are not represented in the crash period (e.g., future years). This

approach gives consideration to any differences in traffic volume, geometry, or traffic control between the study period and the crash period. This procedure yields the expected average crash frequency for each year of the study period.

Apply the severity distribution functions (SDFs), if desired.

The SDFs can be used to compute the expected average crash frequency for each of the following severity levels: fatal, incapacitating injury, non-incapacitating injury, and possible injury. Each SDF includes variables that describe the geometric design and traffic control features of a site. In this manner, the computed distribution gives consideration to the features present at the selected site. The SDFs are described in Section 19.8. They can benefit from being updated based on local data as part of the calibration process. Detailed guidance for the development of the SDF calibration factor is included in Section B.1.4 of Appendix B to Part C.

Apply the crash type distribution, if desired.

Each predictive model includes a default distribution of crash type. This distribution can be used to compute the expected average crash frequency for each of ten crash types (e.g., head-on, fixed object). The distribution is presented in Section 19.6. It can benefit from being updated based on local data as part of the calibration process.

Step 14—If there is another site to be evaluated, return to Step 7; otherwise, proceed to Step 15.

This step creates a loop from Step 7 through Step 14 that is repeated for each site of interest.

Step 15—Apply the project-level EB Method (if applicable) and apply SDFs.

The activities undertaken during this step are the same as undertaken for Step 13 but they occur at the project level (i.e., entire ramp, entire C-D road, or interchange). They are based on estimating the project-level predicted average crash frequency. This crash frequency is computed for each year during the crash period. It is computed as the sum of the predicted average crash frequency for all sites (as computed in Step 11).

The project-level EB Method combines the project-level predicted average crash frequency with the observed crash frequency for all sites within the project limits. It produces a more statistically reliable estimate of the project-level expected average crash frequency. The procedure for applying the project-level EB Method is provided in B.2.5 of Appendix B to Part C.

The decision to apply the project-level EB Method was determined in Step 3. If this method is not used, then the project-level expected average crash frequency for each year of the study period is limited to the project-level predicted average crash frequency for that year, as computed in Step 11.

If the EB Method is used, then the project-level expected average crash frequency is equal to the estimate obtained from the EB Method. An estimate is obtained for each year of the crash period (i.e., the period for which the observed crash data are available). The individual years of the crash period are analyzed one year at a time because the SPFs and some CMFs are dependent on AADT volume, which may change from year to year.

Apply the project-level EB Method to a future time period, if appropriate.

Follow the same guidance as provided in Step 13 using the estimate from the project-level EB Method.

Apply the severity distribution functions, if desired.

Follow the same guidance as provided in Step 13 using the estimate from the project-level EB Method.

Apply the crash type distribution, if desired.

Follow the same guidance as provided in Step 13 using the estimate from the project-level EB Method.

Step 16—Sum all sites and years in the study to estimate total crash frequency.

One outcome of the predictive method is the total expected average crash frequency. The term “total” indicates that the estimate includes all crash types and severities. It is computed from an estimate of the total expected number of crashes, which represents the sum of the total expected average crash frequency for each site and for each year in the study period. The total expected number of crashes during the study period is calculated using Equation 19-18:

$$N_{e, aS, ac, at, as}^* = \sum_{j=1}^{n_s} \left(\sum_{i=1}^{\text{all sites}} N_{e, rps(i), ac, at, as, j} + \sum_{i=1}^{\text{all sites}} N_{e, cds(i), ac, at, as, j} + \sum_{i=1}^{\text{all sites}} N_{e, w(i), ac, at, as, j} \right) \quad \text{Equation 19-18}$$

Where:

$N_{e, aS, ac, at, as}^*$ = total expected number of crashes for all sites aS and all years in the study period (includes all cross sections and control types ac , all crash types at , and all severities as) (crashes);

$N_{e, rps(i), ac, at, as, j}$ = expected average crash frequency of ramp segment i for year j (includes all cross sections ac , all crash types at , and all severities as) (crashes/yr);

$N_{e, cds(i), ac, at, as, j}$ = expected average crash frequency of C-D road segment i for year j (includes all cross sections ac , all crash types at , and all severities as) (crashes/yr);

$N_{e, w(i), ac, at, as, j}$ = expected average crash frequency of crossroad ramp terminal i of site type $w(i)$ ($w = D3ex, D3en, D4, A4, B4, A2, B2$) for year j (includes all control types ac , all crash types at , and all severities as) (crashes/yr); and

n_s = number of years in the study period (yr).

Equation 19-18 is used to compute the total expected number of crashes estimated to occur in the project limits during the study period. The summation of crashes for each terminal type, cross section, control type, crash type, and severity for each site and year is not shown in mathematic terms (but it is implied by the subscripts w , ac , at , and as , respectively).

Equation 19-19 is used to estimate the overall expected average crash frequency within the project limits during the study period.

$$N_{e, aS, ac, at, as} = \frac{N_{e, aS, ac, at, as}^*}{n_s} \quad \text{Equation 19-19}$$

Where:

$N_{e, aS, ac, at, as}$ = overall expected average crash frequency for all sites aS and all years in the study period (includes all cross sections and control types ac , all crash types at , and all severities as) (crashes/yr).

Step 17—Determine if there is an alternative design, treatment, or forecast AADT to be evaluated.

Steps 3 through 17 are repeated as appropriate for the same project limits but for alternative conditions, treatments, periods of interest, or forecast AADT volumes.

Step 18—Evaluate and compare results.

The predictive method is used to provide a statistically reliable estimate of the expected average crash frequency (in total, or by crash type and severity) for the specified project limits, study period, geometric design and traffic control features, and known or estimated AADT volume.

19.4.2. Data Needed to Apply the Predictive Method

The input data needed for the predictive models are identified in this section. These data represent the geometric design features, traffic control features, and traffic demand characteristics that have been found to have some relationship to safety. The data are needed for each site in the project limits. Criteria for defining site boundaries are described in Section 19.5.

The data are described in two subsections. The first subsection describes input data for ramp and C-D road segments. The second subsection describes input data for crossroad ramp terminals.

Features of Ramp and C-D Road Segments

The input data needed for ramp and C-D road segments is described in this subsection. There are several data identified in this section that describe a length along the roadway (e.g., segment length, curve length, weaving section length, etc.). *All of these lengths are measured along the reference line*, which is the right edge of traveled way in the direction of travel. Points that do not lie on the reference line must be projected onto the reference line (along a perpendicular line if the alignment is straight, or along a radial line if the alignment is curved) to facilitate length determination.

- Number of through lanes. The total number of through lanes in the segment. Rural ramp segments are limited to one lane. Urban ramp segments are limited to two lanes. A segment with a lane-add (or lane-drop) taper is considered to have the same number of through lanes as the roadway just downstream of the lane-add (or lane-drop) taper. If the segment ends at a ramp terminal, then the number of through lanes is not based on the lane assignment, or lane markings, at the terminal.
 - Do not include any high-occupancy vehicle (HOV) bypass lanes (see Section 19.11).
 - Do not include any auxiliary lanes that are associated with a C-D road weaving section, unless the weaving section length exceeds 0.30 mi (1,600 ft). If this length is exceeded, then the auxiliary lane is counted as a through lane that starts as a lane-add ramp entrance and ends as a lane-drop ramp exit.
 - Do not include any auxiliary lanes that are developed as a turn bay (for queued vehicle storage) at the crossroad ramp terminal.
 - Do not include the speed-change lane that is associated with a second ramp that merges with (or diverges from) the subject ramp, unless its length exceeds 0.19 mi (1,000 ft). If this length is exceeded, then the speed-change lane is counted as a through lane that starts as a lane-add ramp entrance and ends as a lane drop by taper (or starts as a lane add by taper and ends as a lane-drop ramp exit).

This guidance is illustrated in Figure 19-3 using a portion of an exit ramp. The portion is shown to end at the crossroad ramp terminal. It consists of three segments. The first segment ends at the lane add section and has one lane. The second segment ends at the start of the bay taper and has two lanes. The third segment ends at the crossroad. Four lanes are shown at the downstream end of this segment, but two of the lanes are in turn bays and are not included in the determination of the number of through lanes for the segment. Thus, this segment is considered to have two lanes ($= 4 - 2$) for this application.

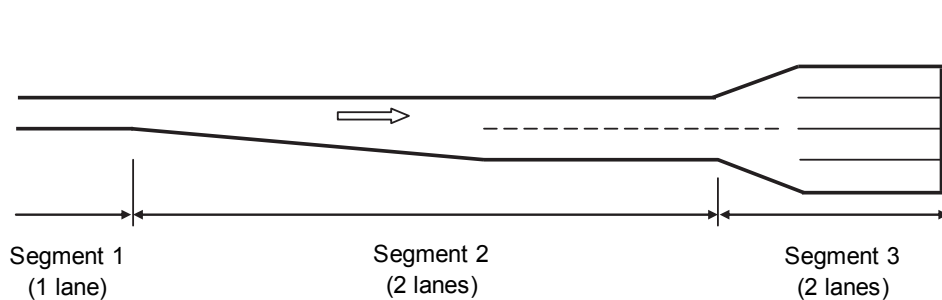


Figure 19-3. Number-of-Lanes Determination for Ramp Segments

- Length of ramp or C-D road segment.
- Average traffic speed on the freeway during off-peak periods of the typical day. This speed is used to compute the speed for each curve (if any) that is present on the ramp. If better information is not available, then this speed can be estimated as the freeway’s maximum speed limit.
- Type of traffic control used at the crossroad ramp terminal to regulate intersecting traffic (none, yield, stop, signal). The term “None” is appropriate if the ramp intersects the crossroad as a speed-change lane or as a lane added (or lane dropped).
- Presence of a horizontal curve prior to (or in) the subject segment. Curves located prior to the segment influence the speed on the subject segment. For each curve located prior to (or in) the segment, the following data are needed:
 - Length of curve.
 - Curve length is measured along the reference line from the point where the tangent ends and the curve begins (i.e., the PC) to the point where the curve ends and the tangent begins (PT).
 - If the curve has spiral transitions, then measure from the “effective” PC point to the “effective” PT point. The effective PC point is located midway between the TS and SC mileposts, where the TS is the point of change from tangent to spiral and the SC is the point of change from spiral to circular curve. The effective PT is located midway between the CS and ST.
 - If the curve is continued from a curve on an intersecting alignment, then consider only the curve length on the subject alignment. For example, if the subject ramp diverges from another ramp and the curvature from the originating ramp continues into the subject ramp, then the curve on the subject ramp is considered to start at the beginning of the subject ramp (i.e., at the gore point).
 - Radius of curve. The radius is defined by the right edge of traveled way. If the curve has spiral transitions, then use the radius of the central circular portion of the curve.
 - Length of curve in segment. The length of the curve within the boundaries of the segment. This length cannot exceed the segment length or the curve length.
 - Milepost of beginning of curve in direction of travel. Measure to the point where the tangent ends and the curve begins. Milepost locations are measured along the right edge of the ramp through lane in the direction of travel (in the absence of tapers and speed-change lanes, this edge coincides with the right edge of traveled way). These mileposts are established for this application, and may or may not coincide with the mileposts (or stations) established for the ramp’s design.

- If the curve is preceded by a spiral transition, then measure to the “effective” curve beginning point. This point is located midway between the TS and SC mileposts, where the TS is the point of change from tangent to spiral and the SC is the point of change from spiral to circular curve.
- For exit ramps, C-D roads, and entrance ramps that diverge from the crossroad using a speed-change lane, milepost 0.0 is referenced to the gore point. The gore point is defined as the point in the gore area where the distance between the near edge of the freeway (or crossroad) traveled way and the ramp traveled way is 2.0 ft. This point is shown in Figure 19-4.
- For entrance ramps that intersect the crossroad, milepost 0.0 is located at the point where the ramp reference line intersects with the near edge of traveled way of the crossroad. The ramp reference line is defined as the right edge of the ramp traveled way. This point is shown in Figure 19-4.
- If there is a choice of two or more points at which milepost 0.0 could be established for a ramp and it is not clearly established by the guidance in the two previous bullets, then choose the one point that is associated with the highest entering ramp volume.

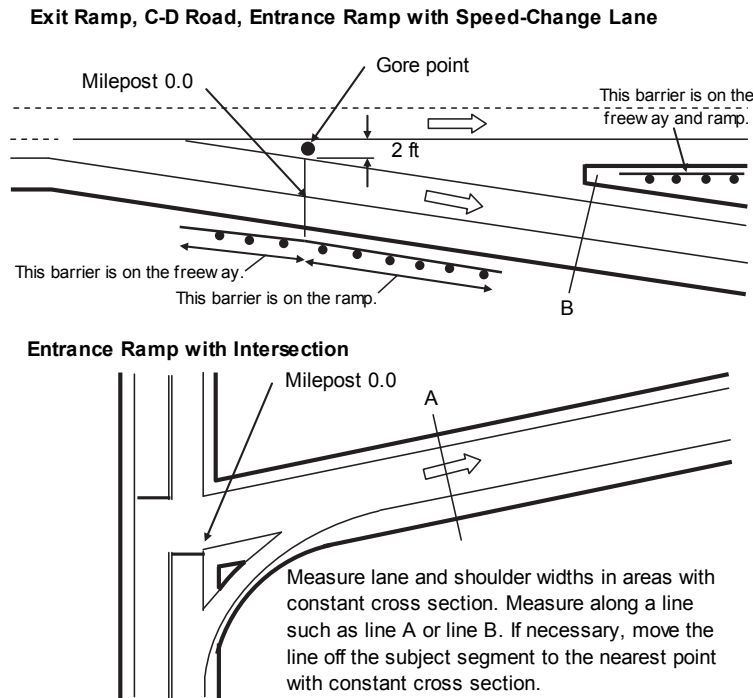


Figure 19-4. Starting Milepost Location on Ramps and C-D Roads

- Widths of lanes, right shoulder, and left shoulder. These elements represent an average for the segment. These widths should be measured where the cross section is constant, such as along line A or line B shown in Figure 19-4. They should not be measured where one or more edges are discontinuous or tapered. If a width varies along the segment (but not enough to justify beginning a new segment), then compute the length-weighted average width. Rules for defining segment boundaries are provided in Section 19.5.2.
- Lane width is an average for all through lanes (as defined at the start of this section).
- Shoulder width represents the paved width.

- Length of (and offset to) the right-side barrier and the left-side barrier. Measured separately for each short piece of barrier and for barrier that continues for the length of the segment (and beyond). Each piece is represented once for a site. Barrier length is measured along the reference line. Offset is measured to the near edge of traveled way.
- Figure 19-5 illustrates these measurements for a barrier element protecting a sign support on the right side of a ramp with right shoulder width W_{rs} . The barrier element has a portion of its length that is parallel to the ramp and a portion of its length that is tapered away from the ramp. To evaluate this element, separate it into two pieces, as shown in Figure 19-5. Each piece is represented by its average offset $W_{off,r,i}$ and length $L_{rb,i}$. Barrier pieces with the same offset can be combined by adding their length and using their common offset.
- A barrier is associated with a ramp if its offset from the near edge of traveled way is 30 ft or less. Barrier adjacent to the freeway but also within 30 ft of the ramp traveled way should also be associated with the ramp. The determination of whether a barrier is adjacent to a freeway speed-change lane or a ramp is based on the gore point, as shown in Figure 19-4.

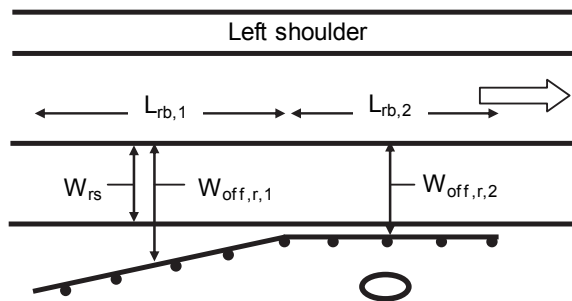


Figure 19-5. Barrier Variables

- Presence of an entrance speed-change lane (due to a second merging ramp). If a speed-change lane is present, then the length of the speed-change lane *in the segment* is needed. Guidance for measuring this length is provided in the following list.
 - Speed-change lane length in the segment is measured between the segment's begin and end points. It cannot exceed the length of the segment, regardless of the length of the speed-change lane. It cannot exceed the length of the speed-change lane.
 - Speed-change lane length is measured along the edge of the subject ramp traveled way from the gore point to the taper point. The gore point is located where the pair of solid white pavement edge markings that separate the subject ramp from the intersecting ramp are 2.0 ft apart. It is shown in Figure 19-6.
 - If the markings do not extend to a point where they are 2.0 ft apart, then the gore point is found by extrapolating both markings until the extrapolated portion is 2.0 ft apart.
 - The taper point is located where the outside edge marking of the intersecting ramp intersects the subject ramp's outside edge marking. It marks the point where the taper ends (or begins). It is shown in Figure 19-6.

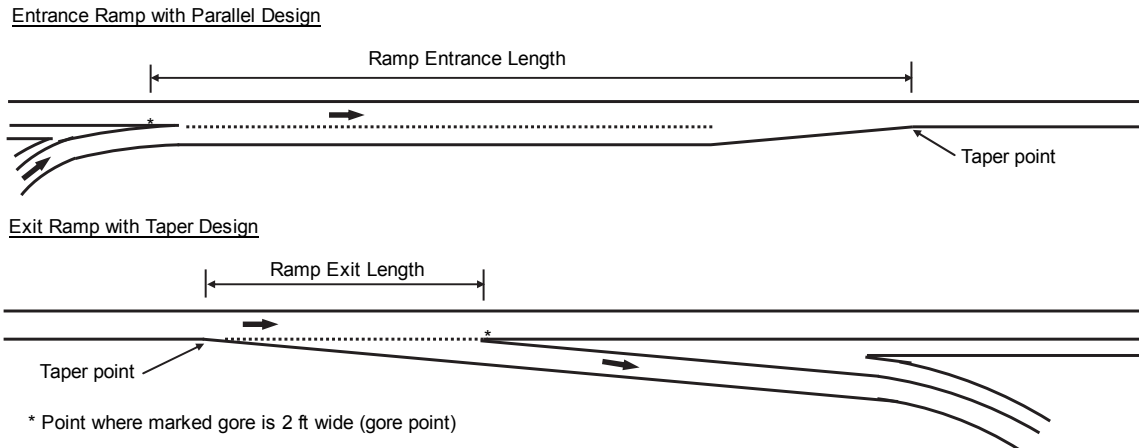
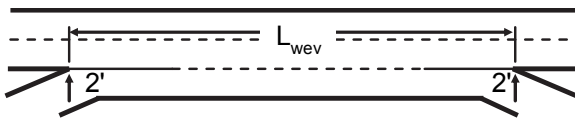


Figure 19-6. Speed-Change Lane Location on Ramps and C-D Roads

- Presence of an exit speed-change lane (due to a second diverging ramp). If a speed-change lane is present, then the length of the speed-change lane *in the segment* is needed. Guidance for measuring this length is the same as for entrance speed-change lanes.
- Lane added to the ramp or C-D road (not as a result of a second merging ramp). If a lane is added, then the length of the taper *in the segment* is needed. Guidance for measuring this length is provided in the following list:
 - This length is measured between the segment's begin and end points. This length cannot exceed the length of the segment. This length cannot exceed the taper length.
 - Taper length is measured along the edge of the ramp traveled way from the point where the traveled way width first begins changing to the point where this width first stops changing. Traveled way width is measured between the solid white pavement edge lines.
- Lane dropped from the ramp or C-D road (not as a result of a second diverging ramp). If a lane is dropped, then the length of the taper *in the segment* is needed. Guidance for measuring this length is the same as for the lane add case.
- Presence of a weaving section on a C-D road segment. If the segment is partially or wholly within a weaving section then the following data are needed:
 - Weaving section length. This length is measured along the edge of the C-D road traveled way from the gore point of the ramp entrance to the gore point of the next ramp exit, as shown in Figure 19-7. The gore point is located where the pair of solid white pavement edge markings that separate the ramp from the C-D road are 2.0 ft apart. If the markings do not extend to a point where they are 2.0 ft apart, then the gore point is found by extrapolating both markings until the extrapolated portion is 2.0 ft apart. If the measured gore-to-gore distance exceeds 0.30 mi (1,600 ft), then a weaving section is not considered to exist. Rather, the entrance ramp is a "lane add" and the exit ramp is a "lane drop."
 - Length of weaving section located *in the segment*, between the segment's begin and end points. This length cannot exceed the length of the segment. This length cannot exceed the length of the weaving section.
- Segment AADT volume.

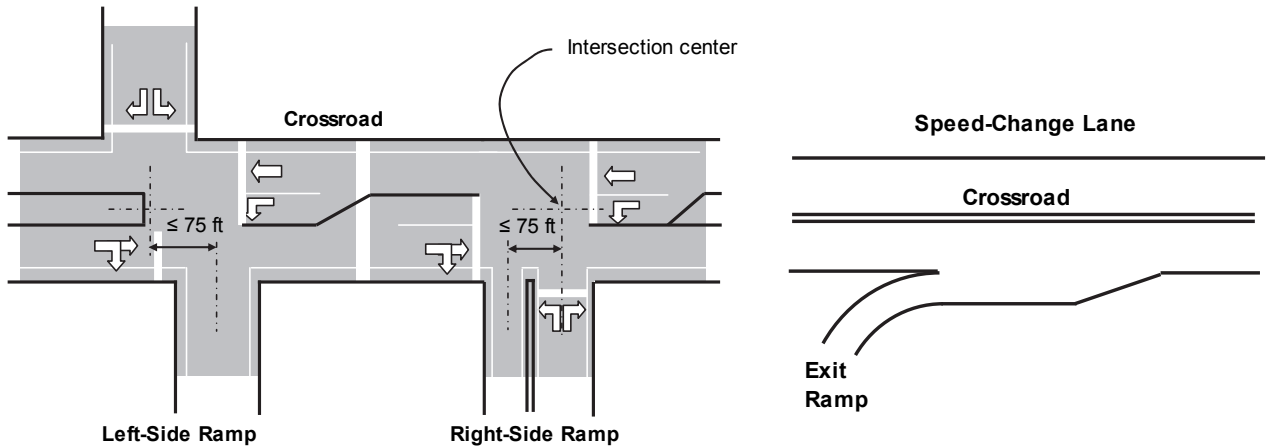


L_{wev} = weaving section length

Figure 19-7. C-D Road Weaving Section Length

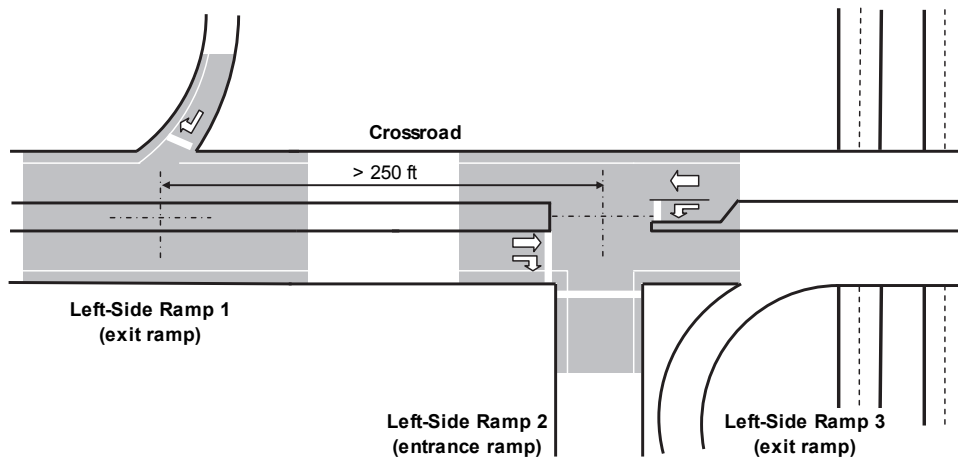
Features of Crossroad Ramp Terminals

The input data that describe a crossroad ramp terminal are described in this subsection. The phrase “crossroad ramp terminal” refers to a controlled terminal between the ramp and crossroad. This type of terminal is addressed by the predictive method. A terminal where the ramp merges with (or diverges from) the crossroad as a speed-change lane is not addressed by the predictive method. Figure 19-8a and Figure 19-8b illustrate these two terminal types.



a. Four-Leg Intersection and Three-Leg Intersection

b. Speed-Change Lane



c. Two Three-Leg Intersections and a Speed-Change Lane

Figure 19-8. Illustrative Ramp Terminals

If the crossroad intersects two ramps that are relatively near one another, there may be some question as to whether the two ramps are part of one intersection or two separate intersections (for the purpose of applying the predictive method). The following guidance is offered to help with this decision; however, some engineering judgment may also be required.

If the centerlines of the two ramps are offset by 75 ft or less, and they are configured to function as one intersection, then both ramps are considered to be part of the same intersection. This point is illustrated in Figure 19-8a for the left-side ramp and the right-side ramp at an interchange. Two intersections are shown in this figure.

If the two ramps are offset by more than 250 ft, then each ramp terminal is considered to form a separate intersection. This point is illustrated in Figure 19-8c for the left-side ramps at a four-quadrant parclo B interchange. Two intersections are shown in this figure.

Occasionally, the ramp offset is between 75 and 250 ft. In this situation, engineering judgment is required to determine whether the two ramps function as one or two intersections. Factors considered in making this determination will include the intersection control, traffic volume level, traffic movements being served (see Figure 19-1), channelization, average queue length, and pavement markings. Higher volume conditions often dictate that the two ramps are controlled as one signalized intersection. Ramp offsets in this range are typically avoided for new designs.

A description of the following geometric design and traffic control features is needed to use the CMFs associated with the predictive model for crossroad ramp terminals:

- Ramp terminal configuration, as described in Figure 19-1.
- Ramp terminal control type (signal, one-way stop control, all-way stop control). The predictive models are calibrated to address signal control and one-way stop control, where the ramp is stop controlled. An interim predictive model is provided in Section 19.10 for all-way stop control.
- Presence of a non-ramp public street leg at the terminal (signal control). This situation occurs occasionally. When it does, the public street leg is opposite from one ramp, and the other ramp either does not exist or is located at some distance from the subject ramp terminal such that it is not part of the terminal. This information is needed only for signalized terminals.
- Exit ramp skew angle (one-way stop control). Skew angle equals 90 minus the intersection angle (in degrees). These angles are shown in Figure 19-9. The intersection angle is the acute angle between the crossroad centerline and a line along the center of an imaginary vehicle stopped at the end of the ramp (i.e., where it joins the crossroad). The vehicle is centered in the traveled way and behind the stop line. If vehicles can exit the ramp as left- or right-turn movements, then use a left-turning vehicle as the vehicle of reference. This information is needed only for terminals with one-way stop control. At a *B4* terminal configuration, the skew angle represents that for the diagonal exit ramp (not the loop exit ramp).

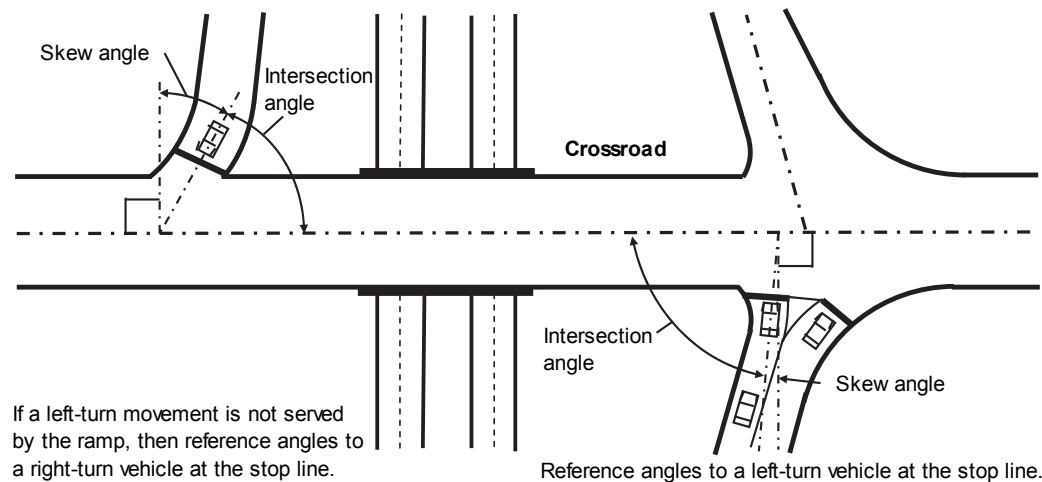


Figure 19-9. Exit Ramp Skew Angle

- Distance to the next public street intersection on the outside crossroad leg. This data element represents the distance between the subject ramp terminal and the nearest public street intersection located in a direction away from the freeway (measured along the crossroad from subject terminal center to intersection center).
- Distance to the adjacent ramp terminal. This data element represents the distance between the subject ramp terminal and the adjacent ramp terminal (measured along the crossroad from terminal center to terminal center). If there is no adjacent ramp terminal, then use the distance to the next public street intersection (located on the crossroad in the direction opposite to the intersection described in the previous bullet).
- Presence of protected left-turn operation (signal control). This information is needed for each crossroad left-turn movement that exists at the terminal. An affirmative response is indicated if the left-turn operates as protected only. If it operates as permissive or protected-permissive, then the response is negative. This information is needed only for signalized terminals.
- Exit ramp right-turn control type. This information is needed only for the exit ramp (at terminals with an exit ramp). It is focused on the right-turn movement, which may have a different control type than the left-turn movement. Control types considered include: free flow, merge, yield, stop, and signal (where free-flow and merge operation are recognized to represent “no control”). The free-flow type is associated with an accepting (or auxiliary) lane on the crossroad for the right-turn movement. The merge type is associated with a speed-change lane for the right-turn movement.
- Crossroad median width. This width is measured along a line perpendicular to the centerline of the crossroad in the vicinity of the intersection. If no median exists, then a width of 0.0 ft is used in the predictive model. If a raised curb is present, then the width is measured from face-of-curb to face-of-curb. If a raised curb is not present, then the width is measured between the near edge of traveled way for the two opposing travel directions. If a left-turn bay is present, then the median width includes the width of the left-turn bay. It is measured from the lane line delineating the bay to the face-of-curb adjacent to (or the near edge of traveled way for) the opposing travel direction. If the median width is different on the two crossroad legs, then use an average of the two widths.
- Number of through lanes on the inside crossroad approach. Number of lanes (shared or exclusive) serving through traffic on the crossroad approach that is nearest to the freeway (i.e., the inside approach). This variable includes only lanes that continue through the intersection. Count the lanes along the crosswalk (or the logical location of the crosswalk if it is not marked).

- Number of through lanes on the outside crossroad approach. Number of lanes (shared or exclusive) serving through traffic on the crossroad approach that is more distant from the freeway (i.e., the outside approach). This variable includes only lanes that continue through the intersection. Count the lanes along the crosswalk (or the logical location of the crosswalk if it is not marked).
- Number of lanes on the exit ramp leg at the terminal. Lanes can serve any movement (left, right, or through). If right-turn channelization is provided, then count the lanes at the last point where all exiting movements are joined (i.e., count at the channelization gore point). All lanes counted must be fully developed for 100 ft or more before they intersect the crossroad. If a lane's development length is less than 100 ft, then it is not counted as a lane for this application. The lane (or lanes) associated with the loop exit ramp at a *B4* terminal configuration are *not* included in this count.
- Presence of right-turn channelization on the inside crossroad approach (signal control). This channelization creates a turning roadway that serves right-turn vehicles. It is separated from the intersection by a triangular channelizing island (delineated by markings or raised curb). The gore point at the upstream end of the island must be within 200 ft of the downstream stop line for right-turn channelization to be considered "present." If this distance exceeds 200 ft, then the right-turn movement is served by a ramp roadway that is separate from the intersection (i.e., it should be evaluated as a ramp). The right-turn movement can be free-flow, stop, or yield controlled. This information is needed only for signalized terminals.
- Presence of right-turn channelization on the outside crossroad approach (signal control). The guidance provided in the previous bullet also applies to this variable. It is needed only for signalized terminals.
- Presence of right-turn channelization on the exit ramp approach (signal control). The guidance provided in the previous bullet also applies to this variable. It is needed only for signalized terminals. The presence of right-turn channelization on the loop exit ramp at a *B4* terminal configuration is *not* considered when determining this input data.
- Presence of a left-turn lane (or bay) on the inside crossroad approach. The lane (or bay) can have one or two lanes. A lane (or bay) is considered to be present when it (a) is for the exclusive use of a turn movement, (b) extends 100 ft or more back from the stop line, and (c) ends at the intersection stop line.
- Presence of a left-turn lane (or bay) on the outside crossroad approach. The guidance provided in the previous bullet also applies to this variable.
- Width of left-turn lane (or bay) on the inside crossroad approach. This variable represents the total width of all lanes that exclusively serve turning vehicles on the subject approach. It is measured from the near edge of traveled way of the adjacent through lane to the near lane marking (or curb face) that delineates the median.
- Width of left-turn lane (or bay) on the outside crossroad approach. The guidance provided in the previous bullet also applies to this variable.
- Presence of a right-turn lane (or bay) on the inside crossroad approach. The lane (or bay) can have one or two lanes. A lane (or bay) is considered to be present when it (a) is for the exclusive use of a turn movement, (b) extends 100 ft or more back from the stop line, and (c) satisfies one of the following rules.
 - If the bay or turn lane does not have island channelization at the intersection, then it must end at the intersection stop line.

- If the bay or turn lane has island channelization at the intersection, then the bay or turn lane must have (a) stop, yield, or signal control at its downstream end, and (b) an exit gore point that is within 200 ft of the intersection.
- Presence of a right-turn lane (or bay) on the outside crossroad approach. The guidance provided in the previous bullet also applies to this variable.
- Number of driveways on the outside crossroad leg (signal control). This number represents the count of unsignalized driveways on the outside crossroad leg and within 250 ft of the ramp terminal. The count is taken on both sides of the leg (i.e., it is a two-way total). The count should only include “active” driveways (i.e., those driveways with an average daily volume of 10 veh/day or more). This information is needed only for signalized terminals.
- Number of public street approaches on the outside crossroad leg. This number represents the count of unsignalized public street approaches on the outside crossroad leg and within 250 ft of the ramp terminal. The count is taken on both sides of the leg (i.e., it is a two-way total). If a public street approach is present at the terminal, then it is not counted for this entry. Rather, it is identified as being present using the “Presence of a non-ramp public street leg at the terminal” data that was discussed previously.
- AADT volume for the inside crossroad leg, AADT volume for the outside crossroad leg, AADT volume for each ramp leg. The inside crossroad leg is the leg that is on the side of the ramp terminal nearest to the freeway. The outside crossroad leg is on the other side of the ramp terminal.

19.5. RAMP SEGMENTS AND RAMP TERMINALS

This section consists of three subsections. The first subsection defines ramp segments, C-D road segments, and crossroad ramp terminals. The second subsection provides guidelines for segmenting the ramp or C-D road. The assignment of crashes to sites is discussed in the last subsection.

19.5.1. Definition of Ramp Segment and Ramp Terminal

When using the predictive method, the ramps and C-D roads within the defined project limits are divided into individual sites. A site is a homogeneous ramp segment, a homogeneous C-D road segment, or a crossroad ramp terminal.

Four ramps and one C-D road are shown in Figure 19-10. This figure represents one side of an interchange. Each ramp is shown to consist of one segment. The C-D road is divided into five segments. The ramp segments are labeled R_{en1} , R_{en2} , R_{ex3} , and R_{ex4} . The C-D road segments are labeled CD_1 to CD_5 . Two of the C-D road segments include a speed-change lane with a ramp. A third C-D road segment includes two speed-change lanes associated with the two loop ramps. The C-D road is not shown to have a weaving section; however, the predictive models can address C-D roads with or without a weaving section.

One crossroad ramp terminal is shown in Figure 19-10. It is labeled In , and is noted to have an influence area that extends 250 ft in each direction along the crossroad and ramps. The terminal has four legs—two crossroad legs and two ramp legs. Given the presence of the loop ramps, it is likely that this terminal serves only right-turn maneuvers to and from the crossroad.

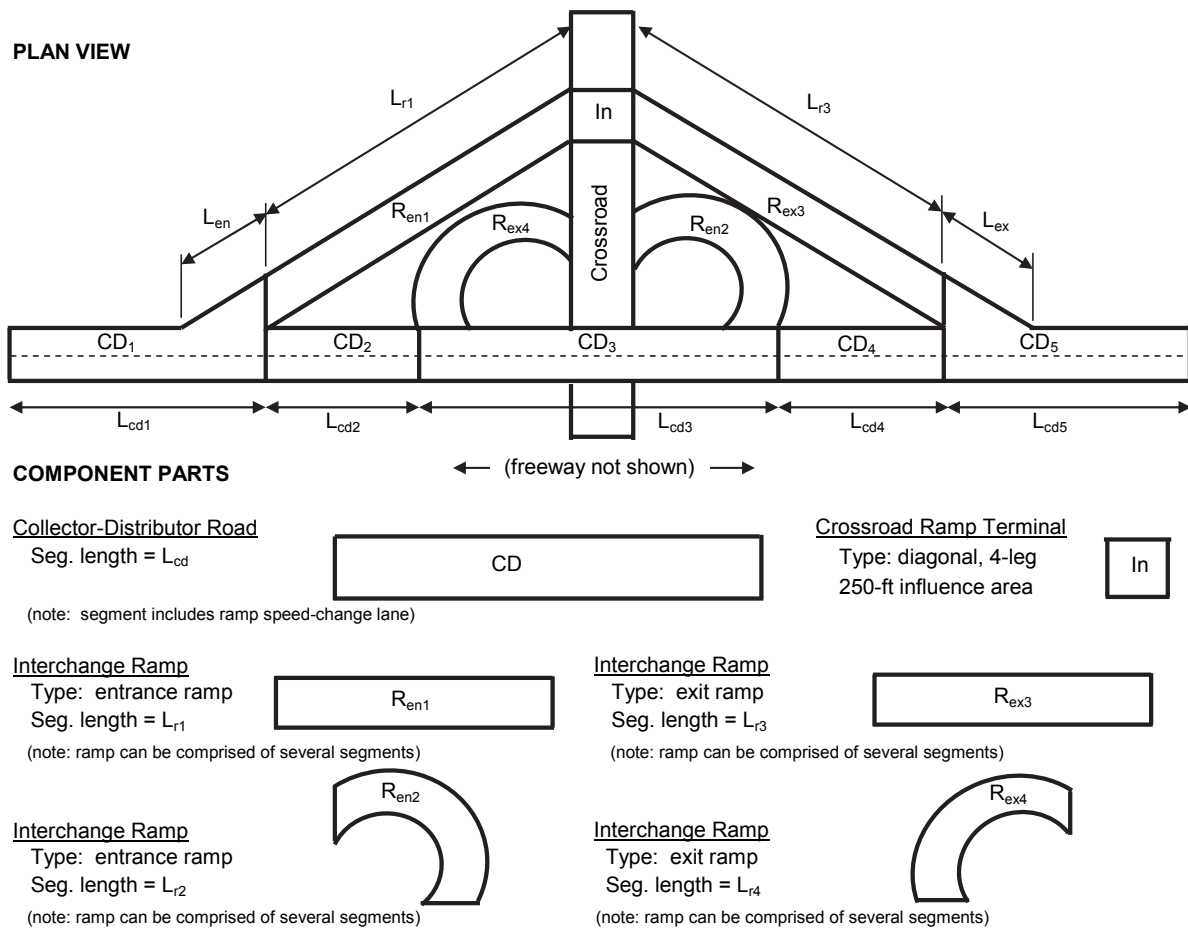


Figure 19-10. Illustrative Ramp Segments and Ramp Terminals

19.5.2 Segmentation Process

The segmentation process produces a set of segments of varying length, each of which is homogeneous with respect to characteristics such as traffic volumes, key geometric design features, and traffic control features. A new homogeneous ramp or C-D road segment begins where there is a change in at least one of the following characteristics of the roadway:

- Number of through lanes. Begin segment at the gore point if the lane is added or dropped at a ramp or C-D road. Begin segment at the upstream start of taper if the lane is added or dropped by taper.
- Lane width. Measure the lane width at successive points along the roadway. Compute an average lane width for each point and round this average to the nearest 0.5 ft. Begin a new segment if the rounded value for the current point changes from that of the previous point (e.g., from 12.5 to 13.0 ft).
- Right shoulder width. Measure the right shoulder width at successive points along the roadway. Round the measured shoulder width at each point to the nearest 1.0 ft. Begin a new segment if the rounded value for the current point changes from that of the previous point (e.g., from 4 to 5 ft).
- Left shoulder width. Measure the left shoulder width at successive points along the roadway. Round the measured shoulder width at each point to the nearest 1.0 ft. Begin a new segment if the rounded value for the current point changes from that of the previous point (e.g., from 4 to 3 ft).

- Merging ramp or C-D road presence. Begin segment at the gore point.
- Diverging ramp or C-D road presence. Begin segment at the gore point.

The presence of a horizontal curve does not necessarily define ramp or C-D road segment boundaries. Application of the “number of through lanes” criterion is shown in Figure 19-3.

When a segment begins or ends at a crossroad ramp terminal, the length of the segment is measured from the near edge of the crossroad traveled way (shown as milepost 0.0 in the lower half of Figure 19-4). When a segment begins or ends at a terminal formed by a merging or diverging ramp or C-D road, then the length of the segment is measured from the gore point, as shown in Figure 19-4. A ramp or C-D road segment can include no more than one ramp entrance with a second ramp and one ramp exit with a second ramp.

Guidance regarding the location of the lane and shoulder width measurement points is provided in Figure 19-4. The rounded lane and shoulder width values are used solely to determine segment boundaries. Once these boundaries are determined, the guidance in the text associated with Figure 19-4 is used to determine the average lane and shoulder width for the segment. The unrounded average for the segment is then used for all subsequent calculations in the predictive method.

19.5.3. Crash Assignment to Sites

Observed crash counts are assigned to the individual sites to apply the site-specific EB Method. Any crashes that occur on a ramp or C-D road are classified as either intersection-related or segment-related crashes. The intersection-related crashes are assigned to the corresponding crossroad ramp terminal. The predictive model for crossroad ramp terminals estimates the frequency of these crashes. The segment-related crashes are assigned to the corresponding ramp or C-D road segment. The ramp segment predictive model estimates the frequency of these crashes. The procedure for assignment of crashes to individual sites is presented in Section B.2.3 in Appendix B to Part C.

Speed-change lanes can occur at locations where ramp segments and C-D road segments connect, or where two ramp segments connect. For the predictive method, these speed-change lanes are considered to be part of the ramp or C-D road segment. Crashes occurring in these speed-change lanes are assigned to the segment.

19.6. SAFETY PERFORMANCE FUNCTIONS

When using the predictive method, the appropriate safety performance functions (SPFs) are used to estimate the predicted average crash frequency of a site with base conditions. Each SPF was developed as a regression model using observed crash data for a set of similar sites as the dependent variable. The SPFs, like all regression models, estimate the value of the dependent variable as a function of a set of independent variables. The independent variables for the ramp and C-D road segment SPFs include the segment AADT volume, segment length, and area type (i.e., rural or urban). The independent variables for the crossroad ramp terminal SPFs include the AADT volume of the intersection legs and area type. The SPFs in this chapter are summarized in Table 19-3.

A detailed discussion of SPFs and their use in the HSM is presented in Section 3.5.2 of Chapter 3, and in Section C.6.3 of Part C.

Some highway agencies may have performed statistically-sound studies to develop their own jurisdiction-specific SPFs. These SPFs may be substituted for the SPFs presented in this chapter. Criteria for the development of SPFs for use in the predictive method are addressed in the calibration procedure presented in Section B.1.2 in Appendix B to Part C.

Each SPF has an associated overdispersion parameter k . The overdispersion parameter provides an indication of the statistical reliability of the SPF. The closer the overdispersion parameter is to zero, the more

statistically reliable the SPF. This parameter is used in the EB Method that is discussed in Section B.2 in Appendix B to Part C.

Table 19-3. Ramp Safety Performance Functions

Site Type (<i>w</i>)	Cross Section and Control Type (<i>x</i>)	Crash Type (<i>y</i>)	SPF Equations
Ramp segments (<i>rps</i>)	Ramp entrance, <i>n</i> lanes (<i>nEN</i>)	Multiple vehicle (<i>mv</i>)	Equation 19-20
		Single vehicle (<i>sv</i>)	Equation 19-24
	Ramp exit, <i>n</i> lanes (<i>nEX</i>)	Multiple vehicle (<i>mv</i>)	Equation 19-20
		Single vehicle (<i>sv</i>)	Equation 19-24
C-D road segments (<i>cds</i>)	<i>n</i> lanes (<i>n</i>)	Multiple vehicle (<i>mv</i>)	Equation 19-22
		Single vehicle (<i>sv</i>)	Equation 19-26
Three-leg terminals with diagonal exit ramp (<i>D3ex</i>)	One-way stop control (<i>ST</i>)	All types (<i>at</i>)	Equation 19-31
	Signal control, <i>n</i> lanes (<i>SGn</i>)	All types (<i>at</i>)	Equation 19-28
Three-leg terminals with diagonal entrance ramp (<i>D3en</i>)	One-way stop control (<i>ST</i>)	All types (<i>at</i>)	Equation 19-31
	Signal control, <i>n</i> lanes (<i>SGn</i>)	All types (<i>at</i>)	Equation 19-28
Four-leg terminals with diagonal ramps (<i>D4</i>)	One-way stop control (<i>ST</i>)	All types (<i>at</i>)	Equation 19-31
	Signal control, <i>n</i> lanes (<i>SGn</i>)	All types (<i>at</i>)	Equation 19-28
Four-leg terminals at four-quadrant parclo A (<i>A4</i>)	One-way stop control (<i>ST</i>)	All types (<i>at</i>)	Equation 19-31
	Signal control, <i>n</i> lanes (<i>SGn</i>)	All types (<i>at</i>)	Equation 19-28
Four-leg terminals at four-quadrant parclo B (<i>B4</i>)	One-way stop control (<i>ST</i>)	All types (<i>at</i>)	Equation 19-31
	Signal control, <i>n</i> lanes (<i>SGn</i>)	All types (<i>at</i>)	Equation 19-28
Three-leg terminals at two-quadrant parclo A (<i>A2</i>)	One-way stop control (<i>ST</i>)	All types (<i>at</i>)	Equation 19-31
	Signal control, <i>n</i> lanes (<i>SGn</i>)	All types (<i>at</i>)	Equation 19-28
Three-leg terminals at two-quadrant parclo B (<i>B2</i>)	One-way stop control (<i>ST</i>)	All types (<i>at</i>)	Equation 19-31
	Signal control, <i>n</i> lanes (<i>SGn</i>)	All types (<i>at</i>)	Equation 19-28

19.6.1. Safety Performance Functions for Ramp Segments

The SPFs for ramp and C-D road segments are presented in this section. Specifically, SPFs are provided for ramp and C-D road segments with 1 or 2 through lanes. The range of AADT volume for which these SPFs are applicable is shown in Table 19-4. Application of the SPFs to sites with AADT volumes substantially outside these ranges may not provide reliable results.

Table 19-4. Applicable AADT Volume Ranges for Ramp SPFs

Area Type	Cross Section (Through Lanes) (<i>x</i>)	Applicable AADT Volume Range (veh/day)
Rural	1	0 to 7,000
Urban	1	0 to 18,000
	2	0 to 32,000

Other types of ramp and C-D road segments may be found at interchanges but are not addressed by the predictive model described in this chapter.

Multiple-Vehicle Crashes on Ramp Segments

The base conditions for the SPFs for multiple-vehicle crashes on ramp segments are:

- Horizontal curve Not present
- Lane width 14 ft
- Right shoulder width 8 ft
- Left shoulder width 4 ft
- Right side barrier Not present
- Left side barrier Not present
- Lane add or drop Not present
- Ramp speed-change lane Not present

The SPFs for multiple-vehicle crashes on ramp segments is represented using the following equation.

$$N_{spf, rps, x, mv, z} = L_r \times \exp(a + b \times \ln[c \times AADT_r] + d [c \times AADT_r]) \quad \text{Equation 19-20}$$

Where:

$N_{spf, rps, x, mv, z}$ = predicted average multiple-vehicle crash frequency of a ramp segment with base conditions, cross section x ($x = nEN$: n -lane entrance ramp, nEX : n -lane exit ramp), and severity z ($z = fi$: fatal and injury, pdo : property damage only) (crashes/yr);

L_r = length of ramp segment (mi);

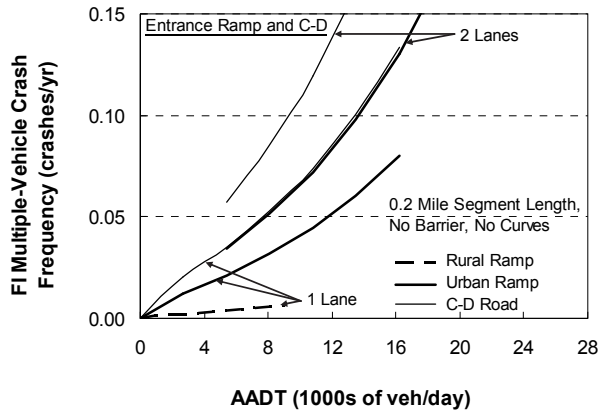
$AADT_r$ = AADT volume of ramp segment (veh/day); and

a, b, c, d = regression coefficients.

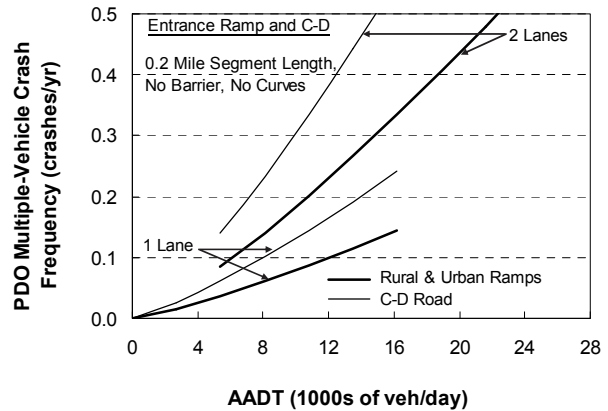
The SPF regression coefficients and inverse dispersion parameter are provided in Table 19-5. The SPFs are illustrated in Figure 19-11 and Figure 19-12.

Table 19-5. SPF Coefficients for Multiple-Vehicle Crashes on Ramp Segments

Crash Severity (<i>z</i>)	Area Type	Cross Section (<i>x</i>)	SPF Coefficient				Inverse Dispersion Parameter $K_{rps, x, mv, z}$ (mi^{-1})
			<i>a</i>	<i>b</i>	<i>c</i>	<i>d</i>	
Fatal and injury (<i>fi</i>)	Rural	One-lane entrance (<i>IEN</i>)	-5.226	0.524	0.001	0.0699	14.6
		One-lane exit (<i>IEX</i>)	-6.692	0.524	0.001	0.0699	14.6
	Urban	One-lane entrance (<i>IEN</i>)	-3.505	0.524	0.001	0.0699	14.6
		One-lane exit (<i>IEX</i>)	-4.971	0.524	0.001	0.0699	14.6
		Two-lane entrance (<i>2EN</i>)	-3.023	0.524	0.001	0.0699	14.6
		Two-lane exit (<i>2EX</i>)	-4.489	0.524	0.001	0.0699	14.6
Property damage only (<i>pdo</i>)	Rural	One-lane entrance (<i>IEN</i>)	-3.819	1.256	0.001	0.00	12.7
		One-lane exit (<i>IEX</i>)	-4.851	1.256	0.001	0.00	12.7
	Urban	One-lane entrance (<i>IEN</i>)	-3.819	1.256	0.001	0.00	12.7
		One-lane exit (<i>IEX</i>)	-4.851	1.256	0.001	0.00	12.7
		Two-lane entrance (<i>2EN</i>)	-2.983	1.256	0.001	0.00	12.7
		Two-lane exit (<i>2EX</i>)	-4.015	1.256	0.001	0.00	12.7

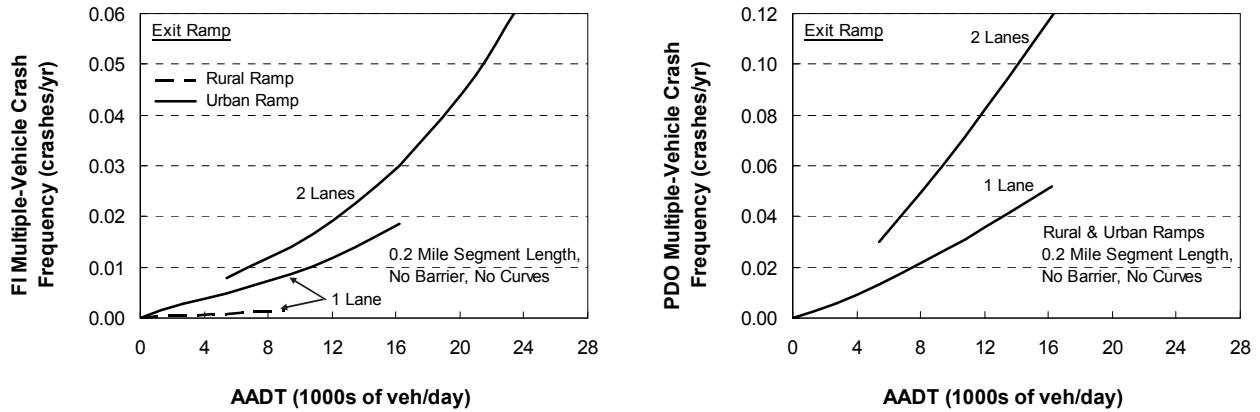


a. Fatal-and-Injury Crash Frequency.



b. Property-Damage-Only Crash Frequency.

Figure 19-11. Graphical Form of the SPFs for Multiple-Vehicle Crashes on Entrance Ramp Segments



a. Fatal-and-Injury Crash Frequency

b. Property-Damage-Only Crash Frequency

Figure 19-12. Graphical Form of the SPFs for Multiple-Vehicle Crashes on Exit Ramp Segments

The value of the overdispersion parameter associated with the SPFs for ramp segments is determined as a function of the segment length. This value is computed using Equation 19-21.

$$k_{rps, x, mv, z} = \frac{1}{K_{rps, x, mv, z} \times L_r} \tag{Equation 19-21}$$

Where:

$k_{rps, x, mv, z}$ = overdispersion parameter for ramp segments with cross section x , multiple-vehicle crashes mv , and severity z ; and

$K_{rps, x, mv, z}$ = inverse dispersion parameter for ramp segments with cross section x , multiple-vehicle crashes mv , and severity z (mi^{-1}).

The crash frequency obtained from Equation 19-20 can be multiplied by the proportions in Table 19-6 to estimate the predicted average multiple-vehicle crash frequency by crash type category.

Table 19-6. Default Distribution of Multiple-Vehicle Crashes by Crash Type for Ramp and C-D Road Segments

Area Type	Crash Type Category	Proportion of Crashes by Severity	
		Fatal and Injury	Property Damage Only
Rural or urban	Head-on	0.015	0.009
	Right-angle	0.010	0.005
	Rear-end	0.707	0.550
	Sideswipe	0.129	0.335
	Other multiple-vehicle crashes	0.139	0.101

Multiple-Vehicle Crashes on C-D Road Segments

The base conditions for the SPFs for multiple-vehicle crashes on C-D road segments are the same as those for multiple-vehicle crashes on ramp segments, as described in the preceding subsection. One additional base condition for this SPF is that there is no weaving section present.

The SPFs for multiple-vehicle crashes on C-D road segments is represented using the following equation.

$$N_{spf, cds, n, mv, z} = L_{cd} \times \exp(a + b \times \ln[c \times AADT_c] + d [c \times AADT_c]) \quad \text{Equation 19-22}$$

Where:

$N_{spf, cds, n, mv, z}$ = predicted average multiple-vehicle crash frequency of a C-D road segment with base conditions, n lanes, and severity z ($z = fi$: fatal and injury, pdo : property damage only) (crashes/yr);

L_{cd} = length of C-D road segment (mi); and

$AADT_c$ = AADT volume of C-D road segment (veh/day).

The SPF regression coefficients and inverse dispersion parameter are provided in Table 19-7. The SPFs are illustrated in Figure 19-11.

Table 19-7. SPF Coefficients for Multiple-Vehicle Crashes on C-D Road Segments

Crash Severity (z)	Area Type	Number of Through Lanes (n)	SPF Coefficient				Inverse Dispersion Parameter $K_{cds, x, mv, z}$ (mi^{-1})
			a	b	c	d	
Fatal and injury (fi)	Rural	1	-4.718	0.524	0.001	0.0699	14.6
	Urban	1	-2.997	0.524	0.001	0.0699	14.6
		2	-2.515	0.524	0.001	0.0699	14.6
Property damage only (pdo)	Rural	1	-3.311	1.256	0.001	0.00	12.7
	Urban	1	-3.311	1.256	0.001	0.00	12.7
		2	-2.475	1.256	0.001	0.00	12.7

The value of the overdispersion parameter associated with the SPFs for C-D road segments is determined as a function of the segment length. This value is computed using Equation 19-23.

$$k_{cds, x, mv, z} = \frac{1}{K_{cds, x, mv, z} \times L_{cd}} \quad \text{Equation 19-23}$$

Where:

$k_{cds, x, mv, z}$ = overdispersion parameter for C-D road segments with cross section x , multiple-vehicle crashes mv , and severity z ; and

$K_{cds, x, mv, z}$ = inverse dispersion parameter for C-D road segments with cross section x , multiple-vehicle crashes mv , and severity z (mi^{-1}).

The crash frequency obtained from Equation 19-22 can be multiplied by the proportions in Table 19-6 to estimate the predicted average multiple-vehicle crash frequency by crash type category.

Single-Vehicle Crashes on Ramp Segments

With one exception, the base conditions for the SPFs for single-vehicle crashes on ramp segments are the same as those for multiple-vehicle crashes on ramp segments, as described in a preceding subsection. The “ramp speed-change lane presence” condition does not apply to the single-vehicle SPFs.

The SPFs for single-vehicle crashes on ramp segments are represented with the following equation.

$$N_{spf, rps, x, sv, z} = L_r \times \exp(a + b \times \ln[c \times AADT_r]) \quad \text{Equation 19-24}$$

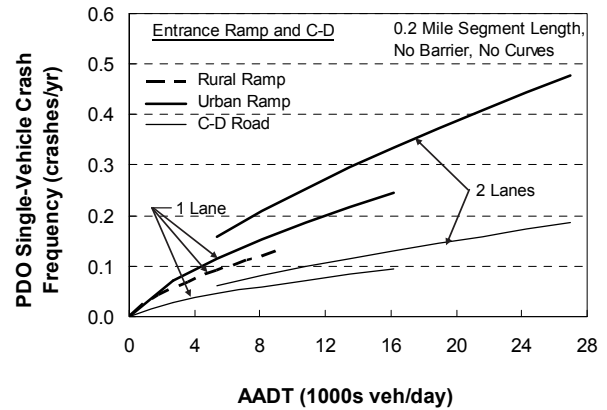
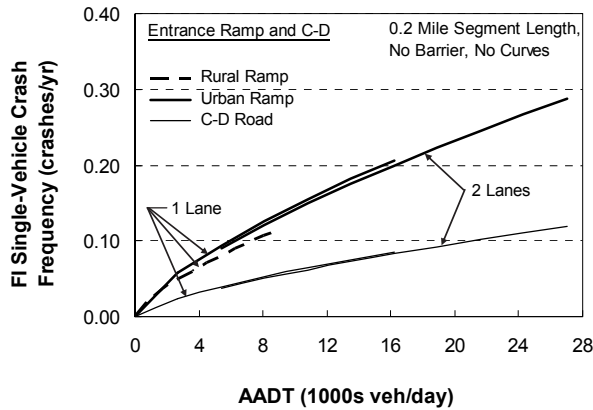
Where:

$N_{spf, rps, x, sv, z}$ = predicted average single-vehicle crash frequency of a ramp segment with base conditions, cross section x ($x = nEN$: n -lane entrance ramp, nEX : n -lane exit ramp), and severity z ($z = fi$: fatal and injury, pdo : property damage only) (crashes/yr).

The SPF regression coefficients and inverse dispersion parameter are provided in Table 19-8. The SPFs are illustrated in Figure 19-13 and Figure 19-14.

Table 19-8. SPF Coefficients for Single-Vehicle Crashes on Ramp Segments

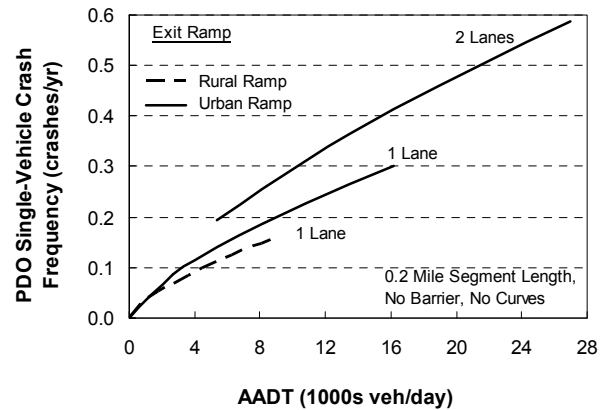
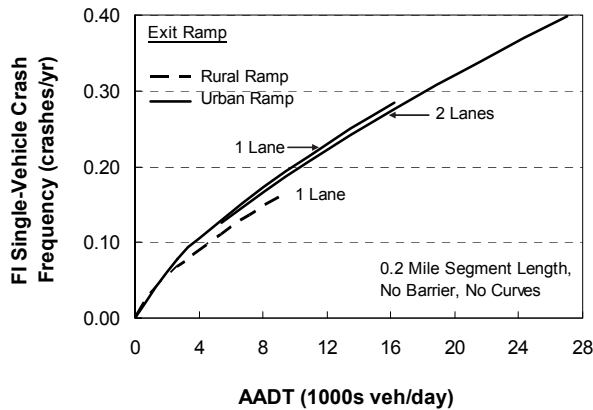
Crash Severity (z)	Area Type	Cross Section (x)	SPF Coefficient			Inverse Dispersion Parameter $K_{rps, x, sv, z}$ (mi^{-1})
			a	b	c	
Fatal and injury (fi)	Rural	One-lane entrance ($1EN$)	-2.120	0.718	0.001	7.91
		One-lane exit ($1EX$)	-1.799	0.718	0.001	7.91
	Urban	One-lane entrance ($1EN$)	-1.966	0.718	0.001	7.91
		One-lane exit ($1EX$)	-1.645	0.718	0.001	7.91
		Two-lane entrance ($2EN$)	-1.999	0.718	0.001	7.91
		Two-lane exit ($2EX$)	-1.678	0.718	0.001	7.91
Property damage only (pdo)	Rural	One-lane entrance ($1EN$)	-1.946	0.689	0.001	9.77
		One-lane exit ($1EX$)	-1.739	0.689	0.001	9.77
	Urban	One-lane entrance ($1EN$)	-1.715	0.689	0.001	9.77
		One-lane exit ($1EX$)	-1.508	0.689	0.001	9.77
		Two-lane entrance ($2EN$)	-1.400	0.689	0.001	9.77
		Two-lane exit ($2EX$)	-1.193	0.689	0.001	9.77



a. Fatal-and-Injury Crash Frequency

b. Property-Damage-Only Crash Frequency

Figure 19-13. Graphical Form of the SPFs for Single-Vehicle Crashes on Entrance Ramp Segments



a. Fatal-and-Injury Crash Frequency

b. Property-Damage-Only Crash Frequency

Figure 19-14. Graphical Form of the SPFs for Single-Vehicle Crashes on Exit Ramp Segments

The value of the overdispersion parameter associated with the SPFs for ramp segments is determined as a function of the segment length. This value is computed using Equation 19-25.

$$k_{rps, x, sv, z} = \frac{1}{K_{rps, x, sv, z} \times L_r} \tag{Equation 19-25}$$

Where:

$k_{rps, x, sv, z}$ = overdispersion parameter for ramp segments with cross section x , single-vehicle crashes mv , and severity z ; and

$K_{rps, x, sv, z}$ = inverse dispersion parameter for ramp segments with cross section x , single-vehicle crashes mv , and severity z (mi^{-1}).

The crash frequency obtained from Equation 19-24 can be multiplied by the proportions in Table 19-9 to estimate the predicted average single-vehicle crash frequency by crash type category.

Table 19-9. Default Distribution of Single-Vehicle Crashes by Crash Type for Ramp and C-D Road Segments

Area Type	Crash Type Category	Proportion of Crashes by Severity	
		Fatal and Injury	Property Damage Only
Rural	Crash with animal	0.012	0.022
	Crash with fixed object	0.422	0.538
	Crash with other object	0.000	0.011
	Crash with parked vehicle	0.024	0.055
	Other single-vehicle crashes	0.542	0.374
Urban	Crash with animal	0.003	0.005
	Crash with fixed object	0.718	0.834
	Crash with other object	0.015	0.023
	Crash with parked vehicle	0.012	0.012
	Other single-vehicle crashes	0.252	0.126

Single-Vehicle Crashes on C-D Road Segments

With one exception, the base conditions for the SPFs for single-vehicle crashes on C-D road segments are the same as those for multiple-vehicle crashes on ramp segments, as described in a preceding subsection. The “ramp speed-change lane presence” condition does not apply to the single-vehicle SPFs. One additional base condition for this SPF is that there is no weaving section present.

The SPFs for single-vehicle crashes on C-D road segments are represented with the following equation.

$$N_{spf, cds, n, sv, z} = L_{cd} \times \exp(a + b \times \ln[c \times AADT_c]) \quad \text{Equation 19-26}$$

Where:

$N_{spf, cds, n, sv, z}$ = predicted average single-vehicle crash frequency of a C-D road segment with base conditions, n lanes, and severity z ($z = fi$: fatal and injury, pdo : property damage only) (crashes/yr).

The SPF regression coefficients and inverse dispersion parameter are provided in Table 19-10. The SPFs are illustrated in Figure 19-13.

Table 19-10. SPF Coefficients for Single-Vehicle Crashes on C-D Road Segments

Crash Severity (z)	Area Type	Number of Through Lanes (n)	SPF Coefficient			Inverse Dispersion Parameter $K_{cds, n, sv, z}$ (mi^{-1})
			a	b	c	
Fatal and injury (fi)	Rural	1	-3.002	0.718	0.001	7.91
	Urban	1	-2.848	0.718	0.001	7.91
		2	-2.881	0.718	0.001	7.91
Property damage only (pdo)	Rural	1	-2.890	0.689	0.001	9.77
	Urban	1	-2.659	0.689	0.001	9.77
		2	-2.344	0.689	0.001	9.77

The value of the overdispersion parameter associated with the SPFs for C-D road segments is determined as a function of the segment length. This value is computed using Equation 19-27.

$$k_{cds, n, sv, z} = \frac{1}{K_{cds, n, sv, z} \times L_{cd}} \quad \text{Equation 19-27}$$

Where:

$k_{cds, x, sv, z}$ = overdispersion parameter for C-D road segments with cross section x , single-vehicle crashes mv , and severity z ; and

$K_{cds, x, sv, z}$ = inverse dispersion parameter for C-D road segments with cross section x , single-vehicle crashes mv , and severity z (mi^{-1}).

The crash frequency obtained from Equation 19-26 can be multiplied by the proportions in Table 19-9 to estimate the predicted average single-vehicle crash frequency by crash type category.

19.6.2. Safety Performance Functions for Ramp Terminals

The SPFs for crossroad ramp terminals are presented in this section. Specifically, SPFs are provided for crossroad ramp terminals with 2 to 6 crossroad through lanes (total of both travel directions). The range of AADT volume for which these SPFs are applicable is shown in Table 19-11. Application of the SPFs to sites with AADT volumes substantially outside these ranges may not provide reliable results.

Other types of crossroad ramp terminal configurations may be found at interchanges but are not addressed by the predictive model described in this chapter.

Table 19-11. Applicable AADT Volume Ranges for Crossroad Ramp Terminal SPFs

Site Type (<i>w</i>)	Control Type (<i>x</i>)	Applicable AADT Volume Range (veh/day)	
		Crossroad	Total All Ramps
Three-leg terminals with diagonal exit ramp (<i>D3ex</i>)	Stop control (<i>ST</i>)	0 to 22,000	0 to 8,000
	Signal control (<i>SG</i>)	0 to 34,000	0 to 16,000
Three-leg terminals with diagonal entrance ramp (<i>D3en</i>)	Stop control (<i>ST</i>)	0 to 22,000	0 to 15,000
	Signal control (<i>SG</i>)	0 to 29,000	0 to 21,000
Four-leg terminals with diagonal ramps (<i>D4</i>)	Stop control (<i>ST</i>)	0 to 18,000	0 to 10,000
	Signal control (<i>SG</i>)	0 to 47,000	0 to 31,000
Four-leg terminals at four-quadrant parcel A (<i>A4</i>)	Stop control (<i>ST</i>)	0 to 21,000	0 to 12,000
	Signal control (<i>SG</i>)	0 to 71,000	0 to 30,000
Four-leg terminals at four-quadrant parcel B (<i>B4</i>)	Stop control (<i>ST</i>)	0 to 20,000	0 to 12,000
	Signal control (<i>SG</i>)	0 to 45,000	0 to 29,000
Three-leg terminals at two-quadrant parcel A (<i>A2</i>)	Stop control (<i>ST</i>)	0 to 17,000	0 to 12,000
	Signal control (<i>SG</i>)	0 to 46,000	0 to 25,000
Three-leg terminals at two-quadrant parcel B (<i>B2</i>)	Stop control (<i>ST</i>)	0 to 26,000	0 to 14,000
	Signal control (<i>SG</i>)	0 to 44,000	0 to 22,000

Signal-Controlled Crossroad Ramp Terminals

The base conditions for the signalized crossroad ramp terminal SPFs are:

- Crossroad left-turn lane (or bay) Not present
- Crossroad right-turn lane (or bay) Not present
- Public street approach presence No public street approaches present
- Driveway presence No driveways present
- Distance to adjacent intersection No adjacent ramp or public street intersection within 6 mi
- Median width (on crossroad) 12 ft
- Protected left-turn phase Not present on either crossroad approach leg
- Channelized right turn on crossroad Not present
- Channelized right turn on exit ramp Not present
- Non-ramp public street leg Not present

The SPFs for crashes at signalized crossroad ramp terminals are presented using the following equation.

$$N_{spf, w, SGn, at, z} = \exp(a + b \times \ln[c \times AADT_{xrd}] + d \times \ln[c \times AADT_{ex} + c \times AADT_{en}]) \quad \text{Equation 19-28}$$

with

$$AADT_{xrd} = 0.5 \times (AADT_{in} + AADT_{out}) \quad \text{Equation 19-29}$$

Where:

$N_{spf, w, SGn, at, z}$ = predicted average crash frequency of a signal-controlled crossroad ramp terminal of site type w ($w = D3ex, D3en, D4, A4, B4, A2, B2$) with base conditions, n crossroad lanes, all crash types at , and severity z ($z = fi$: fatal and injury, pdo : property damage only) (crashes/yr);

$AADT_{xrd}$ = AADT volume for the crossroad (veh/day);

$AADT_{in}$ = AADT volume for the crossroad leg between ramps (veh/day);

$AADT_{out}$ = AADT volume for the crossroad leg outside of interchange (veh/day);

$AADT_{ex}$ = AADT volume for the exit ramp (veh/day); and

$AADT_{en}$ = AADT volume for the entrance ramp (veh/day).

The SPF regression coefficients and inverse dispersion parameter are provided in Table 19-12 to Table 19-15. The SPFs are illustrated in Figure 19-15 to Figure 19-18. The AADT volume of the loop exit ramp at a $B4$ terminal configuration is not included in $AADT_{ex}$. Similarly, the AADT volume of the loop entrance ramp at an $A4$ configuration is not included in $AADT_{en}$.

The Exit ramp capacity CMF is combined with the SPF for fatal-and-injury crashes to create the trend lines shown in the figures for fatal-and-injury crashes. This CMF is a function of exit ramp volume, number of exit ramp lanes, and the traffic control for the exit ramp right turn. These variables in combination do not readily lend themselves to the specification of a representative base condition. For this reason, the CMF is combined with the SPF for the graphical presentation. The Exit ramp capacity CMF is described in Section 19.7.2

Table 19-12. SPF Coefficients for Crashes at Signalized Ramp Terminals—Three-Leg Terminal at Two-Quadrant Parclo A or B (*A2, B2*)

Crash Severity (<i>z</i>)	Area Type	Number of Crossroad Through Lanes (<i>n</i>)	SPF Coefficient				Inverse Dispersion Parameter $K_{w, SGn, at, z}$
			<i>a</i>	<i>b</i>	<i>c</i>	<i>d</i>	
Fatal and injury (<i>fi</i>)	Rural or urban	2	-0.458	0.325	0.001	0.212	2.17
		3	-0.298	0.325	0.001	0.212	2.17
		4	-0.138	0.325	0.001	0.212	2.17
		5 (urban only)	0.022	0.325	0.001	0.212	2.17
		6 (urban only)	0.182	0.325	0.001	0.212	2.17
Property damage only (<i>pdo</i>)	Rural or urban	2	-1.537	0.592	0.001	0.516	4.27
		3	-1.449	0.592	0.001	0.516	4.27
		4	-1.361	0.592	0.001	0.516	4.27
		5 (urban only)	-1.274	0.592	0.001	0.516	4.27
		6 (urban only)	-1.186	0.592	0.001	0.516	4.27

Table 19-13. SPF Coefficients for Crashes at Signalized Ramp Terminals—Three-Leg Terminal with Diagonal Exit Ramp or Four-Leg Terminal at Four-Quadrant Parclo A (*D3ex, A4*)

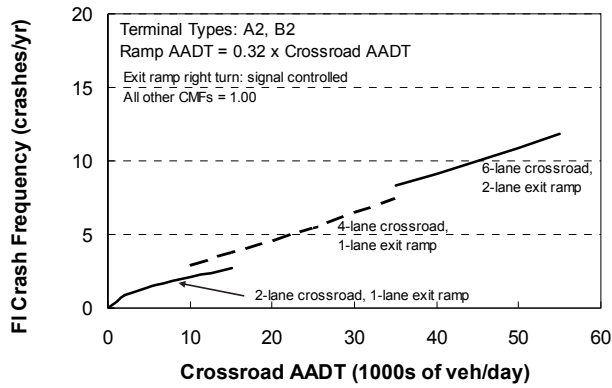
Crash Severity (<i>z</i>)	Area Type	Number of Crossroad Through Lanes (<i>n</i>)	SPF Coefficient				Inverse Dispersion Parameter $K_{w, SGn, at, z}$
			<i>a</i>	<i>b</i>	<i>c</i>	<i>d</i>	
Fatal and injury (<i>fi</i>)	Rural or urban	2	-1.352	0.379	0.001	0.394	8.72
		3	-1.192	0.379	0.001	0.394	8.72
		4	-1.032	0.379	0.001	0.394	8.72
		5 (urban only)	-0.872	0.379	0.001	0.394	8.72
		6 (urban only)	-0.712	0.379	0.001	0.394	8.72
Property damage only (<i>pdo</i>)	Rural or urban	2	-2.247	0.797	0.001	0.384	4.05
		3	-2.159	0.797	0.001	0.384	4.05
		4	-2.071	0.797	0.001	0.384	4.05
		5 (urban only)	-1.984	0.797	0.001	0.384	4.05
		6 (urban only)	-1.896	0.797	0.001	0.384	4.05

Table 19-14. SPF Coefficients for Crashes at Signalized Ramp Terminals–Three-Leg Terminal with Diagonal Entrance Ramp or Four-Leg Terminal at Four-Quadrant Parclo B (*D3en, B4*)

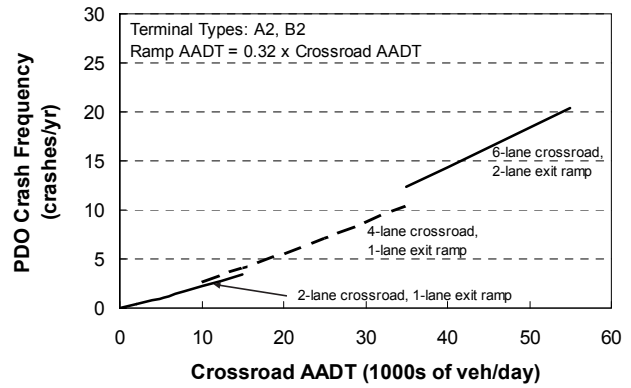
Crash Severity (<i>z</i>)	Area Type	Number of Crossroad Through Lanes (<i>n</i>)	SPF Coefficient				Inverse Dispersion Parameter $K_{Sw, SGn, at, z}$
			<i>a</i>	<i>b</i>	<i>c</i>	<i>d</i>	
Fatal and injury (<i>ft</i>)	Rural or urban	2	-2.068	0.265	0.001	0.905	5.37
		3	-1.908	0.265	0.001	0.905	5.37
		4	-1.748	0.265	0.001	0.905	5.37
		5 (urban only)	-1.588	0.265	0.001	0.905	5.37
		6 (urban only)	-1.428	0.265	0.001	0.905	5.37
Property damage only (<i>pdo</i>)	Rural or urban	2	-2.931	0.741	0.001	0.845	3.72
		3	-2.843	0.741	0.001	0.845	3.72
		4	-2.755	0.741	0.001	0.845	3.72
		5 (urban only)	-2.668	0.741	0.001	0.845	3.72
		6 (urban only)	-2.580	0.741	0.001	0.845	3.72

Table 19-15. SPF Coefficients for Crashes at Signalized Ramp Terminals–Four-Leg Terminal with Diagonal Ramps (*D4*)

Crash Severity (<i>z</i>)	Area Type	Number of Crossroad Through Lanes (<i>n</i>)	SPF Coefficient				Inverse Dispersion Parameter $K_{Sw, SGn, at, z}$
			<i>a</i>	<i>b</i>	<i>c</i>	<i>d</i>	
Fatal and injury (<i>ft</i>)	Rural or urban	2	-2.655	1.191	0.001	0.131	11.5
		3	-2.495	1.191	0.001	0.131	11.5
		4	-2.335	1.191	0.001	0.131	11.5
		5 (urban only)	-2.175	1.191	0.001	0.131	11.5
		6 (urban only)	-2.015	1.191	0.001	0.131	11.5
Property damage only (<i>pdo</i>)	Rural or urban	2	-2.248	0.879	0.001	0.545	7.21
		3	-2.160	0.879	0.001	0.545	7.21
		4	-2.072	0.879	0.001	0.545	7.21
		5 (urban only)	-1.985	0.879	0.001	0.545	7.21
		6 (urban only)	-1.897	0.879	0.001	0.545	7.21

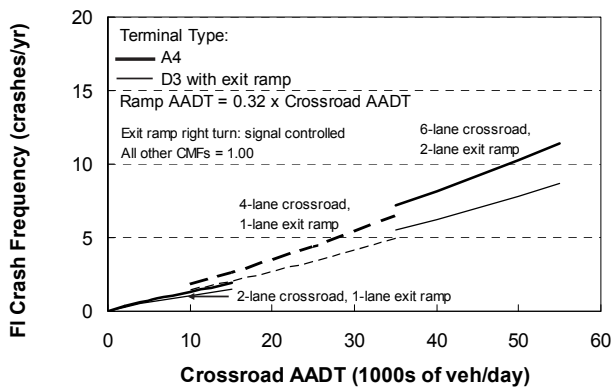


a. Fatal-and-Injury Crash Frequency

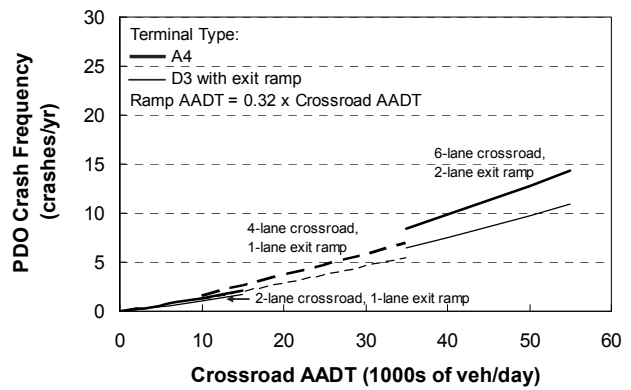


b. Property-Damage-Only Crash Frequency

Figure 19-15. Graphical Form of the SPF for Crashes at Signalized Ramp Terminals—Three-Leg Terminal at Two-Quadrant Parclo A or B (A2, B2)

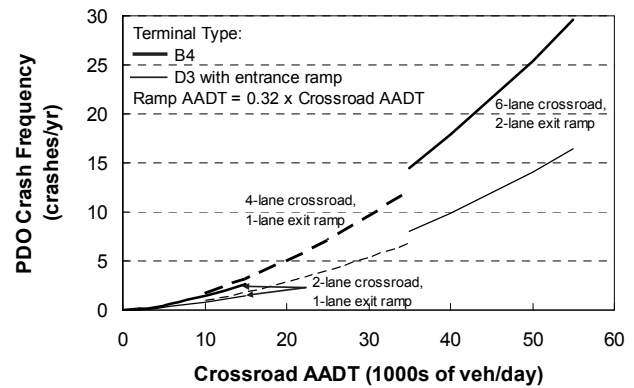
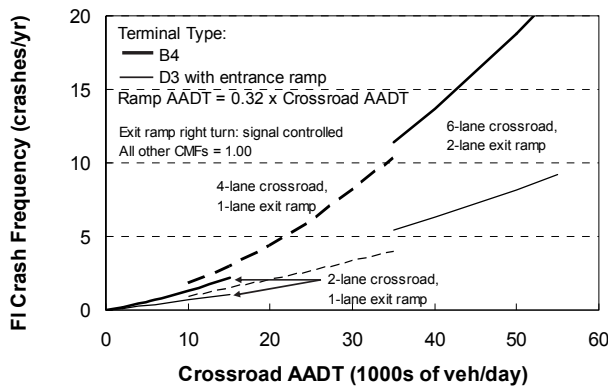


a. Fatal-and-Injury Crash Frequency



b. Property-Damage-Only Crash Frequency

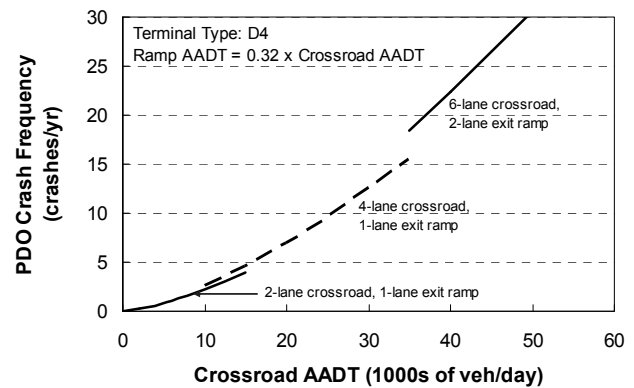
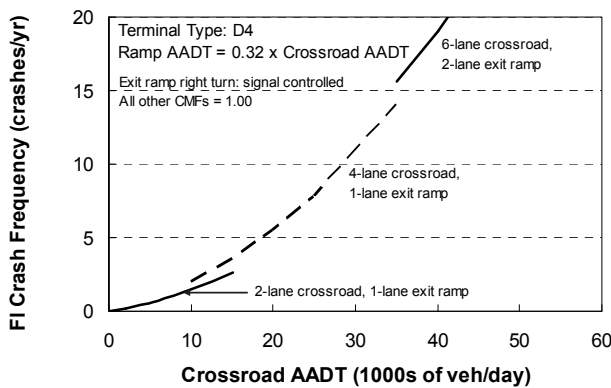
Figure 19-16. Graphical Form of the SPF for Crashes at Signalized Ramp Terminals—Three-Leg Terminal with Diagonal Exit Ramp or Four-Leg Terminal at Four-Quadrant Parclo A (D3ex, A4)



a. Fatal-and-Injury Crash Frequency

b. Property-Damage-Only Crash Frequency

Figure 19-17. Graphical Form of the SPF for Crashes at Signalized Ramp Terminals—Three-Leg Terminal with Diagonal Entrance Ramp or Four-Leg Terminal at Four-Quadrant Parclo B (*D3en, B4*)



a. Fatal-and-Injury Crash Frequency

b. Property-Damage-Only Crash Frequency

Figure 19-18. Graphical Form of the SPF for Crashes at Signalized Ramp Terminals—Four-Leg Terminal with Diagonal Ramps (*D4*)

The value of the overdispersion parameter associated with the SPFs for signalized crossroad ramp terminals is computed using Equation 19-30.

$$k_{w,SGn,at,z} = \frac{1}{K_{w,SGn,at,z}} \tag{Equation 19-30}$$

Where:

$k_{w,SGn,at,z}$ = overdispersion parameter for signal-controlled site of type w , when n crossroad lanes, all crash types at , and severity z ; and

$K_{w,SGn,at,z}$ = inverse dispersion parameter for signal-controlled site of type w , when n crossroad lanes, all crash types at , and severity z .

The crash frequency obtained from Equation 19-28 can be multiplied by the proportions in Table 19-16 to estimate the predicted average signalized crossroad ramp terminal crash frequency by crash type or crash type category.

Table 19-16. Default Distribution of Signal-Controlled Ramp Terminal Crashes by Crash Type

Area Type	Crash Type	Crash Type Category	Proportion of Crashes by Severity	
			Fatal and Injury	Property Damage Only
Rural	Multiple vehicle	Head-on	0.000	0.006
		Right-angle	0.333	0.187
		Rear-end	0.552	0.466
		Sideswipe	0.000	0.219
		Other multiple-vehicle crash	0.014	0.013
	Single vehicle	Crash with animal	0.000	0.000
		Crash with fixed object	0.043	0.077
		Crash with other object	0.000	0.000
		Crash with parked vehicle	0.000	0.013
		Other single-vehicle crashes	0.058	0.019
Urban	Multiple vehicle	Head-on	0.011	0.007
		Right-angle	0.260	0.220
		Rear-end	0.625	0.543
		Sideswipe	0.042	0.149
		Other multiple-vehicle crash	0.009	0.020
	Single vehicle	Crash with animal	0.000	0.000
		Crash with fixed object	0.033	0.050
		Crash with other object	0.001	0.002
		Crash with parked vehicle	0.001	0.002
		Other single-vehicle crashes	0.018	0.007

One-Way Stop-Controlled Crossroad Ramp Terminals

The predictive models described in this section are calibrated to address one-way stop control, where the ramp is stop controlled. An interim predictive model is provided in Section 19.10 for all-way stop control.

The base conditions for the one-way stop-controlled crossroad ramp terminal SPFs are:

- Crossroad left-turn lane (or bay) Not present
- Crossroad right-turn lane (or bay) Not present

- Public street approach presence No public street approaches present
- Distance to adjacent intersection No adjacent ramp or public street intersection within 6 mi
- Median width (on crossroad) 12 ft
- Skew angle 0.0 degrees (no skew)

The SPF for crashes at one-way stop-controlled ramp terminals is applied as follows:

$$N_{spf, w, ST, at, z} = \exp(a + b \times \ln[c \times AADT_{xrd}] + d \times \ln[c \times AADT_{ex} + c \times AADT_{en}]) \tag{Equation 19-31}$$

Where:

$N_{spf, w, ST, at, z}$ = predicted average crash frequency of a one-way stop-controlled crossroad ramp terminal of site type w ($w = D3ex, D3en, D4, A4, B4, A2, B2$) with base conditions, all crash types at , and severity z ($z = fi$: fatal and injury, pdo : property damage only) (crashes/yr).

The SPF regression coefficients and inverse dispersion parameter are provided in Table 19-17 to Table 19-20. The SPFs are illustrated in Figure 19-19 to Figure 19-22.

The Exit ramp capacity CMF is combined with the SPF for fatal-and-injury crashes to create the trend lines shown in the figures for fatal-and-injury crashes. This CMF is a function of exit ramp volume, number of exit ramp lanes, and the traffic control for the exit ramp right turn. These variables in combination do not readily lend themselves to the specification of a representative base condition. For this reason, the CMF is combined with the SPF for the graphical presentation. The Exit ramp capacity CMF is described in Section 19.7.2.

Table 19-17. SPF Coefficients for Crashes at One-Way Stop-Controlled Ramp Terminals–Three-Leg Terminal at Two-Quadrant Parclo A or B ($A2, B2$)

Crash Severity (z)	Area Type	Number of Crossroad Through Lanes (n)	SPF Coefficient				Inverse Dispersion Parameter $K_{w, ST, at, z}$
			a	b	c	d	
Fatal and injury (fi)	Rural	All lanes	-2.363	0.260	0.001	0.947	3.40
	Urban	All lanes	-2.687	0.260	0.001	0.947	3.40
Property damage only (pdo)	Rural	All lanes	-3.055	0.773	0.001	0.878	5.49
	Urban	All lanes	-3.055	0.773	0.001	0.878	5.49

Table 19-18. SPF Coefficients for Crashes at One-Way Stop-Controlled Ramp Terminals–Three-Leg Terminal with Diagonal Exit Ramp or Four-Leg Terminal at Four-Quadrant Parclo A (*D3ex, A4*)

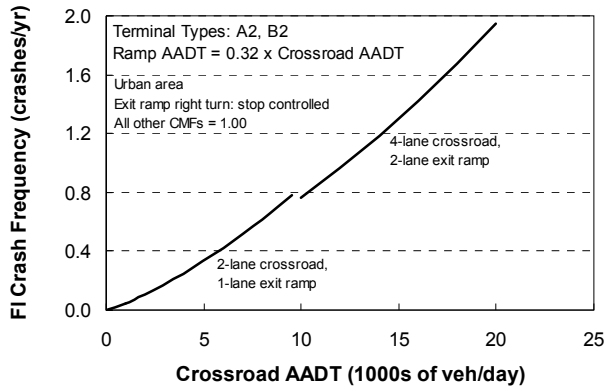
Crash Severity (<i>z</i>)	Area Type	Number of Crossroad Through Lanes (<i>n</i>)	SPF Coefficient				Inverse Dispersion Parameter $K_{w, ST, at, z}$
			<i>a</i>	<i>b</i>	<i>c</i>	<i>d</i>	
Fatal and injury (<i>fi</i>)	Rural	All lanes	-2.899	0.582	0.001	0.899	2.16
	Urban	All lanes	-3.223	0.582	0.001	0.899	2.16
Property damage only (<i>pdo</i>)	Rural	All lanes	-2.670	0.595	0.001	0.937	6.57
	Urban	All lanes	-2.670	0.595	0.001	0.937	6.57

Table 19-19. SPF Coefficients for Crashes at One-Way Stop-Controlled Ramp Terminals–Three-Leg Terminal with Diagonal Entrance Ramp or Four-Leg Terminal at Four-Quadrant Parclo B (*D3en, B4*)

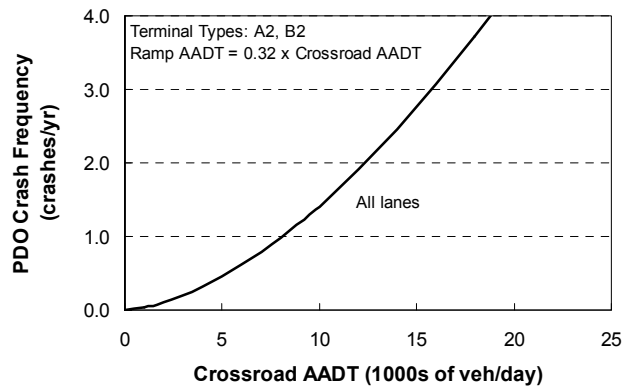
Crash Severity (<i>z</i>)	Area Type	Number of Crossroad Through Lanes (<i>n</i>)	SPF Coefficient				Inverse Dispersion Parameter $K_{w, ST, at, z}$
			<i>a</i>	<i>b</i>	<i>c</i>	<i>d</i>	
Fatal and injury (<i>fi</i>)	Rural	All lanes	-2.817	0.709	0.001	0.730	0.92
	Urban	All lanes	-3.141	0.709	0.001	0.730	0.92
Property damage only (<i>pdo</i>)	Rural	All lanes	-2.358	0.885	0.001	0.350	3.90
	Urban	All lanes	-2.358	0.885	0.001	0.350	3.90

Table 19-20. SPF Coefficients for Crashes at One-Way Stop-Controlled Ramp Terminals–Four-Leg Terminal with Diagonal Ramps (*D4*)

Crash Severity (<i>z</i>)	Area Type	Number of Crossroad Through Lanes (<i>n</i>)	SPF Coefficient				Inverse Dispersion Parameter $K_{w, ST, at, z}$
			<i>a</i>	<i>b</i>	<i>c</i>	<i>d</i>	
Fatal and injury (<i>fi</i>)	Rural	All lanes	-2.740	1.008	0.001	0.177	2.58
	Urban	All lanes	-3.064	1.008	0.001	0.177	2.58
Property damage only (<i>pdo</i>)	Rural	All lanes	-2.432	0.845	0.001	0.476	4.27
	Urban	All lanes	-2.432	0.845	0.001	0.476	4.27

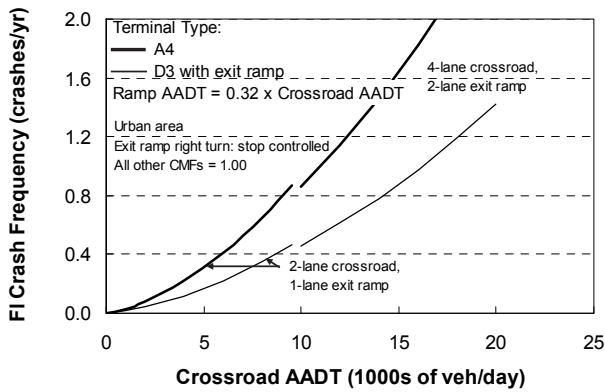


a. Fatal-and-Injury Crash Frequency

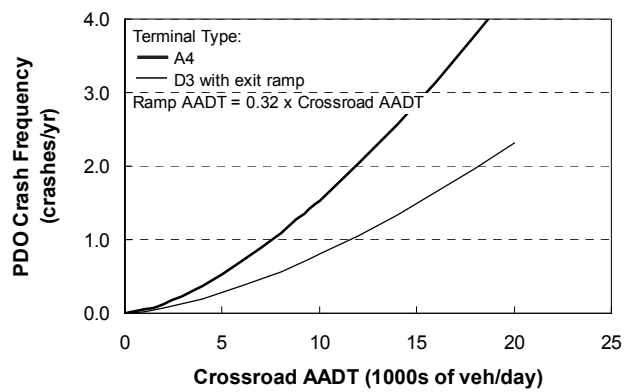


b. Property-Damage-Only Crash Frequency

Figure 19-19. Graphical Form of the SPF Crashes at One-Way Stop-Controlled Ramp Terminals–Three-Leg Terminal at Two-Quadrant Parclo A or B (A2, B2)

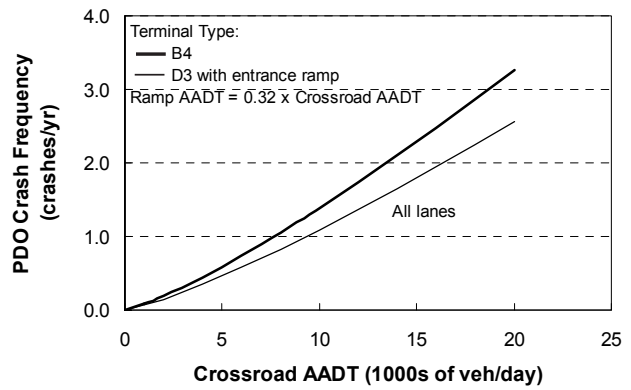
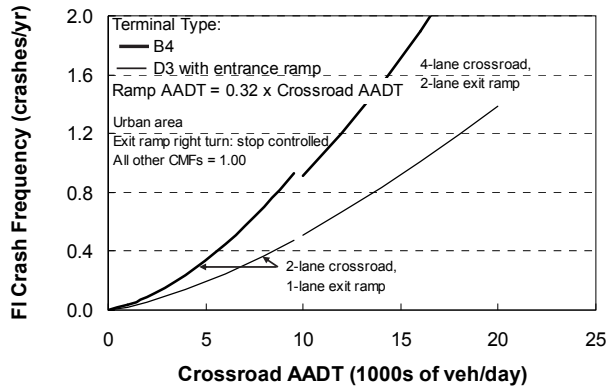


a. Fatal-and-Injury Crash Frequency



b. Property-Damage-Only Crash Frequency

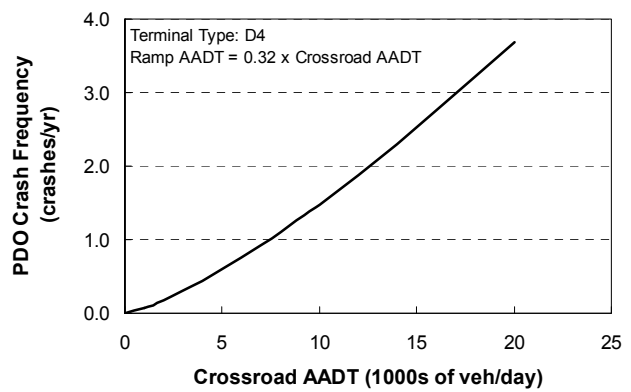
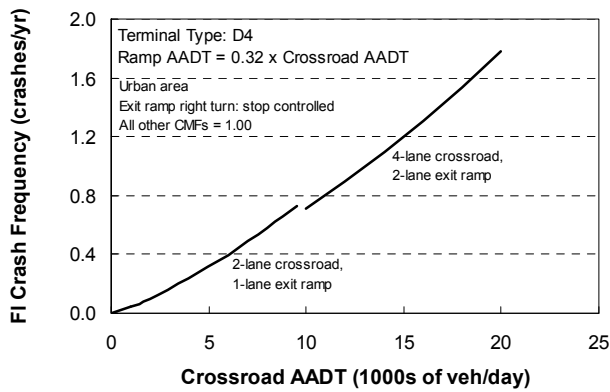
Figure 19-20. Graphical Form of the SPF Crashes at One-Way Stop-Controlled Ramp Terminals–Three-Leg Terminal with Diagonal Exit Ramp or Four-Leg Terminal at Four-Quadrant Parclo A (D3ex, A4)



a. Fatal-and-Injury Crash Frequency

b. Property-Damage-Only Crash Frequency

Figure 19-21. Graphical Form of the SPF Crashes at One-Way Stop-Controlled Ramp Terminals—Three-Leg Terminal with Diagonal Entrance Ramp or Four-Leg Terminal at Four-Quadrant Parclo B (*D3en, B4*)



a. Fatal-and-Injury Crash Frequency

b. Property-Damage-Only Crash Frequency

Figure 19-22. Graphical Form of the SPF Crashes at One-Way Stop-Controlled Ramp Terminals—Four-Leg Terminal with Diagonal Ramps (*D4*)

The value of the overdispersion parameter associated with the SPFs for one-way stop-controlled crossroad ramp terminals is computed using Equation 19-32.

$$k_{w,ST,at,z} = \frac{1}{K_{w,ST,at,z}} \tag{Equation 19-32}$$

Where:

$k_{w,ST,at,z}$ = overdispersion parameter for a stop-controlled site of type w , with n crossroad lanes, and all crash types at and severity z ; and

$K_{w,ST,at,z}$ = inverse dispersion parameter for a stop-controlled site of type w , with n crossroad lanes, and all crash types at and severity z .

The crash frequency obtained from Equation 19-31 can be multiplied by the proportions in Table 19-21 to estimate the predicted average stop-controlled crossroad ramp terminal crash frequency by crash type or crash type category.

Table 19-21. Default Distribution of One-Way Stop-Controlled Ramp Terminal Crashes by Crash Type

Area Type	Crash Type	Crash Type Category	Proportion of Crashes by Severity	
			Fatal and Injury	Property Damage Only
Rural	Multiple vehicle	Head-on	0.020	0.015
		Right-angle	0.522	0.372
		Rear-end	0.275	0.276
		Sideswipe	0.020	0.107
		Other multiple-vehicle crash	0.013	0.026
	Single vehicle	Crash with animal	0.000	0.000
		Crash with fixed object	0.078	0.158
		Crash with other object	0.000	0.005
		Crash with parked vehicle	0.007	0.015
		Other single-vehicle crashes	0.065	0.026
Urban	Multiple vehicle	Head-on	0.017	0.012
		Right-angle	0.458	0.378
		Rear-end	0.373	0.377
		Sideswipe	0.025	0.079
		Other multiple-vehicle crash	0.017	0.016
	Single vehicle	Crash with animal	0.000	0.000
		Crash with fixed object	0.085	0.110
		Crash with other object	0.000	0.000
		Crash with parked vehicle	0.000	0.008
		Other single-vehicle crashes	0.025	0.020

19.7. CRASH MODIFICATION FACTORS

This section describes the CMFs applicable to the SPFs presented in Section 19.6. These CMFs were calibrated along with the SPFs. They are summarized in Table 19-22 and Table 19-23.

Table 19-22. Ramp Segment Crash Modification Factors and their Corresponding SPFs

Applicable SPF(s)	CMF Variable	CMF Description	CMF Equations
Ramp or C-D road segments	$CMF_{1, w, x, y, z}$	Horizontal curve	Equation 19-33
	$CMF_{2, w, x, y, fi}$	Lane width	Equation 19-34
	$CMF_{3, w, x, y, z}$	Right shoulder width	Equation 19-35
	$CMF_{4, w, x, y, z}$	Left shoulder width	Equation 19-36
	$CMF_{5, w, x, y, z}$	Right side barrier	Equation 19-37
	$CMF_{6, w, x, y, z}$	Left side barrier	Equation 19-38
	$CMF_{7, w, x, y, fi}$	Lane add or drop	Equation 19-39
Multiple-vehicle crashes on ramp or C-D Road segments	$CMF_{8, w, x, mv, fi}$	Ramp speed-change lane	Equation 19-40
C-D road segments	$CMF_{9, cds, ac, y, z}$	Weaving section	Equation 19-41

Note: Subscripts to the CMF variables use the following notation:

- Site type w ($w = rps$: ramp segment, cds : C-D road segment),
- Cross section x ($x = n$: n -lane C-D road, nEN : n -lane entrance ramp, nEX : n -lane exit ramp, ac : any cross section),
- Crash type y ($y = sv$: single vehicle, mv : multiple vehicle, at : all types), and
- Severity z ($z = fi$: fatal and injury, pdo : property damage only, as : all severities).

Many of the CMFs in Table 19-22 and Table 19-23 are developed for specific site types, cross sections, crash types, or crash severities. This approach was undertaken to make the predictive model sensitive to the geometric design and traffic control features of specific sites with specific cross sections, in terms of their influence on specific crash types and severities. The subscripts for each CMF variable indicate the sites, cross sections, crash types, and severities to which each CMF is applicable. The subscript definitions are provided in the table footnote. In some cases, a CMF is applicable to several site types, cross sections, crash types, or severities. In these cases, the subscript retains the generic letter w , x , y , or z , as appropriate. The discussion of these CMFs in Section 19.7.1 or 19.7.2 identifies the specific site types, cross sections, crash types, or severities to which they apply.

As indicated in Table 19-22, some of the CMFs apply to both ramp segments and C-D road segments. For some of the CMFs, supplemental calculations must be performed before the CMF value can be computed. For example, to apply the Right side barrier CMF, the proportion of the segment length having barrier on the right side and the length-weighted average barrier offset (as measured from the edge of the outside shoulder) must be computed. Procedures for supplemental calculations are described in Section 19.7.3.

Table 19-23. Crossroad Ramp Terminal Crash Modification Factors and their Corresponding SPFs

Applicable SPF(s)	CMF Variable	CMF Description	CMF Equations
Signal-controlled or one-way stop-controlled ramp terminals	$CMF_{10, w, x, at, fi}$	Exit ramp capacity	Equation 19-42
	$CMF_{11, w, x, at, z}$	Crossroad left-turn lane	Equation 19-45
	$CMF_{12, w, x, at, z}$	Crossroad right-turn lane	Equation 19-48
	$CMF_{13, w, x, at, z}$	Access point frequency	Equation 19-49
	$CMF_{14, w, x, at, z}$	Segment length	Equation 19-50
	$CMF_{15, w, x, at, z}$	Median width	Equation 19-51
Signal-controlled crossroad ramp terminals	$CMF_{16, w, SGn, at, z}$	Protected left-turn operation	Equation 19-53
	$CMF_{17, w, SGn, at, z}$	Channelized right turn on crossroad	Equation 19-55
	$CMF_{18, w, SGn, at, z}$	Channelized right turn on exit ramp	Equation 19-56
	$CMF_{19, w, SGn, at, z}$	Non-ramp public street leg	Equation 19-57
One-way stop-controlled ramp terminals	$CMF_{20, w, ST, at, fi}$	Skew angle	Equation 19-58

Note: Subscripts to the CMF variables use the following notation:

- Site type w ($w = D3ex, D3en, D4, A4, B4, A2, B2$),
- Cross section x ($x = ST$: one-way stop control; SGn : signal control with n -lane crossroad; ac : any cross section),
- Crash type y ($y = sv$: single vehicle, mv : multiple vehicle, at : all types), and
- Severity z ($z = fi$: fatal and injury, pdo : property damage only, as : all severities).

19.7.1. Crash Modification Factors for Ramp Segments

The CMFs for geometric design and traffic control features of freeway segments are presented in this section.

$CMF_{1, w, x, y, z}$ —Horizontal Curve

Four CMFs are used to describe the relationship between horizontal curve geometry and predicted crash frequency. The six fatal-and-injury SPFs to which they apply are identified in the following list:

- SPF for fatal-and-injury multiple-vehicle crashes, n -lane entrance ramp (rps, nEN, mv, fi);
- SPF for fatal-and-injury single-vehicle crashes, n -lane entrance ramp (rps, nEN, sv, fi);
- SPF for fatal-and-injury multiple-vehicle crashes, n -lane exit ramp (rps, nEX, mv, fi);
- SPF for fatal-and-injury single-vehicle crashes, n -lane exit ramp (rps, nEX, sv, fi);
- SPF for fatal-and-injury multiple-vehicle crashes, n -lane C-D road (cds, n, mv, fi); and
- SPF for fatal-and-injury single-vehicle crashes, n -lane C-D road (cds, n, sv, fi).

The six property-damage-only SPFs to which these CMFs apply are not shown in the previous list. However, the only difference is that the fi subscript (shown in parentheses in the previous list) is replaced by pdo .

The base condition is an uncurved (i.e., tangent) segment. The CMFs are described using the following equation.

$$CMF_{l,w,x,y,z} = 1.0 + a \times \frac{1,000}{32.2} \left[\sum_{i=1}^m \left(\frac{v_{ent,i}}{R_i} \right)^2 P_{c,i} \right] \quad \text{Equation 19-33}$$

Where:

$CMF_{l,w,x,y,z}$ = crash modification factor for horizontal curvature on a site of type w , cross section x , crash type y , and severity z ;

$v_{ent,i}$ = average entry speed for curve i (ft/s);

R_i = radius of curve i (ft);

$P_{c,i}$ = proportion of segment length with curve i ; and

m = number of horizontal curves in the segment.

The regression coefficient for Equation 19-33 is provided in Table 19-24. Equation 19-33 is derived to recognize that more than one curve may exist in a segment and that a curve may be located only partially in the segment (and partially on an adjacent segment). The variable $P_{c,i}$ is computed as the ratio of the length of curve i in the segment to the length of the segment (i.e., L_r or L_{cd}). For example, consider a segment that is 0.5 mi long and a curve that is 0.2 mi long. If one-half of the curve is in the segment, then $P_{c,i} = 0.20$ ($= 0.1/0.5$). In fact, this proportion is the same regardless of the curve's length (provided that it is 0.1 mi or longer and 0.1 mi of this curve is located in the segment).

Table 19-24. Coefficients for Horizontal Curve CMF—Ramp and C-D Road Segments

Cross Section (x)	Crash Type (y)	Crash Severity (z)	CMF Variable	Regression Coefficient (a)
Any cross section (ac)	Multiple vehicle (mv)	Fatal and injury (fi)	$CMF_{l,w,ac,mv,fi}$	0.779
		Property damage only (pdo)	$CMF_{l,w,ac,mv,pdo}$	0.545
	Single vehicle (sv)	Fatal and injury (fi)	$CMF_{l,w,ac,sv,fi}$	2.406
		Property damage only (pdo)	$CMF_{l,w,ac,sv,pdo}$	3.136

Details regarding the measurement of radius and curve length are provided in Section 19.4. A procedure for estimating the average curve entry speed is provided in Section 19.7.3. The CMF is applicable to curves with a radius of 100 ft or larger.

$CMF_{2,w,x,y,n}$ —Lane Width

Two CMFs are used to describe the relationship between average lane width and predicted crash frequency. The SPFs to which they apply are identified in the following list:

- SPF for fatal-and-injury multiple-vehicle crashes, n -lane entrance ramp (rps, nEN, mv, fi);
- SPF for fatal-and-injury single-vehicle crashes, n -lane entrance ramp (rps, nEN, sv, fi);

- SPF for fatal-and-injury multiple-vehicle crashes, n -lane exit ramp (rps, nEX, mv, fi);
- SPF for fatal-and-injury single-vehicle crashes, n -lane exit ramp (rps, nEX, sv, fi);
- SPF for fatal-and-injury multiple-vehicle crashes, n -lane C-D road (cds, n, mv, fi); and
- SPF for fatal-and-injury single-vehicle crashes, n -lane C-D road (cds, n, sv, fi).

The base condition is a 14-ft lane width. The CMFs are described using the following equation.

$$CMF_{2, w, x, y, fi} = \exp(a \times [W_l - 14])$$

Equation 19-34

Where:

$CMF_{2, w, x, y, fi}$ = crash modification factor for lane width on a site of type w , cross section x , crash type y , and fatal-and-injury crashes fi ; and

W_l = lane width (ft).

The regression coefficient for Equation 19-34 is provided in Table 19-25. In fact, the coefficient value is the same for both crash types listed in the table, which indicates that the CMF value is the same for the corresponding SPFs. The CMF is applicable to lane widths in the range of 10 to 20 ft.

Table 19-25. Coefficients for Lane Width CMF—Ramp and C-D Road Segments

Cross Section (x)	Crash Type (y)	Crash Severity (z)	CMF Variable	Regression Coefficient (a)
Any cross section (ac)	Multiple vehicle (mv)	Fatal and injury (fi)	$CMF_{2, w, ac, mv, fi}$	-0.0458
	Single vehicle (sv)	Fatal and injury (fi)	$CMF_{2, w, ac, sv, fi}$	-0.0458

$CMF_{3, w, x, y, z}$ —Right Shoulder Width

Four CMFs are used to describe the relationship between average right shoulder width and predicted crash frequency. The six fatal-and-injury SPFs to which they apply are identified in the following list:

- SPF for fatal-and-injury multiple-vehicle crashes, n -lane entrance ramp (rps, nEN, mv, fi);
- SPF for fatal-and-injury single-vehicle crashes, n -lane entrance ramp (rps, nEN, sv, fi);
- SPF for fatal-and-injury multiple-vehicle crashes, n -lane exit ramp (rps, nEX, mv, fi);
- SPF for fatal-and-injury single-vehicle crashes, n -lane exit ramp (rps, nEX, sv, fi);
- SPF for fatal-and-injury multiple-vehicle crashes, n -lane C-D road (cds, n, mv, fi); and
- SPF for fatal-and-injury single-vehicle crashes, n -lane C-D road (cds, n, sv, fi).

The six property-damage-only SPFs to which these CMFs apply are not shown in the previous list. However, the only difference is that the fi subscript (shown in parentheses in the previous list) is replaced by pdo .

The base condition is an 8-ft shoulder width. The CMFs are described using the following equation.

$$CMF_{3,w,x,y,z} = \exp(a \times [W_{rs} - 8]) \quad \text{Equation 19-35}$$

Where:

$CMF_{3,w,x,y,z}$ = crash modification factor for the right shoulder width on a site of type w , cross section x , crash type y , and severity z ; and

W_{rs} = right shoulder width (ft).

The regression coefficient for Equation 19-35 is provided in Table 19-26. For a given severity, the coefficient values are the same for both crash types listed in the table, which indicates that the CMF value is the same for the corresponding SPFs. The CMF is applicable to shoulder widths in the range of 2 to 12 ft.

Table 19-26. Coefficients for Right Shoulder Width CMF—Ramp and C-D Road Segments

Cross Section (x)	Crash Type (y)	Crash Severity (z)	CMF Variable	Regression Coefficient (a)
Any cross section (ac)	Multiple vehicle (mv)	Fatal and injury (fi)	$CMF_{3,w,ac,mv,fi}$	-0.0539
		Property damage only (pdo)	$CMF_{3,w,ac,mv,pdo}$	-0.0259
	Single vehicle (sv)	Fatal and injury (fi)	$CMF_{3,w,ac,sv,fi}$	-0.0539
		Property damage only (pdo)	$CMF_{3,w,ac,sv,pdo}$	-0.0259

$CMF_{4,w,x,y,z}$ —Left Shoulder Width

Four CMFs are used to describe the relationship between average left shoulder width and predicted crash frequency. The six fatal-and-injury SPFs to which they apply are identified in the following list:

- SPF for fatal-and-injury multiple-vehicle crashes, n -lane entrance ramp (rps, nEN, mv, fi);
- SPF for fatal-and-injury single-vehicle crashes, n -lane entrance ramp (rps, nEN, sv, fi);
- SPF for fatal-and-injury multiple-vehicle crashes, n -lane exit ramp (rps, nEX, mv, fi);
- SPF for fatal-and-injury single-vehicle crashes, n -lane exit ramp (rps, nEX, sv, fi);
- SPF for fatal-and-injury multiple-vehicle crashes, n -lane C-D road (cds, n, mv, fi); and
- SPF for fatal-and-injury single-vehicle crashes, n -lane C-D road (cds, n, sv, fi).

The six property-damage-only SPFs to which these CMFs apply are not shown in the previous list. However, the only difference is that the fi subscript (shown in parentheses in the previous list) is replaced by pdo .

The base condition is a 4-ft shoulder width. The CMFs are described using the following equation.

$$CMF_{4,w,x,y,z} = \exp(a \times [W_{ls} - 4]) \quad \text{Equation 19-36}$$

Where:

$CMF_{4, w, x, y, z}$ = crash modification factor for the left shoulder width on a site of type w , cross section x , crash type y , and severity z ; and

W_{ls} = left shoulder width (ft).

The regression coefficient for Equation 19-36 is provided in Table 19-27. For a given severity, the coefficient values are the same for both crash types listed in the table, which indicates that the CMF value is the same for the corresponding SPFs. The CMF is applicable to shoulder widths in the range of 2 to 10 ft.

Table 19-27. Coefficients for Left Shoulder Width CMF–Ramp and C-D Road Segments

Cross Section (x)	Crash Type (y)	Crash Severity (z)	CMF Variable	Regression Coefficient (a)
Any cross section (ac)	Multiple vehicle (mv)	Fatal and injury (fi)	$CMF_{4, w, ac, mv, fi}$	-0.0539
		Property damage only (pdo)	$CMF_{4, w, ac, mv, pdo}$	-0.0259
	Single vehicle (sv)	Fatal and injury (fi)	$CMF_{4, w, ac, sv, fi}$	-0.0539
		Property damage only (pdo)	$CMF_{4, w, ac, sv, pdo}$	-0.0259

$CMF_{5, w, x, y, z}$ —Right Side Barrier

Four CMFs are used to describe the relationship between right side barrier presence and predicted crash frequency. The six fatal-and-injury SPFs to which they apply are identified in the following list:

- SPF for fatal-and-injury multiple-vehicle crashes, n -lane entrance ramp (rps, nEN, mv, fi);
- SPF for fatal-and-injury single-vehicle crashes, n -lane entrance ramp (rps, nEN, sv, fi);
- SPF for fatal-and-injury multiple-vehicle crashes, n -lane exit ramp (rps, nEX, mv, fi);
- SPF for fatal-and-injury single-vehicle crashes, n -lane exit ramp (rps, nEX, sv, fi);
- SPF for fatal-and-injury multiple-vehicle crashes, n -lane C-D road (cds, n, mv, fi); and
- SPF for fatal-and-injury single-vehicle crashes, n -lane C-D road (cds, n, sv, fi).

The six property-damage-only SPFs to which these CMFs apply are not shown in the previous list. However, the only difference is that the fi subscript (shown in parentheses in the previous list) is replaced by pdo .

The base condition is no barrier present on the right side of the ramp. The CMFs are described using the following equation.

$$CMF_{5, w, x, y, z} = (1.0 - P_{rb}) \times 1.0 + P_{rb} \times \exp\left(\frac{a}{W_{rcb}}\right) \quad \text{Equation 19-37}$$

Where:

$CMF_{5, w, x, y, z}$ = crash modification factor for right side barrier on a site of type w , cross section x , crash type y , and severity z ; and

P_{rb} = proportion of segment length with a barrier present on the right side; and

W_{rcb} = distance from edge of right shoulder to barrier face (ft).

The regression coefficient for Equation 19-37 is provided in Table 19-28. For a given severity, the coefficient values are the same for both crash types listed in the table, which indicates that the CMF value is the same for the corresponding SPFs. Guidance for computing the variables P_{rb} and W_{rcb} is provided in Section 19.7.3. The CMF is applicable to W_{rcb} values in the range of 0.75 to 25 ft. This CMF is applicable to cable barrier, concrete barrier, guardrail, and bridge rail.

Table 19-28. Coefficients for Right Side Barrier CMF–Ramp and C-D Road Segments

Cross Section (x)	Crash Type (y)	Crash Severity (z)	CMF Variable	Regression Coefficient (a)
Any cross section (ac)	Multiple vehicle (mv)	Fatal and injury (fi)	$CMF_{5, w, ac, mv, fi}$	0.210
		Property damage only (pdo)	$CMF_{5, w, ac, mv, pdo}$	0.193
	Single vehicle (sv)	Fatal and injury (fi)	$CMF_{5, w, ac, sv, fi}$	0.210
		Property damage only (pdo)	$CMF_{5, w, ac, sv, pdo}$	0.193

CMF_{6, w, x, y, z}—Left Side Barrier

Four CMFs are used to describe the relationship between left side barrier presence and predicted crash frequency. The six fatal-and-injury SPFs to which they apply are identified in the following list:

- SPF for fatal-and-injury multiple-vehicle crashes, n -lane entrance ramp (rps, nEN, mv, fi);
- SPF for fatal-and-injury single-vehicle crashes, n -lane entrance ramp (rps, nEN, sv, fi);
- SPF for fatal-and-injury multiple-vehicle crashes, n -lane exit ramp (rps, nEX, mv, fi);
- SPF for fatal-and-injury single-vehicle crashes, n -lane exit ramp (rps, nEX, sv, fi);
- SPF for fatal-and-injury multiple-vehicle crashes, n -lane C-D road (cds, n, mv, fi); and
- SPF for fatal-and-injury single-vehicle crashes, n -lane C-D road (cds, n, sv, fi).

The six property-damage-only SPFs to which these CMFs apply are not shown in the previous list. However, the only difference is that the fi subscript (shown in parentheses in the previous list) is replaced by pdo .

The base condition is no barrier present on the left side of the ramp. The CMFs are described using the following equation.

$$CMF_{6, w, x, y, z} = (1.0 - P_{lb}) \times 1.0 + P_{lb} \times \exp\left(\frac{a}{W_{lcb}}\right) \quad \text{Equation 19-38}$$

Where:

$CMF_{6, w, x, y, z}$ = crash modification factor for left side barrier on a site of type w , cross section x , crash type y , and severity z ; and

P_{lb} = proportion of segment length with a barrier present on the left side; and

W_{lcb} = distance from edge of left shoulder to barrier face (ft).

The regression coefficient for Equation 19-38 is provided in Table 19-29. For a given severity, the coefficient values are the same for both crash types listed in the table, which indicates that the CMF value is the same for the corresponding SPFs. Guidance for computing the variables P_{lb} and W_{lcb} is provided in Section 19.7.3. The CMF is applicable to W_{lcb} values in the range of 0.75 to 24 ft. This CMF is applicable to cable barrier, concrete barrier, guardrail, and bridge rail.

Table 19-29. Coefficients for Left Side Barrier CMF–Ramp and C-D Road Segments

Cross Section (x)	Crash Type (y)	Crash Severity (z)	CMF Variable	Regression Coefficient (a)
Any cross section (ac)	Multiple vehicle (mv)	Fatal and injury (fi)	$CMF_{\delta, w, ac, mv, fi}$	0.210
		Property damage only (pdo)	$CMF_{\delta, w, ac, mv, pdo}$	0.193
	Single vehicle (sv)	Fatal and injury (fi)	$CMF_{\delta, w, ac, sv, fi}$	0.210
		Property damage only (pdo)	$CMF_{\delta, w, ac, sv, pdo}$	0.193

CMF_{7, w, x, y, fi}—Lane Add or Drop

Two CMFs are used to describe the relationship between a change in lanes and predicted crash frequency. The SPFs to which they apply are identified in the following list:

- SPF for fatal-and-injury multiple-vehicle crashes, n -lane entrance ramp (rps, nEN, mv, fi);
- SPF for fatal-and-injury single-vehicle crashes, n -lane entrance ramp (rps, nEN, sv, fi);
- SPF for fatal-and-injury multiple-vehicle crashes, n -lane exit ramp (rps, nEX, mv, fi);
- SPF for fatal-and-injury single-vehicle crashes, n -lane exit ramp (rps, nEX, sv, fi);
- SPF for fatal-and-injury multiple-vehicle crashes, n -lane C-D road (cds, n, mv, fi); and
- SPF for fatal-and-injury single-vehicle crashes, n -lane C-D road (cds, n, sv, fi).

The base condition is no lane change (i.e., no lanes added or dropped). The CMFs are described using the following equation.

$$CMF_{7, w, x, y, fi} = (1.0 - P_{tpr}) \times 1.0 + P_{tpr} \times \exp(a \times [I_{add} - I_{drop}]) \quad \text{Equation 19-39}$$

Where:

$CMF_{7, w, x, y, fi}$ = crash modification factor for lane add or drop on a site of type w , cross section x , crash type y , and fatal-and-injury crashes fi ;

P_{tpr} = proportion of segment length adjacent to the taper associated with a lane add or drop;

I_{add} = lane add indicator variable (= 1.0 if one or more lanes are added, 0.0 otherwise); and

I_{drop} = lane drop indicator variable (= 1.0 if one or more lanes are dropped, 0.0 otherwise).

The regression coefficient for Equation 19-39 is provided in Table 19-30. In fact, the coefficient value is the same for both crash types listed in the table, which indicates that the CMF value is the same for the corresponding SPFs. The variable P_{tpr} is computed as the ratio of the length of the lane add (or drop) taper in the segment to the length of the segment. If the segment is wholly located in the taper, then this variable is equal to 1.0.

Table 19-30. Coefficients for Lane Add or Drop CMF—Ramp and C-D Road Segments

Cross Section (x)	Crash Type (y)	Crash Severity (z)	CMF Variable	Regression Coefficient (a)
Any cross section (ac)	Multiple vehicle (mv)	Fatal and injury (fi)	$CMF_{7, w, ac, mv, fi}$	-0.231
	Single vehicle (sv)	Fatal and injury (fi)	$CMF_{7, w, ac, sv, fi}$	-0.231

This CMF is not used with the Weaving section CMF. If a C-D road segment is being evaluated, either the Lane add or drop CMF is used for the subject segment or the Weaving section CMF is used.

If a lane add occurs as a result of a ramp-to-ramp merge, then a taper does not exist and this CMF is not used. Similarly, if a lane drop occurs as a result of a ramp-to-ramp diverge, then a taper does not exist and this CMF is not used.

CMF_{8, w, x, mv, fi}—Ramp Speed-Change Lane

One CMF is used to describe the relationship between ramp speed-change lane presence and predicted crash frequency. The SPFs to which it applies are identified in the following list:

- SPF for fatal-and-injury multiple-vehicle crashes, n -lane entrance ramp (rps, nEN, mv, fi);
- SPF for fatal-and-injury multiple-vehicle crashes, n -lane exit ramp (rps, nEX, mv, fi); and
- SPF for fatal-and-injury multiple-vehicle crashes, n -lane C-D road (cds, n, mv, fi).

The base condition is no ramp speed-change lane present. The CMF is described using the following equation.

$$CMF_{8, w, x, mv, fi} = (1.0 - P_{en-ex}) \times 1.0 + P_{en-ex} \times \exp(0.310) \quad \text{Equation 19-40}$$

Where:

$CMF_{8, w, x, mv, fi}$ = crash modification factor for speed-change lane presence on a site of type w , cross section x , and with multiple-vehicle mv fatal-and-injury crashes fi ; and

P_{en-ex} = proportion of segment length that is adjacent to the speed-change lane for a connecting ramp.

This CMF is used to evaluate a ramp or C-D road segment that is being joined by another ramp by way of a speed-change lane. The speed-change lane can be either an acceleration lane or a deceleration lane. This CMF is not used with the Weaving section CMF because the ramps in weaving section are joined by an auxiliary lane (i.e., they do not have a speed-change lane).

The variable P_{en-ex} in Equation 19-40 is computed as the ratio of the length of the ramp speed-change lane in the segment to the length of the segment. If the segment is wholly located in the speed-change lane, then this variable is equal to 1.0. If this CMF is used with the Lane add or drop CMF, then the variable P_{en-ex} is equal to the variable P_{lpr} .

CMF_{9, cds, ac, y, z}—Weaving Section

Two CMFs are used to describe the relationship between weaving section presence and predicted crash frequency. The four SPFs to which they apply are identified in the following list:

- SPF for fatal-and-injury multiple-vehicle crashes, n -lane C-D road (cds, n, mv, fi);
- SPF for property-damage-only multiple-vehicle crashes, n -lane C-D road (cds, n, mv, pdo);
- SPF for fatal-and-injury single-vehicle crashes, n -lane C-D road (cds, n, sv, fi); and
- SPF for property-damage-only single-vehicle crashes, n -lane C-D road (cds, n, sv, pdo).

The base condition is no weaving section on the C-D road segment. The CMFs are described using the following equation.

$$CMF_{9, cds, ac, y, z} = (1.0 - P_{wev}) \times 1.0 + P_{wev} \times \exp\left(\frac{a + b \times \ln[c \times AADT_c]}{L_{wev}}\right) \quad \text{Equation 19-41}$$

Where:

$CMF_{9, cds, ac, y, z}$ = crash modification factor for weaving section presence on a C-D road segment with any cross section ac , crash type y , and severity z ;

$AADT_c$ = AADT volume of C-D road segment (veh/day);

P_{wev} = proportion of segment length within a weaving section; and

L_{wev} = weaving section length (may extend beyond segment boundaries) (mi).

The regression coefficients for Equation 19-41 are provided in Table 19-31. The variable P_{wev} in Equation 19-41 is computed as the ratio of the length of the weaving section in the segment to the length of the segment. If the segment is wholly located in the weaving section, then this variable is equal to 1.0.

Table 19-31. Coefficients for Weaving Section CMF—C-D Road Segments

Cross Section (x)	Crash Type (y)	Crash Severity (z)	CMF Variable	Regression Coefficients		
				a	b	c
Any cross section (ac)	All types (mv)	Fatal and injury (fi)	$CMF_{9, cds, ac, mv, fi}$	0.191	-0.0715	0.001
		Property damage only (pdo)	$CMF_{9, cds, ac, mv, pdo}$	0.187	-0.0580	0.001
	All types (sv)	Fatal and injury (fi)	$CMF_{9, cds, ac, sv, fi}$	0.191	-0.0715	0.001
		Property damage only (pdo)	$CMF_{9, cds, ac, sv, pdo}$	0.187	-0.0580	0.001

This CMF is used to evaluate C-D road segments that have some or all of their length in a weaving section. This CMF is not used with the Ramp speed-change lane CMF or the Lane add or drop CMF.

The variable for weaving section length L_{wev} in Equation 19-41 is intended to reflect the degree to which the weaving activity is concentrated along the C-D road. The CMF is applicable to weaving section lengths in the range from 0.05 to 0.30 mi.

19.7.2. Crash Modification Factors for Ramp Terminals

The CMFs for geometric design and traffic control features of crossroad ramp terminals are presented in this section.

CMF_{10, w, x, at, fi}—Exit Ramp Capacity

Excessively long queues on exit ramps are recognized as sometimes creating unsafe operating conditions. Crash risk tends to increase as the length of ramp available for deceleration to the back of queue is reduced due to long queues at the downstream ramp terminal. The Exit ramp capacity CMF is derived to capture this influence.

Two CMFs are used to describe the relationship between exit ramp capacity and predicted crash frequency. The SPFs applicable to three-leg terminals with a diagonal exit ramp (*D3ex*) are identified in the following list:

- SPF for fatal-and-injury crashes, three-legs with diagonal exit ramp, stop control, n lanes (*D3ex, ST, at, fi*); and
- SPF for fatal-and-injury crashes, three-legs with diagonal exit ramp, signal control, n lanes (*D3ex, SGn, at, fi*).

There are two more SPFs for each of six terminal configurations (i.e., site types) to which these CMFs apply. They are not shown in the previous list. However, the only difference is that the *D3ex* subscript (shown in parentheses in the previous list) is replaced by the other configuration subscripts (*D3en, D4, A4, B4, A2, B2*).

The CMFs are described using the following equation.

$$CMF_{10, w, x, at, fi} = (1.0 - P_{ex}) \times 1.0 + P_{ex} \times \exp \left(a \times \frac{c \times AADT_{ex}}{n_{ex, eff}} \right) \quad \text{Equation 19-42}$$

with,

$$n_{ex, eff} = \begin{cases} 0.5 \times (n_{ex} - 1.0) + 1.0 & : \text{merge or free-flow right turn} \\ 0.5 \times n_{ex} & : \text{signal, stop, or yield-controlled right turn} \end{cases} \quad \text{Equation 19-43}$$

$$P_{ex} = \frac{AADT_{ex}}{AADT_{in} + AADT_{out} + AADT_{en} + AADT_{ex}} \quad \text{Equation 19-44}$$

Where:

$CMF_{10, w, x, at, fi}$ = crash modification factor for exit ramp capacity at a site of type w , control type x , and all types at of fatal-and-injury crashes;

P_{ex} = proportion of total leg AADT on exit ramp leg;

$AADT_{en}$ = AADT volume for the entrance ramp (veh/day);

- $AADT_{ex}$ = AADT volume for the exit ramp (veh/day);
- $AADT_{in}$ = AADT volume for the crossroad leg between ramps (veh/day);
- $AADT_{out}$ = AADT volume for the crossroad leg outside of interchange (veh/day);
- $n_{ex, eff}$ = effective number of lanes serving exit ramp traffic (lanes); and
- n_{ex} = number of lanes serving exit ramp traffic (lanes).

The regression coefficients for Equation 19-42 are provided in Table 19-32. When computing P_{ex} , the AADT volume of the loop exit ramp at a *B4* terminal configuration is not included in $AADT_{ex}$. Similarly, the AADT volume of the loop entrance ramp at an *A4* configuration is not included in $AADT_{en}$.

Table 19-32. Coefficients for Exit Ramp Capacity CMF–Crossroad Ramp Terminals

Control Type (<i>x</i>)	Crash Type (<i>y</i>)	Crash Severity (<i>z</i>)	CMF Variable	Regression Coefficients	
				<i>a</i>	<i>c</i>
One-way stop control (<i>ST</i>)	All types (<i>at</i>)	Fatal and injury (<i>fi</i>)	$CMF_{10, w, ST, at, fi}$	0.151	0.001
Signal control, <i>n</i> lanes (<i>SGn</i>)	All types (<i>at</i>)	Fatal and injury (<i>fi</i>)	$CMF_{10, w, SGn, at, fi}$	0.0668	0.001

The effective number of lanes is based on the number of lanes on the exit ramp at the terminal, and the type of control used for the exit ramp right-turn movement. The constant “0.5” in Equation 19-43 approximately represents the ratio of capacity for a signal, stop, or yield controlled lane to the capacity of a free-flow lane.

Figure 19-23 illustrates the use of Equation 19-43 to calculate the effective number of lanes for various exit ramp configurations. This figure also indicates that all lanes counted need to be fully developed for 100 ft or more upstream from the point at which their respective movement intersects with the crossroad (as discussed in Section 19.4.2).

Figure 19-23 shows eight exit ramps in plan view. The four ramps on the left side of the figure have two lanes serving exit ramp traffic. The four ramps on the right side of the figure have one lane serving exit ramp traffic (because the lane development is less than 100 ft). The two ramps at the bottom of the figure have merge or free-flow operation for the ramp right-turn movement. The other ramps have signal, stop, or yield control for the right-turn movement. The computed number of effective lanes is typically less than the actual lanes (i.e., $n_{ex, eff} \leq n_{ex}$) due to the control used for the ramp movement.

This CMF is applicable to stop-controlled terminals with one or two lanes serving exit ramp traffic. It is applicable to signal-controlled terminals with one, two, three, or four lanes serving exit ramp traffic.

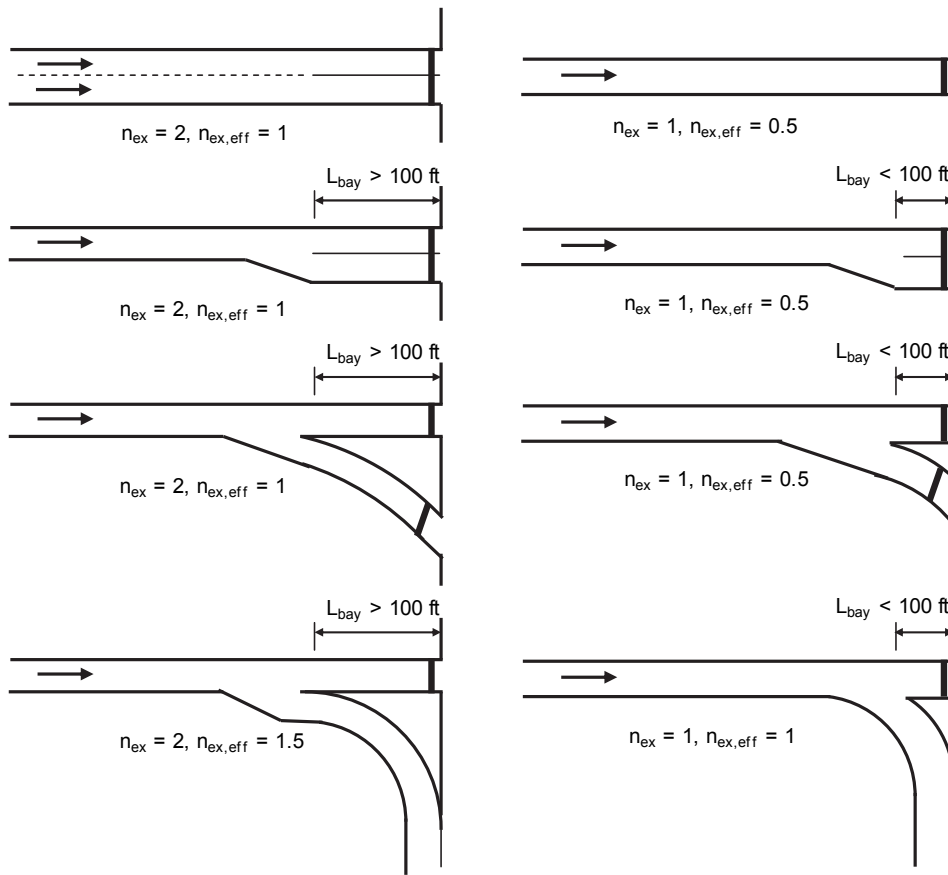


Figure 19-23. Effective Number of Lanes for Various Exit Ramp Configurations

CMF_{11, w, x, at, z}—Crossroad Left-Turn Lane

Eight CMFs are used to describe the relationship between left-turn lane (or bay) presence and predicted crash frequency. The SPFs applicable to three-leg terminals with a diagonal exit ramp (*D3ex*) are identified in the following list:

- SPF for fatal-and-injury crashes, three-legs with diagonal exit ramp, stop control, *n* lanes (*D3ex, ST, at, fi*);
- SPF for property-damage-only crashes, three-legs with diagonal exit ramp, stop control, *n* lanes (*D3ex, ST, at, pdo*);
- SPF for fatal-and-injury crashes, three-legs with diagonal exit ramp, signal control, *n* lanes (*D3ex, SGn, at, fi*); and
- SPF for property-damage-only crashes, three-legs with diagonal exit ramp, signal control, *n* lanes (*D3ex, SGn, at, pdo*).

There are four more SPFs for each of six terminal configurations (i.e., site types) to which these CMFs apply. They are not shown in the previous list. However, the only difference is that the *D3ex* subscript (shown in parentheses in the previous list) is replaced by the other configuration subscripts (*D3en, D4, A4, B4, A2, B2*).

The base condition is no left-turn lane (or bay) present. The CMFs are described using the following equation.

$$CMF_{11, w, x, at, z} = [(1.0 - P_{in}) \times 1.0 + P_{in} \times a]^{I_{bay, lt, in}} \times [(1.0 - P_{out}) \times 1.0 + P_{out} \times a]^{I_{bay, lt, out}} \tag{Equation 19-45}$$

with,

$$P_{in} = \frac{AADT_{in}}{AADT_{in} + AADT_{out} + AADT_{en} + AADT_{ex}} \quad \text{Equation 19-46}$$

$$P_{out} = \frac{AADT_{out}}{AADT_{in} + AADT_{out} + AADT_{en} + AADT_{ex}} \quad \text{Equation 19-47}$$

Where:

$CMF_{11, w, x, at, z}$ = crash modification factor for left-turn lane (or bay) presence at a site of type w , control type x , all crash types at , and severity z ;

P_{in} = proportion of total leg AADT on crossroad leg between ramps;

P_{out} = proportion of total leg AADT on crossroad leg outside of interchange; and

$I_{bay, lt, k}$ = left-turn lane (or bay) indicator variable for crossroad leg k ($k = in$ or out) (= 1.0 if left-turn lane [or bay] is present, 0.0 otherwise).

The regression coefficient for Equation 19-45 is provided in Table 19-33. When computing P_{in} and P_{out} , the AADT volume of the loop exit ramp at a $B4$ terminal configuration is not included in $AADT_{ex}$. Similarly, the AADT volume of the loop entrance ramp at an $A4$ configuration is not included in $AADT_{en}$.

Table 19-33. Coefficients for Crossroad Left-Turn Lane CMF—Crossroad Ramp Terminals

Control Type (x)	Area Type	Crash Type (y)	Crash Severity (z)	CMF Variable	Regression Coefficient (a)
One-way stop control (ST)	Rural	All types (at)	Fatal and injury (fi)	$CMF_{11, w, ST, at, fi}$	0.36
			Property damage only (pdo)	$CMF_{11, w, ST, at, pdo}$	0.55
	Urban	All types (at)	Fatal and injury (fi)	$CMF_{11, w, ST, at, fi}$	0.59
			Property damage only (pdo)	$CMF_{11, w, ST, at, pdo}$	0.58
Signal control, n lanes (SGn)	Rural	All types (at)	Fatal and injury (fi)	$CMF_{11, w, SGn, at, fi}$	0.44
			Property damage only (pdo)	$CMF_{11, w, SGn, at, pdo}$	0.66
	Urban	All types (at)	Fatal and injury (fi)	$CMF_{11, w, SGn, at, fi}$	0.65
			Property damage only (pdo)	$CMF_{11, w, SGn, at, pdo}$	0.68

This CMF is applicable to any crossroad approach that is either signalized or uncontrolled. It is not applicable to a stop-controlled approach. The CMF value is applicable to turn bays that have a design that is consistent with agency policy such that their length adequately provides for vehicle storage or deceleration, as appropriate.

CMF_{12, w, x, at, z}—Crossroad Right-Turn Lane

Eight CMFs are used to describe the relationship between right-turn lane (or bay) presence and predicted crash frequency. The SPFs applicable to three-leg terminals with a diagonal exit ramp ($D3ex$) are identified in the following list:

- SPF for fatal-and-injury crashes, three-legs with diagonal exit ramp, stop control, n lanes ($D3ex, ST, at, fi$);
- SPF for property-damage-only crashes, three-legs with diagonal exit ramp, stop control, n lanes ($D3ex, ST, at, pdo$);
- SPF for fatal-and-injury crashes, three-legs with diagonal exit ramp, signal control, n lanes ($D3ex, SGn, at, fi$); and
- SPF for property-damage-only crashes, three-legs with diagonal exit ramp, signal control, n lanes ($D3ex, SGn, at, pdo$).

There are four more SPFs for each of six terminal configurations (i.e., site types) to which these CMFs apply. They are not shown in the previous list. However, the only difference is that the $D3ex$ subscript (shown in parentheses in the previous list) is replaced by the other configuration subscripts ($D3en, D4, A4, B4, A2, B2$).

The base condition is no right-turn lane (or bay) present. The CMFs are described using the following equation.

$$CMF_{12, w, x, at, z} = [(1.0 - P_{in}) \times 1.0 + P_{in} \times a]^{I_{bay, rt, in}} \times [(1.0 - P_{out}) \times 1.0 + P_{out} \times a]^{I_{bay, rt, out}} \tag{Equation 19-48}$$

Where:

$CMF_{12, w, x, at, z}$ = crash modification factor for right-turn lane (or bay) presence at a site of type w , control type x , all crash types at , and severity z ; and

$I_{bay, rt, k}$ = right-turn lane (or bay) indicator variable for crossroad leg k ($k = in$ or out) (= 1.0 if right-turn lane [or bay] is present, 0.0 otherwise).

The regression coefficient for Equation 19-48 is provided in Table 19-34. The variable P_{in} is computed using Equation 19-46. The variable P_{out} is computed using Equation 19-47.

This CMF is applicable to any crossroad approach that is either signalized or uncontrolled. It is not applicable to a stop-controlled approach. The CMF value is applicable to turn bays that have a design that is consistent with agency policy such that their length adequately provides for vehicle storage or deceleration, as appropriate.

Table 19-34. Coefficients for Crossroad Right-Turn Lane CMF—Crossroad Ramp Terminals

Control Type (x)	Area Type	Crash Type (y)	Crash Severity (z)	CMF Variable	Regression Coefficient (a)
One-way stop control (ST)	Rural	All types (at)	Fatal and injury (fi)	$CMF_{12, w, ST, at, fi}$	0.76
			Property damage only (pdo)	$CMF_{12, w, ST, at, pdo}$	0.63
	Urban	All types (at)	Fatal and injury (fi)	$CMF_{12, w, ST, at, fi}$	0.87
			Property damage only (pdo)	$CMF_{12, w, ST, at, pdo}$	0.69
Signal control, n lanes (SGn)	Rural	All types (at)	Fatal and injury (fi)	$CMF_{12, w, SGn, at, fi}$	0.59
			Property damage only (pdo)	$CMF_{12, w, SGn, at, pdo}$	0.97
	Urban	All types (at)	Fatal and injury (fi)	$CMF_{12, w, SGn, at, fi}$	0.76
			Property damage only (pdo)	$CMF_{12, w, SGn, at, pdo}$	0.94

CMF_{13, w, x, at, z}—Access Point Frequency

Three CMFs are used to describe the relationship between unsignalized access point presence and predicted crash frequency. The SPFs applicable to three-leg terminals with a diagonal exit ramp (*D3ex*) are identified in the following list:

- SPF for fatal-and-injury crashes, three-legs with diagonal exit ramp, stop control, *n* lanes (*D3ex, ST, at, fi*);
- SPF for fatal-and-injury crashes, three-legs with diagonal exit ramp, signal control, *n* lanes (*D3ex, SGn, at, fi*); and
- SPF for property-damage-only crashes, three-legs with diagonal exit ramp, signal control, *n* lanes (*D3ex, SGn, at, pdo*).

There are three more SPFs for each of six terminal configurations (i.e., site types) to which these CMFs apply. They are not shown in the previous list. However, the only difference is that the *D3ex* subscript (shown in parentheses in the previous list) is replaced by the other configuration subscripts (*D3en, D4, A4, B4, A2, B2*).

The base condition is no unsignalized driveways and no unsignalized public street approaches present on the outside leg of the crossroad ramp terminal. The CMFs are described using the following equation.

$$CMF_{13, w, x, at, z} = (1.0 - P_{out}) \times 1.0 + P_{out} \times \exp(a \times n_{dw} + b \times n_{ps}) \tag{Equation 19-49}$$

Where:

CMF_{13, w, x, at, z} = crash modification factor for access point frequency at a site of type *w*, control type *x*, all crash types *at*, and severity *z*;

n_{ps} = number of unsignalized public street approaches to the crossroad leg outside of the interchange and within 250 ft of the ramp terminal; and

n_{dw} = number of unsignalized driveways on the crossroad leg outside of the interchange and within 250 ft of the ramp terminal.

The regression coefficients for Equation 19-49 are provided in Table 19-35. The variable *P_{out}* is computed using Equation 19-47. This CMF applies to any ramp terminal with unsignalized driveways or unsignalized public street approaches on the crossroad leg that is outside of the interchange.

Table 19-35. Coefficients for Access Point Frequency CMF—Crossroad Ramp Terminals

Control Type (<i>x</i>)	Crash Type (<i>y</i>)	Crash Severity (<i>z</i>)	CMF Variable	Regression Coefficients	
				<i>a</i>	<i>b</i>
One-way stop control (<i>ST</i>)	All types (<i>at</i>)	Fatal and injury (<i>fi</i>)	<i>CMF_{13, w, ST, at, fi}</i>	0.00	0.522
Signal control, <i>n</i> lanes (<i>SGn</i>)	All types (<i>at</i>)	Fatal and injury (<i>fi</i>)	<i>CMF_{13, w, SGn, at, fi}</i>	0.158	0.158
		Property damage only (<i>pdo</i>)	<i>CMF_{13, w, SGn, at, pdo}</i>	0.203	0.203

This CMF is applicable when there are four or fewer driveways, and two or fewer unsignalized public street approaches, on the crossroad leg outside of the interchange.

CMF_{14, w, x, at, z}—Segment Length

The distance between the subject ramp terminal and adjacent intersections (or terminals) along the crossroad is logically correlated with crossroad operating speed. This speed is likely to increase as distance increases, and an increase in speed may increase the risk of a crash.

Three CMFs are used to describe the relationship between intersection spacing and predicted crash frequency. The SPFs applicable to three-leg terminals with a diagonal exit ramp (*D3ex*) are identified in the following list:

- SPF for fatal-and-injury crashes, three-legs with diagonal exit ramp, stop control, *n* lanes (*D3ex, ST, at, fi*);
- SPF for fatal-and-injury crashes, three-legs with diagonal exit ramp, signal control, *n* lanes (*D3ex, SGn, at, fi*); and
- SPF for property-damage-only crashes, three-legs with diagonal exit ramp, signal control, *n* lanes (*D3ex, SGn, at, pdo*).

There are three more SPFs for each of six terminal configurations (i.e., site types) to which these CMFs apply. They are not shown in the previous list. However, the only difference is that the *D3ex* subscript (shown in parentheses in the previous list) is replaced by the other configuration subscripts (*D3en, D4, A4, B4, A2, B2*).

The base condition is no adjacent ramp or public street intersection within 6 mi. The CMFs are described using the following equation.

$$CMF_{14, w, x, at, z} = \exp\left(a \times \left[\frac{1.0}{L_{rmp}} + \frac{1.0}{L_{str}} - 0.333 \right] \right) \tag{Equation 19-50}$$

Where:

CMF_{14, w, x, at, z} = crash modification factor for segment length at a site of type *w*, control type *x*, all crash types *at*, and severity *z*;

L_{rmp} = distance between subject ramp terminal and adjacent ramp terminal (measured along the crossroad from terminal center to terminal center) (mi); and

L_{str} = distance between subject ramp terminal and nearest public road intersection in a direction away from freeway (measured along the crossroad from terminal center to intersection center) (mi).

The regression coefficient for Equation 19-50 is provided in Table 19-36.

Table 19-36. Coefficients for Segment Length CMF—Crossroad Ramp Terminals

Control Type (<i>x</i>)	Crash Type (<i>y</i>)	Crash Severity (<i>z</i>)	CMF Variable	Regression Coefficient (<i>a</i>)
One-way stop control (<i>ST</i>)	All types (<i>at</i>)	Fatal and injury (<i>fi</i>)	<i>CMF_{14, w, ST, at, fi}</i>	-0.0141
Signal control, <i>n</i> lanes (<i>SGn</i>)	All types (<i>at</i>)	Fatal and injury (<i>fi</i>)	<i>CMF_{14, w, SGn, at, fi}</i>	-0.0185
		Property damage only (<i>pdo</i>)	<i>CMF_{14, w, SGn, at, pdo}</i>	-0.0186

This CMF describes the relationship between ramp terminal crash frequency and the distance to the adjacent ramp or nearest public street intersection. The adjacent ramp or intersection can be signalized or unsignalized. The CMF is applicable to distances of 0.02 mi or more.

CMF_{15, w, x, at, z}—Median Width

Research indicates that median width at an intersection can influence crash frequency, provided that this width is 14 ft or more (2). At rural unsignalized intersections, an increase in median width is associated with a decrease in crash frequency. In contrast, at urban intersections (unsignalized and signalized), an increase in median width is associated with an increase in crash frequency. This latter trend is contrary to segment-based safety research that shows crash frequency decreases with an increase in median width. Conflict studies have confirmed a tendency for improper use of wide median areas within intersections that, when complicated by high traffic volume, results in an increased propensity for multiple-vehicle crashes (2).

Three CMFs are used to describe the relationship between crossroad median width and predicted crash frequency. The SPFs applicable to three-leg terminals with a diagonal exit ramp (*D3ex*) are identified in the following list:

- SPF for fatal-and-injury crashes, three-legs with diagonal exit ramp, stop control, *n* lanes (*D3ex, ST, at, fi*);
- SPF for fatal-and-injury crashes, three-legs with diagonal exit ramp, signal control, *n* lanes (*D3ex, SGn, at, fi*); and
- SPF for property-damage-only crashes, three-legs with diagonal exit ramp, signal control, *n* lanes (*D3ex, SGn, at, pdo*).

There are three more SPFs for each of six terminal configurations (i.e., site types) to which these CMFs apply. They are not shown in the previous list. However, the only difference is that the *D3ex* subscript (shown in parentheses in the previous list) is replaced by the other configuration subscripts (*D3en, D4, A4, B4, A2, B2*).

The base condition is a 12-ft median width. The CMFs are described using the following equation.

$$CMF_{15, w, x, at, z} = \left[(1.0 - P_{in}) \times 1.0 + P_{in} \times \exp\left[(a + b \times c \times AADT_{in}) \times W_{me, in} \right] \right] \times \left[(1.0 - P_{out}) \times 1.0 + P_{out} \times \exp\left[(a + b \times c \times AADT_{out}) \times W_{me, out} \right] \right] \quad \text{Equation 19-51}$$

with,

$$W_{me, k} = W_m - \max(W_{b, k}, 12) \geq 0.0 \quad \text{Equation 19-52}$$

Where:

$CMF_{15, w, x, at, z}$ = crash modification factor for median width at a site of type *w*, control type *x*, all crash types *at*, and severity *z*;

$W_{me, k}$ = width of median adjacent to turn lane (or bay) for crossroad leg *k* (*k* = *in* or *out*) (ft);

$W_{b, k}$ = left-turn lane (or bay) width for crossroad leg *k* (*k* = *in* or *out*) (= 0.0 if no lane present on leg) (ft); and

W_m = median width (ft).

The regression coefficients for Equation 19-51 are provided in Table 19-37. The variable P_{in} is computed using Equation 19-46. The variable P_{out} is computed using Equation 19-47.

Table 19-37. Coefficients for Median Width CMF–Crossroad Ramp Terminals

Control Type (x)	Crash Type (y)	Crash Severity (z)	CMF Variable	Regression Coefficients		
				a	b	c
One-way stop control (ST)	All types (at)	Fatal and injury (fi)	$CMF_{15, w, ST, at, fi}$	-0.0322	0.00354	0.001
Signal control, n lanes (SGn)	All types (at)	Fatal and injury (fi)	$CMF_{15, w, SGn, at, fi}$	0.0287	-0.00074	0.001
		Property damage only (pdo)	$CMF_{15, w, SGn, at, pdo}$	0.0610	-0.00246	0.001

For signalized ramp terminals, the applicable values for $AADT_{in}$ and $AADT_{out}$ range from 14,000 to 60,000 veh/day. AADT volumes smaller than 14,000 should be set to 14,000 in Equation 19-51.

For unsignalized ramp terminals, the applicable values for $AADT_{in}$ and $AADT_{out}$ range from 0 to 14,000 veh/day. AADT volumes larger than 14,000 should be set to 14,000 in Equation 19-51.

The CMF is applicable to W_m values in the range of 0 to 50 ft. Similarly, it is applicable to $W_{b, k}$ values in the range of 0 to 26 ft.

CMF_{16, w, SGn, at, z}—Protected Left-Turn Operation

Two CMFs are used to describe the relationship between protected-only left-turn operation and predicted crash frequency. The SPFs applicable to three-leg terminals with a diagonal exit ramp (*D3ex*) are identified in the following list:

- SPF for fatal-and-injury crashes, three-legs with diagonal exit ramp, signal control, n lanes (*D3ex, SGn, at, fi*); and
- SPF for property-damage-only crashes, three-legs with diagonal exit ramp, signal control, n lanes (*D3ex, SGn, at, pdo*).

There are two more SPFs for each of six terminal configurations (i.e., site types) to which these CMFs apply. They are not shown in the previous list. However, the only difference is that the *D3ex* subscript (shown in parentheses in the previous list) is replaced by the other configuration subscripts (*D3en, D4, A4, B4, A2, B2*).

The base condition is permissive or protected-permissive left-turn operation (i.e., not protected-only operation). The CMFs are described using the following equation.

$$CMF_{16, w, SGn, at, z} = \left[(1.0 - P_{xrd}) \times 1.0 + P_{xrd} \times \exp(a \times n_{o, in}) \right]^{I_{p, lt, in}} \times \left[(1.0 - P_{xrd}) \times 1.0 + P_{xrd} \times \exp(a \times n_{o, out}) \right]^{I_{p, lt, out}} \tag{Equation 19-53}$$

with,

$$P_{xrd} = \frac{AADT_{in} + AADT_{out}}{AADT_{in} + AADT_{out} + AADT_{en} + AADT_{ex}} \tag{Equation 19-54}$$

Where:

$CMF_{16, w, SGn, at, z}$ = crash modification factor for protected left-turn operation at a signal-controlled site of type w, with n crossroad lanes, all crash types at, and severity z;

- $n_{o, k}$ = number of through traffic lanes that oppose the left-turn movement on crossroad leg k (k = in or out) (lanes);
- P_{xrd} = proportion of total leg AADT on crossroad; and
- $I_{p, lt, k}$ = protected left-turn operation indicator variable for crossroad leg k (k = in or out) (= 1.0 if protected operation exists, 0.0 otherwise).

The regression coefficient for Equation 19-53 is provided in Table 19-38. When computing P_{xrd} , the AADT volume of the loop exit ramp at a $B4$ terminal configuration is not included in $AADT_{ex}$. Similarly, the AADT volume of the loop entrance ramp at an $A4$ configuration is not included in $AADT_{en}$.

Table 19-38. Coefficients for Protected Left-Turn Operation CMF–Crossroad Ramp Terminals

Control Type (x)	Crash Type (y)	Crash Severity (z)	CMF Variable	Regression Coefficient (a)
Signal control, n lanes (SGn)	All types (at)	Fatal and injury (fi)	$CMF_{16, w, SGn, at, fi}$	-0.363
		Property damage only (pdo)	$CMF_{16, w, SGn, at, pdo}$	-0.223

The CMF is applicable to $n_{o, k}$ values in the range of 1 to 3 lanes.

CMF_{17, w, SGn, at, z}—Channelized Right Turn on Crossroad

Two CMFs are used to describe the relationship between crossroad right-turn channelization and predicted crash frequency. The SPFs applicable to three-leg terminals with a diagonal exit ramp ($D3ex$) are identified in the following list:

- SPF for fatal-and-injury crashes, three-legs with diagonal exit ramp, signal control, n lanes ($D3ex, SGn, at, fi$); and
- SPF for property-damage-only crashes, three-legs with diagonal exit ramp, signal control, n lanes ($D3ex, SGn, at, pdo$).

There are two more SPFs for each of six terminal configurations (i.e., site types) to which these CMFs apply. They are not shown in the previous list. However, the only difference is that the $D3ex$ subscript (shown in parentheses in the previous list) is replaced by the other configuration subscripts ($D3en, D4, A4, B4, A2, B2$).

The base condition is no crossroad right-turn channelization. The CMFs are described using the following equation.

$$CMF_{17, w, SGn, at, z} = [(1.0 - P_{in}) \times 1.0 + P_{in} \times \exp(a)]^{I_{ch, in}} \times [(1.0 - P_{out}) \times 1.0 + P_{out} \times \exp(a)]^{I_{ch, out}} \quad \text{Equation 19-55}$$

Where:

$CMF_{17, w, SGn, at, z}$ = crash modification factor for crossroad right-turn channelization at a signal-controlled site of type w , with n crossroad lanes, all crash types at , and severity z ; and

$I_{ch, k}$ = right-turn channelization indicator variable for crossroad leg k (k = in or out) (= 1.0 if right-turn channelization exists, 0.0 otherwise).

The regression coefficient for Equation 19-55 is provided in Table 19-39. The variable P_{in} is computed using Equation 19-46. The variable P_{out} is computed using Equation 19-47.

Table 19-39. Coefficients for Channelized Right Turn on Crossroad CMF—Crossroad Ramp Terminals

Control Type (x)	Crash Type (y)	Crash Severity (z)	CMF Variable	Regression Coefficient (a)
Signal control, <i>n</i> lanes (<i>SGn</i>)	All types (<i>at</i>)	Fatal and injury (<i>fi</i>)	$CMF_{17, w, SGn, at, fi}$	0.466
		Property damage only (<i>pdo</i>)	$CMF_{17, w, SGn, at, pdo}$	0.465

This CMF is applicable to any ramp terminal with right-turn channelization on one or both crossroad legs, where the associated right-turn movement is turning from the crossroad. This CMF can be applied to channelization associated with the loop entrance ramp of the *A4* configuration.

CMF_{18, w, SGn, at, z}—Channelized Right Turn on Exit Ramp

Two CMFs are used to describe the relationship between exit ramp right-turn channelization and predicted crash frequency. The SPFs applicable to three-leg terminals with a diagonal exit ramp (*D3ex*) are identified in the following list:

- SPF for fatal-and-injury crashes, three-legs with diagonal exit ramp, signal control, *n* lanes (*D3ex, SGn, at, fi*); and
- SPF for property-damage-only crashes, three-legs with diagonal exit ramp, signal control, *n* lanes (*D3ex, SGn, at, pdo*).

There are two more SPFs for each of six terminal configurations (i.e., site types) to which these CMFs apply. They are not shown in the previous list. However, the only difference is that the *D3ex* subscript (shown in parentheses in the previous list) is replaced by the other configuration subscripts (*D3en, D4, A4, B4, A2, B2*).

The base condition is no exit ramp right-turn channelization. The CMFs are described using the following equation.

$$CMF_{18, w, SGn, at, z} = [(1.0 - P_{ex}) \times 1.0 + P_{ex} \times \exp(a)]^{I_{ch, ex}} \quad \text{Equation 19-56}$$

Where:

$CMF_{18, w, SGn, at, z}$ = crash modification factor for exit ramp right-turn channelization at a signal-controlled site of type *w*, with *n* crossroad lanes, all crash types *at*, and severity *z*; and

$I_{ch, ex}$ = right-turn channelization indicator variable for exit ramp (= 1.0 if right-turn channelization exists, 0.0 otherwise).

The regression coefficient for Equation 19-56 is provided in Table 19-40. The variable P_{ex} is computed using Equation 19-44.

Table 19-40. Coefficients for Channelized Right Turn on Exit Ramp CMF—Crossroad Ramp Terminals

Control Type (x)	Crash Type (y)	Crash Severity (z)	CMF Variable	Regression Coefficient (a)
Signal control, <i>n</i> lanes (<i>SGn</i>)	All types (<i>at</i>)	Fatal and injury (<i>fi</i>)	$CMF_{18, w, SGn, at, fi}$	0.992
		Property damage only (<i>pdo</i>)	$CMF_{18, w, SGn, at, pdo}$	1.429

This CMF is applicable to any ramp terminal with an exit ramp that has left-turn and right-turn movements and right-turn channelization. This CMF is not applicable to the loop exit ramp of the *B4* configuration.

CMF_{19, w, SGn, at, z}—Non-Ramp Public Street Leg

Two CMFs are used to describe the relationship between public-street leg presence and predicted crash frequency. The SPFs applicable to three-leg terminals with a diagonal exit ramp (*D3ex*) are identified in the following list:

- SPF for fatal-and-injury crashes, three-legs with diagonal exit ramp, signal control, *n* lanes (*D3ex, SGn, at, fi*); and
- SPF for property-damage-only crashes, three-legs with diagonal exit ramp, signal control, *n* lanes (*D3ex, SGn, at, pdo*).

There are two more SPFs for each of six terminal configurations (i.e., site types) to which these CMFs apply. They are not shown in the previous list. However, the only difference is that the *D3ex* subscript (shown in parentheses in the previous list) is replaced by the other configuration subscripts (*D3en, D4, A4, B4, A2, B2*).

The base condition is no public-street leg present. The CMFs are described using the following equation.

$$CMF_{19, w, SGn, at, z} = \exp(a \times I_{ps}) \quad \text{Equation 19-57}$$

Where:

$CMF_{19, w, SGn, at, z}$ = crash modification factor for non-ramp public street leg presence at a signal-controlled site of type *w*, with *n* crossroad lanes, all crash types *at*, and severity *z*; and

I_{ps} = non-ramp public street leg indicator variable (= 1.0 if leg is present, 0.0 otherwise).

The regression coefficient for Equation 19-57 is provided in Table 19-41. The variable P_{ex} is computed using Equation 19-44.

This CMF is applicable to any ramp terminal that has a fourth leg that (a) is a public street serving two-way traffic and (b) intersects with the crossroad at the terminal. This situation occurs occasionally. When it does, the public street leg is opposite from one ramp and the other ramp either does not exist or is located at some distance from the subject ramp terminal such that it is not part of the terminal.

Table 19-41. Coefficients for Non-Ramp Public Street Leg CMF—Crossroad Ramp Terminals

Control Type (<i>x</i>)	Crash Type (<i>y</i>)	Crash Severity (<i>z</i>)	CMF Variable	Regression Coefficient (<i>a</i>)
Signal control, <i>n</i> lanes (<i>SGn</i>)	All types (<i>at</i>)	Fatal and injury (<i>fi</i>)	$CMF_{19, w, SGn, at, fi}$	0.592
		Property damage only (<i>pdo</i>)	$CMF_{19, w, SGn, at, pdo}$	0.520

CMF_{20, w, ST, at, fi}—Skew Angle

One CMF is used to describe the relationship between the exit ramp skew angle and predicted crash frequency. The SPFs applicable to three-leg terminals with a diagonal exit ramp (*D3ex*) are identified in the following list:

- SPF for fatal-and-injury crashes, three-legs with diagonal exit ramp, stop control, *n* lanes (*D3ex, ST, at, fi*).

There is one more SPF for each of six terminal configurations (i.e., site types) to which these CMFs apply. They are not shown in the previous list. However, the only difference is that the $D3ex$ subscript (shown in parentheses in the previous list) is replaced by the other configuration subscripts ($D3en, D4, A4, B4, A2, B2$).

The base condition is no skew in the intersecting alignments (i.e., a skew angle of 0.0 degrees). The CMFs are described using the following equation.

$$CMF_{20,w,ST,at,fi} = (1.0 - P_{ex}) \times 1.0 + P_{ex} \times \exp(0.341 \times \sin[I_{sk}] \times 0.001 \times AADT_{ex}) \quad \text{Equation 19-58}$$

Where:

$CMF_{20,w,ST,at,fi}$ = crash modification factor for skew angle at a stop-controlled site of type w , with n crossroad lanes, and all types at of fatal-and-injury crashes fi ; and

I_{sk} = skew angle between exit ramp and crossroad (degrees).

The variable P_{ex} is computed using Equation 19-44.

This CMF is applicable to any one-way stop-controlled ramp terminal with an exit ramp that has stop or yield control for the “reference” exit ramp movement. The reference movement is the left-turn movement for all terminal configurations except the $B4$ configuration. At a $B4$ ramp terminal, the reference movement is the right-turn movement on the diagonal exit ramp (not the loop exit ramp). This CMF is applicable to skew angles in the range of 0 to 70 degrees.

19.7.3. Supplemental Calculations to Apply Crash Modification Factors

Some of the CMFs in Section 19.7.1 require the completion of supplemental calculations before they can be applied to the SPFs in Section 19.6. These CMFs are: Horizontal curve, Right side barrier, and Left side barrier.

This section consists of two subsections. The first section describes the procedure for calculating the curve entry speed needed for the Horizontal curve CMF. The second section describes the procedure for calculating the barrier-related variables for the Right side Barrier CMF and the Left side Barrier CMF.

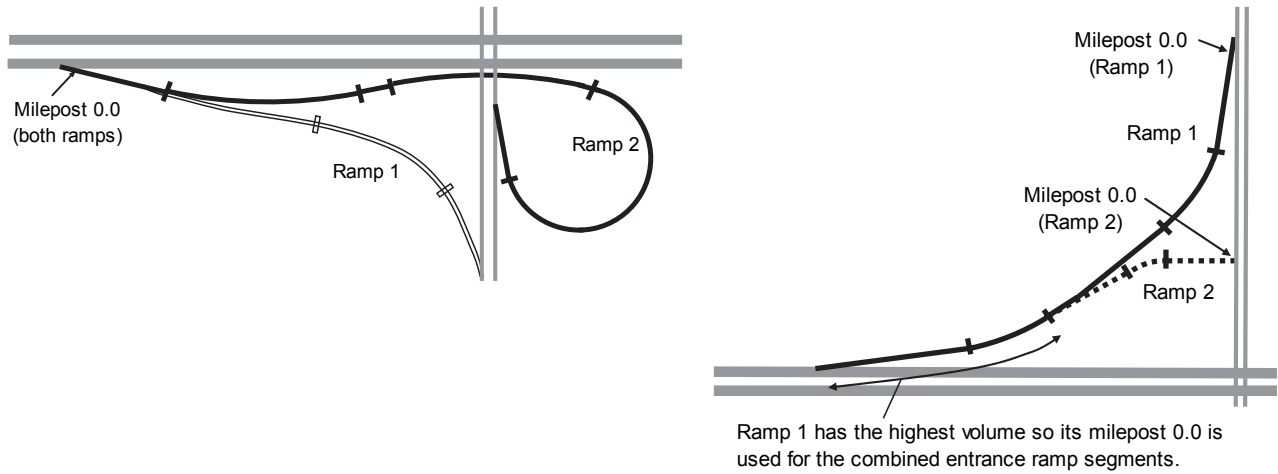
Calculation of Curve Entry Speed

This subsection describes a procedure for predicting the average curve entry speed for each curve on a ramp or C-D road. This procedure is developed for use with the Horizontal curve CMF, as described in Section 19.7.1. It is not intended to be used with other applications, or to predict vehicle speed at other points along a ramp or C-D road.

The speed prediction procedure consists of a sequence of steps that lead to a prediction of average entry speed for each horizontal curve on the subject ramp or C-D road. Each curve is addressed by the procedure in the same sequence as they are encountered when traveling along the ramp or C-D road. In this manner, the speed for all previous curves encountered must be calculated first, before the speed on the subject curve can be calculated. The steps used will vary depending on whether the segment is part of an entrance ramp, exit ramp, connector ramp, or C-D road.

The horizontal curves are located along the ramp or C-D road using a linear referencing system. For exit ramps, the “0.0” milepost is located at the gore point. For entrance ramps that intersect the crossroad, the “0.0” milepost is located at the point where the ramp reference line intersects with the near edge of traveled way of the crossroad. The location of the “0.0” milepost is shown in Figure 19-4 for simple situations. It is shown in Figure 19-24 for more complex ramp and C-D road combinations. When a specific entrance ramp

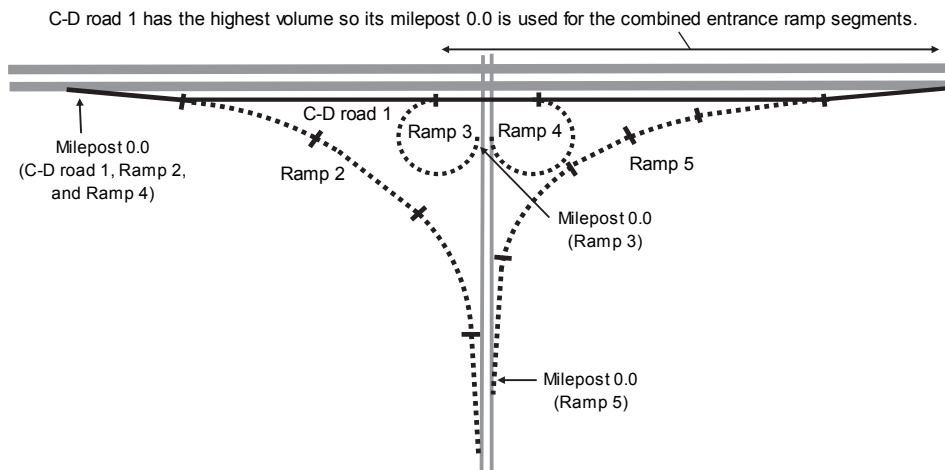
or C-D road segment serves traffic from two or more sources combined, the “0.0” milepost for this segment should be that of the one ramp that is the source of the highest daily traffic volume.



a. Exit Ramp

b. Entrance Ramp

Figure 19-24. Starting Milepost Location for Ramp and C-D Road Combinations



c. Entrance and Exit Ramps with C-D Road

Figure 19-24. Starting Milepost Location for Ramp and C-D Road Combinations *continued*

The input data needed for this procedure are identified in Table 19-42. The first three variables listed represent required input data. Default values are provided for the remaining variables.

Table 19-42. Input Data for Ramp Curve Speed Prediction

Variable	Description	Default Value	Applicable Site Type
X_i	Milepost of the point of change from tangent to curve (PC) for curve i^a (mi)	None	All
R_i	Radius of curve i^b (ft)	None	All
$L_{c,i}$	Length of horizontal curve i (mi)	None	All
V_{frwy}	Average traffic speed on the freeway during off-peak periods of the typical day (mi/h)	Estimate as equal to the speed limit	All
V_{xroad}	Average speed at the point where the ramp connects to the crossroad (mi/h)	15 – ramps with stop-, yield-, or signal-controlled crossroad ramp terminals 30 – all other ramps at service interchanges	Entrance ramp, exit ramp, connector ramp at service interchange
V_{cdroad}	Average speed on C-D road or connector ramp (measured at the mid-point of the C-D road or ramp) (mi/h)	40	C-D road, connector ramp at system interchange

Notes:

- If the curve is preceded by a spiral transition, then X_i is computed as equal to the average of the TS and SC mileposts, where TS is the milepost of the point of change from tangent to spiral and SC is the milepost of the point of change from spiral to curve.
- If the curve has spiral transitions, then R_i is equal to the radius of the central circular portion of the curve.

Entrance Ramp Procedure

This procedure is applicable to entrance ramps and connector ramps at service interchanges that serve motorists traveling from the crossroad to the freeway.

Step 1—Gather Input Data. The input data needed for this procedure are identified in Table 19-42.

Step 2—Compute Limiting Curve Speed. The limiting curve speed is computed for each curve on the ramp using the following equation.

$$v_{\max,i} = 3.24 \times (32.2 \times R_i)^{0.30} \quad \text{Equation 19-59}$$

where $v_{\max,i}$ is the limiting speed for curve i (ft/s).

The analysis proceeds in the direction of travel. The first curve encountered is curve 1 ($i=1$). The value of v_{\max} is computed for all curves prior to, and including, the curve of interest. The value obtained from Equation 19-59 represents an upper limit on the curve speed. The vehicle may reach this speed if the distance between curves is lengthy or the crossroad speed is high.

Step 3—Calculate Curve 1 Entry Speed. The average entry speed at curve 1 is computed using the following equation.

$$v_{ent,1} = \left([1.47 \times V_{xroad}]^3 + 495 \times 5,280 \times X_1 \right)^{1/3} \leq 1.47 \times V_{frwy} \quad \text{Equation 19-60}$$

where $v_{ent,1}$ is the average entry speed for curve 1 (ft/s).

The boundary condition on the right side of the equation indicates that the value computed cannot exceed the average freeway speed.

Step 4—Calculate Curve 1 Exit Speed. The average exit speed at curve 1 is equal to the value obtained from the following equation.

$$v_{ext,1} = \left(v_{ent,1}^3 + 495 \times 5,280 \times L_{c,1} \right)^{1/3} \leq v_{max,1} \quad \text{and} \quad \leq 1.47 \times V_{frwy} \quad \text{Equation 19-61}$$

where $v_{ext,1}$ is the average exit speed for curve 1 (ft/s).

The boundary condition indicates that the value computed should not exceed the limiting curve speed or the average freeway speed.

Step 5—Calculate Curve i Entry Speed. The average entry speed at curve 2 (and all subsequent curves) is computed using the following equation.

$$v_{ent,i} = \left(v_{ext,i-1}^3 + 495 \times 5,280 \times [X_i - X_{i-1} - L_{c,i-1}] \right)^{1/3} \leq 1.47 \times V_{frwy} \quad \text{Equation 19-62}$$

where, $v_{ent,i}$ equals the average entry speed for curve i ($i = 2, 3, \dots$) (ft/s) and $v_{ext,i}$ equals the average exit speed for curve i (ft/s).

Step 6—Calculate Curve i Exit Speed. The average exit speed at curve 2 (and all subsequent curves) is computed using the following equation.

$$v_{ext,i} = \left(v_{ent,i}^3 + 495 \times 5,280 \times L_{c,i} \right)^{1/3} \leq v_{max,i} \quad \text{and} \quad \leq 1.47 \times V_{frwy} \quad \text{Equation 19-63}$$

Step 7—Calculate Speed on Successive Curves. The entry and exit speeds for curve 3 and higher are computed by applying Steps 5 and 6 for each curve. Step 6 does not need to be applied for the last curve because only the entry speed is used in the safety evaluation.

Exit Ramp Procedure

This procedure is applicable to exit ramps and connector ramps at service interchanges that serve motorists traveling from the freeway to the crossroad.

Step 1—Gather Input Data. The input data needed for this procedure are identified in Table 19-42.

Step 2—Compute Limiting Curve Speed. This step is the same as Step 2 for the entrance ramp procedure. A lower curve speed than that obtained from Equation 19-59 is possible due to the deceleration that occurs as the driver transitions from the freeway speed to the crossroad speed.

Step 3—Calculate Curve 1 Entry Speed. The average entry speed at curve 1 is computed using the following equation.

$$v_{ent,1} = 1.47 \times V_{frwy} - 0.034 \times 5,280 \times X_1 \geq 1.47 \times V_{xroad} \quad \text{Equation 19-64}$$

The boundary condition on the right side of the equation indicates that the value computed cannot be less than the average speed at the point where the ramp connects to the crossroad.

Step 4—Calculate Curve 1 Exit Speed. This step is the same as Step 4 for the entrance ramp procedure.

$$v_{ext,1} = v_{ent,1} - 0.034 \times 5,280 \times L_{c,1} \leq v_{max,1} \quad \text{and} \quad \geq 1.47 \times V_{xroad} \quad \text{Equation 19-65}$$

The boundary condition indicates that the value computed should not exceed the limiting curve speed and should not be less than the average speed at the point where the ramp connects to the crossroad.

Step 5—Calculate Curve i Entry Speed. The average entry speed at curve 2 (and all subsequent curves) is computed using the following equation.

$$v_{ent,i} = v_{ext,i-1} - 0.034 \times 5,280 \times (X_i - X_{i-1} - L_{c,i-1}) \geq 1.47 \times V_{xroad} \quad \text{Equation 19-66}$$

Step 6—Calculate Curve i Exit Speed. The average exit speed at curve 2 (and all subsequent curves) is computed using the following equation.

$$v_{ext,i} = v_{ent,i} - 0.034 \times 5,280 \times L_{c,i} \leq v_{max,i} \quad \text{and} \quad \geq 1.47 \times V_{xroad} \quad \text{Equation 19-67}$$

Step 7—Calculate Speed on Successive Curves. This step is the same as Step 7 for the entrance ramp procedure.

C-D Road Procedure

This procedure is applicable to C-D roads and connector ramps at system interchanges.

Step 1—Gather Input Data. The input data needed for this procedure are identified in Table 19-42.

Step 2—Compute Limiting Curve Speed. This step is the same as Step 2 for the entrance ramp procedure.

Step 3—Calculate Curve 1 Entry Speed. The average entry speed at curve 1 is computed using Equation 19-68 or Equation 19-69, depending on the following two conditions.

If $1.47 \times V_{frwy} \leq v_{max,1}$ then:

$$v_{ent,1} = 1.47 \times V_{frwy} \quad \text{Equation 19-68}$$

If $1.47 \times V_{frwy} > v_{max,1}$ then:

$$v_{ent,1} = 1.47 \times V_{frwy} - 0.034 \times 5,280 \times X_1 \geq 1.47 \times V_{cdroad} \quad \text{Equation 19-69}$$

The boundary condition for Equation 19-69 indicates that the value computed cannot be less than the average speed on the C-D road.

Step 4—Calculate Curve 1 Exit Speed. The average exit speed at curve 1 is equal to the entrance speed, provided that it does not exceed the limiting curve speed. The following rule is used to make this determination.

$$v_{ext,1} = v_{ent,1} \leq v_{max,1} \quad \text{Equation 19-70}$$

Step 5—Calculate Curve i Entry Speed. The average entry speed at curve 2 (and all subsequent curves) is computed using Equation 19-71 or Equation 19-72, depending on the following conditions.

If $v_{ext, i-1} \leq v_{max, i}$ then:

$$v_{ent, i} = \left(v_{ext, i-1}^3 + 495 \times 5,280 \times [X_i - X_{i-1} - L_{c, i-1}] \right)^{1/3} \leq 1.47 \times V_{frwy} \quad \text{Equation 19-71}$$

If $v_{ext, i-1} > v_{max, i}$ then:

$$v_{ent, i} = v_{ext, i-1} - 0.034 \times 5,280 \times (X_i - X_{i-1} - L_{c, i-1}) \geq 1.47 \times V_{cdroad} \quad \text{Equation 19-72}$$

Step 6—Calculate Curve i Exit Speed. The average exit speed at curve 2 (and all subsequent curves) is computed using the following equation.

$$v_{ext, i} = v_{ent, i} \leq v_{max, i} \quad \text{Equation 19-73}$$

Step 7—Calculate Speed on Successive Curves. This step is the same as Step 7 for the entrance ramp procedure.

Calculation of Barrier-Related Variables

The two barrier CMFs include variables that describe the presence of barrier on the left or right side of the ramp or C-D road. These variables include barrier offset and length.

Barrier offset represents a lateral distance measured from the near edge of the shoulder to the face of the barrier (i.e., it does not include the width of the shoulder). Barrier length represents the length of lane paralleled by a barrier; it is a total for both travel directions. For example, if the left side barrier extends for the length of the ramp segment, then the left side barrier length equals the segment length.

Two key variables that are needed for the evaluation of barrier presence are the right side barrier offset distance W_{rcb} and the left side barrier offset distance W_{lcb} . As indicated in Equation 19-37 and Equation 19-38, this distance is included as a divisor in the exponential term. This relationship implies that the correlation between distance and crash frequency is an inverse one (i.e., crash frequency decreases with increasing distance to the barrier). When multiple sections of barrier exist along the segment, a length-weighted average of the reciprocal of the individual distances is needed to properly reflect this inverse relationship. The length used to weight the average is the barrier length.

Additional key variables include the proportion of segment length with a barrier present on the right side P_{rb} and the proportion of segment length with a barrier present on the left side P_{lb} . Equations for calculating these proportions and the aforementioned distances are described in the following paragraphs.

The length of segment L used in the following equations is equal to that of the ramp segment L_r or C-D road segment L_{cd} , as appropriate for the CMF to which the calculated value will be applied.

The following equations should be used to estimate W_{rcb} and P_{rb} .

$$W_{rcb} = \frac{\sum L_{rb, i}}{\sum \frac{L_{rb, i}}{W_{off, r, i} - W_{rs}}} \quad \text{Equation 19-74}$$

$$P_{rb} = \frac{\sum L_{rb, i}}{L} \quad \text{Equation 19-75}$$

Where:

W_{rcb} = distance from edge of right shoulder to barrier face (ft);

P_{rb} = proportion of segment length with a barrier present on the right side;

L = length of segment (mi);

$L_{rb, i}$ = length of right side lane paralleled by barrier i (mi);

W_{rs} = right shoulder width (ft); and

$W_{off, r, i}$ = horizontal clearance from the edge of the traveled way to the face of right side barrier i (ft).

Any clearance distance ($= W_{off, r, i} - W_{rs}$) that is less than 0.75 ft should be set to 0.75 ft.

The following equations should be used to estimate W_{lcb} and P_{lb} .

$$W_{lcb} = \frac{\sum L_{lb, i}}{\sum \frac{L_{lb, i}}{W_{off, l, i} - W_{ls}}} \quad \text{Equation 19-76}$$

$$P_{lb} = \frac{\sum L_{lb, i}}{L} \quad \text{Equation 19-77}$$

Where:

W_{lcb} = distance from edge of left shoulder to barrier face (ft);

P_{lb} = proportion of segment length with a barrier present on the left side;

L = length of segment (mi);

$L_{lb, i}$ = length of left side lane paralleled by barrier i (mi);

W_{ls} = left shoulder width (ft); and

$W_{off, l, i}$ = horizontal clearance from the edge of the traveled way to the face of left side barrier i (ft).

Any clearance distance ($= W_{off, l, i} - W_{ls}$) that is less than 0.75 ft should be set to 0.75 ft.

19.8. SEVERITY DISTRIBUTION FUNCTIONS

The severity distribution functions (SDFs) are presented in this section. They are used in the predictive model to estimate the expected average crash frequency for the following severity levels: fatal K , incapacitating injury A , non-incapacitating injury B , and possible injury C . Each SDF was developed as a regression model using observed crash data for a set of similar sites as the dependent variable. The SDF, like all regression models, estimates the value of the dependent variable as a function of a set of independent variables. The independent variables include various geometric features, traffic control features, and area type (i.e., rural or urban). Separate SDFs described in this section for ramp segments and crossroad ramp terminals.

The general model form for the severity distribution prediction is shown in the following equation.

$$N_{e,w,x,y,i} = N_{e,w,x,y,\hat{f}_i} \times P_{w,ac,at,j} \quad \text{Equation 19-78}$$

Where:

$N_{e,w,x,y,j}$ = expected average crash frequency for site type w , cross section or control type x , crash type y , and severity level j ($j = K$: fatal, A : incapacitating injury, B : non-incapacitating injury, C : possible injury) (crashes/yr);

N_{e,w,x,y,\hat{f}_i} = expected average crash frequency for site type w , cross section or control type x , crash type y , and fatal-and-injury crashes \hat{f}_i (crashes/yr); and

$P_{w,x,at,j}$ = probability of the occurrence of severity level j ($j = K$: fatal, A : incapacitating injury, B : non-incapacitating injury, C : possible injury) for all crash types at at site type w with cross section or control type x .

There is one SDF associated with each probability level j in the predictive model. An SDF predicts the probability of occurrence of severity level j for a crash based on various geometric design and traffic control features at the subject site. Each SDF also contains a calibration factor that is used to calibrate it to local conditions.

19.8.1. Severity Distribution Functions for Ramp Segments

The SDFs for ramp and C-D road segments are described by the following equations.

$$P_{rps+cds,ac,at,K} = \frac{\exp(V_{K+A})}{\frac{1.0}{C_{sdf,rps+cds}} + \exp(V_{K+A}) + \exp(V_B)} \times P_{K|K+A,rps+cds,ac,at} \quad \text{Equation 19-79}$$

$$P_{rps+cds,ac,at,A} = \frac{\exp(V_{K+A})}{\frac{1.0}{C_{sdf,rps+cds}} + \exp(V_{K+A}) + \exp(V_B)} \times (1.0 - P_{K|K+A,rps+cds,ac,at}) \quad \text{Equation 19-80}$$

$$P_{rps+cds,ac,at,B} = \frac{\exp(V_B)}{\frac{1.0}{C_{sdf,rps+cds}} + \exp(V_{K+A}) + \exp(V_B)} \quad \text{Equation 19-81}$$

$$P_{rps+cds,ac,at,C} = 1.0 - (P_K + P_A + P_B) \quad \text{Equation 19-82}$$

Where:

V_j = systematic component of crash severity likelihood for severity level j ;

$P_{K|K+A,rps+cds,ac,at}$ = probability of a fatal K crash given that the crash has a severity of either fatal or incapacitating injury A on a ramp or C-D road segment based on all crash types at and any cross section ac ; and

$C_{sdf,rps+cds}$ = calibration factor to adjust SDF for local conditions for ramp and C-D road segments.

The first term Equation 19-79 estimates the probability of a fatal or incapacitating injury crash. The second term (i.e., $P_{K|K+A}$) is used to convert the estimate into the probability of a fatal crash. A value of 0.248 is used for $P_{K|K+A}$ based on an analysis of fatal and incapacitating injury crashes on ramps and C-D road segments.

A model for estimating the systematic component of crash severity V_j for ramp and C-D road segments is described by the following equation.

$$V_j = a + \left(b \times \frac{P_{lb} + P_{rb}}{2} \right) + (c \times n) + (d \times I_{rural}) + (e \times I_{exr}) \tag{Equation 19-83}$$

Where:

- P_{lb} = proportion of segment length with a barrier present on the left side;
- P_{rb} = proportion of segment length with a barrier present on the right side;
- n = number of through lanes in the segment (lanes);
- I_{rural} = area type indicator variable (= 1.0 if area is rural, 0.0 if it is urban);
- I_{exr} = exit ramp indicator variable (= 1.0 if segment is an exit ramp, 0.0 otherwise); and
- a, b, c, d, e = regression coefficients.

The SDF regression coefficients in Equation 19-83 are provided in Table 19-43. Guidance for computing the variables P_{lb} and P_{rb} is provided in Section 19.7.3.

Table 19-43. SDF Coefficients for Ramp Segments

Severity Level (<i>j</i>)	Variable	Regression Coefficients				
		<i>a</i>	<i>b</i>	<i>c</i>	<i>d</i>	<i>e</i>
Fatal or incapacitating injury (<i>K+A</i>)	V_{K+A}	-1.537	-0.481	-0.228	0.668	0.426
Non-incapacitating injury (<i>B</i>)	V_B	0.236	-0.431	-0.435	0.696	0.00

The SDF is applicable to rural ramps and C-D roads with one lane (i.e., $n = 1$), and to urban ramps and C-D roads with one or two lanes (i.e., $n = 1$ or 2).

The sign of a regression coefficient in Table 19-43 indicates the change in the proportion of crashes associated with a change in the corresponding variable. For example, the negative coefficient associated with barrier presence indicates that the proportion of fatal *K* and incapacitating injury *A* crashes decreases with an increase in the proportion of barrier present in the segment. A similar trend is indicated for barrier presence on non-incapacitating injury *B* crashes. By inference, the proportion of possible injury *C* crashes *increases* with an increase in the proportion of barrier present.

19.8.2. Severity Distribution Functions for Ramp Terminals

The SDFs for crossroad ramp terminals are described by the following equations.

$$P_{aS,x,at,K} = \frac{\exp(V_{K+A})}{\frac{1.0}{C_{sdf,aS,x}} + \exp(V_{K+A}) + \exp(V_B)} \times P_{K|K+A,aS,x,at} \quad \text{Equation 19-84}$$

$$P_{aS,x,at,A} = \frac{\exp(V_{K+A})}{\frac{1.0}{C_{sdf,aS,x}} + \exp(V_{K+A}) + \exp(V_B)} \times (1.0 - P_{K|K+A,aS,x,at}) \quad \text{Equation 19-85}$$

$$P_{aS,x,at,B} = \frac{\exp(V_B)}{\frac{1.0}{C_{sdf,aS,x}} + \exp(V_{K+A}) + \exp(V_B)} \quad \text{Equation 19-86}$$

$$P_{aS,x,at,C} = 1.0 - (P_K + P_A + P_B) \quad \text{Equation 19-87}$$

Where:

V_j = systematic component of crash severity likelihood for severity level j ;

$P_{K|K+A,aS,x,at}$ = probability of a fatal K crash given that the crash has a severity of either fatal or incapacitating injury A for all ramp terminal sites aS based on all crash types at and control type x ($x = ST$: one-way stop control; SGn : signal control, n -lane crossroad); and

$C_{sdf,aS,x}$ = calibration factor to adjust SDF for local conditions for all ramp terminal sites aS with control type x ($x = ST$: stop control, SGn : signal control, n -lane crossroad).

The first term Equation 19-84 estimates the probability of a fatal or incapacitating injury crash. The second term (i.e., $P_{K|K+A}$) is used to convert the estimate into the probability of a fatal crash. For signal-controlled ramp terminals, a value of 0.0385 is used for $P_{K|K+A}$ based on an analysis of fatal and incapacitating injury crashes at signalized ramp terminals. For one-way stop-controlled ramp terminals, a value of 0.160 is used for $P_{K|K+A}$ based on a similar analysis.

A model for estimating the systematic component of crash severity V_j for crossroad ramp terminals is described by the following equation.

$$V_j = a + (b \times I_{p,lt}) + (c \times [n_{dw} + n_{ps}]) + (d \times I_{ps}) + (e \times I_{rural}) \quad \text{Equation 19-88}$$

Where:

$I_{p,lt}$ = protected left-turn operation indicator variable for crossroad (= 1.0 if protected operation exists, 0.0 otherwise);

n_{dw} = number of unsignalized driveways on the crossroad leg outside of the interchange and within 250 ft of the ramp terminal;

n_{ps} = number of unsignalized public street approaches to the crossroad leg outside of the interchange and within 250 ft of the ramp terminal; and

I_{ps} = non-ramp public street leg indicator variable (= 1.0 if leg is present, 0.0 otherwise).

The SDF regression coefficients in Equation 19-88 are provided in Table 19-44.

Table 19-44. SDF Coefficients for Crossroad Ramp Terminals

Control Type (<i>x</i>)	Severity Level (<i>j</i>)	Variable	Regression Coefficients				
			<i>a</i>	<i>b</i>	<i>c</i>	<i>d</i>	<i>e</i>
One-way stop control (<i>ST</i>)	Fatal or incapacitating inj. (<i>K+A</i>)	V_{K+A}	-3.168	0.00	0.00	0.00	0.891
	Non-incapacitating injury (<i>B</i>)	V_B	-1.476	0.00	0.00	0.00	0.221
Signal control, <i>n</i> lanes (<i>SGn</i>)	Fatal or incapacitating inj. (<i>K+A</i>)	V_{K+A}	-3.257	-0.288	0.0991	1.171	0.619
	Non-incapacitating injury (<i>B</i>)	V_B	-1.511	-0.193	0.149	0.741	0.416

This SDF is applicable when there are four or fewer driveways, and two or fewer unsignalized public street approaches, on the crossroad leg outside of the interchange.

The variable $I_{p,lt}$ is equal to 1.0 if protected-only left-turn operation is provided on each crossroad leg with a left-turn movement. If permissive or protected-permissive operation is provided on either leg, then the variable equals 0.0.

The variable I_{ps} is equal to 1.0 if the ramp terminal has a fourth leg that (a) is a public street serving two-way traffic and (b) intersects with the crossroad at the terminal. This situation occurs occasionally. When it does, the public street leg is opposite from one ramp and the other ramp either does not exist or is located at some distance from the subject ramp terminal such that it is not part of the terminal.

The sign of a regression coefficient in Table 19-44 indicates the change in the proportion of crashes associated with a change in the corresponding variable. For example, the negative coefficient associated with protected left-turn operation indicates that the proportion of fatal *K* and incapacitating injury *A* crashes decreases when protected-only left-turn operation is provided. A similar trend is indicated for protected-only left-turn operation on non-incapacitating injury *B* crashes. By inference, the proportion of possible injury *C* crashes *increases* when protected-only left-turn operation is provided.

19.9. CALIBRATION OF THE SPFS AND SDFS TO LOCAL CONDITIONS

Crash frequencies, even for nominally similar ramp segments or ramp terminals, can vary widely from one jurisdiction to another. Geographic regions differ markedly in climate, animal population, driver populations, crash-reporting threshold, and crash-reporting practices. These variations may result in some jurisdictions experiencing a different number of traffic crashes on ramps than others. Calibration factors are included in the methodology to allow highway agencies to adjust the SPFs and SDFs to match actual local conditions.

The SPF calibration factors will have values greater than 1.0 for segments or terminals that, on average, experience more crashes than those used in the development of the SPFs. Similarly, the calibration factors for segments or terminals that experience fewer crashes on average than those used in the development of the SPFs will have values less than 1.0. The calibration procedures for SPFs are presented in Section B.1.1 of Appendix B to Part C.

The SDF calibration factors will have values greater than 1.0 for segments or terminals that, on average, experience more severe crashes than those used in the development of the SDFs. Similarly, the calibration factors for segments or terminals that experience fewer severe crashes on average than those used in the development of the SDFs will have values less than 1.0. The calibration procedures for SDFs are presented in Section B.1.4 of Appendix B to Part C.

Default values are also provided for the crash type distributions used in the methodology. These values can also be replaced with locally derived values. The derivation of these values is addressed in Section B.1.3 of Appendix B to Part C.

19.10. INTERIM PREDICTIVE METHOD FOR ALL-WAY STOP CONTROL

Sufficient research has not yet been conducted to form the basis for development of a predictive method for crossroad ramp terminals with all-way stop control. An interim method is presented in this section. It consists of the same steps as described previously in Section 19.4. The discussion below highlights the modifications to these steps when they are applied to an all-way stop-controlled ramp terminal.

Steps 1 to 18—Evaluate the Crossroad Ramp Terminal as One-Way Stop Control. Apply the predictive method described in Section 19.4 to the subject crossroad ramp terminal. The subject crossroad ramp terminal has all-way stop control but it is evaluated using the predictive method for one-way stop control.

Step 10—The following list identifies the CMFs that can be used in Step 10 of the predictive method to evaluate all-way stop-controlled ramp terminals.

- Exit ramp capacity.
- Access point frequency.
- Segment length.
- Median width.

The Crossroad left-turn lane CMF, Crossroad right-turn lane CMF, and Skew angle CMF cannot be used to evaluate all-way stop-controlled ramp terminals.

In addition, the All-way stop control CMF is used in Step 10 of the predictive method. This CMF has a value of 0.686 when applied to fatal-and-injury crashes. Research has not established a value for this CMF when applied to property-damage-only crashes, so the unadjusted estimate from the predictive method is considered to be equally applicable to all-way stop-controlled ramp terminals.

Step 13—The crash-type distribution in Table 19-45 can be used in Step 13 of the predictive method, if desired, to compute the expected average crash frequency for each of ten crash types (e.g., head-on, fixed object).

Table 19-45. Default Distribution of All-Way Stop-Controlled Ramp Terminal Crashes by Crash Type

Area Type	Crash Type	Crash Type Category	Proportion of Crashes by Severity	
			Fatal and Injury	Property Damage Only
Rural	Multiple vehicle	Head-on	0.000	0.000
		Right-angle	0.500	0.375
		Rear-end	0.500	0.405
		Sideswipe	0.000	0.094
		Other multiple-vehicle crash	0.000	0.000
	Single vehicle	Crash with animal	0.000	0.000
		Crash with fixed object	0.000	0.063
		Crash with other object	0.000	0.000
		Crash with parked vehicle	0.000	0.000
		Other single-vehicle crashes	0.000	0.063
Urban	Multiple vehicle	Head-on	0.000	0.000
		Right-angle	0.182	0.333
		Rear-end	0.727	0.500
		Sideswipe	0.000	0.000
		Other multiple-vehicle crash	0.000	0.000
	Single vehicle	Crash with animal	0.000	0.000
		Crash with fixed object	0.000	0.167
		Crash with other object	0.000	0.000
		Crash with parked vehicle	0.000	0.000
		Other single-vehicle crashes	0.091	0.000

19.11. LIMITATIONS OF PREDICTIVE METHOD

The limitations of the predictive method which apply generally across all of the Part C chapters are discussed in Section C.14 of Part C. This section discusses limitations of the predictive models described this chapter.

The predictive method described in this chapter does not account for the influence of the following conditions on ramp safety:

- Ramp or C-D road segments in rural areas with 2 or more lanes.
- Ramp or C-D road segments in urban areas with 3 or more lanes.
- Ramps and C-D roads providing two-way travel.

- Ramp metering.
- A high-occupancy vehicle (HOV) bypass lane on a ramp or C-D road.
- A frontage-road segment.
- A frontage-road ramp terminal.
- A frontage-road crossroad terminal.
- A crossroad speed-change lane.
- A crossroad ramp terminal with 3 or more left-turn lanes on a crossroad approach.
- A crossroad ramp terminal where the crossroad provides one-way travel.
- The crossroad ramp terminal formed by a single-point urban interchange or roundabout.

The predictive method does not distinguish between barrier types (i.e., cable barrier, concrete barrier, guardrail, and bridge rail) in terms of their possible different influence on crash severity.

19.12. APPLICATION OF PREDICTIVE METHOD

The predictive method presented in this chapter is applied to a ramp by following the 18 steps presented in Section 19.4. Worksheets are provided in Appendix 14A for applying calculations in the predictive method. All computations of crash frequencies within these worksheets are conducted with values expressed to three decimal places. This level of precision is needed only for consistency in computations. In the last stage of computations, rounding the final estimates of expected average crash frequency to one decimal place is appropriate.

19.13. SUMMARY

The predictive method for ramps is applied by following the 18 steps of the predictive method presented in Section 19.4. It is used to estimate the expected average crash frequency for a series of contiguous sites, or a single individual site. If a ramp is being evaluated, then it is divided into a series of sites in Step 5 of the predictive method. Predictive models are applied in Steps 9, 10, and 11 of the method to estimate the expected average crash frequency of each site.

Each predictive model consists of a safety performance function (SPF), crash modification factors (CMFs), a severity distribution function (SDF), and calibration factors. The SPF is selected in Step 9. It is used to estimate the predicted average crash frequency for a site with base conditions. CMFs are selected in Step 10. They are combined with the estimate from the SPF to produce the expected average crash frequency for the subject site. Optionally, the SDFs are selected in Step 13. They can be used to estimate the expected average crash frequency for one or more crash severity levels (i.e., fatal, incapacitating injury, non-incapacitating injury, or possible injury crash). Optionally, the crash type distribution can be used in Step 13 to estimate the expected crash frequency for one or more crash types (e.g., head-on, fixed object).

When observed crash data are available, the EB Method is applied in Step 13 or 15 of the predictive method to improve the reliability of the estimated expected average crash frequency. The EB Method can be applied at the site-specific level in Step 13, or at the project level in Step 15. The choice of level will depend on (a) the required reliability of the estimate and (b) the accuracy with which each observed crash can be associated with an individual site. The EB Method is described in Section B.2 of Appendix B to Part C.

The SPF is calibrated to the specific state or geographic region in which the project is located. Calibration accounts for differences in state or regional crash frequencies, relative to the states and regions represented in the data used to define the predictive models described in this chapter. The process for determining calibration factors for the predictive models is described in Section B.1 of Appendix B to Part C.

Section 19.14 presents several sample problems that detail the application of the predictive method. A series of worksheets are used to guide the method application and document the calculations. The use of these worksheets is illustrated in the sample problems. Appendix 19A contains blank worksheets that can be copied to document future method applications.

19.14. SAMPLE PROBLEMS

In this section, six sample problems are presented using the predictive method steps for ramp facilities. Sample Problems 1 through 3 illustrate how to calculate the predicted average crash frequency for ramp segments. Sample Problems 4 through 6 illustrate how to calculate the predicted average crash frequency for ramp terminals.

Table 19-46. List of Sample Problems

Problem No.	Description
1	Predicted average crash frequency for a one-lane exit ramp segment
2	Predicted average crash frequency for a two-lane C-D road segment
3	Predicted average crash frequency for a one-lane entrance ramp segment
4	Predicted average crash frequency for a D4 ramp terminal with signal control
5	Predicted average crash frequency for a A4 ramp terminal with one-way stop control
6	Predicted average crash frequency for a B2 ramp terminal with all-way stop control

19.14.1. Sample Problem 1

The Site/Facility

A one-lane urban exit ramp segment.

The Question

What is the predicted average crash frequency of the ramp segment for a one-year period?

The Facts

The study year is 2011. The conditions present during this year are provided in the following list.

- 0.15-mi length
- 6,750 veh/day
- 65-mi/h average speed on freeway mainline
- Signal control at crossroad ramp terminal
- One off-segment horizontal curve

- 400-ft radius
- 0.025-mi length
- Beginning at milepost 0.07
- One in-segment horizontal curve
 - 400-ft radius
 - 0.07-mi length, entirely in the segment
 - Beginning at milepost 0.19
- 14-ft lane width
- 8-ft right shoulder width
- 4-ft left shoulder width
- No lane adds or lane drops
- No barrier on the right or left sides of the roadway
- No ramp entrances or exits in the segment
- No weaving section

Assumptions

- Crash type distributions used are the default values presented in Table 19-6 and Table 19-9.
- The calibration factor is 1.00.

Results

Using the predictive method steps as outlined below, the predicted average fatal-and-injury crash frequency for the ramp segment in Sample Problem 1 is determined to be 0.2 crashes per year, and the predicted average property-damage-only crash frequency is determined to be 0.2 crashes per year (rounded to one decimal place).

Steps

Step 1 through 8

To determine the predicted average crash frequency of the ramp segment in Sample Problem 1, only Steps 9 through 13 are conducted. No other steps are necessary because only one ramp segment is analyzed for a one-year period and the EB Method is not applied.

Step 9 – For the selected site, determine and apply the appropriate SPF.

For a one-lane urban exit ramp segment, SPF values for multiple-vehicle and single-vehicle crashes are determined.

Multiple-Vehicle Crashes

The SPF for multiple-vehicle fatal-and-injury crashes is calculated from Equation 19-20 and Table 19-5 as follows:

$$\begin{aligned} N_{spf, rps, 1EX, mv, fi} &= L_r \times \exp(a + b \times \ln[c \times AADT_r]) + d[c \times AADT_r] \\ &= 0.15 \times \exp(-4.971 + 0.524 \times \ln[0.001 \times 6,750]) + 0.0699[0.001 \times 6,750] \\ &= 0.005 \text{ crashes/year} \end{aligned}$$

Similarly, the SPF for multiple-vehicle property-damage-only crashes is calculated from Equation 19-20 and Table 19-5 to yield the following result:

$$N_{spf, rps, 1EX, mv, pdo} = 0.013 \text{ crashes/year}$$

Single-Vehicle Crashes

The SPF for single-vehicle fatal-and-injury crashes is calculated from Equation 19-24 and Table 19-8 as follows:

$$\begin{aligned} N_{spf, rps, 1EX, sv, fi} &= L_r \times \exp(a + b \times \ln[c \times AADT_r]) \\ &= 0.15 \times \exp(-1.645 + 0.718 \times \ln[0.001 \times 6,750]) \\ &= 0.114 \text{ crashes/year} \end{aligned}$$

Similarly, the SPF for single-vehicle property-damage-only crashes is calculated from Equation 19-24 and Table 19-8 to yield the following result:

$$N_{spf, rps, 1EX, sv, pdo} = 0.124 \text{ crashes/year}$$

Step 10 – Multiply the result obtained in Step 9 by the appropriate CMFs.

Each CMF used in the calculation of the predicted average crash frequency of the ramp segment is calculated in this step.

Horizontal Curve (CMF_{L, rps, 1EX, y, z})

The limited curve speed for the off-segment horizontal curve (curve 1) is computed using Equation 19-59 as follows:

$$\begin{aligned} v_{max, 1} &= 3.24 \times (32.2 \times R_1)^{0.30} \\ &= 3.24 \times (32.2 \times 400)^{0.30} \\ &= 55.4 \text{ ft/s} \end{aligned}$$

The in-segment horizontal curve (curve 2) has the same radius as curve 1. Hence, its limited speed $v_{max, 2}$ is also equal to 55.4 ft/s.

The average entry speed at curve 1 is computed using Equation 19-64 and the default values in Table 19-42 as follows:

$$\begin{aligned}
 v_{ent,1} &= (1.47 \times V_{frwy} - 0.034 \times 5,280 \times X_1) \geq 1.47 \times V_{xroad} \\
 &= (1.47 \times 65 - 0.034 \times 5,280 \times 0.07) \geq 1.47 \times 15 \\
 &= 83.0 \text{ ft/s}
 \end{aligned}$$

The average exit speed at curve 1 is computed using Equation 19-65 as follows:

$$\begin{aligned}
 v_{ext,1} &= (v_{ent,1} - 0.034 \times 5,280 \times L_{c,1}) \leq v_{max,1} \text{ and } \geq 1.47 \times V_{xroad} \\
 &= (83.0 - 0.034 \times 5,280 \times 0.025) \leq 55.4 \text{ and } \geq 1.47 \times 15 \\
 &= 55.4 \text{ ft/s}
 \end{aligned}$$

The average entry speed at curve 2 is computed using Equation 19-66 and the default values in Table 19-42 as follows:

$$\begin{aligned}
 v_{ent,i} &= v_{ext,i-1} - 0.034 \times 5,280 \times (X_i - X_{i-1} - L_{c,i-1}) \geq 1.47 \times V_{xroad} \\
 &= 55.4 - 0.034 \times 5,280 \times (0.19 - 0.07 - 0.025) \geq 1.47 \times 15 \\
 &= 38.3 \text{ ft/s}
 \end{aligned}$$

$CMF_{1, rps, 1EX, y, fi}$ is calculated using Equation 19-33 as follows:

$$CMF_{1, rps, 1EX, y, fi} = 1.0 + a \times \frac{1,000}{32.2} \left[\sum_{i=1}^m \left(\frac{v_{ent,i}}{R_i} \right)^2 \times P_{c,i} \right]$$

Only curve 2 is included in the summation term. Curve 1 is not in the segment, but its presence upstream of the segment affects vehicle speeds in curve 2. From Table 19-24, $a = 0.779$ for multiple-vehicle fatal-and-injury crashes. $CMF_{1, rps, 1EX, mv, fi}$ is calculated as follows:

$$\begin{aligned}
 CMF_{1, rps, 1EX, mv, fi} &= 1.0 + 0.779 \times \frac{1,000}{32.2} \left(\frac{38.3}{400} \right)^2 \times \frac{0.07}{0.15} \\
 &= 1.104
 \end{aligned}$$

Calculations using the other coefficients from Table 19-24 yield the following results:

$$CMF_{1, rps, 1EX, sv, fi} = 1.320$$

$$CMF_{1, rps, 1EX, mv, pdo} = 1.073$$

$$CMF_{1, rps, 1EX, sv, pdo} = 1.418$$

Lane Width ($CMF_{2, rps, 1EX, y, z}$)

The segment has 14-ft lanes, which is the base condition for the lane width CMF. Hence, $CMF_{2, rps, 1EX, y, fi}$ and $CMF_{2, rps, 1EX, y, pdo}$ are equal to 1.000.

Right Shoulder Width ($CMF_{3, rps, 1EX, y, z}$)

The segment has 8-ft right shoulders, which is the base condition for the right shoulder width CMF. Hence, $CMF_{3, rps, 1EX, y, fi}$ and $CMF_{3, rps, 1EX, y, pdo}$ are equal to 1.000.

Left Shoulder Width ($CMF_{4, rps, 1EX, y, z}$)

The segment has 4-ft left shoulders, which is the base condition for the left shoulder width CMF. Hence, $CMF_{4, rps, 1EX, y, fi}$ and $CMF_{4, rps, 1EX, y, pdo}$ are equal to 1.000.

Right Side Barrier ($CMF_{5, rps, 1EX, y, z}$)

The segment does not have right side barrier. Hence, $CMF_{5, rps, 1EX, y, fi}$ and $CMF_{5, rps, 1EX, y, pdo}$ are equal to 1.000.

Left Side Barrier ($CMF_{6, rps, 1EX, y, z}$)

The segment does not have left side barrier. Hence, $CMF_{6, rps, 1EX, y, fi}$ and $CMF_{6, rps, 1EX, y, pdo}$ are equal to 1.000.

Lane Add or Drop ($CMF_{7, rps, 1EX, y, fi}$)

The segment does not have a lane add or a lane drop. Hence, $CMF_{7, rps, 1EX, y, fi}$ is equal to 1.000.

Ramp Speed-Change Lane ($CMF_{8, rps, 1EX, mv, fi}$)

The segment does not have a speed-change lane. Hence, $CMF_{8, rps, 1EX, mv, fi}$ is equal to 1.000.

Multiple-Vehicle Crashes

The CMFs are applied to the multiple-vehicle fatal-and-injury SPF as follows:

$$\begin{aligned} N_{p^*, rps, 1EX, mv, fi} &= N_{spf, rps, 1EX, mv, fi} \times (CMF_{1, rps, 1EX, mv, fi} \times \dots \times CMF_{8, rps, 1EX, mv, fi}) \\ &= 0.005 \times (1.104 \times 1.000 \times 1.000 \times 1.000 \times 1.000 \times 1.000 \times 1.000 \times 1.000) \\ &= 0.005 \times 1.104 \\ &= 0.005 \text{ crashes/year} \end{aligned}$$

The CMFs are applied to the multiple-vehicle property-damage-only SPF as follows:

$$\begin{aligned} N_{p^*, rps, 1EX, mv, pdo} &= N_{spf, rps, 1EX, mv, pdo} \times (CMF_{1, rps, 1EX, mv, pdo} \times \dots \times CMF_{8, rps, 1EX, mv, pdo}) \\ &= 0.013 \times (1.073 \times 1.000 \times 1.000 \times 1.000 \times 1.000 \times 1.000 \times 1.000 \times 1.000) \\ &= 0.013 \times 1.073 \\ &= 0.014 \text{ crashes/year} \end{aligned}$$

Single-Vehicle Crashes

The CMFs are applied to the single-vehicle fatal-and-injury SPF as follows:

$$\begin{aligned} N_{p^*, rps, 1EX, sv, fi} &= N_{spf, rps, 1EX, sv, fi} \times (CMF_{1, rps, 1EX, sv, fi} \times \dots \times CMF_{8, rps, 1EX, sv, fi}) \\ &= 0.114 \times (1.320 \times 1.000 \times 1.000 \times 1.000 \times 1.000 \times 1.000 \times 1.000 \times 1.000) \\ &= 0.114 \times 1.320 \\ &= 0.151 \text{ crashes/year} \end{aligned}$$

The CMFs are applied to the single-vehicle property-damage-only SPF as follows:

$$\begin{aligned} N_{p^*, rps, 1EX, sv, pdo} &= N_{spf, rps, 1EX, sv, pdo} \times (CMF_{1, rps, 1EX, sv, pdo} \times \dots \times CMF_{8, rps, 1EX, sv, pdo}) \\ &= 0.124 \times (1.418 \times 1.000 \times 1.000 \times 1.000 \times 1.000 \times 1.000 \times 1.000 \times 1.000) \\ &= 0.124 \times 1.418 \\ &= 0.176 \text{ crashes/year} \end{aligned}$$

Step 11 – Multiply the result obtained in Step 10 by the appropriate calibration factor.

It is assumed that a calibration factor of 1.00 has been determined for local conditions. As a result, $N_{p, rps, 1EX, y, z} = N_{p^*, rps, 1EX, y, z}$ for both crash types y ($y = mv$: multiple-vehicle, sv : single-vehicle) and both crash severities z ($z = fi$: fatal-and-injury, pdo : property-damage-only). See Section B.1 of Appendix B to Part C for further discussion on calibration of the predicted models.

Calculation of Predicted Average Crash Frequency

The predicted average crash frequency is calculated using Equation 19-1 based on the results obtained in Steps 9 through 11 as follows.

Fatal-and-injury crashes:

$$\begin{aligned} N_{p, rps, 1EX, at, fi} &= N_{p, rps, 1EX, mv, fi} + N_{p, rps, 1EX, sv, fi} \\ &= 0.005 + 0.151 \\ &= 0.156 \text{ crashes/year} \end{aligned}$$

Property-damage-only crashes:

$$\begin{aligned} N_{p, rps, 1EX, at, pdo} &= N_{p, rps, 1EX, mv, pdo} + N_{p, rps, 1EX, sv, pdo} \\ &= 0.014 + 0.176 \\ &= 0.190 \text{ crashes/year} \end{aligned}$$

Step 12—If there is another year to be evaluated in the evaluation period for the selected site, return to Step 8. Otherwise, proceed to Step 13.

The study period is one year (2011), so steps 8 through 11 need not be repeated.

Step 13—Apply site-specific EB Method (if applicable) and apply SDFs.

This step consists of three optional sets of calculations—site-specific EB Method, severity distribution functions, and crash type distribution.

Apply the site-specific EB Method to a future time period, if appropriate.

The site-specific EB Method is not applied in this sample problem because crash data are not available.

Apply the severity distribution functions (SDFs), if desired.

To apply the SDFs, the systematic component of crash severity likelihood V_j is computed for each severity level j using Equation 19-83 as follows:

$$V_j = a + \left(b \times \frac{P_{lb} + P_{rb}}{2} \right) + (c \times n) + (d \times I_{rural}) + (e \times I_{exr})$$

The coefficients a , b , c , d , and e are obtained from Table 19-43 for each severity level j . The segment does not have barrier, so P_{lb} and P_{rb} are equal to 0.0. V_j is computed for fatal and incapacitating injury crashes as follows:

$$\begin{aligned} V_{K+A} &= -1.537 + \left(-0.481 \times \frac{0.0 + 0.0}{2} \right) + (-0.228 \times 1.0) + (0.668 \times 0.0) + (0.426 \times 1.0) \\ &= -1.339 \end{aligned}$$

Similar calculations using the coefficients from Table 19-43 for non-incapacitating injury crashes yield the following results:

$$V_B = -0.199$$

Using these computed V_{K+A} and V_B values, and assuming a calibration factor $C_{sdf, rps+cds}$ of 1.0, the probability of occurrence of a fatal crash is computed using Equation 19-79 as follows:

$$\begin{aligned} P_{rps+cds, ac, at, K} &= \frac{\exp(V_{K+A})}{\frac{1.0}{C_{sdf, rps+cds}} + \exp(V_{K+A}) + \exp(V_B)} \times P_{K|K+A, rps+cds, ac, at} \\ &= \frac{\exp(-1.339)}{\frac{1.0}{1.0} + \exp(-1.339) + \exp(-0.199)} \times 0.248 \\ &= 0.032 \end{aligned}$$

Similar calculations using Equation 19-80 and Equation 19-81 yield the following results:

$$P_{rps+cds, ac, at, A} = 0.096$$

$$P_{rps+cds, ac, at, B} = 0.391$$

The probability of occurrence of a possible-injury crash is computed using Equation 19-82 as follows:

$$\begin{aligned} P_{rps+cds, ac, at, C} &= 1.0 - (P_{rps+cds, ac, at, K} + P_{rps+cds, ac, at, A} + P_{rps+cds, ac, at, B}) \\ &= 1.0 - (0.032 + 0.096 + 0.391) \\ &= 0.481 \end{aligned}$$

The probability of occurrence of a fatal crash is multiplied by the fatal-and-injury crash frequency obtained in Step 11 using Equation 19-78 as follows:

$$\begin{aligned} N_{e, rps, 1EX, at, K} &= N_{e, rps, 1EX, at, fi} \times P_{rps+cds, ac, at, K} \\ &= 0.156 \times 0.032 \\ &= 0.005 \text{ crashes/year} \end{aligned}$$

Similar calculations using Equation 19-78 and the probabilities of occurrences of the other crash severities yield the following results:

$$N_{e, rps, 1EX, at, A} = 0.015 \text{ crashes/year}$$

$$N_{e, rps, 1EX, at, B} = 0.061 \text{ crashes/year}$$

$$N_{e, rps, 1EX, at, C} = 0.075 \text{ crashes/year}$$

Apply the crash type distribution, if desired.

The crash type distributions are applied by multiplying the default crash type distribution proportions in Table 19-6 and Table 19-9 by the predicted average crash frequencies obtained in Step 11.

Worksheets

The step-by-step instructions are provided to illustrate the predictive method for calculating the predicted average crash frequency for a ramp segment. To apply the predictive method steps to multiple segments, a series of worksheets are provided for determining the predicted average crash frequency. The worksheets include:

- Table 19-47. Ramp Segment Worksheet (1 of 4)—Sample Problem 1
- Table 19-48. Ramp Segment Worksheet (2 of 4)—Sample Problem 1
- Table 19-49. Ramp Segment Worksheet (3 of 4)—Sample Problem 1
- Table 19-50. Ramp Segment Worksheet (4 of 4)—Sample Problem 1

Filled versions of these worksheets are provided below. Blank versions of worksheets used in the Sample Problems are provided in Appendix 19A.

Table 19-47 is a summary of general information about the ramp segment, analysis, input data (i.e., “The Facts”), and assumptions for Sample Problem 1. The input data include area type, crash data, basic roadway data, and alignment data.

Table 19-48 is a summary of general information about the ramp segment, analysis, input data (i.e., “The Facts”), and assumptions for Sample Problem 1. The input data include cross section data, roadside data, ramp access data, and traffic data.

Table 19-49 is a tabulation of the CMF and SPF computations for Sample Problem 1.

Table 19-50 is a tabulation of the crash severity and crash type distributions for Sample Problem 1.

Table 19-47. Ramp Segment Worksheet (1 of 4)—Sample Problem 1

General Information					Location Information					
Analyst					Roadway					
Agency or company					Roadway section					
Date performed					Study year					
Area type		X	Urban		Rural					
Input Data										
Crash Data				Crash Period	Study Year	Complete the study year column. Complete the crash period column if the EB Method is used.				
Crash data time period						First year	--	Last year	--	
Count of multiple-vehicle FI crashes $N_{o, w, n, mv, fi}^*$				--						
Count of single-vehicle FI crashes $N_{o, w, n, sv, fi}^*$				--						
Count of multiple-vehicle PDO crashes $N_{o, w, n, mv, pdo}^*$				--						
Count of single-vehicle PDO crashes $N_{o, w, n, sv, pdo}^*$				--						
Basic Roadway Data										
Number of through lanes n				1		Same value for crash period and study year.				
Segment length L (mi)				--	0.15					
Average traffic speed on the freeway V_{frwy} (mi/h)				--	65					
Segment type				Exit		Choices: Entrance, Exit, C-D road, Connector				
Type of control at crossroad ramp terminal				--	Signal	Choices: Stop, Yield, Signal, None				
Alignment Data										
Horizontal Curve Data										
1	Presence of horizontal curve 1			--	Off Seg.	Choices: No, In segment, Off segment.				
	Curve radius R_1 (ft)			--	400	If "In segment" or "Off segment", enter data for curve radius, length, and milepost.				
	Length of curve L_{c1} (mi)			--	0.025					
	Length of curve in segment $L_{c1, seg}$ (mi)			--	--					
	Milepost of beginning of curve in dir. of travel X_1 (mi)			--	0.07					
2	Presence of horizontal curve 2			--	In Seg.	Choices: No, In segment, Off segment				
	Curve radius R_2 (ft)			--	400	If "In segment" or "Off segment", enter data for curve radius, length, and milepost.				
	Length of curve L_{c2} (mi)			--	0.07					
	Length of curve in segment $L_{c2, seg}$ (mi)			--	0.07					
	Milepost of beginning of curve in dir. of travel X_2 (mi)			--	0.19					
3	Presence of horizontal curve 3			--	No	Choices: No, In segment, Off segment				
	Curve radius R_3 (ft)			--	--	If "In segment" or "Off segment", enter data for curve radius, length, and milepost.				
	Length of curve L_{c3} (mi)			--	--					
	Length of curve in segment $L_{c3, seg}$ (mi)			--	--					
	Milepost of beginning of curve in dir. of travel X_3 (mi)			--	--					
4	Presence of horizontal curve 4			--	No	Choices: No, In segment, Off segment				
	Curve radius R_4 (ft)			--	--	If "In segment" or "Off segment", enter data for curve radius, length, and milepost.				
	Length of curve L_{c4} (mi)			--	--					
	Length of curve in segment $L_{c4, seg}$ (mi)			--	--					
	Milepost of beginning of curve in dir. of travel X_4 (mi)			--	--					

Table 19-48. Ramp Segment Worksheet (2 of 4)—Sample Problem 1

Input Data						
Cross Section Data		Crash Period	Study Year	Complete the study year column. Complete the crash period column if the EB Method is used.		
Lane width W_l (ft)		--	14			
Right shoulder width W_{rs} (ft)		--	8			
Left shoulder width W_{ls} (ft)		--	4			
Presence of lane add or lane drop		--	No	Choices: No, Lane add, Lane drop		
Length of taper in segment $L_{add, seg}$ or $L_{drop, seg}$ (mi)		--	--	If "Lane add" or "Lane drop", enter length.		
Roadside Data						
Presence of barrier on right side of roadway		--	Y/N	N	Y/N	If Yes, then use the ramp barrier worksheet.
Presence of barrier on left side of roadway		--	Y/N	N	Y/N	If Yes, then use the ramp barrier worksheet.
Ramp Access Data						
Ramp Entrance						
Ent. ramp	Presence of speed-change lane in segment	--	Y/N	N	Y/N	If Yes, then enter data in the next row.
	Length of s-c lane in segment $L_{en, seg}$ (mi)	--	--	--	--	
Exit ramp	Presence of speed-change lane in segment	--	Y/N	N	Y/N	If Yes, then enter data in the next row.
	Length of s-c lane in segment $L_{ex, seg}$ (mi)	--	--	--	--	
Weave	Presence of a weaving section in segment	--	Y/N	--	Y/N	If Yes, then enter data in the next two rows.
	Length of weaving section L_{wev} (mi)	--	--	--	--	
	Length of weaving section in seg. $L_{wev, seg}$ (mi)	--	--	--	--	
Traffic Data						
Segment AADT $AAADT_r$ or $AAADT_c$ (veh/day)		--	6,750			

Table 19-49. Ramp Segment Worksheet (3 of 4)—Sample Problem 1

Crash Modification Factors									
Complete the study year column. Complete the crash period column if the EB Method is used. Equation	Fatal and Injury				Property Damage Only				
	Multiple Vehicle		Single Vehicle		Multiple Vehicle		Single Vehicle		
	Crash Period	Study Year	Crash Period	Study Year	Crash Period	Study Year	Crash Period	Study Year	
Horizontal curve $CMF_{1, w, x, y, z}$	19-33	--	1.104	--	1.320	--	1.073	--	1.418
Lane width $CMF_{2, w, x, y, fi}$	19-34	--	1.000	--	1.000				
Right shoulder width $CMF_{3, w, x, y, z}$	19-35	--	1.000	--	1.000	--	1.000	--	1.000
Left shoulder width $CMF_{4, w, x, y, z}$	19-36	--	1.000	--	1.000	--	1.000	--	1.000
Right side barrier $CMF_{5, w, x, y, z}$	19-37	--	1.000	--	1.000	--	1.000	--	1.000
Left side barrier $CMF_{6, w, x, y, z}$	19-38	--	1.000	--	1.000	--	1.000	--	1.000
Lane add or drop $CMF_{7, w, x, y, fi}$	19-39	--	1.000	--	1.000				
Ramp speed-change lane $CMF_{8, w, x, mv, fi}$	19-40	--	1.000						
Weaving section $CMF_{9, cds, ac, y, z}$	19-41	--	1.000	--	1.000	--	1.000	--	1.000
Combined CMF (multiply all CMFs evaluated)		--	1.104	--	1.320	--	1.073	--	1.418
Expected Average Crash Frequency^a									
Complete the study year column. Complete the crash period column if the <i>site-specific</i> EB Method is used.	Fatal and Injury				Property Damage Only				
	Multiple Vehicle		Single Vehicle		Multiple Vehicle		Single Vehicle		
	Crash Period	Study Year	Crash Period	Study Year	Crash Period	Study Year	Crash Period	Study Year	
Calibration factor $C_{w, x, y, z}$		1.00		1.00		1.00		1.00	
Overdispersion parameter $k_{w, x, y, z}$	--		--		--		--		
Observed crash count $N_{o, w, x, y, z}^*$ (cr)	--		--		--		--		
Reference year r	--		--		--		--		
Predicted average crash freq. for reference year $N_{p, w, x, y, z, r}$ (cr/yr)	--		--		--		--		
Predicted number of crashes for crash period (sum all years) $N_{p, w, x, y, z}^*$ (cr)	--		--		--		--		
Equivalent years associated with crash count $C_{b, w, x, y, z, r}$ (yr)	--		--		--		--		
Adjusted average crash freq. for ref. year given $N_{o, w, x, y, z, r}^*$ (cr/yr)	--		--		--		--		
Study year s		2011		2011		2011		2011	
Predicted average crash freq. for study year $N_{p, w, x, y, z, s}$ (cr/yr)		0.005		0.151		0.014		0.175	
Expected average crash freq. for study year $N_{e, w, x, y, z, s}$ (cr/yr)		0.005		0.151		0.014		0.175	
Expected average crash freq. for study year (all crash types) $N_{e, w, x, at, z, s}$ (cr/yr)				0.156				0.189	

Note:

a – If the EB Method is not used, then substitute the word “predicted” for the word “expected” and substitute the subscript “p” for the subscript “e”.

Table 19-50. Ramp Segment Worksheet (4 of 4)—Sample Problem 1**Expected Average Crash Frequency^a****Crash Severity Distribution**

	K	A	B	C	Total FI	PDO	Total FI + PDO
Proportion by injury level	0.032	0.096	0.391	0.481	1.000		
Expected average crash freq. for study year (all crash types) $N_{e, w, x, at, z, s}$ (cr/yr)	0.005	0.015	0.061	0.075	0.156	0.189	0.345

Crash Type Distribution

Crash Type Category	Table	Fatal and Injury		Property Damage Only		Total
		Proportion	Expected Average Crash Frequency for Study Year $N_{e, w, x, y, fi, s}$ (cr/yr)	Proportion	Expected Average Crash Frequency for Study Year $N_{e, w, x, y, pdo, s}$ (cr/yr)	Expected Average Crash Frequency for Study Year $N_{e, w, x, y, as, s}$ (cr/yr)
Multiple-Vehicle Crashes	19-6					
Head-on		0.015	0.000	0.009	0.000	0.000
Right-angle		0.010	0.000	0.005	0.000	0.000
Rear-end		0.707	0.003	0.550	0.008	0.011
Sideswipe		0.129	0.001	0.335	0.005	0.005
Other multiple-vehicle crashes		0.139	0.001	0.101	0.001	0.002
Total		1.000	0.005	1.000	0.014	0.019
Single-Vehicle Crashes	19-9					
Crash with animal		0.003	0.000	0.005	0.001	0.001
Crash with fixed object		0.718	0.108	0.834	0.146	0.254
Crash with other object		0.015	0.002	0.023	0.004	0.006
Crash with parked vehicle		0.012	0.002	0.012	0.002	0.004
Other single-vehicle crashes		0.252	0.038	0.126	0.022	0.060
Total		1.000	0.151	1.000	0.175	0.326

Note:

a – If the EB Method is not used, then substitute the word “predicted” for the word “expected” and substitute the subscript “p” for the subscript “e”.

19.14.2. Sample Problem 2**The Site/Facility**

A two-lane urban C-D road segment.

The Question

What is the predicted average crash frequency of the C-D road segment for a one-year period?

The Facts

The study year is 2011. The conditions present during this year are provided in the following list.

- 0.08-mi length
- 5,500 veh/day

- 60-mi/h average speed on freeway mainline
- One off-segment horizontal curve
 - 1,100-ft radius
 - 0.08-mi length
 - Beginning at milepost 0.09
- 14-ft lane width
- 8-ft right shoulder width
- 4-ft left shoulder width
- No lane adds or lane drops
- No barrier on the right or left sides of the roadway
- No ramp entrances or exits in the segment
- 0.08-mi weaving section along entire length of segment

Assumptions

- Crash type distributions used are the default values presented in Table 19-6 and Table 19-9.
- The calibration factor is 1.00.

Results

Using the predictive method steps as outlined below, the predicted average fatal-and-injury crash frequency for the C-D road segment in Sample Problem 2 is determined to be 0.1 crashes per year, and the predicted average property-damage-only crash frequency is determined to be 0.2 crashes per year (rounded to one decimal place).

Steps

Step 1 through 8

To determine the predicted average crash frequency of the C-D road segment in Sample Problem 2, only Steps 9 through 13 are conducted. No other steps are necessary because only one C-D road segment is analyzed for a one-year period and the EB Method is not applied.

Step 9 – For the selected site, determine and apply the appropriate SPF.

For a two-lane urban C-D road segment, SPF values for multiple-vehicle and single-vehicle crashes are determined.

Multiple-Vehicle Crashes

The SPF for multiple-vehicle fatal-and-injury crashes is calculated from Equation 19-22 and Table 19-7 as follows:

$$\begin{aligned}
 N_{spf, cds, 2, mv, fi} &= L_{cd} \times \exp(a + b \times \ln[c \times AADT_c] + d[c \times AADT_c]) \\
 &= 0.08 \times \exp(-2.515 + 0.524 \times \ln[0.001 \times 5,500] + 0.0699[0.001 \times 5,500]) \\
 &= 0.023 \text{ crashes/year}
 \end{aligned}$$

Similarly, the SPF for multiple-vehicle property-damage-only crashes is calculated from Equation 19-22 and Table 19-7 to yield the following result:

$$N_{spf, cds, 2, mv, pdo} = 0.057 \text{ crashes/year}$$

Single-Vehicle Crashes

The SPF for single-vehicle fatal-and-injury crashes is calculated from Equation 19-26 and Table 19-10 as follows:

$$\begin{aligned}
 N_{spf, cds, 2, sv, fi} &= L_{cd} \times \exp(a + b \times \ln[c \times AADT_c]) \\
 &= 0.08 \times \exp(-2.881 + 0.718 \times \ln[0.001 \times 5,500]) \\
 &= 0.015 \text{ crashes/year}
 \end{aligned}$$

Similarly, the SPF for single-vehicle property-damage-only crashes is calculated from Equation 19-26 and Table 19-10 to yield the following result:

$$N_{spf, cds, 2, sv, pdo} = 0.025 \text{ crashes/year}$$

Step 10 – Multiply the result obtained in Step 9 by the appropriate CMFs.

Each CMF used in the calculation of the predicted average crash frequency of the ramp segment is calculated in this step.

Horizontal Curve ($CMF_{1, cds, 2, y, z}$)

$CMF_{1, cds, 2, y, z}$ is calculated using Equation 19-33 as follows:

$$CMF_{1, cds, 2, y, z} = 1.0 + a \times \frac{1,000}{32.2} \left[\sum_{i=1}^m \left(\frac{v_{ent,i}}{R_i} \right)^2 \times P_{c,i} \right]$$

Only in-segment curves are included in the summation term. The C-D road has a curve upstream of the segment being analyzed, but there are no curves in the segment. Hence, $CMF_{1, cds, 2, y, z}$ is equal to 1.000.

Lane Width ($CMF_{2, cds, 2, y, z}$)

The segment has 14-ft lanes, which is the base condition for the lane width CMF. Hence, $CMF_{2, cds, 2, y, fi}$ and $CMF_{2, cds, 2, y, pdo}$ are equal to 1.000.

Right Shoulder Width ($CMF_{3, cds, 2, y, z}$)

The segment has 8-ft right shoulders, which is the base condition for the right shoulder width CMF. Hence, $CMF_{3, cds, 2, y, fi}$ and $CMF_{3, cds, 2, y, pdo}$ are equal to 1.000.

Left Shoulder Width ($CMF_{4, cds, 2, y, z}$)

The segment has 4-ft left shoulders, which is the base condition for the left shoulder width CMF. Hence, $CMF_{4, cds, 2, y, fi}$ and $CMF_{4, cds, 2, y, pdo}$ are equal to 1.000.

Right Side Barrier ($CMF_{5, cds, 2, y, z}$)

The segment does not have right side barrier. Hence, $CMF_{5, rps, 1EX, y, fi}$ and $CMF_{5, rps, 1EX, y, pdo}$ are equal to 1.000.

Left Side Barrier ($CMF_{6, rps, 1EX, y, z}$)

The segment does not have left side barrier. Hence, $CMF_{6, cds, 2, y, fi}$ and $CMF_{6, cds, 2, y, pdo}$ are equal to 1.000.

Lane Add or Drop ($CMF_{7, cds, 2, y, fi}$)

The segment does not have a lane add or a lane drop. Hence, $CMF_{7, rps, 1EX, y, fi}$ is equal to 1.000.

Ramp Speed-Change Lane ($CMF_{8, cds, 2, mv, fi}$)

The segment does not have a speed-change lane. Hence, $CMF_{8, cds, 2, mv, fi}$ is equal to 1.000.

Weaving Section ($CMF_{9, cds, 2, at, z}$)

$CMF_{9, cds, 2, at, z}$ is calculated using Equation 19-41 as follows:

$$CMF_{9, cds, 2, at, z} = (1.0 - P_{wev}) \times 1.0 + P_{wev} \times \exp\left(\frac{a + b \times \ln[c \times AADT_c]}{L_{wev}}\right)$$

From Table 19-31, $a = 0.191$, $b = -0.0715$, and $c = 0.001$ for multiple-vehicle fatal-and-injury crashes. $CMF_{9, cds, 2, at, z}$ is calculated as follows:

$$\begin{aligned} CMF_{9, cds, 2, at, fi} &= (1.0 - 1.0) \times 1.0 + 1.0 \times \exp\left(\frac{0.191 - 0.0715 \times \ln[0.001 \times 5,500]}{0.08}\right) \\ &= 2.372 \end{aligned}$$

Similar calculations using the property-damage-only coefficients from Table 19-31 yield the following results:

$$CMF_{9, cds, 2, at, pdo} = 3.009$$

Multiple-Vehicle Crashes

The CMFs are applied to the multiple-vehicle fatal-and-injury SPF as follows:

$$\begin{aligned} N_{p^*, cds, 2, mv, fi} &= N_{spf, cds, 2, mv, fi} \times (CMF_{1, cds, 2, mv, fi} \times \dots \times CMF_{9, cds, 2, mv, fi}) \\ &= 0.023 \times (1.000 \times 1.000 \times 2.372) \\ &= 0.023 \times 2.372 \\ &= 0.055 \text{ crashes/year} \end{aligned}$$

The CMFs are applied to the multiple-vehicle property-damage-only SPF as follows:

$$\begin{aligned} N_{p^*, cds, 2, mv, pdo} &= N_{spf, cds, 2, mv, pdo} \times (CMF_{1, cds, 2, mv, pdo} \times \dots \times CMF_{9, cds, 2, mv, pdo}) \\ &= 0.057 \times (1.000 \times 1.000 \times 3.009) \\ &= 0.057 \times 3.009 \\ &= 0.172 \text{ crashes/year} \end{aligned}$$

Single-Vehicle Crashes

The CMFs are applied to the single-vehicle fatal-and-injury SPF as follows:

$$\begin{aligned} N_{p^*, cds, 2, sv, fi} &= N_{spf, cds, 2, sv, fi} \times (CMF_{1, cds, 2, sv, fi} \times \dots \times CMF_{7, cds, 2, sv, fi} \times CMF_{9, cds, 2, sv, fi}) \\ &= 0.015 \times (1.000 \times 1.000 \times 1.000 \times 1.000 \times 1.000 \times 1.000 \times 1.000 \times 2.372) \\ &= 0.015 \times 2.372 \\ &= 0.036 \text{ crashes/year} \end{aligned}$$

The CMFs are applied to the single-vehicle property-damage-only SPF as follows:

$$\begin{aligned} N_{p^*, cds, 2, sv, pdo} &= N_{spf, cds, 2, sv, pdo} \times (CMF_{1, cds, 2, sv, pdo} \times \dots \times CMF_{7, cds, 2, sv, pdo} \times CMF_{9, cds, 2, sv, pdo}) \\ &= 0.025 \times (1.000 \times 1.000 \times 1.000 \times 1.000 \times 1.000 \times 1.000 \times 1.000 \times 3.009) \\ &= 0.025 \times 3.009 \\ &= 0.075 \text{ crashes/year} \end{aligned}$$

Step 11 – Multiply the result obtained in Step 10 by the appropriate calibration factor.

It is assumed that a calibration factor of 1.00 has been determined for local conditions. As a result, $N_{p, cds, 2, y, z} = N_{p^*, cds, 2, y, z}$ for both crash types y ($y = mv$: multiple-vehicle, sv : single-vehicle) and both crash severities z ($z = fi$: fatal-and-injury, pdo : property-damage-only). See Section B.1 of Appendix B to Part C for further discussion on calibration of the predicted models.

Calculation of Predicted Average Crash Frequency

The predicted average crash frequency is calculated using Equation 19-1 based on the results obtained in Steps 9 through 11 as follows.

Fatal-and-injury crashes:

$$\begin{aligned} N_{p, cds, 2, at, fi} &= N_{p, cds, 2, mv, fi} + N_{p, cds, 2, sv, fi} \\ &= 0.055 + 0.036 \\ &= 0.091 \text{ crashes/year} \end{aligned}$$

Property-damage-only crashes:

$$\begin{aligned} N_{p, cds, 2, at, pdo} &= N_{p, cds, 2, mv, pdo} + N_{p, cds, 2, sv, pdo} \\ &= 0.172 + 0.075 \\ &= 0.247 \text{ crashes/year} \end{aligned}$$

Step 12—If there is another year to be evaluated in the evaluation period for the selected site, return to Step 8. Otherwise, proceed to Step 13.

The study period is one year (2011), so steps 8 through 11 need not be repeated.

Step 13—Apply site-specific EB Method (if applicable) and apply SDFs.

This step consists of three optional sets of calculations—site-specific EB Method, severity distribution functions, and crash type distribution.

Apply the site-specific EB Method to a future time period, if appropriate.

The site-specific EB Method is not applied in this sample problem because crash data are not available.

Apply the severity distribution functions (SDFs), if desired.

To apply the SDFs, the systematic component of crash severity likelihood V_j is computed for each severity level j using Equation 19-83 as follows:

$$V_j = a + \left(b \times \frac{P_{lb} + P_{rb}}{2} \right) + (c \times n) + (d \times I_{rural}) + (e \times I_{exr})$$

The coefficients a , b , c , d , and e are obtained from Table 19-43 for each severity level j . The segment does not have barrier, so P_{lb} and P_{rb} are equal to 0.0. V_j is computed for fatal and incapacitating injury crashes as follows:

$$\begin{aligned} V_{K+A} &= -1.537 + \left(-0.481 \times \frac{0.0 + 0.0}{2} \right) + (-0.228 \times 2.0) + (0.668 \times 0.0) + (0.426 \times 0.0) \\ &= -1.993 \end{aligned}$$

Similar calculations using the coefficients from Table 19-43 for non-incapacitating injury crashes yield the following results:

$$V_B = -0.634$$

Using these computed V_{K+A} and V_B values, and assuming a calibration factor $C_{sdf, rps+cds}$ of 1.0, the probability of occurrence of a fatal crash is computed using Equation 19-79 as follows:

$$\begin{aligned} P_{rps+cds, ac, at, K} &= \frac{\exp(V_{K+A})}{\frac{1.0}{C_{sdf, rps+cds}} + \exp(V_{K+A}) + \exp(V_B)} \times P_{K|K+A, rps+cds, ac, at} \\ &= \frac{\exp(-1.993)}{\frac{1.0}{1.0} + \exp(-1.993) + \exp(-0.634)} \times 0.248 \\ &= 0.022 \end{aligned}$$

Similar calculations using Equation 19-80 and Equation 19-81 yield the following results:

$$P_{rps+cds, ac, at, A} = 0.065$$

$$P_{rps+cds, ac, at, B} = 0.315$$

The probability of occurrence of a possible-injury crash is computed using Equation 19-82 as follows:

$$\begin{aligned} P_{rps+cds, ac, at, C} &= 1.0 - (P_{rps+cds, ac, at, K} + P_{rps+cds, ac, at, A} + P_{rps+cds, ac, at, B}) \\ &= 1.0 - (0.022 + 0.065 + 0.315) \\ &= 0.598 \end{aligned}$$

The probability of occurrence of a fatal crash is multiplied by the fatal-and-injury crash frequency obtained in Step 11 using Equation 19-78 as follows:

$$\begin{aligned}
 N_{e,cds,2,at,K} &= N_{e,cds,2,at,fi} \times P_{rps+cds,ac,at,K} \\
 &= 0.091 \times 0.022 \\
 &= 0.002 \text{ crashes/year}
 \end{aligned}$$

Similar calculations using Equation 19-78 and the probabilities of occurrences of the other crash severities yield the following results:

$$N_{e,cds,2,at,A} = 0.006 \text{ crashes/year}$$

$$N_{e,cds,2,at,B} = 0.029 \text{ crashes/year}$$

$$N_{e,cds,2,at,C} = 0.055 \text{ crashes/year}$$

Apply the crash type distribution, if desired.

The crash type distributions are applied by multiplying the default crash type distribution proportions in Table 19-6 and Table 19-9 by the predicted average crash frequencies obtained in Step 11.

Worksheets

The step-by-step instructions are provided to illustrate the predictive method for calculating the predicted average crash frequency for a ramp segment. To apply the predictive method steps to multiple segments, a series of worksheets are provided for determining the predicted average crash frequency. The worksheets include:

- Table 19-51. Ramp Segment Worksheet (1 of 4)—Sample Problem 2
- Table 19-52. Ramp Segment Worksheet (2 of 4)—Sample Problem 2
- Table 19-53. Ramp Segment Worksheet (3 of 4)—Sample Problem 2
- Table 19-54. Ramp Segment Worksheet (4 of 4)—Sample Problem 2

Filled versions of these worksheets are provided below. Blank versions of worksheets used in the Sample Problems are provided in Appendix 19A.

Table 19-51 is a summary of general information about the ramp segment, analysis, input data (i.e., “The Facts”), and assumptions for Sample Problem 2. The input data include area type, crash data, basic roadway data, and alignment data.

Table 19-52 is a summary of general information about the ramp segment, analysis, input data (i.e., “The Facts”), and assumptions for Sample Problem 2. The input data include cross section data, roadside data, ramp access data, and traffic data.

Table 19-53 is a tabulation of the CMF and SPF computations for Sample Problem 2.

Table 19-54 is a tabulation of the crash severity and crash type distributions for Sample Problem 2.

Table 19-51. Ramp Segment Worksheet (1 of 4)—Sample Problem 2

General Information					Location Information				
Analyst					Roadway				
Agency or company					Roadway section				
Date performed					Study year				
Area type		X	Urban		Rural				
Input Data									
Crash Data				Crash Period	Study Year	Complete the study year column. Complete the crash period column if the EB Method is used.			
Crash data time period						First year	--	Last year	--
Count of multiple-vehicle FI crashes $N_{o, w, n, mv, fi}^*$									
Count of single-vehicle FI crashes $N_{o, w, n, sv, fi}^*$									
Count of multiple-vehicle PDO crashes $N_{o, w, n, mv, pdo}^*$									
Count of single-vehicle PDO crashes $N_{o, w, n, sv, pdo}^*$									
Basic Roadway Data									
Number of through lanes n				2		Same value for crash period and study year.			
Segment length L (mi)				0.08					
Average traffic speed on the freeway V_{frwy} (mi/h)				60					
Segment type				C-D Road		Choices: Entrance, Exit, C-D road, Connector			
Type of control at crossroad ramp terminal				--		Choices: Stop, Yield, Signal, None			
Alignment Data									
Horizontal Curve Data									
1	Presence of horizontal curve 1				Off Seg.	Choices: No, In segment, Off segment.			
	Curve radius R_1 (ft)				1,100	If "In segment" or "Off segment", enter data for curve radius, length, and milepost.			
	Length of curve L_{c1} (mi)				0.08				
	Length of curve in segment $L_{c1, seg}$ (mi)				--				
	Milepost of beginning of curve in dir. of travel X_1 (mi)				0.09				
2	Presence of horizontal curve 2				No	Choices: No, In segment, Off segment			
	Curve radius R_2 (ft)				--	If "In segment" or "Off segment", enter data for curve radius, length, and milepost.			
	Length of curve L_{c2} (mi)				--				
	Length of curve in segment $L_{c2, seg}$ (mi)				--				
	Milepost of beginning of curve in dir. of travel X_2 (mi)				--				
3	Presence of horizontal curve 3				No	Choices: No, In segment, Off segment			
	Curve radius R_3 (ft)				--	If "In segment" or "Off segment", enter data for curve radius, length, and milepost.			
	Length of curve L_{c3} (mi)				--				
	Length of curve in segment $L_{c3, seg}$ (mi)				--				
	Milepost of beginning of curve in dir. of travel X_3 (mi)				--				
4	Presence of horizontal curve 4				No	Choices: No, In segment, Off segment			
	Curve radius R_4 (ft)				--	If "In segment" or "Off segment", enter data for curve radius, length, and milepost.			
	Length of curve L_{c4} (mi)				--				
	Length of curve in segment $L_{c4, seg}$ (mi)				--				
	Milepost of beginning of curve in dir. of travel X_4 (mi)				--				

Table 19-52. Ramp Segment Worksheet (2 of 4)—Sample Problem 2

Input Data						
Cross Section Data		Crash Period	Study Year	Complete the study year column. Complete the crash period column if the EB Method is used.		
Lane width W_l (ft)		--	14			
Right shoulder width W_{rs} (ft)		--	8			
Left shoulder width W_{ls} (ft)		--	4			
Presence of lane add or lane drop		--	No	Choices: No, Lane add, Lane drop		
Length of taper in segment $L_{add, seg}$ or $L_{drop, seg}$ (mi)		--	--	If "Lane add" or "Lane drop", enter length.		
Roadside Data						
Presence of barrier on right side of roadway		--	Y/N	N	Y/N	If Yes, then use the ramp barrier worksheet.
Presence of barrier on left side of roadway		--	Y/N	N	Y/N	If Yes, then use the ramp barrier worksheet.
Ramp Access Data						
Ramp Entrance						
Ent. ramp	Presence of speed-change lane in segment	--	Y/N	N	Y/N	If Yes, then enter data in the next row.
	Length of s-c lane in segment $L_{en, seg}$ (mi)	--		--		
Exit ramp	Presence of speed-change lane in segment	--	Y/N	N	Y/N	If Yes, then enter data in the next row.
	Length of s-c lane in segment $L_{ex, seg}$ (mi)	--		--		
Weave	Presence of a weaving section in segment	--	Y/N	Y	Y/N	If Yes, then enter data in the next two rows.
	Length of weaving section L_{wev} (mi)	--		0.08		
	Length of weaving section in seg. $L_{wev, seg}$ (mi)	--		0.08		
Traffic Data						
Segment AADT $AAADT_r$ or $AAADT_c$ (veh/day)		--	5,500			

Table 19-53. Ramp Segment Worksheet (3 of 4)—Sample Problem 2

Crash Modification Factors									
Complete the study year column. Complete the crash period column if the EB Method is used. Equation	Fatal and Injury				Property Damage Only				
	Multiple Vehicle		Single Vehicle		Multiple Vehicle		Single Vehicle		
	Crash Period	Study Year	Crash Period	Study Year	Crash Period	Study Year	Crash Period	Study Year	
Horizontal curve $CMF_{1, w, x, y, z}$	19-33	--	1.000	--	1.000	--	1.000	--	1.000
Lane width $CMF_{2, w, x, y, fi}$	19-34	--	1.000	--	1.000				
Right shoulder width $CMF_{3, w, x, y, z}$	19-35	--	1.000	--	1.000	--	1.000	--	1.000
Left shoulder width $CMF_{4, w, x, y, z}$	19-36	--	1.000	--	1.000	--	1.000	--	1.000
Right side barrier $CMF_{5, w, x, y, z}$	19-37	--	1.000	--	1.000	--	1.000	--	1.000
Left side barrier $CMF_{6, w, x, y, z}$	19-38	--	1.000	--	1.000	--	1.000	--	1.000
Lane add or drop $CMF_{7, w, x, y, fi}$	19-39	--	1.000	--	1.000				
Ramp speed-change lane $CMF_{8, w, x, mv, fi}$	19-40	--	1.000						
Weaving section $CMF_{9, cds, ac, y, z}$	19-41	--	2.372	--	2.372	--	3.009	--	3.009
Combined CMF (multiply all CMFs evaluated)		--	2.372	--	2.372	--	3.009	--	3.009
Expected Average Crash Frequency^a									
Complete the study year column. Complete the crash period column if the <i>site-specific</i> EB Method is used.	Fatal and Injury				Property Damage Only				
	Multiple Vehicle		Single Vehicle		Multiple Vehicle		Single Vehicle		
	Crash Period	Study Year	Crash Period	Study Year	Crash Period	Study Year	Crash Period	Study Year	
Calibration factor $C_{w, x, y, z}$		1.00		1.00		1.00		1.00	
Overdispersion parameter $k_{w, x, y, z}$	--		--		--		--		
Observed crash count $N_{o, w, x, y, z}^*$ (cr)	--		--		--		--		
Reference year r	--		--		--		--		
Predicted average crash freq. for reference year $N_{p, w, x, y, z, r}$ (cr/yr)	--		--		--		--		
Predicted number of crashes for crash period (sum all years) $N_{p, w, x, y, z}^*$ (cr)	--		--		--		--		
Equivalent years associated with crash count $C_{b, w, x, y, z, r}$ (yr)	--		--		--		--		
Adjusted average crash freq. for ref. year given $N_{o, w, x, y, z, r}^*$ (cr/yr)	--		--		--		--		
Study year s		2011		2011		2011		2011	
Predicted average crash freq. for study year $N_{p, w, x, y, z, s}$ (cr/yr)		0.055		0.036		0.172		0.075	
Expected average crash freq. for study year $N_{e, w, x, y, z, s}$ (cr/yr)		0.055		0.036		0.172		0.075	
Expected average crash freq. for study year (all crash types) $N_{e, w, x, at, z, s}$ (cr/yr)		0.091				0.247			

Note:

a – If the EB Method is not used, then substitute the word “predicted” for the word “expected” and substitute the subscript “p” for the subscript “e”.

Table 19-54. Ramp Segment Worksheet (4 of 4)—Sample Problem 2**Expected Average Crash Frequency^a****Crash Severity Distribution**

	K	A	B	C	Total FI	PDO	Total FI + PDO
Proportion by injury level	0.022	0.065	0.315	0.598	1.000		
Expected average crash freq. for study year (all crash types) $N_{e, w, x, at, z, s}$ (cr/yr)	0.002	0.006	0.029	0.055	0.091	0.247	0.338

Crash Type Distribution

Crash Type Category	Table	Fatal and Injury		Property Damage Only		Total
		Proportion	Expected Average Crash Frequency for Study Year $N_{e, w, x, y, fi, s}$ (cr/yr)	Proportion	Expected Average Crash Frequency for Study Year $N_{e, w, x, y, pdo, s}$ (cr/yr)	Expected Average Crash Frequency for Study Year $N_{e, w, x, y, as, s}$ (cr/yr)
Multiple-Vehicle Crashes	19-6					
Head-on		0.015	0.001	0.009	0.002	0.002
Right-angle		0.010	0.001	0.005	0.001	0.001
Rear-end		0.707	0.039	0.550	0.095	0.134
Sideswipe		0.129	0.007	0.335	0.058	0.065
Other multiple-vehicle crashes		0.139	0.008	0.101	0.017	0.025
Total		1.000	0.055	1.000	0.172	0.227
Single-Vehicle Crashes	19-9					
Crash with animal		0.003	0.000	0.005	0.000	0.000
Crash with fixed object		0.718	0.026	0.834	0.062	0.088
Crash with other object		0.015	0.001	0.023	0.002	0.002
Crash with parked vehicle		0.012	0.000	0.012	0.001	0.001
Other single-vehicle crashes		0.252	0.009	0.126	0.009	0.019
Total		1.000	0.036	1.000	0.075	0.111

Note:

a – If the EB Method is not used, then substitute the word “predicted” for the word “expected” and substitute the subscript “p” for the subscript “e”.

19.14.3. Sample Problem 3**The Site/Facility**

A one-lane urban entrance ramp segment.

The Question

What is the predicted average crash frequency of the ramp segment for a one-year period?

The Facts

The study year is 2011. The conditions present during this year are provided in the following list.

- 0.3-mi length
- 7,250 veh/day

- 65-mi/h average speed on freeway mainline
- Yield control at crossroad ramp terminal
- One in-segment horizontal curve
 - 475-ft radius
 - 0.08-mi length, entirely in the segment
 - Beginning at milepost 0.07
- 14-ft lane width
- 8-ft right shoulder width
- 4-ft left shoulder width
- No lane adds or lane drops
- Barrier on both sides of the roadway
 - Right-side barrier length: 0.15 mi
 - Right-side barrier offset: 9 ft
 - Left-side barrier length: 0.15 mi
 - Left-side barrier offset: 5 ft
- No ramp entrances or exits in the segment
- No weaving section

Assumptions

- Crash type distributions used are the default values presented in Table 19-6 and Table 19-9.
- The calibration factor is 1.00.

Results

Using the predictive method steps as outlined below, the predicted average fatal-and-injury crash frequency for the ramp segment in Sample Problem 3 is determined to be 0.3 crashes per year, and the predicted average property-damage-only crash frequency is determined to be 0.5 crashes per year (rounded to one decimal place).

Steps**Step 1 through 8**

To determine the predicted average crash frequency of the ramp segment in Sample Problem 3, only Steps 9 through 13 are conducted. No other steps are necessary because only one ramp segment is analyzed for a one-year period and the EB Method is not applied.

Step 9 – For the selected site, determine and apply the appropriate SPF.

For a one-lane urban exit ramp segment, SPF values for multiple-vehicle and single-vehicle crashes are determined.

Multiple-Vehicle Crashes

The SPF for multiple-vehicle fatal-and-injury crashes is calculated from Equation 19-20 and Table 19-5 as follows:

$$\begin{aligned} N_{spf, rps, 1EN, mv, fi} &= L_r \times \exp(a + b \times \ln[c \times AADT_r] + d[c \times AADT_r]) \\ &= 0.3 \times \exp(-3.505 + 0.524 \times \ln[0.001 \times 7,250] + 0.0699[0.001 \times 7,250]) \\ &= 0.042 \text{ crashes/year} \end{aligned}$$

Similarly, the SPF for multiple-vehicle property-damage-only crashes is calculated from Equation 19-20 and Table 19-5 to yield the following result:

$$N_{spf, rps, 1EN, mv, pdo} = 0.079 \text{ crashes/year}$$

Single-Vehicle Crashes

The SPF for single-vehicle fatal-and-injury crashes is calculated from Equation 19-24 and Table 19-8 as follows:

$$\begin{aligned} N_{spf, rps, 1EN, sv, fi} &= L_r \times \exp(a + b \times \ln[c \times AADT_r]) \\ &= 0.3 \times \exp(-1.966 + 0.718 \times \ln[0.001 \times 7,250]) \\ &= 0.174 \text{ crashes/year} \end{aligned}$$

Similarly, the SPF for single-vehicle property-damage-only crashes is calculated from Equation 19-24 and Table 19-8 to yield the following result:

$$N_{spf, rps, 1EN, sv, pdo} = 0.211 \text{ crashes/year}$$

Step 10 – Multiply the result obtained in Step 9 by the appropriate CMFs.

Each CMF used in the calculation of the predicted average crash frequency of the ramp segment is calculated in this step.

Horizontal Curve (CMF_{L, rps, 1EN, y, z})

The limited curve speed for the in-segment horizontal curve is computed using Equation 19-59 as follows:

$$\begin{aligned} v_{\max, l} &= 3.24 \times (32.2 \times R_1)^{0.30} \\ &= 3.24 \times (32.2 \times 475)^{0.30} \\ &= 58.3 \text{ ft/s} \end{aligned}$$

The average entry speed at the curve is computed using Equation 19-60 and the default values in Table 19-42 as follows:

$$\begin{aligned}
 v_{ent,1} &= \left([1.47 \times V_{xroad}]^3 + 495 \times 5,280 \times X_1 \right)^{1/3} \leq 1.47 \times V_{frwy} \\
 &= \left([1.47 \times 15]^3 + 495 \times 5,280 \times 0.07 \right)^{1/3} \leq 1.47 \times 65 \\
 &= 57.9 \text{ ft/s}
 \end{aligned}$$

The average exit speed at curve 1 is computed using Equation 19-61 as follows:

$$\begin{aligned}
 v_{ext,1} &= \left(v_{ent,1}^3 + 495 \times 5,280 \times L_{c,1} \right)^{1/3} \leq v_{max,1} \text{ and } \leq 1.47 \times V_{frwy} \\
 &= \left(57.9^3 + 495 \times 5,280 \times 0.3 \right)^{1/3} \leq 58.3 \text{ and } \leq 1.47 \times 65 \\
 &= 58.3 \text{ ft/s}
 \end{aligned}$$

$CMF_{1, rps, 1EN, y, fi}$ is calculated using Equation 19-33 as follows:

$$CMF_{1, rps, 1EN, y, fi} = 1.0 + a \times \frac{1,000}{32.2} \left[\sum_{i=1}^m \left(\frac{v_{ent,i}}{R_i} \right)^2 \times P_{c,i} \right]$$

From Table 19-24, $a = 0.779$ for multiple-vehicle fatal-and-injury crashes and 2.406 for single-vehicle fatal-and-injury crashes. $CMF_{1, rps, 1EN, mv, fi}$ is calculated as follows:

$$\begin{aligned}
 CMF_{1, rps, 1EN, mv, fi} &= 1.0 + 0.779 \times \frac{1,000}{32.2} \left(\frac{57.9}{475} \right)^2 \times \frac{0.08}{0.3} \\
 &= 1.096
 \end{aligned}$$

Calculations using the other coefficients from Table 19-24 yield the following results:

$$CMF_{1, rps, 1EN, sv, fi} = 1.296$$

$$CMF_{1, rps, 1EN, mv, pdo} = 1.067$$

$$CMF_{1, rps, 1EN, sv, pdo} = 1.385$$

Lane Width ($CMF_{2, rps, 1EN, y, z}$)

The segment has 14-ft lanes, which is the base condition for the lane width CMF. Hence, $CMF_{2, rps, 1EN, y, fi}$ and $CMF_{2, rps, 1EN, y, pdo}$ are equal to 1.000.

Right Shoulder Width ($CMF_{3, rps, 1EN, y, z}$)

The segment has 8-ft right shoulders, which is the base condition for the right shoulder width CMF. Hence, $CMF_{3, rps, 1EN, y, fi}$ and $CMF_{3, rps, 1EN, y, pdo}$ are equal to 1.000.

Left Shoulder Width ($CMF_{4, rps, 1EN, y, z}$)

The segment has 4-ft left shoulders, which is the base condition for the left shoulder width CMF. Hence, $CMF_{4, rps, 1EN, y, fi}$ and $CMF_{4, rps, 1EN, y, pdo}$ are equal to 1.000.

Right Side Barrier ($CMF_{5, rps, 1EN, y, z}$)

$CMF_{5, rps, 1EN, y, fi}$ is calculated using Equation 19-37 as follows:

$$CMF_{5, rps, 1EN, y, fi} = (1.0 - P_{rb}) \times 1.0 + P_{rb} \times \exp\left(\frac{a}{W_{rcb}}\right)$$

The distance from the edge of the right shoulder to the barrier face W_{rcb} is computed using Equation 19-74 as follows:

$$\begin{aligned} W_{rcb} &= \frac{\sum L_{rb, i}}{\sum \frac{L_{rb, i}}{W_{off, r, i} - W_{rs}}} \\ &= \frac{0.15}{\left(\frac{0.15}{9-8}\right)} \\ &= 1.0 \end{aligned}$$

From Table 19-28, $a = 0.210$ for multiple-vehicle crashes. $CMF_{5, rps, 1EN, y, fi}$ is calculated as follows:

$$\begin{aligned} CMF_{5, rps, 1EN, y, fi} &= \left(1.0 - \frac{0.15}{0.3}\right) \times 1.0 + \frac{0.15}{0.3} \times \exp\left(\frac{0.210}{1.0}\right) \\ &= 1.117 \end{aligned}$$

Similar calculations using the property-damage-only coefficients from Table 19-28 yield the following results:

$$CMF_{5, rps, 1EN, y, pdo} = 1.106$$

Left Side Barrier ($CMF_{6, rps, 1EN, y, z}$)

$CMF_{6, rps, 1EN, y, fi}$ is calculated using Equation 19-38 as follows:

$$CMF_{6, rps, 1EN, y, fi} = (1.0 - P_{lb}) \times 1.0 + P_{lb} \times \exp\left(\frac{a}{W_{lcb}}\right)$$

The distance from the edge of the right shoulder to the barrier face W_{lcb} is computed using Equation 19-76 as follows:

$$\begin{aligned} W_{lcb} &= \frac{\sum L_{lb, i}}{\sum \frac{L_{lb, i}}{W_{off, l, i} - W_{ls}}} \\ &= \frac{0.15}{\left(\frac{0.15}{5-4}\right)} \\ &= 1.0 \end{aligned}$$

From Table 19-29, $a = 0.210$ for multiple-vehicle crashes. $CMF_{6, rps, 1EN, y, fi}$ is calculated as follows:

$$\begin{aligned}
 CMF_{6, rps, 1EN, y, fi} &= \left(1.0 - \frac{0.15}{0.3}\right) \times 1.0 + \frac{0.15}{0.3} \times \exp\left(\frac{0.210}{1.0}\right) \\
 &= 1.117
 \end{aligned}$$

Similar calculations using the property-damage-only coefficients from Table 19-29 yield the following results:

$$CMF_{6, rps, 1EN, y, pdo} = 1.106$$

Lane Add or Drop ($CMF_{7, rps, 1EN, y, fi}$)

The segment does not have a lane add or a lane drop. Hence, $CMF_{7, rps, 1EN, y, fi}$ is equal to 1.000.

Ramp Speed-Change Lane ($CMF_{8, rps, 1EN, mv, fi}$)

The segment does not have a speed-change lane. Hence, $CMF_{8, rps, 1EN, mv, fi}$ is equal to 1.000.

Multiple-Vehicle Crashes

The CMFs are applied to the multiple-vehicle fatal-and-injury SPF as follows:

$$\begin{aligned}
 N_{p^*, rps, 1EN, mv, fi} &= N_{spf, rps, 1EN, mv, fi} \times (CMF_{1, rps, 1EN, mv, fi} \times \dots \times CMF_{8, rps, 1EN, mv, fi}) \\
 &= 0.042 \times (1.096 \times 1.000 \times 1.000 \times 1.000 \times 1.117 \times 1.117 \times 1.000 \times 1.000) \\
 &= 0.042 \times 1.367 \\
 &= 0.058 \text{ crashes/year}
 \end{aligned}$$

The CMFs are applied to the multiple-vehicle property-damage-only SPF as follows:

$$\begin{aligned}
 N_{p^*, rps, 1EN, mv, pdo} &= N_{spf, rps, 1EN, mv, pdo} \times (CMF_{1, rps, 1EN, mv, pdo} \times \dots \times CMF_{8, rps, 1EN, mv, pdo}) \\
 &= 0.079 \times (1.067 \times 1.000 \times 1.000 \times 1.000 \times 1.106 \times 1.106 \times 1.000 \times 1.000) \\
 &= 0.079 \times 1.305 \\
 &= 0.104 \text{ crashes/year}
 \end{aligned}$$

Single-Vehicle Crashes

The CMFs are applied to the single-vehicle fatal-and-injury SPF as follows:

$$\begin{aligned}
 N_{p^*, rps, 1EN, sv, fi} &= N_{spf, rps, 1EN, sv, fi} \times (CMF_{1, rps, 1EN, sv, fi} \times \dots \times CMF_{8, rps, 1EN, sv, fi}) \\
 &= 0.174 \times (1.296 \times 1.000 \times 1.000 \times 1.000 \times 1.117 \times 1.117 \times 1.000 \times 1.000) \\
 &= 0.174 \times 1.617 \\
 &= 0.281 \text{ crashes/year}
 \end{aligned}$$

The CMFs are applied to the single-vehicle property-damage-only SPF as follows:

$$\begin{aligned} N_{p^*, rps, 1EN, sv, pdo} &= N_{spf, rps, 1EN, sv, pdo} \times (CMF_{1, rps, 1EN, sv, pdo} \times \dots \times CMF_{8, rps, 1EN, sv, pdo}) \\ &= 0.211 \times (1.385 \times 1.000 \times 1.000 \times 1.000 \times 1.106 \times 1.106 \times 1.000 \times 1.000) \\ &= 0.211 \times 1.694 \\ &= 0.358 \text{ crashes/year} \end{aligned}$$

Step 11 – Multiply the result obtained in Step 10 by the appropriate calibration factor.

It is assumed that a calibration factor of 1.00 has been determined for local conditions. As a result, $N_{p, rps, 1EN, y, z} = N_{p^*, rps, 1EN, y, z}$ for both crash types y ($y = mv$: multiple-vehicle, sv : single-vehicle) and both crash severities z ($z = fi$: fatal-and-injury, pdo : property-damage-only). See Section B.1 of Appendix B to Part C for further discussion on calibration of the predicted models.

Calculation of Predicted Average Crash Frequency

The predicted average crash frequency is calculated using Equation 19-1 based on the results obtained in Steps 9 through 11 as follows.

Fatal-and-injury crashes:

$$\begin{aligned} N_{p, rps, 1EN, at, fi} &= N_{p, rps, 1EN, mv, fi} + N_{p, rps, 1EN, sv, fi} \\ &= 0.058 + 0.281 \\ &= 0.339 \text{ crashes/year} \end{aligned}$$

Property-damage-only crashes:

$$\begin{aligned} N_{p, rps, 1EN, at, pdo} &= N_{p, rps, 1EN, mv, pdo} + N_{p, rps, 1EN, sv, pdo} \\ &= 0.104 + 0.358 \\ &= 0.462 \text{ crashes/year} \end{aligned}$$

Step 12—If there is another year to be evaluated in the evaluation period for the selected site, return to Step 8. Otherwise, proceed to Step 13.

The study period is one year (2011), so steps 8 through 11 need not be repeated.

Step 13—Apply site-specific EB Method (if applicable) and apply SDFs.

This step consists of three optional sets of calculations—site-specific EB Method, severity distribution functions, and crash type distribution.

Apply the site-specific EB Method to a future time period, if appropriate.

The site-specific EB Method is not applied in this sample problem because crash data are not available.

Apply the severity distribution functions (SDFs), if desired.

To apply the SDFs, the systematic component of crash severity likelihood V_j is computed for each severity level j using Equation 19-83 as follows:

$$V_j = a + \left(b \times \frac{P_{lb} + P_{rb}}{2} \right) + (c \times n) + (d \times I_{rural}) + (e \times I_{extr})$$

The coefficients a , b , c , d , and e are obtained from Table 19-43 for each severity level j . V_j is computed for fatal and incapacitating injury crashes as follows:

$$\begin{aligned} V_{K+A} &= -1.537 + \left(-0.481 \times \frac{0.5 + 0.5}{2} \right) + (-0.228 \times 1.0) + (0.668 \times 0.0) + (0.426 \times 0.0) \\ &= -2.006 \end{aligned}$$

Similar calculations using the coefficients from Table 19-43 for non-incapacitating injury crashes yield the following results:

$$V_B = -0.415$$

Using these computed V_{K+A} and V_B values, and assuming a calibration factor $C_{sdf, rps+cds}$ of 1.0, the probability of occurrence of a fatal crash is computed using Equation 19-79 as follows:

$$\begin{aligned} P_{rps+cds, ac, at, K} &= \frac{\exp(V_{K+A})}{\frac{1.0}{C_{sdf, rps+cds}} + \exp(V_{K+A}) + \exp(V_B)} \times P_{K|K+A, rps+cds, ac, at} \\ &= \frac{\exp(-2.006)}{\frac{1.0}{1.0} + \exp(-2.006) + \exp(-0.415)} \times 0.248 \\ &= 0.018 \end{aligned}$$

Similar calculations using Equation 19-80 and Equation 19-81 yield the following results:

$$P_{rps+cds, ac, at, A} = 0.056$$

$$P_{rps+cds, ac, at, B} = 0.369$$

The probability of occurrence of a possible-injury crash is computed using Equation 19-82 as follows:

$$\begin{aligned} P_{rps+cds, ac, at, C} &= 1.0 - (P_{rps+cds, ac, at, K} + P_{rps+cds, ac, at, A} + P_{rps+cds, ac, at, B}) \\ &= 1.0 - (0.018 + 0.056 + 0.369) \\ &= 0.557 \end{aligned}$$

The probability of occurrence of a fatal crash is multiplied by the fatal-and-injury crash frequency obtained in Step 11 using Equation 19-78 as follows:

$$\begin{aligned} N_{e, rps, 1EN, at, K} &= N_{e, rps, 1EN, at, fi} \times P_{rps+cds, ac, at, K} \\ &= 0.339 \times 0.018 \\ &= 0.006 \text{ crashes/year} \end{aligned}$$

Similar calculations using Equation 19-78 and the probabilities of occurrences of the other crash severities yield the following results:

$$N_{e, rps, 1EN, at, A} = 0.019 \text{ crashes/year}$$

$$N_{e,rps,1EN,at,B} = 0.125 \text{ crashes/year}$$

$$N_{e,rps,1EN,at,C} = 0.189 \text{ crashes/year}$$

Apply the crash type distribution, if desired.

The crash type distributions are applied by multiplying the default crash type distribution proportions in Table 19-6 and Table 19-9 by the predicted average crash frequencies obtained in Step 11.

Worksheets

The step-by-step instructions are provided to illustrate the predictive method for calculating the predicted average crash frequency for a ramp segment. To apply the predictive method steps to multiple segments, a series of worksheets are provided for determining the predicted average crash frequency. The worksheets include:

- Table 19-55. Ramp Segment Worksheet (1 of 4)—Sample Problem 3
- Table 19-56. Ramp Segment Worksheet (2 of 4)—Sample Problem 3
- Table 19-57. Ramp Segment Worksheet (3 of 4)—Sample Problem 3
- Table 19-58. Ramp Segment Worksheet (4 of 4)—Sample Problem 3
- Table 19-59. Ramp Barrier Worksheet—Sample Problem 3

Filled versions of these worksheets are provided below. Blank versions of worksheets used in the Sample Problems are provided in Appendix 19A.

Table 19-55 is a summary of general information about the ramp segment, analysis, input data (i.e., “The Facts”), and assumptions for Sample Problem 3. The input data include area type, crash data, basic roadway data, and alignment data.

Table 19-56 is a summary of general information about the ramp segment, analysis, input data (i.e., “The Facts”), and assumptions for Sample Problem 3. The input data include cross section data, roadside data, ramp access data, and traffic data.

Table 19-57 is a tabulation of the CMF and SPF computations for Sample Problem 3.

Table 19-58 is a tabulation of the crash severity and crash type distributions for Sample Problem 3.

Table 19-59 is used to complete the barrier calculations for Sample Problem 3.

Table 19-55. Ramp Segment Worksheet (1 of 4)—Sample Problem 3

General Information					Location Information				
Analyst					Roadway				
Agency or company					Roadway section				
Date performed					Study year				
Area type		X	Urban		Rural				
Input Data									
Crash Data				Crash Period	Study Year	Complete the study year column. Complete the crash period column if the EB Method is used.			
Crash data time period						First year	--	Last year	--
Count of multiple-vehicle FI crashes $N_{o, w, n, mv, fi}^*$				--					
Count of single-vehicle FI crashes $N_{o, w, n, sv, fi}^*$				--					
Count of multiple-vehicle PDO crashes $N_{o, w, n, mv, pdo}^*$				--					
Count of single-vehicle PDO crashes $N_{o, w, n, sv, pdo}^*$				--					
Basic Roadway Data									
Number of through lanes n				1		Same value for crash period and study year.			
Segment length L (mi)				--	0.3				
Average traffic speed on the freeway V_{frwy} (mi/h)				--	65				
Segment type				Entrance		Choices: Entrance, Exit, C-D road, Connector			
Type of control at crossroad ramp terminal				--	Yield	Choices: Stop, Yield, Signal, None			
Alignment Data									
Horizontal Curve Data									
1	Presence of horizontal curve 1			--	In Seg.	Choices: No, In segment, Off segment.			
	Curve radius R_1 (ft)			--	475	If "In segment" or "Off segment", enter data for curve radius, length, and milepost.			
	Length of curve L_{c1} (mi)			--	0.08				
	Length of curve in segment $L_{c1, seg}$ (mi)			--	0.08				
	Milepost of beginning of curve in dir. of travel X_1 (mi)			--	0.07				
2	Presence of horizontal curve 2			--	No	Choices: No, In segment, Off segment			
	Curve radius R_2 (ft)			--	--	If "In segment" or "Off segment", enter data for curve radius, length, and milepost.			
	Length of curve L_{c2} (mi)			--	--				
	Length of curve in segment $L_{c2, seg}$ (mi)			--	--				
	Milepost of beginning of curve in dir. of travel X_2 (mi)			--	--				
3	Presence of horizontal curve 3			--	No	Choices: No, In segment, Off segment			
	Curve radius R_3 (ft)			--	--	If "In segment" or "Off segment", enter data for curve radius, length, and milepost.			
	Length of curve L_{c3} (mi)			--	--				
	Length of curve in segment $L_{c3, seg}$ (mi)			--	--				
	Milepost of beginning of curve in dir. of travel X_3 (mi)			--	--				
4	Presence of horizontal curve 4			--	No	Choices: No, In segment, Off segment			
	Curve radius R_4 (ft)			--	--	If "In segment" or "Off segment", enter data for curve radius, length, and milepost.			
	Length of curve L_{c4} (mi)			--	--				
	Length of curve in segment $L_{c4, seg}$ (mi)			--	--				
	Milepost of beginning of curve in dir. of travel X_4 (mi)			--	--				

Table 19-56. Ramp Segment Worksheet (2 of 4)—Sample Problem 3

Input Data						
Cross Section Data		Crash Period	Study Year	Complete the study year column. Complete the crash period column if the EB Method is used.		
Lane width W_l (ft)		--	14			
Right shoulder width W_{rs} (ft)		--	8			
Left shoulder width W_{ls} (ft)		--	4			
Presence of lane add or lane drop		--	No	Choices: No, Lane add, Lane drop		
Length of taper in segment $L_{add, seg}$ or $L_{drop, seg}$ (mi)		--	--	If "Lane add" or "Lane drop", enter length.		
Roadside Data						
Presence of barrier on right side of roadway		--	Y/N	Y	Y/N	If Yes, then use the ramp barrier worksheet.
Presence of barrier on left side of roadway		--	Y/N	Y	Y/N	If Yes, then use the ramp barrier worksheet.
Ramp Access Data						
Ramp Entrance						
Ent. ramp	Presence of speed-change lane in segment	--	Y/N	N	Y/N	If Yes, then enter data in the next row.
	Length of s-c lane in segment $L_{en, seg}$ (mi)	--		--		
Exit ramp	Presence of speed-change lane in segment	--	Y/N	N	Y/N	If Yes, then enter data in the next row.
	Length of s-c lane in segment $L_{ex, seg}$ (mi)	--		--		
Weave	Presence of a weaving section in segment	--	Y/N	--	Y/N	If Yes, then enter data in the next two rows.
	Length of weaving section L_{wev} (mi)	--		--		
	Length of weaving section in seg. $L_{wev, seg}$ (mi)	--		--		
Traffic Data						
Segment AADT $AAADT_r$ or $AAADT_c$ (veh/day)		--		7,250		

Table 19-57. Ramp Segment Worksheet (3 of 4)—Sample Problem 3

Crash Modification Factors									
Complete the study year column. Complete the crash period column if the EB Method is used. Equation	Fatal and Injury				Property Damage Only				
	Multiple Vehicle		Single Vehicle		Multiple Vehicle		Single Vehicle		
	Crash Period	Study Year	Crash Period	Study Year	Crash Period	Study Year	Crash Period	Study Year	
Horizontal curve $CMF_{1, w, x, y, z}$	19-33	--	1.096	--	1.296	--	1.067	--	1.385
Lane width $CMF_{2, w, x, y, fi}$	19-34	--	1.000	--	1.000				
Right shoulder width $CMF_{3, w, x, y, z}$	19-35	--	1.000	--	1.000	--	1.000	--	1.000
Left shoulder width $CMF_{4, w, x, y, z}$	19-36	--	1.000	--	1.000	--	1.000	--	1.000
Right side barrier $CMF_{5, w, x, y, z}$	19-37	--	1.117	--	1.117	--	1.106	--	1.106
Left side barrier $CMF_{6, w, x, y, z}$	19-38	--	1.117	--	1.117	--	1.106	--	1.106
Lane add or drop $CMF_{7, w, x, y, fi}$	19-39	--	1.000	--	1.000				
Ramp speed-change lane $CMF_{8, w, x, mv, fi}$	19-40	--	1.000						
Weaving section $CMF_{9, cds, ac, y, z}$	19-41	--	1.000	--	1.000	--	1.000	--	1.000
Combined CMF (multiply all CMFs evaluated)		--	1.367	--	1.617	--	1.305	--	1.694
Expected Average Crash Frequency^a									
Complete the study year column. Complete the crash period column if the <i>site-specific</i> EB Method is used.	Fatal and Injury				Property Damage Only				
	Multiple Vehicle		Single Vehicle		Multiple Vehicle		Single Vehicle		
	Crash Period	Study Year	Crash Period	Study Year	Crash Period	Study Year	Crash Period	Study Year	
Calibration factor $C_{w, x, y, z}$		1.00		1.00		1.00		1.00	
Overdispersion parameter $k_{w, x, y, z}$	--		--		--		--		
Observed crash count $N_{o, w, x, y, z}^*$ (cr)	--		--		--		--		
Reference year r	--		--		--		--		
Predicted average crash freq. for reference year $N_{p, w, x, y, z, r}$ (cr/yr)	--		--		--		--		
Predicted number of crashes for crash period (sum all years) $N_{p, w, x, y, z}^*$ (cr)	--		--		--		--		
Equivalent years associated with crash count $C_{b, w, x, y, z, r}$ (yr)	--		--		--		--		
Adjusted average crash freq. for ref. year given $N_{o, w, x, y, z, r}^*$ (cr/yr)	--		--		--		--		
Study year s		2011		2011		2011		2011	
Predicted average crash freq. for study year $N_{p, w, x, y, z, s}$ (cr/yr)		0.058		0.281		0.103		0.358	
Expected average crash freq. for study year $N_{e, w, x, y, z, s}$ (cr/yr)		0.058		0.281		0.103		0.358	
Expected average crash freq. for study year (all crash types) $N_{e, w, x, at, z, s}$ (cr/yr)		0.339				0.461			

Note:

a – If the EB Method is not used, then substitute the word “predicted” for the word “expected” and substitute the subscript “p” for the subscript “e”.

Table 19-58. Ramp Segment Worksheet (4 of 4)—Sample Problem 3

Expected Average Crash Frequency^a

Crash Severity Distribution

	K	A	B	C	Total FI	PDO	Total FI + PDO
Proportion by injury level	0.018	0.056	0.369	0.557	1.000		
Expected average crash freq. for study year (all crash types) $N_{e, w, x, at, z, s}$ (cr/yr)	0.006	0.019	0.125	0.189	0.339	0.462	0.801

Crash Type Distribution

Crash Type Category	Table	Fatal and Injury		Property Damage Only		Total
		Proportion	Expected Average Crash Frequency for Study Year $N_{e, w, x, y, fi, s}$ (cr/yr)	Proportion	Expected Average Crash Frequency for Study Year $N_{e, w, x, y, pdo, s}$ (cr/yr)	Expected Average Crash Frequency for Study Year $N_{e, w, x, y, as, s}$ (cr/yr)
Multiple-Vehicle Crashes	19-6					
Head-on		0.015	0.001	0.009	0.001	0.002
Right-angle		0.010	0.001	0.005	0.001	0.001
Rear-end		0.707	0.041	0.550	0.057	0.098
Sideswipe		0.129	0.007	0.335	0.035	0.042
Other multiple-vehicle crashes		0.139	0.008	0.101	0.011	0.019
Total		1.000	0.058	1.000	0.104	0.162
Single-Vehicle Crashes	19-9					
Crash with animal		0.003	0.001	0.005	0.002	0.003
Crash with fixed object		0.718	0.202	0.834	0.299	0.501
Crash with other object		0.015	0.004	0.023	0.008	0.012
Crash with parked vehicle		0.012	0.003	0.012	0.004	0.008
Other single-vehicle crashes		0.252	0.071	0.126	0.045	0.116
Total		1.000	0.282	1.000	0.358	0.640

Note:

a – If the EB Method is not used, then substitute the word “predicted” for the word “expected” and substitute the subscript “p” for the subscript “e”.

Table 19-59. Ramp Barrier Worksheet—Sample Problem 3

Input Data			
Segment length L (mi)	0.3	Crash period	X
Left shoulder width W_{ls} (ft)	4	Right shoulder width W_{rs} (ft)	8
Individual Right Side Barrier Element Data			
Barrier Location	Length $L_{rb,i}$ (mi)	Width from Edge of Traveled Way to Face of Right Side Barrier $W_{off,r,i}$ (ft)	Ratio $L_{rb,i}/(W_{off,r,i}-W_{rs})$
1. Bridge	0.10	9	0.10
2. Sign support	0.05	9	0.05
3.			
4.			
5.			
6.			
7.			
Sum1	0.15	Sum2	0.15
Individual Left Side Barrier Element Data			
Barrier Location	Length $L_{lb,i}$ (mi)	Width from Edge of Traveled Way to Face of Left Side Barrier $W_{off,l,i}$ (ft)	Ratio $L_{lb,i}/(W_{off,l,i}-W_{ls})$
1. Bridge	0.10	5	0.10
2. Sign support	0.05	5	0.05
3.			
4.			
5.			
6.			
7.			
Sum3	0.15	Sum4	0.15
Right Side Barrier Calculations			
Proportion of segment length with barrier in median $P_{rb} = \text{Sum1}/L$	0.500	Width from edge of shoulder to barrier face $W_{rcb} = \text{Sum1} / \text{Sum2}$ (ft)	1.000
Left Side Barrier Calculations			
Proportion of segment length with barrier in median $P_{lb} = \text{Sum3}/L$	0.500	Width from edge of shoulder to barrier face $W_{lcb} = \text{Sum3} / \text{Sum4}$ (ft)	1.000

19.14.4. Sample Problem 4

The Site/Facility

A signalized diamond interchange ramp terminal on an urban arterial.

The Question

What is the predicted average crash frequency of the ramp terminal for a one-year period?

The Facts

The study year is 2011. The conditions present during this year are provided in the following list.

- D4 configuration

- No non-ramp public street leg present
- 1.0 mi to the next public street intersection on the outside crossroad leg
- 0.1 mi to the adjacent ramp terminal
- Protected-permissive left-turn operational mode on the inside crossroad leg
 - 12-ft left-turn bay present
- Signal control for the exit ramp right-turn movement
- 12-ft crossroad median width
- 4 through lanes on the crossroad (2 on each approach)
- 3 lanes on the exit ramp approach (developed at a distance of 150 ft from the ramp terminal)
- No right-turn channelization or bays
- No driveways present
- 28,000 veh/day on the crossroad (same for both legs)
- 7,100 veh/day on the exit ramp leg
- 6,750 veh/day on the entrance ramp leg

Assumptions

- Crash type distributions used are the default values presented in Table 19-16.
- The calibration factor is 1.00.

Results

Using the predictive method steps as outlined below, the predicted average fatal-and-injury crash frequency for the ramp terminal in Sample Problem 4 is determined to be 5.3 crashes per year, and the predicted average property-damage-only crash frequency is determined to be 7.1 crashes per year (rounded to one decimal place).

Steps

Step 1 through 8

To determine the predicted average crash frequency of the ramp terminal in Sample Problem 4, only Steps 9 through 13 are conducted. No other steps are necessary because only one ramp terminal is analyzed for a one-year period and the EB Method is not applied.

Step 9 – For the selected site, determine and apply the appropriate SPF.

For a ramp terminal, an SPF value for all crash types is determined. The SPF for fatal-and-injury crashes is calculated from Equation 19-28 and Table 19-15 as follows:

$$\begin{aligned}
 N_{spf, D4, SG4, at, fi} &= \exp(a + b \times \ln[c \times AADT_{xrd}] + d \times \ln[c \times AADT_{ex} + c \times AADT_{en}]) \\
 &= \exp(-2.335 + 1.191 \times \ln[0.001 \times 28,000] + 0.131 \times \ln[0.001 \times 7,100 + 0.001 \times 6,750]) \\
 &= 7.228 \text{ crashes/year}
 \end{aligned}$$

Similarly, the SPF for property-damage-only crashes is calculated from Equation 19-28 and Table 19-15 to yield the following result:

$$N_{spf, D4, SG4, at, pdo} = 9.869 \text{ crashes/year}$$

Step 10 – Multiply the result obtained in Step 9 by the appropriate CMFs.

Each CMF used in the calculation of the predicted average crash frequency of the ramp terminal is calculated in this step.

Exit Ramp Capacity ($CMF_{10, D4, SG4, at, fi}$)

$CMF_{10, D4, SG4, at, fi}$ is calculated from Equation 19-42 as follows:

$$CMF_{10, D4, SG4, at, fi} = (1.0 - P_{ex}) \times 1.0 + P_{ex} \times \exp\left(a \times \frac{c \times AADT_{ex}}{n_{ex, eff}}\right)$$

For a signalized exit-ramp right-turn movement, the effective number of lanes serving exit ramp traffic $n_{ex, eff}$ is computed using the second portion of Equation 19-43 as follows:

$$\begin{aligned}
 n_{ex, eff} &= 0.5 \times n_{ex} \\
 &= 0.5 \times 3 \\
 &= 1.5
 \end{aligned}$$

The proportion of total leg AADT on the exit ramp leg P_{ex} is computed using Equation 19-44 as follows:

$$\begin{aligned}
 P_{ex} &= \frac{AADT_{ex}}{AADT_{in} + AADT_{out} + AADT_{en} + AADT_{ex}} \\
 &= \frac{7,100}{28,000 + 28,000 + 6,750 + 7,100} \\
 &= 0.102
 \end{aligned}$$

From Table 19-32, $a = 0.0668$ and $c = 0.001$ for signal-controlled ramp terminals. $CMF_{10, D4, SG4, at, fi}$ is calculated as follows:

$$\begin{aligned}
 CMF_{10, D4, SG4, at, fi} &= (1.0 - 0.102) \times 1.0 + 0.102 \times \exp\left(0.0668 \times \frac{0.001 \times 7,100}{1.5}\right) \\
 &= 1.038
 \end{aligned}$$

Crossroad Left-Turn Lane ($CMF_{11, D4, SG4, at, z}$)

$CMF_{11, D4, SG4, at, fi}$ is calculated from Equation 19-45 as follows:

$$CMF_{11, D4, SG4, at, fi} = [(1.0 - P_{in}) \times 1.0 + P_{in} \times a]^{I_{bay, lt, in}} \times [(1.0 - P_{out}) \times 1.0 + P_{out} \times a]^{I_{bay, lt, out}}$$

The proportion of total leg AADT on the crossroad leg between ramps P_{in} is computed using Equation 19-46 as follows:

$$\begin{aligned} P_{in} &= \frac{AADT_{in}}{AADT_{in} + AADT_{out} + AADT_{en} + AADT_{ex}} \\ &= \frac{28,000}{28,000 + 28,000 + 6,750 + 7,100} \\ &= 0.401 \end{aligned}$$

The proportion of total leg AADT on the crossroad leg outside of the interchange P_{out} is computed using Equation 19-47 as follows:

$$\begin{aligned} P_{out} &= \frac{AADT_{out}}{AADT_{in} + AADT_{out} + AADT_{en} + AADT_{ex}} \\ &= \frac{28,000}{28,000 + 28,000 + 6,750 + 7,100} \\ &= 0.401 \end{aligned}$$

From Table 19-33, $a = 0.65$ for signal-controlled ramp terminals. $CMF_{11, D4, SG4, at, fi}$ is calculated as follows:

$$\begin{aligned} CMF_{11, D4, SG4, at, fi} &= [(1.0 - 0.401) \times 1.0 + 0.401 \times 0.65]^1 \times [(1.0 - 0.401) \times 1.0 + 0.401 \times 0.65]^0 \\ &= 0.860 \end{aligned}$$

Similar calculations using the property-damage-only coefficient from Table 19-33 yield the following results:

$$CMF_{11, D4, SG4, at, pdo} = 0.872$$

Crossroad Right-Turn Lane ($CMF_{12, D4, SG4, at, z}$)

The ramp terminal does not have right-turn lanes or bays on the crossroad legs, which is the base condition for the crossroad right-turn lane CMF. Hence, $CMF_{12, D4, SG4, at, fi}$ and $CMF_{12, D4, SG4, at, pdo}$ are equal to 1.000.

Access Point Frequency ($CMF_{13, D4, SG4, at, z}$)

The ramp terminal has no unsignalized driveways or unsignalized public street approaches on the outside leg, which are the base conditions for the access point frequency CMF. Hence, $CMF_{13, D4, SG4, at, fi}$ and $CMF_{13, D4, SG4, at, pdo}$ are equal to 1.000.

Segment Length ($CMF_{14, D4, SG4, at, z}$)

$CMF_{14, D4, SG4, at, fi}$ is calculated from Equation 19-50 as follows:

$$CMF_{14, D4, SG4, at, fi} = \exp \left(a \times \left[\frac{1.0}{L_{rmp}} + \frac{1.0}{L_{str}} - 0.333 \right] \right)$$

From Table 19-36, $a = -0.0185$ for fatal-and-injury crashes. $CMF_{14, D4, SG4, at, fi}$ is calculated as follows:

$$\begin{aligned} CMF_{14, D4, SG4, at, fi} &= \exp\left(-0.0185 \times \left[\frac{1.0}{0.1} + \frac{1.0}{1.0} - 0.333\right]\right) \\ &= 0.821 \end{aligned}$$

Similar calculations using the property-damage-only coefficient from Table 19-36 yield the following results:

$$CMF_{14, D4, SG4, at, pdo} = 0.820$$

Median Width ($CMF_{15, D4, SG4, at, z}$)

The crossroad has a 12-ft median, which is the base condition for the median width CMF. Hence, $CMF_{15, D4, SG4, at, fi}$ and $CMF_{15, D4, SG4, at, pdo}$ are equal to 1.000.

Protected Left-Turn Operation ($CMF_{16, D4, SG4, at, z}$)

Protected-only left-turn operational mode is not used on the crossroad legs, which is the base condition for the protected left-turn operation CMF. Hence, $CMF_{16, D4, SG4, at, fi}$ and $CMF_{16, D4, SG4, at, pdo}$ are equal to 1.000.

Channelized Right Turn on Crossroad ($CMF_{17, D4, SG4, at, z}$)

Right-turn channelization is not used on the crossroad legs, which is the base condition for the channelized right turn on crossroad CMF. Hence, $CMF_{17, D4, SG4, at, fi}$ and $CMF_{17, D4, SG4, at, pdo}$ are equal to 1.000.

Channelized Right Turn on Exit Ramp ($CMF_{18, D4, SG4, at, z}$)

Right-turn channelization is not used on the exit-ramp leg, which is the base condition for the channelized right turn on exit ramp CMF. Hence, $CMF_{18, D4, SG4, at, fi}$ and $CMF_{18, D4, SG4, at, pdo}$ are equal to 1.000.

Non-Ramp Public Street Leg ($CMF_{19, D4, SG4, at, z}$)

A non-ramp public street leg is not present at the ramp terminal, which is the base condition for the non-ramp public street leg CMF. Hence, $CMF_{19, D4, SG4, at, fi}$ and $CMF_{19, D4, SG4, at, pdo}$ are equal to 1.000.

Crashes

The CMFs are applied to the fatal-and-injury SPF as follows:

$$\begin{aligned} N_{p^*, D4, SG4, at, fi} &= N_{spf, D4, SG4, at, fi} \times (CMF_{10, D4, SG4, at, fi} \times \dots \times CMF_{19, D4, SG4, at, fi}) \\ &= 7.228 \times (1.038 \times 0.860 \times 1.000 \times 1.000 \times 0.821 \times 1.000 \times 1.000 \times 1.000 \times 1.000 \times 1.000) \\ &= 7.228 \times 0.733 \\ &= 5.294 \text{ crashes/year} \end{aligned}$$

The CMFs are applied to the property-damage-only SPF as follows:

$$\begin{aligned} N_{p^*, D4, SG4, at, pdo} &= N_{spf, D4, SG4, at, pdo} \times (CMF_{10, D4, SG4, at, pdo} \times \dots \times CMF_{19, D4, SG4, at, pdo}) \\ &= 9.869 \times (1.000 \times 0.872 \times 1.000 \times 1.000 \times 0.820 \times 1.000 \times 1.000 \times 1.000 \times 1.000 \times 1.000) \\ &= 9.869 \times 0.715 \\ &= 7.052 \text{ crashes/year} \end{aligned}$$

Step 11 – Multiply the result obtained in Step 10 by the appropriate calibration factor.

It is assumed that a calibration factor of 1.00 has been determined for local conditions. See Section B.1 of Appendix B to Part C for further discussion on calibration of the predicted models.

Calculation of Predicted Average Crash Frequency

The predicted average crash frequency is calculated using Equation 19-1 based on the results obtained in Steps 9 through 11 as follows.

Fatal-and-injury crashes:

$$\begin{aligned} N_{p, D4, SG4, at, fi} &= N_{p^*, D4, SG4, at, fi} \times C_{D4, SG4, at, fi} \\ &= 5.294 \times 1.00 \\ &= 5.294 \text{ crashes/year} \end{aligned}$$

Property-damage-only crashes:

$$\begin{aligned} N_{p, D4, SG4, at, pdo} &= N_{p^*, D4, SG4, at, pdo} \times C_{D4, SG4, at, pdo} \\ &= 7.052 \times 1.00 \\ &= 7.052 \text{ crashes/year} \end{aligned}$$

Step 12—If there is another year to be evaluated in the evaluation period for the selected site, return to Step 8. Otherwise, proceed to Step 13.

The study period is one year (2011), so steps 8 through 11 need not be repeated.

Step 13—Apply site-specific EB Method (if applicable) and apply SDFs.

This step consists of three optional sets of calculations—site-specific EB Method, severity distribution functions, and crash type distribution.

Apply the site-specific EB Method to a future time period, if appropriate.

The site-specific EB Method is not applied in this sample problem because crash data are not available.

Apply the severity distribution functions (SDFs), if desired.

To apply the SDFs, the systematic component of crash severity likelihood V_j is computed for each severity level j using Equation 19-88 as follows:

$$V_j = a + (b \times I_{p,lt}) + (c \times [n_{dw} + n_{ps}]) + (d \times I_{ps}) + (e \times I_{rural})$$

The coefficients a , b , c , d , and e are obtained from Table 19-44 for each severity level j . V_j is computed for fatal and incapacitating injury crashes as follows:

$$\begin{aligned} V_{K+A} &= -3.257 + (-0.288 \times 0.0) + (0.0991 \times [0.0 + 0.0]) + (1.171 \times 0.0) + (0.619 \times 0.0) \\ &= -3.257 \end{aligned}$$

Similar calculations using the coefficients from Table 19-44 for non-incapacitating injury crashes yield the following results:

$$V_B = -1.511$$

Using these computed V_{K+A} and V_B values, and assuming a calibration factor $C_{sdf, aS, x}$ of 1.0, the probability of occurrence of a fatal crash is computed using Equation 19-84 as follows:

$$\begin{aligned} P_{aS, SG, at, K} &= \frac{\exp(V_{K+A})}{\frac{1.0}{C_{sdf, aS, x}} + \exp(V_{K+A}) + \exp(V_B)} \times P_{K|K+A, aS, x, at} \\ &= \frac{\exp(-3.257)}{\frac{1.0}{1.0} + \exp(-3.257) + \exp(-1.511)} \times 0.0385 \\ &= 0.001 \end{aligned}$$

Similar calculations using Equation 19-85 and Equation 19-86 yield the following results:

$$P_{aS, SG, at, A} = 0.029$$

$$P_{aS, SG, at, B} = 0.175$$

The probability of occurrence of a possible-injury crash is computed using Equation 19-87 as follows:

$$\begin{aligned} P_{aS, SG, at, C} &= 1.0 - (P_{aS, SG, at, K} + P_{aS, SG, at, A} + P_{aS, SG, at, B}) \\ &= 1.0 - (0.001 + 0.029 + 0.175) \\ &= 0.794 \end{aligned}$$

The probability of occurrence of a fatal crash is multiplied by the fatal-and-injury crash frequency obtained in Step 11 using Equation 19-78 as follows:

$$\begin{aligned} N_{e, D4, SG4, at, K} &= N_{e, D4, SG4, at, fi} \times P_{aS, SG, at, K} \\ &= 5.294 \times 0.001 \\ &= 0.006 \text{ crashes/year} \end{aligned}$$

Similar calculations using Equation 19-78 and the probabilities of occurrences of the other crash severities yield the following results:

$$N_{e, D4, SG, at, A} = 0.156 \text{ crashes/year}$$

$$N_{e, D4, SG, at, B} = 0.928 \text{ crashes/year}$$

$$N_{e, D4, SG, at, C} = 4.204 \text{ crashes/year}$$

Apply the crash type distribution, if desired.

The crash type distributions are applied by multiplying the default crash type distribution proportions in Table 19-16 by the predicted average crash frequencies obtained in Step 11.

Worksheets

The step-by-step instructions are provided to illustrate the predictive method for calculating the predicted average crash frequency for a ramp terminal. To apply the predictive method steps to multiple terminals, a series of worksheets are provided for determining the predicted average crash frequency. The worksheets include:

- Table 19-60. Ramp Terminal Worksheet (1 of 4)—Sample Problem 4
- Table 19-61. Ramp Terminal Worksheet (2 of 4)—Sample Problem 4
- Table 19-62. Ramp Terminal Worksheet (3 of 4)—Sample Problem 4
- Table 19-63. Ramp Terminal Worksheet (4 of 4)—Sample Problem 4

Filled versions of these worksheets are provided below. Blank versions of worksheets used in the Sample Problems are provided in Appendix 19A.

Table 19-60 is a summary of general information about the ramp terminal, analysis, input data (i.e., “The Facts”), and assumptions for Sample Problem 4. The input data include area type, crash data, basic intersection data, alignment data, traffic control data, and cross section data.

Table 19-61 is a summary of general information about the ramp terminal, analysis, input data (i.e., “The Facts”), and assumptions for Sample Problem 4. The input data include cross section data, access data, and traffic data.

Table 19-62 is a tabulation of the CMF and SPF computations for Sample Problem 4.

Table 19-63 is a tabulation of the crash severity and crash type distributions for Sample Problem 4.

Table 19-60. Ramp Terminal Worksheet (1 of 4)—Sample Problem 4

General Information					Location Information				
Analyst					Roadway				
Agency or company					Intersection				
Date performed					Study year				
Area type		X	Urban		Rural				
Input Data									
Crash Data				Crash Period	Study Year	Complete the study year column. Complete the crash period column if the EB Method is used.			
Crash data time period						First year	--	Last year	--
Count of FI crashes $N_{o, w, x, at, fi}^*$				--					
Count of PDO crashes $N_{o, w, x, at, pdo}^*$				--					
Basic Intersection Data									
Ramp terminal configuration				D4		Choices: D3ex, D3en, D4, A4, B4, A2, B2 Same choice for crash period and study year.			
Ramp terminal traffic control type				Signal		Choices: Signal, One-way-stop, All-way stop			
Presence of a non-ramp public street leg I_{ps}				--	Y/N	N	Y/N		
Alignment Data									
Exit ramp skew angle I_{sk} (degrees)				--	--				
Distance to the next public street intersection on the outside crossroad leg L_{str} (mi)				--	1.0				
Distance to the adjacent ramp terminal L_{rmp} (mi)				--	0.1				
Traffic Control									
Left-Turn Operational Mode									
Crossroad	Inside approach	Prot.-only mode $I_{p, lt, in}$	--	Y/N	N	Y/N			
	Outside approach	Prot.-only mode $I_{p, lt, out}$	--	Y/N	--	Y/N			
Right-Turn Control Type									
Ramp	Exit ramp approach	Right-turn control type	--	Signal			Choices: Signal, Stop, Yield, Merge, Free		
Cross Section Data									
Crossroad median width W_m (ft)				--	12				
Number of Lanes									
Crossroad	Inside approach	Through lanes $n_{th, in}$	2		Same choice for crash period and study year.				
	Outside approach	Through lanes $n_{th, out}$	2		Same choice for crash period and study year.				
Ramp	Exit ramp approach	All lanes n_{ex}	3		Same choice for crash period and study year.				
Right-Turn Channelization									
Crossroad	Inside approach	Chan. present $I_{ch, in}$	--	Y/N	--	Y/N			
	Outside approach	Chan. present $I_{ch, out}$	--	Y/N	N	Y/N			
Ramp	Exit ramp approach	Chan. present $I_{ch, ex}$	--	Y/N	N	Y/N			

Table 19-61. Ramp Terminal Worksheet (2 of 4)—Sample Problem 4

Input Data

Cross Section Data			Crash Period		Study Year		Complete the study year column. Complete the crash period column if the EB Method is used.
Left-Turn Lane or Bay							
Crossroad	Inside approach	Lane or bay present $I_{bay, lt, in}$	--	Y/N	Y	Y/N	If Yes, then enter data in the next row.
		Lane or bay width $W_{b, in}$ (ft)	--		12		
	Outside approach	Lane or bay present $I_{bay, lt, out}$	--	Y/N	N	Y/N	If Yes, then enter data in the next row.
		Lane or bay width $W_{b, out}$ (ft)	--		--		
Right-Turn Lane or Bay							
Crossroad	Inside approach	Lane or bay present $I_{bay, rt, in}$	--	Y/N	--	Y/N	
	Outside approach	Lane or bay present $I_{bay, rt, out}$	--	Y/N	N	Y/N	
Access Data							
Number of driveways on the outside crossroad leg n_{dw}			--		0		
Number of public street approaches on the outside crossroad leg n_{ps}			--		--		
Traffic Data							
Crossroad	Inside leg	$AADT_{in}$ (veh/day)	--		28,000		
	Outside leg	$AADT_{out}$ (veh/day)	--		28,000		
Ramp	Exit ramp	$AADT_{ex}$ (veh/day)	--		7,100		
	Entrance ramp	$AADT_{en}$ (veh/day)	--		6,750		

Table 19-62. Ramp Terminal Worksheet (3 of 4)—Sample Problem 4

Crash Modification Factors					
Complete the study year column. Complete the crash period column if the EB Method is used.	Equation	Fatal and Injury		Property Damage Only	
		Crash Period	Study Year	Crash Period	Study Year
Signal Control					
Exit ramp capacity $CMF_{10, w, SGn, at, fi}$	19-42	--	1.038		
Crossroad left-turn lane $CMF_{11, w, SGn, at, z}$	19-45	--	0.860	--	0.872
Crossroad right-turn lane $CMF_{12, w, SGn, at, z}$	19-48	--	1.000	--	1.000
Access point frequency $CMF_{13, w, SGn, at, z}$	19-49	--	1.000	--	1.000
Segment length $CMF_{14, w, SGn, at, z}$	19-50	--	0.821	--	0.820
Median width $CMF_{15, w, SGn, at, z}$	19-51	--	1.000	--	1.000
Protected left-turn operation $CMF_{16, w, SGn, at, z}$	19-53	--	1.000	--	1.000
Chan. right turn on crossroad $CMF_{17, w, SGn, at, z}$	19-55	--	1.000	--	1.000
Chan. right turn on exit ramp $CMF_{18, w, SGn, at, z}$	19-56	--	1.000	--	1.000
Non-ramp public street leg $CMF_{19, w, SGn, at, z}$	19-57	--	1.000	--	1.000
Stop Control					
Exit ramp capacity $CMF_{10, w, ST, at, fi}$	19-42	--	--		
Crossroad left-turn lane $CMF_{11, w, ST, at, z}$	19-45	--	--	--	--
Crossroad right-turn lane $CMF_{12, w, ST, at, z}$	19-48	--	--	--	--
Access point frequency $CMF_{13, w, ST, at, fi}$	19-49	--	--		
Segment length $CMF_{14, w, ST, at, fi}$	19-50	--	--		
Median width $CMF_{15, w, ST, at, fi}$	19-51	--	--		
Skew angle $CMF_{20, w, ST, at, fi}$	19-58	--	--		
All-way stop-control (exclude $CMF_{11}, CMF_{12}, CMF_{20}$)		--	--		
Combined CMF (multiply all CMFs evaluated)		--	0.733	--	0.715
Expected Average Crash Frequency^a					
Complete the study year column. Complete the crash period column if the <i>site-specific</i> EB Method is used.	Fatal and Injury		Property Damage Only		
	Crash Period	Study Year	Crash Period	Study Year	
Calibration factor $C_{aS, x, at, z}$	1.00		1.00		
Overdispersion parameter $k_{w, x, at, z}$	--		--		
Observed crash count $N_{o, w, x, at, z}^*$ (cr)	--		--		
Reference year r	--		--		
Predicted average crash freq. for reference year $N_{p, w, x, at, z, r}$ (cr/yr)	--		--		
Predicted number of crashes for crash period (sum all years) $N_{p, w, x, y, z}^*$ (cr)	--		--		
Equivalent years associated with crash count $C_{b, w, x, at, z, r}$ (yr)	--		--		
Adjusted average crash freq. for ref. year given $N_{o, N_{a, w, x, at, z, r}}^*$ (cr/yr)	--		--		
Study year s		2011		2011	
Predicted average crash freq. for study year $N_{p, w, x, at, z, s}$ (cr/yr)		5.294		7.052	
Expected average crash freq. for study year $N_{e, w, x, at, z, s}$ (cr/yr)		5.294		7.052	

Note: a – If the EB Method is not used, then substitute “predicted” for “expected” and substitute the subscript “p” for the subscript “e”.

Table 19-63. Ramp Terminal Worksheet (4 of 4)—Sample Problem 4

Expected Average Crash Frequency							
<i>Crash Severity Distribution</i>							
	K	A	B	C	Total FI	PDO	Total FI + PDO
Proportion by injury level	0.001	0.029	0.175	0.794	1.000		
Expected average crash freq. for study year $N_{e, w, x, at, z, s}$ (cr/yr)	0.006	0.156	0.928	4.204	5.294	7.052	12.346
<i>Crash Type Distribution</i>							
Crash Type Category	Table 19-16, 19-21, or 19-45	Fatal and Injury		Property Damage Only		Total	
		Proportion	Expected Average Crash Frequency for Study Year $N_{e, w, x, at, fi, s}$ (cr/yr)	Proportion	Expected Average Crash Frequency for Study Year $N_{e, w, x, at, pdo, s}$ (cr/yr)	Expected Average Crash Frequency for Study Year $N_{e, w, x, at, as, s}$ (cr/yr)	Expected Average Crash Frequency for Study Year $N_{e, w, x, at, as, s}$ (cr/yr)
Multiple-Vehicle Crashes							
Head-on		0.011	0.058	0.007	0.049	0.108	
Right-angle		0.260	1.376	0.220	1.551	2.928	
Rear-end		0.625	3.309	0.543	3.829	7.138	
Sideswipe		0.042	0.222	0.149	1.051	1.273	
Other multiple-vehicle crashes		0.009	0.048	0.020	0.141	0.189	
Single-Vehicle Crashes							
Crash with animal		0.000	0.000	0.000	0.000	0.000	
Crash with fixed object		0.033	0.175	0.050	0.353	0.527	
Crash with other object		0.001	0.005	0.002	0.014	0.019	
Crash with parked vehicle		0.001	0.005	0.002	0.014	0.019	
Other single-vehicle crashes		0.018	0.095	0.007	0.049	0.145	
Total		1.000	0.281	1.000	0.430	0.711	

19.14.5. Sample Problem 5**The Site/Facility**

A one-way stop-controlled partial cloverleaf interchange ramp terminal on an urban arterial.

The Question

What is the predicted average crash frequency of the ramp terminal for a one-year period?

The Facts

The study year is 2011. The conditions present during this year are provided in the following list.

- A4 configuration
- 1.0 mi to the next public street intersection on the outside crossroad leg
- 0.09 mi to the adjacent ramp terminal
- 0-degree skew angle on exit-ramp approach

- Merge control for the exit ramp right-turn movement
- 12-ft crossroad median width
- 4 through lanes on the crossroad
- 2 lanes on the exit ramp approach (developed at a distance of 200 ft from the ramp terminal)
- No right-turn channelization or bays
- 21,500 veh/day on the crossroad (same for both legs)
- 3,400 veh/day on the exit ramp leg
- 3,750 veh/day on the entrance ramp leg

Assumptions

- Crash type distributions used are the default values presented in Table 19-21.
- The calibration factor is 1.00.

Results

Using the predictive method steps as outlined below, the predicted average fatal-and-injury crash frequency for the ramp terminal in Sample Problem 5 is determined to be 1.2 crashes per year, and the predicted average property-damage-only crash frequency is determined to be 2.7 crashes per year (rounded to one decimal place).

Steps

Step 1 through 8

To determine the predicted average crash frequency of the ramp terminal in Sample Problem 5, only Steps 9 through 13 are conducted. No other steps are necessary because only one ramp terminal is analyzed for a one-year period and the EB Method is not applied.

Step 9 – For the selected site, determine and apply the appropriate SPF.

For a ramp terminal, an SPF value for all crash types is determined. The SPF for fatal-and-injury crashes is calculated from Equation 19-31 and Table 19-18 as follows:

$$\begin{aligned}
 N_{spf, A4, ST, at, fi} &= \exp(a + b \times \ln[c \times AADT_{xrd}] + d \times \ln[c \times AADT_{ex} + c \times AADT_{en}]) \\
 &= \exp(-3.223 + 0.582 \times \ln[0.001 \times 21,500] + 0.899 \times \ln[0.001 \times 3,400 + 0.001 \times 3,750]) \\
 &= 1.392 \text{ crashes/year}
 \end{aligned}$$

Similarly, the SPF for property-damage-only crashes is calculated from Equation 19-31 and Table 19-18 to yield the following result:

$$N_{spf, A4, ST, at, pdo} = 2.715 \text{ crashes/year}$$

Step 10 – Multiply the result obtained in Step 9 by the appropriate CMFs.

Each CMF used in the calculation of the predicted average crash frequency of the ramp terminal is calculated in this step.

Exit Ramp Capacity ($CMF_{10, A4, ST, at, fi}$)

$CMF_{10, A4, ST, at, fi}$ is calculated from Equation 19-42 as follows:

$$CMF_{10, A4, ST, at, fi} = (1.0 - P_{ex}) \times 1.0 + P_{ex} \times \exp\left(a \times \frac{c \times AADT_{ex}}{n_{ex, eff}}\right)$$

For a merge-controlled exit-ramp right-turn movement, the effective number of lanes serving exit ramp traffic $n_{ex, eff}$ is computed using the first portion of Equation 19-43 as follows:

$$\begin{aligned} n_{ex, eff} &= 0.5 \times (n_{ex} - 1.0) + 1.0 \\ &= 0.5 \times (2 - 1.0) + 1.0 \\ &= 1.5 \end{aligned}$$

The proportion of total leg AADT on the exit ramp leg P_{ex} is computed using Equation 19-44 as follows:

$$\begin{aligned} P_{ex} &= \frac{AADT_{ex}}{AADT_{in} + AADT_{out} + AADT_{en} + AADT_{ex}} \\ &= \frac{3,400}{21,500 + 21,500 + 3,750 + 3,400} \\ &= 0.068 \end{aligned}$$

From Table 19-32, $a = 0.151$ and $c = 0.001$ for one-way stop-controlled ramp terminals. $CMF_{10, A4, ST, at, fi}$ is calculated as follows:

$$\begin{aligned} CMF_{10, A4, ST, at, fi} &= (1.0 - 0.068) \times 1.0 + 0.068 \times \exp\left(0.151 \times \frac{0.001 \times 3,400}{1.5}\right) \\ &= 1.028 \end{aligned}$$

Crossroad Left-Turn Lane ($CMF_{11, A4, ST, at, z}$)

The ramp terminal does not have left-turn lanes or bays on the crossroad legs, which is the base condition for the crossroad left-turn lane CMF. Hence, $CMF_{11, A4, ST, at, fi}$ and $CMF_{11, A4, ST, at, pdo}$ are equal to 1.000.

Crossroad Right-Turn Lane ($CMF_{12, A4, ST, at, z}$)

The ramp terminal does not have right-turn lanes or bays on the crossroad legs, which is the base condition for the crossroad right-turn lane CMF. Hence, $CMF_{12, A4, ST, at, fi}$ and $CMF_{12, A4, ST, at, pdo}$ are equal to 1.000.

Access Point Frequency ($CMF_{13, A4, ST, at, fi}$)

The ramp terminal has no unsignalized public street approaches on the outside leg, which is the base condition for the access point frequency CMF. Hence, $CMF_{13, A4, ST, at, fi}$ is equal to 1.000.

Segment Length ($CMF_{14, A4, ST, at, fi}$)

$CMF_{14, A4, ST, at, fi}$ is calculated from Equation 19-50 as follows:

$$CMF_{14, A4, ST, at, fi} = \exp\left(a \times \left[\frac{1.0}{L_{rmp}} + \frac{1.0}{L_{str}} - 0.333\right]\right)$$

From Table 19-36, $a = -0.0141$ for fatal-and-injury crashes. $CMF_{14, A4, ST, at, fi}$ is calculated as follows:

$$\begin{aligned} CMF_{14, A4, ST, at, fi} &= \exp\left(-0.0141 \times \left[\frac{1.0}{0.09} + \frac{1.0}{1.0} - 0.333\right]\right) \\ &= 0.847 \end{aligned}$$

Median Width ($CMF_{15, A4, ST, at, fi}$)

The crossroad has a 12-ft median, which is the base condition for the median width CMF. Hence, $CMF_{15, A4, ST, at, fi}$ is equal to 1.000.

Skew Angle ($CMF_{20, A4, ST, at, fi}$)

The ramp terminal has no skew, which is the base condition for the skew angle CMF. Hence, $CMF_{20, A4, ST, at, fi}$ is equal to 1.000.

Crashes

The CMFs are applied to the fatal-and-injury SPF as follows:

$$\begin{aligned} N_{p^*, A4, ST, at, fi} &= N_{spf, A4, ST, at, fi} \times (CMF_{10, A4, ST, at, fi} \times \dots \times CMF_{15, A4, ST, at, fi} \times CMF_{20, A4, ST, at, fi}) \\ &= 1.392 \times (1.028 \times 1.000 \times 1.000 \times 1.000 \times 0.847 \times 1.000 \times 1.000) \\ &= 1.392 \times 0.871 \\ &= 1.212 \text{ crashes/year} \end{aligned}$$

The CMFs are applied to the property-damage-only SPF as follows:

$$\begin{aligned} N_{p^*, A4, ST, at, pdo} &= N_{spf, A4, ST, at, pdo} \times (CMF_{11, A4, ST, at, pdo} \times CMF_{12, A4, ST, at, pdo}) \\ &= 2.715 \times (1.000 \times 1.000) \\ &= 2.715 \times 1.000 \\ &= 2.715 \text{ crashes/year} \end{aligned}$$

Step 11 – Multiply the result obtained in Step 10 by the appropriate calibration factor.

It is assumed that a calibration factor of 1.00 has been determined for local conditions. See Section B.1 of Appendix B to Part C for further discussion on calibration of the predicted models.

Calculation of Predicted Average Crash Frequency

The predicted average crash frequency is calculated using Equation 19-1 based on the results obtained in Steps 9 through 11 as follows.

Fatal-and-injury crashes:

$$\begin{aligned} N_{p, A4, ST, at, fi} &= N_{p^*, A4, ST, at, fi} \times C_{A4, ST, at, fi} \\ &= 1.212 \times 1.00 \\ &= 1.212 \text{ crashes/year} \end{aligned}$$

Property-damage-only crashes:

$$\begin{aligned} N_{p, A4, ST, at, pdo} &= N_{p^*, A4, ST, at, pdo} \times C_{A4, ST, at, pdo} \\ &= 2.715 \times 1.00 \\ &= 2.715 \text{ crashes/year} \end{aligned}$$

Step 12—If there is another year to be evaluated in the evaluation period for the selected site, return to Step 8. Otherwise, proceed to Step 13.

The study period is one year (2011), so steps 8 through 11 need not be repeated.

Step 13—Apply site-specific EB Method (if applicable) and apply SDFs.

This step consists of three optional sets of calculations—site-specific EB Method, severity distribution functions, and crash type distribution.

Apply the site-specific EB Method to a future time period, if appropriate.

The site-specific EB Method is not applied in this sample problem because crash data are not available.

Apply the severity distribution functions (SDFs), if desired.

To apply the SDFs, the systematic component of crash severity likelihood V_j is computed for each severity level j using Equation 19-88 as follows:

$$V_j = a + (b \times I_{p,lt}) + (c \times [n_{dw} + n_{ps}]) + (d \times I_{ps}) + (e \times I_{rural})$$

The coefficients a , b , c , d , and e are obtained from Table 19-44 for each severity level j . V_j is computed for fatal and incapacitating injury crashes as follows:

$$\begin{aligned} V_{K+A} &= -3.168 + (0.00 \times 0.0) + (0.00 \times [0.0 + 0.0]) + (0.00 \times 0.0) + (0.891 \times 0.0) \\ &= -3.168 \end{aligned}$$

Similar calculations using the coefficients from Table 19-44 for non-incapacitating injury crashes yield the following results:

$$V_B = -1.476$$

Using these computed V_{K+A} and V_B values, and assuming a calibration factor $C_{sdf, aS, x}$ of 1.0, the probability of occurrence of a fatal crash is computed using Equation 19-84 as follows:

$$\begin{aligned}
 P_{aS,ST,at,K} &= \frac{\exp(V_{K+A})}{\frac{1.0}{C_{sdf,aS,x}} + \exp(V_{K+A}) + \exp(V_B)} \times P_{K|K+A,aS,x,at} \\
 &= \frac{\exp(-3.168)}{\frac{1.0}{1.0} + \exp(-3.168) + \exp(-1.476)} \times 0.160 \\
 &= 0.005
 \end{aligned}$$

Similar calculations using Equation 19-85 and Equation 19-86 yield the following results:

$$P_{aS,ST,at,A} = 0.028$$

$$P_{aS,ST,at,B} = 0.180$$

The probability of occurrence of a possible-injury crash is computed using Equation 19-87 as follows:

$$\begin{aligned}
 P_{aS,ST,at,C} &= 1.0 - (P_{aS,ST,at,K} + P_{aS,ST,at,A} + P_{aS,ST,at,B}) \\
 &= 1.0 - (0.005 + 0.028 + 0.180) \\
 &= 0.787
 \end{aligned}$$

The probability of occurrence of a fatal crash is multiplied by the fatal-and-injury crash frequency obtained in Step 11 using Equation 19-78 as follows:

$$\begin{aligned}
 N_{e,A4,ST,at,K} &= N_{e,A4,ST,at,fi} \times P_{aS,ST,at,K} \\
 &= 1.212 \times 0.005 \\
 &= 0.006 \text{ crashes/year}
 \end{aligned}$$

Similar calculations using Equation 19-78 and the probabilities of occurrences of the other crash severities yield the following results:

$$N_{e,A4,ST,at,A} = 0.034 \text{ crashes/year}$$

$$N_{e,A4,ST,at,B} = 0.218 \text{ crashes/year}$$

$$N_{e,A4,ST,at,C} = 0.954 \text{ crashes/year}$$

Apply the crash type distribution, if desired.

The crash type distributions are applied by multiplying the default crash type distribution proportions in Table 19-21 by the predicted average crash frequencies obtained in Step 11.

Worksheets

The step-by-step instructions are provided to illustrate the predictive method for calculating the predicted average crash frequency for a ramp terminal. To apply the predictive method steps to multiple terminals, a series of worksheets are provided for determining the predicted average crash frequency. The worksheets include:

- Table 19-64. Ramp Terminal Worksheet (1 of 4)—Sample Problem 5

- Table 19-65. Ramp Terminal Worksheet (2 of 4)—Sample Problem 5
- Table 19-66. Ramp Terminal Worksheet (3 of 4)—Sample Problem 5
- Table 19-67. Ramp Terminal Worksheet (4 of 4)—Sample Problem 5

Filled versions of these worksheets are provided below. Blank versions of worksheets used in the Sample Problems are provided in Appendix 19A.

Table 19-64 is a summary of general information about the ramp terminal, analysis, input data (i.e., “The Facts”), and assumptions for Sample Problem 5. The input data include area type, crash data, basic intersection data, alignment data, traffic control data, and cross section data.

Table 19-65 is a summary of general information about the ramp terminal, analysis, input data (i.e., “The Facts”), and assumptions for Sample Problem 5. The input data include cross section data, access data, and traffic data.

Table 19-66 is a tabulation of the CMF and SPF computations for Sample Problem 5.

Table 19-67 is a tabulation of the crash severity and crash type distributions for Sample Problem 5.

Table 19-64. Ramp Terminal Worksheet (1 of 4)—Sample Problem 5

General Information					Location Information				
Analyst					Roadway				
Agency or company					Intersection				
Date performed					Study year				
Area type		X	Urban		Rural				
Input Data									
Crash Data				Crash Period	Study Year	Complete the study year column. Complete the crash period column if the EB Method is used.			
Crash data time period						First year	--	Last year	--
Count of FI crashes $N_{o,w,x,at,fi}^*$				--					
Count of PDO crashes $N_{o,w,x,at,pdo}^*$				--					
Basic Intersection Data									
Ramp terminal configuration				A4		Choices: D3ex, D3en, D4, A4, B4, A2, B2 Same choice for crash period and study year.			
Ramp terminal traffic control type				One-way stop		Choices: Signal, One-way-stop, All-way stop			
Presence of a non-ramp public street leg I_{ps}				--	Y/N	--	Y/N		
Alignment Data									
Exit ramp skew angle I_{sk} (degrees)				--	0				
Distance to the next public street intersection on the outside crossroad leg L_{str} (mi)				--	1.0				
Distance to the adjacent ramp terminal L_{rmp} (mi)				--	0.09				
Traffic Control									
Left-Turn Operational Mode									
Crossroad	Inside approach	Prot.-only mode $I_{p,lt,in}$	--	Y/N	--	Y/N			
	Outside approach	Prot.-only mode $I_{p,lt,out}$	--	Y/N	--	Y/N			
Right-Turn Control Type									
Ramp	Exit ramp approach	Right-turn control type	--	Merge	Choices: Signal, Stop, Yield, Merge, Free				
Cross Section Data									
Crossroad median width W_m (ft)				--	12				
Number of Lanes									
Crossroad	Inside approach	Through lanes $n_{th,in}$	2		Same choice for crash period and study year.				
	Outside approach	Through lanes $n_{th,out}$	2		Same choice for crash period and study year.				
Ramp	Exit ramp approach	All lanes n_{ex}	2		Same choice for crash period and study year.				
Right-Turn Channelization									
Crossroad	Inside approach	Chan. present $I_{ch,in}$	--	Y/N	--	Y/N			
	Outside approach	Chan. present $I_{ch,out}$	--	Y/N	--	Y/N			
Ramp	Exit ramp approach	Chan. present $I_{ch,ex}$	--	Y/N	--	Y/N			

Table 19-65. Ramp Terminal Worksheet (2 of 4)—Sample Problem 5

Input Data

Cross Section Data			Crash Period		Study Year		Complete the study year column. Complete the crash period column if the EB Method is used.
Left-Turn Lane or Bay							
Crossroad	Inside approach	Lane or bay present $I_{bay, lt, in}$	--	Y/N	--	Y/N	If Yes, then enter data in the next row.
		Lane or bay width $W_{b, in}$ (ft)	--		--		
	Outside approach	Lane or bay present $I_{bay, lt, out}$	--	Y/N	--	Y/N	If Yes, then enter data in the next row.
		Lane or bay width $W_{b, out}$ (ft)	--		--		
Right-Turn Lane or Bay							
Crossroad	Inside approach	Lane or bay present $I_{bay, rt, in}$	--	Y/N	N	Y/N	
	Outside approach	Lane or bay present $I_{bay, rt, out}$	--	Y/N	N	Y/N	
Access Data							
Number of driveways on the outside crossroad leg n_{dw}			--		--		
Number of public street approaches on the outside crossroad leg n_{ps}			--		--		
Traffic Data							
Crossroad	Inside leg	$AADT_{in}$ (veh/day)	--		21,500		
	Outside leg	$AADT_{out}$ (veh/day)	--		21,500		
Ramp	Exit ramp	$AADT_{ex}$ (veh/day)	--		3,400		
	Entrance ramp	$AADT_{en}$ (veh/day)	--		3,750		

Table 19-66. Ramp Terminal Worksheet (3 of 4)—Sample Problem 5

Crash Modification Factors					
Complete the study year column. Complete the crash period column if the EB Method is used.	Equation	Fatal and Injury		Property Damage Only	
		Crash Period	Study Year	Crash Period	Study Year
Signal Control					
Exit ramp capacity $CMF_{10, w, SGn, at, fi}$	19-42	--	--		
Crossroad left-turn lane $CMF_{11, w, SGn, at, z}$	19-45	--	--	--	--
Crossroad right-turn lane $CMF_{12, w, SGn, at, z}$	19-48	--	--	--	--
Access point frequency $CMF_{13, w, SGn, at, z}$	19-49	--	--	--	--
Segment length $CMF_{14, w, SGn, at, z}$	19-50	--	--	--	--
Median width $CMF_{15, w, SGn, at, z}$	19-51	--	--	--	--
Protected left-turn operation $CMF_{16, w, SGn, at, z}$	19-53	--	--	--	--
Chan. right turn on crossroad $CMF_{17, w, SGn, at, z}$	19-55	--	--	--	--
Chan. right turn on exit ramp $CMF_{18, w, SGn, at, z}$	19-56	--	--	--	--
Non-ramp public street leg $CMF_{19, w, SGn, at, z}$	19-57	--	--	--	--
Stop Control					
Exit ramp capacity $CMF_{10, w, ST, at, fi}$	19-42	--	1.028		
Crossroad left-turn lane $CMF_{11, w, ST, at, z}$	19-45	--	1.000	--	1.000
Crossroad right-turn lane $CMF_{12, w, ST, at, z}$	19-48	--	1.000	--	1.000
Access point frequency $CMF_{13, w, ST, at, fi}$	19-49	--	1.000		
Segment length $CMF_{14, w, ST, at, fi}$	19-50	--	0.847		
Median width $CMF_{15, w, ST, at, fi}$	19-51	--	1.000		
Skew angle $CMF_{20, w, ST, at, fi}$	19-58	--	1.000		
All-way stop-control (exclude $CMF_{11}, CMF_{12}, CMF_{20}$)		--	--		
Combined CMF (multiply all CMFs evaluated)		--	0.871	--	1.000
Expected Average Crash Frequency^a					
Complete the study year column. Complete the crash period column if the <i>site-specific</i> EB Method is used.	Fatal and Injury		Property Damage Only		
	Crash Period	Study Year	Crash Period	Study Year	
Calibration factor $C_{aS, x, at, z}$	1.00		1.00		
Overdispersion parameter $k_{w, x, at, z}$	--		--		
Observed crash count $N_{o, w, x, at, z}^*$ (cr)	--		--		
Reference year r	--		--		
Predicted average crash freq. for reference year $N_{p, w, x, at, z, r}$ (cr/yr)	--		--		
Predicted number of crashes for crash period (sum all years) $N_{p, w, x, y, z}^*$ (cr)	--		--		
Equivalent years associated with crash count $C_{b, w, x, at, z, r}$ (yr)	--		--		
Adjusted average crash freq. for ref. year given $N_{o, N_{a, w, x, at, z, r}}^*$ (cr/yr)	--		--		
Study year s		2011		2011	
Predicted average crash freq. for study year $N_{p, w, x, at, z, s}$ (cr/yr)		1.212		2.715	
Expected average crash freq. for study year $N_{e, w, x, at, z, s}$ (cr/yr)		1.212		2.715	

Note: a – If the EB Method is not used, then substitute “predicted” for “expected” and substitute the subscript “p” for the subscript “e”.

Table 19-67. Ramp Terminal Worksheet (4 of 4)—Sample Problem 5

Expected Average Crash Frequency							
<i>Crash Severity Distribution</i>							
	K	A	B	C	Total FI	PDO	Total FI + PDO
Proportion by injury level	0.005	0.028	0.180	0.787	1.000		
Expected average crash freq. for study year $N_{e, w, x, at, z, s}$ (cr/yr)	0.006	0.034	0.218	0.954	1.212	2.715	3.927
<i>Crash Type Distribution</i>							
Crash Type Category	Table 19-16, 19-21, or 19-45	Fatal and Injury		Property Damage Only		Total	
		Proportion	Expected Average Crash Frequency for Study Year $N_{e, w, x, at, fi, s}$ (cr/yr)	Proportion	Expected Average Crash Frequency for Study Year $N_{e, w, x, at, pdo, s}$ (cr/yr)	Expected Average Crash Frequency for Study Year $N_{e, w, x, at, as, s}$ (cr/yr)	Expected Average Crash Frequency for Study Year $N_{e, w, x, at, as, s}$ (cr/yr)
Multiple-Vehicle Crashes							
Head-on		0.017	0.021	0.012	0.033	0.053	
Right-angle		0.458	0.055	0.378	1.026	1.581	
Rear-end		0.373	0.452	0.377	1.023	1.476	
Sideswipe		0.025	0.030	0.079	0.214	0.245	
Other multiple-vehicle crashes		0.017	0.021	0.016	0.043	0.064	
Single-Vehicle Crashes							
Crash with animal		0.000	0.000	0.000	0.000	0.000	
Crash with fixed object		0.085	0.103	0.110	0.299	0.402	
Crash with other object		0.000	0.000	0.000	0.000	0.000	
Crash with parked vehicle		0.000	0.000	0.008	0.022	0.022	
Other single-vehicle crashes		0.025	0.030	0.020	0.054	0.085	
Total		1.000	1.212	1.000	2.715	3.927	

19.14.6. Sample Problem 6**The Site/Facility**

An all-way stop-controlled partial cloverleaf interchange ramp terminal on an urban arterial.

The Question

What is the predicted average crash frequency of the ramp terminal for a one-year period?

The Facts

The study year is 2011. The conditions present during this year are provided in the following list.

- B2 configuration
- 1.0 mi to the next public street intersection on the outside crossroad leg
- 0.15 mi to the adjacent ramp terminal
- Stop control for the exit ramp right-turn movement

- 12-ft crossroad median width
- 4 through lanes on the crossroad
- 2 lanes on the exit ramp approach (developed at a distance of 125 ft from the ramp terminal)
- 14,000 veh/day on the crossroad (same for both legs)
- 1,450 veh/day on the exit ramp leg
- 1,300 veh/day on the entrance ramp leg

Assumptions

- Crash type distributions used are the default values presented in Table 19-45.
- The calibration factor is 1.00.

Results

Using the predictive method steps as outlined below, the predicted average fatal-and-injury crash frequency for the ramp terminal in Sample Problem 6 is determined to be 0.2 crashes per year, and the predicted average property-damage-only crash frequency is determined to be 0.9 crashes per year (rounded to one decimal place).

As stated in the interim predictive method for all-way stop control in Section 19.10, the ramp terminal is evaluated as a one-way stop-controlled terminal, but with a smaller set of CMFs in Step 10. None of the CMFs apply to the property-damage-only SPF.

Steps

Step 1 through 8

To determine the predicted average crash frequency of the ramp terminal in Sample Problem 6, only Steps 9 through 13 are conducted. No other steps are necessary because only one ramp terminal is analyzed for a one-year period and the EB Method is not applied.

Step 9 – For the selected site, determine and apply the appropriate SPF.

For a ramp terminal, an SPF value for all crash types is determined. The SPF for fatal-and-injury crashes is calculated from Equation 19-31 and Table 19-17 as follows:

$$\begin{aligned}
 N_{spf, B2, ST, at, fi} &= \exp(a + b \times \ln[c \times AADT_{xrd}] + d \times \ln[c \times AADT_{ex} + c \times AADT_{en}]) \\
 &= \exp(-2.687 + 0.260 \times \ln[0.001 \times 14,000] + 0.947 \times \ln[0.001 \times 1,450 + 0.001 \times 1,300]) \\
 &= 0.352 \text{ crashes/year}
 \end{aligned}$$

Similarly, the SPF for property-damage-only crashes is calculated from Equation 19-31 and Table 19-17 to yield the following result:

$$N_{spf, B2, ST, at, pdo} = 0.881 \text{ crashes/year}$$

Step 10 – Multiply the result obtained in Step 9 by the appropriate CMFs.

Each CMF used in the calculation of the predicted average crash frequency of the ramp terminal is calculated in this step.

Exit Ramp Capacity (CMF_{10, B2, ST, at, fi})

CMF_{10, B2, ST, at, fi} is calculated from Equation 19-42 as follows:

$$CMF_{10, B2, ST, at, fi} = (1.0 - P_{ex}) \times 1.0 + P_{ex} \times \exp\left(a \times \frac{c \times AADT_{ex}}{n_{ex, eff}}\right)$$

For a stop-controlled exit-ramp right-turn movement, the effective number of lanes serving exit ramp traffic $n_{ex, eff}$ is computed using the second portion of Equation 19-43 as follows:

$$\begin{aligned} n_{ex, eff} &= 0.5 \times n_{ex} \\ &= 0.5 \times 2 \\ &= 1.0 \end{aligned}$$

The proportion of total leg AADT on the exit ramp leg P_{ex} is computed using Equation 19-44 as follows:

$$\begin{aligned} P_{ex} &= \frac{AADT_{ex}}{AADT_{in} + AADT_{out} + AADT_{en} + AADT_{ex}} \\ &= \frac{1,450}{14,000 + 14,000 + 1,300 + 1,450} \\ &= 0.047 \end{aligned}$$

From Table 19-32, $a = 0.151$ and $c = 0.001$ for one-way stop-controlled ramp terminals. CMF_{10, B2, ST, at, fi} is calculated as follows:

$$\begin{aligned} CMF_{10, B2, ST, at, fi} &= (1.0 - 0.047) \times 1.0 + 0.047 \times \exp\left(0.151 \times \frac{0.001 \times 1,450}{1.0}\right) \\ &= 1.012 \end{aligned}$$

Access Point Frequency (CMF_{13, B2, ST, at, fi})

The ramp terminal has no unsignalized public street approaches on the outside leg, which is the base condition for the access point frequency CMF. Hence, CMF_{13, B2, ST, at, fi} is equal to 1.000.

Segment Length (CMF_{14, B2, ST, at, fi})

CMF_{14, B2, ST, at, fi} is calculated from Equation 19-50 as follows:

$$CMF_{14, B2, ST, at, fi} = \exp\left(a \times \left[\frac{1.0}{L_{rmp}} + \frac{1.0}{L_{str}} - 0.333\right]\right)$$

From Table 19-36, $a = -0.0141$ for fatal-and-injury crashes. CMF_{14, B2, ST, at, fi} is calculated as follows:

$$\begin{aligned}
 CMF_{14, B2, ST, at, fi} &= \exp\left(-0.0141 \times \left[\frac{1.0}{0.15} + \frac{1.0}{1.0} - 0.333\right]\right) \\
 &= 0.902
 \end{aligned}$$

Median Width ($CMF_{15, B2, ST, at, fi}$)

The crossroad has a 12-ft median, which is the base condition for the median width CMF. Hence, $CMF_{15, B2, ST, at, fi}$ is equal to 1.000.

All-Way Stop Control (CMF_{awsc})

As stated in Section 19.10, the all-way stop control CMF, CMF_{awsc} , is equal to 0.686. It applies to fatal-and-injury crashes only.

Crashes

The CMFs are applied to the fatal-and-injury SPF as follows:

$$\begin{aligned}
 N_{p^*, B2, ST, at, fi} &= N_{spf, B2, ST, at, fi} \times \left(\begin{array}{l} CMF_{10, B2, ST, at, fi} \times CMF_{13, B2, ST, at, fi} \times \\ CMF_{14, B2, ST, at, fi} \times CMF_{15, B2, ST, at, fi} \times CMF_{awsc} \end{array} \right) \\
 &= 0.352 \times (1.012 \times 1.000 \times 0.902 \times 1.000 \times 0.686) \\
 &= 0.352 \times 0.626 \\
 &= 0.221 \text{ crashes/year}
 \end{aligned}$$

The CMFs are applied to the property-damage-only SPF as follows:

$$\begin{aligned}
 N_{p^*, B2, ST, at, pdo} &= N_{spf, B2, ST, at, pdo} \\
 &= 0.881 \text{ crashes/year}
 \end{aligned}$$

Step 11 – Multiply the result obtained in Step 10 by the appropriate calibration factor.

It is assumed that a calibration factor of 1.00 has been determined for local conditions. See Section B.1 of Appendix B to Part C for further discussion on calibration of the predicted models.

Calculation of Predicted Average Crash Frequency

The predicted average crash frequency is calculated using Equation 19-1 based on the results obtained in Steps 9 through 11 as follows.

Fatal-and-injury crashes:

$$\begin{aligned}
 N_{p, B2, ST, at, fi} &= N_{p^*, B2, ST, at, fi} \times C_{B2, ST, at, fi} \\
 &= 0.221 \times 1.00 \\
 &= 0.221 \text{ crashes/year}
 \end{aligned}$$

Property-damage-only crashes:

$$\begin{aligned}
 N_{p, B2, ST, at, pdo} &= N_{p^*, B2, ST, at, pdo} \times C_{B2, ST, at, pdo} \\
 &= 0.881 \times 1.00 \\
 &= 0.881 \text{ crashes/year}
 \end{aligned}$$

Step 12—If there is another year to be evaluated in the evaluation period for the selected site, return to Step 8. Otherwise, proceed to Step 13.

The study period is one year (2011), so steps 8 through 11 need not be repeated.

Step 13—Apply site-specific EB Method (if applicable) and apply SDFs.

This step consists of three optional sets of calculations—site-specific EB Method, severity distribution functions, and crash type distribution.

Apply the site-specific EB Method to a future time period, if appropriate.

The site-specific EB Method is not applied in this sample problem because crash data are not available.

Apply the severity distribution functions (SDFs), if desired.

To apply the SDFs, the systematic component of crash severity likelihood V_j is computed for each severity level j using Equation 19-88 as follows:

$$V_j = a + (b \times I_{p,lt}) + (c \times [n_{dw} + n_{ps}]) + (d \times I_{ps}) + (e \times I_{rural})$$

The coefficients a , b , c , d , and e are obtained from Table 19-44 for each severity level j . V_j is computed for fatal and incapacitating injury crashes as follows:

$$\begin{aligned} V_{K+A} &= -3.168 + (0.00 \times 0.0) + (0.00 \times [0.0 + 0.0]) + (0.00 \times 0.0) + (0.891 \times 0.0) \\ &= -3.168 \end{aligned}$$

Similar calculations using the coefficients from Table 19-44 for non-incapacitating injury crashes yield the following results:

$$V_B = -1.476$$

Using these computed V_{K+A} and V_B values, and assuming a calibration factor $C_{sdf, aS, x}$ of 1.0, the probability of occurrence of a fatal crash is computed using Equation 19-84 as follows:

$$\begin{aligned} P_{aS, ST, at, K} &= \frac{\exp(V_{K+A})}{\frac{1.0}{C_{sdf, aS, x}} + \exp(V_{K+A}) + \exp(V_B)} \times P_{K|K+A, aS, x, at} \\ &= \frac{\exp(-3.168)}{\frac{1.0}{1.0} + \exp(-3.168) + \exp(-1.476)} \times 0.160 \\ &= 0.005 \end{aligned}$$

Similar calculations using Equation 19-85 and Equation 19-86 yield the following results:

$$P_{aS, ST, at, A} = 0.028$$

$$P_{aS, ST, at, B} = 0.180$$

The probability of occurrence of a possible-injury crash is computed using Equation 19-87 as follows:

$$\begin{aligned}
 P_{aS,ST,at,C} &= 1.0 - (P_{aS,ST,at,K} + P_{aS,ST,at,A} + P_{aS,ST,at,B}) \\
 &= 1.0 - (0.005 + 0.028 + 0.180) \\
 &= 0.787
 \end{aligned}$$

The probability of occurrence of a fatal crash is multiplied by the fatal-and-injury crash frequency obtained in Step 11 using Equation 19-78 as follows:

$$\begin{aligned}
 N_{e,B2,ST,at,K} &= N_{e,B2,ST,at,fi} \times P_{aS,ST,at,K} \\
 &= 0.221 \times 0.005 \\
 &= 0.001 \text{ crashes/year}
 \end{aligned}$$

Similar calculations using Equation 19-78 and the probabilities of occurrences of the other crash severities yield the following results:

$$N_{e,B2,ST,at,A} = 0.006 \text{ crashes/year}$$

$$N_{e,B2,ST,at,B} = 0.040 \text{ crashes/year}$$

$$N_{e,B2,ST,at,C} = 0.174 \text{ crashes/year}$$

Apply the crash type distribution, if desired.

The crash type distributions are applied by multiplying the default crash type distribution proportions in Table 19-45 by the predicted average crash frequencies obtained in Step 11.

Worksheets

The step-by-step instructions are provided to illustrate the predictive method for calculating the predicted average crash frequency for a ramp terminal. To apply the predictive method steps to multiple terminals, a series of worksheets are provided for determining the predicted average crash frequency. The worksheets include:

- Table 19-68. Ramp Terminal Worksheet (1 of 4)—Sample Problem 6
- Table 19-69. Ramp Terminal Worksheet (2 of 4)—Sample Problem 6
- Table 19-70. Ramp Terminal Worksheet (3 of 4)—Sample Problem 6
- Table 19-71. Ramp Terminal Worksheet (4 of 4)—Sample Problem 6

Filled versions of these worksheets are provided below. Blank versions of worksheets used in the Sample Problems are provided in Appendix 19A.

Table 19-68 is a summary of general information about the ramp terminal, analysis, input data (i.e., “The Facts”), and assumptions for Sample Problem 6. The input data include area type, crash data, basic intersection data, alignment data, traffic control data, and cross section data.

Table 19-69 is a summary of general information about the ramp terminal, analysis, input data (i.e., “The Facts”), and assumptions for Sample Problem 6. The input data include cross section data, access data, and traffic data.

Table 19-70 is a tabulation of the CMF and SPF computations for Sample Problem 6.

Table 19-71 is a tabulation of the crash severity and crash type distributions for Sample Problem 6.

Table 19-68. Ramp Terminal Worksheet (1 of 4)—Sample Problem 6

General Information					Location Information				
Analyst					Roadway				
Agency or company					Intersection				
Date performed					Study year				
Area type		X	Urban		Rural				
Input Data									
Crash Data				Crash Period	Study Year	Complete the study year column. Complete the crash period column if the EB Method is used.			
Crash data time period						First year		Last year	
Count of FI crashes $N_{o, w, x, at, fi}^*$									
Count of PDO crashes $N_{o, w, x, at, pdo}^*$									
Basic Intersection Data									
Ramp terminal configuration				B2		Choices: D3ex, D3en, D4, A4, B4, A2, B2 Same choice for crash period and study year.			
Ramp terminal traffic control type				All-way stop		Choices: Signal, One-way-stop, All-way stop			
Presence of a non-ramp public street leg I_{ps}				Y/N	--	Y/N			
Alignment Data									
Exit ramp skew angle I_{sk} (degrees)					--				
Distance to the next public street intersection on the outside crossroad leg L_{str} (mi)					1.0				
Distance to the adjacent ramp terminal L_{rmp} (mi)					0.15				
Traffic Control									
Left-Turn Operational Mode									
Crossroad	Inside approach	Prot.-only mode $I_{p, lt, in}$		Y/N	--	Y/N			
	Outside approach	Prot.-only mode $I_{p, lt, out}$		Y/N	--	Y/N			
Right-Turn Control Type									
Ramp	Exit ramp approach	Right-turn control type		Stop	Choices: Signal, Stop, Yield, Merge, Free				
Cross Section Data									
Crossroad median width W_m (ft)					12				
Number of Lanes									
Crossroad	Inside approach	Through lanes $n_{th, in}$		2	Same choice for crash period and study year.				
	Outside approach	Through lanes $n_{th, out}$		2	Same choice for crash period and study year.				
Ramp	Exit ramp approach	All lanes n_{ex}		2	Same choice for crash period and study year.				
Right-Turn Channelization									
Crossroad	Inside approach	Chan. present $I_{ch, in}$		Y/N	--	Y/N			
	Outside approach	Chan. present $I_{ch, out}$		Y/N	--	Y/N			
Ramp	Exit ramp approach	Chan. present $I_{ch, ex}$		Y/N	--	Y/N			

Table 19-69. Ramp Terminal Worksheet (2 of 4)—Sample Problem 6

Input Data						
Cross Section Data		Crash Period	Study Year	Complete the study year column. Complete the crash period column if the EB Method is used.		
Left-Turn Lane or Bay						
Crossroad	Inside approach	Lane or bay present $I_{bay, lt, in}$	Y/N	--	Y/N	If Yes, then enter data in the next row.
		Lane or bay width $W_{b, in}$ (ft)		--		
	Outside approach	Lane or bay present $I_{bay, lt, out}$	Y/N	--	Y/N	If Yes, then enter data in the next row.
		Lane or bay width $W_{b, out}$ (ft)		--		
Right-Turn Lane or Bay						
Crossroad	Inside approach	Lane or bay present $I_{bay, rt, in}$	Y/N	--	Y/N	
	Outside approach	Lane or bay present $I_{bay, rt, out}$	Y/N	--	Y/N	
Access Data						
Number of driveways on the outside crossroad leg n_{dw}				--		
Number of public street approaches on the outside crossroad leg n_{ps}				--		
Traffic Data						
Crossroad	Inside leg	$AADT_{in}$ (veh/day)		14,000		
	Outside leg	$AADT_{out}$ (veh/day)		14,000		
Ramp	Exit ramp	$AADT_{ex}$ (veh/day)		1,450		
	Entrance ramp	$AADT_{en}$ (veh/day)		1,300		

Table 19-70. Ramp Terminal Worksheet (3 of 4)—Sample Problem 6

Crash Modification Factors

Complete the study year column. Complete the crash period column if the EB Method is used.	Equation	Fatal and Injury		Property Damage Only	
		Crash Period	Study Year	Crash Period	Study Year
Signal Control					
Exit ramp capacity $CMF_{10, w, SGn, at, fi}$	19-42	--	--		
Crossroad left-turn lane $CMF_{11, w, SGn, at, z}$	19-45	--	--	--	--
Crossroad right-turn lane $CMF_{12, w, SGn, at, z}$	19-48	--	--	--	--
Access point frequency $CMF_{13, w, SGn, at, z}$	19-49	--	--	--	--
Segment length $CMF_{14, w, SGn, at, z}$	19-50	--	--	--	--
Median width $CMF_{15, w, SGn, at, z}$	19-51	--	--	--	--
Protected left-turn operation $CMF_{16, w, SGn, at, z}$	19-53	--	--	--	--
Chan. right turn on crossroad $CMF_{17, w, SGn, at, z}$	19-55	--	--	--	--
Chan. right turn on exit ramp $CMF_{18, w, SGn, at, z}$	19-56	--	--	--	--
Non-ramp public street leg $CMF_{19, w, SGn, at, z}$	19-57	--	--	--	--

Stop Control

Exit ramp capacity $CMF_{10, w, ST, at, fi}$	19-42	--	1.012		
Crossroad left-turn lane $CMF_{11, w, ST, at, z}$	19-45	--	--	--	--
Crossroad right-turn lane $CMF_{12, w, ST, at, z}$	19-48	--	--	--	--
Access point frequency $CMF_{13, w, ST, at, fi}$	19-49	--	1.000		
Segment length $CMF_{14, w, ST, at, fi}$	19-50	--	0.902		
Median width $CMF_{15, w, ST, at, fi}$	19-51	--	1.000		
Skew angle $CMF_{20, w, ST, at, fi}$	19-58	--	--		
All-way stop-control (exclude $CMF_{11}, CMF_{12}, CMF_{20}$)		--	0.686		
Combined CMF (multiply all CMFs evaluated)		--	0.626	--	1.000

Expected Average Crash Frequency^a

Complete the study year column. Complete the crash period column if the <i>site-specific</i> EB Method is used.	Fatal and Injury		Property Damage Only	
	Crash Period	Study Year	Crash Period	Study Year
Calibration factor $C_{aS, x, at, z}$	1.00		1.00	
Overdispersion parameter $k_{w, x, at, z}$	--		--	
Observed crash count $N_{o, w, x, at, z}^*$ (cr)	--		--	
Reference year r	--		--	
Predicted average crash freq. for reference year $N_{p, w, x, at, z, r}$ (cr/yr)	--		--	
Predicted number of crashes for crash period (sum all years) $N_{p, w, x, y, z}^*$ (cr)	--		--	
Equivalent years associated with crash count $C_{b, w, x, at, z, r}$ (yr)	--		--	
Adjusted average crash freq. for ref. year given $N_{o, N_{a, w, x, at, z, r}}$ (cr/yr)	--		--	
Study year s		2011		2011
Predicted average crash freq. for study year $N_{p, w, x, at, z, s}$ (cr/yr)		0.221		0.881
Expected average crash freq. for study year $N_{e, w, x, at, z, s}$ (cr/yr)		0.221		0.881

Note: a – If the EB Method is not used, then substitute “predicted” for “expected” and substitute the subscript “p” for the subscript “e”.

Table 19-71. Ramp Terminal Worksheet (4 of 4)—Sample Problem 6

Expected Average Crash Frequency							
<i>Crash Severity Distribution</i>							
	K	A	B	C	Total FI	PDO	Total FI + PDO
Proportion by injury level	0.005	0.028	0.180	0.787	1.000		
Expected average crash freq. for study year $N_{e, w, x, at, z, s}$ (cr/yr)	0.001	0.006	0.040	0.174	0.221	0.881	1.102
<i>Crash Type Distribution</i>							
Crash Type Category	Table 19-16, 19-21, or 19-45	Fatal and Injury		Property Damage Only		Total	
		Proportion	Expected Average Crash Frequency for Study Year $N_{e, w, x, at, fi, s}$ (cr/yr)	Proportion	Expected Average Crash Frequency for Study Year $N_{e, w, x, at, pdo, s}$ (cr/yr)	Expected Average Crash Frequency for Study Year $N_{e, w, x, at, as, s}$ (cr/yr)	Expected Average Crash Frequency for Study Year $N_{e, w, x, at, as, s}$ (cr/yr)
Multiple-Vehicle Crashes							
Head-on		0.017	0.000	0.012	0.000	0.000	0.000
Right-angle		0.458	0.040	0.378	0.293	0.333	0.333
Rear-end		0.373	0.160	0.377	0.440	0.601	0.601
Sideswipe		0.025	0.000	0.079	0.000	0.000	0.000
Other multiple-vehicle crashes		0.017	0.000	0.016	0.000	0.000	0.000
Single-Vehicle Crashes							
Crash with animal		0.000	0.000	0.000	0.000	0.000	0.000
Crash with fixed object		0.085	0.000	0.110	0.147	0.147	0.147
Crash with other object		0.000	0.000	0.000	0.000	0.000	0.000
Crash with parked vehicle		0.000	0.000	0.008	0.000	0.000	0.000
Other single-vehicle crashes		0.025	0.020	0.020	0.000	0.020	0.020
Total		1.000	0.221	1.000	0.881	1.102	1.102

19.15. REFERENCES

- (1) Bonneson, J., S. Geedipally, M. Pratt, and D. Lord. *National Cooperative Highway Research Program Document XXX, Safety Prediction Methodology and Analysis Tool for Freeways and Interchanges*. (Web-Only). NCHRP, Transportation Research Board, Washington, D.C., 2012.
- (2) Harwood, D. W., M. T. Pietrucha, M. D. Wooldridge, R. E. Brydia, and K. Fitzpatrick. *NCHRP Report 375: Median Intersection Design*. National Cooperative Highway Research Association, Transportation Research Board, Washington, D.C., 1995.

APPENDIX 19A—WORKSHEETS FOR PREDICTIVE METHOD FOR RAMPS

Ramp Segment Worksheet (1 of 4)

General Information				Location Information			
Analyst				Roadway			
Agency or company				Roadway section			
Date performed				Study year			
Area type		Urban		Rural			

Input Data

Crash Data	Crash Period	Study Year	Complete the study year column. Complete the crash period column if the EB Method is used.			
Crash data time period			First year		Last year	
Count of multiple-vehicle FI crashes $N_{o, w, n, mv, fi}^*$						
Count of single-vehicle FI crashes $N_{o, w, n, sv, fi}^*$						
Count of multiple-vehicle PDO crashes $N_{o, w, n, mv, pdo}^*$						
Count of single-vehicle PDO crashes $N_{o, w, n, sv, pdo}^*$						

Basic Roadway Data

Number of through lanes n			Same value for crash period and study year.			
Segment length L (mi)						
Average traffic speed on the freeway V_{frwy} (mi/h)						
Segment type			Choices: Entrance, Exit, C-D road, Connector			
Type of control at crossroad ramp terminal			Choices: Stop, Yield, Signal, None			

Alignment Data

Horizontal Curve Data

1	Presence of horizontal curve 1			Choices: No, In segment, Off segment.		
	Curve radius R_1 (ft)			If “In segment” or “Off segment”, enter data for curve radius, length, and milepost.		
	Length of curve L_{c1} (mi)					
	Length of curve in segment $L_{c1, seg}$ (mi)					
	Milepost of beginning of curve in dir. of travel X_1 (mi)					
2	Presence of horizontal curve 2			Choices: No, In segment, Off segment		
	Curve radius R_2 (ft)			If “In segment” or “Off segment”, enter data for curve radius, length, and milepost.		
	Length of curve L_{c2} (mi)					
	Length of curve in segment $L_{c2, seg}$ (mi)					
	Milepost of beginning of curve in dir. of travel X_2 (mi)					
3	Presence of horizontal curve 3			Choices: No, In segment, Off segment		
	Curve radius R_3 (ft)			If “In segment” or “Off segment”, enter data for curve radius, length, and milepost.		
	Length of curve L_{c3} (mi)					
	Length of curve in segment $L_{c3, seg}$ (mi)					
	Milepost of beginning of curve in dir. of travel X_3 (mi)					
4	Presence of horizontal curve 4			Choices: No, In segment, Off segment		
	Curve radius R_4 (ft)			If “In segment” or “Off segment”, enter data for curve radius, length, and milepost.		
	Length of curve L_{c4} (mi)					
	Length of curve in segment $L_{c4, seg}$ (mi)					
	Milepost of beginning of curve in dir. of travel X_4 (mi)					

Ramp Segment Worksheet (2 of 4)

Input Data				
Cross Section Data		Crash Period	Study Year	Complete the study year column. Complete the crash period column if the EB Method is used.
Lane width W_l (ft)				
Right shoulder width W_{rs} (ft)				
Left shoulder width W_{ls} (ft)				
Presence of lane add or lane drop				Choices: No, Lane add, Lane drop
Length of taper in segment $L_{add, seg}$ or $L_{drop, seg}$ (mi)				If "Lane add" or "Lane drop", enter length.
Roadside Data				
Presence of barrier on right side of roadway			Y/N	Y/N
Presence of barrier on left side of roadway			Y/N	Y/N
Ramp Access Data				
Ramp Entrance				
Ent. ramp	Presence of speed-change lane in segment		Y/N	Y/N
	Length of s-c lane in segment $L_{en, seg}$ (mi)			
Exit ramp	Presence of speed-change lane in segment		Y/N	Y/N
	Length of s-c lane in segment $L_{ex, seg}$ (mi)			
Weave	Presence of a weaving section in segment		Y/N	Y/N
	Length of weaving section L_{wev} (mi)			
	Length of weaving section in seg. $L_{wev, seg}$ (mi)			
Traffic Data				
Segment AADT $AAADT_r$ or $AAADT_c$ (veh/day)				

Ramp Segment Worksheet (3 of 4)

Crash Modification Factors

Complete the study year column. Complete the crash period column if the EB Method is used.	Equation	Fatal and Injury				Property Damage Only			
		Multiple Vehicle		Single Vehicle		Multiple Vehicle		Single Vehicle	
		Crash Period	Study Year	Crash Period	Study Year	Crash Period	Study Year	Crash Period	Study Year
Horizontal curve $CMF_{1, w, x, y, z}$	14-33								
Lane width $CMF_{2, w, x, y, fi}$	14-34								
Right shoulder width $CMF_{3, w, x, y, z}$	14-35								
Left shoulder width $CMF_{4, w, x, y, z}$	14-36								
Right side barrier $CMF_{5, w, x, y, z}$	14-37								
Left side barrier $CMF_{6, w, x, y, z}$	14-38								
Lane add or drop $CMF_{7, w, x, y, fi}$	14-39								
Ramp speed-change lane $CMF_{8, w, x, mv, fi}$	14-40								
Weaving section $CMF_{9, cds, ac, y, z}$	14-41								
Combined CMF (multiply all CMFs evaluated)									

Expected Average Crash Frequency^a

Complete the study year column. Complete the crash period column if the <i>site-specific</i> EB Method is used.	Fatal and Injury				Property Damage Only			
	Multiple Vehicle		Single Vehicle		Multiple Vehicle		Single Vehicle	
	Crash Period	Study Year	Crash Period	Study Year	Crash Period	Study Year	Crash Period	Study Year
Calibration factor $C_{w, x, y, z}$								
Overdispersion parameter $k_{w, x, y, z}$								
Observed crash count $N_{o, w, x, y, z}^*$ (cr)								
Reference year r								
Predicted average crash freq. for reference year $N_{p, w, x, y, z, r}$ (cr/yr)								
Predicted number of crashes for crash period (sum all years) $N_{p, w, x, y, z}^*$ (cr)								
Equivalent years associated with crash count $C_{b, w, x, y, z, r}$ (yr)								
Adjusted average crash freq. for ref. year given $N_{o, w, x, y, z, r}^*$, $N_{a, w, x, y, z, r}$ (cr/yr)								
Study year s								
Predicted average crash freq. for study year $N_{p, w, x, y, z, s}$ (cr/yr)								
Expected average crash freq. for study year $N_{e, w, x, y, z, s}$ (cr/yr)								
Expected average crash freq. for study year (all crash types) $N_{e, w, x, at, z, s}$ (cr/yr)								

Note:

a – If the EB Method is not used, then substitute the word “predicted” for the word “expected” and substitute the subscript “p” for the subscript “e”.

Ramp Segment Worksheet (4 of 4)

Expected Average Crash Frequency^a

Crash Severity Distribution

	K	A	B	C	Total FI	PDO	Total FI + PDO
Proportion by injury level					1.000		
Expected average crash freq. for study year (all crash types) $N_{e, w, x, at, z, s}$ (cr/yr)							

Crash Type Distribution

Crash Type Category	Table	Fatal and Injury		Property Damage Only		Total
		Proportion	Expected Average Crash Frequency for Study Year $N_{e, w, x, y, fi, s}$ (cr/yr)	Proportion	Expected Average Crash Frequency for Study Year $N_{e, w, x, y, pdo, s}$ (cr/yr)	Expected Average Crash Frequency for Study Year $N_{e, w, x, y, as, s}$ (cr/yr)
Multiple-Vehicle Crashes	14-6					
Head-on						
Right-angle						
Rear-end						
Sideswipe						
Other multiple-vehicle crashes						
Total		1.000		1.000		
Single-Vehicle Crashes	14-9					
Crash with animal						
Crash with fixed object						
Crash with other object						
Crash with parked vehicle						
Other single-vehicle crashes						
Total		1.000		1.000		

Note:

a – If the EB Method is not used, then substitute the word “predicted” for the word “expected” and substitute the subscript “p” for the subscript “e”.

Ramp Barrier Worksheet

Input Data			
Segment length L (mi)		Crash period	Study year
Left shoulder width W_{ls} (ft)		Right shoulder width W_{rs} (ft)	
Individual Right Side Barrier Element Data			
Barrier Location	Length $L_{rb, i}$ (mi)	Width from Edge of Traveled Way to Face of Right Side Barrier $W_{off, r, i}$ (ft)	Ratio $L_{rb, i} / (W_{off, r, i} - W_{rs})$
1.			
2.			
3.			
4.			
5.			
6.			
7.			
	Sum1		Sum2
Individual Left Side Barrier Element Data			
Barrier Location	Length $L_{lb, i}$ (mi)	Width from Edge of Traveled Way to Face of Left Side Barrier $W_{off, l, i}$ (ft)	Ratio $L_{lb, i} / (W_{off, l, i} - W_{ls})$
1.			
2.			
3.			
4.			
5.			
6.			
7.			
	Sum3		Sum4
Right Side Barrier Calculations			
Proportion of segment length with barrier in median $P_{rb} = \text{Sum1} / L$		Width from edge of shoulder to barrier face $W_{rcb} = \text{Sum1} / \text{Sum2}$ (ft)	
Left Side Barrier Calculations			
Proportion of segment length with barrier in median $P_{lb} = \text{Sum3} / L$		Width from edge of shoulder to barrier face $W_{lcb} = \text{Sum3} / \text{Sum4}$ (ft)	

Ramp Terminal Worksheet (1 of 4)

General Information				Location Information			
Analyst				Roadway			
Agency or company				Intersection			
Date performed				Study year			
Area type		Urban		Rural			
Input Data							
Crash Data				Crash Period	Study Year	Complete the study year column. Complete the crash period column if the EB Method is used.	
Crash data time period						First year	Last year
Count of FI crashes $N_{o, w, x, at, fi}^*$							
Count of PDO crashes $N_{o, w, x, at, pdo}^*$							
Basic Intersection Data							
Ramp terminal configuration						Choices: D3ex, D3en, D4, A4, B4, A2, B2 Same choice for crash period and study year.	
Ramp terminal traffic control mode						Choices: Signal, One-way-stop, All-way stop	
Presence of a non-ramp public street leg I_{ps}				Y/N		Y/N	
Alignment Data							
Exit ramp skew angle I_{sk} (degrees)							
Distance to the next public street intersection on the outside crossroad leg L_{str} (mi)							
Distance to the adjacent ramp terminal L_{rmp} (mi)							
Traffic Control							
Left-Turn Operational Mode							
Crossroad	Inside approach	Prot.-only mode $I_{p, lt, in}$		Y/N		Y/N	
	Outside approach	Prot.-only mode $I_{p, lt, out}$		Y/N		Y/N	
Right-Turn Control Mode							
Ramp	Exit ramp approach	Right-turn control mode				Choices: Signal, Stop, Yield, Merge, Free	
Cross Section Data							
Crossroad median width W_m (ft)							
Number of Lanes							
Crossroad	Inside approach	Through lanes $n_{th, in}$				Same choice for crash period and study year.	
	Outside approach	Through lanes $n_{th, out}$				Same choice for crash period and study year.	
Ramp	Exit ramp approach	All lanes n_{ex}				Same choice for crash period and study year.	
Right-Turn Channelization							
Crossroad	Inside approach	Chan. present $I_{ch, in}$		Y/N		Y/N	
	Outside approach	Chan. present $I_{ch, out}$		Y/N		Y/N	
Ramp	Exit ramp approach	Chan. present $I_{ch, ex}$		Y/N		Y/N	

Ramp Terminal Worksheet (2 of 4)

Input Data

Cross Section Data	Crash Period	Study Year	Complete the study year column. Complete the crash period column if the EB Method is used.
---------------------------	---------------------	-------------------	--

Left-Turn Lane or Bay

Crossroad	Inside approach	Lane or bay present $I_{bay, lt, in}$	Y/N	Y/N	If Yes, then enter data in the next row.
		Lane or bay width $W_{b, in}$ (ft)			
	Outside approach	Lane or bay present $I_{bay, lt, out}$	Y/N	Y/N	If Yes, then enter data in the next row.
		Lane or bay width $W_{b, out}$ (ft)			

Right-Turn Lane or Bay

Crossroad	Inside approach	Lane or bay present $I_{bay, rt, in}$	Y/N	Y/N	
	Outside approach	Lane or bay present $I_{bay, rt, out}$	Y/N	Y/N	

Access Data

Number of driveways on the outside crossroad leg n_{dw}			
Number of public street approaches on the outside crossroad leg n_{ps}			

Traffic Data

Crossroad	Inside leg	$AADT_{in}$ (veh/day)			
	Outside leg	$AADT_{out}$ (veh/day)			
Ramp	Exit ramp	$AADT_{ex}$ (veh/day)			
	Entrance ramp	$AADT_{en}$ (veh/day)			

Ramp Terminal Worksheet (3 of 4)

Crash Modification Factors

Complete the study year column. Complete the crash period column if the EB Method is used.	Equation	Fatal and Injury		Property Damage Only	
		Crash Period	Study Year	Crash Period	Study Year
Signal Control					
Exit ramp capacity $CMF_{10, w, SGn, at, fi}$	14-42				
Crossroad left-turn lane $CMF_{11, w, SGn, at, z}$	14-45				
Crossroad right-turn lane $CMF_{12, w, SGn, at, z}$	14-48				
Access point frequency $CMF_{13, w, SGn, at, z}$	14-49				
Segment length $CMF_{14, w, SGn, at, z}$	14-50				
Median width $CMF_{15, w, SGn, at, z}$	14-51				
Protected left-turn operation $CMF_{16, w, SGn, at, z}$	14-53				
Chan. right turn on crossroad $CMF_{17, w, SGn, at, z}$	14-55				
Chan. right turn on exit ramp $CMF_{18, w, SGn, at, z}$	14-56				
Non-ramp public street leg $CMF_{19, w, SGn, at, z}$	14-57				

Stop Control

Exit ramp capacity $CMF_{10, w, ST, at, fi}$	14-42				
Crossroad left-turn lane $CMF_{11, w, ST, at, z}$	14-45				
Crossroad right-turn lane $CMF_{12, w, ST, at, z}$	14-48				
Access point frequency $CMF_{13, w, ST, at, fi}$	14-49				
Segment length $CMF_{14, w, ST, at, fi}$	14-50				
Median width $CMF_{15, w, ST, at, fi}$	14-51				
Skew angle $CMF_{20, w, ST, at, fi}$	14-58				
All-way stop-control (exclude $CMF_{11}, CMF_{12}, CMF_{20}$)					
Combined CMF (multiply all CMFs evaluated)					

Expected Average Crash Frequency^a

Complete the study year column. Complete the crash period column if the <i>site-specific</i> EB Method is used.	Fatal and Injury		Property Damage Only	
	Crash Period	Study Year	Crash Period	Study Year
Calibration factor $C_{aS, x, at, z}$				
Overdispersion parameter $k_{w, x, at, z}$				
Observed crash count $N_{o, w, x, at, z}^*$ (cr)				
Reference year r				
Predicted average crash freq. for reference year $N_{p, w, x, at, z, r}$ (cr/yr)				
Predicted number of crashes for crash period (sum all years) $N_{p, w, x, y, z}^*$ (cr)				
Equivalent years associated with crash count $C_{b, w, x, at, z, r}$ (yr)				
Adjusted average crash freq. for ref. year given $N_{o, N_{a, w, x, at, z, r}}^*$ (cr/yr)				
Study year s				
Predicted average crash freq. for study year $N_{p, w, x, at, z, s}$ (cr/yr)				
Expected average crash freq. for study year $N_{e, w, x, at, z, s}$ (cr/yr)				

Note:

a – If the EB Method is not used, then substitute the word “predicted” for the word “expected” and substitute the subscript “p” for the subscript “e”.

Ramp Terminal Worksheet (4 of 4)

Expected Average Crash Frequency^a

Crash Severity Distribution

	K	A	B	C	Total FI	PDO	Total FI + PDO
Proportion by injury level					1.000		
Expected average crash freq. for study year $N_{e, w, x, at, z, s}$ (cr/yr)							

Crash Type Distribution

Crash Type Category	Table 14-16, 14-21, or 14-45	Fatal and Injury		Property Damage Only		Total
		Proportion	Expected Average Crash Frequency for Study Year $N_{e, w, x, at, fi, s}$ (cr/yr)	Proportion	Expected Average Crash Frequency for Study Year $N_{e, w, x, at, pdo, s}$ (cr/yr)	Expected Average Crash Frequency for Study Year $N_{e, w, x, at, as, s}$ (cr/yr)
Multiple-Vehicle Crashes						
Head-on						
Right-angle						
Rear-end						
Sideswipe						
Other multiple-vehicle crashes						
Single-Vehicle Crashes						
Crash with animal						
Crash with fixed object						
Crash with other object						
Crash with parked vehicle						
Other single-vehicle crashes						
Total		1.000		1.000		

Note:

a – If the EB Method is not used, then substitute the word “predicted” for the word “expected” and substitute the subscript “p” for the subscript “e”.

APPENDIX E

PROPOSED HSM APPENDIX B FOR PART C

APPENDIX B—SPECIALIZED PROCEDURES COMMON TO CHAPTERS 18 AND 19

TABLE OF CONTENTS

List of Figures.....	ii
List of Tables.....	ii
B.1. Calibration of the Chapter 18 and 19 Predictive Models.....	1
B.1.1. Calibration of Predictive Models.....	1
B.1.2. Development of Jurisdiction-Specific Safety Performance Functions for Use in the Predictive Method.....	8
B.1.3. Replacement of Selected Default Values in the Predictive Methods.....	9
B.1.4. Calibration of Severity Distribution Functions.....	12
B.2. The Empirical Bayes Method.....	15
B.2.1. Determine whether the EB Method is Applicable.....	15
B.2.2. Determine whether Observed Crash Data are Available for the Project and, if so, Obtain those Data.....	16
B.2.3. Assign Crashes to Individual Sites for Use in the EB Method.....	19
B.2.4. Apply the Site-Specific EB Method.....	20
B.2.5. Apply the Project-Level EB Method.....	22
B.2.6. Estimate the Expected Average Crash Frequency for a Future Time Period.....	26
B.2.7. EB Method for Segments with an Odd Number of Lanes.....	29
B.3. References.....	31

LIST OF FIGURES

Figure B-1. Determination of the Appropriate Variation of the EB Method 17

Figure B-2. Definition of Freeway Segments and Speed-Change Lanes 19

LIST OF TABLES

Table B-1. Predictive Models in Chapters 18 and 19 that Need Calibration 3

Table B-2. Data Needs for Calibration of Chapter 18 and 19 Predictive Models 5

Table B-3. Crash Distributions in Chapter 18 and 19 Predictive Models That May Be Calibrated to Local Conditions 10

Appendix B—Specialized Procedures Common to Chapters 18 and 19

This appendix describes two specialized procedures intended for use with the predictive method presented in Chapters 18 and 19. The first procedure is used to calibrate the predictive models in Chapters 18 and 19 to local conditions. The second procedure is the empirical Bayes (EB) Method for combining observed crash frequencies with the estimate provided by the predictive models in Chapters 18 and 19. Both of these procedures are an integral part of the predictive method in Chapters 18 and 19, and are presented in this appendix only to avoid repetition across the chapters.

B.1. CALIBRATION OF THE CHAPTER 18 AND 19 PREDICTIVE MODELS

The predictive models in each of Chapters 18 and 19 consist of safety performance functions (SPFs), crash modification factors (CMFs), and a calibration factor. Each model is developed for a specific site type (i.e., segment or intersection).

The predictive models were developed from the most complete and consistent data sets available. However, the general level of crash frequencies may vary substantially from one jurisdiction to another for a variety of reasons including climate, driver populations, animal populations, crash reporting thresholds, and crash reporting system procedures. Therefore, for these predictive models to provide results that are meaningful and accurate for each jurisdiction, it is important that they be calibrated for application in the jurisdiction in which they are applied. A procedure for determining the calibration factors for the predictive models is presented in Section B.1.1.

Some HSM users may prefer to develop SPFs with data from their jurisdiction for use in the predictive models rather than calibrating the existing SPFs. Calibration of the SPFs in Chapters 18 and 19 will provide satisfactory results. However, SPFs developed directly with data for a specific jurisdiction may provide more reliable estimates for that jurisdiction than calibration of the existing SPFs. Guidance is presented in Section B.1.2 on the development of jurisdiction-specific SPFs that are suitable for use in Chapter 18 and 19.

The predictive method in each of Chapters 18 and 19 consists of a set of predictive models, default distributions, and severity distribution functions (SDFs). Most of the regression coefficients and distribution values used in the predictive methods have been determined through research. Therefore, modification of the regression coefficients is not recommended. However, a few specific quantities, such as the distribution of crashes by collision type, can vary substantially from jurisdiction to jurisdiction. Where local data are available, users are encouraged to replace these default values with locally derived values. A procedure for deriving jurisdiction-specific distribution values is presented in Section B.1.3. A procedure for calibrating the SDFs is described in Section B.1.4.

B.1.1. Calibration of Predictive Models

The calibration procedure is used to derive the value of the calibration factor that is included in each predictive model. A calibration factor represents the ratio of the total observed number of crashes for a selected set of sites to the total predicted number of crashes for the same sites, during the same time period, using the applicable predictive model. Thus, the nominal value of the calibration factor is 1.00 when the

observed and predicted number of crashes happen to be equal. When there are more crashes observed than are predicted by the predictive model, the computed calibration factor will be greater than 1.00. When there are fewer crashes observed than are predicted by the predictive model, the computed calibration factor will be less than 1.00.

It is recommended that new values of the calibration factors be derived at least every two to three years, and some HSM users may prefer to develop calibration factors on an annual basis. The calibration factor for the most recent available period is to be used for all assessment of proposed future projects. If available, calibration factors for the specific time periods included in the evaluation period are to be used in effectiveness evaluations that use the procedures presented in Chapter 9.

If the procedure in Section B.1.3 is used to calibrate a default distribution, then the locally-calibrated values should be used in the calibration process described in this section.

The calibration procedure involves five steps. Each step is described in the following five subsections.

B.1.1.1. Step 1—Identify the predictive models to be calibrated.

Calibration is performed separately for each predictive model described in Chapters 18 and 19. Table B-1 identifies the combinations of site type and cross section or control type represented in each predictive model and for which calibration factors can be derived. The models of interest are identified by the user in this step.

Table B-1. Predictive Models in Chapters 18 and 19 that Need Calibration

Site Type and Cross Section or Control Type	Calibration Factor	
	Symbol	Equation Number
ROADWAY SEGMENTS		
Freeways		
Multiple-vehicle fatal-and-injury crashes, all cross sections	$C_{fs, ac, mv, fi}$	18-3
Multiple-vehicle property-damage-only crashes, all cross sections	$C_{fs, ac, mv, pdo}$	18-5
Single-vehicle fatal-and-injury crashes, all cross sections	$C_{fs, ac, sv, fi}$	18-4
Single-vehicle property-damage-only crashes, all cross sections	$C_{fs, ac, sv, pdo}$	18-6
Ramps		
Entrance ramp, multiple-vehicle fatal-and-injury crashes, all lanes	$C_{rps, EN, mv, fi}$	19-3
Entrance ramp, multiple-vehicle property-damage-only crashes, all lanes	$C_{rps, EN, mv, pdo}$	19-5
Entrance ramp, single-vehicle fatal-and-injury crashes, all lanes	$C_{rps, EN, sv, fi}$	19-4
Entrance ramp, single-vehicle property-damage-only crashes, all lanes	$C_{rps, EN, sv, pdo}$	19-6
Exit ramp, multiple-vehicle fatal-and-injury crashes, all lanes	$C_{rps, EX, mv, fi}$	not shown
Exit ramp, multiple-vehicle property-damage-only crashes, all lanes	$C_{rps, EX, mv, pdo}$	not shown
Exit ramp, single-vehicle fatal-and-injury crashes, all lanes	$C_{rps, EX, sv, fi}$	not shown
Exit ramp, single-vehicle property-damage-only crashes, all lanes	$C_{rps, EX, sv, pdo}$	not shown
C-D road, multiple-vehicle fatal-and-injury crashes, all cross sections	$C_{cds, ac, mv, fi}$	19-8
C-D road, multiple-vehicle property-damage-only crashes, all cross sections	$C_{cds, ac, mv, pdo}$	19-10
C-D road, single-vehicle fatal-and-injury crashes, all cross sections	$C_{cds, ac, sv, fi}$	19-9
C-D road, single-vehicle property-damage-only crashes, all cross sections	$C_{cds, ac, sv, pdo}$	19-11
INTERSECTIONS		
Freeway Speed-Change Lanes		
Ramp entrance speed-change lane, fatal-and-injury crashes of all types	$C_{sc, EN, at, fi}$	18-8
Ramp entrance speed-change lane, property-damage-only crashes of all types	$C_{sc, EN, at, pdo}$	18-9
Ramp exit speed-change lane, fatal-and-injury crashes of all types	$C_{sc, EX, at, fi}$	18-11
Ramp exit speed-change lane, property-damage-only crashes of all types	$C_{sc, EX, at, pdo}$	18-12
Crossroad Ramp Terminals		
One-way stop control, fatal-and-injury crashes of all types	$C_{aS, ST, at, fi}$	19-13
One-way stop control, property-damage-only crashes of all types	$C_{aS, ST, at, pdo}$	19-14
Signal control, fatal-and-injury crashes of all types	$C_{aS, SG, at, fi}$	19-16
Signal control, property-damage-only crashes of all types	$C_{aS, SG, at, pdo}$	19-17

Also established in this step is the calibration period. A calibration period longer than three years is not recommended because the expected average crash frequency is likely to change over time. The calibration period should have a duration that is a multiple of 12 months to avoid seasonal effects. For ease of application, it is recommended that the calibration periods consist of one, two, or three full calendar years. It is recommended to use the same calibration period for all sites, but exceptions may be made where necessary.

B.1.1.2. Step 2—Select sites for calibration of the predictive model.

Calibration sites are selected during this step. One set of calibration sites is assembled for each predictive model identified in Step 1. A given site may be included in more than one set *provided* that all sites in the set are consistent with the model's calibration factor characteristics (as listed in Table B-1). It is desirable that these sites be reasonably representative of the range of site characteristics to which the predictive model will be applied. However, no formal stratification by traffic volume or other site characteristics is needed in selecting the calibration sites. As such, the sites can be selected in a manner to make the data collection needed for Step 3 as efficient as practical.

Each calibration site should be selected without regard to the number of crashes reported during the calibration period. In other words, calibration sites should not be selected to intentionally limit the calibration database to include only sites with either high or low crash frequencies. Where practical, this may be accomplished by selecting calibration sites randomly from a larger set of candidate sites.

The desirable minimum sample size for the calibration database for one predictive model is 30 to 50 sites. For segments, each site should be between 0.1 and 1.0 mi in length. Lengths in this range should be long enough to have statistical validity and short enough to be realistically homogeneous.

For large jurisdictions, such as entire states, with a variety of topographical and climate conditions, it may be desirable to assemble a separate set of calibration sites representing two or three different conditions. In this manner, separate calibration factors are developed for each specific terrain type or geographical region for a given predictive model. For example, a state with distinct plains and mountain regions (or with distinct dry and wet regions), might choose to develop separate calibration factors for those regions. Where separate calibration factors are developed by terrain type or region, this needs to be done consistently for all predictive models applicable to those regions.

B.1.1.3. Step 3—Obtain data for each set of calibration sites for the calibration period.

This step is repeated for each predictive model identified in Step 1 and its associated set of calibration sites assembled in Step 2. For this step, a calibration database is assembled for each set of calibration sites. The calibration data are assembled for a common calibration period for all sites. The calibration database should include the following information for each site represented in the database:

- All target crashes that are reported during the calibration period.
- Site characteristics data needed to apply the predictive model for the same calibration period.

Target crashes are those crashes that are consistent with the predictive model being calibrated. For example, if the predictive model is applicable to multiple-vehicle fatal-and-injury crashes on freeway segments, then the target crashes are multiple-vehicle fatal-and-injury crashes on freeway segments.

For a given site type, the calibration database should include at least 100 target crashes per year. If this minimum is not realized then additional sites should be added to the database following the guidelines in Step 2.

The crash data used for calibration should include all crashes related to each site selected for the calibration database. Crashes should be assigned to specific sites based on the guidelines presented in Section B.2.3.

Table B-2 identifies the site characteristics data that are needed to apply the predictive models. The table classifies each data element as either required or desirable for the calibration procedure. Data for each of the required elements are needed for calibration. For the desirable data elements, it is recommended that actual data be used if available. Assumptions are offered in the table when these data are not available.

Table B-2. Data Needs for Calibration of Chapter 18 and 19 Predictive Models

Chapter	Data Element	Data Need		
		Required	Desirable	Default Assumption
ROADWAY SEGMENTS				
18—Freeways	Area type (rural or urban)	X		Need actual data
	Number of through lanes	X		Need actual data
	Segment length	X		Need actual data
	Length and radii of horizontal curves	X		Need actual data
	Lane width	X		Need actual data
	Inside and outside shoulder width	X		Need actual data
	Median width	X		Need actual data
	Length of rumble strips on inside and outside shoulders		X	Base default on agency policy
	Length of (and offset to) median barrier	X		Need actual data
	Length of (and offset to) outside barrier	X		Need actual data
	Clear zone width		X	Base default on agency policy
	AADT volume of (and distance to) nearest upstream entrance ramp	X		Need actual data
	AADT volume of (and distance to) nearest downstream exit ramp	X		Need actual data
	Presence of speed-change lane	X		Need actual data
	Presence and length of Type B weaving sections	X		Need actual data
Proportion of AADT that occurs during hours where lane volume exceeds 1,000 veh/h/ln		X	Equation for computing default is in Chapter 18, Section 18.4	
Average annual daily traffic (AADT) volume	X		Need actual data	

Table B-2. Data Needs for Calibration of Chapter 18 and 19 Predictive Models *continued*

Chapter	Data Element	Data Need		
		Required	Desirable	Default Assumption
ROADWAY SEGMENTS				
<i>For ramps and collector-distributor (C-D) roads:</i>				
19—Ramps	Area type (rural or urban)	X		Need actual data
	Number of through lanes	X		Need actual data
	Segment length	X		Need actual data
	Average annual daily traffic (AADT) volume	X		Need actual data
	Length and radii of horizontal curves	X		Need actual data
	Lane width	X		Need actual data
	Left and right shoulder width	X		Need actual data
	Length of (and offset to) right side barrier	X		Need actual data
	Length of (and offset to) left side barrier	X		Need actual data
	Presence of lane add or drop		X	Assume not present
Presence of speed-change lane	X		Need actual data	
<i>For C-D roads only:</i>				
	Presence and length of weaving section	X		Need actual data
INTERSECTIONS				
<i>For freeway speed-change lanes:</i>				
18—Freeways	Area type (rural or urban)	X		Need actual data
	Number of through lanes	X		Need actual data
	Segment length	X		Need actual data
	Length and radii of horizontal curves	X		Need actual data
	Lane width	X		Need actual data
	Inside shoulder width	X		Need actual data
	Median width	X		Need actual data
	Presence of rumble strips on inside shoulder		X	Base default on agency policy
	Length of (and offset to) median barrier	X		Need actual data
	AADT volume of ramp in speed-change lane	X		Need actual data
	Presence and length of Type B weaving sections	X		Need actual data
	Proportion of AADT that occurs during hours where lane volume exceeds 1,000 veh/h/ln		X	Equation for computing default is in Chapter 18, Section 18.4
	AADT of freeway adjacent to speed-change lane	X		Need actual data

Table B-2. Data Needs for Calibration of Chapter 18 and 19 Predictive Models *continued*

Chapter	Data Element	Data Need		
		Required	Desirable	Default Assumption
INTERSECTIONS				
<i>For all crossroad ramp terminals:</i>				
	Area type (rural or urban)	X		Need actual data
	Ramp terminal configuration	X		Need actual data
	Type of traffic control	X		Need actual data
	Control for exit ramp right-turn movement	X		Need actual data
	AADT for inside and outside crossroad legs	X		Need actual data
	AADT volume for each ramp leg	X		Need actual data
	Number of through lanes on each crossroad approach	X		Need actual data
	Number of lanes on the exit ramp	X		Need actual data
	Nbr. of crossroad approaches with left-turn lanes	X		Need actual data
	Nbr. of crossroad approaches with right-turn lanes	X		Need actual data
	Number of unsignalized public street approaches to the crossroad leg outside of the interchange		X	Assume no public street approaches present
19— Ramps	Distance to next public street intersection		X	Assume 0.15 mi for urban areas, assume 0.20 mi for rural areas
	Distance to adjacent crossroad ramp terminal		X	Based default on terminal configuration and area type ^a
	Crossroad median width and left-turn lane width	X		Need actual data
<i>For signal-controlled crossroad ramp terminals only:</i>				
	Number of unsignalized driveways on the crossroad leg outside of the interchange		X	Assume no driveways present
	Number of crossroad approaches with protected-only left-turn operation	X		Need actual data
	Number of crossroad approaches with right-turn channelization	X		Need actual data
	Presence of exit ramp right-turn channelization	X		Need actual data
	Presence of a non-ramp public street leg		X	Assume leg not present
<i>For one-way stop-controlled crossroad ramp terminals only:</i>				
	Skew angle	X		Need actual data

Note:

^a Default values by crossroad ramp terminal configuration and area type. Urban areas: $A2 = 0.17$ mi, $A4 = 0.17$ mi, $B2 = 0.19$ mi, $B4 = 0.19$ mi, $D3 = 0.13$ mi, $D4 = 0.11$ mi. Rural areas: $A2 = 0.20$ mi, $A4 = 0.20$ mi, $B2 = 0.22$ mi, $B4 = 0.22$ mi, $D3 = 0.16$ mi, $D4 = 0.17$ mi. Crossroad ramp terminal configurations are shown in Chapter 19, Figure 19-1.

If data for some required elements are not readily available, it may be possible to select sites in Step 2 for which these data are available. For example, in calibrating the predictive models for freeway segments, if data on the radii of horizontal curves are not readily available, the calibration data set could be limited to tangent freeways. Decisions of this type should be made, as needed, to keep the effort required to assemble the calibration data set within reasonable bounds.

B.1.1.4. Step 4—Apply the applicable predictive method to estimate the predicted average crash frequency for each site during the calibration period as a whole.

This step is repeated for each predictive model identified in Step 1 and its associated set of calibration sites assembled in Step 2. The site characteristics data assembled in Step 3 are used to apply the applicable predictive method to each site in the set of calibration sites. For this application, the predictive model should be applied without using the EB Method and without employing a calibration factor (i.e., a calibration factor of 1.00 is assumed). Through this process, the predicted average crash frequency is obtained for each site in the set of calibration sites, and for each year in the calibration period.

B.1.1.5. Step 5—Compute calibration factors for use in the predictive models.

The final step is to compute the calibration factor using the following equation. The appropriate subscripts for this equation are identified in Table B-1 for each predictive model.

$$C_{w,x,y,z} = \frac{\sum_{i=1}^{\text{all sites}} \sum_{j=1}^{n_c} N_{o,w(i),x(i),y,z,j}}{\sum_{i=1}^{\text{all sites}} \sum_{j=1}^{n_c} N_{p,w(i),x(i),y,z,j}} \quad \text{Equation B-1}$$

Where:

- $C_{w,x,y,z}$ = calibration factor to adjust SPF for local conditions for site type w , cross section or control type x , crash type y , and severity z ;
- $N_{o,w(i),x(i),y,z,j}$ = observed crash frequency for site i with site type $w(i)$ and year j (includes cross section or control type $x(i)$ for crash type y , and severity z) (crashes/yr);
- $N_{p,w(i),x(i),y,z,j}$ = predicted average crash frequency for site i with site type $w(i)$ and year j (includes cross section or control type $x(i)$ for crash type y , and severity z) (crashes/yr); and
- n_c = number of years in the crash period (yr).

The computation is performed separately for each predictive model identified in Step 1. The computed calibration factor is rounded to two decimal places for application in the appropriate predictive model.

B.1.2. Development of Jurisdiction-Specific Safety Performance Functions for Use in the Predictive Method

Satisfactory results from the Chapter 18 and 19 predictive methods can be obtained by calibrating the predictive model for each predictive model, as explained in Section B.1.1. However, some users may prefer to develop jurisdiction-specific SPFs using their agency's own data because these SPFs are likely to enhance the reliability of the predictive method. While there is no requirement that this be done, HSM users are welcome to use local data to develop their own SPFs.

Within the first two to three years after a jurisdiction-specific SPF is developed, calibration of the jurisdiction-specific SPF may not be necessary, particularly if other default values in the predictive models were also replaced with locally-derived values, as explained in Section B.1.3.

If jurisdiction-specific SPFs are used in a predictive method, they need to be developed with methods that are statistically valid and developed in such a manner that they fit into the applicable predictive method. The following guidelines for development of jurisdiction-specific SPFs that are acceptable for use in Chapters 18 and 19 include:

- In preparing the crash data to be used for development of jurisdiction-specific SPFs, crashes are assigned to roadway segments and intersections following the definitions explained in Section B.2.3.
- The jurisdiction-specific SPF should be developed with a statistical technique (such as negative binomial regression) that accounts for the overdispersion typically found in crash data, and quantifies an overdispersion parameter.
- The jurisdiction-specific SPF should use the same base conditions as the corresponding SPF in Chapter 18 or 19, or should be capable of being converted to those base conditions.
- The jurisdiction-specific SPF should include the effects of traffic volume. For segments, the average annual daily traffic volume is included. For intersections, the major- and minor-road average annual daily traffic volumes are included.
- The jurisdiction-specific SPF for any roadway segment facility type should have a functional form in which predicted average crash frequency is directly proportional to segment length.

These guidelines are not intended to stifle creativity and innovation in model development. However, a model that does not account for overdispersed data or that cannot be integrated with the rest of the predictive method will not be useful.

Two types of data sets may be used for SPF development. First, SPFs may be developed using only data that represent the base conditions, which are defined for each SPF in Chapters 18 and 19. Second, it is also acceptable to develop models using data for a broader set of conditions than the base conditions. In this approach, all variables that are part of the applicable base-condition definition, but have non-base-condition values, should be included in an initial model. Then, the initial model should be made applicable to the base conditions by substituting values that correspond to those base conditions into the model.

B.1.3. Replacement of Selected Default Values in the Predictive Methods

Table B-3 identifies the specific distributions used in the Chapter 18 and 19 predictive methods. The default distribution values provided in these tables were developed from the most complete and consistent databases available. If desired, these default values may be replaced with locally derived values. This replacement is optional, but it may yield more reliable results.

Any replacement values derived with the procedures presented in this section should be incorporated in the predictive models before the calibration described in Section B.1.1 is performed.

Table B-3. Crash Distributions in Chapter 18 and 19 Predictive Models That May Be Calibrated to Local Conditions

Chapter	Table or Equation Number	Site Type		Distribution That May Be Calibrated to Local Conditions
		Roadway Segments	Intersections	
18—Freeways	Table 18-6	X		Crash type for multiple-vehicle crashes
	Table 18-8	X		Crash type for single-vehicle crashes
	Table 18-10		X	Crash type for ramp-entrance-related crashes
	Table 18-12		X	Crash type for ramp-exit-related crashes
19—Ramps	Table 19-6	X		Crash type for multiple-vehicle crashes
	Table 19-9	X		Crash type for single-vehicle crashes
	Table 19-16		X	Crash type for signal-controlled ramp terminal crashes
	Table 19-21		X	Crash type for one-way stop-controlled ramp terminal crashes
	Table 19-45		X	Crash type for all-way stop-controlled ramp terminal crashes

B.1.3.1. Replacement of Default Values for Freeways

Four default distributions for freeways may be updated with locally-derived replacement values. Procedures to develop each of these replacement values are described in the following subsections.

Crash Type for Multiple-Vehicle Crashes

Table 18-6 presents the distribution of multiple-vehicle crashes by crash type for freeway segments. The distribution is categorized by two crash severity levels and two area types. If sufficient data are available, the values in Table 18-6 may be updated. This table represents a joint distribution of two variables for each area type. Therefore, for a given area type, sufficient data for calibrating the distribution requires a set of freeway segments that have collectively experienced at least 200 multiple-vehicle crashes during a recent one- to three-year period (i.e., 200 crashes in the entire time period).

Crash Type for Single-Vehicle Crashes

Table 18-8 presents the distribution of single-vehicle crashes by crash type for freeway segments. The distribution is categorized by two crash severity levels and two area types. If sufficient data are available, the values in Table 18-8 may be updated. This table represents a joint distribution of two variables for each area type. Therefore, for a given area type, sufficient data for calibrating the distribution requires a set of freeway segments that have collectively experienced at least 200 single-vehicle crashes during a recent one- to three-year period (i.e., 200 crashes in the entire time period).

Crash Type for Ramp-Entrance-Related Crashes

Table 18-10 presents the distribution of ramp-entrance-related crashes by crash type for freeway ramp entrances (and adjacent freeway lanes). The distribution is based on ramp-entrance speed-change lane crashes. It does not include crashes associated with a ramp entrance that adds a lane to the cross section. The distribution is categorized by two crash severity levels and two area types. If sufficient data are available, the values in Table 18-10 may be updated. This table represents a joint distribution of two variables for each area

type. Therefore, for a given area type, sufficient data for calibrating the distribution requires a set of ramp entrances (and adjacent freeway lanes) that have collectively experienced at least 200 crashes during a recent one- to three-year period (i.e., 200 crashes in the entire time period).

Crash Type for Ramp-Exit-Related Crashes

Table 18-12 presents the distribution of ramp-exit-related crashes by crash type for freeway ramp exits (and adjacent freeway lanes). The distribution is based on ramp-exit speed-change lane crashes. It does not include crashes associated with a ramp exit that drops a lane from the cross section. The distribution is categorized by two crash severity levels and two area types. If sufficient data are available, the values in Table 18-12 may be updated. This table represents a joint distribution of two variables for each area type. Therefore, for a given area type, sufficient data for calibrating the distribution requires a set of ramp exits (and adjacent freeway lanes) that have collectively experienced at least 200 crashes during a recent one- to three-year period (i.e., 200 crashes in the entire time period).

B.1.3.2. Replacement of Default Values for Ramps

Five default distributions for ramps may be updated with locally-derived replacement values. Procedures to develop each of these replacement values are described in the following subsections.

Crash Type for Multiple-Vehicle Crashes

Table 19-6 presents the distribution of multiple-vehicle crashes by crash type for ramp and C-D road segments. The distribution is categorized by two crash severity levels. If sufficient data are available, the values in Table 19-6 may be updated. Sufficient data for calibrating the distribution requires a set of ramp and C-D road segments that have collectively experienced at least 200 multiple-vehicle crashes during a recent one- to three-year period (i.e., 200 crashes in the entire time period).

Crash Type for Single-Vehicle Crashes

Table 19-9 presents the distribution of single-vehicle crashes by crash type for ramp and C-D road segments. The distribution is categorized by two crash severity levels and two area types. If sufficient data are available, the values in Table 19-9 may be updated. This table represents a joint distribution of two variables for each area type. Therefore, for a given area type, sufficient data for calibrating the distribution requires a set of ramp and C-D road segments that have collectively experienced at least 200 single-vehicle crashes during a recent one- to three-year period (i.e., 200 crashes in the entire time period).

Crash Type for Signal-Controlled Ramp Terminal Crashes

Table 19-16 presents the distribution of intersection-related crashes by crash type for signal-controlled crossroad ramp terminals. The distribution is categorized by two crash severity levels and two area types. If sufficient data are available, the values in Table 19-16 may be updated. This table represents a joint distribution of two variables for each area type. Therefore, for a given area type, sufficient data for calibrating the distribution requires a set of signal-controlled ramp terminals that have collectively experienced at least 200 intersection-related crashes during a recent one- to three-year period (i.e., 200 crashes in the entire time period).

Crash Type for One-Way Stop-Controlled Ramp Terminal Crashes

Table 19-21 presents the distribution of intersection-related crashes by crash type for one-way stop-controlled crossroad ramp terminals. The distribution is categorized by two crash severity levels and two area types. If sufficient data are available, the values in Table 19-21 may be updated. This table represents a joint distribution of two variables for each area type. Therefore, for a given area type, sufficient data for calibrating the distribution requires a set of one-way stop-controlled ramp terminals that have collectively experienced at least 200 intersection-related crashes during a recent one- to three-year period (i.e., 200 crashes in the entire time period).

Crash Type for All-Way Stop-Controlled Ramp Terminal Crashes

Table 19-45 presents the distribution of intersection-related crashes by crash type for all-way stop-controlled crossroad ramp terminals. The distribution is categorized by two crash severity levels and two area types. If sufficient data are available, the values in Table 19-45 may be updated. This table represents a joint distribution of two variables for each area type. Therefore, for a given area type, sufficient data for calibrating the distribution requires a set of all-way stop-controlled ramp terminals that have collectively experienced at least 200 intersection-related crashes during a recent one- to three-year period (i.e., 200 crashes in the entire time period).

B.1.4. Calibration of Severity Distribution Functions

The SDFs used in the predictive methods of Chapters 18 and 19 were developed from the most complete and consistent databases available. If desired, these SDFs may be calibrated to local conditions. This calibration is optional, but it may yield more reliable estimates of expected average crash frequency by severity level.

The procedure described in this section is used to quantify the calibration factor for an SDF. The procedure consists of five steps. It requires data for a set of sites (i.e., freeway segments, speed-change lanes, ramp segments, or crossroad ramp terminals) that are located in the jurisdiction of interest.

The SDF calibration factors will have values greater than 1.0 for sites that, on average, experience more severe crashes than those used in the development of the SDFs. Similarly, the calibration factors for sites that experience fewer severe crashes on average than those used in the development of the SDFs will have values less than 1.0.

The procedures presented in this subsection should be used *after* the predictive models have been calibrated using the procedures described in Sections B.1.1 and B.1.3. The calibrated predictive models are used to determine the calibration factor for an SDF.

B.1.4.1. Step 1—Identify the site types for which the SDFs are to be calibrated.

Calibration is performed separately for each SDF provided in Chapters 18 and 19. Chapter 18 provides an SDF for freeway segments and speed-change lanes. Chapter 19 provides an SDF for ramp and C-D road segments. It also provides an SDF for one-way stop-controlled crossroad ramp terminals and an SDF for signal-controlled ramp terminals. The site types needed to calibrate a given SDF are identified in this step.

Also established in this step is the calibration period. Because crash severity is likely to change over time, a calibration period longer than three years is not recommended. The calibration period should have a duration that is a multiple of 12 months to avoid seasonal effects. It is recommended to use the same calibration period for all sites, but exceptions may be made where necessary.

B.1.4.2. Step 2—Select sites for calibration of the SDF.

Calibration sites are selected during this step. One set of calibration sites is assembled for each SDF identified in Step 1. It is desirable that these sites be reasonably representative of the range of site characteristics to which the predictive model will be applied. However, no formal stratification by traffic volume or other site characteristics is needed in selecting the calibration sites. As such, the sites can be selected in a manner to make the data collection needed for Step 3 as efficient as practical.

Each calibration site should be selected without regard to the number or severity of crashes reported during the calibration period. In other words, calibration sites should not be selected to intentionally limit the calibration database to include only sites with either high or low crash frequencies. Also, they should not be selected to intentionally limit the database to include sites with either more severe or less severe crashes. Where practical, this may be accomplished by selecting calibration sites randomly from a larger set of candidate sites.

The desirable minimum sample size for the calibration database for one site type is 30 to 50 sites. For segments, each site should be between 0.1 and 1.0 mi in length. Lengths in this range should be long enough to have statistical validity and short enough to be realistically homogeneous.

For large jurisdictions, such as entire states, with a variety of topographical and climate conditions, it may be desirable to assemble a separate set of calibration sites representing two or three different conditions. In this manner, separate calibration factors are developed for each specific terrain type or geographical region for a given site type. For example, a state with distinct plains and mountain regions (or with distinct dry and wet regions), might choose to develop separate calibration factors for those regions. Where separate calibration factors are developed by terrain type or region, this needs to be done consistently for all site types applicable to those regions.

B.1.4.3. Step 3—Obtain data for each set of calibration sites for the calibration period.

This step is repeated for each SDF identified in Step 1 and its associated set of calibration sites assembled in Step 2. For this step, a calibration database is assembled for each set of calibration sites. The calibration data are assembled for a common calibration period for all sites. The calibration database should include the following information for each site represented in the database:

- All fatal or injury crashes that are reported during the calibration period.
- Site characteristics data needed to apply the predictive method for the same calibration period.

Only fatal or injury crashes should be included in the calibration database. Each observation in the database represents one site. It includes the site characteristics as well as the separate count of fatal, incapacitating injury, nonincapacitating injury, and possible injury crashes reported during the calibration period.

For a given site type, the calibration database should include at least 300 fatal or injury crashes per calibration period. If this minimum is not realized then (a) additional sites should be added to the database following the guidelines in Step 2 or (b) the calibration period should be expanded to include additional years of crash data.

The crash data used for calibration should include all fatal or injury crashes related to each site selected for the calibration database. Crashes should be assigned to specific sites based on the guidelines presented in Section B.2.3.

Table B-2 identifies the site characteristics data that are needed to apply the predictive method. The table classifies each data element as either required or desirable for the calibration procedure. Data for each of the required elements are needed for calibration. For the desirable data elements, it is recommended that actual data be used if available. Assumptions are offered in the table when these data are not available.

B.1.1.4. Step 4—Apply the applicable predictive method to estimate the predicted average crash frequency by severity for each site during the calibration period.

This step is repeated for each SDF identified in Step 1 and its associated set of calibration sites assembled in Step 2. The site characteristics data assembled in Step 3 are used to apply the applicable predictive method to each site in the set of calibration sites. For this application, the predictive model should be applied without using the EB Method. The SDF calibration factor is set to 1.00. Through this process, the predicted average crash frequency for each severity level is obtained for each site in the set of calibration sites, and for each year in the calibration period.

B.1.1.5. Step 5—Compute the calibration factors for use in the SDFs.

This step is repeated for each SDF identified in Step 1 and its associated set of calibration sites assembled in Step 2. It consists of three tasks.

During the first task, the observed crash data are used to calculate the observed probability of a severe crash (i.e., fatal K , incapacitating injury A , or nonincapacitating injury B), given that a fatal or injury crash has occurred. Equation B-2 is used for this purpose. In this manner, one overall average value is obtained for all sites represented in the database.

$$P_{o, aS, ac, at, KAB} = \frac{\sum_{i=1}^{all\ sites} \sum_{j=1}^{n_c} (N_{o, w(i), x(i), at, K, j} + N_{o, w(i), x(i), at, A, j} + N_{o, w(i), x(i), at, B, j})}{\sum_{i=1}^{all\ sites} \sum_{j=1}^{n_c} (N_{o, w(i), x(i), at, K, j} + N_{o, w(i), x(i), at, A, j} + N_{o, w(i), x(i), at, B, j} + N_{o, w(i), x(i), at, C, j})} \quad \text{Equation B-2}$$

Where:

$P_{o, aS, ac, at, KAB}$ = observed probability of a severe crash (i.e., K , A , or B) for all crash types at at all sites aS and all cross sections or control types ac ;

$N_{o, w(i), x(i), at, m, j}$ = observed crash frequency for site i with site type $w(i)$ and year j (includes cross section or control type $x(i)$) for all crash types at and severity level m , with $m = K, A, B, C$ (crashes/yr);

n_{sites} = number of sites; and

n_c = number of years in the crash period (yr).

In the second task, the predicted average crash frequency by severity from Step 4 is used to calculate the predicted probability of occurrence of a severe crash, given that a fatal or injury crash has occurred. Equation B-3 is used for this purpose. In this manner, one overall average value is obtained for all sites represented in the database.

$$P_{p, aS, ac, at, KAB} = \frac{\sum_{i=1}^{all\ sites} \sum_{j=1}^{n_c} (N_{p, w(i), x(i), at, K, j} + N_{p, w(i), x(i), at, A, j} + N_{p, w(i), x(i), at, B, j})}{\sum_{i=1}^{all\ sites} \sum_{j=1}^{n_c} (N_{p, w(i), x(i), at, K, j} + N_{p, w(i), x(i), at, A, j} + N_{p, w(i), x(i), at, B, j} + N_{p, w(i), x(i), at, C, j})} \quad \text{Equation B-3}$$

Where:

$P_{p, aS, ac, at, KAB}$ = predicted probability a severe crash (i.e., K , A , or B) for all crash types at at all sites aS and all cross sections or control types ac ; and

$N_{p, w(i), x(i), at, m, j}$ = predicted crash frequency for site i with site type $w(i)$ and year j (includes cross section or control type $x(i)$) for all crash types at and severity level m , with $m = K, A, B, C$ (crashes/yr).

The final step is to compute the calibration factor using the following equation. The appropriate site-type subscript in this equation is uniquely defined for each SDF identified in Step 1.

$$C_{sdf,w} = \frac{P_{o,aS,ac,at,KAB}}{1.0 - P_{o,aS,ac,at,KAB}} \times \frac{1.0 - P_{p,aS,ac,at,KAB}}{P_{p,aS,ac,at,KAB}} \quad \text{Equation B-4}$$

Where:

$C_{sdf,w}$ = calibration factor to adjust SDF for local conditions for site type w .

The computation is performed separately for each SDF identified in Step 1. The computed calibration factor is rounded to two decimal places for application in the appropriate SDF.

B.2. THE EMPIRICAL BAYES METHOD

The EB Method is used to combine the estimate from a predictive model with observed crash data to obtain a more reliable estimate of the expected average crash frequency. The development of the EB Method described in this appendix is documented by Hauer (1).

The EB Method improves the reliability of the estimate of expected average crash frequency by pooling the estimate from a predictive model with the subject site's observed crash data. The model estimate describes the safety of the typical site with attributes matching those of the subject site. However, it has some level of statistical uncertainty due to unexplained differences among the set of similar sites used to calibrate the predictive model. Similarly, an average crash frequency computed from crash data has uncertainty because of the random variability inherent to crash data. The EB Method produces an estimate of the expected average crash frequency that combines the model prediction and the site-specific crash data in proportion to the level of certainty that can be attached to each.

Each of Chapters 18 and 19 presents a four-step process for applying the EB Method. Before the EB Method can be applied, the appropriate predictive model must be used to determine the predicted average crash frequency for each site of interest. Each site's predicted average crash frequency is estimated for each year in a specified crash period. The steps in applying the EB Method are:

- Determine whether the EB Method is applicable.
- Determine whether observed crash data are available for the project or facility for a desired crash period. Acquire the crash data for this crash period.
- Apply the EB Method to estimate the expected average crash frequency by combining the predicted average crash frequency and observed crash data for the crash period.
- Adjust the estimated value of expected average crash frequency to a future time period, if appropriate.

B.2.1. Determine whether the EB Method is Applicable

The applicability of the EB Method to a particular project depends on the type of analysis being performed and the type of future project work that is anticipated. If the analysis is being performed to evaluate the safety of an existing project, then the EB Method should be applied.

If a future project is being planned, then the nature of that future project should be considered in deciding whether to apply the EB Method. Specifically, the EB Method should be applied for the analyses involving the following future project types.

- Sites at which the roadway geometrics and traffic control are not being changed (e.g., the “do-nothing” alternative).
- Projects in which the roadway cross section is modified but the basic number of through lanes remains the same. This could include projects for which lanes or shoulders were widened or the roadside was improved.
- Projects in which minor changes in alignment are made, such as flattening individual horizontal curves while leaving most of the alignment intact.
- Projects in which a weaving section is added to a freeway.
- Any combination of the above improvements.

The EB Method is not applicable to the following types of improvements.

- Projects in which a new alignment is developed for a substantial proportion of the project length.
- Crossroad ramp terminals at which the basic number of intersection legs or type of traffic control is changed as part of a project.

The reason that the EB Method is not used for the two improvement types in the previous list is that the observed crash data for a previous time period is not necessarily indicative of the crash experience that is likely to occur after a major geometric improvement.

If the EB Method is applied to individual sites and some sites within the project limits will not undergo a major geometric improvement, it is acceptable to apply the EB Method to these sites. In other words, the site-specific EB Method can be applied to some sites within the project limits and not applied to other sites.

If alternative improvements are being evaluated for a given project and the EB Method is being considered, then the EB Method will need to be consistently applied to all alternatives being evaluated. If the EB Method cannot be consistently applied to all alternatives, then it should not be used for any alternatives (i.e., the predictive method should be used without EB adjustment). This approach recognizes that there is typically a small difference in the results obtained from the predictive method when it is used with and without the EB Method. If the EB Method is not applied consistently, such differences will likely introduce a small bias in the comparison of expected crash frequency among alternatives.

If the EB Method is not applicable, do not proceed to the remaining steps. Instead, follow the predictive method in Chapter 18 or 19 but skip Steps 6, 13, and 15.

B.2.2. Determine whether Observed Crash Data are Available for the Project and, if so, Obtain those Data

If the EB Method is determined to be applicable to a given project, then it should be determined whether observed crash data are available directly from the jurisdiction’s crash record system, or indirectly from another source. At least two years of observed crash data are desirable to apply the EB Method.

Two variations of the EB Method are available. They are the site-specific EB Method and the project-level EB Method. The appropriate variation to use for a given project depends on the level of detail provided in the crash record system, the site types to which the method is applied, and the crash types associated with the predictive model that will be used. In general, the best results will be obtained if the site-specific EB Method

is used. Figure B-1 provides a flow chart to assist in the determination of whether the site-specific or project-level variation of the EB Method is applicable for a given project.

B.2.2.1. Projects with One Site

Two considerations are discussed in this section. The first consideration relates to crash type. It is included in Figure B-1. The second consideration relates to crash severity. It is not included in the figure, and may only apply in rare instances.

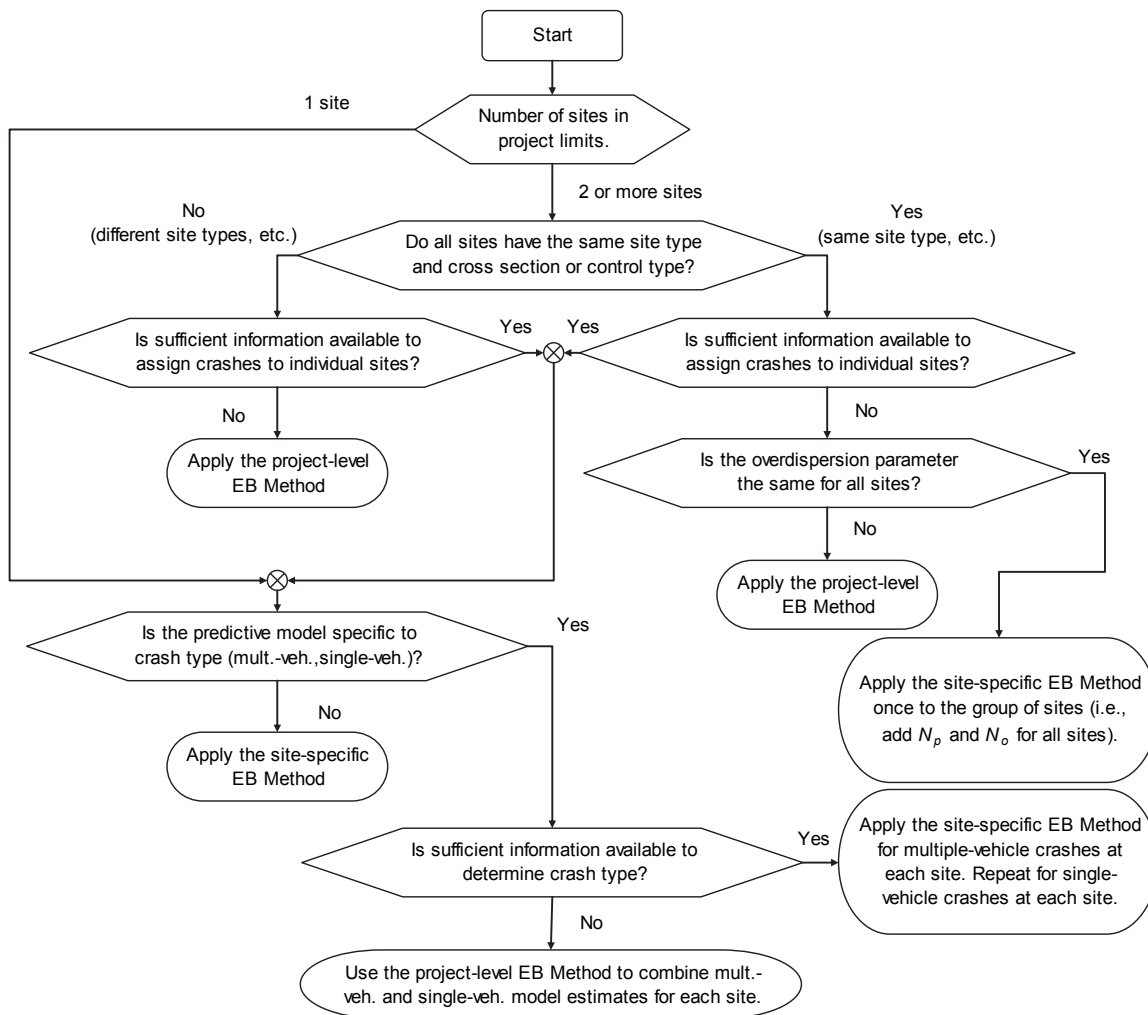


Figure B-1. Determination of the Appropriate Variation of the EB Method

Crash Type Considerations

For projects that consist of one site, Figure B-1 indicates that the first consideration is whether the applicable predictive model is specific to one crash type (i.e., multiple-vehicle crashes or single-vehicle crashes). The predictive methods in Chapters 18 and 19 include some models that are specific to crash type. These models have different overdispersion parameters for each crash type. They are identified in Table B-1.

If the crash record system provides sufficient information to determine crash type for each site and a model with this sensitivity from Chapter 18 or 19 is being used, then the site-specific EB Method is applicable. This method is described in Section B.2.4.

If the crash record system does *not* provide sufficient information to determine crash type and a model with this sensitivity from Chapter 18 or 19 is being used, then the project-level EB Method is applicable. This method is described in Section B.2.5.

Crash Severity Considerations

Although not shown in Figure B-1, another consideration is whether the applicable predictive model is specific to crash severity (i.e., fatal-and-injury crashes or property-damage-only crashes). The predictive methods in Chapters 18 and 19 include models that are specific to crash severity. These models have different overdispersion parameters for each severity.

If the crash record system provides sufficient information to determine crash severity for each site, then the site-specific EB Method is applicable. This method is described in Section B.2.4.

If the crash record system does *not* provide sufficient information to determine crash severity, then the project-level EB Method is applicable. This method is described in Section B.2.5.

Once the total expected average crash frequency is obtained, the estimate of expected average crash frequency for fatal-and-injury crashes is calculated by applying the proportion of predicted average crash frequency for fatal-and-injury crashes (i.e., $N_{p, w, x, y, fi} / N_{p, w, x, y, as}$) to the total expected average crash frequency. Similarly, the estimate of expected average crash frequency for property-damage-only crashes is calculated by applying the proportion of predicted average crash frequency for property-damage-only crashes (i.e., $N_{p, w, x, y, pdo} / N_{p, w, x, y, as}$) to the total expected average crash frequency.

B.2.2.2. Projects with Two or More Sites

For projects that consist of two or more sites, Figure B-1 indicates that there are several considerations when determining the appropriate EB Method variation. The first consideration relates to the site types and cross sections or control types represented within the project limits. In general, a project will consist of many sites that collectively represent different site types, cross sections, and control types. Occasionally, a project may consist of several sites that have the same site type and cross section or control type (e.g., a succession of segments along a specific freeway).

Projects with Different Types of Sites

If a project consists of several sites that collectively have different site types, cross sections or control types, then the next consideration is whether the crash record system provides sufficient information to assign observed crashes to the individual sites. If the crashes can be assigned to individual sites, then the evaluation proceeds on a site-by-site basis. In this situation, the discussion in Section B.2.2.1 applies and the guidance therein is followed to determine the appropriate EB Method variation. Criteria for assigning crashes to individual sites are presented in Section B.2.3.

If the crashes cannot be assigned to individual sites, then the project-level EB Method is applicable. This method is described in Section B.2.5.

Projects with the Same Site Types

If a project consists of several sites that have the same site type and cross section or control type, then the next consideration is whether the crash record system provides sufficient information to assign observed crashes to the individual sites. If the crashes can be assigned to individual sites, then the evaluation proceeds on a site-by-site basis. In this situation, the discussion in Section B.2.2.1 applies and the guidance therein is followed to determine the appropriate EB Method variation. Criteria for assigning crashes to individual sites are presented in Section B.2.3.

If the crashes cannot be assigned to individual sites, then the next consideration is whether the overdispersion parameter is the same for all the sites. The overdispersion parameter is constant for some predictive models; for others it is a function of segment length. For those models in which it is a function of segment length, the length of each segment would have to be the same to produce an overdispersion factor that is the same for all sites.

If the overdispersion parameter is the same for all sites, then the site-specific EB Method can be used. In this application, the predicted average crash frequency for each site is combined into a single estimate for the group of sites. Similarly, the observed crash count for each site is combined into a single estimate for the group of sites.

If the overdispersion parameter is not the same for all sites, then the project-level EB Method is applicable. This method is described in Section B.2.5.

B.2.3. Assign Crashes to Individual Sites for Use in the EB Method

When using the site-specific EB Method, observed crashes for a site are combined with the predictive model estimate of crash frequency for that site to provide a more reliable estimate of its expected average crash frequency. To apply the site-specific EB Method, observed crashes are assigned to each individual site within the facility of interest. This assignment occurs during Step 6 of the predictive method. This section provides guidance for assigning crashes to sites associated with freeway facilities. Similar guidance for assigning crashes to sites associated with street and highway facilities is provided in Section A.2.3 of Appendix A.

Guidance for Assigning Crashes to Freeway Segments and Speed-Change Lanes

Speed-change-related crashes include all crashes that are located between the gore point and the taper point of a speed-change lane and that involve vehicles (a) in the speed-change lane or (b) in the freeway lanes on the same side of the freeway as the speed-change lane. All freeway crashes that are not classified as speed-change-related crashes are considered to be freeway segment crashes.

Figure B-2 illustrates the method used to assign crashes to freeway segments or speed-change lanes. All crashes that occur in Region A are assigned to the speed-change lane. Crashes that occur outside of Region A (i.e., in Region B) are assigned to the freeway segment.

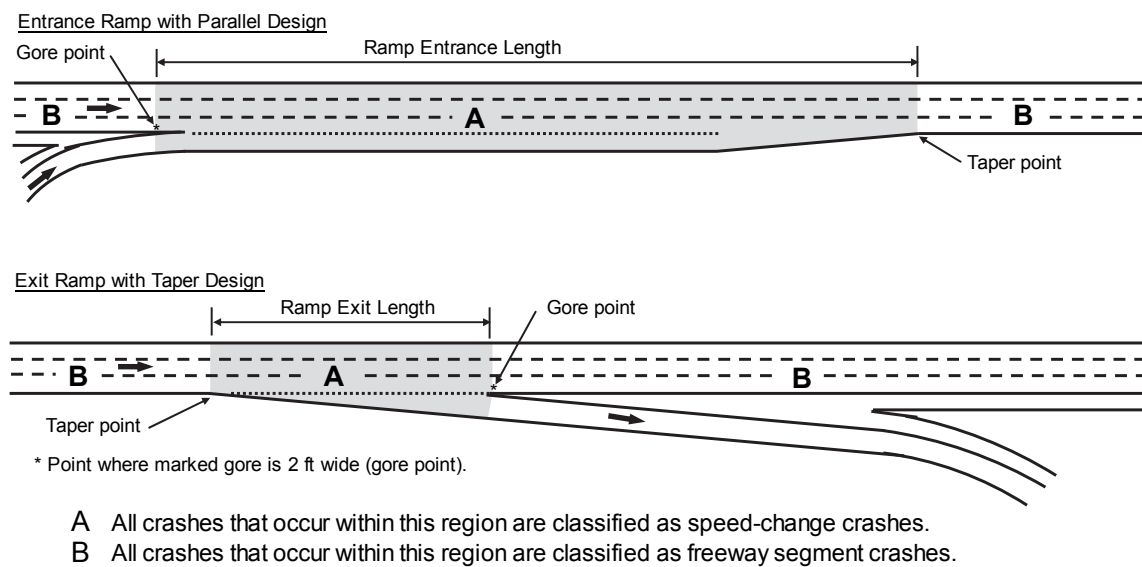


Figure B-2. Definition of Freeway Segments and Speed-Change Lanes

Guidance for Assigning Crashes to Ramp Segments and Crossroad Ramp Terminals

The guidance for assigning crashes to intersections described in Section A.2.3 of Appendix A also applies to assigning crashes to crossroad ramp terminals. Exceptions to this guidance are described in the following paragraphs. Crashes that are not assigned to the crossroad ramp terminal are assigned to the crossroad or intersecting ramp segments.

The predictive models for crossroad ramp terminals include consideration of crashes on the crossroad that are associated with an unsignalized driveway or public street approach located within 250 ft of the crossroad ramp terminal. The interaction between driveway traffic and ramp terminal traffic is complex. As a result, it is often difficult to determine whether crashes between the two traffic streams are related to the driveway or the ramp terminal geometry and traffic control features. Consideration of these crashes in the crossroad ramp terminal predictive models facilitates an examination of the safety implications of these interactions. Therefore, driveway- and public-street-related crashes on the crossroad within 250 ft of the crossroad ramp terminal should be assigned to the crossroad ramp terminal (they should not be assigned to the crossroad segment).

Rear-end crashes on exit ramps should be carefully scrutinized for their relationship to the downstream crossroad ramp terminal. Lengthy queues of stopped vehicles can exist on some ramps during peak traffic demand periods. If the crash is related to the presence of a queue created by the operation of the downstream ramp terminal, then the crash should be assigned to the ramp terminal regardless of the distance between the crash location and the ramp terminal.

In general, a ramp is defined to begin at a gore point and end at (a) another gore point (when ending at another ramp) or (b) the near edge of traveled way of the crossroad (when ending at a crossroad ramp terminal). Exit-ramp-related and entrance-ramp-related crashes represent crashes that occur on a ramp, between the near edge of traveled way of the crossroad and the freeway speed-change lane gore point (this point is shown in Figure B-2). Connector-ramp-related crashes represent all crashes that occur on a connector ramp, between the freeway speed-change lane gore point and the crossroad speed-change lane gore point.

Any crashes that occur in a ramp speed-change lane associated with a ramp-to-ramp junction are assigned to the originating ramp (i.e., they are not assigned to the merging or diverging ramp). The merging ramp ends at the gore point of the ramp speed-change lane. The diverging ramp begins at the gore point of the ramp speed-change lane.

C-D road crashes represent crashes that occur on a C-D road, between the freeway exit gore point and the freeway entrance gore point.

B.2.4. Apply the Site-Specific EB Method

This section describes the EB Method that is used when observed crash data are available for each site of interest. It is used to estimate the expected average crash frequency (in total, or by crash type or severity) for a specific site by combining the predictive model estimate with observed crash data.

The expected average crash frequency for reference year r at a site i with site type $w(i)$ and cross section or control type $x(i)$ for a specified crash type y , and severity z is computed using the following equation.

$$N_{e, w(i), x(i), y, z, r} = w_{w(i), x(i), y, z} \times N_{p, w(i), x(i), y, z, r} + (1.0 - w_{w(i), x(i), y, z}) \times \frac{N_{o, w(i), x(i), y, z}^*}{C_{b, w(i), x(i), y, z, r}} \quad \text{Equation B-5}$$

with,

$$w_{w(i),x(i),y,z} = \frac{1.0}{1.0 + \left(k_{w(i),x(i),y,z} \times \sum_{j=1}^{n_c} N_{p,w(i),x(i),y,z,j} \right)} \quad \text{Equation B-6}$$

$$C_{b,w(i),x(i),y,z,r} = \frac{1.0}{N_{p,w(i),x(i),y,z,r}} \times \sum_{j=1}^{n_c} N_{p,w(i),x(i),y,z,j} \quad \text{Equation B-7}$$

Where:

$N_{e,w(i),x(i),y,z,r}$ = expected average crash frequency for site i with site type $w(i)$ and reference year r (includes cross section or control type $x(i)$ for crash type y , and severity z) (crashes/yr);

$N_{e,w(i),x(i),y,z,j}$ = expected average crash frequency for site i with site type $w(i)$ and year j (includes cross section or control type $x(i)$ for crash type y , and severity z) (crashes/yr);

$N_{p,w(i),x(i),y,z,r}$ = predicted average crash frequency for site i with site type $w(i)$ and reference year r (includes cross section or control type $x(i)$ for crash type y , and severity z) (crashes/yr);

$N_{p,w(i),x(i),y,z,j}$ = predicted average crash frequency for site i with site type $w(i)$ and year j (includes cross section or control type $x(i)$ for crash type y , and severity z) (crashes/yr);

$N_{o,w(i),x(i),y,z}^*$ = total observed number of crashes for site i with site type $w(i)$ and all years in the crash period (includes cross section or control type $x(i)$ for crash type y , and severity z) (crashes);

$C_{b,w(i),x(i),y,z,r}$ = equivalent years in the crash period relative to reference year r at site i with site type $w(i)$ and cross section or control type $x(i)$ for crash type y , and severity z (yr);

$k_{w,x(i),y(i),z}$ = overdispersion parameter for site i with site type $w(i)$, cross section or control type $x(i)$, crash type y , and severity z ;

n_c = number of years in the crash period (yr); and

$w_{w(i),x(i),y,z}$ = weighted adjustment factor for site i with site type $w(i)$ and cross section or control type $x(i)$ for crash type y , and severity z .

The following equation is an alternative form of Equation B-5 that is useful when the expected number of crashes for the crash period is desired.

$$N_{e,w(i),x(i),y,z}^* = w_{w(i),x(i),y,z} \times \left(\sum_{j=1}^{n_c} N_{p,w(i),x(i),y,z,j} \right) + (1.0 - w_{w(i),x(i),y,z}) \times N_{o,w(i),x(i),y,z}^* \quad \text{Equation B-8}$$

Where:

$N_{e,w(i),x(i),y,z}^*$ = total expected number of crashes for site i with site type $w(i)$ and all years in the study period (includes cross section or control type $x(i)$ for crash type y , and severity z) (crashes).

The expected average crash frequency is specific to a given site type w , cross section or control type x , crash type y , and severity z . As a result, the variables used in these equations must all be consistent in their

representation of site type, cross section or control type, crash type, and severity. Also, the reference year r must be one of the years represented in the crash period. The crash period is defined as the consecutive years for which observed crash data are available.

The predicted average crash frequencies used in Equation B-5 to Equation B-7 are obtained from the appropriate predictive model described in Chapter 18 or 19. Similarly, the overdispersion parameter used in Equation B-6 is obtained from the same predictive model as used to estimate the predicted average crash frequencies.

The overdispersion parameter is shown to be specific to site i . This situation will apply whenever it is computed as a function of segment length, which is the case for Chapters 18 and 19. When it is not a function of segment length, the subscript components referencing site i are removed.

Equation B-6 shows an inverse relationship between the overdispersion parameter and the weight w . This implies that when a model with little overdispersion is available, more reliance will be placed on the predictive model estimate N_p and less reliance on the observed crash count N_o^* . The opposite is also the case; when a model with substantial overdispersion is available, less reliance will be placed on the predictive model estimate and more reliance on the observed crash count.

It is important to note in Equation B-6 that, as N_p increases, there is less weight placed on it and more on N_o^* . This might seem counterintuitive at first. However, this implies that for longer sites and for longer study periods, there are more opportunities for crashes to occur. Thus, the observed crash history is likely to be more meaningful and the model prediction less important. So, as N_p increases, the EB Method places more weight on the number of crashes that actually occur. When few crashes are predicted, the observed crash count is not likely to be meaningful, in statistical terms, so greater reliance is placed on the predicted crash frequency.

Chapters 18 and 19 present worksheets that can be used to apply the site-specific EB Method as presented in this section.

Section B.2.6 explains how to use Equation B-5 to estimate the expected average crash frequency for a time period other than the crash period, such as the time period when a proposed future project will be implemented.

B.2.5. Apply the Project-Level EB Method

This section describes an alternative EB Method that is used when observed crash data are aggregated across several sites (e.g., for an entire facility or project). The development of this variation of the EB Method is documented by Hauer et al. (2).

In general, the EB Method described in this section is used when the predictive model and its overdispersion parameter are not uniquely defined for the combined set of sites being evaluated. It is also needed when the predictive model is specific to crash type (or severity) but the information in the crash database is insufficient to make crash type determinations.

When the crash data cannot be disaggregated to the level of the predictive model, the estimates from each of the predictive models for the various sites have different weights. These estimates cannot be directly combined to compute an overall weighted adjustment factor w because they are likely correlated to some degree (e.g., all sites in a given project may be consistently safer [or less safe] than the similar sites used to calibrate the predictive model). Because the degree of correlation is unknown, an approximate method is used to estimate the expected average crash frequency for each of two extreme conditions of correlation. The first condition assumes that the estimates among sites are independent. The second condition assumes that

the estimates among sites are perfectly correlated. The best estimate of expected average crash frequency is rationalized to be the average of these two extreme conditions.

The following procedure describes the sequence of calculations necessary to implement the project-level EB Method. To facilitate the presentation of this procedure, the equations shown in this section have subscripts denoting fatal-and-injury fi crashes of all crash types (i.e., multiple-vehicle and single-vehicle fatal-and-injury crashes combined). The conversion of these equations so that they are applicable to property-damage-only crashes (or crashes of a specific crash type) requires only the substitution of the appropriate subscripts.

Step 1—Sum the predicted average crash frequency and observed crash counts.

The desired crash type w and crash severity z are specified during this step. The crash type chosen must have an associated predictive model. For example, if an estimate of the expected average multiple-vehicle crash frequency is desired, then an SPF that predicts multiple-vehicle crash frequency must be available in the predictive model. Similarly, if an estimate of the expected average fatal-and-injury crash frequency is desired, then an SPF that predicts fatal-and-injury crash frequency is required.

The predicted average crash frequency is summed for each site and year represented in the crash period to obtain the predicted number of crashes for all sites and all years in the crash period. Each site i will have a specific site type $w(i)$ and cross section or control type $x(i)$. Similarly, the observed crash counts are summed for each site and year represented in the crash period to obtain the observed number of crashes for all sites and all years in the crash period. The following equations are used to compute the desired sums for fatal-and-injury crashes of all crash types.

$$N_{p, aS, ac, at, fi}^* = \sum_i^{all\ sites} \sum_k^{all\ crash\ types} \sum_{j=1}^{n_c} N_{p, w(i), x(i), y(k), fi, j} \quad \text{Equation B-9}$$

$$N_{o, aS, ac, at, fi}^* = \sum_i^{all\ sites} \sum_k^{all\ crash\ types} \sum_{j=1}^{n_c} N_{o, w(i), x(i), y(k), fi, j} \quad \text{Equation B-10}$$

Where:

$N_{p, aS, ac, at, fi}^*$ = total predicted number of crashes for all sites aS and all years in the crash period (includes all cross sections ac and fatal-and-injury crashes fi of all crash types at) (crashes);

$N_{p, w(i), x(i), y(k), fi, j}$ = predicted average crash frequency for site i with site type $w(i)$ and year j (includes cross section or control type $x(i)$ for fatal-and-injury crashes fi of crash type $y(k)$) (crashes/yr);

$N_{o, aS, ac, at, fi}^*$ = total observed number of crashes for all sites aS and all years in the crash period (includes all cross sections ac and fatal-and-injury crashes fi of all crash types at) (crashes); and

$N_{o, w(i), x(i), y(k), fi, j}$ = observed crash frequency for site i with site type $w(i)$ and year j (includes cross section or control type $x(i)$ for fatal-and-injury crashes fi of crash type $y(k)$) (crashes/yr).

The predicted average crash frequencies used in Equation B-9 are obtained from the appropriate predictive model described in Chapter 18 or 19. Because the EB Method is applied at the project level, it is likely that observed crashes cannot be associated with specific sites and Equation B-10 cannot be directly used. In this situation, the analyst should use the equation as guidance when consulting crash records to identify crashes

of all types that are associated with one of the sites in the project limits and that occur during the crash period.

Step 2—Compute the variance of the predicted average crash frequency.

Two variance estimates are computed in this step. One estimate is based on the assumption that the sites are independent and the other estimate is based on the assumption that the sites are perfectly correlated. The following equations are used for these computations.

$$V_{0,aS,ac,at,fi} = \sum_i^{\text{all sites}} \sum_k^{\text{all crash types}} k_{w(i),x(i),y(k),fi} \times \left[\sum_{j=1}^{n_c} N_{p,w(i),x(i),y(k),fi,j} \right]^2 \quad \text{Equation B-11}$$

$$V_{1,aS,ac,at,fi} = \left(\sum_i^{\text{all sites}} \sum_k^{\text{all crash types}} \sqrt{k_{w(i),x(i),y(k),fi} \times \left[\sum_{j=1}^{n_c} N_{p,w(i),x(i),y(k),fi,j} \right]^2} \right)^2 \quad \text{Equation B-12}$$

Where:

$V_{0,aS,ac,at,fi}$ = variance of the predicted average crash frequency assuming independence for all sites aS and all years in the crash period (includes all cross sections ac and fatal-and-injury crashes fi of all crash types at) (crashes²/yr²);

$V_{1,aS,ac,at,fi}$ = variance of the predicted average crash frequency assuming perfect correlation for all sites aS and all years in the crash period (includes all cross sections ac and fatal-and-injury crashes fi of all crash types at) (crashes²/yr²); and

$k_{w(i),x(i),y(k),fi}$ = overdispersion parameter for site i with site type $w(i)$ and cross section or control type $x(i)$ for fatal-and-injury crashes of crash type $y(k)$.

The overdispersion parameters used in Equation B-11 and Equation B-12 are obtained from the same predictive model that was used to estimate the predicted average crash frequencies.

Step 3—Compute the weighted adjustment factor.

Two weighted adjustment factors are computed in this step. One factor is based on the assumption that the sites are independent and the other factor is based on the assumption that the sites are perfectly correlated. The following equations are used for these computations.

$$W_{0,aS,ac,at,fi} = \frac{1.0}{1.0 + \frac{V_{0,aS,ac,at,fi}}{N_{p,aS,ac,at,fi}^*}} \quad \text{Equation B-13}$$

$$W_{1,aS,ac,at,fi} = \frac{1.0}{1.0 + \frac{V_{1,aS,ac,at,fi}}{N_{p,aS,ac,at,fi}^*}} \quad \text{Equation B-14}$$

Where:

$w_{0,aS,ac,at,fi}$ = weighted adjustment factor assuming independence for all sites aS and all years in the crash period (includes all cross sections ac and fatal-and-injury crashes fi of all crash types at); and

$w_{1,aS,ac,at,fi}$ = weighted adjustment factor assuming perfect correlation for all sites aS and all years in the crash period (includes all cross sections ac and fatal-and-injury crashes fi of all crash types at).

Step 4—Compute the equivalent years in the crash period.

The equivalent number of years in the crash period reflects changes in traffic volume and other factors during the crash period. The changes are relative to a specified reference year r . Any year in the crash period can be designated as the reference year. It is the year for which the expected average crash frequency will be estimated in Step 5. The equivalent number of years is computed using the following equation.

$$C_{b,aS,ac,at,fi,r} = \frac{N_{p,aS,ac,at,fi}^*}{N_{p,aS,ac,at,fi,r}} \quad \text{Equation B-15}$$

with,

$$N_{p,aS,ac,at,fi,r} = \sum_i^{\text{all sites}} \sum_k^{\text{all crash types}} N_{p,w(i),x(i),y(k),fi,r} \quad \text{Equation B-16}$$

Where:

$C_{b,aS,ac,at,fi,r}$ = equivalent years in the crash period relative to reference year r for all sites aS , all cross sections ac , and fatal-and-injury crashes fi of all crash types at (yr); and

$N_{p,aS,ac,at,fi,r}$ = predicted average crash frequency for all sites aS and reference year r (includes all cross sections ac and fatal-and-injury crashes fi of all crash types at) (crashes/yr).

Step 5—Compute the expected average crash frequency.

The expected average crash frequency for the reference year r is computed in this step. Steps 4 and 5 are repeated for other reference years of interest. The expected average crash frequency is computed as the average of the expected values for the two assumed conditions (i.e., sites are independent and sites are perfectly correlated). The following equation is used for this calculation.

$$N_{e,aS,ac,at,fi,r} = \frac{N_{0,aS,ac,at,fi,r} + N_{1,aS,ac,at,fi,r}}{2} \quad \text{Equation B-17}$$

with,

$$N_{0,aS,ac,at,fi,r} = w_{0,aS,ac,at,fi} \times N_{p,aS,ac,at,fi,r} + (1.0 - w_{0,aS,ac,at,fi}) \times \frac{N_{o,aS,ac,at,fi}^*}{C_{b,aS,ac,at,fi,r}} \quad \text{Equation B-18}$$

$$N_{1,aS,ac,at,fi,r} = w_{1,aS,ac,at,fi} \times N_{p,aS,ac,at,fi,r} + (1.0 - w_{1,aS,ac,at,fi}) \times \frac{N_{o,aS,ac,at,fi}^*}{C_{b,aS,ac,at,fi,r}} \quad \text{Equation B-19}$$

Where:

$N_{e, aS, ac, at, fi, r}$ = expected average crash frequency for all sites aS and reference year r (includes all cross sections ac and fatal-and-injury crashes fi of all crash types at) (crashes/yr);

$N_{0, aS, ac, at, fi, r}$ = expected average crash frequency for all sites aS and reference year r assuming independence among sites (includes all cross sections ac and fatal-and-injury fi crashes of all crash types at) (crashes/yr); and

$N_{1, aS, ac, at, fi, r}$ = expected average crash frequency for all sites aS and reference year r assuming perfect correlation among sites (includes all cross sections ac and fatal-and-injury fi crashes of all crash types at) (crashes/yr).

The following equation is an alternative form of Equation B-17 that is useful when the expected number of crashes for the crash period is desired.

$$N_{e, aS, ac, at, fi}^* = \frac{N_{0, aS, ac, at, fi}^* + N_{1, aS, ac, at, fi}^*}{2} \quad \text{Equation B-20}$$

with,

$$N_{0, aS, ac, at, fi}^* = w_{0, aS, ac, at, fi} \times N_{p, aS, ac, at, fi}^* + (1.0 - w_{0, aS, ac, at, fi}) \times N_{o, aS, ac, at, fi}^* \quad \text{Equation B-21}$$

$$N_{1, aS, ac, at, fi}^* = w_{1, aS, ac, at, fi} \times N_{p, aS, ac, at, fi}^* + (1.0 - w_{1, aS, ac, at, fi}) \times N_{o, aS, ac, at, fi}^* \quad \text{Equation B-22}$$

Where:

$N_{e, aS, ac, at, fi}^*$ = total expected number of crashes for all sites aS and all years in the study period (includes all cross sections ac and fatal-and-injury crashes fi of all crash types at) (crashes);

$N_{0, aS, ac, at, fi}^*$ = total expected number of crashes for all sites aS and all years assuming independence among sites (includes all cross sections ac and fatal-and-injury crashes fi of all crash types at) (crashes); and

$N_{1, aS, ac, at, fi}^*$ = total expected number of crashes for all sites aS and all years assuming perfect correlation among sites (includes all cross sections ac and fatal-and-injury crashes fi of all crash types at) (crashes).

Chapters 18 and 19 present worksheets that can be used to apply the project-level EB Method as presented in this section.

Section B.2.6 explains how to use Equation B-17 to estimate the expected average crash frequency for a time period other than the crash period, such as the time period when a proposed future project will be implemented.

B.2.6. Estimate the Expected Average Crash Frequency for a Future Time Period

The estimate obtained from Equation B-5 or Equation B-17 represents the expected average crash frequency for a given site or project, respectively, during the crash period.

This section describes a procedure that is used to obtain an estimate of the expected average crash frequency during the study period. The study period is defined as the consecutive years for which an estimate of the

expected average crash frequency is desired. This procedure is used when the study period includes years that are not represented in the crash period. Typically, the study period includes one or more future years that are coincident with a proposed or anticipated change in some feature or characteristic of the project.

The procedure yields an estimate of the expected average crash frequency for a specified study year j . This estimate is corrected for (a) any growth or decline in AADTs between the crash period and the study period and (b) any change in geometric design or traffic control features between the crash period and the study period (as represented by the values of the associated CMFs). The estimates for each study year j are added to obtain the expected number of crashes for the study period.

Site-Specific EB Method

The expected average crash frequency for a site for year j can be estimated using the following equation. In this application, the year of interest is year j and the reference year r is any one year in the crash period (by convention, the reference year is typically selected to be the first year in the crash period).

$$N_{e, w(i), x(i), y, z, j} = N_{e, w(i), x(i), y, z, r} \times \frac{N_{p, w(i), x(i), y, z, j}}{N_{p, w(i), x(i), y, z, r}} \quad \text{Equation B-23}$$

Where:

$N_{e, w(i), x(i), y, z, j}$ = expected average crash frequency for site i with site type $w(i)$ and year j (includes cross section or control type $x(i)$ for crash type y , and severity z) (crashes/yr);

$N_{e, w(i), x(i), y, z, r}$ = expected average crash frequency for site i with site type $w(i)$ and reference year r (includes cross section or control type $x(i)$ for crash type y , and severity z) (crashes/yr);

$N_{p, w(i), x(i), y, z, j}$ = predicted average crash frequency for site i with site type $w(i)$ and year j (includes cross section or control type $x(i)$ for crash type y , and severity z) (crashes/yr); and

$N_{p, w(i), x(i), y, z, r}$ = predicted average crash frequency for site i with site type $w(i)$ and reference year r (includes cross section or control type $x(i)$ for crash type y , and severity z) (crashes/yr).

The expected average crash frequency is specific to a given site type w , cross section or control type x , crash type y , and severity z . As a result, the variables used in this equation must all be consistent in their representation of site type, cross section or control type, crash type, and severity.

The predicted average crash frequencies used in Equation B-23 are obtained from the appropriate predictive model described in Chapter 18 or 19. The expected average crash frequency is obtained from Equation B-5.

The expected number of crashes for a site for a specified study period is computed using the following equation.

$$N_{e, w(i), x(i), y, z}^* = \sum_{j=1}^{n_s} N_{e, w(i), x(i), y, z, j} \quad \text{Equation B-24}$$

Where:

$N_{e, w(i), x(i), y, z}^*$ = total expected number of crashes for site i with site type $w(i)$ and all years in the study period (includes cross section or control type $x(i)$ for crash type y , and severity z) (crashes); and

n_s = number of years in the study period (yr).

The expected number of crashes for all sites for a specified study period is computed using the following equation.

$$N_{e, aS, ac, at, as}^* = \sum_i^{\text{all sites}} \sum_k^{\text{all crash types}} \sum_l^{\text{all severities}} N_{e, w(i), x(i), y(k), z(l)}^* \quad \text{Equation B-25}$$

Where:

$N_{e, aS, ac, at, as}^*$ = total expected number of crashes for all sites aS and all years in the study period (includes all cross sections ac , all crash types at , and all severities as) (crashes).

Project-Level EB Method

The following procedure describes the sequence of calculations necessary to adjust the estimate of expected average crash frequency to a future year (or years). To facilitate the presentation of this procedure, the equations shown in this subsection have subscripts denoting fatal-and-injury fi crashes of all crash types (i.e., multiple-vehicle and single-vehicle fatal-and-injury crashes combined). The conversion of these equations so that they are applicable to property-damage-only crashes (or crashes of a specific crash type) requires only the substitution of the appropriate subscripts.

The expected average crash frequency for all sites for year j can be estimated using the following equation. In this application, the year of interest is year j and the reference year r is any one year in the crash period (by convention, the reference year is typically selected to be the first year in the crash period).

$$N_{e, aS, ac, at, fi, j} = N_{e, aS, ac, at, fi, r} \times \frac{N_{p, aS, ac, at, fi, j}}{N_{p, aS, ac, at, fi, r}} \quad \text{Equation B-26}$$

Where:

$N_{e, aS, ac, at, fi, j}$ = expected average crash frequency for all sites aS and year j (includes all cross sections ac and fatal-and-injury crashes fi of all crash types at) (crashes/yr);

$N_{e, aS, ac, at, fi, r}$ = expected average crash frequency for all sites aS and reference year r (includes all cross sections ac and fatal-and-injury crashes fi of all crash types at) (crashes/yr);

$N_{p, aS, ac, at, fi, j}$ = predicted average crash frequency for all sites aS and year j (includes all cross sections ac and fatal-and-injury crashes fi of all crash types at) (crashes/yr); and

$N_{p, aS, ac, at, fi, r}$ = predicted average crash frequency for all sites aS and reference year r (includes all cross sections ac and fatal-and-injury crashes fi of all crash types at) (crashes/yr).

The predicted average crash frequencies used in Equation B-26 are computed using Equation B-16. The expected average crash frequency is obtained from Equation B-17.

The expected number of crashes for all sites for a specified study period is computed using the following equation.

$$N_{e, aS, ac, at, fi}^* = \sum_{j=1}^{n_s} N_{e, aS, ac, at, fi, j}$$

Equation B-27

Where:

$N_{e, aS, ac, at, fi}^*$ = total expected number of crashes for all sites aS and all years in the study period (includes all cross sections ac and fatal-and-injury crashes fi of all crash types at) (crashes).

B.2.7. EB Method for Segments with an Odd Number of Lanes

Most roadway cross sections have an even number of through traffic lanes. As a result, researchers can typically acquire data for segments with even numbers of lanes in sufficient number to permit the development of statistically valid predictive models. On the other hand, some roadways do exist with an odd number of through lanes. The development of statistically valid models for these cross sections is sometimes not possible due to inadequate sample size.

This section describes a procedure for evaluating a segment of interest that has a cross section with an odd number of through lanes. This procedure can be used when a predictive model is not available for the specified cross section. It is described in the form of supplemental equations that are used in the steps of the predictive method. The step numbers of the procedure match those of the predictive method to which they apply. The procedure is viable if the following checks are satisfied.

- The segment has X total lanes that represent Y lanes in one direction and Z lanes in the opposite direction (i.e., $X = Y + Z$) and Y is not equal to Z .
- The predictive model for segments includes an SPF for $2 \times Y$ lanes.
- The predictive model for segments includes an SPF for $2 \times Z$ lanes.

If these checks are satisfied, then the procedure can be applied.

Step 9—For the selected site, determine and apply the appropriate SPF.

The applicable predictive model is identified from the appropriate chapter. The site of interest is determined to have a site type w with an X -lane cross section, and the analysis is focused on crash type y and severity z .

Select an SPF for the subject site based on it being applicable to a cross section of $2 \times Y$ lanes. Select a second SPF for the subject site based on it being applicable to a cross section of $2 \times Z$ lanes. The best estimate of the predicted average crash frequency for base conditions is computed as the average of the estimates from the two SPFs. This calculation is shown using the following equation.

$$N_{spf, w, X, y, z, j} = \frac{N_{spf, w, 2Y, y, z, j} + N_{spf, w, 2Z, y, z, j}}{2}$$

Equation B-28

Where:

$N_{spf, w, n, y, z, j}$ = predicted average crash frequency for year j determined for base conditions of the SPF developed for site type w , n -lane cross section ($n = X, 2Y, 2Z$), crash type y , and severity z (crashes/yr).

Step 10—Multiply the result obtained in Step 9 by the appropriate CMFs.

The predictive model is used to compute the predicted average crash frequency for the subject site. The general form of this model is shown in the equation below. The specific CMFs and calibration factor are obtained from the appropriate chapter.

$$N_{p,w,X,y,z,j} = N_{spf,w,X,y,z,j} \times (CMF_{1,w,X,y,z} \times CMF_{2,w,X,y,z} \times \dots \times CMF_{m,w,X,y,z}) \times C_{w,X,y,z} \quad \text{Equation B-29}$$

Where:

$N_{p,w,X,y,z,j}$ = predicted average crash frequency for year j for site type w , X -lane cross section, crash type y , and severity z (crashes/yr);

$CMF_{m,w,X,y,z}$ = crash modification factors specific to site type w , X -lane cross section, crash type y , and severity z for specific geometric design and traffic control features m ; and

$C_{w,X,y,z}$ = calibration factor to adjust SPF for local conditions for site type w , X -lane cross section, crash type y , and severity z .

Step 13—Apply site-specific EB Method (if applicable) and apply SDFs.

If the EB Method is used in the predictive method, then the variance of the predicted average crash frequency is computed in this step using the following equation.

$$V_{p,w,X,y,z} = \left(\sqrt{k_{w,2Y,y,z} \times \left[\sum_{j=1}^{n_c} (0.5 \times N_{p,w,2Y,y,z,j}) \right]^2} + \sqrt{k_{w,2Z,y,z} \times \left[\sum_{j=1}^{n_c} (0.5 \times N_{p,w,2Z,y,z,j}) \right]^2} \right)^2 \quad \text{Equation B-30}$$

with,

$$N_{p,w,2Y,y,z,j} = N_{spf,w,2Y,y,z,j} \times (CMF_{1,w,X,y,z} \times CMF_{2,w,X,y,z} \times \dots \times CMF_{m,w,X,y,z}) \times C_{w,X,y,z} \quad \text{Equation B-31}$$

$$N_{p,w,2Z,y,z,j} = N_{spf,w,2Z,y,z,j} \times (CMF_{1,w,X,y,z} \times CMF_{2,w,X,y,z} \times \dots \times CMF_{m,w,X,y,z}) \times C_{w,X,y,z} \quad \text{Equation B-32}$$

Where:

$V_{p,w,X,y,z}$ = variance of the predicted average crash frequency for site type w , X -lane cross section, crash type y , and severity z (crashes²/yr²);

$k_{w,n,y,z}$ = overdispersion parameter for site type w , n -lane cross section ($n = X, 2Y, 2Z$), crash type y , and severity z ;

$N_{p,w,n,y,z,j}$ = predicted average crash frequency for a year j for site type w , n -lane cross section ($n = X, 2Y, 2Z$), crash type y , and severity z (crashes/yr); and

n_c = number of years in the crash period (yr).

The overdispersion parameters used in Equation B-30 are obtained from the same predictive model as used to estimate the predicted average crash frequencies.

An overdispersion parameter is needed to apply the EB Method. An equivalent overdispersion parameter that is associated with the predicted average crash frequency from Equation B-29 is computed using the following equation.

$$k_{p,w,X,y,z}^* = \frac{V_{p,w,X,y,z}}{\left[\sum_{j=1}^{n_c} N_{p,w,X,y,z,j} \right]^2} \quad \text{Equation B-33}$$

Where:

$k_{w,X,y,z}^*$ = effective overdispersion parameter for site type w , X -lane cross section, crash type y , and severity z .

The effective overdispersion parameter computed using Equation B-33 is used in Equation B-5 of the site-specific EB Method described in Section B.2.4.

Step 15—Apply the project-level EB Method (if applicable).

The effective overdispersion parameter computed using Equation B-33 is used in Step 2 of the project-level EB Method described in Section B.2.5.

B.3. REFERENCES

- (1) Hauer, E. *Observational Before-After Studies in Road Safety*. Pergamon Press, Elsevier Ltd., Oxford, United Kingdom, 1997.
- (2) Hauer, E., D. Harwood, F. Council, and M. Griffith. "Estimating Safety by the Empirical Bayes Method." In *Transportation Research Record 1784*. TRB, National Research Council, Washington, D.C., 2002, pp. 126–131.

APPENDIX F

ALGORITHM DESCRIPTION

ALGORITHM DESCRIPTION

TABLE OF CONTENTS

List of Figures	ii
List of Tables.....	ii
Algorithm Description for Freeway segments	1
Input Data.....	1
Predictive Models	3
Predictive Method.....	5
Output.....	5
Algorithm Description for Freeway speed-Change Lanes	6
Input Data.....	6
Predictive Models	8
Predictive Method.....	10
Output.....	10
Algorithm Description for Ramp segments	10
Input Data.....	11
Predictive Models	12
Predictive Method.....	14
Output.....	14
Algorithm Description for Crossroad Ramp Terminals.....	14
Input Data.....	15
Predictive Models	17
Predictive Method.....	19
Output.....	19

Software Documentation.....	19
Flowcharts	19
Linkage Lists	23

LIST OF FIGURES

Figure 1. Main Subroutine.....	20
Figure 2. Performance Measures Subroutine	20
Figure 3. Evaluation based on Predictive Model Only	21
Figure 4. Evaluation based on the Site-Specific EB Method	22
Figure 5. Evaluation based on the Project-Level EB Method	23

LIST OF TABLES

Table 1. Linkage List for Key Subroutines	24
Table 2. Subroutines Implementing the Predictive Method	25

ALGORITHM DESCRIPTION

This document provides a description of the algorithms used in the predictive methods for evaluating freeways and ramps. These methods have been implemented in software in the Enhanced Interchange Safety Analysis Tool (ISATe). They are documented in the proposed *HSM* Freeways chapter (Appendix C), proposed *HSM* Ramps chapter (Appendix D), and proposed *HSM* Appendix B for Part C (Appendix E).

The objective of this document is to identify the information needed to implement the predictive methods in software products other than ISATe, such as the Interactive Highway Safety Design Model (IHSDM). This objective is achieved by identifying the input data needed, and predictive models used, when implementing the predictive methods. Extensive reference is made to the content of the proposed documents identified in the previous paragraph, as opposed to repeating that material in this document.

This document consists of five parts. Each part provides the information needed to implement the predictive method for one of the following freeway facility site types.

- Freeway segments.
- Freeway speed-change lanes.
- Ramp or C-D road segments.
- Crossroad ramp terminals.

The fifth part of this document provides a series of flow charts that describe the logic flow used in the ISATe software implementation.

ALGORITHM DESCRIPTION FOR FREEWAY SEGMENTS

This part of the appendix provides information needed to implement the predictive method for freeway segments in software. This method is described in the proposed *HSM* Freeways chapter.

The remainder of this part consists of four sections. The first section identifies the input data needed by the predictive method. The second section presents the crash prediction models. The third section describes the sequence of steps that comprise the predictive method. The last section describes the output data that are available from an application of the predictive method.

Input Data

This section describes the input data for the predictive method. These data are identified using the following categories.

- Evaluation period.
- Evaluation type.
- Crash data.
- Geometric design, traffic control, and traffic volume data.

Evaluation Period

The evaluation period is the set of years in the combined study period and crash period. Every calendar year in the evaluation period is separately evaluated using the methodology.

Specific details about this input are provided in Section 18.4.1, Step 2 of the proposed *HSM* Freeways chapter.

Evaluation Type

The predictive method can be used to evaluate one site, or a contiguous group of sites. The evaluation is described as one of several types, as determined by the analyst. When one site is being evaluated, the evaluation types are:

- A. Evaluation based on using the predictive model only.
- B. Evaluation based on using the predictive model and crash data.

When a group of sites are being evaluated, the evaluation types are:

- A. Evaluation based on using the predictive model only for each site.
- B. Evaluation based on using the predictive model and crash data for each site.
- C. Evaluation based on using the predictive model for each site and crash data for the group of sites.

When crash data are used, the empirical Bayes (EB) Method is used to combine the crash data with the predictive model estimate to obtain a more reliable estimate of the expected crash frequency. The three evaluation types are referred to herein as types A, B, and C. In the HSM, type B evaluation is referred to as the “site-specific” EB Method and type C is referred to as “project-level” EB Method.

There are several factors to be considered when determining whether the EB Method is appropriate for a given project. These criteria are described in Sections B.2.1 and B.2.2 of the proposed *HSM* Appendix B for Part C.

Crash Counts

If evaluation type B is input by the analyst, then the crash data for each site are necessary input data. The criteria for assigning crashes to individual freeway segment sites are described in Section B.2.3 of the proposed *HSM* Appendix B for Part C. If evaluation type C is input, then the crash data for the group of sites is needed.

The crash counts must correspond to the crash period. The crash period can be site-specific; however, for coding convenience, the crash period should be the same for all sites. If the crash period includes multiple years, then the crash data do not have to be separately tabulated for each year at each site. Rather, it is sufficient for the analyst to input the total number of crashes for the crash period.

Geometric Design, Traffic Control, and Traffic Volume Data

The input data describing the geometric design and traffic volume data for freeway segments are identified in the following list.

General

- Area type (urban or rural).

Geometric Design

- Number of through lanes.
- Segment length.
- Length and radius of horizontal curve.
- Lane width.
- Inside and outside shoulder width.
- Median width.
- Length of rumble strips on inside and outside shoulders.
- Length of (and offset to) median barrier.
- Length of (and offset to) outside barrier.
- Clear zone width.
- Presence and length of Type B weaving section.

Traffic Characteristics

- AADT volume of (and distance to) nearest upstream and downstream entrance ramp.
- AADT volume of (and distance to) nearest upstream and downstream exit ramp.
- AADT volume of freeway segment.
- Proportion of AADT that occurs during hours where the lane volume exceeds 1,000 veh/h/ln.

Specific details about these input data are provided in Section 18.4.2 of the proposed *HSM* Freeways chapter. These details include the method of measurement and the value limits for each variable. The AADT volume ranges for the predictive models are listed in Table 18-4 of the proposed *HSM* Freeways chapter.

The units of measurement for all input data are U.S. customary. If input data are provided in metric units, then they should undergo soft conversion to U.S. customary units before their use in the predictive method.

Predictive Models

The general structure of the predictive model is described by Equation 18-1 of the proposed *HSM* Freeways chapter. A more specific structure is described by Equation 18-2.

Safety Performance Functions

Separate safety performance functions (SPFs) are provided for the following conditions:

- Area type (rural or urban).
- Through lanes (4, 6, 8, 10 in urban areas).
- Crash type (multiple-vehicle, single-vehicle).

- Crash severity (fatal-and-injury, property-damage-only).

All total, there are 28 SPFs represented by unique combinations of the four conditions identified in the preceding list. Specific details about the SPF regression coefficients are provided in Section 18.6.1 of the proposed *HSM* Freeways chapter.

Section 18.6.1 of the proposed *HSM* Freeways chapter describes a procedure for extending the SPFs to segments with an odd number of lanes. Section B.2.7 of the proposed *HSM* Appendix B for Part C describes a procedure for applying the EB Method to segments with an odd number of lanes.

The overdispersion parameter is computed as a function of segment length. The equation for this calculation is provided in Section 18.6.1 of the proposed *HSM* Freeways chapter.

A procedure for calibrating the predictive models is described in Section B.1.1 of the proposed *HSM* Appendix B for Part C.

Crash Modification Factors

Eleven crash modification factors (CMFs) are provided in the predictive method. The geometric design features and traffic conditions that they address are identified in the following list.

- Horizontal curvature.
- Lane width.
- Inside shoulder width.
- Median width.
- Median barrier.
- High-volume (congested) conditions.
- Lane change activity related to ramp entrances and ramp exits.
- Outside shoulder width.
- Shoulder rumble strip presence.
- Outside clearance.
- Outside barrier.

Specific details about the CMF formulation and regression coefficients are provided in Section 18.7.1 of the proposed *HSM* Freeways chapter. This section also identifies conditions where a CMF is not applicable.

Supplemental calculations for using the barrier-related CMFs are described in Section 18.7.3 of the proposed *HSM* Freeways chapter.

Crash Type Distribution

The predicted crash frequency from a predictive model can be disaggregated into estimates of crash frequency by crash type. The crash type categories for multiple-vehicle crashes include head-on, right-

angle, rear-end, and sideswipe. The crash type categories for multiple-vehicle crashes include animal, fixed object, other object, and parked vehicle.

Distribution percentages for these crash types are provided in Section 18.6.1 of the proposed *HSM* Freeways chapter. Application of these percentages is described in Sample Problem 1 in Section 18.13.1 of the proposed *HSM* Freeways chapter.

Crash Severity Distribution

The predicted crash frequency from a predictive model can be disaggregated into estimates of crash severity. Specifically, the predicted fatal-and-injury crash frequency can be disaggregated into estimates of fatal (K), incapacitating injury (A), non-incapacitating injury (B), and possible injury (C) crash frequency. A severity distribution function is used for this purpose. The function is an equation that includes some of the same variables used in the predictive model.

The equations that comprise the severity distribution function are described in Section 18.8 of the proposed *HSM* Freeways chapter. Application of these equations is described in Sample Problem 1 in Section 18.13.1 of the proposed *HSM* Freeways chapter.

A procedure for calibrating the severity distribution functions is described in Section B.1.4 of the proposed *HSM* Appendix B for Part C.

Predictive Method

The predictive method for freeway segments is described as a flow chart in Figure 18-1 of the proposed *HSM* Freeways chapter. The flow chart indicates that the method includes 18 steps that are completed in sequence when evaluating one or more sites. The method is described in sufficient generality that it can be applied to one or more sites, for one or more years, with or without the use of crash data.

The steps that comprise the predictive method are described in detail in Section 18.4.1 of the proposed *HSM* Freeways chapter. If the EB Method is used in the method, the related calculations are described in Section B.2 of the proposed *HSM* Appendix B for Part C.

A key step of the predictive method is to divide the facility being evaluated into individual sites (i.e., segments and speed-change lanes). The procedure for dividing the freeway into individual sites is described in Section 18.5 of the proposed *HSM* Freeways chapter.

Application of the predictive method is described in the sample problems in Section 18.13 of the proposed *HSM* Freeways chapter.

Limitations of the predictive method are identified in Section 18.10 of the of the proposed *HSM* Freeways chapter.

Output

The output data computed using the predictive method consists primarily of the expected crash frequency for each site and year in the evaluation period. Only the output data computed for the study period should be summarized given that it is most relevant to the analyst. Data for the crash period (available when the EB Method is used) may be of nominal interest, but its primary purpose to support the calculation of the expected average crash frequency for the *study* period.

The estimated crash frequency for a site can be reported in terms of the following performance measures:

- Total estimated number of crashes for the study period.
- Estimated crash frequency for each year during the study period

Either of these two measures can be further disaggregated in terms of crash severity or crash type. For example, the “total estimated number of crashes for the study period” can be disaggregated into the following measures.

- Total estimated number of crashes for each severity level
- Total estimated number of crashes for each crash type (e.g., head on, fixed object, etc.)

Other combinations of study year, severity level, and crash type can be devised, if desired.

If there are multiple sites, then the aforementioned measures should be computed for all sites combined. This type of project-wide aggregation will provide meaningful summary measures that facilitate the comparison of competing projects or alternatives for a given project.

Detailed output data can also be made available on a site-by-site basis. Of particular note are the crash modification factors. The value of a factor can be used as an indicator of relative crash risk. Collectively, these factors provide insight into geometric design and traffic control features that have potential for safety improvement.

If the input AADT volume data were incomplete (i.e., some years missing) and values were estimated (within the software) for the missing years, then the AADT volume history should be reported so that the analyst can review and confirm the suitability of the estimated volumes. Step 3 in Section 18.4.1 of the proposed *HSM* Freeways chapter provides some rules for estimating missing AADT volumes. These rules are implemented in ISATe.

ALGORITHM DESCRIPTION FOR FREEWAY SPEED-CHANGE LANES

This part of the appendix provides information needed to implement the predictive method for freeway speed-change lanes in software. This method is described in the proposed *HSM* Freeways chapter.

The remainder of this part consists of four sections. The first section identifies the input data needed by the predictive method. The second section presents the crash prediction models. The third section describes the sequence of steps that comprise the predictive method. The last section describes the output data that are available from an application of the predictive method.

Input Data

This section describes the input data for the predictive method. These data are identified using the following categories.

- Evaluation period.
- Evaluation type.
- Crash data.
- Geometric design, traffic control, and traffic volume data.

Evaluation Period

The evaluation period is the set of years in the combined study period and crash period. Every calendar year in the evaluation period is separately evaluated using the methodology.

Specific details about this input are provided in Section 18.4.1, Step 2 of the proposed *HSM* Freeways chapter.

Evaluation Type

The predictive method can be used to evaluate one site, or a contiguous group of sites. The evaluation is described as one of several types, as determined by the analyst. When one site is being evaluated, the evaluation types are:

- A. Evaluation based on using the predictive model only.
- B. Evaluation based on using the predictive model and crash data.

When a group of sites are being evaluated, the evaluation types are:

- A. Evaluation based on using the predictive model only for each site.
- B. Evaluation based on using the predictive model and crash data for each site.
- C. Evaluation based on using the predictive model for each site and crash data for the group of sites.

When crash data are used, the empirical Bayes (EB) Method is used to combine the crash data with the predictive model estimate to obtain a more reliable estimate of the expected crash frequency. The three evaluation types are referred to herein as types A, B, and C. In the *HSM*, type B evaluation is referred to as the “site-specific” EB Method and type C is referred to as “project-level” EB Method.

There are several factors to be considered when determining whether the EB Method is appropriate for a given project. These criteria are described in Sections B.2.1 and B.2.2 of the proposed *HSM* Appendix B for Part C.

Crash Counts

If evaluation type B is input by the analyst, then the crash data for each site are necessary input data. The criteria for assigning crashes to individual freeway speed-change lane sites are described in Section B.2.3 of the proposed *HSM* Appendix B for Part C. If evaluation type C is input, then the crash data for the group of sites is needed.

The crash counts must correspond to the crash period. The crash period can be site-specific; however, for coding convenience, the crash period should be the same for all sites. If the crash period includes multiple years, then the crash data do not have to be separately tabulated for each year at each site. Rather, it is sufficient for the analyst to input the total number of crashes for the crash period.

Geometric Design, Traffic Control, and Traffic Volume Data

The input data describing the geometric design and traffic volume data for freeway speed-change lanes are identified in the following list.

General

- Area type (urban or rural).

Geometric Design

- Number of through lanes.
- Segment length.
- Length and radius of horizontal curve.
- Lane width.
- Inside shoulder width.
- Median width.
- Length of rumble strips on inside shoulders.
- Length of (and offset to) median barrier.
- Presence and length of Type B weaving section.

Traffic Characteristics

- AADT volume of ramp associated with speed-change lane.
- AADT volume of freeway segment.
- Proportion of AADT that occurs during hours where the lane volume exceeds 1,000 veh/h/ln.

Specific details about these input data are provided in Section 18.4.2 of the proposed *HSM* Freeways chapter. These details include the method of measurement and the value limits for each variable. The AADT volume ranges for the predictive models are listed in Table 18-4 of the proposed *HSM* Freeways chapter.

The units of measurement for all input data are U.S. customary. If input data are provided in metric units, then they should undergo soft conversion to U.S. customary units before their use in the predictive method.

Predictive Models

The general structure of the predictive model is described by Equation 18-1 of the proposed *HSM* Freeways chapter. A more specific structure is described by Equation 18-7 and Equation 18-10.

Safety Performance Functions

Separate safety performance functions (SPFs) are provided for the following conditions:

- Area type (rural or urban).
- Through lanes (4, 6, 8, 10 in urban areas).
- Crash type (multiple-vehicle, single-vehicle).
- Crash severity (fatal-and-injury, property-damage-only).

All total, there are 28 SPFs represented by unique combinations of the four conditions identified in the preceding list. Specific details about the SPF regression coefficients are provided in Section 18.6.2 of the proposed *HSM* Freeways chapter.

Section 18.6.1 of the proposed *HSM* Freeways chapter describes a procedure for extending the SPFs to freeways with an odd number of lanes. Section B.2.7 of the proposed *HSM* Appendix B for Part C describes a procedure for applying the EB Method to freeways with an odd number of lanes.

The overdispersion parameter for ramp entrance speed-change lanes is computed as a function of speed-change lane length. The equation for this calculation is provided in Section 18.6.2 of the proposed *HSM* Freeways chapter. The factor for ramp exit speed-change lanes is a constant (i.e., it is not a function of speed-change lane length).

A procedure for calibrating the predictive models is described in Section B.1.1 of the proposed *HSM* Appendix B for Part C.

Crash Modification Factors

Eight crash modification factors (CMFs) are provided in the predictive method. The geometric design features and traffic conditions that they address are identified in the following list.

- Horizontal curvature.
- Lane width.
- Inside shoulder width.
- Median width.
- Median barrier.
- High-volume (congested) conditions.
- Ramp entrance length and side of freeway.
- Ramp exit length and side of freeway.

Specific details about the CMF formulation and regression coefficients are provided in Section 18.7.2 of the proposed *HSM* Freeways chapter. This section also identifies conditions where a CMF is not applicable.

Supplemental calculations for using the barrier-related CMFs are described in Section 18.7.3 of the proposed *HSM* Freeways chapter.

Crash Type Distribution

The predicted crash frequency from a predictive model can be disaggregated into estimates of crash frequency by crash type. The crash type categories for multiple-vehicle crashes include head-on, right-angle, rear-end, and sideswipe. The crash type categories for single-vehicle crashes include animal, fixed object, other object, and parked vehicle.

Distribution percentages for these crash types are provided in Section 18.6.2 of the proposed *HSM* Freeways chapter. Application of these percentages is described in Sample Problem 3 in Section 18.13.3 of the proposed *HSM* Freeways chapter.

Crash Severity Distribution

The predicted crash frequency from a predictive model can be disaggregated into estimates of crash severity. Specifically, the predicted fatal-and-injury crash frequency can be disaggregated into estimates of fatal (K), incapacitating injury (A), non-incapacitating injury (B), and possible injury (C) crash frequency. A severity distribution function is used for this purpose. The function is an equation that includes some of the same variables used in the predictive model.

The equations that comprise the severity distribution function are described in Section 18.8 of the proposed *HSM* Freeways chapter. Application of these equations is described in Sample Problem 3 in Section 18.13.3 of the proposed *HSM* Freeways chapter.

A procedure for calibrating the severity distribution functions is described in Section B.1.4 of the proposed *HSM* Appendix B for Part C.

Predictive Method

The predictive method for freeway speed-change lanes is described as a flow chart in Figure 18-1 of the proposed *HSM* Freeways chapter. The flow chart indicates that the method includes 18 steps that are completed in sequence when evaluating one or more sites. The method is described in sufficient generality that it can be applied to one or more sites, for one or more years, with or without the use of crash data.

The steps that comprise the predictive method are described in detail in Section 18.4.1 of the proposed *HSM* Freeways chapter. If the EB Method is used in the method, the related calculations are described in Section B.2 of the proposed *HSM* Appendix A for Part C.

A key step of the predictive method is to divide the facility being evaluated into individual sites (i.e., segments and speed-change lanes). The procedure for dividing the freeway into individual sites is described in Section 18.5 of the proposed *HSM* Freeways chapter.

Application of the predictive method is described in the sample problems in Section 18.13 of the proposed *HSM* Freeways chapter.

Limitations of the predictive method are identified in Section 18.10 of the of the proposed *HSM* Freeways chapter.

Output

The output data computed using the predictive method consists primarily of the expected crash frequency for each site and year in the evaluation period. Useful performance measures and techniques for presenting this output are presented in the Output section in the previous part of this document.

ALGORITHM DESCRIPTION FOR RAMP SEGMENTS

This part of the appendix provides information needed to implement the predictive method for ramp segments in software. This method is described in the proposed *HSM* Ramps chapter.

The remainder of this part consists of four sections. The first section identifies the input data needed by the predictive method. The second section presents the crash prediction models. The third section describes the sequence of steps that comprise the predictive method. The last section describes the output data that are available from an application of the predictive method.

Input Data

This section describes the input data for the predictive method. These data are identified using the following categories.

- Evaluation period.
- Evaluation type.
- Crash data.
- Geometric design, traffic control, and traffic volume data.

Evaluation Period

The evaluation period is the set of years in the combined study period and crash period. Every calendar year in the evaluation period is separately evaluated using the methodology.

Specific details about this input are provided in Section 19.4.1, Step 2 of the proposed *HSM* Ramps chapter.

Evaluation Type

The predictive method can be used to evaluate one site, or a contiguous group of sites. The evaluation is described as one of several types, as determined by the analyst. When one site is being evaluated, the evaluation types are:

- A. Evaluation based on using the predictive model only.
- B. Evaluation based on using the predictive model and crash data.

When a group of sites are being evaluated, the evaluation types are:

- A. Evaluation based on using the predictive model only for each site.
- B. Evaluation based on using the predictive model and crash data for each site.
- C. Evaluation based on using the predictive model for each site and crash data for the group of sites.

When crash data are used, the empirical Bayes (EB) Method is used to combine the crash data with the predictive model estimate to obtain a more reliable estimate of the expected crash frequency. The three evaluation types are referred to herein as types A, B, and C. In the HSM, type B evaluation is referred to as the “site-specific” EB Method and type C is referred to as “project-level” EB Method.

There are several factors to be considered when determining whether the EB Method is appropriate for a given project. These criteria are described in Sections B.2.1 and B.2.2 of the proposed *HSM* Appendix B for Part C.

Crash Counts

If evaluation type B is input by the analyst, then the crash data for each site are necessary input data. The criteria for assigning crashes to individual ramp segment sites are described in Section B.2.3 of the proposed *HSM* Appendix B for Part C. If evaluation type C is input, then the crash data for the group of sites is needed.

The crash counts must correspond to the crash period. The crash period can be site-specific; however, for coding convenience, the crash period should be the same for all sites. If the crash period includes multiple years, then the crash data do not have to be separately tabulated for each year at each site. Rather, it is sufficient for the analyst to input the total number of crashes for the crash period.

Geometric Design, Traffic Control, and Traffic Volume Data

The input data describing the geometric design and traffic volume data for ramp segments are identified in the following list.

General

- Area type (urban or rural).

Geometric Design

- Number of through lanes.
- Segment length.
- Length and radius of horizontal curve.
- Lane width.
- Left and right shoulder width.
- Length of (and offset to) right side barrier.
- Length of (and offset to) left side barrier.
- Presence of lane add or drop.
- Presence of speed-change lane (associated with a ramp-to-ramp merge or diverge).
- Presence and length of weaving section (only applicable to C-D roads).

Traffic Characteristics

- AADT volume of ramp segment.

Specific details about these input data are provided in Section 19.4.2 of the proposed *HSM Ramps* chapter. These details include the method of measurement and the value limits for each variable. The AADT volume ranges for the predictive models are listed in Table 19-4 of the proposed *HSM Ramps* chapter.

The units of measurement for all input data are U.S. customary. If input data are provided in metric units, then they should undergo soft conversion to U.S. customary units before their use in the predictive method.

Predictive Models

The general structure of the predictive model is described by Equation 19-1 of the proposed *HSM Ramps* chapter. A more specific structure is described by Equation 19-2 and Equation 19-7.

Safety Performance Functions

Separate safety performance functions (SPFs) are provided for the following conditions:

- Area type (rural or urban).
- Ramp type (entrance ramp, exit ramp, C-D road)
- Through lanes (1, 2 in urban areas).
- Crash type (multiple-vehicle, single-vehicle).
- Crash severity (fatal-and-injury, property-damage-only).

All total, there are 36 SPFs represented by unique combinations of the five conditions identified in the preceding list. Specific details about the SPF regression coefficients are provided in Section 19.6.1 of the proposed *HSM Ramps* chapter.

The overdispersion parameter is computed as a function of segment length. The equation for this calculation is provided in Section 19.6.1 of the proposed *HSM Ramps* chapter.

A procedure for calibrating the predictive models is described in Section B.1.1 of the proposed *HSM* Appendix B for Part C.

Crash Modification Factors

Nine crash modification factors (CMFs) are provided in the predictive method. The geometric design features and traffic conditions that they address are identified in the following list.

- Horizontal curvature.
- Lane width.
- Right shoulder width.
- Left shoulder width.
- Right side barrier.
- Left side barrier.
- Lane add or drop.
- Ramp speed-change lane.
- Weaving section.

Specific details about the CMF formulation and regression coefficients are provided in Section 19.7.1 of the proposed *HSM Ramps* chapter. This section also identifies conditions where a CMF is not applicable.

Supplemental calculations for using the barrier-related CMFs and the Horizontal Curve CMF are described in Section 19.7.3 of the proposed *HSM Ramps* chapter.

Crash Type Distribution

The predicted crash frequency from a predictive model can be disaggregated into estimates of crash frequency by crash type. The crash type categories for multiple-vehicle crashes include head-on, right-

angle, rear-end, and sideswipe. The crash type categories for multiple-vehicle crashes include animal, fixed object, other object, and parked vehicle.

Distribution percentages for these crash types are provided in Section 19.6.1 of the proposed *HSM Ramps* chapter. Application of these percentages is described in Sample Problem 1 in Section 19.14.1 of the proposed *HSM Ramps* chapter.

Crash Severity Distribution

The predicted crash frequency from a predictive model can be disaggregated into estimates of crash severity. Specifically, the predicted fatal-and-injury crash frequency can be disaggregated into estimates of fatal (K), incapacitating injury (A), non-incapacitating injury (B), and possible injury (C) crash frequency. A severity distribution function is used for this purpose. The function is an equation that includes some of the same variables used in the predictive model.

The equations that comprise the severity distribution function for ramp segments are described in Section 19.8.1 of the proposed *HSM Ramps* chapter. Application of these equations is described in Sample Problem 1 in Section 19.14.1 of the proposed *HSM Ramps* chapter.

A procedure for calibrating the severity distribution functions is described in Section B.1.4 of the proposed *HSM Appendix A* for Part C.

Predictive Method

The predictive method for ramp segments is described as a flow chart in Figure 19-2 of the proposed *HSM Ramps* chapter. The flow chart indicates that the method includes 18 steps that are completed in sequence when evaluating one or more sites. The method is described in sufficient generality that it can be applied to one or more sites, for one or more years, with or without the use of crash data.

The steps that comprise the predictive method are described in detail in Section 19.4.1 of the proposed *HSM Ramps* chapter. If the EB Method is used in the method, the related calculations are described in Section B.2 of the proposed *HSM Appendix A* for Part C.

A key step of the predictive method is to divide the facility being evaluated into individual sites (i.e., ramp segments and crossroad ramp terminals). The procedure for dividing the ramps into individual sites is described in Section 19.5 of the proposed *HSM Ramps* chapter.

Application of the predictive method is described in the sample problems in Section 19.14 of the proposed *HSM Ramps* chapter.

Limitations of the predictive method are identified in Section 19.11 of the of the proposed *HSM Ramps* chapter.

Output

The output data computed using the predictive method consists primarily of the expected crash frequency for each site and year in the evaluation period. Useful performance measures and techniques for presenting this output are presented in the Output section in the part titled Algorithm Description for Freeway Segments.

ALGORITHM DESCRIPTION FOR CROSSROAD RAMP TERMINALS

This part of the appendix provides information needed to implement the predictive method for crossroad ramp terminals in software. This method is described in the proposed *HSM Ramps* chapter.

The remainder of this part consists of four sections. The first section identifies the input data needed by the predictive method. The second section presents the crash prediction models. The third section describes the sequence of steps that comprise the predictive method. The last section describes the output data that are available from an application of the predictive method.

Input Data

This section describes the input data for the predictive method. These data are identified using the following categories.

- Evaluation period.
- Evaluation type.
- Crash data.
- Geometric design, traffic control, and traffic volume data.

Evaluation Period

The evaluation period is the set of years in the combined study period and crash period. Every calendar year in the evaluation period is separately evaluated using the methodology.

Specific details about this input are provided in Section 19.4.1, Step 2 of the proposed *HSM* Ramps chapter.

Evaluation Type

The predictive method can be used to evaluate one site, or a contiguous group of sites. The evaluation is described as one of several types, as determined by the analyst. When one site is being evaluated, the evaluation types are:

- A. Evaluation based on using the predictive model only.
- B. Evaluation based on using the predictive model and crash data.

When a group of sites are being evaluated, the evaluation types are:

- A. Evaluation based on using the predictive model only for each site.
- B. Evaluation based on using the predictive model and crash data for each site.
- C. Evaluation based on using the predictive model for each site and crash data for the group of sites.

When crash data are used, the empirical Bayes (EB) Method is used to combine the crash data with the predictive model estimate to obtain a more reliable estimate of the expected crash frequency. The three evaluation types are referred to herein as types A, B, and C. In the HSM, type B evaluation is referred to as the “site-specific” EB Method and type C is referred to as “project-level” EB Method.

There are several factors to be considered when determining whether the EB Method is appropriate for a given project. These criteria are described in Sections B.2.1 and B.2.2 of the proposed *HSM* Appendix A for Part C.

Crash Counts

If evaluation type B is input by the analyst, then the crash data for each site are necessary input data. The criteria for assigning crashes to individual crossroad ramp terminal sites are described in Section B.2.3 of the proposed *HSM* Appendix A for Part C. If evaluation type C is input, then the crash data for the group of sites is needed.

The crash counts must correspond to the crash period. The crash period can be site-specific; however, for coding convenience, the crash period should be the same for all sites. If the crash period includes multiple years, then the crash data do not have to be separately tabulated for each year at each site. Rather, it is sufficient for the analyst to input the total number of crashes for the crash period.

Geometric Design, Traffic Control, and Traffic Volume Data

The input data describing the geometric design and traffic volume data for crossroad ramp terminals are identified in the following list.

General

- Area type (urban or rural).
- Ramp terminal configuration.

Geometric Design Data for All Terminals

- Number of through lanes on each crossroad approach.
- Number of lanes on the exit ramp.
- Number of crossroad approaches with left-turn lanes.
- Number of crossroad approaches with right-turn lanes.
- Number of unsignalized public street approaches to the crossroad leg outside of the interchange.
- Distance to the next public street intersection
- Distance to the adjacent crossroad ramp terminal.
- Crossroad median width and left-turn lane width.

Geometric Design Data for Signalized Terminals Only

- Number of unsignalized driveways on the crossroad leg outside of the interchange.
- Number of crossroad approaches with protected-only left-turn operation.
- Number of crossroad approaches with right-turn channelization.
- Presence of exit ramp right-turn channelization.
- Presence of a non-ramp public street leg at the terminal.

Geometric Design Data for Unsignalized Terminals Only

- Skew angle.

Traffic Control

- Type of traffic control (signal, one-way stop, all-way stop).
- Type of control for the exit ramp right-turn movement.

Traffic Characteristics

- AADT volume for the inside and outside crossroad legs
- AADT volume for each ramp leg.

Specific details about these input data are provided in Section 19.4.2 of the proposed *HSM Ramps* chapter. These details include the method of measurement and the value limits for each variable. The AADT volume ranges for the predictive models are listed in Table 19-11 of the proposed *HSM Ramps* chapter.

The units of measurement for all input data are U.S. customary. If input data are provided in metric units, then they should undergo soft conversion to U.S. customary units before their use in the predictive method.

Predictive Models

The general structure of the predictive model is described by Equation 19-1 of the proposed *HSM Ramps* chapter. A more specific structure is described by Equation 19-12 and Equation 19-15.

Safety Performance Functions

Separate safety performance functions (SPFs) are provided for the following conditions:

- Area type (rural or urban).
- Terminal configuration (D3ex, D3en, D4, A4, B4, A2, B2)
- Control mode (signal, one-way stop)
- Crossroad through lanes (2, 3, 4, 5 signalized in urban areas, 6 signalized in urban areas).
- Crash severity (fatal-and-injury, property-damage-only).

All total, there are 196 SPFs represented by unique combinations of the five conditions identified in the preceding list. Specific details about the SPF regression coefficients are provided in Section 19.6.2 of the proposed *HSM Ramps* chapter.

The overdispersion parameter is constant. It is provided in Section 19.6.2 of the proposed *HSM Ramps* chapter.

A procedure for calibrating the predictive models is described in Section B.1.1 of the proposed *HSM Appendix A* for Part C.

Crash Modification Factors

Eleven crash modification factors (CMFs) are provided in the predictive method. The geometric design features, traffic control features, and traffic conditions that they address are identified in the following list.

- Exit ramp capacity.
- Crossroad left-turn lane.
- Crossroad right-turn lane.
- Access point frequency.
- Segment length.
- Median width.
- Protected left-turn operation (signalized terminals only).
- Channelized right turn on crossroad (signalized terminals only).
- Channelized right turn on exit ramp (signalized terminals only).
- Non-ramp public street leg (signalized terminals only).
- Skew angle (unsignalized terminals only).

Specific details about the CMF formulation and regression coefficients are provided in Section 19.7.2 of the proposed *HSM Ramps* chapter. This section also identifies conditions where a CMF is not applicable.

A CMF for all-way stop control is also provided with the predictive model for one-way stop controlled terminals. A procedure for using it is described in Section 19.10 of the proposed *HSM Ramps* chapter. It is an interim procedure to be used to evaluate all-way stop controlled terminals until a better procedure can be developed through research.

Crash Type Distribution

The predicted crash frequency from a predictive model can be disaggregated into estimates of crash frequency by crash type. The crash type categories for multiple-vehicle crashes include head-on, right-angle, rear-end, and sideswipe. The crash type categories for single-vehicle crashes include animal, fixed object, other object, and parked vehicle.

Distribution percentages for these crash types are provided in Section 19.6.2 of the proposed *HSM Ramps* chapter. Application of these percentages is described in Sample Problem 4 in Section 19.14.4 of the proposed *HSM Ramps* chapter.

Crash Severity Distribution

The predicted crash frequency from a predictive model can be disaggregated into estimates of crash severity. Specifically, the predicted fatal-and-injury crash frequency can be disaggregated into estimates of fatal (K), incapacitating injury (A), non-incapacitating injury (B), and possible injury (C) crash frequency. A severity distribution function is used for this purpose. The function is an equation that includes some of the same variables used in the predictive model.

The equations that comprise the severity distribution function for crossroad ramp terminals are described in Section 19.8.2 of the proposed *HSM Ramps* chapter. Application of these equations is described in Sample Problem 4 in Section 19.14.4 of the proposed *HSM Ramps* chapter.

A procedure for calibrating the severity distribution functions is described in Section B.1.4 of the proposed *HSM* Appendix A for Part C.

Predictive Method

The predictive method for crossroad ramp terminals is described as a flow chart in Figure 19-2 of the proposed *HSM* Ramps chapter. The flow chart indicates that the method includes 18 steps that are completed in sequence when evaluating one or more sites. The method is described in sufficient generality that it can be applied to one or more sites, for one or more years, with or without the use of crash data.

The steps that comprise the predictive method are described in detail in Section 19.4.1 of the proposed *HSM* Ramps chapter. If the EB Method is used in the method, the related calculations are described in Section B.2 of the proposed *HSM* Appendix A for Part C.

A key step of the predictive method is to divide the facility being evaluated into individual sites (i.e., ramp segments and crossroad ramp terminals). The procedure for dividing the ramps into individual sites is described in Section 19.5 of the proposed *HSM* Ramps chapter.

Application of the predictive method is described in the sample problems in Section 19.14 of the proposed *HSM* Ramps chapter.

Limitations of the predictive method are identified in Section 19.11 of the of the proposed *HSM* Ramps chapter.

Output

The output data computed using the predictive method consists primarily of the expected crash frequency for each site and year in the evaluation period. Useful performance measures and techniques for presenting this output are presented in the Output section in the part titled Algorithm Description for Freeway Segments.

SOFTWARE DOCUMENTATION

This part of the document uses a series of flow charts and linkage lists to document the logic flow for the ISATe software.

Flowcharts

The calculation sequence is controlled by the subroutine titled `Main_PerformanceCalculations`. It calls other subroutines in the sequence needed to complete the calculations. This subroutine is shown in Figure 1. The subroutines called by this main subroutine are identified by name in parentheses in the flowchart boxes.

When the main subroutine is invoked, it initially clears any data in the output worksheets that is left from a prior evaluation. It also sets all variable values to zero. Next, the main subroutine calls a subroutine that reads the regression coefficients and local calibration factors from the Calibration Factors worksheet. Then, it calls the performance measures subroutine. This subroutine implements the calculations associated with the predictive methods described in the proposed *HSM* chapters. When the calculations are complete, a subroutine is called to write the performance measures to the output worksheets. More information about these subroutines is provided in the section titled Linkage Lists.

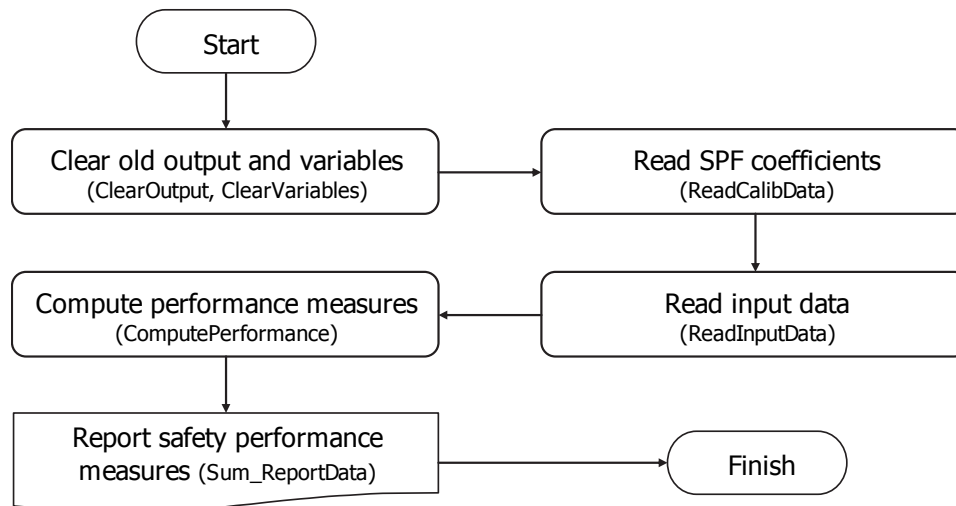


Figure 1. Main Subroutine

The calculation sequence for the performance measures subroutine (i.e., ComputePerformance) is shown in Figure 2. Initially, it checks the input AADT volume data to determine if there are any missing data. If one or more volumes are missing, then a subroutine is called that implements the rules for estimating missing volume. These rules are described in Step 3 in Section 18.4.1 of the proposed *HSM* Freeways chapter.

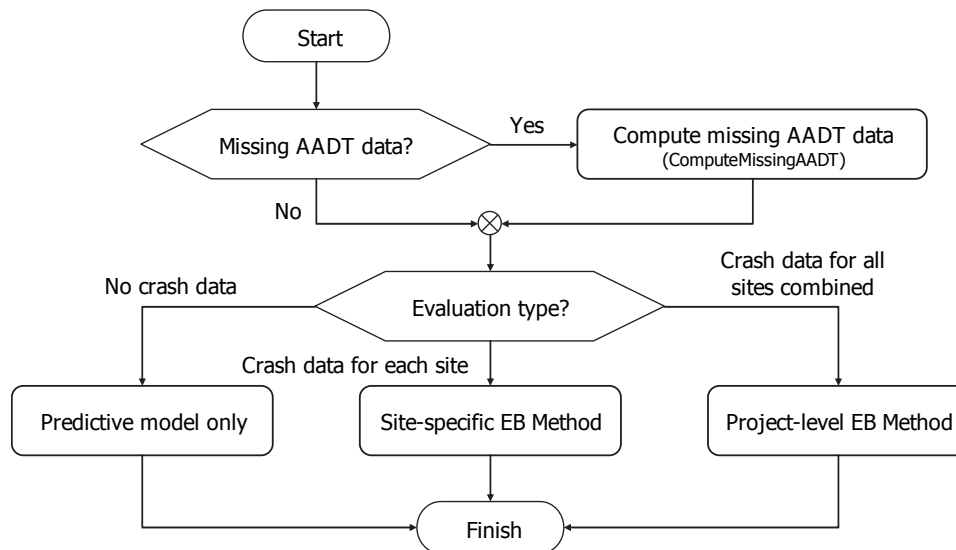


Figure 2. Performance Measures Subroutine

Once the AADT data are determined to be complete, the predictive method is initiated. This method has three variations, depending on whether crash data are available and, if available, whether it can be correctly associated with individual sites. One of three evaluation types is identified based on these three considerations. The choice of evaluation type dictates the subsequent sequence of calculations.

Predictive Model Only

If the evaluation is determined to be based on the predictive model only, then the calculation sequence is shown in Figure 3. Two variations are shown in the figure. One variation applies to freeway segments. The other variation applies to ramp segments. This latter variation includes a subroutine to calculate ramp curve speed. The chart shown in Figure 3b can be applied to crossroad ramp terminals if the subroutine for computing curve speed is removed and the references to “ramp segment” are changed to “ramp terminal.”

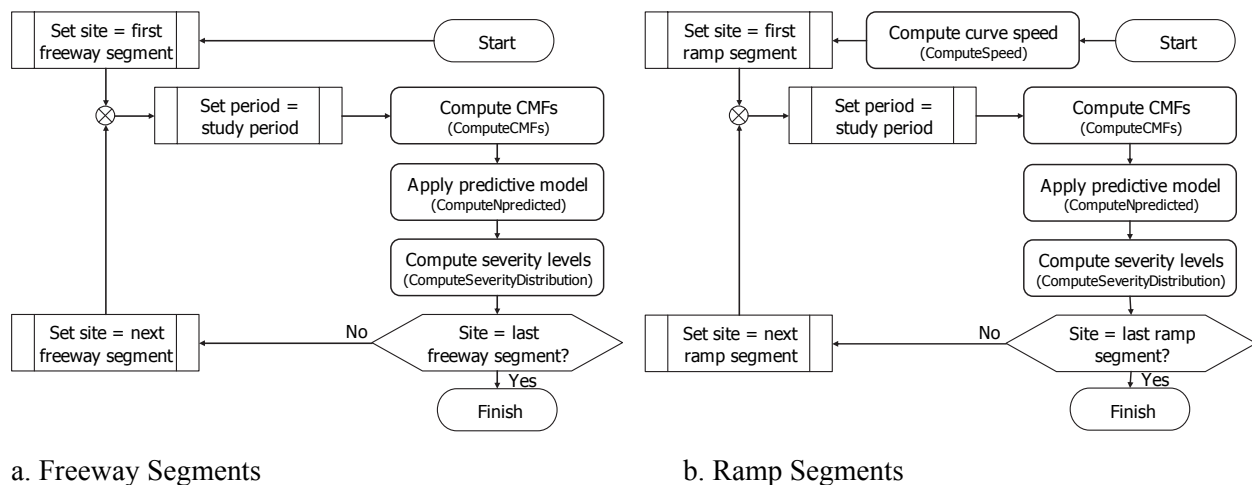


Figure 3. Evaluation based on Predictive Model Only

The subroutine sequence in Figure 3 is shown to be repeated for each site. The first subroutine called in Figure 3a is used to calculate the CMFs for each year at the subject site. These CMFs are then used in the second subroutine to calculate the predicted average crash frequency using the predictive model. Finally, the third subroutine computes the crash severity distribution and combines it with the predicted average crash frequency from the previous subroutine to estimate the crash frequency by severity level. The sequence is repeated until all sites are evaluated.

Site-Specific EB Method

If the evaluation is determined to be based on the site-specific EB Method, then the calculation sequence is shown in Figure 4. Two variations are shown in the figure. One variation applies to freeway segments. It includes a subroutine to calculate an equivalent overdispersion parameter for odd-lane cross sections based on the parameters provided for even-lane SPFs. The other variation applies to ramp segments. This variation includes a subroutine to calculate ramp curve speed. The chart shown in Figure 4b can be applied to crossroad ramp terminals if the subroutine for computing curve speed is removed and the references to “ramp segment” are changed to “ramp terminal.”

The subroutine sequence in Figure 4 is shown to have two looping sequences. In the first loop, the sequence is repeated for each site. Each site is evaluated once for the crash period and once for the study period. The first subroutine called in Figure 4a is used to calculate the CMFs for each year at the subject site. These CMFs are then used in the second subroutine to calculate the predicted average crash frequency using the predictive model. Finally, the third subroutine computes the equivalent overdispersion parameter, as described in the previous paragraph. The sequence is repeated until all sites are evaluated.

In the second loop shown in Figure 4, the sequence is again repeated for each site but only for the study period. The first subroutine implements the EB Method to combine the predicted crash frequency with the crash data to obtain an estimate of the expected average crash frequency. The second subroutine computes the crash severity distribution and combines it with the expected average crash frequency from the previous subroutine to estimate the crash frequency by severity level.

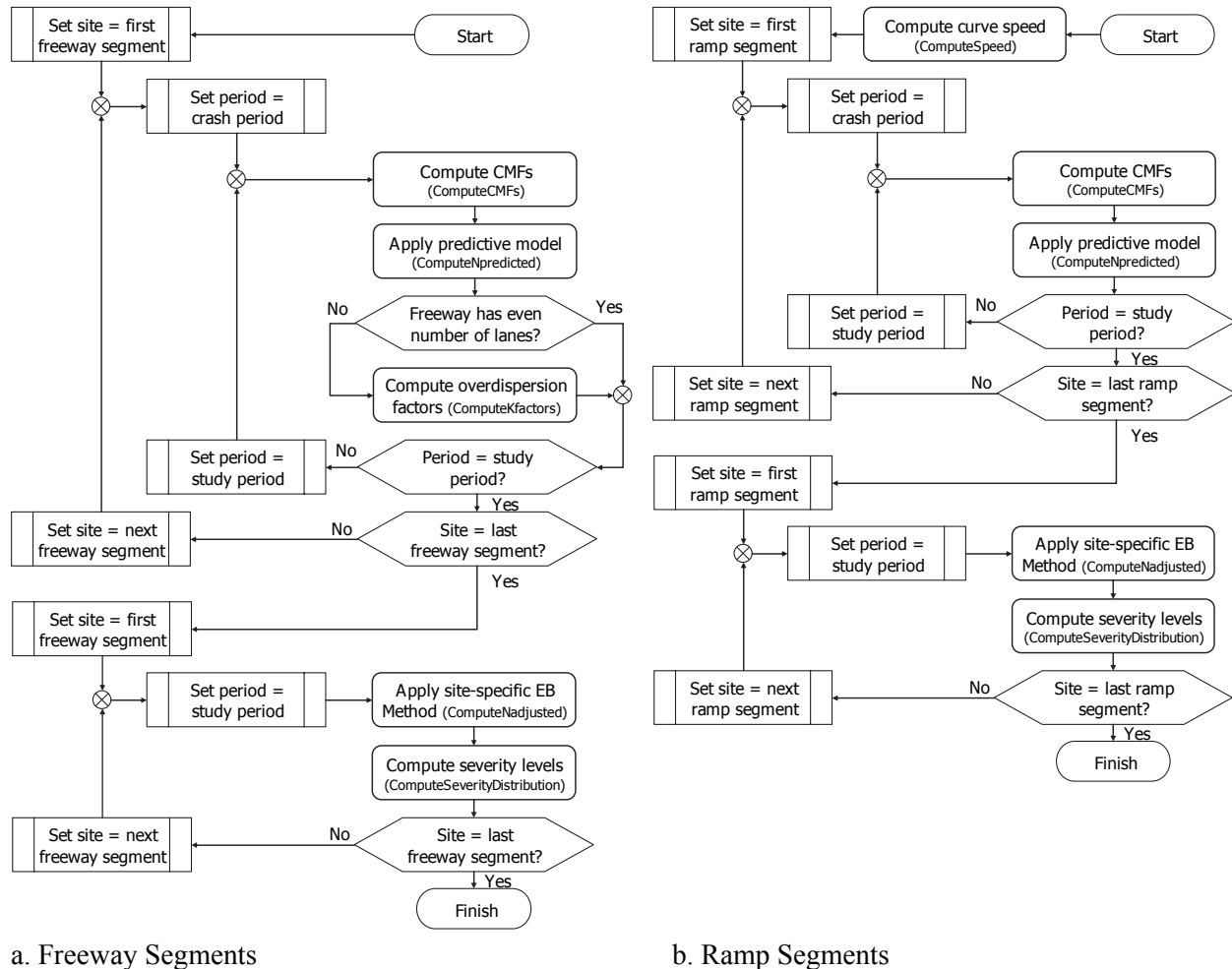


Figure 4. Evaluation based on the Site-Specific EB Method

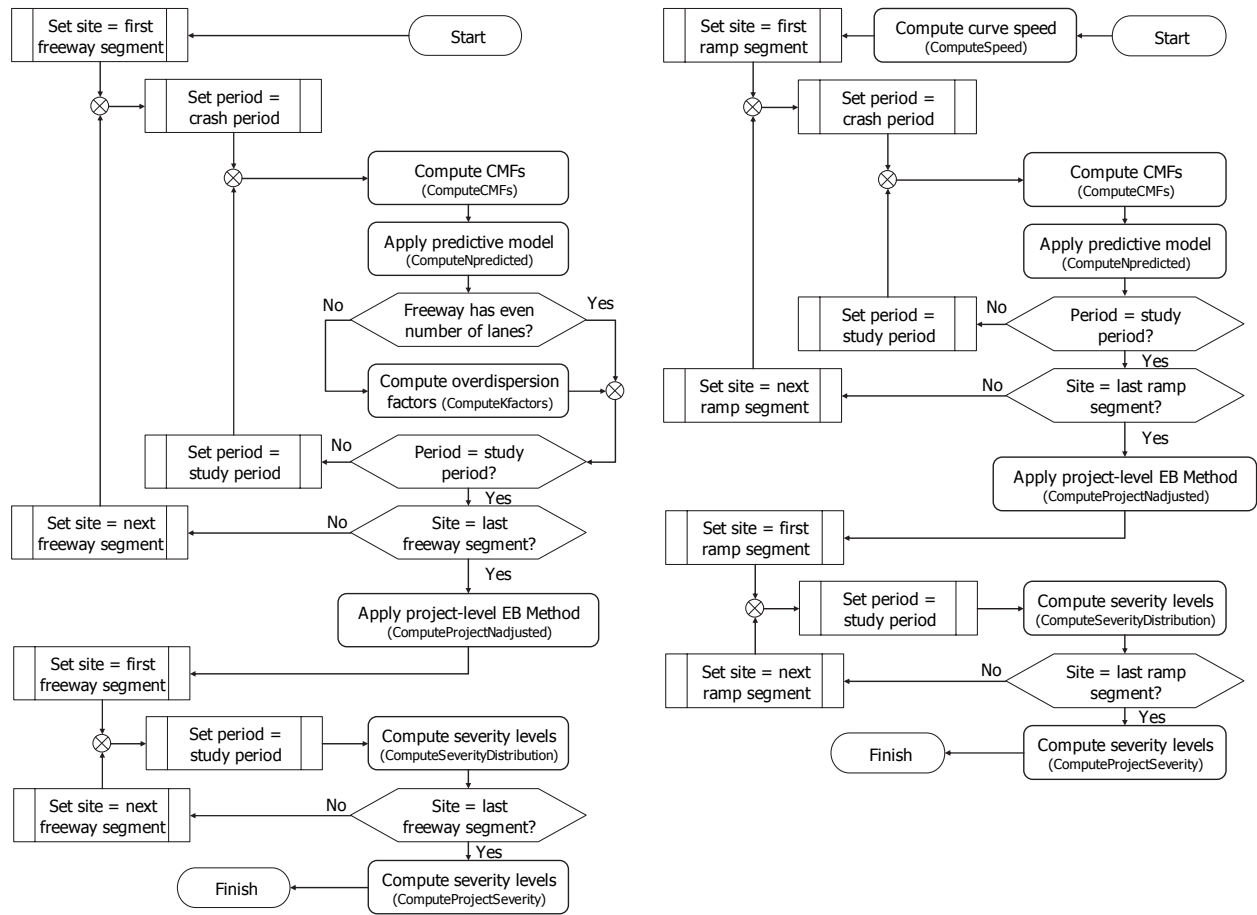
Project-Level EB Method

If the evaluation is determined to be based on the project-level EB Method, then the calculation sequence is shown in Figure 5. Two variations are shown in the figure. One variation applies to freeway segments. It includes a subroutine to calculate an equivalent overdispersion parameter for odd-lane cross sections based on the parameters provided for even-lane SPFs. The other variation applies to ramp segments. This variation includes a subroutine to calculate ramp curve speed. The chart shown in Figure 5b can be applied to crossroad ramp terminals if the subroutine for computing curve speed is removed and the references to “ramp segment” are changed to “ramp terminal.”

The subroutine sequence in Figure 5 is shown to have two looping sequences. In the first loop, the sequence is repeated for each site. Each site is evaluated once for the crash period and once for the study period. This sequence of calculations is described in the discussion associated with Figure 4. When the

loop is completed, the project-level EB Method calculations are completed for the collective set of sites to produce an estimate of the total expected average crash frequency.

In the second loop shown in Figure 5, the sequence is again repeated for each site but only for the study period. The subroutine in this loop computes the crash severity distribution and combines it with the predicted average crash frequency from a previous subroutine to estimate the crash frequency by severity level for each site. After the loop is complete, the last subroutine uses the site estimates of predicted average crash frequency by severity level to compute a total by severity level for the project. The proportion of predicted crashes in each severity level is then multiplied by the total expected average crash frequency to compute the distribution of expected average crash frequency by severity level for the project.



a. Freeway Segments

b. Ramp Segments

Figure 5. Evaluation based on the Project-Level EB Method

Linkage Lists

This section uses linkage lists to describe the main subroutines that comprise the ISATe software. Each list is provided in a table that identifies the main subroutine and the subroutines that it calls. A brief description is provided for each called subroutine.

A linkage list is provided in Table 1 for the subroutines identified in Figure 1. The subroutine naming convention includes a prefix for many subroutines to denote their application to one of the three freeway facility components (i.e., freeway segments, ramp segments, and crossroad ramp terminals). In each case, the subroutine includes the same basic calculations but it is tailored to address some unique elements of the associated facility component. The prefix is not shown in the table because the description offered is sufficiently general as to be applicable to all components.

Table 1. Linkage List for Key Subroutines

Main Subroutine ^a	Called Subroutine ^a	Called Subroutine Description
Main_PerformCalculations	CheckLaneCounts	Check lanes entered for sites and report a warning message for any sites with a lane count that is not consistent with the limits of the predictive model for the input area type.
	<u>ClearOutput</u>	Clear all cells in the output worksheets. Cells are blank (empty) after this subroutine is called.
	<u>ClearVariables</u>	Set all variables and arrays to zero.
	<u>ReadCalibData</u>	Read all regression coefficients, distribution values, and calibration factors in the Calibration Factors worksheet.
	<u>ReadInputData</u>	Read input data from the input worksheets.
	<u>ComputePerformance</u>	Compute performance measures for each year in the evaluation period for each site in the project.
	Sum_ReportData	Combines the freeway, ramp, and ramp terminal performance measures and reports the results at the project level, as total crashes by severity and crash type. Reports results in the Output Summary worksheet.
<u>ReadInputData</u>	GetData	Reads a cell with a blue background. If the background is not blue, then a zero or blank is returned.
Sum_ReportData	<u>Report</u>	Combines site performance measures for a specified freeway component (i.e., freeway, ramp, or ramp terminal) as total crashes by severity and crash type.
<u>Report</u>	ClearMOCDistribution	Clears the manner-of-collision-by-severity array. Sets all a values to zero.
	<u>ComputeMOCDistribution</u>	Computes the manner-of-collision-by-severity array for all years and sites combined.

Note:

a. Underlined subroutine names actually represent three subroutines and have a prefix of "Frwy_," "Ramp_," or "Term_." Each subroutine variation is minor variations to address one of the three freeway components: freeway, ramp, or crossroad ramp terminal.

The linkage list provided in Table 2 is specific to the subroutines called by the performance measures subroutine. These subroutines are identified in Figure 2 to Figure 5.

Table 2. Subroutines Implementing the Predictive Method

Main Subroutine ^a	Called Subroutine ^a	Called Subroutine Description
<u>ComputePerformance</u>	ComputeMissingAADT	Scans the AADT input cells for each year at each site. If an AADT value for a given year is missing, then it is estimated using the rules described in Step 3 of the predictive method.
	<u>ComputeCMFs</u>	Computes the value of each applicable CMF for each year at each site.
	<u>ComputeNpredicted</u>	Combines the CMFs with the SPFs and the calibration factor to compute the predicted average crash frequency for each year at each site.
	Frwy_ComputeKfactors	Used only in the Freeways module when the EB Method is applied. This subroutine computes an effective overdispersion parameter when the segment has an odd number of lanes. It is generalized such that it is called regardless of whether the lane count is even or odd. However, the computed overdispersion parameter is equal to the input factor value when the segment has an even number of lanes.
	<u>ComputeNadjusted</u>	Used when the site-specific EB Method is applied. This subroutine combines the predictive model estimate with the crash count to determine the expected average crash frequency for each year at each site.
	<u>ComputeSeverityDistribution</u>	Uses a severity distribution function to estimate the crash severity distribution. Combines this distribution with the estimated crash frequency to estimate the crash frequency by severity level for each site.
	<u>ComputeProjectSeverity</u>	Uses the predicted crash frequency by severity level for each site from ComputeSeverityDistribution with the total expected number of crashes from ComputeProjectNadjusted to estimate the total crash frequency by severity level for the project.
	<u>ComputeProjectNpredicted</u>	Used when the project-level EB Method is applied. This subroutine combines the predictive model estimates for each year at each site to produce a total estimated number of crashes for the project.
	<u>ComputeProjectNadjusted</u>	Used when the project-level EB Method is applied. This subroutine combines the predictive model estimate with the crash count to determine the total expected number of crashes for the project.
Ramp_ComputeSpeed	Used only in the Ramps module. This subroutine computes the curve entry speed for each ramp curve.	

Note:

- a. Underlined subroutine names actually represent three subroutines and have a prefix of "Frwy_," "Ramp_," or "Term_." Each subroutine variation is minor variations to address one of the three freeway components: freeway, ramp, or crossroad ramp terminal.

